

# ORGANOMETALLICS

Volume 5, Number 3, March 1986

© Copyright 1986  
American Chemical Society

## Photochemistry of Matrix-Isolated $\text{CH}_3\text{Mn}(\text{CO})_5$ : Evidence for Two Isomers of $\text{CH}_3\text{Mn}(\text{CO})_4$

Amanda Horton-Mastin, Martyn Poliakoff,\* and James J. Turner\*

Department of Chemistry, University of Nottingham, Nottingham NG7 2RD, England

Received July 2, 1985

UV photolysis of  $\text{CH}_3\text{Mn}(\text{CO})_5$  isolated in  $\text{CH}_4$  or Ar matrices at 20 K provides IR and UV-vis evidence for two isomers of the coordinatively unsaturated fragment  $\text{CH}_3\text{Mn}(\text{CO})_4$ , with square-pyramidal structures **3b** and **4b**. Both isomers show a large shift between the position of their visible absorption maxima in Ar and  $\text{CH}_4$  matrices, consistent with an interaction of the matrix with the unsaturated metal center.

### Introduction

There is considerable interest, both experimental and theoretical, in the structure of coordinatively unsaturated transition-metal carbonyl species. Matrix isolation has been very successful in providing structural information about such carbonyl fragments and a large amount of work has centered around the geometry of five-coordinate  $d^6$  species.<sup>1</sup>

Early work by Perutz and Turner<sup>2,3</sup> involved  $\text{Cr}(\text{CO})_5$ , generated by UV photolysis of matrix-isolated  $\text{Cr}(\text{CO})_6$ . The structure was shown to be square-pyramidal, **1**, by a combination of  $^{13}\text{C}$  enrichment and IR spectroscopy,<sup>2</sup> a technique which has since been very widely applied.<sup>4</sup> This square-pyramidal structure, **1**, was quickly found to be in agreement with simple molecular orbital predictions.<sup>5</sup> Nevertheless, there have been arguments<sup>6</sup> over the possibility that structure **1** was imposed by the matrix and "free"  $\text{Cr}(\text{CO})_5$  would have a trigonal-bipyramidal structure. These suggestions have been finally disproved by very recent time-resolved infrared experiments<sup>7</sup> which show that "naked"  $\text{Cr}(\text{CO})_5$  has the same  $C_{4v}$  structure in the gas phase as in condensed phases.<sup>2</sup>

The question then arose whether a square-pyramidal or pseudo-square-pyramidal structure would always be the most stable for a five-coordinate 16-electron species con-

taining a  $d^6$  metal center. Would all  $\text{M}(\text{CO})_4\text{R}$  species adopt structures **3** and **4** or would the pseudo-trigonal structure **5** be more stable in some cases?<sup>8</sup> Molecular orbital calculations<sup>9</sup> for  $\text{Mn}(\text{CO})_4\text{X}$  species made the interesting prediction that the trigonal structure **5c** would be the most stable for  $\text{Mn}(\text{CO})_4\text{Br}$  but for  $\text{HMn}(\text{CO})_4$ , structures **3a**, **4a**, and **5a** would all have similar energies. The difference between  $\text{Mn}(\text{CO})_4\text{Br}$  and  $\text{HMn}(\text{CO})_4$  was attributed<sup>9</sup> to  $\pi$ -bonding effects of Br. Subsequent matrix isolation experiments,<sup>10</sup> again involving  $^{13}\text{C}$  enrichment, showed that  $\text{Mn}(\text{CO})_4\text{Br}$  did indeed have the predicted pseudo-trigonal-bipyramidal structure **5c**. More recently  $\text{HMn}(\text{CO})_4$ , generated by photolysis of  $\text{HMn}(\text{CO})_5$ , was shown<sup>11</sup> to have two isomers  $C_s$  and  $C_{4v}$ , **3a** and **4a**, both clearly derived from the square-based-pyramidal  $\text{M}(\text{CO})_5$  structure **1**. Both isomers had UV-visible absorptions and could be interconverted by irradiation with visible light of the appropriate wavelength. In the matrix, the  $C_s$  isomer **3a** appeared to be the more stable.

This work revealed a surprising difference between  $\text{HMn}(\text{CO})_4$  and  $\text{CH}_3\text{Mn}(\text{CO})_4$  which had earlier been reported<sup>12</sup> to have the trigonal structure **5b**, similar to that of  $\text{Mn}(\text{CO})_4\text{Br}$ . This structure implies that  $\text{CH}_3$  is more like Br than H in its effect on molecular geometry, even though  $\text{CH}_3$  is unlikely to have significant  $\pi$  interactions.

$\text{CH}_3\text{Mn}(\text{CO})_4$  is one of the most easily generated carbonyl fragments containing an alkyl group and is poten-

(1) Burdett, J. K. *Coord. Chem. Rev.* 1978, 27, 1. Hitam, R. B.; Mahmoud, K. A.; Rest, A. J. *Ibid.* 1984, 55, 1.

(2) Perutz, R. N.; Turner, J. J. *Inorg. Chem.* 1975, 14, 262.

(3) Perutz, R. N.; Turner, J. J. *J. Am. Chem. Soc.* 1975, 97, 4800.

(4) Burdett, J. K.; Poliakoff, M.; Turner, J. J.; Dubost, H. *Adv. Infrared Raman Spectrosc.* 1976, 2, 1-52.

(5) Burdett, J. K. *J. Chem. Soc., Faraday Trans. 2* 1974, 70, 1599. Elian, M.; Hoffman, R. *Inorg. Chem.* 1975, 14, 1058.

(6) Kundig, E. P.; Ozin, G. A. *J. Am. Chem. Soc.* 1974, 96, 3820. Burdett, J. K.; Graham, M. A.; Perutz, R. N.; Poliakoff, M.; Rest, A. J.; Turner, J. J.; Turner, R. F. *Ibid.* 1975, 97, 4805.

(7) Seder, T. A.; Church, S. P.; Ouderkirk, A. J.; Weitz, E. *J. Am. Chem. Soc.* 1985, 107, 1432.

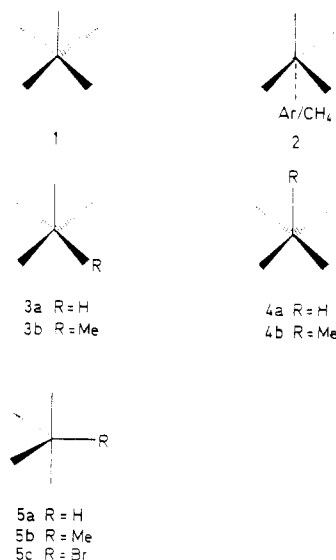
(8) The other possible trigonal isomer with an axial R group and  $C_{3v}$  symmetry would be expected to be Jahn-Teller unstable.

(9) Lichtenberger, D. L.; Brown, T. L. *J. Am. Chem. Soc.* 1978, 100, 366.

(10) McHugh, T. M.; Rest, A. J.; Taylor, D. J. *J. Chem. Soc., Dalton Trans.* 1980, 1803.

(11) Church, S. P.; Poliakoff, M.; Timney, J. A.; Turner, J. J. *Inorg. Chem.* 1983, 22, 3259.

(12) McHugh, T. M.; Rest, A. J. *J. Chem. Soc., Dalton Trans.* 1980, 2823.



tially an excellent model system for studying M-C interactions. This has prompted us to reinvestigate the structure of  $\text{CH}_3\text{Mn}(\text{CO})_4$ . The original workers<sup>12</sup> assigned structure **5b** to  $\text{CH}_3\text{Mn}(\text{CO})_4$  on the basis of  $^{13}\text{CO}$  enrichment. However, our own more recent experiments<sup>11</sup> with  $\text{HMn}(\text{CO})_4$  led to the realization that  $^{13}\text{CO}$ -enrichment techniques cannot always distinguish between a  $C_s$  square-pyramidal structure, such as **3**, and a  $C_{2v}$  trigonal-bipyramidal structure, **5**. In this case, it can be shown that the original  $^{13}\text{CO}$  data<sup>12</sup> for  $\text{CH}_3\text{Mn}(\text{CO})_4$  are equally consistent with the square-pyramidal structure<sup>13</sup> **3b**.

In this paper, we report IR results which show that matrix-isolated  $\text{CH}_3\text{Mn}(\text{CO})_4$  exists in *two* interconvertible isomeric forms, one of which must be the  $C_{4v}$  isomer **4b**.

Both isomers have UV-vis absorption bands, which are substantially blue-shifted when the matrix material is changed from Ar to  $\text{CH}_4$ . In 16-electron, five-coordinate systems, such shifts have always been associated with square-pyramidal or pseudo-square-pyramidal fragments.<sup>2,3,11,14</sup> We therefore assign the square-pyramidal structure **3b** to the second isomer of  $\text{CH}_3\text{Mn}(\text{CO})_4$ .

### Experimental Section

The matrix isolation apparatus at Nottingham has been described previously.<sup>15</sup> IR spectra were obtained with use of a Nicolet 7199 FT-IR interferometer (32K data points, 262K Transform points,  $0.5\text{ cm}^{-1}$  resolution) and UV-vis spectra with Perkin-Elmer Lambda 5 spectrophotometer with a Model 3600 Data Station. All UV spectra were recorded with 2-nm slit width.  $\text{CH}_3\text{Mn}(\text{CO})_5$  was a gift from Dr. J. Spencer, and matrix gases (Messer Griesheim) were used without further purification. The photolysis source was a Philips HPK 125W Hg arc, with Balzers interference filters where appropriate.

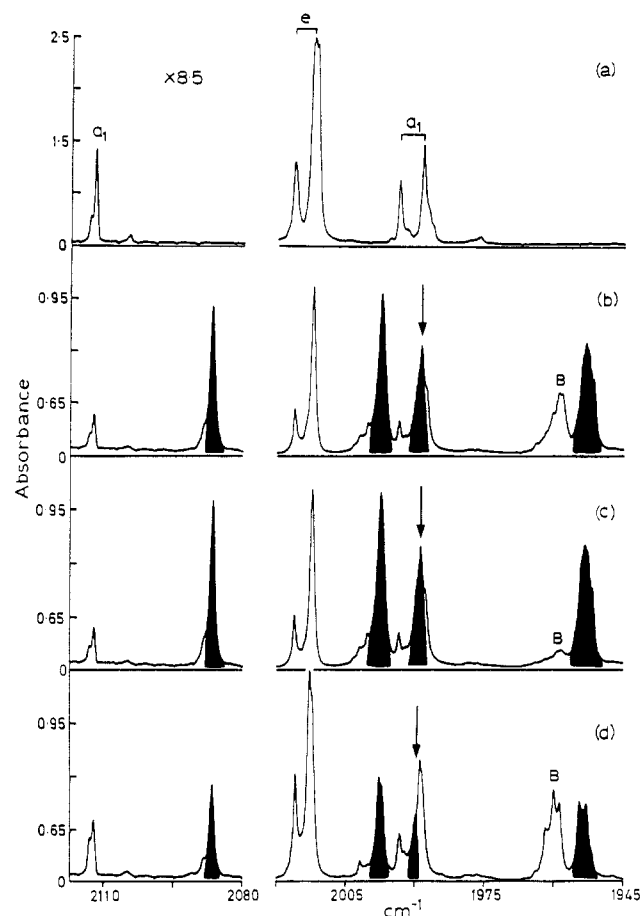
### Results

Figure 1 shows IR spectra produced by UV photolysis of  $\text{CH}_3\text{Mn}(\text{CO})_5$  in a  $\text{CH}_4$  matrix and subsequent irradiation with visible light. Before photolysis, the IR spectrum of  $\text{CH}_3\text{Mn}(\text{CO})_5$  shows the overall pattern ( $2a_1 + e$ ) expected for a square-pyramidal  $\text{Mn}(\text{CO})_5\text{X}$  species with local  $C_{4v}$  symmetry but each mode is somewhat split by

(13) The  $^{13}\text{CO}$  data can be fitted with a  $C_s$  force field<sup>15</sup> with  $k_1 = 1600.2$ ,  $k_2 = 1665.7$ ,  $k_3 = 1593.1$ ,  $k_{1,2} = 40.0$ ,  $k_{1,3} = 56.56$ ,  $k_{2,2} = 53.75$ , and  $k_{2,3} = 25.94\text{ Nm}^{-1}$ , where "2" refers to the two equivalent CO groups. The original workers<sup>12</sup> were unable to find a solution based on a  $C_s$  force field but in the absence of other evidence might have been expected to favor the higher symmetry  $C_{2v}$  solution which has two fewer force constants.

(14) Poliakov, M. *Inorg. Chem.* **1976**, *15*, 2022; **1976**, *15*, 2892.

(15) Church, S. P. Ph.D. Thesis, University of Nottingham, 1982.



**Figure 1.** IR spectra in the C-O stretching region illustrating reversible formation of isomer B of  $\text{CH}_3\text{Mn}(\text{CO})_4$ . Spectra were recorded after photolysis of  $\text{CH}_3\text{Mn}(\text{CO})_5$  isolated in a  $\text{CH}_4$  matrix ( $\text{CH}_3\text{Mn}(\text{CO})_5/\text{CH}_4$ , 1:4000) at 14 K: (a) after deposition; (b) after 12-min UV irradiation, following by 7-min irradiation with  $\lambda = 403\text{ nm}$ ; (c) 7 min further irradiation with  $\lambda = 489\text{ nm}$ ; (d) 20 min more photolysis with  $\lambda = 403\text{ nm}$ . The bands are labeled as follows: B, " $C_{4v}$ " isomer of  $\text{CH}_3\text{Mn}(\text{CO})_4$ ; black,  $C_s$  isomer of  $\text{CH}_3\text{Mn}(\text{CO})_4$ ; unlabeled, unreacted  $\text{CH}_3\text{Mn}(\text{CO})_5$ . (Note the expanded absorbance scale in the high wavenumber region and that a is plotted on a reduced absorbance scale compared to b-d).

"matrix" effects<sup>16</sup> (Figure 1a). On photolysis, new IR bands are observed. Apart from a band at  $2138\text{ cm}^{-1}$  due to free CO (not illustrated), five IR bands can be assigned to  $\nu(\text{C}-\text{O})$  vibrations of primary photoproducts (see Figure 1b where four of the bands are colored black and the fifth band is marked B). On subsequent irradiation, the four black bands remain with constant relative intensities and therefore belong to one molecular species, while the band B changes substantially in intensity suggesting that it may be due to a second species (compare parts c and d of Figure 1). Three of the four black bands correspond almost exactly to those originally reported<sup>12</sup> for  $\text{CH}_3\text{Mn}(\text{CO})_4$  (see Table I) while the fourth band (arrowed in Figure 1) overlaps with an absorption of the parent  $\text{CH}_3\text{Mn}(\text{CO})_5$  and might have easily been missed in the earlier work.<sup>17</sup> Thus, the black bands are reasonably assigned to  $\text{CH}_3\text{Mn}(\text{CO})_4$ .

Is the fifth band (B in Figure 1) due to a distinct chemical species or merely a "matrix splitting"? This question can be answered by examining the UV-vis spectra of the matrix (Figure 2). These spectra show two ab-

(16) See, e.g.: Horton-Mastin, A.; Poliakov, M. *Chem. Phys. Lett.* **1984**, *109*, 587 and references therein.

(17) There is some evidence for the presence of this band, unresolved from that of  $\text{CH}_3\text{Mn}(\text{CO})_5$  in Figure 1 of ref 12.

**Table I. Wavenumbers ( $\text{cm}^{-1}$ ) of  $\text{CH}_3\text{Mn}(\text{CO})_4$  and  $\text{HMn}(\text{CO})_4$  Isolated in  $\text{CH}_4$  Matrices at 20 K**

$\text{CH}_3\text{Mn}(\text{CO})_4$		$\text{HMn}(\text{CO})_4$	assignt
a	b	c	
$C_3$ Isomer 3			
2086.6	2086.9	2089.9	a'
1997.3	1997.4	1996.6 <sup>d</sup>	a''
1989.1	e	e	a'
1952.1 <sup>d</sup>	1952.0	1964.9	a'
$C_{4v}$ Isomer 4			
1960.0 <sup>d</sup>	e	1966.3	e

<sup>a</sup>This work. <sup>b</sup>Reference 12, note that the bands have been re-assigned. <sup>c</sup>Reference 11. <sup>d</sup>Mean value of matrix splitting. <sup>e</sup>Not reported.

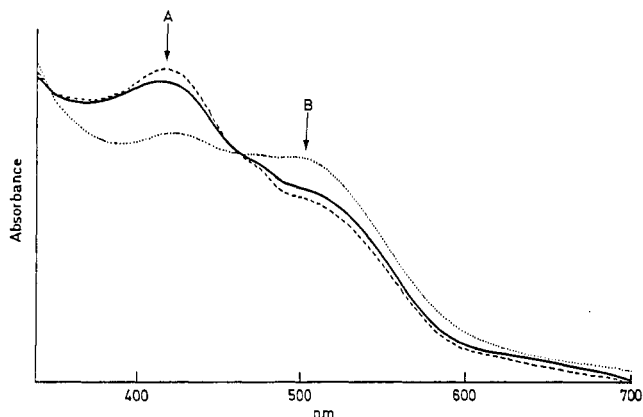
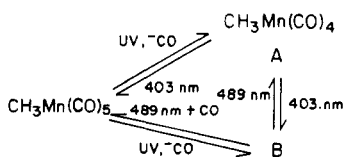


**Figure 2.** UV-visible spectra recorded in the same experiment as the IR spectra in Figure 1: (—) corresponding to 1b; ---, corresponding to 1c; ···, corresponding to 1d. (Note that these spectra have been corrected for background scatter by computer subtraction of the spectrum recorded before any irradiation of the matrix. The two absorption maxima are assigned to isomers A and B of  $\text{CH}_3\text{Mn}(\text{CO})_4$ .)

sorption maxima (marked A and B) which change substantially in relative intensities during the experiment. Matrix-isolated metal carbonyls have broad unresolved electronic absorptions which do not display detectable matrix splittings. Thus the visible absorptions A (414 nm) and B (505 nm) must arise from two different and distinct species. Absorption A is clearly associated with the IR bands of  $\text{CH}_3\text{Mn}(\text{CO})_4$ , while absorption B shows the same growth and decay pattern as the IR band B (Figure 1). What is the nature of this second species B?

B is not  $\text{Mn}(\text{CO})_5$ , the IR bands of which are known.<sup>18</sup> A careful analysis of the IR spectra showed that B was formed from  $\text{CH}_3\text{Mn}(\text{CO})_5$  by loss of CO and that  $\text{CH}_3\text{Mn}(\text{CO})_4$  and B could be interconverted by irradiation with the appropriate wavelength visible light, which also causes some regeneration of the parent  $\text{CH}_3\text{Mn}(\text{CO})_5$ . For example, in  $\text{CH}_4$  matrix



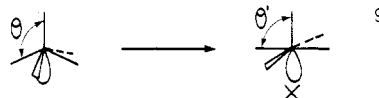
Similar evidence for two photoproducts was obtained in Ar matrices but the IR spectra are somewhat more split by "matrix effects". This scheme is very similar to that observed<sup>11</sup> for the two isomers of  $\text{HMn}(\text{CO})_4$ , 3a and 4a,

and the behavior of B is quite consistent with a second isomer of  $\text{CH}_3\text{Mn}(\text{CO})_4$ . B has only one strong  $\nu(\text{C}-\text{O})$  IR band, which can only be assigned to a  $C_{4v}$  square-pyramidal structure, 4b. Group theory predicts two  $\nu(\text{C}-\text{O})$  bands for this structure ( $a_1 + e$ ) with the  $a_1$  band expected to be very weak. All other plausible structures are predicted to have at least two strong  $\nu(\text{C}-\text{O})$  IR bands. Further support for our assignment is the frequency of the IR band, only  $6 \text{ cm}^{-1}$  from the band of the  $C_{4v}$  isomer of  $\text{HMn}(\text{CO})_4$  (see Table I).

What is the structure of isomer A of  $\text{CH}_3\text{Mn}(\text{CO})_4$ ? We have observed four IR-active  $\nu(\text{C}-\text{O})$  bands for this isomer. The band pattern is similar to that of  $\text{HMn}(\text{CO})_4$  which has structure 3a. However, four IR bands would be equally consistent with the pseudo-square-pyramid 3b ( $3a' + a''$ ) or the pseudo-trigonal-bipyramid 5b ( $2a_1 + b_1 + b_2$ ). Similarly, the  $^{13}\text{CO}$  data<sup>12,13</sup> could be fitted to either structure. We can, however, distinguish between the two structures on the basis of UV-vis spectra.

Perutz and Turner discovered<sup>3</sup> that matrix-isolated  $\text{Cr}(\text{CO})_5$  was not "naked" but interacted with the matrix material via the empty coordination site to give a pseudo-six-coordinate species, 2. The strength of this interaction depended on the matrix material. The interaction, which was less with Ar than with  $\text{CH}_4$  or Xe, manifested itself in a substantial shift in the wavelength of the visible absorption of  $\text{Cr}(\text{CO})_5$  between one matrix and another, e.g.,  $\lambda_{\text{max}} = 533$  (Ar) and 494 nm ( $\text{CH}_4$ ). Similar interactions of  $\text{Cr}(\text{CO})_5$  have since been observed in cryogenic<sup>19</sup> and room-temperature solutions<sup>20,21</sup> and even in the gas phase.<sup>22</sup>

The interaction, which has been discussed in detail previously,<sup>23</sup> involves a  $\sigma$  interaction involving the empty  $a_1$  LUMO of  $\text{Cr}(\text{CO})_5$ , which is largely  $d_{z^2}$  in character. This orbital is raised in energy both by direct interaction with the matrix and also by the change in axial/equatorial bond angle  $\theta$  shown somewhat exaggeratedly in 9, a change which simultaneously raises the energy of the LUMO and lowers the energy of the HOMO.<sup>23</sup>



A similar interaction would be expected for any 16-electron square-pyramidal or pseudo-square-pyramidal fragment, e.g., 3 or 4, and has been observed for several systems, e.g.,  $\text{Cr}(\text{CO})_4\text{CS}$ <sup>14</sup> and  $\text{HMn}(\text{CO})_4$ .<sup>11</sup> By contrast, a trigonal or pseudotrigonal fragment, e.g., 5, does not have a suitable LUMO for interaction with the matrix. Thus we can distinguish between structures 3b and 5b for  $\text{CH}_3\text{Mn}(\text{CO})_4$ . Structure 3b should show a substantial blue-shift in  $\lambda_{\text{max}}$  from Ar to  $\text{CH}_4$  matrices, while structure 5b should not.

The spectra are shown in Figure 3. Between  $\text{CH}_4$  and Ar matrices there were substantial shifts in the UV/visible absorption maxima of both photoproducts. These matrix shifts [ $\text{CH}_4\text{Mn}(\text{CO})_4$  (A), 414 ( $\text{CH}_4$ ) to 457 nm (Ar), 2250  $\text{cm}^{-1}$ ;  $\text{CH}_3\text{Mn}(\text{CO})_4$  (B), 505 ( $\text{CH}_4$ ) to 565 nm (Ar), 2100  $\text{cm}^{-1}$ ] are similar to those of  $\text{Cr}(\text{CO})_5$ <sup>3</sup> ( $\sim 1600 \text{ cm}^{-1}$ ) and  $\text{HMn}(\text{CO})_4$ <sup>11</sup> (3a; 2500  $\text{cm}^{-1}$ ), both of which are known to interact with the matrix. The shift in the band of B, which

(19) Simpson, M. B.; Poliakoff, M.; Turner, J. J.; Maier, W. B. II; McLaughlin, J. G. *J. Chem. Soc., Chem. Commun.* 1983, 1355.

(20) Kelly, J. M.; Long, C.; Bonneau, R. *J. Phys. Chem.* 1983, 87, 3344.

(21) Welch, J. A.; Peters, K. S.; Vaida, V. *J. Phys. Chem.* 1982, 86, 1941.

(22) Breckenridge, W. H.; Sinai, N. *J. Phys. Chem.* 1981, 85, 1351.

(23) Burdett, J. K.; Grzybowski, J. M.; Perutz, R. N.; Poliakoff, M.; Turner, J. J.; Turner, R. F. *Inorg. Chem.* 1978, 17, 147.

(18) Church, S. P.; Poliakoff, M.; Timney, J. A.; Turner, J. J. *J. Am. Chem. Soc.* 1981, 103, 7517.

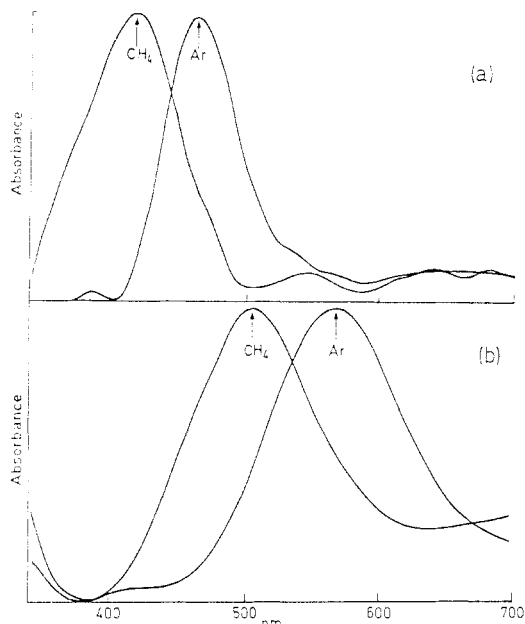


**Figure 3.** UV-visible spectra illustrating the substantial shift in absorption maxima of the two isomers of  $\text{CH}_3\text{Mn}(\text{CO})_4$  between  $\text{CH}_4$  and Ar matrices: (a)  $C_s$  isomer A and (b)  $C_{4v}$  isomer B. Spectra were obtained by computer subtraction of spectra similar to those in Figure 2. Note that the spectra for Ar and  $\text{CH}_4$  matrices were obtained in different experiments.

we have already identified as the  $C_{4v}$  isomer of  $\text{CH}_3\text{Mn}(\text{CO})_4$ , confirms our assignment. The shift in the absorption of the other isomer A is exactly as predicted for structure **3b** and allows us to eliminate the trigonal structure **5b**.

Thus, the isomers of  $\text{CH}_3\text{Mn}(\text{CO})_4$  have structures **3b** and **4b**, both based on a square pyramid. Their photochemical interconversion can readily be explained by the

inverse Berry pseudorotation,  $C_{4v} \rightarrow C_{2v} \rightarrow C_s$ , already invoked in the isomerization of  $\text{Cr}(\text{CO})_4\text{CS}^{14}$  and  $\text{HMn}(\text{CO})_4$ .<sup>12</sup>

### Conclusions

Thus, contrary to earlier reports,  $\text{CH}_3\text{Mn}(\text{CO})_4$  has two isomers, **3b** and **4b**, similar in structure to those of  $\text{HMn}(\text{CO})_4$ <sup>11</sup> and unlike the reported structure<sup>10</sup> of  $\text{Mn}(\text{CO})_4\text{Br}$ . Thus,  $\text{CH}_3$  is finally shown to be more akin to H than Br in its effects on molecular geometry. An interesting theoretical question still remains to be answered, namely, why the  $C_s$  isomers **3a** and **3b** should be the predominant products in our photolysis experiments? Again, the interaction between the unsaturated metal center and the matrix underlines the enormous reactivity of these fragments. In hydrocarbon solution at room temperature, " $\text{CH}_3\text{Mn}(\text{CO})_4$ " will almost certainly be a pseudooctahedral species with a weakly coordinated solvent molecule occupying the vacant coordination site.

Now that the isomers of  $\text{CH}_3\text{Mn}(\text{CO})_4$  have been characterized, they form promising model systems for studying M-C interactions. For example, following the pioneering work of McKean,<sup>24</sup> it should now be possible to use IR bands in the  $\nu(\text{C-H})$  region to examine differences in Mn-CH<sub>3</sub> bonding between the two isomers and  $\text{CH}_3\text{Mn}(\text{CO})_5$ .

**Acknowledgment.** We thank the SERC and BP Research Ltd for support. We are grateful to Dr. S. P. Church, Dr. M. A. Healy, Mr. J. G. Gamble, Dr. G. E. Morris, and Dr. A. J. Rest for their help and comments.

**Registry No.** **3b**, 71518-84-8; **4b**, 99684-96-5;  $\text{CH}_3\text{Mn}(\text{CO})_5$ , 13601-24-6.

(24) Long, C.; Morrison, A. R.; McKean, D. C.; McQuillan, G. P. *J. Am. Chem. Soc.* **1984**, *106*, 7418 and references therein.

## Synthesis of $\text{Os}_3(\text{CO})_{10}(\text{CH}_3)(\mu\text{-I})$ with an $\eta^1$ -Methyl Ligand and Its Insertion of CO To Give Acetyl Derivatives

Eric D. Morrison, Sherri L. Bassner, and Gregory L. Geoffroy\*

Department of Chemistry, The Pennsylvania State University, University Park, Pennsylvania 16802

Received May 24, 1985

Protonation of the anionic cluster  $[\text{Os}_3(\text{CO})_{10}(\mu\text{-CH}_2)(\mu\text{-I})]^-$  with  $\text{HBF}_4 \cdot \text{Et}_2\text{O}$  yields  $\text{Os}_3(\text{CO})_{10}(\text{CH}_3)(\mu\text{-I})$  (**5**), one of the few examples of an alkyl-substituted cluster. Methyl cluster **5** reacts with CO to give predominantly the  $\eta^1$ -acetyl cluster  $\text{Os}_3(\text{CO})_{11}(\eta^1\text{-C}(\text{O})\text{CH}_3)(\mu\text{-I})$  (**7**) along with small amounts of the bridging acetyl cluster  $\text{Os}_3(\text{CO})_{10}(\mu\text{-O}=\text{CCH}_3)(\mu\text{-I})$  (**6**). The bridging acetyl cluster **6** can also be synthesized in high yield from the reaction of  $\text{Os}_3(\text{CO})_{11}(\mu\text{-CH}_2)$  with HI. When the  $\eta^1$ -acetyl cluster **7** is heated under vacuum, it loses CO and gives a mixture of the  $\mu$ -acetyl cluster **6** and the original methyl cluster **5**.

Insertion of CO into metal-alkyl bonds in *mononuclear* complexes is a textbook reaction with numerous examples and many important synthetic applications.<sup>1-3</sup> In contrast, insertion of CO into metal-alkyl bonds in well-charac-

terized alkyl-substituted *clusters* has not been documented. However, CO insertion into *transient* metal-alkyl bonds has been proposed for several cluster reactions. For example, Kaesz et al.<sup>4</sup> observed formation of the  $\mu$ -propionyl complexes  $\text{Ru}_3(\text{CO})_{10}(\mu\text{-O}=\text{CEt})(\mu\text{-X})$  (**2**; X = Cl, Br, I) from the reaction of  $(\mu\text{-H})\text{Ru}_3(\text{CO})_{10}(\mu\text{-X})$  (X = Cl,

(1) Wojcicki, A. *Adv. Organomet. Chem.* **1973**, *11*, 87.

(2) Calderazzo, F. *Angew. Chem., Int. Ed. Engl.* **1977**, *16*, 299.

(3) Collman, J. P.; Hegedus, L. S. "Principles and Applications of Organotransition Metal Chemistry"; University Science Books: Oxford, 1980.

(4) Kampe, C. E.; Boag, N. M.; Kaesz, H. D. *J. Am. Chem. Soc.* **1983**, *105*, 2896.



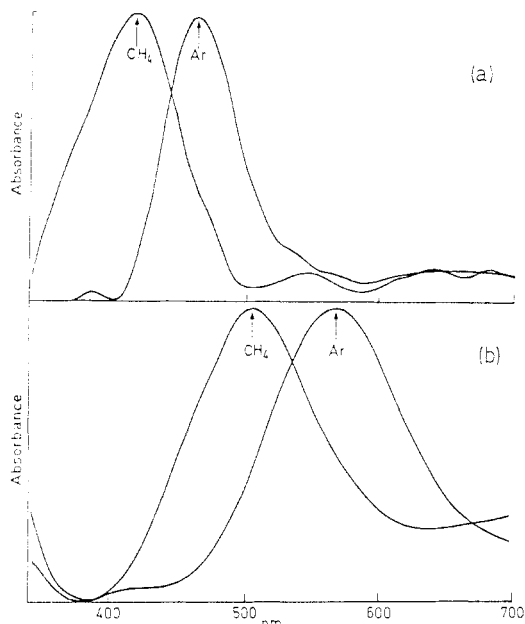


**Figure 3.** UV-visible spectra illustrating the substantial shift in absorption maxima of the two isomers of  $\text{CH}_3\text{Mn}(\text{CO})_4$  between  $\text{CH}_4$  and Ar matrices: (a)  $C_s$  isomer A and (b)  $C_{4v}$  isomer B. Spectra were obtained by computer subtraction of spectra similar to those in Figure 2. Note that the spectra for Ar and  $\text{CH}_4$  matrices were obtained in different experiments.

we have already identified as the  $C_{4v}$  isomer of  $\text{CH}_3\text{Mn}(\text{CO})_4$ , confirms our assignment. The shift in the absorption of the other isomer A is exactly as predicted for structure **3b** and allows us to eliminate the trigonal structure **5b**.

Thus, the isomers of  $\text{CH}_3\text{Mn}(\text{CO})_4$  have structures **3b** and **4b**, both based on a square pyramid. Their photochemical interconversion can readily be explained by the

inverse Berry pseudorotation,  $C_{4v} \rightarrow C_{2v} \rightarrow C_s$ , already invoked in the isomerization of  $\text{Cr}(\text{CO})_4\text{CS}^{14}$  and  $\text{HMn}(\text{CO})_4$ .<sup>12</sup>

### Conclusions

Thus, contrary to earlier reports,  $\text{CH}_3\text{Mn}(\text{CO})_4$  has two isomers, **3b** and **4b**, similar in structure to those of  $\text{HMn}(\text{CO})_4$ <sup>11</sup> and unlike the reported structure<sup>10</sup> of  $\text{Mn}(\text{CO})_4\text{Br}$ . Thus,  $\text{CH}_3$  is finally shown to be more akin to H than Br in its effects on molecular geometry. An interesting theoretical question still remains to be answered, namely, why the  $C_s$  isomers **3a** and **3b** should be the predominant products in our photolysis experiments? Again, the interaction between the unsaturated metal center and the matrix underlines the enormous reactivity of these fragments. In hydrocarbon solution at room temperature, " $\text{CH}_3\text{Mn}(\text{CO})_4$ " will almost certainly be a pseudooctahedral species with a weakly coordinated solvent molecule occupying the vacant coordination site.

Now that the isomers of  $\text{CH}_3\text{Mn}(\text{CO})_4$  have been characterized, they form promising model systems for studying M-C interactions. For example, following the pioneering work of McKean,<sup>24</sup> it should now be possible to use IR bands in the  $\nu(\text{C-H})$  region to examine differences in Mn-CH<sub>3</sub> bonding between the two isomers and  $\text{CH}_3\text{Mn}(\text{CO})_5$ .

**Acknowledgment.** We thank the SERC and BP Research Ltd for support. We are grateful to Dr. S. P. Church, Dr. M. A. Healy, Mr. J. G. Gamble, Dr. G. E. Morris, and Dr. A. J. Rest for their help and comments.

**Registry No.** **3b**, 71518-84-8; **4b**, 99684-96-5;  $\text{CH}_3\text{Mn}(\text{CO})_5$ , 13601-24-6.

(24) Long, C.; Morrison, A. R.; McKean, D. C.; McQuillan, G. P. *J. Am. Chem. Soc.* **1984**, *106*, 7418 and references therein.

## Synthesis of $\text{Os}_3(\text{CO})_{10}(\text{CH}_3)(\mu\text{-I})$ with an $\eta^1$ -Methyl Ligand and Its Insertion of CO To Give Acetyl Derivatives

Eric D. Morrison, Sherri L. Bassner, and Gregory L. Geoffroy\*

Department of Chemistry, The Pennsylvania State University, University Park, Pennsylvania 16802

Received May 24, 1985

Protonation of the anionic cluster  $[\text{Os}_3(\text{CO})_{10}(\mu\text{-CH}_2)(\mu\text{-I})]^-$  with  $\text{HBF}_4 \cdot \text{Et}_2\text{O}$  yields  $\text{Os}_3(\text{CO})_{10}(\text{CH}_3)(\mu\text{-I})$  (**5**), one of the few examples of an alkyl-substituted cluster. Methyl cluster **5** reacts with CO to give predominantly the  $\eta^1$ -acetyl cluster  $\text{Os}_3(\text{CO})_{11}(\eta^1\text{-C}(\text{O})\text{CH}_3)(\mu\text{-I})$  (**7**) along with small amounts of the bridging acetyl cluster  $\text{Os}_3(\text{CO})_{10}(\mu\text{-O}=\text{CCH}_3)(\mu\text{-I})$  (**6**). The bridging acetyl cluster **6** can also be synthesized in high yield from the reaction of  $\text{Os}_3(\text{CO})_{11}(\mu\text{-CH}_2)$  with HI. When the  $\eta^1$ -acetyl cluster **7** is heated under vacuum, it loses CO and gives a mixture of the  $\mu$ -acetyl cluster **6** and the original methyl cluster **5**.

Insertion of CO into metal-alkyl bonds in *mononuclear* complexes is a textbook reaction with numerous examples and many important synthetic applications.<sup>1-3</sup> In contrast, insertion of CO into metal-alkyl bonds in well-charac-

terized alkyl-substituted *clusters* has not been documented. However, CO insertion into *transient* metal-alkyl bonds has been proposed for several cluster reactions. For example, Kaesz et al.<sup>4</sup> observed formation of the  $\mu$ -propionyl complexes  $\text{Ru}_3(\text{CO})_{10}(\mu\text{-O}=\text{CEt})(\mu\text{-X})$  (**2**; X = Cl, Br, I) from the reaction of  $(\mu\text{-H})\text{Ru}_3(\text{CO})_{10}(\mu\text{-X})$  (X = Cl,

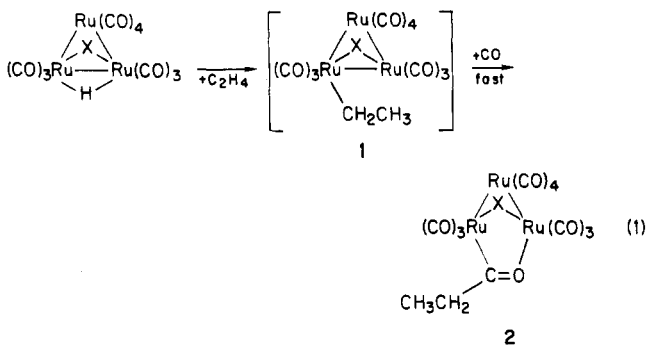
(1) Wojcicki, A. *Adv. Organomet. Chem.* **1973**, *11*, 87.

(2) Calderazzo, F. *Angew. Chem., Int. Ed. Engl.* **1977**, *16*, 299.

(3) Collman, J. P.; Hegedus, L. S. "Principles and Applications of Organotransition Metal Chemistry"; University Science Books: Oxford, 1980.

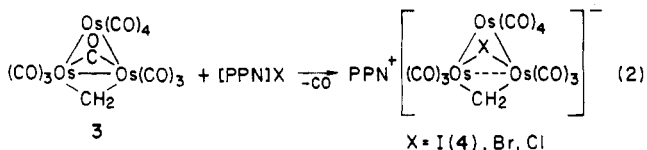
(4) Kampe, C. E.; Boag, N. M.; Kaesz, H. D. *J. Am. Chem. Soc.* **1983**, *105*, 2896.

Br, I) with ethylene and CO. These presumably arise via ethylene insertion into the metal-hydride bond to give the alkyl intermediate 1 which then quickly inserts CO to yield the isolated  $\mu$ -acyl product 2 (eq 1). Similarly, the reac-



tions of  $\text{Na}_2[\text{Fe}_2(\text{CO})_6(\mu\text{-PPh}_2)_2]^5$  and  $\text{Li}[\text{Fe}_2(\text{CO})_6(\mu\text{-PPh}_2)(\text{PPh}_2\text{H})]^6$  with alkylating agents to give acyl-containing products were proposed to proceed through intermediate alkyl complexes although these were not detected.

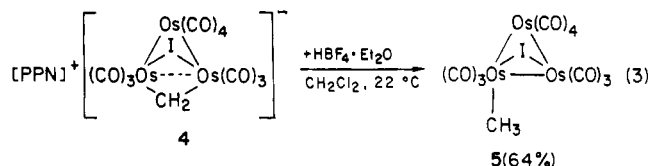
We recently described the synthesis of a series of anionic  $\mu$ -halide,  $\mu$ -methylene clusters by the reaction of  $\text{Os}_3(\text{CO})_{11}(\mu\text{-CH}_2)$  (3) with  $[\text{PPN}]\text{X}$  salts (eq 2).<sup>7a,c</sup> Other



work with *binuclear* complexes has established that the  $\mu$ -methylene ligand can often be protonated to give methyl-substituted derivatives.<sup>8</sup> Herein we demonstrate that this procedure can be extended to cluster compounds. Protonation of  $[\text{PPN}][\text{Os}_3(\text{CO})_{10}(\mu\text{-CH}_2)(\mu\text{-I})]$  gives the methyl cluster  $\text{Os}_3(\text{CO})_{10}(\text{CH}_3)(\mu\text{-I})$  (5) in good yield. Cluster 5 is one of the very few examples of isolable alkyl-substituted clusters. It is also analogous to Kaesz's<sup>4</sup> intermediate 1. Like Kaesz's presumed intermediate, our cluster 5 further reacts with added CO to give first a terminal acetyl derivative which in turn loses CO to give a bridging acetyl complex analogous to Kaesz's compound 2. Details of these studies are described herein.

## Results and Discussion

**Synthesis of  $\text{Os}_3(\text{CO})_{10}(\text{CH}_3)(\mu\text{-I})$  via Protonation of  $[\text{PPN}][\text{Os}_3(\text{CO})_{10}(\mu\text{-CH}_2)(\mu\text{-I})]$ .** All of the complex anions  $[\text{Os}_3(\text{CO})_{10}(\mu\text{-CH}_2)(\mu\text{-X})]^-$  (X = Cl, Br, I, NCO)<sup>7a,c</sup> undergo protonation to yield the corresponding  $\text{Os}_3(\text{CO})_{10}(\text{CH}_3)(\mu\text{-X})$  clusters, but the reaction has been studied in detail only for the X = I derivative. Here the product is  $\text{Os}_3(\text{CO})_{10}(\text{CH}_3)(\mu\text{-I})$  (5), which can be isolated as a slightly air-sensitive maroon-colored solid (eq 3). This reaction is most conveniently carried out by adding an excess of  $\text{HBF}_4 \cdot \text{Et}_2\text{O}$  to a  $\text{CH}_2\text{Cl}_2$  solution of  $[\text{PPN}][\text{Os}_3-$



$(\text{CO})_{10}(\mu\text{-CH}_2)(\mu\text{-I})$ . Complex 5 is stable indefinitely as a dry solid when stored under an  $\text{N}_2$  atmosphere at  $-20^\circ\text{C}$ , but in solution under  $\text{N}_2$  it slowly decomposes over a period of several days to give  $\text{Os}_3(\text{CO})_{10}(\mu\text{-O}=\text{CCH}_3)(\mu\text{-I})$  (6), in 32% yield along with a complex mixture of unidentified products. Complex 5 also slowly decomposes upon chromatography. The best yields of this material were obtained when it was immediately extracted from the product mixture with *n*-pentane and then rapidly chromatographed. Acidification with  $\text{CF}_3\text{SO}_3\text{H}$  also gave 5 but in somewhat lower yield.

The spectroscopic data for 5 are consistent with the formulation given in eq 3. Its mass spectrum shows a parent ion at  $m/z$  992 and fragment ions corresponding to successive loss of 10 CO's. Only terminal  $\nu_{\text{CO}}$  bands are observed in the IR spectrum of 5, and the  $^1\text{H}$  NMR spectrum at  $22^\circ\text{C}$  shows a singlet at  $\delta$  1.34 assigned to the methyl ligand. This signal does not broaden relative to internal  $\text{CHCl}_3$  down to  $-80^\circ\text{C}$ . Although this resonance is downfield from the usual  $\delta$  0.5  $\rightarrow$   $\delta$  -4.0 chemical shift range characteristic of alkyl ligands (e.g.,  $\text{Os}_3(\text{CO})_{10}(\mu\text{-H})(\text{CH}_3)$ ,  $\delta$  -3.68;<sup>9a</sup>  $\text{Os}(\text{CO})_4(\text{CH}_3)_2$ ,  $\delta$  -0.15<sup>9b</sup>), the  $^{13}\text{C}$  NMR resonance of the alkyl carbon at  $\delta$  -39.7 is within the -59.2 to 3.4 range characteristic of methyl complexes of Fe, Ru, and Os.<sup>10,11</sup> Furthermore, this resonance appears as a quartet ( $J_{\text{CH}} = 136.7$  Hz) with coupling to three equivalent hydrogens, confirming its assignment to a  $\text{CH}_3$  group. The  $^{13}\text{C}$  NMR spectrum of 5 further shows ten distinct resonances in the carbonyl region ( $\delta$  169-190) implying that all 10 carbonyl ligands are inequivalent, consistent with the structure drawn in eq 3 but not consistent with a more symmetrical structure, for example, with a  $\mu\text{-CH}_3$  ligand.

The  $^1\text{H}$  NMR spectra of the partially deuterated derivatives  $\text{Os}_3(\text{CO})_{10}(\text{CH}_2\text{D})(\mu\text{-I})$  and  $\text{Os}_3(\text{CO})_{10}(\text{CHD}_2)(\mu\text{-I})$  showed  $^1\text{H}$  NMR resonances at  $\delta$  1.28 and 1.22, respectively, slightly upfield of the  $\delta$  1.34 resonance of 5. Shapley and co-workers have shown that similar upfield shifts of partially deuterated derivatives of  $\text{Os}_3(\text{CO})_{10}(\text{CH}_3)(\mu\text{-H})$  are the result of interaction of one of the carbon-hydrogen bonds of the methyl group with an adjacent osmium atom in the cluster,<sup>12</sup> and such an  $\text{Os}\cdots\text{C}\cdots\text{H}$  interaction could be invoked for 5. However, we do not believe this to be the case since the shift per deuterium substitution in complex 5 is 0.06 ppm, considerably attenuated from the 0.34 ppm shifts observed with the incorporation of each deuterium into the methyl ligand of Shapley's  $\text{Os}_3(\text{CO})_{10}(\text{CH}_3)(\mu\text{-H})$ .<sup>12</sup> Also, the chemical shift difference per deuterium substitution in 5 does not increase significantly upon lowering the temperature from 22 to  $-80^\circ\text{C}$  which it should if a bridging  $\text{C}\cdots\text{H}\cdots\text{Os}$  interaction were present.<sup>12</sup> Shapley's complex  $\text{Os}_3(\text{CO})_{10}(\text{CH}_3)(\mu\text{-H})$  has 46 valence electrons which is two less than the number required to give a closed triangular cluster.<sup>13</sup> This formal two-electron deficiency is compensated by interaction of one of the carbon-hydrogen bonds of the methyl group with an os-

(5) Collman, J. P.; Rothrock, R. K.; Finke, R. G.; Moore, E. J.; Rose-Munch, F. *Inorg. Chem.* **1982**, *21*, 146.

(6) Yu, Y. F.; Gallucci, J.; Wojcicki, A. *J. Am. Chem. Soc.* **1983**, *105*, 4826.

(7) (a) Morrison, E. D.; Geoffroy, G. L.; Rheingold, A. L. *J. Am. Chem. Soc.* **1985**, *107*, 254. (b) Morrison, E. D.; Geoffroy, G. L. *J. Am. Chem. Soc.* **1985**, *107*, 3541. (c) Morrison, E. D.; Geoffroy, G. L.; Rheingold, A. L.; Fultz, W. C. *Organometallics* **1985**, *4*, 1413.

(8) (a) Herrmann, W. A.; Plank, J.; Guggolz, E.; Ziegler, M. L. *Angew. Chem., Int. Ed. Engl.* **1980**, *19*, 651. (b) Herrmann, W. A.; Plank, J.; Ziegler, M. L.; Balbach, B. *J. Am. Chem. Soc.* **1980**, *102*, 5906. (c) Dawkins, G. M.; Green, M.; Orpen, A. G.; Stone, F. G. A. *J. Chem. Soc., Chem. Commun.* **1982**, 41. (d) Hursthouse, M. B.; Jones, R. A.; Abdul Malik, K. M.; Wilkinson, G. *J. Am. Chem. Soc.* **1979**, *101*, 4128.

(9) (a) Calvert, R. B.; Shapley, J. R. *J. Am. Chem. Soc.* **1977**, *99*, 5225. (b) Carter, W. J.; Kelland, J. W.; Okrasinski, S. J.; Warner, K. E.; Norton, J. R. *Inorg. Chem.* **1982**, *21*, 3955.

(10) Calvert, R. B.; Shapley, J. R. *J. Am. Chem. Soc.* **1978**, *100*, 6544.

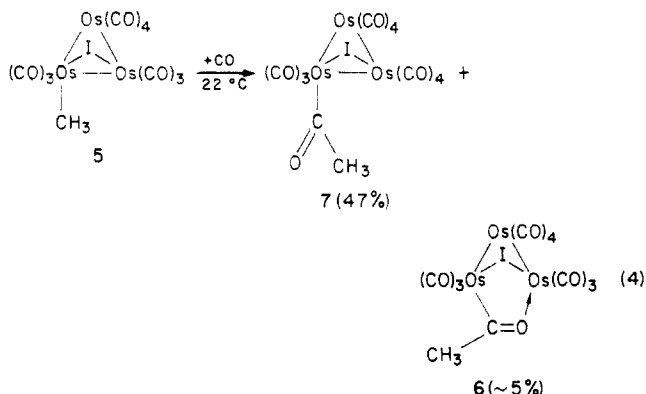
(11) Mann, B. E.; Taylor, B. F.  $^{13}\text{C}$  NMR Data for Organometallic Compounds"; Academic Press: New York, 1981; pp 42-43.

(12) Calvert, R. B.; Shapley, J. R. *J. Am. Chem. Soc.* **1978**, *100*, 7726.

(13) Lauher, J. W. *J. Am. Chem. Soc.* **1978**, *100*, 5305.

mium atom via a two-electron, three-center bond.<sup>12</sup> In contrast, our complex **5** is coordinatively saturated since the four-electron donor  $\mu$ -I ligand in **5** has replaced the 2e donor  $\mu$ -H ligand in Shapley's  $\text{Os}_3(\text{CO})_{10}(\text{CH}_3)(\mu\text{-H})$ .<sup>12</sup> Thus, there is no need for a  $\text{C}\cdots\text{H}\cdots\text{Os}$  interaction in **5**.

**Reaction of  $\text{Os}_3(\text{CO})_{10}(\text{CH}_3)(\mu\text{-I})$  with CO.** Complex **5** reacts with CO over a period of several hours to give the acyl complexes **6** and **7** derived from insertion of CO into the metal-alkyl bond (eq 4). Several other unidentified



compounds were also formed, but they were not isolated in sufficient quantities to characterize. The major product from the reaction is the terminal acetyl complex **7** which is only slightly soluble in  $\text{CH}_2\text{Cl}_2$  or hydrocarbon solvents and slowly precipitates as the reaction proceeds. The terminal acetyl complex **7** readily loses CO upon heating (45 °C, 2 h) under vacuum to yield mainly the  $\mu$ -acetyl complex **6** (~70%) along with some of the deinsertion product **5** (~30%). The  $\mu$ -acetyl complex **6** also forms in high yield (90%) upon addition of HI to  $\text{Os}_3(\text{CO})_{11}(\mu\text{-CH}_2)$  (see Experimental Section). Complex **6** was previously obtained in low yield by Kaesz and co-workers as a minor byproduct in a complex reaction scheme.<sup>14</sup>

These two acyl complexes have been spectroscopically characterized. Both show parent ions in their mass spectra and acetyl  $\nu_{\text{CO}}$  vibrations in their IR spectra. For **7**, this vibration is at 1620  $\text{cm}^{-1}$  within the 1545–1620  $\text{cm}^{-1}$  range typical of  $\eta^1$ -acyl complexes.<sup>5,15</sup> In contrast, the  $\mu$ -acetyl complex **6** shows an acetyl  $\nu_{\text{CO}}$  band at 1499  $\text{cm}^{-1}$  within the 1450–1530  $\text{cm}^{-1}$  region typically found for  $\mu$ -acyl complexes.<sup>4,6,16</sup>

It should be noted that the methyl complex **5** is analogous to Kaesz's<sup>4</sup> unobserved intermediate ethyl complex **1** (eq 1). The insertion of CO into this species to give the  $\mu$ -propionyl complex **2** has been modeled in the results reported here by the **5**  $\rightarrow$  **6**  $\rightarrow$  **7** sequence of transformations. Note also that Shapley and co-workers<sup>17</sup> have shown that the reaction of  $\text{Os}_3(\text{CO})_{10}(\text{CH}_3)(\mu\text{-H})$  with CO proceeds slowly and does not lead to CO insertion. Instead, reductive coupling of the methyl and hydride ligands occurs to give  $\text{CH}_4$ . The rapid reaction of **5** with CO to give acetyl-containing products is thus quite different, and it represents another example of a halide-promoted insertion

reaction, analogous to the recently reported halide promotion of CO insertion into  $\mu\text{-CH}_2$  complexes to give  $\mu$ -ketene derivatives.<sup>7a,b</sup>

## Experimental Section

The complexes  $\text{Os}_3(\text{CO})_{11}(\mu\text{-CH}_2)$  (**3**)<sup>18</sup> and  $[\text{PPN}][\text{Os}_3(\text{CO})_{10}(\mu\text{-CH}_2)(\mu\text{-I})]$  (**4**),<sup>7c</sup> were prepared according to literature procedures. Carbon monoxide (CP grade, Matheson),  $\text{HBF}_4\cdot\text{Et}_2\text{O}$ ,  $[(\text{CH}_3)_3\text{O}][\text{BF}_4]$  (Aldrich Chemical Corp.), and HI (0.8 M in  $\text{CHCl}_3$ , Alfa Chemical Corp.) were purchased and used as received. Solvents were dried and degassed by standard methods. All manipulations, unless otherwise specified, were conducted under prepurified  $\text{N}_2$  by using standard Schlenk techniques. Instruments used in this work have been previously described.<sup>7,18</sup> The complex  $\text{Os}_3(\text{CO})_{10}(\mu\text{-H})(\mu\text{-I})$ <sup>19</sup> was used as an internal standard in the mass spectral analyses of the partially deuterated  $\text{Os}_3(\text{CO})_{10}(\text{CH}_3)(\mu\text{-I})$  derivatives. Elemental analyses were performed by Schwartzkopf Microanalytical Laboratory, Woodside, NY.

**Synthesis of  $\text{Os}_3(\text{CO})_{10}(\text{CH}_3)(\mu\text{-I})$  (**5**).** The salt  $[\text{PPN}][\text{Os}_3(\text{CO})_{10}(\mu\text{-CH}_2)(\mu\text{-I})]$  (0.310 g, 0.203 mmol) was dissolved in 3.0 mL of dry  $\text{CH}_2\text{Cl}_2$  in a 25-mL round-bottom flask in a glovebag under an  $\text{N}_2$  atmosphere.  $\text{HBF}_4\cdot\text{Et}_2\text{O}$  (~0.15 mL, ~1.24 mmol) was added dropwise to the stirred solution, and this gave an orange to red color change. The  $\text{CH}_2\text{Cl}_2$  solvent was immediately removed by rotary evaporation in air, and the resultant red residue was quickly extracted with several ~5-mL portions of *n*-pentane. The pentane soluble material was quickly chromatographed on  $\text{SiO}_2$  using 25%  $\text{CH}_2\text{Cl}_2/n$ -pentane as eluant. Evaporation of solvent from the first red band gave  $\text{Os}_3(\text{CO})_{10}(\text{CH}_3)(\mu\text{-I})$  (**5**) as a maroon-colored microcrystalline solid in 64% yield (0.129 g, 0.130 mmol). This band was followed by a yellow band which was not identified. **5**: IR ( $\nu_{\text{CO}}$  cyclohexane) 2112 m, 2062s, 2045s, 2031 vs, 2000 s, 1985 m  $\text{cm}^{-1}$ ; MS (EI, <sup>190</sup>Os)  $m/z$  992 ( $\text{M}^+$ ) plus fragments corresponding to loss of 10 CO's and  $\text{CH}_3$ ; <sup>1</sup>H NMR ( $\text{CDCl}_3$ )  $\delta$  1.34 (s); <sup>13</sup>C NMR ( $\text{CDCl}_3$ )  $\delta$  -39.7 (q,  $J_{\text{CH}}$  = 136.7 Hz), 189.4 (s, CO), 187.1 (s, CO), 186.1 (s, CO), 184.5 (s, CO), 181.3 (s, CO), 178.8 (s, CO), 176.6 (s, CO), 175.9 (s, CO), 170.0 (s, CO), 169.4 (s, CO). Anal. Calcd for  $\text{C}_{11}\text{H}_3\text{IO}_{10}\text{Os}_3$ : C, 13.30; H, 0.31. Found: C, 13.05; H, 0.60.

**<sup>1</sup>H NMR Characterization of  $\text{Os}_3(\text{CO})_{10}(\text{CHD}_2)(\mu\text{-I})$  and  $\text{Os}_3(\text{CO})_{10}(\text{CH}_2\text{D})(\mu\text{-I})$ .** The salt  $[\text{PPN}][\text{Os}_3(\text{CO})_{10}(\mu\text{-CD}_2)(\mu\text{-I})]$  (0.287 g, 0.188 mmol), prepared by reaction of  $[\text{PPN}]\text{I}$  with  $\text{Os}_3(\text{CO})_{11}(\mu\text{-CD}_2)$ ,<sup>14</sup> was placed in a 50-mL Schlenk flask and dissolved in ~8 mL of dry  $\text{CH}_2\text{Cl}_2$  under an  $\text{N}_2$  atmosphere. The solution was acidified with 0.65 mL of a 0.316 M solution of  $\text{CF}_3\text{SO}_3\text{H}$  in  $\text{CH}_2\text{Cl}_2$ . Workup of the product as described above for  $\text{Os}_3(\text{CO})_{10}(\text{CH}_3)(\mu\text{-I})$  gave a mixture of  $\text{Os}_3(\text{CO})_{10}(\text{CHD}_2)(\mu\text{-I})$  and  $\text{Os}_3(\text{CO})_{10}(\text{CH}_2\text{D})(\mu\text{-I})$  (0.060 g, 0.060 mmol) in 32% yield: <sup>1</sup>H NMR ( $\text{CDCl}_3$ )  $\delta$  1.22 (s, 0.7 H,  $\text{Os}_3(\text{CO})_{10}(\text{CHD}_2)(\mu\text{-I})$ ), 1.28 (s, 1 H,  $\text{Os}_3(\text{CO})_{10}(\text{CH}_2\text{D})(\mu\text{-I})$ ). No resonance was observed at  $\delta$  1.34 for  $\text{Os}_3(\text{CO})_{10}(\text{CH}_3)(\mu\text{-I})$ . Computer simulation of the EI mass spectrum of the sample in the  $m/z$  988–1000 region showed the parent ion envelope to be composed of contributions from individual clusters with molecular weights based on <sup>190</sup>Os of 994 (66%, 5- $d_2$ ), 993 (10%, 5- $d_1$ , (5- $d_2$ ) - H), and 992 (24%, 5, (5- $d_2$ ) - D, (5- $d_1$ ) - H).

**Reaction of  $\text{Os}_3(\text{CO})_{10}(\text{CH}_3)(\mu\text{-I})$  with CO.** The complex  $\text{Os}_3(\text{CO})_{10}(\text{CH}_3)(\mu\text{-I})$  (0.0537 g, 0.0541 mmol) was placed in a 40-mL Schlenk flask, and ~5 mL of  $\text{CH}_2\text{Cl}_2$  was distilled onto the sample from BaO in vacuo. One atmosphere of CO was admitted to the evacuated sample, and a red to orange color change occurred over a 2-h period. After the solution was stirred overnight, the color had changed to light yellow. The  $\text{CH}_2\text{Cl}_2$  solvent was removed by vacuum distillation, and the resultant yellow powder was extracted with several ~3-mL portions of *n*-pentane and then washed with  $\text{CH}_2\text{Cl}_2$  to give  $\text{Os}_3(\text{CO})_{11}(\eta^1\text{-C(O)CH}_3)(\mu\text{-I})$  (**7**; 0.0264 g, 0.0252 mmol) as a light yellow powder in 47% yield. This compound is only slightly soluble in  $\text{CH}_2\text{Cl}_2$  or hydrocarbon solvents. IR ( $\nu_{\text{CO}}$ ,  $\text{CH}_2\text{Cl}_2$ ) 2141 w, 2109 m, 2054 s, 2035 m, 2026 m, 1997 w, 1620 w  $\text{cm}^{-1}$ ; MS (EI, <sup>190</sup>Os)  $m/z$  1048 ( $\text{M}^+$ ) plus

(14) Jensen, C. M.; Knobler, C. B.; Kaesz, H. D. *J. Am. Chem. Soc.* **1984**, *106*, 5926.

(15) (a) Butler, I. S.; Basolo, F.; Pearson, R. G. *Inorg. Chem.* **1967**, *6*, 2074. (b) Green, M. L. H.; Mitchard, L. C.; Swanwick, M. G. *J. Chem. Soc. A* **1971**, 794. (c) Collman, J. P.; Siegl, W. A. *J. Am. Chem. Soc.* **1972**, *94*, 2516. (d) Mayr, A.; Lin, Y. C.; Boag, N. M.; Kaesz, H. D. *Inorg. Chem.* **1982**, *21*, 1704.

(16) (a) Jensen, C. M.; Chen, Y. J.; Kaesz, H. D. *J. Am. Chem. Soc.* **1984**, *106*, 4046. (b) Azam, K. A.; Deeming, A. J.; Rothwell, I. P. *J. Chem. Soc., Dalton Trans.* **1981**, 91. (c) Cook, N.; Smart, L.; Woodward, P. *J. Chem. Soc., Dalton Trans.* **1977**, 1744.

(17) Calvert, R. B. Ph.D. Thesis, University of Illinois, 1978. Shapley, J. R., personal communication.

(18) Steinmetz, G. R.; Morrison, E. D.; Geoffroy, G. L. *J. Am. Chem. Soc.* **1984**, *106*, 2559.

(19) Johnson, B. F. G.; Lewis, J.; Pippard, D. A. *J. Chem. Soc., Dalton Trans.* **1981**, 407.

fragment ions corresponding to the loss of 11 CO's;  $^1\text{H}$  NMR ( $\text{CDCl}_3$ )  $\delta$  2.55 (s). Anal. Calcd for  $\text{C}_{13}\text{H}_3\text{IO}_{12}\text{Os}_3$ : C, 14.88; H, 0.29. Found: C, 15.04; H, 0.38.

The combined *n*-pentane extracts from the above preparation of 7 were chromatographed on a  $\text{SiO}_2$  TLC plate with *n*-pentane as eluant. Nine yellow bands eluted of which only the seventh was identified. Removal of this band from the plate led to isolation of  $\text{Os}_3(\text{CO})_{10}(\mu\text{-O}=\text{CCH}_3)(\mu\text{-I})$  (6) as a light yellow microcrystalline solid in ~5% yield. 6: IR ( $\nu_{\text{CO}}$ , cyclohexane) 2105 w, 2072 s, 2056 m, 2022 s, 2008 s, 1995 m, 1987 w, 1979 w, 1499 w  $\text{cm}^{-1}$ ; MS (EI,  $^{190}\text{Os}$ )  $m/z$  1020 ( $\text{M}^+$ ) plus fragment ions corresponding to the loss of 10 CO's;  $^1\text{H}$  NMR ( $\text{CDCl}_3$ )  $\delta$  2.58 (s). Anal. Calcd for  $\text{C}_{12}\text{H}_3\text{IO}_{11}\text{Os}_3$ : C, 14.11; H, 0.30. Found: C, 14.42; H, 0.59.

**Conversion of 7 into 6 and 5.** The complex  $\text{Os}_3(\text{CO})_{11}(\eta^1\text{-C}(\text{O})\text{CH}_3)(\mu\text{-I})$  (7) (0.020 g, 0.019 mmol) was dissolved in  $\text{THF-}d_8$  and the 200-MHz NMR spectrum recorded. The NMR tube was then freeze-pump-thawed three times and sealed in vacuo. After the solution was heated in a 45 °C oil bath for 2 h, the NMR spectrum was again recorded and showed disappearance of the resonance at  $\delta$  2.55 (s) attributed to 7 and growth of two resonances in a 3:1 intensity ratio at  $\delta$  2.58 (s) due to the  $\mu$ -acetyl complex 6 and  $\delta$  1.28 (s) assigned to 5.

**Thermal Decomposition of  $\text{Os}_3(\text{CO})_{10}(\text{CH}_3)(\mu\text{-I})$ .** The complex  $\text{Os}_3(\text{CO})_{10}(\text{CH}_3)(\mu\text{-I})$  (0.060 g, 0.061 mmol) was dissolved in 0.75 mL of a 1:2  $\text{CDCl}_3/\text{CD}_2\text{Cl}_2$  solution and placed in a 5-mm NMR tube under  $\text{N}_2$ . The sample was degassed by three freeze-pump-thaw cycles and sealed under vacuum and the  $^1\text{H}$  NMR spectrum recorded. The color changed from deep red to orange overnight. The  $^1\text{H}$  NMR spectrum recorded after 1 week showed that all of 5 had decomposed and that  $\text{Os}_3(\text{CO})_{10}(\mu\text{-O}=\text{CCH}_3)(\mu\text{-I})$  (6) was present in 53% yield based upon NMR integration relative to internal  $\text{CDHCl}_2$ . Chromatography (TLC)

on  $\text{SiO}_2$  with 10%  $\text{CH}_2\text{Cl}_2$ /hexane gave 6 (0.020 g, 0.019 mmol) as the fourth bright yellow band in 32% yield. Peach-colored, orange, and tan bands preceding 6 and orange, red, yellow-orange, violet, green, violet, green, violet, and brown bands following 6 were not identified.

**Reaction of  $\text{Os}_3(\text{CO})_{11}(\mu\text{-CH}_2)$  with HI.** The complex  $\text{Os}_3(\text{CO})_{11}(\mu\text{-CH}_2)$  (0.0516 g, 0.0578 mmol) was dissolved in 6.0 mL of  $\text{CH}_2\text{Cl}_2$  and placed in a 40-mL Schlenk flask to which was added via syringe 0.17 mL of a 0.8 M solution of HI in  $\text{CHCl}_3$  (0.136 mmol). The solution changed color from dark red to orange while it was stirred for 14 h. The  $\text{CH}_2\text{Cl}_2$  solvent was then removed by rotary evaporation, and the oily orange residue was chromatographed on  $\text{SiO}_2$  using 5%  $\text{CH}_2\text{Cl}_2$ /*n*-pentane as eluant. This gave an orange band which was poorly separated from a faint red band of  $\text{Os}_3(\text{CO})_{11}(\mu\text{-CH}_2)$  which preceded it. The IR spectrum of the second band showed it to contain a mixture of ~90%  $\text{Os}_3(\text{CO})_{10}(\mu\text{-O}=\text{CCH}_3)(\mu\text{-I})$  (6) and ~10%  $\text{Os}_3(\text{CO})_{11}(\mu\text{-CH}_2)$  (3). Unreacted 3 was converted to  $[\text{PPN}][\text{Os}_3(\text{CO})_{10}(\mu\text{-CH}_2)(\mu\text{-Cl})]$  by treating the solution with excess  $[\text{PPN}]\text{Cl}$  in  $\text{CH}_2\text{Cl}_2$ ,<sup>7</sup> and the  $\text{Os}_3(\text{CO})_{10}(\mu\text{-O}=\text{CCH}_3)(\mu\text{-I})$  product (0.028 g, 0.027 mmol) was obtained from this mixture in 47% yield by extracting with several ~5-mL portions of *n*-pentane.

**Acknowledgment.** We gratefully acknowledge the Department of Energy, Office of Basic Energy Sciences, for support of this research and J. Shapley for helpful discussions.

**Registry No.** 3, 77208-32-3; 4, 96395-21-0; 4-*d*<sub>2</sub>, 99642-95-2; 5, 99642-96-3; 5-*d*<sub>1</sub>, 99642-93-0; 5-*d*<sub>2</sub>, 99642-92-9; 6, 91312-92-4; 7, 99642-97-4;  $[\text{PPN}][\text{Os}_3(\text{CO})_{10}(\mu\text{-CH}_2)(\mu\text{-Cl})]$ , 96395-17-4; Os, 7440-04-2.

## Correlation between the Site of Insertion of the Gas-Phase Ions $\text{Fe}^+$ , $\text{Co}^+$ , and $\text{Ni}^+$ into C-C Bonds in Alkanes and the Ionization Potentials of the Alkyl Radicals Involved

Barbara D. Radecki and John Allison\*

Department of Chemistry, Michigan State University, East Lansing, Michigan 48824

Received June 24, 1985

In the gas-phase chemistry of  $\text{M}^+$  ( $\text{M} = \text{Fe}, \text{Co}, \text{Ni}$ ) with alkanes, the metal ion can insert into a number of the C-C bonds to give intermediates of the type  $\text{R-M}^+-\text{R}'$ . Insertion into some C-C bonds is preferred over others. We note a correlation between the preference for insertion into a particular skeletal bond and the ionization potentials (IP's) of the alkyl radicals formed when the C-C bond is cleaved. The correlation suggests a relationship between  $\text{IP}(\text{C}_n\text{H}_{2n+1})$  and  $D^0(\text{M}^+-\text{C}_n\text{H}_{2n+1})$ , with IP decreasing and bond energy increasing as *n* increases. The relationship between IP and bond energies of alkyl radicals to other cations such as  $\text{Hg}^+$  is noted and supports this suggestion. Thus, the correlation may suggest that the preferred intermediates involve those in which the  $(\text{M}^+-\text{R})$  bonds which are formed are the strongest.

### Introduction

In the numerous reports of the gas-phase chemistry of transition-metal ions with organic molecules which have appeared in the past several years,<sup>1</sup> the metal insertion/ $\beta$ -hydrogen shift/competitive ligand loss reaction sequence<sup>2</sup> has been utilized to explain the formation of the

majority of the product ions. If each step in this sequence were sufficiently understood, products and branching ratios could be predicted a priori. Such predicting ability becomes very important in analytical applications of these reactions in the metal ion chemical ionization technique. The least understood step in this sequence is the metal insertion process, yet it appears to be the dominant factor affecting product distributions.<sup>3</sup> Here, we focus on the metal insertion process occurring in the reactions of first-row transition-metal ions ( $\text{M}^+ = \text{Fe}^+, \text{Co}^+, \text{Ni}^+$ ) with straight-chain alkanes from butane to decane.

(1) Publications representative of the groups currently active in this area include: (a) Freas, R. B.; Ridge, D. P. *J. Am. Chem. Soc.* **1980**, *102*, 7129. (b) Armentrout, P. B.; Beauchamp, J. L. *J. Am. Chem. Soc.* **1981**, *103*, 6624. (c) Jacobson, D. B.; Freiser, B. S. *J. Am. Chem. Soc.* **1983**, *105*, 7484. (d) Grady, W. L.; Bursey, M. M. *Int. J. Mass Spectrom. Ion. Processes* **1983/1984**, *55*, 111. (e) Huang, S. K.; Allison, J. *Organometallics* **1983**, *2*, 883.

(2) Allison, J.; Ridge, D. P. *J. Am. Chem. Soc.* **1976**, *98*, 7445.

(3) Armentrout, P. B.; Beauchamp, J. L. *J. Am. Chem. Soc.* **1981**, *103*, 784.

fragment ions corresponding to the loss of 11 CO's;  $^1\text{H}$  NMR ( $\text{CDCl}_3$ )  $\delta$  2.55 (s). Anal. Calcd for  $\text{C}_{13}\text{H}_3\text{IO}_{12}\text{Os}_3$ : C, 14.88; H, 0.29. Found: C, 15.04; H, 0.38.

The combined *n*-pentane extracts from the above preparation of **7** were chromatographed on a  $\text{SiO}_2$  TLC plate with *n*-pentane as eluant. Nine yellow bands eluted of which only the seventh was identified. Removal of this band from the plate led to isolation of  $\text{Os}_3(\text{CO})_{10}(\mu\text{-O}=\text{CCH}_3)(\mu\text{-I})$  (**6**) as a light yellow microcrystalline solid in ~5% yield. **6**: IR ( $\nu_{\text{CO}}$ , cyclohexane) 2105 w, 2072 s, 2056 m, 2022 s, 2008 s, 1995 m, 1987 w, 1979 w, 1499 w  $\text{cm}^{-1}$ ; MS (EI,  $^{190}\text{Os}$ )  $m/z$  1020 ( $\text{M}^+$ ) plus fragment ions corresponding to the loss of 10 CO's;  $^1\text{H}$  NMR ( $\text{CDCl}_3$ )  $\delta$  2.58 (s). Anal. Calcd for  $\text{C}_{12}\text{H}_3\text{IO}_{11}\text{Os}_3$ : C, 14.11; H, 0.30. Found: C, 14.42; H, 0.59.

**Conversion of 7 into 6 and 5.** The complex  $\text{Os}_3(\text{CO})_{11}(\eta^1\text{-C}(\text{O})\text{CH}_3)(\mu\text{-I})$  (**7**) (0.020 g, 0.019 mmol) was dissolved in  $\text{THF-}d_8$  and the 200-MHz NMR spectrum recorded. The NMR tube was then freeze-pump-thawed three times and sealed in vacuo. After the solution was heated in a 45 °C oil bath for 2 h, the NMR spectrum was again recorded and showed disappearance of the resonance at  $\delta$  2.55 (s) attributed to **7** and growth of two resonances in a 3:1 intensity ratio at  $\delta$  2.58 (s) due to the  $\mu$ -acetyl complex **6** and  $\delta$  1.28 (s) assigned to **5**.

**Thermal Decomposition of  $\text{Os}_3(\text{CO})_{10}(\text{CH}_3)(\mu\text{-I})$ .** The complex  $\text{Os}_3(\text{CO})_{10}(\text{CH}_3)(\mu\text{-I})$  (0.060 g, 0.061 mmol) was dissolved in 0.75 mL of a 1:2  $\text{CDCl}_3/\text{CD}_2\text{Cl}_2$  solution and placed in a 5-mm NMR tube under  $\text{N}_2$ . The sample was degassed by three freeze-pump-thaw cycles and sealed under vacuum and the  $^1\text{H}$  NMR spectrum recorded. The color changed from deep red to orange overnight. The  $^1\text{H}$  NMR spectrum recorded after 1 week showed that all of **5** had decomposed and that  $\text{Os}_3(\text{CO})_{10}(\mu\text{-O}=\text{CCH}_3)(\mu\text{-I})$  (**6**) was present in 53% yield based upon NMR integration relative to internal  $\text{CDHCl}_2$ . Chromatography (TLC)

on  $\text{SiO}_2$  with 10%  $\text{CH}_2\text{Cl}_2$ /hexane gave **6** (0.020 g, 0.019 mmol) as the fourth bright yellow band in 32% yield. Peach-colored, orange, and tan bands preceding **6** and orange, red, yellow-orange, violet, green, violet, green, violet, and brown bands following **6** were not identified.

**Reaction of  $\text{Os}_3(\text{CO})_{11}(\mu\text{-CH}_2)$  with HI.** The complex  $\text{Os}_3(\text{CO})_{11}(\mu\text{-CH}_2)$  (0.0516 g, 0.0578 mmol) was dissolved in 6.0 mL of  $\text{CH}_2\text{Cl}_2$  and placed in a 40-mL Schlenk flask to which was added via syringe 0.17 mL of a 0.8 M solution of HI in  $\text{CHCl}_3$  (0.136 mmol). The solution changed color from dark red to orange while it was stirred for 14 h. The  $\text{CH}_2\text{Cl}_2$  solvent was then removed by rotary evaporation, and the oily orange residue was chromatographed on  $\text{SiO}_2$  using 5%  $\text{CH}_2\text{Cl}_2$ /*n*-pentane as eluant. This gave an orange band which was poorly separated from a faint red band of  $\text{Os}_3(\text{CO})_{11}(\mu\text{-CH}_2)$  which preceded it. The IR spectrum of the second band showed it to contain a mixture of ~90%  $\text{Os}_3(\text{CO})_{10}(\mu\text{-O}=\text{CCH}_3)(\mu\text{-I})$  (**6**) and ~10%  $\text{Os}_3(\text{CO})_{11}(\mu\text{-CH}_2)$  (**3**). Unreacted **3** was converted to  $[\text{PPN}][\text{Os}_3(\text{CO})_{10}(\mu\text{-CH}_2)(\mu\text{-Cl})]$  by treating the solution with excess  $[\text{PPN}]\text{Cl}$  in  $\text{CH}_2\text{Cl}_2$ ,<sup>7</sup> and the  $\text{Os}_3(\text{CO})_{10}(\mu\text{-O}=\text{CCH}_3)(\mu\text{-I})$  product (0.028 g, 0.027 mmol) was obtained from this mixture in 47% yield by extracting with several ~5-mL portions of *n*-pentane.

**Acknowledgment.** We gratefully acknowledge the Department of Energy, Office of Basic Energy Sciences, for support of this research and J. Shapley for helpful discussions.

**Registry No.** **3**, 77208-32-3; **4**, 96395-21-0; **4-*d*<sub>2</sub>**, 99642-95-2; **5**, 99642-96-3; **5-*d*<sub>1</sub>**, 99642-93-0; **5-*d*<sub>2</sub>**, 99642-92-9; **6**, 91312-92-4; **7**, 99642-97-4;  $[\text{PPN}][\text{Os}_3(\text{CO})_{10}(\mu\text{-CH}_2)(\mu\text{-Cl})]$ , 96395-17-4; Os, 7440-04-2.

## Correlation between the Site of Insertion of the Gas-Phase Ions $\text{Fe}^+$ , $\text{Co}^+$ , and $\text{Ni}^+$ into C-C Bonds in Alkanes and the Ionization Potentials of the Alkyl Radicals Involved

Barbara D. Radecki and John Allison\*

Department of Chemistry, Michigan State University, East Lansing, Michigan 48824

Received June 24, 1985

In the gas-phase chemistry of  $\text{M}^+$  ( $\text{M} = \text{Fe}, \text{Co}, \text{Ni}$ ) with alkanes, the metal ion can insert into a number of the C-C bonds to give intermediates of the type  $\text{R-M}^+-\text{R}'$ . Insertion into some C-C bonds is preferred over others. We note a correlation between the preference for insertion into a particular skeletal bond and the ionization potentials (IP's) of the alkyl radicals formed when the C-C bond is cleaved. The correlation suggests a relationship between  $\text{IP}(\text{C}_n\text{H}_{2n+1})$  and  $D^0(\text{M}^+-\text{C}_n\text{H}_{2n+1})$ , with IP decreasing and bond energy increasing as *n* increases. The relationship between IP and bond energies of alkyl radicals to other cations such as  $\text{Hg}^+$  is noted and supports this suggestion. Thus, the correlation may suggest that the preferred intermediates involve those in which the  $(\text{M}^+-\text{R})$  bonds which are formed are the strongest.

### Introduction

In the numerous reports of the gas-phase chemistry of transition-metal ions with organic molecules which have appeared in the past several years,<sup>1</sup> the metal insertion/ $\beta$ -hydrogen shift/competitive ligand loss reaction sequence<sup>2</sup> has been utilized to explain the formation of the

majority of the product ions. If each step in this sequence were sufficiently understood, products and branching ratios could be predicted a priori. Such predicting ability becomes very important in analytical applications of these reactions in the metal ion chemical ionization technique. The least understood step in this sequence is the metal insertion process, yet it appears to be the dominant factor affecting product distributions.<sup>3</sup> Here, we focus on the metal insertion process occurring in the reactions of first-row transition-metal ions ( $\text{M}^+ = \text{Fe}^+, \text{Co}^+, \text{Ni}^+$ ) with straight-chain alkanes from butane to decane.

(1) Publications representative of the groups currently active in this area include: (a) Freas, R. B.; Ridge, D. P. *J. Am. Chem. Soc.* **1980**, *102*, 7129. (b) Armentrout, P. B.; Beauchamp, J. L. *J. Am. Chem. Soc.* **1981**, *103*, 6624. (c) Jacobson, D. B.; Freiser, B. S. *J. Am. Chem. Soc.* **1983**, *105*, 7484. (d) Grady, W. L.; Bursey, M. M. *Int. J. Mass Spectrom. Ion. Processes* **1983/1984**, *55*, 111. (e) Huang, S. K.; Allison, J. *Organometallics* **1983**, *2*, 883.

(2) Allison, J.; Ridge, D. P. *J. Am. Chem. Soc.* **1976**, *98*, 7445.

(3) Armentrout, P. B.; Beauchamp, J. L. *J. Am. Chem. Soc.* **1981**, *103*, 784.



Table I. Reactions of Fe<sup>+</sup>, Co<sup>+</sup>, and Ni<sup>+</sup> with Nonane and Decane

			Fe <sup>+</sup>	Co <sup>+</sup>	Ni <sup>+</sup>
M <sup>+</sup> + <i>n</i> -nonane	→	MC <sub>9</sub> H <sub>18</sub> <sup>+</sup> + H <sub>2</sub>	0.09	0.03	
	→	MC <sub>7</sub> H <sub>14</sub> <sup>+</sup> + C <sub>2</sub> H <sub>6</sub>	0.05	0.03	0.02
	→	MC <sub>6</sub> H <sub>12</sub> <sup>+</sup> + C <sub>3</sub> H <sub>8</sub>	0.04	0.09	0.12
	→	MC <sub>5</sub> H <sub>10</sub> <sup>+</sup> + C <sub>4</sub> H <sub>10</sub>	0.18	0.20	0.56
	→	MC <sub>4</sub> H <sub>8</sub> <sup>+</sup> + C <sub>5</sub> H <sub>12</sub>	0.16	0.33	0.08
	→	MC <sub>4</sub> H <sub>6</sub> <sup>+</sup> + C <sub>5</sub> H <sub>12</sub> + H <sub>2</sub>	0.17	0.03	
	→	MC <sub>3</sub> H <sub>6</sub> <sup>+</sup> + C <sub>6</sub> H <sub>14</sub>	0.20	0.29	0.22
	→	MC <sub>2</sub> H <sub>4</sub> <sup>+</sup> + C <sub>7</sub> H <sub>16</sub>	0.11		
M <sup>+</sup> + <i>n</i> -decane	→	MC <sub>10</sub> H <sub>20</sub> <sup>+</sup> + H <sub>2</sub>	0.16	0.05	
	→	MC <sub>8</sub> H <sub>16</sub> <sup>+</sup> + C <sub>2</sub> H <sub>6</sub>		0.05	
	→	MC <sub>7</sub> H <sub>14</sub> <sup>+</sup> + C <sub>3</sub> H <sub>8</sub>	0.13	0.07	0.12
	→	MC <sub>6</sub> H <sub>12</sub> <sup>+</sup> + C <sub>4</sub> H <sub>10</sub>	0.10	0.18	0.14
	→	MC <sub>5</sub> H <sub>10</sub> <sup>+</sup> + C <sub>5</sub> H <sub>12</sub>	0.26	0.17	0.13
	→	MC <sub>4</sub> H <sub>8</sub> <sup>+</sup> + C <sub>6</sub> H <sub>14</sub>	0.18	0.29	0.20
	→	MC <sub>3</sub> H <sub>6</sub> <sup>+</sup> + C <sub>7</sub> H <sub>16</sub>	0.17	0.19	0.41

Table II. Reactions of Fe<sup>+</sup> with Octane

Fe <sup>+</sup> + <i>n</i> -octane	→		
	→	FeC <sub>5</sub> H <sub>10</sub> <sup>+</sup> + C <sub>3</sub> H <sub>8</sub>	0.18
	→	FeC <sub>5</sub> H <sub>8</sub> <sup>+</sup> + C <sub>3</sub> H <sub>8</sub> + H <sub>2</sub>	0.02
	→	FeC <sub>4</sub> H <sub>8</sub> <sup>+</sup> + C <sub>4</sub> H <sub>10</sub>	0.11
	→	FeC <sub>4</sub> H <sub>6</sub> <sup>+</sup> + C <sub>4</sub> H <sub>10</sub> + H <sub>2</sub>	0.22
	→	FeC <sub>3</sub> H <sub>6</sub> <sup>+</sup> + C <sub>5</sub> H <sub>12</sub>	0.36
	→	FeC <sub>2</sub> H <sub>4</sub> <sup>+</sup> + C <sub>6</sub> H <sub>14</sub>	0.11

Table III. Branching Ratios of Ion/Molecule Reaction Products of Co<sup>+</sup> and *n*-Pentane (Table Indicates Neutral Products Lost)

Co <sup>+</sup> + C <sub>5</sub> H <sub>12</sub> → loss of	H <sub>2</sub>	(H <sub>2</sub> + CH <sub>4</sub> )	CH <sub>4</sub>	C <sub>2</sub> H <sub>6</sub>	C <sub>3</sub> H <sub>8</sub>
laboratory					
Cal Tech <sup>a</sup>	0.30		0.02	0.59	0.08
Purdue <sup>b</sup>	0.19	0.02	0.02	0.67	0.10
MSU <sup>c</sup>	0.23			0.65	0.12

<sup>a</sup>Data taken from ref 3. <sup>b</sup>Data taken from ref 4. <sup>c</sup>Data taken from ref 13.

identified. Conventional double-resonance techniques were used to identify precursors of ion/molecule reaction products. Branching ratios were calculated to determine product distributions and are accurate to within ±10%.

Tricarbonylnitrosylcobalt(0) and tetrakis(trifluorophosphine)nickel were obtained from Alfa Inorganics. Iron pentacarbonyl was purchased from the Aldrich Chemical Co. Butane, pentane, hexane, heptane, octane, nonane, and decane were obtained from the Fluka Chemical Corp. Samples were degassed by multiple freeze-pump-thaw cycles and were used without further purifications.

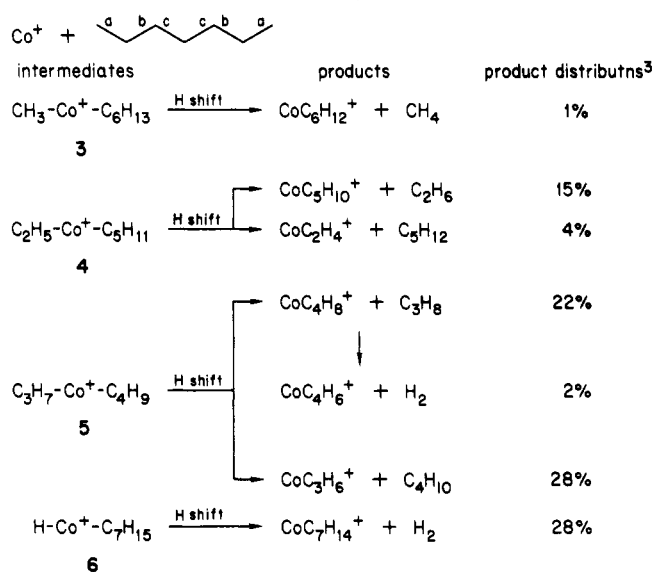
We believe that our results<sup>13</sup> for the reactions of Fe<sup>+</sup>, Co<sup>+</sup>, and Ni<sup>+</sup> with alkanes are consistent with those previously reported in the literature<sup>3-5</sup> and will not be included here. Partial data from our labs have appeared elsewhere.<sup>14</sup> However, the reactions of Fe<sup>+</sup> with octane and Fe<sup>+</sup>, Co<sup>+</sup>, and Ni<sup>+</sup> with nonane and decane have not been reported. These results are listed in Tables I and II.

It should be noted that there are lab-to-lab deviations in such experiments. For example, Table III shows the product distributions for the reactions of Co<sup>+</sup> with *n*-pentane from three laboratories. These results are not identical. Minor products observed in one lab may not be observed in another. However, we have interpreted the published data as we have interpreted our own and we believe that the data in the literature is consistent in that the implications which can be derived concerning preferential formation of specific metal insertion intermediates are the same.

## Results and Discussion

Assuming that the metal insertion/H shift/competitive ligand loss sequence is predominant in the chemistry of

Scheme I



first-row transition-metal ions (M<sup>+</sup>) with alkanes, it has been reported that internal C-C bonds are preferentially attacked by M<sup>+</sup> over terminal C-C bonds.<sup>3-5</sup> (It should be noted that the metal insertion/ $\beta$ -H shift mechanism for explaining the elimination of small alkanes from larger alkanes is speculative, although consistent with a large number of similar reactions which have been reported. The insertion of a metal ion into a C-H bond followed by a  $\beta$ -alkyl shift still remains as a possible mechanism for explaining alkane elimination.) We believe that, in order to understand the metal-insertion process, the preference or ordering of site of attack must be determined. Here, we describe the procedure which was followed for determining the order of preference of M<sup>+</sup> insertion into skeletal bonds of *n*-alkanes. This order of preference for Fe<sup>+</sup>, Co<sup>+</sup>, and Ni<sup>+</sup> with *n*-alkanes from butane to decane will be presented. Finally, a discussion of the trends and a correlation of these trends with alkyl radical ionization potentials will be presented and discussed.

To establish an ordering of the preference of M<sup>+</sup> for insertion into C-C bonds of alkanes, both final product distributions and the mechanisms leading to these prod-

(13) Radecki, B. D. Ph.D. Thesis, Michigan State University, 1985.

(14) Tsarbopoulos, A.; Allison, J. J. *Am. Chem. Soc.* 1985, 107, 5085.



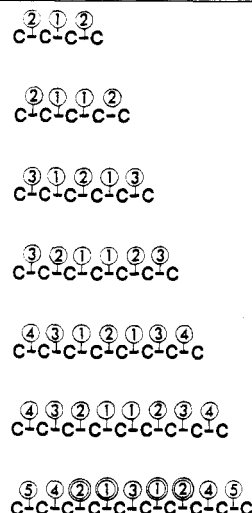
ucts must be known. Consider as an example, the reaction of  $\text{Co}^+$  and heptane. Heptane has three pairs of chemically indistinguishable bonds, labelled as a, b, and c in Scheme I.

Insertion into every C-C bond by  $\text{Co}^+$  should be an exothermic process. Scheme I shows these insertion intermediates, the possible products, and the experimentally observed branching ratios for these products—revealing how the product distributions reflect the distribution of insertion intermediates which are initially formed. Note that products indicative of insertion into all three skeletal bonds are formed. From the product distribution in Scheme I, *disregarding  $\text{H}_2$  elimination*, we would suggest that intermediate 5 (i.e., insertion into the c bond) is formed most often leading to 52% of the products; intermediate 4 follows, producing 19% of the observed products; and insertion into the terminal C-C bond, intermediate 3, only leads to 1% of the products.<sup>3</sup> This naive approach to interpretation of product distributions assumes that only one mechanism is operative. However, extensive work which has appeared in the literature<sup>4,6,7</sup> has shown that  $\text{H}_2$  elimination need not occur through intermediate 6 in Scheme I but may occur through 4 and 5 as well. Also, evidence for alkane elimination by a metal insertion/ $\beta$ -methyl shift mechanism has appeared.<sup>7</sup> Thus, a true distribution of insertion intermediates which are initially formed can be determined by combining information such as the product distributions in Scheme I with the results of labelling and mechanistic studies.

First consider  $\text{H}_2$  elimination. Molecular hydrogen elimination may occur following insertion into C-H bonds (1,2-dehydrogenation)<sup>3</sup> and insertion into C-C bonds (1,4-dehydrogenation)<sup>6</sup> in alkanes. Labeling studies<sup>7</sup> and collision-induced dissociation<sup>4</sup> experiments have been used to distinguish between the mechanisms which are operative in  $\text{H}_2$  elimination for a variety of alkanes reacting with  $\text{Fe}^+$ ,  $\text{Co}^+$ , and  $\text{Ni}^+$ . By examining the branching ratios associated with  $\text{H}_2$ , HD, and  $\text{D}_2$  elimination occurring in the reactions of  $\text{M}^+$  with strategically deuterated alkanes, the intermediates involved in  $\text{H}_2$  elimination should become apparent. The chemistry of deuterated butane, pentane, and hexanes with  $\text{Fe}^+$ ,  $\text{Co}^+$ , and  $\text{Ni}^+$  has been reported.<sup>7</sup> For example, in the chemistry of  $\text{Co}^+$  with  $\text{CD}_3\text{CH}_2\text{CH}_2\text{CD}_3$ , results suggest that 51% of  $\text{H}_2$  elimination results from insertion into the internal C-C bond, with 49% from C-H insertion.  $\text{Ni}^+$  reacts exclusively by  $\text{H}_2$  elimination through the  $\text{C}_2\text{H}_5\text{-Ni}^+\text{-C}_2\text{H}_5$  intermediate. The results for  $\text{Fe}^+$  and  $\text{Co}^+$  with deuterated pentane and hexane are inconclusive, since dehydrogenation products of  $\text{CH}_3\text{C-D}_2\text{CD}_2\text{CD}_2\text{CH}_3$  could be indicative of 1,2- or 1,4-dehydrogenation or both. Also, such results are subject to isotope effects, which appear to alter product distributions—that is, labeling studies provide insights into which mechanisms are operative in the unlabeled alkanes, but not the relative importance of each.

Jacobson and Freiser have used collision-induced dissociation (CID) to probe the structures of the ionic products formed in the dehydrogenation reactions of  $\text{M}^+$  and selected alkanes.<sup>4</sup> Their results suggest that 70% of  $\text{H}_2$  elimination occurs via C-C insertion for  $\text{Fe}^+$ , 90% for  $\text{Co}^+$ , and 100% for  $\text{Ni}^+$ . The CID experiments with  $\text{Fe}^+$  and  $\text{Co}^+$  also indicate which C-C insertions lead to the 1,4-dehydrogenation. Recent studies of the translational energy distributions of product ions have also provided insights into the 1,2- and 1,4- $\text{H}_2$  elimination mechanisms.<sup>15</sup> Therefore, data is available which we used to "deconvolute"

Table IV. Preference<sup>a</sup> of  $\text{Fe}^+$ ,  $\text{Co}^+$ , and  $\text{Ni}^+$  for C-C Bond Insertion in Linear Alkanes<sup>b</sup>



<sup>a</sup> As determined by the method discussed in the text. The ordering is consistent with ICR results from our laboratory and previously reported results<sup>3-5</sup> within experimental uncertainty. <sup>b</sup> Double circles indicate that a different preference for these two bonds was observed for the metal ions studied. In the case of decane,  $\text{Fe}^+$  exhibited equal preference for the two bonds indicated by double circles. In the case of  $\text{Co}^+$  the order is as shown. In the case of  $\text{Ni}^+$  the order of the bonds labeled one and two is reversed.

the branching ratios to determine the relative ordering of insertion intermediates.

A second complication is the metal insertion/ $\beta$ -methyl shift reaction which has been observed in the reactions of  $\text{Fe}^+$  with partially deuterated butane, pentane, and hexane.<sup>7</sup> Fortunately, this process is sufficiently minor such that it can be neglected in analyzing the branching ratios.

The branching ratio data,<sup>3</sup> labeling studies,<sup>7</sup> and CID<sup>4</sup> results have thus been combined to produce the orderings of the preference of  $\text{Fe}^+$ ,  $\text{Co}^+$ , and  $\text{Ni}^+$  for sites of insertion into the C-C bonds of alkanes from butane to decane. These are presented in Table IV. The trends hold for all three metals,  $\text{Fe}^+$ ,  $\text{Co}^+$ , and  $\text{Ni}^+$ , except in the case of decane. For all three metals, the same two bonds have the highest priorities, and there are small deviations which make one slightly preferred over the other.

As indicated in the Introduction, we believe that  $\text{M}^+$  reacts with alkanes through a variety of insertion intermediates, the relative amounts of these intermediates which are formed may reflect their relative stabilities. Since the variation in C-C bond energies in the  $n$ -alkanes is small ( $\leq 5$  kcal/mol),<sup>8</sup> we suggest that the energies of the  $\text{M}^+\text{-R}$  bonds formed upon insertion may be the most significant factor in determining intermediate stabilities.

Experimentally determined bond energies show that  $D(\text{M}^+\text{-H}) < D(\text{M}^+\text{-CH}_3)$ <sup>7</sup> ( $\text{M} = \text{Fe}, \text{Co}, \text{Ni}$ ), contrary to what is observed for the neutral analogues.<sup>8</sup> This has been explained on the basis of the polarizabilities of H and  $\text{CH}_3$ . Since  $\text{CH}_3$  is more polarizable than H, it can better stabilize the positive charge on the metal—this results in a stronger  $\sigma$ -bond to the metal ion. We would expect the polarizability of  $-\text{C}_n\text{H}_{2n+1}$  to increase with increasing  $n$ , and thus we would expect  $D(\text{M}^+\text{-C}_n\text{H}_{2n+1})$  to increase with increasing  $n$ . Unfortunately, alkyl radical polarizabilities are not available. We note that the ionization potentials (IP's) of alkyl radicals reflect, in part, their polarizabilities. The IP ( $\text{C}_n\text{H}_{2n+1}$ ) decreases as  $n$  increases due to the increased polarizability which stabilizes the cation. Thus IP( $\text{C}_n\text{H}_{2n+1}$ ) should correlate with  $D(\text{Co}^+\text{-C}_n\text{H}_{2n+1})$  if the reason for changes in both values (as  $n$  changes) is the



Table V. Alkyl Radical Ionization Potentials and Bond Strengths to Various Atomic Cations

radical (R·)	IP, kcal/mol	D <sup>0</sup> (Cl <sup>+</sup> -R), <sup>e</sup> kcal/mol	D <sup>0</sup> (HO <sup>+</sup> -R), <sup>e</sup> kcal/mol	D <sup>0</sup> (Hg <sup>+</sup> -R), <sup>e</sup> kcal/mol
CH <sub>3</sub>	226.0 ± 0.5 <sup>a</sup>	119.7	137.0	53.2
C <sub>2</sub> H <sub>5</sub>	193.5 ± 0.5 <sup>a</sup>	123.4	144.7	57.0
<i>n</i> -C <sub>3</sub> H <sub>7</sub>	187.5 ± 1.0 <sup>b</sup>	130.4	148.7	65.8 <sup>f</sup>
<i>n</i> -C <sub>4</sub> H <sub>9</sub>	184.7 ± 1.0 <sup>b</sup>	132.4	150.7	
<i>n</i> -C <sub>5</sub> H <sub>11</sub>	183.1 ± 1.4 <sup>c</sup>			
<i>n</i> -C <sub>6</sub> H <sub>13</sub>	182.6 ± 1.4 <sup>c</sup>			
<i>n</i> -C <sub>7</sub> H <sub>15</sub>	182.2 ± 1.4 <sup>c</sup>			
<i>n</i> -C <sub>8</sub> H <sub>17</sub>	182.2 <sup>d</sup>			
<i>n</i> -C <sub>9</sub> H <sub>19</sub>	182.2 <sup>d</sup>			

<sup>a</sup>Data taken from ref 16. <sup>b</sup>Data taken from ref 17. <sup>c</sup>Data taken from ref 18. <sup>d</sup>Extrapolated from a plot of the known IP's (as given in this table) vs. number of carbons. <sup>e</sup>Data taken from ref 8. <sup>f</sup>Bond strength for Hg<sup>+</sup>-(*i*-C<sub>3</sub>H<sub>7</sub>).

changing polarizability. Table V lists the IP's of C<sub>*n*</sub>H<sub>2*n*+1</sub> radicals for *n* = 4–10.

Note that the IP's decrease as *n* increases, implying that *D*(M<sup>+</sup>-C<sub>*n*</sub>H<sub>2*n*+1</sub>) should increase as *n* increases. This is apparently true when alkyl groups are bonded to ions such as Hg<sup>+</sup>, Cl<sup>+</sup>, and OH<sup>+</sup>, as shown in Table V. There is *not* a similar bond energy trend for the analogous neutral species.<sup>8</sup> In addition to the polarizability argument, the trends in bond energies may also suggest that, as IP(R·) decreases, the [HOMO(R·)-LUMO(cation)] gap may decrease, facilitating the formation of a strong bond.<sup>19</sup>

Note, also, the *rate* at which IP(C<sub>*n*</sub>H<sub>2*n*+1</sub>) changes with *n*. IP(C<sub>2</sub>H<sub>5</sub>) < IP(CH<sub>3</sub>) by 32.5 kcal/mol, the largest change for adjacent alkyl radicals. In contrast, IP(C<sub>6</sub>H<sub>13</sub>) is approximately equal to IP(C<sub>5</sub>H<sub>11</sub>), within the experimental limits. Thus, we have extrapolated the IP(C<sub>*n*</sub>H<sub>2*n*+1</sub>) vs. *n* curve to estimate the IP's of the *n* = 8 and 9 species. We suggest that this also would parallel *D*(M<sup>+</sup>-R). We expect the *D*(M<sup>+</sup>-C<sub>*n*</sub>H<sub>2*n*+1</sub>) - *D*(M<sup>+</sup>-C<sub>*n*+1</sub>H<sub>2*n*+3</sub>) difference to be greatest for *n* = 1, and *D*(M<sup>+</sup>-C<sub>8</sub>H<sub>17</sub>) ≈ *D*(M<sup>+</sup>-C<sub>7</sub>H<sub>15</sub>). We see this trend reflected in *D*(HO<sup>+</sup>-R); the difference for consecutive values of *n* decreases as *n* increases (Table V).

We report a direct correlation between the sum of ionization potentials of the alkyl groups bound to M<sup>+</sup> upon insertion and the ordering of M<sup>+</sup> preference for site of insertion into the C-C bonds of alkanes. Figure 1 shows this correlation. Note that, within the experimental error of the thermodynamic information available, the C-C bond most preferred by M<sup>+</sup> for insertion corresponds to that bond which, when cleaved, forms the two radicals for which the sum of their IP's is lowest (implying the sum of their bond energies to the metal ion is highest). Priority for site of insertion decreases as this IP sum increases. Again, consider heptane as an example. If each C-C bond is cleaved and the IP's of the resulting radicals summed (the subscripts of the bracketed sums refer to the bond labels in Scheme I):

$$[\text{IP}(\text{C}_3\text{H}_7) + \text{IP}(\text{C}_4\text{H}_9)]_c < [\text{IP}(\text{C}_2\text{H}_5) + \text{IP}(\text{C}_5\text{H}_{11})]_b < [\text{IP}(\text{CH}_3) + \text{IP}(\text{C}_6\text{H}_{13})]_a$$

Note that the smallest sum corresponds to Intermediate 5 (Scheme I), which accounts for the majority of the products. The largest ΣIP corresponds to intermediate 3, which accounts for the smallest number of products etc.

The correlation may reflect the fact that, when a number of metal insertion intermediates of the type R-M<sup>+</sup>-R' are possible, those in which the *sum* of the two M<sup>+</sup>-R bond

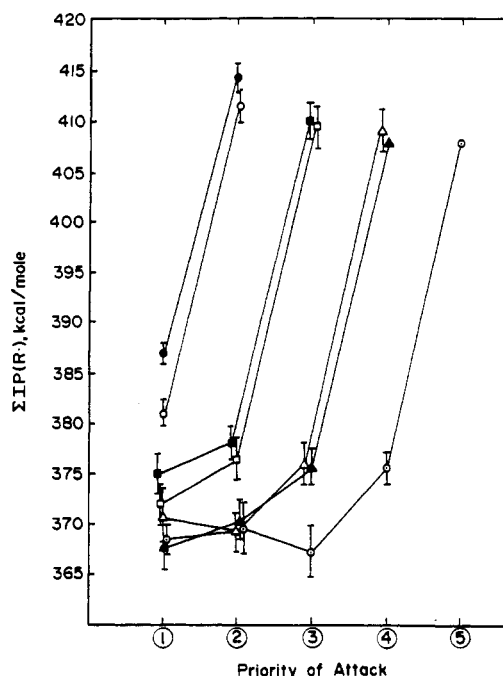


Figure 1. Correlation between priority of attack and the radical ionization potential sums. The C-C bond for which insertion by M<sup>+</sup> (M = Fe, Co, Ni) occurs to the greatest extent is given a priority of ①. The bond next most favored is priority ②, etc. When a C-C bond is cleaved, two alkyl radicals are formed. The sum of the ionization potentials of these two radicals correlates with the extent to which M<sup>+</sup> inserts into that bond. The correlation is shown for butane (●), pentane (○), hexane (■), heptane (□), octane (△), nonane (▲), and decane (○).

energies is greatest are preferentially formed. The IP/polarizability argument would then suggest that the extent to which the various C-C insertion intermediates are formed for heptane reflect the ordering

$$[D^0(\text{M}^+-\text{C}_3\text{H}_7) + D^0(\text{C}_3\text{H}_7\text{M}^+-\text{C}_4\text{H}_9)] > [D^0(\text{M}^+-\text{C}_2\text{H}_5) + D^0(\text{C}_2\text{H}_5\text{M}^+-\text{C}_5\text{H}_{11})] > [D^0(\text{M}^+-\text{CH}_3) + D^0(\text{CH}_3\text{M}^+-\text{C}_6\text{H}_{13})]$$

Note that, in the case of decane, if the experimental uncertainty in IP's are considered, any of three C-C bonds may actually correspond to the lowest ΣIP's, since any differences in IP's for the larger radicals is very small.

In this analysis, statistical factors were not included in the assignment of bond insertion preferences. Alkanes containing even numbers of carbon atoms (*n*) contain [(*n*/2) - 1] pairs of bonds and one unique bond at the center of the chain. If statistical factors were used, the products formed from insertion into the unique center bond would be weighted twice that of those products which were formed by attack of either of two identical C-C bonds. In some cases, the incorporation of statistical

(16) Houle, F. A.; Beauchamp, J. L. *J. Am. Chem. Soc.* 1979, 101, 4067.

(17) Williams, J. M.; Hamill, W. H. *J. Chem. Phys.* 1968, 49, 4467.

(18) Lossing, F. P.; Macoll, A. *Can. J. Chem.* 1976, 54, 990.

(19) Fleming, I. "Frontier Orbitals and Organic Chemical Reactions"; Wiley: New York, 1976.

factors for such alkanes could make the central bond the bond with the highest preference for insertion. Note, in this context, the alkanes in Figure 1 for which the correlation is not exact contain even numbers of C atoms, such as decane.

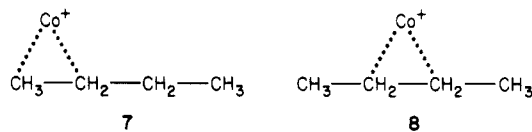
This model shows why  $M^+$  rarely inserts into terminal C-C bonds in alkanes; the high IP suggests that the  $M^+-CH_3$  bond is the weakest of the  $M^+-alkyl$  bonds. Of course, the slightly higher bond energy of that terminal bond must also be a factor to some extent.

It should be noted that such a model does not directly hold when  $M^+$  reacts with polar molecules, where the functional group can have a strong effect in "directing" the site of attack of  $M^+$  into skeletal bonds which would not be attacked to as great an extent in the corresponding alkanes.<sup>20</sup>

We recognize the fact that there may be other explanations for the observed correlation. We believe that the distribution of observed products reflect the ordering of intermediate formation "early" in the reaction. This

(20) Tsarbopoulos, A.; Radecki, B. D.; Allison, J. "32nd Annual Conference on Mass Spectrometry and Allied Topics", San Antonio, 1984, paper TOD 10.

prompts questions such as, how is the initial distribution of insertion intermediates established? There are at least two possibilities. In one case, rapid insertion/"deinsertion" may occur, allowing the metal ion to "sample" all possibilities. A second explanation may involve the formation of those ion-alkane complexes which are most stable. That is, in the case of butane, consider two intermediates 7 and 8.



The same considerations of alkyl polarizabilities may predict that 8 should be more stable than 7. Thus, it may be the distribution of *initial adduct structures* which determine those bonds which are attacked rather than the stabilities of the insertion intermediates which follow. Work is currently underway in our laboratory to model such intermediates, and to determine the influence of ion-induced dipole interactions in such collision complexes.

**Registry No.**  $Fe^+$ , 14067-02-8;  $Co^+$ , 16610-75-6;  $Ni^+$ , 14903-34-5; nonane, 111-84-2; decane, 124-18-5; octane, 111-65-9.

## Gas-Phase Chemistry of Transition-Metal-Containing Anions with Alcohols, Chloroalkanes, and Bifunctional Organic Molecules

Stephen W. McElvany and John Allison\*

Department of Chemistry, Michigan State University, East Lansing, Michigan 48824

Received June 17, 1985

The chemistry of  $Fe(CO)_{3,4}^-$ ,  $Cr(CO)_{3,5}^-$ ,  $Co(CO)_{2,3}^-$ , and  $CoNO(CO)_{1,2}^-$  with a series of *n*-chloroalkanes, *n*-alcohols, 1,*n*-bromochloroalkanes, and 1,*n*-chloro alcohols is reported here. The results suggest that the chemistry of metal-containing anions is similar to that observed for metal-containing cations; metal insertions into bonds of the organic molecule followed by  $\beta$ -H shifts appear to occur. These anions only insert into C-functional group bonds. Charge transfer from the metal to the electronegative group (Cl, Br, OH) appears to be an important step leading to the formation of the observed products. Ligands formed in these reactions, which bond strongly to the analogous cations, are not retained by the anions. Reaction trends are used to suggest an ordering for the electron affinities of the metal-containing species studied here.

### Introduction

The majority of gas-phase organometallic ion/molecule reactions, as studied by ion cyclotron resonance (ICR) mass spectrometry and related methods, have dealt with metal and metal-containing positive ions. Previous studies have observed changes in reactivity as the type of metal,<sup>1</sup> number of ligands on the metal (i.e., ligand effects),<sup>2</sup> and the neutral organic molecule are varied.<sup>3</sup> Relatively few

studies have been performed on the corresponding metal and metal-containing anions, i.e., have determined changes in the chemistry of a metal "center" due to a change in the charge on the metal species. This study reports the ion/molecule reactions observed for various metal-containing anions with a series of *n*-chloroalkanes, *n*-alcohols, 1,*n*-bromochloroalkanes, and 1,*n*-chloro alcohols.

The products which are observed in the positive metal ion reactions can usually be explained by the general mechanism: metal insertion/ $\beta$ -H shift/competitive ligand loss.<sup>4</sup> Metal insertion has been observed into C-C bonds, C-H bonds (e.g., alkanes<sup>1a</sup> and amines<sup>5</sup>), C-functional group bonds (e.g., alkyl halides<sup>6</sup>), and even bonds within functional groups (e.g., nitroalkanes<sup>2c</sup>). The  $\beta$ -H shift mechanism is common in both solution<sup>7</sup> and gas-phase positive metal ion/molecule reactions.<sup>8</sup> The metal in-

(1) (a) Jacobson, D. B.; Freiser, B. S. *J. Am. Chem. Soc.* **1983**, *105*, 5197. (b) Cassady, C. J.; Freiser, B. S. *J. Am. Chem. Soc.* **1985**, *107*, 1566.

(2) (a) Allison, J.; Huang, S. K.; Lombarski, M.; McElvany, S. W.; Radecki, B.; Tsarbopoulos, A. "American Society for Mass Spectrometry Meeting", Boston, 1983. (b) Tsarbopoulos, A.; Allison, J. *Organometallics* **1984**, *3*, 86. (c) Cassady, C. J.; Freiser, B. S.; McElvany, S. W.; Allison, J. *J. Am. Chem. Soc.* **1984**, *106*, 6125.

(3) Publications representative of the groups active in this area include the following: (a) Huang, S. K.; Allison, J. *Organometallics* **1983**, *2*, 883. (b) Jones, R. W.; Staley, R. H. *J. Am. Chem. Soc.* **1980**, *102*, 3794. (c) Jacobson, D. B.; Freiser, B. S. *J. Am. Chem. Soc.* **1983**, *105*, 7484. (d) Wronka, J.; Ridge, D. P. *J. Am. Chem. Soc.* **1984**, *106*, 67. (e) Hanratty, M. A.; Beauchamp, J. L.; Illies, A. J.; Bowers, M. T. *J. Am. Chem. Soc.* **1985**, *107*, 1788. (f) Aristov, N.; Armentrout, P. B. *J. Am. Chem. Soc.* **1984**, *106*, 4065.

(4) Allison, J.; Ridge, D. P. *J. Am. Chem. Soc.* **1976**, *98*, 7445.

(5) Radecki, B.; Allison, J. *J. Am. Chem. Soc.* **1984**, *106*, 946.

(6) Allison, J.; Ridge, D. P. *J. Am. Chem. Soc.* **1979**, *101*, 4998.

(7) Heck, R. F. "Organotransition Metal Chemistry"; Academic Press: New York, 1974; pp 76-110.

factors for such alkanes could make the central bond the bond with the highest preference for insertion. Note, in this context, the alkanes in Figure 1 for which the correlation is not exact contain even numbers of C atoms, such as decane.

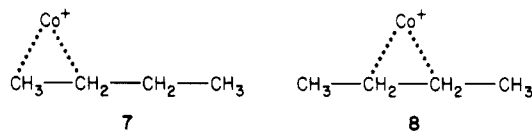
This model shows why  $M^+$  rarely inserts into terminal C-C bonds in alkanes; the high IP suggests that the  $M^+-CH_3$  bond is the weakest of the  $M^+-alkyl$  bonds. Of course, the slightly higher bond energy of that terminal bond must also be a factor to some extent.

It should be noted that such a model does not directly hold when  $M^+$  reacts with polar molecules, where the functional group can have a strong effect in "directing" the site of attack of  $M^+$  into skeletal bonds which would not be attacked to as great an extent in the corresponding alkanes.<sup>20</sup>

We recognize the fact that there may be other explanations for the observed correlation. We believe that the distribution of observed products reflect the ordering of intermediate formation "early" in the reaction. This

(20) Tsarbopoulos, A.; Radecki, B. D.; Allison, J. "32nd Annual Conference on Mass Spectrometry and Allied Topics", San Antonio, 1984, paper TOD 10.

prompts questions such as, how is the initial distribution of insertion intermediates established? There are at least two possibilities. In one case, rapid insertion/"deinsertion" may occur, allowing the metal ion to "sample" all possibilities. A second explanation may involve the formation of those ion-alkane complexes which are most stable. That is, in the case of butane, consider two intermediates 7 and 8.



The same considerations of alkyl polarizabilities may predict that 8 should be more stable than 7. Thus, it may be the distribution of *initial adduct structures* which determine those bonds which are attacked rather than the stabilities of the insertion intermediates which follow. Work is currently underway in our laboratory to model such intermediates, and to determine the influence of ion-induced dipole interactions in such collision complexes.

**Registry No.**  $Fe^+$ , 14067-02-8;  $Co^+$ , 16610-75-6;  $Ni^+$ , 14903-34-5; nonane, 111-84-2; decane, 124-18-5; octane, 111-65-9.

## Gas-Phase Chemistry of Transition-Metal-Containing Anions with Alcohols, Chloroalkanes, and Bifunctional Organic Molecules

Stephen W. McElvany and John Allison\*

Department of Chemistry, Michigan State University, East Lansing, Michigan 48824

Received June 17, 1985

The chemistry of  $Fe(CO)_{3,4}^-$ ,  $Cr(CO)_{3,5}^-$ ,  $Co(CO)_{2,3}^-$ , and  $CoNO(CO)_{1,2}^-$  with a series of *n*-chloroalkanes, *n*-alcohols, 1,*n*-bromochloroalkanes, and 1,*n*-chloro alcohols is reported here. The results suggest that the chemistry of metal-containing anions is similar to that observed for metal-containing cations; metal insertions into bonds of the organic molecule followed by  $\beta$ -H shifts appear to occur. These anions only insert into C-functional group bonds. Charge transfer from the metal to the electronegative group (Cl, Br, OH) appears to be an important step leading to the formation of the observed products. Ligands formed in these reactions, which bond strongly to the analogous cations, are not retained by the anions. Reaction trends are used to suggest an ordering for the electron affinities of the metal-containing species studied here.

### Introduction

The majority of gas-phase organometallic ion/molecule reactions, as studied by ion cyclotron resonance (ICR) mass spectrometry and related methods, have dealt with metal and metal-containing positive ions. Previous studies have observed changes in reactivity as the type of metal,<sup>1</sup> number of ligands on the metal (i.e., ligand effects),<sup>2</sup> and the neutral organic molecule are varied.<sup>3</sup> Relatively few

studies have been performed on the corresponding metal and metal-containing anions, i.e., have determined changes in the chemistry of a metal "center" due to a change in the charge on the metal species. This study reports the ion/molecule reactions observed for various metal-containing anions with a series of *n*-chloroalkanes, *n*-alcohols, 1,*n*-bromochloroalkanes, and 1,*n*-chloro alcohols.

The products which are observed in the positive metal ion reactions can usually be explained by the general mechanism: metal insertion/ $\beta$ -H shift/competitive ligand loss.<sup>4</sup> Metal insertion has been observed into C-C bonds, C-H bonds (e.g., alkanes<sup>1a</sup> and amines<sup>5</sup>), C-functional group bonds (e.g., alkyl halides<sup>6</sup>), and even bonds within functional groups (e.g., nitroalkanes<sup>2c</sup>). The  $\beta$ -H shift mechanism is common in both solution<sup>7</sup> and gas-phase positive metal ion/molecule reactions.<sup>8</sup> The metal in-

(1) (a) Jacobson, D. B.; Freiser, B. S. *J. Am. Chem. Soc.* **1983**, *105*, 5197. (b) Cassady, C. J.; Freiser, B. S. *J. Am. Chem. Soc.* **1985**, *107*, 1566.

(2) (a) Allison, J.; Huang, S. K.; Lombarski, M.; McElvany, S. W.; Radecki, B.; Tsarbopoulos, A. "American Society for Mass Spectrometry Meeting", Boston, 1983. (b) Tsarbopoulos, A.; Allison, J. *Organometallics* **1984**, *3*, 86. (c) Cassady, C. J.; Freiser, B. S.; McElvany, S. W.; Allison, J. *J. Am. Chem. Soc.* **1984**, *106*, 6125.

(3) Publications representative of the groups active in this area include the following: (a) Huang, S. K.; Allison, J. *Organometallics* **1983**, *2*, 883. (b) Jones, R. W.; Staley, R. H. *J. Am. Chem. Soc.* **1980**, *102*, 3794. (c) Jacobson, D. B.; Freiser, B. S. *J. Am. Chem. Soc.* **1983**, *105*, 7484. (d) Wronka, J.; Ridge, D. P. *J. Am. Chem. Soc.* **1984**, *106*, 67. (e) Hanratty, M. A.; Beauchamp, J. L.; Illies, A. J.; Bowers, M. T. *J. Am. Chem. Soc.* **1985**, *107*, 1788. (f) Aristov, N.; Armentrout, P. B. *J. Am. Chem. Soc.* **1984**, *106*, 4065.

(4) Allison, J.; Ridge, D. P. *J. Am. Chem. Soc.* **1976**, *98*, 7445.

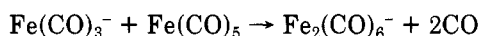
(5) Radecki, B.; Allison, J. *J. Am. Chem. Soc.* **1984**, *106*, 946.

(6) Allison, J.; Ridge, D. P. *J. Am. Chem. Soc.* **1979**, *101*, 4998.

(7) Heck, R. F. "Organotransition Metal Chemistry"; Academic Press: New York, 1974; pp 76-110.

sertion/ $\beta$ -H shift mechanism produces two molecules from one. These two molecules compete as ligands on the metal. The proton affinities of ligands have been shown to be an indication of the strength of the metal-ligand interaction.<sup>2b</sup> Ligands that have low proton affinities are lost preferentially to ligands with higher proton affinities in the competitive ligand loss process. Ligands which are  $\pi$ -donors (e.g., olefins) also form strong interactions with positive metal ions and frequently are preferentially retained in the competitive ligand loss process. At this time one may predict the ion/molecule reaction products which would be observed for a certain metal-organic system by the metal insertion/ $\beta$ -H shift/competitive ligand loss mechanism. To date, there has been no attempt to formulate a general mechanism to describe metal-containing anion/organic molecule interactions.

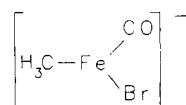
Early mass spectrometric studies have shown that  $M(\text{CO})_{n-1}^-$  is the predominant anion formed by 70-eV electron impact on transition-metal carbonyls,  $M(\text{CO})_n^-$ , with a small percentage of  $M(\text{CO})_{n-2}^-$  also being formed.<sup>9</sup> The first metal anion/molecule reactions studied with ICR were performed by Dunbar<sup>10</sup> and Beauchamp.<sup>11</sup> The stable 17-electron species  $M(\text{CO})_{n-1}^-$  were found to be generally unreactive in the gas phase, whereas the  $M(\text{CO})_{n-2}^-$  anions were observed to react with the neutral  $M(\text{CO})_n$ ,<sup>10</sup> e.g.



Recently Wronka and Ridge<sup>12</sup> have observed sequential anion/molecule reactions in  $\text{Fe}(\text{CO})_5$  up to  $\text{Fe}_4(\text{CO})_{13}^-$ .

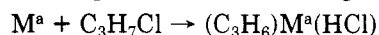
Reactions of these metal-containing anions with organic molecules have been studied by using ICR and flowing afterglow techniques. Weddle and Ridge<sup>13</sup> reported the chemistry of  $\text{Fe}(\text{CO})_3^-$  and  $\text{Fe}(\text{CO})_4^-$  with a series of 13 organic molecules. Ligand substitution of the neutral organic molecule for one or two carbonyl ligands was observed for 9 of the 13 compounds studied. Only one rearrangement-type reaction was reported, ion-induced decarbonylation of maleic anhydride. The predominance of ligand substitution reactions and lack of (apparent) bond-breaking and rearrangement reactions for  $\text{Fe}(\text{CO})_3^-$  and  $\text{Fe}(\text{CO})_4^-$  is not surprising since, in the reactions of positive metal ions, as the number of ligands on the metal increases ligand substitution processes dominate the products observed.<sup>2</sup> Freiser et al.<sup>14</sup> were able to study the proton abstraction reactions of the bare metal anion  $\text{Cr}^-$  with a series of Brønsted acids. The bare metal anion  $\text{Cr}^-$  was formed by performing collision-induced dissociation on the  $\text{Cr}(\text{CO})_5^-$  anion produced from electron impact on  $\text{Cr}(\text{CO})_6$ . Squires et al.<sup>15</sup> have formed metalcarboxylic anions in the gas-phase ( $\text{Fe}(\text{CO})_4\text{COOH}^-$ ) by reacting  $\text{OH}^-$  with neutral  $\text{Fe}(\text{CO})_5$  in a flowing afterglow apparatus in an attempt to study the water gas shift reaction. McDonald et al.<sup>16</sup> have also used a flowing afterglow apparatus

to study the reaction of anions formed by electron impact on  $\text{Fe}(\text{CO})_5$ . The anion  $\text{Fe}(\text{CO})_4^-$  reacts with a series of halomethanes to yield halogen atom transfer products and in some cases ligand substitution with loss of one or two carbonyl ligands.<sup>16a</sup> The reactions of  $\text{Fe}(\text{CO})_3^-$ <sup>16b</sup> were also studied in which adduct products with the neutral molecule were observed due to the termolecular collisional stabilization with the  $\text{He}/\text{CH}_4$  buffer gas, in addition to ligand substitution of the neutral molecule for carbonyl ligands. The reaction of  $\text{Fe}(\text{CO})_3^-$  with  $\text{CH}_3\text{Br}$  yields a ligand substitution product of  $\text{CH}_3\text{Br}$  for two carbonyl ligands and abstraction of a bromine atom from  $\text{CH}_3\text{Br}$ . The mechanism proposed was the formation of an ion/radical collision complex produced by the bromine atom transfer, although oxidative addition is still possible since  $\text{Fe}(\text{CO})_3^-$  has two available coordination sites. It is then suggested that the ion/radical complex could dissociate to produce the bromine abstraction product or the methyl radical could add and displace two carbonyl ligands to yield the substitution product of the neutral  $\text{CH}_3\text{Br}$  in the form:



The present study was initiated in an attempt to obtain an understanding of the reactions and mechanisms of these metal-containing anions. Low-energy (0–5 eV) electron impact was used to produce a greater percentage of the more reactive  $M(\text{CO})_{n-2}^-$  and  $M(\text{CO})_{n-3}^-$  species from  $\text{Co}(\text{CO})_3\text{NO}$ ,  $\text{Fe}(\text{CO})_5$ , and  $\text{Cr}(\text{CO})_6$ .<sup>9</sup> The reactions of these metal-containing anions with a series of 1-chloro-*n*-alkanes, 1-hydroxy-*n*-alkanes, 1-bromo-*n*-chloro-*n*-alkanes, and 1-hydroxy-*n*-chloro-*n*-alkanes were studied in order to propose a general mechanism for the reactions of metal anions with polar organic molecules.

On the basis of the current literature, then, what similarities and differences would be expected in the chemistry of organometallic anions and cations? Metal anions may be expected to insert into bonds similar to cations. There is no evidence in the literature which suggests  $\beta$ -H shifts for anions; however organometallic anions containing M-H bonds have been reported.<sup>17</sup> If a rearrangement such as



occurs when a is (+), ligand loss correlates with the ligands' proton affinities. When a is (-), ligand loss appears to correlate with Lewis acidity.<sup>18</sup> Thus, we may expect both similarities and differences in such anion and cation reactions.

The previous studies mentioned have not addressed the question concerning the location of the negative charge in these anions. In the corresponding positive ion reactions, the positive charge remains on the metal due to the lower ionization potential of the metal compared to the ligands present. In the discussion of the anion reactions, the electron affinities of the metal species and ligands must be considered when determining the location of the negative charge. The pertinent electron affinities which are available are listed in Table I. The amount of electron

(8) Armentrout, P. B.; Beauchamp, J. L. *J. Am. Chem. Soc.* **1981**, *103*, 784.

(9) (a) Pignatoro, S.; Foffani, A.; Grasso, F.; Cantone, B. *Z. Phys. Chem.* **1965**, *47*, 106. (b) Winters, R. E.; Kiser, R. W. *J. Chem. Phys.* **1966**, *44*, 1964. (c) Compton, R. N.; Stockdale, J. A. D. *Int. J. Mass Spectrom. Ion Phys.* **1976**, *22*, 47.

(10) Dunbar, R. C.; Ennever, J. F.; Fackler, J. P. *Inorg. Chem.* **1973**, *12*, 2734.

(11) Foster, M. S.; Beauchamp, J. L. *J. Am. Chem. Soc.* **1975**, *97*, 4808.

(12) Wronka, J.; Ridge, D. P. *J. Am. Chem. Soc.* **1984**, *106*, 67.

(13) Weddle, G. H.; Ridge, D. P. "American Society for Mass Spectrometry Meeting", New York, 1980.

(14) Sallans, L.; Lane, K.; Squires, R. R.; Freiser, B. S. *J. Am. Chem. Soc.* **1983**, *105*, 6352.

(15) Lane, K. R.; Lee, R. E.; Sallans, L.; Squires, R. R. *J. Am. Chem. Soc.* **1984**, *106*, 5767.

(16) (a) McDonald, R. N.; Schell, P. L.; McGhee, W. D. *Organometallics* **1984**, *3*, 182. (b) McDonald, R. N.; Chowdhury, A. K.; Schell, P. L. *J. Am. Chem. Soc.* **1984**, *106*, 6095.

(17) Stevens, A. E.; Feigerle, C. S.; Lineberger, W. C. *J. Chem. Phys.* **1983**, *78*, 5420.

(18) Corderman, R. R.; Beauchamp, J. L. *Inorg. Chem.* **1977**, *16*, 3135.

(19) Stull, D. R.; Prophet, H., Eds. "JANAF Thermochemical Tables"; U.S. Government Printing Office: Washington, D.C.: 1971; NSRDS-NBS 37.

(20) Janousek, B.; Brauman, J. I. "Gas Phase Ion Chemistry"; Bowers, M. T., Ed.; Academic Press: New York, 1979; Vol. 2.

**Table I. Pertinent Electron Affinities (EA, kcal/mol)<sup>a</sup>**

anion (M <sup>-</sup> )	EA (M)	ref
H <sup>-</sup>	17.4	19
Cl <sup>-</sup>	83.3	20
Br <sup>-</sup>	77.6	20
Cr <sup>-</sup>	15.4	21
Co <sup>-</sup>	15.3	22
Fe <sup>-</sup>	3.8	23
Fe(CO) <sup>-</sup>	29.1	23
Fe(CO) <sub>2</sub> <sup>-</sup>	28.1	23
Fe(CO) <sub>3</sub> <sup>-</sup>	41.5	23
Fe(CO) <sub>4</sub> <sup>-</sup>	55.3	23
FeH <sup>-</sup>	21.5	17
CO <sup>-</sup>	31.6	24
HO <sup>-</sup>	42.2	20
CH <sub>3</sub> O <sup>-</sup>	36.7	25
C <sub>2</sub> H <sub>5</sub> O <sup>-</sup>	39.8	26
<i>n</i> -C <sub>3</sub> H <sub>7</sub> O <sup>-</sup>	41.2	26
<i>n</i> -C <sub>4</sub> H <sub>9</sub> O <sup>-</sup>	43.8	27
CH <sub>3</sub> Cl <sup>-</sup>	-79.6	28
CH <sub>3</sub> <sup>-</sup>	26	29
C <sub>2</sub> H <sub>5</sub> <sup>-</sup>	23	29
C <sub>3</sub> H <sub>7</sub> <sup>-</sup>	16	29
C <sub>4</sub> H <sub>9</sub> <sup>-</sup>	15	29
C <sub>2</sub> H <sub>4</sub> <sup>-</sup>	-35.7	30

<sup>a</sup>Electron affinity is defined as  $\Delta H$  for the reaction  $M^- \rightarrow M + e^-$ .

**Table II. Metal-Containing Anions Formed by Low-Energy Electron Impact**

neutral	ionizing energy	anions formed
Fe(CO) <sub>5</sub>	1 eV	Fe(CO) <sub>4</sub> <sup>-</sup> Fe(CO) <sub>3</sub> <sup>-</sup>
Cr(CO) <sub>6</sub>	4.5 eV	Cr(CO) <sub>5</sub> <sup>-</sup> Cr(CO) <sub>4</sub> <sup>-</sup> Cr(CO) <sub>3</sub> <sup>-</sup>
Co(CO) <sub>3</sub> NO	1.5 eV	Co(CO) <sub>2</sub> NO <sup>-</sup> Co(CO) <sub>3</sub> <sup>-</sup> CoCONO <sup>-</sup> Co(CO) <sub>2</sub> <sup>-</sup>

affinity data available on metal carbonyl species is small and incomplete but proves invaluable in explaining the anion/molecule reactions observed. For example, the electron affinities of all three bare metals (Cr, Fe, and Co) have been determined but the various carbonyl-containing species of only one metal (Fe) have been determined. It will be shown that the location of the negative charge and the types of ligands present will play an important role in explaining the reactions and mechanisms observed.

### Experimental Section

All experiments were performed on an ion cyclotron resonance (ICR) mass spectrometer of conventional design (used in the "drift mode") which was constructed at Michigan State University and is described elsewhere.<sup>5</sup> The only experimental condition which had to be changed to detect negative ions instead of positive ions was the polarity of the trapping plates (negative for the negative

(21) Feigerle, C. S.; Corderman, R. R.; Bobashev, S. V.; Lineberger, W. C. *J. Chem. Phys.* **1981**, *74*, 1580.

(22) Corderman, R. R.; Engelking, P. C.; Lineberger, W. C. *J. Chem. Phys.* **1979**, *70*, 4474.

(23) Engelking, P. C.; Lineberger, W. C. *J. Am. Chem. Soc.* **1979**, *101*, 5569.

(24) Refaey, K. M. A.; Franklin, J. L. *Int. J. Mass Spectrom. Ion Phys.* **1976**, *20*, 19.

(25) Janousek, B. K.; Zimmerman, A. H.; Reed, K. J.; Brauman, J. I. *J. Am. Chem. Soc.* **1978**, *100*, 6142.

(26) Ellison, G. B.; Engelking, P. C.; Lineberger, W. C. *J. Phys. Chem.* **1982**, *86*, 4873.

(27) Williams, J. M.; Hamill, W. H. *J. Chem. Phys.* **1968**, *49*, 4467.

(28) Burrow, P. D.; Modelli, A.; Chiu, N. S.; Jordan, K. D. *J. Chem. Phys.* **1982**, *77*, 2699.

(29) Page, F. M. "Free Radicals in Inorganic Chemistry, Advances in Chemistry Series"; Gould, R. F., Ed.; American Chemical Society: Washington D.C., 1962; *Adv. Chem. Ser. No. 36*, pp 68-75.

(30) Burrow, P. D.; Jordan, K. D. *Chem. Phys. Lett.* **1975**, *36*, 594.

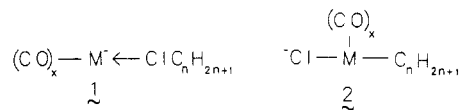
ion studies). All chemicals used in this work were high-purity commercial samples which were used as supplied except for multiple freeze-pump-thaw cycles to remove noncondensable gases.

The reactant metal-containing anions formed by low-energy electron impact on CO(CO)<sub>3</sub>NO, Fe(CO)<sub>5</sub>, and Cr(CO)<sub>6</sub> are shown in Table II along with the ionizing energy utilized. The intensities of the ions formed by low-energy impact are very sensitive to changes in the electron energy<sup>9</sup> and thus are not reported in Table II. Ion/molecule reactions and precursors were identified by using double-resonance techniques. Reported data are results of product ions formed in a 1:1 mixture (by pressure) of the metal carbonyl to organic compound, at a total pressure of approximately  $1 \times 10^{-5}$  torr. Spectra were always taken to masses greater than the sum of the molecular weight of the metal carbonyl and the organic compound. The branching ratios listed in Tables III-IX are accurate to within  $\pm 10\%$ . Although in some cases empirical formulas other than those listed may also be possible for the products, we believe those listed are the most reasonable based on observed reaction trends and the reactions of the other metal anions.

### Results and Discussion

***n*-Chloroalkanes.** The ion/molecule reaction products and their branching ratios for the reactions of chromium, iron, and cobalt-containing anions with a series of *n*-chloroalkanes (*n* = 1-6) are listed in Table III. Three types of reactions are observed for the metal-containing anions with *n*-chloroalkanes: ligand substitution by the chloroalkane molecule for two or three carbonyl ligands (parent substitution); abstraction of chlorine from the chloroalkane (Cl abstraction); and abstraction of chlorine and hydrogen from the chloroalkane (HCl abstraction).

Parent substitution reactions by the chloroalkanes are observed for the metal-containing anions Cr(CO)<sub>3</sub><sup>-</sup>, Fe(CO)<sub>3</sub><sup>-</sup>, and Co(CO)<sub>2</sub><sup>-</sup>. The reaction of Fe(CO)<sub>3</sub><sup>-</sup> and Co(CO)<sub>2</sub><sup>-</sup> are accompanied by a loss of two carbonyl ligands while Cr(CO)<sub>3</sub><sup>-</sup> loses all three carbonyl ligands. Two possible product ion structures are shown, structures 1 and 2 (where *x* = 0 for M = Cr and Co and *x* = 1 for M = Fe).



Structure 1 results from ligand substitution by the chloroalkane for two or three carbonyl ligands with the chloroalkane molecule remaining intact as a ligand on the metal anion. The negative charge must remain on the metal species in structure 1 due to the large *negative* electron affinity of the chloroalkane ligand (e.g., EA(CH<sub>3</sub>Cl) = -79.6 kcal/mol). While an electron pair on the chlorine may form a dative bond to the metal, there will certainly be a strong ion-dipole repulsive interaction in this intermediate. The magnitude of this repulsion is estimated to be 35 kcal/mol for 1-chlorobutane and 29 kcal/mol for 1-butanol.<sup>31</sup> Comparison of the electron affinities for the metal-containing species Fe(CO)<sub>3</sub> (41.5 kcal/mol) and Cl (83.3 kcal/mol) suggests the possibility that, once the metal anion-chloroalkane complex is formed, it is thermodynamically favorable for the charge to be transferred from the metal anion to a chlorine atom. Structure 2 results from metal insertion into the C-Cl bond

(31) The ion-dipole repulsions were calculated from ref 32 with the dipole moment values from 33. The distance between the ion and dipole for these calculations was 2 Å ( $\theta = 0^\circ$ ). Similar calculations for a distance of 5 Å yields ion-dipole repulsions of approximately 6 and 5 kcal/mol for 1-chlorobutane and 1-butanol, respectively.

(32) Benson, S. W. "The Foundations of Chemical Kinetics"; McGraw-Hill: New York, 1960.

(33) West, R. C., Ed. "Handbook of Chemistry and Physics", 56th ed.; CRC Press: Cleveland, 1976.

Table III. Reactions of Chromium-, Iron-, and Cobalt-Containing Anions with *n*-Chloroalkanes

reaction	branching ratios						
	<i>n</i> = 1	<i>n</i> = 2	<i>n</i> = 3	<i>n</i> = 4	<i>n</i> = 5	<i>n</i> = 6	
$\text{Cr}(\text{CO})_3^- + \text{C}_n\text{H}_{2n+1}\text{Cl}$	$\rightarrow \text{CrC}_n\text{H}_{2n+1}\text{Cl}^- + 3\text{CO}$	0.36	0.28	0.27	(0.39) <sup>b</sup>	0.27	0.20
	$\rightarrow \text{Cr}(\text{CO})_2\text{Cl}^- + \text{C}_n\text{H}_{2n+1} + \text{CO}$	0.22	0.23	0.15	0.13	0.10	0.08
	$\rightarrow \text{Cr}(\text{CO})_3\text{Cl}^- + \text{C}_n\text{H}_{2n+1}$	0.42	0.36	0.43	0.48	0.47	0.52
	$\rightarrow \text{Cr}(\text{CO})_2\text{HCl}^- + \text{C}_n\text{H}_{2n} + \text{CO}$		0.13	0.15	(0.39)	0.16	0.20
$\text{Cr}(\text{CO})_4^- + \text{C}_n\text{H}_{2n+1}\text{Cl}$	$\rightarrow$						
$\text{Cr}(\text{CO})_5^- + \text{C}_n\text{H}_{2n+1}\text{Cl}$	$\rightarrow$						
$\text{Fe}(\text{CO})_3^- + \text{C}_n\text{H}_{2n+1}\text{Cl}$	$\rightarrow \text{FeCOC}_n\text{H}_{2n+1}\text{Cl}^- + 2\text{CO}$		(0.25)	0.19	0.12	0.10	0.08
	$\rightarrow \text{Fe}(\text{CO})_3\text{Cl}^- + \text{C}_n\text{H}_{2n+1}$	1.00	0.75	0.70	0.78	0.71	0.70
	$\rightarrow \text{Fe}(\text{CO})_2\text{HCl}^- + \text{C}_n\text{H}_{2n} + \text{CO}$		(0.25)	0.11	0.10	0.19	0.22
$\text{Fe}(\text{CO})_4^- + \text{C}_n\text{H}_{2n+1}\text{Cl}$	$\rightarrow$						
$\text{Co}(\text{CO})_2^- + \text{C}_n\text{H}_{2n+1}\text{Cl}$	$\rightarrow \text{CoC}_n\text{H}_{2n+1}\text{Cl}^- + 2\text{CO}$	0.67	(0.65)	0.26	(0.28)	0.10	0.08
	$\rightarrow \text{CoCOCl}^- + \text{C}_n\text{H}_{2n+1} + \text{CO}$	0.07	0.11				
	$\rightarrow \text{Co}(\text{CO})_2\text{Cl}^- + \text{C}_n\text{H}_{2n+1}$	0.26	0.24	0.26	0.26	0.17	0.20
	$\rightarrow \text{CoCOHCl}^- + \text{C}_n\text{H}_{2n} + \text{CO}$		(0.65)	0.43	0.46	0.61	0.60
	$\rightarrow \text{Co}(\text{CO})_2\text{HCl}^- + \text{C}_n\text{H}_{2n}$			0.05	(0.28)	0.12	0.12
	$\rightarrow \text{CoCONOCl}^- + \text{C}_n\text{H}_{2n+1}$	1.00	0.56	0.39	0.62	0.55	0.53
$\text{Co}(\text{CO})_3^- + \text{C}_n\text{H}_{2n+1}\text{Cl}$	$\rightarrow$						
	$\rightarrow \text{CoNOHCl}^- + \text{C}_n\text{H}_{2n} + \text{CO}$		0.44	0.61	0.38	0.45	0.47
$\text{Co}(\text{CO})_2\text{NO}^- + \text{C}_n\text{H}_{2n+1}\text{Cl}$	$\rightarrow$						
$\rightarrow$	NR						

<sup>a</sup>NR indicates the ion did not undergo any reactions. <sup>b</sup>Values in parentheses are the sum of branching ratios for isobaric product ions.

Table IV. Reactions of Chromium-, Iron-, and Cobalt-Containing Anions with *n*-Alcohols

reaction	branching ratios						
	<i>n</i> = 1	<i>n</i> = 2	<i>n</i> = 3	<i>n</i> = 4	<i>n</i> = 5	<i>n</i> = 6	
$\text{Cr}(\text{CO})_3^- + \text{C}_n\text{H}_{2n+1}\text{OH}$	$\rightarrow \text{Cr}(\text{CO})_2\text{C}_n\text{H}_{2n+1}\text{OH}^- + \text{CO}$	0.43	0.40	0.33	0.33	0.38	0.37
	$\rightarrow \text{Cr}(\text{CO})_2\text{C}_n\text{H}_{2n}\text{O}^- + \text{H}_2 + \text{CO}$	0.53	0.50	0.47	0.28	0.22	0.19
	$\rightarrow \text{Cr}(\text{CO})_2\text{C}_n\text{H}_{2n-2}\text{O}^- + 2\text{H}_2 + \text{CO}$			0.11	0.27	0.22	0.24
	$\rightarrow \text{CrCOC}_n\text{H}_{2n+1}\text{OH}^- + 2\text{CO}$		0.02	0.04	0.06	0.09	0.07
	$\rightarrow \text{CrCOC}_n\text{H}_{2n}\text{O}^- + \text{H}_2 + 2\text{CO}$						0.03
	$\rightarrow \text{CrCOC}_n\text{H}_{2n-2}\text{O}^- + 2\text{H}_2 + 2\text{CO}$						0.05
	$\rightarrow \text{Cr}(\text{CO})_3\text{OH}^- + \text{C}_n\text{H}_{2n+1}$	0.04	0.08	0.05	0.06	0.09	0.05
$\text{Cr}(\text{CO})_4^- + \text{C}_n\text{H}_{2n+1}\text{OH}$	$\rightarrow$						
$\text{Cr}(\text{CO})_5^- + \text{C}_n\text{H}_{2n+1}\text{OH}$	$\rightarrow$						
$\text{Fe}(\text{CO})_3^- + \text{C}_n\text{H}_{2n+1}\text{OH}$	$\rightarrow \text{Fe}(\text{CO})_2\text{C}_n\text{H}_{2n}\text{O}^- + \text{H}_2 + \text{CO}$	<i>n</i> = 1-6					
$\text{Fe}(\text{CO})_4^- + \text{C}_n\text{H}_{2n+1}\text{OH}$	$\rightarrow$						
$\text{Co}(\text{CO})_2^- + \text{C}_n\text{H}_{2n+1}\text{OH}$	$\rightarrow \text{Co}(\text{CO})_2\text{C}_n\text{H}_{2n}\text{O}^- + \text{H}_2$	<i>n</i> = 1-6					
$\text{CoCONO}^- + \text{C}_n\text{H}_{2n+1}\text{OH}$	$\rightarrow \text{CoNOC}_n\text{H}_{2n}\text{O}^- + \text{H}_2 + \text{CO}$	<i>n</i> = 5, 6					
$\text{Co}(\text{CO})_3^- + \text{C}_n\text{H}_{2n+1}\text{OH}$	$\rightarrow$						
$\text{Co}(\text{CO})_2\text{NO}^- + \text{C}_n\text{H}_{2n+1}\text{OH}$	$\rightarrow$						

<sup>a</sup>NR indicates the ion did not undergo any reactions.

Table V. Reactions of Iron- and Chromium-Containing Anions with 1,*n*-Bromochloroalkanes

reaction	branching ratios						
	<i>n</i> = 2; 1,1 <sup>a</sup>	<i>n</i> = 2	<i>n</i> = 3	<i>n</i> = 4	<i>n</i> = 5	<i>n</i> = 6	
$\text{Fe}(\text{CO})_3^- + \text{Br}(\text{CH}_2)_n\text{Cl}$	$\rightarrow \text{FeCOBr}(\text{CH}_2)_n\text{Cl}^- + 2\text{CO}$			0.09	0.28	0.23	0.26
	$\rightarrow \text{FeClBr}^- + \text{C}_n\text{H}_{2n} + 3\text{CO}$		0.15	0.11	0.04	0.11	
	$\rightarrow \text{Fe}(\text{CO})_2\text{Cl}^- + (\text{CH}_2)_n\text{Br} + \text{CO}$	0.04	0.04				
	$\rightarrow \text{Fe}(\text{CO})_3\text{Cl}^- + (\text{CH}_2)_n\text{Br}$	0.44	0.28	0.38	0.28	0.23	0.22
	$\rightarrow \text{Fe}(\text{CO})_2\text{Br}^- + (\text{CH}_2)_n\text{Cl} + \text{CO}$	0.19	0.16	0.04			
	$\rightarrow \text{Fe}(\text{CO})_3\text{Br}^- + (\text{CH}_2)_n\text{Cl}$	0.33	0.37	0.38	0.35	0.30	0.32
$\text{Fe}(\text{CO})_4^- + \text{Br}(\text{CH}_2)_n\text{Cl}$	$\rightarrow \text{Fe}(\text{CO})_2\text{HBr}^- + \text{C}_n\text{H}_{2n-1}\text{Cl} + \text{CO}$				0.05	0.13	0.20
	$\rightarrow$						
	$\rightarrow \text{CrClBr}^- + \text{C}_n\text{H}_{2n} + 3\text{CO}$	0.22	0.21	0.28	0.30	0.33	0.31
	$\rightarrow \text{CrHClBr}^- + \text{C}_n\text{H}_{2n-1} + 3\text{CO}$					0.06	0.05
	$\rightarrow \text{Cr}(\text{CO})_2\text{Cl}^- + (\text{CH}_2)_n\text{Br} + \text{CO}$	0.26	0.19	0.14	0.16	0.09	0.05
	$\rightarrow \text{Cr}(\text{CO})_3\text{Cl}^- + (\text{CH}_2)_n\text{Br}$	0.10	0.10	0.18	0.19	0.19	0.22
$\text{Cr}(\text{CO})_2^- + \text{Br}(\text{CH}_2)_n\text{Cl}$	$\rightarrow \text{Cr}(\text{CO})_2\text{Br}^- + (\text{CH}_2)_n\text{Cl} + \text{CO}$	0.34	0.36	0.26	0.18	0.13	0.09
	$\rightarrow \text{Cr}(\text{CO})_3\text{Br}^- + (\text{CH}_2)_n\text{Cl}$	0.08	0.14	0.14	0.09	0.12	0.15
	$\rightarrow \text{Cr}(\text{CO})_2\text{HCl}^- + \text{C}_n\text{H}_{2n-1}\text{Br} + \text{CO}$				0.04	0.04	0.05
	$\rightarrow \text{Cr}(\text{CO})_2\text{HBr}^- + \text{C}_n\text{H}_{2n-1}\text{Cl} + \text{CO}$				0.04	0.04	0.08
	$\rightarrow \text{Cr}(\text{CO})_3\text{Cl}^- + (\text{CH}_2)_n\text{Br} + \text{CO}$	0.55	0.32	0.33	0.44	0.37	0.36
	$\rightarrow \text{Cr}(\text{CO})_3\text{Br}^- + (\text{CH}_2)_n\text{Cl} + \text{CO}$	0.45	0.68	0.67	0.56	0.63	0.64
$\text{Cr}(\text{CO})_5^- + \text{Br}(\text{CH}_2)_n\text{Cl}$	$\rightarrow$						
$\rightarrow$	NR						

<sup>a</sup>1,1-Bromochloroethane. <sup>b</sup>NR indicates the ion did not undergo any reactions.

(which occurs in positive metal ion reactions) with transfer of the electron to the chlorine atom. Presumably the metal anion insertion/charge-transfer process is sufficiently exothermic such that excess energy results in the loss of

two or three carbonyl ligands.

Following metal insertion into the C-Cl bond, a metal-carbon  $\sigma$ -bond is also formed. Reactions of aliphatic halides with  $\text{Na}_2\text{Fe}(\text{CO})_4$  in solution also proceed through

Table VI. Reactions of Cobalt-Containing Anions with 1,*n*-Bromochloroalkanes

reaction	branching ratios					
	<i>n</i> = 2; 1,1 <sup>a</sup>	<i>n</i> = 2	<i>n</i> = 3	<i>n</i> = 4	<i>n</i> = 5	<i>n</i> = 6
Co(CO) <sub>2</sub> <sup>-</sup> + Br(CH <sub>2</sub> ) <sub><i>n</i></sub> Cl	→ CoBr(CH <sub>2</sub> ) <sub><i>n</i></sub> Cl <sup>-</sup> + 2CO	0.03				
	→ CoClBr <sup>-</sup> + C <sub><i>n</i></sub> H <sub>2<i>n</i></sub> + 2CO	0.15	0.35	0.54	0.40	0.32
	→ CoCOCl <sup>-</sup> + (CH <sub>2</sub> ) <sub><i>n</i></sub> Br + CO	0.18	0.12	0.07		
	→ Co(CO) <sub>2</sub> Cl <sup>-</sup> + (CH <sub>2</sub> ) <sub><i>n</i></sub> Br	0.16	0.11	0.13	0.12	0.08
	→ CoCOBr <sup>-</sup> + (CH <sub>2</sub> ) <sub><i>n</i></sub> Cl + CO	0.36	0.31	0.11	0.10	0.08
	→ Co(CO) <sub>2</sub> Br <sup>-</sup> + (CH <sub>2</sub> ) <sub><i>n</i></sub> Cl	0.12	0.11	0.11	0.09	0.09
	→ CoCOHCl <sup>-</sup> + C <sub><i>n</i></sub> H <sub>2<i>n</i>-1</sub> Br + CO				0.04	0.11
	→ CoCOHBr <sup>-</sup> + C <sub><i>n</i></sub> H <sub>2<i>n</i>-1</sub> Cl + CO			0.04	0.21	0.26
	→ Co(CO) <sub>2</sub> HBr <sup>-</sup> + C <sub><i>n</i></sub> H <sub>2<i>n</i>-1</sub> Cl				0.04	0.06
	→ Co(CO) <sub>2</sub> HCl <sup>-</sup> + C <sub><i>n</i></sub> H <sub>2<i>n</i>-1</sub> Br + CO					0.08
CoCONO <sup>-</sup> + Br(CH <sub>2</sub> ) <sub><i>n</i></sub> Cl	→ CoNOCl <sup>-</sup> + (CH <sub>2</sub> ) <sub><i>n</i></sub> Br + CO	0.08	0.08			
	→ CoCONOCl <sup>-</sup> + (CH <sub>2</sub> ) <sub><i>n</i></sub> Br	0.10	0.19	0.15	0.11	0.09
	→ CoNOBr <sup>-</sup> + (CH <sub>2</sub> ) <sub><i>n</i></sub> Cl + CO	0.47	0.47	0.34	0.14	0.14
	→ CoCONOBr <sup>-</sup> + (CH <sub>2</sub> ) <sub><i>n</i></sub> Cl	0.35	0.26	0.36	0.22	0.20
	→ CoNOHCl <sup>-</sup> + C <sub><i>n</i></sub> H <sub>2<i>n</i>-1</sub> Br + CO			0.15	0.53	0.52
Co(CO) <sub>3</sub> <sup>-</sup> + Br(CH <sub>2</sub> ) <sub><i>n</i></sub> Cl	→ Co(CO) <sub>2</sub> Br <sup>-</sup> + (CH <sub>2</sub> ) <sub><i>n</i></sub> Cl + CO	1.00	1.00	1.00		
	→ Co(CO) <sub>2</sub> HBr <sup>-</sup> + C <sub><i>n</i></sub> H <sub>2<i>n</i>-1</sub> Cl + CO				1.00	1.00
	→ CoCOHBr <sup>-</sup> + C <sub><i>n</i></sub> H <sub>2<i>n</i>-1</sub> Cl + 2CO					0.59
Co(CO) <sub>2</sub> NO <sup>-</sup> + Br(CH <sub>2</sub> ) <sub><i>n</i></sub> Cl	→ Co(CO) <sub>2</sub> NOBr <sup>-</sup> + (CH <sub>2</sub> ) <sub><i>n</i></sub> Cl	1.00	1.00	NR <sup>b</sup>	NR	NR
						0.41

<sup>a</sup> 1,1-Bromochloroethane. <sup>b</sup> NR indicates the ion did not undergo any reactions.

Table VII. A Comparison of the Average Branching Ratios of Cl-Containing and Br-Containing Products and HCl Abstraction and HBr Abstraction Products for the 1,*n*-Bromochloroalkanes (*n* = 1-6)

anion	% of containing products		% of abstraction	
	Cl	Br	HCl	HBr
Fe(CO) <sub>3</sub> <sup>-</sup>	41	59	0	100
Cr(CO) <sub>3</sub> <sup>-</sup>	47	53	45	55
Cr(CO) <sub>4</sub> <sup>-</sup>	40	60		
Co(CO) <sub>2</sub> <sup>-</sup>	35	65	25	75
CoCONO <sup>-</sup>	19	81	19	81
Co(CO) <sub>3</sub> <sup>-</sup>	0	100	0	100

intermediates which have a metal-carbon  $\sigma$ -bond from the alkyl group to the metal anion Fe(CO)<sub>4</sub><sup>-</sup>.<sup>34</sup> The electron affinities of these alkyl ligands (15-26 kcal/mol) indicate that the presence of the alkyl ligand may help delocalize the negative charge in structure 2. Structure 2 seems to be the most reasonable structure from the electron affinity data and the mechanisms predicted from condensed-phase reactions.

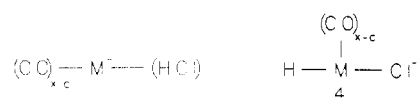
Note that the parent substitution product ion, structure 2, does not consist of an intact parent organic molecule (as predicted from positive ion reactions) but instead is a metal insertion structure which contains the organic molecule as two separate ligands. The remainder of this paper will refer to these metal insertion substitution products simply as "parent substitution".

The amount of excess energy released in the metal anion insertion/charge-transfer process is dependent upon both the exothermicity of the metal insertion (i.e. the bonds which are broken and formed) and the exothermicity of the charge-transfer process (i.e., the difference in the electron affinities of the metal species and the ligand). If the differences in the metal-ligand bond strengths are small for the three metals, then the differences in the exothermicity for the metal insertion/charge-transfer process for the metal species would be an indication of the difference in the electron affinities for the metal species. Since Fe(CO)<sub>3</sub><sup>-</sup> reacts by loss of only two carbonyl ligands and Cr(CO)<sub>3</sub><sup>-</sup> reacts by losing all three carbonyl ligands,

we would infer that the electron affinity of Cr(CO)<sub>3</sub> is less than the electron affinity of Fe(CO)<sub>3</sub> (EA(Cr(CO)<sub>3</sub>) < EA(Fe(CO)<sub>3</sub>) = 41.5 kcal/mol).

Once the metal insertion/charge-transfer intermediate 2 is formed, the excess energy may not only result in loss of carbonyl ligands (parent substitution) but may also lead to loss of the alkyl ligand. A similar process has also been proposed in the corresponding positive metal ion reactions.<sup>2b</sup> Competitive ligand loss of the alkyl ligand with concurrent loss of zero or one carbonyl ligands leads to the chlorine abstraction products (M(CO)<sub>*x*</sub>Cl<sup>-</sup>) observed in Table III.

The third reaction type observed for *n*-chloroalkanes (*n* ≥ 2) is abstraction of HCl. This product may also result from metal insertion into the C-Cl bond as a first step. A common mechanism in both solution and gas-phase organometallic reactions involves the shift of a  $\beta$ -hydrogen atom onto the metal center.<sup>7,8</sup> This apparently occurs in the metal-containing anion reactions as well. In the case of chloromethane the intermediate resulting from metal insertion into the C-Cl bond does not have any  $\beta$ -H's available to shift onto the metal. As a result, the HCl abstraction product is *not* observed for chloromethane (Table III). For the larger *n*-chloroalkanes (*n* = 2-6) however,  $\beta$ -H's are available to shift onto the metal. Once the  $\beta$ -H shift occurs, the alkene ligand produced is lost, yielding the HCl abstraction products (M(CO)<sub>*x*</sub>-HCl<sup>-</sup>). The two possible structures for this product ion are shown in structures 3 and 4. Structure 3 represents the structure



if HCl exists as a single ligand on the metal. The electron affinities of H (17.4 kcal/mol) and Cl (83.3 kcal/mol) (Table I) suggest that structure 4, where H and Cl are separate ligands on the metal, may be the most probable structure. The addition of the hydrogen atom as a ligand, which has a positive electron affinity, may help delocalize the negative charge. This effect is also seen in the comparison of the electron affinities of Fe (3.8 kcal/mol) and FeH (21.5 kcal/mol).

The alkene ligand which is formed following metal insertion and  $\beta$ -H shift in the corresponding positive metal ion reactions is retained preferentially to the HCl ligand.

(34) Collman, J. P. *Acc. Chem. Res.* 1975, 8, 342.

(35) Rosenstock, H. M.; Draxl, K.; Steiner, B. W.; Herron, J. T. J. *Phys. Chem. Ref. Data, Suppl.* 1977, 1, 6.

Table VIII. Reactions of Iron- and Cobalt-Containing Anions with 1,*n*-Chloro Alcohols

reaction	branching ratios						
	<i>n</i> = 2	<i>n</i> = 3	<i>n</i> = 4	<i>n</i> = 5	<i>n</i> = 6		
Fe(CO) <sub>3</sub> <sup>-</sup> + Cl(CH <sub>2</sub> ) <sub>n</sub> OH	→	FeCl(CH <sub>2</sub> ) <sub>n</sub> OH <sup>-</sup> + 3CO	0.04	0.14	0.10	0.17	0.12
	→	Fe(CO) <sub>3</sub> Cl <sup>-</sup> + (CH <sub>2</sub> ) <sub>n</sub> OH	0.84	0.73	0.72	0.76	0.75
	→	Fe(CO) <sub>2</sub> HCl <sup>-</sup> + C <sub>n</sub> H <sub>2n</sub> O + CO	0.05	0.14	0.18	0.07	0.13
	→	Fe(CO) <sub>2</sub> C <sub>n</sub> H <sub>2n</sub> O <sup>-</sup> + HCl + CO	0.07				
Fe(CO) <sub>4</sub> <sup>-</sup> + Cl(CH <sub>2</sub> ) <sub>n</sub> OH	→	NR <sup>a</sup>					
Co(CO) <sub>2</sub> <sup>-</sup> + Cl(CH <sub>2</sub> ) <sub>n</sub> OH	→	CoCl(CH <sub>2</sub> ) <sub>n</sub> OH <sup>-</sup> + 2CO	0.04	0.33	0.19	0.19	0.11
	→	CoCOCl <sup>-</sup> + (CH <sub>2</sub> ) <sub>n</sub> OH + CO	0.14				
	→	Co(CO) <sub>2</sub> Cl <sup>-</sup> + (CH <sub>2</sub> ) <sub>n</sub> OH	0.36	0.38	0.23	0.27	0.24
	→	CoHCl <sup>-</sup> + C <sub>n</sub> H <sub>2n</sub> O + 2CL			0.04	0.04	0.01
	→	CoCOHCl <sup>-</sup> + C <sub>n</sub> H <sub>2n</sub> O + CO	0.17	0.29	0.35	0.32	0.49
	→	Co(CO) <sub>2</sub> HCl <sup>-</sup> + C <sub>n</sub> H <sub>2n</sub> O			0.09	0.18	0.15
	→	CoClOH <sup>-</sup> + C <sub>n</sub> H <sub>2n</sub> + 2CO	0.29				
	→	CoC <sub>n</sub> H <sub>2n</sub> O <sup>-</sup> + HCl + 2CO			0.03		
	→	CoC <sub>n</sub> H <sub>2n-2</sub> O <sup>-</sup> + HCl + H <sub>2</sub> + 2CO			0.07		
CoCONO <sup>-</sup> + Cl(CH <sub>2</sub> ) <sub>n</sub> OH	→	CoCONOCl <sup>-</sup> + (CH <sub>2</sub> ) <sub>n</sub> OH	1.00	0.67	0.57	0.67	0.68
	→	CoNOHCl <sup>-</sup> + C <sub>n</sub> H <sub>2n</sub> O + CO		0.33	0.43	0.33	0.32
Co(CO) <sub>3</sub> <sup>-</sup> + Cl(CH <sub>2</sub> ) <sub>n</sub> OH	→	NR					
Co(CO) <sub>2</sub> NO <sup>-</sup> + Cl(CH <sub>2</sub> ) <sub>n</sub> OH	→	NR					

<sup>a</sup>NR indicates the ion did not undergo any reactions.

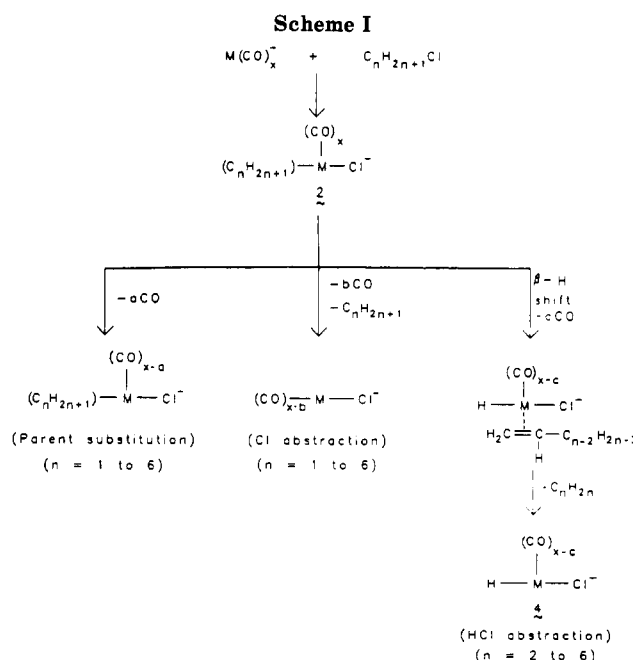
Table IX. Reactions of Chromium-Containing Anions with 1,*n*-Chloro Alcohols

reaction	branching ratios						
	<i>n</i> = 2	<i>n</i> = 3	<i>n</i> = 4	<i>n</i> = 5	<i>n</i> = 6		
Cr(CO) <sub>3</sub> <sup>-</sup> + Cl(CH <sub>2</sub> ) <sub>n</sub> OH	→	CrCl(CH <sub>2</sub> ) <sub>n</sub> OH <sup>-</sup> + 3CO	0.16	0.29	0.22	0.18	0.24
	→	CrClC <sub>n</sub> H <sub>2n-1</sub> O <sup>-</sup> + H <sub>2</sub> + 3CO	0.08	(0.17) <sup>a</sup>	0.17	0.21	0.12
	→	CrClC <sub>n</sub> H <sub>2n-3</sub> O <sup>-</sup> + 2H <sub>2</sub> + 3CO			0.06	0.14	0.03
	→	Cr(CO) <sub>2</sub> Cl(CH <sub>2</sub> ) <sub>n</sub> OH <sup>-</sup> + CO				0.07	0.06
	→	Cr(CO) <sub>2</sub> ClC <sub>n</sub> H <sub>2n-1</sub> O <sup>-</sup> + H <sub>2</sub> + CO				0.05	0.03
	→	Cr(CO) <sub>2</sub> ClC <sub>n</sub> H <sub>2n-3</sub> O <sup>-</sup> + 2H <sub>2</sub> + CO					0.02
	→	Cr(CO) <sub>2</sub> C <sub>n</sub> H <sub>2n</sub> O <sup>-</sup> + HCl + CO	0.06				
	→	Cr(CO) <sub>2</sub> Cl <sup>-</sup> + (CH <sub>2</sub> ) <sub>n</sub> OH + CO	0.16	0.11	0.09	0.04	0.06
	→	Cr(CO) <sub>3</sub> Cl <sup>-</sup> + (CH <sub>2</sub> ) <sub>n</sub> OH	0.28	0.23	0.25	0.21	0.27
	→	CrHCl <sup>-</sup> + C <sub>n</sub> H <sub>2n</sub> O + 3CO		0.16	0.04	0.03	0.04
	→	Cr(CO) <sub>2</sub> HCl <sup>-</sup> + C <sub>n</sub> H <sub>2n</sub> O + CO	0.07	(0.17)	0.11	0.04	0.09
	→	Cr(CO) <sub>3</sub> OH <sup>-</sup> + (CH <sub>2</sub> ) <sub>n</sub> Cl	0.05	0.04	0.06	0.03	0.04
	→	CrClOH <sup>-</sup> + C <sub>n</sub> H <sub>2n</sub> + 3CO	0.14				
Cr(CO) <sub>4</sub> <sup>-</sup> + Cl(CH <sub>2</sub> ) <sub>n</sub> OH	→	Cr(CO) <sub>3</sub> Cl <sup>-</sup> + (CH <sub>2</sub> ) <sub>n</sub> OH + CO	1.00	0.79	1.00	0.60	0.77
	→	Cr(CO) <sub>4</sub> Cl <sup>-</sup> + (CH <sub>2</sub> ) <sub>n</sub> OH		0.21		0.40	0.23
Cr(CO) <sub>5</sub> <sup>-</sup> + Cl(CH <sub>2</sub> ) <sub>n</sub> OH	→	NR <sup>b</sup>					

<sup>a</sup>Values in parentheses are the sum of branching ratios for isobaric product ions. <sup>b</sup>NR indicates the ion did not undergo any reactions.

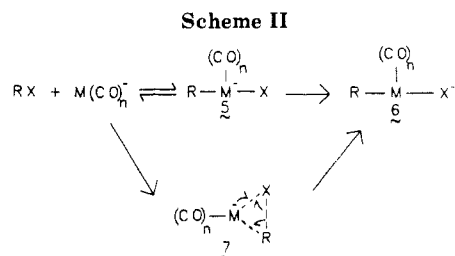
In the metal anion reactions, the alkene ligand is never retained and is always lost in the competitive ligand loss process. This is not unexpected if the electron affinity of the alkene is considered (and structure 4 is assumed to be the HCl abstraction product). The electron affinity of ethylene (-35.7 kcal/mol) suggests that the alkene ligand would be lost preferentially to ligands which possess a positive electron affinity, i.e., those which help to delocalize the negative charge. The difference in metal-ligand bonding in positive and negative metal ions has been studied by Corderman and Beauchamp,<sup>18</sup> suggesting that the competitive ligand loss process for positive and negative metal ions may be quite different. The metal-ligand bond energy in positive ions is determined largely by the  $\pi$ -donor ability of the ligand while back-bonding effects are less important. In the negative ions however, the bond energy is predominantly dependent upon the  $\pi$ -acceptor ability of the ligand with the  $\pi$ -donor ability playing a less important role. Thus, the difference in the metal-ligand bonding in positive and negative ions may be a factor in the retention or loss of the alkene in the positive and negative ion reactions.

Scheme I shows the general mechanism for the reactions of the metal-containing anions with *n*-chloroalkanes (*n* = 1-6). Note that all three types of products observed (parent substitution, Cl abstraction, and HCl abstraction) proceed through intermediate structure 2. Two possible mechanisms for forming structure 2 are presented in



Scheme II. In the first mechanism the metal anion initially inserts into the R-X bond (analogous to positive metal ion insertion) to give structure 5. If the charge transfer from the metal species to X is exothermic, structure 6 (the metal





anion insertion/charge-transfer intermediate) is formed. If the charge transfer is not exothermic, then **5** may reform the metal anion and RX. In the second mechanism (Scheme II), the metal anion interacts with both X and the alkyl R as seen in structure **7**. This type of initial complexation may reduce the ion-dipole repulsive interaction. If the charge transfer is exothermic, an M-X<sup>-</sup> bond is formed concurrent with the cleavage of the R-X bond and formation of the M-R bond yielding structure **6**. Regardless of the order in which charge transfer and bond cleavage occurs, it appears that all reactions observed proceed through intermediate **6** and the driving force for the reactions appears to be the exothermicity of the charge transfer.

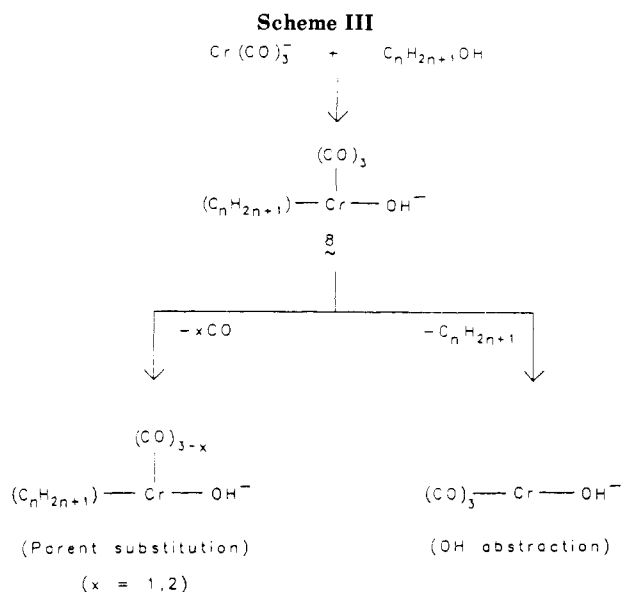
The effects that the number and types of ligands present on the metal have on reactivity and mechanisms in positive metal ion reactions have been described previously.<sup>2</sup> Several ligand effects are also observed in the reaction of metal-containing anions. The carbonyl ligand is lost preferentially to the nitrosyl ligand as seen in the reaction of CoCONO<sup>-</sup> with *n*-chloroalkanes (Table III). This effect is also observed in the positive metal ion reactions. Also, the reactivity of the metal-containing anions decreases as the number of ligands present increase. As expected, the stable 17-electron species M(CO)<sub>*n*-1</sub><sup>-</sup> is unreactive toward the *n*-chloroalkanes.

Additional information may be obtained through trends observed in the branching ratios of product ions as the alkyl chain length (*n*) increases. For all three metal-containing anions, parent substitution and Cl abstraction decrease and HCl abstraction increases as *n* increases. These trends support a mechanism in which all products observed proceed through a common intermediate (structure **2**). One possible explanation for the increase in the amount of HCl abstraction observed may be the thermodynamics of the reaction. Thermodynamic calculations<sup>36</sup> indicate that it is more favorable to form an alkene from the corresponding alkyl chloride as the length of the alkyl chain increases.

In summary, the reactions of the metal-containing anions with chloroalkanes proceed through a mechanism in which the metal inserts into the C-Cl bond with transfer of the electron to the chlorine due to its higher electron affinity. This complex may then undergo rearrangements ( $\beta$ -H shift) and ligand loss processes to yield all products which are observed. In the corresponding positive metal ion reactions with *n*-chloroalkanes,<sup>37</sup> products resulting from metal insertion into C-C and C-H bonds are also seen in addition to C-Cl insertion products. All reactions for metal-containing anions appear to result from interaction with chlorine which has a relatively high electron affinity, and thus no products from C-C or C-H insertion are observed. This may reflect the importance of the charge-transfer step, since, if Fe(CO)<sub>3</sub><sup>-</sup> inserted into a C-C bond,

(36) Thermodynamic calculations from values in ref 35 show that the amount of energy required to make 1-pentene from *n*-chloropentane is 4.3 kcal/mol less than the analogous process for *n*-chloroethane.

(37) Tzarbopoulos, A.; Allison, J. *J. Am. Chem. Soc.* 1985, 107, 5085.



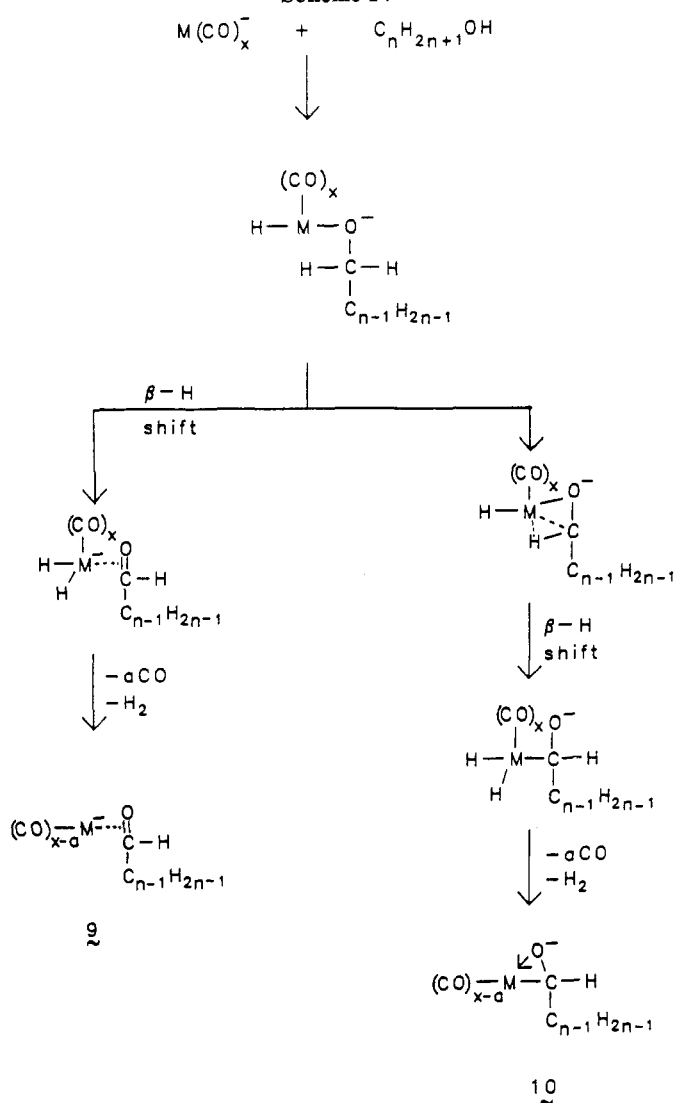
the charge would remain on the metal, and no chemistry from such intermediates is observed.

***n*-Alcohols.** The ion/molecule reaction products and branching ratios for the reactions of chromium-, iron-, and cobalt-containing anions with the series of *n*-alcohols (*n* = 1-6) are listed on Table IV. Parent substitution reactions are observed in the reaction of Cr(CO)<sub>3</sub><sup>-</sup> with the series of *n*-alcohols and are accompanied by the loss of one or two carbonyl ligands. If metal insertion into the C-OH bond is assumed in the parent substitution process (analogous to C-Cl insertion in the chloroalkanes), the electron would be transferred to the OH ligand due to its relatively high electron affinity (42.2 kcal/mol). This intermediate proceeds through a competitive ligand loss process to lose the excess energy produced in the formation of the metal insertion/charge-transfer intermediate. Loss of carbonyl ligands yield parent substitution products (Cr(CO)<sub>*x*</sub>C<sub>*n*</sub>H<sub>2*n*+1</sub>OH<sup>-</sup>) and loss of the alkyl radical (C<sub>*n*</sub>H<sub>2*n*+1</sub>) yields the OH abstraction product (Cr(CO)<sub>3</sub>OH<sup>-</sup>) (similar to Cl abstraction in chloroalkanes). These products are observed *only* for Cr(CO)<sub>3</sub><sup>-</sup> (Table IV), suggesting that the C-OH insertion intermediate **8** (Scheme III) occurs exclusively for the reaction of Cr(CO)<sub>3</sub><sup>-</sup>. Scheme III shows the mechanism for the reaction of Cr(CO)<sub>3</sub><sup>-</sup> with *n*-alcohols to yield the parent substitution and OH abstraction products. The loss of only one or two carbonyl ligands in the parent substitution of *n*-alcohols in contrast to three carbonyls displaced in the chloroalkane reactions is due to a decrease in the energy released in the charge-transfer step, i.e., due to the lower electron affinity of OH (42.2 kcal/mol) compared to Cl (83.3 kcal/mol). Parent substitution reactions are *not* observed for either cobalt- or iron-containing anions, possibly due to the comparable electron affinity of OH (42.2 kcal/mol) and the metal species (e.g., EA(Fe(CO)<sub>3</sub>) = 41.5 kcal/mol).

Since the cobalt anion Co(CO)<sub>2</sub><sup>-</sup> does not react with the alcohols by parent substitution or OH abstraction, the difference in the electron affinity of Co(CO)<sub>2</sub><sup>-</sup> and OH must not be large enough to cause these reactions to occur. Therefore, we may infer (making the same assumptions as in the chloroalkane discussion) that the electron affinity of Cr(CO)<sub>3</sub> is less than the electron affinity of Co(CO)<sub>2</sub> (EA(Cr(CO)<sub>3</sub>) < EA(Co(CO)<sub>2</sub>)).

Products indicative of H<sub>2</sub>O abstraction may be expected in the Cr(CO)<sub>3</sub><sup>-</sup> reactions (similar to HCl abstraction in chloroalkanes) since  $\beta$ -H's are present after the metal inserts into the C-OH bond of the *n*-alcohols (*n* ≥ 2).

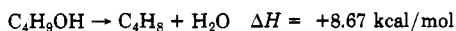
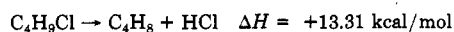
Scheme IV



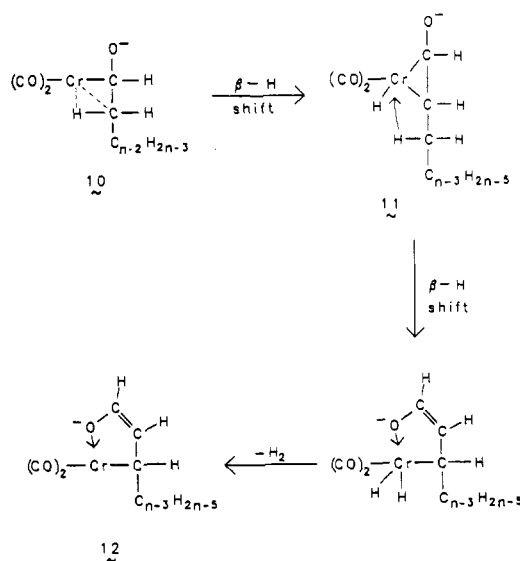
Thermodynamic calculations show that less energy is required to form the alkene from  $n$ -alcohols than from the analogous  $n$ -chloroalkanes.<sup>38</sup> The  $\text{H}_2\text{O}$  abstraction product however is not observed (Table IV). Apparently sufficient energy is released in the electron transfer to the Cl ligand to result in rearrangement ( $\beta$ -H shift) and loss of the alkene ligand in the chloroalkane reactions, but not enough energy is released in the electron transfer to the OH ligand (due to its lower electron affinity) to result in rearrangement and loss of the alkene in the  $n$ -alcohol reactions. That is, a barrier to the  $\beta$ -H shift appears to exist.

The only reaction observed for the cobalt- and iron-containing anions is the elimination of  $\text{H}_2$  from the  $n$ -alcohols ( $n = 1-6$ ) with  $\text{Co}(\text{CO})_2^-$ ,  $\text{CoCONO}^-$ , and  $\text{Fe}(\text{CO})_3^-$ . This hydrogen elimination product is also observed for the chromium anion  $\text{Cr}(\text{CO})_3^-$ . This product is not expected to proceed through metal insertion into the C-OH bond since products indicative of C-OH insertion (parent substitution and OH abstraction) are not observed for the cobalt- or iron-containing anions. Also, note that  $\text{H}_2$

(38) The calculated  $\Delta H$  values for the reaction of producing 1-butene and HCl or  $\text{H}_2\text{O}$  from 1-chlorobutane and 1-butanol using thermodynamic values from ref 35 are shown below. Note that it is thermodynamically more favorable to produce butene from 1-butanol than from 1-chlorobutane.

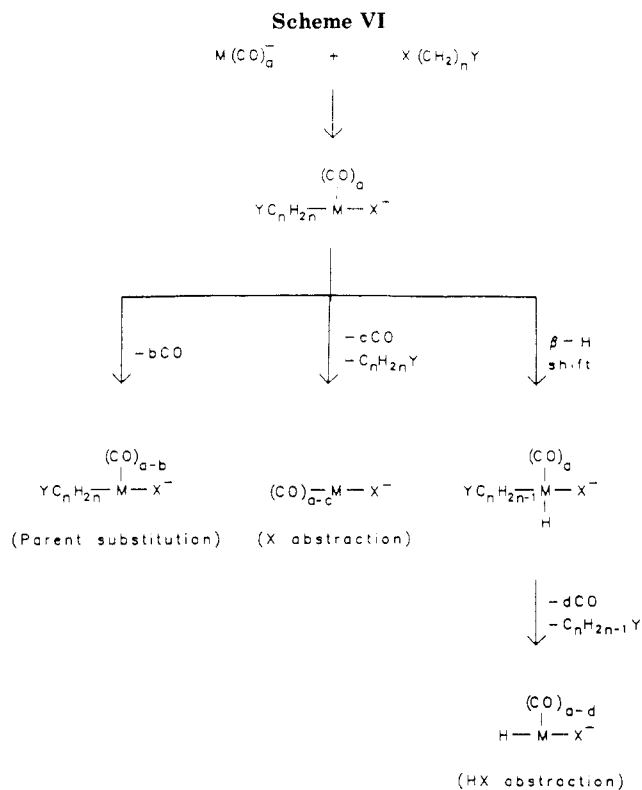


Scheme V



elimination is observed for methanol ( $n = 1$ ), and there are no  $\beta$ -H's available to shift on the metal resulting in  $\text{H}_2$  elimination if the metal inserts into the C-OH bond. A new intermediate is proposed in which the metal inserts into the O-H bond as shown in Scheme IV. This intermediate is predicted to be stable due to the relatively high electron affinities of the alkoxy ( $\sim 40$  kcal/mol) and the hydrogen (17.4 kcal/mol) ligands on the metal following O-H insertion. The charge is then transferred predominantly to the alkoxy ligand due to its relatively high electron affinity. Following metal insertion into the O-H bond and charge transfer, the  $\beta$ -H shift and loss of  $\text{H}_2$  may lead to the two different structures (9 and 10) in Scheme IV. In structure 9, the alkoxy ligand is converted into an aldehyde ( $\pi$ -donor) ligand following the  $\beta$ -H shift with the negative charge being transferred back to the metal. In positive metal ion reactions, these  $\pi$ -donor-type ligands are found to form strong bonds with the metal. In metal anion reactions with chloroalkanes, however, the  $\pi$ -donor alkene ligand produced following the  $\beta$ -H shift to yield HCl was lost preferentially to the other ligands on the metal. In contrast to the positive ion studies, these  $\pi$ -donor ligands do not appear to form strong bonds to the metal in these negative ion studies. The alkyl ligand (metal-carbon bond) appears to be a good ligand in the metal anion reactions, since the alkyl ligand is in some cases retained during the competitive ligand loss process (parent substitution) for chloroalkanes and alcohols. Therefore, structure 10 (Scheme IV) is the more probable structure for the product ion resulting from  $\text{H}_2$  elimination from alcohols. Following the  $\beta$ -H shift, the metal may form a bond to the carbon which is  $\beta$ - to the metal resulting in the metal-alkoxy structure 10. In this structure, the negative charge remains on an alkoxy ligand which has a high electron affinity.

The anion  $\text{Cr}(\text{CO})_3^-$  reacts further with the alcohols to eliminate a second molecule of hydrogen. This product is only observed for  $\text{Cr}(\text{CO})_3^-$  presumably due to its lower electron affinity than the other metal species. Elimination of two hydrogens does not occur for methanol and ethanol but does occur for  $n \geq 3$ . A general mechanism for the elimination of the second molecule of hydrogen is shown in Scheme V. The mechanism begins with structure 10 (elimination of one  $\text{H}_2$ ) which may proceed through a  $\beta$ -H shift to produce structure 11 which has two metal-carbon bonds. Another  $\beta$ -H is now available to shift from the  $\text{C}_3$  carbon to give structure 12. Note that, in the proposed



mechanism, the charge *remains* on the alkoxy oxygen. There appears to be little thermodynamic advantage to this elimination of a second molecule of  $\text{H}_2$  as shown in Scheme V. The double bond does not interact with the metal. We estimate that 5–10 kcal/mol is required to eliminate the second  $\text{H}_2$  molecule, and the electron affinity of the product is only a few kilocalories per mole greater than the alkoxy group prior to  $\text{H}_2$  elimination. Thus, the loss of a second  $\text{H}_2$  appears to be one pathway for *disposal* of excess energy in the complex. Thus, it is only observed for  $\text{Cr}(\text{CO})_3^-$  which releases the most energy on charge transfer due to its low electron affinity.

The ligand effects observed in the reactions of chloroalkanes are also observed for alcohols: the nitrosyl ligand is retained in the reaction of  $\text{CoCONO}^-$  and the stable 17-electron metal anion species are unreactive. Again, the metal anion attacks exclusively at the functional group (no evidence for C–C or C–H insertion) due to the relatively high electron affinities of OH and OR. In comparison to the chloroalkane reactions, the metal is seen to insert into *two* bonds (C–OH and O–H) in the reactions of alcohols.

**1,*n*-Bromochloroalkanes.** The ion/molecule reaction products and branching ratios for the reactions of 1,*n*-bromochloroalkanes ( $n = 2-6$ ), and 1,1-bromochloroethane with iron, and chromium-containing anions and cobalt-containing anions are listed in Tables V and VI, respectively. Parent substitution, bromine or chlorine abstraction, and HCl or HBr abstraction products are observed which are expected from the results of the chloroalkane reactions. A product from abstraction of bromine and chlorine is observed and is unique to the reactions of the 1,*n*-bromochloroalkanes.

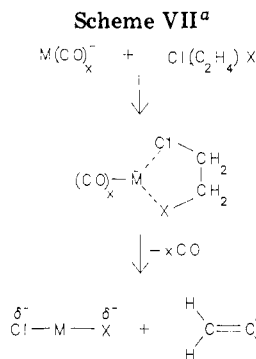
The same mechanism utilized in the chloroalkane reactions may also be used to explain most of the 1,*n*-bromochloroalkane reactions as shown in Scheme VI. The metal anion inserts into the C–X bond ( $X = \text{Cl}$  or  $\text{Br}$ ) with transfer of the electron to the halogen. This ion may undergo either loss of carbonyl and alkyl ligands to yield parent substitution or halogen abstraction products or rearrangement ( $\beta\text{-H}$  shift) to yield HCl or HBr abstraction

products. The presence of two halogen atoms on the neutral molecule is seen to affect the distribution of the observed products when compared to the chloroalkane products. Parent substitution products are *not* observed in the reactions of  $\text{Cr}(\text{CO})_3^-$ . Recall that all three carbonyl ligands were lost in the parent substitution reactions of  $\text{Cr}(\text{CO})_3^-$  with the chloroalkanes. Apparently the metal insertion/charge-transfer process for the bromochloroalkanes is more exothermic than for the chloroalkanes resulting in only X and HX abstraction and no parent substitution.

The reactions of 1,*n*-bromochloroalkanes allow the study of the preference for the site of attack (Br or Cl) by the metal-containing anions. Table VII lists the average branching ratios for products in which either the bromine or chlorine is exclusively attacked by various metal anions with the 1,*n*-bromochloroalkanes. These values are calculated by summing the branching ratios for all the 1,*n*-bromochloroalkanes in which bromine or chlorine is exclusively attacked and calculating the average value. Also listed in Table VII is a comparison of the average amount of HCl and HBr abstraction observed for the 1,*n*-bromochloroalkanes. The preference for attack at the chlorine on the molecule by the metal anion may be expected since the electron affinity of chlorine is 6 kcal/mol greater than that for bromine (Table I). The opposite trend, preference for attack at the bromine, is actually observed as seen in Table VII. This trend may reflect the thermodynamics of the metal insertion into the C–X bond. The C–Br bond strength is 14 kcal/mol less than the C–Cl bond strength.<sup>33</sup> Metal-containing species having relatively high electron affinities ( $\text{Fe}(\text{CO})_3$ ,  $\text{Co}(\text{CO})_2$ ,  $\text{Co}(\text{CO})_3$ , etc.) exhibit a preference for attack at the weaker C–Br bond as seen in Table VII. In contrast,  $\text{Cr}(\text{CO})_3^-$  which reacts as though it has a low electron affinity exhibits virtually no preference for Cl or Br due to the large amount of energy available from electron transfer to *either* Br or Cl. Therefore, it appears that both the strength of the C–X bond which must be broken, and the difference in electron affinity between the metal species and the halogen (i.e., the energy available from the charge-transfer process) determine the preference of attack by the metal anion. The difference in the amount of HCl and HBr abstraction observed also reflects the corresponding electron affinity of the reactant metal anions. Virtually no preference is seen for metal species with a relatively low electron affinity ( $\text{Cr}(\text{CO})_3^-$ ) but HBr abstraction occurs exclusively for metal species with high electron affinities ( $\text{Fe}(\text{CO})_3$  and  $\text{Co}(\text{CO})_3$ ). An ordering of the electron affinities of the metal species is suggested by the results in Table VII:  $\text{EA}(\text{Cr}(\text{CO})_3^-) < \text{EA}(\text{Co}(\text{CO})_2) < \text{EA}(\text{CoCONO}) < \text{EA}(\text{Co}(\text{CO})_3) < \text{EA}(\text{Fe}(\text{CO})_3) = 41.5$  kcal/mol. These relationships are the same as those inferred in the chloroalkane and alcohol reactions.

The product resulting from abstraction of *both* bromine and chlorine from the 1,*n*-bromochloroalkanes is observed for  $\text{Co}(\text{CO})_2^-$ ,  $\text{Cr}(\text{CO})_3^-$ , and  $\text{Fe}(\text{CO})_3^-$  (for  $n = 2-6$ ) and is accompanied by the loss of all carbonyl ligands on the metal. In the reaction of 1,2-bromochloroethane, the metal may complex with the chlorine and bromine simultaneously (Scheme VII) resulting in abstraction of both Br and Cl and loss of a neutral ethylene molecule. A similar product is observed in the reaction of  $\text{Co}^+$  with 1,2-bromochloroethane<sup>39</sup> but is not observed for the larger 1,*n*-bromochloroalkanes ( $n \geq 3$ ). Two possible mechanisms for the reaction of the larger 1,*n*-bromochloroalkanes ( $n = 3-6$ ) with metal-containing anions are shown in Scheme

(39) Lombarski, M.; Allison J. *Int. J. Mass Spectrom. Ion Phys.* 1983, 49, 281.



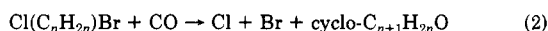
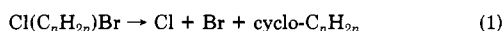
<sup>a</sup> X = Br or OH.

VIII. The first mechanism is similar to Scheme VII for 1,2-bromochloroethane except that the neutrals lost are the corresponding cycloalkane (as opposed to the loss of a biradical species). The second mechanism involves insertion of the metal *and* one of the carbonyl ligands into a C-X (X = Cl or Br) bond. The other halogen (Y) is then transferred to the metal through a cyclic intermediate. The carbonyl ligand is now incorporated in the neutral product which is in the form of a cyclic ketone. In gas-phase positive metal ion reactions, evidence for active participation of carbonyl ligands in insertion processes has occasionally been observed.<sup>2</sup> To this point, it has not been necessary to invoke active participation of ligands on the metal anion to explain the products observed. Thermodynamic calculations indicate that the loss of the cyclic ketone is favored over the loss of the cycloalkane in the reactions of 1,*n*-bromochloroalkanes by 26.2 kcal/mol for *n* = 4, 9.23 kcal/mol for *n* = 5, and 3.27 kcal/mol for *n* = 6.<sup>40</sup> As the alkyl chain length increases, the thermodynamic advantage of forming the cyclic ketone over the cycloalkane decreases due to the decreased difference in ring strain for the two structures. Thus, there is a thermodynamic advantage to utilize the CO in these reactions, although there is no direct experimental evidence for the elimination of a cyclic ketone.

There are, of course, alternate explanations which do not require CO incorporation in the product. For example, it is possible for the metal insertion intermediate to undergo reversible  $\beta$ -H transfers down the length of the carbon chain until it reaches the second functional group. In this process, an alkene is eliminated rather than the cycloalkane or cyclic ketone.

The same ligand effects are observed in the 1,*n*-bromochloroalkane reactions as seen in the chloroalkanes and alcohols: retention of NO in reactions of CoCONO<sup>-</sup> and unreactivity of the 17-electron metal anions. Also, the same trends in the branching ratios are observed as in the chloroalkane reactions, i.e., an increase in HX abstraction and decrease in X abstraction as the alkyl chain length (*n*) increases.

(40) Reaction 1 below shows the formation of Br, Cl, and the cycloalkane from the 1,*n*-bromochloroalkane. Reaction 2 shows the incorporation of CO with the 1,*n*-bromochloroalkane to form Br, Cl, and a cyclic ketone.

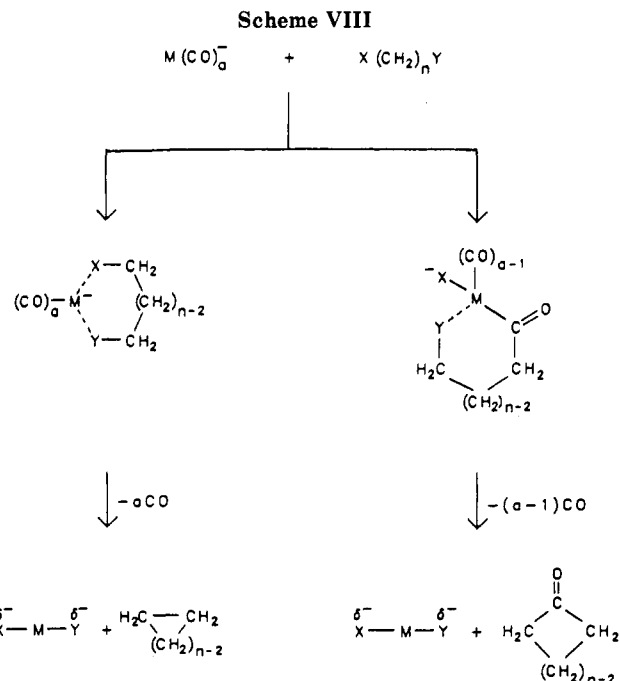


The difference in  $\Delta H$  for these two reactions is given by

$$\Delta H_{\text{diff}} = \Delta H_1 - \Delta H_2 =$$

$$\Delta H(\text{cyclo-C}_n\text{H}_{2n}) - \Delta H(\text{cyclo-C}_{n+1}\text{H}_{2n}\text{O}) + \Delta H(\text{CO})$$

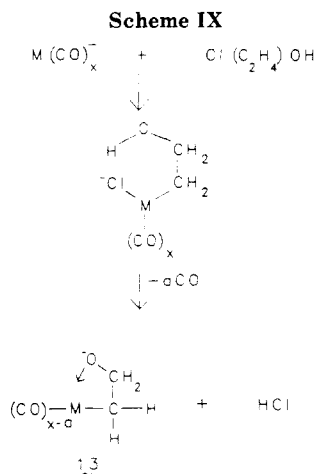
The calculated values of  $\Delta H_{\text{diff}}$  for the 1,*n*-bromochloroalkanes (*n* = 4–6) using thermodynamic values from ref 35 are  $\Delta H = 26.2$  kcal/mol (*n* = 4),  $\Delta H = 9.23$  kcal/mol (*n* = 5), and  $\Delta H = 3.27$  kcal/mol (*n* = 6). Note that it is thermodynamically more favorable to incorporate CO and form a cyclic ketone than to form the cycloalkane, especially for small *n*.



**1,*n*-Chloro Alcohols.** The products and branching ratios for the reactions of 1,*n*-chloro alcohols (*n* = 2–6) with iron- and cobalt-containing anions and chromium-containing anions are listed in Tables VIII and IX, respectively. These studies allow the determination of the preference for attack at Cl or OH by the metal-containing anions. Parent substitution is observed for the three metal anions Cr(CO)<sub>3</sub><sup>-</sup>, Fe(CO)<sub>3</sub><sup>-</sup>, and Co(CO)<sub>2</sub><sup>-</sup> with the loss of all carbonyl ligands. Since parent substitution was not observed in the reactions of Co(CO)<sub>2</sub><sup>-</sup> and Fe(CO)<sub>3</sub><sup>-</sup> with alcohols but was seen for all three metal anions with chloroalkanes, the mechanism for parent substitution in reactions of 1,*n*-chloro alcohols presumably involves metal insertion/charge transfer into the C–Cl bond (and *not* the C–OH bond) with competitive ligand loss of the carbonyl ligands similar to Scheme I. If the metal inserts into the C–Cl bond in the 1,*n*-chloro alcohols, other products typical of chloroalkane reactions would be expected. The abstraction of Cl and HCl from the chloro alcohols by all three metal anions are observed as seen in Tables VIII and IX. These products also result from metal insertion/charge transfer into the C–Cl bond followed by a  $\beta$ -H shift and competitive ligand loss similar to Scheme I for the *n*-chloroalkanes.

The chromium anion Cr(CO)<sub>3</sub><sup>-</sup> reacts with the 1,*n*-chloro alcohols to yield products expected from the *n*-alcohol reactions. These include OH abstraction and elimination of one or two hydrogen molecules. The mechanisms for these reactions are similar to those for the reactions of *n*-alcohols in Schemes III–V. Since both OH abstraction and parent substitution products proceed through the same intermediate (C–OH insertion) in the *n*-alcohol reactions (Scheme III), the parent substitution ion for 1,*n*-chloro alcohols probably consists of both insertion into the C–Cl and C–OH bonds. Products predicted from the reactions of *n*-alcohols (loss of H<sub>2</sub>) are not observed for iron- and cobalt-containing anions with 1,*n*-chloro alcohols.

Products that are unique in the reactions of 1,*n*-chloro alcohols include the abstraction of both Cl and OH and the elimination of HCl. The abstraction of both Cl and OH is observed for the anions Co(CO)<sub>2</sub><sup>-</sup> and Cr(CO)<sub>3</sub><sup>-</sup> with 1,2-chloroethanol and is accompanied by the loss of all carbonyl ligands on the metal. These products are not observed for the larger 1,*n*-chloro alcohols (*n* ≥ 3). A



mechanism for abstraction of Cl and OH is shown in Scheme VII. In this mechanism, the metal does not insert into the C-Cl or C-OH bonds but complexes with both Cl and OH simultaneously. Abstraction of Cl and OH with electron transfer to the ligands with higher electron affinity is accompanied by the loss of a neutral ethylene molecule similar to Br and Cl abstraction in the 1,*n*-bromochloroalkanes. The elimination of HCl from 1,2-chloroethanol is a minor process which is observed for the anions Fe(CO)<sub>3</sub><sup>-</sup> and Cr(CO)<sub>3</sub><sup>-</sup>. Following metal insertion into the C-Cl bond and electron transfer to the chlorine (Scheme IX), a six-member-ring intermediate may form (only for *n* = 2). Cleavage of the C-Cl bond and electron pair transfer results in loss of HCl and structure 13 in which the charge has migrated to the alkoxy ligand. In the previous reactions, HCl was always retained and presumably existed as H and Cl ligands on the metal due to their high electron affinities. In Scheme IX, however, an HCl molecule is formed, but never exists as two ligands, and is lost. A smaller percentage of this HCl elimination product is also formed in the reaction of Co(CO)<sub>2</sub><sup>-</sup> with 1,*n*-chlorobutanol but must proceed through some other intermediate in which an H-Cl bond can be formed.

The reactions of 1,*n*-chloro alcohols indicate that the preference for attack (Cl or OH) by the metal anions is at the chlorine end of the molecule. The preference for chlorine is due to the higher electron affinity of Cl compared to OH (see Table I). The thermodynamics of the metal insertion may also play a role since the C-Cl bond strength is 10 kcal/mol less than the C-OH bond strength.<sup>33</sup> The same ligand effects are observed in the reaction of 1,*n*-chloro alcohols that were seen in the previous reactions.

## Conclusions

The reactions of the metal-containing anions with the four series of organic molecules suggest a general mechanism for the reaction of metal anions in which all products result from the formation of a metal anion insertion/charge-transfer intermediate. The metal anions attack only at the functional group due to the high electron affinities of the ligands which are formed. In contrast, positive metal ions are seen to insert into several bonds (C-C, C-H, C-functional group) with the charge remaining on the metal<sup>3</sup>. The exothermicity of the charge-transfer process appears to determine the products which are observed. An ordering of the electron affinities of the metal containing species may then be predicted from the observed products. Following the formation of the metal anion insertion/charge-transfer intermediate, a β-H may shift onto the metal analogous to reactions of positive metal ions. The ligand loss process which follows is seen to be quite different for metal anions than for the corresponding positive ions (e.g., the loss or retention of π-donor-type ligands). The study of the bifunctional organic molecules suggests that both the C-functional group bond strength and the electron affinities of the ligands formed determine the preference for attack by the metal-containing anions.

Several ligand effects have been observed in the reactions of metal-containing anions. The reactivity of the metal anions decrease as the number of ligands increase (the 17-electron species M(CO)<sub>*n*-1</sub><sup>-</sup> are unreactive). This trend is also observed in the positive metal ion reactions.<sup>2</sup> Thermodynamic calculations suggest the possibility of active participation of a carbonyl ligand in the formation of the metal anion insertion/charge transfer intermediate in the 1,*n*-bromochloroalkane reactions. Active participation of ligands in the metal insertion of positive ions has also been suggested.<sup>2</sup>

**Acknowledgment** is made to the National Science Foundation (CHE-8023704) for partial support of this work.

**Registry No.** Fe(CO)<sub>5</sub>, 13463-40-6; Cr(CO)<sub>6</sub>, 13007-92-6; Co(CO)<sub>3</sub>NO, 14096-82-3; Fe(CO)<sub>4</sub><sup>-</sup>, 71564-27-7; Fe(CO)<sub>3</sub><sup>-</sup>, 53221-56-0; Cr(CO)<sub>5</sub><sup>-</sup>, 51222-95-8; Cr(CO)<sub>4</sub><sup>-</sup>, 53221-57-1; Cr(CO)<sub>3</sub><sup>-</sup>, 53221-59-3; Co(CO)<sub>2</sub>NO<sup>-</sup>, 99632-74-3; Co(CO)<sub>3</sub><sup>-</sup>, 53364-03-7; CoCONO<sup>-</sup>, 99632-75-4; Co(CO)<sub>2</sub><sup>-</sup>, 99632-76-5; CH<sub>3</sub>Cl, 74-87-3; C<sub>2</sub>H<sub>5</sub>Cl, 75-00-3; C<sub>3</sub>H<sub>7</sub>Cl, 540-54-5; C<sub>4</sub>H<sub>9</sub>Cl, 109-69-3; C<sub>5</sub>H<sub>11</sub>Cl, 543-59-9; C<sub>6</sub>H<sub>13</sub>Cl, 544-10-5; CH<sub>3</sub>OH, 67-56-1; C<sub>2</sub>H<sub>5</sub>OH, 64-17-5; C<sub>3</sub>H<sub>7</sub>OH, 71-23-8; C<sub>4</sub>H<sub>9</sub>OH, 71-36-3; C<sub>5</sub>H<sub>11</sub>OH, 71-41-0; C<sub>6</sub>H<sub>13</sub>OH, 111-27-3; BrCH<sub>2</sub>Cl, 74-97-5; Br(CH<sub>2</sub>)<sub>2</sub>Cl, 107-04-0; Br(CH<sub>2</sub>)<sub>3</sub>Cl, 109-70-6; Br(CH<sub>2</sub>)<sub>4</sub>Cl, 6940-78-9; Br(CH<sub>2</sub>)<sub>5</sub>Cl, 54512-75-3; Br(CH<sub>2</sub>)<sub>6</sub>Cl, 6294-17-3; Cl(CH<sub>2</sub>)<sub>2</sub>OH, 107-07-3; Cl(CH<sub>2</sub>)<sub>3</sub>OH, 627-30-5; Cl(CH<sub>2</sub>)<sub>4</sub>OH, 928-51-8; Cl(CH<sub>2</sub>)<sub>5</sub>OH, 5259-98-3; Cl(CH<sub>2</sub>)<sub>6</sub>OH, 2009-83-8.

# Synthesis of Diphenacyl Telluride and Related Substances

Lars Engman

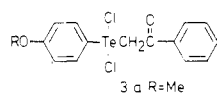
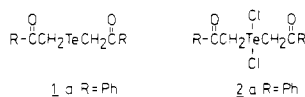
Department of Organic Chemistry, Royal Institute of Technology, S-100 44 Stockholm, Sweden

Received July 2, 1985

Diphenacyl telluride (**1a**) was prepared for the first time by a mild  $\text{Na}_2\text{S}_2\text{O}_5$  reduction of diphenacyltellurium dichloride (**2a**) in a two-phase system. A series of related diorganyltellurium dichlorides ( $\text{ArC(=O)CH}_2)_2\text{TeCl}_2$  (**2**), prepared from tellurium tetrachloride and various acetylaromatic compounds,  $\text{ArC(=O)CH}_3$ , were similarly reduced to tellurides. It was also possible to synthesize the unsymmetrical compounds 4-methoxyphenyl phenacyl telluride (**14a**) and 2-naphthyl phenacyl telluride (**14b**) by a similar procedure. The new materials, although unstable, could be handled and characterized without special precautions. Treatment of diphenacyl telluride with *m*-chloroperbenzoic acid or sodium sulfide caused decomposition with formation of acetophenone. Photolysis in dry benzene under nitrogen also resulted in formation of acetophenone.

## Introduction

An early as in 1901 Rohrbach<sup>1</sup> reported an unsuccessful attempt to prepare diphenacyl telluride (**1a**) by reduction of diphenacyltellurium dichloride (**2a**), which had been synthesized some years earlier by Rust.<sup>2</sup> Morgan has later reported the separation of elemental tellurium upon attempted reduction of the three dichlorides **2** ( $\text{R} = \text{Ph, Me, } t\text{-Bu}$ ).<sup>3</sup> These compounds have recently received renewed

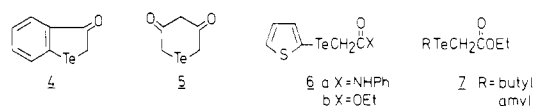


interest as a result of new imaging applications of organotellurium compounds in photography.<sup>4</sup> In a typical non-silver amplification process, diphenacyltellurium dichloride was incorporated with a reducing agent and a catalytic amount of Pd(0) in a polymeric binder. Upon physical development (heating to 100–185 °C) a high-density image of elemental tellurium was produced. Although never isolated, diphenacyl telluride was postulated as an unstable intermediate in this process.<sup>5</sup>

Photodecomposition of diphenacyltellurium dichloride also failed to produce any detectable amount of diphenacyl telluride.<sup>6</sup> Petragani<sup>7</sup> has reported similar difficulties in preparing unsymmetrical tellurides where one of the organic moieties is a phenacyl group. Thus, reduction of compounds **3** ( $\text{R} = \text{Me, Et, Ph}$ ) with a variety of mild reducing agents afforded only decomposition products instead of the expected aryl phenacyl tellurides.

The reported inherent instability of diphenacyl telluride and related tellurides is somewhat surprising in view of the successful isolation of the cyclic tellurides **4**<sup>8</sup> and **5**<sup>9</sup>

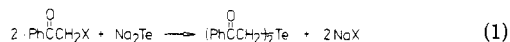
and the closely related  $\alpha$ -telluro amide **6a**<sup>10</sup> and the  $\alpha$ -telluro esters **7**.<sup>11,12</sup>



We felt that it should also be possible to isolate diphenacyl telluride if only sufficiently mild reaction conditions could be found for its formation. In the following we report several different strategies toward this goal.

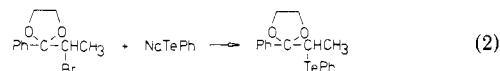
## Results and Discussion

The reaction of sodium telluride,  $\text{Na}_2\text{Te}$ , with 2 equiv of a phenacyl halide would constitute an obvious way to synthesize diphenacyl telluride (eq 1).



However, when sodium telluride, generated in aqueous solution, was allowed to interact at ambient temperature with methanolic phenacyl bromide, only acetophenone (50%) and unreacted phenacyl bromide (39%) were isolated in addition to elemental tellurium. This result was quite expected in view of the known ability of  $\text{NaHTe}^{13}$  and lithium 2-thienyltelluroate<sup>10</sup> to reductively remove a variety of electronegative  $\alpha$ -substituents of carbonyl compounds. A similar disappointing results was obtained when sodium telluride and phenacyl bromide were brought together in dry dimethylformamide.

Uemura has recently demonstrated<sup>14</sup> the successful introduction of tellurium, via a normal substitution reaction, into the  $\alpha$ -position of propiophenone ethylene glycol ketal (eq 2). We similarly prepared bis[(2-phenyl-1,3-dioxa-



lan-2-yl)methyl] telluride (**8**) in 60% yield from sodium telluride. It was our plan to mildly hydrolyze the ketal in order to obtain the desired diphenacyl telluride (**1a**). However, all attempts to carry out this hydrolysis failed. When compound **8** was heated at reflux in dry acetone containing a catalytic amount of *p*-toluenesulfonic acid (transketalization conditions), acetophenone ethylene

(1) Rohrbach, E. *Justus Liebigs Ann. Chem.* **1901**, 315, 9.  
 (2) Rust, E. *Ber. Dtsch. Chem. Ges.* **1897**, 30, 2828.  
 (3) Morgan, G. T.; Elvins, O. C. *J. Chem. Soc.* **1925**, 2625.  
 (4) Gysling, H. J.; Lelental, M.; Mason, M. G.; Gerenser, L. J. *J. Photogr. Sci.* **1982**, 30, 55 and references cited therein.  
 (5) Lelental, M.; Gysling, H. J. *J. Photogr. Sci.* **1980**, 28, 209.  
 (6) Marsh, D. G.; Chu, J. Y. C.; Lewicki, J. W.; Weaver, J. L. *J. Am. Chem. Soc.* **1976**, 98, 8432.  
 (7) Petragani, N. *Tetrahedron* **1961**, 12, 219.  
 (8) Talbot, J. M.; Piette, J. L.; Renson, M. *Bull. Soc. Chim. Fr.* **1976**, 294.  
 (9) Morgan, G. T.; Drew, H. D. K. *J. Chem. Soc.* **1920**, 1456.

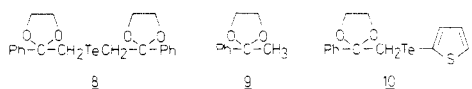
(10) Engman, L.; Cava, M. P. *J. Org. Chem.* **1982**, 47, 3946.  
 (11) Balfe, M. P.; Chaplin, C. A.; Phillips, H. J. *J. Chem. Soc.* **1938**, 341.  
 (12) Balfe, M. P.; Nandi, K. N. *J. Chem. Soc.* **1941**, 70.  
 (13) Osuka, A.; Suzuki, H. *Chem. Lett.* **1983**, 119.  
 (14) Uemura, S.; Fukuzawa, S.; Yamauchi, T.; Hattori, K.; Mizutaki, S.; Tamaki, K. *J. Chem. Soc., Chem. Commun.* **1984**, 426.

Table I. Synthesis of  $(RC(=O)CH_2)_2Te$  (1) by  $Na_2S_2O_5$  Reduction of Compounds 2 [ $(RC(=O)CH_2)_2TeCl_2$ ]

compd	R	yield, %	mp, °C	anal.			
				calcd		found	
				C	H	C	H
1a	phenyl	53	78-79	52.52	3.86	52.53	3.89
1b	4-methylphenyl	63	95	54.88	4.61	54.69	4.65
1c	4-bromophenyl	76	131-132	36.70	2.31	36.24	2.29
1d	4-chlorophenyl	63 <sup>a</sup>	128	44.20	2.78	41.98	2.67
1e	4-methoxyphenyl	75	67-68	50.76	4.26	49.86	4.30
1f	1-naphthyl	51	101	61.86	3.89	61.25	3.88
1g	2-naphthyl	74 <sup>a</sup>	108-110	61.86	3.89	61.52	3.90
1h	2-thienyl	69 <sup>a</sup>	93-94	38.14	2.67	38.01	2.64
1i	9-anthryl	45 <sup>a</sup>	168	67.89	3.92	67.45	4.02
1j	2-benzo[b]furanyl	63 <sup>a</sup>	100-102	53.87	3.16	52.72	3.08

<sup>a</sup>Yield after chromatographic purification.

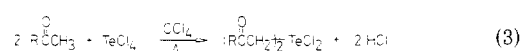
glycol ketal (9) was isolated in 76% yield together with elemental tellurium. Wet acetone containing a trace of sulfuric acid readily produced acetophenone and elemental tellurium. (2-Phenyl-1,3-dioxolan-2-yl)methyl 2-thienyl telluride (10) failed to give any phenacyl 2-thienyl telluride when submitted to hydrolysis or transketalization conditions.



After these initial failures we turned our attention to the old problem of finding a mild reducing agent for the reduction of diphenacyltellurium dichloride to diphenacyl telluride. This type of reduction has been successfully executed in the selenium series using zinc in carbon disulfide<sup>15</sup> or thiourea in acetone.<sup>16</sup> In fact, the reduced species, e.g., diphenacyl selenide, are much more stable than the corresponding Se(IV) dichlorides.

In organic tellurium chemistry diorganyltellurium dichlorides are commonly reduced to diorganyl tellurides employing reagents such as potassium disulfite, sodium hydrogen sulfite, sodium sulfite, or sodium sulfide.<sup>17</sup> The reactions proceed in aqueous alkaline solution at ambient<sup>9</sup> or elevated<sup>18</sup> temperature in the absence of an organic solvent. As already mentioned in the introduction, diphenacyltellurium dichloride is decomposed by using these reaction conditions. However, we felt that the intermediate diphenacyl telluride might survive if it could escape into an added organic solvent. This indeed proved to be the case. When diphenacyltellurium dichloride in dichloromethane was shaken in a separatory funnel with an aqueous solution containing 1.15 equiv of sodium disulfite,  $Na_2S_2O_5$ , the organic phase slowly turned yellow with almost no separation of elemental tellurium. After 15 min of vigorous shaking the organic phase was separated, washed with water, and dried for 5-10 min over  $CaCl_2$  (upon longer drying, the solution darkened considerably as elemental tellurium started to precipitate). Evaporation gave an oil which crystallized in yellow flakes (53% yield) from petroleum ether. The infrared spectrum of diphenacyl telluride showed a remarkably low carbonyl absorption, which appeared as a broad peak at  $1640\text{ cm}^{-1}$ . This lowering effect is less pronounced for its chalcogen analogues diphenacyl selenide ( $1660$  and  $1670\text{ cm}^{-1}$ ) and diphenacyl sulfide ( $1690\text{ cm}^{-1}$ ).

Table I contains yields as well as physical and analytical data of a series of compounds prepared by this reduction procedure. The required diorganyltellurium dichlorides 2 were in all cases prepared from tellurium tetrachloride and an excess (2.2-4.0 equiv) of the appropriate acetylated aromatic compound  $RC(O)CH_3$  (eq 3).



As can be seen from Table I, the analytical data were not always satisfactory ( $\pm 0.4\%$ ) for compounds 1. The microcrystalline materials were especially difficult to obtain in pure form even after several recrystallizations. Some derivatives (Table I) were passed through an  $SiO_2$  column to remove acetylated aromatic compound  $ArC(O)CH_3$ , which was the main byproduct in the reduction. Small amounts of elemental tellurium were always deposited on top of the column during this process.

Bis(4-methoxyphenacyl)telluride was not stable enough to survive drying (0.1 mmHg) at ambient temperature. Very soon the crystals started to darken with separation of elemental tellurium. All compounds 1 could be stored in a freezer ( $-15\text{ }^\circ\text{C}$ ) for several months without any visible decomposition. However, when exposed to daylight in the open air, considerable decomposition occurred within a few days.

It would be of interest to investigate the stability of some derivatives where the carbon atom bonded to tellurium is secondary. Such compounds, as well as their corresponding *Te*, *Te*-dichlorides, were not known at the outset of this project. Therefore, we attempted to react some cycloalkanones with tellurium tetrachloride in order to obtain the 2:1 condensation products 11—all possible candidates for further reduction. These reactions were carried out in refluxing carbon tetrachloride in the presence of some calcium oxide. Considerable amounts of a black insoluble material always were formed, but when the reaction of cyclohexanone was disrupted after 1 h, a 54% yield of 2-(trichlorotelluro)cyclohexanone (12a) could be isolated after filtration, evaporation, and recrystallization of the resulting oily product. When the reaction time was increased to 4 h, no crystalline material could be isolated. Cycloheptanone similarly afforded 2-(trichlorotelluro)cycloheptanone (12b) in 42% yield. Cyclooctanone yielded the desired 2:1-adduct bis(1-oxo-2-cyclooctyl)tellurium dichloride (11c) in 40% yield after 4 h in refluxing  $CCl_4$ . This compound was submitted to the usual  $Na_2S_2O_5$  reduction in a two-phase system. The oily reduction product was very unstable and did not survive passage through an  $SiO_2$  column. The quickly recorded NMR spectrum indicated the complete disappearance of the starting material and the formation of a new compound, presumably the desired bis(1-oxo-2-cyclooctyl) telluride (13). Due to its

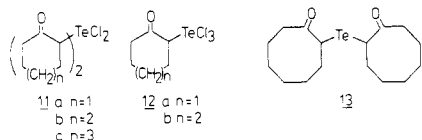
(15) Kuncell, F.; Zimmermann, R. *Justus Liebig's Ann. Chem.* **1901**, 314, 281.

(16) Appa Rao, G. V. N.; Seshasayee, M.; Aravamudan, G.; Sowrirajan, S. *Acta Crystallogr., Sect. C: Cryst. Struct. Commun.* **1983**, C39, 620.

(17) Irgolic, K. J. "The Organic Chemistry of Tellurium"; Gordon and Breach: New York, 1974; p 107.

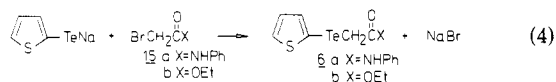
(18) Vernon, R. H. *J. Chem. Soc.* **1920**, 889.





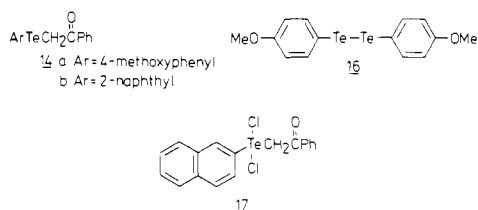
lability, this compound could not be further characterized. However, chlorination of a freshly prepared material with sulfuryl chloride in  $\text{CCl}_4$  regenerated compound **11c** in 54% yield. The stability of a C-Te bond next to a carbonyl is apparently decreased with increasing substitution on carbon.

We also turned our attention to the problem of synthesizing aryl phenacyl tellurides **14**. It was known from previous work that certain  $\alpha$ -halo carbonyl compounds would undergo nucleophilic substitution reactions with telluroate ions. The  $\alpha$ -telluro amide **6a** could be obtained from  $\alpha$ -bromoacetanilide (**15a**) by careful treatment with sodium 2-thienyl telluroate (eq 4).<sup>10</sup> A successful sub-



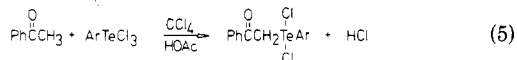
stitution reaction does also occur with ethyl bromoacetate (**15b**), if the product (**6b**) is isolated at low conversion of the starting material. Attempts to increase the conversion resulted in formation of the debrominated ester. However, as soon as the hetero substituent X (NHPh, OEt) was replaced by an aryl group, only products of  $\alpha$ -reduction were isolated.<sup>10</sup> Therefore the nucleophilic substitution approach is not useful for the preparation of compounds **14**.

Petragnani<sup>7</sup> has reported the formation of bis(4-methoxyphenyl) ditelluride (**16**) when (4-methoxyphenyl)phenacyltellurium dichloride (**3a**) was treated with either hydrated sodium sulfide, sodium bisulfite, zinc in chloroform, or hydrazine sulfate. By the use of  $\text{Na}_2\text{S}_2\text{O}_5$  and the two-phase system outlined above, we could readily reduce compound **3a** to 4-methoxyphenyl phenacyl telluride (**14a**) in 72% yield. 2-Naphthyl phenacyl telluride (**14b**) was similarly obtained in 86% yield from compound **17**.

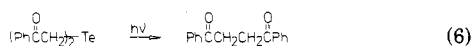


Both compounds **14** survived chromatographic purification, but recrystallization from ethanol always caused formation of the corresponding ditellurides  $\text{ArTeTeAr}$ .

Compounds **3a** and **17** were prepared in excellent yields by the reaction of acetophenone with the corresponding aryltellurium trichloride in refluxing  $\text{CCl}_4$  containing a small amount of acetic acid (eq 5).



Finally, we have also carried out a few chemical reactions with diphenacyl telluride (**1a**). By the use of photochemical tellurium extrusion it was our hope to convert telluride **1a** into dibenzoyl ethane (eq 6). However, all such efforts



met with failure. When the photolysis was carried out in dry benzene for a prolonged time (18 h) at 300 nm under

$\text{N}_2$ , only acetophenone was isolated in addition to some unreacted starting material and precipitated elemental tellurium. Apparently, dimerization of the slowly formed phenacyl radicals cannot compete with hydrogen abstraction.

When diphenacyl telluride was oxidized in methylene chloride with *m*-chloroperbenzoic acid, acetophenone was again formed as the only isolable product (84%).

Some experiments with sodium sulfide nicely exemplify our hypothesis that diphenacyl telluride is incompatible with certain mild reducing agents, even in a two-phase system: when diphenacyltellurium dichloride (**2a**) was reduced in methylene chloride with aqueous  $\text{Na}_2\text{S}$ , only acetophenone (98%) was isolated from the organic phase. Diphenacyl telluride (**1a**), when submitted to the same reaction conditions, was also effectively decomposed to yield acetophenone (96%).

In summary we have shown that diphenacyl telluride and many related compounds can be synthesized by the mild  $\text{Na}_2\text{S}_2\text{O}_5$  reduction of their corresponding  $\text{Te}, \text{Te}$ -dichlorides. These materials, although unstable, can be handled by using ordinary laboratory manipulations. Their significance in organic synthesis has yet to be explored. However, we feel that the weak carbon-tellurium bonds present in these compounds might be of value for carbon-carbon bond-forming reactions.

## Experimental Section

Melting points were uncorrected. NMR spectra were obtained at 200 MHz by using a Bruker WP 200 instrument. They were recorded in  $\text{CDCl}_3$  solutions containing  $\text{Me}_4\text{Si}$  as internal standard and are reported in  $\delta$  units. IR and UV spectra were obtained by using a Perkin-Elmer 257 and a Perkin-Elmer Hitachi 200 instrument, respectively. The photochemical experiment was performed by using a Rayonet photochemical reactor. Elemental analyses were performed by Novo Microanalytical laboratory, Bagsvaerd, Denmark. All acetylated aromatic compounds used were commercially available. 2-(Bromomethyl)-2-phenyl-1,3-dioxolane was prepared by ketalization of phenacyl bromide with ethylene glycol in toluene in the presence of *p*-toluenesulfonic acid: yield 76%; mp 61 °C (lit.<sup>19</sup> 60–61 °C). Di-2-thienyl ditelluride,<sup>20</sup> (4-methoxyphenyl)tellurium trichloride,<sup>21</sup> 2-naphthyltellurium trichloride,<sup>22</sup> diphenacyl sulfide,<sup>23</sup> and diphenacyl selenide<sup>15</sup> were all synthesized by literature methods.

**Phenacyl Bromide and  $\text{Na}_2\text{Te}$ .** Sodium telluride was prepared as previously described<sup>24</sup> from elemental tellurium (1.0 g, 7.8 mmol) and sodium borohydride (0.8 g) in water (15 mL). To this solution was added phenacyl bromide (3.10 g, 15.5 mmol) in MeOH (30 mL) dropwise. A black precipitate of elemental tellurium was immediately formed, and after workup, acetophenone (0.93 g, 50%) and unreacted phenacyl bromide (1.20 g, 39%) were isolated.

**Bis[2-phenyl-1,3-dioxolan-2-yl)methyl] Telluride (8).** Finely pulverized elemental tellurium (0.30 g, 2.3 mmol) and sodium (0.22 g, 9.6 mmol) were stirred under  $\text{N}_2$  in dry DMF (15 mL) at 110 °C until all tellurium metal had disappeared (~15 min). To the resulting yellowish white inhomogeneous solution was added 2-(bromomethyl)-2-phenyl-1,3-dioxolane (1.15 g, 4.7 mmol) in dry THF (10 mL). After 2.5 h at ambient temperature, the reaction mixture was poured into water and extracted with  $\text{CH}_2\text{Cl}_2$ . Chromatographic separation [ $\text{SiO}_2$ ;  $\text{CH}_2\text{Cl}_2$ /petroleum ether (bp 40–60 °C), 1/1] from some unreacted starting material afforded 0.65 g (60%) of telluride **8**: mp 67–68 °C (EtOH);  $^1\text{H}$  NMR  $\delta$  3.14 (s, 2 H), 3.73–3.80 (several peaks, 2 H), 4.04–4.11 (several peaks, 2 H), 7.28–7.35 (several peaks, 3 H), 7.44–7.49 (several peaks, 2 H). Anal. Calcd for  $\text{C}_{20}\text{H}_{22}\text{O}_4\text{Te}$ : C, 52.91; H,

(19) Marquet, A.; Dvolaitzky, M.; Kagan, H. B.; Mamlok, L.; Quannes, C.; Jaques, J. *Bull. Soc. Chim. Fr.* **1961**, 1822.

(20) Engman, L.; Cava, M. P. *Organometallics* **1982**, *1*, 470.

(21) Morgan, G. T.; Kellett, R. E. *J. Chem. Soc.* **1926**, 1080.

(22) Bergman, J.; Engman, L. *Tetrahedron* **1980**, *36*, 1275.

(23) Tafel, J.; Mauritz, A. *Ber. Dtsch. Chem. Ges.* **1890**, 3474.

(24) Bergman, J.; Engman, L. *Org. Prep. Proced. Int.* **1978**, *10*, 289.



4.88. Found: C, 53.02; H, 4.97.

**(2-Phenyl-1,3-dioxolan-2-yl)methyl 2-Thienyl Telluride (10).** A solution of di-2-thienyl ditelluride (0.30 g, 0.71 mmol) in dry DMF (10 mL) under  $N_2$  was heated at 110 °C with sodium (0.08 g, 3.4 mmol) until the red color faded. At this point 2-(bromomethyl)-2-phenyl-1,3-dioxolane (0.35 g, 1.44 mmol) in dry THF (4 mL) was added and the solution stirred at ambient temperature for 2.5 h. Workup as for telluride 8 and chromatography [petroleum ether (bp 40–60 °C)/ $CH_2Cl_2$ , 2/1] yielded 0.24 g (45%) of telluride 10: mp 37–38 °C (EtOH);  $^1H$  NMR  $\delta$  3.46 (s, 2 H), 3.79–3.86 (several peaks, 2 H), 4.12–4.15 (several peaks, 2 H), 6.88 (dd, 1 H,  $J = 3.5$  Hz and  $J = 5.2$  Hz), 7.30–7.40 (several peaks, 5 H), 7.46–7.50 (several peaks, 2 H). Anal. Calcd for  $C_{14}H_{14}O_2S_2Te$ : C, 44.97; H, 3.77. Found: C, 44.91; H, 3.79.

**Attempted Transchelation of Telluride 8.** Telluride 8 (0.20 g, 0.44 mmol) was heated at reflux in dry acetone (10 mL) containing *p*-toluenesulfonic acid (0.015 g). Black elemental tellurium was gradually precipitated, and after 2 h the reaction mixture was poured into an alkaline aqueous solution and extracted with ethyl ether. 2-Methyl-2-phenyl-1,3-dioxolane (9) [0.11 g (76%); mp 63 °C sublimation (lit.<sup>19</sup> 60 °C)] was the only isolable product.

**Preparation of Diorganytellurium Dichlorides 2. Typical Procedure: Diphenacyltellurium Dichloride (2a).**  $TeCl_4$  (5.0 g, 18.5 mmol) and acetophenone (9.0 g, 75.0 mmol) were heated at reflux for 8 h in dry  $CCl_4$  (100 mL). Filtration from a small amount of elemental tellurium and evaporation of the solvent afforded a semisolid which crystallized upon trituration with diethyl ether. The weight of the precipitated diphenacyltellurium dichloride was 5.0 g (62%); mp 195–197 °C dec ( $CHCl_3$ ) (lit.<sup>6</sup> 190 °C dec).

All other compounds 2 were similarly prepared, the relative molar ratio of  $TeCl_4$  and the acetylaromatic compound varying between 1:3 and 1:4. This ratio was lowered to 1:2.2 in the preparation of compounds 2c, 2e, 2g, 2i, and 2j. The yields and melting points ( $CH_2Cl_2$ /petroleum ether) are reported in the following. All compounds seem to gradually decompose with heating, and it is sometimes difficult to determine the melting point [compound no., yield (%), mp (°C)]: 2b, 62, 213–15 dec (lit.<sup>2</sup> 200); 2c, 57, 204–205 dec; 2d, 93, 195–197 dec; 2e, 92, 197 dec; 2f, 84, 205–207 dec (lit.<sup>1</sup> 203–204); 2g, 75, 200–201 dec; 2h, 37, 180–182 dec; 2i, 34, 265–267 dec when dropped on a Kofler bench; 2j, 33, 190–195 dec.

**Preparation of Diorganyl Tellurides 1. Typical Procedure: Diphenacyl Telluride (1a).** Diphenacyltellurium dichloride (1.0 g, 2.3 mmol) was dissolved in  $CH_2Cl_2$  (100 mL) and shaken vigorously in a separatory funnel for 15 min with an aqueous solution (50 mL) of  $Na_2S_2O_5$  (0.50 g, 2.6 mmol). The yellow organic phase was separated, washed once with water, and dried for 5–10 min over  $CaCl_2$ . Evaporation and crystallization from petroleum ether (bp 40–60 °C) afforded 0.44 g of diphenacyl telluride (53%) as yellow flakes: mp 78–79 °C; IR 1640  $cm^{-1}$  (C=O); UV  $\lambda_{max}^{EtOH}$  204, 248 nm;  $^1H$  NMR  $\delta$  4.26 (s, 2 H), 7.44–7.58 (several peaks, 3 H), 7.95–8.00 (several peaks, 2 H).

The other compounds 1 were similarly prepared. Some sparingly soluble  $Te, Te$ -dichlorides were added as solids to the separatory funnel. The insoluble material gradually disappeared as the reduced species was extracted into the organic phase.

As indicated in Table I, some reduction products were passed through an  $SiO_2$  column ( $CH_2Cl_2$ ) to remove some acetylated aromatic compound,  $RC(=O)CH_3$ . The reported yields were those obtained after this process and the following recrystallization (usually from  $CCl_4$ /petroleum ether).  $^1H$  NMR data ( $\delta$ ) of compounds 1b–j: 1b, 2.42 (s, 3 H), 4.23 (s, 2 H), 7.26 (d, 2 H), 7.87 (d, 2 H); 1c, 4.19 (s, 2 H), 7.61 (d, 2 H), 7.83 (d, 2 H); 1d, 4.21 (s, 2 H), 7.45 (d, 2 H), 7.91 (d, 2 H); 1e, 3.88 (s, 3 H), 4.22 (s, 2 H), 6.94 (d, 2 H), 7.96 (d, 2 H); 1f, 4.27 (s, 2 H), 7.42–7.59 (several peaks, 3 H), 7.81–7.90 (several peaks, 2 H), 7.98 (d, 1 H), 8.46 (d, 1 H); 1g, 4.40 (s, 2 H), 7.54–7.61 (several peaks, 2 H), 7.85–8.05 (several peaks, 4 H), 8.53 (s, 1 H); 1h, 4.19 (s, 2 H), 7.15 (dd, 1 H), 7.65 (dd, 1 H), 7.80 (dd, 1 H); 1i, 4.23 (s, 2 H), 7.42–7.50 (several peaks, 4 H), 7.83–7.97 (several peaks, 4 H), 8.39 (s, 1 H); 1j, 4.23 (s, 2 H), 7.32 (t, 1 H), 7.44–7.60 (several peaks, 2 H), 7.65 (s, 1 H), 7.72 (d, 1 H).

**Bis(1-oxo-2-cyclooctyl)tellurium Dichloride (11c).**  $TeCl_4$  (3.0 g, 11.1 mmol), cyclooctanone (4.0 g, 31.7 mmol), and CaO (0.80

g) were heated at reflux in  $CCl_4$  (50 mL) for 4 h. Filtration from 1.1 g of dark insoluble material and evaporation of the solvent afforded an oil which crystallized upon trituration with diethyl ether/petroleum ether (bp 40–60 °C). After recrystallization from  $CCl_4$ /petroleum ether, 2.0 g (40%) of compound 11c (mp 174 °C) was obtained:  $^1H$  NMR  $\delta$  1.47–1.65 (several peaks, 5 H), 1.88–1.98 (several peaks, 3 H), 2.46–2.71 (several peaks, 4 H), 4.49 (dd, 1 H). Anal. Calcd for  $C_{16}H_{26}Cl_2O_2Te$ : C, 42.81; H, 5.84. Found: C, 42.32; H, 5.80.

When cyclohexanone was submitted to the same reaction conditions, the resulting oil did not afford a crystalline product. However, when the reaction was disrupted after 1 h, 2-(trichlorotelluro)cyclohexanone (12a) was obtained in 54% yield; mp 140–143 °C dec ( $CCl_4$ );  $^1H$  NMR  $\delta$  1.71–1.82 (several peaks, 2 H), 2.39–2.97 (several peaks, 6 H), 5.34 (dd, 1 H). Anal. Calcd for  $C_6H_9Cl_3OTe$ : C, 21.77; H, 2.74. Found: C, 21.70; H, 2.76.

Cycloheptanone similarly yielded 2-(trichlorotelluro)cycloheptanone (12b) in 42% yield: mp 123–124 °C dec ( $CCl_4$ /petroleum ether);  $^1H$  NMR  $\delta$  1.47–1.84 (several peaks, 3 H), 1.94–2.16 (several peaks, 2 H), 2.29–3.02 (several peaks, 5 H), 5.48 (dd, 1 H). Anal. Calcd for  $C_7H_{11}Cl_3OTe$ : C, 24.36; H, 3.21. Found: C, 24.44; H, 3.27.

**Bis(1-oxo-2-cyclooctyl) Telluride (13).** Compound 11c (0.50 g, 1.1 mmol) was reduced in a two-phase system with  $Na_2S_2O_5$  (0.22 g, 1.2 mmol) as described above. The yellow oil obtained did not survive passage through an  $SiO_2$  column ( $CH_2Cl_2$ ). The NMR spectrum of some freshly prepared crude material showed the complete disappearance of the signals at 4.49 ppm of the starting material. Instead, there appeared a triplet (4.05 ppm) and a doublet of doublets (3.94 ppm), which we have assigned to the two possible diastereomers of compound 13. When the freshly prepared, crude reduction product was treated with  $SO_2Cl_2$  (0.20 g) in  $CCl_4$  (5 mL), compound 11c (0.27 g, 54%) precipitated.

**Carbethoxymethyl 2-Thienyl Telluride (6b).** To a solution of ethyl bromoacetate (1.0 g, 6.0 mmol) and di-2-thienyl ditelluride (0.126 g, 0.30 mmol) in EtOH (40 mL) under  $N_2$  was added sodium borohydride (5% aqueous) dropwise until the red color faded. Another portion of ditelluride (0.125 g) was then added and the borohydride treatment repeated. After workup with  $CH_2Cl_2$ /water and chromatographic purification, 0.26 g (73%) carbethoxymethyl 2-thienyl telluride was isolated as a yellowish oil:  $^1H$  NMR  $\delta$  1.20 (t, 3 H), 3.44 (s, 2 H), 4.09 (q, 2 H), 6.98 (dd, 1 H), 7.47–7.51 (several peaks, 2 H). At higher conversion of the bromo ester, di-2-thienyl ditelluride was the only isolable product.

**Phenacyl (4-Methoxyphenyl)tellurium Dichloride (3a).** (4-Methoxyphenyl)tellurium trichloride (0.50 g, 1.46 mmol) and acetophenone (0.70 g, 5.8 mmol) were heated at reflux overnight in  $CCl_4$  (10 mL) containing HOAc (0.5 mL). The homogeneous solution was then evaporated and the excess acetophenone pumped off. Trituration with ethyl ether afforded 0.60 g (96%) of phenacyl (4-methoxyphenyl)tellurium dichloride, mp 136–137 °C (lit.<sup>7</sup> 136–137 °C).

By an analogous procedure phenacyl 2-naphthyltellurium dichloride (17) was obtained in 91% yield: mp 147–148 °C (benzene/petroleum ether).

**Phenacyl (4-Methoxyphenyl) Telluride (14a).** Phenacyl(4-methoxyphenyl)tellurium dichloride (0.50 g) was submitted to two-phase reduction with  $Na_2S_2O_5$  (0.23 g) as described above. After chromatography ( $CH_2Cl_2$ ), 0.30 g (72%) of telluride 14a was isolated: mp 56–58 °C (EtOH);  $^1H$  NMR  $\delta$  3.80 (s, 3 H), 4.20 (s, 2 H), 6.74 (d, 2 H), 7.33–7.42 (several peaks, 2 H), 7.50 (m, 1 H), 7.66 (d, 2 H), 7.75–7.81 (several peaks, 2 H). Anal. Calcd for  $C_{15}H_{14}O_2Te$ : C, 50.91; H, 3.93. Found: C, 50.89; H, 4.02.

**Phenacyl 2-naphthyl telluride (14b)** was similarly prepared in 86% yield: mp 53–55 °C (EtOH);  $^1H$  NMR  $\delta$  4.34 (s, 2 H), 7.32 (t, 2 H), 7.44–7.52 (several peaks, 4 H), 7.65–7.83 (several peaks, 5 H), 8.26 (s, 1 H). Anal. Calcd for  $C_{18}H_{14}OTe$ : C, 57.82; H, 3.77. Found: C, 57.09; H, 3.78.

**Oxidation of Diphenacyl Telluride.** To a solution of diphenacyl telluride (0.20 g, 0.55 mmol) in  $CH_2Cl_2$  at 0 °C was added 80% *m*-chloroperbenzoic acid (0.118 g, 0.55 mmol) in  $CH_2Cl_2$  dropwise. After 2 h at 0 °C the solution was extracted with  $NaHCO_3$  (5% aqueous). Acetophenone (0.11 g, 85%) was the only isolated product.

**Reduction of Diphenacyltellurium Dichloride (2a) and Diphenacyl Telluride (1a) with  $Na_2S$ .** Compound 2a (0.50

g, 1.15 mmol) was dissolved in  $\text{CH}_2\text{Cl}_2$  and extracted with water containing  $\text{Na}_2\text{S}\cdot 9\text{H}_2\text{O}$  (1.0 g, 4.16 mmol). Acetophenone (0.27 g, 98%) was the only product contained in the organic phase.

When diphenacyl telluride (1a) was similarly treated, acetophenone was isolated in 96% yield.

**Acknowledgment.** Financial support by the Swedish Natural Science Research Council is gratefully acknowledged.

**Registry No.** 1a, 99766-21-9; 1b, 99766-22-0; 1c, 99766-23-1; 1d, 99766-24-2; 1e, 99766-25-3; 1f, 99766-26-4; 1g, 99766-27-5; 1h, 99766-28-6; 1i, 99766-29-7; 1j, 99766-30-0; 2a, 36362-83-1; 2b, 77017-00-6; 2c, 99766-31-1; 2d, 99766-32-2; 2e, 66839-13-2; 2f, 99766-33-3; 2g, 77840-07-4; 2h, 73537-53-8; 2i, 99766-34-4; 2j,

99766-35-5; 3a, 67096-37-1; 6b, 99766-36-6; 8, 99766-37-7; 9, 3674-77-9; 10, 99766-38-8; 11c, 99766-39-9; 12a, 98797-28-5; 12b, 99766-40-2; 13 (isomer 1), 99766-41-3; 13 (isomer 2), 99766-42-4; 14a, 99766-43-5; 14b, 99766-44-6; 17, 99766-45-7; acetophenone, 98-86-2; 4-methylacetophenone, 122-00-9; 4-bromoacetophenone, 99-90-1; 4-chloroacetophenone, 99-91-2; 4-methoxyacetophenone, 100-06-1; 1-(1-naphthyl)ethanone, 941-98-0; 1-(2-naphthyl)ethanone, 93-08-3; 1-(2-thienyl)ethanone, 88-15-3; 1-(9-anthryl)ethanone, 784-04-3; 1-(2-benzo[b]furan)ethanone, 1646-26-0; phenacyl bromide, 70-11-1; 2-(bromomethyl)-2-phenyl-1,3-dioxolane, 3418-21-1; di-2-thienyl ditelluride, 66697-24-3; cyclooctanone, 502-49-8; cyclohexanone, 108-94-1; cycloheptanone, 502-42-1; ethyl bromoacetate, 105-36-2; (4-methoxyphenyl)tellurium trichloride, 36309-68-9; 2-naphthyltellurium trichloride, 71578-23-9.

## Kinetics and Mechanism of Pyrolysis of 1,3-Disilacyclobutane, 1,3-Dimethyl-1,3-disilacyclobutane, and 1,1,3,3-Tetramethyl-1,3-disilacyclobutane in the Gas Phase

Norbert Auner

Anorganisch-Chemisches Institut, Westfälische Wilhelms-Universität,  
4400 Münster, Federal Republic of Germany

Iain M. T. Davidson,\* Sina Ijadi-Maghsoodi, and F. Timothy Lawrence

Department of Chemistry, The University, Leicester LE1 7RH, Great Britain

Received June 11, 1985

Kinetic data and product analyses are reported for the pyrolysis of the title compounds. Pyrolysis mechanisms are discussed with reference to recent developments in organosilicon chemistry.

### Introduction

There has been considerable interest in the kinetics and mechanism of pyrolysis of silacyclobutanes. While 1,1-dimethylsilacyclobutane is well-known to undergo pyrolysis cleanly to give ethene and dimethylsilene,  $\text{Me}_2\text{Si}=\text{CH}_2$ , which dimerizes quantitatively to 1,1,3,3-tetramethyl-1,3-disilacyclobutane (1),<sup>1</sup> the pyrolysis mechanisms of 1-methylsilacyclobutane<sup>2</sup> and silacyclobutane<sup>3</sup> are considerably more complex, with good evidence for the involvement of silylene intermediates. It has now been established that these complications arise partly because hydridosilenes isomerize reversibly to silylenes<sup>4,5</sup> and partly because hydridosilacyclobutanes can decompose by a silylene-forming 1,2-hydrogen shift as well as by silene formation.<sup>6</sup> Kinetic data for these hydridosilacyclobutanes have been reported.<sup>6</sup>

Less attention has been paid to disilacyclobutanes. Pyrolysis of 1 is known to be complex, yielding methane,  $\text{C}_2$  hydrocarbons, and some high molecular weight products.<sup>7,8</sup> Pyrolysis with added benzaldehyde at 700 °C gave

evidence for the intermediacy of dimethylsilene,<sup>7</sup> as did pyrolysis above 600 °C with added methanol, although the product methoxytrimethylsilane might have resulted from direct reaction of 1 with methanol.<sup>8</sup> The onset of pyrolysis of 1 was observed at 600 °C, as opposed to 450 °C for 1,1-dimethylsilacyclobutane; dimethylsilene was not trapped below 600 °C, indicating that the observed thermal stability of 1 was not attributable to an equilibrium between 1 and dimethylsilene.<sup>8</sup> Extensive pyrolysis of 1 and of 1,1-dimethylsilacyclobutane gave similar products.<sup>9</sup> Analogous results were obtained for the pyrolysis of 1,3-dimethyl-1,3-disilacyclobutane (2), 1,3-disilacyclobutane (3), and their monosilacyclobutane counterparts.<sup>9,10</sup>

We now report kinetic results and further product analysis for the pyrolysis of these three disilacyclobutanes, enabling some mechanistic conclusions to be drawn in the light of recent developments in organosilicon chemistry.

### Experimental Section

Product composition after extensive pyrolysis of 2 and 3 was determined at Münster from pyrolyses in a flow system at ca.  $10^{-2}$  mmHg and 850 °C. Products were trapped at low temperature and analyzed by GC, NMR, IR, and GC/MS. Kinetic experiments and product analysis in the early stages of pyrolysis of 1, 2, and 3 were carried out at Leicester by low-pressure pyrolysis (LPP),<sup>11</sup>

(1) Flowers, M. C.; Gusev, L. E. *J. Chem. Soc. B* 1968, 428, 1396.

(2) Conlin, R. T.; Wood, D. L. *J. Am. Chem. Soc.* 1981, 103, 1843.

(3) Conlin, R. T.; Gill, R. S., *J. Am. Chem. Soc.* 1983, 105, 618.

(4) Davidson, I. M. T.; Ijadi-Maghsoodi, S.; Barton, T. J.; Tillman, N. *J. Chem. Soc., Chem. Commun.* 1984, 478.

(5) Davidson, I. M. T.; Scampton, R. J. *J. Organomet. Chem.* 1984, 271, 249.

(6) Davidson, I. M. T.; Fenton, A.; Ijadi-Maghsoodi, S.; Scampton, R. J.; Auner, N.; Grobe, J.; Tillman, N.; Barton, T. J. *Organometallics* 1984, 3, 1593.

(7) Barton, T. J.; Marquardt, G.; Kilgour, J. A. *J. Organomet. Chem.* 1975, 85, 317.

(8) Nametkin, N. S.; Gusev, L. E.; Volpina, E. A.; Vdovin, V. M. *Dokl. Akad. Nauk SSSR* 1975, 220, 386 (English translation, p 81).

(9) Auner, N.; Grobe, J. *J. Organomet. Chem.* 1980, 197, 13.

(10) Auner, N.; Grobe, J. *Z. Anorg. Allg. Chem.* 1979, 459, 15.

(11) Davidson, I. M. T.; Ring, M. A. *J. Chem. Soc., Faraday Trans. 1* 1980, 76, 1520.

g, 1.15 mmol) was dissolved in  $\text{CH}_2\text{Cl}_2$  and extracted with water containing  $\text{Na}_2\text{S}\cdot 9\text{H}_2\text{O}$  (1.0 g, 4.16 mmol). Acetophenone (0.27 g, 98%) was the only product contained in the organic phase.

When diphenacyl telluride (1a) was similarly treated, acetophenone was isolated in 96% yield.

**Acknowledgment.** Financial support by the Swedish Natural Science Research Council is gratefully acknowledged.

**Registry No.** 1a, 99766-21-9; 1b, 99766-22-0; 1c, 99766-23-1; 1d, 99766-24-2; 1e, 99766-25-3; 1f, 99766-26-4; 1g, 99766-27-5; 1h, 99766-28-6; 1i, 99766-29-7; 1j, 99766-30-0; 2a, 36362-83-1; 2b, 77017-00-6; 2c, 99766-31-1; 2d, 99766-32-2; 2e, 66839-13-2; 2f, 99766-33-3; 2g, 77840-07-4; 2h, 73537-53-8; 2i, 99766-34-4; 2j,

99766-35-5; 3a, 67096-37-1; 6b, 99766-36-6; 8, 99766-37-7; 9, 3674-77-9; 10, 99766-38-8; 11c, 99766-39-9; 12a, 98797-28-5; 12b, 99766-40-2; 13 (isomer 1), 99766-41-3; 13 (isomer 2), 99766-42-4; 14a, 99766-43-5; 14b, 99766-44-6; 17, 99766-45-7; acetophenone, 98-86-2; 4-methylacetophenone, 122-00-9; 4-bromoacetophenone, 99-90-1; 4-chloroacetophenone, 99-91-2; 4-methoxyacetophenone, 100-06-1; 1-(1-naphthyl)ethanone, 941-98-0; 1-(2-naphthyl)ethanone, 93-08-3; 1-(2-thienyl)ethanone, 88-15-3; 1-(9-anthryl)ethanone, 784-04-3; 1-(2-benzo[b]furan)ethanone, 1646-26-0; phenacyl bromide, 70-11-1; 2-(bromomethyl)-2-phenyl-1,3-dioxolane, 3418-21-1; di-2-thienyl ditelluride, 66697-24-3; cyclooctanone, 502-49-8; cyclohexanone, 108-94-1; cycloheptanone, 502-42-1; ethyl bromoacetate, 105-36-2; (4-methoxyphenyl)tellurium trichloride, 36309-68-9; 2-naphthyltellurium trichloride, 71578-23-9.

## Kinetics and Mechanism of Pyrolysis of 1,3-Disilacyclobutane, 1,3-Dimethyl-1,3-disilacyclobutane, and 1,1,3,3-Tetramethyl-1,3-disilacyclobutane in the Gas Phase

Norbert Auner

Anorganisch-Chemisches Institut, Westfälische Wilhelms-Universität,  
4400 Münster, Federal Republic of Germany

Iain M. T. Davidson,\* Sina Ijadi-Maghsoodi, and F. Timothy Lawrence

Department of Chemistry, The University, Leicester LE1 7RH, Great Britain

Received June 11, 1985

Kinetic data and product analyses are reported for the pyrolysis of the title compounds. Pyrolysis mechanisms are discussed with reference to recent developments in organosilicon chemistry.

### Introduction

There has been considerable interest in the kinetics and mechanism of pyrolysis of silacyclobutanes. While 1,1-dimethylsilacyclobutane is well-known to undergo pyrolysis cleanly to give ethene and dimethylsilene,  $\text{Me}_2\text{Si}=\text{CH}_2$ , which dimerizes quantitatively to 1,1,3,3-tetramethyl-1,3-disilacyclobutane (1),<sup>1</sup> the pyrolysis mechanisms of 1-methylsilacyclobutane<sup>2</sup> and silacyclobutane<sup>3</sup> are considerably more complex, with good evidence for the involvement of silylene intermediates. It has now been established that these complications arise partly because hydridosilenes isomerize reversibly to silylenes<sup>4,5</sup> and partly because hydridosilacyclobutanes can decompose by a silylene-forming 1,2-hydrogen shift as well as by silene formation.<sup>6</sup> Kinetic data for these hydridosilacyclobutanes have been reported.<sup>6</sup>

Less attention has been paid to disilacyclobutanes. Pyrolysis of 1 is known to be complex, yielding methane,  $\text{C}_2$  hydrocarbons, and some high molecular weight products.<sup>7,8</sup> Pyrolysis with added benzaldehyde at 700 °C gave

evidence for the intermediacy of dimethylsilene,<sup>7</sup> as did pyrolysis above 600 °C with added methanol, although the product methoxytrimethylsilane might have resulted from direct reaction of 1 with methanol.<sup>8</sup> The onset of pyrolysis of 1 was observed at 600 °C, as opposed to 450 °C for 1,1-dimethylsilacyclobutane; dimethylsilene was not trapped below 600 °C, indicating that the observed thermal stability of 1 was not attributable to an equilibrium between 1 and dimethylsilene.<sup>8</sup> Extensive pyrolysis of 1 and of 1,1-dimethylsilacyclobutane gave similar products.<sup>9</sup> Analogous results were obtained for the pyrolysis of 1,3-dimethyl-1,3-disilacyclobutane (2), 1,3-disilacyclobutane (3), and their monosilacyclobutane counterparts.<sup>9,10</sup>

We now report kinetic results and further product analysis for the pyrolysis of these three disilacyclobutanes, enabling some mechanistic conclusions to be drawn in the light of recent developments in organosilicon chemistry.

### Experimental Section

Product composition after extensive pyrolysis of 2 and 3 was determined at Münster from pyrolyses in a flow system at ca.  $10^{-2}$  mmHg and 850 °C. Products were trapped at low temperature and analyzed by GC, NMR, IR, and GC/MS. Kinetic experiments and product analysis in the early stages of pyrolysis of 1, 2, and 3 were carried out at Leicester by low-pressure pyrolysis (LPP),<sup>11</sup>

(1) Flowers, M. C.; Gusel'nikov, L. E. *J. Chem. Soc. B* 1968, 428, 1396.

(2) Conlin, R. T.; Wood, D. L. *J. Am. Chem. Soc.* 1981, 103, 1843.

(3) Conlin, R. T.; Gill, R. S., *J. Am. Chem. Soc.* 1983, 105, 618.

(4) Davidson, I. M. T.; Ijadi-Maghsoodi, S.; Barton, T. J.; Tillman, N. *J. Chem. Soc., Chem. Commun.* 1984, 478.

(5) Davidson, I. M. T.; Scampton, R. J. *J. Organomet. Chem.* 1984, 271, 249.

(6) Davidson, I. M. T.; Fenton, A.; Ijadi-Maghsoodi, S.; Scampton, R. J.; Auner, N.; Grobe, J.; Tillman, N.; Barton, T. J. *Organometallics* 1984, 3, 1593.

(7) Barton, T. J.; Marquardt, G.; Kilgour, J. A. *J. Organomet. Chem.* 1975, 85, 317.

(8) Nametkin, N. S.; Gusel'nikov, L. E.; Volpina, E. A.; Vdovin, V. M. *Dokl. Akad. Nauk SSSR* 1975, 220, 386 (English translation, p 81).

(9) Auner, N.; Grobe, J. *J. Organomet. Chem.* 1980, 197, 13.

(10) Auner, N.; Grobe, J. *Z. Anorg. Allg. Chem.* 1979, 459, 15.

(11) Davidson, I. M. T.; Ring, M. A. *J. Chem. Soc., Faraday Trans. 1* 1980, 76, 1520.

Table I. Kinetic Data for Decomposition of Disilacyclobutanes

reactant	temp/°C	press/mmHg	log A/s <sup>-1</sup>	E/kJ mol <sup>-1</sup>	k <sub>550°C</sub> /s <sup>-1</sup>	k <sub>rel</sub>
1	664-746	3.0	14.4 ± 0.2	296 ± 3	4.1 × 10 <sup>-5</sup>	1
2	611-663	2.5	13.5 ± 0.2	255 ± 3	2.07 × 10 <sup>-3</sup>	50
3	516-573	2.5	13.3 ± 0.3	230 ± 4	0.05	1220

Table II. Relative Yields of Gaseous Products

reactant	CH <sub>4</sub>	C <sub>2</sub> H <sub>4</sub>	C <sub>3</sub> H <sub>6</sub>	MeSiH <sub>3</sub>	Me <sub>2</sub> SiH <sub>2</sub>	Me <sub>3</sub> SiH
1	40	30	1	~0	1	2
2	30	13	1	1	15	30
3	1	1	~0	5	20	~0

Table III. Additional Products Detected at 850 °C

Pyrolysis of 2						
SiH <sub>4</sub>	C <sub>4</sub> H <sub>10</sub>	H <sub>2</sub> C=C=CH <sub>2</sub>	HC≡CCH <sub>3</sub>			
{H <sub>3</sub> Si}	Me <sub>3</sub> Si	Me <sub>2</sub> (H)Si	HC≡CSiH <sub>3</sub>			HC≡CSiMe <sub>3</sub> <sup>a</sup>
Pyrolysis of 3						
SiH <sub>4</sub>	H <sub>2</sub> (Me)Si	(H <sub>2</sub> SiCH <sub>2</sub> ) <sub>5</sub>	H <sub>3</sub> Si(CH <sub>2</sub> SiH <sub>2</sub> ) <sub>3</sub> SiH <sub>3</sub>	H <sub>3</sub> Si(CH <sub>2</sub> SiH <sub>2</sub> ) <sub>3</sub> CH <sub>2</sub> SiH <sub>3</sub>		
{HC≡CH}	C <sub>3</sub> H <sub>6</sub>	H <sub>2</sub> C=C=CH <sub>2</sub>	HC≡CCH <sub>3</sub>			HC≡CSiH <sub>3</sub> <sup>a</sup>

<sup>a</sup>Trace quantities in braces.

with analysis by quadrupole mass spectrometry, and by pyrolysis in a stirred-flow apparatus (SFR),<sup>12</sup> with analysis by GC and by GC/MS.

## Results

**LPP of 1. Preliminary Experiments.**<sup>13</sup> These pyrolyses were carried out between 662 and 782 °C, with an initial pressure of 1 of 0.14 mmHg. The main products detected were hydrogen, methane, and ethene. In the presence of equal pressures of hydrogen chloride, trimethylchlorosilane was also formed, in approximately equal amount to the methane; in these experiments the formation of hydrogen and ethene was significantly reduced. Likewise, added methoxytrimethylsilane gave the silene insertion product.<sup>14</sup> 1 was found to react slowly with hydrogen chloride in the vacuum line at room temperature, but not in the reaction vessel below pyrolysis temperature. The internal surface of the vacuum line would have more adsorbed water than the reaction vessel; also, the surface of the latter was passivated by pyrolytic deposition. Detailed kinetic measurements were not made, but the half-life for decomposition of 1 at 677 °C was 66 s, increased to 70 s in the presence of hydrogen chloride.

**Kinetics of Pyrolysis of 1-3.** The kinetics of the first-order decomposition of 1, 2, and 3 were measured by LPP, with the results given in Table I.

**Product Formation.** Pyrolysis of 1 in the SFR at 740 °C gave methane, ethene, trimethylsilane, propene, and dimethylsilane, in the approximate ratios of 40:30:2:1:1.

Pyrolysis of 2 in the SFR at 676 °C gave trimethylsilane, methane, dimethylsilane, ethene, propene, and methylsilane in the approximate ratios of 30:30:15:13:1:1. In LPP experiments, significant quantities of hydrogen (undetectable by our GC) was observed.

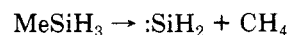
Pyrolysis of 3 in the SFR at 571 °C gave dimethylsilane, methylsilane, methane, and ethene in the approximate ratios of 20:5:1:1. Hydrogen was again observed in significant quantity by LPP, as were several products of high molecular weight. The foregoing results are summarized in Table II.

In all of the above pyrolyses there were also small quantities of other unidentified products. Many of these were identified in Münster in the flow pyrolyses there of 2 and 3 to higher conversion at 850 °C. The new products identified in these experiments are listed in Table III. For simplicity, the products identified in the SFR experiments (Table II) are omitted from Table III but were, of course, also detected in the flow pyrolyses at 850 °C, in the same order of importance.

## Discussion

The kinetic data in Table I relate to the overall decomposition of the three disilacyclobutanes. In view of the obvious complexity of these pyrolyses, the Arrhenius parameters should not be identified with primary processes; their main use is to demonstrate the substantial differences in thermal stability between 1, 2, and 3, as indicated by the relative rate constants in the final column of Table I. Although these pyrolyses were done at the highest pressure possible in our LPP apparatus, there may still have been some unimolecular fall-off; if so, this would have been most pronounced for 3, with 12 atoms in the molecule, and least for 1, with 24 atoms. Consequently, the differences in thermal stability between 1, 2, and 3 may be even greater than indicated in Table I.

A basic reason for these differences is that 2 and 3 can undergo the 1,2-hydrogen shift from silicon to carbon with concomitant formation of a silylene, whereas 1 cannot. This reaction, already shown to be important in the pyrolysis of hydridomonosilacyclobutanes,<sup>6</sup> was first observed as a minor reaction in the pyrolysis of methylsilane:<sup>11</sup>



Arrhenius parameters have now been measured or estimated for this type of reaction in the pyrolysis of methylsilane, dimethylsilane, and trimethylsilane. The activation energy increases with increasing methyl substitution at silicon, from 279 kJ mol<sup>-1</sup> for methylsilane, through 301 for dimethylsilane, to 326 for trimethylsilane.<sup>15</sup> The last two methylsilanes are simple, acyclic analogies for 3 and 2, respectively. Alternative primary processes would involve silicon-carbon bond rupture to form radi-

(12) Baldwin, A. C.; Davidson, I. M. T.; Howard, A. V. *J. Chem. Soc., Faraday Trans. 1* 1975, 71, 972.

(13) Lawrence, F. T. Ph.D. Thesis, University of Leicester, 1983.

(14) Davidson, I. M. T.; Wood, I. T. *J. Chem. Soc., Chem. Commun.* 1982, 550.

(15) Ring, M. A.; O'Neal, H. E.; Rickborn, S. F.; Sawrey, B. A. *Organometallics* 1983, 2, 1891.

Table IV. Arrhenius Parameters for Ring Opening in the Disilacyclopropane, 4

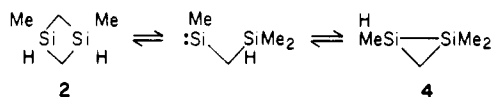
reactn type	log A	E/kJ mol <sup>-1</sup>	k <sub>900K</sub> /s <sup>-1</sup>
H shift, Si → Si	14.0	209-E03	3.65 × 10 <sup>11</sup>
H shift, Si → C	14.3	301-E03	3.33 × 10 <sup>6</sup>
Me shift, Si → Si	13.3	282-E03	4.22 × 10 <sup>6</sup>
Si-Si bond rupture	15.5	337-E03	4.30 × 10 <sup>5</sup>

<sup>a</sup>The values of  $k_{900K}$  (at the mid temperature of the experiments) are based on an estimate<sup>20</sup> of 167 kJ mol<sup>-1</sup> for E03.

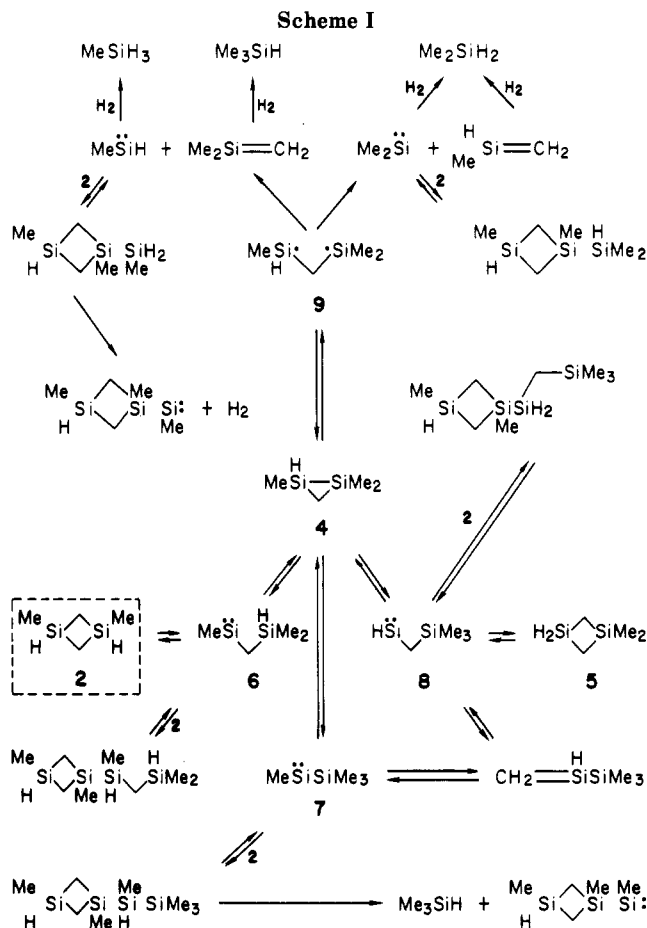
cal, the silicon-carbon bond in the ring being weaker than silicon-methyl because of ring strain. Recent estimates of the silicon-methyl bond dissociation energy, which is not strongly sensitive to substituent effects,<sup>16</sup> vary between 355 and 370 kJ mol<sup>-1</sup>; from recent work on the pyrolysis of trimethylchlorosilane,<sup>17</sup> we now favor 366 kJ mol<sup>-1</sup>.

Hence, the activation energy for the 1,2-hydrogen shift in 3 would be 301-E04 kJ mol<sup>-1</sup>, where E04 is the element of ring strain released on opening the disilacyclobutane ring. The corresponding figure for 2 would be 326-E04 kJ mol<sup>-1</sup>, while for silicon-carbon bond breaking in the ring to form a biradical (the main primary route open to 1), it would be 366-E04 kJ mol<sup>-1</sup>. As E04 is unknown, absolute values are speculative, but the activation energy would be lowest for 3, 25 kJ mol<sup>-1</sup> higher for 2, and a further 40 kJ mol<sup>-1</sup> higher for 1. These are almost exactly the differences that were observed experimentally (Table I). While this trend is interesting, we stress our earlier comment that the Arrhenius parameters in Table I should not be identified with the primary reactions, which would undoubtedly have higher A factors and activation energies.

In the pyrolysis of 2 and 3, the primary 1,2-hydrogen shift would form silylenes that could insert into the silicon-hydrogen bond of the parent disilacyclobutane but could also cyclize to form disilacyclopropane intermediates, as illustrated below for the pyrolysis of 2.



Disilacyclopropanes are well established as key intermediates in intramolecular rearrangements of silylenes,<sup>18</sup> and we have successfully modelled a number of rearrangements involving them by numerical integration,<sup>5,19</sup> including the specific case of 4,<sup>5</sup> which has been very reasonably suggested<sup>18</sup> as an intermediate in the pyrolytic formation of 2 and its unsymmetrical isomer, 5, from Me<sub>4</sub>Si<sub>2</sub>. Recently,<sup>20</sup> we have refined our earlier estimates<sup>5,19</sup> of Arrhenius parameters for reactions involving disilacyclopropanes by applying the methods of thermochemical kinetics.<sup>21</sup> The resulting rate parameters for silylene-forming ring-opening reactions of 4 are in Table IV, together with our estimates for a bond rupture to form a biradical. For the latter, the A factor was taken to be the same as for cyclopropane and 1,1,2,2-tetramethylcyclopropane,<sup>22</sup> while the activation energy is derived from D(Me<sub>3</sub>Si-SiMe<sub>3</sub>) in hexamethyldisilane.<sup>23</sup>



As regards the product composition in the pyrolysis of 2, formation of trimethylsilane and dimethylsilane (Table II) is particularly significant mechanistically. The range of products obtained in flow pyrolyses at 850 °C (Table III) is certainly interesting but not surprising in view of the extensive pyrolysis that took place under these conditions. However, it is noteworthy that both 2 and 3 gave silane, SiH<sub>4</sub>, as a product. Silane would have been undetectable by the analytical methods used in the kinetic experiments.

The foregoing considerations (Tables II and IV) lead to the outline mechanism for the early stages of the pyrolysis of 2 given in Scheme I.

The silylenes 6, 7, and 8 and the biradical 9 are the respective products of the ring-opening reactions of disilacyclopropane 4 in the order listed in Table IV. As the rapid ring opening of 4 to 6 is balanced by equally rapid ring closing,<sup>5,18</sup> 4 and 6 are essentially equilibrated. Consequently, the reactions forming 7, 8, and 9 are not unimportant.<sup>24</sup> While all three silylenes insert into the silicon-hydrogen bond in 2, silylenes 6 and 8 only do so reversibly, while the insertion product of 7 into 2 may also decompose to give trimethylsilane, which therefore emerges as a major gaseous product (Table II). Once biradical 9 has been formed, it will dissociate to a silene and a silylene, aided by the silicon-carbon π-bond energy in the silene and the silylene stabilization energy.<sup>16</sup> These simpler silylenes and silenes provide a further source of methyl-

(16) Walsh, R. *Acc. Chem. Res.* 1981, 14, 246.

(17) Davidson, I. M. T.; Dean, C. E., to be submitted for publication. Dean, C. E. Ph.D. Thesis, University of Leicester, 1983.

(18) Wulff, W. D.; Goure, W. F.; Barton, T. J. *J. Am. Chem. Soc.* 1978, 100, 6236.

(19) Davidson, I. M. T.; Hughes, K. J.; Scampton, R. J. *J. Organomet. Chem.* 1984, 272, 11.

(20) Davidson, I. M. T.; O'Neal, H. E., unpublished work.

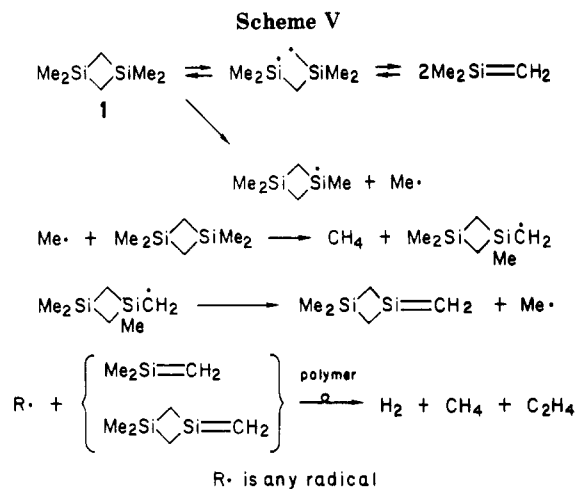
(21) Benson, S. W. "Thermochemical Kinetics", 2nd ed.; Wiley: New York, 1976.

(22) Robinson, P. J.; Holbrook, K. A. "Unimolecular Reactions"; Wiley: London, 1972; p 189.

(23) Davidson, I. M. T.; Howard, A. V. *J. Chem. Soc., Faraday Trans. 1* 1975, 71, 69.

(24) A reviewer has pointed out that Scheme I includes reactions such as the methyl shift converting 4 to 8, previously dismissed<sup>5</sup> as being insignificantly slow; there is no inconsistency in that because in the previous case<sup>5</sup> there was another route to the silylene 7. In the absence of that route, as in Scheme I, conversion of 4 to 8 cannot be ignored.





A very similar silylene chain branching reaction, forming  $\text{:SiMeH}$  instead of  $\text{:SiH}_2$ , would result from reaction of silylsilylene 14 with 3. These features, combined with the lower activation energy for the initial 1,2-hydrogen shift,<sup>15</sup> account for the substantially higher rate of decomposition of 3 (Table I). Formation and secondary decomposition of polymer would also occur with 3, giving mainly hydrogen rather than hydrocarbons. Again, there would be gaseous products of higher molecular weight resulting from further secondary reactions. Such products were observed in LPP experiments and in the flow experiments at 850 °C (Table III).

We have noted above that while the Arrhenius parameters in Table I should not be identified with primary reactions, the trend in activation energies is consistent with these primary reactions being the 1,2-hydrogen shift in 2 and 3 and rupture of the silicon-carbon ring bond in 1 to form a biradical, which then dissociates to give two molecules of dimethylsilylene. In the pyrolysis of 1 we had

evidence for the formation of dimethylsilylene from trapping experiments, as had earlier workers.<sup>7,8</sup> However, the Arrhenius parameters for the decomposition of 1 do not rule out some contribution from silicon-methyl bond rupture. While that activation energy would be higher than for silicon-carbon bond rupture in the ring by an amount equal to EO4, the  $A$  factor would also be higher, ca.  $10^{17} \text{ s}^{-1}$  instead of ca.  $10^{15.5} \text{ s}^{-1}$ . A good analogy is the pyrolysis of tetramethylsilane, which proceeds by a short-chain reaction with kinetic behavior sensitive to experimental conditions.<sup>27</sup> Because the chain is short, a chain length approaching unity can be achieved by raising the temperature, giving Arrhenius parameters approaching those for dissociation of the silicon-methyl bond.<sup>27</sup> At lower temperatures, the Arrhenius parameters for the chain reaction depend on conditions, as shown in Table V.

The observed Arrhenius parameters for the decomposition of 1 are very similar to some of those for the pyrolysis of tetramethylsilane in Table V. The rate constant for the decomposition of 1 at 700 °C would be  $0.032 \text{ s}^{-1}$ . Consequently, a chain reaction initiated by silicon-methyl bond rupture, exactly as in the pyrolysis of tetramethylsilane,<sup>27</sup> cannot be excluded. We therefore agree with earlier suggestions<sup>7,8</sup> that both modes of silicon-carbon bond breaking may occur in the pyrolysis of 1. Our suggestions are embodied in Scheme V. Our observation that added hydrogen chloride had a small effect on the half-life for decomposition of 1, but a greater inhibitory effect on the formation of hydrogen and ethene,<sup>13</sup> confirms that the decomposition of polymer is an important secondary process in the pyrolysis of 1.

**Acknowledgment.** We warmly thank Professors J. Grobe (Westfälische Wilhelms-Universität, Münster) and T. J. Barton (Iowa State University) for stimulating discussions and encouragement. The financial support of the SERC is gratefully acknowledged. We are also grateful to the reviewers for their constructive comments and suggestions.

(29) Clifford, R. P.; Gowenlock, B. G.; Johnson, C. A. F.; Stevenson, J. J. *Organomet. Chem.* 1972, 34, 53.

**Registry No.** 1, 1627-98-1; 2, 68060-11-7; 3, 287-55-8; 4, 1628-01-9.



# Formation of a Bridging Methylidyne Complex and of a Bridging Vinyl Complex from the Reaction of $[(C_5H_5)Fe(NO)]_2(\mu-CH_2)$ with Trityl Cation

Charles P. Casey\* and Dean M. Roddick

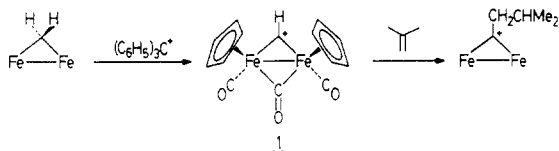
Department of Chemistry, University of Wisconsin, Madison, Wisconsin 53706

Received July 1, 1985

Reaction of methylidene complex  $[(C_5H_5)Fe(NO)]_2(\mu-CH_2)$  (**2**) with trityl cation,  $(C_6H_5)_3C^+PF_6^-$ , at  $-78^\circ C$  in  $CH_2Cl_2$  followed by slow warming to ambient temperature gave an equimolar mixture of bridging vinyl complex  $\{[(C_5H_5)Fe(NO)]_2(\mu-\eta^1, \eta^2-CH=CH_2)\}^+PF_6^-$  (**3**) and  $[(C_5H_5)Fe(\mu-NO)]_2$ . **3** was independently prepared by the reaction of ethylidene complex  $[(C_5H_5)Fe(NO)]_2(\mu-CHCH_3)$  with  $(C_6H_5)_3C^+PF_6^-$ . Reaction of **2** with trityl cation at ambient temperature gave a mixture of **3**, methylidyne complex  $\{[(C_5H_5)Fe(\mu-NO)]_2(\mu-CH)\}^+PF_6^-$  (**4**), and a nitrosyl alkylation product  $\{[(C_5H_5)Fe]_2(\mu-NO)(\mu-CH_2)(C_6H_5)_3NO\}^+PF_6^-$  (**5**). Slow dropwise addition of a  $CH_2Cl_2$  solution of trityl cation to a solution of **2** gave **5** in 42% yield. Reaction of methylidene complex **2** with methylidyne complex **4** did not result in methylene transfer to form **3**. Unlike the carbonyl methylidyne complex  $\{[(C_5H_5)Fe(CO)]_2(\mu-CO)(\mu-CH)\}^+PF_6^-$  (**1**) nitrosyl methylidyne complex **4** did not form stable 1:1 adducts with  $KO-t-Bu$ ,  $NMe_3$ , or  $PMe_3$  and did not react with isobutylene.

## Introduction

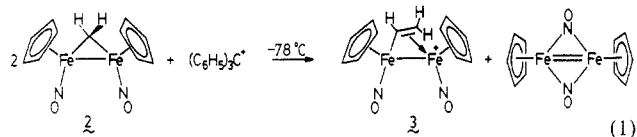
Recently we reported the first synthesis of a dinuclear bridging methylidyne complex by reaction of a bridging methylene complex with the hydride abstracting reagent trityl cation,  $(C_6H_5)_3C^+$ .<sup>1</sup> The resulting methylidyne complex  $[(C_5H_5)_2(CO)_2Fe_2(\mu-CO)(\mu-CH)]^+PF_6^-$  (**1**) is a very reactive electrophile that forms 1:1 adducts with CO,  $NMe_3$ , and  $KO-t-Bu$ .<sup>2</sup> Methylidyne complex **1** also reacts with alkenes to add its C-H bond across the carbon-carbon double bond in a reaction we have called hydrocarbation.<sup>3</sup> Other known dinuclear bridging methylidyne complexes include  $\{[(C_5Me_5)_2(CO)_2Fe_2(\mu-CO)(\mu-CH)]\}^+$ ,<sup>4</sup>  $[(C_5H_5)(C_5Me_5)(CO)_2Fe_2(\mu-CO)(\mu-CH)]^+$ ,<sup>5</sup>  $[(C_5H_5)_2(dppm)Ru_2(\mu-CO)(\mu-CH)]^+$ ,<sup>6</sup> and  $[(C_5H_5)_2(CO)_2Ru_2(\mu-CO)(\mu-CH)]^+$ .<sup>7</sup>



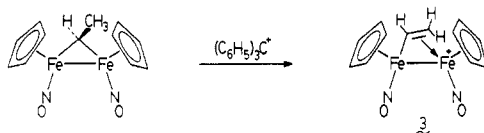
In view of the unique chemistry seen for **1**, we have sought to prepare additional examples of methylidyne complexes to help understand the reactivity patterns of **1**. Here we report a series of reactions of the known methylene complex  $[(C_5H_5)Fe(NO)]_2(\mu-CH_2)$  (**2**)<sup>8</sup> with trityl cation. In contrast to the clean hydride abstraction chemistry found for **1**, the reaction of trityl cation with **2** was quite complex and gave mixtures of  $\{[(C_5H_5)Fe(NO)]_2(\mu-\eta^1, \eta^2-CH=CH_2)\}^+PF_6^-$  (**3**),  $\{[(C_5H_5)Fe(\mu-NO)]_2(\mu-CH)\}^+PF_6^-$  (**4**), and an apparent nitrosyl alkylation product,  $\{[(C_5H_5)Fe]_2(\mu-NO)(\mu-CH_2)(C_6H_5)_3NO\}^+PF_6^-$  (**5**).

## Results

**Bridging Vinyl Complex 3.** Herrmann first prepared the bridging methylene dinitrosyl iron complex  $[(C_5H_5)Fe(NO)]_2(\mu-CH_2)$  (**2**) by reaction of metal-metal double-bonded complex  $[(C_5H_5)Fe(\mu-NO)]_2$ <sup>9</sup> with diazomethane. The reaction of **2** with an equimolar amount of  $(C_6H_5)_3C^+PF_6^-$  at  $-78^\circ C$  in  $CH_2Cl_2$  followed by slow warming to ambient temperature over the course of several hours yielded a 1:1 mixture of  $\{[(C_5H_5)Fe(NO)]_2(\mu-\eta^1, \eta^2-CH=CH_2)\}^+PF_6^-$  (**3**) and  $[(C_5H_5)Fe(\mu-NO)]_2$ . Half of the  $(C_6H_5)_3C^+PF_6^-$  remained unreacted and was identified by <sup>1</sup>H NMR. No other products were observed under these conditions. The reaction of **2** with half the number of moles of  $(C_6H_5)_3C^+PF_6^-$  gave a 74% yield of **3** based on the stoichiometry shown in eq 1. Extraction of **3** into acetone at  $-78^\circ C$  provided an excellent procedure to remove the insoluble coproduct  $[(C_5H_5)Fe(\mu-NO)]_2$ . An



authentic sample of bridging vinyl complex **3** was also independently prepared in good yield from the ethylidene complex  $[(C_5H_5)Fe(NO)]_2(\mu-CHCH_3)$ <sup>10</sup> by hydride abstraction with  $(C_6H_5)_3C^+PF_6^-$ .



The structure of **3** was assigned on the basis of spectroscopic and analytical data. The IR spectrum of **3** displays two strong bands at 1822 and 1774  $cm^{-1}$ , indicative of terminal nitrosyl ligands. The IR bands for these terminal nitrosyl groups in the cationic complex **3** are shifted about 100  $cm^{-1}$  to higher energy than bands for related neutral complexes.<sup>10</sup> The IR spectrum does not allow an unequivocal assignment of the nitrosyl stereochemistry.

(1) Casey, C. P.; Fagan, P. J.; Miles, W. H. *J. Am. Chem. Soc.* **1982**, *104*, 1134.

(2) Casey, C. P.; Fagan, P. J.; Day, V. W. *J. Am. Chem. Soc.* **1982**, *104*, 7360.

(3) Casey, C. P.; Fagan, P. J. *J. Am. Chem. Soc.* **1982**, *104*, 4950.

(4) Casey, C. P.; Colborn, R. E., unpublished results.

(5) Miles, W. H. Ph.D. Thesis, University of Wisconsin at Madison, 1984.

(6) Davies, D. L.; Gracey, B. P.; Guerschais, V.; Knox, S. A. R.; Orpen, A. G. *J. Chem. Soc., Chem. Commun.* **1984**, 841.

(7) Knox, S. A. R.; Hathorn, J. J., private communication.

(8) Herrmann, W. A.; Bauer, C. *J. Organomet. Chem.* **1981**, *204*, C21.

(9) Brunner, H. *J. Organomet. Chem.* **1968**, *14*, 173.

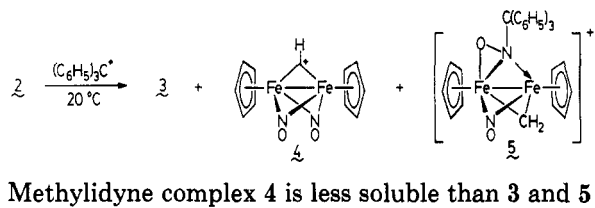
(10) Herrmann, W. A.; Bauer, C. *Chem. Ber.* **1982**, *115*, 14.



The  $^1H$  NMR data for **3** is similar to that of the related vinyl complex  $[(C_5H_5)Fe(CO)]_2(\mu-CO)(\mu-\eta^1, \eta^2-CH=CH_2)^+$ .<sup>11</sup> The vinyl group gives rise to three doublets of doublets at  $\delta$  10.96, 4.98, and 3.65. The far downfield chemical shift ( $\delta$  10.96) of the hydrogen on the vinyl carbon bonded to both irons is particularly characteristic of  $\mu$ -vinyl compounds. In the  $^{13}C$  NMR, resonances at  $\delta$  187.7, (d,  $J = 154$  Hz) and 69.8 (t,  $J = 188$  Hz) were assigned to the CH and  $CH_2$  vinylic carbons.

$\mu$ -Vinyl complex **3** is slightly soluble and moderately stable in methylene chloride or THF. It is more soluble in acetone or  $CH_3CN$  but decomposes within several hours at ambient temperature in these solvents. The only products observed by  $^1H$  NMR were  $[(C_5H_5)Fe(\mu-NO)]_2$ , ferrocene, and vinylcyclopentadiene.<sup>12</sup>

**Bridging Methylidyne Complex 4.** The reaction of **2** with trityl is sensitive to both temperature and concentration. When  $CH_2Cl_2$  was added via syringe to an intimate 1:1 mixture of solids **2** and  $(C_6H_5)_3C^+PF_6^-$  at 20 °C and stirred for 1 h, both **3** and the methylidyne complex  $\{[(C_5H_5)Fe(\mu-NO)]_2(\mu-CH)\}^+PF_6^-$  (**4**) were formed in approximately 30% and 25% crude yield, respectively. In addition to **3** and **4**, a third product with the empirical formula  $\{[(C_5H_5)Fe(NO)]_2(\mu-CH_2)C(C_6H_5)_3\}^+PF_6^-$  (**5**) was observed in varying (5–20%) yield.



Methylidyne complex **4** is less soluble than **3** and **5** in  $CH_2Cl_2$  and was isolated as a dark brown solid from the reaction mixture in 50–70% purity. **4** was obtained in greater than 90% purity by repeated extraction and precipitation from THF. Nonetheless, the carbon analyses for **4** were consistently high (0.9%) despite our best purification efforts.

The structure of methylidyne complex **4** was assigned on the basis of spectroscopic data. The IR spectrum of **4** in KBr exhibits three strong nitrosyl bands at 1617, 1572, and 1518  $cm^{-1}$ , assigned to two bridging nitrosyl ligands. These bands are more than 200  $cm^{-1}$  lower in energy than the terminal nitrosyl bands for **3**. We do not understand why conversion of methylidyne complex **2** to cationic methylidyne complex **4** results in bridging of the nitrosyl ligands. The  $^1H$  NMR spectrum of **4** is quite similar to that of the analogous carbonyl methylidyne complex **1**, with a single low-field resonance at  $\delta$  22.91 (s, 1 H) and a singlet at  $\delta$  5.26 (10 H) for the cyclopentadienyl protons. The  $^{13}C$  resonance for the methylidyne carbon of **4** at  $\delta$  348.1 is substantially upfield from that of **1**, which appears at  $\delta$  490.2.<sup>1</sup>

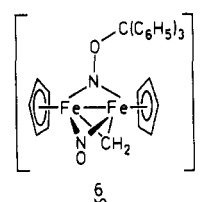
Reactions of **2** with other hydride abstractors were examined in an effort to find a more efficient route to **4**. However, treatment of **2** with either  $C_7H_7^+BF_4^-$  or  $(C_6H_5)_2CH^+SbCl_6^-$  gave complex product mixtures. Treatment with  $(p-CH_3C_6H_4)_3C^+PF_6^-$  afforded essentially the same product mixtures as  $(C_6H_5)_3C^+PF_6^-$ .

(11) (a) Kao, S. C.; Lu, P. P. Y.; Pettit, R. *Organometallics* 1982, 1, 911. (b) Dyke, A. F.; Knox, S. A. R.; Morris, M. J.; Naish, P. J. *J. Chem. Soc., Dalton Trans.* 1983, 1417.

(12) Vinylcyclopentadiene has been tentatively identified as a decomposition product of **3** on the basis of  $^1H$  NMR (500 MHz, acetone- $d_6$ ):  $\delta$  6.64 (dd pentets,  $J = 17.3, 11.0, 0.6$  Hz, 1 H), 6.45 (dt,  $J = 5.4, 1.8$  Hz, 1 H), 6.40 (m, 1 H), 6.30 (dm,  $J = 5.4$  Hz, 1 H), 5.29 (dddd,  $J = 17.3, 1.6, 0.8, 0.6$  Hz, 1 H), 4.95 (ddt,  $J = 10.7, 1.6, 0.5$  Hz, 1 H), 3.10 (dtd,  $J = 1.7, 1.6, 0.6$  Hz, 1 H). The regioisomer assignment (i.e., 1- or 2-vinylcyclopentadiene) was not determined from these data.

**Nitrosyl Alkylation Product 5.** When a dichloromethane solution of  $(C_6H_5)_3C^+PF_6^-$  was slowly added to a stirred solution of methylene complex **2** at ambient temperature, a third product, **5**, was obtained in 42% crude yield. Small amounts of **3** and **4** were removed from the sample by washing with THF, and **5** was isolated as a THF solvate, 95% pure by  $^1H$  NMR spectroscopy.

Spectroscopic data for **5** establish its formulation as  $\{[(C_5H_5)Fe]_2(\mu-NO)(\mu-CH_2)(C(C_6H_5)_3NO)\}^+PF_6^-$ . The  $^1H$  NMR spectrum for **5** exhibits nonequivalent methylene proton resonances at  $\delta$  13.03 (d,  $J = 0.7$  Hz, 1 H) and 11.85 (d,  $J = 0.7$  Hz, 1 H), phenyl resonances at  $\delta$  7.37 (m, 9 H) and 7.02 (m, 6 H), and two resonances at  $\delta$  5.56 (s, 5 H) and 5.05 (s, 5 H) attributed to nonequivalent cyclopentadienyl rings. In the IR spectrum of **5** a single strong band at 1588  $cm^{-1}$  was observed, indicating the presence of only one bridging NO ligand. The structure shown for **5** is consistent with these data.<sup>13</sup> The nitrosyl alkylation product might also be formulated as the O-alkylated structure **6**. A priori, O-alkylation is a reasonable possibility since Gladfelter has demonstrated that  $[Ru(CO)_{10}(\mu-NO)]^-$  can be O-alkylated.<sup>14</sup> However, the restricted rotation about the N–O bond of **6** that would be required to explain the observation of two different Cp resonances seems highly unlikely.



#### Mechanism of Bridging Vinyl Complex Formation.

The stoichiometry of the formation of bridging vinyl complex **3** involves 2 equiv of methylene complex **2** and 1 equiv of  $(C_6H_5)_3C^+PF_6^-$  (eq 1). This stoichiometry suggested the possibility that **3** might be formed by initial hydride abstraction from **2** to produce methylidyne complex **4** which could then abstract a methylene group from a second equivalent of **2** to produce the observed products. The abstraction of methylene from **2** seemed plausible since the methylene abstraction product is the stable metal–metal double-bonded complex  $[(C_5H_5)Fe(\mu-NO)]_2$ . However, this mechanism has been ruled out. When methylene complex **2** and methylidyne complex **4** were stirred together in methylene chloride at ambient temperature, no  $\mu$ -vinyl complex **3** was detected by  $^1H$  NMR spectroscopy. Instead, **2** appears to decompose in the presence of **4** to an uncharacterized mixture of products. Other possible mechanisms for formation of bridging vinyl complex **3** include coupling of the radical cation of **2** with a second molecule of **2** followed by hydrogen atom abstraction and fragmentation.

**Reactivity of Methylidyne Complex 4.** Methylidyne complex **4** is slightly soluble and stable in methylene chloride or THF. It is more soluble in acetone or acetonitrile but decomposes within several hours in these solvents. Unlike the carbonyl methylidyne complex **1** which forms stable 1:1 adducts with nucleophiles, the nitrosyl

(13) We know of no simple examples of N-alkylation of nitrosyl ligands. In a recent review, McCleverty has proposed  $RuBr(CO)(PPh_3)[PhCH_2NO]$  as an intermediate in the reaction of  $Ru(NO)_2(PPh_3)_2$  with  $PhCH_2Br$  under CO. McCleverty, J. A. *J. Mol. Catal.* 1981, 13, 309. Transition-metal complexes with  $(\mu-\eta^1, \eta^2-RNO)$  ligands have been reported: (a) Barrow, M. J.; Mills, O. S. *J. Chem. Soc. A* 1971, 364. (b) Calligaris, M.; Yoshida, T.; Otsuka, S. *Inorg. Chim. Acta* 1974, 11, L15. (14) Stevens, R. E.; Gladfelter, W. L. *J. Am. Chem. Soc.* 1982, 104, 6454.

methylidyne complex **4** decomposes to give predominantly  $[(C_5H_5)Fe(\mu-NO)]_2$  upon treatment with  $KO-t-Bu$ ,  $NMe_3$ ,  $PMe_3$  or  $H_2O$ . Attempted conversion of methylidyne complex **4** to methylene complex **2** by treatment with  $NEt_4^+HFe(CO)_4^-$  also led to formation of  $[(C_5H_5)Fe(\mu-NO)]_2$ . The carbonyl methylidyne complex **1** reacts with CO to form an acylium complex as a 1:1 adduct, but the nitrosyl methylidyne complex **4** showed no evidence of reaction with CO in acetone.

The most unusual reaction of the carbonyl methylidyne complex **1** is its hydrocarbation of alkenes which occurs rapidly at  $-50^\circ C$ . However, nitrosyl methylidyne complex **4** does not react with isobutylene (the most reactive alkene toward **1**) at ambient temperature in acetone.

**Attempted Synthesis of Other Methylidyne Complexes.** Attempted generation of methylidyne complexes by  $(C_6H_5)_3C^+PF_6^-$  mediated hydride abstraction from either  $[(C_5Me_5)(CO)Rh]_2(\mu-CH_2)^{15}$  or  $[(C_5Me_5)CH_3Rh]_2(\mu-CH_2)^{16}$  failed to produce any far downfield  $^1H$  NMR signals attributable to a bridging methylidyne unit.

Since our initial attempts to prepare additional examples of cationic bridging methylidyne complexes related to **1** have proven extremely difficult and since only the closest relatives of **1** undergo hydrocarbation reactions, we are beginning to suspect that the stability and reaction chemistry of methylidyne complex **1** is indeed very special.

### Experimental Section

**General Data.** All manipulations were carried out by using either high vacuum line or glovebox techniques. Solvents were distilled from sodium and benzophenone (THF, ether),  $P_2O_5$  ( $CH_2Cl_2$ ), or  $B_2O_3$  (acetone) prior to use. The 270-MHz  $^1H$  NMR spectra were recorded on a Bruker WP270 spectrometer;  $^{13}C$  NMR spectra were recorded on a JEOL FX200 (50.10 MHz) or a Bruker AM500 (125.76 MHz) spectrometer. Infrared spectra were recorded on a Beckman 4230 IR spectrometer. Elemental analyses were performed by Schwarzkopf Microanalytical Labs.

$\{[(C_5H_5)(NO)Fe]_2(\mu-\eta^1, \eta^2-CH=CH_2)\}^+PF_6^-$  (**3**). **Method A.** A mixture of bridging methylidene complex **2** (237 mg, 0.75 mmol) and  $(C_6H_5)_3C^+PF_6^-$  (146 mg, 0.38 mmol) in 3 mL of  $CH_2Cl_2$  was stirred for 2 h at  $-78^\circ C$  and then slowly warmed to ambient temperature. The solvent was evaporated under vacuum, and the residue was slurried in 3 mL of acetone at  $-78^\circ C$  and filtered to remove insoluble  $[(C_5H_5)Fe(\mu-NO)]_2$ . The acetone was evaporated under vacuum at  $0^\circ C$ , the residue was taken up in 2 mL of  $CH_2Cl_2$ , and 8 mL of ether was added to give **3** (132 mg, 74% based on  $(C_6H_5)_3C^+PF_6^-$  as the limiting reagent) as a red-brown microcrystalline solid.

**Method B.** A solution of bridging ethylidene complex  $[(C_5H_5)(NO)Fe]_2(\mu-CHCH_3)^{10}$  (209 mg, 0.63 mmol) and  $(C_6H_5)_3C^+PF_6^-$  (246 mg, 0.63 mmol) in 5 mL of  $CH_2Cl_2$  was stirred

for 15 min at  $0^\circ C$  and then at ambient temperature for 1 h. A workup procedure similar to that of method A gave **3** (211 mg, 70%):  $^1H$  NMR (acetone- $d_6$ ,  $20^\circ C$ )  $\delta$  10.96 (dd,  $J = 14.3, 7.9$  Hz, 1 H), 5.90 (s, 5 H), 5.88 (s, 5 H), 4.98 (dd,  $J = 7.9, 1.1$  Hz, 1 H), 3.65 (dd,  $J = 14.3, 1.1$  Hz, 1 H);  $^{13}C$  NMR (50.10 MHz, acetone- $d_6$ ,  $0.07$  M  $Cr(acac)_3$ ,  $-10^\circ C$ )  $\delta$  187.7 (d,  $J = 154$  Hz,  $CH=CH_2$ ), 95.1 (d,  $J = 185$  Hz,  $C_5H_5$ ), 94.5 (d,  $J = 181$  Hz,  $C_5H_5$ ), 69.8 (t,  $J = 188$  Hz,  $CH=CH_2$ ); IR (Nujol) 1822, 1774  $cm^{-1}$ .

Anal. Calcd for  $C_{12}H_{13}F_6Fe_2N_2O_2P$ : C, 30.41; H, 2.77; N, 5.91. Found: C, 30.31; H, 2.97; N, 5.73.

$\{[(C_5H_5)Fe(\mu-NO)]_2(\mu-CH)\}^+PF_6^-$  (**4**).  $CH_2Cl_2$  (10 mL) was added via syringe to a solid mixture of bridging methylidene **2** (937 mg, 2.97 mmol) and  $(C_6H_5)_3C^+PF_6^-$  (1.324 g, 3.40 mmol) at ambient temperature with rapid stirring. After 45 min the resulting dark brown solid was isolated by filtration at  $-78^\circ C$ , washed with cold  $CH_2Cl_2$  ( $3 \times 5$  mL), and dried to give crude **4** (665 mg, 70% pure by  $^1H$  NMR). Samples of **4** of greater purity were obtained in low yield by successive THF extractions. For example, 200 mg of 70% pure **4** was stirred with 140 mL of THF at ambient temperature. The THF solution was filtered and evaporated to dryness under vacuum. The resulting solid was dissolved in 5 mL of acetone at  $-78^\circ C$ , and the solution was filtered and evaporated to dryness at  $0^\circ C$ . The resulting solid was slurried with 3 mL of THF at ambient temperature and cooled to  $-78^\circ C$  to give 50 mg of 93% pure **4**:  $^1H$  NMR (acetone- $d_6$ )  $\delta$  22.91 (s, 1 H), 5.26 (s, 10 H);  $^{13}C\{^1H\}$  NMR (125.76 MHz, acetone- $d_6$ , 0.07 M  $Cr(acac)_3$ ,  $-25^\circ C$ )  $\delta$  348.1 ( $Fe_2CH$ ), 96.0 ( $C_5H_5$ ); IR (KBr) 1617 (s), 1572 (m), 1518 (m)  $cm^{-1}$ .

Anal. Calcd for  $C_{11}H_{11}F_6Fe_2N_2O_2P$ : C, 28.73; H, 2.41; N, 6.09. Found: C, 29.69; H, 2.67; N, 6.10.

$\{[(C_5H_5)Fe]_2(\mu-NO)(\mu-CH_2)(C(C_6H_5)_3NO)\}^+PF_6^-$  (**5**). A solution of  $(C_6H_5)_3C^+PF_6^-$  (330 mg, 0.85 mmol) in 5 mL of  $CH_2Cl_2$  was added dropwise to a rapidly stirred solution of bridging methylidene **2** (268 mg, 0.85 mmol) over the course of 30 min at ambient temperature. Solvent was evaporated under vacuum, and the residue was dissolved in 3 mL of acetone at  $-78^\circ C$  and filtered to remove  $[(C_5H_5)Fe(\mu-NO)]_2$  (58 mg, 0.19 mmol). Solvent was evaporated, and the residue was slurried with 5 mL of THF, filtered, and dried for 24 h under high vacuum to give purple-brown crystalline **5** (373 mg, 42%) as a 1:1 THF solvate, contaminated by a small amount of **4**. **5** was further purified by THF extraction as described for **4**:  $^1H$  NMR (acetone- $d_6$ )  $\delta$  13.03 (d,  $J = 0.7$  Hz, 1 H), 11.85 (d,  $J = 0.7$  Hz, 1 H), 7.37 (m, 9 H), 7.02 (m, 6 H), 5.56 (s, 5 H), 5.05 (s, 5 H);  $^{13}C\{^1H\}$  NMR (50.10 MHz, acetone- $d_6$ , 0.07 M  $Cr(acac)_3$ ,  $-20^\circ C$ )  $\delta$  208.9 ( $Fe_2CH_2$ ), 141.1 (ipso), 130.3, 128.6 (ortho, meta), 128.4 (para), 102.8 ( $Ph_3C$ ), 97.9 ( $C_5H_5$ ), 96.7 ( $C_5H_5$ ); IR (KBr) 1588 (s), 1491 (w), 1447 (w), 1431 (w), 836 (s)  $cm^{-1}$ .

Anal. Calcd for  $C_{34}H_{35}Fe_2F_6N_2O_3P$ : C, 52.56; H, 4.54; N, 3.61. Found: C, 51.38; H, 4.51; N, 3.64.<sup>17</sup>

**Acknowledgment.** Research support from the National Science Foundation is gratefully acknowledged.

**Registry No.** **2**, 99748-60-4; **3**, 99766-96-8; **4**, 99748-62-6; **5**, 99748-64-8;  $[(C_5H_5)(NO)Fe]_2(\mu-CHCH_3)$ , 81014-33-7;  $(C_6H_5)_3C^+PF_6^-$ , 437-17-2;  $(p-CH_3C_6H_4)_3C^+PF_6^-$ , 1526-53-0; Fe, 7439-89-6.

(15) Herrmann, W. A.; Bauer, C.; Plank, J.; Kalcher, W.; Speth, D.; Ziegler, M. L. *Angew. Chem., Int. Ed. Engl.* **1981**, *20*, 193.

(16) Isobe, K.; Miguel, A. V. de; Bailey, P. M.; Okeya, S.; Maitlis, P. M. *J. Chem. Soc., Dalton Trans.* **1983**, 1441.

(17) Although samples of **5** were pure by  $^1H$  NMR and gave excellent hydrogen and nitrogen analyses, carbon analyses were consistently low.

# Oxidative Addition of Alkyl Halides in the Presence of Alkenes and the Rate of Addition of an Alkyl Radical to a Platinum(II) Complex

Patrick K. Monaghan and Richard J. Puddephatt\*

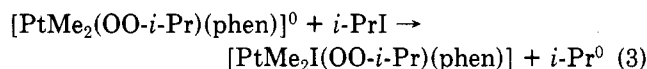
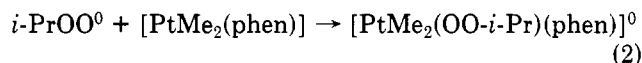
Department of Chemistry, University of Western Ontario, London, Ontario, Canada N6A 5B7

Received July 16, 1985

Dimethyl(1,10-phenanthroline)platinum(II) reacts with isopropyl or *tert*-butyl iodide, RI, in the presence of alkenes [CH<sub>2</sub>=CHX where X = CN, CHO, or C(=O)Me] to give the new functionally substituted organoplatinum(IV) complexes [PtMe<sub>2</sub>(CHXCH<sub>2</sub>R)(phen)] in high yield. The complexes were characterized by NMR and IR spectroscopy and by elemental analysis. The reactions occur by a free radical chain reaction, in which the radical R<sup>0</sup> reacts with CH<sub>2</sub>=CHX to give RCH<sub>2</sub>CHX<sup>0</sup>, which then reacts with [PtMe<sub>2</sub>(phen)] to give [PtMe<sub>2</sub>(CHXCH<sub>2</sub>R)(phen)]<sup>0</sup>; iodine atom abstraction from RI by this platinum(III) radical completes the cycle. A competition experiment, in which radicals R<sup>0</sup> react with either [PtMe<sub>2</sub>(phen)] or CH<sub>2</sub>=CHCN, gives an approximate rate constant for addition of the *i*-Pr<sup>0</sup> radical to [PtMe<sub>2</sub>(phen)] of 10<sup>7</sup> M<sup>-1</sup> s<sup>-1</sup>, one of the first rate constants for radical addition to a diamagnetic transition-metal complex. A second competition experiment shows that the relative rate of iodine abstraction from *t*-BuI and *i*-PrI by the platinum(III) radical is 1.7 ± 0.2. It is suggested that this radical trapping technique will have general use in identifying the free radical mechanism of oxidative addition.

## Introduction

The complex [PtMe<sub>2</sub>(1,10-phenanthroline)]<sup>1</sup> (1) is very reactive toward oxidative addition of alkyl halides, and studies of reactivity and mechanism in such reactions have been made.<sup>2,3</sup> The reaction of *i*-PrI with 1 in the presence of air gave not only the oxidative addition product 2 but also complexes 3 and 4.<sup>4,5</sup> This reaction was shown to occur primarily by a free radical chain mechanism, and complex 3 was formed by the sequence of reactions 1-3.<sup>5,6</sup>



According to this mechanism, it should be possible to "insert" not only oxygen but also other unsaturated molecules A=B during the oxidative addition, provided that they trap the primary *i*-Pr<sup>0</sup> radical efficiently and that the radical *i*-Pr-A-B<sup>0</sup> then adds to platinum rather than reacting with more A=B or undergoing other reactions. In this paper, the results of reactions in which the unsaturated reagents are the activated alkenes CH<sub>2</sub>=CHX, where X = CN, CHO, or C(Me)O, are described. A preliminary account of parts of this work has been published.<sup>5</sup>

## Results and Discussion

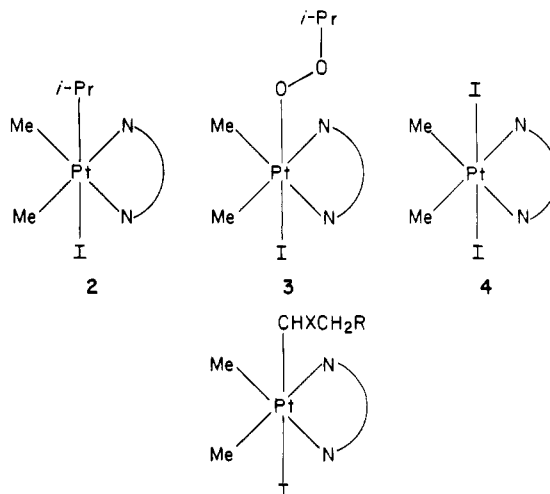
**Synthesis of New Complexes.** In the absence of oxygen, complex 1 in acetone solution reacted with *i*-PrI in diffuse daylight to give 2 in pure form.<sup>4</sup> When the reactions were carried out in the presence of excess alkene CH<sub>2</sub>=CHX, the new products 5a-c were formed in high yield. The concentration of alkene was important in op-

Table I. Products Formed by Reaction of [PtMe<sub>2</sub>(phen)] with *i*-PrI (0.4 M) and CH<sub>2</sub>=CHCN in Acetone at 20 °C

10 <sup>3</sup> [PtMe <sub>2</sub> (Phen)], M	[CH <sub>2</sub> =CHCN], M	product ratio <i>x</i> = 5a/2	<i>k</i> <sub>1</sub> / <i>k</i> <sub>2</sub> <sup>a</sup>
4.2	0.12	2.4	23.8
3.2	0.12	3.8	19.7
2.1	0.12	4.7	24.3
4.2	0.40	7.6	25.0
4.2	0.20	4.6	20.7
4.2	0.10	2.5	19.0
4.2	0.06	1.7	16.8
4.2	0.02	1.0	9.5

$$^a k_1/k_2 = [\text{CH}_2=\text{CHCN}]/0.5[\text{PtMe}_2(\text{phen})]_0.$$

timizing yields. With low concentrations of alkene considerable amounts of 2 were formed (Table I) whereas, with very high concentrations of alkene, some polymer was formed. This polymerization limited the range of substituents, X, in the alkenes CH<sub>2</sub>=CHX, which could be accommodated. For example, styrene and methyl acrylate or methacrylate gave large amounts of polymer and it was not possible to isolate complexes of structure 5.



- 5a. X = CN; R = *i*-Pr  
 b. X = CHO; R = *i*-Pr  
 c. X = C(=O)Me; R = *i*-Pr  
 d. X = CN; R = *t*-Bu  
 e. X = CHO; R = *t*-Bu

(1) Chaudhury, N.; Puddephatt, R. J. *J. Organomet. Chem.* **1975**, *84*, 105.

(2) Jawad, J. K.; Puddephatt, R. J. *J. Organomet. Chem.* **1976**, *117*, 297; *J. Chem. Soc., Dalton Trans.* **1977**, 1466.

(3) Monaghan, P. K.; Puddephatt, R. J. *Inorg. Chim. Acta* **1983**, *76*, L237.

(4) Ferguson, G.; Parvez, M.; Monaghan, P. K.; Puddephatt, R. J. *J. Chem. Soc., Chem. Commun.* **1983**, 267; *Organometallics*, in press.

(5) Monaghan, P. K.; Puddephatt, R. J. *Organometallics* **1983**, *2*, 1698.

(6) Hill, R. H.; Puddephatt, R. J. *J. Am. Chem. Soc.* **1985**, *107*, 1218.

Table II.  $^1\text{H}$  NMR Data for Complexes  $[\text{Pt}(\text{Me})_2\text{CH}_2(\text{X})\text{CH}_2\text{H}_2\text{R}(\text{N}\text{N})]^{\text{a}}$ 

complex	PtMe		R		$\text{H}_\alpha, \text{H}_\beta, \text{H}_\gamma$	
	$\delta$	$^2J(\text{PtH})/\text{Hz}$	$\delta$	$J/\text{Hz}$	$\delta$	$J/\text{Hz}$
[PtMe <sub>2</sub> CH(CN)CH <sub>2</sub> - <i>i</i> -Pr(phen)] <sup>b</sup>	1.68	71	0.40 (CH <sub>3</sub> )	6 [ <sup>3</sup> J(HH)]	2.26 (H <sub>α</sub> )	13 [ <sup>3</sup> J(H <sub>α</sub> H <sub>β</sub> )]
	1.75	72.5	0.70 (CH <sub>3</sub> )	6 [ <sup>3</sup> J(HH)]		4 [ <sup>3</sup> J(H <sub>α</sub> H <sub>γ</sub> )]
			1.43 (CH)	6 [ <sup>3</sup> J(HH)]		92 [ <sup>2</sup> J(PtH)]
					0.08 (H <sub>β</sub> )	4 [ <sup>2</sup> J(H <sub>β</sub> H <sub>γ</sub> )]
						13 [ <sup>2</sup> J(H <sub>β</sub> H)]
					0.65 (H <sub>γ</sub> )	11 [ <sup>3</sup> J(H <sub>γ</sub> H)]
[PtMe <sub>2</sub> CH(CHO)CH <sub>2</sub> - <i>i</i> -Pr(phen)] <sup>c</sup>	1.82	71	0.49 (CH <sub>3</sub> )	6 [ <sup>3</sup> J(HH)]	2.95 (H <sub>α</sub> )	
	1.88	72	0.64 (CH <sub>3</sub> )	6 [ <sup>3</sup> J(HH)]		
			1.17 (CH) <sup>d</sup>			
[PtMe <sub>2</sub> CH(OMe)CH <sub>2</sub> - <i>i</i> -Pr(phen)] <sup>c</sup>	1.74	70	0.52 (CH <sub>3</sub> )	6 [ <sup>3</sup> J(HH)]	2.94 (H <sub>α</sub> )	
	1.85	70.5	0.67 (CH <sub>3</sub> )	6 [ <sup>3</sup> J(HH)]		
[PtMe <sub>2</sub> CH(CN)CH <sub>2</sub> - <i>t</i> -Bu(phen)] <sup>f</sup>	1.68	70.5	0.67 (CH <sub>3</sub> )		3.25 (H <sub>α</sub> )	2 [ <sup>3</sup> J(H <sub>α</sub> H <sub>β</sub> )]
	1.76	71.0				12.5 [ <sup>3</sup> J(H <sub>α</sub> H <sub>β</sub> )]
						96 [ <sup>2</sup> J(PtH <sub>α</sub> )]
					0.23 (H <sub>β</sub> )	13 [ <sup>2</sup> J(H <sub>β</sub> H <sub>α</sub> )]
					0.83 (H <sub>γ</sub> )	48 [ <sup>3</sup> J(PtH)]
[PtMe <sub>2</sub> CH(CHO)CH <sub>2</sub> - <i>t</i> -Bu(phen)] <sup>g</sup>	1.81	71.5			2.86 (H <sub>α</sub> )	
	1.76	71.5	0.57 (CH <sub>3</sub> )			

<sup>a</sup> N = phen; X = CN, CHO, or C(=O)Me; R = *i*-Pr or *t*-Bu. <sup>b</sup> Solvent, CDCl<sub>3</sub>. Spectrum run on Bruker AM250 instrument. <sup>c</sup> Solvent, CDCl<sub>3</sub>;  $\delta$  8.76 [m, <sup>3</sup>J(HH) = 3, <sup>3</sup>J(PtH) = 10 Hz, CHO]. <sup>d</sup> Tentative assignment, due to poor resolution. <sup>e</sup> Solvent, CDCl<sub>3</sub>;  $\delta$  1.40 [s, COMe]. <sup>f</sup> Solvent, CD<sub>2</sub>Cl<sub>2</sub>. <sup>g</sup> Solvent, CD<sub>2</sub>Cl<sub>2</sub>;  $\delta$  8.55 [m, CHO].

Table III.  $^{13}\text{C}\{^1\text{H}\}$  NMR Data for Complexes  $[\text{Pt}(\text{Me})_2\text{C}_\alpha\text{H}(\text{X})\text{C}_\beta\text{H}_2\text{R}(\text{N}\text{N})]^{\text{a}}$ 

complex	Pt-Me		R		$\text{C}_\alpha, \text{C}_\beta$		X	
	$\delta$	$^1J(\text{PtC})/\text{Hz}$	$\delta$	$J(\text{PtC})/\text{Hz}$	$\delta$	$J(\text{PtC})/\text{Hz}$	$\delta$	$J(\text{PtC})/\text{Hz}$
[PtMe <sub>2</sub> CH(CN)CH <sub>2</sub> - <i>i</i> -Pr(phen)] <sup>b</sup>	-4.36	638	27.46 (CH)	60.9 ( <sup>3</sup> J <sub>PtC</sub> )	11.35 (C <sub>α</sub> )	681.3 ( <sup>1</sup> J <sub>PtC</sub> )		
			23.37 (CH <sub>3</sub> )					
[PtMe <sub>2</sub> CH(OMe)CH <sub>2</sub> - <i>i</i> -Pr(phen)] <sup>c</sup>	-4.69	634	20.82 (CH <sub>3</sub> )		41.31 (C <sub>β</sub> )	32.5 ( <sup>2</sup> J <sub>PtC</sub> )		
	-2.57	672	27.98 (CH)	70.3 ( <sup>3</sup> J <sub>PtC</sub> )	44.58 (C <sub>α</sub> )	583.5 ( <sup>1</sup> J <sub>PtC</sub> )	209.39 (C=O)	
[PtMe <sub>2</sub> CH(CHO)CH <sub>2</sub> - <i>i</i> -Pr(phen)] <sup>c</sup>	-4.93	660	21.75 (CH <sub>3</sub> )		40.18 (C <sub>β</sub> )	34.7 ( <sup>2</sup> J <sub>PtC</sub> )	31.34 (CH <sub>3</sub> CO)	
	-3.81	647.9	23.62 (CH <sub>3</sub> )	66.6 ( <sup>3</sup> J <sub>PtC</sub> )	43.94 (C <sub>α</sub> )	553.6 ( <sup>1</sup> J <sub>PtC</sub> )	202.32	50 ( <sup>2</sup> J <sub>PtC</sub> )
[PtMe <sub>2</sub> CH <sub>2</sub> (CHO)CH <sub>2</sub> - <i>t</i> -Bu(phen)] <sup>c</sup>	-6.24	638.9	21.57 (CH <sub>3</sub> )		37.49 (C <sub>β</sub> )	33.3 ( <sup>2</sup> J <sub>PtC</sub> )		
			23.45 (CH <sub>3</sub> )					
[PtMe <sub>2</sub> CH <sub>2</sub> (CHO)CH <sub>2</sub> - <i>t</i> -Bu(phen)] <sup>c</sup>	-3.47	650.5	30.74 [C(CH <sub>3</sub> ) <sub>3</sub> ]		42.74 (C <sub>α</sub> )	543 ( <sup>1</sup> J <sub>PtC</sub> )	201.81	60.2 ( <sup>2</sup> J <sub>PtC</sub> )
	-5.44	652.0	29.64 (CH <sub>3</sub> )		42.17 (C <sub>β</sub> )	34.8 ( <sup>2</sup> J <sub>PtC</sub> )		

<sup>a</sup> R = *i*-Pr or *t*-Bu; X = CN, CHO, or C(=O)Me. <sup>b</sup> Solvent, CDCl<sub>3</sub>. <sup>c</sup> Solvent, CD<sub>2</sub>Cl<sub>2</sub>.

Reaction of *t*-BuI with complex 1 gave only 4, 4' but, in the presence of alkene CH<sub>2</sub>CHX, the complexes 5d and 5e could be prepared without difficulty. In this case, the reactions occurred rapidly even in the dark and dichloromethane was the preferred solvent.

**Characterization of Complexes.** Elemental analyses were consistent with the structures 5, and the major problem in characterization was to determine the structure of the added radical. The radicals RCH<sub>2</sub>CHX<sup>0</sup>, R = *i*-Pr or *t*-Bu, can exist in two resonance forms either of which could be trapped by the platinum center of complex 1. This is illustrated for the acrolein-derived radical in eq 4.



Trialkylboranes, R<sub>3</sub>B, apparently trap the oxygen-centered radical to give RCH<sub>2</sub>CH=CHOBR<sub>2</sub>,<sup>7</sup> but the spectroscopic data for complexes 5 show conclusively that platinum traps the carbon-centered radical. The IR spectra for 5a, 5b, and 5c give typical stretching vibrations for  $\nu(\text{C}\equiv\text{N})$  or  $\nu(\text{C}=\text{O})$  at 2200, 1650, and 1665 cm<sup>-1</sup>, respectively, and the NMR spectra provided conclusive evidence for these structures. A complete assignment of the <sup>1</sup>H and <sup>13</sup>C NMR

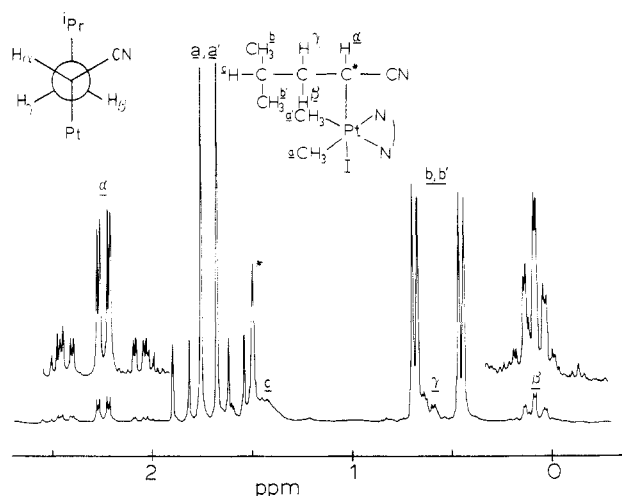
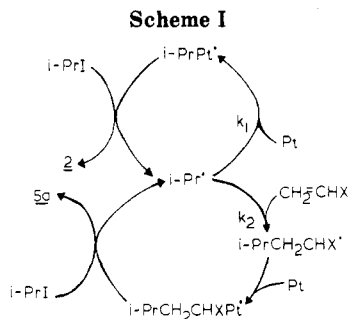


Figure 1.  $^1\text{H}$  NMR spectrum (400 MHz) of complex 5a. The peak labeled with an asterisk is due to water impurity.

spectra of 5a was made by recording the <sup>1</sup>H (250 and 400 MHz), <sup>13</sup>C{<sup>1</sup>H}, and <sup>13</sup>C INEPT spectra and by a two-dimensional heteronuclear <sup>1</sup>H-<sup>13</sup>C chemical shift correlated experiment. Part of the <sup>1</sup>H NMR spectrum is shown in Figure 1, along with the Newman projection of the pro-

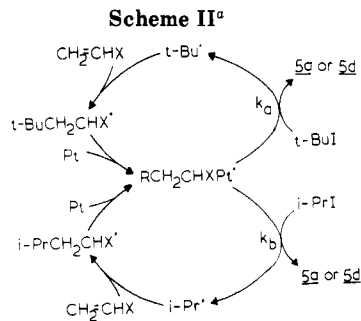


<sup>a</sup>Pt = [PtMe<sub>2</sub>(Phen)].

posed dominant conformer. The chiral carbon, bound to platinum, leads to nonequivalence of the Me<sub>2</sub>Pt, CH<sub>2</sub>, and CHMe<sub>2</sub> groups. The assignments are given in Figure 1 and, for the less intense signals due to H<sub>α</sub>, H<sub>β</sub>, H<sub>γ</sub>, and H<sub>δ</sub>, were confirmed by the 2-D experiment. The spectra are not consistent with the possible N-bonded isomer, the most unambiguous evidence being the observation of <sup>1</sup>J(PtC\*) = 681 Hz. The complete spectral parameters are listed in Tables II and III. The very different vicinal couplings <sup>2</sup>J(H<sub>α</sub>H<sub>β</sub>) = 13 Hz and <sup>2</sup>J(H<sub>α</sub>H<sub>γ</sub>) = 4 Hz (Figure 1, H<sub>α</sub> signal) are expected (from the Karplus equation) if the conformation shown in Figure 1 is dominant. Assignment of the <sup>1</sup>H and <sup>13</sup>C NMR spectra of **5b-e** was straightforward by comparison with the spectra of **5a**.

**The Mechanism of Reaction.** The reactions described above, like those in the absence of alkenes,<sup>4-6</sup> occur by a free radical chain reaction. This has been confirmed by showing that trace amounts of the free radical scavenger 4-methoxyphenol inhibit the reaction of **1** with *i*-PrI and CH<sub>2</sub>=CHCN in diffuse light.<sup>8</sup> The mechanism is shown in Scheme I, and this scheme also shows how a competition experiment, in which the primary *i*-Pr<sup>0</sup> radicals can be trapped by alkene or attack complex **1** directly to yield **5a** or **2**, respectively, can be set up. According to this mechanism, decreasing the concentration of **1** or increasing the concentration of alkene CH<sub>2</sub>=CHX should increase the product ratio **5a**/2. The data in Table I show that this is indeed observed. The product ratio was determined by integration of the resonances due to the methyl protons of the isopropyl groups in the <sup>1</sup>H NMR spectra. Quantitatively, the product ratio,  $x = \frac{5a}{2} = \frac{k_2[\text{CH}_2=\text{CHCN}]}{k_1[\mathbf{1}]}$ , from which  $k_1/k_2 = \frac{[\text{CH}_2=\text{CHCN}]}{x[\mathbf{1}]}$ . The individual values of  $k_1/k_2$  found in this way are listed in Table I and give a mean value of  $k_1/k_2 = 20 \pm 6$ .<sup>9</sup>

An approximate value for  $k_2$  can be estimated. Extrapolation of kinetic data for the reaction Et<sup>0</sup> + CH<sub>2</sub>=CHCN at high temperatures in the gas phase gives  $k_2 \approx 2 \times 10^5 \text{ L mol}^{-1} \text{ s}^{-1}$  at 20 °C.<sup>10</sup> It must then be assumed that *i*-Pr<sup>0</sup> reacts at the same rate as Et<sup>0</sup> and that the rates are equal for acetone solution and the gas phase. Very recently, the rate of reaction of the 5-hexenyl radical with acrylonitrile has been determined directly at 20 °C in solution in CH<sub>2</sub>Cl<sub>2</sub> and CH<sub>3</sub>CN/CH<sub>3</sub>CO<sub>2</sub>H<sup>11</sup> and the second-order rate constant was found to be  $k_2 = 5 \times 10^5 \text{ L mol}^{-1} \text{ s}^{-1}$ ; this is considered a better approximation for the



<sup>a</sup>Pt = [PtMe<sub>2</sub>(phen)] (R = *t*-Bu or *i*-Pr).

rate of the reaction *i*-Pr<sup>0</sup> + CH<sub>2</sub>=CHCN in acetone solution at 20 °C.<sup>12</sup> Hence a value of  $k_1 \approx 1 \times 10^7 \text{ L mol}^{-1} \text{ s}^{-1}$  is calculated under the experimental conditions. This is best regarded only as an order of magnitude estimate of  $k_1$ , but it is significant as one of the first estimates of a rate of free radical addition to a diamagnetic transition metal complex.<sup>13</sup> A similar value has been estimated for addition of the isopropyl radical to [IrCl(CO)(PMe<sub>3</sub>)<sub>2</sub>], and rate constants of similar magnitude have been determined for S<sub>H</sub>2 reactions of main-group metal alkyls, such as trialkylboranes, in which free radical addition to the metal center may be rate determining.<sup>14</sup> For this electron-rich platinum(II) system the platinum(III) radical [PtMe<sub>2</sub>-*i*-Pr(phen)]<sup>0</sup> does not undergo dissociation of an alkyl radical to give an S<sub>H</sub>2 process and regenerate platinum(II) but instead abstracts an iodine atom from *i*-PrI to give the stable platinum(IV) complexes. It is this ability to undergo two-electron oxidation which makes the chemistry of these platinum(II) complexes so different from boron(III).

The reactions with *t*-BuI to give **5d** or **5e** occur by the same mechanism and are faster because of the greater ease of cleavage of the tertiary alkyl-iodide bond. This was confirmed by a study of the competition experiment of Scheme II. Here a mixture of **1** with excess acrylonitrile<sup>15</sup> competes for a mixture of *t*-BuI and *i*-PrI. The selectivity for formation of **5d** or **5a** is governed by the relative rates of iodine atom abstraction by the radical [PtMe<sub>2</sub>CH(CN)CH<sub>2</sub>R](phen)<sup>0</sup> from *t*-BuI or *i*-PrI, and hence the product ratio  $\frac{5d}{5a} = \frac{k_a[t\text{-BuI}]}{k_b[i\text{-PrI}]}$ . Experimental data were in good agreement with this relationship and gave the ratio of rate constants  $k_a/k_b = 1.7 \pm 0.2$ .

The kinetics of reaction of *i*-PrI with complex **1** in the presence of different concentrations of acrylonitrile were studied. The rates were measured by spectrophotometry, as described earlier for reactions in the absence of alkene.<sup>4</sup> As expected for a radical chain reaction the kinetics were complex, but the rates were not much affected by the presence or absence of acrylonitrile. The olefin therefore does not appear to affect the chain length to any significant extent, in marked contrast to the behavior of oxygen described previously.<sup>4</sup> The reactions described here occur remarkably cleanly due to a favorable combination of rate constants. Thus, the electron-rich isopropyl or *tert*-butyl radicals are trapped efficiently by the electrophilic alkenes to give the relatively electron-poor radicals RCH<sub>2</sub>CHX<sup>0</sup>. The rate constant for attack by this radical on more alkene

(8) Typical kinetic data were given in the preliminary communication as supplementary material.<sup>5</sup>

(9) A graph of [CH<sub>2</sub>=CHCN] vs.  $x[\mathbf{1}]$  gives a straight line of slope =  $26 \pm 1$ ,  $r = 0.992$ , but this does not pass through the origin. It is not clear if this is due to a systematic error in integration of NMR signals or to some other effect. As can be seen from Table I, fairly consistent values of  $k_1/k_2$  are obtained except at the lowest concentration of CH<sub>2</sub>=CHCN used. Since [1] decreases from [1]<sub>0</sub> to zero during the reaction, the value used in calculating  $k_1/k_2$  is  $0.5[1]_0$ .

(10) Abell, P. I. *Compr. Chem. Kinet.* 1976, 18, Chapter 3.

(11) Giese, B.; Kretzschmar, G. *Chem. Ber.* 1984, 117, 3160.

(12) The rate of radical attack on simple alkenes is not much different for primary and secondary alkyl radicals, so this approximation should be reasonably good.<sup>10</sup>

(13) Note that a very similar value has since been determined by an independent method.<sup>5</sup>

(14) Labinger, J. A.; Osborn, J. A.; Coville, N. J. *Inorg. Chem.* 1980, 19, 3236. Davies, A. G.; Roberts, B. P. In "Free Radicals"; Kochi, J. K., Ed.; Wiley: New York, 1973; Chapter 10.

(15) So that essentially none of complex **2** is formed under the experimental conditions.

ultimately to give polymers is then much lower than the rate of attack at the nucleophilic platinum center of 1 (note that the propagation rate constant for polymerization of acrylonitrile is ca.  $10^2$  at 20 °C in DMF solvent,<sup>16</sup> much lower than the rate of addition of the 5-hexenyl radical to acrylonitrile of  $5 \times 10^5$  L mol<sup>-1</sup> s<sup>-1</sup>). Hence complexes 5 are formed cleanly with the alkenes.

### Conclusions

The alkene trapping technique developed here has been shown to be useful for synthesizing unusual functionally substituted organometallic compounds. It is also useful as a test for a free radical mechanism of oxidative addition. Thus the alkene inserted compounds are not formed in reactions of 1 with primary alkyl iodides, such as MeI or EtI, or with the secondary alkyl bromide *i*-PrBr, all of which are thought to undergo oxidative addition by the S<sub>N</sub>2 mechanism.<sup>3,4</sup> The method is clearly capable of being extended to oxidative additions of other metal complexes, though complications can be expected when the metal complexes react with the alkenes used here.

If the complexes 5 underwent reductive elimination of RCH<sub>2</sub>CHXI, a catalytic cycle for addition of RI to CH<sub>2</sub>=CHX would be completed. It is possible that a mechanism, as in Schemes I and II, with the additional reductive elimination step could account for the photochemical addition of alkyl halides to acrylonitrile and related alkenes catalyzed by CuCl/PBu<sub>3</sub>. A similar mechanism, but with an initial two-electron oxidative addition step rather than the free radical mechanism established here, was proposed for this reaction.<sup>17</sup>

### Experimental Section

<sup>13</sup>C and <sup>1</sup>H NMR spectra were recorded by using Varian XL200 and XL100 spectrometers, respectively. IR spectra were recorded on a Beckman 4250 instrument. UV-visible spectra were recorded by using a Hewlett-Packard 8450A diode array spectrophotometer. All alkenes were distilled under vacuum before use. Elemental analysis was carried out by Guelph Chemical Laboratories, Ontario. The solvents used were CH<sub>2</sub>Cl<sub>2</sub> and acetone, and they were deoxygenated, before use, by means of several freeze/pump/thaw cycles, and all reactions were performed at ambient temperature and in diffuse daylight unless otherwise stated. *t*-BuI was purified by shaking in contact with a saturated aqueous solution of Na<sub>2</sub>S<sub>2</sub>O<sub>3</sub> and drying over anhydrous MgSO<sub>4</sub>.

**[PtMe<sub>2</sub>{CH(CHO)CH<sub>2</sub>-*i*-Pr}(phen)].** To a solution of [PtMe<sub>2</sub>(phen)] (0.06 g) in deoxygenated acetone (20 mL) was added acrolein (2 mL) followed by *i*-PrI (1 mL). The reaction was carried out under N<sub>2</sub>. The solution turned yellow after 15 min, the solvent removed under vacuum, and the solid residue

redissolved in CH<sub>2</sub>Cl<sub>2</sub> (3 mL). The product was recovered by precipitation using pentane (15 mL): yield 70%; mp 197 °C. Anal. Calcd for C<sub>22</sub>H<sub>25</sub>N<sub>3</sub>IOPt: C, 38.0; H, 4.0; N, 4.4. Found: C, 38.0; H, 3.9; N, 4.5. Similarly were prepared [PtMe<sub>2</sub>{CH(COMe)-CH<sub>2</sub>-*i*-Pr}(phen)] [Anal. Calcd for C<sub>23</sub>H<sub>27</sub>N<sub>3</sub>IOPt: C, 39.0; H, 4.2; N, 4.4. Found: C, 39.0; H, 4.1; N, 4.3.] and [PtMe<sub>2</sub>{CH(CN)-CH<sub>2</sub>-*i*-Pr}(phen)] [Anal. Calcd for C<sub>22</sub>H<sub>24</sub>N<sub>3</sub>IPT: C, 38.2; H, 3.8; N, 6.7. Found: C, 37.6; H, 3.7; N, 6.4.].

**[PtMe<sub>2</sub>{CH(CN)CH<sub>2</sub>-*t*-Bu}(phen)].** To a solution of [PtMe<sub>2</sub>(phen)] (0.09 g) in deoxygenated CH<sub>2</sub>Cl<sub>2</sub> (10 mL) was added acrylonitrile (2.5 mL) followed by freshly purified *t*-BuI (0.2 mL). The reaction was performed under N<sub>2</sub> and in the dark. After 1 h the solvent was reduced in volume (5 mL), and the product precipitated as a pale yellow solid by the addition of pentane (20 mL): yield 78%; mp 246 °C. Anal. Calcd for C<sub>23</sub>H<sub>26</sub>N<sub>3</sub>IPT: C, 39.1; H, 4.0; N, 6.5. Found: C, 38.0; H, 3.6; N, 6.0. In a similar way was prepared [PtMe<sub>2</sub>{CH(CHO)CH<sub>2</sub>-*t*-Bu}(phen)], Anal. Calcd for C<sub>23</sub>H<sub>27</sub>N<sub>3</sub>IOPt: C, 38.5; H, 4.2; N, 4.3. Found: C, 37.6; H, 3.9; N, 4.2.

**Competition Experiments.** Acrylonitrile (1.15 mL) was added to a solution of [PtMe<sub>2</sub>(phen)] (0.035 g) in deoxygenated CH<sub>2</sub>Cl<sub>2</sub> (25 mL). To this was added a mixture of *i*-PrI and *t*-BuI (1.0 mL, 1:1 ratio by volume). The reaction was carried out under N<sub>2</sub>, and the product was recovered by evaporation of the solvent followed by pentane washing of the residue. The product ratio was determined by integration of the <sup>1</sup>H NMR spectra. The procedure was repeated by varying only the relative amounts of *i*-PrI and *t*-BuI.

A similar method but using a constant [*i*-PrI] and varying [CH<sub>2</sub>=CHCN] was used in the competition experiments of Scheme I.

**Kinetic Studies.** To a solution of [PtMe<sub>2</sub>(phen)] (0.008 g) in acetone (35.0 mL) was added acrylonitrile (1.0 mL), and the sample was deoxygenated. The solution was kept under nitrogen. Working in the dark, a portion of the solution (5.0 mL) was transferred to a 1-cm quartz cuvette which was then sealed with a serum cap. Nitrogen gas was bubbled through the sample, and *i*-PrI (1.0 mL) was added. The cuvette was placed in the cell compartment of the UV-visible spectrophotometer. The decay of the band at 473 nm was monitored with time. A plot of log (*A*<sub>*t*</sub> - *A*<sub>∞</sub>) vs. time was made. This procedure was repeated several times by using the same concentrations of [PtMe<sub>2</sub>(phen)] and *i*-PrI but varying that of CH<sub>2</sub>CH(CN).

**Effect of Radical Inhibitor.** To a solution of [PtMe<sub>2</sub>(phen)] (0.004 g) in degassed acetone (20.0 mL) was added distilled CH<sub>2</sub>CH(CN) (0.8 mL). A portion was placed in a 1-cm quartz cuvette and, with use of the same procedure as in the last section, *i*-PrI (0.1 mL) was added. The decay of the band at 473 nm was monitored. This was done in diffuse light. The experiment was repeated by using CH<sub>2</sub>CH(CN) containing the radical scavenger 4-methoxyphenol (approximately 1%).

**Acknowledgment.** We thank NSERC (Canada) for financial support.

**Registry No.** 5a, 87338-36-1; 5b, 87338-37-2; 5c, 87350-68-3; 5d, 87338-38-3; 5e, 87338-39-4; [PtMe<sub>2</sub>(phen)], 52594-55-5; *i*-PrI, 75-30-9; CH<sub>2</sub>=CHC(=O)Me, 78-94-4; CH<sub>2</sub>=CHCN, 107-13-1; *t*-BuI, 558-17-8; acrolein, 107-02-8.

(16) Eastmond, G. C. *Compr. Chem. Kinet.* 1976, 14a, 232.

(17) Mitani, M.; Kato, I.; Koyama, K. *J. Am. Chem. Soc.* 1983, 105, 6719.

# Reactions of Alkyl and Hydride Derivatives of Permethylscandocene and -zirconocene with Nitriles and Amines. Catalytic Hydrogenation of *tert*-Butyl Cyanide with Permethylscandocene Hydride<sup>†</sup>

John E. Bercaw,\* David L. Davies, and Peter T. Wolczanski<sup>‡</sup>

Arthur Amos Noyes Laboratory of Chemical Physics, California Institute of Technology, Pasadena, California 91125

Received June 17, 1985

The compounds Cp\*<sub>2</sub>ScR (Cp\* = η<sup>5</sup>-C<sub>5</sub>Me<sub>5</sub>; R = H, Me, *p*-tol) react readily with nitriles R'CN to provide azomethine complexes Cp\*<sub>2</sub>ScNC(R)R' containing a C=N double bond (ν(CN) 1640–1680 cm<sup>-1</sup>). If Cp\*<sub>2</sub>ScMe is used, further reaction may occur to give products containing two nitriles. The related complex Cp\*<sub>2</sub>ZrH<sub>2</sub> will insert two nitriles in a stepwise manner; however, the dimethyl analogue is unreactive toward nitriles. The compounds Cp\*<sub>2</sub>ScNC(H)R may be hydrogenated under relatively mild conditions to yield the corresponding amide complexes Cp\*<sub>2</sub>ScNHCH<sub>2</sub>R. This transformation is reversible; addition of ethylene leads to dehydrogenation of the amide complex and production of ethane. The amide complexes may be independently synthesized by reaction of Cp\*<sub>2</sub>ScR (R = H, Me) and the corresponding amine, with resultant elimination of hydrogen or methane, respectively. Cp\*<sub>2</sub>ScNHCH<sub>2</sub>CMe<sub>3</sub> will catalytically hydrogenate (4 atm of H<sub>2</sub>) Me<sub>3</sub>CCN to Me<sub>3</sub>CCH<sub>2</sub>NH<sub>2</sub>; however, termination occurs by insertion of the nitrile into the scandium–amide bond to form Cp\*<sub>2</sub>ScNC(CMe<sub>3</sub>)NHCH<sub>2</sub>CMe<sub>3</sub>, the NC bond of which is not hydrogenated under these conditions. Labeling experiments show that hydrogen can add reversibly across the Sc–N bond of the amide, and this step is believed to play a crucial role in the catalytic reaction.

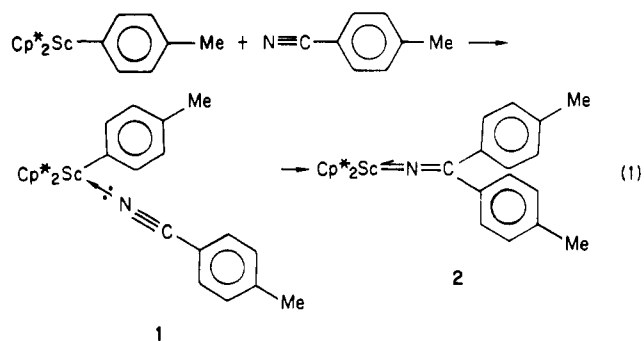
## Introduction

The chemistry of scandium may be expected to be intermediate between that of early transition metals and that of yttrium and the later lanthanide elements.<sup>1</sup> Moreover, coordinatively unsaturated organoscandium compounds appear to be voracious Lewis acids<sup>2</sup> and in this regard resemble the organic compounds of aluminum. We have a long standing interest in the organometallic chemistry of the group IV (4<sup>20</sup>) transition elements, particularly the Cp\*<sub>2</sub>MRR' (Cp\* = η<sup>5</sup>-C<sub>5</sub>Me<sub>5</sub>) derivatives. The chemistry of the group IV metals in their higher oxidation states is dominated by their propensity to form extremely strong bonds with "hard" donor atoms such as O, N, F, and Cl,<sup>3</sup> a similar reactivity would certainly be expected for the even "earlier" member scandium. These strong metal–heteroatom interactions are often invoked as providing the driving forces for many reactions involving substrates containing oxygen or nitrogen. Indeed, it has been generally assumed that products containing M–N or M–O bonds are entirely too inert for such early-transition-metal complexes to function as catalysts for the reduction of substrates containing nitrogen or oxygen. This manuscript describes the reactions of compounds of the general formula Cp\*<sub>2</sub>ScR and Cp\*<sub>2</sub>ZrR<sub>2</sub> with N–H bonds of amines and the C≡N triple bond of nitriles. The catalytic hydrogenation of *tert*-butyl cyanide by Cp\*<sub>2</sub>ScH under moderate conditions is observed, thus belying the previous assumption, at least for nitrogen-containing substrates. A preliminary exploration of some of the reactivity associated with the Sc–N bond in these complexes, particularly that which is relevant to the hydrogenation of nitriles, is described. The general features of the chemistry of scandium appear to be intermediate between those of aluminum and early transition metals.

## Results and Discussion

In the reaction Cp\*<sub>2</sub>Sc-*p*-tol with *p*-tolunitrile, an intermediate adduct, analogous to those found for alumi-

num,<sup>4</sup> may be isolated (eq 1). The <sup>1</sup>H NMR spectrum for



1 displays one signal due to equivalent Cp\* groups, but two resonances for the methyl substituents of the inequivalent *p*-tolyl groups, and the IR spectrum has a band at 2200 cm<sup>-1</sup> characteristic of a C≡N stretching mode. Compound 1 is thus formulated as the nitrile adduct, bound through the lone pair on nitrogen. In solution 1 slowly isomerizes to 2, requiring about 2 days at 25 °C or 2 h at 80 °C. Coordination of the nitrile through the nitrogen lone pair is expected to induce polarization of the NC bond, encouraging a 1,3-alkyl shift from scandium to the carbon of the nitrile. This mechanism is entirely analogous to that proposed for the insertion of nitriles into aluminum–alkyl bonds. A study of the reactions of *para*-substituted phenyl cyanides with Al(NEt<sub>2</sub>)Et<sub>2</sub> suggested that π-coordination of the nitrile was not important.<sup>5</sup>

Permethylscandocene methyl reacts rapidly at room temperature with nitriles RCN (R = Me, CMe<sub>3</sub>, CHCH<sub>2</sub>)

(1) Thompson, M. E.; Bercaw, J. E. *Pure Appl. Chem.* **1984**, *56*, 1.

(2) Holton, J.; Lappert, M. F.; Ballard, D. G. H.; Pearce, R.; Atwood, J. L.; Hunter, W. E. *J. Chem. Soc., Dalton Trans.* **1979**, 54.

(3) Wailes, P. C.; Coutts, R. S. P.; Weigold, H. "Organometallic Chemistry of Titanium, Zirconium, and Hafnium"; Academic Press: New York, 1974.

(4) Lloyd, J. E.; Wade, K. *J. Chem. Soc.* **1965**, 2662.

(5) Hirabayashi, T.; Itoh, K.; Sakai, S.; Ishii, Y. *J. Organomet. Chem.* **1970**, *21*, 273.

<sup>†</sup> Contribution No. 7205.

<sup>‡</sup> Present address: Department of Chemistry, Cornell University, Ithaca, NY 14853.



Table I<sup>a</sup>

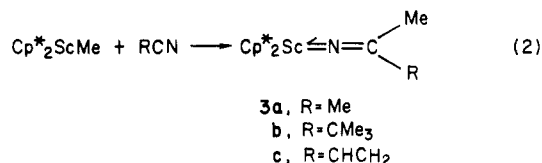
		<sup>1</sup> H NMR	<sup>13</sup> C NMR
1, Cp* <sub>2</sub> ScC <sub>6</sub> H <sub>4</sub> Me(NCC <sub>6</sub> H <sub>4</sub> Me)	Me	1.83 (s)	
	C <sub>5</sub> Me <sub>5</sub>	2.02 (s)	
	Me	2.41 (s)	
	Ph	6.60 (d, <i>J</i> = 9)	
2, Cp* <sub>2</sub> ScNC(C <sub>6</sub> H <sub>4</sub> Me) <sub>2</sub>	Ph	7.29 (d, <i>J</i> = 9)	
	C <sub>5</sub> Me <sub>5</sub>	2.03 (s)	
	Me	2.17 (s)	
	Ph	7.04 (d, <i>J</i> = 8)	
3a, Cp* <sub>2</sub> ScNC(Me) <sub>2</sub>	Ph	7.68 (d, <i>J</i> = 8)	
	Me	1.89 (s)	C <sub>5</sub> Me <sub>5</sub> 11.8
3b, Cp* <sub>2</sub> ScNC(Me)CMe <sub>3</sub>	C <sub>5</sub> Me <sub>5</sub>	1.90 (s)	CMe <sub>2</sub> 29.8
			C <sub>5</sub> Me <sub>5</sub> 117.9
			CMe <sub>2</sub> 159.5
			C <sub>5</sub> Me <sub>5</sub> 11.8
3c, Cp* <sub>2</sub> ScNC(Me)CHCH <sub>2</sub>	CMe <sub>3</sub>	1.20 (s)	C(Me)CMe <sub>3</sub> 24.5
	Me	1.87 (s)	CMe <sub>3</sub> 29.3
	C <sub>5</sub> Me <sub>5</sub>	1.89 (s)	CMe <sub>3</sub> 41.2
			C <sub>5</sub> Me <sub>5</sub> 117.9
4, Cp* <sub>2</sub> ScNHC(C <sub>6</sub> H <sub>4</sub> OMe)CHC(C <sub>6</sub> H <sub>4</sub> OMe)NH	C <sub>5</sub> Me <sub>5</sub>	1.89 (s)	
	C(Me)	2.75 (s)	
	CH <sub>A</sub> H <sub>B</sub>	5.23 (dd, <i>J</i> = 10.5, 3)	
	CH <sub>A</sub> H <sub>B</sub>	5.38 (dd, <i>J</i> = 18, 3)	
5a, Cp* <sub>2</sub> ScNC(H)CMe <sub>3</sub>	CHCH <sub>2</sub>	6.05 (dd, <i>J</i> = 18, 10.5)	
	C <sub>5</sub> Me <sub>5</sub>	1.98 (s)	C <sub>5</sub> Me <sub>5</sub> 12.3 (q, <i>J</i> = 124)
	OMe	3.30 (s)	OMe 55.2 (q, <i>J</i> = 143)
	CH	5.27 (t, <i>J</i> = 2)	CH 91.6 (dt, <i>J</i> = 157, 9.5)
	NH	5.68 (br)	Ph 114.3 (dd, <i>J</i> = 158.5, 4.4)
	Ph	6.78 (dt, <i>J</i> = 8, 1.95)	C <sub>5</sub> Me <sub>5</sub> 118.0 (s)
	Ph	7.61 (dt, <i>J</i> = 8.8, 1.95)	Ph 127.4 (dd, <i>J</i> = 153, 7.3)
			Ph 137.8 (br) <sup>c</sup>
			Ph 160.5 (br)
			(C <sub>6</sub> H <sub>4</sub> OMe) 168.5 (br)
			C <sub>5</sub> Me <sub>5</sub> 11.3
5b, Cp* <sub>2</sub> ScNC(H)C <sub>6</sub> H <sub>4</sub> OMe	C <sub>5</sub> Me <sub>5</sub>	1.90 (s)	CMe <sub>3</sub> 26.8
	CH	8.39 (s)	CMe <sub>3</sub> 39.0
			C <sub>5</sub> Me <sub>5</sub> 117.5
			CH 164.9
6, Cp* <sub>2</sub> Zr(H)NC(H)C <sub>6</sub> H <sub>4</sub> Me	C <sub>5</sub> Me <sub>5</sub>	1.91 (s)	C <sub>5</sub> Me <sub>5</sub> 11.8 (q, <i>J</i> = 125)
	OMe	3.28 (s)	OMe 55.2 (q, <i>J</i> = 143)
	{-C <sub>6</sub> H <sub>4</sub> AA'BB'}	6.79 (d, <i>J</i> = 8)	Ph 114.2 (d, <i>J</i> = 157)
	CH	9.38 (s)	
7, Cp* <sub>2</sub> Zr(I)NC(H)C <sub>6</sub> H <sub>4</sub> Me	CH	7.40 (d, <i>J</i> = 8)	
			C <sub>5</sub> Me <sub>5</sub> 118.3 (s)
			Ph 133.0 (dt, <i>J</i> = 15, 7)
			CH 154.4 (d, 161)
8, Cp* <sub>2</sub> Zr(H)NC(H)C <sub>6</sub> H <sub>4</sub> Me	Ph	160.5 (s)	
	C <sub>5</sub> Me <sub>5</sub>	1.94 (s)	
	Me	2.08 (s)	
	Zr-H	4.82 (s)	
9, Cp* <sub>2</sub> Zr(I)NC(H)C <sub>6</sub> H <sub>4</sub> Me	{-C <sub>6</sub> H <sub>4</sub> AA'BB'}	7.02 (d, <i>J</i> = 8)	
		7.72 (d, <i>J</i> = 8)	
	N=C(H)	9.23 (d, <i>J</i> = 1.1)	
	C <sub>5</sub> Me <sub>5</sub>	1.88 (s)	
10a, Cp* <sub>2</sub> ScNH <sub>2</sub>	Me	2.00 (s)	
	{C <sub>6</sub> H <sub>4</sub> AA'BB'}	6.99 (d, <i>J</i> = 8)	
		7.79 (d, <i>J</i> = 8)	
	N=C(H)	8.54 (s)	
10b, Cp* <sub>2</sub> ScNHMe	C <sub>5</sub> Me <sub>5</sub>	1.82 (s)	
	Me	2.10 (s)	
	{-C <sub>6</sub> H <sub>4</sub> AA'BB'}	7.18 (d, <i>J</i> = 8)	
		7.73 (d, <i>J</i> = 8)	
10c, Cp* <sub>2</sub> ScNMe <sub>2</sub>	N=C(H)	9.69 (s)	
	C <sub>5</sub> Me <sub>5</sub>	1.90 (s) <sup>d</sup>	
	NHMe	3.52 (d, <i>J</i> = 7.6)	C <sub>5</sub> Me <sub>5</sub> 11.3 <sup>f</sup>
	NHMe	4.71 (q, <i>J</i> = 7.6)	NHMe 40.0
10d, Cp* <sub>2</sub> ScNHPh	C <sub>5</sub> Me <sub>5</sub>	1.89 (s)	C <sub>5</sub> Me <sub>5</sub> 118.0
	NMe <sub>2</sub>	2.71 (s)	
	C <sub>5</sub> Me <sub>5</sub>	1.82 (s)	
	NH	4.08 (br, <i>J</i> = 62.5, <sup>15</sup> N-H)	
10e, Cp* <sub>2</sub> ScNHCH <sub>2</sub> CMe <sub>3</sub>	Ph	6.11 (d, <i>J</i> = 7.5)	
	Ph	6.64 (tt, <i>J</i> = 7.2, 1)	
	Ph	7.21 (t, <i>J</i> = 7.3)	
	CMe <sub>3</sub>	1.05 (s)	
10e, Cp* <sub>2</sub> ScNHCH <sub>2</sub> CMe <sub>3</sub>	C <sub>5</sub> Me <sub>5</sub>	1.98 (s)	
	CH <sub>2</sub>	3.47 (d, <i>J</i> = 8)	
	NH	4.75 (br)	

Table I<sup>a</sup> (Continued)

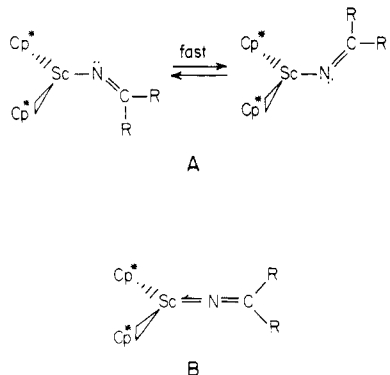
		<sup>1</sup> H NMR	<sup>13</sup> C NMR
10f, Cp* <sub>2</sub> ScNHCH <sub>2</sub> C <sub>6</sub> H <sub>4</sub> OMe	C <sub>5</sub> Me <sub>5</sub>	1.92 (s)	
	OMe	3.39 (s)	
	NH	4.71 (br)	
	CH <sub>2</sub>	4.83 (d, <i>J</i> = 8.3)	
	{C <sub>6</sub> H <sub>4</sub> AA'BB'}	6.94 (d, <i>J</i> = 8.5)	
11, Cp* <sub>2</sub> ScNC(NHCH <sub>2</sub> CMe <sub>3</sub> )CMe <sub>3</sub>	CMe <sub>3</sub>	0.93 (s)	
	CMe <sub>3</sub>	1.20 (s)	
	C <sub>5</sub> Me <sub>5</sub>	1.95 (s)	
	CH <sub>2</sub>	3.30 (br)	
	NH	4.97 (br)	

<sup>a</sup> All spectra are recorded in benzene-*d*<sub>6</sub> at room temperature and referenced to residual protons or carbons of solvent or to Me<sub>4</sub>Si as an internal standard, unless otherwise stated. Multiplicities for <sup>13</sup>C spectra are only reported where coupled spectra were recorded. Chemical shifts are in δ and coupling constants in hertz. <sup>b</sup> Only one peak of doublet observed, *J* calculated from the difference in frequency between line of doublet and single line in decoupled spectrum. <sup>c</sup> Other phenyl signals obscured by solvent resonances. <sup>d</sup> NH<sub>2</sub> protons not observed. <sup>e</sup> Spectrum obtained at -80 °C. <sup>f</sup> In toluene-*d*<sub>6</sub>.

to form directly the azomethine insertion complexes Cp\*<sub>2</sub>ScNC(Me)R (eq 2). Complexes **3a-c** display a



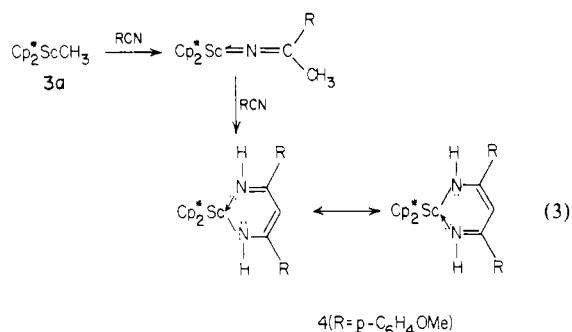
characteristic C=N stretching frequency in the IR spectrum at 1640–1680 cm<sup>-1</sup>. The <sup>1</sup>H and <sup>13</sup>C NMR spectra display equivalent Cp\* resonances in all cases, and for R = Me (**3a**), the methyl groups are also equivalent. The equivalence of Cp\* ligands for **3b** and **3c** indicates structures for which both the Me and R groups lie in the equatorial plane. Moreover, the equivalence of the methyl groups for **3a** suggests either a fluxional structure, A, or an "ylide-heteroallene" structure, B. Collier, Lappert, and



McMeeking<sup>6</sup> have shown that Cp<sub>2</sub>MCl<sub>2</sub> (M = Zr, Ti) react with lithium ketimides (LiNCR<sub>2</sub>; R = Ph, *p*-tol, CMe<sub>3</sub>) to replace one or two chlorides. They suggested that for Cp<sub>2</sub>M(Cl)NCR<sub>2</sub> (M = Zr, Ti), significant M=N=CR<sub>2</sub> π-bonding was unlikely (the <sup>1</sup>H NMR spectrum displayed inequivalent R groups) and therefore proposed a bent MNC arrangement. However, they appear to have overlooked the fact that for these complexes both linear and bent MNC arrangements would possess inequivalent R groups, since in both cases one R would be toward the Cl and the other away. For complexes **3a-c** we favor structure B above, since it not only allows the two substituents on the nitrile carbon to lie in the middle of the wedge between the Cp\* ligands (i.e., in the sterically most favorable positions) but also allows for significant donation of electron density from the nitrogen lone pair into the empty b<sub>2</sub> orbital on scandium.<sup>7</sup>

Although Cp<sub>2</sub>Ti(Cl)NC(Me)Ph has been prepared from Cp<sub>2</sub>TiCl<sub>2</sub> and LiNC(Me)Ph, the same complex was not accessible by insertion of benzonitrile into the Ti-Me bond of Cp<sub>2</sub>Ti(Me)Cl.<sup>6</sup> Moreover, we have found that neither Cp\*<sub>2</sub>ZrMe<sub>2</sub> nor Cp\*<sub>2</sub>HfMe<sub>2</sub> will insert nitriles, possibly due to the decreased Lewis acidity of these 16e metal centers.

In the reaction of Cp\*<sub>2</sub>ScMe with acetonitrile to afford **3a**, it is important to ensure a stoichiometry of 1:1, since excess MeCN reacts further to yield a complex which incorporates a second equivalent of MeCN. An additional competing reaction, which appears to result in loss of Cp\* ligands(s), has precluded the isolation of analytical samples of this new compound.<sup>8</sup> It has proven possible to isolate an analogous compound from the reaction of *p*-anisonitrile with Cp\*<sub>2</sub>ScMe. The expected initial insertion product, observed (NMR) at room temperature, reacts with a second equivalent of *p*-anisonitrile at 80 °C to afford **4** (eq 3). The structure of **4** is based primarily on its spectral



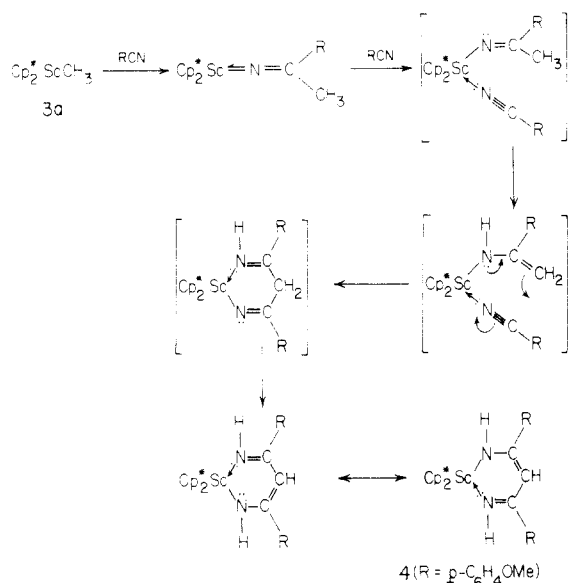
features. Thus bands at 3325 and 3305 cm<sup>-1</sup> in its infrared spectrum indicate the presence of N-H bonds. The absence of absorptions in the ranges 2300–2100 and 1610–1690 cm<sup>-1</sup> suggests a C-N bond order of less than 2. Its <sup>1</sup>H NMR spectrum displays two equivalent OCH<sub>3</sub> groups per [Cp\*<sub>2</sub>Sc] unit, thus indicating a symmetrical arrangement of phenyl substituents. In addition there is a triplet at δ 5.27 (*J* = 2 Hz) with an integrated intensity of one proton and a broad signal at δ 5.68 with intensity two. The <sup>13</sup>C NMR spectrum shows similar features and is consistent with the formulation of the complex as shown in eq 3.

A possible mechanism for the formation of **4** is outlined in Scheme I. Initial coordination of the second nitrile followed by imine-enamine tautomerism (cf. keto-enol tautomerism) would generate an intermediate with a nu-

(7) Lauher, J. W.; Hoffman, R. *J. Am. Chem. Soc.* 1976, 98, 1729.

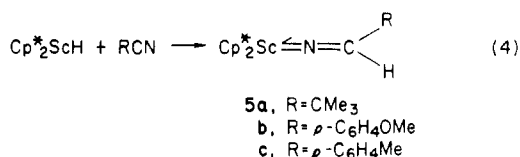
(8) This additional competing reaction is very likely due to the acidic nature of the methyl protons of MeCN causing protonation of one of the Cp\* groups and liberation of C<sub>5</sub>Me<sub>5</sub>H.

Scheme I



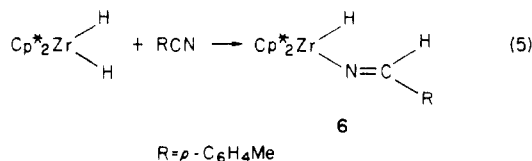
cleophilic methylene center. Attack at the electrophilic carbon of the coordinated nitrile and a second 1,3-hydrogen shift would provide the observed product. A tautomerism via just such a 1,3-hydrogen shift has been previously observed for a titanium metallacycle.<sup>9</sup>

Although Cp\*<sub>2</sub>ScH is unstable at room temperature in the absence of dihydrogen, it may be isolated as a THF adduct.<sup>1</sup> Thus, reactions involving Cp\*<sub>2</sub>ScH were performed at -78 °C in the absence of excess hydrogen. In other cases the THF adduct was used at room temperature (see Experimental Section). Addition of nitrile to Cp\*<sub>2</sub>ScH or Cp\*<sub>2</sub>ScH(THF) produces an instantaneous color change from off-white to bright yellow (eq 4). The NMR spectra



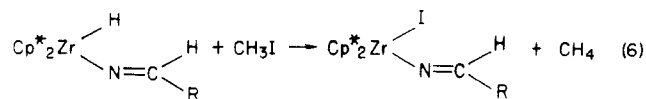
of 5a,b are as expected, with the azomethine hydrogen being observed in the range  $\delta$  8.5–9.5 and the carbon at ca.  $\delta$  160. The C=N stretching frequencies are at 1640–1680 cm<sup>-1</sup>, and the mass spectra show the expected ions.

In a similar manner, Cp\*<sub>2</sub>ZrH<sub>2</sub> reacts at low-temperature (-78 °C) with a stoichiometric amount of *p*-tolunitrile to yield the monoinsertion product Cp\*<sub>2</sub>Zr(H)N=C(H)(*p*-C<sub>6</sub>H<sub>4</sub>Me) (6) (eq 5). Compound 6 exhibits a broad IR



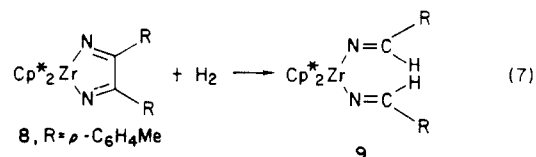
absorption at 1500 cm<sup>-1</sup> and a low-field NMR resonance ( $\delta$  4.82) characteristic of a Zr-H bond. A strong IR band at 1660 cm<sup>-1</sup> is indicative of the C=N bond, and the azomethine proton ( $\delta$  9.23) is coupled to the Zr-H (<sup>4</sup>J = 1.1 Hz). The resonances at  $\delta$  4.82 and 9.23 are absent when *p*-tolunitrile is treated with Cp\*<sub>2</sub>ZrD<sub>2</sub>. The reaction of 6 with CH<sub>3</sub>I yields Cp\*<sub>2</sub>Zr(I)NC(H)(*p*-C<sub>6</sub>H<sub>4</sub>Me) and 0.70 mmol of CH<sub>4</sub>/mmol of 6 (eq 6), again indicative of a Zr-H bond.<sup>10</sup>

(9) Cohen, S. A.; Bercaw, J. E. *Organometallics* 1985, 4, 1006.



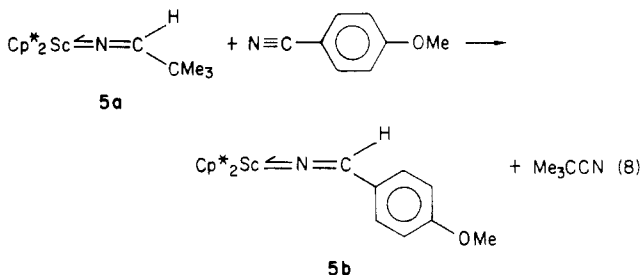
6, R = *p*-C<sub>6</sub>H<sub>4</sub>Me

The zirconacyclobutane 8 obtained via treatment of (Cp\*<sub>2</sub>ZrN<sub>2</sub>)<sub>2</sub>N<sub>2</sub> with 4 equiv of tolunitrile reacts with dihydrogen over a period of 3 days at 70 °C to form the double nitrile insertion product 9 (eq 7). An initial con-

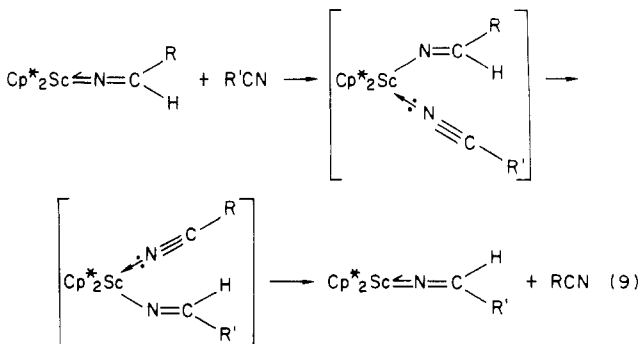


version of 8 to 6 and free *p*-tolunitrile is complete after 1 h at 25 °C, and the subsequent nitrile insertion to form 9 occurs over a period of days.<sup>11</sup> Even under excess dihydrogen, there is no evidence for hydrogenation of the C=N bond to yield an amide although such a complex would be expected to be stable.<sup>12</sup>

The reaction of Cp\*<sub>2</sub>ScNC(H)CMe<sub>3</sub> with *p*-anisonitrile leads to exchange of the nitriles giving Cp\*<sub>2</sub>ScNC(H)C<sub>6</sub>H<sub>4</sub>OMe and Me<sub>3</sub>CCN (eq 8). Unfortunately, at-



tempts to use MeCN to displace either Me<sub>3</sub>CCN or *p*-NCC<sub>6</sub>H<sub>4</sub>OMe were not successful; decomposition occurred and free Cp\*H was observed in solution.<sup>8</sup> Thus, it is not known if the nitrile exchange reaction is driven by steric or electronic factors. Since Cp\*<sub>2</sub>ScH reacts very rapidly with ethylene to form polyethylene,<sup>13</sup> it is significant that Cp\*<sub>2</sub>ScNC(H)R (R = CH<sub>3</sub>, CMe<sub>3</sub>, *p*-C<sub>6</sub>H<sub>4</sub>OMe) do not react with ethylene. We conclude therefore that nitrile exchange does not proceed via the reverse of eq 4. Rather we favor an associative mechanism such as that shown in eq 9.



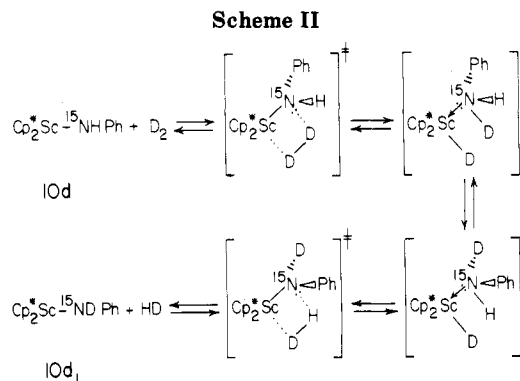
The amide complexes 10a-e can be prepared by reaction of Cp\*<sub>2</sub>ScH or Cp\*<sub>2</sub>ScMe with the corresponding amine,

(10) Bercaw, J. E. *Adv. Chem. Ser.* 1978, No. 167, 136.

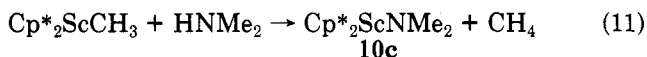
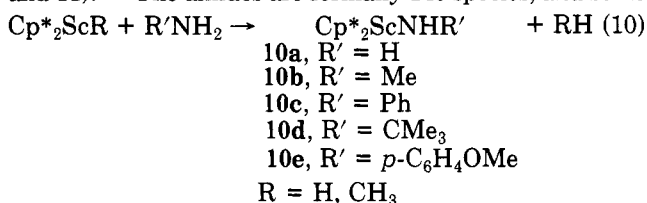
(11) Compound 8 undergoes exchange with free nitrile, suggesting the reductive coupling reaction which generates 8 is reversible. Thus, it is likely that 8 + H<sub>2</sub> leads initially to Cp\*<sub>2</sub>ZrH<sub>2</sub> + free nitrile. Wolczanski, P. T. Ph.D. Thesis, California Institute of Technology, 1981.

(12) Hillhouse, G. L.; Bercaw, J. E. *J. Am. Chem. Soc.* 1984, 106, 5472.

(13) Cp\*<sub>2</sub>ScH reacts very rapidly with ethylene even at -78 °C, effecting fast polymerization at 25 °C (see ref 1).

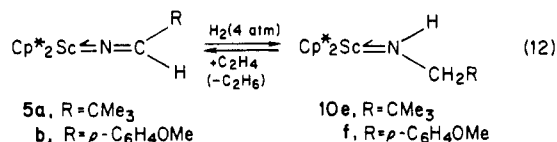


producing 1 equiv of hydrogen or methane, respectively.<sup>14</sup> It is likely that these reactions occur by interaction of the nitrogen lone pair with the scandium center followed by a four-center elimination of hydrogen or methane (eq 10 and 11).<sup>12</sup> The amides are formally 14e species, and some

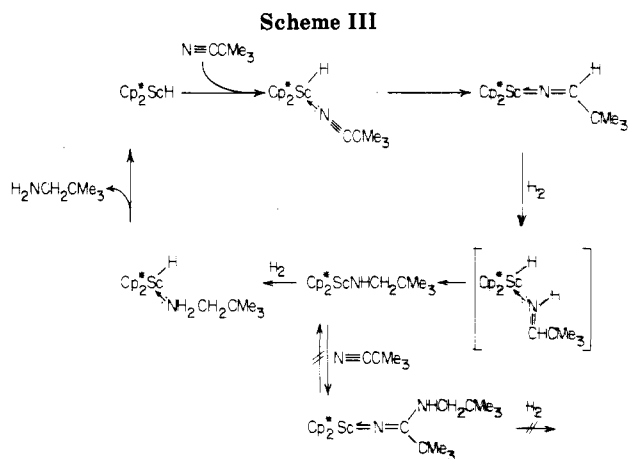


N → Sc π-donation is thus anticipated. However, to allow donation from the nitrogen lone pair, the substituents on nitrogen must be directed toward the Cp\* ligands, i.e., in the sterically least favorable conformation. It has been shown<sup>12</sup> that for the related Cp\*<sub>2</sub>HfH(NR<sub>2</sub>) system, the preferred conformation for R = Me has the methyl groups lying in the equatorial plane between the Cp\* groups, i.e., an orthogonal orientation for π-bonding. However, models for the parent complex Cp\*<sub>2</sub>HfH(NH<sub>2</sub>) suggested no prohibitive steric interactions between the NH<sub>2</sub> hydrogens and the Cp\* groups. Accordingly, the low-temperature <sup>1</sup>H NMR spectra (500 MHz, -90 °C) of Cp\*<sub>2</sub>HfH(NH<sub>2</sub>) displays equivalent amide proton resonances consistent with the Hf=NH<sub>2</sub> conformation. The low-temperature <sup>1</sup>H NMR spectrum of Cp\*<sub>2</sub>ScNHMe (400 MHz, -80 °C) shows equivalent Cp\* moieties, indicating either that the preferred conformer is that with no nitrogen π-donation or that rotation about the Sc-N bond is still rapid at this temperature.

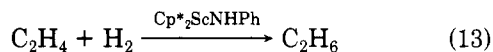
The amide complexes Cp\*<sub>2</sub>ScNHCH<sub>2</sub>R (10e,f) can also be prepared by hydrogenation of the complexes 5a,b. Interestingly, this hydrogenation is reversible, since reaction of the amide with ethylene at 80 °C gives the azomethine and ethane (eq 12).



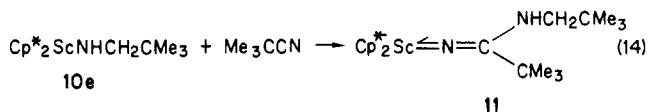
(14) An exception to eq 10 and 11 is the reaction of Cp\*<sub>2</sub>ScCH<sub>3</sub> with *p*-NH<sub>2</sub>CH<sub>2</sub>C<sub>6</sub>H<sub>4</sub>OMe for which the product isolated is the amine adduct Cp\*<sub>2</sub>ScNHCH<sub>2</sub>C<sub>6</sub>H<sub>4</sub>OMe(NH<sub>2</sub>CH<sub>2</sub>C<sub>6</sub>H<sub>4</sub>OMe). The adduct appears to be fluxional (<sup>1</sup>H NMR), hydrogen transfer from amine to amide interconverting the two groups. At low temperature this process can be frozen out (-80 °C, 400 MHz): C<sub>6</sub>Me<sub>3</sub> (δ 2.00, (s)), OMe (δ 3.25 (s)), OMe (δ 3.28 (s)), CH<sub>2</sub> (δ 3.50 (b s)), CH<sub>2</sub> (δ 4.69 (b s)), Ph (δ 6.74), (d, *J* = 8.2 Hz), 6.93 (d, *J* = 8.6 Hz), 6.96 (d, *J* = 8.6 Hz), 7.50 (d, *J* = 8.3 Hz)). Reaction with Cp\*<sub>2</sub>ScMe affords CH<sub>4</sub> and Cp\*<sub>2</sub>ScNHCH<sub>2</sub>C<sub>6</sub>H<sub>4</sub>OMe; however, isolation of the amine adduct of the amide has not been possible. Evidence for other amine-amide adducts has also been obtained from NMR experiments, but their stability is even lower than that for the above compound.



The mechanism for hydrogenation of 5a,b to 10e,f has been probed by treating Cp\*<sub>2</sub>Sc<sup>15</sup>NHPh with D<sub>2</sub>. Rapid exchange to afford Cp\*<sub>2</sub>Sc<sup>15</sup>NDPh and HD is observed by <sup>1</sup>H NMR. No incorporation of deuterium into the Cp\* positions is observed, so that mechanisms involving ligand C-H bonds (i.e., via "tuck-in" intermediates) are eliminated. Thus, we favor a four-center mechanism like that postulated to explain C-H activation by this system<sup>1</sup> (Scheme II). Consistent with the proposed equilibrium between Cp\*<sub>2</sub>ScNHPh, H<sub>2</sub>, and [Cp\*<sub>2</sub>Sc(H)(NH<sub>2</sub>Ph)] in Scheme II is the observation that ethylene is rapidly hydrogenated to ethane by 10d, whereas in the absence of H<sub>2</sub> no reaction between 10d and C<sub>2</sub>H<sub>4</sub> is observed (eq 13).<sup>15</sup>



The observation that 5a,b can be hydrogenated under relatively mild conditions suggests that catalytic hydrogenation of nitriles may be possible in this system. The reaction of Cp\*<sub>2</sub>ScNHCH<sub>2</sub>CMe<sub>3</sub> (5a) with Me<sub>3</sub>CCN under dihydrogen (4 atm) proceeds at 80 °C for a few turnovers to liberate NH<sub>2</sub>CH<sub>2</sub>CMe<sub>3</sub>. However, there is a competing, irreversible reaction which removes the catalytic species, involving insertion of nitrile into the Sc-N bond of the amide to form 11, analogous to similar reactions previously observed<sup>5</sup> for aluminum amides (eq 14).



A likely mechanism for the catalytic cycle, based almost entirely on precedented steps, is shown in Scheme III. It is worth noting once again that the key step in this mechanism is addition of dihydrogen across a Sc-N bond.

## Conclusions

The reactions of permethylscandocene and -zirconocene hydrides with nitriles proceed rapidly to provide the azomethine insertion products. Moreover, permethylscandocene alkyl and aryl complexes react in a similar manner, and in one case, an intermediate nitrile adduct of an aryl complex has been directly observed. These reactions are very similar to those of aluminum hydrides and alkyls with nitriles;<sup>4,5,16</sup> initial nitrile adducts of alu-

(15) An alternative mechanism involving free Cp\*<sub>2</sub>ScH cannot be ruled out; however, it is expected to react much faster and yield polyethylene under these conditions.

minum alkyls have been isolated in several cases which, when heated, give the carbalumination products. As far as we are aware, there are, as yet, no examples of transfer of an alkyl or aryl group from a transition metal to a nitrile. There have, however, been examples of insertion of a nitrile into an actinide-carbon bond; *tert*-butyl cyanide was found to insert into the M-C bond of the metallacycles

$[(\text{Me}_3\text{Si})_2\text{N}]_2\text{MCH}_2\text{Si}(\text{Me}_2)\text{NNSiMe}_3$  (M = Th or U) to give six-membered metallacycles.<sup>17</sup> There are many examples of insertion of a nitrile into a transition-metal hydride bond, although more commonly for cluster compounds.<sup>18</sup> The driving force for the reactions of permethylscandocene and -zirconocene derivatives is presumably the high Lewis acidity of these early transition-metal complexes, which polarizes the N≡C bond and thus encourages alkyl transfer. The reaction of nitriles with Cp\*<sub>2</sub>ScMe is faster than with aluminum alkyls. Accordingly, deprotonation of the α-carbon does not compete with insertion of the nitrile; however, the higher reactivity of the scandium products may result in further reactions with nitriles bearing hydrogens on the α-carbon (e.g., eq 3).

The nucleophilicity of scandium hydrides or alkyls has been used to prepare a variety of amide complexes from the corresponding amines. This same type of reactivity has been observed previously for permethylzirconocene and permethylhafnocene hydrides and may be generally applicable for the synthesis of early metal amide complexes.

The catalytic hydrogenation of nitriles by organometallic complexes is well precedented,<sup>19</sup> and presumably nitrile insertion into metal-hydrogen bonds also occurs in these systems. However, stepwise reduction has only been observed in noncatalytic systems where liberation of the amine leads to decomposition of the complex.<sup>18b,c</sup> Our observation of stepwise hydrogenation of nitriles is believed to be the first in a catalytic system. It is surprising that such catalysis occurs with an early transition metal such as scandium for which the Sc-N bond had been expected to be very resistant to hydrogenation. It is particularly significant that a Sc-N bond undergoes hydrogenolysis under relatively mild conditions. The implication is that under suitable conditions early transition elements may serve as viable homogeneous catalysts, even for substrates containing heteroatoms such as nitrogen.

## Experimental Section

**General Considerations.** All manipulations were performed by using glovebox or high vacuum techniques, as previously described. IR spectra were recorded on a Beckman 4240 spectrophotometer as Nujol mulls and are reported in inverse centimeters. Proton, <sup>2</sup>H, and <sup>13</sup>C NMR spectra were recorded by using a Varian

EM 390 or JEOL GX 400 spectrometer. Spectra were recorded in benzene-*d*<sub>6</sub> or toluene-*d*<sub>8</sub> solution and are referenced to Me<sub>4</sub>Si or residual protons or carbons of solvent. Elemental analyses and mass spectra were recorded by Larry A. Henling at the California Institute of Technology.

Dimethylamine (Eastman Kodak), neopentylamine, aniline, and *p*-methoxybenzylamine (Aldrich) were stored over 4-Å molecular sieves. Anhydrous ammonia and methylamine (Matheson) were freeze-pump-thawed twice before use. <sup>15</sup>N aniline (MSD) was used as supplied. Many of the syntheses reported proceed quantitatively (NMR), but the isolated yields are often low because the compounds are extremely soluble in hydrocarbon solvents.

**Cp\*<sub>2</sub>Sc(*p*-tol)*p*-NCC<sub>6</sub>H<sub>4</sub>Me (1).** Cp\*<sub>2</sub>Sc(*p*-tol) (400 mg, 0.98 mmol) and *p*-tolunitrile (150 mg, 1.28 mmol) were stirred in 10 mL of petroleum ether, giving a yellow precipitate. Recrystallization from petroleum ether gave 1: 407 mg (79%); IR 3020 (s), 2708 (m), 2245 (vs), 1602 (s), 1500 (m), 1405 (m), 1222 (m), 1205 (w), 1172 (s), 1120 (m), 1052 (sh), 1030 (s), 1014 (s), 815 (s), 808 (sh), 778 (s), 712 (w), 582 (w), 545 (m), 480 (m) cm<sup>-1</sup>. Anal. Calcd for C<sub>35</sub>H<sub>37</sub>NSc: C, 80.27; H, 8.47; N, 2.67. Found: C, 79.9; H, 8.55; N, 2.83.

**Cp\*<sub>2</sub>ScNC(*p*-tol)<sub>2</sub> (2).** Cp\*<sub>2</sub>Sc(*p*-tol) (263 mg, 0.65 mmol) and *p*-tolunitrile (104 mg, 0.89 mmol) were heated at 80 °C in toluene (5 mL) for 2.5 h. Recrystallization from petroleum ether gave 2 as an orange-yellow solid: yield 65%; IR 2720 (w), 1638 (vs), 1605 (s), 1567 (w), 1505 (m), 1302 (w), 1281 (w), 1240 (m), 1208 (w), 1175 (s), 1103 (w), 1018 (m), 907 (m), 827 (s), 815 (s), 778 (w), 732 (m), 565 (w), 544 (w), 463 (w), 425 (m) cm<sup>-1</sup>. Anal. Calcd for C<sub>35</sub>H<sub>37</sub>NSc: C, 80.27; H, 8.47; N, 2.67. Found: C, 80.00; H, 8.25; N, 3.66.

**Cp\*<sub>2</sub>ScNC(Me)CHCH<sub>2</sub> (3c).** Acrylonitrile (77 μL, 1.17 mmol) was added to a stirred solution of Cp\*<sub>2</sub>ScMe (387 mg, 1.17 mmol) in petroleum ether (15 mL). After being stirred for 0.5 h, the solution was concentrated to ca. 2 mL, cooled to -78 °C, and filtered to give a yellow solid, 3c: yield 200 mg (45%); IR 3285 (2), 3085 (m), 2722 (m), 1820 (w), 1645 (vs), 1610 (vs), 1345 (s), 1275 (m), 1218 (s), 1162 (w), 1145 (w), 1067 (m), 1020 (s), 992 (s), 944 (m), 908 (s), 795 (m), 740 (w), 705 (m), 675 (sh), 658 (m) cm<sup>-1</sup>. Anal. Calcd for C<sub>24</sub>H<sub>36</sub>NSc: C, 75.16; H, 9.46; N, 3.65. Found: C, 74.46; H, 9.43; N, 3.31.

Similar procedures were used for the preparation of Cp\*<sub>2</sub>ScNC(Me)CMe<sub>3</sub> (3b) and Cp\*<sub>2</sub>ScNC(Me)<sub>2</sub> (3a).

**Compound 3b:** yield 32%; IR 2720 (w), 1672 (vs), 1630 (m), 1433 (s), 1398 (m), 1358 (m), 1343 (m), 1242 (m), 1210 (w), 1195 (w), 1150 (m), 1102 (s), 1058 (m), 1015 (m), 947 (m), 868 (w), 832 (w), 798 (w), 730 (w), 700 (w), 565 (w), 504 (w), 423 (s) cm<sup>-1</sup>. Anal. Calcd for C<sub>26</sub>H<sub>42</sub>NSc: C, 75.51; H, 10.24; N, 3.39. Found: C, 74.33; H, 10.13; N, 3.08.

**Compound 3a:** yield 56%; IR 1790 (w), 1710 (s), 1685 (vs), 1655 (sh), 1648 (sh), 1482 (m), 1340 (s), 1178 (s), 1058 (w), 1020 (s), 892 (w), 798 (w), 530 (m), 478 (s), 415 (s) cm<sup>-1</sup>. Anal. Calcd for C<sub>23</sub>H<sub>36</sub>NSc: C, 74.36; H, 9.77; N, 3.77. Found: C, 73.39; H, 9.54; N, 3.49.

**Cp\*<sub>2</sub>ScN(H)C(C<sub>6</sub>H<sub>4</sub>OMe)C(H)C(C<sub>6</sub>H<sub>4</sub>OMe)N(H) (4).** A mixture of Cp\*<sub>2</sub>ScMe (400 mg, 1.21 mmol) and *p*-NCC<sub>6</sub>H<sub>4</sub>OMe (330 mg, 2.48 mmol) was heated at 80 °C for 3 days in toluene (10 mL). The toluene was removed and the residue extracted with petroleum ether (10 mL). Concentration to ca. 2 mL, cooling to -78 °C, and filtration gave a lemon yellow solid: yield 53%; IR 3325 (w), 3305 (w), 1605 (s), 1575 (m), 1545 (s), 1525 (s), 1498 (vs), 1412 (s), 1398 (s), 1290 (s), 1250 (vs), 1215 (m), 1170 (s), 1102 (w), 1025 (s), 915 (w), 835 (s), 812 (w), 765 (s), 732 (m), 718 (w), 680 (m) cm<sup>-1</sup>. Anal. Calcd for C<sub>37</sub>H<sub>47</sub>N<sub>2</sub>O<sub>2</sub>Sc: C, 74.47; H, 7.94; N, 4.70. Found: C, 71.49; H, 7.53; N, 4.56.

**Cp\*<sub>2</sub>ScNC(H)CMe<sub>3</sub> (5a).** A toluene (10 mL) solution of Cp\*<sub>2</sub>ScMe (404 mg, 1.22 mmol) in a thick walled glass reaction vessel with Teflon needle valve was cooled to -196 °C, dihydrogen (700 torr) was admitted, and the valve was closed. The solution was warmed to room temperature with stirring and was stirred for a further 15 mins. The solution was cooled to -78 °C, and the valve was opened to vacuum to remove dihydrogen. *tert*-Butyl cyanide (140 μL, 1.27 mmol) was added, causing an immediate color change from cream to yellow. The mixture was stirred for 30 min, the toluene was removed, and petroleum ether (5 mL) was added. The solution was transferred to a frit, concentrated

(16) (a) Reinheckel, H.; Jahnke, D. *Chem. Ber.* **1964**, *97*, 2661. (b) Pasynkiewicz, S.; Maciaszek, S. *J. Organomet. Chem.* **1968**, *15*, 301. (c) Miller, A. E. G.; Bliss, J. W.; Schwartzman, L. H. *J. Org. Chem.* **1959**, *24*, 627.

(17) Simpson, S. J.; Andersen, R. A. *J. Am. Chem. Soc.* **1981**, *103*, 4063.

(18) (a) Mays, M. J.; Prest, D. W.; Raithby, P. R. *J. Chem. Soc., Chem. Commun.* **1980**, 171. (b) Andrews, M. A.; Kaesz, H. D. *J. Am. Chem. Soc.* **1979**, *101*, 7238. (c) Bernhardt, W.; Vahrenkamp, H. *Angew. Chem., Int. Ed. Engl.* **1984**, *23*, 381. (d) Evans, W. J.; Meadows, J. H.; Hunter, W. E.; Atwood, J. L. *J. Am. Chem. Soc.* **1984**, *106*, 1291.

(19) (a) Toshikatsu, Y.; Okano, T.; Otsuka, S. *J. J. Chem. Soc., Chem. Commun.* **1979**, 870. (b) Grey, A. R.; Pez, G. P.; Wallo, A. *J. Am. Chem. Soc.* **1981**, *103*, 7536.

(20) In this paper the periodic group notation in parentheses is in accord with recent actions by IUPAC and ACS nomenclature committees. A and B notation is eliminated because of wide confusion. Groups IA and IIA become groups 1 and 2. The d-transition elements comprise groups 3 through 12, and the p-block elements comprise groups 13 through 18. (Note that the former Roman numeral designation is preserved in the last digit of the new numbering: e.g., III → 3 and 13.)

to ca. 2 mL, cooled to  $-78^{\circ}\text{C}$ , and filtered to isolate a pale yellow solid: yield 38%; IR 3360 (w), 2710 (s), 2625 (s), 1748 (m), 1675 (s), 1625 (m), 1240 (m), 1202 (s), 1148 (w), 1082 (m), 1055 (sh), 1024 (s), 885 (sh), 870 (m), 795 (w), 748 (m), 692 (m), 645 (m)  $\text{cm}^{-1}$ . Anal. Calcd for  $\text{C}_{25}\text{H}_{40}\text{NSc}$ : C, 75.15; H, 10.09; N, 3.51. Found: C, 75.00; H, 10.23; N, 3.54.

**$\text{Cp}^*_2\text{ScNC}(\text{H})\text{C}_6\text{H}_4\text{OMe}$  (5b).**  $\text{Cp}^*_2\text{ScMe}$  (1.13 g, 3.42 mmol) was stirred in THF (10 mL) under dihydrogen (1 atm) for 17 h to form  $\text{Cp}^*_2\text{Sc}(\text{H})\text{THF}$ .  $p\text{-NCC}_6\text{H}_4\text{OMe}$  (500 mg, 3.76 mmol) in petroleum ether (10 mL) was added, and the mixture was stirred for 0.5 h. The solution was evaporated to dryness, and petroleum ether (5 mL) was added. Concentration to ca. 2 mL and cooling to  $-78^{\circ}\text{C}$  allowed isolation of a yellow solid: yield 27%; IR 1648 (vs), 1595 (vs), 1572 (s), 1495 (s), 1350 (s), 1302 (s), 1242 (vs), 1152 (s), 1092 (w), 1025 (s), 828 (s), 800 (m), 640 (m)  $\text{cm}^{-1}$ . Anal. Calcd for  $\text{C}_{28}\text{H}_{38}\text{NOSc}$ : C, 74.80; H, 8.52; N, 3.12. Found: C, 71.71; H, 8.21; N, 2.93.

**$\text{Cp}^*_2\text{Zr}(\text{H})\text{NC}(\text{H})\text{C}_6\text{H}_4\text{Me}$  (6).**  $\text{Cp}^*_2\text{ZrH}_2$  (200 mg, 0.550 mmol) and  $p\text{-tolunitrile}$  (64 mg, 0.550 mmol) were placed in a flask, and toluene (15 mL) was distilled in at  $-78^{\circ}\text{C}$ . After the solution was warmed to  $25^{\circ}\text{C}$  and stirred for 1 h, the solvent was removed. Recrystallization from petroleum ether yielded bright yellow 6: yield 57%;  $\nu(\text{C}=\text{N})$  1660,  $\nu(\text{Zr}-\text{H})$  1500  $\text{cm}^{-1}$ . Anal. Calcd for  $\text{C}_{28}\text{H}_{38}\text{NZr}$ : C, 69.94; H, 8.18; N, 2.91. Found: C, 68.77; H, 8.16; N, 1.93.

**$\text{Cp}^*_2\text{Zr}(\text{I})\text{NC}(\text{H})\text{C}_6\text{H}_4\text{Me}$  (7).**  $\text{Cp}^*_2\text{Zr}(\text{H})\text{NC}(\text{H})\text{C}_6\text{H}_4\text{Me}$  (200 mg, 0.416 mmol) was placed in a flask, and toluene (15 mL) was distilled in along with about 4 mmol of MeI. After the solution was warmed to  $25^{\circ}\text{C}$ , the gas was collected (0.291 mmol, 0.70 mmol/mmol of 6). After passage over hot CuO, the volume of gas was unchanged (IR identified  $\text{CH}_4$ ). The solution was filtered, and the toluene was then removed. The resulting yellow powder was slurried in petroleum ether and then collected (160 mg, 63% yield):  $\nu(\text{C}=\text{N})$  1650  $\text{cm}^{-1}$ . Anal. Calcd for  $\text{C}_{28}\text{H}_{38}\text{NIZr}$ : C, 55.43; H, 6.31; N, 2.31. Found: C, 55.49; H, 6.34; N, 2.23.

**$\text{Cp}^*_2\text{Zr}[\text{NC}(\text{H})\text{C}_6\text{H}_4\text{Me}]_2$  (9).** Compound 8 was prepared by treatment of ( $\text{Cp}^*_2\text{ZrN}_2$ ) $_2$  (500 mg, 0.62 mmol) with 290 mg (2.48 mmol) of  $p\text{-tolunitrile}$  in 50 mL of toluene,  $-78 \rightarrow 25^{\circ}\text{C}$ . After 4 h at  $25^{\circ}\text{C}$ , toluene was removed and 8 crystallized from petroleum ether (40 mL). Orange crystalline 8 (650 mg, 82%) was obtained. Anal. Calcd for  $\text{C}_{36}\text{H}_{44}\text{N}_2\text{Zr}$ : C, 72.54; H, 7.46; N, 4.70. Found: C, 72.36; H, 7.57; N, 4.49. A glass bomb reactor (65 mL) containing 173 mg of 8 (0.291 mmol) and 10 mL of toluene was pressurized with 1.254 mmol of  $\text{H}_2$  and heated for 5 days at  $70^{\circ}\text{C}$  to ensure complete reaction. After this time the unreacted  $\text{H}_2$  was Toepler pumped (0.979 mmol); thus, 0.275 mmol of  $\text{H}_2$  were absorbed (0.945 mmol/mmol of 8). The brown solution was then transferred to a flask, and pure 9 was crystallized from toluene/petroleum ether. The brown-orange crystals were collected on a frit (156 mg, 90% yield):  $\nu(\text{C}=\text{N})$  1670  $\text{cm}^{-1}$ .

**Nitrile Exchange.** An NMR tube was loaded with  $\text{Cp}^*_2\text{ScNC}(\text{H})\text{CMe}_3$  (25 mg, 0.05 mmol),  $p\text{-NCC}_6\text{H}_4\text{OMe}$  (9 mg, 0.07 mmol), and 0.3 mL of benzene- $d_6$ . The NMR spectrum showed that complete exchange had occurred; addition of 10 equiv of  $\text{Me}_3\text{CCN}$  did not produce a detectable amount of  $\text{Cp}^*_2\text{ScNC}(\text{H})\text{CMe}_3$ .

**Hydrogenation of  $\text{Cp}^*_2\text{ScNC}(\text{H})\text{R}$  (5a,b).** An NMR tube sealed to a ground-glass joint was loaded with  $\text{Cp}^*_2\text{ScNC}(\text{H})\text{CMe}_3$  (20 mg, 0.05 mmol) and 0.3 mL of benzene- $d_6$ . The tube was cooled to 77 K, 700 torr of  $\text{H}_2$  introduced, and the tube sealed with a torch. The formation of  $\text{Cp}^*_2\text{ScNHCH}_2\text{CMe}_3$  was complete after 24 h at room temperature.

Similarly, hydrogenation of  $\text{Cp}^*_2\text{ScNC}(\text{H})\text{C}_6\text{H}_4\text{OMe}$  to  $\text{Cp}^*_2\text{ScNHCH}_2\text{C}_6\text{H}_4\text{OMe}$  was complete within 6 h at room temperature.

**Dehydrogenation of  $\text{Cp}^*_2\text{ScNHCH}_2\text{CMe}_3$  (10e).** An NMR tube sealed to a ground-glass joint was charged with  $\text{Cp}^*_2\text{ScNHCH}_2\text{CMe}_3$  (20 mg, 0.05 mmol) and 0.3 mL of benzene- $d_6$ . The tube was cooled to 77 K, ethylene (58.6 torr in 15.8 mL, 0.05 mmol) condensed in, and the tube sealed with a torch. The tube was heated at  $80^{\circ}\text{C}$  for 17 h after which time the ethylene had been converted to ethane and complex 10e has been completely converted to  $\text{Cp}^*_2\text{ScNC}(\text{H})\text{CMe}_3$  (5a); no intermediates were observed.

**Catalytic Hydrogenation of *tert*-Butyl Cyanide.** An NMR tube sealed to a ground-glass joint was charged with

$\text{Cp}^*_2\text{ScNHCH}_2\text{CMe}_3$  (20 mg, 0.05 mmol) and 0.4 mL of benzene- $d_6$ . The tube was cooled to 77 K,  $\text{Me}_3\text{CCN}$  (28 torr, 108 mL, 0.16 mmol) was condensed in, 700 torr of  $\text{H}_2$  was introduced, and the tube was sealed with a torch. Complex 5a was observed as soon as the spectrum was recorded. The reaction proceeds slowly at  $25^{\circ}\text{C}$ , and complex 11 could be observed. After 17 h the tube was heated to  $80^{\circ}\text{C}$ , and after a further 24 h of heating there was virtually no *tert*-butyl cyanide left, 2 equiv of  $\text{NH}_2\text{CH}_2\text{CMe}_3$  had been formed, and the major scandium-containing species (>70%) was complex 11.

**$\text{Cp}^*_2\text{ScN}=\text{C}(\text{NHCHCMe}_3)\text{CMe}_3$  (11).** *tert*-Butyl cyanide (75  $\mu\text{L}$ , 0.68 mmol) was added to a stirred solution of  $\text{Cp}^*_2\text{ScNHCH}_2\text{CMe}_3$  (266 mg, 0.66 mmol) in petroleum ether (15 mL). After being stirred for 17 h, the solution was concentrated to ca. 2 mL, cooled to  $-78^{\circ}\text{C}$ , and filtered, to provide 11 as a white solid in 31% yield: IR 3466 (m), 3398 (w), 2718 (w), 1627 (s), 1345 (vs), 1247 (m), 1210 (vs), 1185 (s), 1087 (w), 1063 (w), 1017 (m), 922 (w), 892 (w), 798 (w), 742 (m), 717 (w)  $\text{cm}^{-1}$ . Anal. Calcd for  $\text{C}_{30}\text{H}_{51}\text{N}_2\text{Sc}$ : C, 74.34; H, 10.67; N, 5.78. Found: C, 68.82; H, 9.89; N, 5.29.

**$\text{Cp}^*_2\text{ScNH}_2$  (10a).** Anhydrous ammonia (450 torr in 108 mL, 2.6 mmol) was condensed into a solution of  $\text{Cp}^*_2\text{ScMe}$  (848 mg, 2.57 mmol) in petroleum ether (10 mL) at  $-196^{\circ}\text{C}$ . The solution warmed to room temperature with stirring and was stirred for a further 0.5 h. Recrystallization from petroleum ether gave an off-white solid: yield 26%; IR 3382 (w), 3356 (sh), 3285 (w), 1592 (m), 1525 (vs), 1490 (m), 1220 (m), 1170 (sh), 1155 (s), 1058 (w), 1022 (s), 935 (w), 800 (w), 648 (m)  $\text{cm}^{-1}$ . Anal. Calcd for  $\text{C}_{20}\text{H}_{32}\text{NSc}$ : C, 72.47; H, 9.73; N, 4.23. Found: C, 70.03; H, 9.67; N, 5.19.

Similar procedures were used for the isolation of  $\text{Cp}^*_2\text{ScNHMe}$  (10b) and  $\text{Cp}^*_2\text{ScNMe}_2$  (10c).

**Compound  $\text{Cp}^*_2\text{ScNHMe}$ :** yield 37%; IR 3360 (w), 3270 (w), 2770 (s), 2730 (sh), 1585 (w), 1145 (w), 1085 (s), 1042 (s), 1018 (s), 992 (sh), 970 (m), 800 (w), 655 (m)  $\text{cm}^{-1}$ . Anal. Calcd for  $\text{C}_{21}\text{H}_{34}\text{NSc}$ : C, 73.01; H, 9.92; N, 4.05. Found: C, 72.00; H, 9.55; N, 3.92.

**Compound  $\text{Cp}^*_2\text{ScNMe}_2$ :** yield 38%; IR 2752 (s), 2720 (sh), 1234 (s), 1157 (s), 1116 (w), 1017 (m), 922 (s), 795 (w), 712 (w), 650 (w), 490 (w), 368 (m)  $\text{cm}^{-1}$ . Anal. Calcd for  $\text{C}_{22}\text{H}_{36}\text{NSc}$ : C, 73.50; H, 10.09; N, 3.90. Found: C, 73.33; H, 10.07; N, 3.85.

With the less volatile amines  $\text{NH}_2\text{R}$  ( $\text{R} = \text{Ph}$ ,  $\text{CH}_2\text{CMe}_3$ ,  $p\text{-CH}_2\text{C}_6\text{H}_4\text{OMe}$ ) 1 equiv of amine was syringed into a stirred solution of  $\text{Cp}^*_2\text{ScMe}$ . Recrystallization from petroleum ether provided the corresponding amides  $\text{Cp}^*_2\text{ScNHPh}$  (10d) and  $\text{Cp}^*_2\text{ScNHCHCMe}_3$  (10e). However for  $p\text{-NH}_2\text{CH}_2\text{C}_6\text{H}_4\text{OMe}$  the complex isolated is the adduct  $\text{Cp}^*_2\text{Sc}(\text{NHCH}_2\text{C}_6\text{H}_4\text{OMe})\text{-NH}_2\text{CH}_2\text{C}_6\text{H}_4\text{OMe}$  (12).<sup>14</sup>

**Compound  $\text{Cp}^*_2\text{ScNHPh}$ :** yield 47%; IR 3700 (w), 2720 (w), 1578 (s), 1560 (m), 1342 (m), 1277 (vs), 1192 (w), 1168 (m), 1143 (w), 1058 (w), 1014 (m), 882 (m), 830 (m), 736 (s), 681 (m)  $\text{cm}^{-1}$ . Anal. Calcd for  $\text{C}_{26}\text{H}_{36}\text{NSc}$ : C, 76.62; H, 8.90; N, 3.44. Found: C, 75.59; H, 8.72; N, 3.53.

**Compound  $\text{Cp}^*_2\text{ScNHCH}_2\text{CMe}_3$ :** yield 33%; IR 3370 (w), 3342 (w), 2770 (m), 2720 (w), 1388 (s), 1358 (m), 1318 (w), 1275 (w), 1235 (w), 1207 (w), 1152 (w), 1095 (s), 1018 (m), 1000 (m), 925 (w), 798 (w), 740 (w), 658 (m), 610 (m)  $\text{cm}^{-1}$ . Anal. Calcd for  $\text{C}_{25}\text{H}_{42}\text{NSc}$ : C, 74.78; H, 10.54; N, 3.49. Found: C, 74.00; H, 10.44; N, 3.42.

**Compound  $\text{Cp}^*_2\text{Sc}(\text{NHR})\text{NH}_2\text{R}$  ( $\text{R} = \text{CH}_2\text{C}_6\text{H}_4\text{OMe}$ ):** yield 14%; IR 3705 (w), 3360 (m), 3300 (w), 1608 (s), 1578 (s), 1505 (vs), 1335 (s), 1300 (s), 1238 (vs), 1202 (w), 1172 (s), 1130 (m), 1105 (s), 1072 (s), 1032 (s), 960 (s), 838 (m), 825 (m), 802 (s), 745 (s), 700 (w)  $\text{cm}^{-1}$ . Anal. Calcd for  $\text{C}_{36}\text{H}_{52}\text{N}_2\text{O}_2\text{Sc}$ : C, 71.74; H, 8.90; N, 4.76. Found: C, 71.99; H, 8.82; N, 4.22.

**Reaction of  $\text{Cp}^*_2\text{Sc}(\text{NHR})\text{NH}_2\text{R}$  ( $\text{R} = \text{CH}_2\text{C}_6\text{H}_4\text{OMe}$ ) with  $\text{Cp}^*_2\text{ScMe}$ .**<sup>14</sup> An NMR tube was charged with  $\text{Cp}^*_2\text{ScNHCH}_2\text{C}_6\text{H}_4\text{OMe}(\text{NH}_2\text{CH}_2\text{C}_6\text{H}_4\text{OMe})$  (20 mg, 0.034 mmol),  $\text{Cp}^*_2\text{ScMe}$  (18 mg, 0.054 mmol), and 0.4 mL of benzene- $d_6$ . An immediate reaction occurred with liberation of a gas; observation of the NMR spectrum showed the presence of  $\text{Cp}^*_2\text{ScNHCH}_2\text{C}_6\text{H}_4\text{OMe}$  (10f), methane, and unreacted  $\text{Cp}^*_2\text{ScMe}$ .

**Acknowledgment.** This work was supported by the National Science Foundation (Grant No. CHE-8024869).

Use was made of the Southern California Regional NMR Facility (NSF Grant No. CHE-7916324). D.L.D. acknowledges support through a NATO Postdoctoral Fellowship administered through the Science and Engineering Research Council (U.K.).

**Registry No.** 1, 99706-97-5; 2, 99706-98-6; 3a, 99706-99-7; 3b, 99707-00-3; 3c, 99707-01-4; 4, 99707-02-5; 5a, 99707-03-6; 5b, 99707-04-7; 6, 99707-05-8; 7, 99707-06-9; 8, 99707-07-0; 9,

99707-16-1; 10a, 99707-08-1; 10b, 99707-09-2; 10c, 99707-10-5; 10d, 99707-11-6; 10e, 99707-12-7; 10f, 99707-17-2; 11, 99707-13-8; Cp\*<sub>2</sub>Sc(NHCH<sub>2</sub>C<sub>6</sub>H<sub>4</sub>OMe)NH<sub>2</sub>CH<sub>2</sub>C<sub>6</sub>H<sub>4</sub>OMe, 99725-86-7; Cp\*<sub>2</sub>Sc(*p*-tol), 99707-14-9; Cp\*<sub>2</sub>ScMe, 99707-15-0; Cp\*<sub>2</sub>ZrH<sub>2</sub>, 61396-34-7; (Cp\*<sub>2</sub>ZrN<sub>2</sub>)<sub>2</sub>N<sub>2</sub>, 54387-50-7; *p*-NCC<sub>6</sub>H<sub>4</sub>OMe, 874-90-8; NH<sub>2</sub>CH<sub>2</sub>CMe<sub>3</sub>, 5813-64-9; *p*-tolunitrile, 104-85-8; acrylonitrile, 107-13-1; *tert*-butyl cyanide, 630-18-2; acetonitrile, 75-05-8; ammonia, 7664-41-7; methylamine, 74-89-5; dimethylamine, 124-40-3; aniline, 62-53-3; 4-methoxybenzenemethamine, 2393-23-9.

## Photophysics and Photochemistry of a Series of M(CO)<sub>5</sub>L Complexes Where M = Cr or Mo and L = Pyridine or a Substituted Pyridine

Richard M. Kolodziej and Alistair J. Lees\*

Department of Chemistry, State University of New York at Binghamton, Binghamton, New York 13901

Received July 25, 1985

Electronic absorption data are reported for a series of M(CO)<sub>5</sub>L complexes, where M = Cr and Mo and L = pyridine or a substituted pyridine. Low-lying ligand field (LF) and metal to ligand charge-transfer (MLCT) transitions are observed in the electronic absorption spectra. As the pyridine substituent becomes more electron withdrawing, the MLCT feature shifts to lower energy. For L = pyridine, 4-methylpyridine, 3,5-dichloropyridine, 4-phenylpyridine, 2-cyanopyridine, and 3-cyanopyridine the LF transition is the lowest lying excited state. For L = 4-cyanopyridine, 4-benzoylpyridine, 4-acetylpyridine, and 4-formylpyridine the MLCT transition is at lowest energy. Luminescence has been detected from room-temperature solutions of those complexes with a lowest lying MLCT transition and thus assigned to originate from this state. Upon excitation in the visible region these complexes undergo photosubstitution of the pyridine ligand. The photosubstitution quantum yields are most sensitive to the nature of the lowest energy excited state, being considerably greater when this state is of LF character as opposed to MLCT character. The quantum efficiencies were determined not to be thermally activated following MLCT excitation, suggesting that another state, possibly a LF triplet, is close in energy to the low-lying MLCT transition and is responsible for the photochemistry. Excited-state schemes based on the experimental data are reported.

### Introduction

Unlike classical coordination compounds, the photochemical properties of organometallic species are only poorly understood. Yet a further knowledge of these photoprocesses may be expected to prove extremely valuable toward successful design of synthetically useful and catalytically active transformations. It has been a focus of our research to study excited-state deactivation pathways in transition-metal organometallic complexes and, specifically, to learn of the interrelationship of their photophysical and photochemical behavior.

Luminescence characteristics of transition-metal organometallic complexes have not been explored in detail. Most investigations of the emission behavior of organometallic complexes have been carried out at low temperature in a rigid environment, such as a glass or a matrix, where nonradiative deactivation pathways are substantially reduced.<sup>1</sup> When examples of emission from metal complexes in fluid solution are discovered, valuable information on excited state processes can be obtained.<sup>2,3</sup> In particular, metal carbonyl complexes have not been thought to luminesce in fluid solution due to the relatively high photoreactivity and efficient nonradiative deactivation routes

of their excited states. Only a few complexes are known to emit in room-temperature conditions. The lack of available data has, up to the present time, inhibited models for the excited states of transition-metal carbonyls and their derivatives. Several ClRe(CO)<sub>3</sub>L complexes, where L = 1,10-phenanthroline and related ligands, have been reported to luminesce in fluid solution, and the emission attributed to a low-energy MLCT state with considerable triplet character.<sup>4</sup> Room-temperature luminescence from a MLCT triplet state has also been observed from a series of XRe(CO)<sub>3</sub>L<sub>2</sub> complexes, where X = Cl, Br, I, and L = 4,4'-bipyridine, 4-phenylpyridine, and 3-benzoylpyridine.<sup>5</sup> Upon cooling this system was concluded to undergo substantial reordering of low-lying states; the emission at 77 K attributed to an intraligand ( $\pi$ - $\pi^*$ ) triplet state. Recently emission in fluid solution has been determined from a series of W(CO)<sub>5</sub>L complexes, where L = a pyridine derivative.<sup>6</sup> Noticeably all these examples are of third-row transition-metal systems in which spin-orbit coupling parameters can be expected to be high.<sup>7</sup> We have,

(1) Calvert, J. G.; Pitts, J. N. "Photochemistry"; Wiley-Interscience: New York, 1966; p 240.

(2) Fleischauer, P. D.; Fleischauer, P. *Chem. Rev.* 1970, 70, 199.

(3) Porter, G. B. "Concepts of Inorganic Photochemistry"; Adamson, A. W., Fleischauer, P. D., Eds.; Wiley-Interscience: New York, 1975; p 37.

(4) (a) Wrighton, M.; Morse, D. L. *J. Am. Chem. Soc.* 1974, 96, 998.

(b) Giordano, P. J.; Fredericks, S. M.; Wrighton, M. S.; Morse, D. L. *J. Am. Chem. Soc.* 1978, 100, 2257. (c) Fredericks, S. M.; Luong, J. C.; Wrighton, M. S. *J. Am. Chem. Soc.* 1979, 101, 7415. (d) Luong, J. C.; Faltynek, R. A.; Wrighton, M. S. *J. Am. Chem. Soc.* 1979, 101, 1597.

(5) Giordano, P. J.; Wrighton, M. S. *J. Am. Chem. Soc.* 1979, 101, 2888.

(6) (a) Lees, A. J.; Adamson, A. W. *J. Am. Chem. Soc.* 1980, 102, 6874.

(b) Lees, A. J.; Adamson, A. W. *J. Am. Chem. Soc.* 1982, 104, 3804.

(7) Moore, C. E. "National Standards Reference Data Service"; National Bureau of Standards: Washington, D.C., 1971; Vol. 3.



Use was made of the Southern California Regional NMR Facility (NSF Grant No. CHE-7916324). D.L.D. acknowledges support through a NATO Postdoctoral Fellowship administered through the Science and Engineering Research Council (U.K.).

**Registry No.** 1, 99706-97-5; 2, 99706-98-6; 3a, 99706-99-7; 3b, 99707-00-3; 3c, 99707-01-4; 4, 99707-02-5; 5a, 99707-03-6; 5b, 99707-04-7; 6, 99707-05-8; 7, 99707-06-9; 8, 99707-07-0; 9,

99707-16-1; 10a, 99707-08-1; 10b, 99707-09-2; 10c, 99707-10-5; 10d, 99707-11-6; 10e, 99707-12-7; 10f, 99707-17-2; 11, 99707-13-8; Cp\*<sub>2</sub>Sc(NHCH<sub>2</sub>C<sub>6</sub>H<sub>4</sub>OMe)NH<sub>2</sub>CH<sub>2</sub>C<sub>6</sub>H<sub>4</sub>OMe, 99725-86-7; Cp\*<sub>2</sub>Sc(*p*-tol), 99707-14-9; Cp\*<sub>2</sub>ScMe, 99707-15-0; Cp\*<sub>2</sub>ZrH<sub>2</sub>, 61396-34-7; (Cp\*<sub>2</sub>ZrN<sub>2</sub>)<sub>2</sub>N<sub>2</sub>, 54387-50-7; *p*-NCC<sub>6</sub>H<sub>4</sub>OMe, 874-90-8; NH<sub>2</sub>CH<sub>2</sub>CMe<sub>3</sub>, 5813-64-9; *p*-tolunitrile, 104-85-8; acrylonitrile, 107-13-1; *tert*-butyl cyanide, 630-18-2; acetonitrile, 75-05-8; ammonia, 7664-41-7; methylamine, 74-89-5; dimethylamine, 124-40-3; aniline, 62-53-3; 4-methoxybenzenemethamine, 2393-23-9.

## Photophysics and Photochemistry of a Series of M(CO)<sub>5</sub>L Complexes Where M = Cr or Mo and L = Pyridine or a Substituted Pyridine

Richard M. Kolodziej and Alistair J. Lees\*

Department of Chemistry, State University of New York at Binghamton, Binghamton, New York 13901

Received July 25, 1985

Electronic absorption data are reported for a series of M(CO)<sub>5</sub>L complexes, where M = Cr and Mo and L = pyridine or a substituted pyridine. Low-lying ligand field (LF) and metal to ligand charge-transfer (MLCT) transitions are observed in the electronic absorption spectra. As the pyridine substituent becomes more electron withdrawing, the MLCT feature shifts to lower energy. For L = pyridine, 4-methylpyridine, 3,5-dichloropyridine, 4-phenylpyridine, 2-cyanopyridine, and 3-cyanopyridine the LF transition is the lowest lying excited state. For L = 4-cyanopyridine, 4-benzoylpyridine, 4-acetylpyridine, and 4-formylpyridine the MLCT transition is at lowest energy. Luminescence has been detected from room-temperature solutions of those complexes with a lowest lying MLCT transition and thus assigned to originate from this state. Upon excitation in the visible region these complexes undergo photosubstitution of the pyridine ligand. The photosubstitution quantum yields are most sensitive to the nature of the lowest energy excited state, being considerably greater when this state is of LF character as opposed to MLCT character. The quantum efficiencies were determined not to be thermally activated following MLCT excitation, suggesting that another state, possibly a LF triplet, is close in energy to the low-lying MLCT transition and is responsible for the photochemistry. Excited-state schemes based on the experimental data are reported.

### Introduction

Unlike classical coordination compounds, the photochemical properties of organometallic species are only poorly understood. Yet a further knowledge of these photoprocesses may be expected to prove extremely valuable toward successful design of synthetically useful and catalytically active transformations. It has been a focus of our research to study excited-state deactivation pathways in transition-metal organometallic complexes and, specifically, to learn of the interrelationship of their photophysical and photochemical behavior.

Luminescence characteristics of transition-metal organometallic complexes have not been explored in detail. Most investigations of the emission behavior of organometallic complexes have been carried out at low temperature in a rigid environment, such as a glass or a matrix, where nonradiative deactivation pathways are substantially reduced.<sup>1</sup> When examples of emission from metal complexes in fluid solution are discovered, valuable information on excited state processes can be obtained.<sup>2,3</sup> In particular, metal carbonyl complexes have not been thought to luminesce in fluid solution due to the relatively high photoreactivity and efficient nonradiative deactivation routes

of their excited states. Only a few complexes are known to emit in room-temperature conditions. The lack of available data has, up to the present time, inhibited models for the excited states of transition-metal carbonyls and their derivatives. Several ClRe(CO)<sub>3</sub>L complexes, where L = 1,10-phenanthroline and related ligands, have been reported to luminesce in fluid solution, and the emission attributed to a low-energy MLCT state with considerable triplet character.<sup>4</sup> Room-temperature luminescence from a MLCT triplet state has also been observed from a series of XRe(CO)<sub>3</sub>L<sub>2</sub> complexes, where X = Cl, Br, I, and L = 4,4'-bipyridine, 4-phenylpyridine, and 3-benzoylpyridine.<sup>5</sup> Upon cooling this system was concluded to undergo substantial reordering of low-lying states; the emission at 77 K attributed to an intraligand ( $\pi$ - $\pi^*$ ) triplet state. Recently emission in fluid solution has been determined from a series of W(CO)<sub>5</sub>L complexes, where L = a pyridine derivative.<sup>6</sup> Noticeably all these examples are of third-row transition-metal systems in which spin-orbit coupling parameters can be expected to be high.<sup>7</sup> We have,

(1) Calvert, J. G.; Pitts, J. N. "Photochemistry"; Wiley-Interscience: New York, 1966; p 240.

(2) Fleischauer, P. D.; Fleischauer, P. *Chem. Rev.* **1970**, *70*, 199.

(3) Porter, G. B. "Concepts of Inorganic Photochemistry"; Adamson, A. W., Fleischauer, P. D., Eds.; Wiley-Interscience: New York, 1975; p 37.

(4) (a) Wrighton, M.; Morse, D. L. *J. Am. Chem. Soc.* **1974**, *96*, 998.

(b) Giordano, P. J.; Fredericks, S. M.; Wrighton, M. S.; Morse, D. L. *J. Am. Chem. Soc.* **1978**, *100*, 2257. (c) Fredericks, S. M.; Luong, J. C.; Wrighton, M. S. *J. Am. Chem. Soc.* **1979**, *101*, 7415. (d) Luong, J. C.; Faltynek, R. A.; Wrighton, M. S. *J. Am. Chem. Soc.* **1979**, *101*, 1597.

(5) Giordano, P. J.; Wrighton, M. S. *J. Am. Chem. Soc.* **1979**, *101*, 2888.

(6) (a) Lees, A. J.; Adamson, A. W. *J. Am. Chem. Soc.* **1980**, *102*, 6874.

(b) Lees, A. J.; Adamson, A. W. *J. Am. Chem. Soc.* **1982**, *104*, 3804.

(7) Moore, C. E. "National Standards Reference Data Service"; National Bureau of Standards: Washington, D.C., 1971; Vol. 3.

therefore, initiated a study of the photophysical and photochemical properties of the lighter group 6 metal carbonyl complexes.<sup>8</sup> In this paper we describe the results obtained from a series of  $M(\text{CO})_5\text{L}$  complexes, where  $M = \text{Cr}$  and  $\text{Mo}$  and  $\text{L} =$  a pyridine or a pyridine derivative. The following abbreviations will be used throughout the text for the ligands: py = pyridine; 4-Me-py = 4-methylpyridine; 3,5-Cl<sub>2</sub>-py = 3,5-dichloropyridine; 4-Ph-py = 4-phenylpyridine; 2-CN-py = 2-cyanopyridine; 3-CN-py = 3-cyanopyridine; 4-CN-py = 4-cyanopyridine; 4-Bz-py = 4-benzoylpyridine; 4-Ac-py = 4-acetylpyridine; 4-Fm-py = 4-formylpyridine.

### Experimental Section

**Materials.** The metal hexacarbonyls were obtained from Strem Chemical Co. and used without further purification. The ligands are commercially available (Aldrich or Fisher Chemical Co.) at >99% purity and used without further purification. Solvents used in the synthesis and emission experiments were obtained from J. T. Baker Chemical Co. as HPLC grade and were further purified by several distillations. Carbonyl-containing impurities in these solvents were removed according to a literature procedure.<sup>9</sup> Alumina used in the chromatographic purifications was purchased from Fisher Scientific Co. Nitrogen used in the purging experiments was dried and deoxygenated according to a previously described procedure.<sup>10</sup>

**Synthesis of  $M(\text{CO})_5\text{L}$  Complexes.** The preparation of the  $M(\text{CO})_5\text{L}$  complexes ( $M = \text{Cr}$  or  $\text{Mo}$ ,  $\text{L} =$  pyridine or a pyridine derivative) was carried out via the corresponding tetrahydrofuran complex  $M(\text{CO})_5(\text{THF})$ . A tetrahydrofuran solution (200 mL) of the parent hexacarbonyl (6 mmol) was deoxygenated by purging with purified nitrogen for 15 min and then irradiated with a 200-W medium-pressure Hg lamp until a deep green/yellow color was achieved (~60 min). The solution was continually purged with nitrogen throughout irradiation to avoid any oxidation effects. After the irradiation step a stoichiometric amount of the desired ligand was added to the reaction vessel in the dark. The tetrahydrofuran was then removed by rotary evaporation and the complex redissolved in isooctane and purified via chromatography in the dark on a 3-in. alumina column. Unreacted hexacarbonyl was initially removed from the column by successive isooctane washings; these were monitored by UV spectroscopy. The pentacarbonyl complex was then eluted with benzene and further purified by recrystallization from isooctane/benzene solution. For complexes where  $\text{L} =$  4-cyanopyridine, it was necessary to further remove hexacarbonyl impurities using a sublimation procedure. All the product complexes were moderately stable in the solid form although their long-term stabilities were greatly increased when they were stored in the dark under nitrogen at 273 K. In solution at 298 K the complexes exhibited varying degrees of thermal stability, with the chromium complexes exhibiting the most rapid decomposition.

**Equipment and Procedures.** Infrared spectra were recorded on a Perkin-Elmer Model 283B spectrometer. Reported band maxima are considered to be accurate to  $\pm 2 \text{ cm}^{-1}$ . All complexes were recorded as Nujol mulls between NaCl plates. Electronic absorption spectra were obtained on a Hewlett-Packard 8450A spectrophotometer which incorporates a microprocessor-controlled diode-array detector. This permitted absorption data to be obtained from the thermally sensitive solutions within 5 s of dissolution. Emission spectra were recorded on a SLM Instruments Model 8000/8000S emission spectrophotometer which utilizes a photomultiplier-based photon-counting detector. The emission data were corrected for wavelength variations of detector response, and the band maxima are considered accurate to  $\pm 8 \text{ nm}$ . All spectra were recorded from solutions in a 1-cm clear sided quartz glass cell. The solutions were filtered through a 0.22- $\mu\text{m}$  Millipore filter and purged with nitrogen for 15 min prior to recording

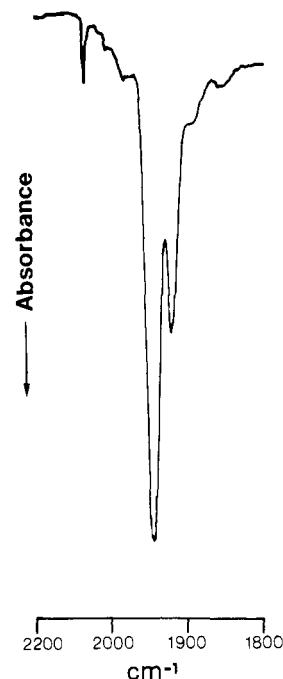


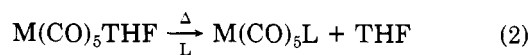
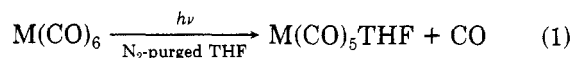
Figure 1. Infrared spectrum of  $\text{Mo}(\text{CO})_5(4\text{-Me-py})$  in Nujol.

emission data. Emission quantum yields were reported relative to the luminescence of  $\text{Ru}(\text{bpy})_3^{2+11}$  and are considered accurate to within  $\pm 10\%$ .

Photolysis experiments were carried out with a 200-W medium-pressure Hg/Xe lamp using Baird Atomic and Rolyn Optics Corp. interference filters (10-nm band-pass) to isolate excitation wavelengths at 405 and 436 nm. Typical light intensities were  $10^{-9}$ – $10^{-8}$  einstein  $\text{s}^{-1}$  determined by ferrioxalate actinometry.<sup>12</sup> Irradiation at 458 nm was performed with a Lexel Corp. Model 95-4 4W argon ion laser with typical laser power at 150 mW. The photon flux was calculated from the laser power, measured by means of an external Lexel Corp. Model 504 power meter. Incident light intensities were further determined by Reineckate actinometry.<sup>13</sup> Sample solutions ( $10^{-4} \text{ M}$  in complex,  $10^{-2} \text{ M}$  in entering ligand) were doubly filtered through 0.22- $\mu\text{m}$  Millipore filters immediately before use and transferred to a 1-cm quartz glass cell. The solutions were deoxygenated by purging with purified nitrogen for 15 min. A Brinkmann Instruments Lauda K-2/R circulating temperature bath was used to control sample temperature to  $\pm 0.2 \text{ K}$ . The concentrations of reactants and products were monitored during the photolysis by UV-visible spectroscopy. Photochemical quantum yields were obtained by monitoring the disappearance of starting complex in the 400–450-nm region. They were corrected for changing degree of light absorption, small inner filter effects due to product formation, and competing thermal reaction, when necessary. For the 405- and 436-nm excitations the quantum yield measurements were made over relatively small conversions. Quantum yields were found to be reproducible to  $\pm 15\%$ .

### Results and Discussion

**a. Synthesis of  $M(\text{CO})_5\text{L}$ .** The complexes were prepared via the corresponding tetrahydrofuran (THF) complex (see eq 1 and 2) according to a literature procedure.<sup>14</sup>



The above method proved more satisfactory than direct

(8) Lees, A. J. *J. Am. Chem. Soc.* **1982**, *104*, 2038.

(9) Perrin, D. D.; Armarego, W. L. F.; Perrin, D. R. "Purification of Laboratory Chemicals", 2nd ed.; Pergamon Press: New York, 1980.

(10) Schadt, M. J.; Gresalfi, N. J.; Lees, A. J. *Inorg. Chem.* **1985**, *24*, 2942.

(11) Van Houten, J.; Watts, R. J. *J. Am. Chem. Soc.* **1976**, *98*, 4853.

(12) Hatchard, C. G.; Parker, C. A. *Proc. R. Soc. London., Ser. A* **1956**, *235*, 518.

(13) Wegner, E. E.; Adamson, A. W. *J. Am. Chem. Soc.* **1966**, *88*, 394.

(14) Strohmeier, W. *Angew. Chem., Int. Ed. Engl.* **1964**, *3*, 730.

**Table I. Infrared Spectral Data in the Carbonyl Stretching Region and Assignments for  $M(\text{CO})_5\text{L}$  ( $M = \text{Cr}, \text{Mo}$ ) Complexes<sup>a</sup>**

complex	stretching freq., <sup>b</sup> $\text{cm}^{-1}$				
	$A_1^1$	B	E	$A_1^2$	
$\text{Cr}(\text{CO})_5(4\text{-Me-py})$	2066 (w)	1981 (vw)	1938 (s)	1920 (m)	
$\text{Cr}(\text{CO})_5(\text{py})$	2067 (w)	c	1940 (s)	1922 (m)	
$\text{Cr}(\text{CO})_5(3,5\text{-Cl}_2\text{-py})$	2070 (w)	1987 (vw)	1947 (s)	1933 (sh)	
$\text{Cr}(\text{CO})_5(4\text{-Ph-py})$	2064 (w)	c	1940 (s)	1920 (sh)	
$\text{Cr}(\text{CO})_5(4\text{-CN-py})$	2242 <sup>d</sup>	2078 (w)	c	1945 (s)	1930 (m)
$\text{Cr}(\text{CO})_5(4\text{-Bz-py})$	2070 (w)	1990 (vw)	1940 (s)	1924 (m)	1672 <sup>e</sup>
$\text{Cr}(\text{CO})_5(4\text{-Ac-py})$	2075 (w)	1990 (vw)	1943 (s)	1928 (m)	1704 <sup>e</sup>
$\text{Cr}(\text{CO})_5(4\text{-Fm-py})$	2070 (w)	1990 (vw)	1943 (s)	1928 (sh)	1715 <sup>e</sup>
$\text{Mo}(\text{CO})_5(4\text{-Me-py})$	2073 (w)	1981 (vw)	1945 (s)	1920 (m)	
$\text{Mo}(\text{CO})_5(\text{py})$	2078 (w)	1985 (vw)	1946 (s)	1922 (m)	
$\text{Mo}(\text{CO})_5(3,5\text{-Cl}_2\text{-py})$	2076 (w)	c	1945 (s)	1928 (sh)	
$\text{Mo}(\text{CO})_5(4\text{-Ph-py})$	2072 (w)	c	1942 (s)	1920 (m)	
$\text{Mo}(\text{CO})_5(2\text{-CN-py})$	2232 <sup>d</sup>	2075 (w)	1987 (vw)	1954 (s)	1910 (sh)
$\text{Mo}(\text{CO})_5(3\text{-CN-py})$	2235 <sup>d</sup>	2072 (w)	1992 (vw)	1956 (s)	1933 (sh)
$\text{Mo}(\text{CO})_5(4\text{-CN-py})$	2241 <sup>d</sup>	2063 (w)	c	1945 (s)	1925 (m)
$\text{Mo}(\text{CO})_5(4\text{-Bz-py})$	2075 (w)	c	1945 (s)	1926 (m)	1670 <sup>e</sup>
$\text{Mo}(\text{CO})_5(4\text{-Ac-py})$	2064 (w)	1984 (w)	1943 (s)	1920 (sh)	1702 <sup>e</sup>
$\text{Mo}(\text{CO})_5(4\text{-Fm-py})$	2070 (w)	1995 (vw)	1945 (s)	1925 (sh)	1715 <sup>e</sup>

<sup>a</sup>In Nujol mulls at 298 K. <sup>b</sup>vw = very weak; w = weak; m = moderate; s = strong; sh = shoulder. <sup>c</sup>Not observed. <sup>d</sup>Cyano stretch of coordinated pyridine ligand. <sup>e</sup>Carbonyl stretch of coordinated pyridine ligand.

**Table II. Electronic Absorption Spectral Data and Assignments for  $M(\text{CO})_5\text{L}$  ( $M = \text{Cr}, \text{Mo}$ ) Complexes in Benzene at 298 K**

complex	absorption maxima, <sup>a</sup> nm		
	$e^4b_2^2 \rightarrow e^3b_2^2b_1^1$	$e^4b_2^2 \rightarrow e^3b_2^2a_1^1$	MLCT
$\text{Cr}(\text{CO})_5(4\text{-Me-py})$	330 (sh)	408	359 (sh)
$\text{Cr}(\text{CO})_5(\text{py})$	331 (sh)	402	368 (sh)
$\text{Cr}(\text{CO})_5(3,5\text{-Cl}_2\text{-py})$	340 (sh)	406	b
$\text{Cr}(\text{CO})_5(4\text{-Ph-py})$	345 (sh)	396	b
$\text{Cr}(\text{CO})_5(4\text{-CN-py})$	350	c	436
$\text{Cr}(\text{CO})_5(4\text{-Bz-py})$	358	c	430
$\text{Cr}(\text{CO})_5(4\text{-Ac-py})$	352	c	438
$\text{Cr}(\text{CO})_5(4\text{-Fm-py})$	356	c	434
$\text{Mo}(\text{CO})_5(4\text{-Me-py})$	322	392	b
$\text{Mo}(\text{CO})_5(\text{py})$	327 (sh)	389	b
$\text{Mo}(\text{CO})_5(3,5\text{-Cl}_2\text{-py})$	336 (sh)	390	b
$\text{Mo}(\text{CO})_5(4\text{-Ph-py})$	343 (sh)	384	b
$\text{Mo}(\text{CO})_5(2\text{-CN-py})$	328	373	b
$\text{Mo}(\text{CO})_5(3\text{-CN-py})$	327 (sh)	381	b
$\text{Mo}(\text{CO})_5(4\text{-CN-py})$	d	392	~435 (sh)
$\text{Mo}(\text{CO})_5(4\text{-Bz-py})$	d	393	~438 (sh)
$\text{Mo}(\text{CO})_5(4\text{-Ac-py})$	d	394	~440 (sh)
$\text{Mo}(\text{CO})_5(4\text{-Fm-py})$	d	392	~447 (sh)

<sup>a</sup>sh = shoulder. <sup>b</sup>Overlaps with  $e^4b_2^2 \rightarrow e^3b_2^2a_1^1$  transition. <sup>c</sup>Overlaps with MLCT transition. <sup>d</sup>Not observed.

irradiation of hexacarbonyl solutions that contained excess ligand; the latter route gave rise to a number of secondary photoproduct impurities of which a major component was identified as *cis*- $M(\text{CO})_4\text{L}_2$ .<sup>15</sup>

**b. Infrared Spectra.** The infrared absorption spectrum in the carbonyl stretching region of  $\text{Mo}(\text{CO})_5(4\text{-Me-py})$  is shown in Figure 1. The three moderate and strong band maxima are characteristic of a  $C_{4v}$  arrangement of the carbonyl ligands at the metal center.<sup>16</sup> Infrared spectra and assignments for all the complexes studied are summarized in Table I. An extremely weak B mode was observed for several of the complexes, indicative of slight perturbation of the  $C_{4v}$  symmetry. The spectral data appear to rule out the possibility of any of the pyridine derivatives being bound through their substituent heteroatoms. That is, carbonyl stretching vibrations of the  $M(\text{CO})_5\text{L}$  complexes, where  $L = 2\text{-CN-py}$ ,

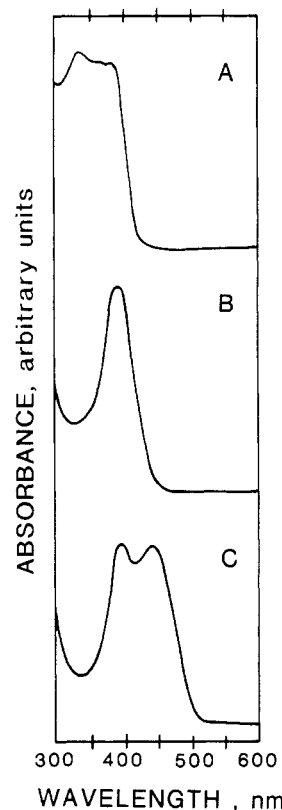


**Figure 2.** Electronic absorption spectra at 298 K of (A)  $\text{Mo}(\text{CO})_5(4\text{-Me-py})$ , (B)  $\text{Mo}(\text{CO})_5(3,5\text{-Cl}_2\text{-py})$ , and (C)  $\text{Mo}(\text{CO})_5(4\text{-CN-py})$  in isoctane.

3-CN-py, 4-CN-py, 4-Bz-py, 4-Ac-py, and 4-Fm-py, are similar to those of the other complexes in this series, and specifically, the  $\text{C}\equiv\text{N}$  or  $\text{C}=\text{O}$  stretching frequencies are concordant to that of the free ligands (2232, 2238, 2241, 1670, 1703, and 1715  $\text{cm}^{-1}$ , respectively).

**c. Electronic Absorption Spectra.** The electronic absorption data obtained from all the  $M(\text{CO})_5\text{L}$  complexes at 298 K are summarized in Table II. Electronic absorption data for the  $\text{Mo}(\text{CO})_5\text{L}$  complexes, where  $L = 4\text{-Me-py}$ ,  $3,5\text{-Cl}_2\text{-py}$ , and  $4\text{-CN-py}$ , are shown in Figure 2. Three distinct transitions can be observed for  $L = 4\text{-Me-py}$ ; the bands centered at 338 and 387 nm are assigned as ligand field (LF)  $e^4b_2^2 \rightarrow e^3b_2^2b_1^1$  and  $e^4b_2^2 \rightarrow e^3b_2^2a_1^1$  transitions, respectively,<sup>17,18</sup> and the band centered at 368

(15) Chun, S.; Getty, E. E.; Lees, A. J. *Inorg. Chem.* 1984, 23, 2155.

(16) Cotton, F. A. "Chemical Applications of Group Theory"; Wiley-Interscience: New York, 1971.

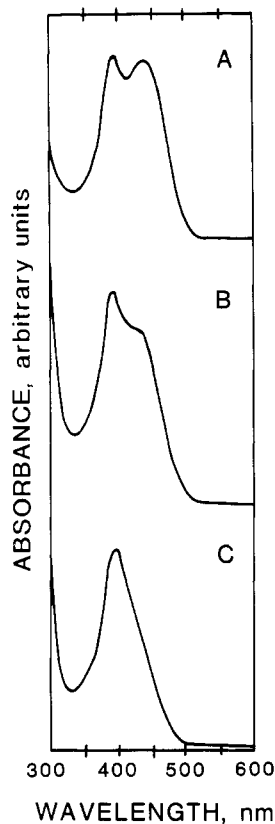


**Figure 3.** Electronic absorption spectra at 298 K of  $\text{Mo}(\text{CO})_5(4\text{-CN-py})$  in (A) isooctane, (B) trichloroethylene, and (C) benzene.

nm is assigned as a metal to ligand charge-transfer (MLCT) transition. As the pyridine substituent becomes more electron withdrawing, the MLCT transition shifts to longer wavelength. In the case of  $\text{L} = 3,5\text{-Cl}_2\text{-py}$  the LF and MLCT transitions overlap substantially. When the pyridine substituent is a strong electron-withdrawing group, e.g., 4-cyano, the MLCT absorption clearly becomes the lowest energy feature. We note that the positions of the LF transitions remain relatively unshifted by changes in the pyridine substituent, although the absorbance in the LF region is greatly affected by overlap with the intense MLCT band. In summary, changes in the electronic character of ligand substituent has a substantial effect on the order of the low-lying energy states in these complexes.

It is noted that the concept of pure LF and MLCT states is implied by the above assignments and discussion. However, as these LF transitions are considerably more intense than that normally observed for metal complexes, it seems likely that there is significant mixing between the LF and MLCT states in these  $M(\text{CO})_5\text{L}$  complexes.

Absorption spectra for the  $\text{Mo}(\text{CO})_5(4\text{-CN-py})$  complex in various solvents are displayed in Figure 3. These are interpreted in terms of the quite different solvent effects on the LF and MLCT transitions.<sup>19</sup> The MLCT transition substantially blue shifts as the solvent polarity or polarizability increases, whereas the LF transition again remains relatively unaffected.<sup>20</sup> Similar large solvent and substituent effects on the energy of the MLCT transition have

(17) Wrighton, M. S.; Abrahamson, H. B.; Morse, D. L. *J. Am. Chem. Soc.* **1976**, *98*, 4105.

(18) Dahlgren, R. M.; Zink, J. I. *Inorg. Chem.* **1977**, *16*, 3154.

(19) Manuta, D. M.; Lees, A. J. *Inorg. Chem.* **1983**, *22*, 3825.

(20) The MLCT absorption energies of zerovalent metal carbonyl complexes have been reported to correlate to high degree with solvent polarizability as well as more established solvent polarity parameters: Manuta, D. M.; Lees, A. J., Biennial Inorganic Chemical Symposium on the Chemistry of Excited States and Reactive Intermediates, Toronto, Canada, June, 1985; see Abstracts, No. 18.

**Table III.** Emission Spectral Data for  $\text{Mo}(\text{CO})_5\text{L}$  Complexes in Benzene at 298 K<sup>a-c</sup>

complex	emission		
	maxima, nm	half width, <sup>d</sup> $\text{cm}^{-1} \times 10^{-3}$	quantum yield $\times 10^4$
$\text{Mo}(\text{CO})_5(4\text{-CN-py})$	630	4.4	1.3
$\text{Mo}(\text{CO})_5(4\text{-Bz-py})$	647	3.7	4.3
$\text{Mo}(\text{CO})_5(4\text{-Ac-py})$	632	4.1	1.6
$\text{Mo}(\text{CO})_5(4\text{-FM-py})$	668	3.8	1.9

<sup>a</sup>The excitation wavelength is 436 nm. Emission spectra were corrected for variation in instrumental response as a function of wavelength. <sup>b</sup> $8 \times 10^{-5} - 2 \times 10^{-4}$  M deaerated solutions. <sup>c</sup>Emission not observed for complexes where  $\text{L} = \text{py}$ , 4-Me-py, 3,5- $\text{Cl}_2\text{-py}$ , 4-Ph-py, 2-CN-py, and 3-CN-py. <sup>d</sup>Width of emission band at half-height.

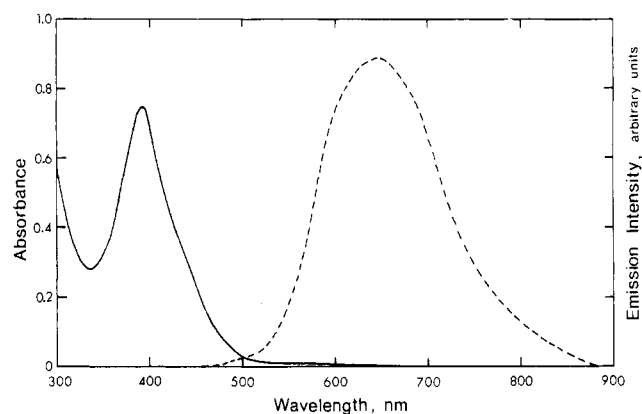


**Figure 4.** Electronic absorption (—) and emission (---) spectra at 298 K of  $10^{-4}$  M  $\text{Mo}(\text{CO})_5(4\text{-Bz-py})$  in benzene. The emission spectrum is corrected for variation in instrumental response as a function of wavelength, and the excitation wavelength is 436 nm.

been observed in the electronic absorption spectra of iso-electronic  $\text{W}(\text{CO})_5\text{L}$ ,<sup>17</sup>  $\text{M}(\text{CO})_4\text{L}_2$  ( $\text{M} = \text{Cr}, \text{Mo}, \text{W}$ ),<sup>15,21</sup>  $\text{Ru}(\text{NH}_3)_5\text{L}^{2+}$ ,<sup>22</sup> and  $\text{Fe}(\text{CN})_5\text{L}^{3-23}$  complexes.

**d. Luminescence Spectra.** Luminescence data have been recorded from room temperature solutions of the series of  $\text{Mo}(\text{CO})_5\text{L}$  complexes, and the results are reported in Table III. Room-temperature emission was not observed from  $\text{Mo}(\text{CO})_5\text{L}$  complexes ( $\text{L} = \text{py}$ , 4-Me-py, 3,5- $\text{Cl}_2\text{-py}$ , 4-Ph-py, 2-CN-py, and 3-CN-py) in which LF states are lowest lying. Figure 4 illustrates the electronic absorption and emission spectra of  $\text{Mo}(\text{CO})_5(4\text{-Bz-py})$  in benzene at 298 K. Each of the emission spectra recorded were typically broad and unstructured. The spectral distribution of the emission of each complex was observed to be independent of excitation wavelengths longer than 300 nm; this is consistent with emission from a single low-lying excited state. The emission data shown in Table III indicate that the emission maxima of  $\text{Mo}(\text{CO})_5\text{L}$  complexes shift to lower energy as the pyridine substituent becomes more electron withdrawing. This result parallels that found in absorption (see Table II), and therefore, we attribute the emission to originate from the MLCT state of each complex. Moreover, the determination of emission exclusively from the complexes in which the MLCT state is at lowest energy (see absorption section) provides further evidence for this assignment. The observation of emission at room temperature suggests that the emitting MLCT state is relatively long-lived and may possess considerable

(21) Abrahamson, H. B.; Wrighton, M. S. *Inorg. Chem.* **1978**, *17*, 3385.

(22) Ford, P. C. *Rev. Chem. Intermed.* **1979**, *2*, 267.

(23) Figard, J. E.; Petersen, J. D. *Inorg. Chem.* **1978**, *17*, 1059.

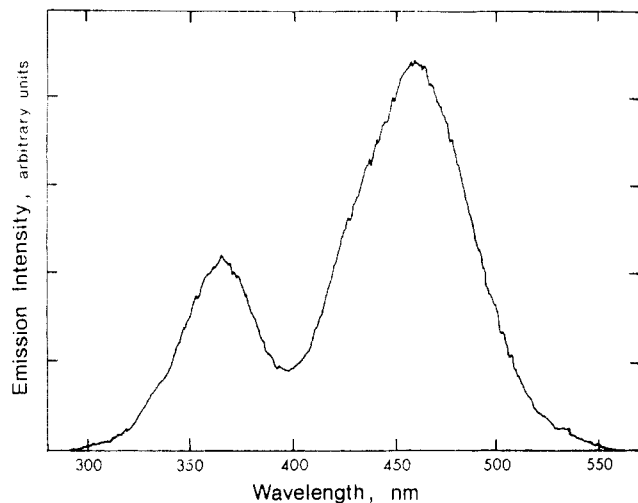
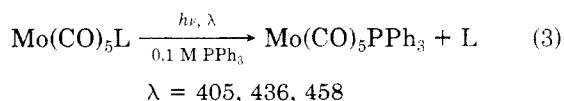


**Figure 5.** Excitation spectrum at 298 K of  $10^{-4}$  M  $\text{Mo}(\text{CO})_5(4\text{-Bz-py})$  in benzene (emission monitored at 640 nm).

triplet character. These complexes appear to be the first examples of second-row transition-metal carbonyls known to luminesce in fluid solution, although a number of these have been reported to emit at low temperature in rigid media.<sup>24-26</sup> The analogous  $\text{Cr}(\text{CO})_5\text{L}$  complexes were very thermally active and decomposed during the time required to acquire emission data. Reproducible emission spectra were unobtainable from these complexes. Emission quantum yields measured for the complexes are shown in Table III. These quantum yields were observed to be independent of temperature in the 283–313 K range, indicating that the emission process is not a thermally activated one.

Figure 5 illustrates an excitation spectrum of  $\text{Mo}(\text{CO})_5(4\text{-Bz-py})$  in benzene at 298 K. The excitation and absorption spectra of this complex are not congruent (see Figures 4 and 5), indicating a wavelength dependence of the emission efficiency. The most intense band centered at 455 nm is assigned to be the emitting MLCT state. An excitation band centered at 366 nm suggests that the higher energy LF state effectively populates the emitting state. The excitation spectrum exhibits a minimum at 398 nm close to that of the lowest energy LF absorption. This result implies that the lowest energy LF excited state does not effectively populate the emitting MLCT state and that its energy degradation is by an alternative route. This LF state may be a reactive one; it has been attributed to be so for the closely related  $\text{W}(\text{CO})_5\text{L}$  complexes<sup>6,17</sup> and in the isoelectronic  $\text{W}(\text{CO})_4\text{L}_2^{15,21}$  and  $\text{Ru}(\text{NH}_3)_5\text{L}^{2+}$  systems.<sup>22</sup>

**e. Photochemistry.** We have determined the quantum efficiencies for reaction 3. These reactions were carried



L = 3-cyanopyridine, 4-cyanopyridine

out at 283 K to minimize thermal substitution effects. The ligands chosen were such that two distinct types of complexes were represented; that is,  $\text{Mo}(\text{CO})_5\text{L}$  complexes with a lowest lying MLCT state (L = 4-CN-py) or with a lowest lying LF state (L = 3-CN-py). For each complex the above photosubstitution reaction (3) was observed to take place exclusively at any of the irradiation wavelengths and no

**Table IV.** Photosubstitution Quantum Yields of  $\text{Mo}(\text{CO})_5\text{L}$  Complexes (L = 3-Cyanopyridine and 4-Cyanopyridine) at 283 K<sup>a</sup>

complex	irradiation wavelength, nm		
	405	436	458
3-cyanopyridine	0.67	0.61	0.40
4-cyanopyridine	0.24	0.12	0.04

<sup>a</sup> Photolyses carried out in benzene solutions containing 0.1 M triphenylphosphine.

evidence was observed for dissociation of CO ligand. However, the photosubstitution quantum efficiency depends substantially on excitation energy. Table IV summarizes the quantum yield results. The data indicate that complexes with a lowest lying LF transition are significantly more photoactive than complexes in which the MLCT state is lowest lying. Furthermore, the quantum yields for each of these complexes decreases as the irradiation wavelength becomes longer. In this respect, the  $\text{Mo}(\text{CO})_5(4\text{-CN-py})$  complex displays a greater quantum efficiency dependence on wavelength than the corresponding  $\text{Mo}(\text{CO})_5(3\text{-CN-py})$  complex. This result is attributed to greater population of the MLCT band following long wavelength irradiation of the 4-CN-py complex. It is concluded from the quantum efficiency data that the LF excited state is significantly more photoreactive than the MLCT excited state. This result is consistent with wavelength dependence studies of  $\text{Mo}(\text{CO})_5\text{L}$  photochemistry previously reported by Boxhoorn et al.<sup>27</sup> Earlier we assigned the lowest energy LF absorption to be a  $e^4b_2^2 \rightarrow e^3b_2^2a_1$  transition; this assignment is consistent with the above photochemical observations, where the weak field (pyridine) ligand is labilized following population of the  $d_{z^2}$  orbital.<sup>18</sup> Furthermore, recent calculations of excited-state distortion in  $\text{W}(\text{CO})_5(\text{py})$  from analyses of preresonance Raman spectra have indicated that the W-py bond undergoes the most severe elongation following low-energy LF excitation.<sup>28</sup>

Quantum yields were obtained for the 458-nm photolysis of  $\text{Mo}(\text{CO})_5(4\text{-CN-py})$  as a function of temperature. At this excitation wavelength it is assumed that the MLCT state is being populated exclusively. The results at 278, 283, 288, 293, and 298 K are 0.05, 0.04, 0.05, 0.05, and 0.04, respectively, indicating that there is very little, if any, thermal activation leading to population of higher energy states. Either the MLCT state is intrinsically (albeit weakly) photoreactive, or another state, possibly a weak LF triplet, is close in energy to the MLCT state and is responsible for the photochemistry. In this connection a triplet state has been implicated in the solution and gas-phase photochemistry of  $\text{Cr}(\text{CO})_6$ .<sup>29,30</sup>

**f. Excited-State Scheme.** Experimental observations have led us to construct energy degradation schemes for the two types of  $\text{M}(\text{CO})_5\text{L}$  complexes; these are presented in Figure 6. Scheme A depicts complexes with a lowest lying MLCT state; i.e., L = 4-CN-py, 4-Ac-py, 4-Bz-py, and 4-Fm-py. Scheme B represents complexes in which the LF state is lowest lying; i.e., L = 4-Me-py, py, 3,5-Cl<sub>2</sub>-py, 4-Ph-py, 2-CN-py, and 3-CN-py. It should also be noted that the relative positions of the LF and MLCT excited states will be further dependent on the solvent medium; the schemes shown in Figure 6 are indicative of the M-

(27) Boxhoorn, G.; Schoemaker, G. C.; Stufkens, D. J.; Oskam, A.; Rest, A. J.; Darensbourg, D. J. *Inorg. Chem.* **1980**, *19*, 3455.

(28) Zink, J. I. *Coord. Chem. Rev.* **1985**, *64*, 93.

(29) Nasielski, J.; Colas, A. *Inorg. Chem.* **1973**, *17*, 237.

(30) Fletcher, T. R.; Rosenfeld, R. N. *J. Am. Chem. Soc.* **1983**, *105*, 6358.

(24) Kaizu, Y.; Fujita, I.; Kobayashi, H. *Z. Phys. Chem.* **1972**, *79*, 298.

(25) Wrighton, M. S.; Morse, D. L. *J. Organomet. Chem.* **1975**, *97*, 405.

(26) Boxhoorn, G.; Oskam, A.; Gibson, E. P.; Narayanaswamy, R.; Rest, A. J. *Inorg. Chem.* **1981**, *20*, 783.

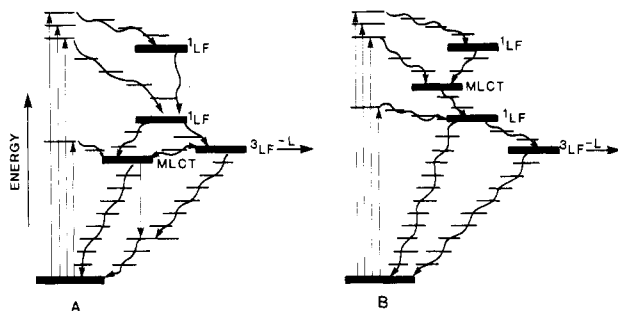


**Figure 6.** Excited-state schemes for  $M(\text{CO})_5\text{L}$  complexes ( $M = \text{Cr}$  or  $\text{Mo}$ ). Vertical and wavy lines represent radiative and nonradiative processes, respectively. Heavy horizontal lines depict thermally equilibrated excited states. Light horizontal lines denote successive complex-solvent cage energies as vibrationally excited states relax (only a few of these lines are shown). Scheme A depicts energy degradation processes in complexes in which the MLCT state is lowest lying ( $L = 4\text{-CN-py}$ ,  $4\text{-Bz-py}$ ,  $4\text{-Ac-py}$ , and  $4\text{-Fm-py}$ ). Scheme B depicts deactivation processes in complexes in which the LF state is at lowest energy ( $L = \text{py}$ ,  $4\text{-Me-py}$ ,  $3,5\text{-Cl}_2\text{-py}$ ,  $4\text{-Ph-py}$ ,  $2\text{-CN-py}$ , and  $3\text{-CN-py}$ ).

$(\text{CO})_5\text{L}$  complexes in a nonpolar solvent.

Scheme A is discussed first. Following absorption into these complexes rapid nonradiative deactivation takes place leading to the lowest lying excited state of MLCT character. From this state the molecule relaxes either by emitting or via further nonradiative processes to the ground state. Although emission was observed from this class of compounds, it is an inefficient route, and it is thus inferred that nonradiative processes are the most efficient mode of deactivation from the MLCT state. Photochemical pathways are also relatively inefficient and may proceed via the low energy LF singlet state. However, intersystem crossing can be anticipated to be very efficient in these heavy-atom complexes<sup>31</sup> and thus lead to efficient formation of the LF triplet. In a study of  $\text{W}(\text{CO})_5\text{L}$  complexes, the LF triplet has been assigned in absorption at 435–445 nm.<sup>17</sup> From the relative positions of the LF singlets in the  $\text{Mo}(\text{CO})_5\text{L}$  and  $\text{W}(\text{CO})_5\text{L}$  species it is estimated that the LF triplet for the molybdenum complexes would appear at 420–435 nm. This transition is spectroscopically unobservable in the  $\text{Mo}(\text{CO})_5\text{L}$  complexes due to the overlapping MLCT and singlet LF transitions. Spin-orbit coupling parameters will be considerably reduced for the lighter complexes<sup>7</sup> and the spin-forbidden singlet  $\rightarrow$  triplet LF absorption can be expected to be very weak. The inference of a photoreactive LF triplet state at  $\sim 430$  nm would account for the wavelength dependence of the quantum yields for the  $\text{Mo}(\text{CO})_5(4\text{-CN-py})$  complex (see Table IV). Short wavelength excitation allows for direct competition between the photochemical and nonradiative routes leading to the emitting state. Longer wavelength photolysis substantially populates the emitting MLCT

state with a reduction in photosubstitution efficiency. The photosubstitution efficiency temperature dependency data illustrates that little or no activation energy barrier exists in populating the photochemically active state. It is, therefore, necessary for us to place the photochemically active state close in energy to the MLCT state (see Scheme A). This again can be interpreted in terms of a low-lying photoreactive LF triplet state. The corresponding LF singlet is approximately 6–7 kcal higher in energy than the MLCT state in this class of complexes, and accordingly this energy gap is too large to infer that it is populated by thermal activation. If indeed a LF triplet is responsible for photoreaction, this would be an analogous situation to many organic molecules in which the photochemistry proceeds via a nonobservable triplet state following initial population of a singlet state and intersystem crossing.

Scheme B represents the other type of complexes which have lowest lying LF states. In these complexes absorption at all three of the wavelengths studied leads to efficient photosubstitution quantum efficiencies of the unique ligand L. After rapid deactivation to the lowest lying LF state, intersystem crossing can once again be assumed to be efficient. The photochemistry can therefore be expected to proceed via the LF triplet state. Emission from the MLCT state was not observed from this class of complexes due to efficient nonradiative processes that lead to the LF singlet and triplet states.

The experimental data has shown that the nature of the lowest energy excited state critically influences the luminescence and photochemical properties of the  $M(\text{CO})_5\text{L}$  series. A minor change in the pyridine substituent (e.g.,  $3\text{-CN-py}$  replaced by  $4\text{-CN-py}$ ) leads to a reordering of excited states in these complexes and quite different photophysical and photochemical behavior. If the lowest energy state is of LF character, photosubstitution pathways are fairly efficient. On the other hand, complexes with a lowest energy MLCT state exhibit emission in room-temperature solution.

**Acknowledgment.** We are grateful to the donors of the Petroleum Research Fund, administered by the American Chemical Society, and to the University Awards Program of the Research Foundation of SUNY for support of this research. We also thank the Research Corp. for a Cottrell Research Grant which contributed to the purchase of the argon ion laser. Gratitude is extended to Mark R. Kagan for help with some of the initial experiments and to the reviewers for some helpful comments.

**Registry No.**  $\text{Cr}(\text{CO})_5(4\text{-Me-py})$ , 64914-26-7;  $\text{Cr}(\text{CO})_5(\text{py})$ , 14740-77-3;  $\text{Cr}(\text{CO})_5(3,5\text{-Cl}_2\text{-py})$ , 99829-62-6;  $\text{Cr}(\text{CO})_5(4\text{-Ph-py})$ , 99829-63-7;  $\text{Cr}(\text{CO})_5(4\text{-CN-py})$ , 88253-55-8;  $\text{Cr}(\text{CO})_5(4\text{-Bz-py})$ , 99829-64-8;  $\text{Cr}(\text{CO})_5(4\text{-Ac-py})$ , 64914-29-0;  $\text{Cr}(\text{CO})_5(4\text{-Fm-py})$ , 99829-65-9;  $\text{Mo}(\text{CO})_5(4\text{-Me-py})$ , 21285-55-2;  $\text{Mo}(\text{CO})_5(\text{py})$ , 14324-76-6;  $\text{Mo}(\text{CO})_5(3,5\text{-Cl}_2\text{-py})$ , 99829-66-0;  $\text{Mo}(\text{CO})_5(4\text{-Ph-py})$ , 14324-76-6;  $\text{Mo}(\text{CO})_5(2\text{-CN-py})$ , 99829-67-1;  $\text{Mo}(\text{CO})_5(3\text{-CN-py})$ , 99829-68-2;  $\text{Mo}(\text{CO})_5(4\text{-CN-py})$ , 80925-83-3;  $\text{Mo}(\text{CO})_5(4\text{-Bz-py})$ , 80925-82-2;  $\text{Mo}(\text{CO})_5(4\text{-Ac-py})$ , 80925-81-1;  $\text{Mo}(\text{CO})_5(4\text{-Fm-py})$ , 80925-84-4;  $\text{Mo}(\text{CO})_5(\text{PPh}_3)$ , 14971-42-7;  $\text{PPh}_3$ , 603-35-0.

(31) Turro, N. J. "Modern Molecular Photochemistry"; Benjamin/Cummings: Menlo Park, CA, 1978; p 192.

# Photochemical Activation of Molecular Hydrogen by $\text{Fe}(\text{CO})_5^\dagger$

Paul J. Krusic,\* David J. Jones, and D. Christopher Roe

Central Research & Development Department, Experimental Station, E. I. du Pont de Nemours & Company, Wilmington, Delaware 19898

Received February 19, 1985

The low-temperature photolysis of pentane solutions of  $\text{Fe}(\text{CO})_5$  under various high pressures of molecular hydrogen or  $\text{H}_2/\text{CO}$  mixtures has been investigated by ESR and NMR using a new sapphire high-pressure cell. The major diamagnetic products identified by proton NMR are the thermally unstable hydrides  $\text{H}_2\text{Fe}(\text{CO})_4$  and  $\text{H}_2\text{Fe}_2(\text{CO})_8$ , while the paramagnetic products identified by ESR are  $\text{HFe}(\text{CO})_4$ ,  $\text{HFe}_2(\text{CO})_8$ ,  $\text{HFe}_3(\text{CO})_{11}$ , and two paramagnetic trihydrides. Isotopic substitution studies with deuterium,  $^{13}\text{C}$ , and  $^{57}\text{Fe}$  were carried out to substantiate the assignments of these labile radical species and to obtain structural information.

The reactions of organometallic compounds with molecular hydrogen play a central role in homogeneous catalysis and are particularly important in processes which utilize hydrogen and carbon monoxide mixtures (synthesis gas) for the production of chemical feedstocks (e.g., the hydroformylation of olefins).<sup>1</sup> After several decades of intensive research there is still much that is not known about hydrogen activation. Spectroscopic investigations, especially on systems undergoing catalysis, have often been hampered by the need of high-pressure cells and by the reactivity of the catalytically active reaction intermediates. We have recently developed a sapphire cell which permits NMR and ESR investigations over a broad temperature range of liquid samples under gaseous pressures up to at least 1500 psi.<sup>2</sup> In this paper we report an ESR study of thermally very unstable paramagnetic iron carbonyl hydrides which were generated in the sapphire cell at low temperatures by UV photolysis of dilute pentane solutions of  $\text{Fe}(\text{CO})_5$  under various pressures of  $\text{H}_2$  and  $\text{CO}$ .

## Experimental Section

Pentane was freed of low-level olefin impurities by repeated shaking with concentrated sulfuric acid. After several washes with distilled water, it was stirred overnight with anhydrous magnesium oxide, and it was then distilled from calcium hydride. Methylcyclohexane- $d_{14}$  and THF- $d_8$  (Merck, Sharp and Dohme Ltd.) were stirred with Na/K alloy overnight and were bulb-to-bulb distilled in a vacuum system. Pentacarbonyliron was bulb-to-bulb distilled several times in a vacuum system and was stored in a refrigerator in a nitrogen atmosphere. Ninety-three percent  $^{13}\text{C}$ -enriched pentacarbonyliron was a custom synthesis by Pressure Chemical Co. Hydrogen, deuterium, carbon monoxide, and anhydrous hydrochloric acid were research grade and were used as received. Ninety-nine percent  $^{13}\text{CO}$  was obtained from Mound Isotopes Inc.  $\text{Na}_2\text{Fe}_2(\text{CO})_8$  and  $[\text{HFe}(\text{CO})_4][\text{PPN}]$  [PPN = bis(triphenylphosphine)nitrogen(1+)] were synthesized as reported in the literature.<sup>3,4</sup> All chemical manipulations were carried out in a  $\text{N}_2$ -filled Vacuum Atmospheres glovebox.

The high-pressure sapphire NMR/ESR tube has been described in detail elsewhere.<sup>2</sup> It consists of tubular single crystal of sapphire (Saphikon Inc., Milford, NH, 5-mm o.d. having a wall thickness of 0.8 mm) fitted to a nonmagnetic Ti-alloy valve via an O-ring flange seal with four bolts. The latter can be easily opened to introduce the sample by syringe. After the valve and tube are reassembled, the valve is attached to a simple pressure manifold for the introduction of the gases at the desired pressure. After charging the gases, the assembly is disconnected from the pressure manifold and is transported to the spectrometer or to the photoreactor inside a Lucite shield.

The low-temperature photoreactor consists of a standard quartz Dewar for variable-temperature ESR surrounded by the coils of a low-pressure Hg discharge tube (mostly 254-nm UV) in the shape

Table I. ESR Parameters of Iron Carbonyl Hydride Radicals

hydride radical	$T$ , °C	$g$	$a(\text{H})$ , G	$a(\text{C})$ , G
$\text{HFe}(\text{CO})_4$	-110	2.0545	22.60 (1 H)	
$\text{HFe}_2(\text{CO})_8$	-110	2.0122	22.22 (1 H)	12.37 (2 C)
$\text{HFe}_3(\text{CO})_{11}$	-80	2.0641	18.95 (1 H)	10.0 (3 C)
$\text{H}_3\text{Fe}(\text{CO})_3$	-80	2.0459	24.9 (2 H), 2.9 (1 H)	
$\text{H}_3\text{Fe}_2(\text{CO})_7$	-80	2.0161	16.7 (1 H), 5.0 (2 H)	

of a tight spiral. The cooling is provided by a flow of cold nitrogen. After irradiation, the sapphire tube is plunged into liquid nitrogen or into dry ice to prevent the contents from warming up before spectral examination.

A Hanau-Heraeus 400-W Hg lamp (Q600) was used for in situ irradiation. Two Suprasil lenses were used to focus the light onto the slotted end-plate of a standard Bruker X-band cavity.

ESR spectra were obtained with a Bruker ER420 spectrometer equipped with accessories to measure precisely the microwave frequency and the magnetic field.

The ESR parameters of the iron carbonyl hydride radicals discussed in this paper are gathered in Table I.

## Results and Discussion

In situ photolysis with a medium-pressure Hg lamp of a  $10^{-3}$  M olefin-free pentane solution of  $\text{Fe}(\text{CO})_5$  under 900 psi of 1:1  $\text{H}_2/\text{CO}$  at  $-110$  °C produces the ESR spectrum of Figure 1A. We assign the broad downfield doublet ( $g = 2.0545$ ,  $a(\text{H}) = 22.60$  G,  $\Delta H = 5.3$  G) to the 17-electron radical  $\text{HFe}(\text{CO})_4$  (I). I decays in the absence of light with a half-life of 12 s at this temperature. The half-life is markedly reduced at higher temperatures ( $t_{1/2} = 7$  s at  $-90$  °C). The proton splitting is strongly temperature dependent, being 21.3 G at  $-80$  °C and 23.1 G at  $-120$  °C. The sharp upfield doublet ( $g = 2.0122$ ,  $a(\text{H}) = 22.22$  G,  $\Delta H = 0.7$  G) was previously assigned to the binuclear radical  $\text{HFe}_2(\text{CO})_8$  (II) with a bridging H atom and two bridging CO's.<sup>5</sup> At  $-110$  °C, II decays in the dark much more slowly than I, and its H splitting is essentially temperature independent. Neither radical can be observed above  $-80$  °C under our conditions.

(1) (a) Falbe, J. "Carbon Monoxide in Organic Synthesis"; Springer-Verlag: New York, 1970. (b) Slocum, D. W., Moser, W. R., Eds. "Catalytic Transition Metal Hydrides"; The New York Academy of Sciences: New York, 1983. (c) Pruetz, R. L. *Adv. Organomet. Chem.* 1979, 17, 1.

(2) Roe, D. C. *J. Magn. Reson.* 1985, 63, 388.

(3) Collman, J. P.; Finke, R. G.; Matlock, P. L.; Wahren, R.; Komoto, R. *J. Am. Chem. Soc.* 1978, 100, 1119.

(4) Darensbourg, M. Y.; Darensbourg, D. J.; Barros, H. L. C. *Inorg. Chem.* 1978, 17, 297.

(5) Krusic, P. J. *J. Am. Chem. Soc.* 1981, 103, 2131.

\* Contribution No. 3654.



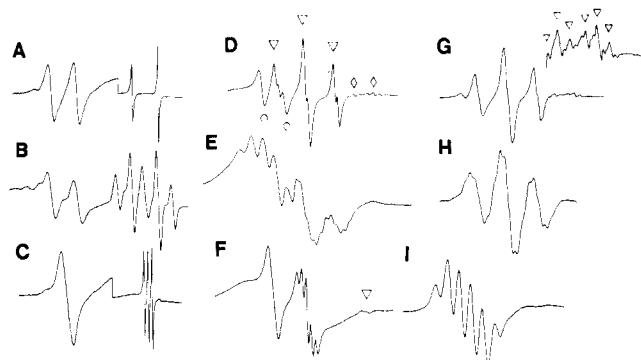


**Figure 1.** ESR spectra of (a)  $\text{HFe}(\text{CO})_4\cdot$  and  $\text{HFe}_2(\text{CO})_8\cdot$  (the step in the base line is due to a change of gain), (b)  $\text{HFe}^{13}\text{CO}_4\cdot$  and  $\text{HFe}_2^{13}\text{CO}_8\cdot$ , (c)  $\text{DFe}(\text{CO})_4\cdot$  and  $\text{DFe}_2(\text{CO})_8\cdot$  (note change of gain), all at  $-110^\circ\text{C}$ , (d)  $\text{HFe}_3(\text{CO})_{11}\cdot$  (circles),  $\text{H}_3\text{Fe}(\text{CO})_3\cdot$  (triangles), and  $\text{H}_3\text{Fe}_2(\text{CO})_7\cdot$  (diamonds), (e)  $\text{HFe}_3^{13}\text{CO}_{11}\cdot$  and  $\text{H}_3\text{Fe}^{13}\text{CO}_3\cdot$ , (f)  $\text{DFe}_3(\text{CO})_{11}\cdot$ ,  $\text{D}_3\text{Fe}(\text{CO})_3\cdot$ , and  $\text{D}_3\text{Fe}_2^{13}\text{CO}_7\cdot$ , (g)  $\text{H}_3\text{Fe}(\text{CO})_3\cdot$  and  $\text{H}_3\text{Fe}_2(\text{CO})_7\cdot$  enriched in  $^{57}\text{Fe}$  ( $\sim 40\%$ ), (h)  $\text{H}_3\text{Fe}^{13}\text{CO}_3\cdot$ , and (i)  $\text{HFe}_3^{13}\text{CO}_{11}\cdot$ , all at  $-80^\circ\text{C}$  in pentane.

In an analogous experiment with 93%  $^{13}\text{C}$ -enriched  $\text{Fe}(\text{CO})_5$  and 900 psi  $\text{H}_2/^{13}\text{CO}$  (99%  $^{13}\text{C}$ )<sup>6</sup> (Figure 1B), the H doublet of I is only slightly broadened by the presence of the  $^{13}\text{C}$  isotope ( $\Delta H = 7.3$  G), while II now shows a coupling to two  $^{13}\text{C}$  atoms which interact appreciably with the unpaired electron ( $a(^{13}\text{C}) = 12.37$  G). The remaining  $^{13}\text{C}$  atoms only cause additional line broadening ( $\Delta H = 3.3$  G). Finally, if the experiment is repeated with  $\text{D}_2/\text{CO}$ , the H doublet of I collapses into a single broad line, since the expected D triplet cannot be resolved with the given line widths, and the spectrum of  $\text{DFe}_2(\text{CO})_8\cdot$  consists of a 1:1:1 triplet ( $a(\text{D}) = 3.4$  G, Figure 1C).

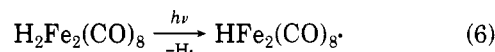
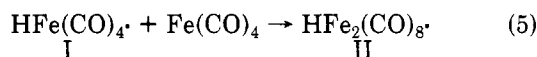
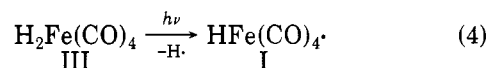
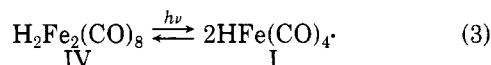
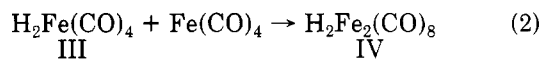
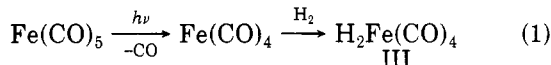
We investigated the diamagnetic products of this photolysis by NMR using the same sapphire cell. A  $10^{-2}$  M methylcyclohexane- $d_{14}$  solution of  $\text{Fe}(\text{CO})_5$  under 500 psi of  $\text{H}_2$  was irradiated for 10 min at  $-80^\circ\text{C}$  in a low-temperature UV photoreactor. When the tube was transferred without warming into the probe of a Nicolet NT-360 NMR spectrometer at  $-80^\circ\text{C}$ , three new proton resonances were detected in the metal hydride region at  $\delta -9.27$ ,  $-9.49$ , and  $-9.53$  (weak shoulder). The first belongs to the thermally very unstable  $\text{H}_2\text{Fe}_2(\text{CO})_8$  hydride (IV) which has been mentioned in the literature as a transient species but which had not been positively identified heretofore.<sup>7</sup> The second and strongest hydrido resonance belongs to the much better characterized albeit also thermally unstable  $\text{H}_2\text{Fe}(\text{CO})_4$  hydride (III).<sup>7</sup> This was established by two similar experiments. Anhydrous HCl (0.08 mmol) was condensed at liquid-nitrogen temperature into an NMR tube attached to a vacuum system containing a suspension of  $\text{Na}_2\text{Fe}_2(\text{CO})_8$  in methylcyclohexane- $d_{14}$ . The tube was sealed with a flame and was agitated in a dry ice/acetone bath to effect the heterogeneous protonation of the insoluble  $\text{Fe}_2(\text{CO})_8^{2-}$  anion thus producing the red hydrocarbon-soluble  $\text{H}_2\text{Fe}_2(\text{CO})_8$ . NMR examination of the sample at  $-80^\circ\text{C}$  without any warming gave a hydrido resonance at  $\delta -9.28$ . This resonance disappears rapidly on warming. An identical procedure with  $[\text{HFe}(\text{CO})_4][\text{P-PN}]$  and HCl produced colorless  $\text{H}_2\text{Fe}(\text{CO})_4$  with  $\delta -9.50$  at  $-80^\circ\text{C}$ .<sup>8</sup>

(6) This gaseous mixture was obtained by opening the cell first to 450 psi of  $^{13}\text{CO}$  and then once more to 900 psi of  $\text{H}_2$ . The second step was carried out quickly to avoid the escape of the  $^{13}\text{CO}$ . The cell was then disconnected from the pressure manifold and was rocked gently in a protective plastic shroud to mix the gases and to equilibrate the system.

(7) Shriver, D. F.; Whitmire, K. H. In "Comprehensive Organometallic Chemistry"; Wilkinson, G.; Stone, F. G. A., Abel, E. W., Eds.; Pergamon Press: Oxford, 1982; Vol. 4, p 243.

A pentane solution of  $\text{H}_2\text{Fe}_2(\text{CO})_8$ , prepared and handled at  $-80^\circ\text{C}$  as described above, was also irradiated in the ESR cavity at  $-100^\circ\text{C}$  in a quartz tube. A complex spectrum was obtained in which the lines of  $\text{HFe}(\text{CO})_4\cdot$  and  $\text{HFe}_2(\text{CO})_8\cdot$  predominated. These lines decayed on shuttering the light leaving a spectrum quite similar to that of Figure 1D which will be discussed below.

These observations strongly implicate reactions 1 through 6 in the photolysis of  $\text{Fe}(\text{CO})_5$  and  $\text{H}_2$ . The



diamagnetic dihydride III is produced initially by oxidative addition of dihydrogen to the 16-electron coordinatively unsaturated  $\text{Fe}(\text{CO})_4$  fragment formed by photoejection of CO from  $\text{Fe}(\text{CO})_5$  (eq 1). This step was previously postulated to explain the photocatalytic hydrogenation of olefins in the presence of  $\text{Fe}(\text{CO})_5$ <sup>9</sup> and was also observed in an IR matrix-isolation study.<sup>10</sup> Dihydride III can plausibly react further with the  $\text{Fe}(\text{CO})_4$  fragment to give the dinuclear dihydride IV (eq 2) observed in the NMR experiment. Light-induced fission of the Fe-Fe bond in the latter compound is probably the major source of the  $\text{HFe}(\text{CO})_4$  radical (eq 3). This is supported by the observation of this radical in the photolysis of  $\text{H}_2\text{Fe}_2(\text{CO})_8$ .<sup>11</sup> A hydrogen atom transfer from III, either by direct UV-induced homolysis of the weak Fe-H bond<sup>13</sup> or by an H atom abstraction by an iron carbonyl fragment in an electronically excited state, is also a possible source of I (eq 4). Finally, the dinuclear radical hydride II can arise either by recombination of I with the  $\text{Fe}(\text{CO})_4$  fragment (eq 5) or, conceivably, by an H atom transfer (eq 6) entirely analogous to that of eq 4. The latter step is consistent with the observation of II in the photolysis of  $\text{H}_2\text{Fe}_2(\text{CO})_8$ .

We consider that the structure of the novel 17-electron  $\text{HFe}(\text{CO})_4\cdot$  radical is most probably represented by a

(8) We carried out the same low-temperature protonations in a homogeneous system using THF- $d_8$  obtaining  $\delta -9.46$  for  $\text{H}_2\text{Fe}_2(\text{CO})_8$ ,  $\delta -9.67$  for  $\text{H}_2\text{Fe}(\text{CO})_4$ , and  $\delta -8.81$  for  $\text{HFe}(\text{CO})_4\cdot$  at  $-80^\circ\text{C}$ . The heterogeneous protonations in methylcyclohexane- $d_{14}$  were chosen in order to eliminate the uncertainties brought about by the appreciable solvent shifts for these hydrido resonances.

(9) Schroeder, M. A.; Wrighton, M. S. *J. Am. Chem. Soc.* 1976, 98, 551. Wrighton, M. S.; Ginley, D. S.; Schroeder, M. A.; Morse, D. L. *Pure Appl. Chem.* 1975, 41, 671.

(10) Sweany, R. L. *J. Am. Chem. Soc.* 1981, 103, 2410.

(11) We have found recently that in situ photolysis of dilute THF solutions of  $\text{Na}_2\text{Fe}_2(\text{CO})_8$  also leads to the fission of the Fe-Fe bond and the formation of the short-lived  $\text{Fe}(\text{CO})_4\cdot$  radical anion which can be considered as the conjugate base of the  $\text{HFe}(\text{CO})_4\cdot$  radical. This radical anion is isoelectronic with the  $\text{Co}(\text{CO})_4\cdot$  radical.<sup>12</sup> It has  $g = 2.0486$ , a line width of 9 G at  $-90^\circ\text{C}$ , and it decays on shuttering the light with a half-life of 2 s at  $-80^\circ\text{C}$  and 10 s at  $-110^\circ\text{C}$ .

(12) Fairhurst, S. A.; Morton, J. R.; Preston, K. F. *J. Magn. Reson.* 1983, 55, 453 and references therein.

(13) (a) Sweany, R. L. *Inorg. Chem.* 1980, 19, 3512. (b) Krusic, P. J.; Briere, R.; Rey, P. *Organometallics* 1985, 4, 801.

(14) Smith, M. B.; Bau, R. *J. Am. Chem. Soc.* 1973, 95, 2388. Darsenbourg, M. Y.; Darsenbourg, D. J.; Barros, H. L. C. *Inorg. Chem.* 1978, 17, 297.

square pyramid (SP) with an axial H atom. A trigonal bipyramid (TB), which is the structure of the diamagnetic  $\text{HFe}(\text{CO})_4^-$  anion with one more electron than  $\text{I}$ ,<sup>12</sup> can be excluded on the basis of our recent study of acyl tetracarbonyliron radicals  $(\text{CO})_4\text{FeCOR}\cdot$  of TB structure with an axial acyl group.<sup>15</sup> These radicals, when prepared from 93%  $^{13}\text{C}$ -enriched  $\text{Fe}(\text{CO})_5$ , displayed a relatively large (11.0 G) hyperfine splitting for three equatorial  $^{13}\text{C}$  atoms. Furthermore,  $^{13}\text{C}$  substitution of the acyl carbon gave no resolvable  $^{13}\text{C}$  hyperfine structure. These results were in good agreement with EHMO calculations for the model (formyl) $\text{Fe}(\text{CO})_4$  radical of TB geometry with an axial CHO group. They showed a SOMO made up mostly of Fe orbitals in the equatorial plane ( $p(x)$ ,  $p(y)$ ,  $d(xy)$ ,  $d(x^2 - y^2)$ ; 52%) and of the orbitals in the equatorial plane of the equatorial CO ligands ( $p(x)$ ,  $p(y)$ ; 41%). The atomic orbitals of the axial CO and CHO groups made only a minor contribution (ca. 3%). The contribution of the 2s orbitals of each equatorial C atom was 1.7% which translates into an isotropic hyperfine  $^{13}\text{C}$  interaction due to direct, positive s orbital contribution of 19 G using the value 1130 G for unit spin population in the  $^{13}\text{C}$  2s orbital.<sup>16</sup> The polarization contribution (negative spin density) to the  $^{13}\text{C}$  isotropic coupling, of course, is not accounted for by the EH method but is presumed to be small. The calculated spin populations of the 2s orbitals of the axial C atoms, on the other hand, were negligible. Since the results of the EH calculations for the  $\text{HFe}(\text{CO})_4\cdot$  radical of TB geometry with  $C_{3v}$  symmetry (see Table I, ref 15) were quite similar to those described above, we conclude that the absence of a relatively large hyperfine interaction for the equatorial  $^{13}\text{C}$  atoms in I precludes a TB structure for this radical.<sup>17</sup>

The EH calculations for  $\text{HFe}(\text{CO})_4\cdot$  of SP geometry with  $C_{4v}$  symmetry (Table I, ref 15), on the other hand, are in much better agreement with the experimental observations for this species. The SOMO is now mostly composed of Fe  $d(z^2)$  and  $p(z)$  orbitals (23% and 7%, respectively) and the  $p(z)$  orbitals of the basal CO ligands (60%). The 1s orbital of the axial H atom is involved to the extent of 6.6%. With use of the isotropic hyperfine interaction of 508 G for unit spin population in the 1s orbital of hydrogen,<sup>16</sup> this represents a hyperfine splitting of 33 G due to direct, positive s orbital contribution which compares favorably with the observed H splitting. Although the delocalization of the unpaired electron over the  $p(z)$  orbitals of the basal CO ligands is quite substantial according to these calculations (60%), the 2s character of each basal C atom is only 0.2%, that is ca. 10 times less than for a TB structure.<sup>15</sup> This contribution translates into a  $^{13}\text{C}$

hyperfine interaction of about 2 G.

The most important point that emerges from these calculations is the absence of an unusually large coupling to the axial hydrogen that might be intuitively expected for  $\text{HFe}(\text{CO})_4\cdot$  of  $C_{4v}$  symmetry. It is noteworthy that a large axial  $^{13}\text{C}$  coupling was also absent in the  $\text{Fe}(\text{CO})_5^+$  radical cation of  $C_{4v}$  symmetry isolated in a  $\text{Cr}(\text{CO})_6$  single crystal.<sup>19</sup> Indeed, the two systems have much in common. Thus, the isotropic  $g$  factors are quite similar (2.0520 vs. 2.0545), and neither species heavily enriched in  $^{13}\text{C}$  gives resolvable  $^{13}\text{C}$  hyperfine structure in solution. In both cases,  $^{13}\text{C}$  substitution merely broadens somewhat the linewidths. For  $\text{Fe}(\text{CO})_5^+$ , this was taken to mean that the radical in solution undergoes rapid interconversion of the five ligands giving rise to a small average isotropic  $^{13}\text{C}$  hyperfine interaction. A similar averaging process may be operative for  $\text{HFe}(\text{CO})_4\cdot$  and may reduce both the isotropic  $^{13}\text{C}$  and H splittings. The reduction would be particularly effective if axial and basal positions should give rise to  $^{13}\text{C}$  and H hyperfine couplings of opposite sign. This nonrigidity is most probably also the source of the substantial temperature dependence of the proton coupling in  $\text{HFe}(\text{CO})_4\cdot$ . The coupling for a bridging hydrogen in a non-fluxional structure such as that of II, on the other hand, would not be expected to be temperature dependence as was indeed observed.

The much greater reactivity at low temperatures of  $\text{HFe}(\text{CO})_4\cdot$  radicals compared with that of (acyl) $\text{Fe}(\text{CO})_4\cdot$  radicals may also be related to their structures. The  $\text{HFe}(\text{CO})_4\cdot$  radical of SP structure has an exposed, localized Fe  $d(z^2)p(z)$  orbital lobe with substantial single electron population pointing in the direction of the missing sixth ligand giving the radical a strong propensity to dimerize or to couple with other Fe carbonyl fragments (cf. eq 3 and 5). The (acyl) $\text{Fe}(\text{CO})_4\cdot$  radicals, on the other hand, have little tendency to dimerize at low temperatures<sup>15</sup> probably because the unpaired electron is more or less evenly smeared over seven equatorial atoms. We presume that an  $\text{HFe}(\text{CO})_4\cdot$  radical of TB structure would be similarly unreactive at low temperatures.

The structure of the binuclear hydride radical  $\text{HFe}_2(\text{C}-\text{O})_8\cdot$  was briefly discussed elsewhere.<sup>5</sup> A structure with a bridging H atom and two bridging CO ligands analogous to that of the diamagnetic  $\text{HFe}_2(\text{CO})_8^-$  anion with one more electron<sup>20</sup> seems most probable. Extended Hückel MO calculations for this structure and for similar binuclear iron carbonyl radicals with a bridging phosphido group<sup>21</sup> indicate that the  $^{13}\text{C}$  atoms with large couplings are those of bridging CO ligands which can accept much more unpaired spin density than terminal CO ligands.

Carbon monoxide was used advisedly in the experiments described so far since it inhibits dramatically the formation of other hydride radicals whose presence would have complicated the analysis of the spectra discussed above. UV photolysis of the same  $\text{Fe}(\text{CO})_5$  solution under 500 psi of  $\text{H}_2$  alone at  $-80^\circ\text{C}$  in the low-temperature photoreactor for 1 min produces three additional hydride radicals which are indefinitely stable at this temperature but decay rapidly on warming: the known  $\text{HFe}_3(\text{CO})_{11}\cdot$  radical (V)<sup>5</sup> (Figure 1D, doublet marked with circles,  $a(\text{H}) = 18.95\text{ G}$ ,  $g = 2.0641$ ) and two new species in which the unpaired electron clearly interacts with three hydrogen atoms (Figure 1D, triangles and diamonds).

(15) Krusic, P. J.; Cote, W. J.; Grand, A. J. *Am. Chem. Soc.* **1984**, *106*, 4642.

(16) Atkins, P. W.; Symons, M. C. R. "The Structure of Inorganic Radicals"; Elsevier: Amsterdam, 1967; p 21.

(17) The d level splitting scheme for a trigonal bipyramid ( $D_{3h}$ ) is well-known.<sup>18</sup> Lowest is the  $e''$  set composed of degenerate  $d(xz)$  and  $d(yz)$  functions. Above is the  $e'$  set composed of the degenerate  $d(x^2 - y^2)$  and  $d(xy)$  functions. Highest is the orbital of  $a_1'$  symmetry. In the formally  $d^7$   $\text{HFe}(\text{CO})_4\cdot$  radical of TB structure, the unpaired electron would be in the degenerate  $e'$  orbitals, and the radical would be expected to undergo a Jahn-Teller distortion. Such a distortion was indeed observed for the isoelectronic  $\text{HCo}(\text{CO})_4^+$  cation radical which was recently detected by K. F. Preston and J. R. Morton in a solid Ar matrix at low temperatures (private communication). This radical was found to have two equivalent  $^{13}\text{C}$  atoms with a very large hyperfine interaction (50 G) which were associated with the equatorial CO ligands of the  $C_{2v}$  distorted TB. If our isoelectronic  $\text{HFe}(\text{CO})_4\cdot$  radical were isostructural with  $\text{HCo}(\text{CO})_4^+$ , we would expect a large triplet splitting for two equivalent equatorial  $^{13}\text{C}$  atoms in the case of a static Jahn-Teller distortion or a substantial average value for three equivalent equatorial  $^{13}\text{C}$  atoms in the more likely case of a dynamic Jahn-Teller effect.

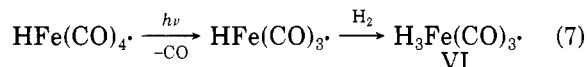
(18) Rossi, A. R.; Hoffmann, R. *Inorg. Chem.* **1975**, *14*, 365.

(19) Lionel, T.; Morton, J. R.; Preston, K. F. *J. Chem. Phys.* **1982**, *76*, 234.

(20) Chin, H. B.; Bau, R. *Inorg. Chem.* **1978**, *17*, 2314.

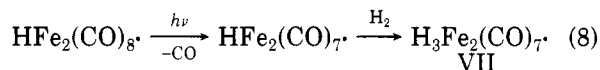
(21) Baker, R. T.; Krusic, P. J.; Calabrese, J. C.; Roe, D. C., submitted to *Organometallics*.

We believe that the paramagnetic trihydride present in higher concentration is the 17-electron H<sub>3</sub>Fe(CO)<sub>3</sub><sup>•</sup> radical (VI) of octahedral geometry. Its spectrum is a large triplet of 24.90 G for the two axial H atoms (Figure 1D, triangles) split into small doublets of 2.9 G by the equatorial H atom. The large *g* factor of 2.0459 is consistent with substantial spin density on the iron atom and is similar to that of other mononuclear iron carbonyl radicals.<sup>15</sup> This radical is formed most logically from the HFe(CO)<sub>4</sub><sup>•</sup> radical by photoejection of a CO ligand followed by the oxidative addition of H<sub>2</sub> to the resulting highly coordinatively unsaturated fragment (eq 7). A related diamagnetic species

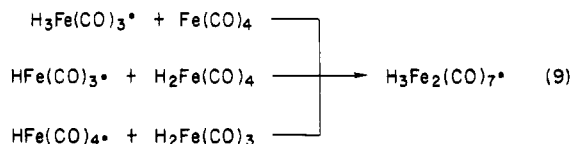


with one more electron, the anion H<sub>3</sub>Fe(CO)<sub>3</sub><sup>-</sup>, has been observed very recently by mass spectrometry in the gas-phase reaction of the coordinatively unsaturated HFe(CO)<sub>3</sub><sup>-</sup> anion with H<sub>2</sub>.<sup>22</sup>

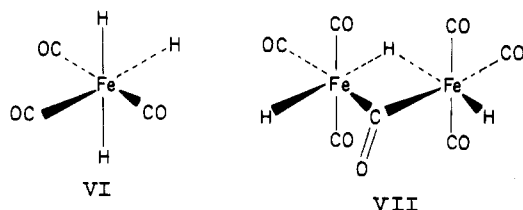
The less abundant trihydride has the small *g* factor of 2.0161 which is similar to that of HFe<sub>2</sub>(CO)<sub>8</sub><sup>•</sup> (2.0122). A *g* factor of this magnitude indicates small spin density on the metal and substantial delocalization of the unpaired electron onto the ligands. Both are more likely for binuclear than mononuclear species. We believe, therefore, that this trihydride is the binuclear H<sub>3</sub>Fe<sub>2</sub>(CO)<sub>7</sub><sup>•</sup> radical (VII) which is related to the HFe<sub>2</sub>(CO)<sub>8</sub><sup>•</sup> radical by having two hydrogen atoms replacing a CO ligand. In agreement with this assignment, the strongest spectrum of this radical was obtained in the photolysis of H<sub>2</sub>Fe<sub>2</sub>(CO)<sub>8</sub> discussed above. It can be formed directly from HFe<sub>2</sub>(CO)<sub>8</sub><sup>•</sup> (eq 8) or by the



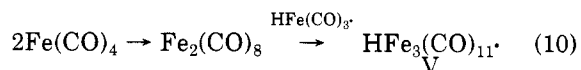
recombination of various fragments which are undoubtedly present in this complex photochemical system (eq 9). Its



spectrum reveals a unique hydrogen atom which gives rise to a large doublet of 16.70 G (Figure 1D, diamonds) each line of which is further split into triplets of 5.0 G by a pair of more weakly interacting H atoms. A possible structure is shown.



The formation of the trinuclear HFe<sub>3</sub>(CO)<sub>11</sub><sup>•</sup> radical is also not entirely clear. Several plausible reaction pathways can be written down including eq 10 which draws attention to the binuclear Fe<sub>2</sub>(CO)<sub>8</sub> fragment as a very likely active intermediate in the low-temperature photolysis of Fe(CO)<sub>5</sub>.<sup>23</sup>



Deuterium substitution, in an analogous experiment with D<sub>2</sub>, produced as expected a single broad line for DFe<sub>3</sub>(CO)<sub>11</sub><sup>•</sup>, a quintet (4.0 G) appropriate for two equivalent axial deuterium atoms for D<sub>3</sub>Fe(CO)<sub>3</sub><sup>•</sup>, and a poorly resolved 1:1:1 triplet for the unique deuterium in D<sub>3</sub>Fe<sub>2</sub>(CO)<sub>7</sub><sup>•</sup> (Figure 1F).

<sup>13</sup>C substitution, in an experiment with 93% <sup>13</sup>C-enriched Fe(CO)<sub>5</sub>, led to the rather complex spectrum of Figure 1E which is the result of the partial superposition of two spectra. Fortunately, the two spectra can be obtained free from interference of the other. A clean spectrum of <sup>13</sup>C-labeled HFe<sub>3</sub>(CO)<sub>11</sub><sup>•</sup> (Figure 1I) was obtained by briefly warming the sample to room temperature to cause the decay of the less stable trihydride radicals. The spectrum is an intermeshing doublet-of-quartets (*a*(H) = 19.0 G, *a*(<sup>13</sup>C) = 10.0 G). Thus, radical HFe<sub>3</sub>(CO)<sub>11</sub><sup>•</sup> has three <sup>13</sup>CO ligands which are equivalent within the rather broad linewidth. The structure is highly fluxional, however, since on raising the temperature to -40 °C, the spectrum changes reversibly into a doublet. These reversible line shape changes were observed previously in THF under considerably worse resolution.<sup>5</sup> The structure of HFe<sub>3</sub>(CO)<sub>11</sub><sup>•</sup> in the slow-exchange limit is probably closely related to that of the diamagnetic HFe<sub>3</sub>(CO)<sub>11</sub><sup>-</sup> anion in which two Fe(CO)<sub>3</sub> units are bridged by a hydrogen, a CO, and an Fe(CO)<sub>4</sub> group.<sup>24</sup> The <sup>13</sup>C quartet could then be caused by the <sup>13</sup>C atoms of two terminal CO's of the Fe(CO)<sub>3</sub> units and by the <sup>13</sup>C atom of the bridging CO having similar couplings.

A clean spectrum of <sup>13</sup>C-labeled H<sub>3</sub>Fe(CO)<sub>3</sub><sup>•</sup> could be obtained by using very dilute starting solutions of 93% <sup>13</sup>C-labeled Fe(CO)<sub>5</sub> (~4 × 10<sup>-4</sup> M) (Figure 1H). This observation also argues in favor of a mononuclear species since agglomeration of iron carbonyl fragments is less likely at such high dilutions. Unfortunately, the resolution was not sufficient for a clear-cut interpretation of the additional hyperfine structure brought about by the <sup>13</sup>C isotopic substitution. It is clear, however, that there is no large <sup>13</sup>C coupling which could be associated with a bridging CO ligand, again in agreement with the proposed mononuclearity of this species.

Finally, we attempted to obtain an experimental confirmation of the nuclearity of the trihydride radicals using <sup>57</sup>Fe-labeled Fe(CO)<sub>5</sub> (<sup>57</sup>Fe has a nuclear spin of 1/2). Unfortunately, the sample available to us was not sufficiently enriched in <sup>57</sup>Fe to provide an unambiguous answer. The spectra of H<sub>3</sub>Fe(CO)<sub>3</sub><sup>•</sup> and H<sub>3</sub>Fe<sub>2</sub>(CO)<sub>7</sub><sup>•</sup> obtained with this starting material are shown in Figure 1G. That for H<sub>3</sub>Fe<sub>2</sub>(CO)<sub>7</sub> shows clearly discernible <sup>57</sup>Fe satellite lines corresponding to a <sup>57</sup>Fe coupling of approximately 3.5 G (see insert in Figure 1G). Given the approximate isotopic composition of 60% <sup>56</sup>Fe and 40% <sup>57</sup>Fe of our Fe(CO)<sub>5</sub> sample, each spectral line of a species having two equivalent <sup>57</sup>Fe nuclei should have all lines split into five lines with relative intensities 1:6:11:6:1. This is the result of the superposition of the spectra of three isotopic species with <sup>56</sup>Fe-<sup>56</sup>Fe (singlet), <sup>56</sup>Fe-<sup>57</sup>Fe (doublet), and <sup>57</sup>Fe-<sup>57</sup>Fe (triplet) in their proper abundances. The available signal-to-noise ratio is clearly insufficient to decide whether the lines labeled with triangles in Figure 1G are indeed such quintets. Similarly, no firm conclusion can be drawn for the <sup>57</sup>Fe-enriched H<sub>3</sub>Fe(CO)<sub>3</sub> radical. The <sup>57</sup>Fe enrichment produced barely visible pairs of shoulders near

(23) (a) Paliakoff, M.; Turner, J. J. *J. Chem. Soc. A* 1971, 2403. (b) Fischer, I.; Hildenbrand, K.; Koerner von Gustorf, E. *Angew. Chem., Int. Ed. Engl.* 1975, 14, 54. (c) Turner, J. J.; Burdett, J. K.; Perutz, R. N.; Paliakoff, M. *Pure Appl. Chem.* 1977, 49, 271.

(24) Dahl, L. F.; Blount, J. F. *Inorg. Chem.* 1965, 4, 1373.

the top and bottom of each line of the triplet (Figure 1G). This allows only a rough estimation of the  $^{57}\text{Fe}$  coupling (ca. 4.5 G). However, the lack of another pair of weaker shoulders near the base of each line, i.e., the outermost lines of the 1:6:11:6:1 quintets mentioned above, seems more consistent with a species with a single iron atom than with two equivalent ones.

**Acknowledgment.** We thank Drs. Keith F. Preston, John R. Morton, and Mr. R. Duttriac for a sample of

$^{57}\text{Fe}$ -enriched  $\text{Fe}(\text{CO})_5$ . We are also grateful to Dr. K. F. Preston, Dr. David Thorn, and Professor Robert Bergman for helpful discussions.

**Registry No.** I, 91199-15-4; I- $^{13}\text{C}_4$ , 99546-49-3; I-d, 99546-51-7; II, 78005-17-1; II- $^{13}\text{C}_8$ , 99546-50-6; II-d, 99546-52-8; III, 12002-28-7; IV, 71500-60-2; V, 77024-06-7; V- $^{13}\text{C}_{11}$ , 99546-53-9; V-d, 99546-55-1; VI, 99546-47-1; VI- $^{13}\text{C}_3$ , 99546-54-0; VI-d $_3$ , 99546-56-2; VII, 99546-48-2; VII-d $_3$ - $^{13}\text{C}_7$ , 99546-57-3;  $\text{Fe}(\text{CO})_5$ , 13463-40-6;  $\text{H}_2$ , 1333-74-0;  $\text{D}_2$ , 7782-39-0; CO, 630-08-0;  $^{13}\text{CO}$ , 1641-69-6.

## Cobalt Hydroformylation Catalyst Supported on a Phosphinated Polyphosphazene. Identification of Phosphorus–Carbon Bond Cleavage as Mode of Catalyst Deactivation<sup>1</sup>

Robert A. Dubois,<sup>†</sup> Philip E. Garrou,<sup>\*†</sup> Karen D. Lavin,<sup>‡</sup> and Harry R. Allcock<sup>\*‡</sup>

Dow Chemical Company, Wayland, Massachusetts 01778, and the Department of Chemistry, The Pennsylvania State University, University Park, Pennsylvania 16802

Received June 18, 1985

The interaction of  $\text{Co}_2(\text{CO})_8$  with  $[\text{NP}(\text{OPh})_{1.7}(\text{OC}_6\text{H}_4\text{PPh}_2)_{0.3}]_n$  (1),  $\text{N}_3\text{P}_3(\text{OPh})_5(\text{OC}_6\text{H}_4\text{PPh}_2)$  (2),  $\text{PPh}_2$ -linked polystyrene (3), or triarylphosphine  $[\text{PPh}_3, \text{P}(p\text{-CH}_3\text{C}_6\text{H}_4)_3]$  yielded species of the type  $\text{Co}_2(\text{CO})_7\text{PR}_3$ ,  $[\text{Co}(\text{CO})_3\text{PR}_3]_2$ , and  $[\text{Co}(\text{CO})_3(\text{PR}_3)_2]^+\text{Co}(\text{CO})_4^-$  as identified by infrared spectroscopy and  $^{31}\text{P}$  NMR. Catalysts derived from 1 were expected to have higher thermal stability based on the inherent thermal stability of 1 vs. 3. A study of the catalyst system 1/ $\text{Co}_2(\text{CO})_8$  for 1-hexene hydroformylation revealed an initial activity equal to its homogeneous analogue. This has been rationalized as due to cleavage of cross-linking P–Co–P sites during reaction with  $\text{CO}/\text{H}_2$  to give soluble hydride  $\text{HCo}(\text{CO})_3\text{PR}_3$  type species. All of the catalysts also revealed a time-dependent decrease in catalytic activity, due to a cobalt-mediated phosphorus–carbon bond cleavage. Benzene, toluene, benzyl alcohol, and  $p\text{-MeC}_6\text{H}_4\text{CH}_2\text{OH}$  were detected as primary cleavage products. When olefin was omitted from these reactions,  $\text{R}_2\text{PH}$  was observed.

### Introduction

Homogeneous transition-metal catalysts have been the focus of much fundamental research during the past decade. However, their use in large scale catalytic transformations has been limited, mainly because of the difficulties encountered in their recovery from the reaction products and unused starting materials.

A possible solution to this problem that has been explored in a number of laboratories is to link transition-metal catalysts to organic macromolecules. Such hybrid polymer–catalyst systems should be easy to recover from reaction media, especially if the macromolecules are lightly cross-linked to form three-dimensional matrices that can be used as solvent-swelled, permeable particles.<sup>2</sup>

The main impediment to the development of this idea lies in the instability of most organic polymers under the sometimes severe reaction conditions employed in important catalytic reactions. Thus, an ideal carrier polymer must be thermally and oxidatively stable and be chemically resistant to substrate and products under the reaction conditions. Not only must the polymer itself be stable under such conditions but so too must be the linkage between the transition metal and the macromolecule.

Largely because of their dominant role in the history of homogeneous catalysis,<sup>3,4</sup> tricoordinate phosphorus units have been used widely as sites for the linkage of metals

to macromolecules.<sup>2,5</sup> In particular, cross-linked phosphinated polystyrene has been the main support material, largely because of its ease of synthesis and its commercial availability.<sup>6</sup>

(Aryloxy)phosphazenes are expected to possess a higher thermooxidative stability than many of the organic polymers studied previously. In this paper, we describe our studies of phosphine-bearing phosphazenes 1 and 2 as carriers for cobalt hydroformylation catalysts, and we compare them to their homogeneous and polystyrene-bound analogues 3. Compound 4 was studied as a control compound.

### Results and Discussion

Polymer 1 and the cyclic model compound 2 were examined as functionalized supports for cobalt catalysts with a view to assessing their catalytic activity and stability. Cobalt catalysts derived from 1 and 2 were catalytically

(1) Some of these results have been published in a preliminary communication, see: Dubois, R. A.; Garrou, P. E.; Lavin, K. D.; Allcock, H. R. *Organometallics* 1984, 3, 649.

(2) Bailey, D. C.; Langer, S. H. *Chem. Rev.* 1981, 81, 109.

(3) Heck, R. F. "Organotransition Metal Chemistry"; Academic Press: New York, 1974.

(4) Parshall, G. W. "Homogeneous Catalysis"; Wiley-Interscience: New York, 1980.

(5) Hodge, P.; Sherrington, D. C., Eds. "Polymer Supported Reactions in Organic Synthesis"; Wiley: New York, 1980.

(6) Polymer-bound triphenylphosphine or styrene–divinylbenzene is made by the Strem Chemical Co. and sold under license of U.S. Patent 3 708 462 owned by the Dow Chemical Co.

<sup>†</sup>Dow Chemical Company.

<sup>‡</sup>The Pennsylvania State University.

the top and bottom of each line of the triplet (Figure 1G). This allows only a rough estimation of the  $^{57}\text{Fe}$  coupling (ca. 4.5 G). However, the lack of another pair of weaker shoulders near the base of each line, i.e., the outermost lines of the 1:6:11:6:1 quintets mentioned above, seems more consistent with a species with a single iron atom than with two equivalent ones.

**Acknowledgment.** We thank Drs. Keith F. Preston, John R. Morton, and Mr. R. Duttriac for a sample of

$^{57}\text{Fe}$ -enriched  $\text{Fe}(\text{CO})_5$ . We are also grateful to Dr. K. F. Preston, Dr. David Thorn, and Professor Robert Bergman for helpful discussions.

**Registry No.** I, 91199-15-4; I- $^{13}\text{C}_4$ , 99546-49-3; I-d, 99546-51-7; II, 78005-17-1; II- $^{13}\text{C}_8$ , 99546-50-6; II-d, 99546-52-8; III, 12002-28-7; IV, 71500-60-2; V, 77024-06-7; V- $^{13}\text{C}_{11}$ , 99546-53-9; V-d, 99546-55-1; VI, 99546-47-1; VI- $^{13}\text{C}_3$ , 99546-54-0; VI-d $_3$ , 99546-56-2; VII, 99546-48-2; VII-d $_3$ - $^{13}\text{C}_7$ , 99546-57-3;  $\text{Fe}(\text{CO})_5$ , 13463-40-6;  $\text{H}_2$ , 1333-74-0;  $\text{D}_2$ , 7782-39-0; CO, 630-08-0;  $^{13}\text{CO}$ , 1641-69-6.

## Cobalt Hydroformylation Catalyst Supported on a Phosphinated Polyphosphazene. Identification of Phosphorus–Carbon Bond Cleavage as Mode of Catalyst Deactivation<sup>1</sup>

Robert A. Dubois,<sup>†</sup> Philip E. Garrou,<sup>\*†</sup> Karen D. Lavin,<sup>‡</sup> and Harry R. Allcock<sup>\*‡</sup>

Dow Chemical Company, Wayland, Massachusetts 01778, and the Department of Chemistry, The Pennsylvania State University, University Park, Pennsylvania 16802

Received June 18, 1985

The interaction of  $\text{Co}_2(\text{CO})_8$  with  $[\text{NP}(\text{OPh})_{1.7}(\text{OC}_6\text{H}_4\text{PPh}_2)_{0.3}]_n$  (1),  $\text{N}_3\text{P}_3(\text{OPh})_5(\text{OC}_6\text{H}_4\text{PPh}_2)$  (2),  $\text{PPh}_2$ -linked polystyrene (3), or triarylphosphine  $[\text{PPh}_3, \text{P}(p\text{-CH}_3\text{C}_6\text{H}_4)_3]$  yielded species of the type  $\text{Co}_2(\text{CO})_7\text{PR}_3$ ,  $[\text{Co}(\text{CO})_3\text{PR}_3]_2$ , and  $[\text{Co}(\text{CO})_3(\text{PR}_3)_2]^+\text{Co}(\text{CO})_4^-$  as identified by infrared spectroscopy and  $^{31}\text{P}$  NMR. Catalysts derived from 1 were expected to have higher thermal stability based on the inherent thermal stability of 1 vs. 3. A study of the catalyst system 1/ $\text{Co}_2(\text{CO})_8$  for 1-hexene hydroformylation revealed an initial activity equal to its homogeneous analogue. This has been rationalized as due to cleavage of cross-linking P–Co–P sites during reaction with  $\text{CO}/\text{H}_2$  to give soluble hydride  $\text{HCo}(\text{CO})_3\text{PR}_3$  type species. All of the catalysts also revealed a time-dependent decrease in catalytic activity, due to a cobalt-mediated phosphorus–carbon bond cleavage. Benzene, toluene, benzyl alcohol, and  $p\text{-MeC}_6\text{H}_4\text{CH}_2\text{OH}$  were detected as primary cleavage products. When olefin was omitted from these reactions,  $\text{R}_2\text{PH}$  was observed.

### Introduction

Homogeneous transition-metal catalysts have been the focus of much fundamental research during the past decade. However, their use in large scale catalytic transformations has been limited, mainly because of the difficulties encountered in their recovery from the reaction products and unused starting materials.

A possible solution to this problem that has been explored in a number of laboratories is to link transition-metal catalysts to organic macromolecules. Such hybrid polymer–catalyst systems should be easy to recover from reaction media, especially if the macromolecules are lightly cross-linked to form three-dimensional matrices that can be used as solvent-swelled, permeable particles.<sup>2</sup>

The main impediment to the development of this idea lies in the instability of most organic polymers under the sometimes severe reaction conditions employed in important catalytic reactions. Thus, an ideal carrier polymer must be thermally and oxidatively stable and be chemically resistant to substrate and products under the reaction conditions. Not only must the polymer itself be stable under such conditions but so too must be the linkage between the transition metal and the macromolecule.

Largely because of their dominant role in the history of homogeneous catalysis,<sup>3,4</sup> tricoordinate phosphorus units have been used widely as sites for the linkage of metals

to macromolecules.<sup>2,5</sup> In particular, cross-linked phosphinated polystyrene has been the main support material, largely because of its ease of synthesis and its commercial availability.<sup>6</sup>

(Aryloxy)phosphazenes are expected to possess a higher thermooxidative stability than many of the organic polymers studied previously. In this paper, we describe our studies of phosphine-bearing phosphazenes 1 and 2 as carriers for cobalt hydroformylation catalysts, and we compare them to their homogeneous and polystyrene-bound analogues 3. Compound 4 was studied as a control compound.

### Results and Discussion

Polymer 1 and the cyclic model compound 2 were examined as functionalized supports for cobalt catalysts with a view to assessing their catalytic activity and stability. Cobalt catalysts derived from 1 and 2 were catalytically

(1) Some of these results have been published in a preliminary communication, see: Dubois, R. A.; Garrou, P. E.; Lavin, K. D.; Allcock, H. R. *Organometallics* 1984, 3, 649.

(2) Bailey, D. C.; Langer, S. H. *Chem. Rev.* 1981, 81, 109.

(3) Heck, R. F. "Organotransition Metal Chemistry"; Academic Press: New York, 1974.

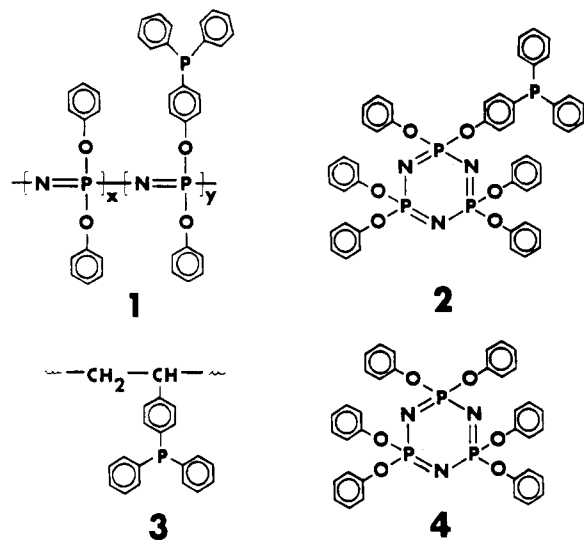
(4) Parshall, G. W. "Homogeneous Catalysis"; Wiley-Interscience: New York, 1980.

(5) Hodge, P.; Sherrington, D. C., Eds. "Polymer Supported Reactions in Organic Synthesis"; Wiley: New York, 1980.

(6) Polymer-bound triphenylphosphine or styrene–divinylbenzene is made by the Strem Chemical Co. and sold under license of U.S. Patent 3 708 462 owned by the Dow Chemical Co.

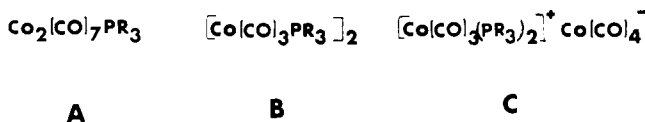
<sup>†</sup>Dow Chemical Company.

<sup>‡</sup>The Pennsylvania State University.



active for the hydroformylation of 1-hexene. However, a decline in catalytic activity with use was detected for both species. We attribute this both to loss of cobalt species from the phosphine unit and to cleavage of phosphine units from the polymeric or cyclic phosphazenes. We believe that this cleavage reaction is a general problem with triarylphosphine-modified catalytic systems. Consequently, a reinterpretation of the industrial viability of phosphinated organic supports for hydroformylation reactions may be needed.

**Reaction of  $\text{Co}_2(\text{CO})_8$  with Phosphine-Bearing Polyphosphazenes.** The reaction of  $\text{Co}_2(\text{CO})_8$  with tertiary phosphines is known<sup>7</sup> to yield three types of compounds, illustrated as species A–C. Each of these is distinguishable



by its characteristic infrared spectrum in the carbonyl region. The known stretching frequencies of the three species, together with those observed for the polyphosphazene–cobalt system, are shown in Table I. The relative concentrations of the three species under hydroformylation conditions depend on temperature, partial pressure of  $\text{CO}/\text{H}_2$ , and on the phosphine/cobalt ratio.<sup>7</sup>

The soluble phosphine-bearing polyphosphazenes  $[\text{NP}(\text{OPh})_{1.7}(\text{OC}_6\text{H}_4\text{PPh}_2)_{0.3}]_n$  reacted with  $\text{Co}_2(\text{CO})_8$  in THF or toluene solution to yield an insoluble brown complex. An infrared spectrum of this material was consistent with the presence of all three cobalt complexes, A, B, and C. It was reported earlier<sup>8</sup> that only species B and C were present in the cobalt carbonyl complexes with (diphenylphosphino)methylated polystyrene. The presence of all three species in the present system is probably a consequence of the higher cobalt to phosphorus ratio. Cobalt carbonyl is known to react with tertiary phosphines to yield bis(phosphine) complexes,<sup>7</sup> and we attribute the insolubility of the polyphosphazene–cobalt system to cross-linking through P–Co–P sites. This type of cross-linking has been described previously for  $[\text{RhCl}(\text{CO})_2]_2$  and  $\text{Fe}(\text{CO})_3(\text{PhCH}=\text{CHC}(\text{O})\text{CH}_3)$  coordinated to this polymer.<sup>9</sup> No evidence was obtained for linkage of cobalt to

Table I

compd	IR (CO), $\text{cm}^{-1}$	<sup>31</sup> P NMR, ppm
$\text{Co}_2(\text{CO})_7\text{PPh}_3$ (A)	2079 (m), 2026 (m), 1996 (s), 1964 (m) <sup>a</sup>	82.4 <sup>a</sup>
$[\text{Co}(\text{CO})_3\text{PPh}_3]_2$ (B)	1960 (s) <sup>a</sup>	71.65 <sup>a</sup>
$[\text{Co}(\text{CO})_3(\text{PPh}_3)_2]^+$ $[\text{Co}(\text{CO})_4]^-$ (C)	1995 (s), 1978 (m), 1890 (s) <sup>a</sup>	
$\text{HCo}(\text{CO})_3\text{PPh}_3$	2041 (m), 1952 (s) <sup>a</sup>	64.4 <sup>b</sup>
$\text{Co}_2(\text{CO})_8 + 1$	2075 (w), 2000 (s), 1980 (sh), 1955 (s), 1890 (s)	
$\text{Co}_2(\text{CO})_8 + 2$		81.2, 70.7

<sup>a</sup> Reference 7. <sup>b</sup> Assigned by analogy to  $\text{PCy}_3$  and  $\text{PET}_3$  systems in ref 7.

the nitrogen atoms of the polymer backbone. Poly(bisphenoxyphosphazene) did not react with  $\text{Co}_2(\text{CO})_8$  under similar conditions.

**Catalyst Activity.** The cobalt–phosphine catalyzed hydroformylation of olefins to aldehydes and alcohols has been studied extensively.<sup>3,4,7,10–12</sup> Hydroformylation of 1-hexene in the presence of cobalt/phosphine catalysts yields hexenes, hexane, heptanal, heptanol, heptyl formate, and higher molecular weight species. From an industrial standpoint, the alcohols are the more desirable products. The initial product of hydroformylation is the linear and branched isomer mixture of heptanal, which is reduced under the reaction conditions to the corresponding isomers of heptanol. The first step to yield heptanal takes place readily at moderate temperatures (110 °C). Alcohol (heptanol) is the main product of hydroformylation at the higher temperatures (170–200 °C). Two complicating side reactions also occur: namely, aldol condensation to higher molecular weight species and formate production.<sup>11</sup> Both of these products are generated from the initial aldehyde.<sup>7,11,13</sup> Product distributions in this study are reported as normalized percentage yields excluding these higher molecular weight species (which normally constituted 7.5 ± 2.5% of the final products).

The results of this study are summarized in Table II.<sup>14</sup> In general, polymer-supported catalysts are less active than their homogeneous analogues, presumably because of mass transfer limitations. However, this was not found to be the case for the polyphosphazene system 1. The cobalt-bound polyphosphazene gave heptanol in 85% yield (reaction 2 in Table II), while the homogeneous cobalt–triphenylphosphine system gave an 87% yield (reaction 4 in Table II) under identical reaction conditions. In addition, the polyphosphazene–cobalt system brought about the reaction of all the initial substrate, 1-hexene. Only a few examples are known where a homogeneous catalyst retains its activity or shows increased activity on an insoluble support, e.g., cobalt-bound 2-vinylpyridine and 2-vinylpyridine–styrene polymer systems.<sup>15</sup>

We propose then that, under these reaction conditions, the cross-linked P–Co–P sites are broken to give the known hydrido  $\text{HCo}(\text{CO})_3\text{PR}_3$  type species. With this now soluble

(9) Allcock, H. R.; Lavin, K. D.; Tollefson, N. M.; Evans, T. L. *Organometallics* 1983, 2, 267.

(10) Paulik, F. E. *Catal. Rev.* 1972, 6, 49.

(11) Wender, I.; Pino, P. "Organic Synthesis Via Metal Carbonyls"; Wiley-Interscience: New York, 1977; Vol. 2, p 43.

(12) Pruet, R. L. "Advances in Organometallic Chemistry"; West, R., Stone, F. G. A., Eds.; Academic Press: New York, 1979; Vol. 17, p 1.

(13) Marko, L.; Szabo, P. *Chem. Technol.* 1961, 13, 482.

(14) Complex reaction profiles which would have given a more quantitative picture of the relative reaction rates were not obtained since it was observed that all of the catalyst systems were degrading with time.

(15) Moffat, A. J. *J. Catal.* 1970, 18, 143, 322.

(7) Wood, C. W.; Garrou, P. E. "Catalytic Conversion of Synthesis-Gas and Alcohols to Chemicals"; Herman, R. G., Ed.; Plenum Press: New York, 1984; p 203.

(8) Evans, G. O.; Pittman, C. U.; McMillan, R.; Beach, R. T.; Jones, R. J.; *J. Organomet. Chem.* 1974, 67, 298.

Table II

reactn	phosphine source	Co, mmol	molar P/Co ratio	product distribution <sup>a</sup>				
				hexenes <sup>b</sup>	hexane	heptanal <sup>c</sup>	heptanol <sup>c</sup>	heptyl formate <sup>c</sup>
1	1	0.10	3.0	3.0	12.8	21.3	62.4	3.7
2	1	0.18	4.0	6.1		3.3	84.7	1.7
3	PPh <sub>3</sub>	0.06	3.8		18.2 <sup>d</sup>	62.4	17.3	2.5
4	PPh <sub>3</sub>	0.18	3.9		4.8		87.2	8.5
5	3 <sup>e</sup>	0.17	2.7		14.7 <sup>d</sup>	33.4	52.1	<1
6	3 <sup>f</sup>	0.31	1.9		38.0 <sup>d</sup>	30.0	31.9	<1
7	3 <sup>f</sup>	0.42	1.2		20.9 <sup>d</sup>	30.7	47.4	1.0

<sup>a</sup> 7 h, 190–195 °C, 2:1 H<sub>2</sub>/CO, 2000 psig. Normalized mol % excluding higher molecular weight species. <sup>b</sup> Mixture of isomers: 1-hexene, *cis*- and *trans*-2-hexene, and *cis*- and *trans*-3-hexene. <sup>c</sup> Mixture of isomers: two branched and one linear. <sup>d</sup> Sum of hexenes and hexane. <sup>e</sup> Styrene-divinylbenzene copolymer (20% cross-linked) substituted with diphenylphosphino groups (0.46 mequiv of P/g of resin) (Strem Chemicals). <sup>f</sup> Styrene-divinylbenzene copolymer (2% cross-linked) substituted with diphenylphosphino groups (0.5 mequiv of P/g of resin) (Strem Chemicals).

polymeric species, the reaction resembles that found for the same concentration of Co<sub>2</sub>(CO)<sub>8</sub>/XPR<sub>3</sub>. With both systems, the concentrations of HCo(CO)<sub>4</sub> should be identical and thus alkene conversion (faster for HCo(CO)<sub>4</sub>) and aldehyde reduction to alcohols (more selective for HCo(CO)<sub>3</sub>PR<sub>3</sub>) would proceed at similar rates for both the homogeneous and phosphazene-bound systems. This explanation is supported by the fact that ~7% of the cobalt-supported phosphazene catalyst, initially insoluble in the reaction mixture at room temperature, was recovered from the solution phase of the cooled reaction mixture after 8 h.

Therefore we believe that these polymeric systems are partially soluble under these conditions, and this avoids the usual mass transfer limitations. However, they are insoluble at room temperature and pressure, and this allows the easy removal of the reaction products. This provides a new approach to the study and use of polymer-immobilized catalysts.

However, this interpretation is complicated by the catalyst recycle data presented in Table III. Although the polyphosphazene-catalyst system 1 revealed better activity and selectivity than the polystyrene system 3 studied, the activity and selectivity of these systems decreased steadily with each cycle. The heptanol yield in the third recycle (34.3–41.7%) for 1 (0.31 mmol of Co) corresponded to the heptanol yield during the first cycle for the 2% cross-linked diphenylphosphinated polystyrene-cobalt systems (0.31 mmol of Co). Elemental analysis confirmed that substantial losses of both cobalt and phosphorus had occurred for both polymer systems. Cobalt loss was higher for 3 (86–88% for 3 vs. 56–60% for 1) while phosphorus loss was higher for the system based on 1 (15–19% for 3 vs. 30% for 1).<sup>16</sup>

**Mode of Catalyst Deactivation.** Although loss of cobalt during polymer-supported hydroformylation would be a serious problem, the loss of phosphine groups would be even more damaging since it would severely limit the regenerative capacity of the polymer. It is important that this decomposition be understood if more stable catalyst systems are to be designed.<sup>17</sup>

Polymers 1 and 3 in the absence of cobalt show excellent stability at 190 °C at hydroformylation temperatures. This is illustrated by the TGA curves in Figure 1. Curve A, for the phosphinated polyphosphazene, shows an onset of decomposition at 400 °C and a maximum rate of decomposition at 460 °C. This is a thermal stability slightly better than that of phosphinated polystyrene (curve B,

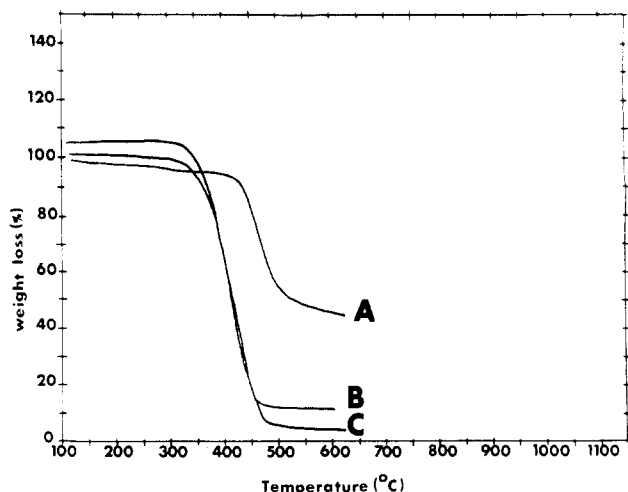


**Figure 1.** TGA curves for phosphinated polymers: (A) diphenylphosphinated polyphosphazene 1; (B) styrene-20% divinylbenzene substituted with diphenylphosphino groups (0.46 mequiv of P/g of resin) (Strem Chemicals); (C) styrene-2% divinylbenzene substituted with diphenylphosphino groups (0.5 mequiv of P/g of resin) (Strem Chemicals).

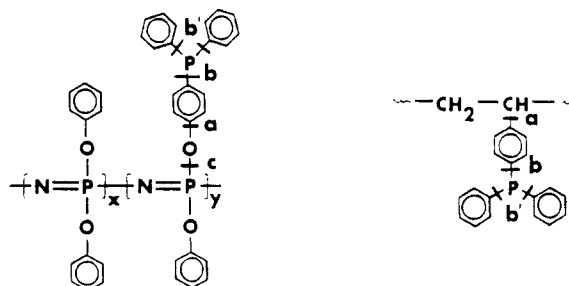


**Figure 2.** Bond scission possibilities.

20% cross-linked; curve C, 2% cross-linked).

Elemental analysis of the catalyst recovered after cycle 6 for 1 (0.31 mmol of Co) showed a 7% drop in carbon and phosphorus, while the nitrogen remained constant. These data indicate that loss of pendent phosphine groups is occurring rather than a random chain scission or depolymerization.

Examination of the <sup>31</sup>P NMR spectra of catalyst solutions of 1 and 2, after exposure to hydroformylation conditions, fails to reveal any signals due to (*p*-OH-C<sub>6</sub>H<sub>5</sub>)PPh<sub>2</sub>. This observation precludes C–O bond cleavage of type c (Figure 2). The detection of PPh<sub>3</sub> (by <sup>31</sup>P NMR spectroscopy and GLC mass spectrometry) after exposure of 1, 2, and 3 to hydroformylation conditions is at least formally consistent with bond cleavage of type a. However, we are not aware of any precedent for it. The most plausible explanation is that PPh<sub>3</sub> is a secondary product

(16) The polyphosphazene system was carried through more recycles since cobalt still remained present.

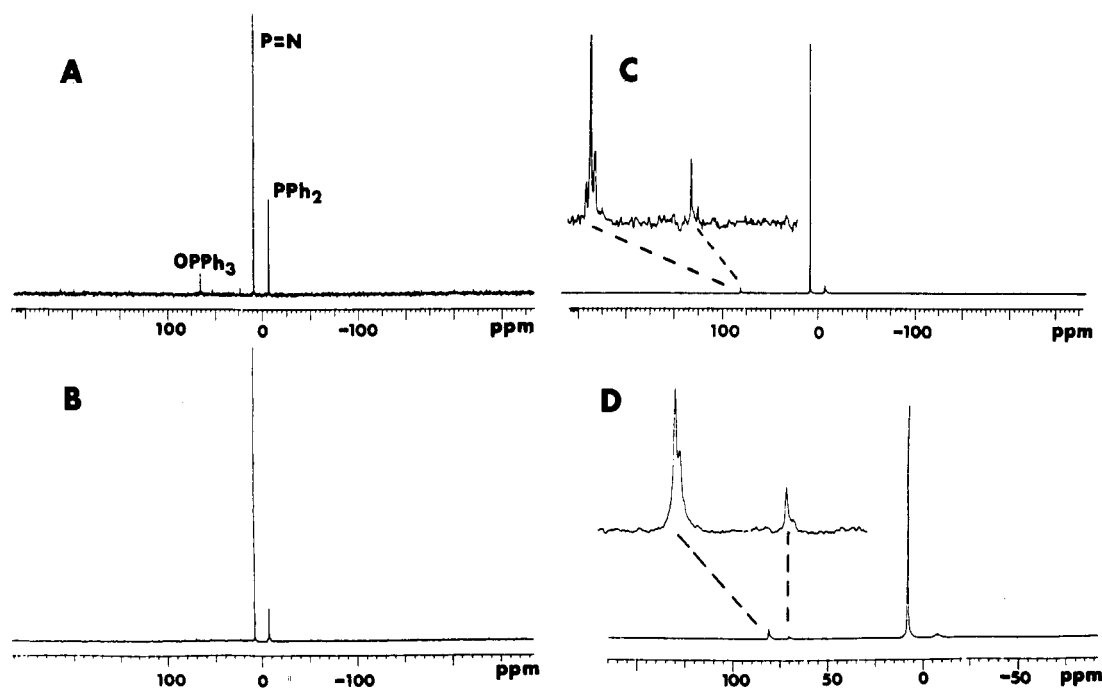
(17) Similar P–C cleavage products have recently been observed during studies on Co-<sup>18</sup> and Rh-catalyzed hydroformylation,<sup>18–20</sup> Ru-catalyzed amine dehydrogenation,<sup>21</sup> and Ir-catalyzed C–H activation.<sup>22</sup>



Table III

polymer support	Co, mmol	molar P/Co ratio	R* <sup>f</sup>	product distribution <sup>a</sup>					P, Co loss
				hexenes	hexanes	heptanal	heptanol	heptyl formate	
1 <sup>b</sup>	0.31	1.9	...	...	9.5	0	89.3	9.0	
			1	...	7.9	12.1	70.7	3.6	
			2	...	9.6	52.6	34.3	1.7	
			3	...	8.3	76.0	13.9	3.4	
			4	...	8.2	73.7	14.4	...	
1 <sup>b</sup>	0.18	4.0	5	...	12.6	78.4	7.5	...	56% Co, 30% P
			1	...	6.1	3.3	84.7	6.5	
			2	...	7.9	7.7	87.6	6.3	
			3	...	17.0 <sup>c</sup>	59.8	21.2	1.9	
			4	...	35.1 <sup>c</sup>	51.7	11.9	1.2	
3 <sup>d</sup>	0.17	2.7	5	...	44.5 <sup>c</sup>	48.0	7.4	...	60% Co, 30% P
			1	...	14.7 <sup>c</sup>	33.4	52.1	<1.0	
			2	...	26.2 <sup>c</sup>	58.6	14.9	...	
			3	...	52.1 <sup>c</sup>	47.6	...	...	
			3 <sup>e</sup>	...	29	9	30.0	31.9	
3 <sup>e</sup>	0.31	1.9	1	29.4	6.8	59.2	8.7	86% Co, 16% P	
			2	23.7	6.5	60.0	9.7		
			3	40.4	5.7	53.8	...		
3 <sup>e</sup>	0.42	1.2	1	20.9	...	30.7	47.4	1.0	88% Co, 19% P
			2	29.9	...	54.1	15.0	1.0	
			3	21.4	...	63.2	14.3	1.2	

<sup>a</sup> 7 h, 190–195 °C, 2:1 CO/H<sub>2</sub>, 2000 psig. Product distribution have been normalized to reflect the 7.5 ± 2.5% higher molecular weight products always present. <sup>b</sup> Polyphosphazene. <sup>c</sup> We were not able to separate hexenes from hexanes. <sup>d</sup> Styrene–divinylbenzene copolymer (2% cross-linked) substituted with diphenylphosphino groups (0.46 mequiv of P/g of resin) (Strem Chemicals). <sup>e</sup> Styrene–divinylbenzene copolymer (20% cross-linked) substituted with diphenylphosphino groups (0.5 mequiv of P/g of resin) (Strem Chemicals). <sup>f</sup> R\* = recycle number.



**Figure 3.** <sup>31</sup>P NMR spectra of a reaction mixture of **2** and Co<sub>2</sub>(CO)<sub>8</sub> after exposure to hydroformylation conditions: (a) at time = 0; (b) at time = 20 h; (c) at time = 35 h; (d) 7 h after the addition of 1-hexene.

of aryl group scrambling after initial P–C bond cleavage of type b and b'. Similar types of P–C bond cleavage has been detected for a variety of transition-metal phosphine complexes.<sup>17</sup> Additional secondary products (i.e., benzene)

and direct products of type b and b' P–C bond cleavage (PPh<sub>2</sub>H) were detected by both <sup>31</sup>P NMR spectroscopy and GLC analysis.

For example, when the cobalt–cyclophosphazene system **2** was subjected to hydroformylation conditions for 35 h, the <sup>31</sup>P NMR resonance for the phosphine groups gradually increased in intensity relative to the ring phosphorus

(18) Sakakura, T.; Kobayashi, T.-A.; Hayashi, T.; Kawahana, Y.; Tanaka, M.; Ogata, I. *J. Organomet. Chem.* **1984**, *267*, 171.

(19) Abatjogolu, A. G.; Billig, E.; Bryant, D. R. *Organometallics* **1984**, *3*, 923.

(20) Ceriotti, A.; Garlaschelli, L.; Longoni, G.; Malzesta, C.; Strumolo, D. *J. Mol. Catal.* **1984**, *24*, 309.

(21) Jung, C. W.; Fellman, J. D.; Garrou, P. E. *Organometallics* **1983**, *2*, 1042.

(22) Burk, M. J.; Crabtree, R. H.; Dion, R. P.; Parnall, C. D.; Urizuk, R. *J. Organometallics* **1984**, *3*, 816.

(23) Garrou, P. E.; Dubois, R. A.; Jung, C. W. *CHEMTECH* **1985**, 123. Garrou, P. E. *Chem. Rev.* **1985**, *85*, 185.

Table IV

complex <sup>a</sup>	Co, mmol	PR <sub>3</sub> , mmol	rxn time, h	product distribution, mmol							
				C <sub>6</sub> H <sub>6</sub>	Ph-Ph	PhCHO	PhCH <sub>2</sub> OH	PhCH <sub>3</sub>	PhCH <sub>2</sub> -CH <sub>2</sub> OH	Ph <sub>2</sub> PH	total <sup>b</sup>
1	4.68	11.8	37	1.74				1.22		+	
3	4.56	11.6	46	2.2			trace	1.74	trace	trace	
PPh <sub>3</sub>	7.8	19.8	56	6.0			0.7	6.9	0.4	+	14.0

<sup>a</sup> Reaction conditions: 190 °C, 1500 psig CO/H<sub>2</sub> (1:1), heptane solvent (for 3); 190 °C, 2000 psig CO/H<sub>2</sub> (1:1), xylene for PPh<sub>3</sub> reaction.

<sup>b</sup> Total organic cleavage products.

resonance, as illustrated in Figure 3. In addition, a small amount of triphenylphosphine was detected by <sup>31</sup>P NMR, apparently the product of aryl group scrambling, as mentioned above. These results are compatible with cleavage of the phosphine unit from the cyclophosphazene ring.

When 1-hexene was added to a catalyst system containing Co<sub>2</sub>(CO)<sub>8</sub> and PPh<sub>3</sub> under these conditions, <sup>31</sup>P NMR examination of the reaction solution showed resonances which were assigned to PPh<sub>2</sub>(CH<sub>2</sub>)<sub>5</sub>CH<sub>3</sub>. This product would result from the reaction of PPh<sub>2</sub>H (a primary product of P-C cleavage) with 1-hexene. In analogous experiments with P(*p*-MeC<sub>6</sub>H<sub>4</sub>)<sub>3</sub> and P(CH<sub>2</sub>Ph)<sub>3</sub>, the secondary phosphines HP(*p*-MeC<sub>6</sub>H<sub>4</sub>)<sub>2</sub> and HP(CH<sub>2</sub>Ph)<sub>2</sub> were detected by <sup>31</sup>P NMR spectroscopy. In addition, substantial quantities of b'-type cleavage products were always detected in the reactions of 1, 2, 3, and PR<sub>3</sub> (Table IV). The production of benzene and toluene could be due to free radical or oxidative addition (P-Ph bond to Co) processes. The benzyl alcohol type products could only result via insertion of CO into a Co-Ph bond to give Co-C(O)Ph followed by elimination and hydrogenation of the resultant aldehyde.<sup>17</sup> A thorough discussion of these reactions is presented in the following paper.<sup>24</sup>

**Conclusions.** Our cobalt-supported polyphosphazene systems and their homogeneous analogues Co<sub>2</sub>(CO)<sub>8</sub>/XPR<sub>3</sub> reveal very similar reactivities, while the polystyrene-bound systems are less reactive. This has been explained by a solubilization of catalysts derived from 1 under the reaction conditions employed due to cleavage of the P-Co-P cross-links and their reformation under ambient conditions. A significant observation was that these phosphine-bound catalysts undergo chemical degradation under the reaction conditions. Examination of a variety of PR<sub>3</sub> systems for the hydroformylation of 1-hexene has revealed the formation of HPR<sub>2</sub>, R<sub>2</sub>P(CH<sub>2</sub>)<sub>5</sub>CH<sub>3</sub>, and products derived from CO insertion such as benzyl alcohol. An increasing amount of evidence suggests that such P-C bond cleavage in phosphine-linked systems is much more common than had been thought previously.<sup>24</sup> The results of this study suggest that a general reevaluation is needed of phosphine-linked transition-metal systems for catalysis.

### Experimental Section

**Materials.** All purchased chemicals were reagent-grade and were used as received. Toluene, tetrahydrofuran, and heptane were degassed and dried over 4-Å molecular sieves. Cobalt octacarbonyl (Strem Chemicals) was either sublimed or recrystallized from hexane. Triphenylphosphine was recrystallized three times from ethanol, and tribenzylphosphine was purified by extraction into hexane. 1-Hexene (Aldrich, Gold Label) was checked for peroxides, flushed with nitrogen, and stored over 4-Å molecular sieves in a drybox. The hydrogen (UHP) and carbon monoxide (UHP) were obtained from Matheson and were used as received. The cyclophosphazenes N<sub>3</sub>P<sub>3</sub>(OPh)<sub>5</sub>(OC<sub>6</sub>H<sub>4</sub>PPh<sub>2</sub>) and N<sub>3</sub>P<sub>3</sub>(OPh)<sub>6</sub> and the polyphosphazene [NP(OPh)<sub>1.7</sub>(OC<sub>6</sub>H<sub>4</sub>PPh<sub>2</sub>)<sub>0.3</sub>]<sub>n</sub> were synthesized according to literature procedures.<sup>9</sup> All reactions under "syn gas" pressure (1:1 CO/H<sub>2</sub>) were carried out with the

use of a glass liner, which was charged with the reagents under an inert atmosphere in a drybox. The liner was then placed in the reactor. After the reactor was sealed, it was purged of air by at least three cycles of pressurization and venting with argon. "Syn gas" was introduced to 1400 psig at room temperature, and this was followed by a 30-min warm-up period at 190 °C, during which time the pressure rose to 2000 psig. Samples were withdrawn from and reagents added to the cooled reaction mixture by syringe under an argon stream.

**Equipment.** The cylindrical glass liners (147 mm long, 41-mm i.d., 45-mm o.d.) were wrapped near the top of the liner with a few turns of Teflon tape to provide a tight fit that would minimize spillover of the contents from the liner into the reaction vessel (a 300 cm<sup>3</sup> Autoclave Engineers, Inc., magnedrive packless autoclave). An external heater was controlled with a LFE series 230 controller, and the reaction temperature was maintained by a Parr temperature controller which circulated water through internal cooling coils. Between reactions, the stirring shaft and cooling coils were periodically immersed in concentrated nitric acid to remove cobalt. Infrared spectra were obtained with a Spectraspan IV dc plasma emission spectrometer equipped with a spectrajert III DC argon plasma emission source. Reaction mixtures were analyzed with the use of a Hewlett-Packard (HP) 5710A (FID) gas chromatograph connected to a HP 3390A reporting integrator and equipped with a HP fused silica capillary column (0.21-mm i.d.) 25 m long, coated with high-temperature SE-30 (0.11 μm thick). Carrier gas (helium) flow rate was 1 mL/min at 15 psig and 100:1 split ratio. Injection port and detector temperatures were 250 and 300 °C, respectively. Octane was used as an internal standard for the GLC analyses. <sup>31</sup>P NMR analyses were obtained by means of a JEOL FX-90Q spectrometer equipped with a broad-band, tunable probe operating at 36.2 MHz. Thermogravimetric analyses (TGA) were obtained by means of a Du Pont 1090 thermal analyzer. Metal analyses on the resin-supported catalysts were performed on a sample (0.050 g) warmed in concentrated nitric acid (1.0 mL) at 50 °C for 2 h. After cooling and dilution to 50 mL with distilled water, the sample was analyzed by emission spectrometry using the 3453.5-Å line for cobalt. The background was determined with 2% nitric acid, and the control was standard solution of CoCl<sub>2</sub> in 2% nitric acid. Metal analyses of the organic reaction mixtures were performed on a measured quantity of material which was warmed in concentrated nitric acid (1.0 mL) at 50 °C for 2 h. After cooling and dilution of the solution to 50 mL with distilled water, the solution was extracted several times with dichloromethane. The solvent was removed, and the material was analyzed as described above for the resin supported catalysts.

**Reaction of Co<sub>2</sub>(CO)<sub>8</sub> with (Diphenylphosphino)polystyrene (3).** The method used was similar to that described previously.<sup>8</sup> In a typical preparation the 2% cross-linked polymer beads (9.0 g, 4.5 mmol of phosphorus) were suspended in heptane (35 mL) for 1 h before adding a concentrated solution of Co<sub>2</sub>(CO)<sub>8</sub> (0.34 g, 2.0 mmol of Co). After the solution was stirred overnight, the dark brown beads were recovered by filtration, washed with copious amounts of toluene, and dried under vacuum at room temperature. Anal. Found: C, 83.2; H, 7.42; P, 2.2; Co, 1.34.

**Reaction of Co<sub>2</sub>(CO)<sub>8</sub> with (Diphenylphosphino)phenoxypolyphosphazene.** A sample of the polymer 1, [NP(OPh)<sub>1.7</sub>(OC<sub>6</sub>H<sub>4</sub>PPh<sub>2</sub>)<sub>0.3</sub>]<sub>n</sub> (1.0 g, 1.03 mmol of phosphine ligand), was dissolved in toluene (50 mL). A concentrated solution of Co<sub>2</sub>(CO)<sub>8</sub> (0.15 g, 0.88 mmol of Co) was added with stirring, and the polymer precipitated from solution. After the mixture was stirred overnight, the cobalt-bound polymer was recovered by filtration and was dried under vacuum at room temperature (0.87 g, 90%): IR 2070 (m), 2000 (vs), 1975 (s), 1905 (sh), 1875 (vs)

(24) Dubois, R. A.; Garrou, P. E., following paper in this issue.

cm<sup>-1</sup>; Co analysis by plasma emission, 1.49%.

**Hexaphenoxycyclotriphosphazene (4) under Hydroformylation Conditions.** A glass liner was filled with 4 (0.85 g, 1.23 mmol), triphenylphosphine (0.35 g, 1.34 mmol), Co<sub>2</sub>(CO)<sub>8</sub> (0.055 g, 0.16 mmol), and toluene (30 mL). It was pressurized to 2000 psig with syn gas at 190 °C for 37 h. A <sup>31</sup>P NMR spectrum contained resonances for the cyclophosphazene (8.5 ppm) and triphenylphosphine (-5.8 ppm). The olefin 1-hexene (5.0 mL) was added, and hydroformylation conditions continued for another 22 h. Two additional resonances appeared in the <sup>31</sup>P NMR spectrum indicative of PPh<sub>2</sub>(CH<sub>2</sub>)<sub>5</sub>CH<sub>3</sub> (-16.9 ppm) and PPh<sub>3</sub>=O (23 ppm). Gas chromatographic analysis showed the presence of hexane (10%), heptanols (83%), and heptyl formates (6.5%).

**(Diphenylphosphino)phenoxycyclotriphosphazene (2) under Hydroformylation Conditions.** The cyclophosphazene 2 (1.0 g, 0.88 mmol), Co<sub>2</sub>(CO)<sub>8</sub> (37.6 mg, 0.11 mmol), and toluene (30 mL) were pressurized to 2000 psig at 190 °C with syn gas for 35 h. Samples were withdrawn at 20 and 35 h for <sup>31</sup>P NMR analysis. Each succeeding sample showed a large decrease in the peak height for the phosphine group (-7 ppm) relative to that for the phosphazene (8.5 ppm) (Figure 3). The phosphine resonance had almost disappeared to the base line at 35 h. Magnification of this peak showed a shoulder at -5.8 ppm for triphenylphosphine. This loss of phosphine was matched by a similar loss in catalytic activity. Addition of 1-hexene (5.0 mL) and application of hydroformylation conditions for 7 h resulted in only a 12% conversion to heptanals (11%) and heptyl formates (1.5%). This reaction mixture was treated with excess hexane, and a dark viscous oil (0.2 g) separated. The hexane-soluble portion was removed to give 0.5 g of a yellow viscous oil whose <sup>31</sup>P NMR spectrum revealed the presence of very small amounts of compound 2 along with cobalt-phosphine complexes (resonances at 70-80 ppm). The black, hexane-insoluble oil (0.2 g) mentioned above had a strong infrared absorption band at 1895 cm<sup>-1</sup> indicative of Co(CO)<sub>4</sub>, and a <sup>31</sup>P NMR spectrum in toluene compatible with the presence of a phosphazene (8.2 ppm) and a cobalt-phosphine complex (81.2, 80.8, 80.7 ppm).

**Decomposition of Triphenylphosphine under Hydroformylation Conditions in the Presence of 1-Hexene.** A glass liner was filled as described above with 1-hexene (10.0 mL), Co<sub>2</sub>(CO)<sub>8</sub> (0.4 g, 1.17 mmol), triphenylphosphine (2.47 g, 9.45 mmol), and heptane (35 mL). The hydroformylation experiment was performed at 190 °C and 1900 psig of syn gas for 8-9 days. At the end of this period, the pressure had decreased to 800 psig. Gas chromatographic analysis showed the expected products hexane, heptanols, and heptyl formates along with benzene (0.17 g, 2.18 mmol, 93% based on cobalt), presumably a decomposition product of triphenylphosphine. A rust brown, crystalline solid, insoluble in most solvents, was also recovered. This gave a strong infrared band at 1950 cm<sup>-1</sup> similar to that found in [Co(PPh<sub>3</sub>)(CO)<sub>3</sub>]<sub>2</sub>.

**Decomposition of (Diphenylphosphino)polystyrene under Hydroformylation Conditions.** A sample of 2% cross-linked (diphenylphosphino)polystyrene beads (9.0 g, 34.3 mmol) was treated with a 3:1 ratio of Co<sub>2</sub>(CO)<sub>8</sub> (0.34 g, 1.0 mmol), 1-hexene (10.0 mL), and heptane (35 mL) and was placed in the reactor at 190 °C under 1500 psig of syn gas for 48 h. Gas chromatographic analysis indicated the presence of the expected products hexane, heptanols, and heptyl formates in addition to the unexpected product benzene (0.070 g, 0.9 mmol, 50% based on cobalt). Elemental analysis of the recovered black beads showed only small losses of cobalt and phosphorus. [Fresh catalyst contained: % C, 83.2; % H, 7.42; % P, 2.2; % Co, 1.34. Used catalyst contained: % C, 83.5; % H, 8.06; % P, 2.1; % Co, 1.26.] An infrared spectrum of the resin beads (KBr pellet) showed absorptions at 2050 (w), 1950 (vs), and 1880 (w) cm<sup>-1</sup>. An attempt was made to recycle these beads, and a quantitative conversion of hexenes to hexane (3%), heptanols (90%), and heptyl formates (2%) was achieved. No benzene was detected. Elemental analysis of these, now blue, twice used beads showed significant losses of cobalt and phosphorus: % C, 85.6; % H, 7.62; % P, 1.71; % Co, 0.85. Another recycle attempt was less successful and yielded after 24 h hexenes-hexane (12%), heptanals (17%), heptanols (53%), and heptyl formates (3%).

**Decomposition of Triphenylphosphine under Hydroformylation Conditions in the Absence of 1-Hexene in**

**Heptane.** The reaction vessel was filled with triphenylphosphine (2.47 g, 9.45 mmol), Co<sub>2</sub>(CO)<sub>8</sub> (0.4 g, 1.17 mmol), and heptane (35 mL) and subjected to 2000 psig of syn gas at 190 °C for 15 h. A sample was withdrawn for <sup>31</sup>P NMR analysis from which crystals of PPh<sub>3</sub> precipitated from solution. The <sup>1</sup>H-decoupled <sup>31</sup>P NMR spectrum contained resonances for PPh<sub>3</sub> at -5.6 ppm and for PPh<sub>2</sub>H at -41.1 ppm (a <sup>1</sup>H-coupled <sup>31</sup>P NMR spectrum contained a doublet with *J*<sub>PH</sub> = 210 Hz). After an additional 96 h of reaction, gas chromatographic analysis indicated the presence of benzene (0.103 g, 1.32 mmol, 57% based on cobalt). A rust brown, insoluble crystalline material (0.11 g) was recovered, with the elemental composition: % C, 62.57; % H, 4.29; % P, 8.11; % Co, 13.85.

**Decomposition of Triphenylphosphine under Hydroformylation Conditions in the Absence of 1-Hexene in Toluene.** The reaction vessel was filled with triphenylphosphine (0.35 g, 1.34 mmol), Co<sub>2</sub>(CO)<sub>8</sub> (0.055 g, 0.16 mmol), and toluene (30 mL). This mixture was placed in the reactor and subjected to 190 °C and 2000 psig of syn gas for 21 h. A <sup>31</sup>P NMR spectrum of the brown-orange solution contained two new resonances, including the resonance assigned to PPh<sub>3</sub>, at 23.9 ppm (assigned to PPh<sub>3</sub>=O), and at 71.7 ppm assigned to [Co(CO)<sub>3</sub>(PPh<sub>3</sub>)<sub>2</sub>]. 1-Hexene (5.0 mL) was added and the experiment was continued for 14 h at 190 °C and 1900 psig. A brown-orange solution was recovered, the <sup>31</sup>P NMR spectrum of which contained several additional resonances: 82.4 and 64.4, assigned to [Co<sub>2</sub>(CO)<sub>7</sub>(PPh<sub>3</sub>)] and [HCo(CO)<sub>3</sub>(PPh<sub>3</sub>)], respectively, 32.9 and 28.0 ppm, and -17 ppm, assigned to PPh<sub>2</sub>(CH<sub>2</sub>)<sub>5</sub>CH<sub>3</sub>. Gas chromatographic analysis indicated that the products were hexane (2%), heptanols (87%), and heptyl formates (9%). The experiment was continued for 19 h at 190 °C and 2200 psig. A <sup>31</sup>P NMR spectrum of the reaction mixture contained resonances for the three cobalt-phosphorus complexes described above at 82.5, 71.7, and 64.6 ppm, with some additional resonances at 81.7, 74.5, and 73.6 ppm which may be derived from the PPh<sub>2</sub>(CH<sub>2</sub>)<sub>5</sub>CH<sub>3</sub> analogues of the cobalt-phosphine complexes. A rust brown solid was recovered (0.050 g) with an infrared absorption at 1950 cm<sup>-1</sup> (Nujol).

**Decomposition of Tri-*p*-tolylphosphine under Hydroformylation Conditions in the Absence of 1-Hexene in Toluene.** The reaction vessel was charged with tri-*p*-tolylphosphine (2.58 g, 9.45 mmol) (a small quantity of the phosphine oxide was present), Co<sub>2</sub>(CO)<sub>8</sub> (0.4 g, 1.17 mmol), and toluene (35 mL). These materials were placed in a reactor, and the experiment was performed at 190 °C under 2000 psig of syn gas for 10 h. A <sup>31</sup>P NMR spectrum of the reaction mixture contained a resonance at -43.2 ppm assigned to di-*p*-tolylphosphine. This resonance disappeared on exposure to the atmosphere.

**Decomposition of Tribenzylphosphine under Hydroformylation Conditions in Heptane in the Absence of 1-Hexene.** The reaction vessel was filled with tribenzylphosphine (1.5 g, 4.93 mmol), Co<sub>2</sub>(CO)<sub>8</sub> (0.4 g, 1.17 mmol), and heptane (35 mL). These materials were introduced into the reactor, and the experiment was performed at 190 °C and 2000 psig of syn gas for 16 h. A <sup>31</sup>P NMR spectrum of the light yellow reaction mixture contained resonances at -15.1 ppm, assigned to the phosphorus atom in tribenzylphosphine, two weak resonances at 61.7 and 42.3 ppm, one resonance at -18.6 ppm, and a resonance at -49.6 ppm, assigned to the phosphorus atom in dibenzylphosphine. The experiment was continued at 190 °C for an additional 20 h, and gas chromatographic analysis indicated the formation of toluene (0.191 g, 2.08 mmol, 89% based on Co).

**Decomposition of Tribenzylphosphine under Hydroformylation Conditions in Toluene in the Absence of 1-Hexene.** The reaction vessel was filled as described above except that toluene replaced heptane as the reaction medium. After 15 h, a sample of the bright red-orange reaction mixture was withdrawn for <sup>31</sup>P NMR analysis. The <sup>31</sup>P NMR spectrum of the sample was complex and contained many resonances in the cobalt-phosphine region (50-75 ppm). In addition, a resonance at -17 ppm and a small resonance at -49.2 ppm were assigned to the phosphorus atom in dibenzylphosphine as described above. The infrared spectrum contained several carbonyl absorption bands at 1930 (w), 1960 (s), 1970 (sh), 1995 (m), and 2050 (w) cm<sup>-1</sup> due to the presence of several different cobalt-phosphine complexes. The experiment was continued at 190 °C for 15 h. The reaction mixture lightened to a yellow-orange color. All absorptions in the infrared spectrum decreased in intensity, except

for the band at  $1930\text{ cm}^{-1}$ . A  $^{31}\text{P}$  NMR spectrum of the reaction mixture was similar to that described above except that two of the cobalt-phosphine resonances (73.2 and 65.4 ppm) had reversed their intensities.

**Solubilization of Polyphosphazene-Supported Cobalt (1) under Hydroformylation Conditions.** The reaction vessel was charged with the cobalt-supported polyphosphazene (0.67 g, 0.69 mmol of phosphine, 5.0% wt Co), 1, and toluene (30 mL). It was placed in a reactor and subjected to 2000 psig of syn gas at  $190^\circ\text{C}$  for 8 h. An infrared spectrum of the reaction mixture contained weak absorptions at 2040 and  $2000\text{ cm}^{-1}$ . A  $^{31}\text{P}$  NMR spectrum contained resonances at  $-5.9$  and  $-19.9$  ppm, assigned to the

phosphorus atom of the pendent phosphine units and the phosphazene phosphorus atoms, respectively.

**Acknowledgment.** We thank the Dow Chemical Co. for its support of the work at the Pennsylvania State University.

**Registry No.** 2, 72796-22-6; 4, 1184-10-7;  $\text{Co}_2(\text{CO})_8$ , 10210-68-1; 1-hexene, 592-41-6; triphenylphosphine, 603-35-0; hexene, 25264-93-1; hexane, 110-54-3; heptanal, 111-71-7; heptanol, 53535-33-4; heptyl formale, 112-23-2; tri-*p*-tolylphosphine, 1038-95-5; tribenzylphosphine, 7650-89-7.

## Cobalt/Arylphosphine Hydroformylation Catalysts: Substituent Effects on the Stability of the Carbon-Phosphorus Bond

Robert A. Dubois and Phillip E. Garrou\*

Dow Chemical Company, Central Research—New England Laboratory, Wayland, Massachusetts 01778

Received June 18, 1985

Triarylphosphines subjected to hydroformylation conditions ( $190^\circ\text{C}$ , 2000 psig of  $\text{CO}/\text{H}_2$ ) in the presence of  $\text{Co}_2(\text{CO})_8$  undergo phosphorus-carbon bond scission to give a variety of hydrogenolysis and CO insertion products as well as secondary products derived from hydrogenation, hydrogenolysis, and homologation. Electron-withdrawing substituents on the aryl groups enhance the initial rate of formation of both the hydrogenolysis and carbonylation products whereas electron-donating groups inhibit such reactions. Aryl group scrambling is observed when  $\text{PR}_3$  and  $\text{PR}'_3$  are subjected to the above hydroformylation conditions. The rate of such scrambling is comparable to the rate of formation of the decomposition products. Product analysis has ruled out contributions by free radical and/or ortho metalation mechanisms. An oxidative addition mechanism is proposed to be operative. Phosphorus-aryl bond cleavage proceeds at a much slower rate when olefin substrate is present.

### Introduction

It has recently become apparent that tertiary phosphines bound to metal complexes are chemically reactive and liable to undergo carbon-phosphorus bond scission, depending on the specific reaction conditions that they are exposed to.<sup>1</sup> It is also becoming more and more apparent that reaction of the phosphorus-carbon bond with the transition metal to which it is bound is a general reaction having profound implications on homogeneous catalysis.<sup>2</sup>

We have shown in a preliminary communication<sup>3</sup> and the preceding paper<sup>4</sup> that phosphorus-carbon bond cleavage is a mode of catalyst deactivation during hydroformylation catalyzed by triarylphosphine-substituted cobalt carbonyl species  $\text{Co}_2(\text{CO})_8/\text{PR}_3$  and the heterogenized catalysts  $\text{Co}_2(\text{CO})_8$  supported on (diphenylphosphino)phenoxyphosphazene or diphenylphosphine-functionalized polystyrene. In this report we wish to present data concerning substituent effects on the rate of cleavage of the phosphorus-carbon bond and discuss some of the possible mechanistic pathways available for this reaction.

The use of homogeneous catalysts in industrial chemical processing necessitates knowledge of the long-term stability of such catalyst systems since reactor downtime to unload

or replace deactivated catalyst can dramatically impact the "operating cost" of the catalyst system. Most researchers are aware of the need to recycle catalysts, but unfortunately very few studies have determined the deactivation vs. time relationship for homogeneous or polymer-supported catalyst systems.

### Discussion

When triarylphosphines are subjected to hydroformylation conditions ( $\text{Co}_2(\text{CO})_8$ ,  $190^\circ\text{C}$ , 2000 psi of  $\text{CO}/\text{H}_2$ ) in the presence or absence of olefinic substrate, they undergo C-P bond cleavage to give a number of products, depicted in Figure 1 and quantified in Table I for reactions in the absence of olefin. Four of the seven products (2, 3, 4, and 8) come directly from the tertiary phosphine by C-P bond cleavage, compounds 2 and 8 come by hydrogenolysis, compound 3 comes by coupling of the two aryl groups at the carbon initially bound to phosphorus, and compound 4 comes by carbonyl insertion into the C-P bond. Reaction profiles for the *m*-Cl- and *m*- $\text{CH}_3$ -substituted triarylphosphines (Figures 2 and 3) are typical for such reactions. They suggest the combination of parallel and consecutive reactions where the amount of hydrogenolysis product, 2, increases smoothly throughout the reaction while the initial carbonylation product, 4, undergoes relatively rapid reduction to the corresponding alcohol<sup>5</sup> 5, which in turn undergoes cobalt-catalyzed ho-

(1) Garrou, P. E.; Dubois, R. A.; Jung, C. W. *CHEMTECH* 1985, 123.

(2) Garrou, P. E. *Chem. Rev.* 1985, 85, 171 and references therein.

(3) Dubois, R. A.; Garrou, P. E.; Lavin, K.; Alcock, H. R., *Organometallics* 1984, 3, 649.

(4) Dubois, R. A.; Garrou, P. E.; Lavin, K.; Alcock, H. R., preceding paper in this issue.

(5) Aldehydes are only observed early on in the reaction. It is assumed that they are rapidly hydrogenated to the corresponding alcohols.

for the band at  $1930\text{ cm}^{-1}$ . A  $^{31}\text{P}$  NMR spectrum of the reaction mixture was similar to that described above except that two of the cobalt-phosphine resonances (73.2 and 65.4 ppm) had reversed their intensities.

**Solubilization of Polyphosphazene-Supported Cobalt (1) under Hydroformylation Conditions.** The reaction vessel was charged with the cobalt-supported polyphosphazene (0.67 g, 0.69 mmol of phosphine, 5.0% wt Co), 1, and toluene (30 mL). It was placed in a reactor and subjected to 2000 psig of syn gas at  $190\text{ }^\circ\text{C}$  for 8 h. An infrared spectrum of the reaction mixture contained weak absorptions at  $2040$  and  $2000\text{ cm}^{-1}$ . A  $^{31}\text{P}$  NMR spectrum contained resonances at  $-5.9$  and  $-19.9$  ppm, assigned to the

phosphorus atom of the pendent phosphine units and the phosphazene phosphorus atoms, respectively.

**Acknowledgment.** We thank the Dow Chemical Co. for its support of the work at the Pennsylvania State University.

**Registry No.** 2, 72796-22-6; 4, 1184-10-7;  $\text{Co}_2(\text{CO})_8$ , 10210-68-1; 1-hexene, 592-41-6; triphenylphosphine, 603-35-0; hexene, 25264-93-1; hexane, 110-54-3; heptanal, 111-71-7; heptanol, 53535-33-4; heptyl formale, 112-23-2; tri-*p*-tolylphosphine, 1038-95-5; tribenzylphosphine, 7650-89-7.

## Cobalt/Arylphosphine Hydroformylation Catalysts: Substituent Effects on the Stability of the Carbon-Phosphorus Bond

Robert A. Dubois and Phillip E. Garrou\*

Dow Chemical Company, Central Research—New England Laboratory, Wayland, Massachusetts 01778

Received June 18, 1985

Triarylphosphines subjected to hydroformylation conditions ( $190\text{ }^\circ\text{C}$ , 2000 psig of  $\text{CO}/\text{H}_2$ ) in the presence of  $\text{Co}_2(\text{CO})_8$  undergo phosphorus-carbon bond scission to give a variety of hydrogenolysis and CO insertion products as well as secondary products derived from hydrogenation, hydrogenolysis, and homologation. Electron-withdrawing substituents on the aryl groups enhance the initial rate of formation of both the hydrogenolysis and carbonylation products whereas electron-donating groups inhibit such reactions. Aryl group scrambling is observed when  $\text{PR}_3$  and  $\text{PR}'_3$  are subjected to the above hydroformylation conditions. The rate of such scrambling is comparable to the rate of formation of the decomposition products. Product analysis has ruled out contributions by free radical and/or ortho metalation mechanisms. An oxidative addition mechanism is proposed to be operative. Phosphorus-aryl bond cleavage proceeds at a much slower rate when olefin substrate is present.

### Introduction

It has recently become apparent that tertiary phosphines bound to metal complexes are chemically reactive and liable to undergo carbon-phosphorus bond scission, depending on the specific reaction conditions that they are exposed to.<sup>1</sup> It is also becoming more and more apparent that reaction of the phosphorus-carbon bond with the transition metal to which it is bound is a general reaction having profound implications on homogeneous catalysis.<sup>2</sup>

We have shown in a preliminary communication<sup>3</sup> and the preceding paper<sup>4</sup> that phosphorus-carbon bond cleavage is a mode of catalyst deactivation during hydroformylation catalyzed by triarylphosphine-substituted cobalt carbonyl species  $\text{Co}_2(\text{CO})_8/\text{PR}_3$  and the heterogenized catalysts  $\text{Co}_2(\text{CO})_8$  supported on (diphenylphosphino)phenoxyphosphazene or diphenylphosphine-functionalized polystyrene. In this report we wish to present data concerning substituent effects on the rate of cleavage of the phosphorus-carbon bond and discuss some of the possible mechanistic pathways available for this reaction.

The use of homogeneous catalysts in industrial chemical processing necessitates knowledge of the long-term stability of such catalyst systems since reactor downtime to unload

or replace deactivated catalyst can dramatically impact the "operating cost" of the catalyst system. Most researchers are aware of the need to recycle catalysts, but unfortunately very few studies have determined the deactivation vs. time relationship for homogeneous or polymer-supported catalyst systems.

### Discussion

When triarylphosphines are subjected to hydroformylation conditions ( $\text{Co}_2(\text{CO})_8$ ,  $190\text{ }^\circ\text{C}$ , 2000 psi of  $\text{CO}/\text{H}_2$ ) in the presence or absence of olefinic substrate, they undergo C-P bond cleavage to give a number of products, depicted in Figure 1 and quantified in Table I for reactions in the absence of olefin. Four of the seven products (2, 3, 4, and 8) come directly from the tertiary phosphine by C-P bond cleavage, compounds 2 and 8 come by hydrogenolysis, compound 3 comes by coupling of the two aryl groups at the carbon initially bound to phosphorus, and compound 4 comes by carbonyl insertion into the C-P bond. Reaction profiles for the *m*-Cl- and *m*- $\text{CH}_3$ -substituted triarylphosphines (Figures 2 and 3) are typical for such reactions. They suggest the combination of parallel and consecutive reactions where the amount of hydrogenolysis product, 2, increases smoothly throughout the reaction while the initial carbonylation product, 4, undergoes relatively rapid reduction to the corresponding alcohol<sup>5</sup> 5, which in turn undergoes cobalt-catalyzed ho-

(1) Garrou, P. E.; Dubois, R. A.; Jung, C. W. *CHEMTECH* 1985, 123.

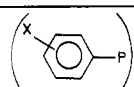
(2) Garrou, P. E. *Chem. Rev.* 1985, 85, 171 and references therein.

(3) Dubois, R. A.; Garrou, P. E.; Lavin, K.; Alcock, H. R., *Organometallics* 1984, 3, 649.

(4) Dubois, R. A.; Garrou, P. E.; Lavin, K.; Alcock, H. R., preceding paper in this issue.

(5) Aldehydes are only observed early on in the reaction. It is assumed that they are rapidly hydrogenated to the corresponding alcohols.

Table I. Products of the Cobalt-Mediated Phosphorus-Carbon Bond Cleavage of Triarylphosphines

		products, mmol									
X	mmol	Co, mmol	time, <sup>a</sup> h	2	3	4	5	6	7	8	total, mmol
<i>p</i> -CF <sub>3</sub>	5.4	2.58	6	1.6			0.3				1.9
<i>m</i> -Cl	6.6	2.58	21	3.3			0.6	tr			3.9
<i>p</i> -Cl	6.2	2.58	28.5	2.8			0.6	1.0			4.4
<i>m</i> -CH <sub>3</sub>	19.1	7.8	62	7.2	tr	tr	0.5	8.6	0.4	tr	16.9
H	19.8	7.8	56	6.0			0.7	6.9	0.4	tr	14.0
<i>p</i> -Me	19.8	7.8	47	3.4			0.3	2.9			6.6
<i>p</i> -OMe	6.8	2.58	60	1.0				2.0			3.0
<i>p</i> -F	7.6	2.58	33	0.8			0.4	0.4			1.6
<i>o</i> -CH <sub>3</sub>	6.6	2.58	27	0.9		tr	0.5	2.7		tr	4.1

<sup>a</sup>At 190 °C and 2000 psig of CO/H<sub>2</sub> (1:1).

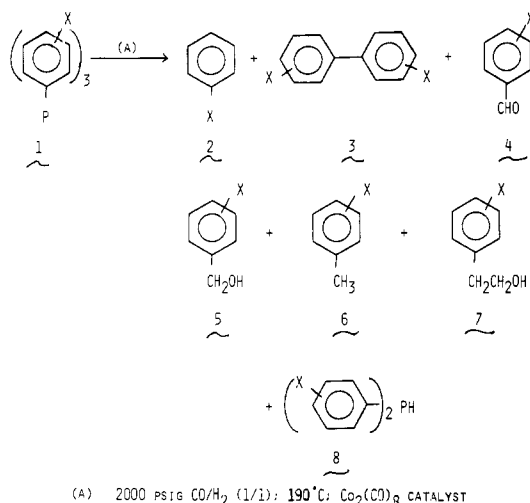


Figure 1. Products of the cobalt-mediated phosphorus-carbon bond cleavage of triarylphosphines.

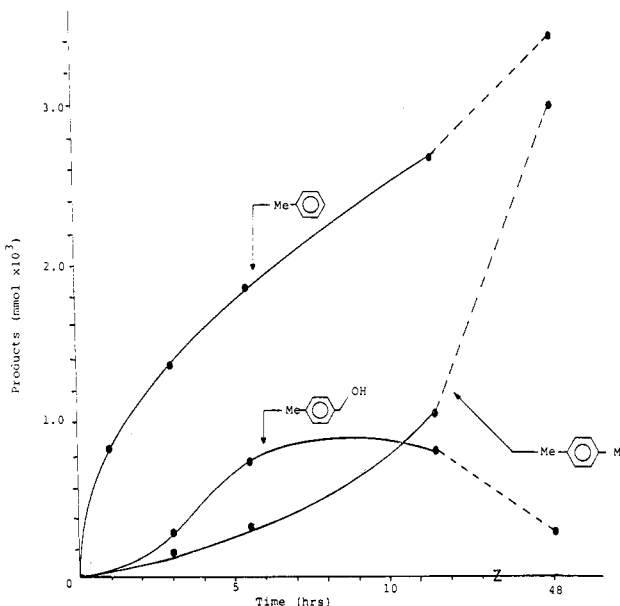


Figure 3. Reaction profile for (*p*-MeC<sub>6</sub>H<sub>4</sub>)<sub>3</sub>P decomposition [Co<sub>2</sub>(CO)<sub>8</sub>, 3.9 mmol; phosphine, 19.8 mmol; 190 °C; 2000 psig of CO/H<sub>2</sub> (1:1); benzene, 120 mL].

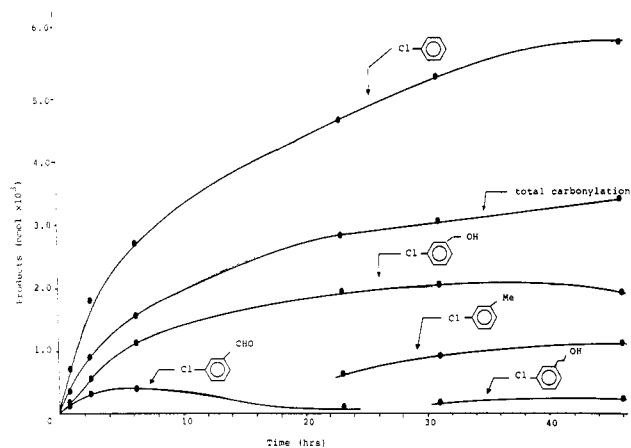


Figure 2. Reaction profile for (*m*-ClC<sub>6</sub>H<sub>4</sub>)<sub>3</sub>P decomposition [Co<sub>2</sub>(CO)<sub>8</sub>, 3.16 mmol; phosphine, 16.1 mmol; benzene, 98 mL; 160 °C; 1800 psig of CO/H<sub>2</sub> (1:1)].

mologation to 7 or hydrogenolysis to 6.<sup>6</sup> Thus compounds 4, 5, 6, and 7 all derive ultimately from the initial carbonyl insertion into the C-P bond. Compound 3 is rarely seen in more than trace quantities, and compound 8 is the phosphine product of the C-P bond scission. Any mechanisms for C-P cleavage must account for the wide variety of products shown in Figure 1 which can be divided into three types: carbonylation, hydrogenolysis, and coupling. We sought to examine potential mechanistic routes to such decomposition products.

(6) Wender, I.; Pino, P. "Organic Synthesis Via Metal Carbonyls"; Wiley-Interscience: New York, 1977.

**Free Radical Pathways.** Free radical processes have been proposed to account for the hydrogenolysis products from Co<sub>2</sub>(CO)<sub>8</sub> catalyzed hydroformylation reactions of compounds that can form stable free radicals such as polycyclic aromatic hydrocarbons<sup>7</sup> and styrene.<sup>8</sup> However for a system that would give less stable free radicals, for example, the decomposition of methyl triarylphosphine cobalt complexes to methane, the intermediacy of free radicals was precluded based on the lack of deuterium incorporation when run in deuterated toluene.<sup>9</sup> We attempted to determine the involvement of free radicals in Co-catalyzed hydroformylation by subjecting Co<sub>2</sub>(CO)<sub>8</sub>/PR<sub>3</sub> to our standard reaction conditions in the presence of ethylbenzene-*d*<sub>10</sub>, a good deuterium source for radicals. A GC/MS examination of the reaction mixtures revealed no deuterium incorporation into the products benzene, diphenylphosphine, or benzyl alcohol. This argues strongly against the presence of phenyl or phosphinyl radicals.

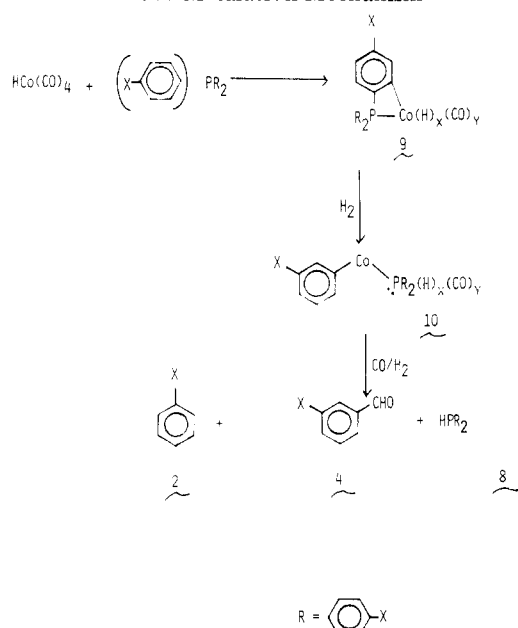
An additional argument against the presence of free aryl radicals can be made on the basis of the aryl-coupled products. In all cases where biaryls were produced only

(7) Feder, H. M.; Halpern, J. *J. Am. Chem. Soc.* 1975, 97, 7186.

(8) Marko, L. In "Fundamental Research in Homogeneous Catalysis"; Gragianzi, M., Grongo, M., Eds.; Plenum Press: New York, 1984; Vol. 4.

(9) Kemmit, R. D. W.; Russell, D. R. "Comprehensive Organometallic Chemistry"; Wilkinson, G., Ed.; Pergamon Press: New York, 1982; Vol. 5, p 70.

## Scheme I. Phosphorus-Carbon Bond Cleavage by an Ortho Metalation Mechanism



those which could arise by coupling of the aryls through the carbons initially bound to the phosphorus were detected; that is, the aryl ring substitution pattern was preserved. No products of coupling between aryl radicals and solvent, benzene or toluene, were detected.<sup>10</sup>

**Ortho Metalation.** Ortho metalation is commonly observed in transition-metal-phosphine catalyst systems; however, P-C bond cleavage products from such intermediates have not been reported.<sup>15</sup> The involvement of ortho metalation intermediates during the generation of hydrogenolysis and CO insertion products was considered as follows. The H of intermediate 9 (Scheme I) could transfer to the aryl carbon bound to phosphorus, and the carbon-phosphorus bond could undergo cleavage to give the aryl cobalt species 10. Species 10 could undergo hydrogenolysis to give 2 or CO insertion to give carbonylation products. If such a process were operative, the carbonylation products would have ring substitution patterns different from starting phosphine. For example, meta-substituted triarylphosphine would afford a mixture of ortho- and para-substituted aryl cobalt intermediates and para-substituted triarylphosphines should give meta-substituted products as shown in Scheme I. In all cases the only experimentally observed carbonylation products detected were those with retained ring substitution pattern. It is highly unlikely that ortho metalation could give rise to aryl cobalt intermediates which could only undergo hydrogenolysis to 2, so we therefore discount ortho metalation as a likely mechanistic route to any of the products derived from tertiary phosphine decomposition.

**Substituent Effects.** The oxidative addition of haloaryls to low oxidation state transition metals has been shown to behave in a manner consistent with nucleophilic substitution where electron-withdrawing groups are rate

(10) Others have used similar coupling arguments to argue against the presence of free radicals.<sup>11-14</sup>

(11) Kikukawa, K.; Yamane, T.; Takagi, M.; Matsuda, T. *Bull. Chem. Soc. Jpn.* **1979**, *52*, 1187.

(12) Lewin, M.; Aizenshtat, Z.; Blum, J. *J. Organomet. Chem.* **1980**, *184*, 255.

(13) Fahey, D.; Mahan, J. *J. Am. Chem. Soc.* **1976**, *98*, 4499.

(14) Michman, M.; Kaufman, V. R.; Nussbaum, S. *J. Organomet. Chem.* **1979**, *182*, 547, 555.

(15) Parshall, G. W. *Acc. Chem. Res.* **1970**, *3*, 139.

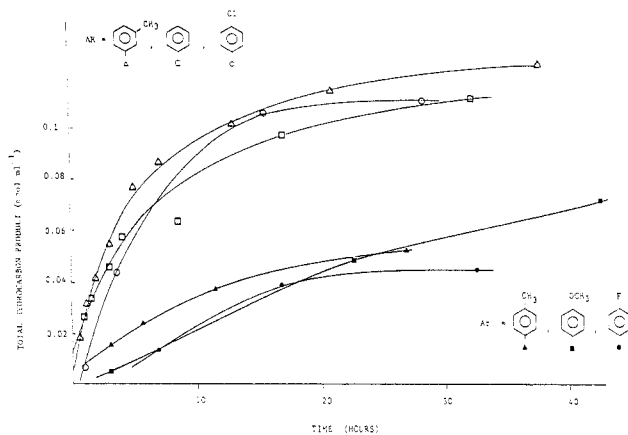


Figure 4. Total decomposition products vs. time for  $\text{PAr}_3$ .

Table II. Substituent Effects on Initial Rates of Product Formation from C-P Bond Cleavage

Ar in $\text{Ar}_3\text{P}$	initial rate formatn, $\text{mmol mL}^{-1} \text{h}^{-1} \times 10^3$		
	hydrogenolysis (2)	carbonylatn (4 + 5 + 6 + 7)	total (2 + 4 + 5 + 6 + 7)
	48	28	76
	12	15.5	27.5
	8.6	3.6	12.2
	5.0	3.5	8.5
	4.4	8.2	12.4
	1.9	1.8	3.7
	NA	NA	2.1
	0.8	0.8	1.6

accelerating and electron-donating groups are rate retarding.<sup>16,17</sup> Substituent effects on electrophilic substitution processes are essentially the reverse; that is, electron-withdrawing groups are rate retarding and electron-donating groups rate accelerating.

The effect of substituents on the overall rate of C-P bond cleavage is shown in Figure 4; a plot of total product formation with time for most of the phosphines are listed in Table I. From such a plot one can construct a relative order of reactivity. Electron-donating substituents (*p*- $\text{CH}_3$ , *p*- $\text{OCH}_3$ , *p*- $\text{F}$ ) effect a roughly fivefold lower rate than

(16) Fitton, P.; Rick, E. A. *J. Organomet. Chem.* **1971**, *28*, 287.

(17) Garrou, P. E.; Heck, R. F. *J. Am. Chem. Soc.* **1975**, *98*, 4115.

(18) Wender, I.; Greenfield, H.; Metlin, S.; Orchin, M. *J. Am. Chem. Soc.* **1952**, *74*, 4079.



Table III. Substituent Effects on the Rate and Selectivity of Cobalt-Catalyzed Homologation of Alcohols

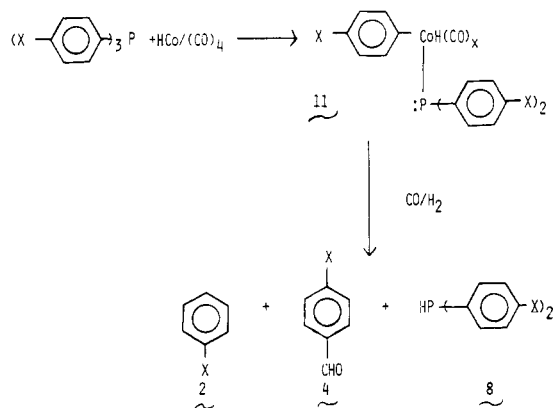
$$\text{C}_6\text{H}_4(\text{X})\text{CH}_2\text{OH} \xrightarrow[\text{CO}/\text{H}_2]{\text{cat.}} \text{C}_6\text{H}_4(\text{X})\text{CH}_3 + \text{C}_6\text{H}_4(\text{X})\text{CH}_2\text{CH}_2\text{OH}$$

5                                  6                                  7

cat.	relative rate						
$\text{Co}_2(\text{CO})_8/\text{P}(\text{C}_6\text{H}_4(\text{X}))_3$	$p\text{-OMe} > p\text{-Me} > \text{H} > m\text{-Me} > m\text{-Cl}$						
$\text{Co}_2(\text{CO})_8^a$	$p\text{-OMe} > p\text{-Me} > m\text{-Me} > \text{H} > p\text{-Cl}$						
	6/7						
cat.	$p\text{-OMe}$	$p\text{-Me}$	$o\text{-Me}$	$m\text{-Me}$	H	$p\text{-Cl}$	$m\text{-OMe}$
$\text{Co}_2(\text{CO})_8/\text{P}(\text{C}_6\text{H}_4(\text{X}))_3$	>100	>100	53	22	22		
$\text{Co}_2(\text{CO})_8^a$	0.2	1.7			2	2.5	10

<sup>a</sup> Reference 12.

### Scheme II. Phosphorus-Carbon Bond Cleavage by an Oxidative Addition Mechanism



those with somewhat lower electron-donating ability ( $\text{Ph}_3\text{P}$ ,  $m\text{-CH}_3$ ,  $p\text{-Cl}$ ). The phosphines with strong electron-withdrawing groups, namely,  $p\text{-CF}_3$  and  $m\text{-Cl}$ , constitute a third group too reactive to be included in this plot. In order to get some idea of the relative rate of the  $m\text{-Cl}$  system, it was necessary to run the reaction thirty degrees lower than the others at 160 °C. With the assumption a doubling of the rate for every ten-degree difference in temperature, the  $m\text{-Cl}$ -substituted phosphine is about six times more reactive than  $\text{PPh}_3$ .

This order of reactivity generally holds for both the initial rates of formation of the hydrogenolysis, 2, and carbonylation, 5, products as shown in Table II. This suggests a common intermediate for both hydrogenolysis and carbonylation as depicted in Scheme II. The ratio of hydrogenolysis to carbonylation products 2/5 + 6 + 7 roughly parallels the reaction rates in Table II; that is, electron-withdrawing groups promote hydrogenolysis vs. carbonylation while electron-donating groups have the opposite effect:

substituent	$p\text{-CF}_3$	$m\text{-Cl}$	$p\text{-Cl}$	$p\text{-Me}$	$m\text{-Me}$	H	$p\text{-OMe}$	$o\text{-Me}$
2/5 + 6 + 7	5.5	5.3	1.9	1.0	0.8	0.8	0.5	0.3

A rate plot for the decomposition of  $(m\text{-MeC}_6\text{H}_4)_3\text{P}$  is shown in Figure 5. Again one clearly observes a pattern of consecutive reactions. Such data can be interpreted in terms of an intermediate such as 11, formed by oxidative addition, initially partitioning between a hydrogenolysis product, 2, and a carbonyl insertion product, 4. The former does not react further, but the latter, present only in very

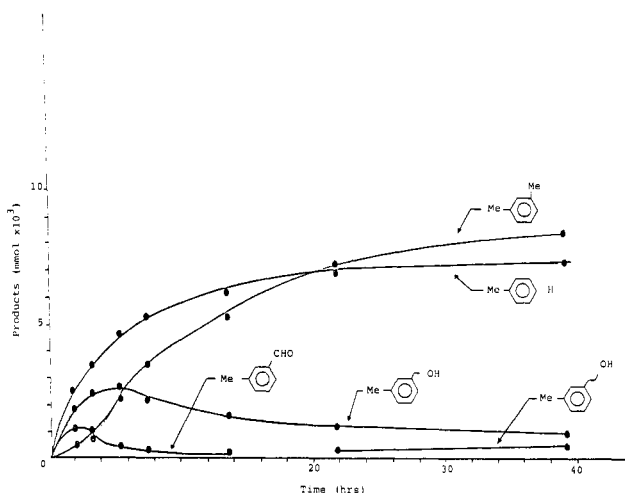


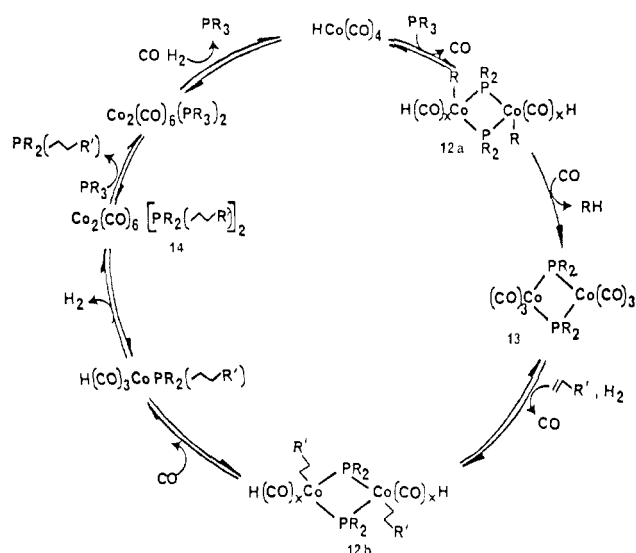
Figure 5. Reaction profile for  $(m\text{-MeC}_6\text{H}_4)_3\text{P}$  [ $\text{Co}_2(\text{CO})_8$ , 3.9 mmol; phosphine, 19.1 mmol; 190 °C; 2000 psig of  $\text{CO}/\text{H}_2$  (1:1); benzene, 120 mL].

low levels when detected, earlier in the reactions, goes on to the benzyl alcohols 5, which often build up to a maximum and then fall off as the hydrogenolysis and homologation products 6 and 7, respectively, build up.

This order is remarkably similar to the aforementioned data reported for attack of Pd on substituted aryl halides, an oxidative addition process, and is in contradistinction to that reported for electrophilic processes.

**Homologation.** As noted above the benzaldehydes initially formed by carbonyl insertion into the C-P are subsequently rapidly reduced to the corresponding alcohols 5 under reaction conditions.

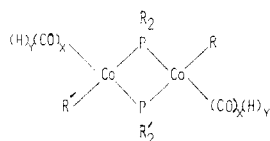
Benzyl alcohols in turn are known to be susceptible to cobalt carbonyl catalyzed hydrogenolysis and homologation to give the observed products 6 and 7. Wender<sup>12</sup> proposed a benzylcarbonium ion intermediate formed by reaction between  $\text{HCo}(\text{CO})_4$  and the benzyl alcohol to account for the effect of substituents on the rate of  $\text{Co}_2(\text{CO})_8$  catalyzed homologation of benzyl alcohols. In our system we similarly observe that electron-withdrawing groups inhibit reaction and electron-donating groups enhance it. For example, for the  $m\text{-Cl}$ -substituted phosphine, only 12% of the benzyl alcohol formed in the reaction mixture had undergone further reaction to 6 or 7 after 10 h of reaction yet, for the triphenylphosphine system, 70% of the benzyl alcohol formed in the reaction had been converted to 6 or 7 in 23 h under identical conditions. Although the orders

Scheme III. Possible Mechanism for  $\text{Co}_2(\text{CO})_8$  Catalyzed P-C Cleavage and/or R Group Scrambling

of reactivity for our system vs. Wenders are similar, the substituent effect on the ratio of products 6/7 derived from the benzyl alcohols are very different (Table III). For the cobalt-phosphine system not only is the ratio substantially higher but also it increases with the electron-donating ability of the substituents while for Wender's system it decreases. The fact that substituent effects on rates of homologation for the two systems are similar yet the product ratios are very different implies a rate limiting step to a common intermediate which then undergoes hydrogenolysis by two different mechanisms. Certainly a closer examination of these observations is called for.

It is interesting to note that the *m*- $\text{CH}_3$ -substituted triarylphosphine gives essentially the same homologation product ratio 6/7 as triphenylphosphine, an expected result based on the electronic similarity of *m*- $\text{CH}_3$  to H.

**Reactions in the Presence of Olefin.** For  $\text{PPh}_3$  in the presence of 1-hexene substrate (a working catalyst), 0.93 mol of benzene was produced per mole of cobalt after 8 days, indicating an obviously slower rate of decomposition.<sup>3,4</sup> It is thus clear that the oxidative addition of the phosphorus-aryl bond when in competition with hydroformylation proceeds at a much slower rate than when the olefin substrate is not present. If the reactions are carried out without the 1-hexene substrate, diarylphosphine,  $\text{R}_2\text{PH}$ , is detected by  $^{31}\text{P}$  NMR. When 1-hexene is present,  $\text{R}_2\text{P}$ (hexyl) is observed by  $^{31}\text{P}$  NMR. The formation of  $\text{R}_2\text{P}$ (hexyl) could occur via catalyzed addition of the 1-hexene to the  $\text{R}_2\text{PH}$  via a phosphido cobalt hydride such as 12 and subsequent elimination. In fact, it is likely that species such as 11 dimerize to species such as 12 ( $\text{R} = \text{R}'$ ).

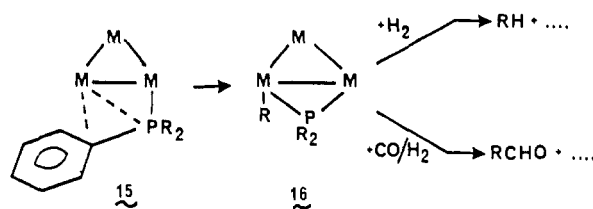


12

This is consistent with the observations of Geoffroy and coworkers,<sup>19</sup> who found that  $\text{Co}_2(\mu\text{-PPh}_2)_2(\text{CO})_6$  (13) reacts

(19) Harley, A. D.; Guskey, G. J.; Geoffroy, G. L. *Organometallics* 1983, 2, 53.

Scheme IV. Possible Cluster-Mediated P-C Bond Cleavage



with 1-hexene under synthesis gas to give  $\text{Co}_2(\text{CO})_6(\text{PPh}_2(\text{hexyl}))_2$  (14). This reaction could occur via an intermediate such as 12 which would give  $\text{HCo}(\text{CO})_3(\text{PPh}_2(\text{hexyl}))$ . Removal of the  $\text{CO}/\text{H}_2$  pressure from the solution of  $\text{HCo}(\text{CO})_3(\text{PPh}_2(\text{hexyl}))$  would result in dimerization to give 14, the observed product.

**Proposed Oxidative Addition Mechanism.** Scheme III is offered as a plausible mechanism for catalytic formation of arene ( $\text{R} = \text{Ph}$ ) and  $\text{PPh}_2(\text{hexyl})$  ( $\text{R}' = \text{C}_4\text{H}_9$ ).  $\text{PPh}_3$  could oxidatively add to an unsaturated  $\text{Co-H}$  to give an intermediate such as 12a ( $\text{R} = \text{Ph}$ ). This could eliminate benzene to give 13. In the absence of olefin an intermediate such as 13 ( $\text{R} = \text{Ph}$ ) could add  $\text{H}_2$  to give a species such as 12a (where R bonded to cobalt is H) which would eliminate  $\text{HCo}(\text{CO})_3(\text{PPh}_2\text{H})$ . Under syn gas, in the presence of excess  $\text{PR}_3$ ,  $\text{HCo}(\text{CO})_3(\text{PPh}_2\text{H})$  would exchange phosphine, leading to the observation of free  $\text{PPh}_2\text{H}$  in solution. Insertion of CO into the  $\text{Co-CH}_2\text{CH}_2\text{R}$  bond to 12b would lead to the elimination of  $\text{CH}(\text{O})\text{CH}_2\text{CH}_2\text{R}$  (hydroformylation). Insertion of CO into the  $\text{Co-Ph}$  bond of 12a would lead to the elimination of benzaldehyde and under reaction conditions subsequent reduction to benzylalcohol.

A cluster-mediated reaction can also be envisaged generating hydrogenolysis and/or CO insertion products. Fachinetti and co-workers<sup>20,21</sup> have observed the presence of the trinuclear cluster  $\text{HCo}_3(\text{CO})_9$  under hydroformylation conditions and have shown that  $\text{HCo}_3(\text{CO})_9$  and  $\text{HCo}(\text{CO})_4$  must both be present for the stoichiometric hydroformylation of 3,3-dimethylbutene. Scheme IV depicts a trimeric cluster, 15 ( $\text{M} = \text{Co}$ ). The interactive phenyl group could easily transfer to the adjacent cobalt atom resulting in a cluster containing a bridging phosphido group, 16. Species 16 could then undergo reaction with either  $\text{H}_2$  or  $\text{CO}/\text{H}_2$  to give the experimentally observed products. Such a mechanism would also result in the maintenance of the stereochemistry around the phenyl ring, i.e., para products from para-substituted substrates.<sup>22</sup>

**Aryl Group Scrambling.** Scheme V is proposed to account for all of the above observations. It is not clear, at this point, which step is rate controlling; the reaction kinetics appear very complex. Since there is a slow plateau of cobalt metal as the reaction progresses, we cannot even say with certainty that the reaction is first order in cobalt concentration. We did want to have a feel for the relative rate of the back reaction  $k_{-1}$  since it has relevance to the rate of aryl group exchange if mixed phosphines were used, i.e.,  $\text{PR}_2\text{R}'$ . We subjected equimolar mixtures of three different pairs of triarylphosphines to our standard hydroformylation conditions and monitored the reactions

(20) Fachinetti, G.; Stefani, A. *Angew. Chem., Int. Ed. Engl.* 1982, 21, 925.

(21) Bradamante, P.; Stefani, A.; Fachinetti, G. *J. Organomet. Chem.* 1984, 266, 303.

(22) Carty has recently described a trimeric hydrido ruthenium cluster similar to 15 which contains a weak phosphorus-phenyl interaction with a ruthenium atom. Reaction of this ruthenium species with  $\text{H}_2$  at 80 °C resulted in the elimination of benzene.<sup>23</sup>

(23) MacLaughlin, S. A.; Carty, A. J.; Taylor, N. J. *Can. J. Chem.* 1982, 60, 88.

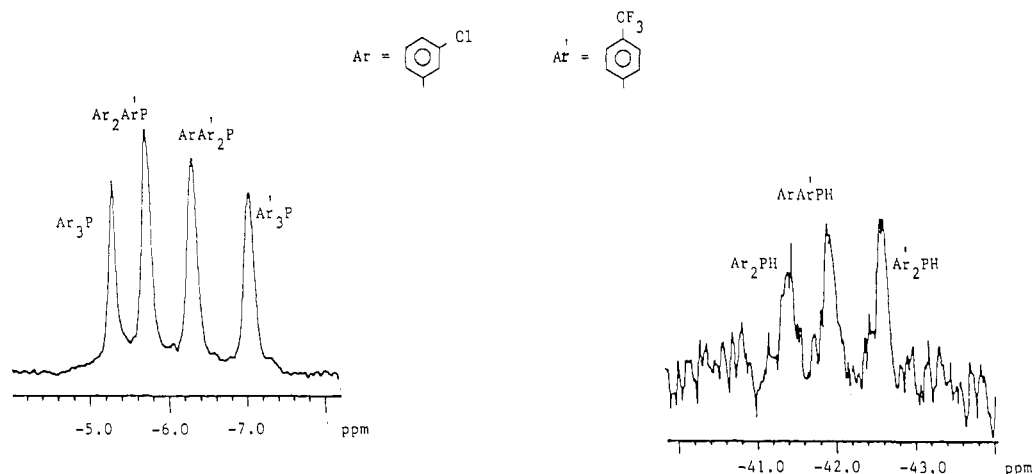
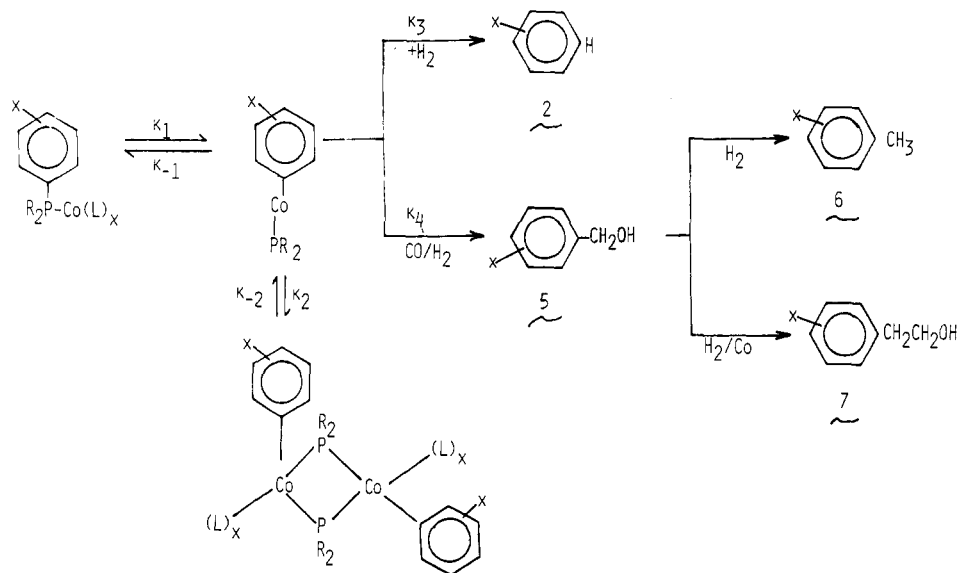


**Figure 6.**  $^{31}\text{P}$  NMR of  $(m\text{-ClC}_6\text{H}_4)_3\text{P}$  +  $(p\text{-CF}_3\text{C}_6\text{H}_4)_3\text{P}$  reaction mixture [1.3 mmol of  $(m\text{-ClC}_6\text{H}_4)_3\text{P}$  + 1.3 mmol of  $(p\text{-CF}_3\text{C}_6\text{H}_4)_3\text{P}$  + 0.47 mmol of  $\text{Co}_2(\text{CO})_8$ ; 3 h; 190 °C; 2000 psig of  $\text{CO}/\text{H}_2$ ; 35 mL of benzene].

**Scheme V. Proposed Mechanism for Phosphorus-Aryl Cleavage by Cobalt Carbonyl**



by  $^{31}\text{P}$  NMR. The pairs were selected on the basis of relative rate of product formation from carbon-phosphorus bond cleavage, that is, one pair of very reactive phosphines, one of moderate reactivity, and one of low reactivity. This order also corresponds roughly with the order of  $\text{p}K_a$ 's and thus allows us to minimize complications that might arise from substantial differences in complexing ability within the phosphine pairs. In each case substantial scrambling was observed. Figure 6 shows the  $^{31}\text{P}$  NMR spectrum obtained from subjecting 1.3 mmol of  $(m\text{-ClC}_6\text{H}_4)_3\text{P}$ , 1.3 mmol of  $(p\text{-CF}_3\text{C}_6\text{H}_4)_3\text{P}$ , and 0.47 mmol of  $\text{Co}_2(\text{CO})_8$  to 3 h at 190 °C and 2000 psig of  $\text{CO}/\text{H}_2$ . Figure 7 reveals  $^{31}\text{P}$  spectra taken over a period of time for the reaction of  $\text{PPh}_3$  and  $(p\text{-ClC}_6\text{H}_4)_3\text{P}$  (1.3 mmol each) under the same conditions. Table IV compares the time to get to 50% scrambling equilibration vs. the time needed to produce 50% of the experimentally observed cleavage products. It is clear that the rates of R group scrambling and the rates of formation of the hydrogenolysis and carbonylation products are comparable.

Abatjoglou and Bryant<sup>24</sup> have recently described similar aryl group exchange catalyzed by group 8 transition metals. It is clearly from their work and ours that the use of "exotic" phosphine modifiers in cobalt- and/or rhodium-

**Table IV. Comparison of R Group Scrambling Rates to Phosphorus-Carbon Cleavage Rates for  $\text{Ar}_3\text{P}$  -  $\text{Ar}'_3\text{P}$  Reactions Studied**

$\text{Ar}_3\text{P} + \text{Ar}'_3\text{P} \rightleftharpoons \text{Ar}_2\text{Ar}'\text{P} + \text{ArAr}'_2\text{P}$		time to, h	
A	B	C	D
Ar	Ar'	50% equilibration	50% product formation
		15	12
		2.75	3.25
		0.6	0.9

<sup>a</sup> Run at 3-fold dilution.

catalyzed hydroformylation would be commercially useless since the R group on the tertiary phosphine will eventually be the same as the olefin substrate.

**Conclusions**

From this study and others<sup>1,2</sup> it is now clear that phosphorus-carbon bond cleavage is a general reaction. Such cleavage does not appear to be free radical in nature

(24) Abatjoglou, A. G.; Bryant, D. R. *Organometallics* 1984, 3, 932.

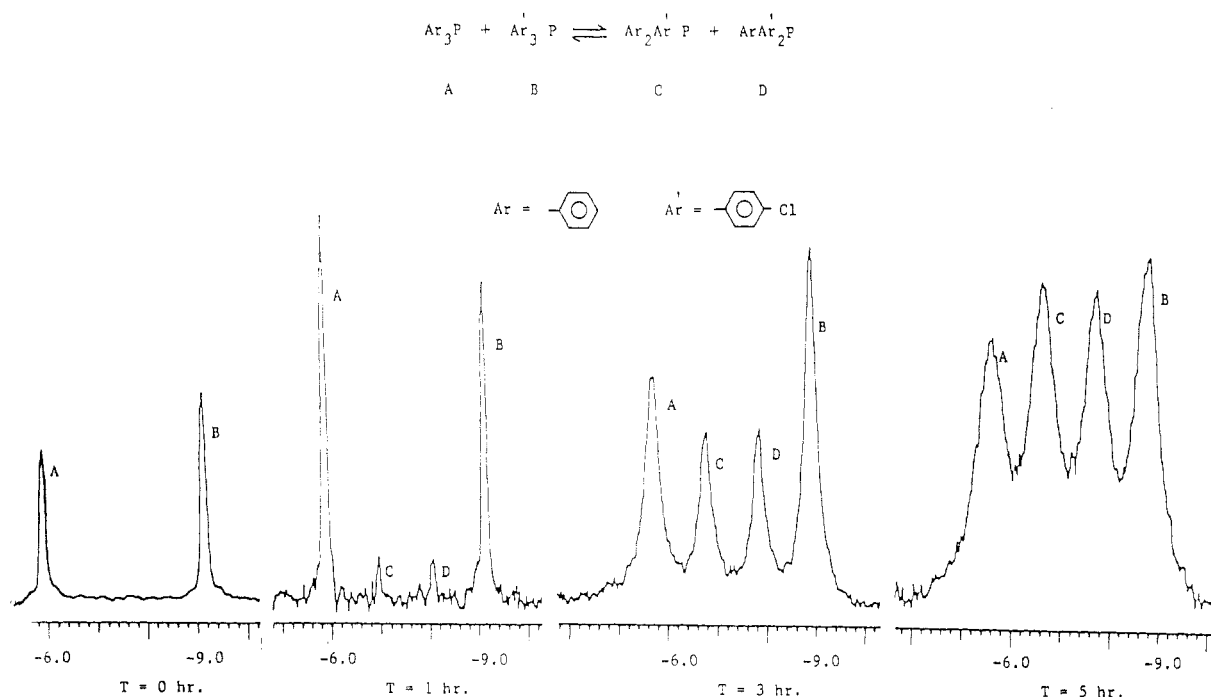


**Figure 7.**  $^{31}\text{P}$  NMR spectra of the reaction of  $\text{PPh}_3 + (p\text{-ClC}_6\text{H}_4)_3\text{P}$  vs. time [3.8 mmol of  $(p\text{-ClC}_6\text{H}_4)_3\text{P} + 3.8$  mmol of  $(\text{PPh}_3) + 1.3$  mmol of  $\text{Co}_2(\text{CO})_8$ ;  $190^\circ\text{C}$ ; 2000 psig of  $\text{CO}/\text{H}_2$ ; 35 mL of *p*-xylene].

**Table V**

phosphines		$^{31}\text{P}$ NMR chemical shifts, $\delta$						
Ar	Ar'	$\text{PAr}_3$	$\text{PAr}_2\text{Ar}'$	$\text{PArAr}'_2$	$\text{PAr}'_3$	$\text{HPAr}_2$	$\text{HPArAr}'$	$\text{HPAr}'_2$
Ph	<i>p</i> -PhCl	-5.9	-6.9	-8.0	-9.2			
<i>m</i> -PhCl	<i>p</i> -PhCF <sub>3</sub>	-5.3	-7.5	-6.3	-7.0	-41.5	-42.0	-42.7
<i>p</i> -PhMe	<i>p</i> -PhOMe	-8.5	-9.2	-10.0	-10.8	-43.3	-44.4	-45.4

but does appear to be influenced electronically by the substituents present on the aryl ring. The reaction appears to fit the traditional requirements of a "oxidative addition" both in its electronic response and its subsequent product distribution.

The cleavage of phosphorus-carbon bonds in tertiary phosphines has obvious implications in the area of homogeneous catalysis in general and more specifically in the areas of polymer-supported homogeneous catalysis<sup>4</sup> and asymmetric catalysis when the site of asymmetry resides on the phosphorus. Future studies in this area should address reactions where extended lifetime studies can be carried out and the specific question of deactivation addressed. Understanding the underlying causes for phosphorus-carbon bond breakage will hopefully point out ways to prevent or retard it.

### Experimental Section

**1. Equipment.** All reactions were run in a 300 cm<sup>3</sup> Autoclave Engineers, Inc., magnedrive packless autoclave, one of which was equipped with a sampling system. Glass liners when used (147 mm long, 41-mm i.d., 45-mm o.d.) were wrapped with a few turns of Teflon tape near the top to provide a tight fit that minimizes spillover of the contents. An external heater was controlled with a LFE series 230 controller, and reaction temperature was maintained by a Parr temperature controller which circulated water through internal cooling coils. The stirring shaft and cooling coils were immersed between runs in concentrated  $\text{HNO}_3$  to remove cobalt. Infrared spectra were obtained on a Beckman 4240 spectrometer. Reaction mixtures were analyzed on a Hewlett-Packard (HP) 5710A (FID) gas chromatograph connected to a HP 3390A reporting integrator and equipped with one of the following 25-m HP fused silica capillary columns: A, high-temperature SE-30 (0.11- $\mu\text{m}$  film); B, Carbowax 20M (0.33- $\mu\text{m}$  film, 0.2-mm i.d.); C, high-temperature 5% methylphenylsilicone (0.33- $\mu\text{m}$  film, 0.2-mm i.d.). Carrier gas (helium) flow rate was

1 mL/min at 15 psi and 100:1 split ratio. Injection port and detector temperatures were 250 and 300  $^\circ\text{C}$ , respectively.  $^{31}\text{P}$  NMR analyses were obtained on a JEOL FX-90Q spectrometer equipped with a broad-band, tunable probe operating at 36.2 MHz. Chemical shifts were measured relative to 85%  $\text{H}_3\text{PO}_4$ . Mass spectra were obtained on a HP Model 5985 capillary gas chromatograph-mass spectrometer.

**2. Reagents.** Unless otherwise specified all chemicals were reagent grade and used as received. Solvents were degassed prior to use. The phosphines were obtained from Strem Chemicals. Triphenylphosphine was recrystallized three times from ethanol. Hydrogen (UHP) and carbon monoxide (UHP) were obtained from Matheson and used as received.

**3. Typical Reaction. Decomposition of Tri-*m*-tolylphosphine under Hydroformylation Conditions.** A reactor was charged under an argon atmosphere with 5.8 g (19.1 mmol) of the phosphine, 1.32 g (3.9 mmol) of  $\text{Co}_2(\text{CO})_8$ , 120 mL of benzene, and 320  $\mu\text{L}$  (224 mg) of *n*-octane as internal GLC standard. After being sealed and pressurized to 1500 psig with a 1:1 mixture of  $\text{CO}$  and  $\text{H}_2$ , the reactor was heated with stirring to 190  $^\circ\text{C}$  at which point the pressure was about 2000 psig. Liquid samples were withdrawn periodically through a sampling port for GLC analysis.

**4. Product Characterization.** The hydrocarbon products 2-7 were characterized by comparison with authentic compounds using a combination of GLC coinjection and GLC-mass spectrometry. The only instances this approach did not work satisfactorily was for the isomers of xylene. Although we were not able to get separation of meta from para, mass spectra confirmed the xylene structure. Assignment of meta or para was based on the fact that the xylenes were derived from the corresponding *m*- or *p*-methylbenzyl alcohols. Similarly for (trifluoromethyl)-toluene, although we did not have any authentic samples, the para assignment was made on the basis of its derivation from the corresponding *p*-(trifluoromethyl)benzyl alcohol.

The secondary phosphine products 8, were characterized by GLC-mass spectrometry and  $^{31}\text{P}$  NMR. Although the only authentic compound available to us was diphenylphosphine. In every

other GLC analysis and  $^{31}\text{P}$  NMR spectra revealed only one peak, indicating only one isomer which we assume to be the one with ring substitution pattern intact.

$^{31}\text{P}$  NMR and mass spectral data for secondary phosphines **8** are as follows [aryl functionality ( $\delta$ ;  $J_{\text{P-H}}$ , Hz,  $\text{M}^+$ ):  $p\text{-C}_6\text{H}_4\text{F}$  (-44.96; 216.3; 222);  $\text{C}_6\text{H}_5$  (-41.35; 210.0; 186),  $p\text{-C}_6\text{H}_4\text{Me}$  (43.14; ...; 214);  $m\text{-C}_6\text{H}_4\text{Cl}$  (-41.5; ...; ...),  $p\text{-C}_6\text{H}_4\text{CF}_3$  (42.0; ...; ...);  $p\text{-C}_6\text{H}_4\text{OMe}$  (-45.4; ...; ...)].

**5. Free Radical Trapping.** A glass liner was charged with 2.5 g (9.54 mmol) of triphenylphosphine, 0.44 g (1.29 mmol) of  $\text{Co}_2(\text{CO})_8$ , 112 mg of *n*-octane as internal standard, 10 g of ethylbenzene- $d_{10}$ , and 20 mL of heptane and pressurized in an autoclave to 1500 psig of a 1:1 mixture of CO and  $\text{H}_2$ . The temperature was raised to 180 °C and held there while stirring for 16 h and then raised to 190 °C for another 15 h. Capillary GLC analysis showed the normal production of benzene, benzyl alcohol, diphenylphosphine, and toluene. A GLC-mass spectral analysis showed no deuterium incorporation into the first three products. We were not able to obtain a mass spectrum of the toluene due to masking by heptane solvent.

**6. Aryl Scrambling.** Three pairs of triarylphosphines were subjected to hydroformylation conditions in the presence of

$\text{Co}_2(\text{CO})_8$  as described here for the pair tris(*p*-chlorophenyl)phosphine and triphenylphosphine. A glass liner was charged under argon with 1.39 g (3.8 mmol) of tri-*p*-chlorophenylphosphine, 0.99 g (3.8 mmol) of triphenylphosphine, 0.44 g (2.58 mmol) of  $\text{Co}_2(\text{CO})_8$ , 112 mg of *n*-octane as internal GLC standard, and 35 mL of *p*-xylene as a solvent, then sealed in an autoclave, and brought up to 190 °C and 2000 psig of a 1:1 mixture of CO and  $\text{H}_2$ . Liquid samples were periodically withdrawn for GLC analysis on capillary column C to monitor the decomposition reaction and for  $^{31}\text{P}$  NMR analysis to monitor aryl scrambling. It was not possible to monitor both by GLC because aryl scrambling takes place in the gas chromatograph. The chemical shifts for each of the phosphines are listed in Table V. Note that the secondary phosphines **8** also suffered aryl scrambling.

**Registry No.** **1** (X = *p*-CF<sub>3</sub>), 13406-29-6; **1** (X = *m*-Cl), 29949-85-7; **1** (X = *p*-Cl), 1159-54-2; **1** (X = *p*-Me), 1038-95-5; **1** (X = *m*-Me), 6224-63-1; **1** (X = H), 603-35-0; **1** (X = *p*-OMe), 855-38-9; **1** (X = *o*-OMe), 6163-58-2; **8** (X = *p*-F), 25186-17-8; **8** (X = H), 829-85-6; **8** (X = *p*-Me), 1017-60-3; **8** (X = *m*-Cl), 99665-67-5; **8** (X = *p*-CF<sub>3</sub>), 99665-68-6; **8** (X = *p*-OMe), 84127-04-8;  $\text{Co}_2(\text{CO})_8$ , 10210-68-1; 1-hexene, 592-41-6.

## Intermediates in the Palladium-Catalyzed Reactions of 1,3-Dienes. 3.<sup>1</sup> The Reaction of ( $\eta^1, \eta^3$ -Octadienediyl)palladium Complexes with Acidic Substrates

P. W. Jolly,\* R. Mynott, B. Raspel, and K.-P. Schick

Max-Planck-Institut für Kohlenforschung, D-4330 Mülheim a.d. Ruhr, West Germany

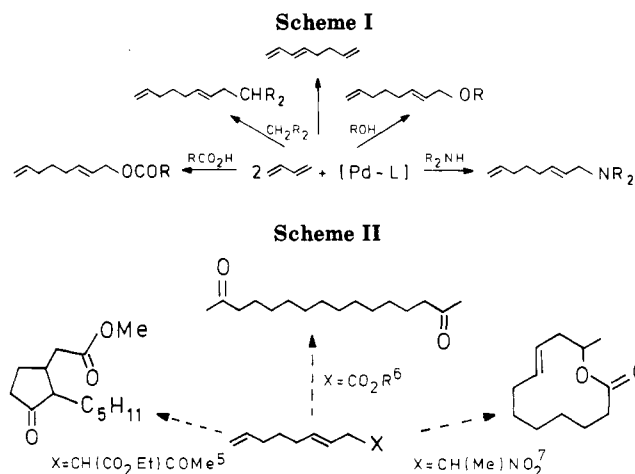
Received April 11, 1985

The stoichiometric reactions of ( $\eta^1, \eta^3$ -octadienediyl)palladium ligand complexes with a variety of acidic substrates, e.g., active methylene compounds, acetylacetone, and alcohols, have been followed by variable-temperature  $^{31}\text{P}$  and  $^{13}\text{C}$  NMR spectroscopy and a number of intermediates, viz., ( $\eta^1$ -octadienediyl)-, ( $\eta^3$ -octadienediyl)-, ( $\eta^2, \eta^3$ -octadienediyl)-, and ( $\eta^2, \eta^2$ -octadiene)palladium ligand complexes, have been identified and characterized. The role of these species in the palladium-catalyzed telomerization of butadiene with the acids to give octadiene derivatives is discussed.

### Introduction

Although a number of transition metals, e.g., Co, Rh, and Ni, are known to form active catalysts for the linear dimerization and telomerization of butadiene, ligand-modified palladium systems are the catalysts of choice. The product of the telomerization reaction is a mixture of 1- and 3-substituted octadiene derivatives in which the terminally substituted isomer predominates (Scheme I).

These reactions, first reported in 1967 by Japanese<sup>2</sup> and American<sup>3</sup> groups, have since been extended to substituted 1,3-dienes and to a wide range of nucleophiles. Although, as far as we are aware, they have not found industrial application, the products have been used as starting materials for a number of natural product syntheses (Scheme II). The field is the subject of a recent review.<sup>4</sup>



The palladium component in these reactions can either be a zerovalent palladium complex, e.g.,  $[\text{Pd}(\text{PPh}_3)_2(\eta^2\text{-maleic anhydride})]$ , or a palladium(II) salt, e.g.,  $\text{PdCl}_2/\text{py}$ , whereby systems containing a P-donor ligand have the

(1) Part 2, see: Benn, R.; Jolly, P. W.; Mynott, R.; Raspel, B.; Schenker, G.; Schick, K. P.; Schroth, G. *Organometallics* 1985, 4, 1945.

(2) Takahashi, S.; Shibano, T.; Hagihara, N. *Tetrahedron Lett.* 1967, 2451.

(3) Smutny, E. J. *J. Am. Chem. Soc.* 1967, 89, 6793.

(4) Behr, A. *Aspects Homogeneous Catal.* 1984, 5, 3.

(5) Tsuji, J.; Kasuga, K.; Takahashi, T. *Bull. Chem. Soc. Jpn.* 1979, 52, 216.

(6) Tsuji, J.; Mizutani, K.; Shimizu, I.; Yamamoto, K. *Chem. Lett.* 1976, 773.

(7) Tsuji, J.; Yamakawa, T.; Mandai, T. *Tetrahedron Lett.* 1978, 565.

other GLC analysis and  $^{31}\text{P}$  NMR spectra revealed only one peak, indicating only one isomer which we assume to be the one with ring substitution pattern intact.

$^{31}\text{P}$  NMR and mass spectral data for secondary phosphines **8** are as follows [aryl functionality ( $\delta$ ;  $J_{\text{P-H}}$ , Hz,  $\text{M}^+$ ):  $p\text{-C}_6\text{H}_4\text{F}$  (-44.96; 216.3; 222);  $\text{C}_6\text{H}_5$  (-41.35; 210.0; 186),  $p\text{-C}_6\text{H}_4\text{Me}$  (43.14; ...; 214);  $m\text{-C}_6\text{H}_4\text{Cl}$  (-41.5; ...; ...),  $p\text{-C}_6\text{H}_4\text{CF}_3$  (42.0; ...; ...);  $p\text{-C}_6\text{H}_4\text{OMe}$  (-45.4; ...; ...)].

**5. Free Radical Trapping.** A glass liner was charged with 2.5 g (9.54 mmol) of triphenylphosphine, 0.44 g (1.29 mmol) of  $\text{Co}_2(\text{CO})_8$ , 112 mg of *n*-octane as internal standard, 10 g of ethylbenzene- $d_{10}$ , and 20 mL of heptane and pressurized in an autoclave to 1500 psig of a 1:1 mixture of CO and  $\text{H}_2$ . The temperature was raised to 180 °C and held there while stirring for 16 h and then raised to 190 °C for another 15 h. Capillary GLC analysis showed the normal production of benzene, benzyl alcohol, diphenylphosphine, and toluene. A GLC-mass spectral analysis showed no deuterium incorporation into the first three products. We were not able to obtain a mass spectrum of the toluene due to masking by heptane solvent.

**6. Aryl Scrambling.** Three pairs of triarylphosphines were subjected to hydroformylation conditions in the presence of

$\text{Co}_2(\text{CO})_8$  as described here for the pair tris(*p*-chlorophenyl)phosphine and triphenylphosphine. A glass liner was charged under argon with 1.39 g (3.8 mmol) of tri-*p*-chlorophenylphosphine, 0.99 g (3.8 mmol) of triphenylphosphine, 0.44 g (2.58 mmol) of  $\text{Co}_2(\text{CO})_8$ , 112 mg of *n*-octane as internal GLC standard, and 35 mL of *p*-xylene as a solvent, then sealed in an autoclave, and brought up to 190 °C and 2000 psig of a 1:1 mixture of CO and  $\text{H}_2$ . Liquid samples were periodically withdrawn for GLC analysis on capillary column C to monitor the decomposition reaction and for  $^{31}\text{P}$  NMR analysis to monitor aryl scrambling. It was not possible to monitor both by GLC because aryl scrambling takes place in the gas chromatograph. The chemical shifts for each of the phosphines are listed in Table V. Note that the secondary phosphines **8** also suffered aryl scrambling.

**Registry No.** **1** (X = *p*- $\text{CF}_3$ ), 13406-29-6; **1** (X = *m*-Cl), 29949-85-7; **1** (X = *p*-Cl), 1159-54-2; **1** (X = *p*-Me), 1038-95-5; **1** (X = *m*-Me), 6224-63-1; **1** (X = H), 603-35-0; **1** (X = *p*-OMe), 855-38-9; **1** (X = *o*-OMe), 6163-58-2; **8** (X = *p*-F), 25186-17-8; **8** (X = H), 829-85-6; **8** (X = *p*-Me), 1017-60-3; **8** (X = *m*-Cl), 99665-67-5; **8** (X = *p*- $\text{CF}_3$ ), 99665-68-6; **8** (X = *p*-OMe), 84127-04-8;  $\text{Co}_2(\text{CO})_8$ , 10210-68-1; 1-hexene, 592-41-6.

## Intermediates in the Palladium-Catalyzed Reactions of 1,3-Dienes. 3.<sup>1</sup> The Reaction of ( $\eta^1, \eta^3$ -Octadienediyl)palladium Complexes with Acidic Substrates

P. W. Jolly,\* R. Mynott, B. Raspel, and K.-P. Schick

Max-Planck-Institut für Kohlenforschung, D-4330 Mülheim a.d. Ruhr, West Germany

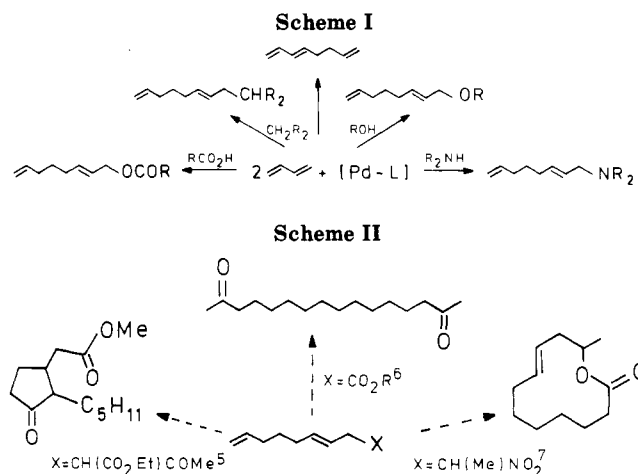
Received April 11, 1985

The stoichiometric reactions of ( $\eta^1, \eta^3$ -octadienediyl)palladium ligand complexes with a variety of acidic substrates, e.g., active methylene compounds, acetylacetone, and alcohols, have been followed by variable-temperature  $^{31}\text{P}$  and  $^{13}\text{C}$  NMR spectroscopy and a number of intermediates, viz., ( $\eta^1$ -octadienyl)-, ( $\eta^3$ -octadienyl)-, ( $\eta^2, \eta^3$ -octadienediyl)-, and ( $\eta^2, \eta^2$ -octadiene)palladium ligand complexes, have been identified and characterized. The role of these species in the palladium-catalyzed telomerization of butadiene with the acids to give octadiene derivatives is discussed.

### Introduction

Although a number of transition metals, e.g., Co, Rh, and Ni, are known to form active catalysts for the linear dimerization and telomerization of butadiene, ligand-modified palladium systems are the catalysts of choice. The product of the telomerization reaction is a mixture of 1- and 3-substituted octadiene derivatives in which the terminally substituted isomer predominates (Scheme I).

These reactions, first reported in 1967 by Japanese<sup>2</sup> and American<sup>3</sup> groups, have since been extended to substituted 1,3-dienes and to a wide range of nucleophiles. Although, as far as we are aware, they have not found industrial application, the products have been used as starting materials for a number of natural product syntheses (Scheme II). The field is the subject of a recent review.<sup>4</sup>



The palladium component in these reactions can either be a zerovalent palladium complex, e.g.,  $[\text{Pd}(\text{PPh}_3)_2(\eta^2\text{-maleic anhydride})]$ , or a palladium(II) salt, e.g.,  $\text{PdCl}_2/\text{py}$ , whereby systems containing a P-donor ligand have the

(1) Part 2, see: Benn, R.; Jolly, P. W.; Mynott, R.; Raspel, B.; Schenker, G.; Schick, K. P.; Schroth, G. *Organometallics* **1985**, *4*, 1945.

(2) Takahashi, S.; Shibano, T.; Hagihara, N. *Tetrahedron Lett.* **1967**, 2451.

(3) Smutny, E. J. *J. Am. Chem. Soc.* **1967**, *89*, 6793.

(4) Behr, A. *Aspects Homogeneous Catal.* **1984**, *5*, 3.

(5) Tsuji, J.; Kasuga, K.; Takahashi, T. *Bull. Chem. Soc. Jpn.* **1979**, *52*, 216.

(6) Tsuji, J.; Mizutani, K.; Shimizu, I.; Yamamoto, K. *Chem. Lett.* **1976**, 773.

(7) Tsuji, J.; Yamakawa, T.; Mandai, T. *Tetrahedron Lett.* **1978**, 565.

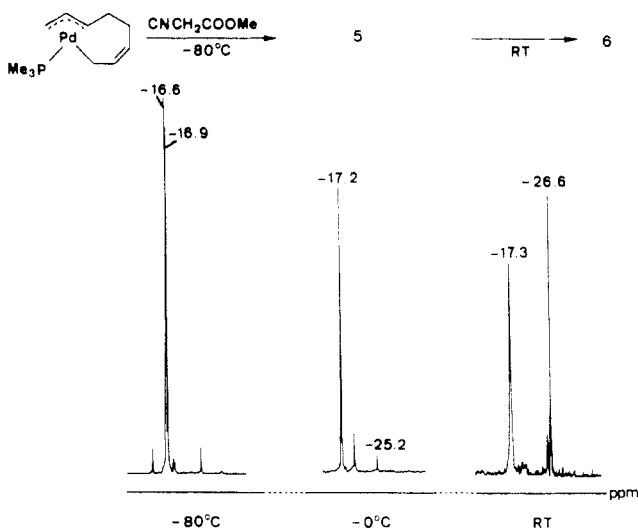
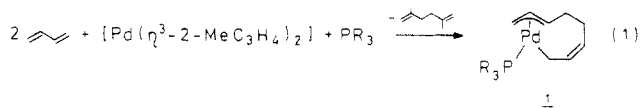


**Figure 1.**  $^{31}\text{P}$  NMR spectra of the reaction of 1 ( $\text{R} = \text{Me}$ ) with  $\text{CNCH}_2\text{CO}_2\text{Me}$  (32.4 MHz, toluene- $d_8$ ).

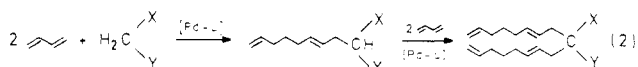
highest activity. Although there is no consensus concerning the mechanism, it is generally assumed that it occurs in a stepwise manner with one of the early steps being the reaction of the two butadiene molecules at the metal to give a  $\text{C}_8$ -Pd species which then reacts further with the nucleophile. In an earlier paper<sup>1</sup> we reported the isolation and characterization of such a species (1, eq 1) and sug-



gested this to be a plausible intermediate in the palladium-catalyzed dimerization and telomerization of butadiene. Here we present evidence supporting this suggestion which has been obtained by studying the stoichiometric reactions of these species with acidic nucleophiles.

## Results and Discussion

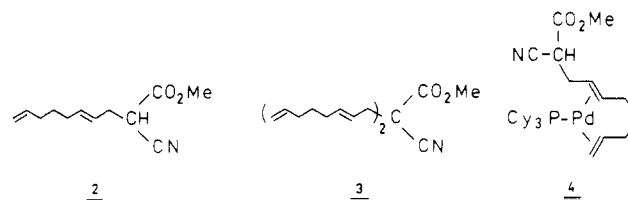
**Telomerization of Butadiene with Active Methylene Compounds.** Both acidic hydrogen atoms present in active methylene compounds can take part in palladium-catalyzed telomerization reactions with butadiene (eq 2). Branched chain products are formed only to a lesser



extent.<sup>4</sup> We have reacted the  $[\text{Pd}(\text{PR}_3)(\eta^1, \eta^3\text{-C}_8\text{H}_{12})]$

complex (1,  $\text{R} = \text{Me}$ , Cy) with a variety of active methylene compounds in a stoichiometric manner and in most cases have followed the course of reaction by variable-temperature  $^{31}\text{P}$  and  $^{13}\text{C}$  NMR spectroscopy. In addition, in selected cases, we have used the same palladium complexes as catalysts for the telomerization reaction.

**Reaction with Cyanoacetic Acid Ester and Related Compounds.** The catalytic telomerization of the methyl ester of cyanoacetic acid with butadiene in the presence of 1 ( $\text{R} = \text{Cy}$ ) in ether at 100 °C led, after 4 days, to the formation of 2 and 3 in approximately equimolar amounts and in good yield.



The product of the stoichiometric reaction of the same palladium complex with the ester at room temperature was fully characterized and shown to be the  $\eta^2, \eta^2$ -diolefin complex 4. More insight into the reaction was obtained by using variable-temperature NMR spectroscopy to follow the course of the reaction of the trimethylphosphine-stabilized complex 1 ( $\text{R} = \text{Me}$ ) with the ester. The result of a  $^{31}\text{P}$  NMR study is shown in Figure 1: the reaction has already occurred at  $-80$  °C to give a first intermediate (5,  $\delta$  ( $^{31}\text{P}$ )  $-16.6/-16.9$ , intensity 1:1; the signal for 1 ( $\text{R} = \text{Me}$ ) occurs at  $\sim -14.0$  ppm at  $-80$  °C), and at  $0$  °C these signals broaden and a new signal appears at  $-25.2$  ppm corresponding to a second intermediate, 6, which upon warming to room temperature becomes the principle product. The nature of 5 and 6 have been established by analysis of their  $^{13}\text{C}$  NMR spectra and comparison with other examples. The  $^{13}\text{C}$  NMR spectrum of 5 is shown in Figure 2. 5 contains an asymmetric carbon atom at C-9. In addition the metal center is chiral: the presence of diastereomers leads to splitting of the signals in both the  $^{31}\text{P}$  and  $^{13}\text{C}$  NMR spectra. The signals at 10.31 and 11.18 ppm are assigned to the palladium-bonded C atom (C-9,  $J_{\text{C,H}} = 144.9$  Hz) and couple with the P atom ( $J_{\text{P,C}} = 5.3$  Hz). The  $\eta^3$ -allyl group gives rise to signals at 53.73/53.38 (C-1), 117.75/117.39 (C-2), and 94.51/93.65 (C-3) ppm. The assignment of C-3 is based partly on the large trans coupling to the phosphorus atom ( $J_{\text{P,C}} = 30.9/29.5$ ; C-1 does not couple to phosphorus). The signals at 138.93/138.91 and 114.99/114.96 ppm are assigned to the olefinic C atoms C-7 and C-8 ( $J_{\text{C,H}} = 151.2$  and 156.6 Hz). An analysis of

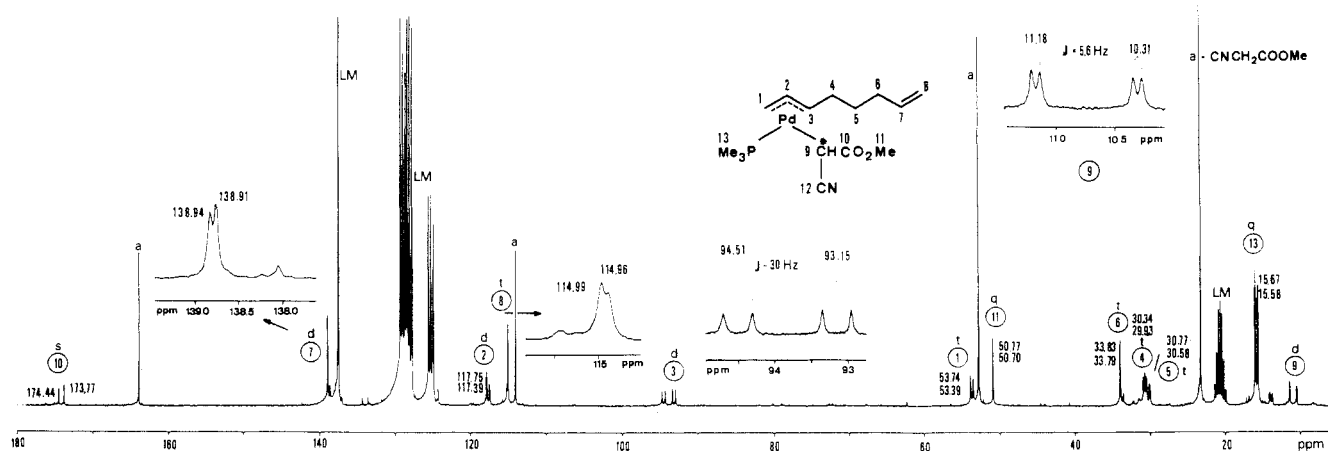


**Figure 2.**  $^{13}\text{C}\{^1\text{H}\}$  NMR spectrum of  $[\text{PdCH}(\text{CN})\text{CO}_2\text{Me}(\text{PMe}_3)(\eta^3\text{-C}_8\text{H}_{13})]$  (5) (75.5 MHz,  $-50$  °C, toluene- $d_8$ ).



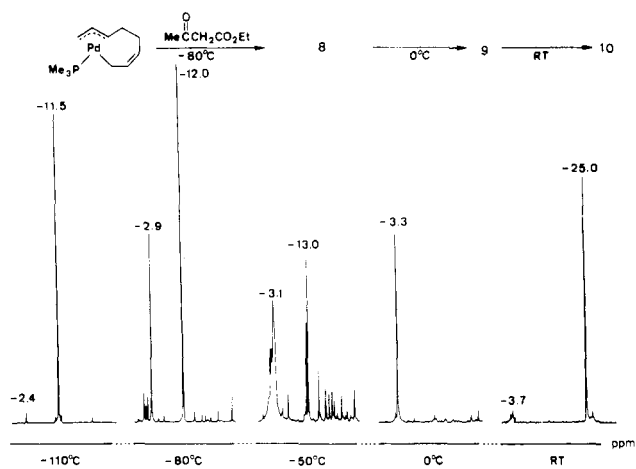
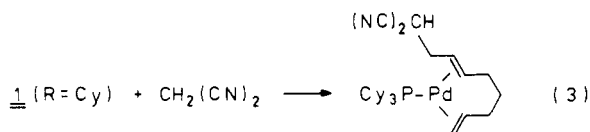


**Figure 3.**  $^{31}\text{P}$  NMR spectra of the reaction of 1 (R = Me) with  $\text{CH}_2(\text{COMe})\text{CO}_2\text{Et}$  (32.4 MHz,  $\text{THF-d}_8$ ).

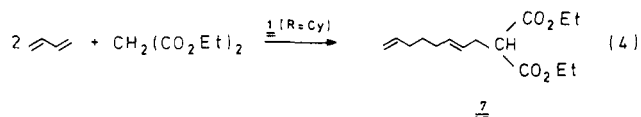
the  $^{13}\text{C}$  NMR spectrum of 6 established it to be the  $\text{PMe}_3$ -stabilized analogue to the  $\eta^2, \eta^2$ -diolefin complex 4: here again the presence of a diastereomeric pair leads to the splitting of practically all the resonances (see Table II).

These results have been incorporated in the catalytic cycle shown in Scheme III for the formation of 2. The formation of 3 is then seen to be the result of the further reaction of 2 with the  $\eta^1, \eta^3$ -octadienediyl species 1.

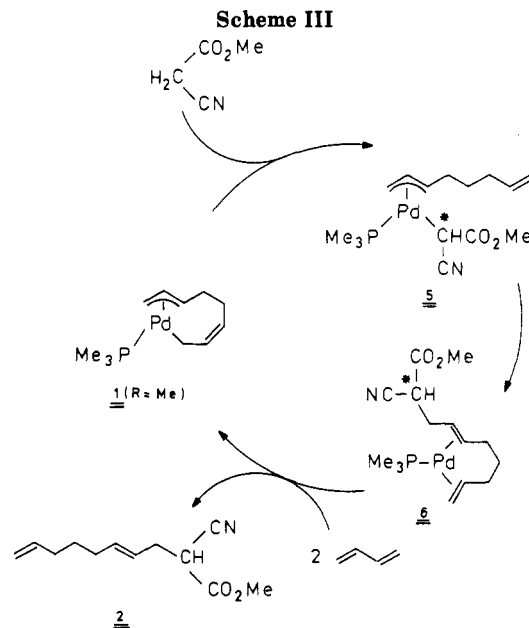
Similar results were obtained from the stoichiometric reaction of the  $\text{PCy}_3$ -stabilized complex 1 (R = Cy) with malonodinitrile: at room temperature the expected  $\eta^2, \eta^2$ -diolefin complex is formed in almost quantitative yield (eq 3) while a variable-temperature  $^{31}\text{P}$  NMR spectroscopic study indicated the low-temperature formation of additional intermediates.



The telomerization of the diethyl ester of malonic acid with butadiene is catalyzed by 1 (R = Cy) at room temperature, and 7 is formed in high yield (eq 4). An ex-



ploratory variable-temperature  $^{31}\text{P}$  NMR spectroscopic



study of the analogous reaction of 1 (R = Me) with the ester led to the generation of signals at  $-17.00$  and  $-25.8$  ppm which suggests here also the intermediacy of species related to 5 and 6.

**Reaction with Ethyl Acetoacetate and Related Compounds.** The catalytic telomerization of ethyl acetoacetate and excess butadiene in the presence of 1 (R = Cy) at room temperature led to a practically quantitative yield of ethyl bis(2,7-octadienyl)acetoacetate after 5 days. Presumably ethyl octadienylacetoacetate is formed first and then reacts further. The catalyst was recovered almost quantitatively at the end of the reaction.

The stoichiometric reaction of the  $\text{PMe}_3$ -stabilized complex 1 (R = Me) with ethyl acetoacetate was monitored by variable-temperature  $^{31}\text{P}$  NMR spectroscopy (Figure 3): at  $-110^\circ\text{C}$  traces of an initial intermediate can be detected ( $\delta -2.4$ ), at  $-50^\circ\text{C}$  this signal broadens while at the same time numerous additional signals having lesser intensity appear, and at  $0^\circ\text{C}$  all of these signals are replaced by a single absorption ( $\delta -3.3$ ) which in turn is converted into a further intermediate which absorbs at  $\delta -25.2$  Hz at room temperature. We interpret these results as implying the intermediacy of three main intermediates. A comparison of the  $^{13}\text{C}$  NMR spectra of the first and third species with those of similar complexes allows them to be identified as the  $\eta^3$ -octadienyl and  $\eta^2, \eta^2$ -octadiene derivatives 8 and 10. The  $^{13}\text{C}$  NMR spectrum of the second

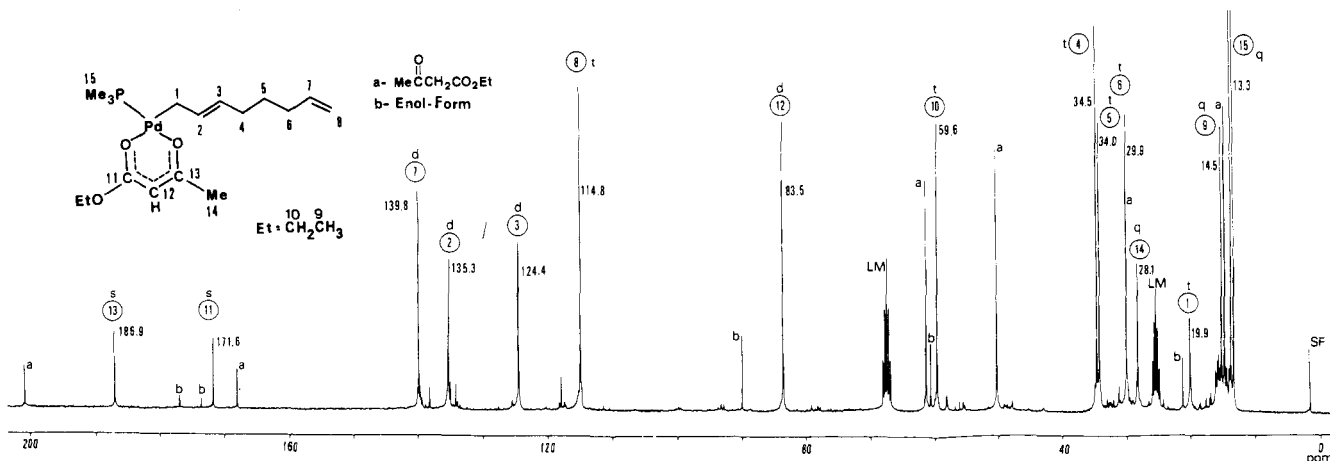


**Figure 4.**  $^{13}\text{C}\{^1\text{H}\}$  NMR spectrum of  $[\text{PdOC}(\text{Me})\text{CHC}(\text{OEt})\text{O}(\text{PMe}_3)(\eta^1\text{-C}_8\text{H}_{13})]$  (9, R = Me) (75.5 MHz,  $-30^\circ\text{C}$ ,  $\text{THF-d}_8$ ).

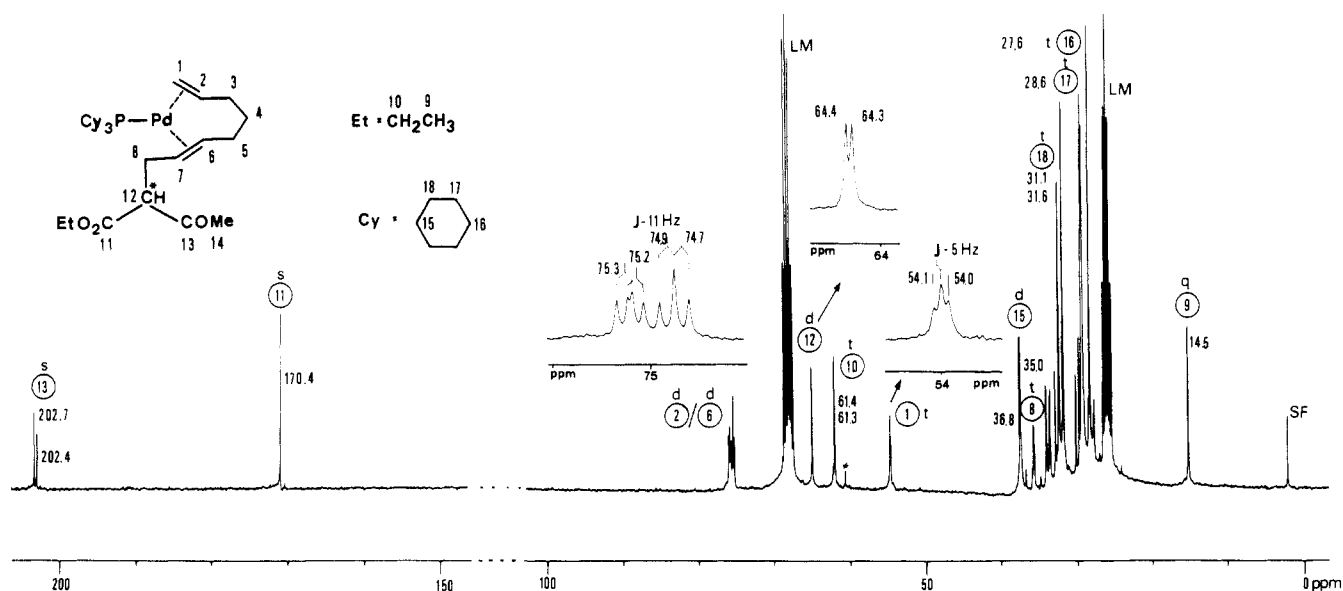
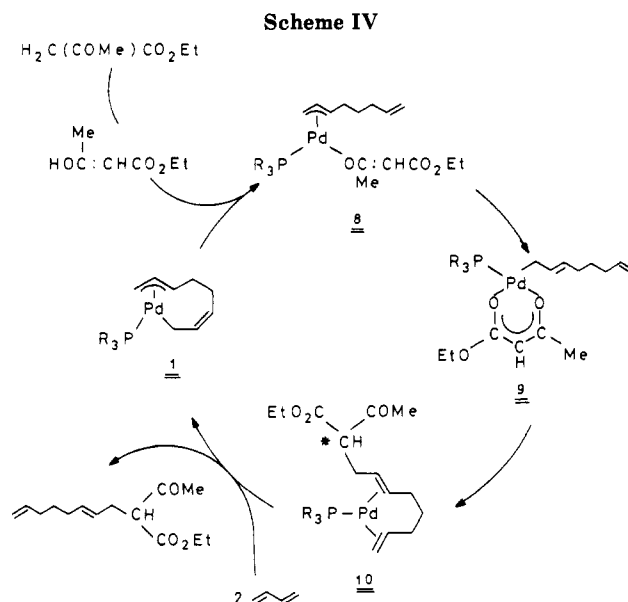
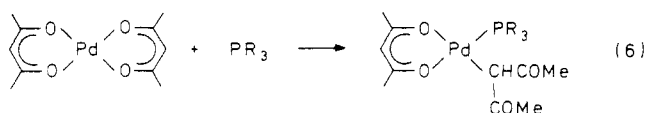
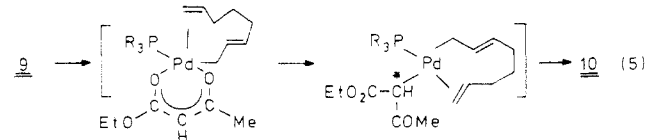


Figure 5.  $^{13}\text{C}\{^1\text{H}\}$  NMR spectrum of  $[\text{Pd}(\text{PCy}_3)(\eta^2, \eta^2\text{-1-EtO}_2\text{C}(\text{MeCO})\text{CHC}_8\text{H}_{13})]$  (**10**,  $\text{R} = \text{Cy}$ ) (75.5 MHz,  $-30^\circ\text{C}$ ,  $\text{THF-}d_6$ ).

intermediate **9** is shown in Figure 4 and indicates that the molecule contains an  $\eta^1$ -octadienyl group. The Pd-bonded carbon atom appears at 19.19 ppm as a doublet with a P-C coupling constant of 3 Hz in keeping with a cis arrangement of the P-donor ligand and C-1. The absorptions at 171.6 and 186.94 ppm are typical for C-11 and C-13 of a chelating ethyl acetoacetate group as is the signal for C-12 at 83.52 ppm which appears as a doublet in the gated-decoupled spectrum. The uncomplexed olefinic C atoms of the  $\eta^2$ -octadienyl chain give rise to signals at 139.76/114.48 and 135.26/124.35 ppm. The impurities (a, b) in the spectrum are due to the presence of ethyl acetoacetate and its enolic form.

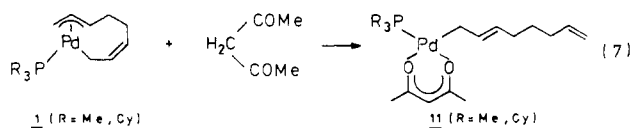
Further information was obtained by studying the stoichiometric reaction of the  $\text{PCy}_3$ -stabilized complex **1** ( $\text{R} = \text{Cy}$ ): complexes **8** and **9** ( $\text{R} = \text{Cy}$ ) were identified spectroscopically while **10** ( $\text{R} = \text{Cy}$ ) was isolated and fully characterized. The  $^{13}\text{C}$  NMR spectrum of **10** ( $\text{R} = \text{Cy}$ ) is shown as Figure 5. **10** exists as a diastereomeric pair, and almost all of the absorptions are split. The absorptions at 75.3/75.2, 67.4/67.3 and 54.1/54.0 ppm are assigned to the metal-bonded olefinic C atoms (C-1, C-2; C-6, C-7) and couple to the phosphorus atom. The asymmetric carbon atom (C-12) is found at 64.4/64.3 ppm.

The results described above enable the catalytic cycle shown as Scheme IV to be formulated. The ethyl acetoacetate reacts as the enol form to give **8**. The further rearrangement of the  $\eta^3$ -allyl group into the  $\eta^1$ -allyl form **9** is presumably triggered by complexation of the ester function to the metal while the further conversion of **9** into **10** is probably preceded by complexation of the terminal olefin in **9** to the metal with rearrangement of the chelating ester followed by reductive coupling of the two organic groups (eq 5). Such donor ligand induced rearrangements of an acetylacetonato group are well documented in palladium chemistry (eq 6).<sup>8</sup>



The product of the catalytic cycle shown in Scheme IV has itself an acidic hydrogen atom and can react with a further ( $\eta^1, \eta^3$ -octadienediyl)palladium ligand molecule to give the bis(octadienyl)acetic acid ester observed in the catalysis.

The palladium-catalyzed telomerization of acetylacetonato with butadiene to give an octadiene derivative has been reported,<sup>4</sup> and the isolation of **11** from the stoichiometric reaction (eq 7) suggests that the mechanism is similar to that shown in Scheme IV, even though the further reaction of **11** to give an  $\eta^2, \eta^2$ -diolefin complex was not observed.



**Reaction with Alcohols.** The tricyclohexylphosphine-stabilized complex **1**, ( $\text{R} = \text{Cy}$ ) catalyzes the telomerization of butadiene and methanol to give mainly

(8) Baba, S.; Ogura, T.; Kawaguchi, S., *Bull. Chem. Soc. Jpn.* 1974, 47, 665.

(9) Jolly, P. W. *Angew. Chem., Int. Ed. Engl.*, 1985, 24, 283.

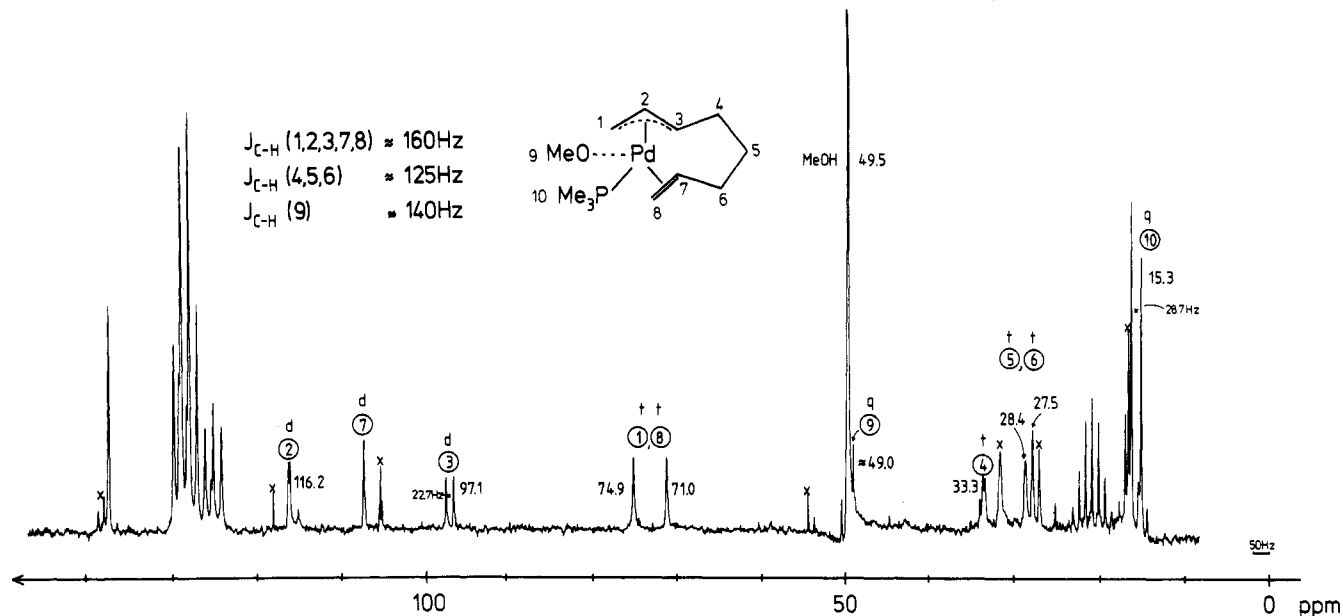
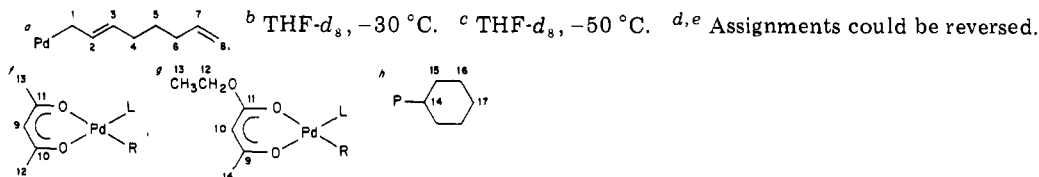


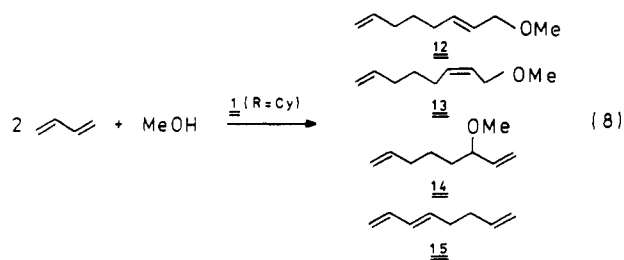
Figure 6.  $^{13}\text{C}\{^1\text{H}\}$  NMR spectrum of  $[\text{PdOMe}(\text{PMe}_3)(\eta^2,\eta^3\text{-C}_8\text{H}_{13})]$  (16) (25.2 MHz,  $-70^\circ\text{C}$ , toluene- $d_8$ ).

Table I. 75.5-MHz  $^{13}\text{C}\{^1\text{H}\}$  NMR Spectral Data for the  $[\text{PdX}(\text{PR}_3)(\eta^1\text{-C}_8\text{H}_{13})]$  Complexes<sup>a</sup>

	$\delta(\text{C}-n)$ ( $J_{\text{C,P}}$ , Hz)		
	$[\text{Pd}(\text{acac})(\text{PCy}_3)(\eta^1\text{-C}_8\text{H}_{13})]$ (11, R = Cy) <sup>b</sup>	$[\text{PdOC}(\text{Me})\text{CHC}(\text{OEt})\text{O}(\text{PCy}_3)(\eta^1\text{-C}_8\text{H}_{13})]$ (9, R = Cy) <sup>b</sup>	$[\text{PdOC}(\text{Me})\text{CHC}(\text{OEt})\text{O}(\text{PMe}_3)(\eta^1\text{-C}_8\text{H}_{13})]$ (9, R = Me) <sup>b</sup>
C-1	18.6 (4.5)	29.17	19.91 (3.0)
C-2	137.2 (1.8) <sup>d</sup>	136.55 <sup>d</sup>	135.26 <sup>d</sup>
C-3	123.9 (2.2) <sup>d</sup>	124.50 <sup>d</sup>	124.35 <sup>d</sup>
C-4	32.8 <sup>e</sup>	34.61 <sup>e</sup>	34.47 <sup>e</sup>
C-5	29.8 <sup>e</sup>	30.54 <sup>e</sup>	34.01 <sup>e</sup>
C-6	34.2	34.36 <sup>e</sup>	29.85 <sup>e</sup>
C-7	139.8	139.76	139.76
C-8	114.7	114.86	114.78
C(X)	99.0 (C-9) <sup>f</sup>	186.64 (C-10) <sup>g</sup>	186.94 (C-9) <sup>g</sup>
	186.5 (C-10,11)	83.44 (C-10)	83.52 (C-10)
	28.3 (C-12,13)	171.47 (C-11)	171.60 (C-11)
		59.77 (C-12)	59.59 (C-12)
C(L)	34.1 (21.5, C-14), 30.3 (C-15) <sup>h</sup>	32.96 (C-14), 30.17 (C-15) <sup>h</sup>	13.28 (31.1, PMe)
	28.4 (12.4, C-16), 27.3 (C-17)	15.04 (C-13)	14.45 (C-13)
		28.21 (C-14)	28.10 (C-14)
		28.35 (C-16), 27.16 (C-17)	



1-methoxy-2,7-octadiene in addition to lesser amounts of 3-methoxy-1,7-octadiene and octatriene (eq 8). If the same

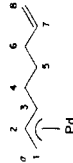


reaction is carried out with  $\text{CH}_3\text{OD}$ , then the product mixture after 1 h at  $70^\circ\text{C}$  (73% 12, 3% 13, 4% 14, 20% 15) is deuterated at C-6 to 83% in the case of the ethers and to 60% in the case of octatriene.

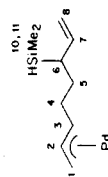
A variable-temperature  $^{31}\text{P}$  NMR investigation of the stoichiometric reaction between the  $\text{PMe}_3$ -stabilized complex 1 (R = Me) and MeOH indicates that the reaction proceeds through two main intermediates ( $\delta -16.0$  at  $-80^\circ\text{C}$ ,  $\delta -25.6$  at  $-35^\circ\text{C}$  in toluene- $d_8$ ; the spectra have been reproduced in ref 9). Although the initial intermediate could not be obtained pure, its  $^{13}\text{C}$  NMR spectrum (Figure 6) suggests it to be 16 in which an  $\eta^2,\eta^3$ -octadienyl group is bonded to the metal. The signals at 74.94, 116.14, and 97.11 ppm are assigned to the C atoms C-1, C-2, and C-3 of the  $\eta^3$ -allyl group: C-3, trans to the P atom, has a large coupling (22.7 Hz) whereas C-1, cis to the P atom does not couple. The complexed olefinic C atoms ( $J_{\text{C,H}} \approx 160$  Hz) absorb at 107.3 and 71.0 ppm. The broad signal at 44.0 ppm is assigned to the  $\text{CH}_3\text{O}$  carbon atom ( $J_{\text{C,H}} \approx 140$  Hz, quartet). The nature of the Pd-O bond in this and related systems has been discussed previously,<sup>1</sup> and we assume

Table II. 75.5-MHz  $^{13}\text{C}\{^1\text{H}\}$ NMR Spectral Data for the  $[\text{PdX}(\text{PR}_3)(\eta^3\text{-C}_8\text{H}_{13})]$  Complexes<sup>a</sup>

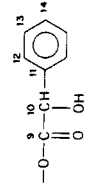
C	$\delta$ (C-n) ( $\nu_{\text{C,P}}$ , Hz)			
	$[\text{PdOCOC}(\text{OH})\text{Ph}(\text{PMe}_3)]$ ( $\eta^3\text{-C}_8\text{H}_{13}$ ) [22, R = Me] <sup>b,d</sup>	$[\text{PdOCOC}(\text{OH})\text{Ph}(\text{PCy}_3)]$ ( $\eta^3\text{-C}_8\text{H}_{13}$ ) [22, R = Cy] <sup>c,d</sup>	$[\text{PdOC}(\text{Me})=\text{CHCO}_2\text{Et}(\text{PCy}_3)]$ ( $\eta^3\text{-C}_8\text{H}_{13}$ ) [8, R = Cy] <sup>b,e</sup>	$[\text{PdCl}(\text{CN})(\text{CO}_2\text{Me})(\text{PMe}_3)]$ ( $\eta^3\text{-C}_8\text{H}_{13}$ ) (5) <sup>c,e</sup>
C-1	43.5	41.21	41.98	53.74 48.6 48.6
C-2	115.9 (4.3)	113.27	115.32 <sup>g</sup>	117.75 (4.5) 115.7 (4.9) 115.4 (4.9)
C-3	101.1 (28.4)	103.1	100.97 (25.4)	99.8 (31.0) 99.6 (30.9)
C-4	31.8 <sup>g</sup>	31.52 <sup>g</sup>	31.93 <sup>h</sup>	29.5 (7.0) 30.2 (7.1)
C-5	29.1 <sup>g</sup>	28.62 (5.1) <sup>g</sup>	30.79 <sup>h</sup>	32.1 (4.0) 32.7 (3.8)
C-6	34.2	33.77	29.65 <sup>h</sup>	33.9 33.79 32.6
C-7	139.1	138.85	139.53	140.6 140.5
C-8	114.4	114.91	115.05 <sup>g</sup>	113.5 113.1
C(X)	177.1 (C-9) <sup>i</sup>	117.18 (C-9) <sup>i</sup>	185.09 (C-9) <sup>j</sup>	-5.81 (C-10)
	74.3 (C-10)	74.89 (C-10)	89.20 (C-10)	-5.85 (C-10)
	114.0 (C-11)	43.81 (C-11)	169.73 (C-11)	-6.27 (C-11)
	128.1 (C-12) <sup>h</sup>	127.85 (C-12) <sup>h</sup>	57.17 (C-12)	-6.34 (C-11)
C(L)	127.1 (C-13,14) <sup>h</sup>	127.20 (C-13) <sup>h</sup>	15.55 (C-13)	15.8 (26.6, PMe)
	15.2 (25.7, PMe)	126.72 (C-14) <sup>h</sup>	28.21 (C-14)	15.8 (26.6, PMe)
		33.81 (C-14), 30.09 (C-15) <sup>i</sup>	33.26 (C-14), 30.17 (C-15) <sup>i</sup>	
		27.59 (11.2, C-16), 26.57 (C-17)	28.48 (C-16), 27.25 (C-17)	



<sup>a</sup> THF-*d*<sub>6</sub>. <sup>b</sup> Toluene-*d*<sub>8</sub>. <sup>c</sup> -30 °C. <sup>d</sup> -50 °C. <sup>e</sup> -50 °C. <sup>f</sup> Assignments could be reversed.

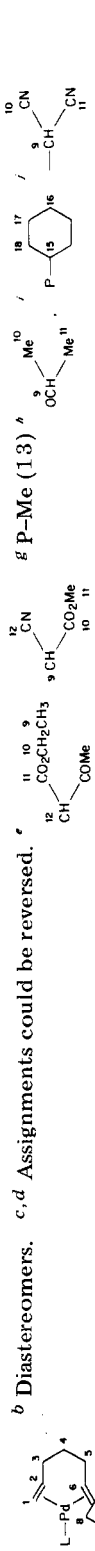


<sup>g</sup> Assignments could be reversed.

Table III. 75.5-MHz  $^{13}\text{C}\{^1\text{H}\}$ NMR Spectral Data for the  $[\text{Pd}(\text{PR}_3)(\eta^2\text{-}^1\text{-R}'\text{C}_8\text{H}_{13})]$  Complexes<sup>a</sup>

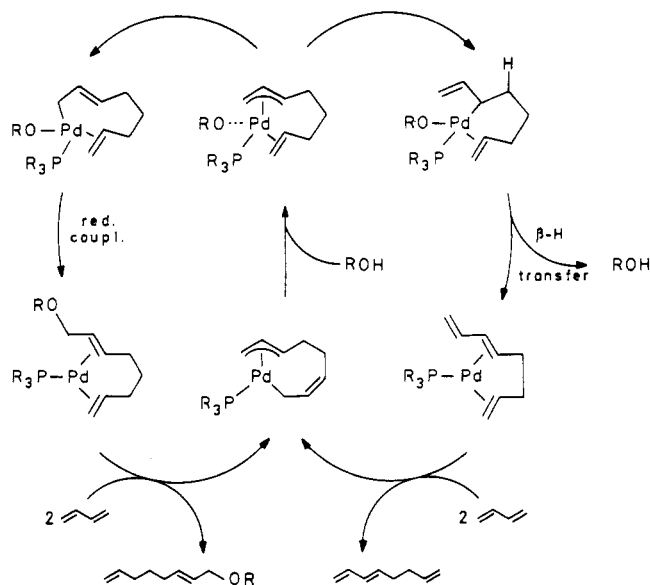
C	$\delta$ (C-n) ( $\nu_{\text{C,P}}$ , Hz)			
	$17^k, \text{R}' = \text{OMe}, \text{R} = \text{Me}$	$18^i, \text{R}' = \text{O-}i\text{-Pr}, \text{R} = \text{Me}$	$5^{b,m}, \text{R}' = \text{CH}(\text{CN})\text{CO}_2\text{Me}, \text{R} = \text{Me}$	$10^{b,o}, \text{R}' = \text{CH}(\text{COMe})\text{CO}_2\text{Et}, \text{R} = \text{Cy}$
C-1	54.61 (3.7)	54.08 (3.7)	54.20 (3.6) 54.09 (4.0)	55.7 (4.6) 55.10
C-2	76.44 (11.5)	75.90 (11.7)	76.06 (11.2) <sup>c</sup> 75.97 (11.2)	76.22 (12.7) <sup>c</sup> 76.08 (13.2)
C-3	32.56 (3.6)	32.62 (3.7)	32.97 (2.6) <sup>d</sup> 32.86 (3.0)	76.08 (13.2) 32.80 <sup>d</sup>
C-4	31.01 (3.4)	31.21 (3.2)	32.54 32.50	33.3 <sup>d</sup> 32.9 (4.9) <sup>d</sup>

C-5	33.08 (8.9)	31.33 (4.0) <sup>d</sup>	33.1 (4.1) <sup>d</sup>	31.2 <sup>d</sup>	32.40 <sup>d</sup>	32.2 <sup>d</sup>
C-6	75.71 (13.7)	31.28 (2.6)	74.70 (12.2) <sup>c</sup>	75.4 (13.2) <sup>c</sup>	75.57 (12.7) <sup>c</sup>	74.9 (11.2) <sup>c</sup>
C-7	67.16 (5.5)	74.67 (13.2) <sup>c</sup>	74.59 (10.1)	61.9 (5.6)	74.94 (12.7)	74.7 (11.2)
C-8	75.81 (8.1)	64.10 (5.5)	63.95	37.1 (3.6)	62.93 (6.1)	67.4 (6.6)
		63.95 (5.6)	34.7 (7.1)	26.9 (C-9) <sup>j</sup>	63.80 (5.6)	67.3 (5.6)
		35.92 (7.6)	15.04 (C-9) <sup>e</sup>	117.15, 116.99 (C-12)	36.90	35.0
C(R)	56.48	41.29, 41.02 (C-9) <sup>f</sup>	61.52, 61.36 (C-10)	115.1, 114.9 (C-10/11)	41.15, 40.85 (C-9) <sup>f</sup>	14.5, 14.5 (C-9) <sup>e</sup>
		166.99, 166.92 (C-10)	68.3 (C-12)	202.4, 202.6 (C-13)	166.91, 166.82 (C-10)	61.4, 61.3 (C-10)
		51.66 (C-11)	29.3, 29.01 (C-14)	18.58 (16.3) <sup>g</sup>	52.42 (C-11)	170.4 (C-11)
C(L)	18.37 (16.5) <sup>g</sup>	18.08 (15.3) <sup>g</sup>	18.53 (16.3)	36.7 (10.7, C-15) <sup>i</sup>	117.15, 116.99 (C-12)	202.7, 202.4 (C-13)
		18.51 (16.5) <sup>g</sup>		27.5 (C-16), 28.5 (4.1)	29.5, 29.0 (C-14)	29.5, 29.0 (C-14)
				28.6 (C-17), 31.6 (3.6)	36.8 (7.8, C-15)	36.8 (7.8, C-15)
				31.0 (C-18)	27.6 (C-16), 28.6 (C-17)	27.6 (C-16), 28.6 (C-17)
					31.14, 30.60 (C-18)	31.6 (3.2, C-18), 31.1 (C-18)



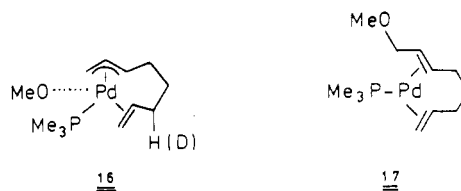
<sup>k</sup> 25.5 MHz, toluene-d<sub>8</sub>, 0 °C. <sup>l</sup> 25.5 MHz, toluene-d<sub>8</sub>, -30 °C. <sup>m</sup> Toluene-d<sub>8</sub>, 0 °C. <sup>n</sup> THF-d<sub>8</sub>, 0 °C. <sup>o</sup> THF-d<sub>8</sub>, -30 °C. <sup>p</sup> Toluene-d<sub>8</sub>, -30 °C.

Scheme V



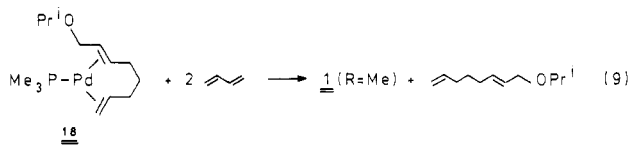
that the bond to the metal is highly polarized.

The second intermediate was fully characterized and shown to be [Pd(PMe<sub>3</sub>)(η<sup>2</sup>,η<sup>2</sup>-1-MeOC<sub>8</sub>H<sub>13</sub>)] (17) by NMR spectroscopy. If the reaction is carried out with MeOD,



then deuteration occurs exclusively at C-6 ( $\delta^{13}\text{C}(\text{H}_2)\text{-6}$ ) 32.56 ( $J_{\text{C,P}} = 3.6$  Hz),  $\delta^{13}\text{C}(\text{HD})\text{-6}$ ) 32.10 ( $^1J_{\text{C,D}} = 19.2$  Hz). Possible mechanisms and personal preferences for this reaction have been discussed in an earlier paper in this series.<sup>1</sup>

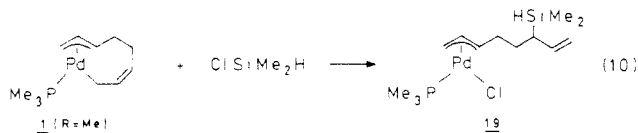
Similar results have been obtained by reacting 1 (R = Me) with 2-propanol: [Pd(PMe<sub>3</sub>)(η<sup>2</sup>,η<sup>2</sup>-*i*-PrOC<sub>8</sub>H<sub>13</sub>)] (18) was isolated in 62% yield. Furthermore it was demonstrated in this case that further reaction of 18 with butadiene at -10 °C results in the displacement of the octadiene derivative with reformation of 1 (R = Me), thereby completing the catalytic cycle (eq 9).



The η<sup>2</sup>,η<sup>3</sup>-octadienyl complex is presumably a common intermediate in the formation of both the alkoxyoctadiene derivatives as well as of octatriene (Scheme V). The nature of the alcohol controls which reaction pathway is preferred, and it has been shown that the proportion of octatriene increases on going from primary to secondary alcohols while in the case of tertiary alcohols only octatriene and no telomer is formed.<sup>4</sup> Some support for this comes from the observation that *tert*-butyl alcohol does not react with 1 (R = Me) below its decomposition point. However, we should mention that the difference in the degree of deuteration of the octatriene and methoxyoctadienes (60% vs. 83%) observed in the catalytic reaction with CH<sub>3</sub>OD described above indicates that an alternative route, presumably direct from the [Pd-(L)(η<sup>1</sup>,η<sup>3</sup>-C<sub>8</sub>H<sub>12</sub>)] species without involvement of the alcohol, is also available for octatriene formation.

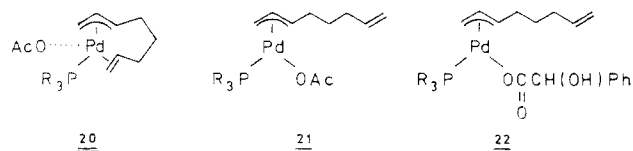
**Miscellaneous Reactions.** Although it was shown that **1** (R = Cy) is an active catalyst for the telomerization of butadiene with secondary amines or with triethylsilane (see Experimental Section), no intermediates could be isolated from stoichiometric reactions. This is particularly regrettable in the case of the reaction involving the silane since the product of the catalytic reaction (after 96 h at 100 °C) is mainly 2,7-octadienyltriethylsilane and not the expected 2,6-isomer.

The stoichiometric reaction of **1** (R = Me) with chlorodimethylsilane took a different course, and cleavage of the Si-Cl bond and not of the Si-H bond occurred to give **19** as a mixture of diastereomers (eq 10). This result is all



the more surprising since it is known, for example, that HSiMeCl<sub>2</sub> reacts with butadiene to give 1-SiMeCl<sub>2</sub>-2,6-octadiene, albeit in low yield.<sup>4,10</sup>

The palladium-catalyzed telomerization of butadiene with organic acids has received considerable attention.<sup>4</sup> The reaction with acetic acid can be modified by the addition of suitable cocatalysts, e.g., tertiary amines, to give acetoxyoctadiene in high yield. The stoichiometric reactions of **1** with acetic acid have been described in a previous publication,<sup>1</sup> and the isolation of **20** and **21** suggests that



the catalytic reaction proceeds through intermediates similar to those described above for other acidic substrates. One can speculate that the role of the tertiary amine in the catalytic reaction is that of a destabilizing ligand in that complexation of an amine molecule to **21** leads to a weakening of the Pd-OAc bond, thereby facilitating reductive coupling. Similar stoichiometric behavior has been observed with mandelic acid: variable-temperature <sup>31</sup>P NMR spectroscopy indicates that various complexes are formed as intermediates but the only complex that could be isolated was **22**.

Preliminary experiments<sup>11</sup> indicate that the complexes analogous to **1** prepared from isoprene, viz., [Pd(L)(η<sup>1</sup>,η<sup>3</sup>-Me<sub>2</sub>C<sub>8</sub>H<sub>10</sub>)],<sup>1</sup> react in a stoichiometric manner with mandelic acid or methanol to give complexes similar to those described here, suggesting strongly that such complexes are also involved as intermediates in the many palladium-catalyzed telomerization reactions of isoprene and nucleophiles.<sup>4</sup> However, these investigations have not been pursued further.

### Experimental Section

General experimental procedures, the NMR instruments employed, and the preparation of [Pd(PR<sub>3</sub>)(η<sup>1</sup>,η<sup>3</sup>-C<sub>8</sub>H<sub>12</sub>)] (**1**, R = Me, Cy) have been described in detail in ref 1.

[Pd(acac)(PCy<sub>3</sub>)(η<sup>1</sup>-C<sub>8</sub>H<sub>13</sub>)] (**11**, R = Cy). **1** (R = Cy) (0.976 g, 1.77 mmol) was dissolved in THF (30 mL) at -30 °C and acetylacetone (1 mL, 0.972 g, 9.71 mmol) was added. The resulting yellow solution was stirred for 4 h and evaporated to dryness, and the yellow solid was washed with cold pentane and dried under high vacuum: yield 0.82 g (78% theory); IR (KBr) ν<sub>C=O</sub> 1580, ν<sub>C=C</sub>

1640 cm<sup>-1</sup>; <sup>31</sup>P NMR (32.4 MHz, THF-d<sub>8</sub>, -30 °C) δ 40.8; <sup>13</sup>C NMR, see Table I. Anal. Calcd for C<sub>31</sub>H<sub>53</sub>O<sub>2</sub>PPd: C, 62.57; H, 8.91; P, 5.21; Pd, 17.89. Found: C, 62.53; H, 9.00; P, 5.30; Pd, 17.68.

[PdOC(OEt)CHC(Me)O(PCy<sub>3</sub>)(η<sup>1</sup>-C<sub>8</sub>H<sub>13</sub>)] (**9**, R = Cy) was prepared in solution by reacting **1** (R = Cy) with ethyl acetoacetone in THF: <sup>13</sup>C NMR, see Table I.

[PdOC(OEt)CHC(Me)O(PMe<sub>3</sub>)(η<sup>1</sup>-C<sub>8</sub>H<sub>13</sub>)] (**9**, R = Me) was prepared in solution by reacting **1** (R = Me) with ethyl acetoacetone in THF: <sup>31</sup>P NMR (32.4 MHz, THF-d<sub>8</sub>, 0 °C) δ -3.3; <sup>13</sup>C NMR, see Table I.

[PdOCOCH(OH)Ph(PMe<sub>3</sub>)(η<sup>3</sup>-C<sub>8</sub>H<sub>13</sub>)] (**22**, R = Me). **1** (R = Me) (0.976 g, 3.36 mmol) was dissolved in ether (20 mL) at -40 °C. *d,l*-Mandelic acid (0.511 g, 3.36 mmol) in ether (10 mL) was added under vigorous stirring. A pale yellow precipitate formed immediately. The reaction mixture was stirred for a further 2 h at -40 °C, cooled to -78 °C, and filtered, and the precipitate was washed with cold pentane. The product was dried at 0 °C under high vacuum: yield 0.81 g (54.4% theory); IR (KBr) ν<sub>OH</sub> 3405 (br), ν<sub>C=O</sub> 1610, ν<sub>allyl</sub> 1495 cm<sup>-1</sup>; <sup>31</sup>P NMR (32.4 MHz, THF-d<sub>8</sub>, -30 °C) δ -12.5; <sup>13</sup>C NMR, see Table II. Anal. Calcd for C<sub>19</sub>H<sub>29</sub>O<sub>3</sub>PPd: C, 51.64; H, 6.58; P, 6.88; Pd, 23.85. Found: C, 51.54; H, 6.60; P, 6.99; Pd, 24.03.

[PdOCOCH(OH)Ph(PCy<sub>3</sub>)(η<sup>3</sup>-C<sub>8</sub>H<sub>13</sub>)] (**22**, R = Cy) was prepared by reacting **1** (R = Cy) with *d,l*-mandelic acid in 43% yield: IR (KBr) ν<sub>OH</sub> 3400, ν<sub>CO</sub> 1612, ν<sub>C=C</sub> 1635, ν<sub>allyl</sub> 1527 cm<sup>-1</sup>; <sup>31</sup>P NMR (32.4 MHz, toluene-d<sub>8</sub>, -30 °C) δ 41.1; <sup>13</sup>C NMR, see Table II. Anal. Calcd for C<sub>34</sub>H<sub>52</sub>O<sub>3</sub>PPd: C, 63.10; H, 8.25; P, 4.79; Pd, 16.44. Found: C, 63.05; H, 8.23; P, 4.69; Pd, 16.28.

[PdCl(PMe<sub>3</sub>)(η<sup>3</sup>-6-Me<sub>2</sub>HSiC<sub>8</sub>H<sub>12</sub>)] (**19**). Me<sub>2</sub>SiHCl (0.511 g, 5.40 mmol) was added to a solution of **1** (R = Me) (1.089 g, 3.75 mmol) in ether (20 mL) at -78 °C. The reaction mixture was stirred overnight and concentrated, and the resulting white precipitate was isolated, washed with precooled pentane (5 mL), and dried under high vacuum at -50 °C: yield 0.64 g (44% theory); IR (KBr, -45 °C) ν<sub>allyl</sub> 1527, ν<sub>C=C</sub> 1626, 1640, ν<sub>SiH</sub> 2110 cm<sup>-1</sup>; <sup>31</sup>P NMR (32.4 MHz, THF-d<sub>8</sub>, -50 °C) δ -11.6 (d, separated by 0.03 ppm); <sup>13</sup>C NMR, see Table II. Anal. Calcd for C<sub>13</sub>H<sub>28</sub>ClPPdSi: C, 40.53; H, 7.28; Cl 9.20; P, 8.06; Pd, 27.65; Si, 7.28. Found: C, 40.66; H, 7.36; Cl, 9.28; P, 8.19; Pd, 27.43; Si, 7.08.

[PdOC(Me):CHCO<sub>2</sub>Et(PCy<sub>3</sub>)(η<sup>3</sup>-C<sub>8</sub>H<sub>13</sub>)] (**8**, R = Cy) was prepared in solution by reacting **1** (R = Cy) with ethyl acetoacetate at low temperature in THF: <sup>13</sup>C NMR, see Table II.

[PdCH(CN)CO<sub>2</sub>Me(PMe<sub>3</sub>)(η<sup>3</sup>-C<sub>8</sub>H<sub>13</sub>)] (**5**) was prepared in solution by reacting **1** (R = Me) with cyanoacetic acid at low temperature in toluene: <sup>31</sup>P NMR (32.4 MHz, toluene-d<sub>8</sub>, -80 °C) δ -16.6/-16.9; <sup>13</sup>C NMR, see Table II.

[Pd(PCy<sub>3</sub>)(η<sup>2</sup>,η<sup>2</sup>-1-EtO<sub>2</sub>C(COMe)CHC<sub>8</sub>H<sub>13</sub>)] (**10**, R = Cy). Ethyl acetoacetate (1 mL, 7.90 mmol) was added to **1** (R = Cy) (0.932 g, 1.88 mmol) in THF (40 mL) at -30 °C. The resulting yellow solution was stirred at room temperature for 40 h and then evaporated to dryness. Addition of cold (-30 °C) pentane gave a pale yellow suspension which was collected, washed with cold pentane, and dried under high vacuum: yield 0.41 g (35% theory); IR (KBr) ν<sub>C=O</sub> 1712, 1742, ν<sub>C=C</sub> 1504, 1445, ν<sub>COC</sub> 1245 cm<sup>-1</sup>; <sup>31</sup>P NMR (32.4 MHz, THF-d<sub>8</sub>, -30 °C) δ 33.7/33.2; <sup>13</sup>C NMR, see Table III. Anal. Calcd for C<sub>35</sub>H<sub>55</sub>O<sub>3</sub>PPd: C, 61.48; H, 8.87; P, 4.95; Pd, 17.02. Found: C, 61.65; H, 8.73; P, 4.95; Pd, 16.92.

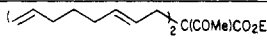
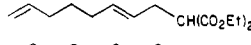
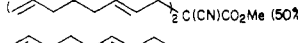
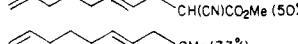
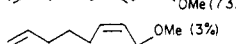
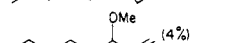
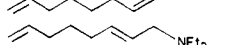
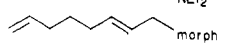
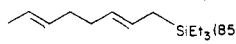
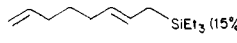

[Pd(PCy<sub>3</sub>)(η<sup>2</sup>,η<sup>2</sup>-1-MeO<sub>2</sub>CC(CN)HC<sub>8</sub>H<sub>13</sub>)] (**4**). Cyanoacetic acid (1 mL, 11.2 mmol) was added under vigorous stirring to **1** (R = Cy) (0.719 g, 1.45 mmol) in THF (40 mL) at -30 °C. The reaction mixture was stirred for a further 30 h at room temperature, concentrated, and cooled to -30 °C. Pentane (5 mL) was added, and a beige precipitate formed which was collected, washed several times with pentane, and dried under high vacuum: yield 0.59 g (68.6% theory); IR (KBr) ν<sub>C=C</sub> 1504, 1493, ν<sub>C=N</sub> 2245, ν<sub>C=O</sub> 1742 cm<sup>-1</sup>; <sup>31</sup>P NMR (32.4 MHz, toluene-d<sub>8</sub>, -30 °C) δ 33.2/33.4; <sup>13</sup>C NMR, see Table III. Anal. Calcd for C<sub>30</sub>H<sub>50</sub>N<sub>2</sub>O<sub>2</sub>PPd: C, 60.85; H, 8.48; N, 2.36; P, 5.21; Pd, 17.91. Found: C, 60.51; H, 8.56; N, 2.24; P, 5.08; Pd, 17.76.

[Pd(PCy<sub>3</sub>)(η<sup>2</sup>,η<sup>2</sup>-1-(CN)<sub>2</sub>CHC<sub>8</sub>H<sub>13</sub>)] (**4**). Malonodinitrile (0.3 mL, 5.41 mmol) was added to **1** (R = Cy) (0.594 g, 1.20 mmol) in THF (40 mL) at -30 °C. The clear yellow solution was stirred at room temperature for 40 h during which time it became orange. The reaction mixture was concentrated, pentane (5 mL) was added, and the resulting pale yellow solid was isolated, washed with

(10) Tsuji, J.; Hara, M.; Ohno, K. *Tetrahedron* 1974, 30, 2143.

(11) Schenker, G., unpublished results (1984).

Table IV.  $[\text{Pd}(\text{PCy}_3)(\eta^1, \eta^3\text{-C}_8\text{H}_{12})]$  (1) Catalyzed Telomerization of Butadiene

telomer	conditns <sup>a</sup>	solv	telomer:BD	product
H <sub>2</sub> C(COMe)CO <sub>2</sub> Et	RT, 120 h	ether	1:10	
H <sub>2</sub> C(CO <sub>2</sub> Et) <sub>2</sub>	RT, 120 h	ether	1:10	
H <sub>2</sub> C(CN)CO <sub>2</sub> Me	100 °C, 96 h	ether	1:2.5	 
MeOH	70 °C, 1 h	none	1:2	  
Et <sub>2</sub> NH	90 °C, 70 h	none	1:2.5	
morpholine	100 °C, 48 h	ether	1:2.5	
Et <sub>3</sub> SiH	100 °C, 96 h	ether	1:3	 

<sup>a</sup> RT = room temperature.

pentane, and dried under high vacuum: yield 0.66 g (98% theory); IR (KBr)  $\nu_{\text{C}=\text{C}}$  1504, 1493,  $\nu_{\text{C}=\text{N}}$  2155, 2200  $\text{cm}^{-1}$ ; <sup>31</sup>P NMR (32.4 MHz, THF-*d*<sub>6</sub>, -30 °C)  $\delta$  33.7; <sup>13</sup>C NMR, see Table III. Anal. Calcd for C<sub>29</sub>H<sub>47</sub>N<sub>2</sub>PPd: C, 62.08; H, 8.44; N, 4.99; P, 5.52; Pd, 18.96. Found: C, 61.96; H, 8.35; N, 5.05; P, 5.67; Pd, 19.05.

$[\text{Pd}(\text{PMe}_3)(\eta^2, \eta^2\text{-1-MeOC}_8\text{H}_{13})]$  (17). Methanol (1 mL) was added at -30 °C to a stirred solution of 1 (R = Cy) (0.872 g, 3.00 mmol) in ether (20 mL). The solution was evaporated to dryness after 12 h and the resulting red oil taken up in a little ether and filtered through Florisil at -30 °C. Concentration of the solution at -30 °C gave the product as a yellow solid: yield 0.484 g (52.7% theory); Raman (-40 °C)  $\nu_{\text{C}=\text{C}}$  1500, 1440, 1410,  $\nu_{\text{C}=\text{O}}$  1230  $\text{cm}^{-1}$ ; <sup>31</sup>P NMR (32.4 MHz, toluene-*d*<sub>8</sub>, -30 °C)  $\delta$  -25.6. <sup>13</sup>C NMR, see Table III; <sup>1</sup>H NMR (400 MHz, toluene-*d*<sub>8</sub>, -40 °C; for numbering scheme see footnote a of Table III)  $\delta$  3.10 (H-1,  $J_{1,2} = 0.5$ ,  $J_{1,3} = 8.6$ ,  $J_{1,P} = 7.0$  Hz), 2.85 (H-2,  $J_{2,3} = 12.9$ ,  $J_{2,P} = 5.7$  Hz), 3.8 (H-3), 2.57, 2.54 (H-4/8,  $J_{4,5}/J_{8,9} = 16.5$ ,  $J_{4,6}/J_{8,6} = 3.0$ ,  $J_{4,7}/J_{8,7} = 3.5$ ,  $J_{4,P}/J_{8,P} = 10.0$ ,  $J_{8,10} = 2.5$  Hz), 0.8 (H-5/9,  $J_{5,6}/J_{9,6} = 13.5$ ,  $J_{5,7}/J_{9,7} = 3.5$  Hz), 1.77 (H-6,  $J_{6,7} = 13.5$  Hz), 1.89 (H-7), 3.61 (H-10,  $J_{10,11} = 11.2$ ,  $J_{10,P} = 5.7$  Hz), 3.8 (H-11,  $J_{11,12} = 4.1$ ,  $J_{11,13} = 9.9$  Hz), 4.36 (H-12,  $J_{12,13} = 10.3$  Hz), 3.26 (H-13), 3.38 (OMe). Anal. Calcd for C<sub>12</sub>H<sub>26</sub>OPPd: C, 44.69; H, 7.83; P, 9.60; Pd, 33.00. Found: C, 44.74; H, 7.93; P, 9.60; Pd, 32.91.

$[\text{Pd}(\text{PMe}_3)(\eta^2, \eta^2\text{-1-}i\text{-PrOC}_8\text{H}_{13})]$  (18). 2-Propanol (6 mL) was added to 1 (R = Me) (1.350 g, 4.64 mmol) in ether (20 mL) at -25 °C and stirred for 12 h. The color of the solution changed from yellow to orange. The solution was filtered through Florisil at -30 °C and concentrated, and the resulting pale yellow solid was dried under high vacuum: yield 1.006 g (61.8% theory); <sup>31</sup>P NMR (32.4 MHz, toluene-*d*<sub>8</sub>, -30 °C)  $\delta$  25.3; <sup>13</sup>C NMR, see Table III; <sup>1</sup>H NMR (400 MHz, toluene-*d*<sub>8</sub>, -35 °C, for numbering scheme see footnote a of Table III)  $\delta$  3.06 (H-1,  $J_{1,2} = 1.1$ ,  $J_{1,3} = 8.7$ ,  $J_{1,P} = 6.9$  Hz), 2.80 (H-2,  $J_{2,3} = 12.8$ ,  $J_{2,P} = 5.7$  Hz), 3.83 (H-3), 2.53, 2.50 (H-4/8,  $J_{4,6}/J_{8,6} = 3.1$ ,  $J_{4,7}/J_{8,7} = 3.4$ ,  $J_{8,10} = 2.6$  Hz), 0.85, 0.81 (H-5/9,  $J_{5,6}/J_{9,6} = 13.1$ ,  $J_{5,7}/J_{9,7} = 3.4$ ,  $J_{9,10} = 11.1$ ,  $J_{9,11} = 3.1$  Hz), 1.75 (H-6,  $J_{6,7} = -13.6$  Hz), 1.88 (H-7), 3.64 (H-10,  $J_{10,11} = 11.1$ ,  $J_{10,P} = 5.7$  Hz), 3.85 (H-11,  $J_{11,12} = 4.4$ ,  $J_{11,13} = 9.4$  Hz), 4.18 ( $J_{12,13} = 10.0$  Hz), 3.46 (H-13), 3.73 (Me<sub>2</sub>CH,  $J = 6.0$ , 6.1 Hz), 1.19, 1.24 (Me<sub>2</sub>C), 1.02 (PMe,  $J_{H,P} = 5.9$  Hz). Anal. Calcd for C<sub>14</sub>H<sub>28</sub>OPPd: C, 47.93; H, 8.35; P, 8.83; Pd, 30.33. Found: C, 47.86; H, 8.18; P, 8.75; Pd, 30.31.

$[\text{Pd}(\text{PMe}_3)(\eta^2, \eta^2\text{-1-EtO}_2\text{C}(\text{COMe})\text{CHC}_8\text{H}_{13})]$  (10, R = Me) was prepared in solution by reacting 1 (R = Me) with ethyl acetoacetate in THF: <sup>31</sup>P NMR (32.4 MHz, THF-*d*<sub>8</sub>, room tem-

perature)  $\delta$  -25.0; <sup>13</sup>C NMR, see Table III.

$[\text{Pd}(\text{PMe}_3)(\eta^2, \eta^2\text{-1-MeO}_2\text{C}(\text{CN})\text{HC}_8\text{H}_{13})]$  (5) was prepared in solution by reacting 1 (R = Me) with cyanoacetic acid in toluene: <sup>31</sup>P NMR (32.4 MHz, toluene-*d*<sub>8</sub>, room temperature)  $\delta$  26.6; <sup>13</sup>C NMR, see Table III.

**Catalytic Reactions.** The results of the catalytic reactions described in the text are summarized in Table IV. Most examples represent one-off experiments, and no attempt was made to optimize the yields. Typical is the reaction between butadiene and the methyl ester of cyanoacetic acid. Butadiene (40 mL, 0.54 mol), H<sub>2</sub>C(CN)CO<sub>2</sub>Me (20 mL, 0.23 mol), and ether (10 mL) were transferred to an autoclave with the catalyst 1 (0.18 g, 0.37 mmol), and the mixture was stirred at 100 °C for 96 h. The maximum pressure reached was 5 atm. The reaction mixture was distilled under high vacuum and separated by preparative gas chromatography, and the products were identified by <sup>1</sup>H NMR spectroscopy. Cyanoacetic acid ester (31.5%) had been converted into a mixture of methyl esters of 2,7-octadienylcyanoacetic acid (9.1 g) and bis(2,7-octadienyl)cyanoacetic acid (8.7 g).

The remaining examples shown in Table IV were carried out similarly.

**Registry No.** 1 (R = Cy), 80191-14-6; 1 (R = Me), 80181-65-3; 4, 99641-61-9;  $\eta^3$ -5, 99641-59-5;  $\eta^2, \eta^2$ -5, 99655-17-1; 8 (R = Cy), 99641-58-4; 9 (R = Cy), 99641-53-9; 9 (R = Me), 99641-54-0; 10 (R = Cy), 99641-60-8; 10 (R = Me), 99655-16-0; 11 (R = Cy), 99641-52-8; 17, 80181-67-5; 18, 99655-15-9; 19, 99641-57-3; 22 (R = Cy), 99641-56-2; 22 (R = Me), 99641-55-1; Me<sub>2</sub>SiHCl, 1066-35-9;  $[\text{Pd}(\text{PCy}_3)(\eta^2, \eta^2\text{-1-(CN)}_2\text{CHC}_8\text{H}_{13})]$ , 99655-14-8; (CH<sub>2</sub>=CH(CH<sub>2</sub>)<sub>3</sub>CH=CHCH<sub>2</sub>)<sub>2</sub>C(COMe)CO<sub>2</sub>Et, 29085-22-1; CH<sub>2</sub>=CH(CH<sub>2</sub>)<sub>3</sub>CH=CHCH<sub>2</sub>CH(COOEt)<sub>2</sub>, 26450-19-1; (CH<sub>2</sub>=CH(CH<sub>2</sub>)<sub>3</sub>CH=CHCH<sub>2</sub>)<sub>2</sub>C(CN)CO<sub>2</sub>Me, 99631-99-9; CH<sub>2</sub>=CH(CH<sub>2</sub>)<sub>3</sub>CH=CHCH<sub>2</sub>CH(CN)CO<sub>2</sub>Me, 99632-00-5; CH<sub>2</sub>=CH(CH<sub>2</sub>)<sub>3</sub>CH=CHCH<sub>2</sub>OMe (isomer 1), 35702-75-1; CH<sub>2</sub>=CH(CH<sub>2</sub>)<sub>3</sub>CH=CHCH<sub>2</sub>OMe (isomer 2), 99685-93-5; CH<sub>2</sub>=CH(CH<sub>2</sub>)<sub>3</sub>CH(OMe)CH=CH<sub>2</sub>, 20202-62-4; CH<sub>2</sub>=CH(CH<sub>2</sub>)<sub>3</sub>CH=CHCH<sub>2</sub>NET<sub>2</sub>, 25017-02-1; CH<sub>2</sub>=CH(CH<sub>2</sub>)<sub>3</sub>CH=CHCH<sub>2</sub>morph, 25017-06-5; CH<sub>3</sub>CH=CH(CH<sub>2</sub>)<sub>2</sub>CH=CHCH<sub>2</sub>SiEt<sub>3</sub>, 21882-23-5; CH<sub>2</sub>=CH(CH<sub>2</sub>)<sub>3</sub>CH=CHCH<sub>2</sub>SiEt<sub>3</sub>, 99632-01-6; Et<sub>3</sub>SiH, 617-86-7; H<sub>2</sub>C(CO<sub>2</sub>Et)<sub>2</sub>, 105-53-3; Et<sub>2</sub>NH, 109-89-7; H<sub>2</sub>C(CN)CO<sub>2</sub>Me, 105-34-0; morpholine, 110-91-8; butadiene, 106-99-0; 2-propanol, 67-63-0; methanol, 67-56-1; malonodinitrile, 109-77-3; cyanoacetic acid, 372-09-8; *d,l*-mandelic acid, 611-72-3; ethyl acetoacetate, 141-97-9; acetylacetone, 123-54-6.



# New Ferrocenyl Thio- and Selenoether Ligands. Preparation, Characterization, and Their Palladium(II) Complexes as Catalysts for Selective Hydrogenation and Grignard Cross-Coupling

Robert V. Honeychuck, Michael O. Okoroafor, Lie-Hang Shen, and Carl H. Brubaker, Jr.\*

Department of Chemistry, Michigan State University, East Lansing, Michigan 48824

Received July 1, 1985

A number of previously unknown ferrocenyl thioethers and selenoethers,  $(\eta^5\text{-C}_5\text{H}_5)\text{Fe}(\eta^5\text{-C}_5\text{H}_3\text{-1-CH}_2\text{NMe}_2\text{-2-SR})$  (R = Me, Et, *i*-Pr, *i*-Bu, isopentyl, and Ph),  $(R,S)\text{-}(\eta^5\text{-C}_5\text{H}_5)\text{Fe}(\eta^5\text{-C}_5\text{H}_3\text{-1-CH}(\text{CH}_3)\text{-NMe}_2\text{-2-SR})$  (R = Me, Et, *i*-Pr, Ph, and  $\text{CH}_2\text{Ph}$ ),  $(\eta^5\text{-C}_5\text{H}_5)\text{Fe}(\eta^5\text{-C}_5\text{H}_3\text{-1-CH}_2\text{NMe}_2\text{-2-SeR})$  (R = Me, Ph, and 4-chlorophenyl),  $(S,R)\text{-}(\eta^5\text{-C}_5\text{H}_5)\text{Fe}(\eta^5\text{-C}_5\text{H}_3\text{-1-CH}(\text{CH}_3)\text{NMe}_2\text{-2-SePh})$ ,  $(\eta^5\text{-C}_5\text{H}_4\text{SeR})_2\text{Fe}$  (R = Me and Ph), and  $(\eta^5\text{-C}_5\text{H}_5)\text{Fe}(\eta^5\text{-C}_5\text{H}_4\text{SeMe})$ , have been made from the appropriate ferrocene precursors via lithiation and reaction with RSSR or RSeSeR. The following techniques were used for characterization:  $^1\text{H}$  and  $^{13}\text{C}$  NMR, IR, MS, and elemental analysis. The  $\text{PdCl}_2$  complex of  $(\eta^5\text{-C}_5\text{H}_5)\text{Fe}(\eta^5\text{-C}_5\text{H}_3\text{-1-CH}_2\text{NMe}_2\text{-2-S-}i\text{-Pr})$  is a selective hydrogenation catalyst under homogeneous and heterogeneous conditions for the reduction of dienes to monoenes. The  $\text{PdCl}_2$  complexes of  $(R,S)\text{-}(\eta^5\text{-C}_5\text{H}_5)\text{Fe}(\eta^5\text{-C}_5\text{H}_3\text{-1-CH}(\text{CH}_3)\text{NMe}_2\text{-2-SPh})$  and  $(S,R)\text{-}(\eta^5\text{-C}_5\text{H}_5)\text{Fe}(\eta^5\text{-C}_5\text{H}_3\text{-1-CH}(\text{CH}_3)\text{NMe}_2\text{-2-SePh})$  are effective Grignard cross-coupling agents coupling 1-chloro-1-phenylethane with allylmagnesium bromide and allylmagnesium chloride in high yield. The preparation of the  $\text{PdCl}_2$  complexes of  $(\eta^5\text{-C}_5\text{H}_4\text{SePh})_2\text{Fe}$  and  $(\eta^5\text{-C}_5\text{H}_5)\text{Fe}(\eta^5\text{-C}_5\text{H}_3\text{-1-CH}_2\text{NMe}_2\text{-2-SeR})$  (R = Me and 4-chlorophenyl) is also described. This paper presents the first transition-metal-catalyzed Grignard cross-coupling reaction that used a ferrocenyl thioether or selenoether as a ligand.

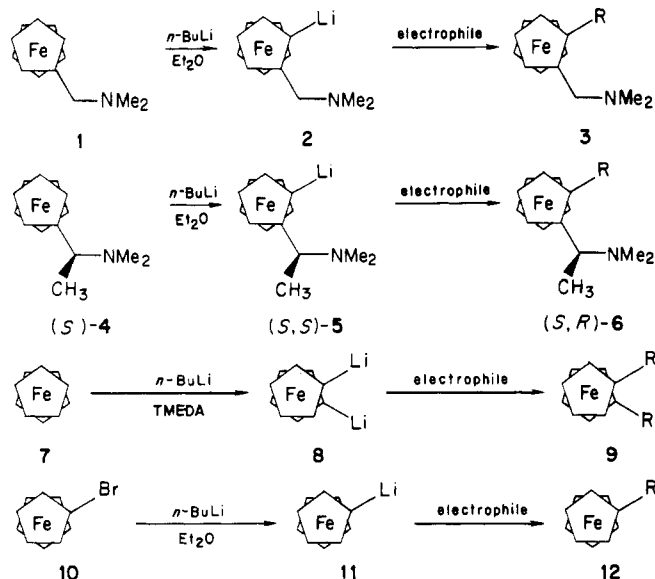
## Introduction

Since the first appearance of [(dimethylamino)methyl]ferrocene (1),<sup>1</sup> [1-(dimethylamino)ethyl]ferrocene (4),<sup>2</sup> ferrocene (7),<sup>3</sup> and bromoferrocene (10),<sup>4</sup> much effort has been expended on the reactions of their lithiation products 2, 5, 8, and 11. For example, electrophiles have been used to give 3 (R =  $\text{PPh}_2$ ,<sup>5</sup>  $\text{SiMe}_3$ ,<sup>6</sup> 2-pyridyl,<sup>7</sup>  $\text{C}(\text{OH})\text{Ph}_2$ ,<sup>8</sup>  $\text{Cl}$ ,<sup>9</sup> and  $\text{B}(\text{OH})_2$ ,<sup>10</sup> Various stereoisomers of 6 have been known for years.<sup>11,55a</sup> Their popularity as chiral ligands in catalysis stems from the ready resolution

of 4 into its *R* and *S* enantiomers.<sup>12</sup> Among the many compounds 9 derived from 1,1'-dilithioferrocene (8) are those where the electrophilic atom comes from the transition metals (9, R =  $\text{AuPPh}_3$ ,<sup>13</sup> and  $\text{Cu}^{14}$ ), the actinides (9, R =  $\text{UCp}_3$ ,<sup>15</sup> group IVA (14<sup>61</sup>) (9, R = organic groups<sup>16</sup> and silyl groups<sup>17</sup>), and group VA (15<sup>61</sup>) (9, R =  $\text{AsMe}_2$ ,  $\text{AsPh}_2$ ,  $\text{PMe}_2$ ,  $\text{PPh}_2$ ,<sup>18</sup> and  $\text{P}(t\text{-Bu})_2$ ,<sup>19</sup>). Ferrocenyllithium (11), upon reaction with appropriate electrophiles, gives 12 (R =  $\text{CO}_2\text{H}$ ,  $\text{SiPh}_3$ ,  $\text{SiMe}_3$ ,  $\text{CPh}_2\text{OH}$ ,<sup>20</sup> D, and Cl).<sup>21</sup> Group VIA (16<sup>61</sup>) atoms were not used as electrophiles with 2, 5, 8, and 11 until recently when it was found in this laboratory<sup>22-24</sup> that 8 and 11 react with alkyl disulfides, phenyl disulfide, and thiuram disulfides. As an extension

- (1) Hauser, C. R.; Lindsay, J. K. *J. Org. Chem.* **1956**, *21*, 382-383.  
 (2) Hauser, C. R.; Lindsay, J. K. *J. Org. Chem.* **1957**, *22*, 906-908.  
 (3) Kealy, T. J.; Pauson, P. L. *Nature (London)* **1951**, *168*, 1039-1040.  
 (4) Nesmeyanov, A. N.; Perevalova, E. G.; Nesmeyanova, O. A. *Dokl. Akad. Nauk SSSR* **1975**, *84*, 255-267.  
 (5) Kotz, J. C.; Nivert, C. L.; Lieber, J. M.; Reed, R. C. *J. Organomet. Chem.* **1975**, *84*, 255-257.  
 (6) Marr, G. J. *Organomet. Chem.* **1967**, *9*, 147-152.  
 (7) Booth, D. J.; Rockett, B. W. *Inorg. Nucl. Chem. Lett.* **1970**, *6*, 121-124.  
 (8) Slocum, D. W.; Rockett, B. W.; Hauser, C. R. *Chem. Ind. (London)* **1964**, 1831-1832.  
 (9) Gay, R. L.; Crimmins, T. F.; Hauser, C. R. *Chem. Ind. (London)* **1966**, 1635.  
 (10) Booth, D. J.; Marr, G.; Rockett, B. W.; Rushworth, A. *J. Chem. Soc. C* **1969**, 2701-2703.  
 (11) Hayashi, T.; Yamamoto, K.; Kumada, M. *Tetrahedron Lett.* **1974**, 4405-4408. Hayashi, T.; Tajika, M.; Tamao, K.; Kumada, M. *J. Am. Chem. Soc.* **1976**, *98*, 3718-3719. Hayashi, T.; Kumada, M. *Fundam. Res. Homogeneous Catal.* **1978**, *2*, 159-180. Hayashi, T.; Mise, T.; Fukushima, M.; Kagotani, M.; Nagashima, N.; Hamada, Y.; Matsumoto, A.; Kawakami, S.; Konishi, M.; Yamamoto, K.; Kumada, M. *Bull. Chem. Soc. Jpn.* **1980**, *53*, 1138-1151. Cullen, W. R.; Yeh, E.-S. *J. Organomet. Chem.* **1977**, *139*, C13-C16. Cullen, W. R.; Einstein, F. W. B.; Huang, C.-H.; Willis, A. C.; Yeh, E.-S. *J. Am. Chem. Soc.* **1980**, *102*, 988-993. Cullen, W. R.; Woollins, J. D. *Coord. Chem. Rev.* **1981**, *39*, 1-30. Cullen, W. R.; Woollins, J. D. *Can. J. Chem.* **1982**, *60*, 1793-1799. Butler, I. R.; Cullen, W. R.; Reglinski, J.; Rettig, S. J. *J. Organomet. Chem.* **1983**, *249*, 183-194. Marquarding, D.; Klusacek, H.; Gokel, G.; Hoffmann, P.; Ugi, I. *J. Am. Chem. Soc.* **1970**, *92*, 5389-5393. Gokel, G.; Hoffmann, P.; Klusacek, H.; Ugi, I. *Angew. Chem., Int. Ed. Engl.* **1970**, *9*, 64-65. Valkovich, P. B.; Gokel, G. W.; Ugi, I. K. *Tetrahedron Lett.* **1973**, 2947-2950. Battelle, L. F.; Bau, R.; Gokel, G. W.; Oyakawa, R. T.; Ugi, I. K. *J. Am. Chem. Soc.* **1973**, *95*, 482-486. Stuber, S.; Ugi, I. *Synthesis* **1973**, 309. Knowles, W. S. *Acc. Chem. Res.* **1983**, *16*, 106-112. Yamamoto, K.; Wakatsuki, J.; Sugimoto, R. *Bull. Chem. Soc. Jpn.* **1980**, *53*, 1132-1137.

- (12) Gokel, G. W.; Ugi, I. K. *J. Chem. Educ.* **1972**, *49*, 294-296.  
 (13) Perevalova, E. G.; Lemnovskii, D. A.; Afanasova, O. B.; Dyadchenko, V. P.; Grandberg, K. I.; Nesmeyanov, A. N. *Izv. Akad. Nauk SSSR, Ser. Khim.* **1972**, *21*, 2594-2596.  
 (14) Sedova, N. N.; Moiseev, S. K.; Sazonova, V. A. *J. Organomet. Chem.* **1982**, *224*, C53-C56.  
 (15) Tsutsui, M.; Ely, M. *J. Am. Chem. Soc.* **1974**, *96*, 3650-3651.  
 (16) Nesmeyanov, A. N.; Perevalova, E. G.; Golovnya, R. V.; Nesmeyanova, O. A. *Dokl. Akad. Nauk SSSR* **1954**, *97*, 459-461. Okuhara, K. *J. Org. Chem.* **1976**, *41*, 1487-1494. Sosin, I. L.; Alekseeva, V. P.; Litvinova, M. D.; Korshak, V. V.; Zhigach, A. F. *Vysokomol. Soedin., Ser. B* **1976**, *18*, 703-707. Hanlan, A. J. L.; Ugolick, R. C.; Fulcher, J. G.; Togashi, S.; Bocarsly, A. B.; Gladysz, J. A. *Inorg. Chem.* **1980**, *19*, 1543-1551. Cassens, A.; Eilbracht, P.; Mueller-Westerhoff, U. T.; Nazzari, A.; Neuenschwander, M.; Prossdorf, W. *J. Organomet. Chem.* **1981**, *205*, C17-C20.  
 (17) Goldberg, S. I.; Mayo, D. W.; Vogel, M.; Rosenberg, H.; Rausch, M. *J. Org. Chem.* **1959**, *24*, 824-826. Rausch, M.; Vogel, M.; Rosenberg, H. *J. Org. Chem.* **1957**, *22*, 900-903. Wrighton, M. S.; Palazzotto, M. C.; Bocarsly, A. B.; Bolts, J. M.; Fischer, A. B.; Nadjio, L. *J. Am. Chem. Soc.* **1978**, *100*, 7264-7271.  
 (18) Bishop, J. J.; Davison, A.; Katcher, M. L.; Lichtenberg, D. W.; Merrill, R. E.; Smart, J. C. *J. Organomet. Chem.* **1971**, *27*, 241-249.  
 (19) Cullen, W. R.; Kim, T.-J.; Einstein, F. W. B.; Jones, T. *Organometallics* **1983**, *2*, 714-719.  
 (20) Seyferth, D.; Hofmann, H. P.; Burton, R.; Helling, J. F. *Inorg. Chem.* **1962**, *1*, 227-231.  
 (21) Hedberg, F. L.; Rosenberg, H. *Tetrahedron Lett.* **1969**, 4011-4012.  
 (22) McCulloch, B.; Ward, D. L.; Woollins, J. D.; Brubaker, C. H., Jr. *Organometallics* **1985**, *4*, 1425-1432.  
 (23) McCulloch, B.; Brubaker, C. H., Jr. *Organometallics* **1984**, *3*, 1707-1711.  
 (24) McCulloch, B. Ph.D. Thesis, Michigan State University, 1983.



of this work, it has now been discovered that **2**, **5**, **8**, and **11** react with various disulfides and diselenides, yielding new ferrocenyl thioethers and selenoethers. The preparation and characterization of these compounds and some of their  $\text{PdCl}_2$  complexes are presented in this paper. The successful use of some of the  $\text{PdCl}_2$  complexes in selective hydrogenation and Grignard cross-coupling is also described.

### Experimental Section

Proton and  $^{13}\text{C}$  NMR spectra were obtained by use of a Bruker WM 250 spectrometer in chloroform-*d* with  $\text{Me}_4\text{Si}$  as internal standard. Infrared spectra were recorded by use of a Perkin-Elmer 457 machine. Mass spectra were obtained by means of a Finnigan 4021 instrument with INCOS data system. Elemental analyses were performed by Spang Microanalytical Laboratory, Eagle Harbor, MI, and Galbraith Laboratories, Knoxville, TN. Gas chromatography was carried out by using a Hewlett-Packard 5880A instrument. [(Dimethylamino)methyl]ferrocene was made by the standard method<sup>25</sup> or was purchased. Amine **4** was made and resolved as previously described.<sup>12</sup> Solvents were dried and distilled by standard methods.<sup>26</sup> The (1,3-cyclooctadiene + cyclooctene):cyclooctane ratios in the hydrogenations were determined by gas chromatography. The 1,3-cyclooctadiene:cyclooctene ratios were determined by integration of the olefinic region of the  $^1\text{H}$  NMR spectra.

**1-[(Dimethylamino)methyl]-2-(methylseleno)ferrocene (13, R = Me).** A 2.7 M solution of *n*-BuLi in hexane (4.1 mL, 11 mmol) was added over a half-hour period to a solution of [(dimethylamino)methyl]ferrocene (**1**, 2.7 g, 11 mmol) in 150 mL of dry ether under argon in a 250-mL round-bottomed Schlenk flask equipped with a magnetic stirring bar. The suspension was stirred for 3 h at room temperature, and then a solution of methyl diselenide (2.07 g, 11.0 mmol) in 20 mL of ether was added dropwise over a 30-min period at  $-78^\circ\text{C}$ . The reaction mixture was further stirred for 30 h. The mixture was filtered, and the filtrate was slowly added to aqueous  $\text{NaHCO}_3$  carbonate with cooling in an ice bath. The resulting organic layer and ether extracts from the aqueous layer were combined, washed with ice water, dried over anhydrous  $\text{MgSO}_4$ , and concentrated in vacuo to afford a brown oil, which was chromatographed on a silica gel column by gradient elution (hexane/benzene/ether). The product was obtained as brown-yellow plates: yield 80%; mp  $75\text{--}76^\circ\text{C}$ ; IR (Nujol) 460, 495, 510, 528, 820, 1002, 1022, 1110, 1180, 1208, 1305  $\text{cm}^{-1}$ ; MS, *m/e* (relative intensity) 44 (44,  $\text{NMe}_2$ ), 56 (93, Fe), 58 (75,  $\text{CH}_2\text{NMe}_2$ ), 65 (113,  $\text{C}_5\text{H}_5$ ), 95 (11, SeMe), 121 (100,  $\text{C}_5\text{H}_5\text{Fe}$ ), 242 (30,  $\text{M}^+ - \text{SeMe}$ ), 279 (3,  $\text{M}^+ - \text{CH}_2\text{NMe}_2$ ), 293 (7,

$\text{M}^+ - \text{NMe}_2$ ), 337 (13,  $\text{M}^+$ ). Anal. Calcd for  $\text{C}_{14}\text{H}_{19}\text{FeNSe}$ : C, 50.64; H, 5.70. Found: C, 49.95; H, 5.79.

**1-[(Dimethylamino)methyl]-2-(phenylseleno)ferrocene (13, R = Ph).** A 2.7 M solution of *n*-BuLi in hexane (4.1 mL, 11 mmol) was added over a half-hour period to a solution of [(dimethylamino)methyl]ferrocene (**1**, 2.7 g, 11 mmol) in 100 mL of dry ether under nitrogen in a 250-mL round-bottomed Schlenk flask equipped with a magnetic stirring bar. The suspension was stirred for 3 h at room temperature under nitrogen, and then a solution of phenyl diselenide (3.43 g, 11.0 mmol) in 20 mL of ether was added dropwise over a 30-min period at  $-78^\circ\text{C}$ . The reaction mixture was further stirred for 12 h. The mixture was filtered, and the filtrate was washed four times with 10-mL portions of ice-cold distilled  $\text{H}_2\text{O}$ . The organic layer was evaporated to a brown-yellow oil, which was chromatographed on a silica gel column by gradient elution (hexane/benzene). The product was obtained as a brown-yellow solid: yield 65%; mp  $42\text{--}44^\circ\text{C}$ ; IR (Nujol, CsI) 690, 735, 820, 1000, 1025, 1108, 1180, 1264, 1583  $\text{cm}^{-1}$ ; MS, *m/e* (relative intensity) 399 (45,  $\text{M}^+$ ). Anal. Calcd for  $\text{C}_{19}\text{H}_{21}\text{FeNSe}$ : C, 57.32; H, 5.32. Found: C, 57.63; H, 5.13.

**1-[(Dimethylamino)methyl]-2-[(4-chlorophenyl)seleno]ferrocene (13, R = 4-Chlorophenyl).** A 2.7 M solution of *n*-BuLi in hexane (2.4 mL, 6.4 mmol) was added over a half-hour period to a solution of [(dimethylamino)methyl]ferrocene (**1**, 1.2 mL, 5.8 mmol) in 80 mL of dry ether under argon in a 250-mL round-bottomed Schlenk flask equipped with a magnetic stirring bar. The suspension was stirred for 3 h at room temperature, and then a solution of bis(4-chlorophenyl) diselenide (2.02 g, 5.30 mmol) in 100 mL of dry ether was added dropwise over a 30-min period at  $-78^\circ\text{C}$ . The reaction mixture was then stirred for 30 h. After 4 h of heating under reflux, 50 mL of aqueous  $\text{NaHCO}_3$  was slowly added and cooled in an ice bath. The resulting organic layer and ether extracts from the aqueous layer were combined, washed with ice water, dried over anhydrous  $\text{Na}_2\text{SO}_4$ , and concentrated in vacuo to afford an orange-brown oil. The oil was chromatographed on a silica gel column by gradient elution (hexane/benzene/ether). The product was obtained as a dark brown oil, which solidified on cooling: yield 63%; IR (neat) 460, 493, 530, 810, 825, 1012, 1090, 1110, 1180, 1240, 1264, 1364, 1358, 1478, 1570, 1667–2000, 2770, 2820, 2860, 2950, 2980, 3050–3100  $\text{cm}^{-1}$ ; MS, *m/e* (relative intensity) 44 (8,  $\text{NMe}_2$ ), 56 (37, Fe), 58 (57,  $\text{CH}_2\text{NMe}_2$ ), 65 (7,  $\text{C}_5\text{H}_5$ ), 121 (79,  $\text{C}_5\text{H}_5\text{Fe}$ ), 191 (4,  $\text{SeC}_6\text{H}_4\text{Cl}$ ), 242 (100,  $\text{M}^+ - \text{SeC}_6\text{H}_4\text{Cl}$ ), 389 (11,  $\text{M}^+ - \text{NMe}_2$ ), 433 (39,  $\text{M}^+$ ). Anal. Calcd for  $\text{C}_{19}\text{H}_{20}\text{ClFeNSe}$ : C, 52.75; H, 4.66. Found: C, 52.85; H, 4.71.

**1-[(Dimethylamino)methyl]-2-ferrocenyl Thioethers (14).** Thioether derivatives **14** were prepared by lithiation of [(dimethylamino)methyl]ferrocene (**1**) in diethyl ether with 1.1 equiv of *n*-BuLi (1.6 M in hexane) under  $\text{N}_2$  in Schlenk flasks with rubber septa. After 12 h, 1.0 equiv of alkyl disulfide (neat) or phenyl disulfide (in 250 mL of  $\text{Et}_2\text{O}$ ) was added via cannula at  $25^\circ\text{C}$ . Because of the exothermic nature of the reaction with the disulfides, it is advisable to cool large scale preparations to  $0^\circ\text{C}$ . Four hours later, 100–200 mL of  $\text{H}_2\text{O}$  was added, the mixture in each case was filtered, and the organic layer was separated and dried ( $\text{Na}_2\text{SO}_4$ ). Solvents were removed on the rotary evaporator. The alkyl derivatives were purified on silica gel columns by using  $\text{CH}_2\text{Cl}_2/\text{MeOH}$ . An analytical sample of **14**, R = Ph, was obtained by repeated column chromatography with benzene/ethyl ether. The yield reported in the latter case is the yield of the analytical sample.

**1-[(Dimethylamino)methyl]-2-(methylthio)ferrocene (14, R = Me).** [(Dimethylamino)methyl]ferrocene (9.2 mL, 0.046 mol) gave 2.27 g (17%) of the product as a yellow solid: mp  $77\text{--}78^\circ\text{C}$ ; IR (Nujol, CsI) 719, 805, 888, 946, 996, 1102  $\text{cm}^{-1}$ ; MS, *m/e* (relative intensity) 44 (10,  $\text{NMe}_2$ ), 47 (1,  $\text{SMe}$ ), 56 (15, Fe), 58 (15,  $\text{CH}_2\text{NMe}_2$ ), 65 (2,  $\text{C}_5\text{H}_5$ ), 121 (41,  $\text{C}_5\text{H}_5\text{Fe}$ ), 231 (2,  $\text{M}^+ - \text{CH}_2\text{NMe}_2$ ), 242 (44,  $\text{M}^+ - \text{SMe}$ ), 245 (37,  $\text{M}^+ - \text{NMe}_2$ ), 289 (89,  $\text{M}^+$ ). Anal. Calcd for  $\text{C}_{14}\text{H}_{19}\text{FeNS}$ : C, 58.14; H, 6.62. Found: C, 58.08; H, 6.81.

**1-[(Dimethylamino)methyl]-2-(ethylthio)ferrocene (14, R = Et).** [(Dimethylamino)methyl]ferrocene (8.1 mL, 0.041 mol) gave 5.60 g (45%) of brown oil: IR (Nujol, CsI) 720, 808, 888, 946, 998, 1103, 1178, 1264  $\text{cm}^{-1}$ ; MS, *m/e* (relative intensity) 44 (23,  $\text{NMe}_2$ ), 56 (61, Fe), 58 (76,  $\text{CH}_2\text{NMe}_2$ ), 65 (21,  $\text{C}_5\text{H}_5$ ), 121 (100,  $\text{FeCp}$ ), 242 (41,  $\text{M}^+ - \text{SEt}$ ), 259 (20,  $\text{M}^+ - \text{NMe}_2$ ), 274 (4,  $\text{M}^+ - \text{Et}$ ), 303 (61,  $\text{M}^+$ ). Anal. Calcd for  $\text{C}_{15}\text{H}_{21}\text{FeNS}$ : C, 59.41; H, 6.98;

(25) Lednicher, D.; Hauser, C. R. *Org. Synth.* 1973, 5, 434–436.

(26) Gorgon, A. J.; Ford, P. A. "The Chemist's Companion"; Wiley: New York, 1972; pp 445–447.

S, 10.57. Found: C, 59.61; H, 7.15; S, 10.48.

**1-[(Dimethylamino)methyl]-2-(isopropylthio)ferrocene (14, R = *i*-Pr).** [(Dimethylamino)methyl]ferrocene (6.3 mL, 0.082 mol) gave 8.22 g (32%) of brown crystals: mp 82–83 °C; IR (Nujol, KBr) 662, 815, 891, 998, 1018, 1103, 1180, 1260, 3095 cm<sup>-1</sup>; MS, *m/e* (relative intensity) 43 (32, *i*-Pr), 44 (8, NMe<sub>2</sub>), 56 (26, Fe), 58 (28, CH<sub>2</sub>NMe<sub>2</sub>), 65 (4, C<sub>5</sub>H<sub>5</sub>), 121 (52, C<sub>5</sub>H<sub>5</sub>Fe), 196 (9, M<sup>+</sup> - C<sub>5</sub>H<sub>5</sub>Fe), 242, (48, M<sup>+</sup> - *S*-*i*-Pr), 259 (3, M<sup>+</sup> - CH<sub>2</sub>NMe<sub>2</sub>), 273 (23, M<sup>+</sup> - NMe<sub>2</sub>), 274 (24, M<sup>+</sup> - *i*-Pr), 302 (3, M<sup>+</sup> - CH<sub>3</sub>), 317 (100, M<sup>+</sup>). Anal. Calcd for C<sub>16</sub>H<sub>23</sub>FeNS: C, 60.57; H, 7.31; S, 10.10. Found: C, 60.54; H, 7.40; S, 10.16.

**1-[(Dimethylamino)methyl]-2-(isobutylthio)ferrocene (14, R = *i*-Bu).** [(Dimethylamino)methyl]ferrocene (16.3 mL, 0.0823 mol) gave 12.0 g (43.9%) of brown oil: IR (Nujol, CsI) 718, 808, 888, 945, 993, 1103 cm<sup>-1</sup>; MS, *m/e* (relative intensity) 43 (8, *i*-Pr), 44 (11, NMe<sub>2</sub>), 56 (45, Fe), 58 (48, CH<sub>2</sub>NMe), 65 (6, C<sub>5</sub>H<sub>5</sub>), 121 (100, M<sup>+</sup>). Anal. Calcd for C<sub>17</sub>H<sub>25</sub>FeNS: C, 61.63; H, 7.61; S, 9.68. Found: C, 61.17; H, 7.69; S, 9.82.

**1-[(Dimethylamino)methyl]-2-(isopentylthio)ferrocene (14, R = Isopentyl).** [(Dimethylamino)methyl]ferrocene (18.4 mL, 0.0930 mol) gave 10.2 g (31.7%) of brown oil: IR (Nujol, CsI) 720, 810, 888, 947, 995, 1103 cm<sup>-1</sup>; MS, *m/e* (relative intensity) 56 (17, Fe), 53 (19, CH<sub>2</sub>NMe<sub>2</sub>), 65 (3, C<sub>5</sub>H<sub>5</sub>), 121 (20, FeCp), 153 (3, M<sup>+</sup> - FeCp-isopentyl), 242 (15, M<sup>+</sup> - *S*-isopentyl), 274 (2, M<sup>+</sup> - NMe<sub>2</sub>), 345 (20, M<sup>+</sup>). Anal. Calcd for C<sub>18</sub>H<sub>27</sub>FeNS: C, 62.61; H, 7.88; S, 9.28. Found: C, 62.82; H, 8.07; S, 9.42.

**1-[(Dimethylamino)methyl]-2-(phenylthio)ferrocene (14, R = Ph).** [(Dimethylamino)methyl]ferrocene (16.3 mL, 0.0823 mol) gave 0.030 g (0.10%) of a yellow solid: mp 66–68 °C; IR (neat) 690, 740, 820, 1000, 1025, 1104, 1176, 1260, 1375, 1480, 1580, 2760, 2810, 2940, 3050–3100 cm<sup>-1</sup>; MS, *m/e* (relative intensity) 56 (43, Fe), 58 (32, CH<sub>2</sub>NMe<sub>2</sub>), 121 (78, C<sub>5</sub>H<sub>5</sub>Fe), 242 (94, M<sup>+</sup> - SPh), 351 (92, M<sup>+</sup>). Anal. Calcd for C<sub>15</sub>H<sub>21</sub>FeNS: C, 64.96; H, 6.03; S, 9.13. Found: C, 65.27; H, 5.87; S, 9.14.

**(S)-1-[(Dimethylamino)ethyl]ferrocene [(S)-4].** Amine **4** was prepared and resolved by using (+)-tartaric acid as described by Gokel and Ugi.<sup>12</sup> The amine was recrystallized twice to give a dark brown oil that partly solidified on cooling: <sup>1</sup>H NMR δ 1.44 (d, 3 H, CH<sub>3</sub>), 2.09 (s, 6 H, NMe<sub>2</sub>), 3.60 (q, 1 H, CH), 4.11 (s, 5 H, C<sub>5</sub>H<sub>5</sub>), 4.12 (m, 4 H, C<sub>5</sub>H<sub>4</sub>); [α]<sub>D</sub><sup>25</sup> -14.0° (lit.<sup>12</sup> [α]<sub>D</sub><sup>25</sup> -14.1°). The *R* isomer was isolated similarly.<sup>12</sup>

**(R,S)-1-[1-(Dimethylamino)ethyl]-2-(methylthio)ferrocene (15, R = Me).** Amine (*R*)-**4** (1.5 g, 5.8 mmol) was dissolved in 50 mL of dry ether and placed in a 100-mL round-bottomed flask equipped with a side arm. The solution was cooled to -78 °C, and 4.0 mL (6.4 mmol) of *n*-BuLi was added slowly via syringe. The orange suspension was allowed to reach room temperature and stirred overnight. Methyl disulfide (0.53 mL, 5.9 mmol) was added dropwise via syringe at -78 °C. The solution was allowed to reach room temperature and stirred for 12 h, after which 20 mL of H<sub>2</sub>O was added. The organic layer was separated, dried, and evaporated to give a dark oily residue. The oil was separated on alumina, with hexane/CH<sub>2</sub>Cl<sub>2</sub> to give the product which upon recrystallization from hexane/petroleum ether gave yellow crystals: yield 45%; mp 64–66 °C; MS, *m/e* (relative intensity) 303 (19, M<sup>+</sup>). Anal. Calcd for C<sub>15</sub>H<sub>21</sub>FeNS: C, 59.41; H, 6.93. Found: C, 59.54; H, 6.89.

**(R,S)-1-[1-(Dimethylamino)ethyl]-2-(ethylthio)ferrocene (15, R = Et).** The procedure was the same as for **15**, R = Me, except that 0.73 mL (5.9 mmol) of Et<sub>2</sub>S<sub>2</sub> was used: yield 45%; MS, *m/e* (relative intensity) 40 (100), 56 (17, Fe), 72 (9, CH(CH<sub>3</sub>)NMe<sub>2</sub>), 121 (29, FeCp), 272 (44, M<sup>+</sup> - HNMe<sub>2</sub>), 302 (23, M<sup>+</sup> - CH<sub>3</sub>), 317 (53, M<sup>+</sup>).

**(R,S)-1-[1-(Dimethylamino)ethyl]-2-(isopropylthio)ferrocene (15, R = *i*-Pr).** The procedure was the same as for **15**, R = Me, except that 0.94 mL (5.9 mmol) of (*i*-Pr)<sub>2</sub>S<sub>2</sub> was used. The product was recrystallized from hexane at -78 °C to give orange needles: yield 50%; mp 34–35 °C; MS, *m/e* (relative intensity) 56 (35, Fe), 121 (78, FeCp), 244 (48, M<sup>+</sup> - CH(CH<sub>3</sub>)NMe<sub>2</sub>), 286 (60, M<sup>+</sup> - HNMe<sub>2</sub>), 331 (35, M<sup>+</sup>). Anal. Calcd for C<sub>17</sub>H<sub>25</sub>FeNS: C, 61.63; H, 7.55; S, 9.67. Found: C, 61.70; H, 7.75; S, 9.90.

**(R,S)-1-[1-(Dimethylamino)ethyl]-2-(phenylthio)ferrocene (15, R = Ph).** Amine (*R*)-**4** (1.5 g, 5.8 mmol) was dissolved in 30 mL of dry ether and placed in a 200-mL round-bottomed flask equipped with a side arm. The solution was cooled

to -40 °C, and 4.0 mL (6.4 mmol) of *n*-BuLi was added slowly via syringe. The orange suspension was allowed to reach room temperature and stirred overnight. Ph<sub>2</sub>S<sub>2</sub> (1.29 g, 5.91 mmol), dissolved in 30 mL of warm hexane, was added dropwise via cannula to the orange suspension at -78 °C. The resulting solution was allowed to reach 25 °C and then heated under reflux overnight. The reaction mixture was cooled, and 20 mL of H<sub>2</sub>O was added. The organic layer was separated, dried, and evaporated to give a dark oily residue. Unreacted Ph<sub>2</sub>S<sub>2</sub> was removed by sublimation. The oil was chromatographed on activated alumina, by eluting first with hexane and then with CH<sub>2</sub>Cl<sub>2</sub>, to give the product: yield 55%; mp 40–41 °C; MS, *m/e* (relative intensity) 56 (45, Fe), 72 (100, CH(CH<sub>3</sub>)NMe<sub>2</sub>), 121 (54, FeCp), 212 (31), 320 (78, M<sup>+</sup> - HNMe<sub>2</sub>), 365 (70, M<sup>+</sup>). Anal. Calcd for C<sub>20</sub>H<sub>23</sub>FeNS: C, 65.75; H, 6.30. Found: C, 65.32; H, 6.21.

**(R,S)-1-[1-(Dimethylamino)ethyl]-2-(benzylthio)ferrocene (15, R = CH<sub>2</sub>Ph).** The procedure was the same as for **15**, R = Ph, except that 1.45 g (5.88 mmol) of (PhCH<sub>2</sub>)<sub>2</sub>S<sub>2</sub> was used. The product was obtained as a brown oil: yield 0.90 g (60%); IR (neat) 1490, 3000–3090 cm<sup>-1</sup>; MS, *m/e* (relative intensity) 56 (54, Fe), 72 (84, CH(CH<sub>3</sub>)NMe<sub>2</sub>), 91 (100, CH<sub>2</sub>Ph), 121 (57, FeCp), 244 (39), 334 (54, M<sup>+</sup> - HNMe<sub>2</sub>), 379 (25, M<sup>+</sup>). Anal. Calcd for C<sub>21</sub>H<sub>25</sub>FeNS: C, 66.49; H, 6.60. Found: C, 66.52; H, 6.65.

**(S,R)-1-[1-(Dimethylamino)ethyl]-2-(phenylseleno)ferrocene (16).** A hexane solution of *n*-BuLi (2.7 M, 4.0 mL, 11 mmol) was added to a solution of 3.43 g (13.3 mmol) of (*S*)-**4** in 150 mL of dry ether at -78 °C over a period of 30 min. The suspension was stirred for 12 h at 25 °C and cooled to -78 °C, and then 3.40 g (11.0 mmol) of Ph<sub>2</sub>Se<sub>2</sub> in 40 mL of ether was added dropwise over a 30-min period. The reaction mixture was stirred under N<sub>2</sub> for 3 h at 25 °C and filtered. The filtrate was washed with H<sub>2</sub>O, and the organic layer was separated and evaporated to a brown oil. The oil was separated on a silica gel column by gradient elution (hexane/benzene/ether), giving **16** as brown crystals: yield 60%; mp 45–46 °C; IR (neat) 460, 504, 540, 685, 730, 818, 925, 962, 1000, 1020, 1102, 1150, 1190, 1240, 1260, 1364, 1480, 1580, 2770, 2810, 2850, 2930, 2965, 3050–3090 cm<sup>-1</sup>; MS, *m/e* (relative intensity) 44 (89, NMe<sub>2</sub>), 56 (63, Fe), 121 (77, FeCp), 212 (16, vinylferrocene), 288 (38, M<sup>+</sup> - HNMe<sub>2</sub> - Se), 368 (100, M<sup>+</sup> - HNMe<sub>2</sub>). Anal. Calcd for C<sub>20</sub>H<sub>23</sub>FeNSe: C, 58.28; H, 5.62. Found: C, 58.25; H, 5.77.

**1,1'-Bis(methylseleno)ferrocene (17, R = Me).** A solution of TMEDA (1.28 g, 11.0 mmol) and 2.7 M *n*-BuLi in hexane (4.1 mL, 11 mmol) was added over a half-hour period to 1.0 g (5.3 mmol) of ferrocene in 50 mL of dry ether under argon in a 150-mL round-bottomed Schlenk flask. The mixture was stirred for 3 h at room temperature, and a solution of Me<sub>2</sub>Se<sub>2</sub> (2.07 g, 11.0 mmol) in 20 mL of dry ether was added dropwise at -78 °C. The mixture was stirred for 12 h at room temperature and filtered. The filtrate was washed with H<sub>2</sub>O, and the organic layer was separated and evaporated to a brown oil. The oil was separated on a silica gel column by gradient elution (hexane/ether). The products obtained were yellow-brown plates (10.2% yield, monosubstituted compound **17**) and a dark brown oil (51.4% yield, disubstituted compound **18**, R = Me). For **17**, R = Me: <sup>1</sup>H NMR δ 2.15 (s, 6 H, CH<sub>3</sub>), 4.20 (m, 4 H, H<sub>3</sub>, H<sub>4</sub>), 4.31 (m, 4 H, H<sub>2</sub>, H<sub>5</sub>); <sup>13</sup>C NMR 8.9 (q, Me), 71.2 (d, C<sub>2</sub>, C<sub>5</sub>), 75.0 (d, C<sub>3</sub>, C<sub>4</sub>), 75.5 (s, C<sub>1</sub>); IR (neat) 500, 616, 823, 883, 910, 1023, 1054, 1155, 1278, 1305, 1375, 1420, 2820, 2938, 3010, 2100 cm<sup>-1</sup>; MS, *m/e* (relative intensity) 56 (100, Fe), 65 (5, C<sub>5</sub>H<sub>5</sub>), 95 (13, SeMe), 121 (49, C<sub>5</sub>H<sub>5</sub>Fe), 184 (32, M<sup>+</sup> - 2 SeMe), 264 (11, M<sup>+</sup> - SeMe - Me), 344 (24, M<sup>+</sup> - 2 Me), 359 (8, M<sup>+</sup> - H), 374 (33, M<sup>+</sup>). Anal. Calcd for C<sub>12</sub>H<sub>14</sub>FeSe<sub>2</sub>: C, 38.76; H, 3.79. Found: C, 39.04; H, 3.93.

**1,1'-Bis(phenylseleno)ferrocene (17, R = Ph).** A solution of TMEDA (1.28 g, 11.0 mmol) and 2.7 M *n*-BuLi in hexane (4.1 mL, 11 mmol) was added over a half-hour period to 1.0 g (5.30 mmol) of ferrocene in 50 mL of hexane under N<sub>2</sub> in a 150-mL Schlenk flask. The mixture was stirred for 3 h at room temperature, and a solution of Ph<sub>2</sub>Se<sub>2</sub> (3.43 g, 11.0 mmol) in 20 mL of ether was added dropwise at -78 °C. The mixture was stirred for 12 h at room temperature and filtered. The filtrate was washed with H<sub>2</sub>O and the organic layer was separated and evaporated. Unreacted ferrocene was removed by sublimation. The product was recrystallized from benzene/hexane giving orange plates: yield 80.0%; mp 147–149 °C; <sup>1</sup>H NMR δ 4.33 (t, 4 H, H<sub>3</sub>, H<sub>4</sub>), 4.47 (t, 4 H, H<sub>2</sub>, H<sub>5</sub>), 7.00–7.41 (m, 10 H, Ph); IR (Nujol, CsI) 466, 493,

685, 729, 820, 1010, 1150, 1575  $\text{cm}^{-1}$ ; MS,  $m/e$  (relative intensity) 56 (40, Fe), 121 (10, CpFe), 264 (14,  $\text{M}^+ - \text{SePh} - \text{Ph}$ ), 498 (38,  $\text{M}^+$ ). Anal. Calcd for  $\text{C}_{22}\text{H}_{18}\text{FeSe}_2$ : C, 53.27; H, 3.66. Found: C, 53.23; H, 3.55.

**(Methylseleno)ferrocene (18).** A 2.7 M solution of *n*-BuLi in hexane (4.1 mL, 11 mmol) was added to a solution of bromoferrocene<sup>27</sup> (2.91 g, 11.0 mmol) in 150 mL of dry ether at  $-78^\circ\text{C}$  under argon in a 250-mL round-bottomed Schlenk flask equipped with a magnetic stirring bar. The suspension was stirred for 30 min at  $0^\circ\text{C}$ , and then a solution of  $\text{Me}_2\text{Se}_2$  (2.07 g, 11.0 mmol) in 20 mL of ether was added dropwise over a 30-min period at  $-78^\circ\text{C}$ . The mixture was further stirred for 24 h and filtered. The filtrate was washed with ice water, and the organic layer was separated and evaporated to a brown oil. The oil was separated on a silica gel column with hexane to give the product as yellow-brown plates: yield 70.3%; mp  $34\text{--}36^\circ\text{C}$ ;  $^1\text{H NMR}$   $\delta$  2.14 (s, 3 H, Me), 4.18 (m, 7 H,  $\text{C}_5\text{H}_5$ ,  $\text{H}_3$ ,  $\text{H}_4$ ), 4.32 (m, 2 H,  $\text{H}_2$ ,  $\text{H}_5$ );  $^{13}\text{C NMR}$   $\delta$  9.0 (q, Me), 69.8 (d,  $\text{C}_2$ ,  $\text{C}_5$ ), 70.0 (d,  $\text{C}_5\text{H}_5$ ), 73.9 (d,  $\text{C}_3$ ,  $\text{C}_4$ ), 74.4 (s,  $\text{C}_1$ ); IR (Nujol) 500, 820, 885, 1005, 1022, 1110, 1155, 1270, 1305  $\text{cm}^{-1}$ ; MS,  $m/e$  (relative intensity) 56 (66, Fe), 65 (7,  $\text{C}_5\text{H}_5$ ), 95 (13, SeMe), 121 (75,  $\text{C}_5\text{H}_5\text{Fe}$ ), 185 (4,  $\text{M}^+ - \text{SeMe}$ ), 265 (82,  $\text{M}^+ - \text{Me}$ ), 280 (63,  $\text{M}^+$ ). Anal. Calcd for  $\text{C}_{11}\text{H}_{12}\text{FeSe}$ : C, 47.36; H, 4.34. Found: C, 47.10; H, 4.51.

**[1-[(Dimethylamino)methyl]-2-(isopropylthio)ferrocene]palladium Dichloride (19).** A 125-mL Erlenmeyer flask with a stir bar was placed in an oil bath at  $100^\circ\text{C}$ . To this was added 1.00 g ( $3.07 \times 10^{-3}$  mol) of  $\text{K}_2\text{PdCl}_4$  in 75 mL of  $\text{H}_2\text{O}$ . A solution of 0.973 g ( $3.07 \times 10^{-3}$  mol) of 14,  $\text{R} = i\text{-Pr}$ , in 45 mL of acetone was added dropwise over 15 min. The mixture was heated for 10 min and left overnight at  $25^\circ\text{C}$ . Filtration and washes with 20 mL of  $\text{H}_2\text{O}$  and 10 mL of hexane gave fine brown crystals of the product: yield 0.902 g (59.6%); mp  $165\text{--}167^\circ\text{C}$ ; IR (Nujol, CsI) 300, 331, 469, 718, 814, 992, 1103, 1168  $\text{cm}^{-1}$ ; MS,  $m/e$  (relative intensity) 43 (41, *i*-Pr), 44 (55,  $\text{NMe}_2$ ), 56 (21, Fe), 58 (18,  $\text{CH}_2\text{NMe}_2$ ), 65 (24,  $\text{C}_5\text{H}_5$ ), 106 (2, Pd), 121 (26,  $\text{C}_5\text{H}_5\text{Fe}$ ), 196 (4,  $\text{M}^+ - \text{C}_5\text{H}_5\text{Fe} - \text{PdCl}_2$ ), 242 (15,  $\text{M}^+ - \text{S-}i\text{-Pr} - \text{PdCl}_2$ ), 273 (6,  $\text{M}^+ - \text{NMe}_2 - \text{PdCl}_2$ ), 274 (7,  $\text{M}^+ - i\text{-Pr} - \text{PdCl}_2$ ), 317 (20,  $\text{M}^+ - \text{PdCl}_2$ ). Anal. Calcd for  $\text{C}_{16}\text{H}_{23}\text{FeNSPdCl}_2$ : C, 38.86; H, 4.69. Found: C, 38.98; H, 4.57.

**(R,S)-[1-[1-(Dimethylamino)ethyl]-2-(phenylthio)ferrocene]palladium Dichloride (20).** Complex 20 was prepared from a benzene solution of  $(\text{PhCN})_2\text{PdCl}_2$  and (*R,S*)-amine thioether 15,  $\text{R} = \text{Ph}$ . The molar ratio of  $(\text{PhCN})_2\text{PdCl}_2$ :15,  $\text{R} = \text{Ph}$ , was 1:1.1. The reaction mixture was stirred for 10 h, and the resulting precipitate was filtered, washed with benzene and then petroleum ether, and recrystallized from  $\text{CH}_2\text{Cl}_2$ /hexane by slow evaporation to give greenish black crystals; yield 85%; mp  $165\text{--}166^\circ\text{C}$  dec. Anal. Calcd for  $\text{C}_{20}\text{H}_{23}\text{FeSNPdCl}_2$ : C, 44.25; H, 4.24. Found: C, 44.18; H, 3.96.

**(S,R)-[1-[1-(Dimethylamino)ethyl]-2-(phenylseleno)ferrocene]palladium Dichloride (21).** To a solution of 0.383 g (1.00 mmol) of  $(\text{PhCN})_2\text{PdCl}_2$  in 10 mL of benzene was added a solution of 0.413 g (1.00 mmol) of (*S,R*)-amine selenoether 16 in 20 mL of benzene. After 20 h of stirring at room temperature, the dark brown precipitate formed was collected by filtration, washed with benzene, and dried in vacuo. The precipitate was recrystallized from  $\text{CH}_2\text{Cl}_2$ /hexane to give 21 as dark brown needles: yield 70%; mp  $160\text{--}162^\circ\text{C}$ ; IR (Nujol, CsI) 305, 330, 467, 493, 518, 538, 685, 740, 830, 900, 1000, 1020, 1104, 1170, 1247, 1304, 1578  $\text{cm}^{-1}$ ; MS,  $m/e$  (relative intensity) 44 (83,  $\text{NMe}_2$ ), 56 (12, Fe), 121 (8, FeCp), 212 (2, vinyl ferrocene), 288 (1,  $\text{M}^+ - \text{PdCl}_2 - \text{HNMe}_2 - \text{Se}$ ), 368 (1,  $\text{M}^+ - \text{PdCl}_2 - \text{HNMe}_2$ ). Anal. Calcd for  $\text{C}_{20}\text{H}_{23}\text{FeSeNPdCl}_2$ : C, 40.75; H, 3.93. Found: C, 41.31; H, 3.69.

**[1,1'-Bis(phenylseleno)ferrocene]palladium Dichloride (22).** To a solution of 0.383 g (1.00 mmol) of  $(\text{PhCN})_2\text{PdCl}_2$  in 10 mL of benzene was added a solution of 0.498 g (1.00 mmol) of 1,1'-bis(phenylseleno)ferrocene (17,  $\text{R} = \text{Ph}$ ) in 20 mL of benzene. After 12 h of stirring at room temperature, the reddish brown precipitate formed was collected by filtration, washed with benzene, and dried in vacuo. The precipitate was recrystallized from  $\text{CH}_2\text{Cl}_2$ /hexane to give 22 as brick red needles: yield 85%; mp  $195\text{--}197^\circ\text{C}$  dec; IR (Nujol, CsI) 270, 302, 345, 460, 482, 500,

685, 730, 836, 1000, 1020  $\text{cm}^{-1}$ ; MS,  $m/e$  (relative intensity) 44 (7,  $\text{NMe}_2$ ), 56 (42, Fe), 65 (11, Cp), 121 (17, CpFe), 184 (3,  $\text{M}^+ - \text{PdCl}_2 - 2 \text{SePh}$ ), 498 (2,  $\text{M}^+ - \text{PdCl}_2$ ). Anal. Calcd for  $\text{C}_{22}\text{H}_{18}\text{FeSe}_2\text{PdCl}_2$ : C, 39.24; H, 2.69. Found: C, 38.97; H, 2.58.

**[1-[(Dimethylamino)methyl]-2-(methylseleno)ferrocene]palladium Dichloride (23,  $\text{R} = \text{Me}$ ).** To a solution of 0.383 g (1.00 mmol) of  $(\text{PhCN})_2\text{PdCl}_2$  in 10 mL of dry benzene was added a solution of 0.336 g (1.00 mmol) 13,  $\text{R} = \text{Me}$ , in 20 mL of dry benzene. After 20 h of stirring at room temperature, the red-brown precipitate formed was collected by filtration, washed with benzene, and dried in vacuo. The powder was recrystallized from  $\text{CH}_2\text{Cl}_2$ /hexane to give 23,  $\text{R} = \text{Me}$ , as dark brown crystals: yield 75%; mp  $182\text{--}184^\circ\text{C}$ ;  $^1\text{H NMR}$   $\delta$  2.32 (s, 3 H, SeMe), 2.75 (s, 3 H, NMe), 2.80 (d,  $J = 13 \text{ Hz}$ , 1 H, NCH), 3.11 (s, 3 H, NMe), 4.00 (d,  $J = 13 \text{ Hz}$ , 1 H, NCH), 4.24 (s, 5 H,  $\text{C}_5\text{H}_5$ ), 4.38, 4.50 (m, 3 H,  $\text{H}_3$ ,  $\text{H}_4$ ,  $\text{H}_5$ );  $^{13}\text{C NMR}$   $\delta$  19.3 (q, SeMe), 48.5 (q, NMe), 54.9 (q, NMe), 65.8 (t, NCH<sub>2</sub>), 68.5 (d,  $\text{C}_3$ ,  $\text{C}_4$ ,  $\text{C}_5$ ), 69.1 (d,  $\text{C}_3$ ,  $\text{C}_4$ ,  $\text{C}_5$ ), 70.5 (d,  $\text{C}_3$ ,  $\text{C}_4$ ,  $\text{C}_5$ ), 71.5 (d,  $\text{C}_5\text{H}_5$ ), 82.0 (s,  $\text{C}_2$ ), 91.4 (s,  $\text{C}_1$ ); IR (Nujol) 263, 320, 470, 498, 510, 520, 530, 678, 830, 995, 1073, 1102, 1160, 1242  $\text{cm}^{-1}$ ; MS,  $m/e$  (relative intensity) 44 (100,  $\text{NMe}_2$ ), 56 (24, Fe), 58 (59,  $\text{CH}_2\text{NMe}_2$ ), 65 (41,  $\text{C}_5\text{H}_5$ ), 95 (22,  $\text{SeCH}_3$ ), 106 (12, Pd), 121 (40,  $\text{C}_5\text{H}_5\text{Fe}$ ), 242 (27,  $\text{M}^+ - \text{SeCH}_3 - \text{PdCl}_2$ ), 293 (5,  $\text{M}^+ - \text{NMe}_2 - \text{PdCl}_2$ ), 337 (16,  $\text{M}^+ - \text{PdCl}_2$ ). Anal. Calcd for  $\text{C}_{14}\text{H}_{19}\text{Cl}_2\text{FeNPdSe}$ : C, 32.76; H, 3.73. Found: C, 32.47; H, 3.65.

**[1-[(Dimethylamino)methyl]-2-[4-chlorophenyl]seleno]ferrocene]palladium Dichloride (23,  $\text{R} = 4\text{-Chlorophenyl}$ ).** To a solution of 0.383 g (1.00 mmol) of  $(\text{PhCN})_2\text{PdCl}_2$  in 10 mL of dry benzene was added a solution of 0.433 g (1.00 mmol) of 13,  $\text{R} = 4\text{-chlorophenyl}$ , in 20 mL of dry benzene. After 20 h of stirring at room temperature, the gold-brown precipitate formed was collected by filtration, washed with benzene, and dried in vacuo. The product was recrystallized from  $\text{CH}_2\text{Cl}_2$ /hexane to give 23,  $\text{R} = 4\text{-chlorophenyl}$ , as dark brown needles: yield 83%; mp  $162\text{--}164^\circ\text{C}$  dec;  $^1\text{H NMR}$   $\delta$  2.45 (s, 3 H, NMe), 2.83 (d,  $J = 14 \text{ Hz}$ , 1 H, NCH), 3.13 (s, 3 H, NMe), 4.10 (d,  $J = 14 \text{ Hz}$ , 1 H, NCH), 4.16 (m, 1 H,  $\text{H}_3$ ,  $\text{H}_4$ ,  $\text{H}_5$ ), 4.32 (m, 1 H,  $\text{H}_3$ ,  $\text{H}_4$ ,  $\text{H}_5$ ), 4.34 (s, 5 H,  $\text{C}_5\text{H}_5$ ), 4.41 (m, 1 H,  $\text{H}_3$ ,  $\text{H}_4$ ,  $\text{H}_5$ ), 7.35–7.83 (m, 4 H, Ph); IR (Nujol, CsI) 260, 324, 472, 290, 520, 540, 810, 840, 1012, 1092, 1110, 1180, 1240, 1266  $\text{cm}^{-1}$ ; MS,  $m/e$  (relative intensity) 44 (62,  $\text{NMe}_2$ ), 56 (16, Fe), 58 (16,  $\text{CH}_2\text{NMe}_2$ ), 65 (34,  $\text{C}_5\text{H}_5$ ), 106 (5, Pd), 121 (35,  $\text{C}_5\text{H}_5\text{Fe}$ ), 190 (18,  $\text{SeC}_6\text{H}_4\text{Cl}$ ), 242 (20,  $\text{M}^+ - \text{PdCl}_2 - \text{SeC}_6\text{H}_4\text{Cl}$ ), 389 (2,  $\text{M}^+ - \text{NMe}_2 - \text{PdCl}_2$ ), 433 (3,  $\text{M}^+ - \text{PdCl}_2$ ). Anal. Calcd for  $\text{C}_{19}\text{H}_{20}\text{Cl}_3\text{NSeFePd}$ : C, 37.42; H, 3.31. Found: C, 36.57; H, 3.46.

**Palladium Complexes 19–23.** Palladium complex 19 was made by using the same procedure as for *o*-(methylthio)aniline.<sup>42</sup> An acetone solution of the ferrocene was added dropwise to a hot aqueous solution of potassium tetrachloropalladate. The acetone boiled off, and the product precipitated immediately as fine brown crystals with a clearly defined melting point of  $165\text{--}167^\circ\text{C}$ . Complexes 20–23 were made by using  $(\text{PhCN})_2\text{PdCl}_2$  as the source of Pd. Precipitates formed after several hours of stirring. Amine complexes 19–21 did not give simple  $^1\text{H NMR}$  spectra. Deposition of a black precipitate began immediately on dissolution in chloroform-*d* (possibly Pd metal). Compounds 23 gave satisfactory NMR data.

**Hydrogenation of 1,3-Cyclooctadiene with 19 in  $\text{CH}_2\text{Cl}_2$  at 101 psi.** Ferrocene-palladium complex 19 (0.010 g,  $2.0 \times 10^{-5}$  mol), methylene chloride (9.0 mL), and 1,3-cyclooctadiene (1.00 mL, 0.00815 mol) were added to a 100-mL pressure bottle with a pressure gauge and stirring bar. The bottle was evacuated and filled several times with  $\text{H}_2$  to a pressure of 101 psi. No  $\text{H}_2$  uptake was observed in 27.4 h, so 0.0036 mL ( $2.0 \times 10^{-4}$  mol) of  $\text{H}_2\text{O}$  was added and the bottle was refilled with  $\text{H}_2$ . Uptake began immediately and slowed after absorption of 0.00815 mol of  $\text{H}_2$ . The initial turnover rate was 27 mol/mol of Pd/h.

**Hydrogenation of 1,3-Cyclooctadiene with 19 in Acetone at 14.7 psi.** Ferrocene-palladium complex 19 (0.010 g,  $2.0 \times 10^{-5}$  mol), acetone (9.0 mL), and 1,3-cyclooctadiene (1.00 mL, 0.00815 mol) were added to a 100-mL round-bottomed magnetically stirred flask on a 1-atm hydrogenation line fitted with a mercury manometer. The system was evacuated and filled several times with  $\text{H}_2$  to 1 atm. Uptake began after the red solution became red-brown. The turnover rate in the linear region was 1.9 mol/mol of Pd/h. Product analysis at the end of reaction showed 0%

(27) Fish, R. W.; Rosenblum, M. *J. Org. Chem.* 1965, 30, 1253–1254.

(28) Kawakami, K.; Kawata, N.; Maruza, K.-I.; Mizoroki, T.; Ozaki, A. *J. Catal.* 1975, 39, 134–140.

1,3-cyclooctadiene, 100% cyclooctene, and 0% cyclooctane.

**Hydrogenation of 1,3-Cyclooctadiene with 19 in Acetone at 61 psi.** Ferrocene-palladium complex 19 (0.010 g,  $2.0 \times 10^{-5}$  mol), acetone (9.0 mL), and 1,3-cyclooctadiene (1.00 mL, 0.00815 mol) were added to a 100-mL pressure bottle with a pressure gauge and stirring bar. The bottle was evacuated and filled several times with  $H_2$  to a pressure of 61 psi. Uptake began immediately and slowed after absorption of 0.0055 mol of  $H_2$ . The initial turnover rate was 422 mol/mol of Pd/h. Product analysis at the end of reaction showed 6.5% 1,3-cyclooctadiene, 72.4% cyclooctene, and 21.1% cyclooctane.

**Isomerization-Hydrogenation of 1,5-Cyclooctadiene with 19.** Ferrocene-palladium complex 19 (0.010 g,  $2.0 \times 10^{-5}$  mol), acetone (9.6 mL), and 1,5-cyclooctadiene (0.50 mL, 0.0041 mol) were added to a 100-mL pressure bottle with a pressure gauge and stirring bar. The bottle was evacuated and filled several times with  $H_2$  to a pressure of 60 psi. Uptake began immediately and ceased after absorption of 0.0025 mol of  $H_2$ . The initial turnover rate was 9.0 mol/mol of Pd/h. Product analysis at the end of reaction showed 17.0% 1,5-cyclooctadiene, 10.2% 1,4-cyclooctadiene, 10.0% 1,3-cyclooctadiene, 52.4% cyclooctene, and 10.4% cyclooctane.

**Grignard Cross-Coupling Reaction with Thioether-Palladium Complex 20 and Allylmagnesium Chloride To Give 4-Phenyl-1-pentene.** Complex 20 (0.0271 g, 0.0499 mmol) was placed in a 100-mL round-bottomed Schlenk flask equipped with a stirring bar and a septum. The vessel was evacuated and filled with Ar several times. After being cooled to  $-78^\circ C$ , the reaction vessel was charged with 1.41 g (10.0 mmol) of 1-phenylethyl chloride in 20 mL of dry ether and stirred for 2 h at room temperature before addition of allylmagnesium chloride (920 mmol, 10 mL at 2 M solution in THF) via syringe at  $-78^\circ C$ . The reaction mixture was allowed to warm to  $0^\circ C$ , stirred for 40 h, and hydrolyzed with 10% HCl. The organic layer and ether extracts from the aqueous layer were combined, washed with saturated NaHCl<sub>3</sub> solution and water, and dried over Na<sub>2</sub>SO<sub>4</sub>. Evaporation of solvent and chromatography on a silica gel column gave 1.32 g (93%) of 4-phenyl-1-pentene:  $^1H$  NMR  $\delta$  1.25 (d, 3 H, CH<sub>3</sub>), 2.35 (m, 2 H, CH<sub>2</sub>), 2.80 (m, 1 H, CHCH<sub>3</sub>), 5.00 (m, 2 H, CH=CH<sub>2</sub>), 5.70 (m, 1 H, CH=CH<sub>2</sub>), 7.25 (m, 5 H, Ph) [lit.<sup>28</sup>  $^1H$  NMR  $\delta$  1.24 (d, 3 H, CH<sub>3</sub>), 2.32 (m, 2 H, CH<sub>2</sub>), 2.75 (sex, 1 H, CHCH<sub>3</sub>), 4.80 (s, 1 H, CH=CH<sub>2</sub>), 4.92 (split d, 1 H, CH=CH<sub>2</sub>), 5.52 (m, 1 H, CH=CH<sub>2</sub>), 7.00 (5 H, Ph)]; MS, *m/e* (relative intensity) 41 (5, CH<sub>2</sub>CH=CH<sub>2</sub>), 77 (15, C<sub>6</sub>H<sub>5</sub>), 105 (100, PhCHCH<sub>3</sub>), 146 (15, M<sup>+</sup>).

**Grignard Cross-Coupling Reaction with Selenoether-Palladium Complex 21 and Allylmagnesium Chloride To Give 4-Phenyl-1-pentene.** The procedure was identical with that above employing 20, with substitution of 22.7 mg (0.0385 mmol) of 21 for 20. After the allylmagnesium chloride was added at  $-78^\circ C$ , the reaction mixture was stirred at  $10^\circ C$  for 25 h. Workup as above gave 1.30 g (91.6%) of 4-phenyl-1-pentene with a proton NMR identical with that from 20.

**Grignard Cross-Coupling Reaction with Selenoether-Palladium Complex 21 and Allylmagnesium Bromide To Give 4-Phenyl-1-pentene.** The procedure was identical with that above employing 20, with substitution of 27.6 mg (0.0468 mmol) of 21 for 20 and 20 mmol (20 mL of a 1 M ether solution) of allylmagnesium bromide for allylmagnesium chloride. Workup gave 1.39 g (98%) of 4-phenyl-1-pentene.

## Results and Discussion

Alkyl disulfides, phenyl disulfide, methyl diselenide, and aryl diselenides react with 1-[(dimethylamino)methyl]-2-lithioferrocene (2) and 1-[1-(dimethylamino)ethyl]-2-lithioferrocene (5), yielding ferrocenyl sulfides 14 and 15 and ferrocenyl selenides 13 and 16. Dilithioferrocene 8 reacts with methyl and phenyl diselenide to give ferrocenyl selenides 17. Ferrocenyllithium (11) with methyl diselenide yields selenide 18. Bidentate ligand 14, R = *i*-Pr, forms a PdCl<sub>2</sub> complex that isomerizes 1,5-cyclooctadiene to 1,3-cyclooctadiene under homogeneous conditions and selectively hydrogenates 1,3-cyclooctadiene to cyclooctene under homogeneous and heterogeneous conditions. The

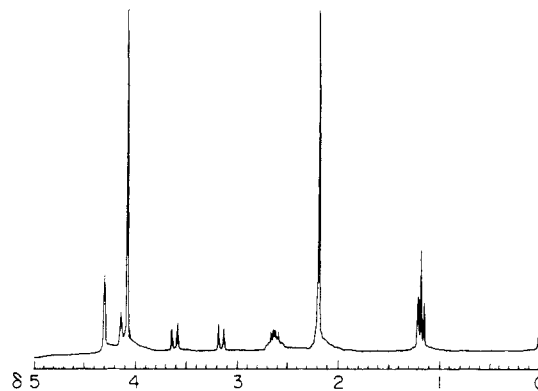
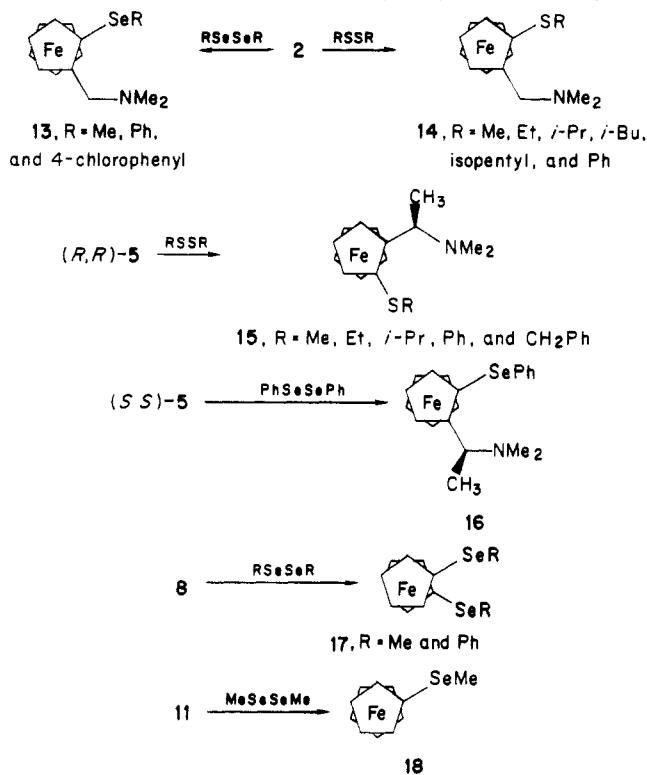


Figure 1. 250-MHz  $^1H$  NMR (chloroform-*d*, Me<sub>4</sub>Si) of 14 (R = Et).

PdCl<sub>2</sub> complexes of 15, R = Ph, and 16 are effective Grignard cross-coupling agents coupling 1-chloro-1-phenylethane with allylmagnesium bromide and allylmagnesium chloride. Disubstituted selenoferrocene 17, R = Ph, and amine selenoethers 13 (R = Me and 4-chlorophenyl) react with (PhCN)<sub>2</sub>PdCl<sub>2</sub> to give PdCl<sub>2</sub> complexes 22 and 23, R = Me and 4-chlorophenyl, respectively.



**Ferrocenyl Sulfides and Selenides 13–18.** Tables I and II present 250-MHz  $^1H$  NMR data for compounds 13–16. The spectrum of 14, R = Et (Figure 1), is typical of the given data. The most striking feature of this spectrum is the large shift (0.39 ppm) between the two diastereotopic protons of the aminomethylene group in the 3–4 ppm region. The value of  $\Delta\nu/J^{29}$  here is 7.5, resulting in two clearly defined doublets. In phenylthio derivative 14, R = Ph,  $\Delta\nu/J = 1.0$ , and in phenylseleno derivative 13, R = Ph,  $\Delta\nu/J < 1.0$ . These are cases in which the outside peaks are small and nonexistent, respectively. The methylene protons of 13, R = Ph, therefore appear as singlets. The large shift between aminomethylene protons, as in compounds 14, R = alkyl, has also been exhibited in

(29) Silverstein, R. M.; Bassler, G. C.; Morrill, T. C. "Spectrometric Identification of Organic Compounds", 4th ed.; Wiley: New York, 1981.

Table I. 250-MHz <sup>1</sup>H NMR Data for (η<sup>5</sup>-C<sub>5</sub>H<sub>5</sub>)Fe(η<sup>5</sup>-C<sub>5</sub>H<sub>3</sub>-1-CH<sub>2</sub>NMe<sub>2</sub>-2-ER) (13 and 14) in CDCl<sub>3</sub>/Me<sub>4</sub>Si [δ (J, Hz)]

compd	CH <sub>3</sub>	CH <sub>2</sub> CH-Me <sub>2</sub>	CH	NMe <sub>2</sub>	SCH <sub>2</sub>	NCH <sub>2</sub>	C <sub>5</sub> H <sub>5</sub>	C <sub>5</sub> H <sub>3</sub>	Ar
FeCpC <sub>5</sub> H <sub>3</sub> (CH <sub>2</sub> NMe <sub>2</sub> )(SeMe)	2.12 s			2.20 s		3.27 d (13)	4.10 s	4.18 t <sup>a</sup> 4.32 d <sup>b</sup>	
FeCpC <sub>5</sub> H <sub>3</sub> (CH <sub>2</sub> NMe <sub>2</sub> )(SePh)				2.04 s		3.45 s	4.16 s	4.34 t <sup>a</sup> 4.46 m <sup>b</sup>	7.00-7.90 m
FeCpC <sub>5</sub> H <sub>3</sub> (CH <sub>2</sub> NMe <sub>2</sub> )(Se-4-CIPh)				2.03 s		3.44 d(13)		4.42 dd <sup>a</sup> 4.46 dd <sup>a</sup>	
FeCpC <sub>5</sub> H <sub>3</sub> (CH <sub>2</sub> NMe <sub>2</sub> )(SMe)	2.27 s			2.31 s		3.73 d (13)	4.12 s	4.20 m <sup>a</sup> 4.35 m <sup>a</sup> 4.43 m <sup>a</sup>	
FeCpC <sub>5</sub> H <sub>3</sub> (CH <sub>2</sub> NMe <sub>2</sub> )(SEt)				2.19 s	2.64 m	3.21 d (13) 3.60 d (13)	4.09 s	4.16 t <sup>a</sup> 4.32 d <sup>b</sup>	
FeCpC <sub>5</sub> H <sub>3</sub> (CH <sub>2</sub> NMe <sub>2</sub> )(S- <i>i</i> -Pr)	1.15 d (6) 1.19 d (7)		3.02 m	2.18 s		3.14 d (13) 3.61 d (13)	4.08 s	4.16 s <sup>a</sup> 4.32 s <sup>b</sup>	
FeCpC <sub>5</sub> H <sub>3</sub> (CH <sub>2</sub> NMe <sub>2</sub> )(S- <i>i</i> -Bu)	0.94 d (7) 0.99 d (7) 0.99 d (7)		1.77 h (7)	2.19 s	2.45 dd (12.8) 2.45 dd (12.8)	3.20 d (13) 3.20 d (13)	4.09 s	4.14 t <sup>a</sup> 4.14 t <sup>a</sup> 4.30 m <sup>b</sup>	
FeCpC <sub>5</sub> H <sub>3</sub> (CH <sub>2</sub> NMe <sub>2</sub> )(S- <i>i</i> -pent)	0.85 d (7)	1.42 m 1.65 m	1.42 m	2.19 s	2.59 ddd (12.87) 2.70 ddd (12.87)	3.17 d (13) 3.62 d (13)	4.08 s	4.14 t <sup>a</sup> 4.30 d <sup>b</sup>	
FeCpC <sub>5</sub> H <sub>3</sub> (CH <sub>2</sub> NMe <sub>2</sub> )(SPh)				2.02 s		3.40 d (13) 3.46 d (13)	4.16 s	4.32 t <sup>a</sup> 4.46 m <sup>a</sup> 4.51 m <sup>a</sup>	6.98-7.17 m

<sup>a</sup> 1 H. <sup>b</sup> 2 H.Table II. 250-MHz <sup>1</sup>H NMR Data (δ) for (η<sup>5</sup>-C<sub>5</sub>H<sub>5</sub>)Fe(η<sup>5</sup>-C<sub>5</sub>H<sub>3</sub>-1-CH(Me)NMe<sub>2</sub>-2-ER) (15 and 16) in CDCl<sub>3</sub>/Me<sub>4</sub>Si

compd	SCCH <sub>3</sub>	NCCH <sub>3</sub>	NMe <sub>2</sub>	SCH <sub>3</sub>	SCH <sub>2</sub>	CHMe <sub>2</sub>	NCH	C <sub>5</sub> H <sub>5</sub>	C <sub>5</sub> H <sub>3</sub>	Ph
FeCpC <sub>5</sub> H <sub>3</sub> [CH(Me)NMe <sub>2</sub> ](SMe)		1.40 d	2.13 s	2.30 s			3.94 q	4.10 s	4.25 m	
FeCpC <sub>5</sub> H <sub>3</sub> [CH(Me)NMe <sub>2</sub> ](SEt)	1.15 t	1.35 d	2.10 s		2.60 q 2.75 q		3.95 q	4.10 s	4.20 m	
FeCpC <sub>5</sub> H <sub>3</sub> [CH(Me)NMe <sub>2</sub> ](S- <i>i</i> -Pr)	1.15 d 1.22 d	1.34 d	2.12 s			3.20 m	4.00 q	4.08 s	4.17-4.33 m	
FeCpC <sub>5</sub> H <sub>3</sub> [CH(Me)NMe <sub>2</sub> ](SPh)		1.45 d	1.90 s				3.85 q	4.18 s	4.30-4.53 m	7.05-7.25 m
FeCpC <sub>5</sub> H <sub>3</sub> [CH(Me)NMe <sub>2</sub> ](SBz)		1.39 d	2.21 s		3.86-4.00 m <sup>a</sup>		2.21 s	4.06 s	4.10 m	7.18 m
FeCpC <sub>5</sub> H <sub>3</sub> [CH(Me)NMe <sub>2</sub> ](SePh)		1.45 d	1.93 s				3.86 q	4.16 s	4.20-4.50 m	7.00-7.50 m

<sup>a</sup> Obscured.Table III. <sup>13</sup>C NMR Data for (η<sup>5</sup>-C<sub>5</sub>H<sub>5</sub>)Fe(η<sup>5</sup>-C<sub>5</sub>H<sub>3</sub>-1-CH<sub>2</sub>NMe<sub>2</sub>-2-ER) (13 and 14) in CDCl<sub>3</sub>/Me<sub>4</sub>Si (δ)

compd	CH <sub>3</sub>	CH	CH <sub>2</sub> CHMe <sub>2</sub>	SCH <sub>2</sub>	NMe <sub>2</sub>	NCH <sub>2</sub>	C <sub>3</sub> , C <sub>4</sub> , C <sub>5</sub>	C <sub>5</sub> H <sub>5</sub>	C <sub>2</sub>	C <sub>1</sub>	Ar
FeCpC <sub>5</sub> H <sub>3</sub> (CH <sub>2</sub> NMe <sub>2</sub> )(SeMe)	9.6 q				45.1 q	58.1 t	68.4 d 70.5 d 73.9 d	69.8 d	75.1 s	87.2 s	
FeCpC <sub>5</sub> H <sub>3</sub> (CH <sub>2</sub> NMe <sub>2</sub> )(Se-4-CIPh)					45.3 q	58.5 t	70.4 d 72.5 d 77.2 d	70.7 d	72.4 s	89.5 s	129.4 d 131.9 d 132.1 s 134.6 s
FeCpC <sub>5</sub> H <sub>3</sub> (CH <sub>2</sub> NMe <sub>2</sub> )(SMe)	20.2 q				44.2 q	56.6 t	68.0 d 70.8 d 71.9 d	70.0 d	83.6 s	84.3 s	
FeCpC <sub>5</sub> H <sub>3</sub> (CH <sub>2</sub> NMe <sub>2</sub> )(SEt)	14.8 q			30.7 t	45.1 q	57.2 t	67.4 d 70.6 d 73.7 d	69.8 d	80.5 s	87.0 s	
FeCpC <sub>5</sub> H <sub>3</sub> (CH <sub>2</sub> NMe <sub>2</sub> )(S- <i>i</i> -Pr)	22.8 q 23.6 q	39.4 d			45.3 q	57.3 t	67.6 d 70.9 d 75.1 d	69.6 d	79.0 s	88.0 s	
FeCpC <sub>5</sub> H <sub>3</sub> (CH <sub>2</sub> NMe <sub>2</sub> )(S- <i>i</i> -Bu)	21.8 q 22.3 q	28.5 d		46.3 t	45.2 q	57.3 t	67.5 d 70.6 d 73.3 d	70.0 d	81.9 s	87.1 s	
FeCpC <sub>5</sub> H <sub>3</sub> (CH <sub>2</sub> NMe <sub>2</sub> )(S- <i>i</i> -pent)	22.1 q 22.4 q	27.2 d	35.1 t	38.6 t	45.2 q	57.3 t	67.4 d 70.7 d 73.6 d	69.9 d	81.2 s	87.2 s	
FeCpC <sub>5</sub> H <sub>3</sub> (CH <sub>2</sub> NMe <sub>2</sub> )(SPh) (14)					45.0 q	56.7 t	69.0 d 71.3 d 75.6 d	70.3 d	76.4 s	87.6 s	124.8 d <sup>a</sup> 128.4 d <sup>b</sup> 126.2 d <sup>c</sup> 140.1 s <sup>d</sup>

<sup>a</sup> Para. <sup>b</sup> Meta. <sup>c</sup> Ortho. <sup>d</sup> S-C.1-[(dimethylamino)methyl]-2-(diphenylphosphino)-ferrocene.<sup>30</sup>

Inversion of the pyramidal N of derivatives 13-16 is faster than the NMR time scale, so the nitrogen methyls

appear as singlets in the 1.9-2.3 ppm region. Assignments of the substituted ring protons H<sub>3</sub>, H<sub>4</sub>, and H<sub>5</sub> in 13-16 have not been made since a number of studies<sup>31-33</sup> of(31) Rausch, M. D.; Siegel, A. *J. Organomet. Chem.* **1969**, *17*, 117-125.(32) Slocum, D. W.; Ernst, C. R. *Adv. Organomet. Chem.* **1972**, *10*, 79-114.(30) Marr, G.; Hunt, T. *J. Chem. Soc. C* **1969**, 1070-1072.



Table IV. Homogeneous Selective Hydrogenation of Dienes to Monoenes

initial rate, mol/mol of Pd/h/psi	substrate	T, °C	metal	solvent	additive	ref
6.92	1,3-COD	27	Pd <sup>2+</sup>	acetone		this work
8.99	1,3-COD	22	Pd <sup>0</sup>	toluene	H <sub>2</sub> O	47
3.45–5.52	isoprene	22	Pd <sup>0</sup>	toluene		45
0.0011	1,4-cyclohexadiene	65	Pd <sup>2+</sup>	toluene		53

<sup>a</sup> COD = cyclooctadiene. Ligands vary from case to case. Complex 19 was used in the first entry.

monosubstituted ferrocenes have shown that a single substituent may deshield or shield positions 2 and 5 and may deshield or shield positions 3 and 4, in any combination relative to ferrocene.

Carbon-13 NMR spectra of compounds 13 and 14 are given in Table III. Since the molecules have a C<sub>1</sub> symmetry due to planar chirality,<sup>34</sup> groups such as isopropyl methyls are diastereotopic and appear at different chemical shifts. As in the proton spectra, the NMe<sub>2</sub> carbons are equivalent due to fast inversion. Broad-band and either gated<sup>35,36</sup> or off-resonance decoupled spectra were recorded. Methyl singlets in the broad-band decoupled spectra appear as quartets in the gated or off-resonance decoupled spectra, methylenes as triplets, etc. Aside from the aryl carbons, the two most downfield peaks in Table III are due to substituted ring carbons C<sub>2</sub> and C<sub>1</sub>, with the shift of C<sub>1</sub> greater than that of C<sub>2</sub> for Se analogue while C<sub>2</sub> is greater than C<sub>1</sub> for S analogue. These assignments are firm and are based on the following observations: (1) the decoupled spectra reveal the two peaks as singlets (substituted carbons), (2) the Se–S change in Table III occurs in the C<sub>1</sub> column, not C<sub>2</sub>, and (3) C<sub>2</sub> of 13, R = Me (Table III) appears at 75.1 ppm, C<sub>1</sub> of 17, R = Me (Experimental Section) at 75.5 ppm, and C<sub>1</sub> of 18 (Experimental Section) at 74.4 ppm. The constancy of chemical shift of the ring carbon atoms attached to selenium in these last three compounds in the face of the alternative assignment of 13, R = Me (87.2 ppm), provides particularly convincing evidence that the assignments are correct.

Carbons 3, 4, and 5 in Table III are, on the other hand, difficult to assign, even on comparison with known assignments in [(dimethylamino)methyl]ferrocene<sup>37</sup> and with an extensive body of literature on  $\pi$ -polarization.<sup>38,39</sup> The proton assignments H<sub>3</sub>, H<sub>4</sub>, and H<sub>5</sub>, if known, would be of no help. In some cases the chemical shift ordering is the same, but in ferrocenecaraldehyde, for example, the carbon order is C<sub>3</sub> > C<sub>2</sub>,<sup>40</sup> whereas the proton order is H<sub>2</sub> > H<sub>3</sub>.<sup>31–33</sup>

Comparison of 13, R = Me, and 14, R = Me, in Table III shows, as expected, that the inductive effect of Se is less than that of S. Carbons attached to Se appear upfield of analogous carbons attached to S (methyls,  $\delta$  9.6 and 20.2;

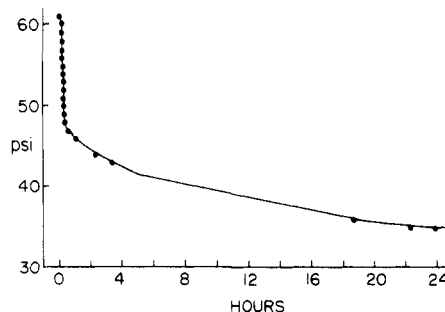


Figure 2. H<sub>2</sub> uptake plot for the hydrogenation of 1,3-cyclooctadiene with 19 in acetone.

C<sub>2</sub>,  $\delta$  72.1 and 83.6).

The infrared spectra of the compounds of this paper are given in the Experimental Section. Compounds 13, 15, 14, 16, and 18 obey the "1000, 1100 rule"<sup>41</sup> which states that ferrocenes containing an unsubstituted ring will have two peaks, one near 1000 cm<sup>-1</sup> due to C–H bend parallel to the C<sub>5</sub>H<sub>5</sub> ring and another near 1100 cm<sup>-1</sup> due to an antisymmetric C<sub>5</sub>H<sub>5</sub> ring breathing mode. Thioethers have a C–S stretch near 660 cm<sup>-1</sup>, usually too weak to be of use,<sup>29</sup> as is the case here.

The mass spectra of these compounds exhibit molecular ions, expected fragments, and smaller peaks consistent with isotopes <sup>54</sup>Fe, <sup>57</sup>Fe, <sup>34</sup>S, and <sup>78</sup>Se.

**Hydrogenation and Isomerization by Using Palladium Complex 19.** Hydrogenation by homogeneous catalysts is well developed.<sup>43</sup> Of the many known complexes, those of group VIII (8–10<sup>61</sup>) metals with amines and sulfides have been used with varying degrees of success. In 1967 PtCl<sub>2</sub>(SPh<sub>2</sub>)<sub>2</sub> was found to be selective for the hydrogenation of dienes to monoenes in the presence of SnCl<sub>2</sub>.<sup>44</sup> Treatment of PdCl<sub>2</sub> or Na<sub>2</sub>PdCl<sub>4</sub> with tertiary amines resulted in an active selective catalyst.<sup>45</sup> The same was true of PdCl<sub>2</sub> when treated with 2,2'-bipyridine and NaBH<sub>4</sub>.<sup>46</sup> Palladium chloride and thioethers gave complexes which, upon reduction by diisobutylaluminum hydride, were selective catalysts.<sup>47</sup> The thioether–rhodium complex RhCl<sub>3</sub>(SEt<sub>2</sub>)<sub>3</sub> hydrogenates maleic acid, provided maleic acid is present in excess.<sup>48–51</sup>

(33) Slocum, D. W.; Ernst, C. R. *Organomet. Chem. Rev. A* 1970, 6, 337–353.

(34) Testa, B. "Principles of Organic Stereochemistry"; Marcel Dekker: New York, 1979; Chapter 7.

(35) Gunther, H. "NMR Spectroscopy"; Wiley: Chichester, 1980; pp 359–360.

(36) Levy, G. C.; Lichter, R. L.; Nelson, G. L. "Carbon-13 Nuclear Magnetic Resonance Spectroscopy", 2nd ed.; Wiley: New York, 1980; Chapter 1.

(37) Koridze, A. A.; Petrovskii, P. V.; Mokhov, A. I.; Lutsenko, A. I. *J. Organomet. Chem.* 1977, 136, 57–63.

(38) Bromilow, J.; Brownlee, R. T. C.; Craik, D. J.; Fiske, P. R.; Rowe, J. E.; Sadek, M. *J. Chem. Soc., Perkin Trans. 2* 1981, 753–759.

(39) Craik, D. J.; Brownlee, R. T. C. *Prog. Phys. Org. Chem.* 1983, 14, 1–73.

(40) Koridze, A. A.; Mokhov, A. I.; Petrovskii, P. V.; Fedin, E. I. *Izv. Akad. Nauk SSSR, Ser. Khim.* 1974, 2156.

(41) Rosenblum, M. "Chemistry of the Iron Group Metalloenes"; Wiley: New York, 1965; pp 37–40.

(42) Lindoy, L. F.; Livingstone, S. E.; Lockyer, T. N. *Aust. J. Chem.* 1967, 20, 471–478.

(43) Parshall, G. W. "Homogeneous Catalysis"; Wiley: New York, 1980.

(44) Tayim, H. A.; Bailar, J. C., Jr. *J. Am. Chem. Soc.* 1967, 89, 4330–4338.

(45) Frolov, V. M.; Parenago, O. P.; Bonarenko, G. N.; Kovaleva, L. S.; El'natanova, A. I.; Shiukina, L. P.; Cherkashin, G. M.; Mirskaya, E. Y. *Kinet. Katal.* 1981, 22, 1356–1357.

(46) Shuikina, L. P.; El'natanova, A. I.; Kovaleva, L. S.; Parenago, O. P.; Frolov, V. M. *Kinet. Katal.* 1981, 22, 177–182.

(47) Shuikina, L. P.; Cherkashin, G. M.; Parenago, O. P.; Frolov, V. M. *Dokl. Akad. Nauk SSSR* 1981, 257, 655–659.

(48) James, B. R.; Ng, F. T. T.; Rempel, G. L. *Inorg. Nucl. Chem. Lett.* 1968, 4, 197–199.

(49) James, B. R.; Ng, F. T. T. *J. Chem. Soc., Dalton Trans.* 1972, 355–359.

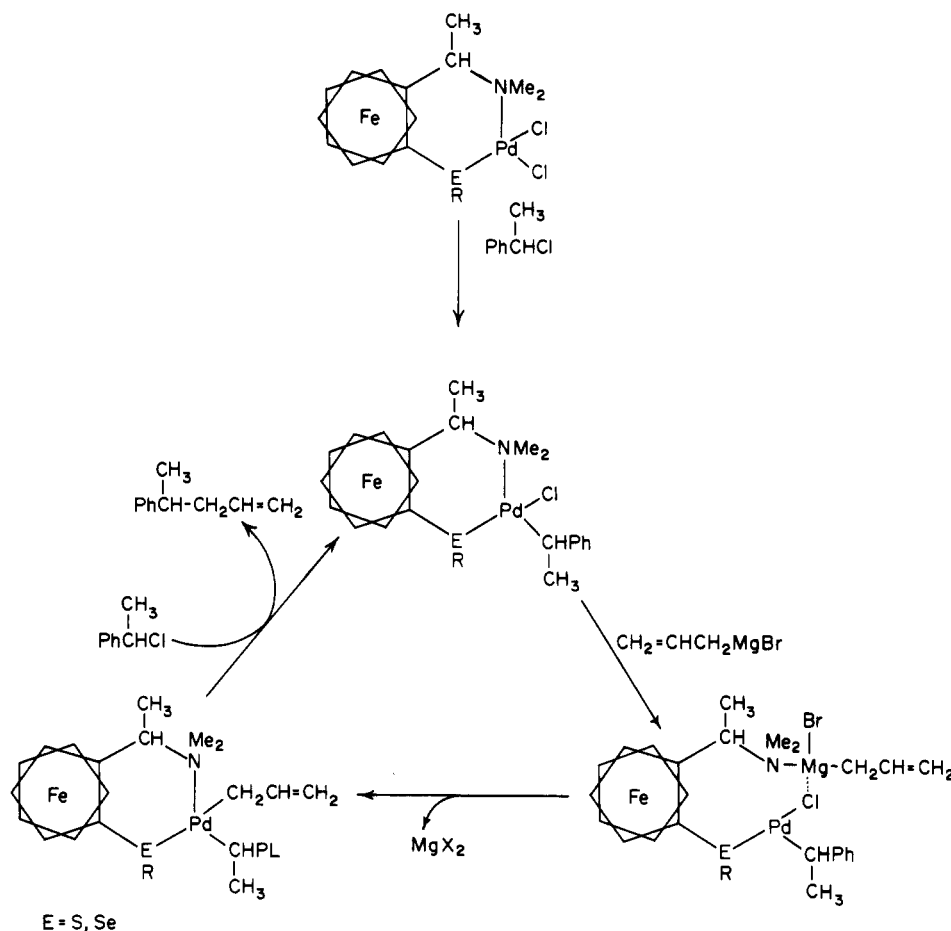
(50) James, B. R.; Ng, F. T. T. *J. Chem. Soc., Dalton Trans.* 1972, 1321–1324.

(51) Cross, R. J. *Int. Rev. Sci.: Inorg. Chem., Ser. Two* 1974, 5, 147–170.

(52) Chatt, J.; Leigh, G. J.; Storace, A. P. *J. Chem. Soc. A* 1971, 1380–1389.



Scheme I. Proposed Mechanism for Grignard Cross-Coupling Reaction

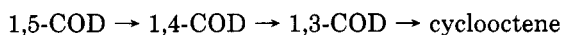


In view of the selective hydrogenation activity of amine-palladium and thioether-palladium complexes when treated with hydride reducing agents,<sup>46,47</sup> a number of similar procedures were tried by using ferrocene-palladium complex 19 and  $\text{NaH}_2\text{Al}(\text{OCH}_2\text{CH}_2\text{OCH}_3)_2$  in various solvents at various temperatures and pressures.

Complex 19 was inactive in  $\text{CH}_2\text{Cl}_2$  (without a reducing agent) at 101 psi but became active after 10 mol of  $\text{H}_2\text{O}$  per mol of Pd was added. This is a heterogeneous system with a black precipitate (possibly Pd metal) which hydrogenates 1,3-cyclooctadiene to cyclooctene, but only at a slow rate. The complex also forms an active heterogeneous system in acetone at 1 atm. The original red solution became cloudy after 36 h and  $\text{H}_2$  uptake began. Here again, though, the rate was low.

Hydrogenation of 1,3-cyclooctadiene became conveniently fast in acetone at 61 psi. This is a homogeneous system with no  $\text{H}_2\text{O}$  or reducing agents, and reaction proceeds at a useful rate (422 mol/mol of Pd/h). As time passed the red solution became brown but remained homogeneous. Most of the product at the end of reaction was cyclooctene, but some cyclooctane was present. The hydrogen uptake plot for the reaction is given in Figure 2.

Complex 19 isomerized and hydrogenated 1,5-cyclooctadiene according to



This is a homogeneous reaction that proceeds at a low rate.

In order to assess its effectiveness as a selective hydrogenation catalyst, complex 19 is compared to previous homogeneous Pd catalysts in Table IV. The initial rates have been normalized as much as possible by dividing by the number of moles of Pd and the pressure. The catalyst

in this work and that of the second entry (PdCl<sub>2</sub> complexed by undecylamine, reduced by diisobutylaluminum hydride, and hydrolyzed)<sup>47</sup> have rates of the same order of magnitude with 1,3-cyclooctadiene. The third (catalyst = PdCl<sub>2</sub> complexed by trialkylamines)<sup>45</sup> and fourth [catalyst =  $(\text{Ph}_2\text{PCH}_2\text{Ph}_2)\text{PdCl}_2$ ]<sup>53</sup> entries are not as comparable to this work as the second entry. As has been pointed out,<sup>53</sup> rates and selectivities are affected most by substrates and to a smaller extent by ligands, oxidation state of the metal, and solvents. With this in mind, the catalyst in this work appears to be at least as fast as the amine catalyst in entry 3 and 3 orders of magnitude faster than the chelating bis(phosphine) in entry 4.

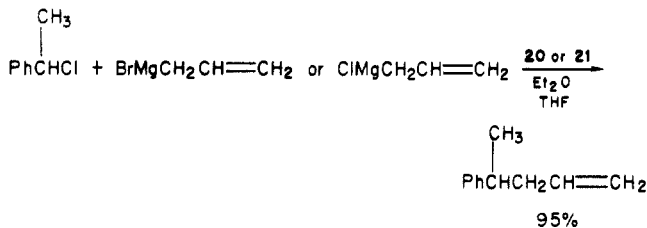
It is possible that the homogeneous hydrogenation proceeds in acetone but not methylene chloride because the acetone replaces the amine or the thioether as a Pd ligand. According to this scheme,  $\text{H}_2$  adds to the acetone-amine-Pd complex or acetone-thioether-Pd complex but not to the amine-thioether-Pd complex. The heterogeneous reaction with  $\text{H}_2\text{O}$  and  $\text{CH}_2\text{Cl}_2$  may proceed via hydrolysis of a Pd-Cl bond,<sup>47</sup> making a hydroxo ligand and HCl. The acid causes formation of an amine hydrochloride, which either precipitates directly or loses its ability to coordinate Pd.

**Grignard Cross-Coupling Reactions by Using Palladium Complexes 20 and 21.** Since the first report in 1975 that Pd complexes catalyze the coupling of Grignard reagents with organic halides,<sup>54</sup> the method has been used on a variety of Grignard reagents and halogenated species. Kumada's group has done important work with many

(53) Stern, E. W.; Maples, P. K. *J. Catal.* 1972, 27, 120-133.

(54) Yamamura, M.; Mirotoni, I.; Murahashi, S.-I. *J. Organomet. Chem.* 1975, 91, C39-C42.

ligands and substrates,<sup>55</sup> and chloropyridines,<sup>56</sup> bromopurpur nucleosides,<sup>57</sup> and iodine carborane<sup>58</sup> have also been used. In these papers, all of the Pd donor atoms come from group VA (15<sup>61</sup>) (N and P). We have now expanded this to group VIA (16<sup>61</sup>) (S and Se).



Thioether-amine-palladium complex **20** catalyzed formation of 4-phenyl-1-pentene from 1-phenyl-1-chloroethane and allylmagnesium chloride at 0 °C in high yield (93%) in 40 h. The selenium analogue **21** was just as effective (91.6% with allylmagnesium chloride at 10 °C for 25 h). Allylmagnesium bromide with **21** gave an even better yield (98%) after 40 h at 0 °C. These are homogeneous reactions. The postulated mechanism<sup>55a</sup> in phosphine-amine-palladium complexes involves breaking the N-Pd bond and making an N-Mg bond, while the P-Pd bond remains intact. The analogous situation here

involves an intact ion of a S-Pd or a Se-Pd bond. Although thioethers have a lower  $\pi$ -acceptor capacity than tertiary phosphines,<sup>59</sup> the strength of the S-Pd bond, and presumably the Se-Pd bond, is still significant and results in high yields.<sup>60</sup> Scheme I illustrates the proposed mechanism for the cross-coupling reaction.

**Registry No.** 1, 1271-86-9; (R)-4, 31886-58-5; (s)-4, 31886-57-4; 7, 102-54-5; 10, 1273-73-0; 13 (R = Me), 100113-86-8; 13 (R = Ph), 100113-87-9; 13 (R = 4-chlorophenyl), 100113-88-0; 14 (R = Me), 12248-18-9; 14 (R = Et), 100113-89-1; 14 (R = *i*-Pr), 100113-90-4; 14 (R = *i*-Bu), 100113-91-5; 14 (R = isopentyl), 100113-92-6; 14 (R = Ph), 100113-93-7; 15 (R = Me), 100113-94-8; 15 (R = Et), 100113-95-9; 15 (R = *i*-Pr), 100113-96-0; 15 (R = Ph), 100113-97-1; 15 (R = CH<sub>2</sub>Ph), 100113-98-2; 16, 100113-99-3; 17 (R = me), 100114-00-9; 17 (R = Ph), 100114-02-1; 18, 100114-01-0; 19, 100165-36-4; 20, 100165-37-5; 21, 100165-38-6; 22, 100165-39-7; 23 (R = Me), 100114-03-2; 23 (R = 4-chlorophenyl), 100165-40-0; Me<sub>2</sub>Se<sub>2</sub>, 7101-31-7; Ph<sub>2</sub>Se<sub>2</sub>, 1666-13-3; Me<sub>2</sub>S<sub>2</sub>, 624-92-0; Et<sub>2</sub>S<sub>2</sub>, 110-81-6; (*i*-Pr)<sub>2</sub>S<sub>2</sub>, 4253-89-8; (*i*-Bu)<sub>2</sub>S<sub>2</sub>, 1518-72-5; Ph<sub>2</sub>S<sub>2</sub>, 882-33-7; (4-chlorophenyl)<sub>2</sub>S<sub>2</sub>, 20541-49-5; (isopentyl)<sub>2</sub>S<sub>2</sub>, 2051-04-9; (PhCH<sub>2</sub>)<sub>2</sub>S<sub>2</sub>, 150-60-7; K<sub>2</sub>PdCl<sub>4</sub>, 10025-98-6; (PhCN)<sub>2</sub>PdCl<sub>2</sub>, 14220-64-5; 1,3-cyclooctadiene, 1700-10-3; cyclooctene, 931-88-4; cyclooctane, 292-64-8; 1,5-cyclooctadiene, 111-78-4; 1,4-cyclooctadiene, 1073-07-0; 1-phenylethyl chloride, 672-65-1; allylmagnesium chloride, 2622-05-1; 4-phenyl-1-pentene, 10340-49-5; allylmagnesium bromide, 1730-25-2.

(55) (a) Hayashi, T.; Mitsuo, K.; Fukushima, M.; Mise, T.; Kagotani, M.; Tajika, M.; Kumada, M. *J. Am. Chem. Soc.* **1982**, *104*, 180-186. (b) Hayashi, T.; Okamoto, Y.; Kumada, M. *Tetrahedron Lett.* **1983**, *24*, 807-808. (c) Hayashi, T.; Konishi, M.; Kobori, Y.; Kumada, M.; Higuchi, T.; Hirotsu, K. *J. Am. Chem. Soc.* **1984**, *106*, 158-163.

(56) Isobe, K.; Kawaguchi, S. *Heterocycles* **1981**, *16*, 1603-1612.

(57) Cong-Danh, N.; Beaucourt, J.-P.; Pichat, L. *Tetrahedron Lett.* **1979**, 3159-3162.

(58) Zakharkin, L. I.; Kovredov, A. I.; Ol'shevskaya, V. A.; Shaugum-bekova, Z. S. *J. Organomet. Chem.* **1982**, *226*, 217-222.

(59) Murray, S. G.; Hartley, F. R. *Chem. Rev.* **1981**, *81*, 365-414.

(60) Efforts are under way to determine the enantiomeric excess present in the 4-phenyl-1-pentene made in these reactions.

(61) In this paper the periodic group notation (in parentheses) is in accord with recent actions by IUPAC and ACS nomenclature committees. A and B notation is eliminated because of wide confusion. Groups IA and IIA became groups 1 and 2. The d-transition elements comprise groups 3 through 12, and the p-block elements comprise groups 13 through 18. (Note that the former Roman number designation is preserved in the last digit of the new numbering: e.g., III $\rightarrow$ 3 and 13.)

## $\pi$ -Facial Stereoselectivity Operational during Conversion of Isodicyclopentadienes to Metallocene Derivatives<sup>1</sup>

Leo A. Paquette,\* Paulo F. T. Schirch, Susan J. Hathaway, Leh-Yeh Hsu,<sup>2</sup> and Judith C. Gallucci<sup>2</sup>

Evans Chemical Laboratories, The Ohio State University, Columbus, Ohio 43210

Received May 21, 1985

Reaction of the isodicyclopentadienide anion with Fe<sup>II</sup>(acac)<sub>2</sub>(py)<sub>2</sub>, RuCl<sub>3</sub>, and OsCl<sub>4</sub> is shown to provide the corresponding metallocene derivatives. The first two complexes are unequivocally established to be the end result of exo complexation to both ligands. The air sensitivity of the osmocene derivative, particularly in solution, precluded its complete characterization. The reactions of 4-(dimethylamino)isodicyclopentafulvene with ( $\eta^5$ -cyclopentadienyl)( $\eta^6$ -*p*-xylene)iron(II) hexafluorophosphate and ( $\eta^5$ -cyclopentadienyl)tris(acetonitrile)ruthenium(III) hexafluorophosphate were also investigated. In the first instance, a 65:35 mixture of *exo*- and *endo*-( $\eta^5$ -cyclopentadienyl)( $\eta^5$ -4-formyltricyclo[5.2.1.0<sup>2,6</sup>]deca-2,4-dien-6-yl)iron (**29** and **30**) was produced after alkaline hydrolysis. These isomers were separated following conversion to their alcohols, with the respective three-dimensional structures being established by X-ray analysis of the dimeric ether derived from the major alcohol. In the ruthenium example, a higher proportion of the *exo* complex **35** (86%) was obtained. Purification was achieved by recrystallization, allowing for crystallographic structural confirmation.

### Introduction

The isodicyclopentadiene ring system (**1**) is of fundamental importance as the result of differing electronic

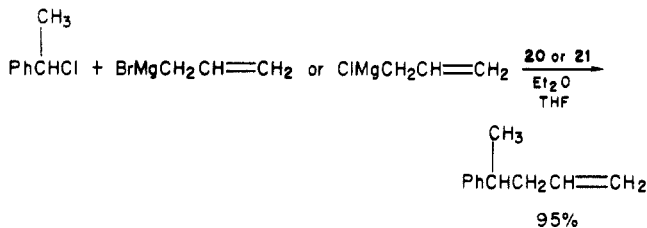
densities on the surfaces of its cyclopentadiene ring and the appreciable  $\pi$ -facial stereoselectivity exhibited during cycloaddition reactions.<sup>3</sup> That ground-state electronic influences are not identical above and below the dienyl

(1) Electronic Control of Stereoselectivity. 32. For part 31, see: Paquette, L. A.; Kravetz, T. M.; Hsu, L.-Y. *J. Am. Chem. Soc.* **1985**, *107*, 6598.

(2) Authors to whom inquiries concerning the X-ray crystal structure analyses should be directed: L.-Y. Hsu for structures **21** and **33** and J. C. Gallucci for structure **35**.

(3) (a) Paquette, L. A. In "Stereochemistry and Reactivity of Pi Systems"; Watson, W. H., Ed.; Verlag Chemie: Deerfield Beach, FL, 1983; pp 41-73. (b) Gleiter, R.; Paquette, L. A. *Acc. Chem. Res.* **1983**, *16*, 328.

ligands and substrates,<sup>55</sup> and chloropyridines,<sup>56</sup> bromopurpur nucleosides,<sup>57</sup> and iodine carborane<sup>58</sup> have also been used. In these papers, all of the Pd donor atoms come from group VA (15<sup>61</sup>) (N and P). We have now expanded this to group VIA (16<sup>61</sup>) (S and Se).



Thioether-amine-palladium complex **20** catalyzed formation of 4-phenyl-1-pentene from 1-phenyl-1-chloroethane and allylmagnesium chloride at 0 °C in high yield (93%) in 40 h. The selenium analogue **21** was just as effective (91.6% with allylmagnesium chloride at 10 °C for 25 h). Allylmagnesium bromide with **21** gave an even better yield (98%) after 40 h at 0 °C. These are homogeneous reactions. The postulated mechanism<sup>55a</sup> in phosphine-amine-palladium complexes involves breaking the N-Pd bond and making an N-Mg bond, while the P-Pd bond remains intact. The analogous situation here

involves an intact ion of a S-Pd or a Se-Pd bond. Although thioethers have a lower  $\pi$ -acceptor capacity than tertiary phosphines,<sup>59</sup> the strength of the S-Pd bond, and presumably the Se-Pd bond, is still significant and results in high yields.<sup>60</sup> Scheme I illustrates the proposed mechanism for the cross-coupling reaction.

**Registry No.** 1, 1271-86-9; (R)-4, 31886-58-5; (s)-4, 31886-57-4; 7, 102-54-5; 10, 1273-73-0; 13 (R = Me), 100113-86-8; 13 (R = Ph), 100113-87-9; 13 (R = 4-chlorophenyl), 100113-88-0; 14 (R = Me), 12248-18-9; 14 (R = Et), 100113-89-1; 14 (R = *i*-Pr), 100113-90-4; 14 (R = *i*-Bu), 100113-91-5; 14 (R = isopentyl), 100113-92-6; 14 (R = Ph), 100113-93-7; 15 (R = Me), 100113-94-8; 15 (R = Et), 100113-95-9; 15 (R = *i*-Pr), 100113-96-0; 15 (R = Ph), 100113-97-1; 15 (R = CH<sub>2</sub>Ph), 100113-98-2; 16, 100113-99-3; 17 (R = me), 100114-00-9; 17 (R = Ph), 100114-02-1; 18, 100114-01-0; 19, 100165-36-4; 20, 100165-37-5; 21, 100165-38-6; 22, 100165-39-7; 23 (R = Me), 100114-03-2; 23 (R = 4-chlorophenyl), 100165-40-0; Me<sub>2</sub>Se<sub>2</sub>, 7101-31-7; Ph<sub>2</sub>Se<sub>2</sub>, 1666-13-3; Me<sub>2</sub>S<sub>2</sub>, 624-92-0; Et<sub>2</sub>S<sub>2</sub>, 110-81-6; (*i*-Pr)<sub>2</sub>S<sub>2</sub>, 4253-89-8; (*i*-Bu)<sub>2</sub>S<sub>2</sub>, 1518-72-5; Ph<sub>2</sub>S<sub>2</sub>, 882-33-7; (4-chlorophenyl)<sub>2</sub>S<sub>2</sub>, 20541-49-5; (isopentyl)<sub>2</sub>S<sub>2</sub>, 2051-04-9; (PhCH<sub>2</sub>)<sub>2</sub>S<sub>2</sub>, 150-60-7; K<sub>2</sub>PdCl<sub>4</sub>, 10025-98-6; (PhCN)<sub>2</sub>PdCl<sub>2</sub>, 14220-64-5; 1,3-cyclooctadiene, 1700-10-3; cyclooctene, 931-88-4; cyclooctane, 292-64-8; 1,5-cyclooctadiene, 111-78-4; 1,4-cyclooctadiene, 1073-07-0; 1-phenylethyl chloride, 672-65-1; allylmagnesium chloride, 2622-05-1; 4-phenyl-1-pentene, 10340-49-5; allylmagnesium bromide, 1730-25-2.

(55) (a) Hayashi, T.; Mitsuo, K.; Fukushima, M.; Mise, T.; Kagotani, M.; Tajika, M.; Kumada, M. *J. Am. Chem. Soc.* **1982**, *104*, 180-186. (b) Hayashi, T.; Okamoto, Y.; Kumada, M. *Tetrahedron Lett.* **1983**, *24*, 807-808. (c) Hayashi, T.; Konishi, M.; Kobori, Y.; Kumada, M.; Higuchi, T.; Hirotsu, K. *J. Am. Chem. Soc.* **1984**, *106*, 158-163.

(56) Isobe, K.; Kawaguchi, S. *Heterocycles* **1981**, *16*, 1603-1612.

(57) Cong-Danh, N.; Beaucourt, J.-P.; Pichat, L. *Tetrahedron Lett.* **1979**, 3159-3162.

(58) Zakharkin, L. I.; Kovredov, A. I.; Ol'shevskaya, V. A.; Shaugum-bekova, Z. S. *J. Organomet. Chem.* **1982**, *226*, 217-222.

(59) Murray, S. G.; Hartley, F. R. *Chem. Rev.* **1981**, *81*, 365-414.

(60) Efforts are under way to determine the enantiomeric excess present in the 4-phenyl-1-pentene made in these reactions.

(61) In this paper the periodic group notation (in parentheses) is in accord with recent actions by IUPAC and ACS nomenclature committees. A and B notation is eliminated because of wide confusion. Groups IA and IIA became groups 1 and 2. The d-transition elements comprise groups 3 through 12, and the p-block elements comprise groups 13 through 18. (Note that the former Roman number designation is preserved in the last digit of the new numbering: e.g., III $\rightarrow$ 3 and 13.)

## $\pi$ -Facial Stereoselectivity Operational during Conversion of Isodicyclopentadienes to Metallocene Derivatives<sup>1</sup>

Leo A. Paquette,\* Paulo F. T. Schirch, Susan J. Hathaway, Leh-Yeh Hsu,<sup>2</sup> and Judith C. Gallucci<sup>2</sup>

Evans Chemical Laboratories, The Ohio State University, Columbus, Ohio 43210

Received May 21, 1985

Reaction of the isodicyclopentadienide anion with Fe<sup>II</sup>(acac)<sub>2</sub>(py)<sub>2</sub>, RuCl<sub>3</sub>, and OsCl<sub>4</sub> is shown to provide the corresponding metallocene derivatives. The first two complexes are unequivocally established to be the end result of exo complexation to both ligands. The air sensitivity of the osmocene derivative, particularly in solution, precluded its complete characterization. The reactions of 4-(dimethylamino)isodicyclopentafulvene with ( $\eta^5$ -cyclopentadienyl)( $\eta^6$ -*p*-xylene)iron(II) hexafluorophosphate and ( $\eta^5$ -cyclopentadienyl)tris(acetonitrile)ruthenium(III) hexafluorophosphate were also investigated. In the first instance, a 65:35 mixture of *exo*- and *endo*-( $\eta^5$ -cyclopentadienyl)( $\eta^5$ -4-formyltricyclo[5.2.1.0<sup>2,6</sup>]deca-2,4-dien-6-yl)iron (**29** and **30**) was produced after alkaline hydrolysis. These isomers were separated following conversion to their alcohols, with the respective three-dimensional structures being established by X-ray analysis of the dimeric ether derived from the major alcohol. In the ruthenium example, a higher proportion of the *exo* complex **35** (86%) was obtained. Purification was achieved by recrystallization, allowing for crystallographic structural confirmation.

### Introduction

The isodicyclopentadiene ring system (**1**) is of fundamental importance as the result of differing electronic

densities on the surfaces of its cyclopentadiene ring and the appreciable  $\pi$ -facial stereoselectivity exhibited during cycloaddition reactions.<sup>3</sup> That ground-state electronic influences are not identical above and below the dienyl

(1) Electronic Control of Stereoselectivity. 32. For part 31, see: Paquette, L. A.; Kravetz, T. M.; Hsu, L.-Y. *J. Am. Chem. Soc.* **1985**, *107*, 6598.

(2) Authors to whom inquiries concerning the X-ray crystal structure analyses should be directed: L.-Y. Hsu for structures **21** and **33** and J. C. Gallucci for structure **35**.

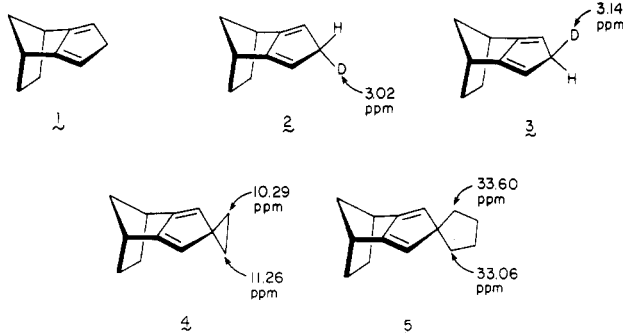
(3) (a) Paquette, L. A. In "Stereochemistry and Reactivity of Pi Systems"; Watson, W. H., Ed.; Verlag Chemie: Deerfield Beach, FL, 1983; pp 41-73. (b) Gleiter, R.; Paquette, L. A. *Acc. Chem. Res.* **1983**, *16*, 328.

Table I. Comparative  $^1\text{H}$  NMR Spectral Data for 16 and 22 ( $\text{CDCl}_3$  Solution,  $\delta$ )

proton	16 <sup>a</sup>	22 <sup>b</sup>
central cyclopentadienide (2)	3.95 (s)	4.28 (s)
peripheral cyclopentadienide (4)	3.74 (s)	4.23 (s)
bridgehead (4)	2.85 (s)	2.76 (s)
syn-methano bridge (4)	2.28 (d, $J = 8$ Hz)	
exo-ethano bridge (4)	1.74–1.69 (m)	1.79–1.66 (m)
anti-ethano bridge (2)	1.35 (d, $J = 8$ Hz)	1.28 (d, $J = 8$ Hz)
endo-ethano bridge (4)	1.02–0.95 (m)	1.17 (dd, $J = 8$ and 2 Hz)

<sup>a</sup> At 200 MHz. <sup>b</sup> At 300 MHz.

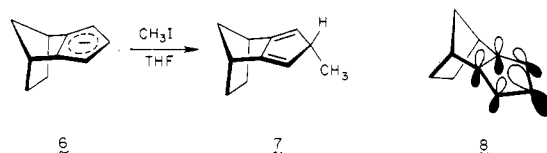
moiety is readily discerned by  $^2\text{H}$  and  $^{13}\text{C}$  NMR spectroscopy in simple derivatives such as 2–5.<sup>4</sup> Especially



relevant is recognition that the affected atoms differ only in their relative spatial disposition to a methano or ethano bridge at the other, remote end of the structure. Theoretical calculations suggest disrotatory terminal  $\pi$ -orbital tilting to be responsible.<sup>5</sup> Although the strained norbornane  $\sigma$ -electron network is the chief perpetrator of this interesting phenomenon, contributions arising from other alkyl groups must also be considered.<sup>6</sup> These effects are thought to be manifested as well in cycloaddition transition states and to be responsible for preferred below-plane Diels–Alder capture of 1<sup>6–9</sup> and above-plane [6 + 4] bonding to tropone and oxallyl cations.<sup>10</sup> Other inter-

pretations of this stereoselectivity have been advanced.<sup>7,8,11</sup>

The derived anion 6 is likewise recognized to possess an ensemble of  $p\pi$  orbitals intrinsically capable of face selectivity toward diverse electrophilic reagents.<sup>6a,12</sup> Its proclivity for below-plane bond formation is exemplified by the exclusive formation of 7 upon reaction with methyl iodide in tetrahydrofuran solution. INDO calculations



again reveal that high-lying norbornyl  $\sigma$  orbitals in 6 are strongly coupled to the neighboring  $\pi$  fragment. As a result of this relatively substantial  $\sigma/\pi$  mixing, the peripheral  $p$  lobes in  $\psi_1$  experience disrotatory tilting toward the methano bridge as illustrated in 8. This deformation leads to group overlap integrals more conducive to below-plane nucleophilic attack.

The unique orbital construct in 8 has prompted us to initiate investigations designed to elucidate the level of stereoelectronic control, if any, that can operate during metal complexation of this species.<sup>13,14</sup> Although earlier workers have utilized isodicyclopentadiene as an  $\eta^5$ -ligand,<sup>15–18</sup> the relevant stereochemical features of the products have often remained unclarified. In general, X-ray crystal analysis is mandated, since structural assignment founded only upon  $^1\text{H}$  and  $^{13}\text{C}$  NMR spectroscopy can be seriously misleading. A case in point is the tricarbonyliron complexation study of 9 and 12 first described by Hansen et al.<sup>19</sup> On the basis of coordination shifts observed in the  $^1\text{H}$  and  $^{13}\text{C}$  NMR spectra of 10/11 and 13/14, these authors formulated 11 and 13 as the respective major products. A more recent chemical and X-ray analytical examination of this stereoselectivity question by Vogel and co-workers<sup>20</sup> has resulted in reversal of the originally proposed configurations. The correct product distributions are given below the formulas.

(4) Paquette, L. A.; Charumilind, P. *J. Am. Chem. Soc.* **1982**, *104*, 3749.

(5) (a) Gleiter, R.; Böhm, M. C. *Pure Appl. Chem.* **1983**, *55*, 237. (b) Gleiter, R.; Böhm, M. C. In "Stereochemistry and Reactivity of Pi Systems"; Watson, W. H., Ed.; Verlag Chemie: Deerfield Beach, FL, 1983; pp 105–146.

(6) (a) Paquette, L. A.; Charumilind, P.; Kravetz, T. M.; Böhm, M. C.; Gleiter, R. *J. Am. Chem. Soc.* **1983**, *105*, 3126. (b) Paquette, L. A.; Charumilind, P.; Böhm, M. C.; Gleiter, R.; Bass, L. S.; Clardy, J. *Ibid.* **1983**, *105*, 3136. (c) Paquette, L. A.; Hayes, P. C.; Charumilind, P.; Böhm, M. C.; Gleiter, R.; Blount, J. F. *Ibid.* **1983**, *105*, 3148.

(7) (a) Sugimoto, T.; Kobuke, Y.; Furukawa, J. *J. Org. Chem.* **1976**, *41*, 1457. (b) Watson, W. H.; Galloy, J.; Bartlett, P. D.; Roof, A. A. M. *J. Am. Chem. Soc.* **1981**, *103*, 2022. (c) Subramanyam, R.; Bartlett, P. D.; Iglesias, G. Y. M.; Watson, W. H.; Galloy, J. *J. Org. Chem.* **1982**, *47*, 4491.

(8) (a) Avenati, M.; Hagenbuch, J.-P.; Mahaim, C.; Vogel, P. *Tetrahedron Lett.* **1980**, 3167. (b) Hagenbuch, J.-P.; Vogel, P.; Pinkerton, A. A.; Schwarzenbach, D. *Helv. Chim. Acta* **1981**, *64*, 1819. (c) Avenati, M.; Vogel, P. *Ibid.* **1982**, *65*, 204. (d) Mahaim, C.; Vogel, P. *Ibid.* **1982**, *65*, 866.

(9) (a) Paquette, L. A.; Carr, R. V. C.; Böhm, M. C.; Gleiter, R. *J. Am. Chem. Soc.* **1980**, *102*, 1186. (b) Böhm, M. C.; Carr, R. V. C.; Gleiter, R.; Paquette, L. A. *Ibid.* **1980**, *102*, 7218. (c) Paquette, L. A.; Carr, R. V. C.; Arnold, E.; Clardy, J. *J. Org. Chem.* **1980**, *45*, 4907. (d) Paquette, L. A.; Bellamy, F.; Böhm, M. C.; Gleiter, R. *Ibid.* **1980**, *45*, 4913. (e) Paquette, L. A.; Carr, R. V. C.; Charumilind, P.; Blount, J. F. *Ibid.* **1980**, *45*, 4922. (f) Paquette, L. A.; Carr, R. V. C. *J. Am. Chem. Soc.* **1980**, *102*, 7553. (g) Paquette, L. A.; Kravetz, T. M.; Böhm, M. C.; Gleiter, R. *J. Org. Chem.* **1983**, *48*, 1250. (h) Hayes, P. C.; Paquette, L. A. *Ibid.* **1983**, *48*, 1257. (i) Paquette, L. A.; Schaefer, A. G.; Blount, J. F. *J. Am. Chem. Soc.* **1983**, *105*, 3642. (j) Hathaway, S. J.; Paquette, L. A. *Tetrahedron* **1985**, *41*, 2037. (k) Paquette, L. A.; Green, K. E.; Hsu, L.-Y. *J. Org. Chem.* **1984**, *49*, 3650. (l) Charumilind, P.; Paquette, L. A. *J. Am. Chem. Soc.* **1984**, *106*, 8225. (m) Paquette, L. A.; Green, K. E.; Gleiter, R.; Schaefer, W.; Gallucci, J. *Ibid.* **1984**, *106*, 8232.

(10) (a) Paquette, L. A.; Hathaway, S. J.; Kravetz, T. M.; Hsu, L.-Y. *J. Am. Chem. Soc.* **1984**, *106*, 5741. (b) Paquette, L. A.; Hsu, L.-Y.; Gallucci, J.; Korp, J. D.; Bernal, I.; Kravetz, T. M.; Hathaway, S. J. *Ibid.* **1984**, *106*, 5743.

(11) (a) Houk, K. N.; Paddon-Row, M. N.; Caramella, P.; Rondan, N. G. *J. Am. Chem. Soc.* **1981**, *103*, 2436. (b) Houk, K. N.; Rondan, N. G.; Paddon-Row, M. N.; Caramella, P.; Mareda, J.; Mueller, P. H. *Ibid.* **1982**, *104*, 4974. (c) Brown, F. K.; Houk, K. N. *Ibid.* **1985**, *107*, 1971.

(12) (a) Paquette, L. A.; Charumilind, P.; Gallucci, J. C. *J. Am. Chem. Soc.* **1983**, *105*, 7364. (b) Bartlett, P. D.; Wu, C. *Ibid.* **1983**, *105*, 100. (c) Washburn, W. N.; Hillson, R. A. *Ibid.* **1984**, *106*, 4575.

(13) Hsu, L.-Y.; Hathaway, S. J.; Paquette, L. A. *Tetrahedron Lett.* **1984**, 259.

(14) Paquette, L. A.; Hathaway, S. J.; Schirch, P. F. T.; Gallucci, J. C., following paper in this issue.

(15) Reimschneider, R. *Z. Naturforsch., B: Anorg. Chem., Org. Chem., Biochem., Biophys., Biol.* **1962**, *17B*, 133.

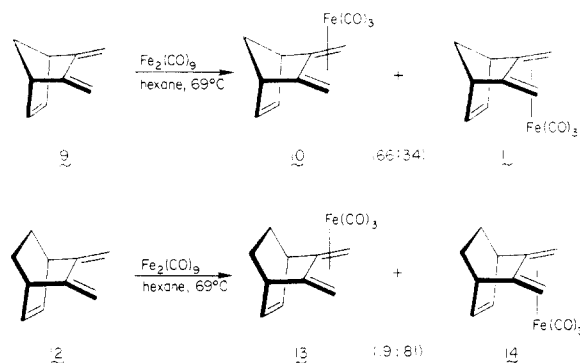
(16) Katz, T. J.; Mrowca, J. J. *J. Am. Chem. Soc.* **1967**, *89*, 1105.

(17) Scroggins, W. T.; Rettig, M. F.; Wing, R. M. *Inorg. Chem.* **1976**, *15*, 1381.

(18) Kohler, F. *J. Organomet. Chem.* **1976**, *110*, 235.

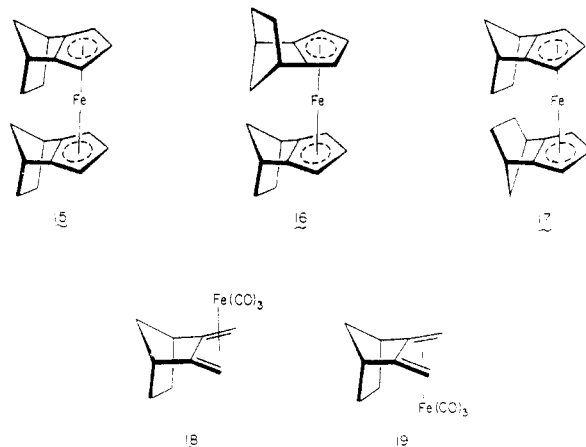
(19) Steiner, U.; Hansen, H.-J.; Bachmann, K.; von Phillipsborn, W. *Helv. Chim. Acta* **1977**, *60*, 643.

(20) Barras, C. A.; Roulet, R.; Carrupt, P.-A.; Berchier, F.; Vogel, P. *Helv. Chim. Acta* **1984**, *67*, 986.

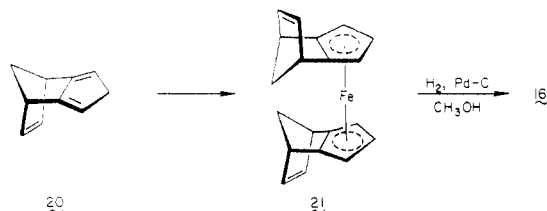


## Results

When **1** was treated with ethylmagnesium bromide and  $\text{Fe}^{\text{II}}(\text{acac})_2(\text{py})_2$  in xylene solution according to Riemenschneider (2 days at 20 °C, 1 h at 65–70 °C,  $\text{N}_2$  atmosphere),<sup>15</sup> a single ferrocene was isolated in 33% yield as golden plates. This substance was clearly identical to the lone ferrocene derivative produced by reaction of thallium isodicyclopentadienide in tetrahydrofuran with ferrous chloride.<sup>16</sup> Although the symmetry apparent in the high-field  $^1\text{H}$  and  $^{13}\text{C}$  NMR spectra of this substance required it to possess *exo,exo* (**16**) or *endo,endo* stereochemistry (**17**), the chemical shifts were viewed as inadequately diagnostic of stereochemistry (Table I). The spectral properties of **15**, the minor sandwich complex isolated by Katz and Mrocaw from reaction of **1** with *n*-butyllithium followed by ferrous chloride,<sup>16</sup> were not of assistance in this regard. Extrapolation from the spectral parameters of **18** and **19**<sup>19</sup> was similarly considered unreliable.



When no crystals of the symmetric metallocene suitable for X-ray analysis could be grown, attention was turned to its dehydro congener, tricyclo[5.2.1.0<sup>2,6</sup>]deca-2,5,8-triene (**20**), which was submitted to the identical reaction conditions. The only detectable ferrocene was isolated as large yellow-brown prisms and identified as **21** by X-ray diffraction analysis. As the ORTEP drawing in Figure 1 re-



veals, the two  $\text{C}_{10}\text{H}_9$  residues are indeed enantiomerically related and possess individual pseudomirror planes. The two cyclopentadienide moieties are fully planar and virtually parallel to each other (dihedral angle = 3.6°). The

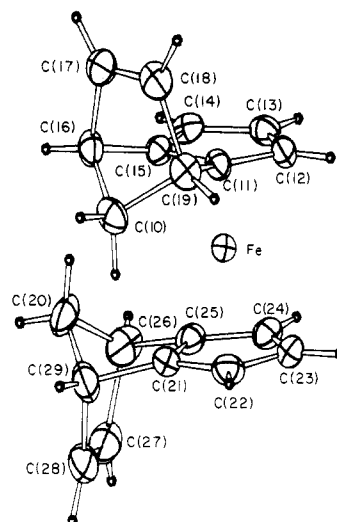


**Figure 1.** A computer-generated perspective side view of the final X-ray model of **21**.

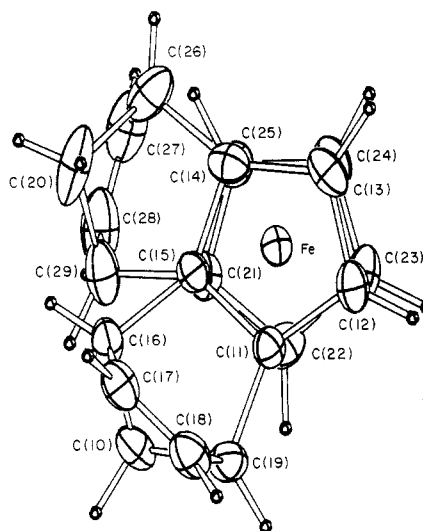


**Figure 2.** A computer-generated perspective top view of the final X-ray model of **21**.

centers of the five-membered rings are 3.31 (7) Å apart, mirroring the situation in ferrocene itself,<sup>21</sup> with the iron atom equidistant between them.

When the sandwich complex is viewed from above (Figure 2), one set of cyclopentadienide carbon atoms is seen to be positioned almost directly above the other. This effect, which may be the norm for ferrocene systems,<sup>21,22</sup> is best reflected in the torsion angle of 60° observed between the C(11)–C(15) and C(21)–C(25) bonds. Since the distance between C(10) and C(20) is large (4.297 Å) and van der Waals compression is not at issue, steric factors appear unimportant. The proximity of the two methano carbons may arise from intermolecular crystal packing forces and/or intramolecular attractive (London) forces.

A final point of interest is the dihedral angle relationship of the ethano bridge [the C(16)–C(15)–C(11)–C(19) plane]

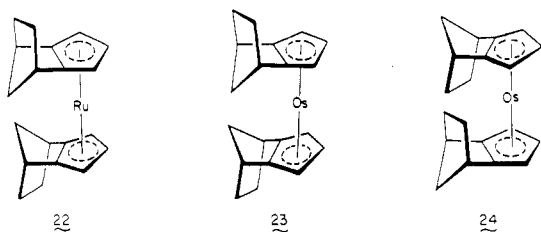
(21) See for example: (a) The parent molecule: Seiler, P.; Dunitz, J. D. *Acta Crystallogr., Sect. B: Struct. Crystallogr. Cryst. Chem.* **1979**, *B35*, 1068. Seiler, P.; Dunitz, J. D. *Ibid.* **1979**, *B35*, 2020. Takusagawa, F.; Koetzle, T. F. *Ibid.* **1979**, *B35*, 1074. (b) Ferrocenedicarboxylic acid: Palenik G. J. *Inorg. Chem.* **1969**, *8*, 2744. (c) Diacetylferrocene: Palenik, G. J. *Ibid.* **1970**, *9*, 2424.

(22) Eclipsing is especially encountered when an interlocking bridge is present, e.g., as in 1,1-(1',3'-cyclopentylene)ferrocene [Batail, P.; Grandjean, D.; Astruc, D.; Dabard, R. *J. Organomet. Chem.* **1975**, *102*, 79].

to the cyclopentadienide moiety in the top half ( $10.1^\circ$ ) relative to the state of affairs in the lower segment ( $\theta = 9.3^\circ$ ). All of the other bond angles and distances are normal.

That a common stereochemical infrastructure exists in the two ferrocenes was established by catalytic hydrogenation of **21** over 10% palladium on carbon. The tetrahydro product, necessarily **16**, was identical with the metallocene obtained by direct synthesis. Consequently, a strong preference exists for above-plane complexation to iron in both halves of the sandwich.

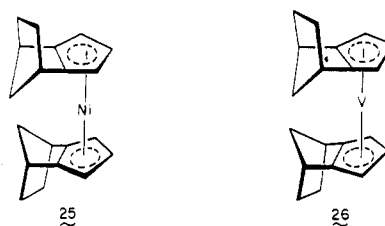
With establishment of the three-dimensional structure of **16**, specific attention was next directed to complexation to ruthenium in order to determine if metals of larger atomic diameter would continue to prefer above-plane coordination to **1**. Reaction of the lithium anion of isocyclopentadiene with ruthenium trichloride and ruthenium metal in 1,2-dimethoxyethane according to precedent<sup>23</sup> provided **22** exclusively, although with low (11.5%) efficiency. The stereochemical assignment to **22** follows in particular from the very close identity of its <sup>13</sup>C NMR spectrum to that of **16** (Table IV). Thus, the observation of only six signals attests to the level of symmetry present in **22**. Should the substance be instead the twofold below-plane stereoisomer, the chemical shifts of the carbon atoms within the methano and ethano bridges should be differently shielded, despite the greater intraring distance in the ruthenocene. This is not observed. The <sup>1</sup>H NMR properties of **22** (Table I) reflect a greater sensitivity to the nature of the metal, as expected from the earlier work referred to above.



Reaction of **6** with osmium tetrachloride<sup>24</sup> in dry 1,2-dimethoxyethane (reflux, 6 days)<sup>23</sup> gave in approximately 10% yield a red solid that proved to be exceptionally labile while in solution. Consequently, all attempts at recrystallization resulted in destruction of the substance. Acquisition of an X-ray quality crystal was thereby precluded. The <sup>13</sup>C NMR data for this metallocene, recorded immediately after dissolution in purified CDCl<sub>3</sub> under nitrogen, showed the major substance to be symmetrical and to possess chemical shifts compatible with structural assignment **23** (Table IV). However, three of the signals were twinned with lower intensity absorptions. It was not possible to deduce the origin of these weaker signals. If they were due to the presence of **24**, why were the additional three peaks not seen? Were the absorptions arising from a decomposition product? If so, its gross structural features were not apparent. Nor was the <sup>1</sup>H NMR spectrum helpful in this regard. For these reasons, we choose not to claim that the stereochemistry of the osmocene is known with any degree of certainty.

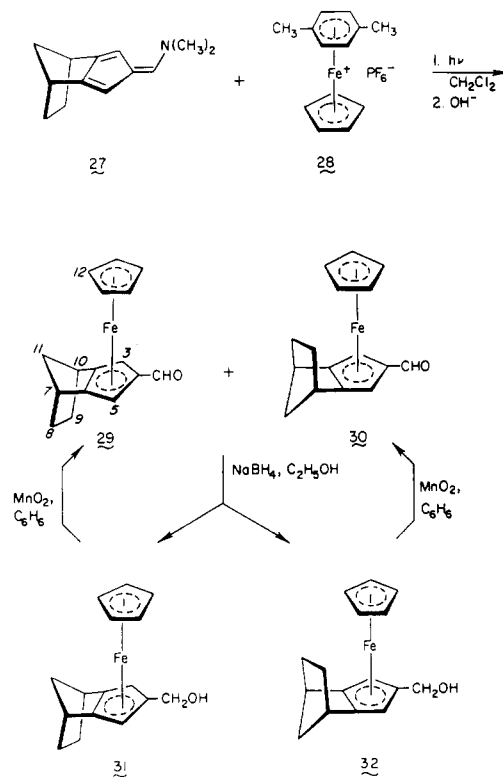
Anion **6** (as the lithium salt) has been shown to react with NiBr<sub>2</sub>(glyme) to give **25**.<sup>17</sup> X-ray crystal structure analysis of this nickelocene indicates that the substance adopts a conformation in the crystal not too dissimilar

from that of **21**.<sup>17</sup> Kohler has also described the preparation of **28**.<sup>18</sup> In his hands, the series was extended to



include the cobaltocene, chromocene, and vanadocene analogues. However, the limited spectral properties reported for these compounds do not allow us to deduce convincingly that they are isostructural with **25**, although they may well be. In this connection, Professor Rettig has informed us that a single crystal of the vanadocene has been found in his laboratory to be isomorphous with those of **25**.<sup>25</sup> Accordingly, the real possibility exists that they share the same three-dimensional stereochemistry (see **26**).

In an effort to broaden the scope of this study, 4-(dimethylamino)isocyclopentafulvene (**27**) was prepared and subjected to  $\pi$ -complexation processes likely to proceed by different mechanistic pathways. Sunlamp irradiation of **27** in the presence of ( $\eta^5$ -cyclopentadienyl)( $\eta^6$ -*p*-xylene)iron(II) hexafluorophosphate (**28**) resulted in ligand exchange on the transition metal<sup>26</sup> and formation after alkaline hydrolysis of a 65:35 mixture of **29** and **30**. Although these isomers could not be separated



chromatographically, the assignment of <sup>1</sup>H NMR shifts to the individual complexes was uncomplicated. The relevant information is compiled in Table V. When recourse was made to sodium borohydride reduction of this aldehyde mixture, the resulting alcohols **31** and **32** could be separated by HPLC and individually reoxidized with manga-

(23) Bullitz, D. E.; McEwen, W. E.; Kleinberg, J. *Org. Synth.* 1961, 41, 46.

(24) Colton, R.; Farthing, R. H. *Aust. J. Chem.* 1967, 21, 589.

(25) Rettig, M. F., private communication of January 21, 1984.

(26) Bickert, P.; Hildebrandt, B.; Hafner, K. *Organometallics* 1984, 3, 653.

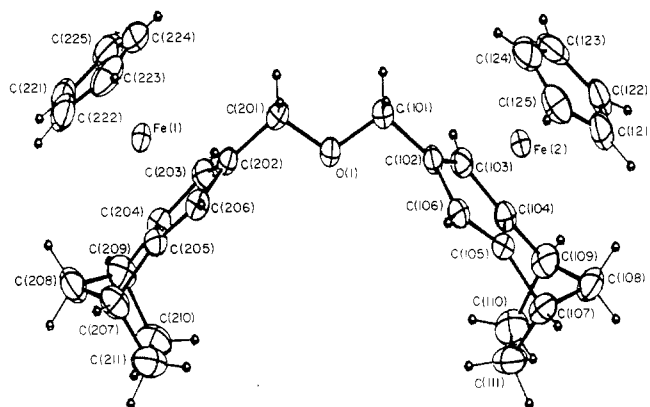


**Figure 3.** A computer-generated perspective side view of the final X-ray model of **33**.

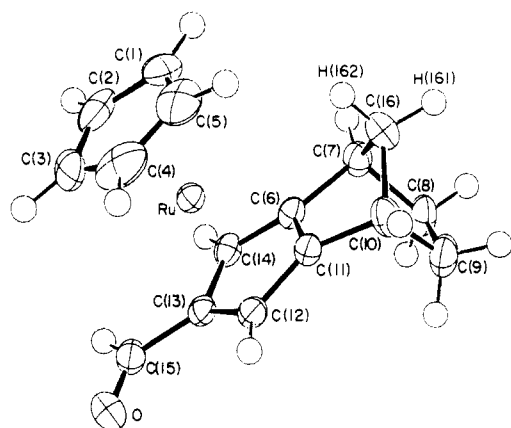
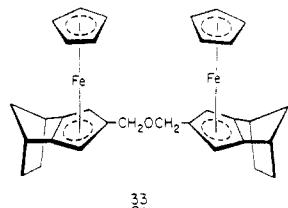


**Figure 4.** A computer-generated perspective side view of the final X-ray model of **35**.

nese dioxide. In this way pure samples of **29** and **30** could be routinely obtained.

When numerous attempts to prepare X-ray quality crystals of **29–32** were not rewarded, alcohol **31** was transformed into the dimeric ether **33** by reaction with 0.5



molar equiv of *p*-toluenesulfonyl chloride in the presence of triethylamine. The beautiful pale yellow prismatic crystals of this substance allowed definitive structural assignment as the product of above-plane complexation to **27** (Figure 3). Consequently, this is the preferred stereochemical course for coordination of the isodicyclopentafulvene to the reactive intermediate generated upon photolysis of **28**.

Ether **33** possesses pseudo- $C_{2v}$  point symmetry. The coordinating five-membered rings of the substituted isodicyclopentadienide moieties are essentially planar, and each is virtually parallel to a capping  $C_5H_5$  moiety. The relevant dihedral angles are  $3.0^\circ$  and  $2.3^\circ$ . The centers of the pairs of metallocene rings are 3.308 and 3.306 Å apart with the two Fe atoms equidistant between them. When both halves of the molecule are viewed from above the respective  $C_5H_5$  rings, the carbon atoms of both cyclopentadienide units are seen to be superimposed, much like the conformational situation noted earlier for **21**. Once again, downward pyramidalization about C(104)/C(105)

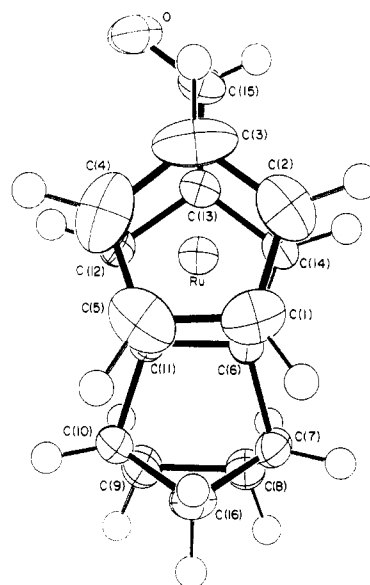
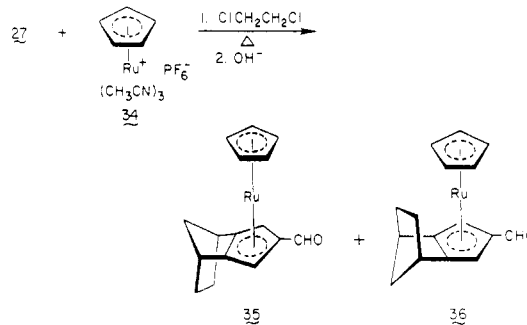


**Figure 5.** A computer-generated perspective top view of the final X-ray model of **35**.

and C(204)/C(205) is clearly evident. The extent of  $\pi$  deformation is  $8.5^\circ$  and  $9.1^\circ$ , respectively. The angle between the two five-membered rings of the isodicyclopentadienide groups is  $85.8^\circ$ .

In the unit cell, the two molecules align with their long axes approximately parallel to the *b* axis. A solvent molecule ( $CH_3CN$ ) occupies the region between the norbornane fragments of each molecule. All of the intermolecular atom-atom distances are beyond the sum of van der Waals radii.

When **27** was heated with ( $\eta^5$ -cyclopentadienyl)tris(acetonitrile)ruthenium(II) hexafluorophosphate (**34**) in 1,2-dichloroethane for 14 h, transfer of the cyclopentadienyl unit again occurred to deliver an 86:14 mixture of **35** and **36**. In this instance, it proved an easy matter



to obtain the major component in isomerically pure form by simple recrystallization from ethyl acetate. A single crystal of this substance, grown from acetonitrile solution at room temperature, was subjected to X-ray analysis and identified as **35** (Figures 4 and 5).

If the aldehyde functionality is discounted, the molecule is seen to contain a noncrystallographic mirror plane which bisects the C(6)–C(11), C(8)–C(9), and C(1)–C(5) bonds and contains atoms C(13), C(16), and C(3). The ruthenium atom is sandwiched between the two five-membered rings and resides syn to C(16) of the norbornane fragment. The unencumbered cyclopentadienide ring and the five-membered cycle containing atoms C(6)–C(11)–C(12)–C(13)–C(14) are eclipsed with respect to each other and are essentially parallel. The dihedral angle between the least-squares planes through each ring is  $1.0^\circ$ , and each ring is planar. The distance between these two five-membered rings is 3.619 Å. The ruthenium atom is 1.815 Å from the



centroid of the unsubstituted cyclopentadienide ring and 1.805 Å from the centroid of the isodicyclopentadienide five-membered ring. Interestingly, the aldehyde group lies significantly out of the least-squares plane containing the C(6)–C(11)–C(12)–C(13)–C(14) atoms and in the direction of the ruthenium atom.

Also worthy of note is the fact that the mutually planar C(7)–C(6)–C(11)–C(10) atoms of the isodicyclopentadiene frame are not coplanar with the neighboring fused five-membered ring. The relevant dihedral angle is 9.5°. The closest approach between the hydrogens of C(16) and the hydrogens of the cyclopentadienide ring is 2.73 Å for H(162)⋯HC(5) and 2.86 Å for H(162)⋯HC(1).

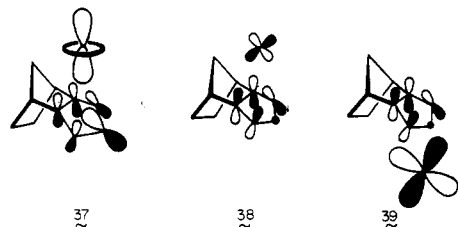
Thus, the involvement of ruthenium as a central atom and the utilization of thermal reaction conditions lead to a greater proportion of above-plane coordination relative to photoinduced iron cyclopentadienide transfer. Since 34 is unreactive to light and 28 unreactive to heat when handled as described above, it was not possible to examine the consequences of reaction mode on product stereochemistry.

### Discussion

Reaction of the isodicyclopentadienide anion with metal salts has proven to be a serviceable method for affecting the synthesis of metallocenes carrying a 1,2-fused bicyclo[2.2.1]heptene moiety in both halves. Furthermore, the complexation process proceeds with stereocontrolled incorporation of the pair of ligands. In all of the examples closely scrutinized so far, coordination has clearly occurred on the exo surface of both segments.

A similar trend is encountered with fulvene 27. Its reaction with the cyclopentadienyl metal transfer reagents 28 and 34 under photochemical and thermal conditions, respectively, also eventuates in preferential above-plane coordination, although not to a comparably overwhelming degree. Does the proportionately larger relative amount of exo adduct 35 in the ruthenocene example signal that larger metals have a greater predilection for complexation to the exo surface? The companion study provides added corroboration of this trend.<sup>14</sup> Certainly, the rings comprising the sandwich complex become more distant as the size of the metal increases. However, this fact alone does not give rise to an obvious explanation for the increased preference in top-side bonding.

We had originally considered the possible interplay of product-determinative options.<sup>13</sup> Should overlap control be dominant and orbital tilting be restricted to the  $\psi_1$  level as in 8, all metals ions might well prefer approach from above-plane because their  $d_{z^2}$ ,  $s$ , and  $p_z$  orbitals (all of which are related to  $\psi_1$  by symmetry) would, under these circumstances, be directed to the center of the more electron-rich cyclopentadienide core (see 37). Alternatively,



tively, should the  $p\pi$  orbitals in  $\psi_2$  also be somewhat tilted (unlikely)<sup>5</sup> and capable of overriding the effect of  $\psi_1$ , the resulting  $d_{\pi}-\psi_2$  interactions could exert their usual dominance over the customarily lesser important  $d_{\sigma}-\psi_1$  interactions. In this event, a metallic species with contracted  $d_{\pi}$  orbitals, viz., a small metal or one in a high oxidation

state, would likely favor top-side bonding as in 38. On the other hand, a metal with diffuse  $d_{\pi}$  orbitals could engage in better overlap on the endo face (39). The second of these considerations clearly runs contrary to the experimental findings reported herein. We caution, however, that the first option has hardly been proven.

Of more than passing interest is the bending of the carboxaldehyde group in 35 toward the ruthenium atom, much like the ring hydrogen atoms in ferrocene are bent toward the metal.<sup>21a</sup> However, the norbornane fragment folds in the opposite direction—a characteristic structural feature of all three complexes examined by X-ray methods. A discussion of this phenomenon follows in the adjoining paper.

### Experimental Section

**Bis( $\eta^5$ -tricyclo[5.2.1.0<sup>2,6</sup>]deca-2,4-dien-6-yl)iron (16).** Ethylmagnesium bromide was prepared from 1.2 g (0.05 mol) of magnesium turnings and 5.5 g (0.05 mol) of ethyl bromide in 25 mL of anhydrous ether. The Grignard reagent was allowed to stir for 1 h, then dry xylene (distilled from CaH<sub>2</sub> and stored over 4-Å molecular sieves, 25 mL) was added, and the ether was removed by distillation up to the boiling point of xylene. While being heated at the reflux temperature, a solution of 1 (5.0 g, 37.9 mmol) in dry xylene (25 mL) was added dropwise. The tan mixture was heated for 2 h, cooled to 15 °C, and treated with Fe<sup>II</sup>(acac)<sub>2</sub>(py)<sub>2</sub> (6.0 g, 14.5 mmol) in the same solvent (50 mL). The yellow-brown mixture was stirred at room temperature for 4.5 h and then allowed to stand under nitrogen at room temperature for 2 days.

The reaction mixture was heated to 65–70 °C for 1 h and poured onto ice and saturated ammonium chloride solution. The xylene was separated, washed with water, and dried. Concentration of the clear red solution in vacuo afforded a viscous black gum that contained some brown crystals. This material was dissolved from ethyl acetate, from which solution a light colored solid precipitated. The solid was dissolved in hot acetone (400 mL) and stored in a freezer overnight. There was isolated in three crops a total of 1.53 g (33%) of 16. <sup>1</sup>H NMR analysis was utilized at each case in an attempt to detect the presence of a second stereoisomer, but to no avail.

Ferrocene 16 crystallized as shiny gold plates, mp 167.5–169 °C; for NMR spectra see the tables.

**Bis( $\eta^5$ -tricyclo[5.2.1.0<sup>2,6</sup>]deca-2,5,8-trien-6-yl)iron (21).** A procedure identical in scale was utilized for 20 up to the point of dissolution in ethyl acetate. The ferrocene was too soluble, and no crystals were deposited. Ethyl acetate was removed, and the red oil was allowed to stand at room temperature. Large crystals formed from which the residual oil was decanted. Recrystallization from hot acetone furnished 21 as large yellow-brown prisms (110 mg, 12%): mp 162.5–163.5 °C; <sup>1</sup>H NMR (200 MHz, CDCl<sub>3</sub>)  $\delta$  6.43–6.41 (m, 4 H), 4.02 (br s, 2 H), 3.82 (br s, 4 H), 3.41 (br s, 4 H), 2.97 (d,  $J = 7$  Hz, 2 H), 2.23 (d,  $J = 7$  Hz, 2 H).

Anal. Calcd for C<sub>20</sub>H<sub>18</sub>Fe: C, 76.45; H, 5.78. Found: C, 76.47; H, 5.84.

The remaining oil was chromatographed on silica gel (elution with 5% ethyl acetate in petroleum ether) to give an additional 50 mg of 21 (total yield 17.4%). No other identifiable product was isolated.

**Hydrogenation of 21.** A solution of 21 (50 mg, 0.16 mmol) in methanol (75 mL) containing 10% palladium on charcoal (10 mg) was hydrogenated at atmospheric pressure for 5 min. Filtration of the reaction mixture through Celite and concentration of the filtrate in vacuo afforded 38 mg of golden plates spectroscopically identical in all respects with 16.

**X-ray Crystal Structure Analysis of 21.** A needle-like prismatic crystal of approximate dimensions 0.20 × 0.25 × 0.55 mm was mounted on a tip of a thin glass fiber. Analysis was conducted at room temperature. The cell parameters and standard deviations (Table II) were determined by a least-squares fit of the diffractometer setting angles for 24 reflections, well distributed in reciprocal space and lying in the  $2\theta$  range between 24 and 30°. The intensity data were corrected for Lorentz and polarization effects, as well as for absorption by using an empirical

**Table II. Experimental Crystallographic Data for 21, 33, and 35<sup>a</sup>**

	21	33	35
space group	$P\bar{1}$	$P\bar{1}$	$P2_1/n$
<i>a</i> , Å	9.137 (1)	11.592 (3)	5.867 (1)
<i>b</i> , Å	11.692 (2)	14.127 (2)	13.394 (2)
<i>c</i> , Å	7.348 (2)	9.401 (2)	16.386 (2)
$\alpha$ , deg	93.62 (2)	105.61 (1)	
$\beta$ , deg	105.31 (2)	101.16 (2)	99.59 (1)
$\gamma$ , deg	69.53 (1)	104.69 (2)	
vol., Å <sup>3</sup>	709	1377	1270
<i>Z</i>	2	2	4
mol wt	314.21	584.35	325.38
$D_{\text{calcd}}$ , g cm <sup>-3</sup>	1.47	1.41	1.70
$\mu$ , cm <sup>-1</sup>	10.51	10.80	11.94
$2\theta$ range, deg	4-55	4-50	4-55
data collected	$\pm h, \pm k, +l$	$\pm h, \pm k, +l$	$+h, +k, +l$
scan type	$\omega-2\theta$	$\omega-2\theta$	$\omega-2\theta$
scan range	$0.75 + 0.35 \tan \theta$	$0.75 + 0.35 \tan \theta$	1.0° below $K\alpha_1$ to 1.1° above $K\alpha_2$
scan speed, deg min <sup>-1</sup>	0.65-5 (in $\omega$ )	0.65-5 (in $\omega$ )	2-24 (in $2\theta$ )
unique reflectns	3507	4853	2939
reflectns obsd <sup>b</sup>	3220	3492	2463
<i>R</i> ( $R_w$ )	0.026 (0.038)	0.032 (0.039)	0.022 (0.027)

<sup>a</sup>Data for the first two structures were collected on an Enraf-Nonius CAD-4 diffractometer. The data for complex 35 was collected with a Syntex  $P\bar{1}$  diffractometer. All experiments were carried out at  $\sim 20^\circ\text{C}$  with graphite-monochromated Mo  $K\alpha$  radiation. <sup>b</sup>Reflections were regarded as significant if  $F_o^2 > 3.0\sigma(F_o^2)$ .

**Table III. Bond Distances (Å) in 21<sup>a</sup>**

atom 1	atom 2	dist	atom 1	atom 2	dist	atom 1	atom 2	dist
Fe1	C11	2.054 (1)	C15	C16	1.523 (1)	C22	H22	0.935 (12)
Fe1	C12	2.061 (1)	C16	C17	1.535 (2)	C23	C24	1.418 (2)
Fe1	C13	2.031 (1)	C16	H16	0.896 (14)	C23	H23	0.94 (2)
Fe1	C14	2.056 (1)	C17	C18	1.319 (2)	C24	C25	1.408 (2)
Fe1	C15	2.059 (1)	C17	H17	0.901 (14)	C24	H24	1.011 (15)
Fe1	C21	2.054 (1)	C18	C19	1.531 (2)	C25	C26	1.524 (2)
Fe1	C22	2.041 (1)	C18	H18	0.963 (14)	C26	C27	1.531 (2)
Fe1	C23	2.026 (1)	C19	H19	0.957 (13)	C26	H26	0.923 (15)
Fe1	C24	2.065 (1)	C20	C26	1.561 (2)	C27	C28	1.297 (2)
Fe1	C25	2.058 (1)	C20	C29	1.537 (2)	C27	H27	0.888 (15)
C10	C16	1.547 (2)	C20	H201	0.86 (2)	C28	C29	1.531 (2)
C10	C19	1.547 (2)	C20	H202	0.910 (15)	C28	H28	0.96 (2)
C10	H101	0.919 (12)	C21	C22	1.409 (2)	C29	H29	0.95 (2)
C10	H102	1.026 (14)	C21	C25	1.417 (2)			
C11	C12	1.411 (1)	C21	C29	1.524 (2)			
C11	C15	1.416 (1)	C22	C23	1.427 (2)			
C11	C19	1.525 (1)						
C12	C13	1.425 (2)						
C12	H12	0.927 (14)						
C13	C14	1.431 (2)						
C13	H13	0.937 (14)						
C14	C15	1.416 (1)						
C14	H14	0.915 (11)						

<sup>a</sup>Numbers in parentheses are estimated standard deviations in the least significant digits.

**Table IV. Comparative <sup>13</sup>C NMR Spectral Data for 16, 22, and 23 (CDCl<sub>3</sub> Solution, ppm)**

carbon	16	22	23 <sup>a</sup>
ethano bridge	28.24	28.35	28.93
bridgehead	37.64	37.57	38.91
methano bridge	47.69	48.82	44.21
quaternary cyclopentadienide	98.62	101.53	101.32
peripheral cyclopentadienide	59.61	62.22	159.21
central cyclopentadienide	67.65	70.58	151.57

<sup>a</sup>Twinned signals were also apparent at 28.95, 44.32, and 101.36 ppm.

**Table V. Comparative <sup>1</sup>H NMR Spectral Data for 29, 30, 35, and 36 (300 MHz, CDCl<sub>3</sub> Solution,  $\delta$ )<sup>a</sup>**

proton	29	30	35	36
-CHO	9.92 (s, 1 H)	9.99 (s, 1 H)	9.60 (s, 1 H)	9.60 (s, 1 H)
H-3,5	4.46 (s, 2 H)	4.61 (s, 2 H)	4.85 (s, 2 H)	5.00 (s, 2 H)
H-12	4.22 (s, 5 H)	4.22 (s, 5 H)	4.60 (s, 5 H)	4.60 (s, 5 H)
H-7,10	2.99 (s, 2 H)	2.91 (s, 2 H)	2.85 (s, 2 H)	2.90 (s, 2 H)
H-8,9( <i>exo</i> )	2.12 (d, $J = 8$ Hz, 2 H)	2.12 (d, $J = 8$ Hz, 2 H)	1.82 (d, $J = 8$ Hz, 2 H)	(2.1-1.9)
H-8,9( <i>endo</i> )	1.04 (d, $J = 7$ Hz, 2 H)	1.91 (d, $J = 7$ Hz, 2 H)	1.23 (d, $J = 8$ Hz, 2 H)	(2.1-1.9) <sup>b</sup>
H-11( <i>syn</i> )	2.12 (d, $J = 8$ Hz, 1 H)	1.91 (d, $J = 7$ Hz, 2 H)	1.60 (d, $J = 8$ Hz, 1 H)	2.20 (d, $J = 8$ Hz, 1 H)
H-11( <i>anti</i> )	1.42 (d, $J = 7$ Hz, 1 H)	1.85 (d, $J = 7$ Hz, 1 H)	1.33 (d, $J = 8$ Hz, 1 H)	(2.1-1.9) <sup>b</sup>

<sup>a</sup>See 29 for numbering. <sup>b</sup>Mutually overlapping peaks that ultimately comprise a multiplet of relative area 5.

Table VI. Bond Distances (Å) in 33<sup>a</sup>

atom 1	atom 2	dist	atom 1	atom 2	dist	atom 1	atom 2	dist
O1	C101	1.426 (3)	C122	C123	1.417 (4)	C211	H2111	0.92 (3)
O1	C201	1.431 (3)	C122	H122	1.02 (3)	C211	H2112	0.94 (3)
C101	C102	1.490 (3)	C123	C124	1.415 (5)	C221	C222	1.396 (4)
C101	H1011	1.06 (3)	C123	H123	0.91 (3)	C221	C225	1.387 (4)
C101	H1012	1.00 (3)	C124	C125	1.395 (5)	C221	H221	0.95 (3)
C102	C103	1.430 (3)	C124	H124	0.86 (3)	C222	C223	1.387 (5)
C102	C106	1.436 (3)	C125	H125	0.92 (3)	C222	H222	0.92 (3)
C103	C104	1.412 (3)	C201	C202	1.483 (3)	C223	C224	1.434 (5)
C103	H103	0.91 (2)	C201	H2011	0.91 (3)	C223	H223	0.88 (3)
C104	C105	1.410 (3)	C201	H2012	1.06 (2)	C224	C225	1.395 (6)
C104	C109	1.509 (3)	C202	C203	1.433 (3)	C224	H224	0.72 (3)
C105	C106	1.408 (3)	C202	C206	1.436 (3)	C225	H225	0.89 (3)
C105	C107	1.508 (3)	C203	C204	1.410 (3)	C1	N1	1.058 (9)
C106	H106	0.97 (2)	C203	H203	0.84 (3)	C1	C2	1.411 (9)
C107	C108	1.540 (4)	C204	C205	1.414 (3)	C2	N2	1.06 (1)
C107	C111	1.548 (4)	C204	C209	1.503 (3)	C2	C21	1.37 (1)
C107	H107	0.95 (2)	C205	C206	1.409 (3)			
C108	C109	1.541 (4)	C205	C207	1.507 (3)			
C108	H1081	0.92 (3)	C206	H206	0.93 (2)			
C108	H1082	1.01 (3)	C207	C208	1.533 (4)			
C109	C110	1.540 (4)	C207	C211	1.542 (4)			
C109	H109	0.92 (3)	C207	H207	0.94 (3)			
C110	C111	1.541 (4)	C208	C209	1.545 (4)			
C110	H1101	0.94 (3)	C208	H2081	0.98 (3)			
C110	H1102	0.97 (2)	C208	H2082	0.97 (3)			
C111	H1111	0.96 (3)	C209	C210	1.537 (4)			
C111	H1112	0.98 (3)	C209	H209	0.92 (3)			
C121	C122	1.410 (4)	C210	C211	1.551 (5)			
C121	C125	1.394 (4)	C210	H2101	0.96 (3)			
C121	H121	0.99 (3)	C210	H2102	0.96 (3)			

<sup>a</sup>Numbers in parentheses are estimated standard deviations in the least significant digits.

method based on crystal orientation and measured psi scans.<sup>27</sup> The reflections used, their  $2\theta$  values, and their maximum to minimum intensity ratios of  $\psi$  scans were as follows: 10 $\bar{2}$ , 5.64, 1:0.89; 20 $\bar{4}$ , 11.33, 1:0.90; 30 $\bar{6}$ , 16.98, 1:0.91; 40 $\bar{8}$ , 22.70, 1:0.90; 51 $\bar{9}$ , 26.29, 1:0.84.

The analytical form of the scattering factors for neutral atoms was used throughout the analysis, and both  $\Delta f'$  and  $i\Delta f''$  terms were included for all atoms.<sup>28</sup> All crystallographic computations were carried out on a PDP 11/44 computer using the Enraf-Nonius structure determination package.

Although the intensity statistics suggested the likely space group to be noncentrosymmetric  $P1$ , the completed structural analysis showed the true space group to be centrosymmetric  $P\bar{1}$ . The structure was solved via MULTAN 82 in space group  $P1$ .<sup>29</sup> Two iron and several of the carbon atoms were first located in the  $E$  map. After several cycles of full-matrix least-squares refinements, the other atoms including hydrogens appeared on the difference electron density maps. At this stage, it was already clear that these two independent molecules were actually related by a center of symmetry. Therefore, the coordinates of these two molecules were averaged and the inversion center was located at the origin.

The function minimized during the least-squares refinement process was  $\sum w(|F_o| - |F_c|)^2$ , where the assigned weights are given as  $w = [\sigma^2(I) + (pI)^2]^{-1/2}$ , and  $p = 0.02$  was chosen to make  $\sum w\Delta F^2$  uniformly distributed in  $|F_o|$ ,  $(\sin \theta)/\lambda$ , and parity class of the crystallographic indices. The final full-matrix least-squares refinement cycle with anisotropic thermal parameters for all non-hydrogens, isotropic for hydrogen atoms, gave  $R_F = 0.026$  and  $R_{wF} = 0.038$ , where  $R_F = \sum ||F_o| - |F_c|| / \sum |F_o|$  and  $R_{wF} = \sum w^{1/2} ||F_o| - |F_c|| / \sum w^{1/2} |F_o|$ . The final difference Fourier map showed no significant features, with a maximum peak height of  $0.33 \text{ e } \text{\AA}^{-3}$  at the vicinity of the iron atom.

The final positional and thermal parameters for 21 are listed in Tables XIV and XV, respectively (supplementary material). Table XVI (supplementary material) contains values of  $10F_o$  and  $10F_c$ .

(27) North, A. C. T.; Phillips, D. C.; Mathews, F. S. *Acta Crystallogr., Sect. A: Cryst. Phys. Diffr., Theor. Gen. Crystallogr.* 1968, A24, 351.

(28) "International Tables for X-Ray Crystallography"; Kynoch Press: Birmingham, England, 1974; Vol. IV.

(29) Frenz, B. A., Enraf-Nonius User's Guide, 1982.

#### Bis( $\eta^5$ -tricyclo[5.2.1.0<sup>2,6</sup>]deca-2,4-dien-6-yl)ruthenium (22).

A solution of isodicyclopentadiene (3.4 g, 25.8 mmol) in dry 1,2-dimethoxyethane (25 mL) contained in a flame-dried flask under a nitrogen atmosphere was cooled to  $-78^\circ\text{C}$ , and *n*-butyllithium (16 mL of 1.6 M in ether, 24.8 mmol) was introduced slowly via syringe. The solution was stirred for 10 min at  $-78^\circ\text{C}$  and allowed to warm to room temperature. A mixture of anhydrous ruthenium trichloride (1.0 g, 4.8 mmol) and ruthenium metal (0.17 g, 1.7 mmol) was added all at once and heating at the reflux temperature with stirring was maintained for 3.5 days. The solvent was removed in vacuo, and the sticky black residue was partitioned between water and toluene. The aqueous phase was extracted with toluene, the toluene was removed in vacuo, and the residue was chromatographed on silica gel (elution with toluene-petroleum ether, 1:1). The initial fraction, a rapidly moving red band, was evaporated and crystallized from toluene to give 200 mg (11.5%) of 22 as light golden brown prisms, mp  $173.5$ – $175^\circ\text{C}$ . For NMR spectra, see the tables.

Anal. Calcd for  $\text{C}_{20}\text{H}_{18}\text{Ru}$ : C, 66.09; H, 6.11. Found: C, 66.08; H, 6.10.

**4-(Dimethylamino)isodicyclopentafulvene (27).**<sup>30</sup> Dimethylformamide (dried over 4-Å molecular sieves, 7.3 g, 0.1 mol) was placed in a flame-dried flask, heated to  $50$ – $60^\circ\text{C}$ , and treated dropwise with dimethyl sulfate (12.6 g, 0.1 mol) while mechanically stirred. The yellow solution was heated at  $70$ – $80^\circ\text{C}$  for 2 h and allowed to cool to room temperature. In a second flask, *n*-butyllithium (67 mL of 1.5 M in hexane, 0.1 mol) was added to a cold ( $-78^\circ\text{C}$ ), stirred solution of 1 (13.2 g, 0.1 mol) in dry tetrahydrofuran (70 mL). After 10 min at  $-78^\circ\text{C}$ , this solution was allowed to warm to  $-10^\circ\text{C}$ , and the first solution was introduced dropwise. When addition was complete, the mixture was allowed to stir at room temperature for 4 h and filtered. The filtrate was concentrated in vacuo and the residue crystallized on standing in the refrigerator. The solid was dissolved in petroleum ether (150 mL), decolorized with charcoal, and set in a freezer. There precipitated 9.9 g (53%) of 27 as fine yellow crystals: mp  $75$ – $76^\circ\text{C}$ ;  $^1\text{H}$  NMR (300 MHz,  $\text{CDCl}_3$ )  $\delta$  6.84 (s, 1 H), 6.10 (s, 1 H), 5.82 (s, 1 H), 3.15 (s, 8 H), 1.88 (d,  $J = 8 \text{ Hz}$ , 2 H), 1.81 (d,  $J = 8 \text{ Hz}$ ,

(30) This procedure is modeled after that described for cyclopentadiene: Hafner, K.; Vopel, K. H.; Ploss, G.; Koning, C. "Organic Syntheses"; Wiley: New York, 1973; Coll. Vol. V, p 431.

Table VII. Bond Distances (Å) in 35

Ru...C1	2.172 (2)	C6-C7	1.509 (3)
Ru...C2	2.171 (3)	C7-C8	1.556 (3)
Ru...C3	2.172 (3)	C8-C9	1.555 (3)
Ru...C4	2.174 (3)	C9-C10	1.554 (4)
Ru...C5	2.168 (3)	C10-C11	1.496 (3)
Ru...C6	2.193 (2)	C6-C11	1.423 (3)
Ru...C11	2.191 (2)	C11-C12	1.417 (3)
Ru...C12	2.182 (2)	C12-C13	1.444 (3)
Ru...C13	2.138 (2)	C13-C14	1.444 (3)
Ru...C14	2.177 (2)	C6-C14	1.419 (3)
C1-C2	1.391 (4)	C13-C15	1.452 (3)
C2-C3	1.412 (5)	C15-O	1.212 (3)
C3-C4	1.415 (5)	C7-C16	1.539 (3)
C4-C5	1.404 (5)	C10-C16	1.542 (3)
C5-C1	1.392 (5)	C15-HC15	0.86 (3)

1 H), 1.69 (d,  $J = 8$  Hz, 1 H), 1.37 (d,  $J = 8$  Hz, 2 H);  $^{13}\text{C}$  NMR ( $\text{CDCl}_3$ ) 152.46, 145.77, 144.62, 120.02, 110.13, 100.72, 48.86, 42.91, 39.68, 39.11 (2 C), 29.53, 29.36 ppm.

Anal. Calcd for  $\text{C}_{13}\text{H}_{17}\text{N}$ : C, 83.37; H, 9.15. Found: C, 83.07; H, 9.12.

( $\eta^5$ -Cyclopentadienyl)( $\eta^5$ -4-formyltricyclo[5.2.1.0<sup>2,6</sup>]deca-2,4-dien-6-yl)iron (29 and 30). A solution of 27 (561 mg, 3.0 mmol) and 28<sup>31</sup> (1.45 g, 3.0 mmol) in dichloromethane was deoxygenated by bubbling nitrogen through for 10 min. While under a nitrogen atmosphere, the magnetically stirred solution was irradiated with a 300-W GE sunlamp for 24 h. The heat of the lamp was adequate to maintain constant reflux. The cooled reaction mixture was filtered, and the clear orange filtrate was added to ethanol (15 mL) containing 2 N sodium hydroxide solution (15 mL). Following a 90-min period of stirring, water (100 mL) was added and the product was extracted into dichloromethane (2  $\times$  50 mL). The combined organic layers were washed with water (2  $\times$  50 mL), dried, and concentrated. Chromatography on alumina (elution with hexane-dichloromethane (1:1)) delivered a 65:35 mixture of 29 and 30 ( $^1\text{H}$  NMR analysis). Sublimation at 80 °C and 0.5 torr furnished a red-orange powder: mp 113–116 °C (464 mg, 55%); IR (KBr,  $\text{cm}^{-1}$ ) 2995, 1665, 1658, 1438, 1385, 1358, 1285, 1120, 1100, 823, 652;  $^1\text{H}$  NMR data, see Table VI;  $^{13}\text{C}$  NMR ( $\text{CDCl}_3$ ) 196.11, 195.33, 111.84, 102.91, 70.17, 69.65, 62.10, 59.70, 57.96, 47.68, 38.30, 37.66, 31.94, 28.22 ppm;  $m/z$  calcd ( $\text{M}^+$ ) 280.0550, obsd 280.0556.

Anal. Calcd for  $\text{C}_{16}\text{H}_{16}\text{FeO}$ : C, 68.56; H, 5.76. Found: C, 68.77; H, 5.83.

( $\eta^5$ -Cyclopentadienyl)( $\eta^5$ -4-(hydroxymethyl)tricyclo[5.2.1.0<sup>2,6</sup>]dien-6-yl)iron (31 and 32). A solution of the 29/30 mixture (100 mg, 0.357 mmol) in 95% ethanol (20 mL) was treated with sodium borohydride (20 mg, 0.528 mmol) and stirred at room temperature for 30 min. Water (100 mL) was added, and the products were extracted into ether (2  $\times$  50 mL). The ether phase was washed with water (2  $\times$  100 mL), dried, and concentrated to leave a yellow crystalline solid (98 mg, 97.7%). The two alcohols were separated by HPLC (silica gel, elution with 25% ethyl acetate in hexane).

Major isomer 31: mp 122.5–123.5 °C; IR (KBr,  $\text{cm}^{-1}$ ) 3480, 3360, 3000, 2980, 2970, 1120, 1105;  $^1\text{H}$  NMR (300 MHz,  $\text{CDCl}_3$ ) sample somewhat paramagnetic—peaks somewhat broadened.

Minor isomer 32: mp 134.0–135.0 °C; IR (KBr,  $\text{cm}^{-1}$ ) 3525, 3340, 2990, 2975, 1105, 990;  $^1\text{H}$  NMR (300 MHz,  $\text{CDCl}_3$ )  $\delta$  4.18 (s, 7 H), 4.12 (s, 2 H), 2.78 (s, 2 H), 2.15 (d,  $J = 6$  Hz, 2 H), 1.91 (br s, 2 H), 1.68 (d,  $J = 8$  Hz, 2 H), 1.38 (br s, 2 H).

**Oxidation of 31.** A solution of 31 (50 mg, 0.177 mmol) in benzene (20 mL) containing activated manganese dioxide (61.6 mg, 0.709 mmol) was deoxygenated by bubbling argon for 10 min and stirred at room temperature for 14 h under argon. The mixture was filtered and concentrated to give 45.9 mg (92.6%) of 29 as a red crystalline solid, pure by  $^1\text{H}$  NMR analysis.

**Oxidation of 32.** Alcohol 32 (20 mg, 0.071 mmol) and manganese dioxide (43.5 mg, 0.500 mmol) were suspended in benzene

(20 mL). By means of the procedure described above, there was isolated 18 mg (90.6%) of 30 as a red crystalline solid, pure by  $^1\text{H}$  NMR analysis.

**Dehydrative Dimerization of 31.** A solution of 31 (21.3 mg, 0.0755 mmol), *p*-toluenesulfonyl chloride (7.3 mg, 0.0377 mmol), and triethylamine (4 drops) in dry benzene (20 mL) was deoxygenated by bubbling argon through for 10 min. The resulting pale yellow mixture was stirred at room temperature under argon for 20 h. Water was added, and the product was extracted into ethyl acetate (3  $\times$  30 mL). The combined organic layers were dried and concentrated to leave a pale yellow solid. This material was dissolved in ethyl acetate and filtered through a small wad of alumina. Solvent evaporation and recrystallization from deoxygenated ethyl acetate afforded 18.4 mg (89%) of ether 33 as pale yellow crystals: mp 201.5–202.5 °C; IR (KBr,  $\text{cm}^{-1}$ ) 2980, 2880, 1390, 1340, 1290, 1105, 1055, 1000, 945, 505;  $^1\text{H}$  NMR (300 MHz,  $\text{CDCl}_3$ )  $\delta$  4.21 (br s, 4 H), 4.06 (s, 10 H), 3.92 (s, 4 H), 2.82 (s, 4 H), 2.22 (br s, 2 H), 1.67 (d,  $J = 7$  Hz, 4 H), 1.31 (d,  $J = 8$  Hz, 2 H), 1.01 (br s, 4 H).

**X-ray Crystal Structure Analysis of 33.** A prismatic colorless crystal of approximate dimensions 0.03  $\times$  0.25  $\times$  0.50 mm was mounted on the tip of a thin glass fiber. Both X-ray examination of the crystal and data collection were carried out on an Enraf-Nonius CAD4 diffractometer using graphite-monochromated Mo  $K\alpha$  radiation. At room temperature, the cell parameters and standard deviations were determined by least-squares fitting from 24 reflections, well distributed in reciprocal space and lying in the  $2\theta$  range between 25° and 30°. Intensity data were collected in the  $\omega$ - $2\theta$  scan mode with the  $2\theta$  range lying between 4° and 50°. A total of 4853 independent reflections was measured with 3492 unique data having  $F_o^2 > 3.0\sigma(F_o^2)$ . Details of data collection are given in Table II. The data were corrected for Lorentz and polarization effects as well as absorption.

The analytical form of the scattering factors for neutral atoms was used throughout the analysis, and both  $\Delta f'$  and  $i\Delta f''$  terms were included for all atoms. All of the crystallographic computations were carried out on a PDP 11/44 computer using the SDP (structure determination package).

The statistic distribution of reflection intensities indicated that the space group might be  $P\bar{1}$ . The final structure shows that the space group is indeed  $P\bar{1}$ . The structure was solved with the aid of MULTAN 82. The two iron atoms were located in the *E* map. After several cycles of full-matrix least-squares refinement of the positional and isotropic thermal parameters for these two atoms, all the non-hydrogen atoms appeared in the difference electron density maps.

Following several cycles of full-matrix least-squares refinement of the positional parameters and anisotropic thermal parameters for the iron atoms and the isotropic thermal parameters for the carbon and oxygen atoms, the converged *R* value was determined to be 0.094. The difference electron density maps showed four significant peaks (electron densities = 3.35, 2.94, 1.87, 1.35  $\text{e}/\text{Å}^3$ ) besides the hydrogen atoms. After several cycles of refinement of these four peaks following assumption of carbon atoms, the isotropic thermal parameters were 7.6, 8.6, 14.2, and 17.9, and the *R* value was 0.071. Finally, these four peaks were assumed to be disordered solvent ( $\text{CH}_3\text{CN}$ ) molecules. The multiplicities were assumed to be 0.5 and 0.5.

The function minimized during the least-squares refinement process was  $\sum w(|F_o| - |F_c|)^2$ , where the assigned weights are given as  $w = 4F_o^2/[\sigma^2(I) + (pI)^2]$ , and  $p = 0.03$  was chosen as previously described. The final full-matrix least-squares refinement cycle with anisotropic thermal parameters for all non-hydrogens, fixed isotropic for solvent atoms and hydrogen atoms, gave  $R_F = 0.032$  and  $R_{wF} = 0.039$ , for 3492 reflections with 477 variable parameters, where  $R_F = \sum ||F_o| - |F_c|| / \sum |F_o|$  and  $R_{wF} = \sum w^{1/2} ||F_o| - |F_c|| / w^{1/2} \sum |F_o|$ . The largest shift vs error was 0.51. The final difference Fourier map showed no significant features (highest electron density = 0.33  $\text{e}/\text{Å}^3$ ).

Final positional and thermal parameters are listed in Tables XVII and XVIII (supplementary material). Table XIX (supplementary material) contains the relevant values of  $10F_o$  and  $10F_c$ .

( $\eta^5$ -Cyclopentadienyl)( $\eta^5$ -4-formyltricyclo[5.2.1.0<sup>2,6</sup>]deca-2,4-dien-6-yl)ruthenium (35 and 36). A solution of 27 (100 mg, 0.75 mmol) and 34<sup>33</sup> (300 mg, 0.70 mmol) in 1,2-dichloroethane

(31) (a) Sutherland, R. G. *J. Organomet. Chem. Libr.* 1977, 3, 311. (b) Gill, T. P.; Mann, K. R. *Inorg. Chem.* 1980, 19, 3007. (c) Lee, C. C.; Gill, U. S.; Iqbal, M.; Azogu, C. I.; Sutherland, R. G. *J. Organomet. Chem.* 1982, 231, 151.

(32) Gill, T. P.; Mann, K. R. *Organometallics* 1982, 1, 485.

(40 mL) was heated at the reflux temperature under a nitrogen atmosphere for 14 h. The cooled reaction mixture was filtered, and the filtrate was added to ethanol (15 mL) containing 2 N sodium hydroxide solution. Following a 90-min period of stirring and workup as described above, the pale brown solid was chromatographed on alumina (elution with dichloromethane). There was isolated an 86:14 mixture of **35** and **36** ( $^1\text{H}$  NMR analysis). Recrystallization from ether-ethyl acetate (1:1) gave pure **35** as pale yellow crystals (82 mg, 33%): mp 155.0–155.5 °C; IR (KBr,  $\text{cm}^{-1}$ ) 2999, 2990, 2950, 1680, 1665, 1435, 1375, 1358, 1348, 1288, 1252, 1120, 1100, 825, 815, 650;  $^1\text{H}$  NMR data, see Table VII;  $^{13}\text{C}$  NMR ( $\text{CDCl}_3$ ) (pure **35**) 190.91, 105.60, 85.12, 72.57, 62.48, 48.93, 37.56, 27.92 ppm;  $m/z$  calcd ( $M^+$ ) 326.0238, obsd 326.0238.

Anal. Calcd for  $\text{C}_{16}\text{H}_{16}\text{ORu}$ : C, 58.89; H, 4.94. Found: C, 59.03; H, 5.13.

**X-ray Crystal Structure Analysis of 35.** The crystals of **35** were pale yellow, clear rods. The crystal used for data collection was cut from the end of one rod and measured approximately 0.15 mm  $\times$  0.42 mm  $\times$  0.46 mm. Preliminary examination of the crystal on a Syntex P1 diffractometer indicated a monoclinic crystal system with systematic absences  $h0l$ ,  $h + l = 2n + 1$ , and  $0k0$ ,  $k = 2n + 1$ , which uniquely determines the space group as  $P2_1/n$ . The unit cell constants  $a = 5.867$  (1) Å,  $b = 13.394$  (2) Å,  $c = 16.386$  (2) Å, and  $\beta = 99.59$  (1)° were determined by the least-squares fit of the diffractometer setting angles at room temperature for 25 reflections in the  $2\theta$  range 20–30° with Mo  $K\alpha$  radiation ( $\lambda(\text{K}\alpha) = 0.71069$  Å).

The  $\omega$ - $2\theta$  scan technique was used to measure intensities on the Syntex P1 diffractometer. The data were corrected for Lorentz and polarization effects and put onto an absolute scale by means of a Wilson plot.<sup>33</sup> Four reflections were omitted from the data set, (002), (021), (101), and (111), since they saturated the detector during data collection. The measurement of six standard reflections after every 100 reflections gave no indication of crystal decomposition. Other crystallographic details are presented in Table II.

The position of the Ru atom was located by MULTAN 80.<sup>34</sup> This one atom was then phased on in the DIRDIF program<sup>35</sup> and the

remainder of the non-hydrogen atoms were easily located in the electron density map. The SHELX-76 package<sup>36</sup> was used for full-matrix least-squares refinements. Isotropic refinement of the model converged to an  $R$  factor of 0.065. An absorption correction was applied at this point by means of the Gaussian grid method with an  $8 \times 8 \times 8$  grid. Transmission factors ranged from 0.63 to 0.85. Isotropic refinement on the absorption corrected data set then converged at  $R = 0.059$ .

After one cycle of anisotropic refinement, the hydrogen atoms were located on a difference electron density map. The aldehyde hydrogen atom was allowed isotropic refinement; the remainder of the hydrogen atoms were included in the model as fixed contributions in their calculated positions with C–H = 1.00 Å and  $B_{\text{H}} = B_{\text{C(iso)}} + 1.0$  Å<sup>2</sup>. The final refinement cycle resulted in agreement indices (based on  $F$ ) of  $R = 0.022$  and  $R_w = 0.027$  for the 2463 intensities with  $F_o^2 > 3\sigma(F_o^2)$  and the 167 variable parameters, where  $R = \sum ||F_o| - |F_c|| / \sum |F_o|$  and  $R_w = [\sum w(|F_o| - |F_c|)^2 / \sum w|F_o|^2]^{1/2}$  with  $w = 1/\sigma^2(F_o)$ . [Final positional and thermal parameters are listed in Table XX (supplementary material) while Table XXI (supplementary material) contains values of  $10F_o$  and  $10F_c$ ]. The maximum and minimum peak heights in the final difference electron density map are 0.31 and  $-0.38$  e/Å<sup>3</sup>. Scattering factors for the ruthenium, oxygen, and carbon atoms<sup>28</sup> and for the hydrogen atoms<sup>37</sup> are from the usual sources. Anomalous dispersion values for all non-hydrogen atoms were included in the calculations.

**Acknowledgment.** We thank the National Institutes of Health for their support of this research program through Grant CA-12115.

**Registry No.** 1, 75725-33-6; 16, 89709-01-3; 20, 6675-71-4; 21, 89669-80-7; 22, 99746-98-2; 27, 99747-02-1; 28, 34978-37-5; 29, 99746-99-3; 30, 99782-55-5; 31, 99747-00-9; 32, 99782-56-6; 33, 99764-86-0; 34, 80049-61-2; 35, 99747-01-0; 36, 99782-57-7; Fe<sup>II</sup>-(acac)<sub>2</sub>(py)<sub>2</sub>, 14843-55-1; RuCl<sub>3</sub>, 10049-08-8; Ru, 7440-18-8; ethyl bromide, 74-96-4.

**Supplementary Material Available:** Stereodrawings of the unit cells for **21**, **33**, and **35** (Figures 6–8) together with bond angles (Tables VIII, X, and XII), weighted least-squares planes (Tables IX, XI, and XIII), final positional and thermal parameters (Tables XIV, XVII, and XX), refined temperature factor expressions (Tables XV (21) and XVIII (33)), and observed and calculated structure factors (Tables XVI, XIX, and XI) for all three complexes (79 pages). Ordering information is given on any current masthead page.

(33) Sheldrick, G. M. "SHELX-76. Program for Crystal Structure Determination"; University Chemical Laboratory: Cambridge, England, 1976.

(37) Stewart, R. F.; Davidson, E. R.; Simpson, W. T. *J. Chem. Phys.* 1965, 42, 3175.

(33) The programs used for data reduction are from the CRYM crystallographic computing package (Duchamp, D. J.; Trus, B. L.; Westphal, B. J., California Institute of Technology, Pasadena, CA) and modified by G. G. Christoph at The Ohio State University, Columbus, OH.

(34) Main, P.; Fiske, S. J.; Hull, S. E.; Lessinger, L.; Germain, G.; Declercq, J.-P.; Woolfson, M. M. "MULTAN 80, A System of Computer Programs for the Automatic Solution of Crystal Structures from X-ray Diffraction Data"; University of York, England, and University of Louvain, Belgium, 1980.

(35) Beurskens, P. T.; Bosman, W. P.; Doesburg, H. M.; Gould, R. O.; Van den Hark, Th. E. M.; Prick, P. A. J.; Noordik, J. H.; Beurskens, G.; Parthasarathi, V.; Bruins Slot, H. J.; Hiltiwanger, R. C. "DIRDIF: Direct Methods for Difference Structures"; Crystallography Laboratory, University of Nijmegen: The Netherlands, 1983.

# 4-(Dimethylamino)isodicyclopentafulvene and the 4-Methylisodicyclopentadienyl Anion as $\pi$ Ligands. Stereochemical Course of Their Complexation to Group 6 Transition-Metal Carbonyls<sup>1</sup>

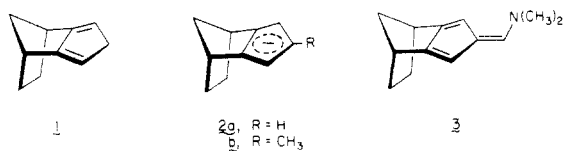
Leo A. Paquette,\* Susan J. Hathaway, Paulo F. T. Schirch, and Judith C. Gallucci<sup>2</sup>

Evans Chemical Laboratories, The Ohio State University, Columbus, Ohio 43210

Received May 21, 1985

The new ligands 4-methylisodicyclopentadienide and 4-(dimethylamino)isodicyclopentafulvene were complexed with group 6 transition-metal carbonyls in order to assess  $\pi$ -facial stereoselectivity. In the first instance where isolation was conducted following conversion to the nitrosyl dicarbonyl derivatives, Cr was found to exhibit the most modest above-plane coordination ability (53%) and W was found to exhibit the greatest (89%). The three-dimensional character of these structures was deduced by the combination of a crystallographic analysis of *exo*-(4-CH<sub>3</sub>C<sub>10</sub>H<sub>10</sub>)W(CO)<sub>2</sub>NO (**4c**) and <sup>1</sup>H/<sup>13</sup>C NMR correlations. Direct condensation of the fulvene with the same triad of metal hexacarbonyls gave rise exclusively to *exo* complexes, as determined by submission of *exo*-(4-CH=N(CH<sub>3</sub>)<sub>2</sub>C<sub>10</sub>H<sub>10</sub>)Mo(CO)<sub>3</sub> (**6b**) to an X-ray structure determination. Both of the molecules examined in detail possess a pyramidalized central double bond ( $\theta = 11-12^\circ$ ). A reasonable level of appreciation for the stereochemical course of metal coordination to isodicyclopentadiene derivatives is beginning to evolve.

Isodicyclopentadiene (**1**), its anion (**2a**), and fulvene **3** have proven useful as ligands for the analysis of  $\pi$ -face stereoselectivity in complexation to metal centers.<sup>1,3,4</sup> As a direct result of fusion of the unsaturated ring to positions 2 and 3 of the norbornyl framework, considerable bias is introduced for kinetically controlled coordination *syn* to the methano bridge. For example, the face selectivity observed during the conversion of **2a** to metallocene derivatives is impressively high. Included within this group are ferrocene, ruthenocene, nickelocene, and vanadocene systems, amongst others. When **3** is irradiated in the presence of ( $\eta^5$ -cyclopentadienyl)( $\eta^6$ -*p*-xylene)iron(II) hexafluorophosphate, less tendency was exhibited for bonding to the *exo* surface (65%). An intermediate stereochemical outcome (86% above-plane) was encountered when **3a** was heated with ( $\eta^5$ -cyclopentadienyl)tris(acetonitrile)ruthenium(II) hexafluorophosphate.

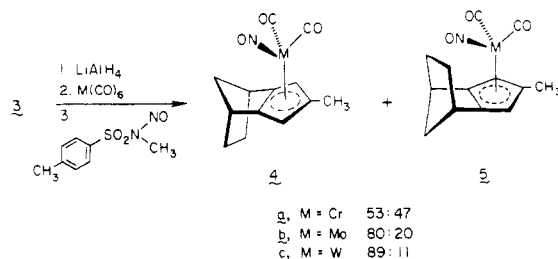


In an effort to shed greater light on the possible root cause of this interesting kinetic preference, we have now proceeded beyond the realm of sandwich complexes and herein report in detail on the stereochemical course of complexation of transition-metal carbonyl fragments to **2b** and **3**. The selection of both an anionic system and a neutral substrate was purposeful in that a broader range of ligand reactivity seemed warranted at this stage of our investigation.

## Results

Fischer and co-workers were the first to describe the preparation of ( $\eta^5$ -cyclopentadienyl)dicarbonylnitrosyl-metal complexes of chromium, molybdenum, and tungsten.<sup>5</sup> In line with that report and more recent descriptions of related chemistry,<sup>6</sup> tetrahydrofuran solutions of **2b** were heated with Cr(CO)<sub>6</sub> at the reflux temperature for 24 h and the tricarbonyl complex so produced was nitrosylated at once with *N*-methyl-*N*-nitroso-*p*-toluenesulfonamide. At the outset, anion **2b** was generated directly in this solvent by LiAlH<sub>4</sub> reduction of **3**.<sup>1</sup> Following solvent evaporation and chromatography of the residue on Florisil, the pair of red-colored complexes **4a** and **5a** were isolated in good yield (90%). These air-sensitive compounds, which decomposed when stored in a freezer under nitrogen, were produced in a ratio of 53:47. The major isomer was determined to be the above-plane complex **4a** on the basis of the closer correspondence of its <sup>1</sup>H NMR spectrum to that of **4c** whose stereochemical features were unequivocally established by X-ray analysis. Comparable trends in chemical shift appear in the <sup>1</sup>H NMR spectra of **5a** and **5c** (see Experimental Section).

Treatment of **2b** with Mo(CO)<sub>6</sub> in an entirely comparable manner produced the more stable complexes **4b** and **5b** with similar efficiency. In this instance, the more dominant *exo* stereoisomer **4b** was formed in somewhat greater proportion (80%) relative to **5b** (20%). Once



again, coordination from above as in **4** has the effect of causing the pair of symmetry-related cyclopentadienide

(1) Electronic Control of Stereoselectivity. 33. For part 32, see: Paquette, L. A.; Schirch, P. F. T.; Hathaway, S. J.; Hsu, L.-Y.; Gallucci, J. C., preceding paper in this issue.

(2) Author to whom inquiries concerning the X-ray crystal structure analyses should be directed.

(3) Hsu, L.-Y.; Hathaway, S. J.; Paquette, L. A. *Tetrahedron Lett.* **1984**, 259.

(4) (a) Reimschneider, R. Z. *Naturforsch., B: Anorg. Chem., Org. Chem., Biochem., Biol.* **1962**, *17B*, 133. (b) Katz, T. J.; Mrowca, J. J. *J. Am. Chem. Soc.* **1967**, *89*, 1105. (c) Scroggins, W. T.; Rettig, M. F.; Wing, R. M. *Inorg. Chem.* **1976**, *15*, 1381. (d) Kohler, F. H. *J. Organomet. Chem.* **1976**, *110*, 235.

(5) Fischer, E. O.; Becker, O.; Hafner, W.; Stahl, H. O. *Z. Naturforsch., B: Anorg. Chem., Org. Chem., Biochem., Biophys., Biol.* **1955**, *10B*, 598.

(6) (a) Rausch, M. D.; Mintz, E. A.; Macomber, D. W. *J. Org. Chem.* **1980**, *45*, 689. (b) Macomber, D. W.; Rausch, M. D. *Organometallics* **1983**, *2*, 1523.

Table I. Experimental Crystallographic Data for 4c and 6b<sup>c</sup>

	4c	6b
space group	$P\bar{1}$	$P2_1/n$
a, Å	6.160 (1)	5.959 (1)
b, Å	15.313 (2)	14.823 (3)
c, Å	6.877 (1)	17.107 (3)
$\alpha$ , deg	93.02 (1)	
$\beta$ , deg	85.87 (1)	97.47 (1)
$\gamma$ , deg	97.72 (1)	
vol, Å <sup>3</sup>	641	1498
Z	2	4
mol wt	415.10	367.26
$D_{\text{calcd}}$ , g cm <sup>-3</sup>	2.15	1.63
linear abs coeff, cm <sup>-1</sup>	92.05	8.62
transmission factors	0.099–0.537	0.730–0.778
cryst size, mm	0.07 × 0.30 × 0.54	0.33 × 0.37 × 0.42
2 $\theta$ range, deg	4–55	4–55
scan speed, deg min <sup>-1</sup> in 2 $\theta$	4.0–24.0	4.0–24.0
scan range	( $K\alpha_1 - 1.0^\circ$ ) to ( $K\alpha_2 + 1.0^\circ$ )	( $K\alpha_1 - 1.0^\circ$ ) to ( $K\alpha_2 + 1.1^\circ$ )
data collected	+h, ±k, ±l	+h, +k, ±l
unique data	2947	3458
unique data with $F_o^2 > 3\sigma(F_o^2)$	2598	2858
final no. of variables	163	190
$R(R_w)^b$	0.023 (0.027)	0.024 (0.031)
error in observn of unit weight, e	1.43	1.73

<sup>c</sup> Both data sets were collected on a Syntex P1 diffractometer using Mo  $K\alpha$  radiation at 20 °C [graphite monochromator,  $\lambda(K\alpha_1) = 0.70926$  Å]. <sup>b</sup>  $R = \sum ||F_o| - |F_c|| / \sum |F_o|$  and  $R_w = [\sum w(|F_o| - |F_c|)^2 / \sum w|F_o|^2]^{1/2}$  with  $w = 1/\sigma^2(F_o)$ .

vinyl protons to resonate at higher field than their counterparts in 5. A further diagnostic is the greater deshielding experienced by the methyl group in 4 relative to that in 5.

The reaction between 2b and  $W(CO)_6$  produced an 89:11 mixture of 4c and 5c. The major isomer could be secured in a pure state by recrystallization. The orange crystals proved suitable for crystallographic analysis (Table I and Figure 1). Despite the fact that the carbonyl and nitrosyl ligands in these types of molecules are frequently disordered, the location of the nitrogen atom was indicated by the shorter length of the W–N bond (1.839 Å) as compared with the two proximal W–C bonds (Table II).

The cyclopentadienide ring in 4c is planar within experimental error. Methyl carbon C(13) lies significantly out of this plane and in the direction away from the W atom. The dihedral angle between the least-squares plane defined by the C(4), C(3), C(7), and C(6) atoms and that least-squares plane containing atoms C(8), C(7), C(3), and C(11) is 168.4°. The disposition of the Cp ring with respect to the W atom is such that the W–C bond lengths are inequivalent. The W–C(3) and W–C(7) bond lengths are the shortest at 2.334 (4) and 2.327 (4) Å, respectively. The W–C(4) and W–C(6) bond lengths are slightly longer (2.354 (4) and 2.353 (4) Å). Finally, the W–C(5) length of 2.370 Å exceeds all of the others. This indication that the cyclopentadienide ring may well have five nonequivalent carbon atoms was observed previously in an entirely different context by Atwood and co-workers.<sup>7</sup> The distance between the tungsten atom and the centroid of the unsaturated five-membered ring (2.015 Å) compares favorably with similar structures.<sup>8</sup>

Apical carbon C(12) of the norbornyl fragment is clearly seen to lie on the same side of the hydrocarbon ligand as the W atom. The isodicyclopentadienyl ligand contains a noncrystallographic mirror plane that bisects the C-

Table II. Bond Distances (Å) in 4c

W–C1	1.931 (5)	C3–C4	1.428 (6)
W–C2	1.978 (5)	C4–C5	1.422 (7)
W–N	1.839 (4)	C5–C13	1.500 (7)
W–C3	2.334 (4)	C5–C6	1.426 (7)
W–C4	2.354 (4)	C6–C7	1.397 (6)
W–C5	2.370 (4)	C7–C3	1.406 (5)
W–C6	2.353 (4)	C7–C8	1.504 (6)
W–C7	2.327 (4)	C8–C9	1.552 (6)
C1–O1	1.157 (7)	C9–C10	1.551 (7)
C2–O2	1.130 (6)	C10–C11	1.561 (6)
N–O3	1.186 (5)	C3–C11	1.504 (6)
W–R <sup>a</sup>	2.015	C8–C12	1.560 (6)
		C11–C12	1.547 (7)

<sup>a</sup> R is the centroid of the cyclopentadiene ring.

(3)–C(7) and C(9)–C(10) bonds and contains the carbon of the methano bridge and the C(5) and C(13) atoms. The worst agreement with respect to this pseudomirror plane is for the C(3)–C(4) and C(6)–C(7) bond lengths: 1.428 (6) and 1.397 (6) Å. A possible reason for the longer C(3)–C(4) bond is suggested by the projected view of the molecule in Figure 1a. In projection the W–C(2) bond approximately bisects the C(3)–C(4) bond and brings both centers into close proximity of C(2): the C(2)⋯C(3) distance is 3.17 Å, while that for C(2)⋯C(4) is only 3.10 Å. The W–N bond is situated such that the N atom lies close only to C(7), which is 3.17 Å away. Also notable is the C(1)⋯C(5) distance (3.09 Å) and the near eclipsing of the C(1)–O(1) bond by the C(5)–C(13) bond. The torsion angle defined by C(13)–C(5)–C(1)–O(1) is –8.1°.

When electron-rich 4-(dimethylamino)isodicyclopentadiene (3) was treated directly with  $Cr(CO)_3(CH_3CN)_3$ , ligand exchange on the transition metal was readily achieved.<sup>9</sup> The related Mo and W reagents behaved comparably as expected.<sup>9–11</sup> In each instance, a single crystalline adduct was isolated. As a result of the development of immonium ion character in the product complexes and the attendant increase in the barrier to rotational isomerization (the magnitude of which is likely dependent upon

(7) Atwood, J. L.; Shakir, R.; Malito, J. T.; Haberhold, M.; Kremnitz, W.; Bernhagen, W. P. E.; Alt, H. G. *J. Organomet. Chem.* 1979, 165, 65.

(8) (a) Greenhough, T. J.; Kolthammer, B. W. S.; Legzdins, P.; Trotter, J. *Acta Crystallogr., Sect. B: Struct. Crystallogr. Crystl. Chem.* 1980, B36, 795. (b) Wilford, J. B.; Powell, H. M. *J. Chem. Soc. A.* 1969, 8. (c) Malito, J. T.; Shakir, R.; Atwood, J. L. *J. Chem. Soc., Dalton Trans.* 1980, 1253. (d) Semion, V. A.; Struchkov, Yu. T. *Zh. Strukt. Khim.* 1968, 9, 1046.

(9) (a) Edelmann, F.; Behrens, U. *Chem. Ber.* 1984, 117, 3463. (b) Lubke, B.; Edelmann, F.; Behrens, U. *Ibid.* 1983, 116, 11.

(10) Setkina, V. N.; Strunin, B. N.; Kursanov, D. N. *J. Organomet. Chem.* 1980, 186, 325.

(11) King, R. B.; Fronzaglia, A. *Inorg. Chem.* 1966, 5, 1837.



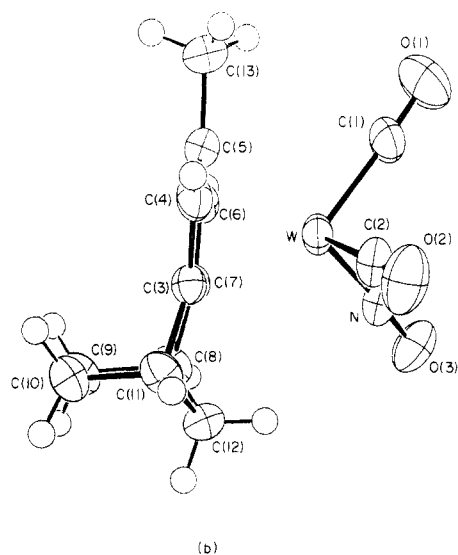
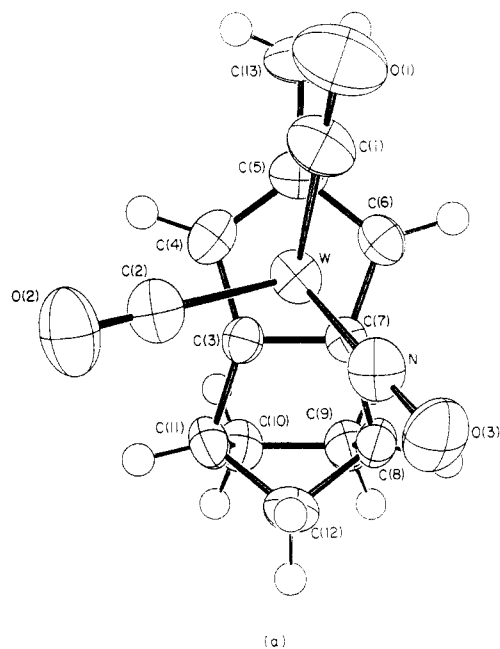


**Figure 1.** ORTEP drawings of **4c**: (a) top view; (b) side view. Non-hydrogen atoms are represented by 50% probability thermal ellipsoids, while the hydrogen atoms are drawn with an artificial radius.

**Table V. Bond Distances (Å) in 6b**

Mo...C1	1.936 (3)	Mo...C6	2.293 (2)
Mo...C2	1.938 (3)	Mo...C7	2.349 (2)
Mo...C3	1.932 (3)	Mo...C8	2.396 (2)
Mo...C4	2.420 (2)	Mo...R <sup>a</sup>	2.026
Mo...C5	2.343 (2)		
Cl-O1	1.153 (3)		
C2-O2	1.149 (3)		
C3-O3	1.162 (4)		
C4-C5	1.388 (3)	C8-C7	1.398 (3)
C5-C6	1.453 (3)	C7-C6	1.453 (3)
C6-C14	1.415 (3)		
C14-N	1.308 (3)		
N-C15	1.450 (4)	N-C16	1.465 (4)
C4-C8	1.433 (3)		
C4-C12	1.505 (3)	C8-C9	1.508 (3)
C12-C11	1.556 (3)	C9-C10	1.546 (3)
C12-C13	1.535 (4)	C9-C13	1.541 (3)
C10-C11	1.551 (3)		

<sup>a</sup>R is the centroid of the cyclopentadiene ring.

the metal involved),<sup>12</sup> the NMR spectra of **6** are no longer as simplified as those of **4** and **5**. The greatest spectral

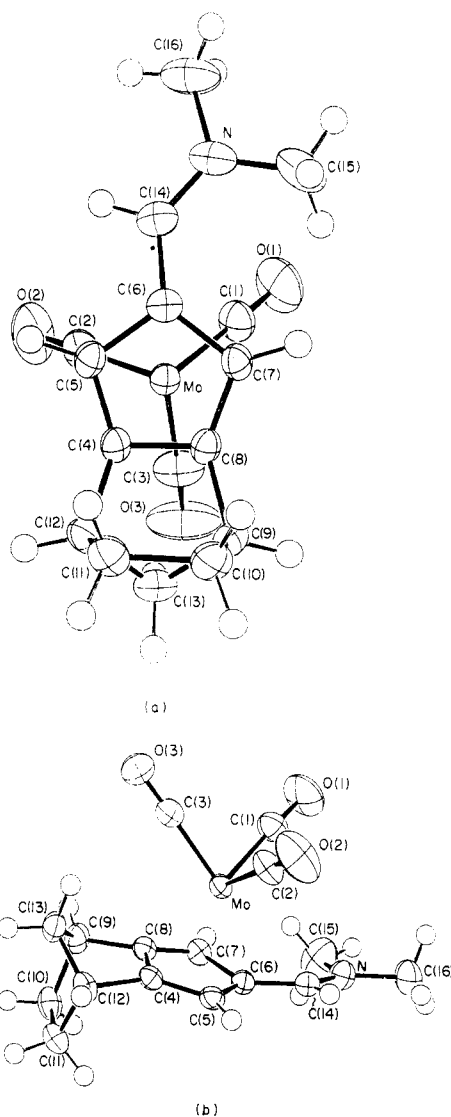
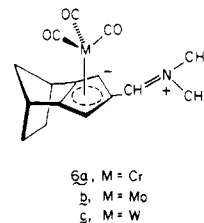


**Figure 2.** ORTEP drawings of **6b**: (a) top view down the Mo-ring centroid axis; (b) side view. Non-hydrogen atoms are represented by 50% probability thermal ellipsoids, while the hydrogen atoms are drawn with an artificial radius.

changes are seen in the progression from Cr to Mo. For the other pair (**6b** and **6c**), the <sup>1</sup>H NMR features are almost superimposable. No surprises were noted and all three substances therefore appeared to partake of the identical stereochemical character. Accordingly, the central member of the series (**6b**) was selected for X-ray crystallographic analysis.



A noncrystallographic mirror plane was found to exist in the isodicyclopentadienyl fragment of **6b** as a result of good agreement between chemically equivalent bond

(12) Strunin, B. N.; Bakhmutov, V. I.; Setkina, V. N.; Kursanov, D. *N. J. Organomet. Chem.* 1981, 208, 81.

(13) The structure of tricarbonyl(6-(dimethylamino)fulvene)chromium has been determined by single-crystal X-ray analysis and provides an interesting comparison: Lubke, B.; Behrens, U. *J. Organomet. Chem.* 1978, 149, 327.

lengths (Table V) and bond angles. The molybdenum atom is without doubt located *syn* to the methano bridge (Figure 2). The Mo-C distances for the three carbonyl groups are equivalent, while the Mo-C distances for the carbon atoms of the cyclopentadienide ring vary from 2.293 to 2.420 Å. While the Mo atom is closest to the C(6) atom of this ring (2.293 Å), it is equidistant from C(5) and C(7) (2.343 and 2.349 Å, respectively) and slightly closer to C(8) (2.396 Å) than to C(4) (2.420 Å). The distance between the Mo atom and the centroid of this ring is 2.026 Å.

The least-squares plane through this cyclopentadienide-like ring indicates that it is essentially planar. The N and C(14) atoms lie significantly out of this plane and in the direction of the Mo atom. The C(9) and C(12) atoms also reside significantly out of this plane but in the opposite direction. In fact, the C(9)-C(8)-C(4)-C(12) atoms of the norbornane fragment are not quite coplanar, the torsion angle being 2.1°. The least-squares plane through these four atoms makes a dihedral angle of 169.0° with the least-squares plane through the attached five-membered ring. The analogous four atoms of the other half of the norbornane fragment are also not coplanar; i.e., the C(9)-C(10)-C(11)-C(12) torsion angle is 2.3°.

Noteworthy, the C(6) atom of the five-membered ring is not coplanar with its substituents. In particular, the C(7)-C(6)-C(14) angle has opened to 131.5° to accommodate the -N(CH<sub>3</sub>)<sub>2</sub> group. Even so, the C(7)···C(15) intramolecular distance is still rather short at 3.14 Å.

### Discussion

Although the cyclopentadienide anion and its permethylated homologue have been intensively examined as ligands for group 6 metals, complexation involving a related system having two intrinsically different surfaces has not been accorded prior attention. The readily available conjugate bases of isodicyclopentadiene (**2a**) and its 4-methyl derivative (**2b**) possess this interesting property and consequently serve as potentially informative probes of stereoselectivity in the course of their coordination to various metals. The ease with which **2b** reacts with Cr(CO)<sub>6</sub>, Mo(CO)<sub>6</sub>, and W(CO)<sub>6</sub> parallels that of C<sub>5</sub>H<sub>5</sub><sup>-</sup>. Subsequent direct nitrosation of the reaction mixtures resulted in the formation of binary product mixtures in which *exo* isomer **4** became increasingly favored (53% → 89%) as the size of the metal was made larger. The greatest change in product distribution occurred during progression from the chromium to the molybdenum examples. A similar, although less complete trend had been noted in the accompanying report.<sup>1</sup> We made note on that occasion that the preference for above-plane coordination conformed to our tilted orbital hypothesis but did not constitute proof of the theory. The situation here is entirely analogous.

It is interesting that direct coordination of the same group of three metal carbonyls to the neutral, although highly polarized substrate **3** leads to exclusive formation of compounds **6a-c**. As usual, there is a possibility that small amounts (~3%) of below-plane adducts could have escaped spectroscopic detection. Nevertheless the degree of stereoselectivity is impressive. Future studies will hopefully define the limits to which this control of  $\pi$ -facial complexation can be expected to operate.

The detailed geometries of **4c** and **6b** reveal a particularly noteworthy structural feature. Both molecules are seen to be folded about their central bond, with the downward pyramidalization amounting to 11.6 and 11.0°, respectively. The magnitude of this bending compares closely to that observed for the three *exo* complexes structurally characterized in the preceding paper.<sup>1</sup> Recent

studies have shown *syn*-sesquinorbornenes ( $\theta = 16$ – $18^\circ$ )<sup>14</sup> and -norbornadienes ( $\theta = 22^\circ$ ),<sup>15,16</sup> as well as the parent *syn*-sesquinorbornatriene ( $\theta > 22^\circ$ )<sup>17</sup> to exhibit somewhat larger deviations from planarity, a phenomenon that has attracted considerable theoretical interest.<sup>18-22</sup> In particular, Houk has advanced the notion that these phenomena arise in order to minimize torsional repulsions between the relevant sp<sup>2</sup>-hybridized carbon orbitals and the allylic bond orbitals.<sup>23</sup> It may well be that the norbornyl subunits within **4c** and **6b** partake of a similar need to relieve energetically unfavorable influences, such that the resultant small increase in *exo* HOMO orbital extension induces the observed pyramidalization.

Some comment regarding the possible role of steric effects in directing the stereoselectivity of complexation is warranted. To estimate the extent of steric congestion in **4c** that would arise if the isodicyclopentadiene framework remained folded during below-plane complexation, the C(3)-C(4)-C(5)-C(6)-C(7) five-membered ring was treated as a mirror plane and the W(CO)<sub>2</sub>(NO) unit was reflected across this plane. The distances calculated for this geometry are W···C(9) = 2.69 Å, W···C(10) = 2.69 Å, N···C(9) = 2.06 Å, O(3)···C(9) = 2.38 Å, C(2)···C(10) = 2.65 Å, and O(2)···C(10) = 3.20 Å. Given the van der Waals radii for these atoms (C, 1.7; N, 1.55; O, 1.5),<sup>31</sup> it is patently clear that these intramolecular contacts are much too short as anticipated.

If the norbornene segment of this hypothetical structure is additionally rotated about the C(3)-C(7) bond such that the C(8) and C(11) atoms are moved into the plane of the five-membered ring, the new distances become 3.06, 3.06, 2.56, 2.83, 3.11, and 3.62 Å, respectively. Although steric congestion is still in evidence, some alleviation of this phenomenon could be arrived at by suitable rotation of the W(CO)<sub>2</sub>(NO) moiety.

Further flexing about the C(3)-C(7) bond so that the dihedral angle between the least-squares plane through the C(3)-C(4)-C(5)-C(6)-C(7) atoms and that through the C(8)-C(7)-C(3)-C(11) atoms is 167.7° generates distances (3.41, 3.41, 3.05, 3.31, 3.54, 4.03 Å, respectively) that are now quite reasonable in magnitude. Again, further small adjustments could be arrived at by rotation of the W(CO)<sub>2</sub>(NO) fragment about that axis passing through the W atom and the center of the five-membered ring. Thus, it can be concluded that if the isodicyclopentadiene framework can flex in an *exo* direction as much as it obviously does in an *endo* direction, there would be no steric impedence to below-plane complexation.

An analogous technique was utilized to analyze the ruthenium complex **35** described in the preceding paper.<sup>1</sup> When its C(6)-C(11)-C(12)-C(13)-C(14) ring was treated as an approximate mirror plane and the Ru(Cp) unit was reflected across this plane to obtain the exact below-plane counterpart, the key distances were calculated to be

(14) Paquette, L. A.; Green, K. E.; Hsu, L.-Y. *J. Org. Chem.* **1984**, *49*, 3650 and pertinent references cited therein.

(15) Bartlett, P. D.; Combs, G. L., Jr. *J. Org. Chem.* **1984**, *49*, 625.

(16) Paquette, L. A.; Green, K. E.; Gleiter, R.; Schäfer, W.; Gallucci, J. C. *J. Am. Chem. Soc.* **1984**, *106*, 8232.

(17) Paquette, L. A.; Künzer, H.; Green, K. E. *J. Am. Chem. Soc.* **1985**, *107*, 4788.

(18) Burkert, U. *Angew. Chem., Int. Ed. Engl.* **1981**, *20*, 572.

(19) Spanget-Larsen, J.; Gleiter, F. *Tetrahedron Lett.* **1982**, 927, 2435.

(20) Bartlett, P. D.; Roof, A. A. M.; Winter, W. J. *J. Am. Chem. Soc.* **1981**, *103*, 6520.

(21) Hagenbuch, J.-P.; Vogel, P.; Pinkerton, A. A.; Schwarzenbach, D. *Helv. Chim. Acta* **1981**, *64*, 1818.

(22) Houk, K. N.; Rondan, N. G.; Brown, F. K.; Jorgensen, W. L.; Madura, J. D.; Spellmeyer, D. C. *J. Am. Chem. Soc.* **1983**, *105*, 5980.

(23) The italicized shifts denote the signals due to the major isomer where both are obvious.

Ru...C(8) = 2.85 Å, Ru...C(9) = 2.84 Å, C(1)...C(8) = 2.62 Å, and C(5)...C(9) = 2.55 Å. While bringing atoms C(7) and C(10) into the "plane" of the isodicyclopentadiene Cp ring only partially alleviates the prevailing steric compressions (3.12, 3.11, 3.02, and 2.94 Å, respectively), further rotation until a dihedral angle of 170.3° is reached gives distances that are again quite respectable (3.38, 3.37, 3.41, and 3.34 Å, respectively). For comparison, the Ru...C distances in **35** are 3.46 and 3.07 Å to C(16) and C(15). Thus, the Cp group in **35** presents no more of a steric problem than the (CO)<sub>2</sub>(NO) group in **4c** when positioned below-plane. However, the isodicyclopentadiene nucleus must be willing to undergo some  $\pi$ -orbital pyramidalization in the exo direction to allow uncongested coordination to the metal.

It is coincidental that all five isodicyclopentadiene-transition-metal complexes examined in detail to this time share the same exo stereochemistry. The strikingly comparable endo bending of the central  $\pi$  bond has encouraged us to undertake the preparation of select endo complexes and to determine by X-ray analysis if the fused norbornyl ring will now experience pyramidalization toward the metal. This study is in progress.

### Experimental Section

( $\eta^5$ -4-Methylisodicyclopentadienyl)dicarbonylnitrosyl Metal Complexes (M = Cr, Mo, and W). A solution of **3** (935 mg, 5 mmol) in dry tetrahydrofuran (5 mL) was added dropwise to a cold (0 °C), magnetically stirred suspension of lithium aluminum hydride (190 mg, 5 mmol) under a nitrogen atmosphere. The mixture was allowed to warm to room temperature and was stirred for 21 h. M(CO)<sub>6</sub> (5 mmol) was added, and the reflux temperature was maintained for 24 h. Diazald (1.07 g, 5 mmol) was added in small portions, and stirring was continued for an additional hour. The solvent was removed in vacuo, and the residue was taken up in deoxygenated ether. Florisil was added, and the solvent was evaporated. This solid was placed atop a Florisil column, and the product was eluted (10% ether in hexane) under nitrogen. The rapidly moving colored band was collected and concentrated to afford the pair of complexes. Yields in all cases were approximately 90%.

For M = Cr: 53:47 **4a/5a**; <sup>1</sup>H NMR (300 MHz, CDCl<sub>3</sub>)<sup>23</sup>  $\delta$  4.61 (s, 2 H), 4.51 (s, 2 H), 3.04 (br s, 2 H), 2.93 (br s, 2 H), 2.27–2.24 (m, 2 H), 2.04–2.00 (m, 2 H), 1.93 (s, 2 H), 1.91–1.86 (m, 1 H), 1.90 (s, 3 H) 1.49 (dd,  $J$  = 8 and 2.5 Hz, 1 H), 1.36–1.21 (m, 3 H).

For **4a** (major): <sup>13</sup>C NMR (20 MHz, CDCl<sub>3</sub>) 215.44, 120.50, 111.59, 78.89, 49.65, 38.08, 28.33, 14.12 ppm.

For **5a** (minor): <sup>13</sup>C NMR (20 MHz, CDCl<sub>3</sub>) 215.07, 130.46, 103.28, 81.85, 59.64, 39.51, 32.07, 13.99 ppm.

For M = Mo: 80:20 **4b/5b**; <sup>1</sup>H NMR (300 MHz, CDCl<sub>3</sub>)<sup>23</sup>  $\delta$  5.22 (s, 2 H), 5.09 (s, 2 H), 3.10 (br s, 2 H), 3.09 (br s, 1 H), 2.27–2.07 (m), 2.05 (s, 3 H), 1.97 (s, 3 H), 1.89–1.84 (m), 1.38–1.32 (dt), 1.30–1.18 (m);  $m/z$  calcd (M<sup>+</sup>) 330.9971, 322.9958, obsd 331.0018, 322.9994.

For **4b** (major): <sup>13</sup>C NMR (20 MHz, CDCl<sub>3</sub>) 225.42, 124.67, 115.27, 82.70, 50.33, 38.87, 28.48, 14.49 ppm.

For **5b** (minor): <sup>13</sup>C NMR (20 MHz, CDCl<sub>3</sub>) 225.19, 134.98, 105.78, 85.84, 59.28, 39.81, 34.02, 14.09 ppm.

For M = W: 89:11 **4c/5c**; <sup>1</sup>H NMR (300 MHz, CDCl<sub>3</sub>)<sup>23</sup>  $\delta$  5.29 (s, 2 H), 5.19 (s, 2 H), 3.08 (br s, 2 H), 3.07 (br s, 2 H), 2.21 (s, 3 H), 2.14 (s, 3 H), 1.90 (dd,  $J$  = 9 and 2 Hz, 2 H), 1.43 (dt,  $J$  = 9 and 1.5 Hz, 1 H), 1.33–1.22 (m, 3 H).

For **4c** (major): <sup>13</sup>C NMR (20 MHz, CDCl<sub>3</sub>) 219.83, 123.37, 113.12, 81.84, 50.66, 38.90, 28.69, 14.32 ppm.

**X-ray Crystal Structure Analysis of 4c.** Crystals of **4c**, mp 89–90.5 °C, are clear, orange, thin plates. Preliminary precession photographs with Mo K $\alpha$  radiation indicated the Laue symmetry  $\bar{1}$ , which restricts the space group possibilities to P1 and P $\bar{1}$ . The crystal used for data collection was cut from a larger plate. The unit cell constants  $a$  = 6.160 (1) Å,  $b$  = 15.313 (2) Å,  $c$  = 6.877 (1) Å,  $\alpha$  = 93.02 (1)°,  $\beta$  = 85.87 (1)°, and  $\gamma$  = 97.72 (1)° were determined by the least-squares fit of the diffractometer setting angles for 25 reflections in the  $2\theta$  range 20–30° with Mo K $\alpha$

radiation ( $\lambda(K\alpha)$  = 0.71069 Å).

Intensities were measured by the  $\theta$ - $2\theta$  scan technique on a Syntex P $\bar{1}$  diffractometer. The data were corrected for Lorentz and polarization effects and put on an absolute scale by means of a Wilson plot.<sup>24</sup> Three reflections are not included in the data set, (001), (1 $\bar{2}$ 0), and (100), as they saturated the detector during data collection. From the measurement of six standard reflections after every 100 reflections there was no indication of crystal decomposition.

The space group P $\bar{1}$  was initially assumed to be correct. Successful solution and refinement of the structure in this space group supports this choice. The intensity statistics indicated a noncentrosymmetric space group, which is an expected result for a molecule containing one heavy atom.<sup>25</sup> The tungsten atom was located by the Patterson method; the remainder of the non-hydrogen atoms were located by standard Fourier techniques.

The SHELX-76 package<sup>26</sup> was used for full-matrix least-squares refinements. Isotropic refinement of the model converged to an  $R$  factor of 0.167. An absorption correction was applied at this point by the Gaussian grid method,<sup>27</sup> with an 8 × 8 × 8 grid. Further isotropic refinement on this absorption corrected data set converged at  $R$  = 0.085.

In these isotropic refinements an attempt was made to identify the NO group by initially treating the nitrogen atom as a carbon atom. The "W-C" bond lengths then converged to the following values: 1.834 (14), 1.924 (20), and 1.965 (17) Å. The thermal parameter for the carbon atom involved in the shortest bond to tungsten was also smaller than the thermal parameters for the remaining two carbon atoms: 2.8 Å<sup>2</sup> vs. 4.4 and 4.0 Å<sup>2</sup>. On the basis of these results, that carbon atom was changed to a nitrogen atom and treated as such for the remainder of the calculations.

After one cycle of anisotropic refinement, all the hydrogen atoms were located on a difference electron density map. The hydrogen atoms were included in the model as fixed contributions with C-H = 1.00 Å and  $B_H = B_{C(iso)} + 1.0$  Å<sup>2</sup>. A very strong low order reflection (020) was removed from the data set as it appeared to be suffering from extinction. The final refinement cycle on the anisotropic non-hydrogen atoms resulted in agreement indices of  $R$  = 0.023 and  $R_w$  = 0.027 (based on  $F$ ) for the 2598 intensities with  $F_o^2 > 3\sigma(F_o^2)$  and 163 variables. The final difference electron density map contains peaks ranging from 0.75 to 1.40 e/Å<sup>3</sup> in the immediate vicinity of the tungsten atom. The maximum peak height for the rest of the map is 0.62 e/Å<sup>3</sup>. Scattering factors for the tungsten, oxygen, nitrogen, and carbon atoms<sup>28a</sup> and for the hydrogen atoms<sup>28b</sup> are from the usual sources. Anomalous dispersion corrections for all the non-hydrogen atoms were included by using values for  $f'$  and  $f''$ .<sup>28a</sup>

**Direct Coordination to 3.** A solution of M(CO)<sub>6</sub> in acetonitrile (25 mL) was deoxygenated by bubbling nitrogen through for 10 min. The mixture was subsequently heated at the reflux temperature for 36–72 h under an argon atmosphere, cooled to room temperature, and freed of solvent in vacuo. The residual yellow crystalline solid was dissolved in dry tetrahydrofuran (40 mL) and **3** was added. The mixture, which immediately turned red-brown, was again deoxygenated for 10 min and heated at reflux (5–12 h). After cooling and filtration, the filtrate was concentrated to afford a dark red-brown solid. This material was kept at 0.1 torr for 2 h, suspended in hot deoxygenated acetone (100 mL), and filtered under nitrogen to give a deep red solution. Overnight cooling at -20 °C afforded deep red crystals.

For M = Cr: Cr(CO)<sub>6</sub> (500 mg, 2.20 mmol); **3** (290 mg, 2.50 mmol); heating 36 and 12 h; 46% yield of **6a**; mp >230 °C dec (from hexane-ethyl acetate); IR (KBr, cm<sup>-1</sup>) 1820, 1625, 1415, 1405, 1155, 1105, 615; <sup>1</sup>H NMR (300 MHz, acetone-*d*<sub>6</sub>)  $\delta$  7.69 (s, 1 H),

(24) The programs used for data reduction are from the CRYM crystallographic computing package [Duchamp, D. J.; Trus, B. L.; Westphal, B. J., California Institute of Technology, Pasadena, CA, 1964] and modified by G. G. Christoph at The Ohio State University.

(25) Hargreaves, A. *Acta Crystallogr.* 1955, 8, 12.

(26) Sheldrick, G. M. "SHELX-76, Program for Crystal Structure Determination"; University Chemical Laboratory: Cambridge, England, 1976.

(27) Busing, W. R.; Levy, H. A. *Acta Crystallogr.* 1957, 10, 180.

(28) (a) "International Tables for X-Ray Crystallography"; The Kynoch Press: Birmingham, England, 1974; Vol. IV. (b) Stewart, R. F.; Davidson, E. R.; Simpson, W. T. *J. Chem. Phys.* 1965, 42, 3175.

5.10–4.85 (br, 1 H), 4.70–4.45 (br, 1 H), 3.38 (s, 3 H), 3.21 (s, 3 H), 2.89 (br s, 2 H), 2.22 (d,  $J = 9$  Hz, 1 H), 1.95 (d,  $J = 8$  Hz, 2 H), 1.37 (d,  $J = 9$  Hz, 1 H), 1.24 (d,  $J = 5$  Hz, 2 H);  $^{13}\text{C}$  NMR (20 MHz, acetone- $d_6$ ) 232.32, 153.91, 81.04, 47.61, 47.37, 40.79, 39.35, 30.65 ppm;  $m/z$  ( $\text{M}^+$ ) calcd 323.0617, obsd 323.0625.

Anal. Calcd for  $\text{C}_{16}\text{H}_{17}\text{CrNO}_3$ : C, 59.44; H, 5.30. Found: C, 59.31; H, 5.41.

For  $\text{M} = \text{Mo}$ :  $\text{Mo}(\text{CO})_6$  (1.073 g, 4.06 mmol); **3** (536 mg, 4.06 mmol); heating 36 and 8 h; 77% yield of **6b**; mp  $>230$  °C dec (from hexane–ethyl acetate); IR (KBr,  $\text{cm}^{-1}$ ) 1945, 1820, 1625, 1445, 1415, 1405, 1350, 1150, 1105, 620;  $^1\text{H}$  NMR (300 MHz, acetone- $d_6$ )  $\delta$  7.70 (s, 1 H), 5.71 (br s, 1 H), 5.12 (br s, 1 H), 3.30 (s, 3 H), 3.17 (s, 3 H), 2.99 (d,  $J = 8$  Hz, 2 H), 2.81 (d,  $J = 10$  Hz, 1 H), 1.96 (br s, 2 H), 1.46 (d,  $J = 9$  Hz, 1 H), 1.25 (br s, 2 H);  $^{13}\text{C}$  NMR (20 MHz, acetone- $d_6$ ) 230.86, 153.92, 81.06, 47.62, 47.37, 40.79, 39.36 ppm.

Anal. Calcd for  $\text{C}_{16}\text{H}_{17}\text{MoNO}_3$ : C, 52.33; H, 4.66. Found: C, 51.84, H, 4.87.

For  $\text{M} = \text{W}$ :  $\text{W}(\text{CO})_6$  (1.244 g, 3.54 mmol); **3** (467 mg, 3.54 mmol); heating 72 and 8 h; 63% yield of **6c**; mp  $>230$  °C dec (from hexane–ethyl acetate); IR (KBr,  $\text{cm}^{-1}$ ) 1935, 1820, 1625, 1415, 1405, 1350, 1150, 1120, 1105;  $^1\text{H}$  NMR (300 MHz, acetone- $d_6$ )  $\delta$  7.79 (s, 1 H), 5.73 (br s, 1 H), 5.09 (br s, 1 H), 3.22 (s, 3 H), 3.10 (s, 3 H), 3.00 (s, 2 H), 2.81 (d,  $J = 10$  Hz, 1 H), 2.00 (s, 2 H), 1.52 (d,  $J = 9$  Hz, 1 H), 1.33 (br s, 2 H).

Anal. Calcd for  $\text{C}_{16}\text{H}_{17}\text{NO}_3\text{W}$ : C, 42.22; H, 3.76. Found: C, 42.34; H, 3.85.

**X-ray Crystal Structure Analysis of 6b.** Crystals of **6b** are dark red rectangular rods. The data collection crystal was cut from the end of one rod. Preliminary examination of the diffraction pattern on a Syntex P1 diffractometer indicated a monoclinic crystal system with systematic absences  $h0l$ ,  $h + l = 2n + 1$ , and  $0k0$ ,  $k = 2n + 1$ . The space group is uniquely determined to be  $P2_1/n$ . The unit cell constants are  $a = 5.959$  (1) Å,  $b = 14.823$  (3) Å,  $c = 17.107$  (3) Å, and  $\beta = 97.48$  (1)°, as determined by the least-squares fit of the diffractometer setting angles for 26 reflections in the  $2\theta$  range 21–30° with Mo  $K\alpha$  radiation ( $\lambda(K\alpha) = 0.71069$  Å). For comparison, ( $\eta^5$ -cyclopentadienyl)( $\eta^5$ -4-formyltricyclo[5.2.1.0<sup>2,16</sup>]deca-2,4-dien-6-yl)ruthenium<sup>1</sup> also crystallizes in  $P2_1/n$  with unit cell constants similar to those determined here.

Intensities were measured by the  $\theta$ - $2\theta$  scan technique on the Syntex P1 diffractometer. The data were corrected for Lorentz and polarization effects and put onto an absolute scale by means of a Wilson plot.<sup>24</sup> The following reflections saturated the detector during data collections and are omitted from the data set: (004), (012), (020), (103), (101), (111), (121), (133), and (141). Six standard reflections were measured after every 100 reflections and indicated that crystal decomposition was negligible.

The Mo atom was located by MULTAN 80<sup>29</sup> and then phased

on in the DIRDIF procedure.<sup>30</sup> The remainder of the non-hydrogen atoms were easily located on the electron density map generated by DIRDIF. The SHELX-76 package<sup>26</sup> was used for all full-matrix least-squares refinements. Isotropic refinement of the non-hydrogen atoms converged to an  $R$  factor of 0.065. At this point an absorption correction was applied by means of the Gaussian grid method<sup>27</sup> with an  $8 \times 8 \times 8$  grid. Isotropic refinement on the absorption corrected data set then converged at  $R = 0.064$ .

After one cycle of anisotropic refinement all the hydrogen atoms, except for those on the methyl carbon (C15), were easily found on a difference electron density map. Only one hydrogen atom on C(15) was apparent at this point. The hydrogen atoms, except for the six methyl hydrogens, were next included in the model as fixed contributions in calculated positions with C–H = 1.00 Å and  $B_{\text{H}} = B_{\text{C}(\text{iso})} + 1.0$  Å<sup>2</sup>. The six methyl hydrogens then appeared on a weighted difference electron density map after a further cycle of refinement. These hydrogen positions were idealized as described above and included in the model. The final refinement cycle resulted in agreement indices of  $R = 0.024$  and  $R_w = 0.031$  (based on  $F$ ) for the 2858 intensities with  $F_o^2 > 3\sigma(F_o^2)$  and the 190 variables (anisotropic non-hydrogen atoms, all hydrogen atoms fixed). The maximum and minimum peak heights in the final difference electron density map are 0.32 and  $-0.39$  e/Å<sup>3</sup>. Scattering factors for the molybdenum, oxygen, nitrogen, and carbon atoms<sup>28a</sup> and for the hydrogen atoms<sup>28b</sup> are from the usual sources. Anomalous dispersion values for all non-hydrogen atoms were included in the calculations.<sup>28a</sup>

**Acknowledgment.** We thank the National Institutes of Health for their support of this research program through Grant CA-12115.

**Registry No.** **3**, 99747-02-1; **4a**, 99829-28-4; **4b**, 99829-29-5; **4c**, 99829-30-8; **5a**, 99883-30-4; **5b**, 99883-31-5; **5c**, 99883-32-6; **6a**, 99829-31-9; **6b**, 99829-32-0; **6c**, 99829-33-1;  $\text{Cr}(\text{CO})_6$ , 13007-92-6;  $\text{Mo}(\text{CO})_6$ , 13939-06-5;  $\text{W}(\text{CO})_6$ , 14040-11-0.

**Supplementary Material Available:** Stereodrawings of the unit cells for **4c** and **6b** (Figures 3 and 4) together with the bond angles (Tables III and VI), least-squares planes (Tables IV and VII), final positional and thermal parameters (Tables VIII and X), and observed and calculated structure factors (Tables IX and XI) for both complexes (34 pages). Ordering information is given on any current masthead page.

(30) Beurskens, P. T.; Bosman, W. P.; Doesburg, H. M.; Gould, R. O.; Van den Hark, Th. E. M.; Prick, P. A. J.; Noordik, J. H.; Beurskens, G.; Parthasarathi, V.; Bruins Slot, H. J.; Hiltiwanger, R. C. "DIRDIF: Direct Methods for Difference Structures"; Crystallography Laboratory, University of Nijmegen: The Netherlands, 1983.

(31) Bondi, A. *J. Phys. Chem.* **1964**, *68*, 441.

(29) Main, P.; Fiske, S. J.; Hull, S. E.; Lessinger, L.; Germain, G.; Declercq, J.-P.; Woolfson, M. M. "MULTAN 80, A System of Computer Programs for the Automatic Solution of Crystal Structures from X-Ray Diffraction Data", University of York, England, and University of Louvain, Belgium, 1980.

# Properties and the Crystal and Molecular Structure of the Pentaammineruthenium(II) Dimethyl Acetylenedicarboxylate Complex $[(\text{NH}_3)_5\text{Ru}(\text{DMAD})](\text{PF}_6)_2$

Wayne W. Henderson,<sup>1a</sup> Barbara T. Bancroft,<sup>1b</sup> Rex E. Shepherd,\*<sup>1a</sup> and John P. Fackler, Jr.\*<sup>1b</sup>

Departments of Chemistry, University of Pittsburgh, Pittsburgh, Pennsylvania 15260, and Texas A&M University, College Station, Texas 77843

Received April 24, 1985

The crystal and molecular structure of the dimethyl acetylenedicarboxylate complex  $[(\text{NH}_3)_5\text{Ru}(\text{DMAD})](\text{PF}_6)_2$  has been determined from 4025 reflections ( $\text{MoK}\alpha$ ) to  $R = 0.0422$  ( $R_w = 0.0451$ ); the space group is  $P2_1/c$ . Unit cell parameters  $a$ ,  $b$ , and  $c$  are 10.7103 (8), 11.8553 (11), and 16.4087 (10) Å, respectively. The number of molecules per unit cell,  $Z$ , is 4. The central  $\text{C}\equiv\text{C}$  bond length is 1.238 (7) Å and exhibits the anticipated increase in distance relative to the free ligand upon coordination to the back-bonding  $(\text{NH}_3)_5\text{Ru}^{\text{II}}$  moiety. The trans  $\text{NH}_3$ -Ru distance is 2.163 (5) Å while the cis  $\text{NH}_3$ 's average 2.139 Å. The DMAD ligand is found to be rotated by 24.7° relative to the "in-plane" N1-N3-N4-Ru centers. ASED-MO calculations found an electronic and steric energy minimization at 30° rotation in good agreement with the observed 24.7° twist. The two  $\text{CH}_3\text{OC}(\text{O})$  groups of the coordinated DMAD ligand are bent back 35.0° and 28.5°. In-plane  $\text{NH}_3$  ligands are bent back by 7° in the  $(\text{NH}_3)_5\text{Ru}^{2+}$  moiety. The  $\nu_{\text{C}\equiv\text{C}}$  at 1947  $\text{cm}^{-1}$  for DMAD shows the DMAD is a better  $\pi$ -acceptor among substituted alkynes,  $\text{RC}\equiv\text{CR}$ , according to the order  $\text{R} = \text{CH}_3\text{OC}(\text{O}) > \text{Ph} > \text{H} > \text{C}_2\text{H}_5$ . The reduction potential of  $\text{Ru}(\text{NH}_3)_5(\text{DMAD})^{3+}$  is 1.00 V ( $\mu = 0.10$ ,  $T = 25.0^\circ\text{C}$ ) with  $E^\circ$  for  $\text{Ru}(\text{NH}_3)_5(\text{alkyne})^{3+/2+}$  series following the order  $\text{R} = \text{CH}_3\text{OC}(\text{O})$  (1.00 V)  $> \text{Ph}$  (0.95)  $> \text{C}_2\text{H}_5$  (0.78 V)  $> \text{H}$  (0.665 V). The trans  $\text{NH}_3$  exhibits its  $^1\text{H}$  resonance at 4.63 ppm while cis  $\text{NH}_3$ 's have their resonance at 3.08 ppm in acetone- $d_6$ . The position of the trans  $\text{NH}_3$  resonance is sensitive to the ligand  $\pi$ -acceptor power, implicating the  $\pi$ -acceptor order for  $\text{RC}\equiv\text{CR}$  as  $\text{R} = \text{CH}_3\text{OC}(\text{O}) > \text{H} \approx \text{Ph} > \text{C}_2\text{H}_5$ . The position of the cis  $\text{NH}_3$   $^1\text{H}$  is also influenced by the ligand  $\pi$ -acceptor power, but less than the trans  $\text{NH}_3$  resonance.

## Introduction

The  $\text{Ru}(\text{NH}_3)_5^{2+}$  moiety is particularly good as a  $\pi$ -donor metal center toward a  $\pi$ -acceptor ligand; the pyridine and pyrazine complexes of  $(\text{NH}_3)_5\text{Ru}^{2+}$  have been extensively studied.<sup>2</sup> Correlations between spectral and chemical properties of these N-heterocyclic complexes of  $(\text{NH}_3)_5\text{Ru}^{2+}$  to the  $\pi$ -acceptor power of the ligands have been made.<sup>3</sup> The use of  $(\text{NH}_3)_5\text{Ru}^{2+}$  as a probe of the  $\pi$ -acceptor nature of olefins and acetylenes would appear to be an obvious extension of its chemistry. Yet it is surprising when one considers the long history of olefin and acetylenic complexes that olefin and acetylene complexes of  $(\text{NH}_3)_5\text{Ru}^{2+}$  were reported by Ludi et al. rather late in the development of the Ru(II)- $\pi$ -acceptor chemical studies.<sup>4</sup> The main attention in the Ludi study was the  $(\text{NH}_3)_5\text{Ru}(\text{fumaric acid})^{2+}$  complex which exhibited an increase in the central  $\text{C}=\text{C}$  distance of  $\text{HO}_2\text{CCH}=\text{CHCO}_2\text{H}$  from 1.348 Å in the free ligand to 1.413 Å in the complex.<sup>4</sup> This change is typical of the same change on coordination of  $\text{C}_2\text{H}_4$  in many organometallic complexes.<sup>5</sup> We report here concerning the coordination of the substituted acetylene dimethyl acetylenedicarboxylate ester (DMAD) toward  $(\text{NH}_3)_5\text{Ru}^{2+}$ .

## Experimental Section

**$[\text{Ru}(\text{NH}_3)_5(\text{DMAD})](\text{PF}_6)_2$ .** The title complex was prepared by the addition of excess dimethyl acetylenedicarboxylate ligand (Aldrich) to an aqueous suspension of  $\text{Ru}(\text{NH}_3)_5\text{Cl}_3$  over Zn/Hg, as described in the literature.<sup>2</sup> The  $\text{PF}_6^-$  salt was precipitated by the addition of a small amount of saturated  $\text{NH}_4\text{PF}_6$  solution. The yellow powder was recrystallized from hot water to yield yellow-orange single crystals. An elemental analysis was performed by Galbraith Labs. Anal. Calcd for  $\text{RuC}_4\text{H}_{21}\text{O}_4\text{N}_5\text{P}_2\text{F}_{12}$  (Found): Ru, 16.35 (16.58); C, 11.66 (11.45); H, 3.42 (3.38); N, 11.33 (11.13).

**Instrumentation.** UV-visible spectra were obtained on a Varian-Cary 118C spectrophotometer using thermostated quartz cells. IR spectra were obtained on a Beckman Acculab 4 spectrophotometer. The electrochemical studies were carried out with a glassy carbon working electrode vs. a saturated NaCl SCE standard. The  $E_{1/2}$  values were measured via differential pulse polarography on an IBM 225 Electrochemical Analyzer. The ionic strength was maintained at 0.10 with NaCl, and the temperature was held at  $25.0 \pm 0.1^\circ\text{C}$ .

$^{13}\text{C}$  and  $^1\text{H}$  nuclear magnetic resonance spectra were obtained on a Bruker WH-300 spectrometer operating at 75.45 and 300.0 MHz, respectively. Dimethyl- $d_6$  sulfoxide, acetone- $d_6$ , and  $\text{D}_2\text{O}$  (Stohler Isotope Chemicals) were used as solvents for both the  $^{13}\text{C}$  and  $^1\text{H}$  methods with  $p$ -dioxane and  $\text{Me}_4\text{Si}$  as the standards. The  $^{13}\text{C}$  resonances are reported vs. external  $\text{Me}_4\text{Si}$  using the relationship  $\delta_{\text{ext, Me}_4\text{Si}} = \delta_{\text{int, dioxane}} + 66.5$ , and the  $^1\text{H}$  resonances are reported in parts per million downfield relative to internal  $\text{Me}_4\text{Si}$ . Spectra of the complexes were obtained at concentrations near saturation and at ambient probe temperature.

**X-ray Crystallography.** A crystal from the preparation analyzed by Galbraith was selected having a size ca.  $0.2 \times 0.2 \times 0.1$  mm. The crystals appear to be board-like in structure. Data were collected ( $hkl$ ,  $hk-l$ ) on a Nicolet R3m-E diffractometer using graphite-monochromated  $\text{Mo K}\alpha$  radiation ( $\lambda = 0.71069$  Å). A total of 4025 reflections having  $3.0 < 2\theta < 50.0$  were measured, using the Wyckoff<sup>20</sup>  $\omega$  scan method. During the data collection three standard reflections were monitored every 97 reflections. The intensities were reduced by applying polarization and decay corrections as well as a psi scan empirical absorption correction. Cell parameters and systematic absences were consistent with the

(1) (a) University of Pittsburgh. (b) Texas A&M University.

(2) (a) Ford, P. C.; Rudd, DeF. P.; Gaunder, R.; Taube, H. *J. Am. Chem. Soc.* **1968**, *90*, 1187-1194. (b) Ford, P. C. *Coord. Chem. Rev.* **1970**, *5*, 75-99. (c) Taube, H. "Survey of Progress in Chemistry"; Scott, A. F. Ed.; Academic Press: New York, 1973; Vol. 6 Chapter 1. (d) Gaunder, R.; Taube, H. *Inorg. Chem.* **1970**, *9*, 2627-2637. (e) Shepherd, R. E.; Taube, H. *Inorg. Chem.* **1973**, *12*, 1392-1401.

(3) (a) Wishart, J. F.; Taube, H.; Breslauer, K. J.; Isied, S. S. *Inorg. Chem.* **1984**, *23*, 2997-3001. (b) Reference 7e. (c) Kuehn, C.; Taube, H. *J. Am. Chem. Soc.* **1975**, *98*, 689-702. (d) Drago, R. S.; Cosmano, R.; Tesler, J. *Inorg. Chem.* **1984**, *23*, 4514-4518.

(4) Lehmann, H.; Shenk, K. J.; Chapuis, G.; Ludi, A. *J. Am. Chem. Soc.* **1979**, *101*, 6197-6202.

(5) (a) Ittel, S. D.; Ibers, J. A. *Adv. Organomet. Chem.* **1976**, *14*, 33-61; (b) Stalick, J. K.; Ibers, J. A. *J. Am. Chem. Soc.* **1970**, *18*, 5333-5338.

Table I

formula	$\text{Ru}(\text{NH}_3)_5(\text{C}_6\text{O}_4\text{H}_6)(\text{PF}_6)_2$
space group	$P2_1/c$
$a$ , Å	10.7103 (8)
$b$ , Å	11.8553 (11)
$c$ , Å	16.4087 (10)
$\beta$ , deg	107.002 (5)
$V$ , Å <sup>3</sup>	1992.42 (25)
mol wt	618.26
$Z$	4
$d$ (calcd), g/cm <sup>3</sup>	2.06
$d$ (obsd) g/cm <sup>3</sup>	2.09
cryst size	0.20 × 0.20 × 0.10
color	yellow-orange
radiatn	Mo K $\alpha$
$\mu$ , absorptn coeff	9.3 cm <sup>-1</sup>
data range	3.0 < $2\theta$ < 50.0
centered on	25 reflectns, $2\theta$ of 20–30°
no. of data	4025
no. of unique data $F_o^2 > 3\sigma(F_o^2)$	2621
no. of parameters refined	272
max transmissn	0.807
min transmissn	0.787
$g$	0.0005

monoclinic system, space group  $P2_1/a$ . The data were collected in this space group and transformed to the standard group  $P2_1/c$  (No. 14).

The position of Ru was determined by SHELXTL direct methods. The remaining positions of non-hydrogen atoms were obtained from a difference Fourier synthesis. The positions of the hydrogen atoms were calculated by using an idealized sp<sup>3</sup>-hybridized geometry and fixed bond lengths of 0.96 Å. A least-squares refinement of 272 parameters using anisotropic thermal parameters for all atoms except hydrogens gave  $R = 0.0422$  and  $R_w = 0.0451$  with quality of fit of 1.599.

The SHELXTL program minimized  $\sum w_i(|F_o| - |F_c|)^2$  using  $w_i = 1/\sigma_i$  values.  $\sigma_i$  values were estimated from the diffractometer intensity measurements assuming the errors are from counting statistics after the polarization and decay corrections were included. SHELXTL programs use the International Tables for scattering factors,  $f_o$ ,  $f'$ , and  $f''$ .

Table I summarizes the data collection at room temperature.

## Results and Discussion

**Infrared Spectrum.** The following IR vibrations (cm<sup>-1</sup>) are observed for  $[\text{Ru}(\text{NH}_3)_5(\text{DMAD})](\text{PF}_6)_2$  in KBr:  $\nu_{\text{C}\equiv\text{C}} = 1947, 1935$  sh;  $\nu_{\text{C}=\text{O}} = 1708, 1695$ ;  $\delta_{\text{degNH}_3} = 1648, 1640$ ;  $\delta_{\text{symNH}_3} = 1325$ ;  $\nu_{\text{P}-\text{F}} = 848$ . The  $\nu_{\text{C}\equiv\text{C}}$  of DMAD is lowered 310 cm<sup>-1</sup> in the complex relative to the free ligand. The extent of the  $\pi$ -back-bonding to DMAD and other acetylenes has been discussed in terms of the lowering of the  $\nu_{\text{C}\equiv\text{C}}$ ,<sup>6</sup> as much as a 500 cm<sup>-1</sup> decrease has been observed depending on the metal and other ligands.<sup>6-10</sup> If L = acetylene, the lowering of  $\nu_{\text{C}\equiv\text{C}}$  from the free ligand value to that of the complex is 199 cm<sup>-1</sup>, for phenylacetylene the lowering is 229 cm<sup>-1</sup>, and for 3-hexyne the lowering is 123 cm<sup>-1</sup>.<sup>4</sup> The change is much larger for the dimethyl acetylenedicarboxylate case, indicating that DMAD is a better  $\pi$ -acceptor than other alkynes. A rough order of  $\pi$ -acid strength would be DMAD > PhC $\equiv$ CH ~ HC $\equiv$ CH > EtC $\equiv$ CEt.

**Electrochemistry.** The reduction potential of  $[\text{Ru}(\text{NH}_3)_5(\text{DMAD})]^{3+/2+}$  was measured to be +1.00 V vs. the

Table II. IR Frequencies of  $[\text{Ru}(\text{NH}_3)_5(\text{DMAD})](\text{PF}_6)_2$ 

$\nu$ , cm <sup>-1</sup>	
1947	
1935	ligand C $\equiv$ C
1708	
1695	ligand C=O
1648	
1640	Ru <sup>II</sup> A <sub>5</sub> moiety
1443	ligand
1362	
1325	Ru <sup>II</sup> A <sub>5</sub> moiety
1252	ligand
1038	ligand
848	PF <sub>6</sub> <sup>-</sup> ion
750	ligand
715	
660	ligand

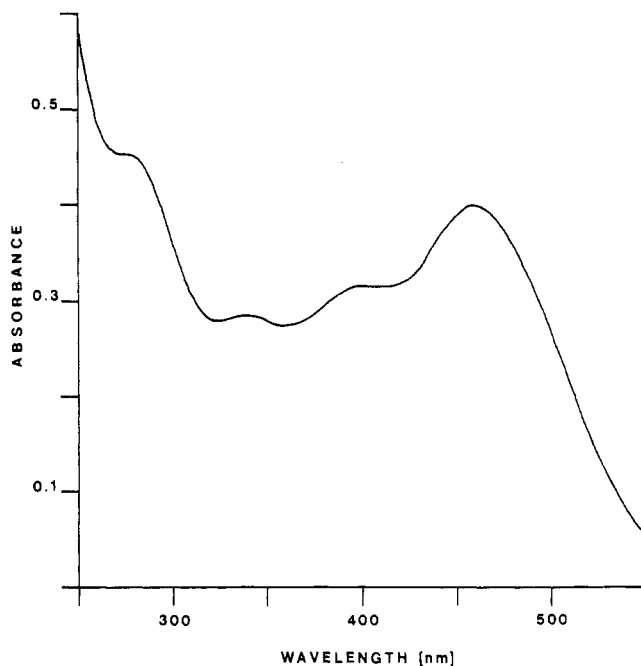


Figure 1. UV-visible spectrum of  $(\text{NH}_3)_5\text{Ru}(\text{DMAD})^{2+}$  ( $3.88 \times 10^{-4}$  M in H<sub>2</sub>O at 25 °C).

NHE. Electrochemical studies by Anson et al.,<sup>11</sup> Taube et al.,<sup>3c</sup> and Shepherd et al.<sup>12</sup> have previously shown that a large positive value for  $E^\circ$ , Ru(III)/Ru(II) is indicative of significant  $\pi$ -back-bonding to the ligand which stabilizes the Ru(II) oxidation state. A comparison of  $\text{Ru}(\text{NH}_3)_5(\text{DMAD})^{3+/2+}$  with other  $\text{Ru}(\text{NH}_3)_5(\text{alkyne})^{3+/2+}$  complexes shows the reduction potential to decrease as L = DMAD (1.00 V) > phenylacetylene (0.95 V) > 3-hexyne (0.78 V) > acetylene (0.665 V).<sup>4</sup>

**UV-Visible Spectra.** The spectrum of  $\text{Ru}(\text{NH}_3)_5(\text{DMAD})^{2+}$  in H<sub>2</sub>O is shown in Figure 1. The peak at 460 nm ( $\epsilon$  1025) is assigned to the MLCT and the peaks at 400, 335, and 275 nm are most likely d-d transitions superimposed upon the charge-transfer absorption envelopes. The MLCT is shifted toward lower energy as the energy of the ligand  $\pi^*$ -orbital is decreased. The dimethyl acetylenedicarboxylate complex has a larger bathochromic shift of the MLCT compared to acetylene.<sup>9</sup> This suggests that  $\pi$ -back-donation is relatively more important for the complex with L = DMAD, in agreement with the infrared evidence and the electrochemistry of the complex.

(6) (a) Davidson, G. *Organomet. Chem. Rev., Sect. A* 1972, 303. (b) Nakamoto, K. "The Infrared and Raman Spectra of Inorganic and Coordination Compounds", 3rd. ed.; Wiley: New York, 1978; p 387.

(7) Sullivan, B. P.; Kober, E. M.; Meyer, T. J. *Organometallics* 1982, 1, 1011-1013.

(8) Sullivan, B. P.; Smythe, R. S.; Kober, E. M.; Meyer, T. J. *J. Am. Chem. Soc.* 1982, 104, 4701-4703.

(9) Bruce, M. I.; Hambley, T. W.; Rodgers, J. R.; Snow, M. R.; Wong, F. S. *Aust. J. Chem.* 1982, 35, 1323-1333.

(10) Herrick, R. S.; Templeton, J. L. *Organometallics* 1982, 1, 842-851.

(11) Lim, H. S.; Barclay, D. J.; Anson, F. C. *Inorg. Chem.* 1972, 11, 1460-1466.

(12) Johnson, C. R.; Shepherd, R. E. *Synth. React. Inorg. Met.-Org. Chem.* 1984, 14(3), 339-353.

The MLCT transition is a function of solvent and shows a bathochromic shift as the Gutmann donor number of the solvent increases. The absorption band shifts from 452 nm in acetonitrile (donor number = 14.1) to 455 nm in acetone (17.0), 460 nm in H<sub>2</sub>O (18.0), and 469 nm in dimethyl sulfoxide (29.8). This trend has been explained for Ru(II) and Ru(III) amines in terms of greater solvent-NH<sub>3</sub> hydrogen bonding.<sup>13,14</sup> The sensitivity of the Ru(NH<sub>3</sub>)<sub>5</sub>(DMAD)<sup>2+</sup> visible and UV spectrum to the choice of solvent establishes the charge-transfer character of these bands as metal to ligand, being more complete in the excited state with the ruthenium center taking on more Ru(III) character.

**NMR Spectra.** The proton signals of the ammonia ligands in Ru(NH<sub>3</sub>)<sub>5</sub>L<sup>2+</sup> complexes can be seen in acetone-*d*<sub>6</sub> or dimethyl-*d*<sub>6</sub> sulfoxide and appear as two absorptions of relative ratio 12:3 (cis:trans). Ludi supports the view that the cis NH<sub>3</sub> peak is independent of the sixth ligand, while the trans NH<sub>3</sub> peak is shifted downfield as the  $\pi$ -back-bonding capacity of L increases.<sup>4</sup> Presumably the synergistic effect of increased  $\pi$ -donation,  $\sigma$ -acceptance from the metal to the ligand L causes the metal-trans NH<sub>3</sub>  $\sigma$ -bonding to be more polarized, resulting in lower field trans NH<sub>3</sub> <sup>1</sup>H resonances. For DMAD this trend continues: the cis resonance is 3.07 ppm and the trans resonance is 4.63 ppm in acetone-*d*<sub>6</sub>. The trans NH<sub>3</sub> resonances establish an order of  $\pi$ -back-bonding in Ru(NH<sub>3</sub>)<sub>5</sub>L<sup>2+</sup> of CH<sub>3</sub>CH<sub>2</sub>C $\equiv$ CCH<sub>2</sub>CH<sub>3</sub><sup>4</sup> (3.40 ppm) < C<sub>6</sub>H<sub>5</sub>C $\equiv$ CH<sup>4</sup> (3.97 ppm)  $\approx$  HC $\equiv$ CH<sup>4</sup> (3.98 ppm) < DMAD (4.63 ppm). The cis NH<sub>3</sub> resonances do vary from 2.40 ppm for 3-hexyne to 3.07 ppm for DMAD and thus are not completely invariant with the nature of L as suggested by Ludi et al.<sup>4</sup>

The ligand <sup>1</sup>H and <sup>13</sup>C resonances have been used to measure  $\pi$ -back-bonding in these types of complexes also.<sup>15</sup> Donation of electron density to the metal occurs via  $\sigma$ -interaction and causes downfield shifts;  $\pi$ -back-bonding can replace the electron density on the ligand, attenuating or even cancelling the downfield effect. In addition, for acetylenes, the loss of axial symmetry in the ligand by coordination can cause a downfield shift.<sup>16</sup> For DMAD there is essentially no shift of the methyl <sup>1</sup>H resonances upon coordination:  $\delta$  3.88 (free ligand) and  $\delta$  3.91 (complex in acetone-*d*<sub>6</sub>). Whether this is a consequence of the several factors effectively cancelling or isolation of the methyl groups from the changes in electron density by the -OC(O)- groups cannot be determined from the <sup>1</sup>H NMR spectra.

<sup>13</sup>C NMR spectra were measured in an attempt to resolve these questions about  $\pi$ -back-donation. The Ru(NH<sub>3</sub>)<sub>5</sub>(DMAD)<sup>2+</sup> complex showed only two resonances in D<sub>2</sub>O/H<sub>2</sub>O solvent: a singlet at 98.46 ppm assigned to the acetylene carbons and a quartet centered at 53.65 ppm assigned to the methyl carbons. The carbonyl carbon resonance was not observed; the carbonyl C appears at 151.83 ppm for the free ligand in Me<sub>2</sub>SO. The free ligand value of the acetylene carbon is 74.35 ppm (Me<sub>2</sub>SO sol-

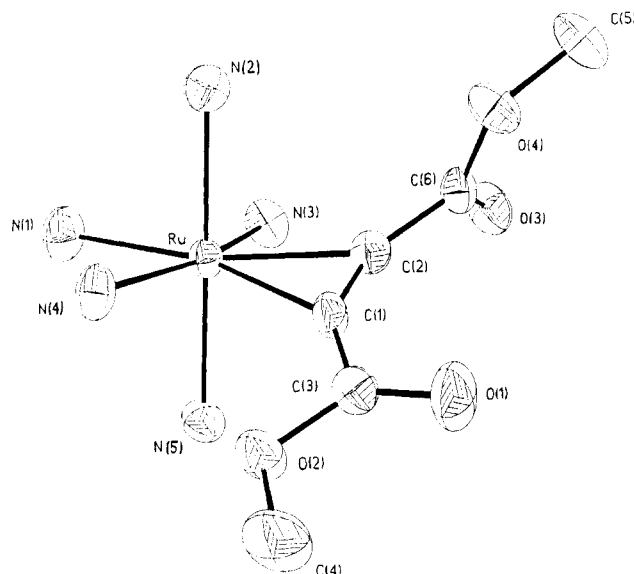


Figure 2. Thermal ellipsoid drawing of [(NH<sub>3</sub>)<sub>5</sub>Ru(DMAD)]<sup>2+</sup>(PF<sub>6</sub>)<sub>2</sub>.

Table III. Atom Coordinates ( $\times 10^4$ ) and Temperature Factors ( $\text{\AA}^2 \times 10^3$ ) for Ru(NH<sub>3</sub>)<sub>5</sub>(C<sub>6</sub>H<sub>6</sub>O<sub>4</sub>)(PF<sub>6</sub>)<sub>2</sub>

atom	x	y	z	U <sub>ij</sub> , $\text{\AA}^2$
Ru	2519 (1)	-9534 (1)	949 (1)	22 (1) <sup>a</sup>
N(1)	2109 (3)	-11183 (4)	144 (5)	40 (2) <sup>a</sup>
N(2)	3759 (3)	-9877 (4)	772 (5)	34 (2) <sup>a</sup>
N(3)	2781 (3)	-10397 (4)	2778 (4)	32 (2) <sup>a</sup>
N(4)	2149 (3)	-9070 (4)	-1066 (4)	35 (2) <sup>a</sup>
N(5)	1285 (3)	-9202 (4)	1170 (6)	43 (2) <sup>a</sup>
C(1)	2658 (3)	-7764 (5)	1183 (5)	27 (2)
C(2)	3137 (4)	-8178 (4)	2194 (5)	27 (2)
C(3)	2228 (4)	-6793 (5)	411 (5)	26 (2) <sup>a</sup>
C(4)	1232 (5)	-5312 (6)	327 (7)	49 (3) <sup>a</sup>
C(5)	4681 (4)	-8634 (6)	5388 (7)	53 (3)
C(6)	3739 (4)	-7931 (5)	3456 (5)	30 (2) <sup>a</sup>
O(1)	2315 (3)	-6513 (4)	-613 (4)	40 (2)
O(2)	1710 (3)	-6293 (4)	989 (4)	38 (2)
O(3)	3876 (3)	-6983 (4)	3874 (4)	48 (2) <sup>a</sup>
O(4)	4110 (3)	-8837 (3)	4108 (4)	36 (1) <sup>a</sup>
P(1)	3599 (1)	-3584 (1)	2199 (2)	40 (1) <sup>a</sup>
F(11)	3315 (3)	-4810 (4)	2371 (5)	108 (3)
F(12)	2675 (3)	-3177 (5)	2108 (7)	143 (4)
F(13)	3856 (3)	-2312 (3)	2070 (5)	80 (2) <sup>a</sup>
F(14)	3848 (5)	-3413 (5)	3709 (4)	166 (5)
F(15)	4516 (3)	-3936 (5)	2355 (9)	144 (4) <sup>a</sup>
F(16)	3334 (5)	-3719 (5)	719 (4)	140 (4) <sup>a</sup>
P(2)	334 (1)	-2096 (2)	2314 (2)	38 (1) <sup>a</sup>
F(21)	2 (4)	-844 (4)	2153 (8)	127 (4)
F(22)	1226 (3)	-1681 (6)	3133 (7)	134 (3) <sup>a</sup>
F(23)	653 (3)	-3326 (4)	2472 (9)	147 (4) <sup>a</sup>
F(24)	-550 (3)	-2470 (5)	1457 (8)	146 (4) <sup>a</sup>
F(25)	640 (8)	-1859 (10)	1123 (8)	216 (7)
F(26)	43 (7)	-2206 (10)	3509 (8)	222 (7) <sup>a</sup>

<sup>a</sup> Equivalent isotropic U defined as one-third of the trace of the orthogonalized U<sub>ij</sub> tensor.

vent), giving a  $\Delta\delta$  of 24 ppm downfield upon coordination. Clearly this shift indicates that  $\sigma$ -donation and loss of axial symmetry are important effects. The methyl value of 53.65 ppm (H<sub>2</sub>O solvent) is close to the value of the resonances in other DMAD complexes and 54.07 ppm (Me<sub>2</sub>SO solvent) for the free ligand. It suggests the effect of  $\pi$ -back-bonding is not very important at positions 4 atoms remote to the metal.

**Structure of [Ru(NH<sub>3</sub>)<sub>5</sub>(DMAD)](PF<sub>6</sub>)<sub>2</sub>.** The thermal ellipsoid drawing of the Ru(NH<sub>3</sub>)<sub>5</sub>(DMAD)<sup>2+</sup> complex as determined by the crystal structure of its PF<sub>6</sub><sup>-</sup> salt is shown in Figure 2. The molecular packing is available in supplementary materials (Figure A). The PF<sub>6</sub><sup>-</sup> anions are

(13) Curtis, J. C.; Sullivan, B. P.; Meyer, T. J. *Inorg. Chem.* **1983**, *22*, 224-236.

(14) Shepherd, R. E.; Hoq, M. F.; Hoblack, N.; Johnson, C. R. *Inorg. Chem.* **1984**, *23*, 3249-3252.

(15) (a) McDonald, J. W.; Corbin, J. L.; Newton, W. E. *J. Am. Chem. Soc.* **1975**, *97*, 1970-1971. (b) McDonald, J. W.; Newton, W. E.; Creedy, C. T. C.; Corbin, J. L. *J. Organomet. Chem.* **1975**, *92*, C25. (c) Ricard, L.; Weiss, R.; Newton, W. E.; Chen, G. J.-J.; McDonald, J. W. *J. Am. Chem. Soc.* **1978**, *100*, 1318-1320. (d) Templeton, J. L.; Ward, B. C.; Chen, G. J.-J.; McDonald, J. W.; Newton, W. E. *Inorg. Chem.* **1981**, *20*, 1248-1253. (e) Templeton, J. L.; Ward, B. C. *J. Am. Chem. Soc.* **1980**, *102*, 3288-3290. (f) Chisholm, M. H.; Clark, H. C.; Manzer, L. E.; Stothers, J. B. *J. Am. Chem. Soc.* **1972**, *94*, 5087-5089.

(16) (a) Borg, A.; Lindblom, T.; Vestin, R. *Acta Chem. Scand., Ser. A* **1975**, *A29*, 475. (b) Reference 9.



Table IV. Energy Minimization by ASED Calculation

$\theta$ , deg	energy, eV	$\theta$ , deg	energy, eV
0	0.1552	50	0.1250
5	0.1401	55	0.1971
10	0.1024	60	0.2935
15	0.0588	65	0.4168
20	0.0240	70	0.5584
25	0.0042	75	0.6959
30	0.0	80	0.803
35	0.0102	85	0.8657
40	0.0340	90	0.8853
45	0.0718		

considerably disordered. Positional parameters are listed in Table III. The dimethyl acetylenedicarboxylate ligand is seen to be twisted with respect to the two planes created by N(2)–N(1)–N(5)–Ru and N(3)–N(1)–N(4)–Ru, but it is not in the position of equilibrium ( $45^\circ$ ) arising from steric interactions with the  $\text{NH}_3$  groups. It is at  $24.7^\circ$  to the N(3)–N(1)–N(4)–Ru plane and  $68.6^\circ$  to the N(2)–N(1)–N(5)–Ru plane. The two nitrogens closest to the Ru–C(1)–C(2) plane (N(3), N(4)) are bent back by  $7^\circ$  each, forming an N(3)–Ru–N(4) angle of  $165.9^\circ$ . The C(1)–C(2)–C(6) and C(2)–C(1)–C(3) bonds are bent back forming angles of  $151.5^\circ$  and  $145.6^\circ$ , respectively. This combined with the lengthening of the C(1)–C(2) acetylene bond to 1.238 (7) Å supports the anticipated intermediate bond order between the acetylene carbon atoms, lower than ca. 1.20 Å of  $\text{C}\equiv\text{C}$  and higher than 1.34 Å of  $\text{C}=\text{C}$ . The Ru–C(1) and Ru–C(2) bond lengths vary slightly since they are not required by the symmetry to be identical, but this variation is statistically insignificant. No hydrogen bonding has been observed.

ASED-MO calculations were carried out to seek the electronic and steric energy minimization of the  $(\text{NH}_3)_5\text{Ru}^{2+}$  and DMAD ligand fragments. Details of the program and the methods have been given elsewhere.<sup>17</sup> ASED-MO calculations do not suggest anything unusual about the twist of  $25^\circ$ , other than that it indeed is the sterically preferred orientation when only two nitrogens are bent back. Parameters used in the ASED calculations are specified in supplementary materials (Table A). The difference in total energy of the  $(\text{NH}_3)_5\text{Ru}(\text{DMAD})^{2+}$  complex as DMAD is rotated about the Ru to  $\text{C}\equiv\text{C}$  axis is given in Table IV. In these calculations  $\theta = 0^\circ$  corresponds to the plane containing Ru–N(3)–N(4) with the nitrogens bent back;  $\theta = 90^\circ$  corresponds to the Ru–N(2)–N(5) plane which has nondistorted  $\text{NH}_3$  ligands. The equilibrium position by the ASED calculation ( $E = 0$ ) occurs at  $30^\circ$  which is close to the experimental value of  $24.7^\circ$ . Since the ASED-MO calculations find the minimum at about  $30^\circ$  instead of  $0^\circ$  or  $45^\circ$  for the twist, symmetry requires  $\sigma$ -donation from the filled  $\pi$ -level of the  $\text{C}\equiv\text{C}$  bond of DMAD into the  $d_{x^2-y^2}$ ,  $d_{z^2}$ -hybridized metal orbitals together with  $\pi$ -bonding interaction between the  $d_{xz}$  and  $d_{xy}$  metal orbitals and the ligand  $\pi^*$ -level. Steric perturbations occur as well. The argument for a steric effect is supported by the N(3)–Ru–N(5) angle of  $85.9^\circ$  and N(2)–Ru–N(4) angle of  $87.5^\circ$  while the other angles bisected

Table V. Bond Lengths (Å)

Ru–N(1)	2.163 (5)	Ru–N(2)	2.136 (5)
Ru–N(3)	2.140 (5)	Ru–N(4)	2.136 (5)
Ru–N(5)	2.143 (6)	Ru–C(1)	2.117 (6)
Ru–C(2)	2.144 (5)		
C(1)–C(2)	1.238 (7)	C(1)–C(3)	1.472 (7)
C(2)–C(6)	1.452 (7)	C(3)–O(1)	1.193 (8)
C(3)–O(2)	1.329 (8)	C(4)–O(2)	1.464 (8)
C(5)–O(4)	1.437 (7)	C(6)–O(3)	1.205 (7)
C(6)–O(4)	1.328 (7)	P–F(av)	1.545 (25)

Table VI. Bond Angles (deg)

N(1)–Ru–N(2)	89.2 (2)	N(1)–Ru–N(3)	83.6 (2)
N(2)–Ru–N(3)	92.8 (2)	N(1)–Ru–N(4)	82.4 (2)
N(2)–Ru–N(4)	87.5 (2)	N(3)–Ru–N(4)	165.9 (2)
N(1)–Ru–N(5)	90.9 (2)	N(2)–Ru–N(5)	178.7 (2)
N(3)–Ru–N(5)	85.9 (2)	N(4)–Ru–N(5)	93.8 (2)
N(1)–Ru–C(1)	162.4 (2)	N(2)–Ru–C(1)	97.3 (2)
N(3)–Ru–C(1)	112.3 (2)	N(4)–Ru–C(1)	81.6 (2)
N(5)–Ru–C(1)	83.0 (2)	N(1)–Ru–C(2)	163.9 (2)
N(2)–Ru–C(2)	84.8 (2)	N(3)–Ru–C(2)	81.8 (2)
N(4)–Ru–C(2)	112.3 (2)	N(5)–Ru–C(2)	94.8 (2)
C(1)–Ru–C(2)	33.8 (2)	Ru–C(1)–C(2)	74.3 (4)
Ru–C(1)–C(3)	133.7 (4)	C(2)–C(1)–C(3)	151.5 (5)
Ru–C(2)–C(1)	71.9 (3)	Ru–C(2)–C(6)	143.1 (4)
C(1)–C(2)–C(6)	145.0 (5)	C(1)–C(3)–O(1)	124.6 (6)
C(1)–C(3)–O(2)	110.7 (5)	O(1)–C(3)–O(2)	124.7 (5)
C(2)–C(6)–O(3)	122.4 (5)	C(2)–C(6)–O(4)	114.1 (5)
O(3)–C(6)–O(4)	123.5 (5)	C(3)–O(2)–C(4)	117.0 (5)
C(5)–O(4)–C(6)	115.9 (5)	F–P–F(av)	90.0 (21)

by DMAD are  $93.8^\circ$  and  $92.8^\circ$ . The twist of one of the carboxylate groups of  $69^\circ$  with respect to the RuC(1)C(2) plane seems to be a result of a random orientation. The theoretical calculations are not influenced significantly by rotation of this group.

The anisotropic temperature factors (Table B), hydrogen coordinates and temperature factors (Table C), and the observed and calculated structure factors (Table D) used to refine the structure leading to the ORTEP drawing in Figure 2 are available as supplementary material on microfilm. Ordering information is given below. Bond lengths for  $[(\text{NH}_3)_5\text{Ru}(\text{DMAD})](\text{PF}_6)_2$  are given in Table V; bond angles are supplied in Table VI. The trans  $\text{NH}_3$ , N(1), at 2.163 (5) Å is slightly longer than the cis  $\text{NH}_3$  ligands which average 2.139 Å. This is consistent with the  $^1\text{H}$  NMR results mentioned above and the known labilization of the trans  $\text{NH}_3$  position when a strong  $\pi$ -acceptor ligand coordinates to  $(\text{NH}_3)_5\text{Ru}^{2+}$ .<sup>19</sup> The crucial C(1)–C(2) distance of 1.238 (7) Å is indeed longer than the free ligand value (ca. 1.20 Å) while the average of the C(4)–O(2) and C(5)–O(4) of 1.450 Å is slightly perturbed from the normal C–O single bond value of 1.43 Å. A slight difference in the Ru–C(1) distance (2.117 (6) Å) vs. Ru–C(2) (2.144 (5) Å) as well as the modest difference for the Ru–C(1)–C(3) angle of  $133.7 (4)^\circ$  compared to Ru–C(2)–C(6) of  $143.1 (4)^\circ$  reinforces the idea that packing distortions are present in the structure.

## Conclusions

The most substantial influence of  $\text{R} = \text{CH}_3\text{OC}(\text{O})$  in the  $(\text{NH}_3)_5\text{Ru}(\text{DMAD})^{2+}$  complex is manifest in its strong stabilization of the Ru(II) half of the (III/II) reduction potential.

The electrochemistry shows that for  $\text{Ru}(\text{NH}_3)_5(\text{alkynes})^{3+/2+}$  complexes,  $\text{R} = \text{CH}_3\text{OC}(\text{O}) > \text{Ph} > \text{C}_2\text{H}_5 > \text{H}$  in tuning the reduction potential over a 0.34 V range. For comparison with other  $(\text{NH}_3)_5\text{RuL}^{2+}$  complexes, a 0.43 V more favorable reduction potential is achieved by changing L from  $\text{NH}_3$  (no  $\pi$ -acceptor power) to L = pyrazine<sup>3c,11</sup> or a 0.51 V change is achieved on changing from L = pyrazine to L =  $\text{Me}_2\text{SO}$ .<sup>3c,11</sup> These are considered to be dramatic

(17) Trzcinska, B. M.; Fackler, J. P., Jr.; Anderson, A. B. *Organometallics* 1984, 3, 319–323.

(18) (a) Johnson, C. R.; Shepherd, R. E. *Inorg. Chem.* 1983, 22, 2439–2444. (b) Johnson, C. R.; Shepherd, R. E. *Inorg. Chem.* 1983, 22, 1117–1123. (c) Johnson, C. R.; Shepherd, R. E. *Inorg. Chem.* 1983, 22, 3506–3513. (d) Henderson, W. W.; Shepherd, R. E. *Inorg. Chem.* 1985, 24, 2398–2404.

(19) (a) Isied, S. S.; Taube, H. *Inorg. Chem.* 1976, 15, 3070–3075. (b) Isied, S. S.; Taube, H. *Inorg. Chem.* 1974, 13, 1545–1551. (c) Isied, S. S.; Taube, H. *Inorg. Chem.* 1975, 14, 2561–2562.

(20) Wycoff, H. W.; Tsenaglou, D.; Hanson, A. W.; Knox, J. R.; Lee, B.; Richards, F. M. *J. Biol. Chem.* 1970, 245, 305–328.

differences in  $\pi$ -acceptor power, contributing factors of about 3 kcal/mol stabilization per ligand change.<sup>3a</sup> Therefore the modest changes in R substituents in  $\text{RC}\equiv\text{CR}$  appear to create major differences in the  $\pi$ -acceptor ability of DMAD vs. acetylene, for example, as detected by the measured reduction potentials. The substituent effect of R in various acetylenes is much greater than R groups attached to the pyridine ring. For example, R =  $(\text{O})\text{CNH}_2$  vs. H in the para position of the pyridine ring raises the reduction potential by 0.135 V<sup>12</sup> compared to the R =  $(\text{O})\text{COCH}_3$  vs. H shift of 0.34 V for coordinated acetylenes.

The same order of the influence of R in  $\text{RC}\equiv\text{CR}$  on the trans  $\text{NH}_3$  <sup>1</sup>H resonance is observed ( $\text{CH}_3\text{OC}(\text{O}) > \text{Ph} > \text{H} > \text{C}_2\text{H}_5$ ) as determined by infrared and approximately so by differential pulse voltammetry of the (III/II) complexes. The acetylenic carbons exhibit a 24 ppm downfield <sup>13</sup>C shift upon coordination of DMAD in  $(\text{NH}_3)_5\text{Ru}(\text{DMAD})^{2+}$ , indicative of good  $\sigma$ -donation of DMAD to Ru(II). The other observed shift for the  $\text{CH}_3$  groups of DMAD is virtually unchanged, indicative of a rapid diminution of the influence of the metal's  $\pi$ -donation in DMAD over three more atom positions from the site of coordination. Interestingly enough, a small difference is still observed in the  $\text{CH}_3\text{-O}$  bond distance in the coordinated ligand for the structure of  $[(\text{NH}_3)_5\text{Ru}(\text{DMAD})](\text{PF}_6)_2$  compared to normal  $\text{CH}_3\text{-O}$  bonds. The key features of this structure appear to be as follows: (1) the  $\text{C}\equiv\text{C}$  bond is increased ca. 0.04 Å upon coordination; (2) the structure about the Ru(II) center is approximately seven-coordinate with the  $\text{C}\equiv\text{C}$  donor occupying one position of an octa-

hedral set of ligands; (3) the "trans"  $\text{NH}_3$  is about 0.024 Å further away from Ru(II) than the "cis" set. The two  $\text{NH}_3$ 's nearest the  $\text{C}\equiv\text{C}$  donor are bent away toward the trans  $\text{NH}_3$  by 7° while two other  $\text{NH}_3$ 's are nearly axial; (4) the DMAD is off a strict plane containing the trans  $\text{NH}_3$ , Ru(II), and the in-plane cis  $\text{NH}_3$  ligands with a twist to about 24° instead of a 45° bisection of all adjacent  $\text{NH}_3$ 's; (5) the ligand bend-back angles of the R group average 31° in  $(\text{NH}_3)_5\text{Ru}(\text{DMAD})^{2+}$  which is about normal for other coordinated acetylenes.<sup>5</sup> (Bend-back angles usually fall in the range of 12° to 40°.)

Curiously enough, the activated  $\text{C}\equiv\text{C}$  unit in  $(\text{NH}_3)_5\text{Ru}(\text{DMAD})^{2+}$  has resisted attack by external electrophiles and nucleophiles in several tests. We believe that this result once again emphasizes the importance of synergism in describing the  $\pi$ -back-bonding situation with Ru(II) and "small atom" units such as CO,  $\text{N}_2$ ,  $\text{CN}^-$ , and  $\text{RC}\equiv\text{CR}$ .<sup>3c,12,18</sup>

**Acknowledgment.** We gratefully acknowledge support of this work via NSF Grant CHE 802183 (Pittsburgh) and NSF Grant CHE8408414 (Texas A&M). The center for Energy and Minerals Research (Texas A&M) also has supported this study.

**Registry No.**  $[\text{Ru}(\text{NH}_3)_5(\text{DMAD})](\text{PF}_6)_2$ , 99642-84-9.

**Supplementary Material Available:** Figure A, molecular packing of  $\text{Ru}(\text{NH}_3)_5(\text{DMAD})^{2+}$ , Table A, parameters used in ASED calculations, Table B, anisotropic temperature factors, Table C, hydrogen coordinates and temperature factors, and Table D, observed and calculated structure factors (22 pages). Ordering information is given on any current masthead page.

## Cobaltadihydroquinoline Derivatives from Carbenoid Cobalt Precursors. X-ray Crystal Structure of $\text{C}_5\text{H}_5(\text{PMe}_3)\text{CoCH}_2\text{-2-C}_6\text{H}_3(4\text{-CH}_3)\text{N}=\text{C}(\text{OCH}_3)^1$

Helmut Werner\* and Lothar Hofmann

*Institut für Anorganische Chemie der Universität, Am Hubland, D-8700 Würzburg, Germany*

Manfred L. Ziegler and Thomas Zahn

*Anorganisch-chemisches Institut der Universität, Im Neuenheimer Feld 270, D-6900 Heidelberg 1, Germany*

Received May 31, 1985

The reaction of  $\text{C}_5\text{H}_5\text{Co}(\text{PMe}_3)\text{CO}$  with aryl isocyanides  $\text{CNAr}$  ( $\text{Ar} = \text{C}_6\text{H}_5$ ,  $\text{C}_6\text{H}_4\text{-4-CH}_3$ ) and  $\text{CH}_2\text{ClI}$  in benzene produces the cationic carbenoid cobalt complexes  $[\text{C}_5\text{H}_5\text{CoCH}_2\text{Cl}(\text{PMe}_3)\text{CNAr}]^+$  which are isolated as the  $\text{PF}_6$  salts 4 and 5. Addition of KOH to a suspension of 4 or 5 in methanol leads to the formation of the cobaltadihydroquinoline derivatives  $\text{C}_5\text{H}_5(\text{PMe}_3)\text{CoCH}_2\text{-2-C}_6\text{H}_3(4\text{-R})\text{N}=\text{C}(\text{OCH}_3)$  (6, R = H; 7, R =  $\text{CH}_3$ ) in ca. 70% yield. The molecular structure of 7 has been determined by an X-ray investigation. 7 crystallizes in the space group  $P2_1/c$  with  $a = 8.776$  (3) Å,  $b = 14.285$  (5) Å,  $c = 14.758$  (7) Å, and  $\beta = 91.38$  (3)°. The bicyclic ring system is nonplanar and bent along the  $\text{N}\cdots\text{C}$  axis of the 1-aza-3-cobaltacyclohexadiene ring. The coordination geometry of the metal is slightly distorted octahedral with bond angles between 84.0 and 95.0°. Under mass spectroscopic conditions, 6 and 7 decompose to give  $[\text{C}_5\text{H}_5\text{Co}(\text{PMe}_3)]^+$  and the corresponding 2-methoxyindolenine derivative, thus suggesting the possibility of using the new complexes as precursors for these heterocycles.

### Introduction

Cyclopentadienylcobalt(I) and -rhodium(I) complexes of the general type  $\text{C}_5\text{H}_5\text{M}(\text{PMe}_3)\text{L}$  ( $\text{M} = \text{Co}, \text{Rh}$ ;  $\text{L} = \text{PR}_3$ ,  $\text{P}(\text{OR})_3$ , CO, CNR,  $\text{C}_2\text{H}_4$ , etc.) are strong metal bases and

react with various electrophiles by oxidative addition or oxidative substitution to form the corresponding cobalt(III) and rhodium(III) derivatives.<sup>2</sup> By using dihalomethanes  $\text{CH}_2\text{XX}'$  as electrophiles, either cationic or neutral car-

(1) Part 55 of the series "Basic Metals". Part 54: Werner, H.; Scholz, H. J.; Zolk, R. *Chem. Ber.* 1985, 118, 4531.

(2) Werner, H. *Angew. Chem.* 1983, 95, 932; *Angew. Chem., Int. Ed. Engl.* 1983, 22, 927.

differences in  $\pi$ -acceptor power, contributing factors of about 3 kcal/mol stabilization per ligand change.<sup>3a</sup> Therefore the modest changes in R substituents in  $RC\equiv CR$  appear to create major differences in the  $\pi$ -acceptor ability of DMAD vs. acetylene, for example, as detected by the measured reduction potentials. The substituent effect of R in various acetylenes is much greater than R groups attached to the pyridine ring. For example, R = (O)CNH<sub>2</sub> vs. H in the para position of the pyridine ring raises the reduction potential by 0.135 V<sup>12</sup> compared to the R = (O)COCH<sub>3</sub> vs. H shift of 0.34 V for coordinated acetylenes.

The same order of the influence of R in  $RC\equiv CR$  on the trans NH<sub>3</sub> <sup>1</sup>H resonance is observed (CH<sub>3</sub>OC(O) > Ph > H > C<sub>2</sub>H<sub>5</sub>) as determined by infrared and approximately so by differential pulse voltammetry of the (III/II) complexes. The acetylenic carbons exhibit a 24 ppm downfield <sup>13</sup>C shift upon coordination of DMAD in (NH<sub>3</sub>)<sub>5</sub>Ru(DMAD)<sup>2+</sup>, indicative of good  $\sigma$ -donation of DMAD to Ru(II). The other observed shift for the CH<sub>3</sub> groups of DMAD is virtually unchanged, indicative of a rapid diminution of the influence of the metal's  $\pi$ -donation in DMAD over three more atom positions from the site of coordination. Interestingly enough, a small difference is still observed in the CH<sub>3</sub>-O bond distance in the coordinated ligand for the structure of [(NH<sub>3</sub>)<sub>5</sub>Ru(DMAD)](PF<sub>6</sub>)<sub>2</sub> compared to normal CH<sub>3</sub>-O bonds. The key features of this structure appear to be as follows: (1) the C $\equiv$ C bond is increased ca. 0.04 Å upon coordination; (2) the structure about the Ru(II) center is approximately seven-coordinate with the C $\equiv$ C donor occupying one position of an octa-

hedral set of ligands; (3) the "trans" NH<sub>3</sub> is about 0.024 Å further away from Ru(II) than the "cis" set. The two NH<sub>3</sub>'s nearest the C $\equiv$ C donor are bent away toward the trans NH<sub>3</sub> by 7° while two other NH<sub>3</sub>'s are nearly axial; (4) the DMAD is off a strict plane containing the trans NH<sub>3</sub>, Ru(II), and the in-plane cis NH<sub>3</sub> ligands with a twist to about 24° instead of a 45° bisection of all adjacent NH<sub>3</sub>'s; (5) the ligand bend-back angles of the R group average 31° in (NH<sub>3</sub>)<sub>5</sub>Ru(DMAD)<sup>2+</sup> which is about normal for other coordinated acetylenes.<sup>5</sup> (Bend-back angles usually fall in the range of 12° to 40°.)

Curiously enough, the activated C $\equiv$ C unit in (NH<sub>3</sub>)<sub>5</sub>Ru(DMAD)<sup>2+</sup> has resisted attack by external electrophiles and nucleophiles in several tests. We believe that this result once again emphasizes the importance of synergism in describing the  $\pi$ -back-bonding situation with Ru(II) and "small atom" units such as CO, N<sub>2</sub>, CN<sup>-</sup>, and RC $\equiv$ CR.<sup>3c,12,18</sup>

**Acknowledgment.** We gratefully acknowledge support of this work via NSF Grant CHE 802183 (Pittsburgh) and NSF Grant CHE8408414 (Texas A&M). The center for Energy and Minerals Research (Texas A&M) also has supported this study.

**Registry No.** [Ru(NH<sub>3</sub>)<sub>5</sub>(DMAD)](PF<sub>6</sub>)<sub>2</sub>, 99642-84-9.

**Supplementary Material Available:** Figure A, molecular packing of Ru(NH<sub>3</sub>)<sub>5</sub>(DMAD)<sup>2+</sup>, Table A, parameters used in ASED calculations, Table B, anisotropic temperature factors, Table C, hydrogen coordinates and temperature factors, and Table D, observed and calculated structure factors (22 pages). Ordering information is given on any current masthead page.

## Cobaltadihydroquinoline Derivatives from Carbenoid Cobalt Precursors. X-ray Crystal Structure of C<sub>5</sub>H<sub>5</sub>(PMe<sub>3</sub>)CoCH<sub>2</sub>-2-C<sub>6</sub>H<sub>3</sub>(4-CH<sub>3</sub>)N=C(OCH<sub>3</sub>)<sup>1</sup>

Helmut Werner\* and Lothar Hofmann

*Institut für Anorganische Chemie der Universität, Am Hubland, D-8700 Würzburg, Germany*

Manfred L. Ziegler and Thomas Zahn

*Anorganisch-chemisches Institut der Universität, Im Neuenheimer Feld 270, D-6900 Heidelberg 1, Germany*

Received May 31, 1985

The reaction of C<sub>5</sub>H<sub>5</sub>Co(PMe<sub>3</sub>)CO with aryl isocyanides CNAr (Ar = C<sub>6</sub>H<sub>5</sub>, C<sub>6</sub>H<sub>4</sub>-4-CH<sub>3</sub>) and CH<sub>2</sub>ClI in benzene produces the cationic carbenoid cobalt complexes [C<sub>5</sub>H<sub>5</sub>CoCH<sub>2</sub>Cl(PMe<sub>3</sub>)CNAr]<sup>+</sup> which are isolated as the PF<sub>6</sub> salts 4 and 5. Addition of KOH to a suspension of 4 or 5 in methanol leads to the formation of the cobaltadihydroquinoline derivatives C<sub>5</sub>H<sub>5</sub>(PMe<sub>3</sub>)CoCH<sub>2</sub>-2-C<sub>6</sub>H<sub>3</sub>(4-R)N=C(OCH<sub>3</sub>) (6, R = H; 7, R = CH<sub>3</sub>) in ca. 70% yield. The molecular structure of 7 has been determined by an X-ray investigation. 7 crystallizes in the space group P2<sub>1</sub>/c with a = 8.776 (3) Å, b = 14.285 (5) Å, c = 14.758 (7) Å, and  $\beta$  = 91.38 (3)°. The bicyclic ring system is nonplanar and bent along the N...C axis of the 1-aza-3-cobaltacyclohexadiene ring. The coordination geometry of the metal is slightly distorted octahedral with bond angles between 84.0 and 95.0°. Under mass spectroscopic conditions, 6 and 7 decompose to give [C<sub>5</sub>H<sub>5</sub>Co(PMe<sub>3</sub>)]<sup>+</sup> and the corresponding 2-methoxyindolenine derivative, thus suggesting the possibility of using the new complexes as precursors for these heterocycles.

### Introduction

Cyclopentadienylcobalt(I) and -rhodium(I) complexes of the general type C<sub>5</sub>H<sub>5</sub>M(PMe<sub>3</sub>)L (M = Co, Rh; L = PR<sub>3</sub>, P(OR)<sub>3</sub>, CO, CNR, C<sub>2</sub>H<sub>4</sub>, etc.) are strong metal bases and

react with various electrophiles by oxidative addition or oxidative substitution to form the corresponding cobalt(III) and rhodium(III) derivatives.<sup>2</sup> By using dihalomethanes CH<sub>2</sub>XX' as electrophiles, either cationic or neutral car-

(1) Part 55 of the series "Basic Metals". Part 54: Werner, H.; Scholz, H. J.; Zolk, R. *Chem. Ber.* 1985, 118, 4531.

(2) Werner, H. *Angew. Chem.* 1983, 95, 932; *Angew. Chem., Int. Ed. Engl.* 1983, 22, 927.

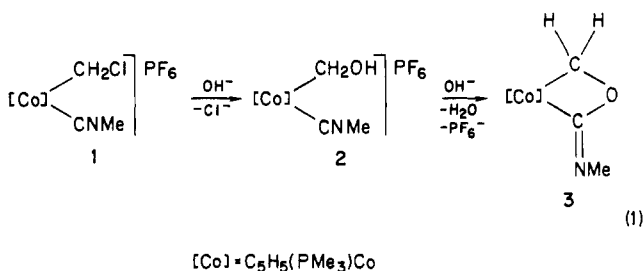
Table I.  $^1\text{H}$  NMR Data of Compounds 4-7 in Acetone- $d_6$ <sup>a</sup>

compd	$\delta(\text{C}_5\text{H}_5)$	$J(\text{PH})$	$\delta(\text{PMe}_3)$	$J(\text{PH})$	$\delta(\text{C}_6\text{H}_4\text{R})$	$\delta(\text{CH}_2)$	$J(\text{PH})$	$J(\text{HH})$
4	5.58 (d)	0.5	1.75 (d)	11.8	7.20 (s, br)	4.27 (dd)	5.5	5.5
5	5.68 (d)	0.6	1.86 (d)	11.5	7.32 <sup>b</sup>	4.58 (dd)	4.5	5.5
					7.59 <sup>b</sup>	4.29 (dd)	5.6	5.6
6 <sup>c</sup>	4.38 (d)	0.4	1.42 (d)	10.1	2.39 (s, br)	1.58 (dd)	14.3	8.7
					7.05 (m)	2.66 (dd)	2.1	8.7
7 <sup>d</sup>	4.38 (d)	0.4	1.36 (d)	10.2	6.75 (s, br), <sup>e</sup>	1.46 (dd)	15.0	8.5
					7.00 (s, br) <sup>f</sup>	2.54 (dd)	2.0	8.5
					2.24 (s, br)			

<sup>a</sup> 60 MHz, 25 °C;  $\delta$  in ppm, internal  $\text{Me}_3\text{Si}$ ;  $J$  in Hz. <sup>b</sup> AA'BB' pattern, each signal corresponding to 2 H. <sup>c</sup>  $\delta(\text{OMe})$  3.89 (s). <sup>d</sup>  $\delta(\text{OMe})$  3.83 (s). <sup>e</sup> Relative intensity 2 H, protons ortho to C-Me. <sup>f</sup> Relative intensity 1 H, proton ortho to C-N.

benoid metal compounds  $[\text{C}_5\text{H}_5\text{MCH}_2\text{X}(\text{PMe}_3)\text{L}]^+$  and  $\text{C}_5\text{H}_5\text{MCH}_2\text{X}(\text{PMe}_3)\text{X}'$  are obtained. In most cases, they contain a highly reactive C-X bond and can thus be used as starting materials for the synthesis of ylide cobalt and rhodium complexes which are not accessible by other routes.<sup>3,4</sup>

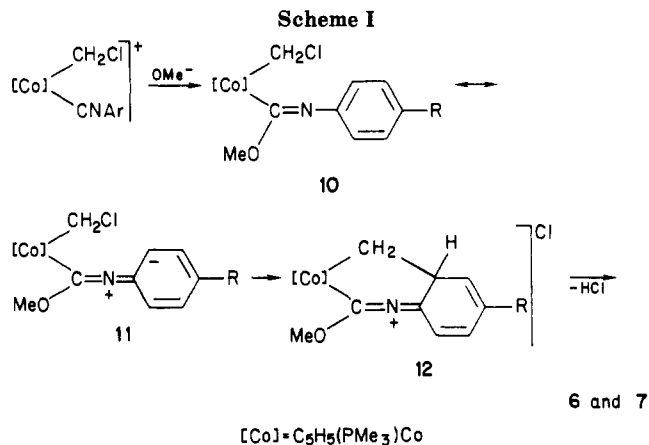
As a continuation of our previous studies, the present work was aimed at finding out whether it is possible to displace the halide of the cationic carbenoid cobalt complex **1**<sup>4</sup> by hydroxide and to abstract a proton from the intermediary species **2** to form the cobaltaoxetane derivative **3**. Analogous four-membered ring compounds  $\text{C}_5\text{H}_5(\text{PMe}_3)_2\text{CoC}(\text{OMe})_2\text{OC}(=\text{NR})$  (R = Me, Ph, Tol) are probably the main products in the reaction of  $[\text{C}_5\text{H}_5\text{CoCOOMe}(\text{PMe}_3)\text{CNR}]\text{PF}_6$  with KOMe formed by nucleophilic attack of the methoxide ion at the COOMe carbon atom.<sup>5</sup>



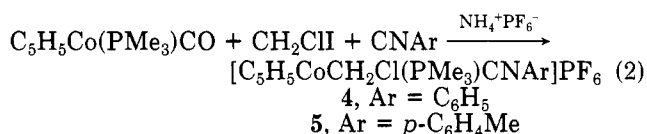
## Results and Discussion

**Synthesis.** The reaction of **1** with KOH in either THF or MeOH does not lead to the expected substitution of the chloride and subsequent formation of the corresponding metallacycle. The starting compound is surprising inert toward  $\text{OH}^-$  and  $\text{OMe}^-$  and complexes such as  $[\text{C}_5\text{H}_5\text{CoCl}(\text{CH}_2\text{PMe}_3)\text{CNMe}]\text{PF}_6$ ,  $[\text{C}_5\text{H}_5\text{CoCH}_2\text{OMe}(\text{PMe}_3)\text{CNMe}]\text{PF}_6$  or  $\text{C}_5\text{H}_5\text{CoCH}_2\text{OMe}(\text{PMe}_3)[\text{C}(\text{OMe})=\text{NMe}]$  are not detected (by NMR) as one of the reaction products.<sup>3,4</sup>

To find out whether these experiments failed owing to the dominating donor properties of the methyl isocyanide ligand (which reduces the electrophilic nature of the  $\text{CH}_2\text{Cl}$  carbon atom), we prepared the aryl isocyanide complexes



**4** and **5**. They are obtained in ca. 80% yield according to eq 2.



Compounds **4** and **5** form yellow, air-stable solids which are easily soluble in polar organic solvents (e.g., acetone and nitromethane) and behave in  $\text{CH}_3\text{NO}_2$  as 1:1 electrolytes. The  $^1\text{H}$  NMR data are summarized in Table I.

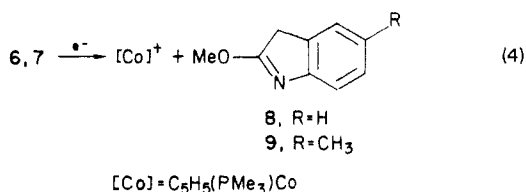
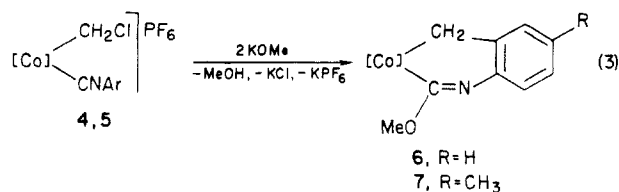
Addition of KOH to a suspension of **4** or **5** in methanol rapidly results in the formation of a yellow solution from which the nonionic complexes **6** and **7** forming orange-yellow crystals are isolated in ca. 70% yield. However, as before, both elemental analyses and mass spectra confirm that a cobaltaoxetan derivative similar to **3** has not been produced. The main fragmentation process occurring under mass spectroscopic conditions is the formation of  $[\text{C}_5\text{H}_5\text{Co}(\text{PMe}_3)]^+$  and the 2-methoxyindolenine derivatives **8** and **9** which strongly supports the structural proposal shown in eq 3. In the  $^1\text{H}$  NMR spectra of **6** and **7** (see Table I) two signals corresponding to the diastereotopic Co- $\text{CH}_2$  protons are observed which differ significantly not only in their chemical shifts but also in their PH coupling constants. Similar results have been found for other chiral cyclopentadienylcobalt complexes containing  $\text{CH}_2\text{X}$  (X = Cl, OMe) and  $\text{CH}_2\text{PMe}_3$  as ligands.<sup>4</sup> In contrast to the spectrum of **5** in which two signals of equal intensity are observed for the CH protons of the  $\text{C}_6\text{H}_4\text{Me}$  ring (AA'BB' spin system), the spectrum of **7** shows two signals with the intensity ratio of 2:1 in the aromatic CH region. The  $^{13}\text{C}$  NMR off-resonance spectrum is also in agreement with the presence of a trisubstituted benzene ring.

The proposed mechanism for the formation of the new metallaheterocycles is summarized in Scheme I. The first step is assumed to be a nucleophilic addition of the

(3) M = Rh: (a) Feser, R.; Werner, H. *Angew. Chem.* 1980, 92, 960; *Angew. Chem., Int. Ed. Engl.* 1980, 19, 940. (b) Werner, H.; Feser, R.; Paul, W.; Hofmann, L. *J. Organomet. Chem.* 1981, 219, C29. (c) Werner, H.; Hofmann, L.; Paul, W. *J. Organomet. Chem.* 1982, 236, C65. (d) Werner, H.; Paul, W.; Feser, R.; Zolk, R.; Thometzek, P. *Chem. Ber.* 1985, 118, 261. (e) Werner, H.; Hofmann, L.; Feser, R.; Paul, W. *J. Organomet. Chem.* 1985, 281, 317.

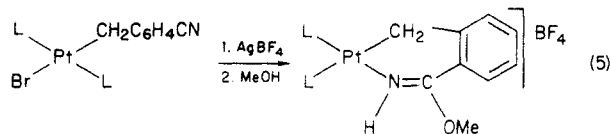
(4) M = Co: Hofmann, L.; Werner, H. *J. Organomet. Chem.* 1985, 289, 141.

(5) Hofmann, L.; Werner, H., manuscript in preparation. See: Hofmann, L. Ph.D. Thesis, Universität Würzburg, 1984.



methoxide ion at the isocyanide carbon atom which is followed by electrophilic attack of the chloromethyl group at the position ortho to the C-N bond of the arene ring. Cyclization of 10 to 12 may then occur, the driving force being the partial negative charge at the ortho positions of the benzene ring (resonance form 11). This process is probably base-catalyzed and is similar in a formal sense to the electrophilic substitution of aniline which also preferentially occurs at the ortho position. The metal atom seems not to be directly involved in the ring-forming reaction, and this led us to speculate that other organometallic compounds of general composition [MCH<sub>2</sub>Cl(CNAr)L<sub>n</sub>]X may react similarly.

A platinum complex containing a six-membered ring system similar to that found in 6 and 7 has previously been obtained by reaction of *trans*-[PtBr(CH<sub>2</sub>C<sub>6</sub>H<sub>4</sub>CN)(PPh<sub>3</sub>)<sub>2</sub>] with AgBF<sub>4</sub> and methanol (eq 5).<sup>6</sup>



**Crystal Data and Structure Determination of 7.** Suitable single crystals of 7 were obtained by cooling a THF-pentane solution (1:15) slowly to -78 °C, and one with the dimensions of 0.1 × 0.15 × 0.4 mm was used for the structure determination. It is monoclinic with *a* = 8.776 (3) Å, *b* = 14.285 (5) Å, *c* = 14.578 (7) Å, β = 91.38 (3)°, and *V* = 1849.6 Å<sup>3</sup>. A total of 1937 independent reflections were collected on a Syntex P3 four-circle automatic diffractometer (Mo Kα radiation, λ = 0.71069 Å, graphite monochromator) in the range 3° ≤ 2θ ≤ 55°. The data were corrected for absorption (μ = 10.11 cm<sup>-1</sup>; transmission factors 0.827–1.000; empirical absorption correction, ψ scans of four reflections) and for Lorentz and polarization factors. The structure was solved by the Patterson method. The hydrogen positions were calculated according to ideal geometry. Refinement of the non-hydrogen atoms by full-matrix least squares resulted in *R*<sub>1</sub> = 0.040 and *R*<sub>2</sub> = 0.053 for 1809 structure factors with *I*<sub>o</sub> ≥ 2.5σ(*I*<sub>o</sub>). Structure factors for uncharged atoms according to "International Tables of Crystallography" were used, corrected for anomalous dispersion. Final positional parameters are given in Table II and selected interatomic bond lengths and angles in Table III.

The molecular structure of 7 is shown in Figure 1. The cobalt atom is part of a 1-aza-3-cobaltacyclohexadiene ring system which is bent along the N-C(2) axis. The dihedral angles between the plane containing N, C(8), C(3), and C(2) and the corresponding planes through N, C(2), and C(1) and N, C(2), and Co are 149.7° and 128.3°, respec-

**Table II. Positional Parameters and Their Estimated Standard Deviations for Non-Hydrogen Atoms in 7**

	<i>x</i>	<i>y</i>	<i>z</i>
Co	0.09033 (9)	0.01783 (5)	0.21810 (5)
P	-0.1553 (2)	0.0222 (1)	0.2137 (1)
N	0.1937 (5)	0.2098 (3)	0.2034 (3)
O	0.0395 (4)	0.1548 (2)	0.0890 (3)
C(1)	0.1158 (6)	0.1417 (4)	0.1722 (4)
C(2)	0.0902 (7)	0.0821 (4)	0.3390 (4)
C(3)	0.2348 (7)	0.1340 (4)	0.3519 (4)
C(4)	0.3298 (7)	0.1231 (4)	0.4274 (4)
C(5)	0.4646 (8)	0.1728 (5)	0.4398 (4)
C(6)	0.5032 (7)	0.2360 (4)	0.3751 (4)
C(7)	0.4130 (7)	0.2470 (4)	0.2969 (4)
C(8)	0.2798 (6)	0.1959 (4)	0.2840 (4)
C(9)	0.5620 (9)	0.1600 (5)	0.5260 (4)
C(10)	-0.2477 (8)	0.1359 (4)	0.2067 (6)
C(11)	-0.2407 (7)	-0.0318 (5)	0.3118 (4)
C(12)	-0.2462 (7)	-0.0382 (5)	0.1193 (4)
C(13)	0.0594 (8)	0.2441 (4)	0.0455 (4)
C(14)	0.3067 (6)	-0.0397 (4)	0.2280 (5)
C(15)	0.2692 (7)	-0.0272 (4)	0.1357 (4)
C(16)	0.1402 (7)	-0.0806 (4)	0.1148 (4)
C(17)	0.0969 (8)	-0.1275 (4)	0.1968 (5)
C(18)	0.2028 (7)	-0.1030 (4)	0.2656 (5)

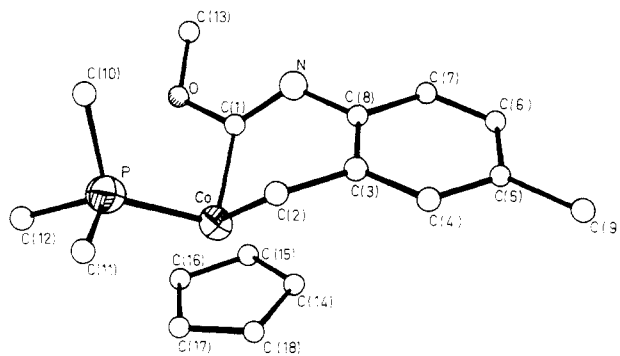


**Figure 1.** X-ray crystal structure of 7. The hydrogen atoms have been omitted for clarity.

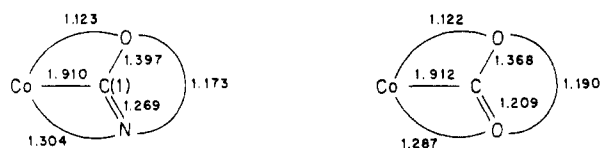


**Figure 2.** Bond lengths (Å) and angles (deg) of the Co-C(OMe)=N fragment in 7 and one of the Co-C(OMe)=O units in C<sub>5</sub>H<sub>5</sub>(PMe<sub>3</sub>)Co(CO<sub>2</sub>CH<sub>3</sub>)<sub>2</sub>.

tively. The atoms N and C(2) together with the carbon atoms C(3)–C(8) of the six-membered ring are almost coplanar. The coordination geometry of the metal is slightly distorted octahedral with bond angles P-Co-C(1), P-Co-C(2), and C(1)-Co-C(2) between 84.0 and 95.0°. Similar values are found in other metallacycles in which the C<sub>5</sub>H<sub>5</sub>(PMe<sub>3</sub>)Co unit is part of a five- or six-membered ring.<sup>7</sup> The Co-P distance (2.156 (2) Å) is slightly shorter than that in C<sub>5</sub>H<sub>5</sub>(PMe<sub>3</sub>)Co(CO<sub>2</sub>CH<sub>3</sub>)<sub>2</sub> (2.173 (1) Å)<sup>8</sup> whereas the Co-C distances in this complex (1.912 (4) and 1.907 (4) Å) and the Co-C(1) distance are nearly identical. There is generally a striking similarity in the bond lengths and bond angles between the Co-C(OMe)=N fragment of 7 and the Co-C(OMe)=O units in C<sub>5</sub>H<sub>5</sub>(PMe<sub>3</sub>)Co(CO<sub>2</sub>CH<sub>3</sub>)<sub>2</sub>, as is shown in Figure 2. It should be noted

(7) (a) Burschka, Ch.; Leonhard, K.; Werner, H. *Z. Anorg. Allg. Chem.* **1980**, *464*, 30. (b) Werner, H.; Heiser, B.; Schubert, U.; Ackermann, K. *Chem. Ber.* **1985**, *118*, 1517. (c) Heiser, B.; Kühn, A.; Werner, H. *Chem. Ber.* **1985**, *118*, 1531.

(8) Werner, H.; Hofmann, L.; Zolk, R. *Chem. Ber.*, accepted for publication.

(6) Ros, R.; Renaud, J.; Roulet, R. *J. Organomet. Chem.* **1975**, *87*, 379.

Table III. Selected Bond Distances (Å) and Bond Angles (deg) with Estimated Standard Deviations

		Bond Distances			
Co-P	2.156 (2)	N-C(1)	1.269 (7)	C(3)-C(8)	1.400 (8)
Co-C(1)	1.910 (5)	N-C(8)	1.409 (7)	C(4)-C(5)	1.389 (9)
Co-C(2)	2.007 (5)	O-C(1)	1.397 (6)	C(5)-C(6)	1.362 (8)
Co-C(Cp)	2.071 (6)-2.127 (6)	O-C(13)	1.441 (7)	C(5)-C(9)	1.527 (9)
		C(2)-C(3)	1.479 (8)	C(6)-C(7)	1.392 (8)
		C(3)-C(4)	1.384 (8)	C(7)-C(8)	1.388 (8)
		Bond Angles			
C(1)-Co-P	95.0 (2)	O-C(1)-N	117.3 (4)	C(4)-C(5)-C(9)	120.4 (6)
C(2)-Co-P	89.5 (2)	Co-C(2)-C(3)	108.9 (4)	C(6)-C(5)-C(9)	121.4 (6)
C(1)-Co-C(2)	84.0 (2)	C(2)-C(3)-C(4)	123.0 (5)	C(5)-C(6)-C(7)	120.7 (5)
C(1)-N-C(8)	118.2 (4)	C(2)-C(3)-C(8)	118.8 (5)	C(6)-C(7)-C(8)	120.9 (5)
C(1)-O-C(13)	116.7 (4)	C(4)-C(3)-C(8)	118.2 (5)	N-C(8)-C(3)	122.6 (5)
Co-C(1)-N	130.4 (4)	C(3)-C(4)-C(5)	122.9 (6)	N-C(8)-C(7)	118.3 (5)
Co-C(1)-O	112.3 (3)	C(4)-C(5)-C(6)	118.2 (6)	C(3)-C(8)-C(7)	119.0 (5)

that although the C(1)—N distance is exactly the same as that of an unconjugated C=N double bond, the distance C(8)—N is significantly shorter than would be expected for a C—N single bond.<sup>9</sup>

The bonding parameters at the methylene carbon atom C(2) also deserve some comment. The Co—C(2) distance is identical with the Co—CH<sub>2</sub> distance in C<sub>5</sub>H<sub>5</sub>(PPh<sub>2</sub>R)-CoCH<sub>2</sub>CH<sub>2</sub>CHR'(O) (R = N(Me)CHMePh, R' = C(OH)H-*t*-Bu)<sup>10</sup> although in this complex a five-membered metallacycle is present. The C(2)—C(3) distance, however, is shorter than that of a C—C single bond as can be seen, e.g., by comparison with the C(5)—C(9) distance. The methylene carbon seems to be exactly sp<sup>3</sup> hybridized as the Co—C(2)—C(3) angle is 108.9 (4)°.

### Conclusion

The present study has confirmed that the exceptional reactivity of the C—X bond in complexes of the general type [C<sub>5</sub>H<sub>5</sub>MCH<sub>2</sub>X(PMe<sub>3</sub>)L]<sup>+</sup> can also be used to form novel metal-containing ring systems. The building blocks for the cobaltadihydroquinolines found in **6** and **7** are the aryl isocyanide, the methoxide ion, and the CoCH<sub>2</sub> unit which provides the prerequisite for ring closure. Although we have no evidence, as yet, that under controlled thermal conditions the metallacycles **6** and **7** react to produce the corresponding indolenine derivative (observed in the mass spectra), it is conceivable that bicyclic systems of this type can be prepared via appropriate carbenoid metal precursors.

### Experimental Section

NMR spectra were recorded on a Varian EM 360 L (<sup>1</sup>H) spectrometer and a Bruker Cryospec WM 400 (<sup>13</sup>C) spectrometer and IR spectra on a Perkin-Elmer 457 spectrometer. The starting materials C<sub>5</sub>H<sub>5</sub>Co(PMe<sub>3</sub>)CO<sup>11</sup> and CNAr (Ar = C<sub>6</sub>H<sub>5</sub>, *p*-C<sub>6</sub>H<sub>4</sub>Me)<sup>12</sup> were prepared by published methods.

**Preparation of [C<sub>5</sub>H<sub>5</sub>CoCH<sub>2</sub>Cl(PMe<sub>3</sub>)CNAr]PF<sub>6</sub> (**4** and **5**).** A solution of C<sub>5</sub>H<sub>5</sub>Co(PMe<sub>3</sub>)CO (0.228 g, 1.0 mmol) and CNAr (1.5 mmol) in 10 mL of benzene was treated dropwise with CH<sub>2</sub>ClI (109 μL, 1.5 mmol). After the mixture was stirred for 1 h, the resulting precipitate was filtered, repeatedly washed with ether, and dried in vacuo. The solid residue together with a slight excess

of NH<sub>4</sub>PF<sub>6</sub> (ca. 200 mg, 1.23 mmol) was dissolved in 5 mL of methanol and the solution stirred for 10 min. After addition of 20 mL of ether, a yellow precipitate was formed which was recrystallized from acetone/ether; yield 80%.

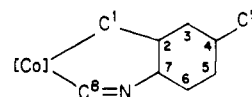
**4:** equivalent conductivity (CH<sub>3</sub>NO<sub>2</sub>) Λ = 91 cm<sup>2</sup>·Ω<sup>-1</sup>·mol<sup>-1</sup>; decomp temp (DTA) 112 °C; IR (KBr) ν(CN) 2165 cm<sup>-1</sup>. Anal. Calcd for C<sub>16</sub>H<sub>21</sub>ClCoF<sub>6</sub>NP<sub>2</sub>: C, 38.69; H, 4.26; Co, 11.86; N, 2.82. Found: C, 39.30; H, 4.56; Co, 12.08; N, 3.11.

**5:** equivalent conductivity (CH<sub>3</sub>NO<sub>2</sub>) Λ = 96 cm<sup>2</sup>·Ω<sup>-1</sup>·mol<sup>-1</sup>; decomp temp (DTA) 103 °C; IR (KBr) ν(CN) 2160 cm<sup>-1</sup>. Anal. Calcd for C<sub>17</sub>H<sub>23</sub>ClCoF<sub>6</sub>NP<sub>2</sub>: C, 39.90; H, 4.53; Co, 11.52; N, 2.74. Found: C, 39.58; H, 4.40; Co, 11.62; N, 3.06.

**Preparation of C<sub>5</sub>H<sub>5</sub>(PMe<sub>3</sub>)CoCH<sub>2</sub>-2-C<sub>6</sub>H<sub>3</sub>(4-R)N=C(OCH<sub>3</sub>) (**6** and **7**).** A solution of **4** or **5** (0.5 mmol) in 5 mL of methanol was treated with KOH (168 mg, 3.0 mmol) and stirred for 2 h at room temperature. After the solvent was removed, the solid residue was extracted with 50 mL of pentane. The solution was filtered, concentrated in vacuo, and cooled to -78 °C. Orange-yellow, moderately air-stable crystals were formed; yield 70%.

**6:** mp 101 °C dec; MS (70 eV), *m/e* (*I*<sub>r</sub>) 347 (12; M<sup>+</sup>), 271 (29; M<sup>+</sup> - PMe<sub>3</sub>), 200 (100; C<sub>5</sub>H<sub>5</sub>(PMe<sub>3</sub>)Co<sup>+</sup>), 147 (57; C<sub>9</sub>H<sub>9</sub>NO<sup>+</sup>), 135 (7; (PMe<sub>3</sub>)Co<sup>+</sup>), 124 (28; C<sub>5</sub>H<sub>5</sub>Co<sup>+</sup>); IR (KBr) ν(CN) 1528 cm<sup>-1</sup>. Anal. Calcd for C<sub>17</sub>H<sub>23</sub>CoNOP: C, 57.80; H, 6.68; Co, 16.97; N, 4.03. Found: C, 58.04; H, 7.20; Co, 17.20; N, 4.32.

**7:** mp 101 °C dec; MS (70 eV), *m/e* (*I*<sub>r</sub>) 361 (14; M<sup>+</sup>), 285 (40; M<sup>+</sup> - PMe<sub>3</sub>), 200 (100; C<sub>5</sub>H<sub>5</sub>(PMe<sub>3</sub>)Co<sup>+</sup>), 161 (8; C<sub>10</sub>H<sub>11</sub>NO<sup>+</sup>), 135 (5; (PMe<sub>3</sub>)Co<sup>+</sup>), 124 (24; C<sub>5</sub>H<sub>5</sub>Co<sup>+</sup>); IR (KBr) ν(CN) 1531 cm<sup>-1</sup>; <sup>13</sup>C NMR (acetone-*d*<sub>6</sub>, -40 °C) δ 199.96 (d, *J*(PC) = 31.3 Hz, C<sup>8</sup>), 151.37 (s, C<sup>7</sup>), 140.42 (s, C<sup>4</sup>), 130.59 (s, C<sup>2</sup>), 125.43, 124.74, 123.82 (each s; C<sup>3</sup>, C<sup>5</sup>, C<sup>6</sup>, exact assignment not possible), 87.24 (s, C<sub>5</sub>H<sub>5</sub>), 54.92 (s, OCH<sub>3</sub>), 21.20 (s, C<sup>9</sup>), 17.16 (d, *J*(PC) = 29.8 Hz, PMe<sub>3</sub>), 7.52 (d, *J*(PC) = 21.2 Hz, C<sup>1</sup>). Anal. Calcd for C<sub>18</sub>H<sub>25</sub>CoNOP: C, 59.84; H, 6.97; Co, 16.31; N, 3.88. Found: C, 59.56; H, 7.27; Co, 16.45; N, 4.12. For C<sup>1</sup>-C<sup>9</sup> assignment according to



**Acknowledgment.** We thank the Deutsche Forschungsgemeinschaft and the Fonds der Chemischen Industrie for financial support, Dr. D. Scheutzw for the 400-MHz NMR spectrum, Mrs. U. Neumann and R. Schedl for the elemental analysis, and H. Otto and R. Zolk for valuable discussions.

**Registry No.** 1, 99898-19-8; 4, 99923-01-0; 5, 99923-03-2; 6, 99923-04-3; 7, 99923-05-4; C<sub>5</sub>H<sub>5</sub>Co(PMe<sub>3</sub>)CO, 66652-86-6; CNC<sub>6</sub>H<sub>5</sub>, 931-54-4; CN-*p*-C<sub>6</sub>H<sub>4</sub>CH<sub>3</sub>, 7175-47-5.

**Supplementary Material Available:** Listings of the structure factors and of thermal parameters for **7** (15 pages). Ordering information is given on any current masthead page.

(9) Häfeler, G. *Chem. Ber.* 1970, 103, 2902.

(10) Theopold, K. H.; Becker, P. N.; Bergman, R. G. *J. Am. Chem. Soc.* 1982, 104, 5252.

(11) Spencer, A.; Werner, H. *J. Organomet. Chem.* 1979, 171, 219.

(12) Weber, W. P.; Gokel, G. W.; Ugi, I. K. *Angew. Chem.* 1972, 84, 587; *Angew. Chem., Int. Ed. Engl.* 1972, 11, 530.

# Octadienyl-Bridged Bimetallic Complexes of Palladium as Intermediates in Telomerization Reactions of Butadiene

Arno Behr,<sup>†</sup> Godard v. Ilsemann,<sup>†</sup> Wilhelm Keim,<sup>\*†</sup> Carl Krüger,<sup>‡</sup> and Yi-Hung Tsay<sup>‡</sup>

*Institute of Technical Chemistry and Petrochemistry, Technical University Aachen, D-5100 Aachen, Federal Republic of Germany, and Max-Planck-Institut für Kohlenforschung, D-4330 Mülheim a.d. Ruhr, Federal Republic of Germany*

Received June 14, 1985

The synthesis and characterization of two bimetallic complexes **1** [ $(\mu-1-3-\eta:6-8-\eta-C_8H_{12})(\mu-OOCCH_3)_2Pd$ ] and **6** [ $(\mu-1-3-\eta:6-8-\eta-C_8H_{12})(F_3CCOCHCOCF_3)_2Pd_2$ ] are reported. Both complexes contain a bridging octadienyl chain and differ only in one having a palladium-palladium bond and the other possessing two isolated palladium atoms. Experiments are described converting **1** into **6**, thus illustrating the ease of metal-metal bond splitting. With the addition of triisopropylphosphine the 1:1 and 1:2 adducts of **6** could be isolated. Complexes **1** and **6** were applied in the telomerization of butadiene with acetic acid yielding acetoxyoctadienes. Complex **1** is discussed as a potential intermediate in this telomerization. Further support rests on results obtained with deuterated butadiene. Complex **1** in the absence of acetic acid reacts with butadiene yielding complex **5** in which a  $C_{12}$  chain is bis  $\eta^3$ -bonded to two palladium atoms. A reaction path for the oligomerization compared to the telomerization is discussed. Compound **6** has been characterized by an X-ray structure analysis (space group  $P2_1/n$  with  $a = 4.6574$  (4) Å,  $b = 9.354$  (1) Å,  $c = 27.113$  (2) Å,  $\beta = 94.573$  (6)°, and  $Z = 2$ ).

## Introduction

Since the early days of homogeneous catalysis monometallic transition-metal complexes have been discussed as key intermediates in mechanistic reaction schemes. Here the mechanism to oligomerize butadiene by Wilke et al. or the hydroformylation reaction may serve as examples.<sup>1</sup> In recent years various multimetallic clusters of transition metals have been invoked as intermediates in catalytic reactions.<sup>2</sup> However, it must be stated that unambiguous proof for a cluster catalysis is lacking so far.

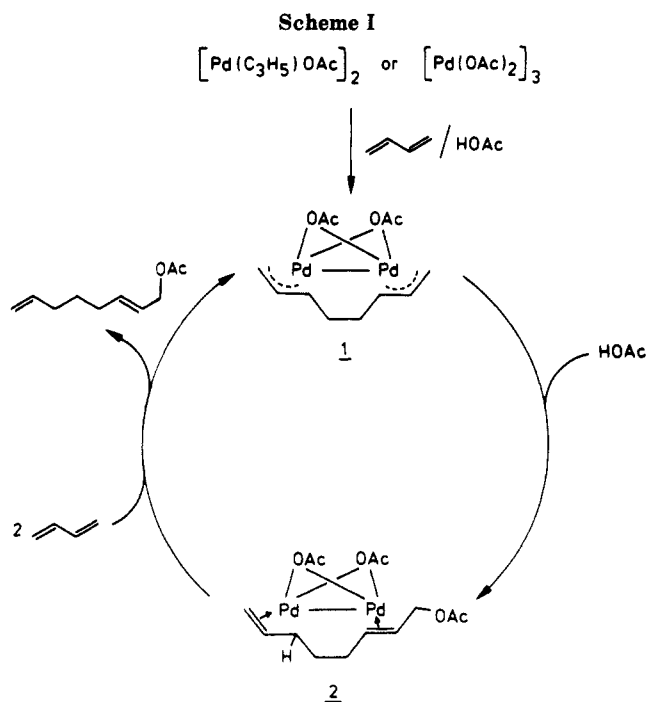
For many years we have been interested in the study of bimetallic complexes in olefin reactions.<sup>3</sup> We believe that it will be useful and easier prior to the understanding of multimetallic clusters to study bimetallic systems, which can be expected to be less complex. However, one must keep in mind that the number of metals or the size of the cluster can be important in determining catalytic properties and that the use of bimetallic compounds may not be generalized. For instance, in a recent paper it was reported that the size of the clusters affected reactions occurring on the surface of the multimetallic species.<sup>4</sup>

For the palladium-catalyzed telomerization of butadiene with acetic acid yielding acetoxyoctadienes we proposed the bimetallic mechanism outlined in Scheme I.<sup>3</sup> In this paper, we want to describe the synthesis of **1**, which has not been reported as yet. In addition, further experiments involving complex **1** dealing with bimetallic species will be presented.

## Experimental Section

The  $^1H$  NMR spectra were recorded at 90 MHz on a Varian Model EM 390 and the  $^{13}C$  NMR spectra at 200 MHz on a Bruker Model CXF 200.  $CDCl_3$  was used as solvent. The shifts are expressed as  $\delta$  values relative to  $Me_4Si$ . The IR spectra were performed on a Perkin-Elmer 577 using KBr pellets. Mass spectra were recorded on a Varian MAT 112 combined with the Varian Spectro System MAT 188 by using an ion source with a temperature of 210 °C, a pressure of  $10^{-5}$  torr, and an ion energy of 70 eV. Elemental analysis was carried out on an Elemental Analyzer Carlo Erba 1106.

**Preparation of  $(\mu-1-3-\eta:6-8-\eta-C_8H_{12})(\mu-OOCCH_3)_2Pd$  (**1**).** (a) Starting from Bis[( $\eta^3$ -allyl)palladium acetate)]. In a



60-mL glass autoclave a sample of 0.5 g (1.2 mmol) of bis[( $\eta^3$ -allyl)palladium acetate] was dissolved in 30 mL of benzene. To the cooled, homogeneous solution were added 0.45 g (7.5 mmol) of acetic acid and 1.5 g (28 mmol) of butadiene. After the yellow

(1) (a) Jolly, P. W. In "Comprehensive Organometallic Chemistry"; Wilkinson, G., Ed.; Pergamon Press: Oxford, 1982; Vol. 8, p 671. (b) Tkatchenko, I. In "Comprehensive Organometallic Chemistry"; Wilkinson, G., Ed.; Pergamon Press: Oxford 1982; Vol. 8, p 101.

(2) (a) Gates, B. C.; Lieto, J. *ChemTech* 1980, 195, 248. (b) Beach, D. L.; Kobylinski, T. P. *J. Chem. Soc. Chem. Commun.* 1980, 933. (c) Hamilton, J. F.; Baetzold, R. C. *Science (Washington, D.C.)* 1979, 205, 1213. (d) Jackson, S. D.; Wells, P. B.; Whyman, R.; Worthington, P. *Catal. (London)* 1981, 4, 75. (e) Muettterties, E. L.; Krause, M. *J. Angew. Chem.* 1983, 95, 135. (f) Muettterties, E. L. *Catal. Rev.—Sci. Eng.* 1981, 23, 69. (g) Whyman, R. *Philos. Trans. R. Soc. London, Ser. A* 1982, 308, 131. (h) Ugo, R.; Psaro, R. *J. Mol. Catal.* 1983, 20, 53.

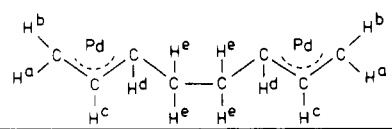
(3) (a) Keim, W. In "Transition Metals in Homogeneous Catalysis"; Schrauzer, G. N., Ed.; Marcel Dekker: New York, 1971; p 59. (b) Keim, W.; Behr, A.; Röper, M. In "Comprehensive Organometallic Chemistry"; Wilkinson, G., Ed.; Pergamon Press: Oxford, 1982; Vol. 8, p 311.

(4) *Chem. Eng. News* 1985, Jan 21, 51.

<sup>†</sup>Institute of Technical Chemistry and Petrochemistry.

<sup>‡</sup>Max-Planck-Institut für Kohlenforschung.



Table I.  $^1\text{H}$  NMR Spectral Data of the Octadienyl Chain of Complex 1


signal	a, d	b	c	e
$\delta$	3.1–3.9	2.4–2.9	4.8–5.5	1.8
$n$ H	4	2	2	4

solution was stirred for 45 min at 45 °C, the volatile components were distilled off at  $10^{-2}$  torr. After addition of *n*-pentane, complex 1 precipitated as a white amorphous solid (0.23 g, 0.54 mmol; 45% yield).

(b) **Starting from  $[\text{Pd}(\text{OAc})_2]_3$ .** In the same manner as described in a, 0.4 g (1.8 mmol) of  $[\text{Pd}(\text{OAc})_2]_3$ , 3.0 g (54 mmol) of butadiene, and 0.4 g (7.5 mmol) of acetic acid were reacted in 30 mL of acetone for 13 h at 50 °C forming complex 1 in a 42% yield. The workup followed preparation under a.

The IR spectrum of complex 1 shows a weak absorption at 2920  $\text{cm}^{-1}$  caused by the saturated C–H bond and strong absorptions of the acetate groups at 1575 and 1410  $\text{cm}^{-1}$ . The  $^1\text{H}$  NMR spectrum (solvent  $\text{CDCl}_3$ ) shows the signal of the methyl groups stemming from the acetate bridges ( $\delta$  2.0; six protons) and four signals of the octadienyl chain (Table I). The allyl fragments are characterized by the two antiprotons  $\text{H}^b$  at 2.4–2.9 ppm, the broad multiplet of the syn protons  $\text{H}^a$  and  $\text{H}^d$  at 3.1–3.9 ppm, and the two protons  $\text{H}^c$  at 4.8–5.5 ppm. It is remarkable that the octadienyl chain is twisted in such a way that proton  $\text{H}^d$  appears in the range of the syn protons. In the mass spectrum the signal at  $m/e$  108 confirms the presence of the octadienyl chain ( $\text{C}_8\text{H}_{12}$ ).

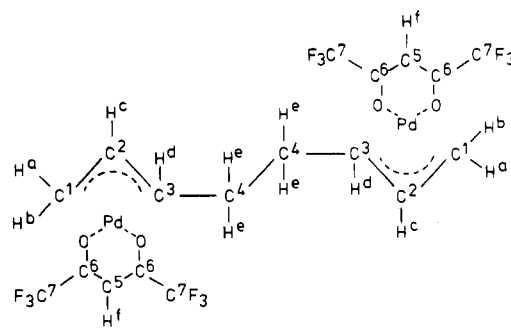
Complex 1 has a decomposition point of 165 °C. Its elemental analysis confirms the composition  $\text{Pd}_2(\text{OAc})_2\text{C}_8\text{H}_{12}$ . (Anal. Calcd: C, 32.8; H, 4.13. Found: C, 33.4; H, 4.20.) Upon hydrogenation quantitative yields of *n*-octane and palladium metal were formed.

**Reaction of Complex 1 with Butadiene Yielding Complex 5.** In a 60-mL glass autoclave 0.1 g (2.2 mmol) of complex 1 was reacted with 2.5 g (46 mmol) of butadiene in 25 mL of benzene. After being stirred for 6 h at 50 °C, the solution was evaporated. Upon addition of *n*-pentane, complex 5 precipitated (0.05 g, 0.1 mmol; 45% yield). The IR and  $^1\text{H}$  NMR spectra were identical with the literature data.<sup>8</sup>

**Preparation of  $(\mu-1-3-\eta^6-8-\eta-\text{C}_8\text{H}_{12})(\text{F}_3\text{CCOCHCOCF}_3)_2\text{Pd}_2$  (6).** In a 60-mL glass autoclave 0.5 g (0.95 mmol) of bis(hexafluoroacetylacetonate)palladium was dissolved in 5 mL of methanol and reacted with 1.0 g (18.5 mmol) of butadiene at 0 °C. The brownish orange solution darkened after a reaction time of 90 min and showed a deep red color after 2 h. After further being stirred for 2 h, the solution turned yellow and the white complex 6 began to precipitate. After evaporation of butadiene and the greater part of the methanol, *n*-pentane was added to get optimum precipitation. After filtration and drying at  $10^{-2}$  torr, complex 6 was obtained in 61% yield (0.21 g). Recrystallization was performed in a 2:1 mixture of chloroform and *n*-pentane at –5 °C, yielding needle-shaped crystals. Anal. Calcd: C, 29.44; H, 1.92. Found: C, 29.44; H, 1.90. The IR spectrum consists absorptions due to the C–O bonds at 1520 and 1670  $\text{cm}^{-1}$ . The  $^1\text{H}$  NMR shows the syn protons  $\text{H}^a$  as a doublet at 4.1 ppm and  $\text{H}^d$  as a multiplet at 3.9 ppm (Table II). The anti protons  $\text{H}^b$  are shifted to a higher field at 3.05 ppm. This assignment is confirmed by decoupling of the methylene protons  $\text{H}^e$  at 2.05 ppm which changes the multiplet at 3.9 ppm into a doublet. The coupling constants of the signals of  $\text{H}^a$ ,  $\text{H}^b$ , and  $\text{H}^c$  are characteristic for  $\eta^3$ -allylic systems. The  $^{13}\text{C}$  NMR (Table II) shows the expected shifts and multiplicities, confirmed by further decoupling experiments. The mass spectrum contains the signal  $m/e$  528, which corresponds to the fragment  $[\text{Pd}_2(\text{C}_8\text{H}_{12})(\text{CF}_3\text{COCHCOCF}_3)]^+$ . Complex 6 decomposes at 160 °C.

**Preparation of  $(\mu-1-3-\eta^6,6,7-\eta^8-\eta-\text{C}_6\text{H}_{12})(\text{F}_3\text{CCOCHCOCF}_3)_2(\text{P}-i\text{-Pr})_2\text{Pd}_2$  (8).** A solution of 0.2 g (0.26 mmol) of complex 6 in 15 mL of tetrahydrofuran was reacted at room temperature with 0.042 g (0.26 mmol) of triisopropylphosphine. After a reaction time of 2.5 h the solvent of the brownish, homogeneous solution was distilled off at  $10^{-2}$  torr. The oily residue was crystallized in a 1:2 mixture of ether and *n*-pentane yielding 0.16 g (0.17 mmol;

Table II. NMR Spectral Data of Complex 6



$^1\text{H}$ NMR Spectral Data			
H	$\delta$	$n$ H	multipl
a	4.1	2	d, $J(a,c) = 6$ Hz
b	3.05	2	d, $J(b,c) = 12$ Hz
c	5.8–5.4	2	m
d	3.9	2	m, $J(c,d) = 12$ Hz
e	2.05	4	m
f	6.1	2	s

$^{13}\text{C}$ NMR Spectral Data		
C	$\delta$	multipl (coupled)
1	56.5	t
2	89.8	d
3	79.6	d
4	29.6	t
5	112.4	d
6	109.4–123.0	q
7	175.4–176.1	q

65%) of white crystals of 8 with a melting point at 103 °C. Anal. Calcd: C, 36.22; H, 3.94. Found: C, 36.58; H, 3.93. The IR spectrum contains nearly the same absorptions as the starting complex 6, however, with a supplementary absorption at 2960  $\text{cm}^{-1}$  typical for C–H bonds in the isopropyl substituents. The  $^1\text{H}$  NMR spectrum shows the signals of the  $\eta^3$ -allyl and the  $\eta^1$ -allyl group (Table III). The  $\text{H}^i$  protons of the methylene group which is  $\eta^1$ -bonded to the palladium afford a characteristic doublet at 2.8 ppm. The two methine protons of the hexafluoroacetylacetonate ligands in complex 6 gave a single singlet at 6.1 ppm. In complex 8, the methine proton  $\text{H}^k$ , which is close to the phosphine, is shifted to a higher field (singlet at 5.75 ppm), whereas proton  $\text{H}^j$  has furthermore a signal at 6.1 ppm. This shift of the methine proton agrees with data reported for  $\text{Pd}(\text{F}_3\text{Cacac})_2\text{PR}_3$ .<sup>9</sup>

**Preparation of  $(\mu-1-\eta^2,3-\eta^6,7-\eta^8-\eta-\text{C}_6\text{H}_{12})(\text{F}_3\text{CCOCHCOCF}_3)(\text{P}-i\text{-Pr})_2\text{Pd}_2$  (9).** The reaction is almost identical with the synthesis of complex 8: however, 0.084 g (0.52 mmol) of *P*-*i*- $\text{Pr}_3$  was used. The pale yellow precipitate (0.098 g, 0.094 mmol; 37% yield) has a melting point of 120 °C. The elemental analysis supports the proposed structure. (Anal. Calcd: C, 40.96; H, 5.34. Found: C, 40.32; H, 5.32.) The  $^1\text{H}$  NMR spectrum (Table III) shows a single singlet of the two shifted methine protons  $\text{H}^e$  at 5.68 ppm. Allylic protons (at about 4.0 and 3.0 ppm) are not observed, whereas the olefinic protons  $\text{H}^b$  and  $\text{H}^c$  appear at 4.6 or 5.5 ppm, respectively.

**Reaction of Complex 1 with Hexafluoroacetylacetonate Yielding Complex 6.** A 0.18-g (0.41-mmol) sample of complex 1 was reacted at room temperature with 0.17 g (0.90 mmol) of hexafluoroacetylacetonate in 10 mL of  $\text{CHCl}_3$ . After the solution was stirred for 16 h, the solvent was evaporated and the residue washed with *n*-pentane. Complex 6 is obtained in a 98% yield (0.3 g, 0.4 mmol).

**Experimental Performance of the Telomerization Reactions.** A 0.045-mmol sample of complex 1 or 6 and 0.09 mmol of tri-*o*-tolyl phosphite were dissolved in 10 mL of acetonitrile. The solution was poured into a 60-mL glass autoclave equipped with a magnetic stirrer. Acetic acid (18 mmol) and butadiene (37 mmol) were added. After a reaction time of 16 h at a temperature of 60 °C the autoclave was opened, the nonreacted butadiene was evaporated, and the remaining acetic acid was washed out with water. The organic layer was analyzed by gas chromatography

Table III.  $^1\text{H}$  NMR Spectra of Complexes 8 and 9

8

9

signal	$\delta$	$n$ H	multipl	signal	$\delta$	$n$ H	multipl
a	4.2-3.8	1	d	a	2.35-1.17	4	m
b	3.0	1	d	b	4.85-4.3	2	m
c	5.6-5.25	1	m	c	5.5-5.1	2	m
d	4.2-3.8	1	d	d	2.75	4	d
e		2	m	e	5.68	2	s
f	2.4-1.7	2	m	f	1.4-1.0	36	q
g	4.85-4.4	1	m	g	2.35-1.75	6	m
h	5.6-5.25	1	m				
i	2.8	2	d				
j	6.1	1	s				
k	5.75	1	s				
l	2.4-1.7	3	m				
m	1.45-1.15	18	d				

using a 50-m basic WG-11 capillary column and a temperature program of 100–230 °C (6 min isothermal, 8 °C/min).

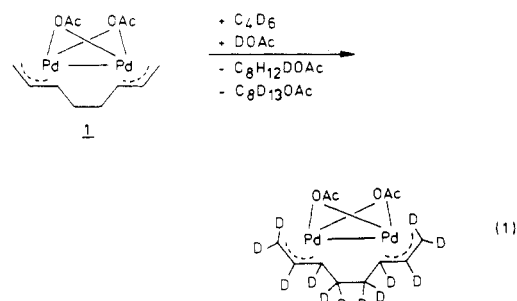
### Results and Discussion

The telomerization of 1,3-dienes with a great variety of nucleophiles is known and has been reviewed recently.<sup>5</sup> For a better understanding of the reaction mechanism, we have studied the telomerization of acetic acid and butadiene in more detail. The chosen system can be regarded as representative for other nucleophiles and dienes. By reacting butadiene and acetic acid with bis[( $\eta^3$ -allyl)palladium acetate] or palladium acetate, complex 1 (Scheme I) could be isolated out of the catalytically active reaction mixture. The X-ray structure<sup>6</sup> showed a Pd–Pd distance of 2.9 Å, which permits the discussion of a palladium–palladium metal bond similar to that in bis[( $\eta^3$ -allyl)palladium acetate].<sup>7</sup> However, in complex 1 palladium is formally in the oxidation state III which does not agree with the good NMR spectra, indicating that the compound is not paramagnetic. So far, the kind of bonding between the palladium atoms is not fully understood.

Complex 1 can be considered as one key intermediate in the telomerization of butadiene with acetic acid. Complex 1 can exist in the  $\eta^3$ -allyl form (Scheme I), the  $\eta^1$ -allyl form, and the  $\eta^1$ - $\eta^3$ -allyl form. The  $\eta^1$ -allyl form originates from coordination of butadiene or phosphines as is discussed below. This coordination looses the  $\text{C}_8$  chain, thus enabling an attack of the nucleophiles giving intermediate 2. The proton always bonds to carbon atom 6 as evidenced from the labeling experiments. The acetato group has the choice between carbon atoms 1 and 3, thus forming the two telomers observed, 1-acetoxyoctadiene and 3-acetoxyoctadiene. After the nucleophile acetic acid has been

added, incoming butadiene closes the catalytic circle via return to 1.

Further support for this mechanism is gained from using deuterated butadiene depicted in eq 1. Complex 1 reacts



with  $\text{C}_4\text{D}_6$  in DOAc yielding  $\text{C}_8\text{H}_{12}\text{DOAc}$  and complex 3 confirmed by MS and  $^1\text{H}$  NMR spectroscopy and gas chromatography. These results prove that the  $\text{C}_8$  chain present in complex 1 is also found in the reaction product  $\text{C}_8\text{H}_{12}\text{DOAc}$ .<sup>3</sup>

Interestingly, reaction of 1 with butadiene omitting acetic acid yielded complex 5, which has been described by Medema and van Helden (Scheme II).<sup>8</sup> They also started from bis[( $\eta^3$ -allyl)palladium acetate] and showed that in the first step complex 4 was formed by addition of butadiene to the allyl moiety. In a second step the two  $\text{C}_7$  fragments are displaced by three incoming molecules of butadiene, thus yielding 5. They proposed route b to account for the catalytic formation of linear  $\text{C}_{12}$  oligomers. In the presence of acetic acid, however, the reaction path alters giving  $\text{C}_8\text{H}_{13}\text{OAc}$  telomers via the interceptable complex 1 (route a).

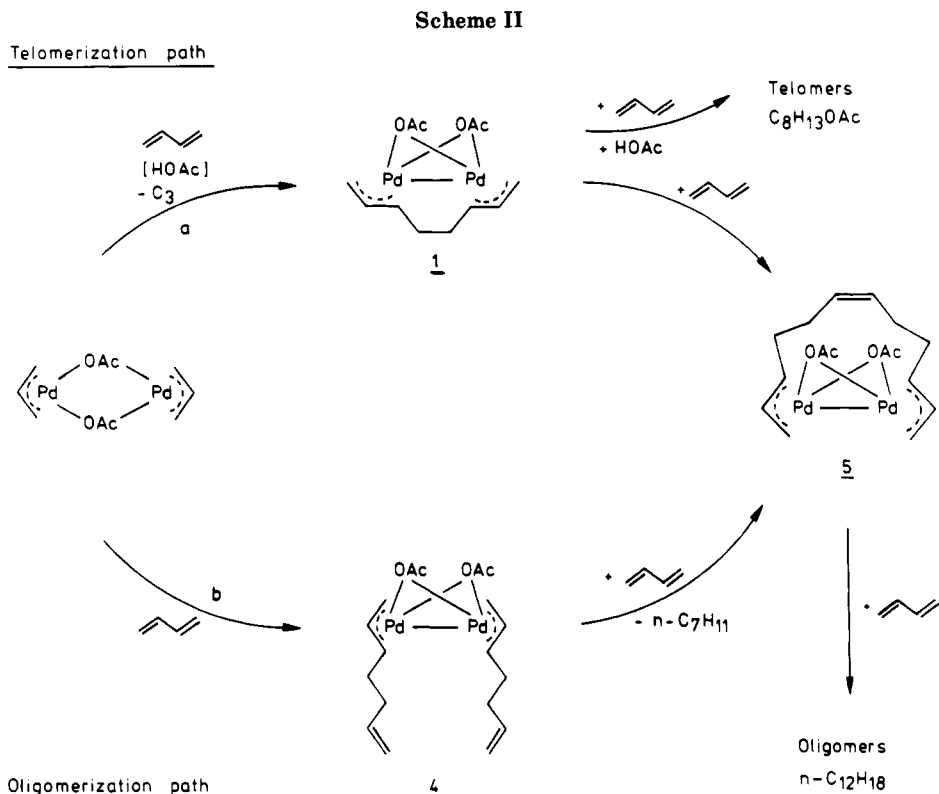
(5) Behr, A. *Aspects Homogeneous Catal.* 1984, 5, 3.

(6) Complex 1 was isolated first by W.K. during his time at Shell Development, but the preparative method was not reported. W.K. is grateful to A. E. Smith for the X-ray data which also have not been published.

(7) Churchill, M. R.; Mason, R. *Nature (London)* 1964, 204, 777.

(8) (a) Medema, D.; van Helden, R.; Kohll, C. F. *Inorg. Chim. Acta* 1969, 3, 255. (b) Medema, D.; van Helden, R. *Recl. Trav. Chim. Pays-Bas* 1971, 90, 324.

(9) Siedle, A. R.; Newmark, R. A.; Pignolet, L. H. *J. Am. Chem. Soc.* 1982, 104, 6584.

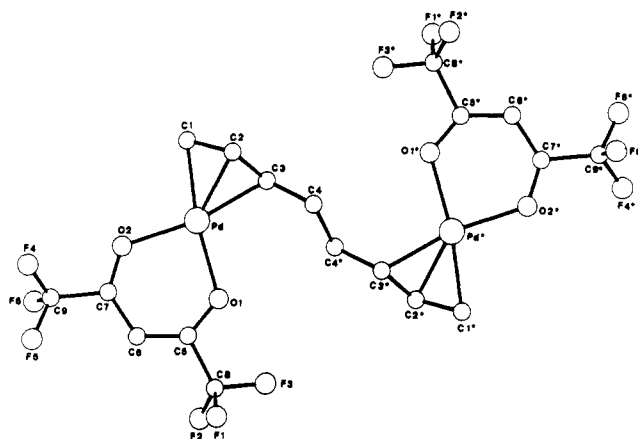
**Table IV. X-ray Diffraction Data for  $C_{18}H_{14}O_4F_{12}Pd_2$  (6)<sup>a</sup>**

crystal size	$0.11 \times 0.28 \times 0.48$ mm
crystal system	monoclinic
space group	$P2_1/n$ (no. 14)
<i>a</i>	4.6574 (4) Å
<i>b</i>	9.354 (1) Å
<i>c</i>	27.113 (2) Å
$\beta$	94.573 (6)°
<i>V</i>	1177.4 Å <sup>3</sup>
<i>Z</i>	2
$d_{\text{calcd}}$	2.07 g cm <sup>-3</sup>
$\mu(\text{Mo})$	16.2 cm <sup>-1</sup>
empirical absorptn correctn	0.875 <sub>min</sub> - 1.286 <sub>max</sub>
diffractometer	Enraf-Nonius CAD-4
graphite-monochromated Mo radiatn	$\lambda = 0.71069$ Å
scan mode	$\omega$ -2 $\theta$
<i>T</i>	21 °C
$\theta$ range	1.0-34.0°
measd reflctns	5105 ( $\pm h, +k, +l$ )
unique reflctns	4768
obsd reflctns ( $I \geq 2\sigma(I)$ )	3132
no. of variables	181
<i>R</i>	0.042
$R_w$ ( $w = 1/\sigma^2(F_o)$ )	0.048
goodness of fit	2.3
residual electron density	0.6 e Å <sup>-3</sup>

<sup>a</sup>Structure solved by heavy-atom method, and hydrogen atom positions were located and kept fixed in the final refinement stages; all fluorine atoms were highly disordered and refined isotropically with partial occupancies.

In the present mechanism, bimetallic palladium complexes possessing palladium-palladium bonds are proposed as intermediates. It appeared of interest to prepare related bimetallic palladium complexes with isolated palladium atoms and to compare the catalytic properties of these complexes.

The reaction of bis(hexafluoroacetylacetonato)palladium in methanol with butadiene gave complex 6, which as the X-ray structure<sup>10</sup> confirms, lies on a crystallographic center

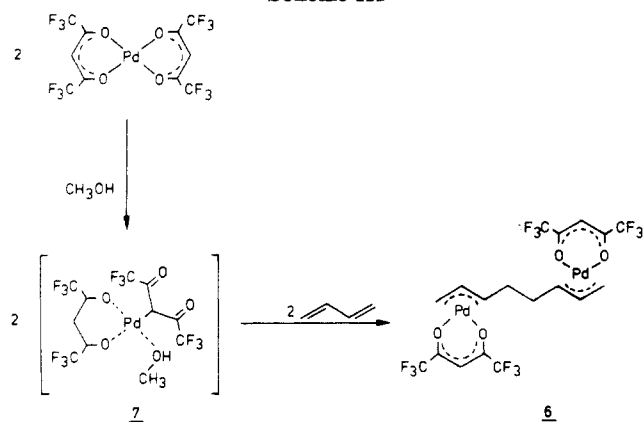
**Figure 1. Structure of complex 6.****Table V. Selected Bond Lengths (Å) and Angles (deg) for 6**

Bond Lengths			
Pd-O1	2.121 (3)	C1-C2	1.393 (6)
Pd-O2	2.102 (3)	C2-C3	1.395 (5)
Pd-C1	2.099 (4)	C3-C4	1.502 (6)
Pd-C2	2.103 (4)	C4-C4*	1.522 (5)
Pd-C3	2.131 (4)	C5-C6	1.367 (7)
O1-C5	1.261 (5)	C6-C7	1.394 (7)
O2-C7	1.251 (5)		
Bond Angles			
O1-Pd-O2	88.3 (1)	Pd-C3-C4	120.2 (3)
C1-Pd-C2	38.7 (2)	C2-C3-C4	123.9 (3)
C1-Pd-C3	68.7 (2)	C4*-C4-C3	113.5 (3)
C2-Pd-C3	38.4 (1)	O1-C5-C6	130.4 (4)
Pd-O1-C5	123.5 (3)	C5-C6-C7	123.6 (4)
Pd-O2-C7	124.8 (3)	O2-C7-C6	129.3 (4)
C1-C2-C3	117.8 (4)		

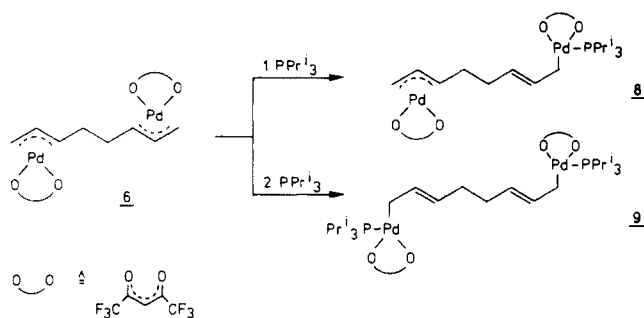
of inversion. Each Pd atom is  $\eta^3$ -bonded to one end of an octa-1,7-dienyl ligand. The molecular structure, together with the atomic numbering scheme, is depicted in Figure 1. Similar complexes of palladium and nickel with a bridging octadienyl chain have been described by White<sup>11</sup>

(10) Computer programs used in this investigation are summarized in: Erker, G.; Dorf, U.; Engel, K.; Krüger, C.; Müller, G. *Organometallics* 1985, 4, 215.

Scheme III



Scheme IV

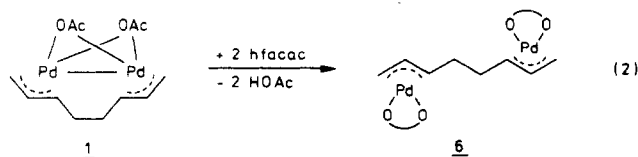


and Green.<sup>12</sup> Details of the X-ray structural analysis are summarized in Table IV. Selected bond distances and angles are given in Table V.

In the synthesis of complex 6, besides methanol, ethanol can also be used as a suitable solvent, whereas nonpolar solvents such as pentane or benzene fail to give 6. "In situ" IR measurements in methanol show a shift of the carbonyl frequency of  $\text{Pd}(\text{F}_6\text{acac})_2$  from 1605 to 1680  $\text{cm}^{-1}$ , which is in agreement with the formation of a palladium-carbon bond as shown in 7 (Scheme III).

The reaction of 6 with equimolar amounts of triisopropylphosphine gave complex 8, in which only one palladium metal is coordinated by the phosphine (Scheme IV). The  $^1\text{H}$  NMR spectrum confirms that  $\eta^3$ -allyl and  $\eta^1$ -allyl groups are present. When the same reaction is carried out with 2 equiv of  $\text{P-}i\text{-Pr}_3$  both  $\eta^3$ -allyl groups convert to  $\eta^1$ -allyl systems selectively yielding complex 9.

The interconversion of complex 1, containing a palladium-palladium bond, into 6, with two isolated palladium atoms, could also be demonstrated by reacting 1 with hexafluoroacetylacetone. In this reaction the acetate bridges are displaced by the diketone and the Pd-Pd bond is broken (eq 2).



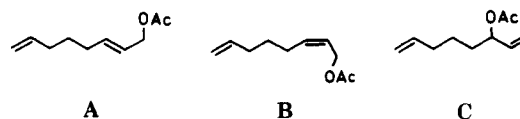
(11) (a) White, D. J. *Chem. Res., Synop.* 1977, 226. (b) White, D. J. *Chem. Res., Miniprint* 1977, 2401.

(12) Green, M. L. H. *J. Coord. Chem.* 1972, 2, 43.

Table VI. Telomerization of Butadiene and Acetic Acid Using Bimetallic catalysts<sup>a</sup>

cat.	yield, %	selectivity, <sup>b</sup>		
		A	B	C
1	97	63	8	29
6	87	65	9	26

<sup>a</sup> Catalyst: 0.045 mmol of complex + 0.09 mmol of tri-*o*-tolyl phosphite. <sup>b</sup>



As was pointed out above one aim of this investigation was directed toward whether bimetallic palladium complexes having palladium-palladium bonds, as in 1, compared to bimetallic complexes possessing two isolated palladium atoms, as in 6, show a different catalytic behavior. For this study both complexes 1 and 6 were reacted under identical conditions with butadiene and acetic acid. As shown in Table VI three telomers are obtained with similar conversions and selectivities.

Unfortunately, this result does not allow conclusions to be drawn favoring palladium-palladium bonds in catalytic cycles. On the other hand, it cannot be ruled out either that a palladium-palladium bond may be formed under catalytic reaction conditions starting from 6 and, of course, vice versa. Bearing in mind that catalytically active intermediates can be formed in either thermodynamically or kinetically controlled reactions and, where several intermediates are involved, those having the highest reactivities would be present in the lowest concentrations, it will always be difficult to confirm a reaction mechanism from the isolated complexes. However, the isolated complexes can be regarded as good models for individual steps in catalytic cycles, thus advancing our understanding and proposing new reactions. The results obtained with deuterated butadiene certainly allow the discussion of a bimetallic mechanism vs. a monometallic one. Furthermore, this paper shows that the interconversion of a bimetallic species having a metal-metal bond into a bimetallic one exhibiting nonbonded metal atoms is rather easy.

**Acknowledgment.** We wish to thank the Bundesministerium für Forschung und Technologie for supporting this work. A generous gift of palladium dichloride by the Degussa AG (Hanau) is gratefully acknowledged. We also thank Dr. W. Meltzow for carrying out the GC work, W. Falter for the GC/MS data and M. Sistig and B. Dederichs for the  $^1\text{H}$  and  $^{13}\text{C}$  NMR data.

**Registry No.** 1, 99632-71-0; 5, 99632-72-1; 6, 94698-82-5; 8, 94715-89-6; 9, 99632-73-2;  $\text{Pd}_2(\text{OAc})_2(\eta^3\text{-C}_3\text{H}_5)_2$ , 12084-71-8;  $[\text{Pd}(\text{OAc})_2]_3$ , 53189-26-7;  $\text{Pd}(\text{F}_6\text{CCOCHCOCF}_3)_2$ , 64916-48-9;  $\text{CF}_3\text{CCOCH}_2\text{COCF}_3$ , 1522-22-1; (*E*)- $\text{CH}_2=\text{CH}(\text{CH}_2)_3\text{CH}=\text{CH}_2\text{OAc}$ , 30460-73-2; (*Z*)- $\text{CH}_2=\text{CH}(\text{CH}_2)_3\text{CH}=\text{CH}_2\text{OAc}$ , 30460-72-1;  $\text{CH}_2=\text{CH}(\text{CH}_2)_3\text{CH}(\text{OAc})\text{CH}=\text{CH}_2$ , 3491-26-7; tri-*o*-tolyl phosphite, 2622-08-4; butadiene, 106-99-0.

**Supplementary Material Available:** Detailed information on the crystal structure determination of 6 including tables of final atomic positional parameters, final thermal parameters, and interatomic distances and angles and lists of observed and calculated structure factors (38 pages). Ordering information is given on any current masthead page.

# Reversible Binding of SO<sub>2</sub> to Arylplatinum(II) and -nickel(II) Complexes. X-ray Crystal Structure of the Five-Coordinate Platinum(II)-Sulfur Dioxide Complex [PtBr(C<sub>6</sub>H<sub>3</sub>(CH<sub>2</sub>NMe<sub>2</sub>)<sub>2</sub>-*o,o'*)( $\eta^1$ -SO<sub>2</sub>)]

Jos Terheijden, Gerard van Koten,\* Wilhelmus P. Mul, and Derk J. Stufkens

Anorganisch Chemisch Laboratorium, J. H. van't Hoff Institute, University of Amsterdam, 1018 WV Amsterdam, The Netherlands

Fred Muller and Casper H. Stam

Laboratorium voor Kristallografie, J. H. van't Hoff Institute, University of Amsterdam, 1018 WV Amsterdam, The Netherlands

Received September 9, 1985

Reactions of the platinum(II) and nickel(II) complexes [MX(C<sub>6</sub>H<sub>3</sub>(CH<sub>2</sub>NMe<sub>2</sub>)<sub>2</sub>-*o,o'*)] (1) with SO<sub>2</sub> afford the  $\eta^1$ -pyramidal-bonded SO<sub>2</sub> complexes [MX(C<sub>6</sub>H<sub>3</sub>(CH<sub>2</sub>NMe<sub>2</sub>)<sub>2</sub>-*o,o'*)( $\eta^1$ -SO<sub>2</sub>)] (2). The binding of the SO<sub>2</sub> to the metal d<sup>8</sup> center is reversible at room temperature. IR, Raman, <sup>1</sup>H NMR, and UV spectra were recorded, and the structure of **2b** (M = Pt; X = Br) was determined by X-ray methods. The crystals of **2b** are monoclinic with space group P2<sub>1</sub>/c and cell constants *a* = 14.215 (1) Å, *b* = 9.840 (1) Å, *c* = 11.985 (1) Å,  $\beta$  = 113.15 (1)°, *V* = 1541.4 (5) Å<sup>3</sup>, *Z* = 4, *D*(calcd) = 2.28 g cm<sup>-3</sup>, and *F*(000) = 1000 electrons. Final *R* = 0.043 for 2063 reflections. The five-coordinate platinum center has an approximately square-pyramidal geometry with two trans N atoms, a Br atom, and a C atom in the base and the S atom of the  $\eta^1$ -bonded SO<sub>2</sub> ligand at the apex (long Pt-S bond of 2.613 (7) Å) (see Figure 4a). The binding of the SO<sub>2</sub> to Pt(II) and Ni(II) centers points to an enhanced basicity of these metals. This arises from the presence of the two hard N donor ligands while the metal(II) center is also bonded to the relatively hard C(ipso) center. Neither insertion of SO<sub>2</sub> in the M-C bond nor formation of sulfato complexes by reactions of **2** with O<sub>2</sub> was observed.

## Introduction

Recent studies have shown that the bonding mode of the SO<sub>2</sub> ligand is a useful probe into the electronic properties of transition-metal complexes.<sup>1-4</sup> Structural features of the coordinated ligand (e.g., bent or planar (L)<sub>n</sub>M-SO<sub>2</sub> geometries and M-S and O-S bond lengths as well as O-S-O bond angles) reflect the specific orbital arrangement that the metal unit L<sub>n</sub>M has available for bonding.

The greater part of the [MSO<sub>2</sub>] (M is a d<sup>8</sup> metal, Rh(I) or Ir(I))<sup>5</sup> type of complexes are five-coordinate and have square-pyramidal structures with axial  $\eta^1$ -pyramidal-bonded SO<sub>2</sub>. The  $\eta^1$ -pyramidal geometry results from M-to-S(O)<sub>2</sub>  $\sigma$ -donation with rehybridization of the S orbitals to sp<sup>3.5</sup>.

In principle the platinum(II) center in PtX<sub>2</sub>L<sub>2</sub> complexes has a too low basicity to form stable PtX<sub>2</sub>L<sub>2</sub>(SO<sub>2</sub>) complexes. This is apparent from the fact that only three platinum(II) complexes have been reported: i.e., *cis*-[(2-Me<sub>2</sub>NCH<sub>2</sub>)<sub>2</sub>C<sub>6</sub>H<sub>4</sub>]<sub>2</sub>Pt( $\eta^1$ -SO<sub>2</sub>),<sup>6</sup> [(Pt<sub>2</sub>(P<sub>2</sub>O<sub>5</sub>H<sub>2</sub>)<sub>4</sub>)(SO<sub>2</sub>)<sub>2</sub>]<sup>4,7</sup> and [Pt(Me)(PPh<sub>3</sub>)<sub>2</sub>(I-SO<sub>2</sub>)].<sup>8</sup>

In the course of our chemistry with NCN'M(d<sup>8</sup>)X complexes, in which NCN' is the monoanionic terdentate ligand system *o,o'*-(Me<sub>2</sub>NCH<sub>2</sub>)<sub>2</sub>C<sub>6</sub>H<sub>3</sub>, we have found that the metal center has an enhanced nucleophilic character as

compared with corresponding MX<sub>2</sub>L<sub>2</sub> complexes. The NCN' ligand system places the metal d<sup>8</sup> center in a pincerlike position with a rigid structure consisting of two hard, mutually trans positioned N donor centers and a hard C donor. This geometry and electronic properties give rise to very specific reactions because the rigid planar NCNM arrangement also blocks subsequent stereoisomerizations of the NCNM(electrophile) complexes. In the final products this NCNM arrangement is invariably present.

It has been observed that, whereas interesting reactions of NCN'PtX have been found with X<sub>2</sub>,<sup>9</sup> MeX,<sup>10,11</sup> and metal salts,<sup>12-14</sup> no reaction occurs with O<sub>2</sub>, CO, N<sub>2</sub>, BF<sub>3</sub>, or HCl.

In this paper we report the syntheses and characterization of arylplatinum(II) and -nickel(II) sulfur dioxide complexes and present the first example of a structurally characterized arylplatinum(II)  $\eta^1$ -sulfur dioxide complex.

## Experimental Section

**General Data.** Compounds of the formula [PtX(C<sub>6</sub>H<sub>3</sub>(CH<sub>2</sub>NMe<sub>2</sub>)<sub>2</sub>-*o,o'*)] (X = Cl (1a), Br (1b), I (1c)) and [NiX(C<sub>6</sub>H<sub>3</sub>(CH<sub>2</sub>NMe<sub>2</sub>)<sub>2</sub>-*o,o'*)] (X = Cl (1d), Br (1e), I (1f)) were prepared as previously described.<sup>10,15</sup> Sulfur dioxide and other

- (1) Mingos, D. M. P. *Transition Met. Chem. (N.Y.)* **1978**, *3*, 1.
- (2) Ryan, R. R.; Kubas, G. J.; Moody, D. C.; Eller, P. G. *Struct. Bonding (Berlin)* **1981**, *46*, 48-100.
- (3) Kubas, G. J. *Inorg. Chem.* **1979**, *18*, 183.
- (4) Muir, K. W.; Ibers, J. A. *Inorg. Chem.* **1969**, *8*, 1921.
- (5) Nappier, T. E., Jr.; Meek, D. W.; Kirchner, R. M.; Ibers, J. A. *J. Am. Chem. Soc.* **1973**, *95*, 4194.
- (6) Longoni, G.; Fantucci, P.; Chini, P.; Canziani, F. *J. Organomet. Chem.* **1972**, *39*, 413.
- (7) Alexander, K. A.; Stein, P.; Hedden, D. B.; Roundhill, D. M. *Polyhedron* **1983**, *2*, 1389.
- (8) Snow, M. R.; Ibers, J. A. *Inorg. Chem.* **1973**, *12*, 224.

- (9) Terheijden, J.; van Koten, G.; de Booy, J. L.; Ubbels, H. J. C.; Stam, H. C. *Organometallics* **1983**, *2*, 1882.
- (10) Grove, D. M.; van Koten, G.; Louwen, J. N.; Noltes, J. G.; Spek, A. L.; Ubbels, H. J. C. *J. Am. Chem. Soc.* **1982**, *104*, 6609.
- (11) Terheijden, J.; van Koten, G.; Vinke, I. C.; Spek, A. L. *J. Am. Chem. Soc.* **1985**, *107*, 2891.
- (12) van der Ploeg, A. F. M. J.; van Koten, G.; Vrieze, K.; Spek, A. L. *Inorg. Chem.* **1982**, *21*, 2014.
- (13) van der Ploeg, A. F. M. J.; van Koten, G.; Vrieze, K. *Inorg. Chem.* **1982**, *21*, 2026.
- (14) van der Ploeg, A. F. M. J.; van Koten, G.; Vrieze, K. *Inorg. Chim. Acta* **1982**, *58*, 35.
- (15) Grove, D. M.; van Koten, G.; Ubbels, H. J. C.; Zoet, R.; Spek, A. L. *Organometallics* **1984**, *3*, 1003.

**Table I. Crystal Data and Details of the Structure Determination of [PtBr(C<sub>6</sub>H<sub>3</sub>(CH<sub>2</sub>NMe<sub>2</sub>)<sub>2-o,o'</sub>)( $\eta^1$ -SO<sub>2</sub>)] (2b)**

a. Crystal Data	
formula	C <sub>12</sub> H <sub>19</sub> N <sub>2</sub> BrPtSO <sub>2</sub>
mol wt	530.34
space group	P <sub>2</sub> <sub>1</sub> /c
cryst system	monoclinic
a/Å	14.215 (1)
b/Å	9.840 (1)
c/Å	11.985 (1)
$\beta$ /deg	113.15 (1)
V/Å <sup>3</sup>	1541.4 (5)
D(calcd), g cm <sup>-3</sup>	2.28
Z	4
F(000), electrons	1000
$\mu$ (Mo K $\alpha$ ), cm <sup>-1</sup>	119.0
cryst vol, mm <sup>3</sup>	0.01
cryst size/mm	0.25 × 0.20 × 0.20
b. Data Collection	
$\theta_{\min}$ , $\theta_{\max}$ , deg	1.1, 35
radiatn/Å	Mo K $\alpha$ , $\lambda$ = 0.71069
ref reflectns	200
total reflectn data	6586
total unique reflectns	6586
obsd data ( $I > 2.5\sigma(I)$ )	2063
c. Refinement	
no. of refined parameters	231
weighting scheme	$w = (4.6 + F_o + 0.039F_o)^{-1}$
final $R_F$ and $R_wF$	0.043 and 0.062

reagents were purchased commercially and used as received. Infrared spectra of the compounds were measured either as Nujol mulls between NaCl windows or in KBr pellets on a Perkin-Elmer 283 instrument. <sup>1</sup>H NMR spectra of solutions in CDCl<sub>3</sub> were recorded on a Varian T-60 spectrometer. Raman spectra of solutions in CH<sub>2</sub>Cl<sub>2</sub> were measured on a Jobin-Yvon Ramanor HG 2S instrument using the 4880 Å line of an argon ion laser. Electronic spectra of solutions in CH<sub>2</sub>Cl<sub>2</sub> were measured on a Perkin-Elmer Lambda 5 UV/vis spectrophotometer. Elemental analyses were carried out by the Analytical Department of the Institute for Applied Chemistry, TNO, Zeist, The Netherlands.

**Preparation of [MX(C<sub>6</sub>H<sub>3</sub>(CH<sub>2</sub>NMe<sub>2</sub>)<sub>2-o,o'</sub>)( $\eta^1$ -SO<sub>2</sub>)] (M = Pt, X = Cl (2a), Br (2b), I (2c); M = Ni, X = Cl (2d), Br (2e), I (2f)).** The complex [MX(C<sub>6</sub>H<sub>3</sub>(CH<sub>2</sub>NMe<sub>2</sub>)<sub>2-o,o'</sub>)] (1a-f; 0.2 mmol) was dissolved in 2 mL of CH<sub>2</sub>Cl<sub>2</sub> which provided a colorless (Pt compounds) or dark orange-brown (Ni compounds) solution. Upon bubbling gaseous SO<sub>2</sub> through the solution the color of the mixture changed to orange (Pt) or dark red (Ni). Addition of pentane (5 mL) resulted in the precipitation of orange (Pt) or dark red (Ni) solids which were filtered off and stored under SO<sub>2</sub> atmosphere. Products were identified by IR, Raman, UV/vis, and <sup>1</sup>H NMR as [MX(C<sub>6</sub>H<sub>3</sub>(CH<sub>2</sub>NMe<sub>2</sub>)<sub>2-o,o'</sub>)( $\eta^1$ -SO<sub>2</sub>)] (2a-f).

Reaction of solid 1a-f with excess of gaseous SO<sub>2</sub> afforded orange (Pt) or dark red (Ni) products. These products were identified by IR spectroscopy as 2a-f.

**Synthesis of [(Pt(C<sub>6</sub>H<sub>3</sub>(CH<sub>2</sub>NMe<sub>2</sub>)<sub>2-o,o'</sub>))<sub>2</sub>( $\mu$ -SO<sub>4</sub>)]·4H<sub>2</sub>O (3).** Complex 1b (446 mg, 1 mmol) dissolved in acetone (5 mL) was reacted with 0.6 equiv of Ag<sub>2</sub>SO<sub>4</sub> for 24 h. The AgBr was removed by filtration and the filtrate evaporated in vacuo. The

white product was extracted by CH<sub>2</sub>Cl<sub>2</sub> (3 mL). Upon addition of pentane (10 mL) a white solid precipitated which was filtered off and dried in vacuo: yield 48%. Anal. Calcd for C<sub>24</sub>H<sub>46</sub>N<sub>4</sub>Pt<sub>2</sub>SO<sub>8</sub>: C, 30.64; H, 4.93; N, 5.95. Found: C, 30.25; H, 4.81; N, 5.61.

**Reversibility of the SO<sub>2</sub> Binding and Reactions with Oxygen.** The orange complex 2b was exposed to air for 24 h whereby the color changed to white. The resulting white product appeared to be the starting complex [PtBr(C<sub>6</sub>H<sub>3</sub>(CH<sub>2</sub>NMe<sub>2</sub>)<sub>2-o,o'</sub>)] (checked by <sup>1</sup>H NMR and IR). When the white product was flushed with gaseous SO<sub>2</sub>, the orange product was formed again. The whole procedure could be repeated several times without any observable decomposition. When 2b was heated, the release of SO<sub>2</sub> was observed to start at a temperature of 82 °C (heating rate 3 °C/min). The analogous nickel complex 2e loses SO<sub>2</sub> at a temperature of 62 °C. At room temperature 2e already released SO<sub>2</sub> after 10 min without any observable decomposition, which points to a less stable SO<sub>2</sub> binding in the nickel compounds.

It is noteworthy that a similar procedure can be applied to a solution of 2. For example complex 1b was dissolved in CH<sub>2</sub>Cl<sub>2</sub> (4 mL) which provided a colorless solution. When gaseous SO<sub>2</sub> was bubbled through the colorless solution, the color of the mixture changed to orange. This color disappeared on bubbling a rapid stream of nitrogen (or oxygen or air) through the solution. The resulting white product obtained from the colorless solution appeared to be the starting complex 1b (checked by <sup>1</sup>H NMR and IR). The whole procedure could be repeated several times, i.e., saturation with SO<sub>2</sub> followed by flushing of the solution with nitrogen, without any observable decomposition.

The complex [PtBr(C<sub>6</sub>H<sub>3</sub>(CH<sub>2</sub>NMe<sub>2</sub>)<sub>2-o,o'</sub>)( $\eta^1$ -SO<sub>2</sub>)] (0.1 mmol) in oxygen-saturated benzene (5 mL) was allowed to stand for several days. The mixture was worked up by evaporating the solvent in vacuo. The remaining white solid was washed with pentane (5 mL) and dried in vacuo. The product was identified by <sup>1</sup>H NMR and IR as [PtBr(C<sub>6</sub>H<sub>3</sub>(CH<sub>2</sub>NMe<sub>2</sub>)<sub>2-o,o'</sub>)].

**Crystal Preparation.** A sample of the complex [PtBr(C<sub>6</sub>H<sub>3</sub>(CH<sub>2</sub>NMe<sub>2</sub>)<sub>2-o,o'</sub>)] (0.75 mmol) was dissolved in a mixture of toluene/SO<sub>2</sub> at low temperature (-50 °C). The dark orange-red solution was slowly warmed up to room temperature. Over a period of 3 days bright red crystals of the complex [PtBr(C<sub>6</sub>H<sub>3</sub>(CH<sub>2</sub>NMe<sub>2</sub>)<sub>2-o,o'</sub>)( $\eta^1$ -SO<sub>2</sub>)] were formed which were then isolated and stored under gaseous SO<sub>2</sub>. A crystal of dimensions 0.25 × 0.20 × 0.20 mm was coated with an inert resin to avoid decomposition and sealed in a capillary.

**X-ray Measurements and Refinement of [PtBr(C<sub>6</sub>H<sub>3</sub>(CH<sub>2</sub>NMe<sub>2</sub>)<sub>2-o,o'</sub>)( $\eta^1$ -SO<sub>2</sub>)] (2b).** Crystals of the title compound are monoclinic, space group P<sub>2</sub><sub>1</sub>/c, with four molecules in a unit cell of dimensions  $a = 14.215$  (1) Å,  $b = 9.840$  (1) Å,  $c = 11.985$  (1) Å,  $\beta = 113.15$  (1)°,  $V = 1541.4$  (5) Å<sup>3</sup>,  $D(\text{calcd}) = 2.28$  g cm<sup>-3</sup>, and  $F(000) = 1000$  electrons. A total of 2063 reflections with  $\theta < 35^\circ$  and intensities above the 2.5 $\sigma(I)$  limit were measured on a Nonius CAD4 diffractometer using graphite-monochromated Mo K $\alpha$  radiation; for details see Table I.

The position of Pt and Br were derived from an E<sup>2</sup> Patterson synthesis, and the remaining non-hydrogen atoms were found from subsequent  $\Delta F$  syntheses. After isotropic block-diagonal least-squares refinement an empirical absorption correction was applied.<sup>16</sup> Subsequent anisotropic refinement converged to R =

**Table II. Positional Parameters of the Atoms in Fractional Coordinates<sup>a</sup>**

atoms	x	y	z	atoms	x	y	z
Pt	0.20586 (3)	0.03884 (5)	-0.04689 (4)	C(3)	0.4370 (9)	0.191 (2)	0.2662 (11)
Br	0.0500 (2)	0.0254 (2)	-0.2428 (2)	C(4)	0.4655 (10)	0.079 (2)	0.3410 (11)
S(1)	0.3548 (4)	-0.0006 (4)	-0.1181 (4)	C(5)	0.4166 (10)	-0.048 (2)	0.3042 (11)
O(1)	0.298 (2)	-0.007 (2)	-0.2498 (12)	C(6)	0.3424 (9)	-0.0610 (14)	0.1866 (12)
O(2)	0.3981 (11)	-0.127 (2)	-0.0659 (12)	C(7)	0.3322 (10)	0.2852 (14)	0.0504 (12)
N(1)	0.2248 (7)	0.2498 (11)	-0.0436 (9)	C(8)	0.2930 (11)	-0.194 (2)	0.1220 (13)
N(2)	0.1962 (9)	-0.1597 (11)	0.0117 (11)	C(9)	0.1464 (12)	0.307 (2)	0.001 (2)
C(1)	0.3158 (9)	0.0548	0.1141 (10)	C(10)	0.2080 (12)	0.317 (2)	-0.1616 (14)
C(2)	0.3630 (8)	0.1782 (13)	0.1490 (10)	C(11)	0.1075 (11)	-0.156 (2)	0.053 (2)
				C(12)	0.178 (2)	-0.268 (2)	-0.080 (2)

<sup>a</sup> Estimated standard deviations in parentheses.

Table III. IR, Raman, and <sup>1</sup>H NMR Data of [MX(C<sub>6</sub>H<sub>3</sub>(CH<sub>2</sub>NMe<sub>2</sub>)<sub>2</sub>-o,o')]<sup>c</sup>

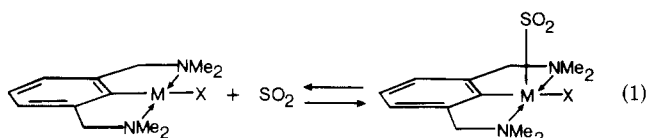
compd.	color	IR			Raman		<sup>1</sup> H NMR <sup>b</sup>		
		ν <sub>a</sub> (SO <sub>2</sub> ), cm <sup>-1</sup>	ν <sub>s</sub> (SO <sub>2</sub> ), cm <sup>-1</sup>	ν <sub>g</sub> (SO <sub>2</sub> ), cm <sup>-1</sup>	δ(SO <sub>2</sub> ), cm <sup>-1</sup>	δ(C <sub>6</sub> H <sub>3</sub> )	δ(CH <sub>2</sub> )	δ(NMe <sub>2</sub> )	
[PtCl(C <sub>6</sub> H <sub>3</sub> (CH <sub>2</sub> NMe <sub>2</sub> ) <sub>2</sub> -o,o')(η <sup>1</sup> -SO <sub>2</sub> )]	orange	1231 (1235)	1074 (1078)	1092	535	6.9 m	4.15 (42)	3.16 (33)	
[PtBr(C <sub>6</sub> H <sub>3</sub> (CH <sub>2</sub> NMe <sub>2</sub> ) <sub>2</sub> -o,o')(η <sup>1</sup> -SO <sub>2</sub> )]	orange	1230 (1236)	1072 (1077)	1080	535	6.9 m	4.03 (43)	3.10 (35)	
[PtI(C <sub>6</sub> H <sub>3</sub> (CH <sub>2</sub> NMe <sub>2</sub> ) <sub>2</sub> -o,o')(η <sup>1</sup> -SO <sub>2</sub> )]	orange	1235 (1237)	1075 (1077)	1090	535	6.9 m	4.16 (43)	3.29 (36)	
[NiCl(C <sub>6</sub> H <sub>3</sub> (CH <sub>2</sub> NMe <sub>2</sub> ) <sub>2</sub> -o,o')(η <sup>1</sup> -SO <sub>2</sub> )] <sup>c</sup>	red	1246 (1244)	1060 (1060)						
[NiBr(C <sub>6</sub> H <sub>3</sub> (CH <sub>2</sub> NMe <sub>2</sub> ) <sub>2</sub> -o,o')(η <sup>1</sup> -SO <sub>2</sub> )] <sup>c</sup>	red	1240 (1238)	1055 (1053)						
[NiI(C <sub>6</sub> H <sub>3</sub> (CH <sub>2</sub> NMe <sub>2</sub> ) <sub>2</sub> -o,o')(η <sup>1</sup> -SO <sub>2</sub> )] <sup>c</sup>	dark red	1241 (1245)	1056 (1057)						
[(Pt(C <sub>6</sub> H <sub>3</sub> (CH <sub>2</sub> NMe <sub>2</sub> ) <sub>2</sub> -o,o') <sub>2</sub> (μ-SO <sub>4</sub> )] <sup>d</sup>	white					6.8 m	4.00 (46)	3.13 (38)	
free SO <sub>2</sub> <sup>e</sup>		1340	1150		524				

<sup>a</sup> IR spectra were measured as Nujol mulls between NaCl windows (or in KBr pellets). The IR bands are strong. Raman spectra were measured in CH<sub>2</sub>Cl<sub>2</sub>. The Raman bands were weak. <sup>b</sup> Pt compounds were measured in CDCl<sub>3</sub>; Ni compounds gave broad signals in CDCl<sub>3</sub>. Chemical shifts are relative to Me<sub>4</sub>Si and *J*(PtH) values (Hz) between parentheses (m = multiplet). <sup>c</sup> The nickel complexes decomposed during the Raman measurements. <sup>d</sup> IR data: 950, 1010, 1105, 1190 cm<sup>-1</sup>. <sup>e</sup> Literature values: Lippincott, E. R.; Welsh, F. E. *Spectrochim. Acta* 1961, 17, 123 (IR). Reference 1 (Raman).

0.043. A weighting scheme  $w = (4.6 + F_o + 0.039F_o^2)^{-1}$  was applied ( $wR = 0.062$ ). The anomalous dispersion of Pt, Br, and S was taken into account, and an extinction correction was applied. The final values of the refined positional parameters are given in Table II (for thermal parameters, see supplementary material). The programs used were from XRAY 76.<sup>17</sup>

## Results and Discussion

**General Information.** The air-stable neutral complexes [MX(C<sub>6</sub>H<sub>3</sub>(CH<sub>2</sub>NMe<sub>2</sub>)<sub>2</sub>-o,o')] (M = Pt, X = Cl (**1a**), Br (**1b**), I (**1c**); M = Ni, X = Cl (**1d**), Br (**1e**), I (**1f**)) react readily with gaseous SO<sub>2</sub> to form the novel organometallic complexes [MX(C<sub>6</sub>H<sub>3</sub>(CH<sub>2</sub>NMe<sub>2</sub>)<sub>2</sub>-o,o')(η<sup>1</sup>-SO<sub>2</sub>)] (M = Pt, X = Cl (**2a**), Br (**2b**), I (**2c**); M = Ni, X = Cl (**2d**), Br (**2e**), I (**2f**); see eq 1.



M = Pt; X = Cl (**1a**),

Br (**1b**), I (**1c**)

M = Ni; X = Cl (**1d**),

Br (**1e**), I (**1f**)

M = Pt; X = Cl (**2a**),

Br (**2b**), I (**2c**)

M = Pt; X = Cl (**2d**),

Br (**2e**), I (**2f**)

The orange platinum(II) or red nickel(II) complexes are stable under SO<sub>2</sub> atmosphere, but on exposure to air at room temperature they slowly lose SO<sub>2</sub> with reformation of complex **1**. Reversible SO<sub>2</sub> uptake and release was found to occur for both the solid and the dissolved (in CH<sub>2</sub>Cl<sub>2</sub> or C<sub>6</sub>H<sub>6</sub>) compounds; this behavior prompted us to further investigate the properties of these SO<sub>2</sub> adducts.

It was observed that in the reaction of **1** with SO<sub>2</sub> no products originating from M-C bond cleavage were obtained. Also products originating from insertion of SO<sub>2</sub> into the M-C bond were not found. A number of examples of the latter type of reaction has been reported for various arylplatinum(II) or alkylnickel(II) complexes. For example, *trans*-[PtCl(Ph)(PEt<sub>3</sub>)<sub>2</sub>] reacted with SO<sub>2</sub> to give a red solution, which afforded after 6 h at 50 °C the white product *trans*-[PtCl(PhSO<sub>2</sub>)(PEt<sub>3</sub>)<sub>2</sub>].<sup>18</sup>

Exposure of a solution of **2b** in benzene to oxygen for several days gave no reaction: the starting product could be recovered from the solution almost quantitatively. In an attempt to see whether the possible product from this

reaction, i.e., [Pt<sup>IV</sup>Br(SO<sub>4</sub>)(C<sub>6</sub>H<sub>3</sub>(CH<sub>2</sub>NMe<sub>2</sub>)<sub>2</sub>-o,o')], would exist, we reacted the platinum(IV) complexes [Pt<sup>IV</sup>Br<sub>3</sub>(C<sub>6</sub>H<sub>3</sub>(CH<sub>2</sub>NMe<sub>2</sub>)<sub>2</sub>-o,o')] with Ag<sub>2</sub>SO<sub>4</sub>. This, however, did not provide the expected complex but instead gave a mixture of unknown products. Probably the rigid structure of the terdentate ligand prevents the formation of a complex containing such a bidentate-bonded sulfato ligand.<sup>19</sup>

These findings contrast with those reported by Kubas et al., who showed that Pt(0) complexes with a reversible, metal-bound SO<sub>2</sub> ligand form bidentate Pt(II) sulfato complexes upon reaction with oxygen.<sup>3</sup> Only the ligand-bound SO<sub>2</sub> complex [Pt(Me)(I-SO<sub>2</sub>)(PPh<sub>3</sub>)<sub>2</sub>], in which the SO<sub>2</sub> ligand is likewise reversibly bound, does not oxidize to the sulfato complex. Our efforts to synthesize a platinum(II) sulfato complex led to the isolation of [(Pt(C<sub>6</sub>H<sub>3</sub>(CH<sub>2</sub>NMe<sub>2</sub>)<sub>2</sub>-o,o')<sub>2</sub>(μ-SO<sub>4</sub>)]<sub>2</sub>. This latter white complex is the result of a metathesis reaction between [PtBr(C<sub>6</sub>H<sub>3</sub>(CH<sub>2</sub>NMe<sub>2</sub>)<sub>2</sub>-o,o')] and 0.5 equiv of Ag<sub>2</sub>SO<sub>4</sub>. Elemental analyses of the product pointed to a dinuclear compound.

In order to get a better understanding of the correlation between structural and physicochemical properties of **2a-f** a spectroscopic study was carried out and the structure of one of the complexes was crystallographically studied.

**IR and Raman Spectra.** IR spectra of **2a-f** (in KBr pellets or in Nujol mulls between NaCl windows) show two strong absorption bands in the region 1231–1245 and 1053–1078 cm<sup>-1</sup>, respectively, which can be assigned to the asymmetric and symmetric S-O stretching vibration (see Table III) of the coordinated SO<sub>2</sub> molecule.

From these ν(SO) data it is not directly apparent that the SO<sub>2</sub> ligand is bound in the η<sup>1</sup>-pyramidal coordination mode as has been structurally established for [Pt(SO<sub>2</sub>)<sub>2</sub>(PPh<sub>3</sub>)<sub>2</sub>].<sup>20</sup>

Kubas et al. have shown that a simple relation exists between ν(SO) frequencies and the MSO<sub>2</sub> geometry.<sup>3</sup> It then appears that the ν(SO) values for **2a-f** are just outside the upper limits (1225–1150/1065–990 cm<sup>-1</sup>) given by Kubas et al. as the region for η<sup>1</sup>-pyramidal-bound SO<sub>2</sub> in a [MSO<sub>2</sub>]<sup>18</sup> fragment. These values are rather in the region (1325–1210/1145–1060 cm<sup>-1</sup>) for ligand-bound SO<sub>2</sub>, thus demonstrating that these ranges have to be applied judiciously.

Only a limited number of metal-SO<sub>2</sub> complexes have been studied by Raman spectroscopy. For the platinum compounds **2a-c** Raman spectra of CH<sub>2</sub>Cl<sub>2</sub> solutions saturated with SO<sub>2</sub> could be recorded. The SO<sub>2</sub> bending

(16) Walker, N.; Stuart, D. *Acta Crystallogr., Sect. A* 1983, A39, 158.

(17) Stewart, J. M., Ed. "The X-RAY 76 System", Technical Report TR 466; Computer Science Center, University of Maryland: College Park, MD, 1976.

(18) Faraone, F.; Silvestro, L.; Sergi, S.; Pietropaolo, R. *J. Organomet. Chem.* 1972, 46, 379.

(19) We have found that other bidentate ligands such as formamidine or triazenido also coordinate via one donor atom to the platinum center.

(20) Moody, D. C.; Ryan, R. R. *Inorg. Chem.* 1976, 15, 1823.



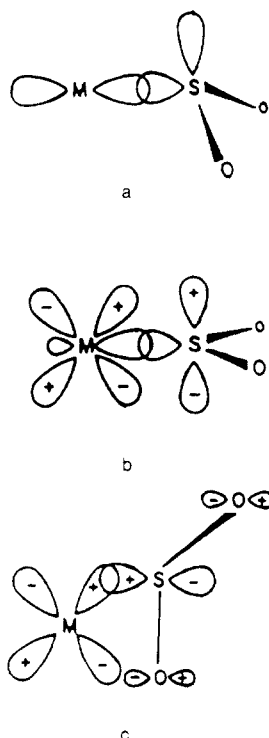


**Figure 1.** The three modes of  $\text{SO}_2$  bonding to mononuclear transition-metal complexes: a,  $\eta^1$ -pyramidal  $\text{SO}_2$ ; b,  $\eta^1$ -planar  $\text{SO}_2$ ; c,  $\eta^2$ - $\text{SO}_2$ .<sup>2</sup>

mode was found at  $535\text{ cm}^{-1}$  in all three complexes. This value is well in the range proposed for this mode:  $525\text{--}585\text{ cm}^{-1}$ .<sup>2</sup> The high-energy frequency regions of the Raman spectra show a strong emission at  $1150\text{ cm}^{-1}$  along with a broad band at  $1090\text{ (}1080\text{)}\text{ cm}^{-1}$  (Table III). The latter band is due to the symmetric (SO) stretching mode of the coordinated  $\text{SO}_2$  molecule, and the band at  $1150\text{ cm}^{-1}$  is the corresponding vibration of the free dissolved gaseous  $\text{SO}_2$  in  $\text{CH}_2\text{Cl}_2$  solution.<sup>2</sup> The corresponding values for the nickel(II) complexes could not be obtained as a result of the decomposition of the compounds in the laser beam. This instability of complexes in Raman measurements is a common feature and may account for the limited number of  $\nu(\text{SO})$  values reported as yet.

It must be noted that in the series **2a–c** and **2d–f** it is only the X that changes. Within each series the IR and Raman data for the M– $\text{SO}_2$  fragment seem almost to be insensitive to the nature of X and therefore the alternative structure containing ligand bound  $\text{SO}_2$  can be excluded. Ryan and Kubas have pointed out that a correlation also exists between sulfato formation, the  $\text{SO}_2$  lability, and the  $\text{SO}_2$  bonding mode, i.e.,  $\eta^1$ -pyramidal vs. planar.  $\eta^1$ -Pyramidal  $\text{SO}_2$  complexes with low-valent metals Pt(0) and Rh(I) generally do undergo sulfato reactions. It is apparent that the platinum and nickel complexes presented here are counter-examples of this generalization, while it is interesting to note that also  $\text{RhCl}(\text{ttp})\text{SO}_2$ <sup>21</sup> which likewise contains a terdentate ligand system fails to react with  $\text{O}_2$  to form a sulfato complex.

The IR spectra of  $[(\text{Pt}(\text{C}_6\text{H}_3(\text{CH}_2\text{NMe}_2)_{2-o,o'})_2(\mu\text{-SO}_4)]$  (**3**) show four strong bands in the  $\nu(\text{SO})$  region at  $950$ ,  $1010$ ,  $1105$ , and  $1190\text{ cm}^{-1}$ . Similar absorption bands have been found in the IR spectra of the nickel analogue,<sup>15</sup> for which a dinuclear structure was proposed with a bridging sulfato ligand. These findings and the fact that other dinuclear species with the  $\text{NCN}'$  ligand are known<sup>22</sup> make a similar

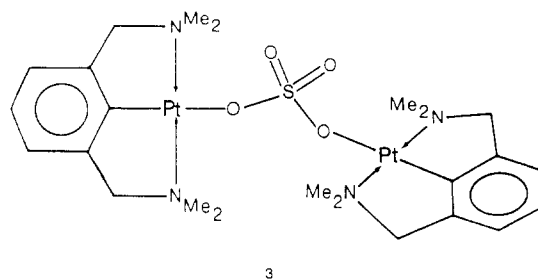


**Figure 2.** Schematic structure of  $[(\text{PtC}_6\text{H}_3(\text{CH}_2\text{NMe}_2)_{2-o,o'})_2(\mu\text{-SO}_4)]$  (**3**).

structure for **3** (see Figure 2), as for the nickel analogue, likely.

**<sup>1</sup>H NMR Spectrometric Measurements.** In the <sup>1</sup>H NMR spectra (60 MHz,  $\text{SO}_2$ -saturated  $\text{CDCl}_3$  solution) of **2a–c** the aryl protons appear as a multiplet signal at 6.9 ppm, while the  $\text{CH}_2$  H and  $\text{NMe}_2$  Me groups give singlet signals at 4.15 and 3.16 ppm (see Table III). Both the  $\text{NCH}_2$  and  $\text{NMe}_2$  groups show sharp <sup>195</sup>Pt ( $I = 1/2$ , 34% abundance) satellites with characteristic  $J(^{195}\text{Pt}, ^1\text{H})$  values for the  $\text{CH}_2\text{NMe}_2$  substituents coordinated to Pt(II). For the platinum(II) complexes **1a–c**<sup>10</sup> these values fall in the ranges 38–40 Hz ( $\text{NMe}_2$ ) and 46–52 Hz ( $\text{NCH}_2$ ), whereas for the platinum(IV) complexes  $[\text{PtX}_3(\text{C}_6\text{H}_3(\text{CH}_2\text{NMe}_2)_{2-o,o'})]$ <sup>9</sup> this range is 29–32 Hz ( $\text{NMe}_2$ ) and 30–34 Hz ( $\text{NCH}_2$ ), respectively.

In general the multiplicity and number of the <sup>1</sup>H NMR signals of the  $\text{CH}_2$  and  $\text{NMe}_2$  groups in the spectra of metal complexes with the terdentate ligand  $\text{NCN}'$  can give information about the symmetry of the metal center and the surrounding groupings (see ref 10).

For example, the square-planar platinum(II) complexes **1a–c** show in the <sup>1</sup>H NMR spectra a pattern of singlets for the  $\text{CH}_2$  H and  $\text{NMe}_2$  Me groups, respectively, because of the presence of an apparent molecular symmetry plane in the molecule, which coincides with the Pt coordination plane. The latter plane is absent in square-pyramidal complexes with the  $\text{NCN}'$  ligand which then results in diastereotopic  $\text{CH}_2$  and  $\text{NMe}_2$  groupings. This will be reflected in the <sup>1</sup>H NMR spectra of these compounds as an AB pattern for the  $\text{CH}_2$  H and two singlets for the  $\text{NMe}_2$  Me groups, respectively.

In the spectra of square-pyramidal (see also IR) **2a–c** this complex pattern is not found. Low-temperature measurements (195 K, toluene- $d_8$ ) gave an <sup>1</sup>H NMR spectrum with an analogous pattern as was found in the spectra at room temperature. A possible explanation might be the fact that the <sup>1</sup>H NMR spectra were measured in  $\text{SO}_2$ -saturated  $\text{CDCl}_3$  solutions. As a result a second  $\text{SO}_2$  molecule can attack the remaining coordination site of the platinum center and eventually result in dissociation of the initially coordinated  $\text{SO}_2$  molecule (and vice versa). If this process in solution is rapid on NMR time scale (assuming that the N–Pt bonds are inert on the NMR time scale), an apparent molecular symmetry plane coinciding with the  $\text{NCN}'\text{Pt}$  system is created, thereby rendering the diastereotopic groupings (in the five-coordinate structures) enantiotopic; i.e., singlet resonances will be observed for both the  $\text{CH}_2$  H and the  $\text{NMe}_2$  Me groups (routes 2 and 3 in Scheme I).

An <sup>1</sup>H NMR spectrum of **2b** in pure  $\text{CDCl}_3$  (thus without using an excess of  $\text{SO}_2$ ) shows a pattern which has been

(21) (a) Tiethof, J. A.; Peterson, J. L.; Meek, D. W. *Inorg. Chem.* **1976**, *15*, 1365. (b) Blum, P. R.; Meek, D. W. *Inorg. Chim. Acta* **1977**, *24*, L75.

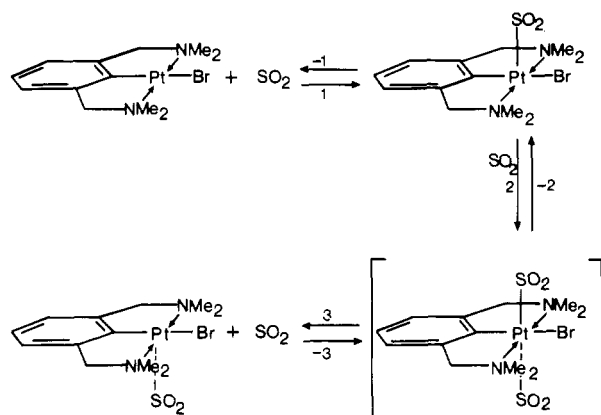
(22) A short communication has already been published about these bridging complexes containing a hydrogen, halogen, or cyanide group as bridging ligand: Grove, D. M.; van Koten, G.; Ubbels, H. J. C.; Spek, A. L. *J. Am. Chem. Soc.* **1982**, *104*, 4285.

Table IV. Electronic Absorption Data of [MX(C<sub>6</sub>H<sub>3</sub>(CH<sub>2</sub>NMe<sub>2</sub>)<sub>2</sub>-o,o')(η<sup>1</sup>-SO<sub>2</sub>)] and [MX(C<sub>6</sub>H<sub>3</sub>(CH<sub>2</sub>NMe<sub>2</sub>)<sub>2</sub>-o,o')]<sup>c</sup>

compd	λ <sub>max</sub> , nm			compound	λ <sub>max</sub> , nm	ε <sub>max</sub>
[PtCl(C <sub>6</sub> H <sub>3</sub> (CH <sub>2</sub> NMe <sub>2</sub> ) <sub>2</sub> -o,o')(η <sup>1</sup> -SO <sub>2</sub> )]	326	352	411 sh	[PtCl(C <sub>6</sub> H <sub>3</sub> (CH <sub>2</sub> NMe <sub>2</sub> ) <sub>2</sub> -o,o')]	279	9701
[PtBr(C <sub>6</sub> H <sub>3</sub> (CH <sub>2</sub> NMe <sub>2</sub> ) <sub>2</sub> -o,o')(η <sup>1</sup> -SO <sub>2</sub> )]	327	362	410 sh	[PtBr(C <sub>6</sub> H <sub>3</sub> (CH <sub>2</sub> NMe <sub>2</sub> ) <sub>2</sub> -o,o')]	280	9770
[PtI(C <sub>6</sub> H <sub>3</sub> (CH <sub>2</sub> NMe <sub>2</sub> ) <sub>2</sub> -o,o')(η <sup>1</sup> -SO <sub>2</sub> )]	324	365	410 sh	[PtI(C <sub>6</sub> H <sub>3</sub> (CH <sub>2</sub> NMe <sub>2</sub> ) <sub>2</sub> -o,o')]	290	12823
[NiCl(C <sub>6</sub> H <sub>3</sub> (CH <sub>2</sub> NMe <sub>2</sub> ) <sub>2</sub> -o,o')(η <sup>1</sup> -SO <sub>2</sub> )]	323		440	[NiCl(C <sub>6</sub> H <sub>3</sub> (CH <sub>2</sub> NMe <sub>2</sub> ) <sub>2</sub> -o,o')]	308	4383
[NiBr(C <sub>6</sub> H <sub>3</sub> (CH <sub>2</sub> NMe <sub>2</sub> ) <sub>2</sub> -o,o')(η <sup>1</sup> -SO <sub>2</sub> )]	326		444	[NiBr(C <sub>6</sub> H <sub>3</sub> (CH <sub>2</sub> NMe <sub>2</sub> ) <sub>2</sub> -o,o')]	308	c
[NiI(C <sub>6</sub> H <sub>3</sub> (CH <sub>2</sub> NMe <sub>2</sub> ) <sub>2</sub> -o,o')(η <sup>1</sup> -SO <sub>2</sub> )]	324	364	445	[NiI(C <sub>6</sub> H <sub>3</sub> (CH <sub>2</sub> NMe <sub>2</sub> ) <sub>2</sub> -o,o')]	282	16285
[Pt <sub>2</sub> (P <sub>2</sub> O <sub>5</sub> H <sub>2</sub> ) <sub>4</sub> (SO <sub>2</sub> ) <sub>2</sub> ] <sup>14-b</sup>			428			

<sup>a</sup> Measured in saturated CH<sub>2</sub>Cl<sub>2</sub> solution (0.1 M); see also ref 24 for the estimated ε<sub>max</sub> values of 2a-f. <sup>b</sup> Measured in H<sub>2</sub>O. <sup>c</sup> Not determined.

### Scheme I. Proposed Dissociation-Association Process for the Five-Coordinate [PtX(C<sub>6</sub>H<sub>3</sub>(CH<sub>2</sub>NMe<sub>2</sub>)<sub>2</sub>-o,o')(η<sup>1</sup>-SO<sub>2</sub>)] Complexes



identified as a mixture of **1b** and the SO<sub>2</sub> complex **2b**. This indicates the existence of equilibrium 1 shown in Scheme I. The spectrum of **2b** again fails to reflect the expected diastereotopicity of the NMe<sub>2</sub> and CH<sub>2</sub> groupings for a square-pyramidal structure. Accordingly, the observation that **1b** and **2b** can be seen separately shows that the process involving exchange between the five- and four-coordinate species (routes 1 and -1) is slow on the NMR time scale and that the process which involves attack of **2b** by the dissociated free SO<sub>2</sub> (route 2) is fast on the NMR time scale even at low temperatures.

In the <sup>1</sup>H NMR spectra of the nickel(II) sulfur dioxide complexes broad signals were found from which it was not possible to obtain accurate data.<sup>23</sup>

The <sup>1</sup>H NMR data of the bis(platinum(II)) sulfato complexes **3** show singlets for the NCH<sub>2</sub> and NMe<sub>2</sub> groups at 4.00 and 3.13 ppm, respectively, both with platinum satellites (*J*(<sup>195</sup>Pt,<sup>1</sup>H) = 46 and 38 Hz) as well as a multiplet at 6.8 ppm for the aryl protons. These observations are in accord with the proposed dimeric structure for **3**.

**Electronic Absorption Spectra.** The electronic absorption data of the starting complexes **1a-f** and their SO<sub>2</sub> products **2a-f** as recorded in SO<sub>2</sub>-saturated CH<sub>2</sub>Cl<sub>2</sub> (0.1 M) solution are presented in Table IV (see ref 24).

For complexes **1a-f** a strong absorption band is observed between 270 and 310 nm. Above 310 nm only weak absorption bands are found for **1a-f** which are assigned to d-d transitions (note that the platinum complexes are white while the nickel complexes are orange or red brown). Below 220 nm the solvent starts to absorb. The electronic

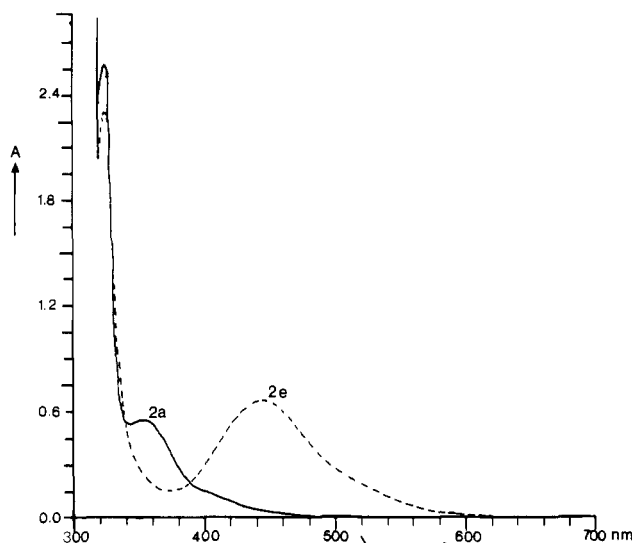


Figure 3. UV/visible spectra of **2a** and **2e** in CH<sub>2</sub>Cl<sub>2</sub>. Both solutions were saturated with SO<sub>2</sub>.

absorption spectra of the platinum(II) and nickel(II) sulfur dioxide complexes **2a-f** show new bands in the region 300–500 nm<sup>24</sup> (see also Figure 3). The bands at 324 and 362 nm undergo no significant changes upon varying the metal or halogen and belong to the free dissolved SO<sub>2</sub> chromophore. A noticeable change for the new absorption band at 410 nm in the spectra of the platinum complexes **2a-c** was found on going from platinum to nickel. In the spectra of **2e,f** this band was found at 444 nm, which is the expected shift for a M(II)-to-SO<sub>2</sub> MLCT transition going from Pt(II) to Ni(II).<sup>25</sup> This MLCT character is confirmed by the appearance of a strong resonance Raman effect for ν<sub>s</sub>(SO<sub>2</sub>) upon excitation into this band (vide supra). Furthermore the absorption bands of **2a-c** agree with the absorption band found for the platinum(II) adduct [Pt<sub>2</sub>(P<sub>2</sub>O<sub>5</sub>H<sub>2</sub>)<sub>4</sub>(η<sup>1</sup>-SO<sub>2</sub>)<sub>2</sub>]<sup>14-</sup> (428.5 nm (ε<sub>max</sub> 41 000)).

**Molecular Geometry of [(PtBr(C<sub>6</sub>H<sub>3</sub>(CH<sub>2</sub>NMe<sub>2</sub>)<sub>2</sub>-o,o')(η<sup>1</sup>-SO<sub>2</sub>)] (**2b**).** Figure 4a gives the adopted numbering scheme. Thermal vibrational ellipsoids are shown in an ORTEP drawing (Figure 4c, supplementary material).

The crystal data and details of the data collection and structure refinement are summarized in Table I. Relevant bond distances and bond angles are listed in Table V. The five-coordinate platinum compound has a square-pyramidal structure with the terdentate ligand NCN' donor sites and the Br at the basal positions and the SO<sub>2</sub> ligand bonded via sulfur at the apex of the square pyramid. The principal distortion from the latter square-pyramidal geometry arises from the small N-Pt-C(1) bite angles of the two five-membered chelate rings (81.7 (5)° and 82.9 (5)°,

(23) The broad signals in the NMR spectra of the nickel compounds are due to small impurities of paramagnetic Ni(III) species; see ref 15.

(24) Accurate ε<sub>max</sub> values for **2a-f** could not be obtained because of the interference of the bands of the compounds and the tail of the band of free SO<sub>2</sub>. Assuming a 100% product formation, we found for the absorption bands at 441 nm [ε<sub>max</sub> = 2566 (**2a**)], 410 nm [ε<sub>max</sub> = 2330 (**2b**)], 440 nm [ε<sub>max</sub> = 7661 (**2d**)], 444 nm [ε<sub>max</sub> = 3550 (**2e**)], and 445 nm [ε<sub>max</sub> = 4109 (**2f**)].

(25) See: Gray, H. B. In "Transition Metal Chemistry"; Marcel Dekker: New York, 1965; Vol. 1, pp 240–287.

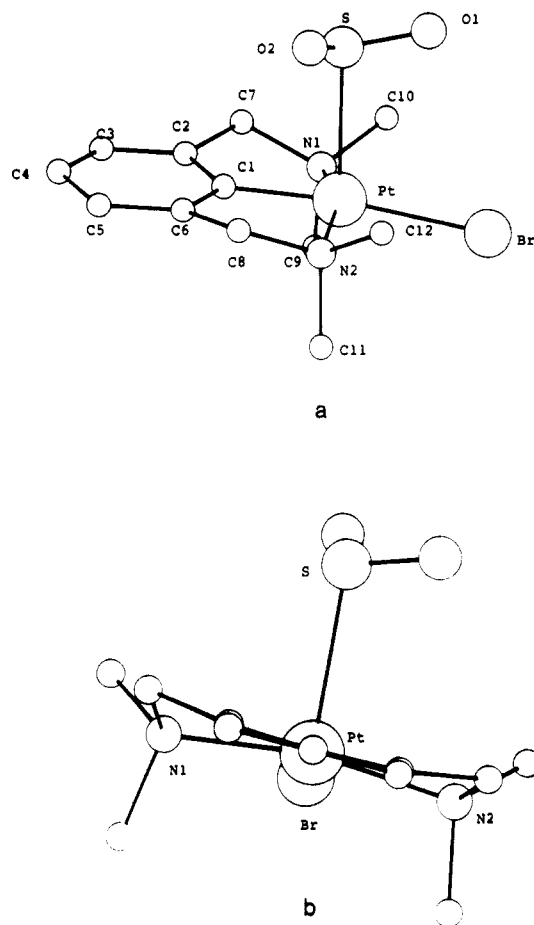


**Figure 4.** a. Pluto drawing of the molecular structure of  $[\text{PtBr}(\text{C}_6\text{H}_3(\text{CH}_2\text{NMe}_2)_2\text{-}o,o')(\eta^1\text{-SO}_2)]$  along with the adopted numbering scheme. b. Projection along the Pt-C(1) axis showing the puckering of the five-membered cyclometalated rings and the conformation of the Pt-SO<sub>2</sub> part of the molecule.

respectively). Another feature is that the Pt center lies ca. 0.18 Å above the approximate plane formed by the basal ligands. This distance is shorter than that found in other square-pyramidal complexes, viz., 0.26 Å for Rh in  $[\text{RhCl}(\eta^1\text{-SO}_2)(\text{tpp})]$ ,<sup>26</sup> but larger than that found in  $[\text{PtBr}(\text{C}_6\text{H}_3(\text{CH}_2\text{NMe}_2)_2\text{-}o,o')(\mu\text{-}(p\text{-tolyl})\text{NC}(\text{H})\text{N}(\text{isopropyl})\text{HgBrCl})]$  (0.09 Å).<sup>27</sup>

The puckering in the two neighboring five-membered chelate rings that has been observed in complexes of the terdentate ligand *NCN'* may be of either the mirror plane or the twofold axis symmetry variety. Examples of the latter type are found in square-planar  $[\text{NiO}_2\text{CH}(\text{C}_6\text{H}_3(\text{CH}_2\text{NMe}_2)_2\text{-}o,o')]$ <sup>15</sup> or octahedral  $[\text{PtCl}_3(\text{C}_6\text{H}_3(\text{CH}_2\text{NMe}_2)_2\text{-}o,o')]$ <sup>9</sup> structures, whereas the square-pyramidal complexes, i.e., the present compound (see Figure 4b) as well as the Pt<sup>II</sup>Hg complex (vide supra) are examples of the former symmetry variety. A characteristic difference of these two possible structures is the position of the two NMe<sub>2</sub> methyl groups with respect to the *NCN'* plane. The structure of **2b** (see Figure 4b) shows that the mirror plane variety results in two axially positioned methyl groups at different N centers opposite the apical ligand.

The Pt-C and Pt-N bond lengths are similar to the corresponding bond lengths found in the square-pyramidal Pt<sup>II</sup>Hg complex, viz. Pt-C(1) = 1.96 (1) vs. 1.91 (1) Å as well as Pt-N(1) = 2.09 (1) and Pt-N(2) = 2.10 (1) vs. 2.097 (9) and 2.08 (1) Å, respectively.

**Table V. Interatomic Distances (Å) and Bond Angles (deg)<sup>a</sup>**

a. Bond Lengths			
Pt-Br	2.522 (7)	C(6)-C(8)	1.54 (2)
Pt-N(1)	2.09 (1)	C(7)-N(1)	1.54 (1)
Pt-N(2)	2.10 (1)	C(8)-N(2)	1.53 (2)
Pt-C(1)	1.96 (1)	C(9)-N(1)	1.52 (2)
C(1)-C(2)	1.37 (2)	C(10)-N(1)	1.50 (2)
C(2)-C(6)	1.40 (2)	C(11)-N(2)	1.53 (2)
C(2)-C(3)	1.39 (2)	C(12)-N(2)	1.48 (3)
C(2)-C(7)	1.52 (2)	Pt-S	2.613 (7)
C(3)-C(4)	1.39 (2)	S-O(1)	1.47 (1)
C(4)-C(5)	1.41 (2)	S-O(2)	1.42 (2)
C(5)-C(6)	1.40 (2)		
b. Bond Angles			
Br-Pt-N(1)	97.4 (2)	C(2)-C(1)-C(6)	124 (1)
Br-Pt-N(2)	96.6 (3)	C(1)-C(2)-C(3)	118 (1)
Br-Pt-C(1)	173.3 (4)	C(1)-C(2)-C(7)	115 (9)
N(1)-Pt-N(2)	160.4 (5)	C(3)-C(2)-C(7)	127 (1)
N(1)-Pt-C(1)	81.7 (5)	C(2)-C(3)-C(4)	120 (1)
N(2)-Pt-C(1)	82.8 (5)	C(3)-C(4)-C(5)	121 (1)
Pt-N(1)-C(7)	108.7 (7)	C(4)-C(5)-C(6)	119 (1)
Pt-N(1)-C(9)	105.6 (9)	C(1)-C(6)-C(5)	118 (1)
Pt-N(1)-C(10)	116.6 (8)	C(1)-C(6)-C(8)	115 (1)
C(7)-N(1)-C(9)	108 (1)	C(5)-C(6)-C(8)	127 (1)
C(7)-N(1)-C(10)	110 (1)	N(1)-C(7)-C(2)	108 (1)
C(9)-N(1)-C(10)	108 (1)	N(2)-C(8)-C(6)	109 (1)
Pt-N(2)-C(8)	110 (1)	C(1)-Pt-S	84.5 (5)
Pt-N(2)-C(11)	107 (1)	N(1)-Pt-S	92.2 (3)
Pt-N(2)-C(12)	116 (1)	N(2)-Pt-S	98.2 (4)
C(8)-N(2)-C(11)	107 (1)	Br-Pt-S	102.2 (2)
C(8)-N(2)-C(12)	109 (1)	O(1)-S-O(2)	114 (1)
Pt-C(1)-C(2)	119 (1)	Pt-S-O(1)	101 (2)
Pt-C(1)-C(6)	118 (1)	Pt-S-O(2)	104.6 (8)

<sup>a</sup> Estimated standard deviations between parentheses.

The Pt-SO<sub>2</sub> geometry is typical<sup>1-3</sup> for  $\eta^1$ -pyramidal SO<sub>2</sub> bonding in a square-pyramidal structure. The bond angles around sulfur are close to the tetrahedral values. The Pt-S vector makes an angle of 114° with the SO<sub>2</sub> plane which affords a good bonding interaction between the filled Pt(d<sub>2</sub>) orbital and the low-lying SO<sub>2</sub> orbital of 2b<sub>1</sub> type, leading to the observed rehybridization of the sulfur center to sp<sup>3</sup>.

A noticeable feature of **2b** is the long Pt-S bond of 2.604 (5) Å, which is much longer than other M-S distances reported for  $\eta^1$ -pyramidal {M(SO<sub>2</sub>)<sup>8</sup>} complexes, viz., 2.48 (8) Å in IrCl(CO)(PPh<sub>3</sub>)<sub>2</sub>(SO<sub>2</sub>)<sup>17</sup> and 2.326 (5) Å in Rh(ttp)(SO<sub>2</sub>) containing the terdentate neutral ttp ligand.<sup>26</sup>

This long Pt-SO<sub>2</sub> distance, which to our knowledge is the longest M-SO<sub>2</sub> distance observed so far, is in agreement with the reversibility of the SO<sub>2</sub> binding in **2**. Furthermore, the  $\nu(\text{SO})$  frequencies of **2a-f** (vide supra) are higher than those observed for related {M(SO<sub>2</sub>)<sup>8</sup>} (M = Rh(I) and Ir(I)) complexes,<sup>1</sup> which points also to a weaker M-SO<sub>2</sub> donation. It must be noted that the basicity of the platinum(II) center in square-planar platinum(II) complexes PtX<sub>2</sub>L<sub>2</sub> generally is too low to give rise to stable five-coordinate PtX<sub>2</sub>L<sub>2</sub>(SO<sub>2</sub>) complexes (see Introduction). The observation that in the case of the platinum compounds **2a-c** as well as for the nickel complexes **2d-f** stable SO<sub>2</sub> complexes could be isolated points to an enhanced basicity of these metal d<sup>8</sup> centers as a result of the presence of exclusively hard donor ligands in the monoanionic terdentate *NCN'* ligand. The basal  $\sigma$ -donor ligands in **2** all have electron-releasing character, i.e., the two trans positioned N donor atoms and to a lesser extent Br and aryl also, which causes enhanced nucleophilic character of the metal d<sup>8</sup> center through its filled d<sub>2</sub> orbital. Accordingly, the metal-to-SO<sub>2</sub> donation, which is the important binding factor for  $\eta^1$ -bound SO<sub>2</sub>,<sup>1</sup> is enhanced. Interestingly, the only other stable Pt<sup>II</sup>SO<sub>2</sub> compound reported has likewise a combination of hard N and C donors bound to

(26) Eller, P. G.; Ryan, R. R. *Inorg. Chem.* 1980, 19, 142.

(27) van der Ploeg, A. F. M. J.; van Koten, G.; Vrieze, K.; Spek, A. L.; Duisenberg A. J. M. *Organometallics* 1982, 1, 1066.

the Pt(II) center (see Introduction).

That the NiSO<sub>2</sub> bonds in the Ni complexes **2d-f** are less stable can be explained by a lower basicity of the Ni d<sub>2</sub><sup>2</sup> orbital in **1d-f** as compared with that of the Pt d<sub>2</sub><sup>2</sup> orbital in the analogous complexes **1a-c**. This view seems to be substantiated by the observation that complexes **1a-c** have a high-energy d<sub>2</sub><sup>2</sup> orbital in the photoelectron spectra (IP = 8.05 eV) which is not present in the spectra of the corresponding nickel complexes **1d-f**.<sup>28</sup>

The orientation of the SO<sub>2</sub> ligand is noteworthy because it has been demonstrated that the relative position of the SO<sub>2</sub> nuclei and ligands in the basal plane is related to the MSO<sub>2</sub> bonding interactions in the complex.<sup>26</sup> The S-O(1)

and S-O(2) bonds of 1.47 (1) and 1.42 (2) Å are positioned above the Pt-Br and Pt-N(1) bond, respectively, an arrangement which so far has not been observed in other {MSO<sub>2</sub>}<sup>8</sup> complexes.

**Acknowledgment.** Thanks are due to Professor K. Vrieze for his interest in this work.

**Registry No.** **1a**, 82112-96-7; **1b**, 67507-09-9; **1c**, 82112-97-8; **1d**, 84500-92-5; **1e**, 84500-93-6; **1f**, 84500-94-7; **2a**, 100228-95-3; **2b**, 100228-96-4; **2c**, 100228-97-5; **2d**, 100228-98-6; **2e**, 100228-99-7; **2f**, 100229-00-3; **3**, 100229-01-4.

**Supplementary Material Available:** Listings of observed and calculated structure factors, thermal parameters, fractional coordinates, and bond distances and angles for C<sub>12</sub>H<sub>19</sub>N<sub>2</sub>PtBrSO<sub>2</sub> (**2b**) as well as an ORTEP drawing (Figure 4c) (16 pages). Ordering information is given on any current masthead page.

(28) Louwen, J. N.; Grove, D. M.; Ubbels, H. J. C.; Stufkens, D. J.; Oskam, A. Z. *Naturforsch., B: Struct. Sci.* 1983, 388, 85.

## Preparation and Crystal Structure Determination of the Indium Methylene Complexes Cl<sub>2</sub>InCH<sub>2</sub>InCl<sub>2</sub>·2tmen and Cl(Br)InCH<sub>2</sub>InCl<sub>2</sub>·2tmen (tmen = N,N,N',N'-Tetramethylethanediamine)

Masood A. Khan, Clovis Peppe, and Dennis G. Tuck\*

Department of Chemistry, University of Windsor, Windsor, Ontario, Canada N9B 3P4

Received July 1, 1985

The reaction of InCl<sub>3</sub> with InX (X = Cl, Br, I) in a dichloromethane/toluene/*N,N,N',N'*-tetramethylethanediamine (tmen) mixture yields the bis(tmen) adducts of Cl(X)InCH<sub>2</sub>InCl<sub>2</sub>. X-ray crystallography of compounds with X = Cl and Br has shown that these are the first examples of diindium methylene structures, with an average In-C-In angle of 117.6°. For Cl<sub>2</sub>InCH<sub>2</sub>InCl<sub>2</sub>·2tmen: cell constants *a* = 7.782 (1) Å, *b* = 21.192 (3) Å, *c* = 14.366 (3) Å; space group *Pccn*; *R* = 0.021, *R*<sub>w</sub> = 0.021. For Cl(Br)InCH<sub>2</sub>InCl<sub>2</sub>·2tmen: cell constants *a* = 7.849 (2) Å, *b* = 21.205 (3) Å, *c* = 14.374 (4) Å; space group *Pccn*; *R* = 0.024, *R*<sub>w</sub> = 0.027. The structural results are compared with those for other organoindium species, and the mechanism of the formation of these compounds is discussed in terms of the available preparative and spectroscopic evidence.

### Introduction

The indium(I) halides (InX, X = Cl, Br, I) are insoluble and intractable materials, rarely used in synthetic chemistry, but we have recently shown<sup>1</sup> that these compounds have an appreciable solubility in mixtures of an aromatic solvent and a neutral base such as *N,N,N',N'*-tetramethylethanediamine (tmen). The resultant solutions are stable below ca. -20 °C but react with a variety of organic and inorganic substrates as the temperature approaches ambient. Some of the synthetic applications of these systems have been discussed elsewhere.<sup>1-3</sup> The present investigation represents a development of this work and of concomitant studies of the synthesis of neutral adducts of In<sub>2</sub>X<sub>4</sub> and In<sub>2</sub>X<sub>3</sub>Y via the reaction of InX with InX<sub>3</sub> or InY<sub>3</sub> species (Y = Br, I),<sup>3-5</sup> since we have now been able

to prepare adducts of the indium methylene complexes Cl<sub>2</sub>InCH<sub>2</sub>InCl<sub>2</sub> and Cl(Br)InCH<sub>2</sub>InCl<sub>2</sub>. The results of spectroscopic and crystal structure studies are also reported.

### Experimental Section

The preparation of InX and InX<sub>3</sub> and the general experimental, analytical, and spectroscopic methods, were as described in previous papers.<sup>2,3</sup>

**Reaction of InX with CH<sub>2</sub>X<sub>2</sub> (X = Cl, Br).** (i) InCl-CH<sub>2</sub>Cl<sub>2</sub>·tmen. InCl (0.78 g, 5.21 mmol) was suspended in 20 mL of dichloromethane at ca. -80 °C, 2 mL of tmen added, and the mixture stirred. The cold bath was removed slowly until room temperature was reached (time of reaction 6-7 h), during which the deep red solution which initially formed at -80 °C gradually gave way to a clear colorless solution at ca. 25 °C; if the cold bath were removed too quickly, indium metal deposited. Any solid impurities were removed at this point by filtration. All the volatile components of the solution phase were then removed by pumping in vacuo, and the white solid so obtained was washed thoroughly with Et<sub>2</sub>O and dried under vacuum; Yield 1.8 g (84%), based on

(1) Peppe, C.; Tuck, D. G.; Victoriano, L. *J. Chem. Soc., Dalton Trans.* 1982, 2165.

(2) Peppe, C.; Tuck, D. G. *Can. J. Chem.* 1984, 62, 2793.

(3) Peppe, C.; Tuck, D. G. *Can. J. Chem.* 1984, 62, 2798.

(4) Taylor, M. J.; Tuck, D. G.; Victoriano, L. *Can. J. Chem.* 1982, 60, 691.

(5) Khan, M. A.; Peppe, C.; Tuck, D. G. *Can. J. Chem.* 1984, 62, 601.

the Pt(II) center (see Introduction).

That the NiSO<sub>2</sub> bonds in the Ni complexes **2d-f** are less stable can be explained by a lower basicity of the Ni d<sub>2</sub><sup>2</sup> orbital in **1d-f** as compared with that of the Pt d<sub>2</sub><sup>2</sup> orbital in the analogous complexes **1a-c**. This view seems to be substantiated by the observation that complexes **1a-c** have a high-energy d<sub>2</sub><sup>2</sup> orbital in the photoelectron spectra (IP = 8.05 eV) which is not present in the spectra of the corresponding nickel complexes **1d-f**.<sup>28</sup>

The orientation of the SO<sub>2</sub> ligand is noteworthy because it has been demonstrated that the relative position of the SO<sub>2</sub> nuclei and ligands in the basal plane is related to the MSO<sub>2</sub> bonding interactions in the complex.<sup>26</sup> The S-O(1)

and S-O(2) bonds of 1.47 (1) and 1.42 (2) Å are positioned above the Pt-Br and Pt-N(1) bond, respectively, an arrangement which so far has not been observed in other {MSO<sub>2</sub>}<sup>8</sup> complexes.

**Acknowledgment.** Thanks are due to Professor K. Vrieze for his interest in this work.

**Registry No.** **1a**, 82112-96-7; **1b**, 67507-09-9; **1c**, 82112-97-8; **1d**, 84500-92-5; **1e**, 84500-93-6; **1f**, 84500-94-7; **2a**, 100228-95-3; **2b**, 100228-96-4; **2c**, 100228-97-5; **2d**, 100228-98-6; **2e**, 100228-99-7; **2f**, 100229-00-3; **3**, 100229-01-4.

**Supplementary Material Available:** Listings of observed and calculated structure factors, thermal parameters, fractional coordinates, and bond distances and angles for C<sub>12</sub>H<sub>19</sub>N<sub>2</sub>PtBrSO<sub>2</sub> (**2b**) as well as an ORTEP drawing (Figure 4c) (16 pages). Ordering information is given on any current masthead page.

(28) Louwen, J. N.; Grove, D. M.; Ubbels, H. J. C.; Stufkens, D. J.; Oskam, A. Z. *Naturforsch., B: Struct. Sci.* 1983, 388, 85.

## Preparation and Crystal Structure Determination of the Indium Methylene Complexes Cl<sub>2</sub>InCH<sub>2</sub>InCl<sub>2</sub>·2tmen and Cl(Br)InCH<sub>2</sub>InCl<sub>2</sub>·2tmen (tmen = N,N,N',N'-Tetramethylethanediamine)

Masood A. Khan, Clovis Peppe, and Dennis G. Tuck\*

Department of Chemistry, University of Windsor, Windsor, Ontario, Canada N9B 3P4

Received July 1, 1985

The reaction of InCl<sub>3</sub> with InX (X = Cl, Br, I) in a dichloromethane/toluene/*N,N,N',N'*-tetramethylethanediamine (tmen) mixture yields the bis(tmen) adducts of Cl(X)InCH<sub>2</sub>InCl<sub>2</sub>. X-ray crystallography of compounds with X = Cl and Br has shown that these are the first examples of diindium methylene structures, with an average In-C-In angle of 117.6°. For Cl<sub>2</sub>InCH<sub>2</sub>InCl<sub>2</sub>·2tmen: cell constants *a* = 7.782 (1) Å, *b* = 21.192 (3) Å, *c* = 14.366 (3) Å; space group *Pccn*; *R* = 0.021, *R*<sub>w</sub> = 0.021. For Cl(Br)InCH<sub>2</sub>InCl<sub>2</sub>·2tmen: cell constants *a* = 7.849 (2) Å, *b* = 21.205 (3) Å, *c* = 14.374 (4) Å; space group *Pccn*; *R* = 0.024, *R*<sub>w</sub> = 0.027. The structural results are compared with those for other organoindium species, and the mechanism of the formation of these compounds is discussed in terms of the available preparative and spectroscopic evidence.

### Introduction

The indium(I) halides (InX, X = Cl, Br, I) are insoluble and intractable materials, rarely used in synthetic chemistry, but we have recently shown<sup>1</sup> that these compounds have an appreciable solubility in mixtures of an aromatic solvent and a neutral base such as *N,N,N',N'*-tetramethylethanediamine (tmen). The resultant solutions are stable below ca. -20 °C but react with a variety of organic and inorganic substrates as the temperature approaches ambient. Some of the synthetic applications of these systems have been discussed elsewhere.<sup>1-3</sup> The present investigation represents a development of this work and of concomitant studies of the synthesis of neutral adducts of In<sub>2</sub>X<sub>4</sub> and In<sub>2</sub>X<sub>3</sub>Y via the reaction of InX with InX<sub>3</sub> or InY<sub>3</sub> species (Y = Br, I),<sup>3-5</sup> since we have now been able

to prepare adducts of the indium methylene complexes Cl<sub>2</sub>InCH<sub>2</sub>InCl<sub>2</sub> and Cl(Br)InCH<sub>2</sub>InCl<sub>2</sub>. The results of spectroscopic and crystal structure studies are also reported.

### Experimental Section

The preparation of InX and InX<sub>3</sub> and the general experimental, analytical, and spectroscopic methods, were as described in previous papers.<sup>2,3</sup>

**Reaction of InX with CH<sub>2</sub>X<sub>2</sub> (X = Cl, Br).** (i) InCl·CH<sub>2</sub>Cl<sub>2</sub>·tmen. InCl (0.78 g, 5.21 mmol) was suspended in 20 mL of dichloromethane at ca. -80 °C, 2 mL of tmen added, and the mixture stirred. The cold bath was removed slowly until room temperature was reached (time of reaction 6-7 h), during which the deep red solution which initially formed at -80 °C gradually gave way to a clear colorless solution at ca. 25 °C; if the cold bath were removed too quickly, indium metal deposited. Any solid impurities were removed at this point by filtration. All the volatile components of the solution phase were then removed by pumping in vacuo, and the white solid so obtained was washed thoroughly with Et<sub>2</sub>O and dried under vacuum; Yield 1.8 g (84%), based on

(1) Peppe, C.; Tuck, D. G.; Victoriano, L. *J. Chem. Soc., Dalton Trans.* 1982, 2165.

(2) Peppe, C.; Tuck, D. G. *Can. J. Chem.* 1984, 62, 2793.

(3) Peppe, C.; Tuck, D. G. *Can. J. Chem.* 1984, 62, 2798.

(4) Taylor, M. J.; Tuck, D. G.; Victoriano, L. *Can. J. Chem.* 1982, 60, 691.

(5) Khan, M. A.; Peppe, C.; Tuck, D. G. *Can. J. Chem.* 1984, 62, 601.

the initial amount of InCl. (Anal. Calcd for  $\text{Cl}_2\text{InCH}_2\text{Cl}\cdot 1.5\text{tmen}$ : In, 28.1; Cl, 26.0. Found: In, 27.9; Cl, 24.6).

Under the same conditions, reactions involving pyridine, triethylamine, or  $\text{Me}_2\text{SO}$  gave indium metal as the result of disproportionation of the InCl species in solution (cf. ref 1).

(ii) **InBr- $\text{CH}_2\text{Br}_2\cdot\text{Me}_2\text{SO}$ .** A suspension of InBr (1.25 g, 6.4 mmol) in 10 mL of  $\text{CH}_2\text{Br}_2$  was frozen to ca.  $-80^\circ\text{C}$ , 1.5 mL of  $\text{Me}_2\text{SO}$  added and the cold bath gradually removed. The suspension was stirred as soon as the melting of the solvent allowed and the stirring continued until the bath reached room temperature. At this point small quantities of indium metal were observed, but this redissolved on further stirring over 1 h to give a clear colorless solution. All the volatiles were removed under vacuo to give an oil, which solidified on stirring with petroleum ether. This white solid was collected, washed thoroughly with  $\text{Et}_2\text{O}$ , and dried under vacuo; yield = 2.6 g (99%), based on the initial amount of InBr. (Anal. Calcd for  $\text{Br}_2\text{InCH}_2\text{Br}\cdot 3\text{Me}_2\text{SO}$ : In, 19.1; Br 39.8. Found: In 20.2; Br, 38.2).

Under the same conditions, addition of tmen causes rapid quaternization of the nitrogen ligand by  $\text{CH}_2\text{Br}_2$ , and this system was not investigated further.

**Preparation of  $\text{Cl(X)InCH}_2\text{InCl}_2$  Adducts.** Equimolar amounts of InX and  $\text{InCl}_3$  (5.5–8.0 mmol) were suspended in 50 mL of dichloromethane–toluene (1:1, v/v) at  $-80^\circ\text{C}$  (X = Cl) or  $-20^\circ\text{C}$  (X = Br, I), 3 mL of tmen was added via a hypodermic syringe, and the mixture was stirred. The cold bath was gradually removed to allow the reaction mixture to reach room temperature, after which stirring was maintained for one further hour (total reaction time 3–4 h). The small amount of indium metal deposited in the case of  $\text{InCl}/\text{InCl}_3$  was removed by filtration. The products were isolated from the solution phase by the procedures described below.

**InCl/ $\text{InCl}_3$ :** colorless crystals of  $\text{Cl}_2\text{InCH}_2\text{InCl}_2\cdot 2\text{tmen}$  (1) precipitated spontaneously from solution on standing. The crystals were collected and dried under vacuo; yield 0.35 g (0.57 mmol) from 5.38 mmol of InCl. (Anal. Calcd for  $\text{C}_{13}\text{H}_{34}\text{N}_4\text{In}_2\text{Cl}_4$ : C, 25.26; H, 5.55, N, 9.07, In, 37.2, Cl, 23.0. Found: C, 25.31; H, 5.44; N, 9.11, In, 37.8; Cl, 23.3).

Addition of diethyl ether to the mother liquor yielded 2.0 g of a white powder, whose composition [anal. found: In, 26.8; Cl, 23.5 (Cl: In = 2.7)] suggested that it was a mixture. Recrystallization from dichloromethane gave a further 0.3 g (0.49 mmol) of 1, raising the overall yield to 20%.

A secondary product of this reaction was isolated in a separate experiment using equimolar quantities (5.6 mmol) of InCl and  $\text{InCl}_3$ . Addition of petroleum ether (10 mL) to the clear solution obtained from this reaction resulted in the precipitation of 2.6 g of an unidentified white powder [anal. found: In, 32.0; Cl, 23.1 (Cl: In = 2.33)]. Crystals of a solvated tmen adduct of  $\text{InCl}_3$  precipitated from the filtrate on standing and were identified as  $\text{InCl}_3\cdot 0.67\text{tmen}\cdot 0.67\text{CH}_2\text{Cl}_2$ . (Anal. Calcd: C, 25.66; H, 5.60; N, 9.29, Cl, 23.6. Found: C, 25.65; H, 5.76; N, 9.28, Cl, 23.5.) The values for chlorine do not include any contribution from  $\text{CH}_2\text{Cl}_2$  since this is not measured in the Volhard titrimetric method used).

**InBr/ $\text{InCl}_3$ :** colorless crystals deposited from the solution on standing and were collected and dried in vacuo; yield 2.1 g from 6.2 mmol of InBr, 36% based on the total initial amount of indium. Anal. Found: C, 25.93; H, 5.60; N 10.39; In, 31.2. These results agree reasonably well with the composition  $\text{In}_3\text{Cl}_6\text{Br}(\text{CH}_2)_4\text{tmen}$ . (calcd; C, 26.88; H, 5.91; N, 10.04), as do values for total halogen (calcd, 26.3; found, 26.3), but the product is clearly a mixture since crystals subsequently identified as  $\text{Cl}(\text{Br})\text{InCH}_2\text{InCl}_2\cdot 2\text{tmen}$  were selected for X-ray analysis.

**InI/ $\text{InCl}_3$ :** addition of excess of petroleum ether to the final solution gave a yellow precipitate which was collected and dried under vacuo. Again the analytical results obtained agree with the formulation  $\text{In}_3\text{Cl}_6\text{I}(\text{CH}_2)_4\text{tmen}$  (anal. calcd: In, 29.7; total halogen, 29.2. found: In, 30.0; halogen, 29.8), but we were unable to obtain crystalline material from either petroleum ether or  $\text{CH}_2\text{Cl}_2$ /petroleum ether solutions; yield 5.5 g, from 8.0 mmol of InI, corresponding to 90% of total initial quantity of indium.

**Related Experiments. (i) Attempted Preparation of  $\text{Cl}_2\text{InCH}_2\text{InCl}_2\cdot 2\text{tmen}$  from InCl in Presence of Catalytic Amounts of  $\text{InCl}_3$ .** Indium(I) chloride (0.69 g, 4.6 mmol, and ca. 20 mg of  $\text{InCl}_3$ ) was suspended in 25 mL of  $\text{CH}_2\text{Cl}_2$  at  $-80^\circ\text{C}$ ; tmen (2 mL) was added and the cold bath slowly removed until

the reaction mixture reached room temperature over a period of ca. 2 h. Under these conditions, metallic indium (0.26 g, 2.3 mmol) was thrown out of solution. Subsequent addition of diethyl ether caused the precipitation of 0.14 g of  $\text{Cl}_2\text{InCH}_2\text{InCl}_2\cdot 2\text{tmen}$  (0.23 mmol, 10%) based on the initial quantity of InCl) which was collected and dried.

(ii) **Attempted Preparation of In- $\text{CH}_2$ -In Species from Neutral Adducts of  $\text{In}_2\text{X}_4$  and InX.**  $\text{In}_2\text{Br}_4\cdot 2\text{tmen}$  (0.65 g, 0.83 mmol) and an equimolar amount of InBr were suspended in 50 mL of  $\text{CH}_2\text{Cl}_2$  at  $-80^\circ\text{C}$ , tmen (1 mL) was syringed in, and the cold bath was removed so that the reaction mixture reached room temperature over a period of 2 h, yielding a clear yellow solution. All the volatile materials were removed under vacuo. The  $^1\text{H}$  NMR spectrum of the off-white solid thus obtained showed a singlet at 0.24 ppm, characteristic of the In- $\text{CH}_2$ -In unit (see below), in addition to resonances (2.2–3.5 ppm) assigned to tmen ligand. Attempts to obtain crystalline materials from  $\text{CH}_2\text{Cl}_2$ /diethyl ether mixtures were unsuccessful.

(iii) **Attempted Preparation of Norcarane from InCl/ $\text{CD}_2\text{Cl}_2$ /tmen/Cyclohexene.** The reaction between InCl and cyclohexene in a  $\text{CD}_2\text{Cl}_2$ /tmen phase was monitored by  $^1\text{H}$  NMR spectroscopy for the disappearance of the olefinic resonances of cyclohexene and/or the formation of a cyclopropane ring. In a typical experiment, 20 mg of InCl and equimolar amount of cyclohexene were suspended in 0.5 mL of  $\text{CD}_2\text{Cl}_2$ , the suspension was cooled to ca.  $-80^\circ\text{C}$ , a threefold excess of tmen was added via a syringe, and the temperature was allowed to reach  $25^\circ\text{C}$ . The  $^1\text{H}$  NMR spectrum of the solution so obtained showed no evidence of reaction. Analogous experiments with the solid products from the system  $\text{InX}/\text{CH}_2\text{X}_2$ /ligand (see above) gave similar negative results.

**Crystallographic Measurements.** Crystals of  $\text{Cl}_2\text{InCH}_2\text{InCl}_2\cdot 2\text{tmen}$  (1) and  $\text{Cl}(\text{Br})\text{InCH}_2\text{InCl}_2\cdot 2\text{tmen}$  (2), which are air-stable colorless parallelepipeds, were mounted on glass fibers for crystallographic study (see Table I for details). Data were collected on a Syntex P2<sub>1</sub> diffractometer following the procedure described elsewhere.<sup>6</sup> The following parameters not listed in Table I were the same for both experiments: radiation,  $\text{Mo K}\alpha$  ( $\lambda = 0.71069 \text{ \AA}$ ); number of reflections, and  $2\theta$  range, for cell constant determination, 15 and  $18\text{--}26^\circ$ , respectively;  $2\theta_{\text{max}} = 50^\circ$ ; scan speed =  $2.02\text{--}4.88^\circ \text{ min}^{-1}$ ; background time/scan time = 0.5; scan type and width as noted in ref 6. The intensities of three monitor reflections did not change significantly during data collection. The data were corrected for Lorentz and polarization effects, and analytical absorption corrections were applied. Densities were determined by the flotation method.

The space group *Pccn* (no. 56) was established for both 1 and 2 from the systematic absences ( $0kl, l = 2n + 1$ ;  $h0l, l = 2n + 1$ ;  $hk0, h + k = 2n + 1$ ). The data clearly showed that the two compounds are isostructural, and this was confirmed by the final refinements. Both structures were solved by the heavy-atom method. In each case, the position of the indium atom was obtained from a sharpened Patterson synthesis, and the positions of the other non-hydrogen atoms were identified from subsequent difference Fourier maps. Compound 2 is disordered in all the four sites involving halogen ligand, since the molecule has a crystallographically required  $C_2$  symmetry. Tests based in various models showed that this disorder is similar to that observed in a salt of the  $\text{InBrCl}_3^-$  anion,<sup>7</sup> and the refinement was therefore based on a model halogen atom consisting of 75% Cl and 25% Br. Both structures were refined anisotropically by a full-matrix least-squares method. The hydrogen atom of the methylene bridge (H(7)) was located on the difference map and refined isotropically. In the final cycle, all non-hydrogen atoms were refined anisotropically, H(7) was refined isotropically, and all other hydrogen atoms were included in idealized positions (C–H = 0.95 Å) with the isotropic temperature factor free to refine. The function minimized in the refinement was  $\sum w(|F_o| - |F_c|)^2$  and the final cycles used weights derived from the counting statistics;  $w = [\sigma^2(F) + pF^2]^{-1}$ , with a final value of  $p = 0.01$  in each case. The final refinements gave  $R = 0.021$  and  $R_w = 0.021$  for 1 and  $R = 0.024$

(6) Khan, M. A.; Steevensz, R. C.; Tuck, D. G.; Noltes, J. G.; Corfield, P. W. R. *Inorg. Chem.* **1980**, *19*, 3407.

(7) Khan, M. A.; Tuck, D. G. *Acta Crystallogr., Sect. B: Struct. Sci.* **1982**, *B38*, 803.

Table I. Summary of Crystal Data, Intensity Collection, and Structural Refinement for the Bis(tmen) Adducts of Cl(X)InCH<sub>2</sub>InCl<sub>2</sub> (X = Cl, Br)

	X = Cl (1)	X = Br (2)
cell constants		
<i>a</i> , Å	7.782 (2)	7.849 (2)
<i>b</i> , Å	21.192 (3)	21.205 (3)
<i>c</i> , Å	14.366 (3)	14.374 (4)
cell vol Å <sup>3</sup>	2369.2 (9)	2392.4 (11)
space group	<i>Pccn</i> (no. 56)	<i>Pccn</i>
<i>Z</i>	4	4
<i>M<sub>r</sub></i>	617.9	662.4
$\rho$ (calcd), g cm <sup>-3</sup>	1.732	1.839
$\rho$ (measd), g cm <sup>-3</sup>	1.74	1.83
abs coeff, cm <sup>-1</sup>	22.2	40.2
min/max abs correct	1.094/1.286	1.696/3.626
cryst dimens, mm	0.36 × 0.12 × 0.04	0.40 × 0.31 × 0.12
total reflectns measd ( <i>h, k, ±l</i> )	4862	4865
unique av data ( <i>F<sub>o</sub></i> <sup>2</sup> > 3σ( <i>F<sub>o</sub></i> ) <sup>2</sup> )	1235	1469
no. of parameters ( <i>n</i> )	125	125
$R = \sum   F_o  -  F_c   / \sum  F_o $	0.021	0.024
$R_w = [\sum w( F_o  -  F_c )^2 / \sum w F_o^2]^{1/2}$	0.021	0.027
$S = [\sum (w F_o  -  F_c )^2 / (m - n)]^{1/2}$	1.6	1.5
$\rho_{max}$ , e Å <sup>-3</sup>	0.5	0.4
shift/error (max)	0.1	0.1

Table II. Final Atomic Coordinates for 1 and 2 with Standard Deviations in Parentheses

(a) 1			
	<i>x</i>	<i>y</i>	<i>z</i>
In(1)	0.26081 (1)	0.16351 (1)	0.21731 (1)
Cl(1)	0.0038 (2)	0.1841 (1)	0.3215 (1)
Cl(2)	0.1279 (2)	0.0698 (1)	0.1514 (1)
N(1)	0.4021 (5)	0.1249 (2)	0.3461 (3)
N(2)	0.5418 (5)	0.1249 (2)	0.1545 (3)
C(1)	0.3200 (7)	0.0641 (2)	0.3715 (4)
C(2)	0.3883 (8)	0.1673 (2)	0.4287 (3)
C(3)	0.5860 (6)	0.1148 (3)	0.3242 (4)
C(4)	0.6118 (7)	0.0860 (3)	0.2303 (3)
C(5)	0.6539 (7)	0.1806 (3)	0.1388 (5)
C(6)	0.5340 (9)	0.0878 (3)	0.0687 (4)
C(7)	0.2500 (0)	0.2500 (0)	0.1399 (5)

(b) 2			
	<i>x</i>	<i>y</i>	<i>z</i>
Tn(1)	0.26033 (4)	0.16351 (1)	0.21243 (2)
X(1)	0.0014 (1)	0.1840 (1)	0.3176 (1)
X(2)	0.1257 (1)	0.0676 (0)	0.1445 (1)
N(1)	0.3984 (4)	0.1255 (2)	0.3410 (2)
N(2)	0.5397 (5)	0.1257 (2)	0.1503 (2)
C(1)	0.3201 (7)	0.0646 (2)	0.3667 (4)
C(2)	0.3858 (7)	0.1680 (2)	0.4228 (4)
C(3)	0.5819	0.1158 (3)	0.3193 (3)
C(4)	0.6098 (7)	0.0864 (3)	0.2263 (3)
C(5)	0.6516 (7)	0.1805 (2)	0.1342 (5)
C(6)	0.5348 (8)	0.0880 (3)	0.0644 (4)
C(7)	0.2500 (0)	0.2500 (0)	0.1349 (5)

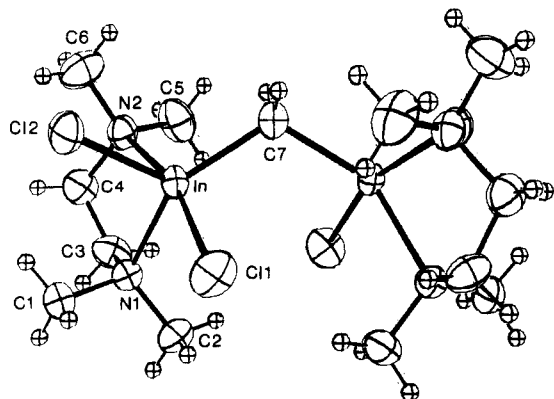


Figure 1. Molecular structure of 1.

Table III. Interatomic Distances (Å) and Angles (deg) for the Bis(tmen) Adducts of Cl(X)InCH<sub>2</sub>InCl<sub>2</sub> (X = Cl, Br)

	X = Cl (1)	X = Br (2)
(a) Interatomic Distances		
In-X(1)	2.536 (1)	2.587 (1)
In-X(2)	2.430 (1)	2.492 (1)
In-X(1)	2.303 (4)	2.288 (3)
In-N(2)	2.503 (4)	2.499 (4)
In-C(7)	2.147 (4)	2.148 (4)
N(1)-C(1)	1.484 (6)	1.477 (6)
N(1)-C(2)	1.492 (6)	1.485 (6)
N(1)-C(3)	1.481 (6)	1.488 (6)
N(2)-C(4)	1.470 (6)	1.479 (6)
N(2)-C(5)	1.485 (6)	1.475 (6)
N(2)-C(6)	1.463 (6)	1.472 (6)
C(3)-C(4)	1.494 (7)	1.492 (7)
C(7)-H(7)	0.89 (5)	0.87 (5)
(b) Angles		
X(1)-In-X(2)	92.0 (1)	91.7 (0)
X(1)-In-N(1)	87.9 (1)	87.9 (1)
X(1)-In-N(2)	163.4 (1)	163.6 (1)
X(1)-In-C(7)	97.3 (1)	97.4 (1)
X(2)-In-N(1)	103.1 (1)	103.3 (1)
X(2)-In-N(2)	88.0 (1)	88.3 (1)
X(2)-In-C(7)	118.6 (2)	118.5 (1)
N(1)-In-N(2)	75.9 (1)	76.1 (1)
In-N(1)-C(1)	107.4 (3)	108.2 (3)
In-N(1)-C(2)	113.0 (3)	113.2 (3)
In-N(1)-C(3)	109.9 (3)	109.8 (3)
In-N(2)-C(4)	103.8 (3)	104.1 (3)
In-N(2)-C(5)	108.0 (3)	109.0 (3)
In-N(2)-C(6)	116.3 (4)	116.8 (3)
C(1)-N(1)-C(2)	107.3 (4)	107.7 (4)
C(1)-N(1)-C(3)	110.1 (4)	109.5 (4)
C(4)-N(2)-C(5)	109.9 (5)	109.8 (4)
C(4)-N(2)-C(6)	109.8 (5)	108.8 (4)
N(1)-C(3)-C(4)	112.4 (5)	112.8 (4)
N(2)-C(4)-C(3)	113.0 (5)	111.8 (4)
In-C(7)-In <sup>a</sup>	117.6 (4)	117.5 (3)
In-C(7)-H(7)	109 (4)	105 (4)

<sup>a</sup> Symmetry equivalent position is 0.5 - *x*, 0.5 - *y*, *z*.

and  $R_w = 0.027$  for 2. The scattering factors, and the programs used in the calculations were those quoted previously.<sup>8</sup>

The atomic coordinates are given in Table II and important interatomic distances and angles in Table III. Figure 1 shows the molecular structure of 1 with the atomic numbering scheme,



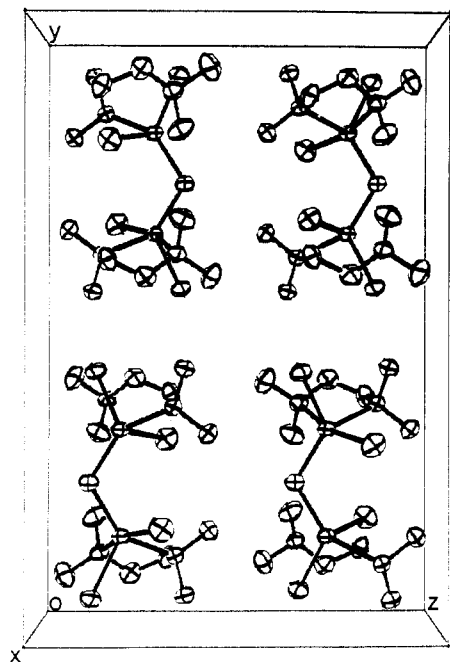


Figure 2. Crystal packing of 1.

and Figure 2 gives the crystal packing. Tables of hydrogen atom coordinates, anisotropic temperature factors, and calculated and observed structure factors have been deposited as supplementary material.

## Results and Discussion

**Crystal Structures.** The structures of compounds 1 and 2 are a convenient starting point for the discussion, in that they provide unambiguous proof that these are the first examples of  $\text{InCH}_2\text{In}$  systems. The local stereochemistry at indium is essentially trigonal bipyramidal, with an  $\text{InX}_2\text{N}_2\text{C}$  kernel in which the equatorial plane formed by In, X(2), N(1), and C(7) (see Figure 1) has the indium atom displaced by approximately 0.077 Å from the median plane (Table IV). This stereochemistry is very similar to that<sup>5</sup> found in  $\text{Br(I)InInBr}_2 \cdot 2\text{tmen}$ , in which indium is in the +II state. Five-coordination is also found in other organoindium compounds, including bis[2-[(dimethylamino)methyl]phenyl]chloroindium,<sup>6</sup>  $\text{C}_2\text{H}_5\text{InX}_2 \cdot \text{tmen}$  (X = Br, I),<sup>9</sup>  $[(\text{CH}_3)_2\text{InCl}]_2$ ,<sup>10</sup>  $[\text{CH}_3\text{InCl}_2]_2$ ,<sup>11</sup>  $(\text{C}_2\text{H}_5)_2\text{InO(S)CCH}_3$ ,<sup>12</sup> and  $[(\text{CH}_3)_2\text{In}(\text{ON}=\text{CHC}_5\text{H}_4\text{N})_2]_2$ .<sup>13</sup> The solid-state structure of  $(\text{CH}_3)_3\text{In}$ <sup>14</sup> and  $(\text{C}_6\text{H}_5)_3\text{In}$ <sup>15</sup> also give rise to five-coordination at indium, so that the evidence points increasingly to the importance of this stereochemistry in the organometallic chemistry of the element.

The bond lengths and angles in 1 and 2 are essentially the same, except for a predictable slight increase in the In-X distances in 2, presumably due to the contribution of bromine to the mixed-halide substituent. The average In-C(7) distance of 2.148 (4) Å is readily comparable to the In-C bond lengths in alkyindium chloride species such as  $[(\text{CH}_3)_2\text{InCl}]_2$  (2.179 (7) Å),<sup>10</sup>  $[\text{CH}_3\text{InCl}_2]_2$  (2.059 (9) Å),<sup>11</sup> and  $\text{C}_2\text{H}_5\text{InX}_2 \cdot \text{tmen}$  (2.17 (1) Å for both X = Br and I,<sup>9</sup>

Table IV. The <sup>1</sup>H NMR Spectra of the Indium(III) Products Obtained from the Systems  $\text{InX}$  (and  $\text{InX/InCl}_3$ )/ $\text{CH}_2\text{X}_2$ /Ligand

product	solv	resonances <sup>a</sup>
$\text{Br}_2\text{InCH}_2\text{Br} \cdot \text{Me}_2\text{SO}$	$\text{D}_2\text{O}$	2.7 (s, 9 H)
	$\text{CD}_3\text{CN}^b$	3.8 (s, 1 H)
		2.6 (s, 9 H)
$\text{Cl}_2\text{InCH}_2\text{Cl} \cdot 1.5\text{tmen}^c$	$\text{D}_2\text{O}$	3.6 (s, 1 H)
		2.95 (s, 28 H)
		3.36 (s, 19 H)
		3.49 (s, 4 H)
		3.56 (s, 7 H)
$\text{Cl}_2\text{InCH}_2\text{InCl}_2 \cdot 2\text{tmen}$	$\text{CD}_2\text{Cl}_2$	3.97 (s, br, 2 H)
		0.40 (s, 1 H)
		2.68 (s, 12 H)
$\text{InCl}_3 \cdot 1.5\text{tmen} \cdot 0.67\text{CH}_2\text{Cl}_2$	$\text{CD}_3\text{CN}$	2.78 (s, 4 H)
		2.51 (s)
		2.75 (s)
		3.20 (s)
		5.39 (s, 1 H)
$\text{In}_3\text{BrCl}_6(\text{CH}_2)_4\text{tmen}^d$	$\text{CD}_2\text{Cl}_2$	0.57 (s, 1 H)
		2.64 (s)
		2.75 (s)
		2.87 (s)
		2.87 (s)
$\text{In}_3\text{ICl}_6(\text{CH}_2)_4\text{tmen}^d$	$\text{CD}_2\text{Cl}_2$	0.56 (s, 1 H)
		2.64 (s)
		2.78 (s, br)
		2.78 (s, br)

<sup>a</sup> In ppm from  $\text{Me}_4\text{Si}$ ; s = singlet, br = broad; numbers in parentheses show relative integrated intensities. <sup>b</sup> Slightly soluble in  $\text{CD}_3\text{CN}$ . <sup>c</sup> Integration not precise. <sup>d</sup> Integration not precise; these mixtures contain  $\text{Cl(X)InCH}_2\text{InCl}_2$  as shown by X-ray crystallography.

all of which are five-coordinate, and in the four-coordinate  $\text{CH}_3\text{InCl}_3^-$  (2.19 (2) Å)<sup>16</sup> and  $\text{C}_2\text{H}_5\text{In}_3^-$  (2.213 (9) Å).<sup>9</sup>

The equatorial In-Cl(2) distance of 2.430 (1) Å found in 1 is within the range for a number of other indium(III) complexes which display trigonal-bipyramidal symmetry, such as  $\text{InCl}_3 \cdot 2\text{PPh}_3$ <sup>17</sup> (2.377 (5), 2.382 (5), 2.391 (5) Å), bis(2-[(dimethylamino)methyl]phenyl)chloroindium(III) (2.465 (1) Å),<sup>6</sup> and  $\text{Cl}_2\text{In}(\text{O}_2\text{CC}_6\text{H}_5) \cdot 2\text{py}$  (2.390 (2), 2.392 (2) Å).<sup>8</sup> The axial In-Cl(1) distance of 2.536 (1) Å is considerably longer than the equatorial distance, in keeping with the general trend that the apical bonds in trigonal-bipyramidal complexes are generally weaker than those in the equatorial plane. A direct comparison with other neutral pentacoordinate species containing an axial In-Cl bond is not possible, since there appears to be no X-ray results for such species, but the bond length is in fact close to the average values of 2.521 (5)<sup>18</sup> and 2.533 (14) Å<sup>19</sup> found in  $\text{InCl}_6^{3-}$ .

The In-N distances and the bite angle (N-In-N) of the tmen ligand are close to those previously reported for adducts of this ligand with  $\text{C}_2\text{H}_5\text{InX}_2$  (X = Br, In-N = 2.30 (1), 2.49 (1) Å, N-In-N = 75.0 (4)°; X = I, In-N = 2.33 (1), 2.44 (1) Å, N-In-N = 75.2 (4)°)<sup>9</sup> and  $\text{In}_2\text{Br}_3\text{I}$  (In-N(av) = 2.33 (2), 2.48 (2) Å, N-In-N(av) 74.7 (6)°)<sup>5</sup> and call for no comment. We have noted in these earlier papers the unusual C-C and C-N distances in the ligand, and the present structures again show such effects. The average C-C bond length in 1 and 2 is 1.493 (7) Å, the average N-C(1,2,3) is 1.479 (6) Å, and N-C(3,4) is 1.477 (6) Å, all of which values are shorter than the conventional single bond distances. Master and Waters<sup>20</sup> have discussed sim-

(9) Khan, M. A.; Peppe, C.; Tuck, D. G. *J. Organomet. Chem.* 1985, 280, 17.

(10) Hausen, H. D.; Mertz, K.; Veigel, E.; Weidlein, J. Z. *Anorg. Allg. Chem.* 1974, 410, 156.

(11) Mertz, K.; Schwartz, W.; Zettler, F.; Hausen, H. D. Z. *Naturforsch., B: Anorg. Chem., Org. Chem.* 1975, 30B, 159.

(12) Hausen, H. D. Z. *Naturforsch., B: Anorg. Chem., Org. Chem., Biochem., Biophys., Biol.* 1972, 27B, 82.

(13) Shearer, H. M. M.; Twiss, J.; Wade, K. *J. Organomet. Chem.* 1980, 184, 309.

(14) Amma, E. L.; Rundle, R. E. *J. Am. Chem. Soc.* 1958, 80, 4141.

(15) Malone, J. F.; McDonald, W. S. *J. Chem. Soc. A* 1970, 3363.

(16) Guder, H. J.; Schwartz, W.; Weidlein, J.; Widler, H. J.; Hausen, H. D. Z. *Naturforsch., B: Anorg. Chem., Org. Chem.* 1976, 31B, 1185.

(17) Veidis, M. V.; Palenik, G. J. *J. Chem. Soc. D* 1969, 586.

(18) Contreras, J. G.; Einstein, F. W. B.; Gilbert, M. M.; Tuck, D. G. *Acta Crystallogr., Sect. B: Struct. Crystallogr. Cryst. Chem.* 1977, B33, 1648.

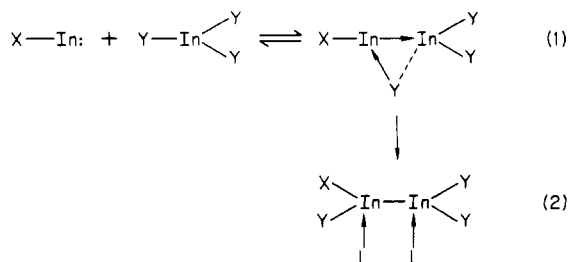
(19) Schlimper, H. V.; Ziegler, M. L. Z. *Naturforsch. B: Anorg. Chem., Org. Chem., Biochem., Biophys., Biol.* 1972, B27, 377.

ilar results for ethanediamine complexes, and more recent results, notably on copper complexes, have been summarized elsewhere.<sup>5</sup>

Finally, and most importantly, the stereochemistry at the bridging carbon C(7) is clearly distorted tetrahedral ( $H-C-H(av) = 107^\circ$ ,  $In-C-In(av) = 117.6^\circ$ ), establishing that we are dealing with a methylene derivative, rather than a dimetalcyclopropane, and incidentally also identifying 1 and 2 as organoindium(III) species. In keeping with this, the In-In distance of 3.672 Å is much longer than the In-In bond lengths found in  $In_2X_4$  derivatives,<sup>5</sup> showing the absence of any In-In bonding. Such methylene compounds are relatively rare amongst the p-group metals. Bis(trimethylstannyl)methane and a number of other  $SnCX_2Sn$  and  $Sn(CH_2)_nSn$  species<sup>21</sup> have been prepared, and their spectroscopic properties been explored. In group III, the reaction of aluminum metal with  $CH_2X_2$  ( $X = Cl, Br$ ) gives  $X_2AlCH_2AlX_2$ , and the mechanism of this reaction has been discussed<sup>22-24</sup> (see below), and the preparation of  $In[CH_2Sn(CH_3)_3]_3$ ,  $CH_3In[CH_2Sn(CH_3)_2]_2$ , and  $R_2InCH_2Sn(CH_3)_3$  from  $(CH_3)_3SnCH_2Li$  and  $InCl_3$ ,  $CH_3InCl_2$ , or  $R_2InCl$  ( $R = CH_3, t-C_4H_9$ ) has recently been reported.<sup>25</sup>

**Formation of  $X_2InCH_2X(Y)$  Compounds.** The fortuitous synthesis of compounds 1 and 2 occurred during unsuccessful attempts to prepare adducts of  $In_2Cl_4$  by methods which work for  $In_2Br_4$  and  $In_2I_4$ , namely, the reaction of  $InX$  and  $InX_3$  or  $InY_3$  in nonaqueous basic media.<sup>2</sup> This reaction does not take place with  $InCl_3$  and any of the indium(I) halides. The following discussion brings together the known experimental facts in explaining these different reaction routes, but does not purport to be a detailed mechanistic discussion. The nature of the system prevented such a study, since such obvious variations as change of temperature and/or solvent are not possible.

The reaction between  $InX$  ( $X = Cl, Br, I$ ) and  $InY_3$  ( $Y = Br, I$ ) was previously<sup>3</sup> described in terms of an insertion reaction, eq 1 and 2, in which the significant factors include



the donation of an electron pair from indium(I), the acceptor properties of indium(III), and the leaving group ability of Y in the final halide transfer process. The failure of  $InCl_3$  to yield  $In_2Cl_4$  species<sup>2</sup> and the ease of decomposition of  $In_2Cl_4$  adducts prepared by other methods<sup>26</sup> establish that the equilibrium (1) lies to the left and that the concentration of  $In_2Cl_4$  or its adduct in solution is very small.

The tentative explanation is based on the reaction of  $InX$  with  $CH_2X_2$  ( $X = Cl, Br$ ) (see Experimental Section). Although the products isolated do not give precise ana-

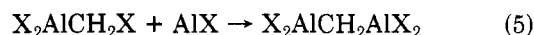
lytical results, it seems clear that  $X_2InCH_2X$  adducts are formed in the absence of the competing reaction between  $CH_2X_2$  and base (see ref 27 for a discussion of such reactions involving tmen and  $CH_2Cl_2$  and Experimental Section for evidence of reaction between tmen +  $CH_2Br_2$ ). It follows that in the presence of tmen, the insertion product  $X_2InCH_2X$  is only important in the  $InCl/CH_2Cl_2/tmen$  system and was properly ignored in the synthesis of  $In_2X_4$  ( $X = Br, I$ ). Such  $X_nMCH_2X$  molecules are well-known<sup>28</sup> for  $Zn/CH_2I_2$ , where the importance of  $IZnCH_2I$  as a methylene transfer reagent has been demonstrated<sup>28,29</sup> by the formation of norcarane from cyclohexene (although we were unable to detect any such reaction in  $InX/CH_2X_2$  systems (see Experimental Section)). A second analogue is found in the reaction of aluminum metal with  $CH_2X_2$  ( $X = Cl, Br$ ). Ort and Mottus<sup>22,23</sup> have proposed that  $AlX$  is generated as an intermediate by



followed by



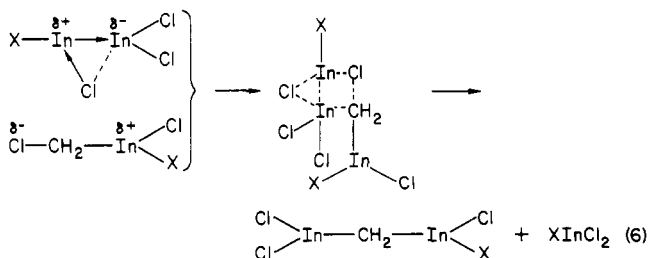
and



Unfortunately, direct evidence for the existence of  $AlX$  in these systems is lacking, and this reaction scheme depends on product analysis for the identification of  $:CH_2$  formed in eq 3.

The structure of  $X_2InCH_2X \cdot nL$  ( $X = Cl, Br$ ) in the solid state is at present unknown, since crystalline material could not be obtained for X-ray studies. The  $^1H$  NMR spectra of both compounds (Table IV) show the expected resonance for the ligands, but there are no resonances in the 0-1 ppm region where signals from the  $CH_2$  group of  $In-CH_2-In$  are detected (see below). The compound  $Cl_2InCH_2Cl \cdot 1.5tmen$  compound shows a complicated pattern (see Table IV) which gives no structural information. For  $Br_2InCH_2Br \cdot 3Me_2SO$  in either  $CD_3CN$  or  $D_2O$ , resonance signals reasonably attributed to the  $CH_2$  and  $Me_2SO$  protons are observed at 3.8 and 2.7 ppm, respectively. A tentative explanation of these preparative and spectroscopic results is that  $InX$  reacts with  $CH_2X_2$  in the presence of base to give a soluble and possibly monomeric solvated species  $X_2InCH_2X$ . On removal of the solvent, a polymeric and relatively unreactive material is obtained, and the NMR spectra observed are therefore those of these polymers, not of the original monomers. Lehmkuhl and Schafer<sup>24</sup> have proposed that the products of the reaction of aluminum with  $CH_2Cl_2$  include  $(AlClCH_2)_n$  polymers, in addition to  $Cl_2AlCH_2AlCl_2$ .

We suggest that  $Cl_2InCH_2Cl$  is the first product in the  $InCl/InCl_3/CH_2Cl_2/tmen$  system is  $Cl(X)InCH_2Cl$ , which reacts with the  $InX/InCl_3$  intermediate as shown in eq 6.



In keeping with this scheme, we find (see Experimental

(20) Maslen, H. S.; Waters, T. N. *Coord. Chem. Rev.* 1975, 17, 137.

(21) Gielen, M.; Nasielski, J. "Organotin Compounds"; Sawyer, A. K., Ed.; Marcel Dekker: New York, 1972; Vol. III, p 625.

(22) Mottus, E. H.; Ort, M. R. *J. Electrochem. Soc.* 1970, 117, 885.

(23) Ort, M. R.; Mottus, E. H. *J. Organomet. Chem.* 1973, 50, 47.

(24) Lehmkuhl, H.; Schafer, R. *Tetrahedron Lett.* 1966, 21, 2315.

(25) Schumann, H.; Mohtachemi, R. *Z. Naturforsch., B: Anorg. Chem., Org. Chem.* 1984, 39B, 798.

(26) Sinclair, I.; Worrall, I. J. *Can. J. Chem.* 1982, 60, 695.

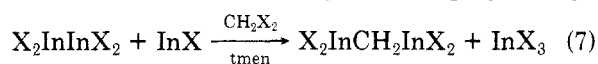
(27) Khan, M. A.; Peppe, C.; Tuck, D. G. *Can. J. Chem.* 1984, 62, 1662.

(28) Simmons, H. E.; Smith, R. D. *J. Am. Chem. Soc.* 1958, 80, 5323; 1959, 81, 4256.

(29) Doehring, W. von E.; LaFlamme, P. M. *Tetrahedron* 1958, 2, 75.

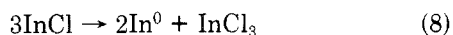
Section) that the product is in fact a mixture whose composition (e.g.,  $\text{In}_3\text{Cl}_6\text{Br}(\text{CH}_2)_4\text{tmen}$ ) corresponds to an equimolar mixture of  $\text{In}_2\text{Cl}_3\text{Br}(\text{CH}_2)_2\text{tmen}$  and  $\text{InCl}_3 \cdot 2\text{tmen}$ , from which the methylene-bridged species could be selected for identification by X-ray crystallography. In principle, the mixture resulting from the reaction of  $\text{InCl}_3$  and  $\text{InX}$  ( $\text{X} = \text{Cl}, \text{Br}, \text{I}$ ) could contain  $\text{InCl}_3$ ,  $\text{InCl}_{3-n}\text{X}_n$ ,  $\text{Cl}(\text{X})\text{InCH}_2\text{InCl}_3$ , and possibly  $\text{Cl}(\text{X})\text{InCH}_2\text{In}(\text{X})\text{Cl}$ , all as the appropriate tmen adducts. The problem of achieving a complete and quantitative separation of these products has not been solved, which in itself presents a major barrier to interpreting the reaction pathway.

A simple qualitative test for the postulated scheme involves reaction 7. The tmen complexes of  $\text{In}_2\text{Br}_4$  and  $\text{In}_2\text{I}_4$



are obvious starting materials, but reactions involving either of these and the corresponding dihalomethane are complicated by the rapid quaternization of the tmen ligand by  $\text{CH}_2\text{Br}_2$  or  $\text{CH}_2\text{I}_2$  (see Experimental Section and above), and the reaction investigated was therefore that between  $\text{In}_2\text{Br}_4 \cdot 2\text{tmen}$  and  $\text{InBr}$  in  $\text{CH}_2\text{Cl}_2 + \text{tmen}$ . A complete separation of the products could not be achieved, but the  $^1\text{H}$  NMR spectrum of the mixture of products showed a resonance signal at 0.24 ppm from  $\text{Me}_4\text{Si}$ , reasonably attributed to the  $\text{In}-\text{CH}_2-\text{In}$  unit. This lends some support to the postulated mechanism but still leaves many unanswered questions.

The possible formation of  $\text{X}_2\text{InCH}_2\text{InX}_2$  compounds from the repeated reaction of  $\text{InX}$  and  $\text{CH}_2\text{X}_2$  via  $\text{X}_2\text{InCH}_2\text{X}$ , with  $\text{InX}_3$  playing only a catalytic role, is difficult to prove, since the reaction of  $\text{InCl}$  with  $\text{CH}_2\text{Cl}_2$  in the presence of catalytic amounts of  $\text{InCl}_3$  deposited  $\text{In}^0$ , which itself has previously been taken as evidence of the disproportionation (8). Under these circumstances the



formation of  $\text{InCl}_3$  gives rise to a system which is essentially identical with one in which  $\text{InCl}$  and  $\text{InCl}_3$  are the starting materials. The experiment therefore sheds no light on the matter of formation of  $\text{In}-\text{CH}_2-\text{In}$  compounds but does show that the presence of  $\text{InCl}_3$  in the reaction mixture is fundamentally important.

Given the reservations expressed initially, we believe that the processes outlined in (6) represent a mechanism which is compatible with the results of these and previous studies.<sup>2,3</sup>

**Some Properties of  $\text{In}-\text{CH}_2-\text{In}$  Compounds.** The compounds  $\text{Cl}_2\text{InCH}_2\text{InCl}_2 \cdot 2\text{tmen}$  (1) and  $\text{Cl}(\text{Br})\text{InCH}_2\text{InCl}_2 \cdot 2\text{tmen}$  (2) find close analogues in bis(trimethylstannyl)methane [ $(\text{Me}_3\text{Sn})_2\text{CH}_2$ ] and bis(dihaloaluminum)methane. The  $^1\text{H}$  NMR spectrum of 1 (Table IV) is consistent with the presence of an  $\text{In}-\text{CH}_2-\text{In}$  unit. The  $\text{CH}_2$  resonance is observed as a singlet at 0.40 ppm, and this value is in good agreement with those of -0.28 ppm for  $(\text{Me}_3\text{Sn})_2\text{CH}_2$  and of -1.14 ppm for the dietherate of

$(\text{Cl}_2\text{Al})_2\text{CH}_2$ . An interesting feature of the spectrum of 1 is that if the sample is left in solution for periods of 30 min, the singlet resonance at 0.4 ppm splits into several less intense lines in the range 0.1–0.5 ppm. A similar behavior was reported for  $(\text{Cl}_2\text{Al})_2\text{CH}_2$ , for which the spectrum consisted of two lines at -0.44 and -1.14 ppm, and the acid-catalyzed equilibrium (9) was proposed to explain  $\text{Cl}_2\text{AlCH}_2\text{AlCl}_2 \rightarrow \text{AlCl}_3 + \text{Cl}_2\text{AlCH}_2\text{Al}(\text{Cl})\text{CH}_2\text{AlCl}_2$  (9)

these results.<sup>22,23</sup> It is possible that similar arguments apply here, although the presence of several lines in the spectrum of the indium compound is consistent with higher polymeric substances  $[-\text{In}(\text{Cl})\text{CH}_2-]_n$  with varying values of  $n$ . We attempted to extend this study by  $^{13}\text{C}$  NMR spectroscopy but were unable to detect any resonance which could be unambiguously assigned to an  $\text{In}-\text{CH}_2-\text{In}$  unit.

The reaction of 1 with excess aqueous hydrochloric acid did not yield any gaseous products, showing that  $\text{CH}_4$  is not formed. This interesting result lead us to record the  $^1\text{H}$  NMR spectrum of 1 in  $\text{DCl}$  solution; no  $\text{In}-\text{CH}_2-\text{In}$  resonance was observed. Again, it is possible that the polymerization to  $[-\text{In}(\text{Cl})\text{CH}_2-]_n$  (see above) is taking place or that H/D exchange between the  $\text{In}-\text{CH}_2-\text{In}$  unit and  $\text{DCl}$  is occurring. No reaction products were identified. Treatment of 1 ( $\text{CCl}_4$  solution) with a stream of chlorine gas gave a white solid [anal. found:  $\text{In}, 30.0; \text{Cl}, 38.0$  ( $\text{Cl}:\text{In} = 4.1$ )], but  $^1\text{H}$  NMR spectroscopy did not indicate the formation of  $\text{CH}_2\text{Cl}_2$ . These reactions suggests that 1 does not decompose by extrusion of the  $\text{CH}_2$  unit. In keeping with this, an equimolar mixture of 1 and cyclohexene in  $\text{CD}_2\text{Cl}_2$  was monitored for the formation of norcaradiene; no reaction of any sort was detected. We therefore conclude that compounds such as 1 and 2 have no chemistry in which the  $\text{CH}_2$  bridge plays a critical role.

**NMR Spectroscopy.** Proton NMR spectroscopy played an important part in identifying reaction products and in establishing their chemistry, and Table IV records the relevant experimental data. Other than those comments already made, the results call for no discussion at this point.

**Acknowledgment.** This work was supported in part by Operating Grants (to D.G.T.) from the Natural Sciences and Engineering Research Council of Canada. C.P. thanks the Conselho Nacional de Desenvolvimento Científico e Tecnológico (Brasil) for the award of a scholarship.

**Registry No.** 1, 99666-60-1; 2, 99666-61-2;  $\text{InCl}$ , 13465-10-6;  $\text{InBr}$ , 14280-53-6;  $\text{InI}$ , 13966-94-4; tmen, 110-18-9;  $\text{CH}_2\text{Cl}_2$ , 75-09-2;  $\text{CH}_2\text{Br}_2$ , 74-95-3;  $\text{Me}_2\text{SO}$ , 67-68-5;  $\text{Br}_2\text{InCH}_2\text{Br} \cdot 3\text{Me}_2\text{SO}$ , 99666-59-8;  $\text{InCl}_3$ , 10025-82-8;  $\text{In}_2\text{InCH}_2\text{InI}_2 \cdot 2\text{tmen}$ , 99666-62-3;  $\text{In}_2\text{Br}_4 \cdot 2\text{tmen}$ , 81985-78-6; pyridine, 110-86-1; triethylamine, 121-44-8; cyclohexane, 110-83-8.

**Supplementary Material Available:** Tables of hydrogen atom coordinates, anisotropic temperature factors, and calculated and observed structure factors (21 pages). Ordering information is given on any current masthead page.

## Structural and Chemical Properties of 1,3-Cyclodisiloxanes

Michael J. Michalczyk,<sup>†</sup> Mark J. Fink,<sup>†</sup> Kenneth J. Haller,<sup>†</sup> Robert West,<sup>\*†</sup> and Josef Michl<sup>†</sup>

Departments of Chemistry, University of Wisconsin, Madison, Wisconsin 53706, and University of Utah, Salt Lake City, Utah 84112

Received February 7, 1985

The synthesis and X-ray crystal structures for tetramesitylcyclodisiloxane, **4**, *trans*-1,3-dimesityl-1,3-di-*tert*-butylcyclodisiloxane, **5a**, and *cis*-1,3-bis[bis(trimethylsilyl)amino]-1,3-dimesitylcyclodisiloxane, **6b**, are reported. Crystals of **4** are tetragonal of space group  $I4_1/a$ ; crystals of **5a** and **6b** are triclinic of space group  $P\bar{1}$ . Both **4** and **6b** have slightly puckered four-membered rings while the ring in **5a** is planar. The silicon-silicon nonbonded distances in **4**, **5a**, and **6b** are 230.6, 239.6, and 234.9 pm, respectively, close to the values seen for normal silicon-silicon single bonds (234-235 pm). These short distances are believed to arise from ring distortions due to an antibonding interaction between the oxygen atoms. Some representative chemical reactions of **4**, **5a**, and **6b** are also presented.

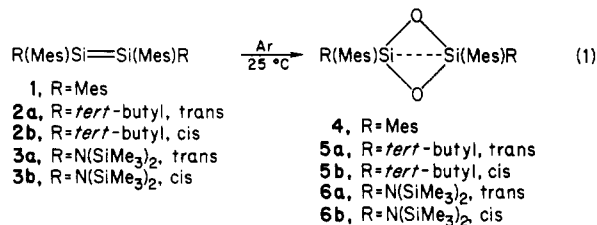
The cyclic siloxanes,  $(R_2SiO)_n$ , have great commercial importance as precursors to high molecular weight silicone polymers.<sup>1</sup> Many examples of rings with  $n = 3-8$ , obtained by condensation of silanediols, are known, and several have been the subject of X-ray crystallographic<sup>2</sup> and <sup>29</sup>Si NMR studies.<sup>3</sup> These rings are also obtained from reactions believed to involve stepwise polymerization of silanones ( $R_2Si=O$ ) generated either in solution as transients<sup>4</sup> or in matrices at 14 K.<sup>5</sup> However, the first members of the series, the 1,3-cyclodisiloxanes, are almost unknown. Although this four-membered ring structure has previously been suggested for a few silicon-oxygen containing compounds,<sup>6</sup> definite evidence for its existence was obtained only recently, from the oxidation of tetramesityldisilene, **1**.<sup>7</sup>

When **1**, either as a solid or in solution, is exposed to air, it rapidly decolorizes producing 1,3-cyclodisiloxane **4** in nearly quantitative yield. In a preliminary account<sup>7c</sup> we reported the structure of **4** and its unusual short silicon-silicon distance, which raises interesting questions concerning the nature of bonding in these ring systems.

In order to investigate whether other cyclodisiloxanes showed unusual structural features, we have determined the crystal structures of *trans*-1,3-di-*tert*-butyl-1,3-dimesitylcyclodisiloxane, **5a**, and *cis*-1,3-bis[bis(trimethylsilyl)amino]-1,3-dimesitylcyclodisiloxane, **6b**. In this paper we report our structural findings and other results bearing on the problem of silicon-silicon interaction in the rings.

## Results and Discussion

Cyclodisiloxanes **4-6** were synthesized by the air oxidation of the corresponding disilenes in the solid, according to eq 1.<sup>7</sup> The reaction is highly stereospecific for **2** and



**3**; disilene **2a** only produces **5a** when oxidized and **3b** oxidizes to a single compound **6b**. Oxidation of **2b** and **3a** also proceeds stereospecifically to give isomers of **5a** and **6b**, believed to be **5b** and **6a**, respectively. The mechanism of oxidation is unknown but may involve an intermediate

Table I. Interatomic Distances and Close Intramolecular Contacts (pm) for **4** (Esd's in Parentheses)

Si	Si	230.6 (3)	C(14)	C(18)	149.2 (9)
Si	O	172.1 (4)	C(15)	C(16)	138.2 (7)
Si	O <sup>a</sup>	165.8 (4)	C(16)	C(19)	151.0 (7)
O	O <sup>a</sup>	246.0 (8)	C(21)	C(22)	140.6 (6)
Si	C(11)	186.7 (4)	C(21)	C(26)	142.5 (6)
Si	C(21)	185.6 (5)	C(22)	C(23)	136.6 (7)
C(11)	C(12)	140.9 (6)	C(22)	C(27)	152.4 (7)
C(11)	C(16)	141.5 (6)	C(23)	C(24)	137.7 (8)
C(12)	C(13)	139.3 (7)	C(24)	C(25)	136.1 (8)
C(12)	C(17)	150.8 (8)	C(24)	C(28)	151.5 (9)
C(13)	C(14)	137.5 (7)	C(25)	C(26)	137.4 (7)
C(14)	C(15)	136.8 (7)	C(26)	C(29)	149.9 (8)
Contacts					
O-C(17)	296.70	O-C(19)	354.7		
O-C(27)	319.6	C(19)-C(29)	373.7		
O-C(29)	303.1				

<sup>a</sup>C(*n*)' is the symmetry-related position of C(*n*).

perepoxide or 1,2-siladioxetane.<sup>8</sup>

**Structure of Tetramesitylcyclodisiloxane, 4.** Figure 1 is an ORTEP diagram of **4** showing the silicon-oxygen ring. The structure consists of a roughly square cyclodisiloxane ring orthogonal to a slightly distorted planar skeleton containing the silicons and their pendant carbons. The mesityl rings are disposed in a roughly helical fashion about this skeleton. Angles between the rings and the silicon-

(1) Noll, W. "Chemistry and Technology of Silicones"; Academic Press: New York, 1968.

(2) (a) Bokii, N. G.; Zakharova, G. N.; Struchkov, Y. T. *Z. Strukt. Khim.* 1972, 13, 291. (b) Steinfink, H.; Post, B.; Fankuchen, I. *Acta Crystallogr.* 1955, 8, 420. (c) Kiss, J.; Mencez, G. *Acta Crystallogr., Sect. B: Struct. Crystallogr. Cryst. Chem.* 1975, B31, 1214. (d) Hossain, M. A.; Hursthouse, M. D.; Malik, K. M. A. *Ibid.* 1979, B35, 522.

(3) (a) Harns, R. K.; Kimber, B. J.; Wood, M. D.; Holt, A. *J. Organomet. Chem.* 1976, 116, 291. (b) Pestunovich, V. A.; Larin, M. F.; Voronkov, M. G.; Engelhardt, G.; Jancke, H.; Mileshekevich, V. P.; Yuzhelevskii, Y. A. *Zh. Strukt. Khim.* 1977, 18, 578. (c) Burton, D. J.; Harris, R. K.; Dodgson, K.; Pellow, C. J.; Semylen, J. A. *Polym. Commun.* 1983, 24, 278. (d) Engelhardt, G.; Magi, M.; Lippmaa, E. *J. Organomet. Chem.* 1973, 54, 115.

(4) For examples, see: Soysa, H. D. S.; Okinoshima, H.; Weber, W. P. *J. Organomet. Chem.* 1977, 133, C17. Okinoshima, H.; Weber, W. P. *Ibid.* 1978, 155, 165. Ando, W.; Ikeno, M.; Hamada, Y. *J. Chem. Soc., Chem. Commun.* 1981, 621. Tomadze, A.; Yablokova, N. V.; Yablokov, V. A.; Razuvaev, G. A. *J. Organomet. Chem.* 1981, 212, 43.

(5) Arrington, C. A.; West, R.; Michl, J. *J. Am. Chem. Soc.* 1983, 105, 6176.

(6) Weiss, V. A. Weiss, A. *Z. Anorg. Allg. Chem.* 1954, 276, 93. Schwartz, R.; Kuchen, W. *Ibid.* 1955, 279, 84. Sharp, R. R.; Margrave, J. L. *J. Inorg. Nucl. Chem.* 1971, 33, 2813. Andrianov, K. A.; Vasileva, T. V.; Katashuk, N. M.; Snigireva, T. V.; Dyachenko, B. I. *Vysokomol. Soedin., Ser. A* 1976, 18, 1270.

(7) (a) West, R.; Fink, M. J.; Michl, J. *Science (Washington, D.C.)* 1981, 214, 1343. (b) Fink, M. J.; De Young, D. J.; West, R.; Michl, J. *J. Am. Chem. Soc.* 1983, 105, 1070. (c) Fink, M. J.; Haller, K. J.; West, R.; Michl, J. *Ibid.* 1984, 106, 823.

(8) Michalczyk, M. J.; West, R.; Michl, J. *J. Chem. Soc., Chem. Commun.* 1984, 22, 1525.

<sup>†</sup>University of Wisconsin.

<sup>†</sup>University of Utah.

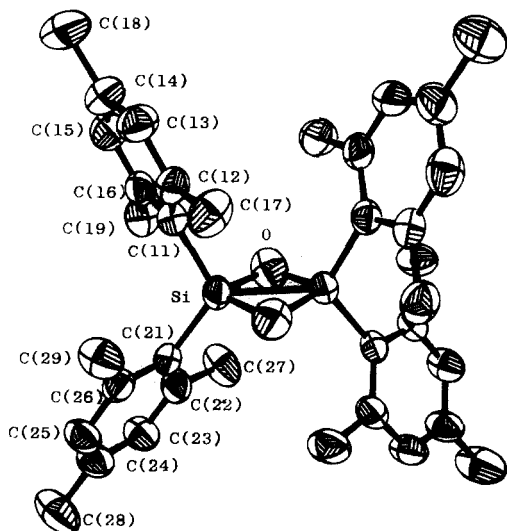


Figure 1. ORTEP drawing of 4. Atoms are represented by their 50% probability ellipsoids.

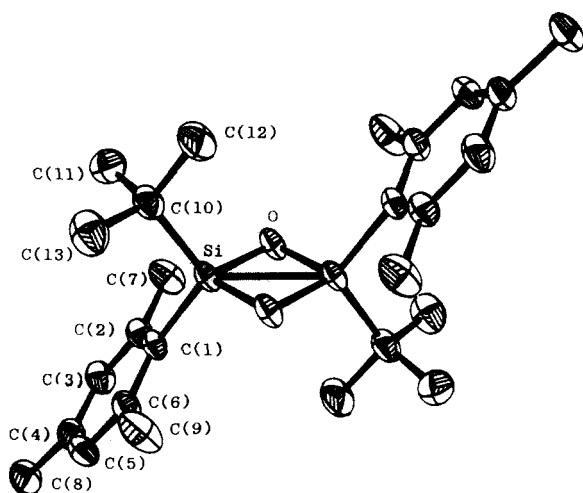


Figure 2. ORTEP drawing of 5a. Atoms are represented by their 50% probability ellipsoids.

carbon framework are 57 and 67°. The two sets of rings are nearly orthogonal to each other, the angle formed by the intersection of the mean planes of the geminal rings being 83°.

A twofold symmetry axis passes through the centroid of the siloxane ring, which is nearly planar, with a dihedral angle between the two Si-Si-O planes of 6°. The endocyclic Si-O-Si and O-Si-O angles are 86.2 (2)°, and 94.5 (1)°, respectively. Each silicon is coplanar with its pendant carbon atoms and the other silicon atom. A slight twist (11°) about the silicon-silicon axis is observed for the two C-Si-C planes.

A most striking feature to this structure is the silicon-silicon distance of 230.6 (3) pm. The two independent silicon-oxygen bond lengths are 165.8 (4) and 172.1 (4) pm. The carbon-carbon distances in the mesityl rings are all normal. Other bond lengths and angles are given in Tables I and II.

**Structure of 5a.** Molecules of 5a possess a center of symmetry midway between the two silicons. Figure 2 is an ORTEP drawing showing 5a in the crystal. The siloxane ring is planar as is the attached orthogonal silicon-carbon framework. The *trans*-mesityl rings are perpendicular to the silicon-carbon framework, the angle subtended by the mesityl rings and the framework plane being 90°.

The endocyclic Si-O-Si and O-Si-O angles are 91.13 (7) and 88.87 (7)°, respectively. The silicon-silicon distance

Table II. Interatomic Angles (deg) in 4 (Esd's in Parentheses)

Si'	O	Si	86.2 (2)
Si'	Si	C(11)	126.76 (13)
Si'	Si	C(21)	117.66 (14)
Si'	Si	O	45.85 (14)
Si'	Si	O'	48.10 (13)
O	Si	C(11)	114.56 (20)
O	Si	C(21)	106.09 (20)
O	Si	O'	94.49 (13)
C(11)	Si	C(11)	115.45 (20)
Si	C(11)	C(16)	117.97 (33)
C(12)	C(11)	C(16)	117.68 (42)
C(11)	C(12)	C(13)	119.34 (46)
C(11)	C(12)	C(17)	122.44 (48)
C(13)	C(12)	C(17)	117.79 (49)
C(12)	C(13)	C(14)	123.31 (49)
C(13)	C(14)	C(15)	116.47 (48)
C(13)	C(14)	C(18)	121.69 (55)
C(15)	C(14)	C(18)	121.83 (58)
C(14)	C(15)	C(16)	123.71 (52)
C(11)	C(16)	C(15)	119.48 (43)
C(11)	C(16)	C(19)	121.39 (45)
C(15)	C(16)	C(19)	119.12 (48)
Si	C(21)	C(22)	117.84 (34)
Si	C(21)	C(26)	124.56 (35)
C(22)	C(21)	C(26)	117.45 (41)
C(21)	C(22)	C(23)	120.50 (48)
C(21)	C(22)	C(27)	120.68 (47)
C(23)	C(22)	C(27)	118.81 (50)
C(22)	C(23)	C(24)	122.42 (55)
C(23)	C(24)	C(25)	117.08 (53)
C(23)	C(24)	C(28)	120.79 (71)
C(25)	C(24)	C(28)	122.07 (72)
C(24)	C(25)	C(26)	124.06 (60)
C(21)	C(26)	C(25)	118.52 (49)
C(21)	C(26)	C(29)	123.17 (50)
C(25)	C(26)	C(29)	118.30 (55)

Table III. Interatomic Distances and Close Intramolecular Contacts (pm) for 5a (Esd's in Parentheses)

Si-Si'	239.6 (11)	C(2)-C(7)	151.8 (4)
Si-O	167.6 (15)	C(3)-C(4)	138.2 (3)
Si-O'	167.9 (15)	C(4)-C(5)	137.8 (3)
Si-C(1)	187.6 (20)	C(4)-C(8)	151.6 (3)
Si-C(10)	187.4 (25)	C(5)-C(6)	139.7 (3)
O-O'	234.9 (3)	C(6)-C(9)	150.4 (3)
C(1)-C(2)	140.9 (3)	C(10)-C(11)	153.7 (4)
C(1)-C(6)	141.0 (3)	C(10)-C(12)	153.5 (3)
C(2)-C(3)	139.5 (3)	C(10)-C(13)	153.5 (4)

Contacts			
O-C(10) <sup>a</sup>	294.4	O-C(12) <sup>a</sup>	325.9
O-C(10)	294.9	O-C(12)	327.2
O-C(9) <sup>a</sup>	311.4	C(9)-C(13)	357.9
O-C(7)	312.9	C(11)-C(7)	363.5

<sup>a</sup> C(n)' is the symmetry-related position of C(n).

Table IV. Interatomic Angles (deg) in 5a (Esd's in Parentheses)

Si'-Si-C(1)	125.97 (8)	C(2)-C(3)-C(4)	122.05 (22)
O'-Si-O	88.87 (7)	C(3)-C(4)-C(5)	117.96 (20)
O'-Si-C(1)	114.90 (9)	C(3)-C(4)-C(8)	120.88 (25)
O'-Si-C(10)	111.77 (9)	C(5)-C(4)-C(8)	121.13 (26)
O-Si-C(1)	114.69 (9)	C(4)-C(5)-C(6)	122.28 (23)
O-Si-C(10)	112.21 (9)	C(1)-C(6)-C(5)	119.52 (21)
C(1)-Si-C(10)	112.40 (10)	C(1)-C(6)-C(9)	122.88 (20)
Si'-O-Si	91.13 (7)	C(5)-C(6)-C(9)	117.59 (22)
Si-C(1)-C(2)	121.09 (16)	Si-C(10)-C(11)	110.71 (20)
Si-C(1)-C(6)	120.41 (16)	Si-C(10)-C(12)	109.56 (18)
C(2)-C(1)-C(6)	118.39 (19)	Si-C(10)-C(13)	110.38 (18)
C(1)-C(2)-C(3)	119.76 (22)	C(11)-C(10)-C(12)	108.97 (24)
C(1)-C(2)-C(7)	122.94 (20)	C(11)-C(10)-C(13)	108.77 (23)
C(3)-C(2)-C(7)	117.30 (22)	C(12)-C(10)-C(13)	108.41 (25)

is 239.6 (11) pm, and the independent silicon-oxygen distances are 167.6 (15) and 167.9 (15) pm. All other bond distances and angles are unexceptional and are listed in

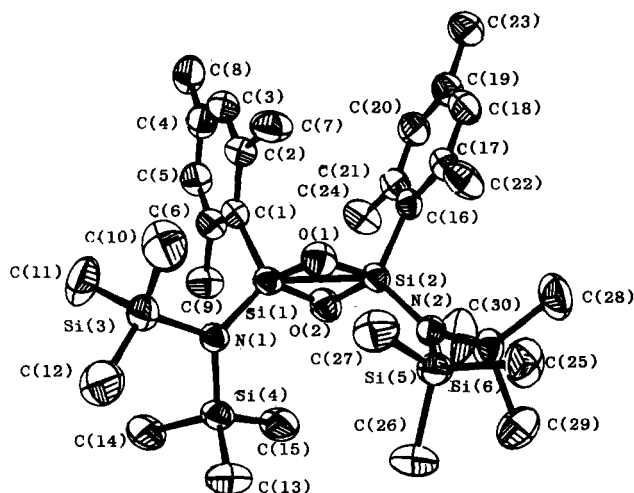


Figure 3. ORTEP drawing of **6b**. Atoms are represented by their 50% probability ellipsoids.

Table V. Interatomic Distances and Close Intramolecular Contacts (pm) for **6b** (Esd's in Parentheses)

Si(1)–Si(2)	234.9 (1)	Si(3)–C(10)	184.1 (4)
Si(1)–O(1)	166.3 (3)	Si(3)–C(11)	186.8 (4)
Si(1)–O(2)	166.7 (3)	Si(3)–C(12)	185.7 (4)
Si(1)–C(1)	188.6 (3)	Si(4)–C(13)	184.8 (5)
Si(1)–N(1)	171.3 (3)	Si(4)–C(14)	185.0 (5)
Si(2)–O(1)	166.8 (3)	Si(4)–C(15)	183.4 (5)
Si(2)–O(2)	167.2 (3)	C(16)–C(17)	141.8 (5)
Si(2)–C(16)	187.2 (3)	C(16)–C(21)	141.7 (5)
Si(2)–N(2)	171.5 (3)	C(17)–C(18)	137.7 (5)
O(1)–O(2)	235.8 (4)	C(17)–C(22)	152.6 (5)
C(1)–C(2)	141.7 (5)	C(18)–C(19)	137.3 (6)
C(1)–C(6)	141.2 (5)	C(18)–H(18)	77.6 (36)
C(2)–C(3)	137.8 (5)	C(19)–C(20)	138.1 (6)
C(2)–C(7)	151.1 (5)	C(19)–C(23)	150.5 (5)
C(3)–C(4)	138.5 (5)	C(20)–C(21)	138.9 (5)
C(3)–H(3)	85.0 (36)	C(20)–H(20)	81.0 (35)
C(4)–C(5)	135.8 (5)	C(21)–C(24)	150.1 (5)
C(4)–C(8)	151.3 (5)	N(2)–Si(5)	177.2 (3)
C(5)–C(6)	139.9 (5)	N(2)–Si(6)	176.1 (3)
C(5)–H(5)	90.2 (35)	Si(5)–C(25)	184.9 (4)
C(6)–C(9)	151.1 (5)	Si(5)–C(26)	183.6 (4)
N(1)–Si(3)	176.3 (3)	Si(5)–C(27)	184.4 (5)
N(1)–Si(4)	176.9 (3)	Si(6)–C(28)	184.8 (4)
		Si(6)–C(29)	186.5 (4)
		Si(6)–C(30)	183.9 (4)

Contacts			
O(1)–C(10)	289.2	C(22)–C(27)	364.6
O(2)–C(30)	291.8	C(9)–C(15)	368.1
O(1)–C(22)	294.1	C(7)–C(13)	376.9
O(2)–C(9)	299.5	C(24)–C(25)	386.8
O(2)–C(24)	334.2	C(12)–C(29)	387.1

<sup>a</sup> There are also very short intramolecular methyl–methyl contact of 295–300 pm between the three methyls on a silicon atom.

Tables III and IV, respectively.

**Structure of 6b.** Figure 3 shows an ORTEP view of **6b**. Molecules of **6b** possess no symmetry element; the center of symmetry lies in the lattice midway between two molecules of **6b**. The siloxane ring is nonplanar, with a dihedral angle between the two Si–O–O planes of 10°. The attached silicon–carbon–nitrogen framework is nearly planar, the C(10)–Si(1)–Si(2)–C(16) and N(1)–Si(1)–Si(2)–N(2) torsional angles being 4.3 (2) and –1.7 (2)°, respectively. Both N–Si<sub>3</sub> fragments are slightly nonplanar, with a dihedral angle between the two Si–N–Si planes of 3°.

There is a slight distortion within the N(SiMe<sub>3</sub>)<sub>2</sub> groups, as shown by the Si(2)–Si(1)–N(1) and Si(1)–Si(2)–N(2) angles of 130.4 (1) and 132.1 (1)°, respectively. The independent endocyclic Si–O–Si angles are 89.7 (1) and 89.4

Table VI. Interatomic Angles (deg) for **6b** (Esd's in Parentheses)

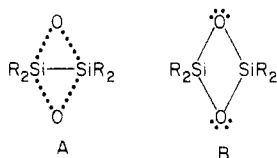
Si(2)–Si(1)–O(1)	45.2 (1)	Si(3)–N(1)–Si(4)	118.8 (2)
Si(2)–Si(1)–O(2)	45.4 (1)	N(1)–Si(3)–C(10)	114.3 (2)
Si(2)–Si(1)–C(1)	114.6 (1)	N(1)–Si(3)–C(11)	110.1 (2)
Si(2)–Si(1)–N(1)	130.4 (1)	N(1)–Si(3)–C(12)	111.9 (2)
O(1)–Si(1)–O(2)	90.2 (1)	C(10)–Si(3)–C(11)	105.5 (2)
O(1)–Si(1)–C(1)	108.8 (1)	C(10)–Si(3)–C(12)	107.0 (2)
O(1)–Si(1)–N(1)	113.7 (1)	C(11)–Si(3)–C(12)	107.7 (2)
O(2)–Si(1)–C(1)	112.0 (1)	N(1)–Si(4)–C(13)	111.9 (2)
O(2)–Si(1)–N(1)	114.7 (1)	N(1)–Si(4)–C(14)	113.1 (2)
C(1)–Si(1)–N(1)	114.9 (1)	N(1)–Si(4)–C(15)	110.2 (2)
Si(1)–Si(2)–O(1)	45.0 (1)	C(13)–Si(4)–C(14)	106.8 (3)
Si(1)–Si(2)–O(2)	45.2 (1)	C(13)–Si(4)–C(15)	106.9 (3)
Si(1)–Si(2)–C(16)	113.2 (1)	C(14)–Si(4)–C(15)	107.6 (3)
Si(1)–Si(2)–N(2)	132.1 (1)	Si(2)–C(16)–C(17)	124.6 (3)
O(1)–Si(2)–O(2)	89.8 (1)	Si(2)–C(16)–C(21)	117.4 (3)
O(1)–Si(2)–C(16)	110.9 (1)	C(17)–C(16)–C(21)	117.3 (3)
O(1)–Si(2)–N(2)	115.8 (1)	C(16)–C(17)–C(18)	119.6 (4)
O(2)–Si(2)–C(16)	108.2 (1)	C(16)–C(17)–C(22)	123.9 (3)
O(2)–Si(2)–N(2)	114.9 (1)	C(18)–C(17)–C(22)	116.5 (3)
C(16)–Si(2)–N(2)	114.6 (1)	C(17)–C(18)–C(19)	123.4 (4)
Si(1)–O(1)–Si(2)	89.7 (1)	C(18)–C(19)–C(20)	117.5 (4)
Si(1)–O(1)–O(2)	45.0 (1)	C(18)–C(19)–C(23)	121.4 (4)
Si(2)–O(1)–O(2)	45.2 (1)	C(20)–C(19)–C(23)	121.1 (4)
Si(1)–O(2)–Si(2)	89.4 (1)	C(19)–C(20)–C(21)	121.9 (4)
Si(1)–O(2)–O(1)	44.8 (1)	C(16)–C(21)–C(20)	120.3 (4)
Si(2)–O(2)–O(1)	45.0 (1)	C(16)–C(21)–C(24)	121.9 (3)
Si(1)–C(1)–C(2)	117.9 (3)	C(20)–C(21)–C(24)	117.7 (3)
Si(1)–C(1)–C(6)	124.4 (3)	Si(2)–N(2)–Si(5)	116.1 (2)
C(2)–C(1)–C(6)	117.3 (3)	Si(2)–N(2)–Si(6)	125.4 (2)
C(1)–C(2)–C(3)	120.5 (3)	Si(5)–N(2)–Si(6)	118.4 (2)
C(1)–C(2)–C(7)	122.1 (3)	N(2)–Si(5)–C(25)	111.7 (2)
C(3)–C(2)–C(7)	117.3 (3)	N(2)–Si(5)–C(26)	112.5 (2)
C(2)–C(3)–C(4)	122.3 (4)	N(2)–Si(5)–C(27)	109.6 (2)
C(3)–C(4)–C(5)	117.3 (4)	C(25)–Si(5)–C(26)	108.2 (3)
C(3)–C(4)–C(8)	121.1 (4)	C(25)–Si(5)–C(27)	108.4 (3)
C(5)–C(4)–C(8)	121.5 (4)	C(26)–Si(5)–C(27)	106.2 (3)
C(4)–C(5)–C(6)	123.4 (4)	N(2)–Si(6)–C(28)	109.7 (2)
C(1)–C(6)–C(5)	119.2 (3)	N(2)–Si(6)–C(29)	111.5 (2)
C(1)–C(6)–C(9)	125.0 (3)	N(2)–Si(6)–C(30)	113.6 (2)
C(5)–C(6)–C(9)	115.8 (3)	C(28)–Si(6)–C(29)	108.3 (2)
Si(1)–N(1)–Si(3)	124.6 (2)	C(28)–Si(6)–C(30)	106.9 (2)
Si(1)–N(1)–Si(4)	116.6 (2)	C(29)–Si(6)–C(30)	106.5 (2)

(1)°, while the O–Si–O angles are 90.2 (1) and 89.8 (1)°. The silicon–silicon internuclear distance is 234.9 (1) pm, and the four independent Si–O distances are all between 166.3 and 167.2 pm. A complete list of distances and angles is given in Tables V and VI, respectively.

**Discussion of Structures.** The solid-state structures of **4**, **5a**, and **6b** are quite similar. The silicon–silicon distance of 234.9 pm in **6b** is normal for a Si–Si single bond (234–235 pm).<sup>9</sup> In **4** the Si–Si distance is even shorter, 230.6 pm, whereas in **5a** it is slightly longer, 239.6 pm. Short O...O separations of 246.0, 234.9, and 235.8 pm are also seen for **4**, **5a**, and **6b**, respectively. The Si–O distances in the cyclodisiloxanes are slightly larger than the normal bond lengths found for other cyclic siloxanes (161–165 pm).<sup>2</sup> The Si–O–Si angles in all three compounds are a highly constrained 86.2° in **4**, 91.1° in **5a**, and 84.4 or 89.7° in **6b** compared to normal siloxane bond angles of about 145°. Two extreme qualitative explanations for the structures of **4**, **5a**, and **6b** come to mind: (1) there is a sigma bond between the silicon atoms, and the Si–O

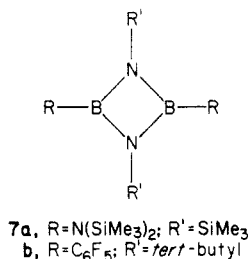
(9) The Si–Si bond length is normally ~234–235 pm in unstrained organosilanes, but longer distances, up to 240 pm, are found in sterically hindered silanes and in the extreme case of hexa-*tert*-butylcyclotrisilane,  $r_{\text{Si-Si}} = 251.1$  pm: Schäfer, A.; Weidenbruch, M.; Peters, K.; Schnering, H.-G. V. *Angew. Chem., Int. Ed. Engl.* 1984, 23, 302. Substitution with strongly electronegative substituents decreases the Si–Si bond length, for example, in hexachlorodisilane,  $r_{\text{Si-Si}} = 230$  pm: Morino, Y.; Hirota, E. *J. Chem. Phys.* 1958, 28, 185. For a discussion of Si–Si bond lengths see: Shafiee, F.; Damewood, J. R., Jr.; Haller, K. J.; West, R. *J. Am. Chem. Soc.* 1985, 107, 6950.

bonds are necessarily electron deficient (structure A); or (2) strong repulsions between the oxygen atoms cause the silicon atoms to be close together, but there is no bonding between them (structure B).

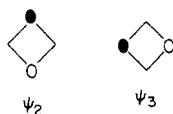


Our earlier MNDO calculations on the parent cyclodisiloxane,  $H_4Si_2O_2$ , provided no evidence for bonding between the silicon atoms.<sup>7c</sup> In agreement with this, recent ab initio calculations on  $H_4Si_2O_2$  indicate that the cyclodisiloxane is best described as containing four equivalent localized Si–O bonds with no appreciable  $\sigma$  bonding between the silicons.<sup>10</sup> However the calculated Si–O–Si angle ( $91.5^\circ$ ) and Si...Si distance (239.4 pm), while similar to those observed for **5a**, are larger than those in **4** and **6b**. A possible qualitative explanation for the acute Si–O–Si angle observed in **4** may be found in comparing the cyclodisiloxanes to the diazadiboretidines.

Planar ring structures are seen in the solid-state structures of diazadiboretidines **7a** and **7b**.<sup>11</sup> Both **7a** and **7b**



have acute B–N–B angles of  $81.9$  and  $82.4^\circ$  in **7a** and  $84.3^\circ$  in **7b**. The B...B and N...N nonbonded separations are similar in **7a** and in **7b**, being 192 and 212 pm, respectively.<sup>12</sup> The elongation of **7a** and **7b** along the N...N axis resulting in BNB valence angles of less than  $90^\circ$  has been rationalized by considering the molecular orbitals of the isoelectronic analogue cyclobutadiene. In cyclobutadiene there are four  $\pi$  molecular orbitals, two of which are nonbonding unless the ring distorts to remove this degeneracy. When the carbon atoms are replaced by less electronegative atoms such as boron and more electronegative atoms such as nitrogen in a 1.3 fashion, the degeneracy of the nonbonded orbitals  $\psi_2$  and  $\psi_3$  is removed.



Two electrons now occupy  $\psi_2$ , which has nodes at boron and is antibonding between the nitrogen atoms. There is no compensating antibonding interaction between the boron atoms since  $\psi_3$  is unoccupied; the N–N antibonding interaction thus leads to a long N–N distance and hence small B–N–B angles.

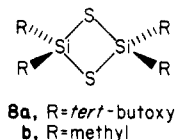
(10) Kudo, T.; Nagase, S. *J. Am. Chem. Soc.* **1985**, *107*, 2589. Bacharach, S. M.; Streitwieser, A., Jr. *Ibid.* **1985**, *107*, 1186. This question may not be closed, however, as recent very high-level calculations may indicate the presence of significant Si–Si bonding; Binkley, S., unpublished results. (We thank Dr. Binkley for permission to cite his work in advance of publication.)

(11) (a) Hess, H. *Acta Crystallogr., Sect. B: Struct. Crystallogr. Cryst. Chem.* **1969**, *B25*, 2342. (b) Paetzold, P.; Richter, A.; Thijssen, T.; Würtenberg, S. *Chem. Ber.* **1979**, *112*, 3811.

(12) The B–B distances in **7a** and **7b** are also longer than the B–B single bond lengths in  $B_2Cl_4$  (170 pm) and  $B_2Br_4$  (169 pm). See: Danielson, D. D.; Hedberg, K. *J. Am. Chem. Soc.* **1979**, *101*, 3199.

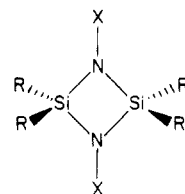
A similar model can be applied to the cyclodisiloxanes. The 3p orbitals of  $\pi$  symmetry on silicon have low electron density compared to the 2p orbitals on oxygen so that the diagonal antibonding interactions between oxygens are stronger than between the silicon atoms, leading to the diamond-shaped distortion found for **4**. The differences seen among **4**, **5a**, and **6b** in their Si–O–Si angles and Si...Si separations could result from crystal packing or steric effects. All three cyclodisiloxanes show short intramolecular oxygen–methyl separations of 289–330 pm (Tables I, II, and V), less than the van der Waals separation of 340 pm. Close methyl–methyl contacts are also seen in **5a** and **6b**, the shortest being 357.9 pm for C(9)–C(13) in **5a** and 364.6 pm for C(22)–C(27) in **6b**. There are few intermolecular contacts in **6b**, and both **4** and **5a** show only one close contact of 366.8 pm [C(18)–C(28)] and 356.3 [C(12)–C(12)], respectively. Tentatively we contribute the differences between **4**, **5a**, and **6b** to the short intramolecular contacts observed, and the different steric requirements of mesityl compared to the *tert*-butyl and  $N(SiMe_3)_2$  groups.

The distortions seen in **4**, **7a**, and **7b** are also observed in the cyclodisilathianes.<sup>13</sup> Planar diamond-shaped structures are found for both **8a**<sup>13a</sup> and **8b**.<sup>13b</sup> In **8a** the



Si–S–Si angle is  $82.2(1)^\circ$  while in **8b** the angle is  $82.41(6)^\circ$ . Both angles are even more acute than the corresponding angle in **4**,  $86.2^\circ$ . Cyclodisilathianes **8a** and **8b** have normal Si–S distances in the range of 213–215 pm<sup>14</sup> and Si...Si separations of 280.9 pm for **8a** and 283.7 pm for **8b**. The distortions seen here are consistent with the model presented for the cyclodisiloxanes where the lone-pair orbitals are now on sulfur instead of oxygen.

On the other hand, in cyclodisilazanes **9a–f**<sup>15</sup> the Si–N–



**9a**,  $R = R' = Me$ ;  $X = Ph$   
**b**,  $R = R' = Ph$ ;  $X = Ph$   
**c**,  $R = R' = Me$ ;  $X = 3,5$ -dimethylphenyl  
**d**,  $R = R' = Me$ ;  $X = SiMe_3$   
**e**,  $R = R' = [NMe(SiMe_3)]$ ;  $X = \textit{tert}$ -butyl  
**f**,  $R = F$ ;  $R' = \textit{tert}$ -butyl;  $X = \textit{mesityl}$

Si angles are all greater than  $90^\circ$ , the largest being  $95.8^\circ$  in **9b**<sup>15b</sup> and the smallest being  $91.7$  in **9d**.<sup>15d</sup> Thus the analogy to  $B_2N_2$  rings fails in this case; the ring elongations

(13) (a) Wojnowski, W.; Peters, K.; Weber, D.; Von Schnering, H. G. *Z. Anorg. Allg. Chem.* **1984**, *519*, 134. (b) Schklower, W. E.; Strutschkow, Y. T.; Guseynikov, L. E.; Wolkowa, W. W.; Awakyan, W. G. *Ibid.* **1983**, *501*, 153. (c) Peters, J.; Krebs, B. *Acta Crystallogr., Sect. B: Struct. Crystallogr. Cryst. Chem.* **1982**, *B38*, 1270. (d) Peters, J.; Mandt, J.; Meyring, M.; Krebs, B. *Z. Kristallogr.* **1981**, *156*, 90.

(14) Compare to  $(PhMeSiS)_3$ ; Pazdernik, L.; Brisse, F.; Rivest, R. *Acta Crystallogr., Sect. B: Struct. Crystallogr. Cryst. Chem.* **1977**, *B33*, 1780.

(15) (a) Parkanyi, L.; Argay, G.; Hencsei, P.; Nagy, J. *J. Organomet. Chem.* **1976**, *116*, 299. (b) Parkanyi, L.; Dunaj-Jurev, M.; Bihatsi, L.; Hencsei, P. *Cryst. Struct. Commun.* **1980**, *9*, 1049. (c) Clegg, W.; Klingebiel, U.; Sheldrick, G. M.; Vater, N. *Z. Anorg. Allg. Chem.* **1981**, *482*, 88. (d) Wheatley, P. J. *J. Chem. Soc.* **1962**, 1721. (e) Clegg, W.; Haase, M.; Klingebiel, U.; Neemann, J.; Sheldrick, G. M. *J. Organomet. Chem.* **1983**, *251*, 281.





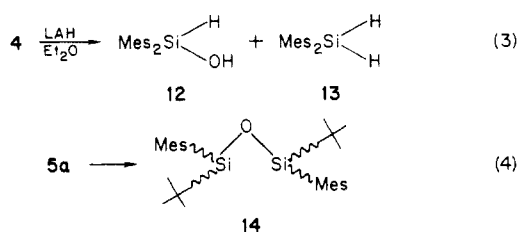
Table VIII. Fractional Coordinates for 4<sup>a</sup>

atom	x	y	z	B <sub>iso</sub> , Å <sup>2</sup>
Si	0.4568 (1)	0.1651 (1)	0.10635 (2)	
C(11)	0.4243 (4)	0.0801 (4)	0.07785 (8)	
C(12)	0.3678 (4)	0.1194 (4)	0.05627 (9)	
C(13)	0.3506 (5)	0.0497 (5)	0.03562 (9)	
C(14)	0.3863 (5)	-0.0569 (4)	0.03503 (9)	
C(15)	0.4404 (5)	-0.0937 (5)	0.05621 (9)	
C(16)	0.4613 (4)	-0.0296 (4)	0.07737 (8)	
C(17)	0.3273 (9)	0.2356 (6)	0.0541 (2)	
C(18)	0.367 (1)	-0.1287 (8)	0.0124 (2)	
C(19)	0.5227 (6)	-0.0787 (6)	0.0996 (1)	
C(21)	0.4128 (4)	0.1090 (3)	0.13746 (8)	
C(22)	0.2994 (4)	0.1010 (4)	0.14186 (9)	
C(23)	0.2607 (5)	0.0644 (5)	0.1648 (1)	
C(24)	0.3290 (5)	0.0366 (5)	0.1846 (1)	
C(25)	0.4387 (6)	0.0455 (5)	0.1805 (1)	
C(26)	0.4841 (4)	0.0804 (4)	0.15791 (9)	
C(27)	0.2176 (5)	0.1340 (6)	0.1213 (1)	
C(28)	0.283 (1)	-0.007 (1)	0.2095 (2)	
C(29)	0.6065 (5)	0.0875 (7)	0.1561 (2)	
C(1 E)	0	1/4	-0.010 (2)	
C(2)	-0.022 (4)	0.320 (5)	-0.005 (1)	
C(3 C)	-0.023 (2)	0.344 (3)	0.0238 (8)	
C(4)	0	1/4	0.037 (1)	
C(5 A)	0	1/4	0.0607 (7)	
C(B)	-0.038 (3)	0.371 (4)	0.051 (1)	
C(D)	0	1/4	0.152 (8)	
O	0.4108 (3)	0.2974 (3)	0.10511 (7)	
H(13)	0.317 (3)	0.080 (3)	0.0224 (8)	4 (1)
H(15)	0.463 (4)	-0.164 (5)	0.0565 (9)	6 (1)
H(17A)	0.282 (5)	0.238 (6)	0.064 (1)	7 (2)
H(17B)	0.275 (4)	0.239 (4)	0.0419 (9)	5 (1)
H(17C)	0.374 (7)	0.299 (8)	0.051 (1)	12 (3)
N(18A)	0.418 (8)	-0.110 (8)	0.001 (2)	16 (4)
H(18B)	0.367 (6)	-0.198 (7)	0.015 (1)	10 (2)
H(18C)	0.304 (7)	-0.133 (8)	0.004 (2)	14 (4)
H(19A)	0.548 (4)	-0.149 (4)	0.0917 (9)	5 (1)
H(19B)	0.565 (5)	-0.028 (5)	0.110 (1)	9 (2)
H(19C)	0.473 (7)	-0.104 (7)	0.117 (2)	14 (3)
H(23)	0.189 (5)	0.064 (4)	0.1694 (9)	6 (1)
H(25)	0.486 (4)	0.033 (4)	0.190 (1)	5 (1)
H(27A)	0.231 (5)	0.098 (5)	0.101 (1)	8 (1)
H(27B)	0.160 (7)	0.090 (7)	0.127 (1)	13 (3)
H(27C)	0.225 (7)	0.207 (8)	0.117 (2)	14 (3)
H(28A)	0.323 (5)	0.008 (6)	0.221 (1)	9 (2)
H(28B)	0.235 (5)	0.038 (5)	0.215 (1)	7 (2)
H(28C)	0.293 (6)	-0.082 (6)	0.209 (1)	9 (2)
H(29A)	0.642 (6)	0.054 (6)	0.167 (1)	10 (2)
H(29B)	0.642 (5)	0.063 (5)	0.144 (1)	8 (2)
H(29C)	0.640 (5)	0.157 (5)	0.158 (1)	8 (2)

<sup>a</sup>The estimated standard deviations of the least significant digits are given in parentheses.

at room temperature, although it decomposes to a complex mixture when refluxed in a THF/H<sub>2</sub>O (4:1) solution for 16 h.

Reduction of 4 with lithium aluminum hydride (LAH) produces silanol 12 and silane 13 (eq 3) while similar reduction of 5a proceeds to the partially reduced product 14 (eq 4). The difference may reflect the greater steric



shielding by *tert*-butyl groups than by mesityl groups, leading to lower reactivity for 5a compared to 4. Cyclodisiloxane 6b also reacts with LAH; however, in this case Si-N cleavage competes with ring opening.

Table IX. Fractional Coordinates for 5a<sup>a</sup>

atom	x	y	z	B <sub>iso</sub> , Å <sup>2</sup>
Si	0.93635 (9)	0.39841 (5)	-0.00480 (10)	2.07
O	0.91866 (21)	0.44716 (13)	-0.18980 (22)	2.32
C(1)	1.0516 (3)	0.29712 (19)	0.0084 (3)	2.21
C(2)	1.0082 (3)	0.20121 (21)	-0.1818 (4)	2.67
C(3)	1.0822 (4)	0.11963 (23)	-0.1679 (4)	2.99
C(4)	1.1999 (3)	0.13026 (22)	0.0284 (4)	2.81
C(5)	1.2459 (4)	0.22633 (23)	0.2143 (4)	2.92
C(6)	1.1747 (3)	0.31004 (21)	0.2094 (4)	2.57
C(7)	0.8836 (6)	0.1817 (3)	-0.4051 (5)	3.88
C(8)	1.2707 (5)	0.0363 (3)	0.0378 (7)	3.59
C(9)	1.2353 (5)	0.41155 (29)	0.4227 (4)	3.40
C(10)	0.7020 (3)	0.32361 (21)	-0.0262 (4)	2.84
C(11)	0.5576 (4)	0.19205 (28)	-0.2318 (5)	4.16
C(12)	0.6167 (5)	0.4117 (3)	-0.0351 (7)	3.98
C(13)	0.7331 (5)	0.3055 (3)	0.1720 (5)	3.96
H(3)	1.052 (3)	0.0581 (2)	-0.301 (4)	2.7 (5)
H(5)	1.330 (4)	0.2398 (25)	0.353 (5)	4.5 (6)
H(7A)	0.741 (8)	0.132 (5)	-0.450 (8)	12.4 (17)
H(7B)	0.872 (6)	0.249 (4)	-0.422 (7)	10.2 (12)
H(7C)	0.906 (6)	0.142 (4)	-0.501 (7)	9.6 (12)
H(8A)	1.311 (5)	0.022 (3)	-0.055 (6)	7.0 (10)
H(8B)	1.382 (6)	0.073 (4)	0.176 (7)	8.9 (12)
H(8C)	1.174 (5)	-0.039 (3)	0.008 (5)	6.9 (9)
H(9A)	1.294 (5)	0.399 (3)	0.528 (6)	7.5 (10)
H(9B)	1.296 (8)	0.495 (5)	0.446 (8)	13.6 (18)
H(9C)	1.133 (6)	0.411 (4)	0.426 (6)	8.6 (11)
H(11A)	0.539 (4)	0.2030 (27)	-0.363 (5)	4.9 (7)
H(11B)	0.436 (5)	0.154 (3)	-0.248 (5)	6.2 (8)
H(11C)	0.606 (4)	0.1304 (29)	-0.242 (5)	5.2 (7)
H(12A)	0.703 (5)	0.498 (3)	0.099 (5)	6.1 (8)
H(12B)	0.594 (4)	0.4212 (27)	-0.158 (5)	4.3 (7)
H(12C)	0.492 (5)	0.368 (3)	-0.048 (5)	6.4 (8)
H(13A)	0.824 (5)	0.388 (8)	0.313 (5)	5.7 (8)
H(13B)	0.784 (4)	0.2436 (28)	0.184 (5)	5.2 (7)
H(13C)	0.608 (5)	0.2711 (27)	0.155 (5)	5.0 (7)

<sup>a</sup>The estimated standard deviations of the least significant digits are given in parentheses. Isotropic equivalents are given for the atoms that were refined anisotropically.

All three cyclodisiloxanes are inert to extended photolysis at 254 nm. Compound 5a also remains unchanged when irradiated at 254 nm in the presence of methanol. Attempts to form the cyclodisiloxane ring by dehydration of 11a or by oxidation of 14 proved unsuccessful.

### Experimental Section

Proton NMR spectra were recorded on a Bruker WP-200 or WP-270 FT spectrometer; <sup>29</sup>Si spectra were recorded on a JEOL FX-200 FT spectrometer. Mass spectra were determined by using a Kratos MS-90 spectrometer. Absorption spectra were taken in cyclohexane using a Cary 14 spectrometer. All solvents were dried and distilled prior to use. Analyses were carried out by Galbraith Laboratories, Inc., Knoxville, TN. Melting points are uncorrected. For those compounds identified by high-resolution mass spectra, the NMR spectra indicated purity of ≥95%.

Disilenes 1, 2, and 3 were synthesized by methods previously reported.<sup>18</sup> Photolyses were done either in quartz NMR tubes using C<sub>6</sub>D<sub>12</sub> as the solvent or in quartz photolysis cells using 3-methylpentane. HPLC separations were carried out by using a Whatman M-20 10/50 semiprep column equipped with a Waters pumping system.

**Synthesis of Cyclodisiloxanes 4-6.** Compounds 4-6 are prepared by the exposure of disilenes 1-3 to ambient air. Powdered disilene when oxidized this way gives near quantitative yields of 4-6. If pure solid disilene is oxidized, no further purification is necessary. If crude disilene is used, recrystallization from either dry hexane, THF, or pentane yields cyclodisiloxanes 4-6 as white powders. 4: mp 215 °C; <sup>1</sup>H NMR (CDCl<sub>3</sub>) δ 2.20 (s, 12 H), 2.30 (s, 24 H), 6.66 (s, 8 H); <sup>29</sup>Si NMR (CDCl<sub>3</sub>) δ -22.02;

(18) (a) Fink, M. J.; Michalczuk, M. J.; Haller, K. J.; West, R.; Michl, J. *Organometallics* 1984, 3, 793. (b) Michalczuk, M. J.; West, R.; Michl, J. *Organometallics* 1985, 4, 826.

Table X. Fractional Coordinates for 6b

atom	x	y	z	atom	x	y	z
Si(1)	0.64189 (9)	0.26502 (7)	0.32863 (9)	H(8C)	0.9196 (20)	0.4420 (16)	0.0624 (19)
Si(2)	0.43343 (9)	0.23532 (6)	0.19659 (9)	H(9A)	0.6764 (22)	0.1528 (15)	0.1132 (12)
O(1)	0.51421 (23)	0.32183 (17)	0.31313 (23)	H(9B)	0.6044 (11)	0.2068 (21)	0.0097 (19)
O(2)	0.55990 (23)	0.17314 (17)	0.22547 (24)	H(9C)	0.7277 (22)	0.1627 (17)	0.0199 (21)
C(1)	0.72657 (28)	0.32237 (23)	0.26427 (31)	H(10A)	0.5715 (28)	0.4228 (12)	0.5461 (21)
C(2)	0.77797 (32)	0.41172 (25)	0.33000 (34)	H(10B)	0.5593 (27)	0.3909 (17)	0.6529 (13)
C(3)	0.83089 (36)	0.46046 (28)	0.28142 (39)	H(10C)	0.4930 (17)	0.3358 (18)	0.5159 (17)
C(4)	0.83314 (34)	0.42650 (29)	0.16621 (38)	H(11A)	0.8879 (21)	0.3089 (16)	0.7532 (26)
C(5)	0.78378 (36)	0.34092 (30)	0.10297 (39)	H(11B)	0.8457 (28)	0.4049 (11)	0.7234 (28)
C(6)	0.73168 (32)	0.28665 (26)	0.14835 (33)	H(11C)	0.8120 (29)	0.3701 (18)	0.8158 (18)
C(7)	0.77270 (41)	0.45901 (28)	0.45190 (36)	H(12A)	0.5952 (18)	0.1577 (17)	0.5730 (12)
C(8)	0.88695 (40)	0.48328 (33)	0.11256 (44)	H(12B)	0.6028 (19)	0.2103 (28)	0.7024 (18)
C(9)	0.68360 (43)	0.19250 (29)	0.6594 (39)	H(12C)	0.7147 (18)	0.1570 (18)	0.6930 (20)
N(1)	0.72761 (24)	0.24770 (19)	0.47643 (25)	H(13A)	1.0119 (28)	0.3088 (19)	0.6315 (13)
Si(3)	0.69033 (10)	0.28859 (7)	0.60417 (10)	H(13B)	0.9684 (28)	0.3073 (20)	0.4909 (23)
C(10)	0.56447 (40)	0.37071 (31)	0.57526 (43)	H(13C)	1.0672 (19)	0.2396 (22)	0.5531 (26)
C(11)	0.82409 (41)	0.35214 (36)	0.74158 (39)	H(14A)	0.9101 (27)	0.1536 (23)	0.6995 (16)
C(12)	0.64708 (45)	0.19296 (31)	0.65293 (44)	H(14B)	0.8422 (17)	0.0795 (16)	0.5784 (31)
Si(4)	0.86646 (10)	0.18953 (8)	0.50162 (12)	H(14C)	0.9836 (15)	0.0874 (20)	0.6386 (30)
C(13)	0.99518 (41)	0.27044 (38)	0.55148 (52)	H(15A)	0.7836 (17)	0.0744 (19)	0.3329 (35)
C(14)	0.91043 (49)	0.12106 (39)	0.62253 (53)	H(15B)	0.8477 (28)	0.1334 (26)	0.2872 (26)
C(15)	0.85451 (51)	0.11034 (41)	0.35633 (51)	H(15C)	0.9245 (17)	0.0729 (20)	0.3810 (34)
C(16)	0.38543 (29)	0.26539 (23)	0.04136 (31)	H(22A)	0.3715 (14)	0.4559 (19)	0.1478 (24)
C(17)	0.39842 (32)	0.35434 (25)	0.02490 (34)	H(22B)	0.4583 (19)	0.4874 (15)	0.1001 (24)
C(18)	0.37747 (36)	0.36554 (31)	-0.09171 (39)	H(22C)	0.5093 (12)	0.4337 (19)	0.2063 (15)
C(19)	0.34530 (34)	0.29412 (31)	-0.19524 (36)	H(23A)	0.3395 (21)	0.3721 (6)	-0.3174 (29)
C(20)	0.33152 (37)	0.20729 (31)	-0.18047 (36)	H(23B)	0.2511 (10)	0.2870 (16)	-0.3809 (21)
C(21)	0.34967 (33)	0.19169 (26)	-0.06567 (32)	H(23C)	0.3903 (16)	0.2738 (14)	-0.3389 (26)
C(22)	0.44110 (43)	0.44013 (26)	0.13126 (38)	H(24A)	0.4097 (13)	0.0709 (18)	-0.0036 (16)
C(23)	0.32989 (41)	0.30911 (38)	-0.31919 (37)	H(24B)	0.2749 (14)	0.0940 (20)	-0.0300 (19)
C(24)	0.33640 (43)	0.09422 (26)	-0.05855 (37)	H(24C)	0.3103 (19)	0.0563 (17)	-0.1403 (10)
N(2)	0.31956 (24)	0.18784 (18)	0.21387 (25)	H(25A)	0.0579 (28)	0.1589 (6)	-0.0204 (34)
Si(5)	0.18318 (9)	0.25102 (8)	0.18170 (10)	H(25B)	0.1154 (28)	0.2441 (21)	-0.0301 (32)
C(25)	0.07794 (42)	0.22272 (43)	0.01347 (42)	H(25C)	0.0056 (17)	0.2561 (18)	0.0047 (34)
C(26)	0.10126 (46)	0.23077 (43)	0.27019 (51)	H(26A)	0.0862 (25)	0.1678 (7)	0.2638 (35)
C(27)	0.21993 (49)	0.37575 (31)	0.22859 (62)	H(26B)	0.1594 (21)	0.2568 (20)	0.3525 (16)
Si(6)	0.32546 (10)	0.08051 (7)	0.25308 (10)	H(26C)	0.0273 (14)	0.2635 (17)	0.2526 (31)
C(28)	0.19079 (41)	0.00843 (29)	0.13594 (42)	H(27A)	0.2334 (28)	0.3943 (27)	0.1658 (25)
C(29)	0.32630 (46)	0.09469 (32)	0.40990 (38)	H(27B)	0.2905 (17)	0.3903 (26)	0.3059 (17)
C(30)	0.46131 (41)	0.01405 (30)	0.25788 (50)	H(27C)	0.1520 (28)	0.4074 (24)	0.2372 (27)
H(3)	0.8562 (34)	0.5123 (26)	0.3318 (26)	H(28A)	0.1952 (17)	0.0025 (18)	0.0585 (16)
H(5)	0.7910 (34)	0.3181 (27)	0.0309 (34)	H(28B)	0.1123 (14)	0.0294 (19)	0.1280 (28)
H(18)	0.3905 (34)	0.4118 (26)	-0.1031 (35)	H(28C)	0.2040 (26)	-0.0498 (10)	0.1581 (27)
H(20)	0.3105 (35)	0.1646 (27)	-0.2410 (25)	H(29A)	0.3769 (18)	0.1475 (10)	0.4610 (24)
H(7A)	0.8121 (18)	0.4226 (15)	0.5123 (21)	H(29B)	0.2483 (12)	0.1032 (17)	0.4107 (30)
H(7B)	0.6903 (8)	0.4678 (15)	0.4399 (27)	H(29C)	0.3624 (19)	0.0417 (11)	0.4414 (28)
H(7C)	0.8137 (18)	0.5173 (8)	0.4806 (25)	H(30A)	0.4640 (29)	0.0000 (18)	0.1788 (13)
H(8A)	0.8233 (18)	0.5171 (15)	0.0618 (19)	H(30B)	0.4513 (27)	-0.0415 (11)	0.2784 (22)
H(8B)	0.9495 (15)	0.5248 (14)	0.1761 (20)	H(30C)	0.5354 (18)	0.0444 (18)	0.3198 (18)

IR 1018–1082  $\text{cm}^{-1}$  (br, Si–O–Si); UV–visible ( $\text{C}_6\text{H}_{12}$ ) 208 nm ( $\epsilon$  115 000), 234 (25 000); MS (30 eV),  $m/e$  (relative intensity) 564 ( $m^+$ , 5), 444 ( $m^+$  –  $\text{C}_9\text{H}_{12}$ , 100), 325 ( $m^+$  –  $\text{C}_9\text{H}_{12}$  –  $\text{C}_9\text{H}_{11}$ , 95); exact mass for  $\text{C}_{36}\text{H}_{44}\text{Si}_2\text{O}_2$  calcd  $m/e$  564.2868, found  $m/e$  564.2882. Anal. Calcd for  $\text{C}_{36}\text{H}_{44}\text{Si}_2\text{O}_2$ : C, 76.54; H, 7.85. Found: C, 76.75; H, 7.76. **5a**: mp 176–187 °C;  $^1\text{H}$  NMR ( $\text{C}_6\text{D}_6$ )  $\delta$  0.99 (s, 18 H), 2.08 (s, 6 H), 2.72 (s, 12 H), 6.76 (s, 4 H);  $^{29}\text{Si}$  NMR ( $\text{CDCl}_3$ )  $\delta$  +12.4; IR ( $\text{CCl}_4$ ) 1000–1080  $\text{cm}^{-1}$  (br, Si–O–Si); UV–visible ( $\text{C}_6\text{H}_{12}$ ) 204 ( $\epsilon$  42 000), 220 (16 000); MS (30 eV),  $m/e$  (relative intensity) 440 ( $m^+$ , 12.8), 383 ( $m^+$  – *tert*-butyl, 100), 327 [( $m^+$  – *tert*-butyl) – 56, 12.5]; exact mass for  $\text{C}_{26}\text{H}_{40}\text{Si}_2\text{O}_2$  calcd  $m/e$  440.2556, found  $m/e$  440.2569. Anal. Calcd for  $\text{C}_{26}\text{H}_{40}\text{Si}_2\text{O}_2$ : C, 70.85; H, 9.15; Si, 12.74. Found: C, 70.55; H, 9.05; Si, 12.58. **5b**:  $^1\text{H}$  NMR ( $\text{C}_6\text{D}_6$ )  $\delta$  1.21 (s, 18 H), 2.10 (s, 6 H), 2.65 (s, 12 H), 6.52 (s, 4 H). **6a**: mp 207–210 °C;  $^1\text{H}$  NMR ( $\text{C}_6\text{D}_6$ )  $\delta$  0.20 (s, 36 H), 2.07 (s, 6 H), 2.84 (s, 12 H), 6.78 (s, 2 H). **6b**: mp 198–192 °C;  $^1\text{H}$  NMR ( $\text{C}_6\text{D}_6$ )  $\delta$  0.39 (s, 36 H), 1.96 (s, 6 H), 2.52 (s, 12 H), 6.59 (s, 4 H); UV–visible ( $\text{C}_6\text{H}_{12}$ ) 202 nm ( $\epsilon$  106 000), 229 (19 900); MS (70 eV),  $m/e$  (relative intensity) 646 ( $m^+$ , 2), 631 ( $m^+$  –  $\text{CH}_3$ , 26.6), 526 ( $m^+$  –  $\text{C}_9\text{H}_{12}$ , 9), 511 [( $m^+$  –  $\text{C}_9\text{H}_{12}$ ) –  $\text{CH}_3$ , 45.4], 407 [( $m^+$  –  $\text{C}_9\text{H}_{12}$ ) –  $\text{C}_9\text{H}_{11}$ , 22.6]; exact mass for  $\text{C}_{30}\text{H}_{58}\text{O}_2\text{N}_2\text{Si}_6$  calcd  $m/e$  646.3098, found  $m/e$  646.3116. Anal. Calcd for  $\text{C}_{30}\text{H}_{58}\text{O}_2\text{N}_2\text{Si}_6$ : C, 55.67; H, 9.03; N, 4.33; Si, 26.03. Found: C, 55.50; H, 9.11; N, 4.32; Si, 25.87.

**Hydrolysis of 4.** A solution of 20 mg ( $3.5 \times 10^{-5}$  mol) of 4 in a (6:1) THF/ $\text{H}_2\text{O}$  mixture was stirred at 25 °C for 6 h. The solvent

was removed in vacuo leaving a white solid.  $^1\text{H}$  NMR analysis showed that the major product was diol **11a** (60%). Recrystallization from pentane gave 10 mg (50%) of **11a**. Compound **11a** was also identified by comparison with an authentic sample synthesized from the hydrolysis of  $(\text{Mes})_2\text{SiCl}_2$  with water:  $^1\text{H}$  NMR ( $\text{CDCl}_3$ )  $\delta$  2.24 (s, 12 H), 2.28 (s, 24 H), 3.44 (s, 2 H), 6.72 (s, 8 H); IR 3670 (sh, Si–OH), 940–1080 (br, Si–O–Si); MS (30 eV),  $m/e$  (relative intensity) 463 ( $m^+$  –  $\text{C}_9\text{H}_{11}$ , 3.4), 462 ( $m^+$  –  $\text{C}_9\text{H}_{12}$ , 9.9), 342 ( $m^+$  –  $2(\text{C}_9\text{H}_{12})$ , 100). A peak match was obtained from the  $m/e$  462 fragment since the parent is not seen; exact mass for  $\text{C}_{27}\text{H}_{34}\text{O}_3\text{Si}_2$  calcd  $m/e$  462.2037, found  $m/e$  462.2048.

**Hydrolysis of 5a.** Hydrolysis of **5a** (10.0 mg,  $2.3 \times 10^{-5}$  mol) was carried out as described above for 4. Workup yielded 90% of diol **11b** as a clear oil:  $^1\text{H}$  NMR ( $\text{C}_6\text{D}_6$ )  $\delta$  1.15 (s, 18 H), 2.05 (s, 6 H), 2.52 (s, 12 H), 2.64 (br, 2 H), 6.71 (s, 4 H); MS (30 eV),  $m/e$  (relative intensity) 458 ( $m^+$ , >0.1), 457 ( $m^+$  – H, 4.4), 456 ( $m^+$  –  $\text{H}_2$ , 4.9), 455 ( $m^+$  – 3, 14.9), 401 ( $m^+$  – *tert*-butyl, 4.5), 164 [( $m^+$  –  $2(\text{C}_9\text{H}_{11})$ ) – 56, 72.3]. Because of the lack of a parent ion a peak match on the  $m/e$  401 fragment was obtained; exact mass for  $\text{C}_{22}\text{H}_{30}\text{O}_3\text{Si}_2$  calcd  $m/e$  401.1959, found  $m/e$  401.1959.

**Reduction of 5a with Lithium Aluminum Hydride (LAH).** A solution of 48.9 mg ( $1.1 \times 10^{-4}$  mol) of **5a** in 35 mL of  $\text{Et}_2\text{O}$  was cooled to –78 °C, and a cold (–78 °C) mixture of 25 mg ( $6.6 \times 10^{-4}$  mol) of LAH in 3 mL of  $\text{Et}_2\text{O}$  was quickly added. The resulting mixture was stirred for 10 min and then slowly warmed to 25 °C. The organic layer was extracted with hexane, washed

with distilled water, and dried over  $\text{MgSO}_4$ . Removal of the solvent in vacuo yielded 39 mg (80%) of **14** as an off-white solid:  $^1\text{H NMR}$  ( $\text{CDCl}_3$ )  $\delta$  0.95 (s, 9 H), 1.01 (s, 9 H), 2.25 (s, 6 H), 2.4 (s, 3 H), 2.46 (s, 3 H), 2.49 (s, 6 H), 5.30 (s, 1 H), 6.79 (s, 4 H); IR 3700 (br, Si-OH), 2160 (s, Si-H), 1000–1100  $\text{cm}^{-1}$  (br, Si-O-Si); MS (30 eV),  $m/e$  (relative intensity) 442 ( $m^+$ , >0.1), 385 ( $m^+$ -*tert*-butyl, 100%); exact mass for  $\text{C}_{26}\text{H}_{32}\text{O}_2\text{Si}_2$  calcd  $m/e$  442.2712, found  $m/e$  442.2467. A peak match was also obtained for  $m/e$  385; exact mass for  $\text{C}_{22}\text{H}_{30}\text{O}_2\text{Si}_2$  calcd  $m/e$  385.2010, found  $m/e$  385.2018.

**Reduction of 4 with LAH.** The procedure was similar to that given for **5a**, starting with 100 mg ( $1.8 \times 10^{-4}$  mol) of **4**. After 2 h at  $-78^\circ\text{C}$ , the mixture was warmed to  $25^\circ\text{C}$ . GLC analysis of the crude mixture showed two products (95%) in a 0.8:1.0 ratio. The crude mixture was separated by preparative HPLC using a 4.7:0.3 (mL) MeOH/THF solvent mixture (200- $\mu\text{L}$  injections) giving two products which were determined to be **12** and a minor amount of silane **13**. **12**:  $^1\text{H NMR}$  ( $\text{C}_6\text{D}_6$ )  $\delta$  2.09 (s, 6 H), 2.40 (s, 12 H), 5.10 (br, 1 H), 5.68 (s, 1 H), 6.65 (s, 4 H); IR 3690 (br, Si-OH), 2158 (br, Si-H), 1010–1030  $\text{cm}^{-1}$  (br, Si-O); MS (30 eV),  $m/e$  (relative intensity) 284 ( $m^+$ , 0.5), 164 ( $m^+$  -  $\text{C}_9\text{H}_{12}$ , 71.9); exact mass for  $\text{C}_{18}\text{H}_{24}\text{OSi}$  calcd  $m/e$  284.1590, found  $m/e$  284.1598. **13**: IR 2140  $\text{cm}^{-1}$  (br, Si-H); MS (30 eV),  $m/e$  (relative intensity) 268 ( $m^+$ , 35), 148 ( $m^+$  -  $\text{C}_9\text{H}_{12}$ , 100).

**Photolysis of 5a with MeOH.** A solution containing 16.0 mg ( $3.6 \times 10^{-5}$  mol) of **5a** and 0.2 mL of MeOH in 4.0 of 2-methyltetrahydrofuran was degassed and irradiated with 254-nm light at  $-60^\circ\text{C}$ . Aliquots of the mixture were removed approximately every hour and analyzed by GLC. After 5 h of irradiation **5a** was still present and no new compounds were seen. The solution was then irradiated for 1 h at  $25^\circ\text{C}$  and analyzed by GLC. Only **5a** was present in the mixture.

**Photolysis of 6b.** Approximately 15 mg ( $2.3 \times 10^{-5}$  mol) of **6b** was dissolved in 1 mL of  $\text{C}_6\text{D}_{12}$  and placed in a quartz NMR tube. The solution was degassed, and the NMR tube was sealed to ensure that no oxygen was present. The tube was irradiated (254 nm) at  $25^\circ\text{C}$  for 15 min after which a proton spectrum was taken showing no decomposition of **6b**. Irradiation continued for 2 h and 20 min. After this time **6b** was still unchanged, as seen from the NMR spectrum.

**Attempted Formation of 4 from 11a.** A solution consisting of 14.8 mg ( $2.8 \times 10^{-5}$  mol) of **11a** and 8 mg ( $3.9 \times 10^{-5}$  mol) of  $N,N'$ -dicyclohexylcarbodiimide in 7 mL of THF was refluxed for 12 h. After the solution was cooled to  $25^\circ\text{C}$ , the solvent was removed and  $\text{C}_6\text{D}_6$  was added.  $^1\text{H NMR}$  analysis ( $\text{CDCl}_3$ ) showed only **11a** to be present.

**Attempted Formation of 5a from 14.** A solution of 17.4 mg ( $3.9 \times 10^{-5}$  mol) of **12** in 3.0 mL of benzene was slowly added to a mixture of 9.9 mg ( $4.4 \times 10^{-5}$  mol) of 2,3-dichloro-5,6-dicyano-1,4-benzoquinone (DDQ) dissolved in 5.0 mL of benzene. Following addition the resulting orange solution was refluxed for 12 h since it still had the original color of DDQ. After cooling, the solution was still orange. The solvent was removed in vacuo, and  $\text{C}_6\text{D}_6$  was added.  $^1\text{H NMR}$  analysis showed only **14** and no **5a**.

**X-ray Data Collection.** Single crystals of **4**, **5a**, and **6b** were grown by slow cooling of saturated solutions in toluene at  $0^\circ\text{C}$ . Those of **4** contained one molecule of toluene per molecule of cyclodisiloxane. Suitably sized crystals were taken from the solution and mounted on a thin glass thread with cyanoacrylate cement.

Crystallographic studies were carried out on a Syntex-Nicolet  $P\bar{1}$  diffractometer with a modified LT-1 low-temperature cooling system, using  $\text{Mo K}\alpha$  radiation. Unit cell parameters were obtained from least-squares refinements based on the setting angles of 60 reflections. For **4** the space group was uniquely determined by the systematic absences in the data; for **5a** and **6b**  $P\bar{1}$  was

assumed and confirmed by successful structure solution and refinement. The crystal dimensions, unit cell parameters, and other crystal data are given in Table VII. Throughout data collection four standard reflections were measured every 50 reflections to monitor stability. The structures were solved by direct methods using the MULTAN program system.  $E$  maps revealed the positions of the silicon and carbon atoms. Compound **4** was isomorphous to the corresponding disilene<sup>17a</sup> except for the presence of the bridging oxygen atoms; the disilene also has the same disordered toluene of crystallization. Starting parameters for the disordered toluene were taken from the disilene structure. After preliminary full-matrix refinements, electron density difference maps revealed most of the nonsolvent hydrogen atom positions in all structures. In **4** and **5a** the hydrogen parameters (coordinates and isotropic thermal parameters) were included with the parameters being refined. All refinements for all three molecules were carried out by using full-matrix least-squares refinement techniques and utilizing standard atomic form factors<sup>19</sup> and all data with  $F_o > 3\sigma(F_o)$ .

In the final cycles of refinement for **4** and **5a** all non-hydrogen atoms were assumed to vibrate anisotropically, and all hydrogen atoms were assumed to vibrate isotropically. Compound **6b** was refined by using RAELS<sup>20</sup> to take advantage of its capability to model the thermal motion of the trimethylsilyl and mesityl groups with a single reorientable thermal libration axial system (TL model)<sup>21</sup> centered on the atoms to which the groups are attached. All 58 hydrogen atoms were included in the thermal libration groups. The methyl hydrogen atoms were included in the model as rigid groups having idealized C-H distances (0.95 Å) and idealized angles ( $109.5^\circ$ ) and centered on the appropriate carbon atoms. The group origin was constrained to move with the attached carbon atom, and the group orientation was refined by allowing it to rotate about the vector from the methyl carbon atom to the attached atom. The final values of the discrepancy indices,  $R_1 = \sum ||F_o| - |F_c|| / \sum |F_o|$  and  $R_2 = [\sum w(|F_o| - |F_c|)^2 / \sum w(F_o)^2]^{1/2}$ , are also included in Table VII. The final coordinates for **4**, **5a**, and **6b** are listed in Tables VIII, IX, and X, respectively. Tables of the anisotropic thermal parameters and of  $10|F_o|$  and  $10|F_c|$  for each structure are available as supplementary material.

**Acknowledgment.** Research was sponsored by the Air Force Office of Scientific Research, Air Force Systems Command, USAF under Contracts F49620-83-C-0004 (R.W.) and AFOSR 84-0065 (J.M.), and by the National Science Foundation under Grant CHE-8318820. The United States Government is authorized to reproduce and distribute reprints for governmental purposes notwithstanding any copyright notation thereon.

**Registry No.** **1**, 80785-72-4; **2a**, 88526-23-2; **2b**, 88526-24-3; **3a**, 88526-25-4; **3b**, 88526-26-5; **4**, 84537-22-4; **5a**, 95206-56-7; **5b**, 99798-79-5; **6a**, 99798-80-8; **6b**, 99798-81-9; **11a**, 88589-60-0; **11b**, 99798-84-2; **12**, 88589-59-7; **13**, 99798-82-0; **14**, 99798-83-1.

**Supplementary Material Available:** Tables of anisotropic thermal parameters, fractional coordinates, bond lengths and angles, and structure factor amplitudes for **4**, **5a**, and **6b** (63 pages). Ordering information is given on any current masthead page.

(19) Atomic form factors were from: Cromer, D. T.; Mann, J. B. "International Tables for X-Ray Crystallography"; Kynoch Press: Birmingham, England, 1974; Vol. 4, pp 99–101, Table 2.2B. The atomic form factor for hydrogen was from: Stewart, R. F.; Davidson, E. R.; Simpson, W. T. *J. Chem. Phys.* **1965**, *42*, 3175.

(20) Rae, A. D. "RAELS, A Comprehensive Constrained Least Squares Refinement Program", University of New South Wales, 1976.

(21) Rae, A. D. *Acta Crystallogr., Sect. A: Cryst. Phys., Diffr., Theor. Gen. Crystallogr.* **1975**, *A31*, 560.

# The Bridging Sulfide Anion Reactivity of Roussin's Red Salt

Dietmar Seyferth\* and Michael K. Gallagher

Department of Chemistry, Massachusetts Institute of Technology, Cambridge, Massachusetts 02139

Martin Cowie

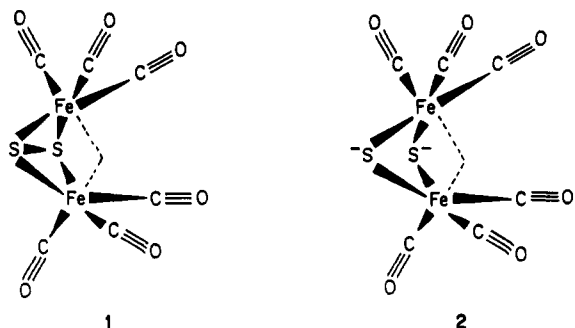
Department of Chemistry, University of Alberta, Edmonton, Alberta, Canada T6G 2G2

Received June 19, 1985

Reactions of Roussin's red sodium salt with organic halides gave  $(\mu\text{-RS})_2\text{Fe}_2(\text{NO})_4$  (two isomers) in good yield, while reactions with  $\text{R}_3\text{SnX}$  ( $\text{R} = \text{Ph}, \text{Me}$ ),  $\text{Ph}_3\text{PbBr}$ , and  $\text{RHgX}$  ( $\text{R} = \text{Ph}, \text{Me}$ ) and with  $[\eta^5\text{-C}_5\text{H}_5\text{Fe}(\text{CO})_2\text{THF}]\text{BF}_4$  yielded the expected organometal derivatives. Reactions with  $(\text{OC})_4\text{FeI}_2$  and  $\text{CpCo}(\text{CO})\text{I}_2$  ( $\text{Cp} = \eta^5\text{-C}_5\text{H}_5$  and  $\eta^5\text{-C}_5\text{Me}_5$ ) gave metal sulfur cluster complexes in low yield. The structure of one of these,  $(\mu_3\text{-S})_2(\eta^5\text{-C}_5\text{Me}_5\text{Co})_2[(\text{ON})_2\text{Fe}]$ , was determined by X-ray diffraction. Other methods for the preparation of organic and organometallic derivatives of Roussin's red salt were investigated: nitrosylation of the corresponding hexacarbonyl compounds; reaction of  $(\mu\text{-Me}_3\text{SnS})_2\text{Fe}_2(\text{NO})_4$  with halides; piperidine-induced Michael additions of  $(\mu\text{-HS})_2\text{Fe}_2(\text{NO})_4$  to  $\alpha,\beta$ -unsaturated olefins. The complex  $(\eta^5\text{-C}_5\text{Me}_5)_2\text{Co}_2(\mu_3\text{-S})_2\text{Fe}(\text{NO})_2$  crystallizes in the space group  $C2/c$  with  $a = 32.951(5) \text{ \AA}$ ,  $b = 8.755(1) \text{ \AA}$ ,  $c = 17.619(2) \text{ \AA}$ ,  $\beta = 112.23(1)^\circ$ , and  $Z = 8$ . Refinement has converged at  $R = 0.028$  and  $R_w = 0.039$  for 262 variables and 3662 unique observations. The structure consists of a trigonal-bipyramidal  $\text{Co}_2\text{FeS}_2$  core in which the  $\text{Co}_2\text{Fe}$  triangle is capped above and below by triply bridging sulfido groups. One  $\text{C}_5\text{Me}_5$  group is bound in an  $\eta^5$ -fashion to each Co center and the two partially bent nitrosyls (average  $\text{Fe-N-O}$  angle =  $159.8^\circ$ ) are bound to Fe.

## Introduction

In earlier work, we had discovered that treatment of  $(\mu\text{-dithio})\text{bis}(\text{tricarboxyliron})$ , **1**, with sodium or with metal



hydrides leads to formation of the sulfur-bridged dianion **2**.<sup>1</sup> Complex **1** had first been reported in 1958.<sup>2</sup> Consideration of the earlier literature showed that a bis(sulfido ion)-bridged  $\text{Fe}_2(\text{NO})_4$  complex had been prepared one hundred years earlier by the French chemist Z. Roussin.<sup>3</sup> Initially, the constitution of "Roussin's red salt" was uncertain,<sup>4</sup> but in 1882 Pavel,<sup>5</sup> on the basis of careful purification and analysis, reported the correct constitution of the potassium salt as " $\text{Fe}(\text{NO})_2\text{SK} + 2\text{H}_2\text{O}$ ". The presence of a dimer, formulated as " $\text{Fe}(\text{NO})_2\text{S}, \text{Fe}(\text{NO})_2$ , and  $\text{K}_2\text{S}$ " was suggested. Recently, the structure of the tetramethylammonium salt  $[\text{Me}_4\text{N}]_2[\text{Fe}_2\text{S}_2(\text{NO})_4]$  was determined by Chinese workers.<sup>6</sup> It was found that the iron and sulfur atoms form a planar array with  $\text{Fe-S-Fe}$  angles of  $74^\circ$  and  $\text{S-Fe-S}$  angles of  $105.5^\circ$ . The distance between

the iron atoms,  $\text{Fe}\dots\text{Fe}$ , is  $2.71 \text{ \AA}$ , while the  $\text{Fe-S}$  bond length is  $2.24 \text{ \AA}$ .

The potassium salt was found by Pavel to react with ethyl iodide to give a red, crystalline diethyl derivative,  $(\mu\text{-C}_2\text{H}_5\text{S})_2\text{Fe}_2(\text{NO})_4$ .<sup>5</sup> Its dimeric constitution was confirmed by Hofmann and Wiede,<sup>7</sup> and its structure was determined by means of X-ray crystallography in 1958.<sup>8</sup>

In spite of the fact that Roussin's red salts had been known for 125 years, very little study had been devoted to their chemical reactivity. Only the reaction with ethyl iodide to give  $(\mu\text{-C}_2\text{H}_5\text{S})_2\text{Fe}_2(\text{NO})_4$  had been reported when we began our work in this area.

Although the  $(\mu\text{-RS})_2\text{Fe}_2(\text{CO})_6$  and the  $(\mu\text{-RS})_2\text{Fe}_2(\text{NO})_4$  complexes and the  $[(\mu\text{-S})_2\text{Fe}_2(\text{CO})_6]^{2-}$  and the  $[(\mu\text{-S})_2\text{Fe}_2(\text{NO})_4]^{2-}$  anions are formally similar, structurally they are quite different. In the nitrosyl complexes, the iron atoms are tetrahedrally coordinated (excluding a possible  $\text{Fe-Fe}$  bond) and a planar  $\text{S}_2\text{Fe}_2$  ring results. In the diethyl derivative the  $\text{Fe}\dots\text{Fe}$  distance is  $2.72 \text{ \AA}$ , and the  $\text{S}\dots\text{S}$  nonbonded distance is  $3.633 \text{ \AA}$ .<sup>8</sup> In contrast, in  $(\mu\text{-C}_2\text{H}_5\text{S})_2\text{Fe}_2(\text{CO})_6$  and, presumably, in the dianion, the iron atoms are octahedrally coordinated and the  $\text{S}_2\text{Fe}_2$  ring is puckered. In  $(\mu\text{-C}_2\text{H}_5\text{S})_2\text{Fe}_2(\text{CO})_6$  the  $\text{Fe}\dots\text{Fe}$  distance is  $2.54 \text{ \AA}$ ; the  $\text{S}\dots\text{S}$  nonbonded distance is  $2.93 \text{ \AA}$ .<sup>9</sup> The structures of the  $\text{S}_2\text{Fe}_2(\text{NO})_4$  units in  $(\mu\text{-C}_2\text{H}_5\text{S})_2\text{Fe}_2(\text{NO})_4$  and  $[\text{Me}_4\text{N}]_2[(\mu\text{-S})_2\text{Fe}_2(\text{NO})_4]$  are not markedly different, and we assume that this also is true for the  $\text{S}_2\text{Fe}_2(\text{CO})_6$  units in  $(\mu\text{-C}_2\text{H}_5\text{S})_2\text{Fe}_2(\text{CO})_6$  and the  $[(\mu\text{-S})_2\text{Fe}_2(\text{CO})_6]^{2-}$  anion. That being the case, then one might expect the chemistries of the two dianions to be quite different. The nitrosyl analogue  $[(\mu\text{-S})_2\text{Fe}_2(\text{NO})_4]^{2-}$  should be able to react with more hindered electrophiles, but the close proximity of the bridging  $\text{S}^-$  ligands in  $[(\mu\text{-S})_2\text{Fe}_2(\text{CO})_6]^{2-}$  should make reactions with hindered electrophiles unfavorable. On the other hand, the proximity of the bridging  $\text{S}^-$  ligands in  $[(\mu\text{-S})_2\text{Fe}_2(\text{CO})_6]^{2-}$ , we know, facilitates reactions with difunctional reactants to form products in which an organic

(1) Seyferth, D.; Henderson, R. S.; Song, L.-C. *Organometallics* 1982, 1, 125.

(2) (a) Hieber, W.; Gruber, J. Z. *Anorg. Allg. Chem.* 1958, 296, 91. (b) Brendel, G. Ph.D. Dissertation, Technische Hochschule München, 1956.

(3) Roussin, Z. C. R. *Hebd. Seances Acad. Sci.* 1858, 46, 224; *Justus Liebigs Ann. Chem.* 1858, 107, 120; *Ann. Chim. Phys.* 1858, [3] 52, 258.

(4) For a history of development of this area, see: "Gmelin Handbook of Inorganic Chemistry", 8th ed. Vol. 59, Iron, Part B, pp 471-477, 517 (1932).

(5) Pavel, O. *Ber. Dtsch. Chem. Ges.* 1882, 15, 2600.

(6) Lin, X.; Huang, J.; Lu, J. *Acta Crystallogr., Sect. A: Cryst. Phys., Diffraction, Theor. Gen. Crystallogr.* 1981, A37, C-232.

(7) Hofmann, K. A.; Wiede, D. F. Z. *Anorg. Chem.* 1895, 9, 295.

(8) Thomas, J. T.; Robertson, J. H.; Cox, E. G. *Acta Crystallogr.* 1958, 11, 599.

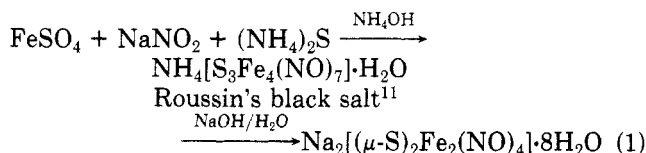
(9) Dahl, L. F.; Wei, C. F. *Inorg. Chem.* 1963, 2, 328.

group or a heteroatom has bridged the two sulfur atoms.<sup>1</sup> Such bridging reactions should not be possible in the case of  $[(\mu\text{-S})_2\text{Fe}_2(\text{NO})_4]^{2-}$ , in which the bridging S<sup>-</sup> ligands are much farther apart, at least not without a change in S<sub>2</sub>Fe<sub>2</sub> geometry from a planar to a puckered ring.

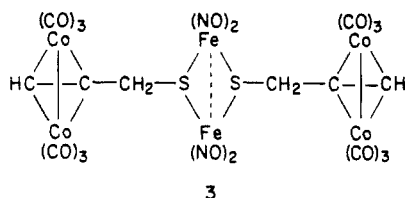
With such considerations in mind, we embarked on a study of the chemistry of the  $[(\mu\text{-S})_2\text{Fe}_2(\text{NO})_4]^{2-}$  anion.

### Results and Discussion

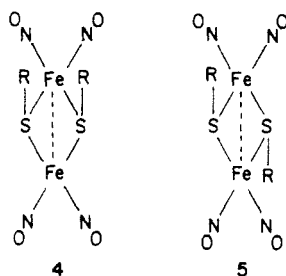
This work was carried out for the most part by using Roussin's red sodium salt prepared as shown in eq 1, which



is the original Roussin preparation as described by Seel.<sup>10</sup> The reaction with reactive organic halides to give  $(\mu\text{-RS})_2\text{Fe}_2(\text{NO})_4$  complexes we found to be a general one which gives high yields. In our various reactions R = CH<sub>3</sub> (91%), C<sub>2</sub>H<sub>5</sub> (91%), CH<sub>2</sub>=CHCH<sub>2</sub> (91%), PhCH<sub>2</sub> (93%), HC≡CCH<sub>2</sub> (91%), Me<sub>3</sub>SiCH<sub>2</sub> (97%), and CH<sub>3</sub>C(O)CH<sub>2</sub> (95%). All of these compounds were isolated as red-black, crystalline solids. Reaction of the propargyl derivative with Co<sub>2</sub>(CO)<sub>8</sub> gave the acetylene complex 3.



In principle, the  $(\mu\text{-RS})_2\text{Fe}_2(\text{NO})_4$  complexes can exist as syn, 4, and anti, 5, isomers. The structural study of



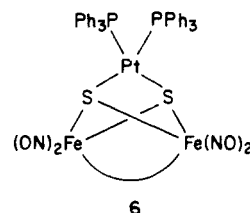
$(\mu\text{-C}_2\text{H}_5\text{S})_2\text{Fe}_2(\text{NO})_4$  in the solid state showed evidence only for the anti isomer.<sup>8</sup> However, the NMR spectra of solutions of such complexes show the presence of two isomers. For instance, the proton NMR spectrum (in CDCl<sub>3</sub>) of  $(\mu\text{-CH}_3\text{S})_2\text{Fe}_2(\text{NO})_4$  showed this compound to exist as a mixture of the syn and anti isomers. Thus the 250-MHz NMR spectrum of this complex (in C<sub>6</sub>D<sub>6</sub>) showed singlets at  $\delta$  2.08 and 2.14 in 44:56 integrated intensity ratio. Examination of the temperature-dependent 250-MHz NMR spectrum of  $(\mu\text{-CH}_3\text{S})_2\text{Fe}_2(\text{NO})_4$  showed the two isomers to interconvert rapidly. The 250-MHz <sup>1</sup>H NMR spectra of all other  $(\mu\text{-RS})_2\text{Fe}_2(\text{NO})_4$  complexes showed that both isomers were present in their solutions. Furthermore, the <sup>13</sup>C NMR spectra of these complexes very often showed two different carbon atoms bound to the sulfur atoms, giving confirmation of the presence of isomers in the alkyl esters of Roussin's red salt.

The organic derivatives of Roussin's red salt,  $(\mu\text{-RS})_2\text{Fe}_2(\text{NO})_4$ , also may be prepared directly from Roussin's black salt, without prior preparation of Roussin's red salt. Thus the reaction of NH<sub>4</sub>[Fe<sub>4</sub>S<sub>3</sub>(NO)<sub>7</sub>]·H<sub>2</sub>O with potassium hydride in ~1:4 molar ratio in THF solution at room temperature for 12 h, followed by addition of ethyl iodide, gave  $(\mu\text{-C}_2\text{H}_5\text{S})_2\text{Fe}_2(\text{NO})_4$  in 56% yield. The methyl derivative  $(\mu\text{-CH}_3\text{S})_2\text{Fe}_2(\text{NO})_4$  also was prepared by this procedure.

Roussin's red sodium salt reacted readily with organometallic halides to give products of type  $(\mu\text{-R}_n\text{MS})_2\text{Fe}_2(\text{NO})_4$ . Prepared in such reactions were  $(\mu\text{-Me}_3\text{SnS})_2\text{Fe}_2(\text{NO})_4$ ,  $(\mu\text{-Ph}_3\text{SnS})_2\text{Fe}_2(\text{NO})_4$ ,  $(\mu\text{-Ph}_3\text{PbS})_2\text{Fe}_2(\text{NO})_4$ ,  $(\mu\text{-PhHgS})_2\text{Fe}_2(\text{NO})_4$ , and  $(\mu\text{-CH}_3\text{HgS})_2\text{Fe}_2(\text{NO})_4$ . The structure of the last of these, determined by X-ray crystallography, has been reported.<sup>11</sup> It was found that isomer 5 (R = CH<sub>3</sub>Hg) was present. While electron-impact mass spectroscopy was very useful in the characterization of the organic derivatives of Roussin's red salt (the molecular ion and fragment ions of type  $[\text{M}^+ - n\text{NO}]$  ( $n = 1\text{-}4$ ) were observed), in the case of these less volatile metal derivatives we had to resort to field desorption (FD) techniques.<sup>12</sup> In the FD mass spectra the molecular ions, M<sup>+</sup>, were observed.

Reactions of Roussin's red salt with dihalides such as Me<sub>2</sub>SnCl<sub>2</sub> and Ph<sub>2</sub>PbCl<sub>2</sub> were not successful in that the expected bridged products were not isolated. Presumably, the long S...S nonbonded distance in the dianion<sup>6</sup> is the critical factor responsible for this.

Attempted reactions with several transition-metal halides, e.g.,  $\eta^5\text{-C}_5\text{H}_5\text{Fe}(\text{CO})_2\text{Br}$ , Mn(CO)<sub>5</sub>Br,  $\eta^3\text{-C}_3\text{H}_5\text{Fe}(\text{CO})_3\text{I}$ ,  $\eta^5\text{-C}_5\text{H}_5\text{Mo}(\text{CO})_3\text{I}$ , and  $\eta^5\text{-C}_5\text{H}_5\text{Ni}(\text{Ph}_3\text{P})\text{Br}$ , with Roussin's red salt were not successful. This may be because these halides are too hindered or not potent enough electrophiles. In this connection it is significant that  $[\eta^5\text{-C}_5\text{H}_5\text{Fe}(\text{CO})_2\text{-(THF)}]\text{BF}_4$ , a more potent electrophile than  $\eta^5\text{-C}_5\text{H}_5\text{Fe}(\text{CO})_2\text{Br}$ , did react with Roussin's red sodium salt in THF to give  $[\mu\text{-}\eta^5\text{-C}_5\text{H}_5\text{Fe}(\text{CO})_2\text{S}]_2\text{Fe}_2(\text{NO})_4 \cdot \text{CH}_2\text{Cl}_2$  in high yield. So it is not a matter of product instability in the case of the  $\eta^5\text{-C}_5\text{H}_5\text{Fe}(\text{CO})_2\text{Br}/[\text{S}_2\text{Fe}_2(\text{NO})_4]^{2-}$  reaction. Attempted reactions of Roussin's red sodium salt with transition-metal dihalides met with only limited success. A reaction with *cis*-(Ph<sub>3</sub>P)<sub>2</sub>PtCl<sub>2</sub> gave (Ph<sub>3</sub>P)<sub>2</sub>Pt( $\mu_3\text{-S}$ )<sub>2</sub>Fe<sub>2</sub>(NO)<sub>4</sub> (6) as an



air-sensitive, red-black crystalline solid in 97% yield. Full details of this reaction as well as of the structure determination of 6 by X-ray crystallography already have been reported.<sup>13</sup> However, similar reactions with (Ph<sub>3</sub>P)<sub>2</sub>NiCl<sub>2</sub> and (Ph<sub>3</sub>P)<sub>2</sub>PdCl<sub>2</sub> did not give an isolable product.

A more complicated reaction course was observed when metal carbonyl dihalides were allowed to react with Roussin's red sodium salt. In the reaction of (OC)<sub>4</sub>FeI<sub>2</sub> with Na<sub>2</sub>[( $\mu\text{-S}$ )<sub>2</sub>Fe<sub>2</sub>(NO)<sub>4</sub>]·8H<sub>2</sub>O three products were isolated, but only in low yield:  $(\mu\text{-S}_2)\text{Fe}_2(\text{CO})_6$  (10%),  $(\mu_3\text{-S})_2\text{Fe}_3(\text{CO})_9$  (1%), and S<sub>4</sub>Fe<sub>4</sub>(NO)<sub>4</sub> (1%). The latter is a cubane-type cluster which had been prepared earlier by Dahl and co-workers by the reaction of S<sub>8</sub> with Hg[Fe(C-

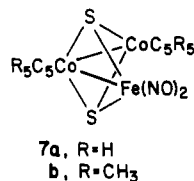
(10) Seel, F. In "Handbook of Preparative Inorganic Chemistry": 2nd ed., Brauer, G., Ed.; Academic Press: New York, 1965: Vol. 2, pp 1763-1764.

(11) Mak, T. C. W.; Book, L.; Chieh, C.; Gallagher, M. K.; Song, L.-C.; Seyferth, D. *Inorg. Chim. Acta* 1983, 73, 159.

(12) Costello, C. E. "Spectra"; Finnigan MAT Corp.: Sunnyvale, CA, 1982: Vol. 8, No. 1, p 28.

(13) Mazany, A. M.; Fackler, J. P., Jr.; Gallagher, M. K.; Seyferth, D. *Inorg. Chem.* 1983, 22, 2593.

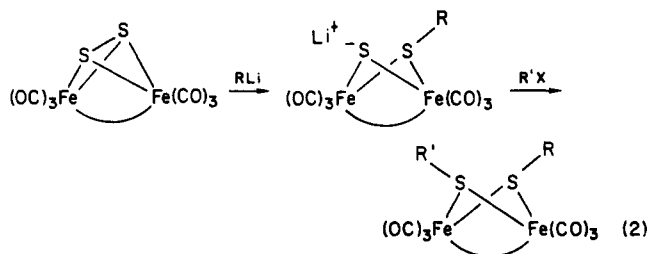
$O)_3NO)_2$ .<sup>14</sup> The cobalt complexes  $\eta^5\text{-C}_5\text{H}_5\text{Co}(\text{CO})\text{I}_2$  and  $\eta^5\text{-C}_5\text{Me}_5\text{Co}(\text{CO})\text{I}_2$  reacted with Roussin's red sodium salt to give the unexpected  $(\text{ON})_2\text{Fe}(\mu\text{-S})_2\text{Co}_2(\eta^5\text{-C}_5\text{R}_5)_2$  (**7**) in



low yield (11–25%, R = H; 12%, R = CH<sub>3</sub>). Although the mechanism of the formation of **7** is not clear, we found the yield of **7** to be quite dependent on reactant stoichiometry. Initially a 1:1 stoichiometry was used, and the yields reported above were obtained. The fact that the products actually obtained contained Co and Fe in 2:1 ratio led us to examine 2:1  $\eta^5\text{-C}_5\text{H}_5\text{Co}(\text{CO})\text{I}_2/\text{Na}_2[\text{S}_2\text{Fe}(\text{NO})_4]\cdot 8\text{H}_2\text{O}$  reactions. These, however, gave no **7**, and instead, the known<sup>15</sup>  $(\mu^3\text{-S})_2\text{Co}_3(\eta^5\text{-C}_5\text{H}_5)_3$  was isolated in 5% yield.

The structure shown for **7** at first was based only on spectroscopic data. Confirmation was provided by an X-ray diffraction study of **7b** which also revealed some interesting structural and bonding features (vide infra).

Finally, we note three other routes to complexes of type  $(\mu\text{-RS})_2\text{Fe}_2(\text{NO})_4$ . The scope of these routes has not been investigated, so it remains to be seen if they are more generally applicable. The route with the greatest potential for general applicability is based on the nitrosylation of the easily prepared  $(\mu\text{-RS})_2\text{Fe}_2(\text{CO})_6$  complexes. This reaction was used first by Hieber and Beutner<sup>16</sup> to convert  $(\mu\text{-H}_2\text{N})_2\text{Fe}_2(\text{CO})_6$  to  $(\mu\text{-H}_2\text{N})_2\text{Fe}_2(\text{NO})_4$ . We found this procedure to be quite useful in the conversion of  $(\mu\text{-RS})_2\text{Fe}_2(\text{CO})_6$  to  $(\mu\text{-RS})_2\text{Fe}_2(\text{NO})_4$ . For instance, for the R = CH<sub>3</sub> case, the yield of the nitrosylation reaction was 97% when NO was bubbled into a refluxing benzene solution of  $(\mu\text{-CH}_3\text{S})_2\text{Fe}_2(\text{CO})_6$ . This procedure served well in the preparation of unsymmetrical alkyl and aryl derivatives of Roussin's red salt, compounds which cannot be prepared directly from the  $[(\mu\text{-S})_2\text{Fe}_2(\text{NO})_4]^{2-}$  anion. The corresponding hexacarbonyl complexes are easily prepared from  $(\mu\text{-S})_2\text{Fe}_2(\text{CO})_6$  as shown in eq 2.<sup>17</sup> Using



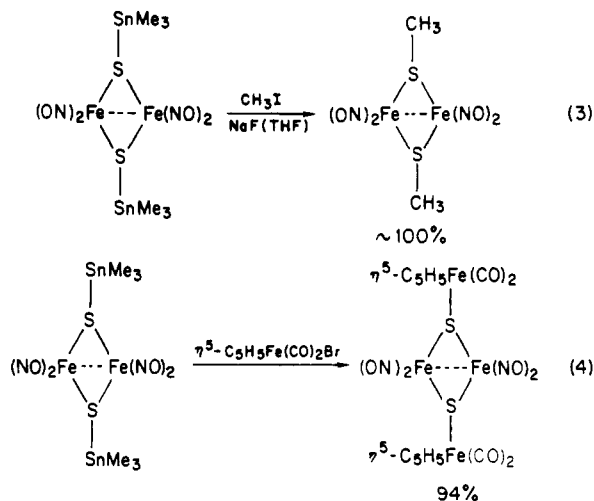
the nitrosylation reaction,  $(\mu\text{-CH}_3\text{S})(\mu\text{-C}_6\text{H}_5\text{S})\text{Fe}_2(\text{CO})_6$  and  $(\mu\text{-CH}_3\text{S})(\mu\text{-p-CH}_3\text{C}_6\text{H}_4\text{S})\text{Fe}_2(\text{CO})_6$  were converted to the respective tetranitrosyl complexes in yields of 65% and 83%, respectively. Such CO-by-NO replacement via nitric oxide also could be used to convert  $(\mu\text{-CH}_3\text{Se})_2\text{Fe}_2(\text{CO})_6$  to  $(\mu\text{-CH}_3\text{Se})_2\text{Fe}_2(\text{NO})_4$  in 83% yield. Nitrosylation of the carbonyl complexes was in particular very successful in the synthesis of  $(\text{Ph}_3\text{P})_2\text{Pt}(\mu\text{-S})_2\text{Fe}_2(\text{NO})_4$  from  $(\text{Ph}_3\text{P})_2\text{Pt}(\mu\text{-S})_2\text{Fe}_2(\text{CO})_6$  (90% yield) and of  $(\mu\text{-S})_2(\eta^5\text{-C}_5\text{H}_5)_2\text{Co}_2\text{Fe}(\text{NO})_2$  (**7**) from  $(\mu^3\text{-S})_2(\eta^5\text{-C}_5\text{H}_5)\text{CoFe}_2(\text{CO})_6$  in

79% yield (based on cobalt). This is a superior route to **7** than that based on the  $[(\mu\text{-S})_2\text{Fe}_2(\text{NO})_4]^{2-}/\eta^5\text{-C}_5\text{H}_5\text{Co}(\text{CO})\text{I}_2$  reaction. It also is an unexpected reaction in that an  $\text{S}_2\text{CoFe}_2$  cluster is converted in this way to an  $\text{S}_2\text{Co}_2\text{Fe}$  cluster.

The nitrosyl analogue of  $(\mu\text{-S}_2)\text{Fe}_2(\text{CO})_6$  has not yet been reported. We investigated the reaction of  $(\mu\text{-S}_2)\text{Fe}_2(\text{CO})_6$  with nitric oxide in order to try and form the nitrosyl analogue directly. Initially, we observed no reaction between the hexacarbonyl and NO with our standard conditions. But, when we allowed  $(\mu\text{-S}_2)\text{Fe}_2(\text{CO})_6$  to react with NO and trimethylamine *N*-oxide in refluxing methylene chloride, we observed the formation of  $(\mu\text{-S})_4\text{Fe}_4(\text{NO})_4$  in 12% yield. This suggests that  $(\mu\text{-S})_2\text{Fe}_2(\text{NO})_4$  may have been formed during the reaction but that the sulfur-sulfur bond is not strong enough to maintain the distorted tetrahedral geometry about the iron atoms, and the complex dimerizes with the loss of NO to give the observed cubane cluster instead.

After this study had been completed, other workers<sup>18,19</sup> reported a similar  $(\mu\text{-RS})_2\text{Fe}_2(\text{CO})_6$  to  $(\mu\text{-RS})_2\text{Fe}_2(\text{NO})_4$  conversion.

In another approach, a neutral, anhydrous alternative to the  $\text{Na}_2[(\mu\text{-S})_2\text{Fe}_2(\text{NO})_4]\cdot 8\text{H}_2\text{O}$  reagent was sought. Abel et al.<sup>20</sup> and others<sup>21</sup> have shown the tin-sulfur bond to be susceptible to cleavage by alkyl metal and metalloidal halides to give a tin halide and products with carbon-sulfur, metal-sulfur, and metalloidal-sulfur bonds, respectively.  $(\mu\text{-Me}_3\text{SnS})_2\text{Fe}_2(\text{NO})_4$ , which we had prepared from Roussin's red salt, reacted in similar fashion (eq 3 and 4). More general applicability seems probable.



Finally, we examined the possibility of using the bridging thiol complex  $(\mu\text{-HS})_2\text{Fe}_2(\text{NO})_4$  (**8**) as a synthetic intermediate in base-catalyzed Michael additions to  $\alpha,\beta$ -unsaturated olefins. In the hexacarbonyl family of compounds,  $(\mu\text{-HS})_2\text{Fe}_2(\text{CO})_6$  had been found to be a useful starting material for the preparation of diverse  $\text{Fe}_2(\text{CO})_6$  complexes containing bridging organosulfur ligands,<sup>22</sup> so the nitrosyl analogue also might show useful reactivity. However, it had been demonstrated that the  $[(\mu\text{-S})_2\text{Fe}_2(\text{NO})_4]^{2-}$  anion is very sensitive to acid, and in the absence

(18) Butler, A. R.; Glidewell, C.; McGinnis, J. *Inorg. Chim. Acta* **1982**, *64*, L77.

(19) Butler, A. R.; Glidewell, C.; Hyde, A. R.; McGinnis, J.; Seymour, J. E. *Polyhedron* **1983**, *1045*.

(20) Abel, E. W.; Brady, D. B.; Crosse, B. C. *J. Organomet. Chem.* **1966**, *5*, 260.

(21) Balcombe, C. I.; Macmullin, E. C.; Peach, M. E. *J. Inorg. Nucl. Chem.* **1975**, *37*, 1353.

(22) Seyferth, D.; Henderson, R. S. *J. Organomet. Chem.* **1981**, *218*, C34.

(14) Gall, R. S.; Chu, C. T.-W.; Dahl, L. F. *J. Am. Chem. Soc.* **1974**, *96*, 4019.

(15) Otsuka, S.; Nakamura, A.; Yoshida, T. *Justus Liebigs Ann. Chem.* **1968**, *719*, 54.

(16) Hieber, W.; Beutner, H. Z. *Anorg. Allg. Chem.* **1962**, *317*, 63.

(17) (a) Seyferth, D.; Henderson, R. S. *J. Am. Chem. Soc.* **1979**, *101*, 508. (b) Seyferth, D.; Henderson, R. S.; Song, L.-C.; Womack, G. B. *J. Organomet. Chem.*, in press.



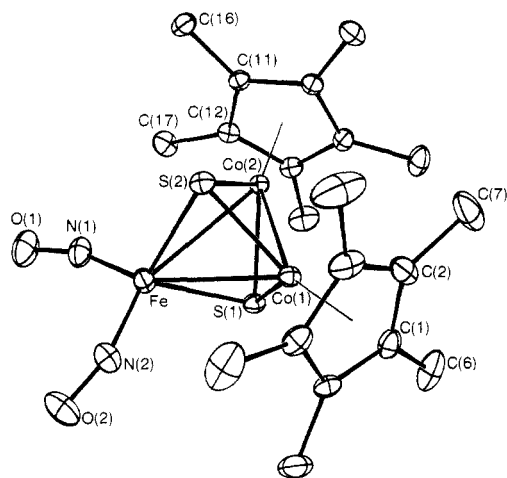


**Figure 1.** Perspective view of  $(\eta^5\text{-C}_5\text{Me}_5)_2\text{Co}_2(\mu_3\text{-S})_2\text{Fe}(\text{NO})_2$  showing the numbering scheme used. Carbon atoms within each cyclopentadienyl group are numbered sequentially around the ring such that for group 1 the ring atoms are C(1)–C(5) with attached methyl carbons as C(6)–C(10) and for group 2 the ring atoms are C(11)–C(15) with attached methyls as C(16)–C(20). Thermal ellipsoids are shown at the 20% level.

**Table I. Summary of Crystal Data and Details of Intensity Collection for  $(\eta^5\text{-C}_5\text{Me}_5)_2\text{Co}_2(\mu_3\text{-S})_2\text{Fe}(\text{NO})_2$**

compd	$(\eta^5\text{-C}_5\text{Me}_5)_2\text{Co}_2(\mu_3\text{-S})_2\text{Fe}(\text{NO})_2$
fw	568.32
space group	$C2/c$ (no. 15)
$a$ , Å	32.951 (5)
$b$ , Å	8.755 (1)
$c$ , Å	17.619 (2)
$\beta$ , deg	112.23 (1)
$V$ , Å <sup>3</sup>	4705.0
$\rho_{\text{calc}}$ , g/cm <sup>3</sup>	1.604
radiatn	Mo K $\alpha$ , $\bar{\alpha} = 0.71073$ Å
detector aperture, mm	4 (2.00 + 1.00 tan $\theta$ )
$2\theta$ limit, deg	52.0°
scan type	$\omega/2\theta$
scan width, deg	(0.70 + 0.347 tan $\theta$ ) in $\omega$
bkgd	25% on low- and high-angle sides
indices collected	$h, k, \pm l$
reflectns obsd	3662
abs coeff $\mu$ , cm <sup>-1</sup>	21.91
cryst dimens, mm	0.23 × 0.38 × 0.30
grid size	8 × 8 × 8
range in trans factors	0.601–0.730
final no. of parameters varied	262
errors in obsvn of unit weight	1.772
$R$	0.028
$R_w$	0.039

of an excess of base it has been found to decompose to the anion of Roussin's black salt,  $[\text{Fe}_4\text{S}_3(\text{NO})_7]^-$ . In particular, our attempts to isolate **8**, either from a THF solution of Roussin's red sodium salt acidified with  $\text{CF}_3\text{CO}_2\text{H}$  or from an aqueous solution acidified with HCl gave no isolable products. At the time of these experiments Beck and co-workers<sup>23</sup> reported the synthesis of **8** by acidification of  $[\text{Ph}_4\text{As}]_2[(\mu\text{-S})_2\text{Fe}_2(\text{NO})_4]$  in pentane at  $-40$  °C, but in only 5–10% yield. In view of the apparent poor stability of **8**, we focused our further efforts on its *in situ* utilization. This approach was successful. In one such experiment, a solution of Roussin's red sodium salt and methyl acrylate in THF was acidified at  $-78$  °C. Subsequently, an excess of piperidine was added. The product which was isolated was that of a Michael addition reaction ( $\mu\text{-MeO}_2\text{CCH}_2\text{CH}_2\text{S})_2\text{Fe}_2(\text{NO})_4$ , in 97% yield. A similar reaction in which acrylonitrile was the  $\alpha,\beta$ -unsaturated olefin

**Table II. Positional Parameters and Equivalent Isotropic  $B$ 's for Non-Hydrogen Atoms**

atom	$x$	$y$	$z$	$B$ , Å <sup>2</sup>
Co(1)	0.40558 (1)	0.37074 (4)	0.56021 (2)	2.646 (7)
Co(2)	0.33667 (1)	0.48742 (4)	0.45606 (2)	2.245 (6)
Fe	0.37704 (1)	0.24782 (5)	0.40468 (2)	3.357 (8)
S(1)	0.40061 (2)	0.48595 (8)	0.44757 (4)	2.85 (1)
S(2)	0.34422 (2)	0.25036 (7)	0.49677 (4)	2.86 (1)
O(1)	0.32728 (8)	0.1828 (3)	0.2395 (1)	6.38 (7)
O(2)	0.43942 (9)	0.0293 (4)	0.4072 (2)	9.40 (9)
N(1)	0.34283 (8)	0.2297 (3)	0.3070 (1)	4.38 (6)
N(2)	0.41796 (9)	0.1235 (3)	0.4209 (2)	5.39 (7)
C(1)	0.45734 (9)	0.4868 (3)	0.6456 (2)	3.75 (7)
C(2)	0.42615 (9)	0.4492 (4)	0.6811 (2)	4.76 (7)
C(3)	0.42127 (9)	0.2889 (4)	0.6780 (2)	4.74 (8)
C(4)	0.44993 (9)	0.2251 (3)	0.6433 (2)	3.97 (7)
C(5)	0.47195 (8)	0.3476 (3)	0.6239 (2)	3.31 (6)
C(6)	0.4728 (1)	0.6430 (4)	0.6349 (2)	6.4 (1)
C(7)	0.4048 (1)	0.5604 (6)	0.7187 (2)	8.7 (1)
C(8)	0.3923 (1)	0.1988 (6)	0.7100 (2)	9.1 (1)
C(9)	0.4564 (1)	0.0591 (4)	0.6325 (3)	7.4 (1)
C(10)	0.50613 (9)	0.3305 (5)	0.5865 (2)	5.47 (9)
C(11)	0.26937 (7)	0.5104 (3)	0.4128 (2)	2.63 (5)
C(12)	0.28588 (7)	0.5806 (3)	0.3575 (1)	2.82 (5)
C(13)	0.31528 (8)	0.6983 (3)	0.4012 (2)	3.04 (5)
C(14)	0.31705 (8)	0.7006 (3)	0.4832 (2)	3.04 (6)
C(15)	0.28864 (7)	0.5843 (3)	0.4904 (1)	2.77 (5)
C(16)	0.23560 (8)	0.3862 (3)	0.3919 (2)	3.76 (6)
C(17)	0.27362 (9)	0.5391 (4)	0.2693 (2)	4.24 (7)
C(18)	0.3391 (1)	0.8080 (4)	0.3668 (2)	5.04 (8)
C(19)	0.3421 (1)	0.8159 (4)	0.5467 (2)	4.70 (8)
C(20)	0.27939 (8)	0.5497 (4)	0.5660 (2)	3.94 (6)

<sup>a</sup> Anisotropically refined atoms are given in the form of their equivalent isotropic thermal parameter defined as  $\frac{1}{3}[a^2B(1,1) + b^2B(2,2) + c^2B(3,3) + ab(\cos \gamma)B(1,2) + ac(\cos \beta)B(1,3) + bc(\cos \alpha)B(2,3)]$ .

**Table III. Selected Distances (Å) in  $(\eta^5\text{-C}_5\text{Me}_5)_2\text{Co}_2(\mu_3\text{-S})_2\text{Fe}(\text{NO})_2$**

Co(1)–Co(2)	2.5326 (4)	N(2)–O(2)	1.169 (3)
Co(1)–Fe	2.7571 (4)	C(1)–C(2)	1.429 (4)
Co(2)–Fe	2.8107 (4)	C(2)–C(3)	1.411 (4)
Co(1)–S(1)	2.1765 (6)	C(3)–C(4)	1.419 (4)
Co(1)–S(2)	2.1768 (6)	C(4)–C(5)	1.407 (3)
Co(2)–S(1)	2.1679 (5)	C(5)–C(1)	1.415 (3)
Co(2)–S(2)	2.1792 (5)	C(11)–C(12)	1.423 (3)
Fe–S(1)	2.2532 (6)	C(12)–C(13)	1.424 (3)
Fe–S(2)	2.2649 (6)	C(13)–C(14)	1.425 (3)
Co(1)–C(1)	2.064 (2)	C(14)–C(15)	1.421 (3)
Co(1)–C(2)	2.091 (2)	C(15)–C(11)	1.426 (3)
Co(1)–C(3)	2.068 (2)	C(1)–C(6)	1.495 (3)
Co(1)–C(4)	2.070 (2)	C(2)–C(7)	1.495 (4)
Co(1)–C(5)	2.056 (2)	C(3)–C(8)	1.503 (4)
Co(2)–C(11)	2.064 (2)	C(4)–C(9)	1.491 (4)
Co(2)–C(12)	2.069 (2)	C(5)–C(10)	1.512 (3)
Co(2)–C(13)	2.079 (2)	C(11)–C(16)	1.498 (3)
Co(2)–C(14)	2.089 (2)	C(12)–C(17)	1.495 (3)
Co(2)–C(15)	2.077 (2)	C(13)–C(18)	1.505 (3)
Fe–N(1)	1.670 (2)	C(14)–C(19)	1.501 (3)
Fe–N(2)	1.671 (2)	C(15)–C(20)	1.505 (3)
N(1)–O(1)	1.177 (2)		

used gave  $(\mu\text{-NCCH}_2\text{CH}_2\text{S})_2\text{Fe}_2(\text{NO})_4$ .

As the discussion above has shown, one can develop a fair amount of new chemistry with the long-known Roussin's red salt. This chemistry is limited due to the structure of the anion, i.e., by the long S...S distance and by the fact that the anion is not stable in acid solution.

We note also interesting published contributions by other workers to the chemistry of Roussin's red salt which appeared during the course of our work: by Beck et al.,<sup>23</sup> by Rauchfuss and Weatherill,<sup>24</sup> and by Glidewell and his co-workers.<sup>18,19</sup> As a result of these investigations and of

(23) Beck, W.; Grenz, R.; Gotzfried, F.; Vilsmaier, E. *Chem. Ber.* 1981, 114, 3184.

(24) Rauchfuss, T. B.; Weatherill, T. D. *Inorg. Chem.* 1982, 21, 827.

Table IV. Selected Angles (deg) in  $(\eta^5\text{-C}_5\text{Me}_5)_2\text{Co}_2(\mu_3\text{-S})_2\text{Fe}(\text{NO})_2$

Co(2)-Co(1)-Fe	64.03 (1)	Fe-N(1)-O(1)	160.2 (2)
Co(2)-Co(1)-S(1)	54.18 (2)	Fe-N(2)-O(2)	159.4 (3)
Co(2)-Co(1)-S(2)	54.49 (2)	C(2)-C(1)-C(5)	107.1 (2)
Fe-Co(1)-S(1)	52.77 (2)	C(2)-C(1)-C(6)	126.9 (3)
Fe-Co(1)-S(2)	53.09 (2)	C(5)-C(1)-C(6)	126.0 (3)
S(1)-Co(1)-S(2)	91.22 (2)	C(1)-C(2)-C(3)	107.6 (2)
Co(1)-Co(2)-Fe	61.87 (1)	C(1)-C(2)-C(7)	125.5 (3)
Co(1)-Co(2)-S(1)	54.50 (2)	C(3)-C(2)-C(7)	126.8 (3)
Co(1)-Co(2)-S(2)	54.41 (2)	C(2)-C(3)-C(4)	108.9 (2)
Fe-Co(2)-S(1)	51.88 (2)	C(2)-C(3)-C(8)	125.9 (3)
Fe-Co(2)-S(2)	52.14 (2)	C(4)-C(3)-C(8)	125.2 (3)
S(1)-Co(2)-S(2)	91.39 (2)	C(3)-C(4)-C(5)	107.0 (2)
Co(1)-Fe-Co(2)	54.10 (1)	C(3)-C(4)-C(9)	126.1 (3)
Co(1)-Fe-S(1)	50.27 (2)	C(5)-C(4)-C(9)	126.9 (3)
Co(1)-Fe-S(2)	50.21 (2)	C(1)-C(5)-C(4)	109.4 (2)
Co(1)-Fe-N(1)	154.77 (8)	C(1)-C(5)-C(10)	126.0 (2)
Co(1)-Fe-N(2)	97.73 (9)	C(4)-C(5)-C(10)	124.6 (2)
Co(2)-Fe-S(1)	49.20 (1)	C(12)-C(11)-C(15)	108.3 (2)
Co(2)-Fe-S(2)	49.43 (2)	C(12)-C(11)-C(16)	125.8 (2)
Co(2)-Fe-N(1)	100.69 (8)	C(15)-C(11)-C(16)	125.8 (2)
Co(2)-Fe-N(2)	151.70 (9)	C(11)-C(12)-C(13)	107.5 (2)
S(1)-Fe-S(2)	87.03 (2)	C(11)-C(12)-C(17)	125.7 (2)
S(1)-Fe-N(1)	116.50 (7)	C(13)-C(12)-C(17)	126.8 (2)
S(1)-Fe-N(2)	113.06 (8)	C(12)-C(13)-C(14)	108.5 (2)
S(2)-Fe-N(1)	114.83 (7)	C(12)-C(13)-C(18)	126.6 (2)
S(2)-Fe-N(2)	117.20 (9)	C(14)-C(13)-C(18)	124.9 (2)
N(1)-Fe-N(2)	107.5 (1)	C(13)-C(14)-C(15)	107.8 (2)
Co(1)-S(1)-Co(2)	71.32 (2)	C(13)-C(14)-C(19)	124.4 (2)
Co(1)-S(1)-Fe	76.96 (2)	C(15)-C(14)-C(19)	127.7 (2)
Co(2)-S(1)-Fe	78.92 (2)	C(11)-C(15)-C(14)	108.0 (2)
Co(1)-S(2)-Co(2)	71.10 (2)	C(11)-C(15)-C(20)	126.2 (2)
Co(1)-S(2)-Fe	76.71 (2)	C(14)-C(15)-C(20)	125.7 (2)
Co(2)-S(2)-Fe	78.44 (2)		

the present study much more is known about the interesting salts which Roussin discovered 127 years ago.

**Description of Structure.** The complex  $(\eta^5\text{-C}_5\text{Me}_5)_2\text{Co}_2(\mu_3\text{-S})_2\text{Fe}(\text{NO})_2$  (**7b**) crystallizes in the space groups  $C2/c$  with eight molecules, separated by normal van der Waals contacts, in the unit cell. Figure 1 shows a perspective view of the complex, and the relevant bond lengths and angles are shown in Tables III and IV. This heteronuclear cluster consists of an inner  $\text{Co}_2\text{FeS}_2$  core having a distorted trigonal-bipyramidal structure in which the triangular  $\text{Co}_2\text{Fe}$  moiety is capped above and below by the triply bridging sulfido groups. Each Co atom is symmetrically bonded in an  $\eta^5$ -fashion to one of the two  $\text{C}_5\text{Me}_5$  groups, and the Fe atom has two terminal nitrosyl groups attached. The geometry about each Co atom is essentially identical and can be described as that of a four-legged piano stool in which the "legs" are described by the two Co-S bonds and the Co-Co and the Co-Fe bonds. This arrangement is rather symmetrical with all angles between the "legs" being near  $53^\circ$ . If the Co-Fe bonds are ignored, the Co geometries become distorted three-legged piano stools, but with obviously open sites where the Co-Fe bonds should be. About Fe the geometry is perhaps best described, without inclusion of the Co-Fe bonds, as distorted tetrahedral. In this geometry the N(1)-Fe-N(2) angle, at  $107.5 (1)^\circ$ , and the N-Fe-S angles (average  $115.4^\circ$ ) are close to the idealized value although the tetrahedron is flattened at the sulfur atoms with a small S(1)-Fe-S(2) angle of  $87.02 (2)^\circ$ .

All parameters associated with the  $\text{C}_5\text{Me}_5$  groups are essentially normal; the Co(1)-C distances range from 2.056 (2) to 2.091 (2) Å and the Co(2)-C distances range from 2.064 (2) to 2.089 (2) Å. In each case the longest Co-C distance is associated with the side of the two rings (C(2) and C(14), respectively) at which the closest approach between these rings occurs, indicating that the rings tilt somewhat to minimize nonbonded contacts with each

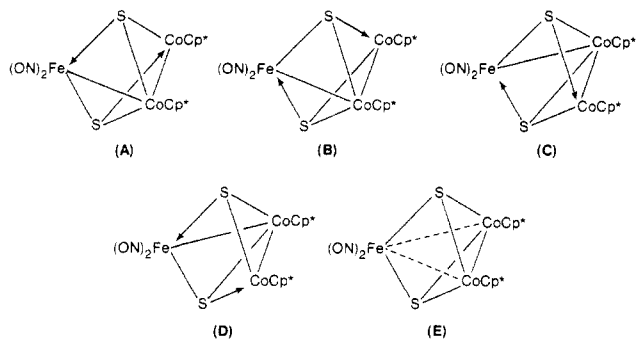
other. All C-C distances within the  $\text{C}_5$  rings, as well as those involving the methyl groups, are normal (average 1.420 and 1.500 Å, respectively).

Both nitrosyl groups are bent slightly with Fe-N-O angles of near  $160^\circ$ . Using the notation of Enemark and Feltham,<sup>25</sup> the iron nitrosyl fragment can be designated  $\{\text{Fe}(\text{NO})_2\}^9$  (vide infra) and as such the parameters involving the nitrosyl ligands are within the range of values previously reported for such species.<sup>26-30</sup> The geniculation of the two nitrosyl groups is also as expected<sup>31</sup> for a quasi-tetrahedral complex in which the N-M-N angle is less than  $130^\circ$ , with the oxygen atoms bent toward each other giving an O(1)-Fe-O(2) angle ( $90.89 (8)^\circ$ ) which is less than the N(1)-Fe-N(2) angle.

Within the  $\text{Co}_2\text{FeS}_2$  cluster the pattern of parameters seems somewhat unusual; although the Co and Fe atoms have essentially the same covalent radius, the metrical parameters involving these atoms in this structure differ considerably. The Co(1)-Co(2) distance (2.5326 (4) Å) is essentially as we would expect for a single bond, being comparable to the Co-Co distances in  $\text{Co}_2(\text{CO})_8$  (2.52 Å),<sup>32</sup>  $\text{Co}_4(\text{CO})_{12}$  (2.49 Å),<sup>33</sup> and  $\text{Co}_3(\text{CO})_9(\mu_3\text{-CCH}_3)$  (2.467 Å),<sup>34</sup> for example. However, the Co-Fe distances (2.7571 (4), 2.8107 (4) Å) are significantly longer than the Co-Co distance, suggesting weaker interactions for the former. These Co-Fe distances by themselves are not particularly unusual, being comparable to such distances in other CoFe clusters,<sup>35-39</sup> where a range from ca. 2.44 to 2.72 Å seems typical, and also being comparable to Fe-Fe distances in some iron nitrosyl complexes where bonding distances between 2.683 (2) and 2.747 (1) Å,<sup>27,29,47</sup> and even up to 3.089 (7) Å,<sup>28</sup> have been observed. However, the large difference between the two types of bonds within the same molecule does seem surprising. It may be that the observed difference is related to the different oxidation states of the atoms involved. Although the oxidation states of the metals in such a cluster are equivocal, it is clear that with linear nitrosyls, the oxidation state of Fe is lower than that of the Co atoms. As such, the covalent radius of Fe would be larger than that of Co. In agreement with this, the Fe-S distances (average 2.26 Å) are also larger than the Co-S distances (average 2.175 Å).

The observed discrepancy in metal-metal distances can also be explained if we consider the valence bond structures for the cluster which will give favorable 18-electron configurations at the metals. The four most reasonable structures, shown in A-D, give iron a -I oxidation state,

- (25) Enemark, J. H.; Feltham, R. D. *Coord. Chem. Rev.* **1974**, *13*, 339.  
 (26) Kopf, J.; Schmidt, J. Z. *Naturforsch., B: Anorg. Chem., Org. Chem.* **1975**, *30B*, 149.  
 (27) Clegg, W. *Inorg. Chem.* **1976**, *15*, 2928.  
 (28) Dahl, L. F.; de Gil, E. R.; Feltham, R. D. *J. Am. Chem. Soc.* **1969**, *91*, 1653.  
 (29) Thomas, J. T.; Robertson, J. H.; Cox, E. G. *Acta Crystallogr.* **1958**, *11*, 599.  
 (30) Chong, K. S.; Rettig, S. J.; Storr, A.; Trotter, J. *Can. J. Chem.* **1979**, *57*, 3119.  
 (31) Feltham, R. D.; Enemark, J. H. *Top. Stereochem.* **1981**, *12*, 156-215.  
 (32) Sumner, G. G.; Klug, H. P.; Alexander, L. E. *Acta Crystallogr.* **1964**, *17*, 732.  
 (33) Wei, C. H.; Dahl, L. F. *J. Am. Chem. Soc.* **1966**, *88*, 1821.  
 (34) Sutton, P. W.; Dahl, L. F. *J. Am. Chem. Soc.* **1967**, *89*, 261.  
 (35) Beurich, V. H.; Richter, F.; Vahrenkamp, H. *Acta Crystallogr., Sect. B: Struct. Crystallogr. Cryst. Chem.* **1982**, *B38*, 3012.  
 (36) Brun, P.; Dawkins, G. M.; Green, M.; Mills, R. M.; Salaün, J.-Y.; Stone, F. G. A.; Woodward, P. *J. Chem. Soc., Dalton Trans.* **1983**, 1357.  
 (37) Aime, S.; Osella, D.; Milone, L.; Lanfredi, A. M. M.; Tiripicchio, A. *Inorg. Chim. Acta* **1983**, *71*, 141.  
 (38) Vahrenkamp, H.; Wucherer, E. J.; Wolters, D. *Chem. Ber.* **1983**, *116*, 1219.  
 (39) Richter, F.; Beurich, H.; Müller, M.; Gärtner, N.; Vahrenkamp, H. *Chem. Ber.* **1983**, *116*, 3774.



consistent with the  $[\text{Fe}(\text{NO})_2]_3^9$  formalism alluded to earlier. As can be seen in the resonance structure (E) this results in a normal Co-Co bond but in only  $1/2$  bond orders for the Co-Fe bonds, consistent with these long distances. It is also worthy of note that a perusal of structures A-D shows that the Fe-S bonds differ from the Co-S bonds in the degree of dative bonding, so they too should differ, as is observed. Complex 7b is an interesting intermediate case between  $\text{S}_2\text{Fe}_3(\text{CO})_9$  (two metal-metal bonds) and  $\text{S}_2\text{Co}_3\text{Cp}_3$  (three metal-metal bonds of order  $2/3$ ). Throughout this discussion of the bonding we have tacitly assumed that the nitrosyl groups were functioning as normal linear nitrosyls, i.e., as three-electron donors. However, these groups are distinctly nonlinear and it is not at all clear how this influences the bonding within the cluster.

Apart from the asymmetry imparted to the bridging sulfido groups as alluded to above, the parameters involving these groups are normal for such triply bridging groups<sup>37,40</sup> in which the angles at sulfur are generally near  $75^\circ$ . The range in angles in the present structure ( $71.10(2)^\circ$ – $78.92(2)^\circ$ ) is again due to the differing Co-Fe and Co-Co distances with the larger angles being the Fe-S-Co values.

### Experimental Section

**General Comments.** All reactions were carried out under an atmosphere of prepurified nitrogen unless otherwise indicated. Air- and/or moisture-sensitive materials were handled either in a Vacuum Atmospheres HE-43 Dri-Lab glovebox or by using standard Schlenk techniques. Benzene, toluene, and tetrahydrofuran (THF) were purified by distillation from potassium or sodium/benzophenone ketyl under a nitrogen atmosphere. Pentane, hexane, and diethyl ether were purified by distillation from lithium aluminum hydride under a nitrogen atmosphere. All other solvents were of reagent grade and were used without further purification unless oxygen-free solvent was needed; then the solvent was purged with nitrogen for ca. 15 min. For the more stable compounds, thin-layer chromatography (TLC) could be used to monitor the progress of the reaction being studied (J.T. Baker silica gel plates) and column chromatography could be used to isolate the desired product using silicic acid as the support (Mallinckrodt reagent, 100–200 mesh). Air-sensitive compounds were chromatographed under nitrogen using Florisil (Fisher reagent, 100 mesh) as the support. The colors of the compounds made visualization of the chromatographs straightforward.

Proton nuclear magnetic resonance spectra were recorded at 60 MHz on a Varian Associates T-60 spectrometer. High-field proton NMR spectra were recorded at 250-MHz on a Bruker WM-250 operating in the Fourier transform mode. Chemical shifts are reported in  $\delta$  units, parts per million downfield from tetramethylsilane or using the solvent as the reference signal. Carbon-13 NMR spectra were recorded on a Bruker WM-270 operating at 67.9 MHz in the Fourier transform mode. Infrared spectra were obtained by using a Perkin-Elmer 457A, 283 or 1430 double-beam grating spectrophotometer. Solution samples were contained in 0.1-mm path length sodium chloride solution cells.

Mass spectra were recorded on a Varian MAT-44 or a Finnigan MAT 8200 mass spectrometer operating at 70 eV. Field desorption mass spectra were recorded on a Finnigan MAT 731 mass spectrometer. The relative intensities in FD mass spectra were determined by a ratio of the peak heights, normalizing the largest peak to 100%. Melting points were determined by using analytically pure samples, which were sealed in evacuated or nitrogen-filled capillaries, on a Büchi melting point apparatus and are uncorrected. Microanalyses were performed by Scandinavian Microanalytical Laboratories, Herlev, Denmark, or Galbraith Laboratories, Inc., Knoxville, TN. Samples were sent sealed in evacuated or nitrogen-filled vials.

**Preparation of Roussin's Red Sodium Salt.** A 4-L Erlenmeyer flask was charged with 36.0 g (0.52 mol) of  $\text{NaNO}_2$  and 160 mL of distilled water. The solid was dissolved, and then 40 mL of a 22% solution of  $(\text{NH}_4)_2\text{S}$  in 120 mL of distilled water was added to the solution. The pale yellow solution was heated at reflux until the solution turned a dark cherry-red. While this solution was being heated, a 1-L beaker was charged with 80 g (0.29 mol) of  $\text{FeSO}_4$  and 640 mL of distilled water. The solid was dissolved to give a pale green-blue solution which was added to the first solution when it had turned deep cherry-red. Instantly, upon addition of the ferrous sulfate solution the reaction mixture turned black. The solution was stirred while it was heated with a Bunsen burner. After 30 s, 100 mL of a 22%  $\text{NH}_4\text{OH}$  solution was added in small portions with stirring. The solution was heated at reflux for 10 min and then filtered (hot), quickly through folded paper towels (filter paper was found to be too fine and would clog almost instantly). The red-brown solid  $\text{Fe}(\text{OH})_3$  was discarded, and the black-brown solution was allowed to stand overnight. The black crystalline solid was collected and dried under vacuum to give 5.33 g (0.01 mol) of  $\text{NH}_4[\text{Fe}_4\text{S}_3(\text{NO})_7]$ . The compound was used without further purification.

A 200-mL beaker was charged with 21.13 g (0.037 mol) of  $\text{NH}_4[\text{Fe}_4\text{S}_3(\text{NO})_7]$  and 70 mL of a 10% NaOH solution. The mixture was stirred and heated in a water bath at  $80^\circ\text{C}$  until ammonia was no longer released, ca. 4 h. The solution was filtered hot and then reduced to half of its initial volume. After the mixture was left standing at room temperature overnight, red-brown crystals had formed and were collected. A second batch of crystals was obtained by reducing the volume of the solution. The solid was washed with diethyl ether and dried under vacuum to give 18.4 g (0.037 mol) of  $\text{Na}_2(\mu\text{-S})_2\text{Fe}_2(\text{NO})_4 \cdot 8\text{H}_2\text{O}$  as a red-brown solid. The solid was further purified by dissolution in THF (0.25 g/mL) under nitrogen. The deep red solution was filtered, and the solvent was removed under reduced pressure. The solid was dried under vacuum and stored in the drybox where it was found to be stable for several months.

**Reactions between Roussin's Red Sodium Salt and Organic Halides.** The preparation of  $(\mu\text{-CH}_3)_2\text{Fe}_2(\text{NO})_4$  is described as an example of the general procedure used. A 200-mL Schlenk flask equipped with a serum stopper and a stir-bar was charged with 1.0 g (2.06 mmol) of  $\text{Na}(\mu\text{-S})_2\text{Fe}_2(\text{NO})_4 \cdot 8\text{H}_2\text{O}$  and then flushed with nitrogen. THF (75 mL) was added, and a deep red solution was formed. To the stirred solution was added 0.31 mL (4.95 mmol) of methyl iodide dropwise by syringe. The solution was stirred for 5 h, and solvent was removed under reduced pressure. The dark solid was chromatographed (silicic acid-pentane) to yield 0.61 g (91% yield) of  $(\mu\text{-CH}_3)_2\text{Fe}_2(\text{NO})_4$  as a black-red crystalline solid which was recrystallized from *n*-pentane: mp  $92\text{--}93^\circ\text{C}$  (lit. mp  $88\text{--}89^\circ\text{C}$ ,<sup>23</sup>  $93.5^\circ\text{C}$ <sup>41</sup>).  $^1\text{H}$  NMR ( $\text{CDCl}_3$ ) (60 MHz):  $\delta$  2.87 (s,  $\text{CH}_3\text{S}$ ), 2.91 (s,  $\text{CH}_3\text{S}$ ), in  $\text{C}_6\text{D}_6$  (250 MHz),  $\delta$  2.08 (s,  $\text{CH}_3\text{S}$ ), 2.14 (s,  $\text{CH}_3\text{S}$ ) (isomer ratio = 44:56).  $^{13}\text{C}$  NMR ( $\text{C}_6\text{D}_6$ ) (67.9 MHz):  $\delta_{\text{C}}$  27.05 (q,  $J = 142.3$  Hz,  $\text{CH}_3$ ), 27.30 (q,  $J = 142.3$  Hz,  $\text{CH}_3$ ). IR ( $\text{CHCl}_3$ ) (nitrosyl region): 1780 vs, 1755 vs  $\text{cm}^{-1}$ . Mass spectrum,  $m/z$  (relative intensity): 326 (8.1,  $\text{M}^+$ ), 296 (15.9,  $\text{M}^+ - \text{NO}$ ), 266 (16.2,  $\text{M}^+ - 2\text{NO}$ ), 236 (33.4,  $\text{M}^+ - 3\text{NO}$ ), 206 (24.9,  $\text{M}^+ - 4\text{NO}$ ), 191 (65.3,  $\text{MeS}_2\text{Fe}_2^+$ ), 176 (100.0,  $\text{S}_2\text{Fe}_2^+$ ), 144 (62.7,  $\text{SFe}_2^+$ ), 103 (30.8,  $\text{MeSFe}^+$ ), 88 (13.1,  $\text{SFe}^+$ ), 56 (47.4,  $\text{Fe}^+$ ). Anal. Calcd for  $\text{C}_2\text{H}_6\text{Fe}_2\text{N}_4\text{O}_4\text{S}_2$ : C, 7.36; H, 1.86; N, 17.19. Found: C, 7.42; H, 1.96; N, 17.02.

This complex may be prepared directly from Roussin's black salt, albeit in lower yield.

(40) Chu, C. T.-W.; Dahl, L. F. *Inorg. Chem.* 1977, 16, 3245.

(41) Wang, G.-H.; Zhang, W.-X.; Chai, W.-G. *Adv. Mass Spectrom.* 1980, 8B, 1369.

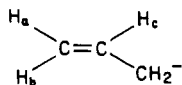
A 250-mL Schlenk flask equipped with a magnetic stir-bar and a serum stopped was charged with 1.00 g (1.77 mmol) of  $\text{NH}_4\text{[Fe}_4\text{S}_3(\text{NO})_7\text{]}\cdot\text{H}_2\text{O}$  and 0.30 g (7.5 mmol) of KH (Alfa) in the drybox. The flask was removed from the drybox and flushed with nitrogen. THF (75 mL) was added by syringe, and the resulting solution was stirred for 12 h. Then 2.5 mL (40 mmol) of methyl iodide was added by syringe, and the mixture was stirred for 4 h. The solvent was removed under reduced pressure and the residue chromatographed (silicic acid). Pentane eluted a red-brown band which, upon removal of solvent, gave 0.194 g (34%) of red-black  $(\mu\text{-CH}_3\text{S})_2\text{Fe}_2(\text{NO})_4$  which was recrystallized from pentane, mp 90–91.5 °C, and identified by comparison of its spectroscopic properties with those of an authentic sample.

Other  $(\mu\text{-RS})_2\text{Fe}_2(\text{NO})_4$  were prepared by using this general procedure for the alkylation of Roussin's red sodium salt.

$(\mu\text{-C}_2\text{H}_5\text{S})_2\text{Fe}_2(\text{NO})_4$ : red-black crystalline, moderately air-sensitive solid, in 91% yield. The complex was recrystallized from *n*-pentane: mp 78.5–80 °C (lit.<sup>10</sup> mp 78–80 °C).  $^1\text{H NMR}$  ( $\text{CDCl}_3$ ) (60 MHz):  $\delta$  1.63 (t,  $J = 7.4$  Hz, 3 H,  $\text{CH}_3$ ), 3.09 (q,  $J = 7.3$  Hz, 2 H,  $\text{CH}_2$ ); in  $\text{C}_6\text{D}_6$ ,  $\delta$  1.07 (t,  $J = 7.2$  Hz, 3 H,  $\text{CH}_3$ ), 1.09 (t,  $J = 7.3$  Hz, 3 H,  $\text{CH}_3$ ), 2.44 (d,  $J = 7.2$  Hz, 2 H,  $\text{CH}_2$ ), 2.52 (d,  $J = 7.3$  Hz, 2 H,  $\text{CH}_2$ ) (isomer ratio = 46:54).  $^{13}\text{C NMR}$  ( $\text{C}_6\text{D}_6$ ) (67.9 MHz):  $\delta_{\text{C}}$  18.99 (q,  $J = 128$  Hz,  $\text{CH}_3$ ), 39.49 (t,  $J = 142$  Hz,  $\text{CH}_2$ ), 40.20 (t,  $J = 142$  Hz,  $\text{CH}_2$ ). IR ( $\text{CHCl}_3$ ) nitrosyl region: 1778 vs, 1750 vs  $\text{cm}^{-1}$ . Mass spectrum,  $m/z$  (relative intensity): 354 (2.1,  $\text{M}^+$ ), 324 (3.5,  $\text{M}^+ - \text{NO}$ ), 294 (4.8,  $\text{M}^+ - 2\text{NO}$ ), 264 (3.7,  $\text{M}^+ - 3\text{NO}$ ), 234 (5.0,  $\text{M}^+ - 4\text{NO}$ ), 205 (16.0,  $\text{EtS}_2\text{Fe}_2^+$ ), 176 (100.0,  $\text{S}_2\text{Fe}_2^+$ ), 144 (64.8,  $\text{SFe}_2^+$ ), 56 (45.3,  $\text{Fe}^+$ ).

This compound also was prepared from Roussin's black ammonium salt in 56% yield by using the procedure described for the analogous preparation of the methyl derivative.

$(\mu\text{-CH}_2=\text{CHCH}_2\text{S})_2\text{Fe}_2(\text{NO})_4$ : a red-black, moderately air-sensitive, crystalline solid in 91% yield. The compound was recrystallized from pentane: mp 57–58 °C.  $^1\text{H NMR}$  ( $\text{CDCl}_3$ ) (60 MHz):  $\delta$  3.71 (d,  $J = 6$  Hz, 2 H,  $\text{CH}_2$ ), 5.11 (m, 1 H,  $\text{H}_\alpha$ ), 5.32 (m, 1 H,  $\text{H}_\beta$ ), 5.59–6.22 (m, 1 H,  $\text{H}_\gamma$ ). (The isomer ratio could not be determined).  $^{13}\text{C NMR}$  ( $\text{C}_4\text{D}_8\text{O}_2$ ) (67.9 MHz):  $\delta_{\text{C}}$  46.61 (t,



$J = 143$  Hz,  $\text{CH}_2$ ), 47.72 (t,  $J = 144$  Hz,  $\text{CH}_2$ ), 119.30 (t,  $J = 158$  Hz,  $=\text{CH}_2$ ), 136.50 (d,  $J = 159$  Hz,  $=\text{CH}$ ). IR ( $\text{CDCl}_3$ ) (nitrosyl region): 1782 vs, 1754 vs,  $\nu(\text{C}=\text{C})$  1660  $\text{cm}^{-1}$ . Mass spectrum,  $m/z$  (relative intensity): 378 (0.3,  $\text{M}^+$ ), 348 (2.6,  $\text{M}^+ - \text{NO}$ ), 318 (1.6,  $\text{M}^+ - 2\text{NO}$ ), 288 (1.8,  $\text{M}^+ - 3\text{NO}$ ), 258 (2.9,  $\text{M}^+ - 4\text{NO}$ ), 216 (1.7,  $\text{C}_3\text{H}_4\text{S}_2\text{Fe}_2^+$ ), 176 (0.9,  $\text{S}_2\text{Fe}_2^+$ ), 144 (0.4,  $\text{SFe}_2^+$ ), 56 (1.0,  $\text{Fe}^+$ ), 41 (55.0,  $\text{C}_3\text{H}_5^+$ ), 39 (100.0,  $\text{C}_3\text{H}_3^+$ ). Anal. Calcd. for  $\text{C}_8\text{H}_{10}\text{Fe}_2\text{N}_4\text{O}_4\text{S}_2$ : C, 19.67; H, 2.67; N, 14.82. Found: C, 19.54; H, 2.78; N, 14.70.

$(\mu\text{-PhCH}_2\text{S})_2\text{Fe}_2(\text{NO})_4$ : a red-purple, slightly air-sensitive, crystalline solid in 93% yield. The complex was recrystallized from  $\text{CH}_2\text{Cl}_2$ /pentane (1:4): mp 148–150 °C.  $^1\text{H NMR}$  ( $\text{CDCl}_3$ ) (60 MHz):  $\delta$  4.09 (s, 2 H,  $\text{CH}_2$ ), 4.15 (s, 2 H,  $\text{CH}_2$ ), 7.28–7.60 (m, 3 H,  $\text{C}_6\text{H}_5$ ); in  $\text{C}_4\text{D}_8\text{O}_2$ ,  $\delta$  4.23 (s, 2 H,  $\text{CH}_2$ ), 4.26 (s, 2 H,  $\text{CH}_2$ ), 7.15–7.48 (m, 5 H,  $\text{C}_6\text{H}_5$ ) (isomer ratio = 43:57). IR ( $\text{CDCl}_3$ ) (nitrosyl region): 1781 vs, 1753 vs  $\text{cm}^{-1}$ . Mass spectrum,  $m/z$  (relative intensity): 478 (0.4,  $\text{M}^+$ ), 448 (10.1,  $\text{M}^+ - \text{NO}$ ), 418 (9.0,  $\text{M}^+ - 2\text{NO}$ ), 388 (7.0,  $\text{M}^+ - 3\text{NO}$ ), 358 (13.5,  $\text{M}^+ - 4\text{NO}$ ), 267 (17.2,  $\text{PhCH}_2\text{S}_2\text{Fe}_2^+$ ), 175 (4.0,  $\text{S}_2\text{Fe}_2^+$ ), 91 (100.0,  $\text{PhCH}_3^+$ ), 56 (2.1,  $\text{Fe}^+$ ). Anal. Calcd. for  $\text{C}_{11}\text{H}_{14}\text{Fe}_2\text{N}_4\text{O}_4\text{S}_2$ : C, 35.17; H, 2.95; N, 11.72. Found: C, 35.20; H, 3.05; N, 11.45.

$(\mu\text{-HC}\equiv\text{CCH}_2\text{S})_2\text{Fe}_2(\text{NO})_4$ : a red-black crystalline solid. Recrystallization from dichloromethane/pentane gave 0.424 g (1.1 mmol) of  $(\mu\text{-HC}\equiv\text{C-CH}_2\text{S})_2\text{Fe}_2(\text{NO})_4$  as a slightly air-sensitive solid: mp 74–75 °C: 91% yield.  $^1\text{H NMR}$  ( $\text{CDCl}_3$ ) (60 MHz):  $\delta$  2.20–2.38 (m, 1 H,  $\text{HC}\equiv$ ), 3.40–4.20 (m, 2 H,  $\text{CH}_2\text{S}$ ); in  $\text{C}_6\text{D}_6$  (250 MHz),  $\delta$  1.70 (t,  $J = 2.7$  Hz, 1 H,  $\text{HC}\equiv$ ), 1.75 (t,  $J = 2.5$  Hz, 1 H,  $\text{HC}\equiv$ ), 3.06 (d,  $J = 2.7$  Hz, 2 H,  $\text{CH}_2\text{S}$ ), 3.11 (d,  $J = 2.5$  Hz, 2 H,  $\text{CH}_2\text{S}$ ) (isomer ratio = 43:57).  $^{13}\text{C NMR}$  ( $\text{C}_6\text{D}_6$ ) (67.9 MHz):  $\delta_{\text{C}}$  29.10 (t,  $J = 148$  Hz,  $\text{CH}_2$ ), 31.27 (t,  $J = 148$  Hz,  $\text{CH}_2$ ), 72.82 (d,  $J = 64$  Hz,  $\text{HC}\equiv$ ), 76.50 (d,  $J = 60$  Hz,  $\text{HC}\equiv$ ), 80.82 (s,  $\text{HC}\equiv\text{C}$ ), 81.55 (s,  $\text{HC}\equiv\text{C}$ ). IR ( $\text{CDCl}_3$ ) (nitrosyl region): 1788 vs, 1760 vs  $\text{cm}^{-1}$ . Mass spectrum,  $m/z$  (relative intensity): 374 (1.0,  $\text{M}^+$ ), 344 (10.0,  $\text{M}^+ - \text{NO}$ ), 314 (18.0,  $\text{M}^+ - 2\text{NO}$ ), 284 (11.7,  $\text{M}^+ - 3\text{NO}$ ), 254 (28.7,  $\text{M}^+ - 4\text{NO}$ ), 214 (12.8,  $\text{C}_3\text{H}_3\text{S}_2\text{Fe}_2^+$ ), 176

(100.0,  $\text{S}_2\text{Fe}_2^+$ ), 144 (3.0,  $\text{SFe}_2^+$ ). Anal. Calcd. for  $\text{C}_6\text{H}_6\text{Fe}_2\text{N}_4\text{O}_4\text{S}_2$ : C, 19.27; H, 1.62; N, 14.98. Found: C, 19.53; H, 1.75; N, 14.82.

$(\mu\text{-CH}_3\text{C}(\text{O})\text{CH}_2\text{S})_2\text{Fe}_2(\text{NO})_4$ : a brown-red crystalline, air-sensitive solid. Recrystallization from dichloromethane/pentane gave pure product, mp 133–135 °C, in 95% yield.  $^1\text{H NMR}$  ( $\text{CD}_2\text{Cl}_2$ ) (60 MHz):  $\delta$  2.25 (s, 3 H,  $\text{CH}_3$ ), 3.78 (s, 2 H,  $\text{CH}_2$ ). (The isomer ratio could not be determined.) IR ( $\text{CH}_2\text{Cl}_2$ ) (nitrosyl region): 1788 vs, 1759 vs,  $\nu(\text{C}=\text{O})$  1720 (sh)  $\text{cm}^{-1}$ . Anal. Calcd. for  $\text{C}_8\text{H}_{10}\text{Fe}_2\text{N}_4\text{O}_4\text{S}_2$ : C, 17.58; H, 2.46. Found: C, 17.70; H, 2.55.

$(\mu\text{-Me}_3\text{SiCH}_2\text{S})_2\text{Fe}_2(\text{NO})_4$ : a red-black crystalline, slightly air-sensitive solid, mp 95.5–96.5 °C (from  $\text{CH}_2\text{Cl}_2$ /pentane), in 97% yield.  $^1\text{H NMR}$  ( $\text{CDCl}_3$ ) (60 MHz):  $\delta$  0.21 (s, 9 H,  $(\text{CH}_3)_3\text{Si}$ ), 2.37 (s, 2 H,  $\text{CH}_2\text{S}$ ); in  $\text{C}_6\text{D}_6$  (250 MHz),  $\delta$  0.10 (s, 9 H,  $\text{CH}_3\text{Si}$ ), 0.12 (s, 9 H,  $\text{CH}_3\text{Si}$ ), 2.18 (s, 2 H,  $\text{CH}_2\text{S}$ ), 2.23 (s, 2 H,  $\text{CH}_2\text{S}$ ) (isomer ratio = 56:44).  $^{13}\text{C NMR}$  ( $\text{C}_6\text{D}_6$ ) (67.9 MHz):  $\delta_{\text{C}}$  2.11 (q,  $J = 120$  Hz,  $\text{CH}_3\text{Si}$ ), 33.28 (t,  $J = 131$  Hz,  $\text{CH}_2$ ), 33.39 (t,  $J = 131$  Hz,  $\text{CH}_2$ ). IR ( $\text{CHCl}_3$ ) (nitrosyl region): 1774 vs, 1749 vs,  $\text{cm}^{-1}$ . Anal. Calcd. for  $\text{C}_8\text{H}_{22}\text{Fe}_2\text{N}_4\text{O}_4\text{S}_2\text{Si}_2$ : C, 20.43; H, 4.72; N, 11.91. Found: C, 20.57; H, 4.76; N, 11.66.

**Reaction between [ $\mu\text{-Di}(2\text{-propynethiolato})$ ]bis(dinitrosyliron) and Dicobalt Octacarbonyl.** A 50-mL round-bottomed flask equipped with a magnetic stir-bar was charged with 0.294 g (0.79 mmol) of  $(\mu\text{-HC}\equiv\text{CCH}_2\text{S})_2\text{Fe}_2(\text{NO})_4$  and 0.610 g (1.78 mmol) of  $\text{Co}_2(\text{CO})_8$  in the drybox. Upon the addition of  $\text{Et}_2\text{O}$  (25 mL) gas evolution was observed for 15 min. The red-brown solution was stirred for 2 h, and then the solvent was removed under reduced pressure. The red-brown residue was chromatographed on Florisil and eluted with pentane to give a small amount of  $\text{Co}_2(\text{CO})_8$ . A second, red-brown band was eluted with 10% dichloromethane/pentane. Removal of the solvent under reduced pressure gave a red-brown solid which was dried under vacuum to yield 0.60 g (81%) 3. The solid was recrystallized from dichloromethane/diethyl ether to give a red-brown crystalline solid, mp 128–130 °C dec.  $^1\text{H NMR}$  ( $\text{CD}_2\text{Cl}_2$ ) (90 MHz):  $\delta$  4.35 (s, 2 H,  $\text{CH}_2$ ), 4.40 (s, 2 H,  $\text{CH}_2$ ), 6.35 (s, 1 H,  $\text{CH}$ ) (isomer ratio = 48:52). IR ( $\text{CD}_2\text{Cl}_2$ ): 1133 w, 955 m, 688 m; carbonyl region, 2102 m, 2063 s, 2038 s; nitrosyl region, 1882 s, 1855 s  $\text{cm}^{-1}$ . Anal. Calcd. for  $\text{C}_{18}\text{H}_6\text{Co}_4\text{Fe}_2\text{N}_4\text{O}_{16}\text{S}_2$ : C, 22.86; H, 0.64; N, 5.92. Found: C, 23.13; H, 0.77; N, 5.85.

**Reactions between Roussin's Red Sodium Salt and Organometallic Halides. (a) Triphenyltin Chloride.** A 300-mL Schlenk flask equipped with a serum stopper and a magnetic stir-bar ("standard apparatus") was charged with 1.00 g (2.06 mmol) of  $\text{Na}_2[(\mu\text{-S})_2\text{Fe}_2(\text{NO})_4]\cdot 8\text{H}_2\text{O}$  and then flushed with nitrogen. THF (75 mL) was added by syringe, followed by the addition of triphenyltin chloride (5 mmol) against a counterflow of nitrogen to the stirred solution. The solution was stirred for 2 h, and then the solvent was removed under reduced pressure. The residue was chromatographed (silicic acid–20%  $\text{CH}_2\text{Cl}_2$ /pentane). Dichloromethane eluted a red-brown band which, upon removal of solvent, gave 1.60 g (1.61 mmol) of  $(\mu\text{-Ph}_3\text{SnS})_2\text{Fe}_2(\text{NO})_4$  in 78% yield. The complex was recrystallized from dichloromethane/pentane to give a red-purple, air-sensitive, crystalline solid, mp 187–189 °C.  $^1\text{H NMR}$  ( $\text{CD}_2\text{Cl}_2$ ) (60 MHz):  $\delta$  7.12–7.55 (m,  $\text{C}_6\text{H}_5$ ). IR ( $\text{CD}_2\text{Cl}_2$ ) (nitrosyl region): 1760 vs, 1732  $\text{cm}^{-1}$ . FD mass spectrum (20 mA,  $\text{CH}_2\text{Cl}_2$ ),  $m/z$ : 990 ( $^{118}\text{Sn}$ ,  $^{116}\text{Sn}$ ), 991 ( $^{116}\text{Sn}$ ,  $^{117}\text{Sn}$ ), 992 ( $^{116}\text{Sn}$ ,  $^{118}\text{Sn}$ ) ( $^{117}\text{Sn}$ ,  $^{117}\text{Sn}$ ), 993 ( $^{117}\text{Sn}$ ,  $^{118}\text{Sn}$ ) ( $^{116}\text{Sn}$ ,  $^{119}\text{Sn}$ ), 994 ( $^{117}\text{Sn}$ ,  $^{119}\text{Sn}$ ) ( $^{118}\text{Sn}$ ,  $^{118}\text{Sn}$ ), 995 ( $^{118}\text{Sn}$ ,  $^{119}\text{Sn}$ ), 996 ( $^{118}\text{Sn}$ ,  $^{122}\text{Sn}$ ) ( $^{119}\text{Sn}$ ,  $^{119}\text{Sn}$ ), 997 ( $^{117}\text{Sn}$ ,  $^{124}\text{Sn}$ ), 998 ( $^{118}\text{Sn}$ ,  $^{122}\text{Sn}$ ) ( $^{116}\text{Sn}$ ,  $^{124}\text{Sn}$ ), 999 ( $^{117}\text{Sn}$ ,  $^{124}\text{Sn}$ ) ( $^{119}\text{Sn}$ ,  $^{122}\text{Sn}$ ). Anal. Calcd. for  $\text{C}_{36}\text{H}_{30}\text{Fe}_2\text{N}_4\text{O}_4\text{S}_2\text{Sn}_2$ : C, 43.42; H, 3.04; N, 5.63. Found: C, 43.06; H, 3.00; N, 5.67.

**(b) Trimethyltin Bromide.** The standard apparatus was charged with 1.00 g (2.06 mmol) of  $\text{Na}_2[(\mu\text{-S})_2\text{Fe}_2(\text{NO})_4]\cdot 8\text{H}_2\text{O}$  and then flushed with nitrogen. THF (75 mL) was added, followed by the dropwise addition of trimethyltin bromide (5 mmol) to the stirred solution. The mixture was stirred for 2 h and turned from a deep red to brown. Solvent was removed under reduced pressure, and a brown-black solid was obtained. The residue was extracted with  $\text{CH}_2\text{Cl}_2$  (4  $\times$  10 mL) and filtered under nitrogen. The red solution was reduced to 25 mL, and pentane (50 mL) was layered on top. The flask was placed in the freezer overnight at –30 °C. The solution was cannulated into another Schlenk flask leaving behind gleaming black crystals which were washed with pentane (5  $\times$  10 mL) and dried under vacuum to yield 0.77 g (60%) of  $(\mu\text{-Me}_3\text{SnS})_2\text{Fe}_2(\text{NO})_4$  as a purple-black, air-sensitive,

crystalline solid, mp 183–185 °C.  $^1\text{H NMR}$  ( $\text{CDCl}_3$ ) (60 MHz):  $\delta$  0.54 (s,  $^2J_{117\text{Sn},119\text{Sn}} = 52, 56$  Hz,  $\text{CH}_3\text{Sn}$ ). IR ( $\text{CDCl}_3$ ) (nitrosyl region): 1765 vs., 1735 vs  $\text{cm}^{-1}$ . Anal. Calcd for  $\text{C}_6\text{H}_{18}\text{Fe}_2\text{N}_4\text{O}_4\text{S}_2\text{Sn}_2$ : C, 11.55; H, 2.91; N, 8.99. Found: C, 11.54; H, 3.00; N, 8.94.

**(c) Triphenyllead Bromide.** The procedure described in (a) was used in the reaction of 2.06 mmol of  $\text{Na}_2[(\mu\text{-S})_2\text{Fe}_2(\text{NO})_4]\cdot 8\text{H}_2\text{O}$  with 2.58 g (4.9 mmol) of  $\text{Ph}_3\text{PbBr}$  in 75 mL of THF. After 2 h the solvent was removed under reduced pressure, and the brown-black residue was chromatographed (silicic acid–20%  $\text{CH}_2\text{Cl}_2$ /pentane). A red-purple band was eluted with pure dichloromethane which, upon removal of solvent, gave 2.40 g (2.04 mmol) of  $(\mu\text{-Ph}_3\text{PbS})_2\text{Fe}_2(\text{NO})_4$  as a dark purple-red, air-sensitive solid in 99% yield. The complex was recrystallized from dichloromethane/*n*-pentane under nitrogen: mp 180 °C dec. IR ( $\text{CHCl}_3$ ) (nitrosyl region): 1758 vs, 1723 vs,  $\text{cm}^{-1}$ . Molecular weight (determined by vapor pressure lowering in  $\text{CH}_2\text{Cl}_2$  at 0 °C):  $M_r = 1140 \pm 50$  (calcd 1172.88). FD mass spectrum (20 mA,  $\text{CH}_2\text{Cl}_2$ ),  $m/z$  (relative intensity, calculated intensity): 1171 (9.8, 10.6), 1172 (37.3, 29.7), 1173 (29.5, 23.6), 1174 (23.4, 27.6). Anal. Calcd for  $\text{C}_{36}\text{H}_{30}\text{Fe}_2\text{N}_4\text{O}_4\text{Pb}_2\text{S}_2$ : C, 36.86; H, 2.58; N, 4.78. Found: C, 36.80; H, 2.57; N, 4.76.

**(d) Phenylmercuric Bromide.** The same procedure as in (a) was used in the reaction of 2.06 mmol of  $\text{Na}_2[(\mu\text{-S})_2\text{Fe}_2(\text{NO})_4]\cdot 8\text{H}_2\text{O}$  with 1.50 g (4.19 mmol) of  $\text{PhHgBr}$ . After 10 h at room temperature, the brown residue left after solvent removal was purified by column chromatography (silicic acid). A red-brown band eluted with 1:4 dichloromethane/pentane which, upon removal of solvent, gave 0.58 g (0.81 mmol) of  $(\mu\text{-PhHgS})_2\text{Fe}_2(\text{NO})_4$ , as a very air-sensitive, red solid in 33% yield. It was recrystallized from dichloromethane/pentane: mp 195–200 °C dec. IR ( $\text{CHCl}_3$ ) (nitrosyl region): 1770 vs, 1740 vs  $\text{cm}^{-1}$ . Anal. Calcd for  $\text{C}_{12}\text{H}_{10}\text{Fe}_2\text{Hg}_2\text{N}_4\text{O}_4\text{S}_2$ : C, 16.93; H, 1.18. Found: C, 16.82; H, 1.29.

The preparation of  $(\mu\text{-CH}_3\text{HgS})_2\text{Fe}_2(\text{NO})_4$  has been described previously.<sup>11</sup>

**(e) ( $\eta^5$ -Cyclopentadienyl)iron Dicarbonyl Tetrahydrofuran Tetrafluoroborate.** The usual Schlenk flask was charged with 1.00 g (2.06 mmol) of  $\text{Na}_2[(\mu\text{-S})_2\text{Fe}_2(\text{NO})_4]\cdot 8\text{H}_2\text{O}$  and then flushed with nitrogen. THF (75 mL) was added by syringe, and a deep red solution was formed. To the stirred solution was added 1.41 g (4.20 mmol) of  $[\text{CpFe}(\text{CO})_2\cdot\text{THF}]^+ \text{BF}_4^-$  against a counterflow of nitrogen. The mixture was stirred for 15 h by which time a precipitate had formed and the solution had turned a deep orange-red. Solvent was removed on a rotary evaporator and the residue purified by column chromatography (silicic acid). Dichloromethane eluted a red-purple band which, upon removal of solvent, gave 1.34 g (1.83 mmol, 90%) of  $(\mu\text{-CpFe}(\text{CO})_2)_2\text{Fe}_2(\text{NO})_4\cdot\text{CH}_2\text{Cl}_2$  as a purple-red, air-stable, crystalline solid which has recrystallized from acetone/dichloromethane: mp 165–168 °C dec.  $^1\text{H NMR}$  [ $(\text{CD}_3)_2\text{C}=\text{O}$ ] (60 MHz):  $\delta$  5.36 (s, 2 H,  $\text{CH}_2\text{Cl}_2$ ), 5.60 (s, 10 H,  $\text{C}_5\text{H}_5$ ). IR ( $\text{CH}_2\text{Cl}_2$ ): (terminal carbonyl region) 2060 vs, 2020 vs; (nitrosyl region) 1745 vs, 1720 vs  $\text{cm}^{-1}$ . FD mass spectrum (20 mA,  $\text{CH}_2\text{Cl}_2$ ),  $m/z$  (relative intensity): 648 (29.0,  $\text{M}^+ - \text{CH}_2\text{Cl}_2$ ), 649 (100.0,  $\text{M}^+ - \text{CH}_2\text{Cl}_2$ ), 650 (36.0,  $\text{M}^+ - \text{CH}_2\text{Cl}_2$ ), 652 (14.0,  $\text{M}^+ - \text{CH}_2\text{Cl}_2$ ) [same as calcd spectrum for  $^{54}\text{Fe} = 5.8$ ,  $^{56}\text{Fe} = 91.7$ ,  $^{57}\text{Fe} = 2.1\%$ ]. Anal. Calcd for  $\text{C}_{15}\text{H}_{12}\text{Cl}_2\text{Fe}_2\text{N}_4\text{O}_8\text{S}_2$ : C, 24.52; H, 1.65; N, 7.63; Cl, 9.65. Found: C, 24.52; H, 1.64; N, 7.40; Cl, 8.65.

**(f) Tetracarbonyliron Diiodide.** The usual Schlenk flask was charged with 1.00 g (2.06 mmol) of  $\text{Na}_2[(\mu\text{-S})_2\text{Fe}_2(\text{NO})_4]\cdot 8\text{H}_2\text{O}$  and 1.00 g (2.4 mmol) of  $\text{Fe}(\text{CO})_4\text{I}_2$ .<sup>43</sup> The flask was flushed with nitrogen, and then THF (75 mL) was added by syringe. The resulting solution was stirred overnight, and then the solvent was removed under reduced pressure. The residue was chromatographed (silicic acid), and pentane eluted three products. The first band eluted from the column after removal of the solvent afforded 0.0098 g (0.02 mmol) of  $(\mu_3\text{-S})_4\text{Fe}_4(\text{NO})_4$  (6) as a black crystalline solid in 1% yield. The second product was identified as  $(\mu\text{-S})_2\text{Fe}_2(\text{CO})_6$  (0.070 g, 10% yield) by comparison of its IR spectrum and melting point with those of an authentic sample. The third product  $(\mu_3\text{-S})_2\text{Fe}_3(\text{CO})_9$  was identified only by its IR spectrum since it was obtained in 1% yield. No other products

were isolated from this reaction. Mass spectrum of  $(\mu_3\text{-S})_4\text{Fe}_4(\text{NO})_4$ ,  $m/z$  (relative intensity): 472 (9.7,  $\text{M}^+$ ), 442 (11.9,  $\text{M}^+ - \text{NO}$ ), 412 (10.0,  $\text{M}^+ - 2 \text{NO}$ ), 382 (12.0,  $\text{M}^+ - 3 \text{NO}$ ), 352 (50.0,  $\text{M}^+ - 4 \text{NO}$ ), 320 (11.5,  $\text{Fe}_4\text{S}_3^+$ ), 264 (23.5,  $\text{Fe}_3\text{S}_3^+$ ), 232 (36.2,  $\text{Fe}_3\text{S}_2$ ), 208 (22.3,  $\text{Fe}_2\text{S}_3^+$ ), 176 (68.5,  $\text{S}_2\text{Fe}_2^+$ ), 144 (11.0,  $\text{Fe}_3\text{S}^+$ ), 119 (6.5,  $\text{FeS}_2^+$ ), 88 (8.4,  $\text{SFe}^+$ ), 56 (100.0,  $\text{Fe}^+$ ). IR ( $\text{CH}_2\text{Cl}_2$ ) of  $(\mu_3\text{-S})_4\text{Fe}_4(\text{NO})_4$ :  $\nu_{\text{NO}}$  1780  $\text{cm}^{-1}$ .

**(g) ( $\eta^5$ -Cyclopentadienyl)cobalt Carbonyl Diiodide.** The usual Schlenk flask was charged with 1.00 g of  $\text{Na}_2[(\mu\text{-S})_2\text{Fe}_2(\text{NO})_4]\cdot 8\text{H}_2\text{O}$  and then flushed with nitrogen. THF (75 mL) was added, followed by 0.84 g (2.06 mmol) of  $\text{CpCo}(\text{CO})\text{I}_2$ ,<sup>44</sup> against a counterflow of nitrogen. The solution was stirred for 12 h, and the solvent was removed under reduced pressure. The black residue was chromatographed (silicic acid–dichloromethane), and the solvent was removed under reduced pressure. The residue was rechromatographed (silicic acid). A 1:1 mixture of dichloromethane/pentane eluted a dark green band as the major product. Removal of the solvent under reduced pressure gave 0.219 g (0.51 mmol) of  $(\text{C}_5\text{H}_5)_2\text{Co}_2(\mu_3\text{-S})_2\text{Fe}(\text{NO})_2$  (7a) as a black, very air-sensitive, crystalline solid in 25% yield (the yield of the reaction was variable, with observed yields of 11–25%). Dichloromethane eluted a brown band which, upon removal of solvent, gave 0.023 g (2.5%) of  $(\mu_3\text{-S})_2\text{Co}_2\text{Cp}_3$  as a dark brown crystalline solid. This compound was identified by its mass spectrum ( $M_r = 436$ , EI MS (70 eV)  $m/z$  436 ( $\text{M}^+$ )). The first product was recrystallized from dichloromethane/pentane: mp 201–203 °C.  $^1\text{H NMR}$  ( $\text{CD}_2\text{Cl}_2/\text{Me}_3\text{Si}$ ) (60 MHz):  $\delta$  5.02 (s,  $\text{C}_5\text{H}_5$ ). IR ( $\text{CH}_2\text{Cl}_2$ ) (nitrosyl region): 1748 vs, 1669 vs  $\text{cm}^{-1}$ . FD mass spectrum (10 mA,  $\text{CH}_2\text{Cl}_2$ ),  $m/z$  (relative intensity): 428 (100.0,  $\text{M}^+$ ), 398 (3.0,  $\text{M}^+ - \text{NO}$ ). Anal. Calcd for  $\text{C}_{10}\text{H}_{10}\text{Co}_2\text{FeN}_2\text{O}_2\text{S}_2$ : C, 28.05; H, 2.35; N, 6.54. Found: C, 28.23; H, 2.63; N, 6.24.

**(h) ( $\eta^5$ -Pentamethylcyclopentadienyl)cobalt Carbonyl Diiodide.** The usual Schlenk flask was charged with 1.00 g (2.06 mmol) of  $\text{Na}_2[(\mu\text{-S})_2\text{Fe}_2(\text{NO})_4]\cdot 8\text{H}_2\text{O}$  and 0.959 g (2.06 mmol) of  $\text{Me}_5\text{C}_5\text{Co}(\text{CO})\text{I}_2$  in the drybox. The flask was removed from the drybox and flushed with nitrogen. THF was added by syringe, and the resulting deep red solution was stirred for 12 h. Solvent was removed under reduced pressure, and the dark residue was chromatographed on Florisil under nitrogen. Benzene eluted two bands. The first, a green-brown band, was obtained in a minute amount and discarded. The second band, also green in color, eluted with benzene and upon the removal of solvent afforded 0.140 g (0.25 mmol) of  $(\text{Me}_5\text{C}_5)_2\text{Co}_2(\mu_3\text{-S})_2\text{Fe}(\text{NO})_2$  (7b) as a black, air-sensitive, crystalline solid in 12% yield which was recrystallized from dichloromethane/pentane: mp 285 °C dec.  $^1\text{H NMR}$  ( $\text{CD}_2\text{Cl}_2$ ) (250 MHz):  $\delta$  1.65 (s,  $\text{CH}_3$ ).  $^{13}\text{C NMR}$  ( $\text{CD}_2\text{Cl}_2$ ) (67.9 MHz):  $\delta$  9.93 (q,  $J = 127.7$  Hz,  $\text{CH}_3$ ), 92.04 (s,  $\text{C}_5\text{Me}_5$ ). Anal. Calcd for  $\text{C}_{20}\text{H}_{30}\text{Co}_2\text{FeN}_2\text{O}_2\text{S}_2$ : C, 42.27; H, 5.32. Found: C, 42.01; H, 5.31.

**Nitrosylation Reactions.** **(a)  $(\mu\text{-CH}_3\text{S})_2\text{Fe}_2(\text{CO})_6$ .** A nitrogen line was connected by latex tubing to a Pyrex T-tube which in turn was connected to a nitric oxide cylinder (Matheson) and a 14/20 Pyrex trap. The trap, which was filled with anhydrous silica gel, was cooled to  $-78$  °C in a dry ice/acetone slush bath. (This was done to dry the gas and to remove the higher oxides of nitrogen,  $\text{NO}_x$ .) The outlet of the trap was connected to a 8-mm glass tube which had been inserted through a 19-mm rubber septum. The septum was attached to a 300-mL three-necked round-bottomed flask which was also equipped with a magnetic stir-bar, a serum stopper, and a reflux condenser. The entire system was flushed with nitrogen, which exited through a gas outlet tube atop the reflux condenser and passed through an oil bubbler. The oil bubbler was vented then to the top of the hood. (In the following reactions involving the use of nitric oxide this shall be known as the “standard apparatus”). The flask was charged with 1.001 g (2.68 mmol) of  $(\mu\text{-CH}_3\text{S})_2\text{Fe}_2(\text{CO})_6$  against a counterflow of nitrogen. Benzene (100 mL) was added by syringe, and then nitric oxide was bubbled through the stirred solution at a rate of  $\sim 1$  L/h. The reaction mixture was heated at reflux, and the progress of the reaction was monitored by infrared spectroscopy. After 5 h the complete disappearance of the carbonyl bands was observed, and the reaction mixture was allowed to cool to room temperature. The solvent was removed

(42) Reger, D. L.; Colman, C. *J. Organomet. Chem.* **1977**, *131*, 153.

(43) Eisch, J. J.; King, R. B. “Organometallic Syntheses”: Academic Press, New York, 1965; Vol. 1.

(44) Rausch, M. D.; Genetti, R. A. *J. Org. Chem.* **1970**, *35*, 3888.



under reduced pressure, and the brown residue was chromatographed (silicic acid). Pentane eluted only one product, a red band which, upon removal of solvent, afforded 0.839 g (97%) of  $(\mu\text{-CH}_3\text{S})_2\text{Fe}_2(\text{NO})_4$  as a red-brown crystalline solid which was recrystallized from pentane, mp 92–94 °C, and identified by comparison of its spectroscopic properties with those of an authentic sample.

(b)  $(\mu\text{-CH}_3\text{S})(\mu\text{-C}_6\text{H}_5\text{S})\text{Fe}_2(\text{CO})_6$ . A solution of 1.079 g (2.47 mmol) of  $(\mu\text{-CH}_3\text{S})(\mu\text{-C}_6\text{H}_5\text{S})\text{Fe}_2(\text{CO})_6$  in 150 mL of benzene was prepared, and nitric oxide was bubbled through it at a rate of ~1 L/h at the reflux temperature. After 6 h the solvent was removed under reduced pressure and the residue purified by column chromatography (silicic acid). Pentane eluted a minor red band, which was discarded, followed by the major product. Solvent was removed to give 0.624 g (65%) of  $(\mu\text{-CH}_3\text{S})(\mu\text{-C}_6\text{H}_5\text{S})\text{Fe}_2(\text{NO})_4$  as a red-brown, moderately air-sensitive solid. The complex was recrystallized from pentane.  $^1\text{H NMR}$  ( $\text{CDCl}_3$ ) (60 MHz):  $\delta$  2.84 (s, 3 H,  $\text{CH}_3$ ), 7.02–7.35 (m, 5 H,  $\text{C}_6\text{H}_5$ ). IR ( $\text{CHCl}_3$ ) (nitrosyl region): 1782 vs, 1757 vs  $\text{cm}^{-1}$ . Mass spectrum,  $m/z$  (relative intensity): 388 (1.0,  $\text{M}^+$ ), 358 (13.1,  $\text{M}^+ - \text{NO}$ ), 328 (9.2,  $\text{M}^+ - 2\text{NO}$ ), 298 (6.8,  $\text{M}^+ - 3\text{NO}$ ), 268 (16.3,  $\text{M}^+ - 4\text{NO}$ ), 253 (21.2,  $\text{PhS}_2\text{Fe}_2^+$ ), 191 (7.4,  $\text{MeS}_2\text{Fe}_2^+$ ), 176 (23.9,  $\text{S}_2\text{Fe}_2^+$ ), 144 (8.1,  $\text{SFe}_2^+$ ), 109 (100.0,  $\text{PhS}^+$ ), 77 (46.5,  $\text{C}_6\text{H}_5^+$ ), 56 (11.3,  $\text{Fe}^+$ ), 47 (28.2,  $\text{MeS}^+$ ). Anal. Calcd for  $\text{C}_7\text{H}_9\text{Fe}_2\text{N}_4\text{O}_4\text{S}_2$ : C, 21.67; H, 2.08; N, 14.44. Found: C, 21.77; H, 2.13; N, 14.25.

(c)  $(\mu\text{-CH}_3\text{S})(\mu\text{-}p\text{-CH}_3\text{C}_6\text{H}_4\text{S})\text{Fe}_2(\text{CO})_6$ . The standard apparatus was charged with 1.15 g (2.54 mmol) of  $(\mu\text{-}p\text{-CH}_3\text{C}_6\text{H}_4\text{S})(\mu\text{-CH}_3\text{S})\text{Fe}_2(\text{CO})_6$  and 130 mL of benzene. The stirred solution was heated a reflux while nitric oxide was bubbled through it at a rate of 1 L/h. After 12 h all of the starting material had been consumed (by IR). Workup as in (a) followed. On column chromatography, pentane eluted a red-brown band which, upon removal of solvent, gave 0.853 g (84%)  $(\mu\text{-}p\text{-CH}_3\text{C}_6\text{H}_4\text{S})(\mu\text{-CH}_3\text{S})\text{Fe}_2(\text{NO})_4$  as a black-red crystalline solid, mp 116–118 °C.  $^1\text{H NMR}$  ( $\text{C}_6\text{D}_6$ ) (60 MHz):  $\delta$  2.79 (s, 3 H,  $p\text{-CH}_3\text{C}_6\text{H}_4$ ), 3.17 (s, 3 H,  $\text{CH}_3$ ), 7.46–7.90 (m, 4 H,  $p\text{-CH}_3\text{C}_6\text{H}_4$ ). IR ( $\text{CHCl}_3$ ) (nitrosyl region): 1785 vs, 1757 vs  $\text{cm}^{-1}$ . Mass spectrum,  $m/z$  (relative intensity): 402 (2.1,  $\text{M}^+$ ), 372 (5.8,  $\text{M}^+ - \text{NO}$ ), 342 (5.2,  $\text{M}^+ - 2\text{NO}$ ), 312 (3.9,  $\text{M}^+ - 3\text{NO}$ ), 282 (7.0,  $\text{M}^+ - 4\text{NO}$ ), 176 (2.1,  $\text{S}_2\text{Fe}_2^+$ ), 144 (1.9,  $\text{SFe}_2^+$ ), 124 (34.5,  $p\text{-CH}_3\text{C}_6\text{H}_4\text{S}^+$ ), 91 (100.0,  $p\text{-CH}_3\text{C}_6\text{H}_4^+$ ), 56 (4.0,  $\text{Fe}^+$ ). Anal. Calcd for  $\text{C}_9\text{H}_{11}\text{Fe}_2\text{N}_4\text{O}_4\text{S}_2$ : C, 23.90; H, 2.51; N, 13.94. Found: C, 24.55; H, 2.55; N, 13.91.

(d)  $(\mu\text{-CH}_3\text{Se})_2\text{Fe}_2(\text{CO})_6$ . A refluxing solution of 0.590 g (1.26 mmol) of  $(\mu\text{-CH}_3\text{Se})_2\text{Fe}_2(\text{CO})_6$  in 100 mL of benzene was treated with nitric oxide at a rate of 0.36 L/h. After 12 h, the solvent was removed under reduced pressure and the solid residue was purified by column chromatography (silicic acid). Pentane eluted a red-brown band which, upon removal of solvent, afforded a red-brown, malodorous solid which was redissolved in pentane under nitrogen and filtered through a small pad of Celite. The solvent was removed under reduced pressure to give 0.44 g (83%) of  $(\mu\text{-CH}_3\text{Se})_2\text{Fe}_2(\text{NO})_4$  as a red-purple, vile smelling, crystalline solid. The complex was recrystallized from pentane: mp 93–95 °C.  $^1\text{H NMR}$  ( $\text{CDCl}_3$ ) (60 MHz):  $\delta$  2.60 (s,  $\text{CH}_3\text{Se}$ ), 2.65 (s,  $\text{CH}_3\text{Se}$ ); in  $\text{C}_6\text{D}_6$  (250 MHz),  $\delta$  2.08 (s,  $\text{CH}_3\text{Se}$ ), 2.17 (s,  $\text{CH}_3\text{Se}$ ) (isomer ratio = 29:71).  $^{13}\text{C NMR}$  ( $\text{C}_6\text{D}_6$ ) (67.9 MHz):  $\delta$  14.11 (q,  $J = 144.2$  Hz,  $\text{CH}_3$ ), 14.63 (q,  $J = 144.5$  Hz,  $\text{CH}_3$ ). IR ( $\text{CHCl}_3$ ) (nitrosyl region): 1778 vs, 1747 vs  $\text{cm}^{-1}$ . Mass spectrum,  $m/z$  (relative intensity): 422 (4.0,  $\text{M}^+$ ,  $^{80}\text{Se}$ ), 420 (4.1,  $\text{M}^+$ ,  $^{78}\text{Se}$ ), 392 (11.0,  $\text{M}^+ - \text{NO}$ ), 390 (11.5,  $\text{M}^+ - \text{NO}$ ), 362 (5.5,  $\text{M}^+ - 2\text{NO}$ ), 360 (5.5,  $\text{M}^+ - 2\text{NO}$ ), 332 (3.5,  $\text{M}^+ - 3\text{NO}$ ), 330 (3.5,  $\text{M}^+ - 3\text{NO}$ ), 302 (11.1,  $\text{M}^+ - 4\text{NO}$ ), 300 (11.0,  $\text{M}^+ - 4\text{NO}$ ), 287 (11.2,  $\text{MeSe}_2\text{Fe}_2^+$ ), 285 (11.4,  $\text{MeSe}_2\text{Fe}_2^+$ ), 272 (25.0,  $\text{Se}_2\text{Fe}_2^+$ ), 270 (24.9,  $\text{Se}_2\text{Fe}_2^+$ ), 192 (12.9,  $\text{SeFe}_2^+$ ), 190 (13.0,  $\text{SeFe}_2^+$ ), 80 (4.2,  $^{80}\text{Se}^+$ ), 78 (1.8,  $^{78}\text{Se}^+$ ), 56 (100.0,  $\text{Fe}^+$ ). Anal. Calcd for  $\text{C}_2\text{H}_6\text{Fe}_2\text{N}_4\text{O}_4\text{Se}_2$ : C, 5.72; H, 1.44; N, 13.35. Found: C, 6.14; H, 1.58; N, 13.16.

(e)  $\eta^5\text{-C}_5\text{H}_5\text{Co}(\mu_3\text{-S})_2\text{Fe}_2(\text{CO})_6$ . The standard apparatus was charged with 0.500 g (1.07 mmol) of  $\text{CpCo}(\mu_3\text{-S})_2\text{Fe}_2(\text{CO})_6^1$  against a counter flow of nitrogen. Benzene (50 mL) was added, and the resulting deep cherry-red solution was stirred and heated to reflux. Nitric oxide then was bubbled through it at a rate of 1 L/h. The progress of the reaction was monitored by the disappearance of carbonyl bands in the infrared spectrum. After 5 h the starting material had been consumed and the solvent was removed under reduced pressure. The residue was purified by column chromatography (silicic/pentane). Dichloromethane eluted a green band

which, upon removal of solvent, gave 0.180 g (79% based cobalt) of  $\text{Cp}_2\text{Co}(\mu_2\text{-S})_2\text{Fe}_2(\text{NO})_2$ , as a black, air-sensitive crystalline solid which was recrystallized from dichloromethane/pentane, mp 202 °C dec. Its  $^1\text{H NMR}$ , IR, and mass spectra were identical with those of an authentic sample (see above).

**Preparation of  $[(\eta^5\text{-C}_5\text{H}_5\text{Fe}(\text{CO})_2\text{S})_2\text{Fe}_2(\text{NO})_4\text{-CH}_2\text{Cl}_2$  via  $(\mu\text{-Me}_3\text{SnS})_2\text{Fe}_2(\text{NO})_4$ .** A 200-mL Schlenk flask equipped with a magnetic stir-bar and a serum stopper was charged with 1.00 g (1.60 mmol) of  $(\mu\text{-Me}_3\text{SnS})_2\text{Fe}_2(\text{NO})_4$  and 1.03 g (4.0 mmol) of  $\text{CpFe}(\text{CO})_2\text{Br}^{43}$  and then flushed with nitrogen. THF (100 mL) was added, and the resulting solution was heated at reflux overnight. The progress of the reaction was monitored by TLC. After all of  $(\mu\text{-Me}_3\text{SnS})_2\text{Fe}_2(\text{NO})_4$  had been consumed, the solvent was removed under reduced pressure and the residue was purified by column chromatography (silicic acid). A 4:1 mixture of pentane/dichloromethane eluted the excess  $\text{CpFe}(\text{CO})_2\text{Br}$ . Subsequent elution with dichloromethane afforded a red-purple band which gave, upon removal of solvent, 1.11 g (94%) of  $(\text{CpFe}(\text{CO})_2\text{S})_2\text{Fe}_2(\text{NO})_4\text{-CH}_2\text{Cl}_2$  as a black, crystalline solid. The complex was recrystallized from acetone/dichloromethane to give the product as the 1:1 dichloromethane solvate. It was identified by comparison of its spectroscopic properties with those of an authentic sample (see above).

**Michael Additions of  $(\mu\text{-HS})_2\text{Fe}_2(\text{NO})_4$ .** (a) **To Methyl Acrylate.** A 100-mL Schlenk flask equipped with a magnetic stir-bar and a serum stopper was charged with 0.50 g (1.03 mmol) of  $\text{Na}_2[(\mu\text{-S})_2\text{Fe}_2(\text{NO})_4]\cdot 8\text{H}_2\text{O}$  in the drybox. THF (30 mL) was added, and the flask was removed from the drybox and attached to a Schlenk manifold. At room temperature, 2.40 mL (26 mmol) of methyl acrylate was added by syringe and the reaction mixture was stirred for 1 h. Then the flask was cooled to -78 °C in a dry ice/acetone slush bath and stirred for 30 min before 0.2 mL (2.5 mmol) of  $\text{CF}_3\text{COOH}$  was added by syringe. The solution was stirred for 15 min, and then 0.25 mL (4.0 mmol) of piperidine was added by syringe. The reaction mixture was stirred for an additional hour at -78 °C and then allowed to warm slowly to room temperature. The progress of the reaction was followed by TLC, and after 2 days the reaction was stopped. Removal of the solvent under reduced pressure yielded a black, oily solid which was chromatographed (Florisol-pentane). A 1:1 mixture of dichloromethane/pentane eluted an orange-brown band which, upon removal of solvent, afforded 0.473 g (98%) of  $(\mu\text{-CH}_3\text{OC}(\text{O})\text{-CH}_2\text{CH}_2\text{S})_2\text{Fe}_2(\text{NO})_4$ , as a brown, slightly air-sensitive, crystalline solid which was recrystallized from dichloromethane/pentane; mp 65.5–67 °C.  $^1\text{H NMR}$  ( $\text{CD}_2\text{Cl}_2$ ) (250 MHz):  $\delta$  2.40 (t,  $J = 7.1$  Hz, 2 H,  $\text{C}(\text{O})\text{CH}_2$ ), 2.42 (t,  $J = 7.2$  Hz, 2 H,  $\text{C}(\text{O})\text{CH}_2$ ), 2.80 (t,  $J = 7.2$  Hz, 2 H,  $\text{CH}_2\text{S}$ ), 2.84 (t,  $J = 7.1$  Hz, 2 H,  $\text{CH}_2\text{S}$ ), 3.27 (s, 3 H,  $\text{CH}_3\text{O}$ ), 3.28 (s, 3 H,  $\text{CH}_3\text{O}$ ) (isomer ratio = 49:51).  $^{13}\text{C NMR}$  ( $\text{CDCl}_3$ ) (22.5 MHz):  $\delta$  37.97 ( $\text{CH}_2$ ), 39.70 ( $\text{CH}_2$ ), 52.09 ( $\text{CH}_3\text{O}$ ), 171.29 ( $\text{OC}(\text{O})$ ). IR ( $\text{CHCl}_3$ ) (nitrosyl region): 1782 vs, 1755 vs  $\text{cm}^{-1}$ . Mass spectrum,  $m/z$  (relative intensity): 440 (0.8,  $\text{M}^+ - \text{NO}$ ), 410 (80.3,  $\text{M}^+ - 2\text{NO}$ ), 380 (64.7,  $\text{M}^+ - 3\text{NO}$ ), 350 (30.5,  $\text{M}^+ - 4\text{NO}$ ), 294 (8.6,  $\text{MeOC}(\text{O})\text{CH}_2\text{CH}_2\text{S}_2\text{Fe}_2(\text{NO})^+$ ), 264 (25.6,  $\text{MeOC}(\text{O})\text{CH}_2\text{CH}_2\text{S}_2\text{Fe}_2^+$ ), 236 (22.9,  $\text{S}_2\text{Fe}_2(\text{NO})_2^+$ ), 207 (4.5,  $\text{MeOC}(\text{O})\text{CH}_2\text{CH}_2\text{S}_2\text{Fe}_2^+$ ), 176 (4.9,  $\text{S}_2\text{Fe}_2^+$ ), 87 (30.4,  $\text{MeOC}(\text{O})\text{CH}_2\text{CH}_2^+$ ), 56 (100.0,  $\text{Fe}^+$ ). Anal. Calcd for  $\text{C}_8\text{H}_{14}\text{Fe}_2\text{N}_4\text{O}_8\text{S}_2$ : C, 20.44; H, 3.00. Found: C, 20.67; H, 3.07.

(b) **To Acrylonitrile.** As in (a), a solution of 0.94 mmol of  $\text{Na}[(\mu\text{-S})_2\text{Fe}_2(\text{NO})_4]\cdot 8\text{H}_2\text{O}$  in 50 mL of THF was cooled to -78 °C and then 1.01 mL (20 mmol) of acrylonitrile was added by syringe, followed immediately by the addition of 0.15 mL (2.0 mmol) of trifluoroacetic acid by syringe. The solution was stirred for 30 min, and then 0.12 mL (2.0 mmol) of piperidine was added by syringe. The reaction mixture was stirred for an additional hour at -78 °C and then allowed to warm slowly to room temperature. The progress of the reaction was followed by TLC, and after 3 days a product was visible. Solvent was removed under reduced pressure, and the residue was chromatographed (Florisil). Dichloromethane eluted a red-brown band which, upon removal of solvent, afforded 0.147 g (39%) of  $(\mu\text{-N}\equiv\text{CCH}_2\text{CH}_2\text{S})_2\text{Fe}_2(\text{NO})_4$  as a red-brown, slightly air-sensitive solid. The solid was recrystallized from dichloromethane/pentane to give 0.12 g (34%).  $^1\text{H NMR}$  ( $\text{CD}_2\text{Cl}_2$ ) (250 MHz):  $\delta$  2.91 (t,  $J = 7.0$  Hz, 2 H,  $\text{CH}_2$ ), 3.19 (t,  $J = 7.0$  Hz, 2 H,  $\text{CH}_2$ ). (Isomer ratio could not be determined by NMR.)  $^{13}\text{C NMR}$  ( $\text{CD}_2\text{Cl}_2$ ):  $\delta$  22.08 (t,  $J = 139$  Hz,  $\text{CH}_2\text{CN}$ ), syn and anti isomers, 39.54 (t,  $J = 142$  Hz,  $\text{CH}_2\text{S}$ ), 39.71

( $t$ ,  $J = 142$  Hz,  $\text{CH}_2\text{S}$ ), 117.46 (s,  $\text{C}\equiv\text{N}$ ). IR ( $\text{CH}_2\text{Cl}_2$ ) (nitrosyl region): 1785 vs, 1754 vs,  $\nu(\text{C}\equiv\text{N})$  2264  $\text{cm}^{-1}$ . Mass spectrum,  $m/z$  (relative intensity): 374 (1.7,  $\text{M}^+ - \text{NO}$ ), 344 (7.2,  $\text{M}^+ - 2$  NO), 314 (7.8,  $\text{M}^+ - 3$  NO), 284 (6.5,  $\text{M}^+ - 4$  NO), 230 (9.0,  $\text{N}\equiv\text{CCH}_2\text{CH}_2\text{S}_2\text{Fe}_2^+$ ), 176 (4.6,  $\text{S}_2\text{Fe}_2$ ), 87 (30.0,  $\text{SFe}^+$ ), 53 (100.0,  $\text{C}_3\text{H}_3\text{N}^+$ ). Anal. Calcd for  $\text{C}_6\text{H}_8\text{Fe}_2\text{N}_2\text{O}_4\text{S}_2$ : C, 17.84; H, 2.00; N, 20.80. Found: C, 18.21; H, 2.18; N, 20.51.

**X-ray Data Collection.** A suitable quality black crystal of  $(\eta^5\text{-C}_5\text{Me}_5)_2\text{Co}_2(\mu_3\text{-S})_2\text{Fe}(\text{NO})_2$ , bound by 10 faces of the form  $\{100\}$ ,  $\{20\bar{1}\}$ ,  $\{001\}$ , and  $\{110\}$  and obtained from  $\text{CH}_2\text{Cl}_2/\text{pentane}$ , was mounted in air on a glass fiber. Unit cell parameters were obtained from a least-squares analysis of the setting angles of 24 reflections in the range  $18.53 \leq 2\theta \leq 25.31^\circ$ , which were accurately centered at  $22^\circ\text{C}$  on an Enraf-Nonius CAD4 diffractometer using  $\text{Mo K}\alpha$  radiation. The  $2/m$  diffraction symmetry and the systematic absences ( $hkl$ ,  $h+k=2n+1$ ;  $h0l$ ,  $l=2n+1$ ) were consistent with the space groups  $Cc$  and  $C2/c$ , the latter of which was established as the more probable one based on the successful refinement of the structure with acceptable parameters and the location of all hydrogen atoms.

Intensity data were collected at  $22^\circ\text{C}$  on the CAD4 diffractometer in the bisecting mode employing the  $\omega-2\theta$  scan technique and using  $\text{Mo K}\alpha$  radiation. Background were scanned for 25% of the peak width on each end of the peak scans. The intensities of three standard reflections, measured every 1 h of exposure as a check for crystal decomposition or movement, showed no significant variations so no correction was applied. A total of 4590 unique reflections was measured and processed in the usual way using a value of 0.04 for  $p$ .<sup>45</sup> Of these, 3662 were considered to be observed and were used in subsequent calculations. See Table I for pertinent crystal data and details of intensity collection.

**Structure Solution and Refinement.** The structure was solved in space group  $C2/c$ , by using MULTAN 80 to locate the Co, Fe, and S atoms.<sup>46</sup> All other atoms were located on subsequent difference Fourier calculations. Full-matrix, least-squares techniques were used for the refinements, utilizing the usual scattering factors and anomalous dispersion terms. The non-hydrogen atoms were refined anisotropically. Although the hydrogen atoms were located, they were not refined but were input in their idealized positions derived from the observed ones by using  $sp^3$  geometries about the carbon atoms and C-H distances of 0.95 Å. The hydrogen positions were allowed to ride on the attached carbon atoms, with the positional changes in the latter being applied to the former after each cycle of refinement. Isotropic thermal parameters of  $1 \text{ \AA}^2$  greater than the equivalent isotropic  $B$  of the attached carbon atom were assigned to each hydrogen. Absorption corrections were applied to the data by using Gaussian integration.

The structure, in space group  $C2/c$ , refined to  $R = 0.028$  and  $R_w = 0.039$ . A comparison of the observed and calculated structure

amplitudes showed no unusual features. On the final difference Fourier map the top ten residuals ( $0.26\text{--}0.37 \text{ e \AA}^{-3}$ ) lay in the vicinities of the two pentamethylcyclopentadienyl groups; by comparison, a carbon atom on earlier maps had an intensity between 4.0 and  $7.2 \text{ e \AA}^{-3}$ .

The positional parameters and the equivalent isotropic  $B$ 's of the non-hydrogen atoms are given in Table II. Tables of anisotropic thermal parameters, hydrogen parameters, and a listing of observed and calculated structure amplitudes are available.

**Acknowledgment.** We are grateful to the National Science Foundation for support of the preparative work at M.I.T., to the University of Alberta and the Natural Sciences and Engineering Research Council of Canada for support of the structural study at University of Alberta, and to the M.I.T. Mass Spectrometry Facility (supported by N.I.H. Division of Research Resources, Grant No. RR 00317; K. Biemann, principal investigator) for mass spectra. M.C. also thanks NSERC for partial funding of the diffractometer.

**Registry No.** 3, 99619-56-4; 4 (R =  $\text{C}_2\text{H}_5$ ), 88643-18-9; 4 (R =  $\text{CH}_3$ ), 88643-17-8; 4 (R =  $\text{CH}_2\text{CH}=\text{CH}_2$ ), 99664-08-1; 4 (R =  $\text{CH}_2\text{Ph}$ ), 88568-33-6; 4 (R =  $\text{CH}_2\equiv\text{CH}$ ), 99664-09-2; 4 (R =  $\text{CH}_2\text{C}(\text{O})\text{CH}_3$ ), 99664-10-5; 4 (R =  $\text{CH}_2\text{SiMe}_3$ ), 99664-11-6; 5 (R =  $\text{CH}_3$ ), 88643-72-5; 5 (R =  $\text{C}_2\text{H}_5$ ), 88643-19-0; 5 (R =  $\text{CH}_2\text{CH}=\text{CH}_2$ ), 99619-52-0; 5 (R =  $\text{CH}_2\text{Ph}$ ), 88643-23-6; 5 (R =  $\text{CH}_2\text{C}\equiv\text{CH}$ ), 99619-53-1; 5 (R =  $\text{CH}_2\text{C}(\text{O})\text{CH}_3$ ), 99619-54-2; 5 (R =  $\text{CH}_2\text{SiMe}_3$ ), 99619-55-3; 6, 53276-80-5; 7a, 99619-57-5; 7b, 99619-58-6;  $\text{Na}_2[(\mu\text{-s})_2\text{Fe}_2(\text{NO})_4]$ , 58204-17-4;  $\text{NH}_4[\text{Fe}_4\text{S}_3(\text{NO})_7]$ , 99619-51-9;  $\text{Co}_2(\text{CO})_8$ , 10210-68-1;  $(\mu\text{-Ph}_3\text{Sn})_2\text{Fe}_2(\text{NO})_4$ , 79827-02-4;  $(\mu\text{-Me}_3\text{Sn})_2\text{Fe}_2(\text{NO})_4$ , 79827-01-3;  $\text{Ph}_3\text{SnCl}$ , 639-58-7;  $\text{Me}_3\text{SnBr}$ , 1066-44-0;  $\text{Ph}_3\text{PbBr}$ , 894-06-4;  $(\mu\text{-Ph}_3\text{Pb})_2\text{Fe}_2(\text{NO})_4$ , 79827-03-5;  $\text{MeNO}_2$ , 7632-00-0;  $(\text{NH}_4)_2\text{S}$ , 12135-76-1;  $\text{FeSO}_4$ , 7720-78-7;  $\text{MeI}$ , 74-88-4;  $\text{PhHgBr}$ , 1192-89-8;  $(\mu\text{-PhHgS})_2\text{Fe}_2(\text{NO})_4$ , 79827-04-6;  $[\text{CpFe}(\text{CO})_2\text{THF}]\text{BF}_4$ , 63313-71-3;  $(\mu\text{-CpFe}(\text{CO})_2)_2\text{Fe}_2(\text{NO})_4$ , 79827-05-7;  $\text{Fe}(\text{CO})_4\text{I}_2$ , 14878-30-9;  $(\mu\text{-S}_2)\text{-Fe}_2(\text{CO})_6$ , 14243-23-3;  $(\mu_3\text{-S})_2\text{Fe}_3(\text{CO})_9$ , 22309-04-2;  $\text{CpCo}(\text{CO})\text{I}_2$ , 12012-77-0;  $(\mu_3\text{-S})_2\text{Co}_3\text{Cp}_3$ , 11105-79-6;  $(\text{C}_5\text{Me}_5)\text{Co}(\text{CO})\text{I}_2$ , 35886-64-7;  $(\mu\text{-CH}_3\text{S})_2\text{Fe}_2(\text{CO})_6$ , 14878-96-7;  $(\mu\text{-CH}_3\text{S})(\mu\text{-C}_6\text{H}_5\text{S})\text{Fe}_2(\text{CO})_6$ , 98302-46-6;  $(\mu\text{-CH}_3\text{S})(\mu\text{-C}_6\text{H}_5\text{S})\text{Fe}_2(\text{NO})_4$ , 99619-59-7;  $(\mu\text{-CH}_3\text{S})(\mu\text{-}p\text{-CH}_2\text{C}_6\text{H}_4\text{S})\text{Fe}_2(\text{CO})_6$ , 95762-95-1;  $(\mu\text{-}p\text{-CH}_3\text{C}_6\text{H}_4\text{S})(\mu\text{-CH}_3\text{S})\text{Fe}_2(\text{NO})_4$ , 99619-60-0;  $(\mu\text{-CH}_3\text{Se})_2\text{Fe}_2(\text{CO})_6$ , 38497-97-1;  $(\mu\text{-CH}_3\text{Se})_2\text{Fe}_2(\text{NO})_4$ , 98716-15-5;  $\text{CpCo}(\mu_3\text{-S})_2\text{Fe}_2(\text{CO})_6$ , 79391-48-3;  $\text{CpFe}(\text{CO})_2\text{Br}$ , 12078-20-5;  $(\text{CpFe}(\text{CO})_2)_2\text{Fe}_2(\text{NO})_4$ , 79827-05-7;  $(\mu\text{-CH}_3\text{OC}(\text{O})\text{CH}_2\text{CH}_2\text{S})_2\text{Fe}_2(\text{NO})_4$ , 99619-61-1; *anti*- $(\mu\text{-N}\equiv\text{CCH}_2\text{CH}_2\text{S})_2\text{Fe}_2(\text{NO})_4$ , 99619-62-2; *syn*- $(\mu\text{-N}\equiv\text{CCH}_2\text{CH}_2\text{S})_2\text{Fe}_2(\text{NO})_4$ , 99664-12-7; Co, 7440-48-4; Fe, 7439-89-6; methyl acrylate, 96-33-3; acrylonitrile, 107-13-1.

**Supplementary Material Available:** Listings of observed and calculated structure factors, anisotropic thermal parameters, and idealized hydrogen parameters (22 pages). Ordering information is given on any current masthead page.

(45) Doedens, R. J.; Ibers, J. A. *Inorg. Chem.* **1967**, *6*, 204.

(46) Programs used were those of the Enraf-Nonius Structure Determination Package by B. A. Frenz and some local programs by R. G. Ball.



# Actinide Diene (2-Butene-1,4-diyl) Complexes. Synthesis Including a Methyl-Induced $\beta$ -Hydrogen Elimination Reaction, Structures, Structural Dynamics, Thermochemistry, and Reactivity

Gregory M. Smith,<sup>1a</sup> Hiroharu Suzuki,<sup>1a,b</sup> David C. Sonnenberger,<sup>1a,c</sup> Victor W. Day,<sup>\*1d</sup> and Tobin J. Marks<sup>\*1a</sup>

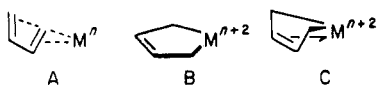
Department of Chemistry, Northwestern University, Evanston, Illinois 60201, Crystallitics Company, Lincoln, Nebraska 68501, the Department of Chemistry, University of Nebraska, Lincoln, Nebraska 68588, and the Chemistry Division, Argonne National Laboratory, Argonne, Illinois 60439

Received August 16, 1985

The synthesis and properties of the actinide *s-cis*-diene/*cis*-2-butene-1,4-diyl complexes  $\text{Cp}'_2\text{U}(\eta^4\text{-C}_4\text{H}_6)$  (2),  $\text{Cp}'_2\text{Th}(\eta^4\text{-C}_4\text{H}_6)$  (3), and  $\text{Cp}'_2\text{Th}(\eta^4\text{-CH}_2\text{CMeCMeCH}_2)$  (4) ( $\text{Cp}' = \eta^5\text{-(CH}_3)_5\text{C}_5$ ) are described. They can be readily prepared from  $\text{Cp}'_2\text{MCl}_2$  ( $\text{M} = \text{U, Th}$ ) and the appropriate  $(\text{THF})_2\text{Mg}(\text{CH}_2\text{CRCRCH}_2)$  reagent. Complex 2 but not 3 can also be prepared from the methane-eliminating reaction of  $\text{Cp}'_2\text{U}(\text{Me})\text{Cl}$  and 3-butenyl Grignard. The molecular structure of 3 has been determined by single-crystal X-ray diffraction.  $\text{Cp}'_2\text{Th}(\eta^4\text{-C}_4\text{H}_6)$  crystallizes in the monoclinic space group  $P2_1/c-C_{2h}^5$  (no. 14) with four molecules in a unit cell of dimensions  $a = 9.236$  (3) Å,  $b = 14.720$  (4) Å,  $c = 17.437$  (4) Å, and  $\beta = 105.48$  (2)°. Least-squares refinement led to a value for the conventional  $R$  index (on  $F$ ) of 0.049 for 2450 reflections having  $2\theta_{\text{MoK}\alpha} < 50.7^\circ$  and  $I > 3\sigma(I)$ . The molecular structure consists of an unexceptional "bent sandwich"  $\text{Cp}'_2\text{Th}$  fragment coordinated to an *s-cis*- $\eta^4$ -butadiene ligand. The average Th-C distance to the terminal carbon atoms of the butadiene ligand, 2.57 (3, 3, 3, 2) Å, is only slightly less than that to the internal carbon atoms, 2.74 (3, 1, 1, 2) Å. The actinide butadiene complexes undergo inversion of the metallacyclopentene ring which is rapid on the NMR time scale at higher temperatures;  $\Delta G^\ddagger$ , kcal mol<sup>-1</sup> ( $T_c$ , K) =  $17.0 \pm 0.3$  (394, 2),  $15.0 \pm 0.3$  (299, 3), and  $10.5 \pm 0.3$  (208, 4). Thermochemical studies of the thorium-butadiene bond disruption enthalpy in 3 and 4 using anaerobic batch-titration (*t*-BuOH) calorimetry indicate that the thorium-butadiene interaction enjoys no special stabilization.  $D(\text{Th-butadiene})$  is comparable to that for relatively "weak" thorium-to-carbon  $\sigma$  bonds. No evidence for *s-trans*-butadiene coordination is found in any of the actinide butadiene complexes. While the actinide-butadiene linkage undergoes facile hydrogenolysis and protonolysis, the activation of C-H bonds on exogenous hydrocarbon molecules is not observed. The bond disruption enthalpy data indicate that such process are thermodynamically unfavorable.

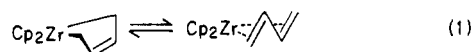
## Introduction

In contrast to the diene chemistry of middle and late transition elements, that of the early transition elements has received only recent attention.<sup>2</sup> However, this field is now in a stage of rapid development, and the picture which is emerging is one of distinctive structural, bonding and reactivity contrasts vis-à-vis middle and late transition elements. It is clear that the conventional  $\pi$  olefin/low-valent metal picture of the bonding (A) is inadequate for early transition metals<sup>2b,3</sup> and that *s-cis*- $\sigma^2$ -metallacyclopentene (2-butene-1,4-diyl) (B) and  $\sigma^2, \pi$ -metallacyclopentene (C) descriptions are major contributors to the



bonding. Furthermore, the relative contributions of these limiting descriptions appear to be subtle functions of the metal (in group 4,  $\text{Cp}_2\text{Hf}$  complexes exhibit greater me-

tallacyclopentene character than those of  $\text{Cp}_2\text{Zr}^{2a}$ ) and diene substituents (substitution at the 2- and 3-positions enhances the metallacyclopentene character<sup>4</sup>). Equilibration between *s-cis*- and *s-trans*-butadiene structures has also been identified for zirconium (eq 1)<sup>5</sup> and further il-



lustrates the richness of this chemistry. Typical synthetic routes to group 4 diene complexes also underscore this point and involve reduction of the precursor complex in the presence of diene by chemical<sup>2a,4</sup> or photochemical<sup>5e</sup> means, the use of magnesium diene reagents,<sup>2b,6,7</sup> the use of pentadienyl reagents,<sup>8a</sup> metal atom vapor techniques,<sup>8b</sup> and the rearrangement of transitory divinyl complexes.<sup>9</sup>

(4) Erker, G.; Engel, K.; Küger, C.; Müller, G. *Organometallics* 1984, 3, 128-133.

(5) (a) Dorf, U.; Engel, K.; Erker, G. *Organometallics* 1983, 2, 462-463. (b) Yasuda, H.; Kajihara, Y.; Mashima, K.; Nagasuna, K.; Lee, K.; Nakamura, A. *Organometallics* 1982, 1, 388-396. (c) Erker, G.; Wicher, J.; Engel, K.; Krüger, C. *Chem. Ber.* 1982, 115, 3300-3310. (d) Dorf, U.; Engel, K.; Erker, G. *Organometallics* 1983, 2, 462-463. (e) Erker, G.; Wicher, J.; Engel, K.; Rosenfeldt, F.; Dietrich, W.; Krüger, C. *J. Am. Chem. Soc.* 1980, 102, 6346-6348.

(6) (a) Datta, S.; Fischer, M. B.; Wreford, S. S. *J. Organomet. Chem.* 1980, 188, 353-366. (b) Beatty, R. P.; Datta, S.; Wreford, S. S. *Inorg. Chem.* 1979, 18, 3139-3145. (c) Datta, S.; Wreford, S. S.; Beatty, R. P.; McNeese, T. J. *J. Am. Chem. Soc.* 1979, 101, 1053-1054.

(7) Wreford, S. S.; Whitney, J. F. *Inorg. Chem.* 1981, 20, 3918-3924. (8) (a) Yasuda, H.; Nagasuna, K.; Akita, M.; Lee, K.; Nakamura, A. *Organometallics* 1984, 3, 1470-1478. (b) Skell, P. S.; McGlinchey, M. J. *Angew. Chem., Int. Ed. Engl.* 1975, 14, 195-196.

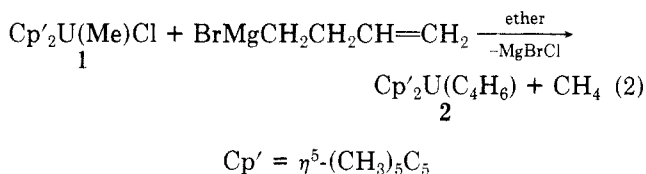
(9) (a) Beckhaus, R.; Thiele, K.-H. *J. Organomet. Chem.* 1984, 268, C7-C8. (b) Czisch, P.; Erker, G.; Korth, H.-G.; Sustmann, R. *Organometallics* 1984, 3, 945-947.

(1) (a) Northwestern University. (b) Present address: Research Laboratories of Resources Utilization, Tokyo Institute of Technology, 4259 Nagatsuta, Midori-ku, Yokohama 227, Japan. (c) Argonne National Laboratory. (d) Crystallitics Co. and the University of Nebraska.

(2) (a) Krüger, C.; Müller, G.; Erker, G.; Dorf, U.; Engel, K. *Organometallics* 1985, 4, 215-223. (b) Yasuda, H.; Tatsumi, K.; Nakamura, A. *Acc. Chem. Res.* 1985, 18, 120-126. (c) Nakamura, A.; Yasuda, H.; Tatsumi, K.; Noda, I.; Mashima, K.; Akita, M.; Nagasuna, K. In "Organometallic Compounds, Synthesis, Structure and Theory"; Shapiro, B. L., Ed.; Texas A&M University Press: College Station, TX, 1983; Vol. 1, pp 29-45. (d) Benn, R.; Schroth, G. *J. Organomet. Chem.* 1982, 228, 71-85 and references therein. (e) Yasuda, H.; Tatsumi, K.; Okamoto, T.; Mashima, K.; Lee, K.; Nakamura, A.; Yasushi, K.; Hanehisa, N.; Kasai, N. *J. Am. Chem. Soc.* 1985, 107, 2410-2422.

(3) Tatsumi, K.; Yasuda, H.; Nakamura, A. *Isr. J. Chem.* 1983, 23, 145-150.

The similarities as well as contrasts between group 4 and actinide<sup>10</sup> organometallic chemistries raise the intriguing question of whether 5f-element diene complexes might exist and if so, what the structural and chemical properties of such molecules would be like. Several years ago, we discovered a route to a uranium butadiene complex (2) via the reaction of complex 1 with a 3-butenyl Grignard reagent (eq 2).<sup>11</sup> This observation prompted a more ex-



tensive study of synthetic approaches to and the properties of actinide diene complexes with a view toward comparisons with group 4 phenomenology. In this contribution, we present a full discussion of our results, including actinide diene complex synthesis by three different routes, the molecular structure of  $\text{Cp}'_2\text{Th}(\eta^4\text{-C}_4\text{H}_6)$  by single-crystal X-ray diffraction, observations on the spectroscopic and molecular dynamical properties of actinide diene complexes, the first thermochemical measurement of actinide-diene bond disruption enthalpies, and information on the reaction chemistry of actinide diene complexes. Although some parallels between actinide and group 4 chemistry are found, a number of unexpected and informative differences also emerge.

### Experimental Section

**General Methods.** All manipulations were carried out using standard air-free methodology in a nitrogen-filled Vacuum Atmospheres Model HE-43-2 Dri-Lab, on a Schlenk line, or in Schlenk-type apparatus interfaced to a high vacuum line ( $<10^{-5}$  torr). The glovebox atmosphere was recirculated through a Vacuum Atmospheres Model HE-193-1 Dri-Train, while the argon used in vacuum line manipulations was purified by passage first through a column of MnO on vermiculite<sup>12</sup> and then through a column of activated Davison type 4-Å molecular sieves. Prepurified grade argon (Matheson) was used without further purification for normal Schlenk manipulations. The glassware used for Schlenk-type manipulations on the vacuum line was constructed with greaseless Teflon joints and valves and in general consisted of a double ended 20- (or 10-) mm glass frit with magnetic stir bar equipped flasks of appropriate size at either end, a side arm and valve connecting opposite sides of the frit, and an adaptor for connection to the vacuum line. All solvents were thoroughly dried and deaerated by conventional techniques<sup>13</sup> before use.

Unless otherwise noted, all reagents were obtained from commercial suppliers. Butadiene was purified by passing through MnO/vermiculite and 4-Å molecular sieve columns. The 2,3-dimethylbutadiene was distilled immediately before use. (*E,E*)-1,4-diphenylbutadiene was obtained from Aldrich and was recrystallized from THF. All alkyl halides were dried over  $\text{P}_4\text{O}_{10}$  before use and were stored under argon. Tin(IV) chloride was distilled immediately before use. Pentamethylcyclopentadiene,<sup>14</sup>

$\text{Cp}'_2\text{ThCl}_2$ ,  $\text{Cp}'_2\text{UCl}_2$ ,  $\text{Cp}'_2\text{Th}(\text{Me})\text{Cl}$ , and  $\text{Cp}'_2\text{U}(\text{Me})\text{Cl}$  were prepared by our usual procedures.<sup>13</sup> One-to-one adducts of butadiene and 2,3-dimethylbutadiene with magnesium were prepared in THF according to the procedure of Nakamura and co-workers.<sup>5b</sup> We obtained adequate results with an overhead stirrer and a cooling bath maintained between 5 and 20 °C in a large Dewar by the periodic removal of water and addition of portions of ice. Vinyl lithium was prepared by the method of Seyferth and Weiner<sup>15</sup> with modifications as noted below. 3-Butenyl Grignard was prepared from 1-bromo-3-butene and magnesium metal in the usual manner, and the effective concentration of the product solution determined by simple acid-base titration.

Proton NMR spectra were recorded at 90 MHz on a Varian Instruments Model EM-390 or on a JEOL Model FX-90Q instrument and at 270 MHz on a JEOL Model FX-270 instrument. Variable-temperature proton NMR spectra were measured on the FX-90Q instrument, using a thermocouple immersed in solvent within a 5-mm NMR tube to measure the probe temperature immediately after each spectrum. Carbon NMR spectra of diamagnetic compounds were recorded at 67.80 MHz on the JEOL Model FX-270 instrument. Carbon NMR spectra of uranium complexes were obtained at 22.49 MHz on the FX-90Q to exploit the larger chemical shift window available on this instrument. The <sup>13</sup>C spectra of the paramagnetic uranium complexes were obtained by using conventional pulse sequences; however, the sampling pulse was increased to ca.  $\pi/2$  and only an extremely short pulse delay (pulse delay = acquisition time) was used between pulses. The combination of short acquisition times (due to the extremely wide spectral windows) and fast relaxation times of the carbon nuclei in these complexes allowed pulse rates of ca. 5 s<sup>-1</sup>. As a consequence, it was a simple matter to collect a decoupled spectrum of a relatively concentrated sample in a 5-mm NMR tube in a matter of hours, while a coupled spectrum required overnight. All proton chemical shifts were measured relative to the internal signal from residual protons in the deuterated solvent, while <sup>13</sup>C NMR shifts were measured relative to the signal due to solvent carbon atoms. GC analyses were obtained with a Varian Model 3700 gas chromatograph equipped with FID detection and a Hewlett-Packard Model 3390A digital recorder/integrator, using either a 1.8-m (3-mm i.d.) column with 12.5% w/w SE-30 liquid phase on a Chromosorb P support or a 50 cm (3-mm i.d.) column of 80–100 mesh Spherocarb activated carbon packing. GC-MS measurements were made on a Hewlett-Packard Model 5985A GC-MS system using electron-impact ionization at 70 eV unless otherwise noted. The SE-30 column was also employed in this instrument. Elemental analyses were performed by Dornis and Kolbe Mikroanalytisches Laboratorium, Mülheim/Ruhr, West Germany.

**$\text{Cp}'_2\text{Th}(\eta^4\text{-C}_4\text{H}_6)$  (3).** In the glovebox, a 30-mL round-bottom flask was charged with  $\text{Cp}'_2\text{ThCl}_2$  (2.00 g, 3.49 mmol) and  $(\text{THF})_2\text{Mg}(\text{CH}_2\text{CH}=\text{CHCH}_2)$  (0.790 g, 3.49 mmol). The flask was connected to a vacuum frit apparatus, and the apparatus closed and then brought out of the box. The apparatus was connected to the vacuum line and evacuated. THF (20 mL) was then slowly condensed onto the white solids while they were cooled in a dry ice-acetone bath ( $-78$  °C). The resulting mixture was stirred and allowed to warm to room temperature. The initially colorless mixture slowly became orange as it warmed and was allowed to stir for an hour after reaching room temperature. The THF was evaporated in vacuo and the orange residue dried for ca. 30 min. After this time, toluene (15 mL) was condensed into the flask and the resulting orange mixture stirred for a few minutes at room temperature and filtered through the frit, separating a clear orange solution from the black insoluble salts. The salts were washed once with toluene (5 mL) condensed into the upper part of the apparatus and the combined filtrate and washings evaporated in vacuo. Once dry, the insoluble salts were off-white. Pentane (5 mL) was condensed into the orange residue and the resulting orange slurry stirred at room temperature to break up clumps. After cooling to  $-78$  °C to bring all of the product out of solution, cold filtration followed by drying in vacuo afforded 1.47 g (75% yield) of orange microcrystalline powder. This compound may be recrystallized by extraction with toluene,

(10) (a) Marks, T. J.; Fragalà, I. L., Eds. "Fundamental and Technological Aspects of Organo-f-Element Chemistry"; D. Reidel Publishing Co.: Dordrecht, 1985. (b) Marks, T. J.; Ernst, R. D. In "Comprehensive Organometallic Chemistry"; Wilkinson, G. W., Stone, F. G. A., Abel, E. W., Eds.; Pergamon Press: Oxford, 1982; Chapter 21. (c) Marks, T. J. *Science (Washington, D.C.)* **1982**, *217*, 989–997.

(11) Suzuki, H.; Marks, T. J., unpublished results in 1982–1983.

(12) (a) McIlwrick, C. R.; Phillips, C. S. G. *J. Phys. E* **1973**, *6*, 1208–1210. (b) He, M.-Y.; Xiong, G.; Toscano, P. J.; Burwell, R. L., Jr.; Marks, T. J. *J. Am. Chem. Soc.* **1985**, *107*, 641–652.

(13) Fagan, P. J.; Manriquez, J. M.; Maatta, E. A.; Seyam, A. M.; Marks, T. J. *J. Am. Chem. Soc.* **1981**, *103*, 6650–6667.

(14) Mintz, E. A.; Schertz, L. D.; Marks, T. J., manuscript in preparation.

(15) Seyferth, D.; Weiner, M. A. *J. Am. Chem. Soc.* **1961**, *83*, 3583–3586.

followed by isolation from cold pentane, in the same manner as in the workup. This reaction may be run on a scale of from 0.5 to 3.0 g of  $\text{Cp}'_2\text{ThCl}_2$  without modification, giving the same or slightly better yield. This compound is thermochromic in the solid state, reversibly becoming almost yellow on cooling to  $-78^\circ\text{C}$  and returning to an orange color at room temperature.

$^1\text{H}$  NMR ( $\text{C}_7\text{D}_8$ , 298 K, 90 MHz):  $\delta$  4.93 (complex m, 2 H,  $\text{CH}_2\text{CH}=\text{CHCH}_2$ ), 3.46 (br s, 2 H,  $\text{Th}-\text{CH}_A\text{H}_B$ ), 1.96 (br s, 15 H,  $((\text{CH}_3)_5\text{C}_5)_A$ ), 1.80 (br s, 15 H,  $((\text{CH}_3)_5\text{C}_5)_B$ ),  $-0.52$  (br s, 2 H,  $\text{Th}-\text{CH}_A\text{H}_B$ ).  $^{13}\text{C}$  NMR ( $\text{C}_7\text{D}_8$ , 233 K, 67.80 MHz):  $\delta$  122.2 (s,  $(\text{Me}_5\text{C}_5)_A$ ), 121.5 (s,  $(\text{Me}_5\text{C}_5)_B$ ), 120.0 (d,  $^1J_{\text{CH}} = 177$  Hz,  $\text{CH}_2\text{CH}=\text{CHCH}_2$ ), 68.7 (dd,  $^1J_{\text{CH}} = 131, 153$  Hz,  $\text{ThCH}_A\text{H}_B$ ), 11.9 (d,  $^1J_{\text{CH}} = 127$  Hz,  $((\text{CH}_3)_5\text{C}_5)_A$ ), 11.0 (q,  $^1J_{\text{CH}} = 127$  Hz,  $((\text{CH}_3)_5\text{C}_5)_B$ ).

Anal. Calcd for  $\text{C}_{24}\text{H}_{36}\text{Th}$ : C, 51.79; H, 6.52. Found: C, 51.76; H, 6.53.

**$\text{Cp}'_2\text{U}(\eta^4\text{-C}_4\text{H}_6)$  (2). Method A.** In the glovebox, a 100-mL round-bottom flask (this size was used to accommodate the pressure increase of evolved methane) equipped with a Teflon vacuum valve side arm was charged with  $\text{Cp}'_2\text{U}(\text{Me})\text{Cl}$  (0.220 g, 0.394 mmol) and closed with a  $90^\circ$  adaptor having a Teflon vacuum valve. The flask was removed from the glovebox and connected to the high vacuum line. Next, the flask was evacuated and diethyl ether (15 mL) condensed into the flask, after which argon was admitted. The resulting red slurry was allowed to stir for several minutes at  $-78^\circ\text{C}$  to ensure that the entire mixture was cold. Under an argon flush, 3-butenylmagnesium bromide (2.0 mL of a 0.25 M solution in ether, 0.50 mmol) was then slowly added via syringe through the side arm of the flask. The reaction mixture (still red) was exposed to vacuum while still at  $-78^\circ\text{C}$  and stirred until a satisfactory vacuum ( $<10^{-3}$  torr) was achieved. The reaction vessel was then tightly closed. Finally, the reaction was allowed to warm to room temperature and stirred overnight.

The dark green reaction mixture was next connected to a Toepler pump, and the volatiles from the reaction pumped first through a  $-78^\circ\text{C}$  trap (to remove most of the ether) and then through a liquid-nitrogen-cooled U-trap (to remove the last traces of ether) before being collected in a closed calibrated volume of 22.2 mL. The pressure stabilized at 317 mmHg (297.80 K), corresponding to 0.335 mmol (85% yield) of gas. Analysis of this gas via GC over an activated carbon support and comparison to a known standard showed this gas to be exclusively ( $>99\%$ ) methane.

To isolate the organometallic product, the green-black residue was thoroughly dried in vacuo, taken up in 5 mL of toluene, and filtered through a small (10-mm o.d.) frit on the vacuum line to separate a green-black solution from the gray solids. The solids were washed twice with toluene (2 mL), and the combined filtrate and washings were evaporated in vacuo. Finally, pentane (5 mL) was condensed onto the residue and the mixture stirred and cooled to  $-78^\circ\text{C}$ . Cold filtration afforded 0.165 g (75% yield) of the green-black microcrystalline product which was identical by NMR to the material synthesized by method B (*vide infra*).

**$\text{Cp}'_2\text{U}(\eta^4\text{-C}_4\text{H}_6)$  (2). Method B.** In the glovebox, a 50-mL round-bottom flask was charged with  $\text{Cp}'_2\text{UCl}_2$  (2.50 g, 4.31 mmol) and  $(\text{THF})_2\text{Mg}(\text{CH}_2\text{CH}=\text{CHCH}_2)$  (1.0 g, 4.41 mmol). The flask was connected to a vacuum line frit apparatus and removed from the box. On the vacuum line, the flask was evacuated and THF (25 mL) was condensed onto the red and white solids, immediately giving a bright forest green mixture. The reaction mixture was stirred and then allowed to warm to room temperature, during which time it became a darker brown-green in color. After the mixture was stirred at room temperature for ca. 1 h, the THF was removed in vacuo and the residue dried for ca. 30 min. A 1:1 mixture of pentane and toluene (total volume ca. 10 mL) was next condensed onto the residue and the resulting mixture vigorously stirred to break up the solid. The solvent was then removed in vacuo and replaced with toluene (ca. 15 mL). The resulting dark green-black mixture was filtered through the frit, and the insoluble light-brown salts were washed twice with toluene (10 mL). After the solvent was removed in vacuo, isolation as above gave 1.32 g (54% yield) of a nearly black microcrystalline powder. Subsequent experiments suggest that reducing the amount of magnesium butadiene reagent to the exact stoichiometric quantity significantly improves the purity of the initially isolated material.

$^1\text{H}$  NMR ( $\text{C}_6\text{D}_6$ , 298 K, 90 MHz):  $\delta$  47.5 ( $w_{1/2} = 27$  Hz, 2 H,  $\text{CH}_2\text{CH}=\text{CHCH}_2$ ), 8.4 ( $w_{1/2} = 15$  Hz, 15 H,  $((\text{CH}_3)_5\text{C}_5)_A$ ),  $-2.0$  ( $w_{1/2} = 12$  Hz, 15 H,  $((\text{CH}_3)_5\text{C}_5)_B$ ),  $-125.6$  ( $w_{1/2} = 25$  Hz, 2 H,  $\text{U}-\text{CH}_A\text{H}_B$ ),  $-168.9$  ( $w_{1/2} = 25$  Hz, 2 H,  $\text{U}-\text{CH}_A\text{H}_B$ ).  $^{13}\text{C}$  NMR ( $\text{C}_6\text{H}_6$ , 273 K, 22.49 MHz):  $\delta$  871.5 (t,  $^1J_{\text{CH}} = 135$  Hz,  $\text{U}-\text{CH}_2$ ), 427.0 (s,  $(\text{Me}_5\text{C}_5)_A$ ), 209.0 ( $\text{Me}_5\text{C}_5)_B$ ), 194.8 (d,  $^1J_{\text{CH}} = 177$  Hz,  $\text{CH}_2\text{CH}=\text{CHCH}_2$ ), 11.5 (q,  $^1J_{\text{CH}} = 127$  Hz,  $((\text{CH}_3)_5\text{C}_5)_A$ ),  $-50.0$  (q,  $^1J_{\text{CH}} = 127$  Hz,  $((\text{CH}_3)_5\text{C}_5)_B$ ).

Anal. Calcd for  $\text{C}_{24}\text{H}_{36}\text{U}$ : C, 51.23; H, 6.46. Found: C, 51.30; H, 6.50.

**$\text{Cp}'_2\text{Th}(\eta^4\text{-CH}_2\text{CMeCMeCH}_2)$  (4).** In the glovebox, a 30-mL round-bottom flask was charged with  $\text{Cp}'_2\text{ThCl}_2$  (1.00 g, 1.74 mmol) and  $(\text{THF})_2\text{Mg}(\text{CH}_2\text{CMe}=\text{CMeCH}_2)$  (0.437 g, 1.74 mmol). The flask was connected to a vacuum frit containing a pad of Celite as a filter aid, with a  $90^\circ$  adaptor between the flask and frit to prevent the Celite from falling into the reaction mixture. On the vacuum line, the flask was evacuated, and THF (15 mL) was condensed onto the white solids at  $-78^\circ\text{C}$ . A yellow mixture immediately formed (typical of the magnesium reagent in THF), which darkened through orange to red as the solution was allowed to warm to room temperature. After the solution was stirred at room temperature for ca. 1 h, the THF was removed in vacuo from the nearly homogeneous solution. After thoroughly drying the red residue, heptane (20 mL) was condensed into the flask and the mixture warmed slightly above room temperature with stirring to break up the solids. Now the reaction mixture was filtered, and the insoluble gray solids were washed thoroughly ( $3 \times 10$  mL) with heptane condensed into the upper part of the frit. The heptane was removed in vacuo from the bright red combined filtrate and washings and replaced with pentane (10 mL). The mixture was vigorously agitated with the aid of an external magnet to loosen the product from the sides of the flask and then slowly cooled to  $-78^\circ\text{C}$ . Cold filtration afforded 0.91 g (89% yield) of orange-red microcrystalline product. This reaction may be scaled up, but it is important to keep the stoichiometric ratio of reactants at 1.0:1.0 to avoid complications in the workup.

$^1\text{H}$  NMR ( $\text{C}_6\text{D}_6$ , 298 K, 90 MHz):  $\delta$  2.17 (6 H,  $\text{CCH}_3$ ), 1.94 (30 H,  $(\text{CH}_3)_5\text{C}_5$ ), 1.15 (4 H,  $\text{Th}-\text{CH}_2$ ).  $^{13}\text{C}$  NMR ( $\text{C}_6\text{H}_6$ , 273 K, 67.80 MHz):  $\delta$  122.4 (s,  $(\text{Me}_5\text{C}_5)$ ), 121.2 (s,  $\text{CH}_2\text{CCH}_3$ ), 77.8 (t,  $^1J_{\text{CH}} = 133$  Hz,  $\text{Th}-\text{CH}_2$ ), 24.99 (q,  $^1J_{\text{CH}} = 125$  Hz,  $\text{CCH}_3$ ), 11.6 (q,  $^1J_{\text{CH}} = 126$  Hz,  $((\text{CH}_3)_5\text{C}_5)$ ). At 193 K, both  $^1J_{^{13}\text{C}-\text{H}}$  values for  $\text{Th}-\text{CH}_2$  can be discerned: 123 and 140 Hz.

Anal. Calcd for  $\text{C}_{26}\text{H}_{40}\text{Th}$ : C, 53.42; H, 6.90. Found: C, 53.23; H, 6.79.

**Preparation and Isolation of  $\text{LiCH}=\text{CH}_2$ .** The following two organoactinide syntheses require pure  $\text{LiCH}=\text{CH}_2$  in solid form so that stoichiometrically precise amounts of reagents may be employed. The following modification of the procedure of Seyferth and Weiner<sup>15</sup> was found to be useful in this regard. A 100-mL round-bottom flask with a Teflon vacuum valve side arm was connected to the usual vacuum frit apparatus, evacuated, and flame dried on the vacuum line. Pentane (30 mL) was condensed into the flask and an argon atmosphere admitted. At room temperature, tetravinyltin<sup>16</sup> (2.2 mL,  $d = 1.267$ ) and then  $n\text{-BuLi}$  (15.4 mL of a 1.6 M solution in hexane) were added to the stirring pentane via syringe under an argon flush, giving a clear, pale yellow solution. After an hour, significant amounts of precipitate had formed, and the mixture was concentrated in vacuo to ca. 10 mL. Filtration at room temperature separated a white powder from the pale yellow filtrate. After being washed with pentane (5 mL) condensed into the upper portion of the frit, the powder was dried in vacuo and collected in the glovebox: 1.02 g (121% apparent yield based on  $n\text{-BuLi}$ ). To purify this material, it was transferred in the glovebox to a 30-mL round-bottom flask and connected to a fresh frit assembly. On the vacuum line, this material was taken up in diethyl ether (10 mL) and filtered. After removal of the ether, collection as above from 5 mL of pentane gave 0.72 g (86% yield) of pure (by  $^1\text{H}$  NMR) material. We find that the vinyl lithium is stable for months when refrigerated. Although we did not attempt it, we foresee no problems with scaling up this reaction.

$^1\text{H}$  NMR ( $\text{THF}-d_6$ , 298 K, 90 MHz). The spectrum exhibits a completely resolved ABX pattern consisting of three doublets

of doublets:  $\delta$  7.28 (dd, 1 H,  $\text{LiCH}=\text{CH}_{\text{cis}}\text{H}_{\text{trans}}$ ,  $^3J_{\text{HH}_{\text{cis}}}\text{H}_{\text{trans}} = 19$  Hz,  $^3J_{\text{HH}_{\text{trans}}}\text{H}_{\text{cis}} = 23$  Hz), 6.64 (dd, 1 H,  $\text{LiCH}=\text{CH}_{\text{cis}}\text{H}_{\text{trans}}$ ,  $^3J_{\text{HH}_{\text{cis}}}\text{H}_{\text{trans}} = 19$  Hz,  $^2J_{\text{HH}_{\text{gem}}}\text{H}_{\text{trans}} = 8$  Hz), 5.89 (dd, 1 H,  $\text{LiCH}=\text{CH}_{\text{cis}}\text{H}_{\text{trans}}$ ,  $^3J_{\text{HH}_{\text{trans}}}\text{H}_{\text{cis}} = 23$  Hz,  $^2J_{\text{HH}_{\text{gem}}}\text{H}_{\text{trans}} = 8$  Hz). In this assignment, cis and trans refer to the relative orientations of the hydrogen atoms.

**$\text{Cp}'_2\text{Th}(\text{CH}=\text{CH}_2)_2$  (5).** In the glovebox, a 30-mL round-bottom flask was charged with  $\text{Cp}'_2\text{ThCl}_2$  (1.00 g, 1.74 mmol) and  $\text{LiCH}=\text{CH}_2$  (0.124 g, 3.65 mmol), and connected to a vacuum frit apparatus. On the vacuum line, the flask was evacuated and diethyl ether (15 mL) condensed onto the colorless reagents at  $-78^\circ\text{C}$ . The mixture was stirred and allowed to warm slowly to  $0^\circ\text{C}$ . After the solution had stirred at  $0^\circ\text{C}$  for ca. 45 min, the ether was removed in vacuo from the yellow mixture. Pentane (20 mL) was condensed into the flask and the resulting yellow mixture then filtered at room temperature. The cream-colored salts were washed once with pentane (5 mL) and the combined filtrate and washing concentrated just until crystals began to form at room temperature. The product was then crystallized by slowly cooling the solution to  $-78^\circ\text{C}$  and collected by cold filtration after standing for several hours. The yield after drying the product in vacuo was 0.76 g (78% yield).

$^1\text{H}$  NMR ( $\text{C}_6\text{D}_6$ , 298 K, 90 MHz). The spectrum exhibited a partially resolved ABX pattern consisting of a doublet of doublets for the X proton and doublets for the A and B protons: 8.08 (dd, 2 H,  $\text{ThCH}=\text{CH}_{\text{cis}}\text{H}_{\text{trans}}$ ,  $^3J_{\text{HH}_{\text{cis}}}\text{H}_{\text{trans}} = 16$  Hz,  $^3J_{\text{HH}_{\text{trans}}}\text{H}_{\text{cis}} = 22$  Hz), 6.20 (d, 2 H,  $\text{ThCH}=\text{CH}_{\text{cis}}\text{H}_{\text{trans}}$ ,  $^3J_{\text{HH}_{\text{cis}}}\text{H}_{\text{trans}} = 19$  Hz,  $^2J_{\text{HH}_{\text{gem}}}\text{H}_{\text{trans}}$  apparent but not resolved), 5.89 (d, 2 H,  $\text{ThCH}=\text{CH}_{\text{cis}}\text{H}_{\text{trans}}$ ,  $^3J_{\text{HH}_{\text{trans}}}\text{H}_{\text{cis}} = 22$  Hz,  $^2J_{\text{HH}_{\text{gem}}}\text{H}_{\text{trans}}$  apparent but not resolved), 1.91 (s, 30 H,  $(\text{CH}_3)_5\text{C}_5$ ). In this assignment, cis and trans refer to the relative orientations of the hydrogen atoms.  $^{13}\text{C}$  NMR ( $\text{C}_6\text{D}_6$ , 298 K, 67.80 MHz):  $\delta$  123.2 (s,  $\text{Me}_5\text{C}_5$ ), 122.7 (ddd coupled to all three vinyl hydrogens,  $^1J_{\text{CH}} = 157$ , 143 Hz,  $^2J_{\text{CH}} = 7$  Hz,  $\text{CH}=\text{CH}_2$ ), 11.4 (q,  $^1J_{\text{CH}} = 127$  Hz,  $(\text{CH}_3)_5\text{C}_5$ ), 8.0 (br d,  $^1J_{\text{CH}} = 132$  Hz,  $\text{Th}-\text{CH}=\text{CH}_2$ ).

Anal. Calcd for  $\text{C}_{24}\text{H}_{36}\text{Th}$ : C, 51.79; H, 6.52. Found: C, 51.78; H, 6.47.

**$\text{Cp}'_2\text{U}(\text{CH}=\text{CH}_2)_2$  (6).** Working in a manner exactly analogous to that used for the thorium compound 5, reaction of dark red  $\text{Cp}'_2\text{UCl}_2$  (0.750 g, 126 mmol) with vinylolithium (0.102 g, 3.00 mmol) gave 0.48 g (66%) of a burgundy-red product.

$^1\text{H}$  NMR ( $\text{C}_6\text{D}_6$ , 298 K, 90 MHz):  $\delta$  3.74 ( $w_{1/2} = 15$  Hz, 30 H,  $(\text{CH}_3)_5\text{C}_5$ ), -18.9 ( $w_{1/2} = 15$  Hz, 2 H,  $\text{U}-\text{CH}=\text{CH}_A\text{H}_B$ ), -113.4 ( $w_{1/2} = 36$  Hz, 2 H,  $\text{U}-\text{CH}=\text{CH}_A\text{H}_B$ ), -130.8 ( $w_{1/2} = 36$  Hz, 2 H,  $\text{U}-\text{CH}=\text{CH}_A\text{H}_B$ ).  $^{13}\text{C}$  NMR ( $\text{C}_6\text{D}_6$ , 298 K, 22.49 MHz):  $\delta$  420.9 (s,  $\text{Me}_5\text{C}_5$ ), -31.45 (q,  $^1J_{\text{CH}} = 127$  Hz,  $(\text{CH}_3)_5\text{C}_5$ ), -177.0 (t,  $^1J_{\text{CH}} = 127$  Hz,  $\text{U}-\text{CH}=\text{CH}_2$ ), -215.2 (d,  $^1J_{\text{CH}} = 137$  Hz,  $\text{U}-\text{CH}=\text{CH}_2$ ).

Anal. Calcd for  $\text{C}_{24}\text{H}_{36}\text{U}$ : C, 51.23; H, 6.46. Found: C, 51.11; H, 6.38.

**Reaction of  $\text{Cp}'_2\text{Th}(\text{Me})\text{Cl}$  with 3-Butenyl Grignard.** In an experiment to test for methyl-induced  $\beta$ -hydride elimination in a thorium complex, a 30-mL round-bottom flask equipped with a Teflon vacuum valve side arm was charged with  $\text{Cp}'_2\text{ThCl}_2$  (0.500 g, 0.904 mmol) and connected to the usual frit apparatus. On the vacuum line, the flask was evacuated and diethyl ether (10 mL) condensed into the flask. The mixture was stirred with cooling to  $-78^\circ\text{C}$  and argon admitted to the flask. The Grignard reagent (3.6 mL of 0.25 M solution in ether, 0.90 mmol) was then slowly added to the reaction mixture via syringe under a strong argon flush. The reaction mixture was stirred and allowed to warm slowly to room temperature. The resulting yellow mixture was then allowed to stir at room temperature for several hours, with no apparent change in color. If the expected butadiene complex were forming, the mixture would become orange. Since the reaction appeared complete, it was worked up as follows, on the assumption that reaction had halted with formation of  $\text{Cp}'_2\text{Th}(\text{Me})(\text{CH}_2\text{CH}_2\text{CH}=\text{CH}_2)$  (or some similar material). The ether was removed in vacuo, and the yellow residue was thoroughly extracted with toluene (15 mL). The resulting slurry was filtered, and the insoluble white salts were washed with toluene ( $3 \times 10$  mL) condensed into the upper part of the frit apparatus. Our experience with dialkyl complexes of thorium convinces us that this extraction would be sufficient to separate a solution of a bis(pentamethylcyclopentadienyl)thorium alkyl from any salts that had formed. After the toluene was removed from the yellow filtrate in vacuo, however, there was only a small amount of residue. Isolation of this material from cold pentane gave only

a few tens of milligrams of product, which gave a complex and uninterpretable  $^1\text{H}$  NMR spectrum. The same batch of Grignard reagent was subsequently used to prepare the uranium butadiene complex in high yield.

In an attempt to determine the fate of the butenyl ligand in the above procedure, a reaction was carried out with 0.150 g of  $\text{Cp}'_2\text{Th}(\text{Me})\text{Cl}$ . The reaction was performed as above, but after the ether was removed in vacuo, the pale yellow residue was hydrolyzed with a little water in methylcyclohexane. The volatiles from the hydrolysis were collected and analyzed by GC-MS. This analysis revealed only methane, solvent, ether,  $\text{Cp}'\text{H}$ , and butenes.

In another experiment, the  $\text{Cp}'_2\text{Th}(\text{Me})\text{Cl}$  + 3-butenyl Grignard reaction was carried out as described above. After 8 h at room temperature, a Toepler pump experiment was carried out on the reaction mixture as described for the analogous uranium system (vide supra). No methane was detected ( $\leq 5\%$  yield).

**Thermolyses and Photolyses of Divinyl Compounds.** For thermolysis experiments, a sample of the subject compound was placed in an NMR tube, dissolved in ca. 0.5 mL of  $\text{C}_6\text{D}_{12}$  or  $\text{C}_6\text{D}_6$ , and sealed off in vacuo. For  $\text{Cp}'_2\text{Th}(\text{CH}=\text{CH}_2)_2$ , heating in the dark at  $50^\circ\text{C}$  led only to decomposition as determined by  $^1\text{H}$  NMR. In a similar manner, dilute samples of the compounds were prepared in methylcyclohexane and irradiated in a water bath with a high-pressure mercury lamp through both quartz and Pyrex. Here, too, only decomposition occurred. No characterizable products were formed. In the case of  $\text{Cp}'_2\text{U}(\text{CH}=\text{CH}_2)_2$ , thermolysis at  $50^\circ\text{C}$  led to a complex mixture of products as monitored by  $^1\text{H}$  NMR. However,  $\text{Cp}'_2\text{U}(\eta^4\text{-C}_4\text{H}_6)$  could be clearly identified at the completion of the reaction in  $30 \pm 10\%$  yield.

**Hydrolysis Studies of Diene Complexes.** Samples of compounds 2, 3, 4,  $(\text{THF})_2\text{Mg}(\text{CH}_2\text{CH}=\text{CHCH}_2)$ , and  $(\text{THF})_2\text{Mg}(\text{CH}_2\text{CMe}=\text{CMeCH}_2)$  were hydrolyzed so that the evolved butenes could be analyzed by GC and GC-MS. The same procedure was used for each compound, and the volatile products were identified in the GC via GC-MS and comparison to known compounds. Thus, ca. 50 mg of a compound was placed in a small Carius tube which was then connected to the vacuum line. Methylcyclohexane (ca. 0.5 mL) was condensed onto the compound, followed by ca. 2-3 equiv of water. As the tube warmed, it was shaken vigorously so that when the ice melted, hydrolysis rapidly occurred. The volatiles were immediately transferred in vacuo to a clean Carius tube, from which they were removed and immediately analyzed.

**X-ray Crystallographic Study of  $\text{Cp}'_2\text{Th}(\eta^4\text{-C}_4\text{H}_6)$  (3).**<sup>17</sup> Large plates of this compound could be grown by slow cooling of a hot saturated heptane solution containing a small amount (ca. 10%) of toluene. A small fragment, suitable for X-ray studies, was cut from one of the crystals, glued into a thin-walled glass capillary, and sealed under nitrogen. This crystal had dimensions of  $0.31 \times 0.38 \times 0.09$  mm. At room temperature ( $20 \pm 1^\circ\text{C}$ ) the crystals are monoclinic, space group  $P2_1/c-C_{2h}^5$  (No. 14),<sup>18</sup> with  $a = 9.236$  (3) Å,  $b = 14.720$  (4) Å,  $c = 17.437$  (4) Å,  $\beta = 105.48$  (2)°, and  $Z = 4$  ( $d_{\text{calcd}} = 1.619$  g  $\text{cm}^{-3}$ ;  $\mu(\text{Mo K}\alpha)^{19a} = 6.8$   $\text{mm}^{-1}$ ). The unit cell parameters were refined by using least-squares techniques from 15 computer-centered reflections with  $2\theta_{\text{MoK}\alpha} > 25^\circ$ .

Intensity measurements were made on a computer-controlled four-circle Nicolet autodiffractometer using  $0.90^\circ$  wide  $\omega$  scans and graphite-monochromated  $\text{Mo K}\alpha$  radiation. A total of 4190 independent reflections having  $2\theta_{\text{MoK}\alpha} < 50.7^\circ$  were measured in two concentric shells of  $2\theta$ . A scanning rate of  $6^\circ \text{min}^{-1}$  was used for the first 0.5 limiting  $\text{Cu K}\alpha$  spheres ( $3^\circ < 2\theta < 43.0^\circ$ ), and a scanning rate of  $3.0^\circ \text{min}^{-1}$  was used for the remainder of the reflections ( $0.5-0.8$  limiting  $\text{Cu K}\alpha$  spheres ( $43.0^\circ < 2\theta < 50.7^\circ$ )). The scan width and step-off for measuring background counts were both  $0.90^\circ$ , and the ratio of total background counting time to net counting time was 0.50. The intensity data were corrected empirically for absorption effects using psi scans for six reflections having  $2\theta$  values between  $5.6^\circ$  and  $26.1^\circ$ , after which data were reduced to relative squared amplitudes,  $|F_o|^2$ , by means of standard

(17) See paragraph at end regarding supplementary material.

(18) "International Tables for X-ray Crystallography"; Kynoch Press: Birmingham, England, 1969; Vol. I, p 99.

(19) "International Tables for X-ray Crystallography"; Kynoch Press: Birmingham, England, 1974; Vol. IV: (a) pp 55-66. (b) pp 99-101. (c) pp 149-150.

**Table I. Fractional Atomic Coordinates for Non-Hydrogen Atoms in Crystalline  $[\eta^5-(\text{C}_6\text{H}_5)_5\text{C}_5]_2\text{Th}(\eta^4-\text{C}_4\text{H}_6)$  (3)<sup>a</sup>**

atom type <sup>b</sup>	10 <sup>3</sup> x	10 <sup>3</sup> y	10 <sup>3</sup> z	B, Å <sup>2</sup>
Th	257.3 (1)	320.7 (1)	315.2 (1)	3.5 (1)
C <sub>a1</sub>	43 (3)	393 (1)	184 (1)	8 (1)
C <sub>a2</sub>	-3 (3)	426 (1)	251 (2)	7 (1)
C <sub>a3</sub>	109 (3)	489 (1)	287 (1)	6 (1)
C <sub>a4</sub>	219 (2)	495 (1)	243 (1)	6 (1)
C <sub>a5</sub>	174 (3)	436 (1)	178 (1)	7 (1)
C <sub>b1</sub>	132 (2)	213 (1)	418 (1)	5 (1)
C <sub>b2</sub>	143 (2)	301 (1)	449 (1)	5 (1)
C <sub>b3</sub>	285 (3)	322 (2)	481 (1)	8 (1)
C <sub>b4</sub>	373 (2)	249 (3)	472 (1)	11 (1)
C <sub>b5</sub>	272 (4)	179 (1)	429 (1)	10 (1)
C <sub>ma1</sub>	-51 (4)	331 (1)	121 (2)	19 (1)
C <sub>ma2</sub>	-150 (3)	406 (2)	261 (2)	17 (2)
C <sub>ma3</sub>	110 (4)	550 (1)	354 (1)	15 (2)
C <sub>ma4</sub>	347 (3)	562 (1)	262 (2)	20 (2)
C <sub>ma5</sub>	250 (4)	440 (2)	108 (2)	17 (2)
C <sub>mb1</sub>	-6 (4)	158 (2)	379 (1)	19 (2)
C <sub>mb2</sub>	21 (5)	362 (2)	470 (2)	23 (2)
C <sub>mb3</sub>	341 (4)	408 (2)	530 (1)	19 (2)
C <sub>mb4</sub>	538 (2)	241 (3)	507 (2)	24 (2)
C <sub>mb5</sub>	323 (6)	90 (2)	420 (2)	29 (3)
C <sub>1</sub>	539 (2)	323 (2)	332 (1)	13 (1)
C <sub>2</sub>	485 (2)	304 (2)	243 (2)	13 (1)
C <sub>3</sub>	371 (3)	241 (2)	202 (2)	10 (1)
C <sub>4</sub>	314 (4)	176 (2)	243 (1)	13 (1)

<sup>a</sup> Numbers in parentheses are the estimated standard deviations in the last significant digit. <sup>b</sup> Atoms are labeled in agreement with Figure 1. <sup>c</sup> Equivalent isotropic thermal parameter is one-third of the trace of the orthogonalized  $B_{ij}$  tensor.

Lorentz and polarization corrections. The range of relative transmission factors in the absorption correction was 0.125–1.000.

The structure was solved by using the "heavy-atom" technique. Unit-weighted isotropic cascade block-diagonal least-squares refinement of the parameters for the thorium atom converged to  $R_1$  (unweighted, based on  $F$ )<sup>20</sup> = 0.179 and  $R_2$  (weighted, based on  $F$ )<sup>21</sup> = 0.213 for 1761 independent reflections having  $2\theta < 43^\circ$  and  $I > 3\sigma(I)$ .<sup>22</sup> At this point the positions of the remaining 24 carbon atoms were clear in a difference map. Inclusion of these atoms into the model with isotropic thermal parameters and the use of anisotropic thermal parameters for the thorium atom gave  $R_1 = 0.073$  and  $R_2 = 0.092$ . Final cycles of counting-statistics weighted<sup>23</sup> cascade block-diagonal least-squares refinement of the model included anisotropic thermal parameters<sup>24</sup> for all non-hydrogen atoms and gave  $R_1 = 0.049$  and  $R_2 = 0.047$  for the complete set of 2450 reflections ( $2\theta_{\text{MoK}\alpha} < 50.7^\circ$ ) with  $I > 3\sigma(I)$ . The final cycles included an extinction correction.<sup>25</sup> Table I lists the final atomic positional parameters, and Table II lists the anisotropic thermal parameters.<sup>17</sup> Observed and calculated structure factor amplitudes are given in Table III.<sup>17</sup>

All structure factor calculations employed recent tabulations<sup>19b</sup> of atomic form factors, including anomalous dispersion corrections<sup>19c</sup> to the scattering factors of the thorium atom. All calculations were performed on a Data General Eclipse S-200 computer with 64K of 16-bit words, a parallel floating-point processor for 32- and 64-bit arithmetic, and a Data General disk with 10 million 16-bit words. Data set manipulations and model refinement were accomplished with versions of either the Nicolet (Syntex) E-XTL or the SHELXTL interactive crystallographic software packages as modified at Crystalitics Company.

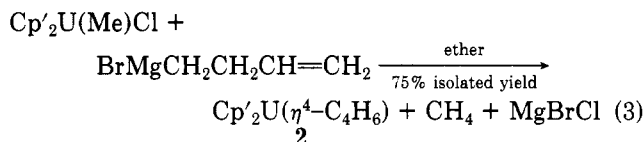
**Titration Calorimetry.** The specially designed anaerobic isoperibol solution batch titration calorimeter and general pro-

cedures for organoactinides have been described elsewhere.<sup>26</sup> The titrant, *t*-BuOH, was purified as outlined previously.<sup>26a</sup> The accuracy of the calorimeter was checked by measuring (i) the enthalpy of solution of potassium chloride (NBS Standard, Lot 999) in water and (ii) the enthalpy of reaction of tris(hydroxymethyl)aminomethane (NBS Standard, Lot 724), THAM, with hydrochloric acid. In the former, our value, based upon four measurements, for  $\Delta H^\circ$  ( $\infty$ , 298.15) is  $4.13 \pm 0.02$  kcal/mol, which compares well with the accepted value of  $4.118 \pm 0.004$  kcal/mol.<sup>27a</sup> In the latter case, our value for  $\Delta H_i$  of THAM<sup>+</sup> is  $11.33 \pm 0.03$  kcal/mol, which agrees excellently with the value reported by Ojelund and Wadsö of  $11.45 \pm 0.01$  kcal/mol.<sup>27b</sup>

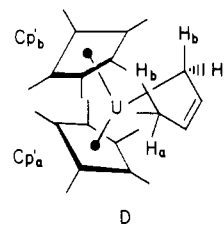
## Results and Discussion

### Synthetic Pathways to Actinide Diene Complexes.

The reaction between  $\text{Cp}'_2\text{U}(\text{Me})\text{Cl}$  and 3-butenylmagnesium bromide in ether proceeds smoothly to produce the dark green-black uranium butadiene complex **2** in high yield (eq 3).

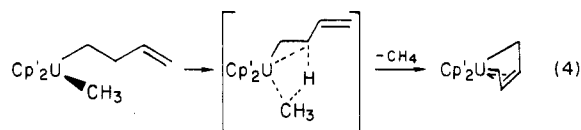


Toepler pump measurements verify the formation of methane in 85% yield. Complex **2** was characterized by standard analytical and NMR spectroscopic methodology (see Experimental Section for details). The generally well-resolved <sup>1</sup>H and <sup>13</sup>C NMR spectra of **2** exhibit some of the largest isotropic shifts yet observed for a U(IV) (5f<sup>2</sup>) organometallic. At room temperature, the NMR data are consistent with a folded, metallacyclopentene structure (D)



having magnetically nonequivalent Cp' ligands and  $\alpha$ -methylene protons. Further comparative static and dynamic aspects of the NMR spectra are discussed below. Independent synthesis of **2** by a more conventional route (vide infra) confirms this formulation.

The most reasonable pathway from complex **1** to **2** would appear to involve initial halide displacement to form the dialkyl  $\text{Cp}'_2\text{U}(\text{Me})\text{CH}_2\text{CH}_2\text{CH}=\text{CH}_2$ , a process for which there is considerable precedent.<sup>13</sup> A subsequent, intramolecular C–H activation/cyclometalation process, involving the weak, allylic C–H bond<sup>28</sup> of the butenyl ligand, followed by metallacyclic ring closure would then yield **2** (e.g., eq 4). Such a process is estimated to be exothermic



(vide infra). Intramolecular  $\gamma$ -C–H activation/cyclome-

(26) (a) Bruno, J. W.; Marks, T. J.; Morss, L. R. *J. Am. Chem. Soc.* **1983**, *105*, 6824–6832. (b) Sonnenberger, D. C.; Morss, L. R.; Marks, T. J. *Organometallics* **1985**, *4*, 352–355.

(27) (a) Kilday, M. V. *J. Res. Natl. Bur. Stand. (U.S.)* **1980**, *85*, 467–481. (b) Ojelund, G.; Wadsö, I. *Acta Chem. Scand.* **1968**, *22*, 2691–2699.

(28) McMillen, D. F.; Golden, D. M. *Annu. Rev. Phys. Chem.* **1982**, *33*, 493–532.

(20)  $R_1 = \sum ||F_o| - |F_c|| / \sum |F_o|$ .

(21)  $R_2 = (\sum w(|F_o| - |F_c|)^2 / \sum w|F_o|^2)^{1/2}$ .

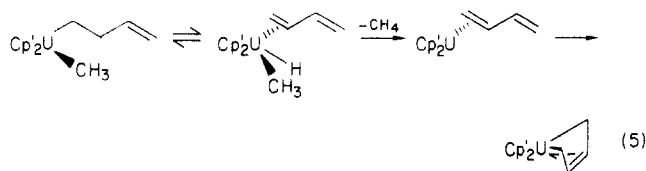
(22) The standard deviation in the intensity is computed from  $\sigma^2(I) = (C_i + k^2B)$  where  $C_i$  is the total scan count,  $k$  is the ratio of scan time to background time, and  $B$  is the total background count.

(23) For weights based on counting statistics,  $\sigma_F = \{[F_o]\}^{1/2} + [0.01|F_o|]^{1/2}$ .

(24) The anisotropic thermal parameter is of the form  $\exp[-0.25(B_{11}h^2a^{*2} + B_{22}k^2b^{*2} + B_{33}l^2c^{*2} + 2B_{12}hka^{*}b^{*} + 2B_{13}hla^{*}c^{*} + 2B_{23}k lb^{*}c^{*})]$ .

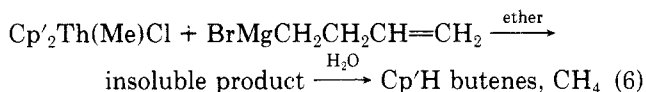
(25) Larson, A. C. *Acta Crystallogr.* **1967**, *23*, 664–665.

tation processes have considerable precedent in organoactinide chemistry,<sup>29</sup> and we have also reported examples of allylic C-H activation by organolanthanides.<sup>30</sup> An alternative process would involve  $\beta$ -H elimination (kinetically viable<sup>10,13,29d,31,32</sup> but thermodynamically unfavorable<sup>13,26</sup> for many organoactinides), followed by reductive elimination and ring closure (e.g., eq 5). While



U(IV)  $\rightarrow$  U(III), presumably bimolecular examples of H<sub>2</sub> elimination are known,<sup>13,33</sup> U(IV)  $\rightarrow$  U(II) eliminations are as yet unknown as are isolable U(II) organometallics<sup>10,34</sup> (divalent uranium has been suggested as a possible intermediate in reductive coupling processes involving U(III) complexes<sup>33</sup>). Ligand-induced M(IV)  $\rightarrow$  M(II) alkane elimination is, however, known for zirconium and hafnium.<sup>35,36</sup> In the case of eq 5, it is also possible to invoke metallacycle closure in concert with methane elimination so as to formally avoid the mechanistic requirement of divalent uranium.

Since Th(IV) is more resistant than U(IV) to formal changes in oxidation state<sup>10,34</sup> and since Th(IV) complexes are generally less labile,<sup>10,34</sup> the thorium analogue of eq 3 was investigated (eq 6). Surprisingly, neither Cp'<sub>2</sub>Th-



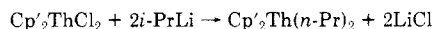
(Me)CH<sub>2</sub>CH<sub>2</sub>CH=CH<sub>2</sub> nor Cp'<sub>2</sub>Th( $\eta^4$ -C<sub>4</sub>H<sub>6</sub>) could be isolated from this reaction, although the latter complex can be prepared by an alternative procedure (vide infra) and is stable under the reaction conditions. Methane is not evolved in this reaction, and hydrolysis of the toluene-insoluble product produces butenes, pentamethylcyclopentadiene, methane, and solvent. This reaction was not investigated further.

(29) (a) Bruno, J. W.; Marks, T. J.; Day, V. W. *J. Am. Chem. Soc.* **1982**, *104*, 7357-7360. (b) Bruno, J. W.; Duttera, M. R.; Fendrick, C. M.; Smith, G. M.; Marks, T. J. *Inorg. Chim. Acta* **1984**, *94*, 271-277. (c) Bruno, J. W.; Smith, G. M.; Marks, T. J.; Fair, C. K.; Schultz, A. J.; Williams, J. M. *J. Am. Chem. Soc.* **1986**, *108*, 40-56. (d) Marks, T. J.; Day, V. W., in ref 10a, pp 115-157. (e) Simpson, S. J.; Turner, H. W.; Andersen, R. A. *Inorg. Chem.* **1981**, *20*, 2991-2995.

(30) Jeske, G.; Lauke, H.; Mauermann, H.; Swepston, P. N.; Schumann, H.; Marks, T. J. *J. Am. Chem. Soc.* **1985**, *107*, 8091-8103.

(31) (a) Bruno, J. W.; Kalina, D. G.; Mintz, E. A.; Marks, T. J. *J. Am. Chem. Soc.* **1982**, *104*, 1860-1869. (b) Seyam, A. M. *Inorg. Chim. Acta* **1980**, *77*, L123-L125. (c) Maatta, E. A.; Marks, T. J. *J. Am. Chem. Soc.* **1981**, *103*, 3576-3578. (d) Marks, T. J.; Seyam, A. M. *J. Organomet. Chem.* **1974**, *67*, 61-66.

(32) (a) Bruno, J. W. Ph.D. Thesis, Northwestern University, 1983.



(b) Jeske, G.; Lauke, H.; Mauermann, H.; Schumann, H. Marks, T. J. *J. Am. Chem. Soc.* **1985**, *107*, 8111-8118.

(33) (a) Fagan, P. J.; Manriquez, J. M.; Marks, T. J.; Day, C. S.; Vollmer, S. H.; Day, V. W. *Organometallics* **1982**, *1*, 170-180. (b) Of course, electron-transfer processes cannot be rigorously excluded with the data at hand.

(34) (a) Marks, T. J., Fischer, R. D., Eds. "Organometallics of the f-Elements"; D. Reidel Publishing Co.: Dordrecht, 1979. (b) Marks, T. J. *Prog. Inorg. Chem.* **1979**, *25*, 224-333

(35) Gell, K. I.; Schwartz, J. *J. Chem. Soc., Chem. Commun.* **1979**, 244-245.

(36) Roddick, D. M.; Fryzuk, M. D.; Seidler, P. F.; Hillhouse, G. L.; Bercaw, J. E. *Organometallics* **1985**, *4*, 97-107 and references therein.

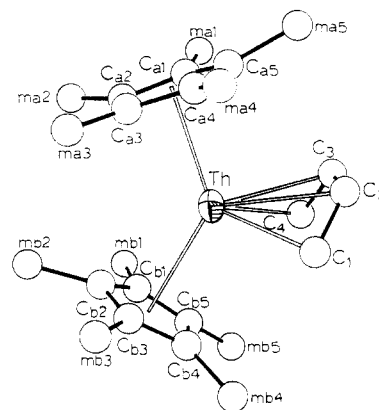
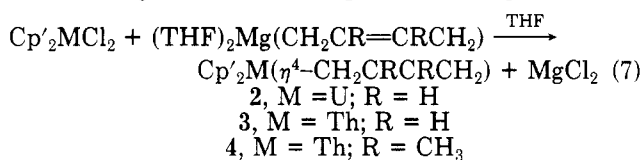
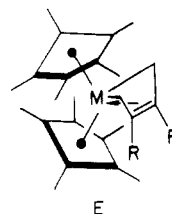


**Figure 1.** Perspective drawing of the non-hydrogen atoms in the solid-state structure of  $[\eta^5\text{-(CH}_3)_5\text{C}_5]_2\text{Th}(\eta^4\text{-C}_4\text{H}_6)$  (**3**). The thorium atom is represented by a thermal vibrational ellipsoid drawn to encompass 50% of the electron density. All carbon atoms are represented by arbitrarily sized spheres for purposes of clarity. The pentamethylcyclopentadienyl rings and butadiene carbon atoms are designated by their atomic symbols with literal and/or numerical subscripts. Pentamethylcyclopentadienyl methyl carbon atoms are labeled only by subscripts (m and a or b followed by a number).

More conventional routes to actinide diene complexes utilized magnesium diene reagents<sup>2b,6,7,37</sup> (eq 7). These



reactions proceed in high (54-89%) yield, and the products can be readily characterized by standard analytical and NMR spectroscopic techniques. The latter data (vide infra) are in accord with instantaneous, folded *s-cis*-metallacyclopentene molecular geometries (E). <sup>1</sup>H NMR

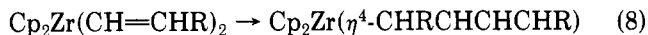


spectroscopy gives no evidence in any of these reactions for an *s-trans* isomer under normal work-up conditions. Curiously, when eq 7 was attempted with Cp'<sub>2</sub>UCl<sub>2</sub> and (THF)<sub>2</sub>Mg(CH<sub>2</sub>CMe=MeCH<sub>2</sub>), a complex mixture was obtained (all U(IV) compounds as judged by the <sup>1</sup>H NMR line widths), and no single product could be isolated by fractional crystallization. Although hydrolysis yields products (butenes) indicative that a butadiene complex is among the products, the NMR spectra are far more complex than expected from structure E (M = U, R = CH<sub>3</sub>) and/or the corresponding *s-trans* isomer.

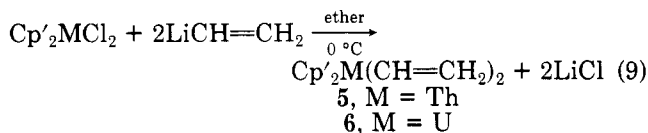
Evidence that transitory divinyl zirconium complexes are precursors to diene complexes (eq 8)<sup>9</sup> prompted an

(37) (a) Yasuda, H.; Kajihara, Y.; Mashima, K.; Lee, K.; Nakamura, A. *Chem. Lett.* **1981**, 519-522. (b) Yasuda, H.; Nakano, Y.; Natsukawa, K.; Tani, H. *Macromolecules* **1978**, *11*, 586-592. (c) Fujita, K.; Ohnuma, Y.; Yasua, H.; Tani, H. *J. Organomet. Chem.* **1976**, *113*, 201-213. (d) Akutagawa, S.; Otsuka, S. *J. Am. Chem. Soc.* **1976**, *98*, 7420-7421. (e) Baker, R.; Cookson, R. C.; Saunders, A. D. *J. Chem. Soc., Perkin Trans. 1* **1976**, 1809-1814. (f) Nakano, Y.; Natsukawa, K.; Yasuda, H.; Tani, H. *Tetrahedron Lett.* **1972**, 2833-2836. (g) Yang, M.; Ando, M.; Takase, K. *Tetrahedron Lett.* **1971**, 3529-3532. (h) Yang, M.; Yamamoto, K.; Otake, M.; Ando, M.; Takase, K. *Tetrahedron Lett.* **1970**, 3843-3846. (i) Ramsden, H. E. U.S. Patent 3388279, 1968.

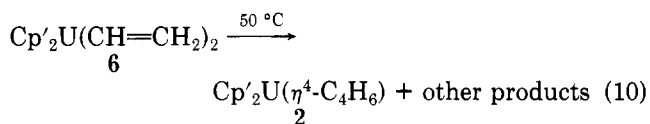




investigation of a similar approach for actinide diene complexes. Synthesis of the requisite thorium and uranium divinyl complexes was straightforward (eq 9), and



the new compounds could be characterized by standard procedures (see Experimental Section for details). For thorium complex 5, thermolysis at 50 °C in C<sub>6</sub>D<sub>12</sub> or C<sub>6</sub>D<sub>6</sub> or photolysis in methylcyclohexane (in quartz or Pyrex) yields, as judged by <sup>1</sup>H NMR, a complex mixture of products. Importantly, butadiene complex 3 is not detectable by <sup>1</sup>H NMR spectroscopy. In the case of uranium divinyl 6, thermolysis in C<sub>6</sub>D<sub>12</sub> or C<sub>6</sub>D<sub>6</sub> also gives a complex mixture of products. However, significant quantities (30 ± 10% yield) of the corresponding butadiene complex 2 are evident in the <sup>1</sup>H NMR of the reaction mixture (eq 10).



**Molecular Structure of [η<sup>5</sup>-(CH<sub>3</sub>)<sub>5</sub>C<sub>5</sub>]<sub>2</sub>Th(η<sup>4</sup>-C<sub>4</sub>H<sub>6</sub>) (3).** Single crystals of 3 suitable for X-ray diffraction were grown by slowly cooling a hot, saturated heptane solution of 3 containing ca. 10% toluene. The X-ray structural analysis reveals that single crystals of 3 are composed of discrete Cp'<sub>2</sub>Th(η<sup>4</sup>-C<sub>4</sub>H<sub>6</sub>) molecules such as that shown in Figure 1. The complex adopts the familiar bent sandwich coordination geometry with an η<sup>4</sup>-C<sub>4</sub>H<sub>6</sub><sup>2-</sup> fragment bound between the Cp' rings to the thorium. Final atomic coordinates and anisotropic thermal parameters for non-hydrogen atoms in crystalline 3 are presented in Tables I and II,<sup>17</sup> respectively. Bond lengths and angles are compiled in Table IV employing the labeling scheme shown in Figure 1.

The metrical parameters associated with the Cp'<sub>2</sub>Th fragment of 3 are unexceptional. Thus, the C<sub>g</sub>-Th-C<sub>g</sub> (C<sub>g</sub> = ring center-of-gravity) angle of 132°, the average Th-C(ring) distance of 2.84 (2, 2, 4, 10)<sup>38</sup> Å, and the average Th-C<sub>g</sub> distance of 2.58 (-, 2, 2, 2) Å are typical of Cp'<sub>2</sub>ThX<sub>2</sub> complexes.<sup>10,29,33,39</sup> The butadiene ligand of 3 is clearly coordinated in a η<sup>4</sup> fashion with an average Th-C distance to the terminal carbon atoms (C<sub>1</sub>, C<sub>4</sub>) of 2.57 (3, 3, 3, 2) Å and to the internal carbon atoms (C<sub>2</sub>, C<sub>3</sub>) of 2.74 (3, 1, 1, 2) Å. In relation to the "equatorial girdle" plane which bisects the C<sub>g</sub>-Th-C<sub>g</sub> angle, C<sub>1</sub> and C<sub>4</sub> lie below this plane by 0.36 and 0.38 Å, respectively, and C<sub>2</sub> and C<sub>3</sub> lie above the plane by 0.67 and 0.71 Å, respectively. Hence, the strongest metal-ligand interaction is to the carbon atoms closest to the equatorial girdle. Even though the precision obtained for the structure of 3 is at best average for an organometallic molecule containing a very heavy actinide

**Table IV. Bond Lengths (Å) and Angles (deg) Involving Non-Hydrogen Atoms in Crystalline [η<sup>5</sup>-(CH<sub>3</sub>)<sub>5</sub>C<sub>5</sub>]<sub>2</sub>Th(η<sup>4</sup>-C<sub>4</sub>H<sub>6</sub>) (3)<sup>a</sup>**

parameter <sup>b</sup>	value	parameter <sup>b</sup>	value
Bond Lengths			
Th-C <sub>a1</sub>	2.80 (2)	C <sub>a1</sub> -C <sub>a2</sub>	1.43 (4)
Th-C <sub>a2</sub>	2.83 (2)	C <sub>a1</sub> -C <sub>a5</sub>	1.39 (4)
Th-C <sub>a3</sub>	2.80 (2)	C <sub>a2</sub> -C <sub>a3</sub>	1.40 (3)
Th-C <sub>a4</sub>	2.84 (2)	C <sub>a3</sub> -C <sub>a4</sub>	1.43 (3)
Th-C <sub>a5</sub>	2.87 (2)	C <sub>a4</sub> -C <sub>a5</sub>	1.39 (3)
Th-C <sub>b1</sub>	2.85 (2)	C <sub>b1</sub> -C <sub>b2</sub>	1.39 (2)
Th-C <sub>b2</sub>	2.82 (2)	C <sub>b1</sub> -C <sub>b5</sub>	1.35 (4)
Th-C <sub>b3</sub>	2.83 (2)	C <sub>b2</sub> -C <sub>b3</sub>	1.32 (3)
Th-C <sub>b4</sub>	2.85 (2)	C <sub>b3</sub> -C <sub>b4</sub>	1.38 (4)
Th-C <sub>b5</sub>	2.86 (2)	C <sub>b4</sub> -C <sub>b5</sub>	1.45 (4)
Th-C <sub>ga</sub> <sup>c</sup>	2.56 (...)	C <sub>a1</sub> -C <sub>ma1</sub>	1.52 (3)
Th-C <sub>gb</sub> <sup>c</sup>	2.59 (...)	C <sub>a2</sub> -C <sub>ma2</sub>	1.44 (4)
		C <sub>a3</sub> -C <sub>ma3</sub>	1.48 (3)
		C <sub>a4</sub> -C <sub>ma4</sub>	1.52 (3)
Th-C <sub>1</sub>	2.54 (2)	C <sub>a5</sub> -C <sub>ma5</sub>	1.57 (4)
Th-C <sub>2</sub>	2.73 (2)	C <sub>b1</sub> -C <sub>mb1</sub>	1.51 (3)
Th-C <sub>3</sub>	2.74 (3)	C <sub>b2</sub> -C <sub>mb2</sub>	1.56 (4)
Th-C <sub>4</sub>	2.60 (3)	C <sub>b3</sub> -C <sub>mb3</sub>	1.54 (3)
		C <sub>b4</sub> -C <sub>mb4</sub>	1.49 (3)
C <sub>1</sub> -C <sub>2</sub>	1.52 (4)	C <sub>b5</sub> -C <sub>mb5</sub>	1.43 (4)
C <sub>2</sub> -C <sub>3</sub>	1.44 (3)		
C <sub>3</sub> -C <sub>4</sub>	1.40 (4)	Bond Angles	
		C <sub>b5</sub> C <sub>b1</sub> C <sub>b2</sub>	109 (2)
C <sub>ga</sub> ThC <sub>gb</sub> <sup>c</sup>	132 (...)	C <sub>b1</sub> C <sub>b2</sub> C <sub>b3</sub>	110 (2)
		C <sub>b2</sub> C <sub>b3</sub> C <sub>b4</sub>	108 (2)
C <sub>ga</sub> ThC <sub>1</sub> <sup>c</sup>	116 (...)	C <sub>b3</sub> C <sub>b4</sub> C <sub>b5</sub>	107 (2)
C <sub>ga</sub> ThC <sub>4</sub> <sup>c</sup>	117 (...)	C <sub>b4</sub> C <sub>b5</sub> C <sub>b1</sub>	106 (2)
		C <sub>a5</sub> C <sub>a1</sub> C <sub>ma1</sub>	124 (2)
C <sub>ga</sub> ThC <sub>2</sub> <sup>c</sup>	99 (...)	C <sub>a2</sub> C <sub>a1</sub> C <sub>ma1</sub>	124 (2)
C <sub>ga</sub> ThC <sub>3</sub> <sup>c</sup>	98 (...)	C <sub>a1</sub> C <sub>a2</sub> C <sub>ma2</sub>	122 (2)
		C <sub>a3</sub> C <sub>a2</sub> C <sub>ma2</sub>	134 (3)
C <sub>gb</sub> ThC <sub>1</sub> <sup>c</sup>	102 (...)	C <sub>a2</sub> C <sub>a3</sub> C <sub>ma3</sub>	127 (3)
C <sub>gb</sub> ThC <sub>4</sub> <sup>c</sup>	101 (...)	C <sub>a4</sub> C <sub>a3</sub> C <sub>ma3</sub>	122 (2)
		C <sub>a3</sub> C <sub>a4</sub> C <sub>ma4</sub>	124 (2)
C <sub>1</sub> ThC <sub>4</sub>	75 (1)	C <sub>a5</sub> C <sub>a4</sub> C <sub>ma4</sub>	129 (2)
		C <sub>a4</sub> C <sub>a5</sub> C <sub>ma5</sub>	121 (2)
C <sub>2</sub> ThC <sub>3</sub>	31 (1)	C <sub>a1</sub> C <sub>a5</sub> C <sub>ma5</sub>	131 (2)
		C <sub>b5</sub> C <sub>b1</sub> C <sub>mb1</sub>	122 (2)
C <sub>1</sub> ThC <sub>2</sub>	33 (1)	C <sub>b2</sub> C <sub>b1</sub> C <sub>mb1</sub>	129 (2)
C <sub>4</sub> ThC <sub>3</sub>	30 (1)	C <sub>b1</sub> C <sub>b2</sub> C <sub>mb2</sub>	130 (2)
		C <sub>b3</sub> C <sub>b2</sub> C <sub>mb2</sub>	117 (2)
C <sub>1</sub> ThC <sub>3</sub>	61 (1)	C <sub>b2</sub> C <sub>b3</sub> C <sub>mb3</sub>	126 (2)
C <sub>2</sub> ThC <sub>4</sub>	55 (1)	C <sub>b4</sub> C <sub>b3</sub> C <sub>mb3</sub>	125 (2)
		C <sub>b3</sub> C <sub>b4</sub> C <sub>mb4</sub>	126 (3)
C <sub>a5</sub> C <sub>a1</sub> C <sub>a2</sub>	111 (2)	C <sub>b5</sub> C <sub>b4</sub> C <sub>mb4</sub>	127 (3)
C <sub>a1</sub> C <sub>a2</sub> C <sub>a3</sub>	104 (2)	C <sub>b4</sub> C <sub>b5</sub> C <sub>mb5</sub>	122 (3)
C <sub>a2</sub> C <sub>a3</sub> C <sub>a4</sub>	110 (2)	C <sub>b1</sub> C <sub>b5</sub> C <sub>mb5</sub>	131 (3)
C <sub>a3</sub> C <sub>a4</sub> C <sub>a5</sub>	107 (2)	C <sub>1</sub> C <sub>2</sub> C <sub>3</sub>	129 (2)
C <sub>a4</sub> C <sub>a5</sub> C <sub>a1</sub>	107 (2)	C <sub>2</sub> C <sub>3</sub> C <sub>4</sub>	121 (2)

<sup>a</sup> Numbers in parentheses are the estimated standard deviation in the last significant digit. <sup>b</sup> Atoms are labeled in agreement with Tables I and II and Figure 1. <sup>c</sup> C<sub>ga</sub> and C<sub>gb</sub> are used to designate the centers of gravity for the five-membered rings of (CH<sub>3</sub>)<sub>5</sub>C<sub>5</sub><sup>-</sup> ligands a and b, respectively.

atom, and there are no bis(cyclopentadienyl) group 4 structures of unsubstituted butadienes with which to compare, a number of significant, comparative comments can be made about the butadiene ligation in 3 vis-à-vis Zr and Hf butadiene complexes. First, the thorium-to-terminal carbon atom distances are significantly shorter than those to the internal carbon atoms (Δ = 0.17 (3) Å). As can be seen in Table V, this is a common feature of group 4 diene complexes. However, Δ is generally larger for the group 4 complexes, the only exception being the 16-electron (dmpe)Hf(η<sup>4</sup>-C<sub>4</sub>H<sub>6</sub>)<sub>2</sub> complex.<sup>7</sup> This parameter (Δ) is also comparable to 3 in 16-electron CpTaCl<sub>2</sub>(η<sup>4</sup>-C<sub>4</sub>H<sub>6</sub>)<sub>2</sub>.<sup>2e</sup> In contrast, structures of zerovalent metal diene

(38) The first number in parentheses following an average value of a bond length or angle is the root-mean-square estimated standard deviation of an individual datum. The second and third numbers, when given, are the average and maximum deviations from the averaged value, respectively. The fourth number represents the number of individual measurements which are included in the average value.

(39) (a) Bruno, J. W.; Marks, T. J.; Day, V. W. *J. Organomet. Chem.* **1983**, *250*, 237-246. (b) Fagan, P. J.; Manriquez, J. M.; Vollmer, S. H.; Day, C. S.; Day, V. W.; Marks, T. J. *J. Am. Chem. Soc.* **1981**, *103*, 2206-2220. (c) Marks, T. J.; Manriquez, J. M.; Fagan, P. J.; Day, V. W.; Day, C. S.; Vollmer, S. H. *ACS Symp. Ser.* **1980**, *No. 131*, 1-29.

(40) Lappert, M. F.; Martin, T. R.; Atwood, J. L.; Hunter, W. E. *J. Chem. Soc., Chem. Commun.* **1980**, 476-477.



**Table V. Important Metrical Parameters in Early-Transition-Metal *s-cis*-Butadiene Complexes<sup>a</sup>**

compound	$\Delta[(M-C_1, C_4) - (M-C_2, C_3)], \text{Å}$	$C_1-C_2, C_3-C_4, \text{Å}$	$C_2-C_3, \text{Å}$	ref
$Cp_2Zr(\eta^4-CH_2CMeCMeCH_2)$	0.297 (3)	1.451 (4)	1.398 (4)	2a
$Cp_2Hf(\eta^4-CH_2CMeCMeCH_2)$	0.374 (5)	1.472 (8)	1.378 (8)	2a
$Cp_2Zr[\eta^4-1,2\text{-bis(methylene)cyclohexane}]$	0.356 (4)	1.462 (5), 1.459 (5)	1.378 (6)	2a
$Cp_2Hf[\eta^4-1,2\text{-bis(methylene)cyclohexane}]$	0.461 (7)	1.47 (1), 1.45 (1)	1.37 (1)	2a
$Cp_2Zr(\eta^4-2,3\text{-diphenylbutadiene})$	0.425 (2)	1.469 (2), 1.476 (2)	1.393 (2)	4
$Cp_2Zr(\eta^4-2,3\text{-dimethylenebicyclo[2.2.1]heptane})$	0.258 (3)	1.456 (2)	1.391 (2)	4
$Cp_2Zr(\eta^4\text{-tetramethyl-3,4-dimethylenetricyclo-[3.1.0]hexane})$	0.233 (3)	1.444 (1), 1.447 (6)	1.398 (4)	4
$(dmpe)Hf(\eta^4-C_4H_6)_2$	0.035 (6)	1.437 (3) (av)	1.383 (4) (av)	7
$CpTaCl_2(\eta^4-C_4H_6)$	0.159 (12)	1.458 (16)	1.375 (16)	2e
$Cp_2Zr(CH_2\text{-}o\text{-}C_6H_4CH_2)$	0.560 (2)	1.48 (2)	1.42 (2)	4, 40
13 (diene)Fe(CO) <sub>3</sub> structures	-0.080 (11) (av)	$[C_1-C_2, C_3-C_4] - [C_2-C_3] = 0.021$ (2) (av)		41a
$Cp^*Th(\eta^4-C_4H_6)$ (3)	0.17 (3)	1.46 (4, 6, 6, 2)	1.44 (3)	this work

<sup>a</sup> Carbon atom numbering scheme:**Table VI. Thorium-Carbon  $\sigma$ -Bond Lengths (Å) in Thorium Hydrocarbyls**

compound	Th-C(alkyl)	Th-C(aryl)	ref
$Cp^*_2Th(CH_2SiMe_3)_2$	2.46 (1), 2.51 (1)		39a
$Cp^*_2Th(CH_2CMe_3)_2$	2.543 (4), 2.446 (4)		29c
$Cp^*_2Th(CH_2CMe_3)\text{-}(CH_2SiMe_3)$	2.44 (3), ( $CH_2CMe_3$ ) 2.47 (3), ( $CH_2SiMe_3$ )		29c
$Cp^*_2Th(CH_2SiMe_2\text{-}o\text{-}C_6H_4)$	2.493 (11)	2.449 (12)	29c
$Cp^*_2Th(CH_2SiMe_2CH_2)$	2.463 (13), 2.485 (14)		29a
$(Li^+\text{TMEDA})_3ThMe_7^{3-}$	2.571 (9) <sup>a</sup>		42
$Cp^*_2Th(\eta^4-C_4H_6)$ (3)	2.55 (3, 3, 3, 2) <sup>b</sup>		this work

<sup>a</sup> Terminal Th-CH<sub>3</sub> ligand. <sup>b</sup> Th-C<sub>1</sub>, Th-C<sub>4</sub>.

complexes (e.g., (diene)Fe(CO)<sub>3</sub><sup>41</sup>) exhibit shorter metal-carbon contacts to the internal carbon atoms of the diene fragment ( $\Delta \approx -0.080$  (11),<sup>41a</sup> Table V). The Th-C<sub>1</sub> and Th-C<sub>4</sub> distances in **3** are compared to typical Th-C(alkyl) distances in Table VI. It can be seen that the Th-C-(terminal) contacts in **3** are in the range of Th-alkyl  $\sigma$  bond distances—perhaps at the long end of that range. Similar trends have been noted for group 4 diene complexes.<sup>2a,4</sup> The average C<sub>1</sub>-C<sub>2</sub>, C<sub>3</sub>-C<sub>4</sub> bond length in **3** is 1.46 (4, 6, 6, 2) Å, a value in the range reported for group 4 analogues (Table V). This parameter is not significantly longer than C<sub>2</sub>-C<sub>3</sub> in **3** (1.44 (3) Å), although it usually is in group 4 analogues (Table V).

An examination of nonbonded contacts in **3** is also illuminating in regard to the butadiene ligation. Particularly close contacts are C<sub>1</sub>-C<sub>mb4</sub> = 3.29 (3) Å, C<sub>4</sub>-C<sub>mb5</sub> = 3.32 (3) Å, C<sub>2</sub>-C<sub>ma4</sub> = 3.39 (3) Å, and C<sub>3</sub>-C<sub>ma5</sub> = 3.39 (3) Å between the Cp' and butadiene ligands. As a point of reference, the methyl van der Waals radius is 2.0 Å and that for carbon, 1.7 Å. Deviations of Cp' methyl groups from C<sub>5</sub> mean-square planes appear to reflect repulsive interactions with the  $\eta^4-C_4H_6$  and other Cp' ligand. For Cp'<sub>a</sub> these are (Å in the direction away from Th) 0.14 (2) (ma1), 0.26 (2)

(41) (a) Cotton, F. A.; Day, V. W.; Frenz, B. A.; Hardcastle, K. I.; Troup, J. M. *J. Am. Chem. Soc.* **1973**, *95*, 4522-4528 and references therein. (b) Krüger, C.; Barnett, B. L.; Brauer, D. In "The Organic Chemistry of Iron"; Koerner von Gustorf, E. A., Grevels, F.-W., Fischler, I., Eds.; Academic Press: New York, 1978; Vol. 1, pp 1-112.

(42) Lauke, H.; Swepston, P. N.; Marks, T. J. *J. Am. Chem. Soc.* **1984**, *106*, 6841-6843.

**Table VII. Coupling Constants <sup>1</sup>J<sub>CH</sub> to  $\alpha$ -Carbon Atoms in Butadiene Complexes**

complex	<sup>1</sup> J <sub>CH</sub> , Hz	ref
$Me_3Si(CH_2CH=CHCH_2)$	125	43
$(\eta^4-C_4H_6)Fe(CO)_3$	168	44
$Cp_2Zr[\eta^4-1,2\text{-bis(methylene)cyclohexane}]$	139	5c
$Cp_2Zr(\eta^4-CH_2CMeCMeCH_2)$	140	2a
$Cp_2Zr(\eta^4\text{-tetramethyl-3,4-dimethylenetricyclo[3.1.0.0]hexane})$	143	5c
$Cp_2Zr(\eta^4-C_4H_6)$	144	5b
$Cp_2Hf[\eta^4-1,2\text{-bis(methylene)cyclohexane}]$	132	2a
$Cp_2Hf(\eta^4-CH_2CMeCMeCH_2)$	136	2a
$Cp_2Hf(\eta^4-C_4H_6)$	140	5b
$Cp^*_2U(\eta^4-C_4H_6)$ (2)	135	this work
$Cp^*_2Th(\eta^4-C_4H_6)$ (3)	142 (131, 153) <sup>a</sup>	this work
$Cp^*_2Th(\eta^4-CH_2CMeCMeCH_2)$ (4)	133 (123, 140) <sup>a</sup>	this work

<sup>a</sup> Values in parentheses recorded at the slow-exchange limit.

(ma2), 0.15 (2) (ma3), 0.11 (2) (ma4), and 0.30 (2) (ma5), and for Cp'<sub>b</sub> these are (Å in the direction away from Th) 0.07 (2) (mb1), 0.34 (2) (mb2), 0.17 (2) (mb3), 0.17 (2) (mb4), and 0.20 (2) (mb5).

**NMR Spectra. Static and Dynamic Aspects.** The one-bond coupling constant between C<sub>1</sub>, C<sub>4</sub> and the  $\alpha$ -hydrogen atoms is another physical parameter that has been used to characterize the bonding in metal diene complexes.<sup>2b</sup> The limiting cases are represented by pure  $\sigma$  bonding (structure B) in  $Me_3Si(CH_2CH=CHCH_2)$  (<sup>1</sup>J<sub>C-H</sub> = 125 Hz)<sup>43</sup> and  $\eta^4$   $\pi$ -bonding (structure A) as in  $(\eta^4-C_4H_6)Fe(CO)_3$  (<sup>1</sup>J<sub>C-H</sub>  $\approx$  168 Hz for both "inner" and "outer" hydrogen atoms).<sup>44</sup> It can be seen in Table VII that <sup>1</sup>J<sub>C-H</sub> values for group 4 diene complexes fall almost midway between the two extremes, with  $J_{Zr} > J_{Hf}$ . To the extent that this parameter may qualitatively assess  $\sigma$  bond character, it is interesting to note that <sup>1</sup>J<sub>C-H</sub> for the Th butadiene complex **3** falls between the Zr and Hf analogues, while that for the 2,3-dimethylbutadiene complex falls slightly below the values for the Zr and Hf analogues. While such relationships may be to some degree inform-

(43) (a) Panasenko, A. A.; Khaililov, L. M.; Tsyrlina, E. M.; Yurev, V. P. *Izv. Akad. Nauk SSSR, Ser. Khim.* **1981**, 424-430. (b) Filleux-Blanchard, M. L.; Nguyen, D. A.; Manuel, G. *J. Organomet. Chem.* **1977**, *137*, 11-22.

(44) (a) Bachmann, K.; von Philipsborn, W. *Org. Magn. Reson.* **1976**, *8*, 648-654. (b) Marks, T. J., in ref 41b, pp 113-119. (c) Interestingly, terminal carbon <sup>1</sup>J<sub>C-H</sub> values differ little between the iron tricarbonyl complex and the free diene.

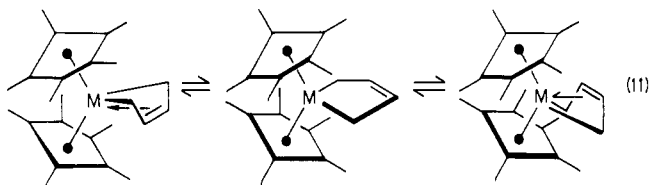
**Table VIII. Free Energies of Activation,  $\Delta G^\ddagger$  ( $T_c$ ), for Metallacyclopentene Ring Inversion in Diene Complexes<sup>a</sup>**

complex	$\Delta G^\ddagger$ ( $T_c$ )	ref
$\text{Cp}_2\text{Zr}[\eta^4\text{-tetramethyl-3,4-dimethylene-tricyclo[3.1.0.0]hexane}]$	14.3 (284)	45
$\text{Cp}_2\text{Zr}(\eta^4\text{-C}_4\text{H}_6)$	12.6 (253)	2a
$\text{Cp}_2\text{Zr}(\eta^4\text{-CH}_2\text{CMeCMeCH}_2)$	11.5 (231)	2a
$\text{Cp}_2\text{Zr}[\eta^4\text{-1,2-bis(methylene)cyclohexane}]$	10.8 (216)	2a
$\text{Cp}_2\text{Zr}(\eta^4\text{-2,3-diphenylbutadiene})$	8.0 (161)	45
$\text{Cp}_2\text{Zr}[\eta^4\text{-1,2-bis(methylene)tetramethylbenzene}]$	6.5 (133)	45
$\text{Cp}_2\text{Hf}(\eta^4\text{-C}_4\text{H}_6)$	8.1 (165)	2a
$\text{Cp}_2\text{Hf}(\eta^4\text{-CH}_2\text{CMeCMeCH}_2)$	8.3 (168)	2a
$\text{Cp}_2\text{Hf}[\eta^4\text{-1,2-bis(methylene)cyclohexane}]^b$	7.6 (152)	2a
$\text{Cp}'_2\text{U}(\eta^4\text{-C}_4\text{H}_6)$ (2)	17.0 (394)	this work
$\text{Cp}'_2\text{Th}(\eta^4\text{-C}_4\text{H}_6)$ (3)	15.0 (299)	this work
$\text{Cp}'_2\text{Th}(\eta^4\text{-CH}_2\text{CMeCMeCH}_2)$ (4)	10.5 (208)	this work

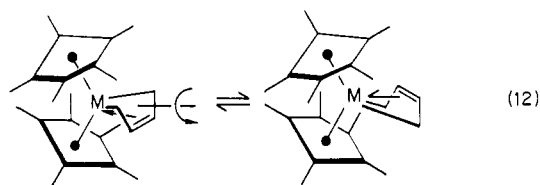
<sup>a</sup>In kcal mol<sup>-1</sup>. Estimated uncertainties are usually  $\pm 0.3$  kcal mol<sup>-1</sup>.  $T_c$  in K.

ative, the actual situation for early transition element and actinide diene complexes differs from structures A and B in that the measured room-temperature  $^1\text{J}_{\text{C-H}}$  values are actually a time average of two quantities which may be quite different (vide infra).

A number of the group 4 diene complexes exhibit fluxional behavior which has been ascribed to rapid ring inversion, presumably occurring via a planar metallacyclopentene structure (eq 11).<sup>2a,b,5a,45</sup> As can be seen in Figure



2, complexes 3 and 2 also exhibit dynamic behavior, as does 4 (not shown). Rapid interchange of both the magnetically nonequivalent Cp' ligands and  $\alpha$ -methylene protons is observed. Simple rotation of the  $\eta^4$ -diene unit<sup>46</sup> about an axis in the equatorial girdle would average Cp' ligands but not methylene protons (eq 12). For complexes 2, 3, and



4 the free energy of activation for Cp' interchange can be calculated at coalescence using the standard modified Bloch equation formalism,<sup>47</sup> and the results are shown in Table VIII. A similar treatment of the methylene proton exchange processes (chemical shift differences are far in excess of the proton-proton coupling constants) yields rates which are the same, within experimental error, to those for Cp' interchange in the same compound. Hence, there is no evidence for significant diene rotation in the actinide complexes.

(45) (a) Erker, G.; Engel, K.; Krüger, C.; Chiang, A.-P. *Chem. Ber.* **1982**, *115*, 3311-3323. (b) Lubke, B.; Edelmann, F.; Behrens, U. *Chem. Ber.* **1983**, *116*, 11-26.

(46) (a) Marks, T. J., in ref 44 b, pp 131-132. (b) Ittel, S. D.; Van-Catledge, F. A.; Jesson, J. P. *J. Organomet. Chem.* **1979**, *168*, C25-C29. (c) Katzian, M.; Kreiter, C. G.; Özkar, S. *J. Organomet. Chem.* **1982**, *229*, 29-42.

(47) (a) Küppert, R. *J. Magn. Reson.* **1982**, *47*, 91-102 and references therein. (b) Binsch, G. In "Dynamic Nuclear Magnetic Resonance Spectroscopy"; Jackman, L. M., Cotton, F. A., Eds.; Academic Press: New York, 1975; Chapter 3.

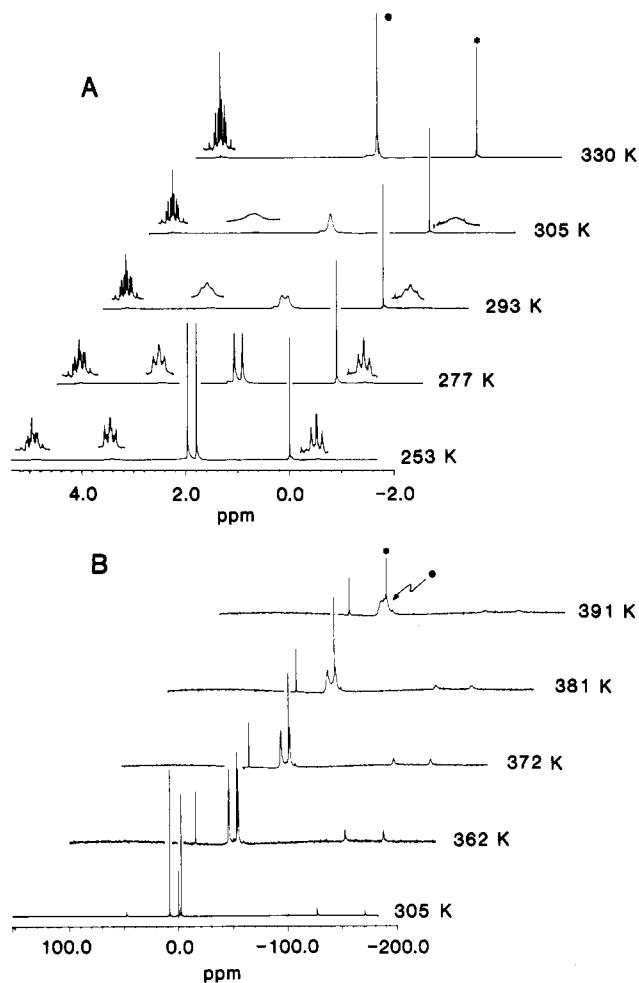


**Figure 2.** Variable-temperature 90-MHz  $^1\text{H}$  NMR spectra of A,  $\text{Cp}'_2\text{Th}(\eta^4\text{-C}_4\text{H}_6)$  (3) in toluene- $d_8$ , and B,  $\text{Cp}'_2\text{U}(\eta^4\text{-C}_4\text{H}_6)$  (2) in benzene- $d_6$ . Asterisks denote  $\text{Me}_4\text{Si}$  and filled circles, coalesced  $\text{Cp}'$  resonances.

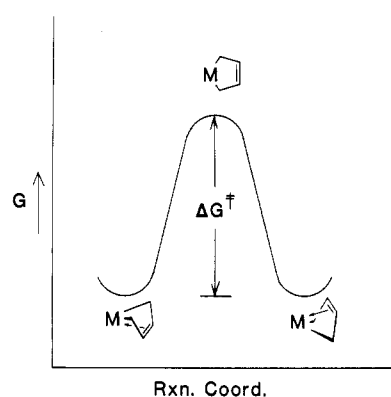


**Figure 3.** Schematic reaction coordinate for ring inversion in butadiene complexes.

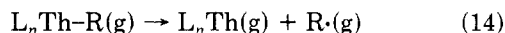
The  $\Delta G^\ddagger$  data in Table VIII reveal several interesting trends. First, the inversion barriers for 2 and 3 are significantly higher than found for the zirconium and hafnium butadiene complexes. One reason is likely to be the greater  $\eta^4$  character of the bonding in the actinide complexes, as suggested by the structural data. As shown in the schematic reaction coordinate of Figure 3, the free energy requirements to reach the metallacyclopentene transition state should decrease as the  $\eta^2$  ( $\sigma^2$ ) character of the ground state increases (all other factors being equal). Similar arguments have been advanced to explain  $\Delta G^\ddagger$  differences between Zr and Hf for identical diene ligands (Tables V and VIII).<sup>2a</sup> The reason for the  $\Delta G^\ddagger$  difference between

2 and 3 (uranium and thorium) is not immediately obvious. The lower barrier in complex 4 appears to reflect steric repulsion in the ground state ( $\text{Cp}'\text{CH}_3$ -butadiene- $\text{CH}_3$ , cf. Figure 1), which should raise  $\Delta G^\circ$  of the ground state relative to the less congested transition state. This is also evident in the thermochemical results (vide infra). This butadiene  $\rightarrow$  dimethylbutadiene effect is not as large in the group 4 systems (Table VIII), possibly because of the smaller steric demands of Cp ligands. However, analogous steric effects are probably operative for some of the more highly substituted dienes.<sup>2a</sup>

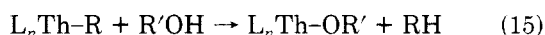
Returning to the question of bonding information afforded by room-temperature  $\alpha$ -carbon  $^1J_{\text{C-H}}$  values, low-temperature  $^{13}\text{C}$  NMR spectroscopy of the actinide diene complexes allows measurement of the individual (rather than averaged) coupling constants in the static molecular structures (Table VII). While the  $^{13}\text{C}$  spectrum of 2 is too broad for accurate  $J_{\text{C-H}}$  measurements, the data for 3 and 4 reveal a surprising dispersion in  $^1J_{\text{C-H}}$  with one value tending toward  $\sigma^2$  limit and the other toward the  $\eta^4$  limit. This situation differs markedly from the equivalences or near equivalences observed in  $\sigma^2$  structures,<sup>43</sup>  $\eta^4$ -diene structures,<sup>44</sup> and the free dienes.<sup>44</sup> The results suggest that caution should be exercised when drawing conclusions about bonding from the averaged, room-temperature data.

**Thermochemistry.** As discussed in detail elsewhere,<sup>26,48</sup> batch titration calorimetry can be employed to measure  $L_n\text{Th-R}$  bond disruption enthalpies ( $D(L_n\text{Th-R})$ )<sup>49</sup> for a wide variety of R functionalities and supporting ligands. The bond disruption enthalpy is formally defined as in eq 13 for the gas-phase homolytic process depicted in eq 14. If the alcoholysis of the organothorium complex

$$D(L_n\text{Th-R}) = \Delta H_f^\circ(L_n\text{Th})(g) + \Delta H_f^\circ(\text{R}\cdot)(g) - \Delta H_f^\circ(L_n\text{Th-R})(g) \quad (13)$$



is rapid, quantitative, and selective for the Th-R bond (eq 15), then it is possible to relate the measured heat of al-



coholysis to solution-phase bond disruption enthalpies (eq 16)<sup>26</sup> or, using measured/tabulated heats of solution along

$$-\Delta H_{\text{rxn}} = D(L_n\text{Th-O})_{\text{soln}} + D(\text{R-H})_{\text{soln}} - D(L_n\text{Th-R})_{\text{soln}} - D(\text{O-H})_{\text{soln}} \quad (16)$$

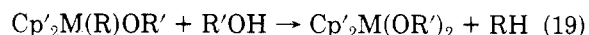
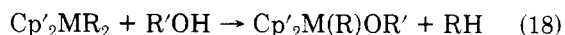
with reasonable assumptions about (or tabulated) heats of vaporization,<sup>26</sup> to gas-phase bond disruption enthalpies (eq 17). Gas-phase  $D$ 's may bear slightly greater uncer-

$$-\Delta H_{\text{gas}}^\circ = D(L_n\text{Th-O}) + D(\text{R-H}) - D(L_n\text{Th-R}) - D(\text{O-H}) \quad (17)$$

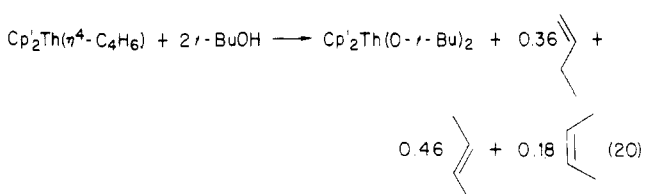
tainties<sup>26</sup> and are frequently superfluous for understanding chemical processes in solution. The quantities  $D(\text{R-H})$  and  $D(\text{O-H})$  are tabulated<sup>28,50</sup> or can be reasonably estimated.<sup>26</sup> Thus, it is straightforward to obtain a relative ordering of  $D(L_n\text{Th-R})$  values for constant  $L_n$ . Moreover, a reasonable estimate of  $D(L_n\text{Th-O}) = 124 \text{ kcal mol}^{-1}$ <sup>26,51</sup>

then yields absolute  $D(L_n\text{Th-R})$  values. An extensive body of such data now exists for  $\text{Cp}'_2\text{ThR}_2$  and  $\text{Cp}'_2\text{Th(R)OR}'$  systems,<sup>26a,48</sup> and it was of interest to obtain data on actinide butadiene complexes 3 and 4 for comparative purposes.

For  $\text{Cp}'_2\text{MR}_2$  systems, the most informative alcoholysis pattern for calorimetry is stepwise M-R protolysis (eq 18 and 19). Unfortunately, such selectivity is not always



observed,<sup>26a,48</sup> and in the case of 3 and  $t$ -BuOH, the second alcoholysis appears by  $^1\text{H}$  NMR to be somewhat more rapid than the first, so that clean, sequential Th-R titration is not possible. Nevertheless, the reaction is rapid and selective for the butadiene ligand so that valuable thermochemical information can still be obtained. The reaction stoichiometry is determined to be as shown in eq 20 by  $^1\text{H}$  NMR and GC. The butene distribution no doubt



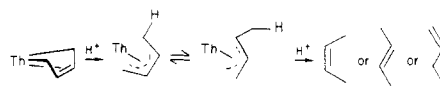
reflects the stepwise nature of the protonolysis process.<sup>5b,52a</sup> The enthalpy of solution of 3 ( $\Delta H_{\text{soln}}^\circ$ )<sup>26</sup> was determined to be 3.1 (1)<sup>52b</sup> kcal mol<sup>-1</sup> and the heat of reaction for eq 20, ( $\Delta H_{\text{rxn}}^\circ$ ), -35.1 (1.9)<sup>52b</sup> kcal mol<sup>-1</sup> of  $t$ -BuOH. The gas-phase reaction enthalpy can then be obtained via a thermodynamic cycle<sup>26</sup> as expressed by eq 21. The

$$\Delta H_{\text{gas}}^\circ = \Delta H_{\text{rxn}} - \left\{ \sum_{\text{products}} \Delta H_{\text{soln}}^\circ - \sum_{\text{reactants}} \Delta H_{\text{soln}}^\circ \right\} + \left\{ \sum_{\text{products}} \Delta H_{\text{sub}}^\circ - \sum_{\text{reactants}} \Delta H_{\text{sub}}^\circ \right\} \quad (21)$$

standard enthalpies of solution ( $\Delta H_{\text{soln}}^\circ$ ) of  $t$ -BuOH<sup>26a</sup> and the butenes<sup>53</sup> are known or can be reasonably estimated.<sup>26</sup>  $\Delta H_{\text{soln}}^\circ$  for  $\text{Cp}'_2\text{Th}(\text{O-}t\text{-Bu})_2$  has also been measured.<sup>26a</sup> For the organometallic species we did not measure  $\Delta H_{\text{soln}}^\circ$ , the enthalpy of solution at infinite dilution, but dilution corrections are expected to be negligible and, in addition, these corrections cancel for they are of opposite sign in eq 21.<sup>26</sup> The enthalpy of sublimation of  $t$ -BuOH is available,<sup>54</sup>

(51) As discussed elsewhere,<sup>26</sup> this parameter is probably not accurate to better than 10 kcal mol<sup>-1</sup>. However, any inaccuracy will be constant throughout a closely related series of molecules, and relative  $D(\text{Th-R})$  values, which describe the chemistry occurring between members of the series, should be reliable.

(52) (a) This process presumably occurs via a thorium allyl which can then undergo rearrangement or suffer protonolysis, e.g.



The product distribution will depend on the regiochemistry of protonolysis and the allyl isomer distribution. The product distribution for 3/ $\text{H}_2\text{O}$  is 76% 1-butene, 7% *cis*-2-butene, and 20% *trans*-2-butene and for 2/ $\text{H}_2\text{O}$  is 71% 1-butene, 6% *cis*-2-butene, and 23% *trans*-2-butene. The composition of the butenes is in between the group 4 hydrolysis products,<sup>5b</sup> which are richer in 1-butene, and those for the magnesium butadiene reagent, which are richer in 2-butenes (mostly *cis*).<sup>5b</sup> (b) The numbers in parentheses represent 2 $\sigma$ .

(53) Hannaert, H.; Haccuria, M.; Mathieu, M. P. *Ind. Chim. Belge* 1967, 156-164.

(54) Thermodynamic Research Center Data Tables, Texas A&M University, College Station, TX.

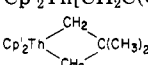
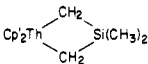


(55) Connor, J. A.; Zarafani-Moattar, M. T.; Bickerton, J.; El Saied, N. I.; Surodi, S.; Carson, R.; Takhin, G. A.; Skinner, H. H. *Organometallics* 1982, 1, 1166-1174.

(48) Sonnenberger, D. C.; Morss, L. R.; Marks, T. J., submitted for publication.

(49) (a) Pilcher, G.; Skinner, H. A. In "The Chemistry of the Metal-Carbon Bond"; Hartley, F. R., Patai, S., Eds.; Wiley: New York, 1982; pp 43-90. (b) Connor, J. A. *Top. Curr. Chem.* 1977, 71, 71-110. (c) Kochi, J. K. "Organometallic Mechanisms and Catalysts"; Academic Press: New York, 1978; Chapter 11.

(50) (a) Larson, C. W.; Harwidge, E. A.; Rabinovitch, B. S. *J. Chem. Phys.* 1969, 50, 2769-2770. (b) Golden, D. M.; Benson, S. W. *Chem. Rev.* 1969, 69, 125-134. (c) Doncaster, A. M.; Walsh, R. J. *Chem. Soc., Faraday Trans. 1* 1976, 72, 2908-2916.

Table IX. Bond Disruption Enthalpy Data for Cp<sub>2</sub>ThR<sub>2</sub> Complexes<sup>a</sup>

compound	$D(\text{Cp}'_2\text{Th}(\text{R})-\text{R})$	$D(\text{Cp}'_2\text{Th}(\text{OR}')-\text{R})$	$\bar{D}(\text{Th}-\text{R})^b$	ref
Cp <sub>2</sub> Th(CH <sub>3</sub> ) <sub>2</sub>	81.2 (0.8)	83.6 (0.9)	82.4 (0.9)	26a
Cp <sub>2</sub> Th(C <sub>2</sub> H <sub>5</sub> ) <sub>2</sub>	73.5 (1.6)	76.3 (1.6)	74.9 (1.6)	26a
Cp <sub>2</sub> Th[CH <sub>2</sub> C(CH <sub>3</sub> ) <sub>3</sub> ] <sub>2</sub>	72.3 (3.8)	76.9 (3.7)	74.6 (3.8)	26a
	65.3 (2.3)	78.6 (2.6)	72.0 (2.5)	26a
Cp <sub>2</sub> Th[CH <sub>2</sub> Si(CH <sub>3</sub> ) <sub>3</sub> ] <sub>2</sub>	80.0 (3.1)	82.2 (3.1)	81.1 (3.1)	26a
	75.5 (3.2)	83.0 (3.4)	79.3 (3.3)	26a
Cp <sub>2</sub> Th(C <sub>6</sub> H <sub>5</sub> ) <sub>2</sub>	88.9 (2.4)	92.4 (2.1)	90.7 (2.3)	26a
Cp <sub>2</sub> Th(CHCH <sub>2</sub> CH <sub>2</sub> ) <sub>2</sub>	88.0 (5.0)		88.0 (5.0)	57
Cp <sub>2</sub> Th(Cl)CH <sub>2</sub> C <sub>6</sub> H <sub>5</sub>	68.2 (1.4)		68.2 (1.4)	26a
Cp <sub>2</sub> Th  (3)			76.1 (2.4)	this work
Cp <sub>2</sub> Th  (4)			65.5 (3.2)	this work

<sup>a</sup> Solution phase. Numbers in parentheses refer to  $2\sigma$ . <sup>b</sup> Average of  $D(\text{Cp}'_2\text{Th}(\text{R})-\text{R})$  and  $D(\text{Cp}'_2\text{Th}(\text{OR}')-\text{R})$ .

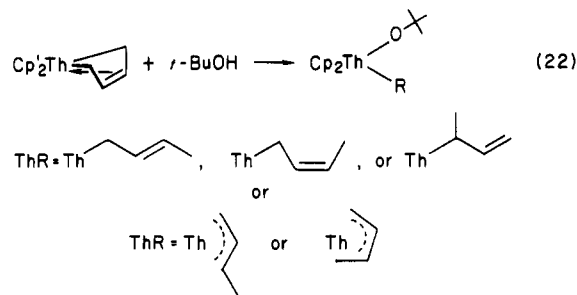
and the butenes are gases at 25 °C ( $\Delta H^\circ_{\text{sub}} = 0$ ). In addition, we make the reasonable assumption<sup>26</sup> that  $\Delta H^\circ_{\text{sub}}(\mathbf{3}) \approx \Delta H^\circ_{\text{sub}}(\text{Cp}'_2\text{Th}(\text{O}-t\text{-Bu})_2)$ . Thus, the  $\Delta H^\circ_{\text{sub}}$  terms for the organometallics in eq 21 will cancel. These considerations lead to  $\Delta H^\circ_{\text{gas}} = -37.9$  (2.3) kcal mol<sup>-1</sup> of *t*-BuOH.

Solution and gas-phase Th-butadiene bond disruption enthalpies can next be calculated via eq 16 and 17, bearing in mind that the derived values are averages for the combined processes depicted in eq 18 and 19.  $D(\text{O}-\text{H})$  for *t*-BuOH was taken to be 105.1 (1) kcal mol<sup>-1</sup>.<sup>28</sup> The  $D(\text{R}-\text{H})$  values used for the butenes were taken from the literature<sup>28,50</sup> and were weighted in the calculation by the stoichiometry of eq 20.<sup>56</sup> The average values  $\bar{D}(\text{Th}-\text{butadiene})_{\text{soln}} = 76.1$  (2.4)<sup>52b</sup> kcal mol<sup>-1</sup> and  $\bar{D}(\text{Th}-\text{butadiene}) = 73.4$  (2.7)<sup>52b</sup> kcal mol<sup>-1</sup> are obtained. The reaction of 4 with *t*-BuOH is also rapid and nonsequential, with a tetramethylethylene:2,3-dimethyl-1-butene ratio of 0.54:0.46 formed upon alcoholysis. For 4, we find that  $\Delta H_{\text{soln}} = 4.1$  (1) kcal mol<sup>-1</sup>,  $\Delta H_{\text{rxn}} = -38.8$  (1.9) kcal mol<sup>-1</sup> of *t*-BuOH, and a treatment as described above yields  $\Delta H^\circ_{\text{gas}} = -36.6$  (2.5) kcal mol<sup>-1</sup> of *t*-BuOH. Analysis of these data as for 3<sup>56</sup> yields the average values  $\bar{D}(\text{Th}-2,3\text{-dimethylbutadiene})_{\text{soln}} = 65.5$  (3.2)<sup>52b</sup> kcal mol<sup>-1</sup> and  $\bar{D}(\text{Th}-2,3\text{-dimethylbutadiene}) = 67.7$  (3.6)<sup>52b</sup> kcal mol<sup>-1</sup>. Comparing these  $\bar{D}$  results to those for other Cp<sub>2</sub>ThR<sub>2</sub> complexes in Table IX (gas-phase data follow a similar trend), it is immediately apparent that the *Th-butadiene interaction enjoys no special stabilization*. Indeed, the  $D(\text{Th}-\text{butadiene})$  interaction is among the group of "weaker" Th-R bonds, which includes strained thoracyclobutanes and crowded<sup>29c,39a</sup> dialkyls. An alternate approach to  $\bar{D}(\text{Th}-\text{butadiene})$  and  $\bar{D}(\text{Th}-2,3\text{-dimethylbutadiene})$ , which circumvents acknowledged uncertainties in  $D(\text{vinyl}-\text{H})$ ,<sup>28</sup> would be to base the calculation upon protonolysis exclusively to *cis*-2-butene and tetramethylethylene and to then partially "isomerize" these products to the actual product distribution, correcting thermodynamically with tabulated<sup>56b</sup>  $\Delta H_f^\circ$  data for the various butenes. This approach yields solution and gas-phase  $\bar{D}(\text{Th}-\text{butadiene})$  values which are ca. 5 kcal mol<sup>-1</sup> lower than those derived above.

(56) (a) The following  $D(\text{R}-\text{H})$  values<sup>28</sup> (kcal mol<sup>-1</sup>) were employed in the calculations: R = 2-butenyl, 85.6 ± 1.5; vinyl, 110 ± 2 (for 1-butenyl and 2,3-dimethyl-1-butenyl); R = *n*-propyl, 97.9 ± 1 (for 3-butenyl and 2,3-dimethyl-3-butenyl); R = 2,3-dimethyl-2-butenyl, 78.0 ± 1.1. (b) Cox, J. D.; Pilcher, G. "Thermochemistry of Organic and Organometallic Compounds"; Academic Press: New York, 1970; p 143.  
(57) Sonnenberger, D. C.; Marks, T. J., manuscript in preparation.

While the result does not greatly affect conclusions we will draw about the thermodynamics of various transformations involving 3 and 4 (vide infra), it suggests that  $\bar{D}(\text{Th}-\text{butadiene})$  and  $\bar{D}(\text{Th}-2,3\text{-dimethylbutadiene})$  may be even "weaker".

$\bar{D}(\text{Th}-\text{butadiene})$  is, of course, a composite of two disruption enthalpies, the first of which ( $D(\text{Th}-\text{butadiene})$ ) presumably involves protolysis to form an isomeric mixture of  $\eta^1$  or  $\eta^3$ -allyls (e.g., eq 22, vide infra). The exact mo-



lecular structures of the Cp<sub>2</sub>Th(X)(allyl) complexes prepared to date<sup>58</sup> ( $\eta^1$  or  $\eta^3$ ) are unknown since they are fluxional with low barriers to rearrangement (infrared data suggest  $\eta^3$  bonding for X = alkyl<sup>58</sup>). In regard to bonding energetics,  $D(\text{Th}-\eta^1\text{-allyl})$  here is likely to be similar to the  $D(\text{Th}-\text{benzyl})$  in Table IX, corrected<sup>26</sup> for the Cl and O-*t*-Bu ligands, i.e., ca. 76 kcal mol<sup>-1</sup>.  $D(\text{Th}-\eta^3\text{-allyl})$  is likely to be somewhat larger, considering the greater metal-ligand interaction and barriers to fluxional processes in f-element  $\eta^3$ -allyls.<sup>10,30,34,59</sup> These considerations imply that  $D(\text{Th}-\eta^1\text{-allyl})$  and  $D(\text{Th}-\eta^3\text{-allyl})$  are likely to be greater than  $\bar{D}(\text{Th}-\text{butadiene})$ , hence the first bond disruption enthalpy,  $D(\text{Th}-\text{butadiene})$ , is likely to be less than  $\bar{D}(\text{Th}-\text{butadiene})$ . In summary, the "strength" of the actinide-butadiene bonding is typical of a relatively "weak" actinide-to-carbon  $\sigma$  bond.

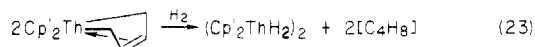
The thermochemical results also reveal a significant difference between  $\bar{D}(\text{Th}-\text{butadiene})$  and  $\bar{D}(\text{Th}-2,3\text{-dimethylbutadiene})$ . A major portion of this difference is likely due to repulsive interactions between the butadiene methyl substituents and Cp' methyl groups. As already noted, this destabilization of the  $\eta^4$  structure would be expected to decrease  $\Delta G^\ddagger$  for ring inversion, and it is

(58) Fendrick, C. M.; Marks, T. J. *J. Am. Chem. Soc.*, in press.

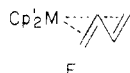
(59) Watson, P. L.; Parshall, G. W. *Acc. Chem. Res.* 1985, 18, 51-56.

noteworthy for **3** and **4** that differences in  $\Delta G^\ddagger$  are roughly comparable to differences in  $\bar{D}$ .

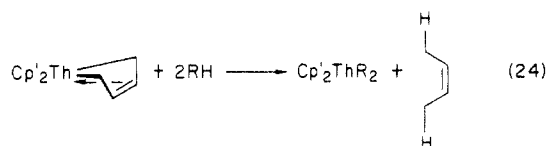
**Chemical Reactions of Actinide Butadiene Complexes.** Hydrogenolysis of actinide-to-carbon  $\sigma$  bonds is generally facile for  $\text{Cp}'_2\text{MR}_2$  systems, and complex **3** reacts rapidly with hydrogen at 1 atm, 25 °C, to yield the corresponding hydride<sup>13</sup> (identified by NMR, eq 23). Under these conditions, the liberated butene is expected to be hydrogenated.<sup>13,60a</sup>



The thermal properties of **2** and **3** were also of interest, first because *s-cis*  $\rightleftharpoons$  *s-trans* equilibration occurs in analogous zirconium systems (eq 1,  $\Delta G^\ddagger \approx 18$ –23 kcal mol<sup>-1</sup>)<sup>5</sup> and second because some actinide metallacycles (e.g.,  $\text{Cp}'_2\text{ThCH}_2\text{C}(\text{CH}_3)_2\text{CH}_2$ ) readily undergo C–H bond activating reactions with arenes and saturated hydrocarbons.<sup>29a,58,60b</sup> It is found that complexes **2** and **3** exhibit remarkable thermal stability. Thus, heating **2** for 4 h in  $\text{C}_6\text{D}_6/\text{Me}_4\text{Si}$  at 120 °C or **3** for 20 h in  $\text{C}_6\text{D}_5\text{CD}_3/\text{Me}_4\text{Si}$  at 140 °C results in negligible decomposition or reaction as monitored by <sup>1</sup>H NMR. In regard to *s-cis*  $\rightarrow$  *s-trans* conversion, the implied very high barrier to and/or apparent instability of the *s-trans* product reasonably reflects the diene complex, divalent character expected<sup>3</sup> for such species F. Such a ground-state electronic structure would appear to be energetically unfavorable for an actinide.<sup>34,61</sup>



With the thermochemical data now at hand, the problem of why complexes such as **3** do not readily activate hydrocarbons can be explored. For processes such as eq 24,



$\Delta H$  values can be estimated for the most reactive hydrocarbons such as benzene,  $\text{SiMe}_4$ , and cyclopropane.<sup>29a,57,60b</sup>

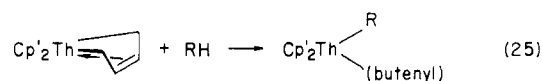
$$\Delta H(\text{C}_6\text{H}_6) \approx +22 \text{ kcal mol}^{-1}$$

$$\Delta H(\text{SiMe}_4) \approx +16 \text{ kcal mol}^{-1}$$

$$\Delta H(\text{C}_3\text{H}_6) \approx +16 \text{ kcal mol}^{-1}$$

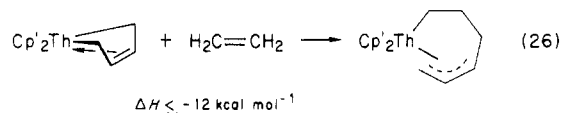
$D(\text{Th-R})_{\text{soln}}$ ,  $D(\text{R-H})$ , and  $D(\text{C-H, cis-2 butene})$  are taken from the literature<sup>28,50,56</sup>;  $D(\text{Th-C, 3})$  is estimated to be 75 kcal mol<sup>-1</sup> (vide supra). These reactions are found to be endothermic. In addition, an unfavorable  $T\Delta S$  contribution to  $\Delta G$  of ca. +12 kcal mol<sup>-1</sup> is expected for loss of rotational and translational entropy (3 particles  $\rightarrow$  2).<sup>58,61,62a-d</sup> A major reason for the inadequate driving force is the relatively weak C–H bonds which are formed in *cis*-2-butene ( $D = 85.6 \pm 1.5$  kcal mol<sup>-1</sup>).<sup>28,62e</sup> For reactions

such as eq 25, a similar calculation reveals that under



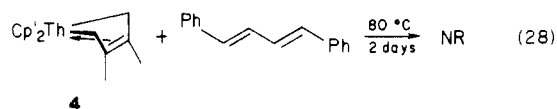
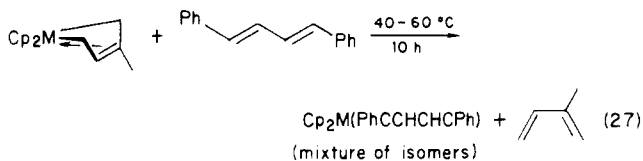
typical reaction conditions,<sup>62</sup>  $D(\text{Th-}\eta^1\text{- or } \eta^3\text{-butenyl})$  must be in excess of ca. 98 kcal mol<sup>-1</sup> ( $\text{C}_6\text{H}_6$ ), 95 kcal mol<sup>-1</sup> ( $\text{SiMe}_4$ ), or 95 kcal mol<sup>-1</sup> ( $\text{C}_3\text{H}_6$ ) for eq 25 to be exergonic. These appear to be unrealistically high disruption enthalpies for a Th–butenyl linkage.

Although olefin insertion processes<sup>2b,58</sup> were not investigated experimentally for the present systems, reactions as in eq 26 are calculated to be exothermic by at least 12

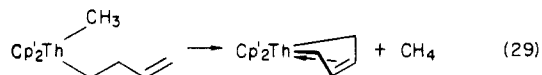


kcal mol<sup>-1</sup>, depending upon how much  $D(\text{Th-allyl})$  exceeds  $D(\text{Th-C, 3})$ . This is likely to render the process exergonic, and it is thus not surprising that group 4 diene complexes undergo olefin insertion.<sup>2b</sup>

Diene exchange reactions are also known for group 4 diene complexes (e.g., eq 27).<sup>5b</sup> In contrast, no reaction was detected between **4** and (*E,E*)-1,4-diphenylbutadiene after 72 h at 80 °C (eq 28). The reluctance of Th(IV) to undergo reductive elimination<sup>34</sup> is a plausible explanation for the diminished reactivity.



It is also possible with the thermochemical data to inquire to what degree processes as in eq 29 (cf. eq 3) are thermodynamically favorable. Using  $D(\text{Th-3-butenyl}) \approx D(\text{Th-}n\text{-butyl})$ ,<sup>26</sup> we estimate  $\Delta H \approx -14$  kcal mol<sup>-1</sup>, with a significant entropic contribution to  $\Delta G$  ( $\sim 12$  kcal mol<sup>-1</sup>) anticipated as well.



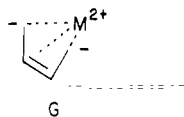
## Conclusions

This study indicates that actinide butadiene complexes are synthetically accessible by several routes. In comparison to the tetravalent bis(cyclopentadienyl) group 4 systems studied to date, it appears that the actinide complexes (at least complexes **2** and **3**) can more closely approach the  $\eta^4$  limit as judged by metrical data and dynamic NMR results. However, unlike many transition-metal-butadiene systems, the  $\eta^4$  limit does not necessarily imply increased involvement of lower formal metal oxidation states, and all evidence suggests that actinide butadiene chemistry closely approaches a tetravalent limit (more so than zirconium). The  $\eta^4$  bonding appears rather to reflect the tendency of the larger, more coordinatively unsaturated (sterically, electronically) actinide ions to assume higher formal coordination numbers. It may be reinforced by electrostatic aspects of the relatively polar actinide–ligand bonding (G). Nevertheless, the thermochemical data indicate that at least for thorium, the magnitude of the actinide–butadiene interaction is not especially great but

(60) (a) Fendrick, C. M.; Marks, T. J., unpublished results. (b) Fendrick, C. M.; Marks, T. J. *J. Am. Chem. Soc.* **1984**, *106*, 2214–2216.

(61) Recent theoretical studies support this picture: Tatsumi, K., private communication.

(62) (a) This contribution<sup>62b-d</sup> is estimated assuming reactants are in the ca. 0.1 M concentration range with  $T \approx 100$  °C. Higher temperatures will favor the reverse reaction while higher RH concentrations will obviously increase the amount of ring-opened product. (b) Ibers, J. A.; DiCosimo, R.; Whitesides, G. M. *Organometallics* **1982**, *1*, 13–20. (c) Page, M. I. In "The Chemistry of Enzyme Action"; Page, M. I., Ed.; Elsevier: New York, 1984; pp 1–54. (d) Page, M. I.; Jencks, W. P. *Proc. Natl. Acad. Sci. U.S.A.* **1971**, *68*, 1678–1683. (e) For the tetramethyl-ethylene from **4**,  $D(\text{C-H})$  is even less, 78.0  $\pm$  1.1 kcal mol<sup>-1</sup>.<sup>56a</sup>



is comparable to that of relatively "weak" actinide-to-carbon  $\sigma$  bonds. Much of the chemistry of actinide and by implication, group 4, diene complexes can be understood on the basis of this characteristic as well as the relatively weak C-H bonds which would be formed on transferring hydrogen atoms (or ions) to the termini of the butadiene fragment.

**Acknowledgment.** This research was supported by the National Science Foundation under Grant CHE8306255 to T.J.M. and by the Office of Basic Energy Sciences,

Division of Chemical Sciences, U.S. Department of Energy, under Contract W-31-109-ENG-38 at Argonne National Laboratory. We thank Dr. Lester Morss for helpful comments.

**Registry No.** 1, 67506-91-6; 2, 99829-51-3; 3, 99668-63-0; 4, 99829-52-4; 5, 99837-57-7; 6, 99837-58-8; Cp<sub>2</sub>ThCl<sub>2</sub>, 67506-88-1; Cp<sub>2</sub>UCl<sub>2</sub>, 67506-89-2; Cp<sub>2</sub>Th(Me)Cl, 79301-20-5; (THF)<sub>2</sub>Mg(C-H<sub>2</sub>CH=CHCH<sub>2</sub>), 83995-88-4; (THF)<sub>2</sub>Mg(CH<sub>2</sub>CMe=CMech<sub>2</sub>), 99829-53-5; LiCH=CH<sub>2</sub>, 917-57-7; 3-butenylmagnesium bromide, 7103-09-5; tetravinyltin, 1112-56-7.

**Supplementary Material Available:** A table of anisotropic thermal parameters for non-hydrogen atoms (Table II) and a listing of observed and calculated structure factors from the final cycle of least-squares refinement (Table III) (12 pages). Ordering information is given on any current masthead page.

## Kinetics of Intramolecular Interconversion of Two Isomers of ( $\mu$ -H)M<sub>3</sub>( $\mu$ -CNMe<sub>2</sub>)(CO)<sub>9</sub>L (M = Ru, L = PR<sub>3</sub>, AsPh<sub>3</sub>, or SbPh<sub>3</sub>; M = Os, L = AsPh<sub>3</sub>)

Mark R. Shaffer and Jerome B. Keister\*

Department of Chemistry, University at Buffalo, State University of New York, Buffalo, New York 14214

Received July 31, 1985

The clusters ( $\mu$ -H)M<sub>3</sub>( $\mu$ -CNMe<sub>2</sub>)(CO)<sub>9</sub>L (M = Ru, L = PPh<sub>3</sub>, PMePh<sub>2</sub>, PMe<sub>2</sub>Ph, PBU<sub>3</sub>, PCyc<sub>3</sub>, P(OMe)<sub>3</sub>, P(O-*i*-Pr)<sub>3</sub>, P(OPh)<sub>3</sub>, AsPh<sub>3</sub>, SbPh<sub>3</sub>; M = Os, L = AsPh<sub>3</sub>) exist in solution as equilibrium mixtures of two isomers, L being coordinated to the nonbridged metal atom in one (n-e isomer) and to the bridged metal atom in the other (b-e isomer). The n-e isomer is the kinetic product formed by addition of L to ( $\mu$ -H)M<sub>3</sub>( $\mu$ -CNMe<sub>2</sub>)(CO)<sub>9</sub>L' (M = Ru, L' = py; M = Os, L' = NCMe). The kinetics of the intramolecular rearrangements of the n-e isomers to the equilibrium mixtures have been determined. The equilibrium constant depends upon the identity of L, increasing in the order SbPh<sub>3</sub> (0.37) < PMe<sub>2</sub>Ph (0.59) < PBU<sub>3</sub> (0.67) < PMePh<sub>2</sub> (1.75) < AsPh<sub>3</sub> (2.5) < P(OMe)<sub>3</sub> (3.2) < P(OPh)<sub>3</sub> (4.5) < P(O-*i*-Pr)<sub>3</sub> (6.9) < PCyc<sub>3</sub> (7.2) < PPh<sub>3</sub> (7.5), and values of the forward rate constant  $10^4 k_f$  (s<sup>-1</sup>) vary slightly (at 5 °C): SbPh<sub>3</sub> (0.27) < AsPh<sub>3</sub> (0.87) < PMe<sub>2</sub>Ph (1.1) < PBU<sub>3</sub> (1.4) < P(O-*i*-Pr)<sub>3</sub> (1.9) < PMePh<sub>2</sub> (2.7)  $\approx$  PPh<sub>3</sub> (2.7)  $\lesssim$  P(OPh)<sub>3</sub> (2.8) < P(OMe)<sub>3</sub> (3.6) < PCyc<sub>3</sub>. These trends indicate that both steric and electronic factors are important,  $K_{eq}$  and  $k_f$  increasing as the size and hardness of L increase. Activation parameters for  $k_f$  for rearrangement of ( $\mu$ -H)M<sub>3</sub>( $\mu$ -CNMe<sub>2</sub>)(CO)<sub>9</sub>(AsPh<sub>3</sub>) are  $\Delta H^\ddagger = 20.7$  (M = Ru) and 15.5 kcal/mol (M = Os) and  $\Delta S^\ddagger = -3.2$  (M = Ru) and -27 eu (M = Os). The deuterium isotope effect  $^H k_f / ^D k_f$  for the Ru complex is 1.24. The proposed mechanism involves migration of hydride, methylidyne, and carbonyl ligands through pairwise bridge opening to form intermediates having only terminally bound ligands.

One of the most active areas of research concerning metal cluster chemistry has been ligand migrations, most commonly involving carbonyls, hydrides, or hydrocarbon fragments, the rates of which are frequently rapid on the NMR time scale.<sup>1</sup> It has been recognized for some time that ligand migration may play an important role in ligand substitution or other reactions of metal clusters,<sup>2</sup> but because ligand migration processes are frequently orders of magnitude faster than substitutions of strongly bound ligands such as CO, there has been little definitive evidence regarding this.

We have shown that ( $\mu$ -H)Ru<sub>3</sub>( $\mu$ -CNMe<sub>2</sub>)(CO)<sub>9</sub>L (L = py, PPh<sub>3</sub>, and other group 15 donor ligands) exist in solution as three isomeric forms in which the ligand L is

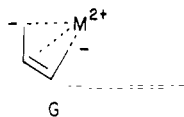
coordinated (1) on a bridged metal atom in the axial position trans to the CNMe<sub>2</sub> ligand (Figure 1, bridged-axial (b-a) isomer), (2) on a bridged metal atom in the equatorial position trans to the Ru(CO)<sub>4</sub> unit (Figure 1, bridged-equatorial (b-e) isomer), or (3) on the nonbridged metal atom in the equatorial position (Figure 1, nonbridged-equatorial (n-e) isomer).<sup>3,4</sup> The only cluster for which the b-a isomer has been found to be the most stable is ( $\mu$ -H)Ru<sub>3</sub>( $\mu$ -CNMe<sub>2</sub>)(CO)<sub>9</sub>(py). In general, when L is a phosphine, phosphite, arsine, or stibine, the b-e and n-e isomers are both present in solution, and thermally induced substitution on ( $\mu$ -H)Ru<sub>3</sub>( $\mu$ -CNMe<sub>2</sub>)(CO)<sub>10</sub> by L produces the equilibrium mixture. However, the kinetic product from replacement of py from ( $\mu$ -H)Ru<sub>3</sub>( $\mu$ -CNMe<sub>2</sub>)(CO)<sub>9</sub>(py) by L at 25 °C is exclusively the n-e

(1) (a) Band, E.; Muetterties, E. L. *Chem. Rev.* 1978, 78, 639. (b) Evans, J. *Adv. Organomet. Chem.* 1977, 16, 319.

(2) (a) Sonnenberger, D.; Atwood, J. D. *J. Am. Chem. Soc.* 1980, 102, 3484. (b) Sonnenberger, D. C.; Atwood, J. D. *Ibid.* 1982, 104, 2113. (c) Sonnenberger, D. C.; Atwood, J. D. *Organometallics* 1982, 1, 694. (d) Atwood, J. D.; Brown, T. L. *J. Am. Chem. Soc.* 1976, 98, 3160.

(3) Dalton, D. M.; Barnett, D. J.; Duggan, T. P.; Keister, J. B.; Malik, P. T.; Modi, S. P.; Shaffer, M. R.; Smesko, S. A. *Organometallics* 1985, 4, 1854.

(4) Churchill, M. R.; Fettingner, J. C.; Keister, J. B. *Organometallics* 1985, 4, 1867.



is comparable to that of relatively "weak" actinide-to-carbon  $\sigma$  bonds. Much of the chemistry of actinide and by implication, group 4, diene complexes can be understood on the basis of this characteristic as well as the relatively weak C-H bonds which would be formed on transferring hydrogen atoms (or ions) to the termini of the butadiene fragment.

**Acknowledgment.** This research was supported by the National Science Foundation under Grant CHE8306255 to T.J.M. and by the Office of Basic Energy Sciences,

Division of Chemical Sciences, U.S. Department of Energy, under Contract W-31-109-ENG-38 at Argonne National Laboratory. We thank Dr. Lester Morss for helpful comments.

**Registry No.** 1, 67506-91-6; 2, 99829-51-3; 3, 99668-63-0; 4, 99829-52-4; 5, 99837-57-7; 6, 99837-58-8; Cp<sub>2</sub>ThCl<sub>2</sub>, 67506-88-1; Cp<sub>2</sub>UCl<sub>2</sub>, 67506-89-2; Cp<sub>2</sub>Th(Me)Cl, 79301-20-5; (THF)<sub>2</sub>Mg(C-H<sub>2</sub>CH=CHCH<sub>2</sub>), 83995-88-4; (THF)<sub>2</sub>Mg(CH<sub>2</sub>CMe=CMech<sub>2</sub>), 99829-53-5; LiCH=CH<sub>2</sub>, 917-57-7; 3-butenylmagnesium bromide, 7103-09-5; tetravinyltin, 1112-56-7.

**Supplementary Material Available:** A table of anisotropic thermal parameters for non-hydrogen atoms (Table II) and a listing of observed and calculated structure factors from the final cycle of least-squares refinement (Table III) (12 pages). Ordering information is given on any current masthead page.

## Kinetics of Intramolecular Interconversion of Two Isomers of $(\mu\text{-H})\text{M}_3(\mu\text{-CNMe}_2)(\text{CO})_9\text{L}$ ( $\text{M} = \text{Ru}$ , $\text{L} = \text{PR}_3$ , $\text{AsPh}_3$ , or $\text{SbPh}_3$ ; $\text{M} = \text{Os}$ , $\text{L} = \text{AsPh}_3$ )

Mark R. Shaffer and Jerome B. Keister\*

Department of Chemistry, University at Buffalo, State University of New York, Buffalo, New York 14214

Received July 31, 1985

The clusters  $(\mu\text{-H})\text{M}_3(\mu\text{-CNMe}_2)(\text{CO})_9\text{L}$  ( $\text{M} = \text{Ru}$ ,  $\text{L} = \text{PPh}_3$ ,  $\text{PMePh}_2$ ,  $\text{PMe}_2\text{Ph}$ ,  $\text{PBU}_3$ ,  $\text{PCyc}_3$ ,  $\text{P(OMe)}_3$ ,  $\text{P(O-}i\text{-Pr)}_3$ ,  $\text{P(OPh)}_3$ ,  $\text{AsPh}_3$ ,  $\text{SbPh}_3$ ;  $\text{M} = \text{Os}$ ,  $\text{L} = \text{AsPh}_3$ ) exist in solution as equilibrium mixtures of two isomers, L being coordinated to the nonbridged metal atom in one (n-e isomer) and to the bridged metal atom in the other (b-e isomer). The n-e isomer is the kinetic product formed by addition of L to  $(\mu\text{-H})\text{M}_3(\mu\text{-CNMe}_2)(\text{CO})_9\text{L}'$  ( $\text{M} = \text{Ru}$ ,  $\text{L}' = \text{py}$ ;  $\text{M} = \text{Os}$ ,  $\text{L}' = \text{NCMe}$ ). The kinetics of the intramolecular rearrangements of the n-e isomers to the equilibrium mixtures have been determined. The equilibrium constant depends upon the identity of L, increasing in the order  $\text{SbPh}_3$  (0.37) <  $\text{PMe}_2\text{Ph}$  (0.59) <  $\text{PBU}_3$  (0.67) <  $\text{PMePh}_2$  (1.75) <  $\text{AsPh}_3$  (2.5) <  $\text{P(OMe)}_3$  (3.2) <  $\text{P(OPh)}_3$  (4.5) <  $\text{P(O-}i\text{-Pr)}_3$  (6.9) <  $\text{PCyc}_3$  (7.2) <  $\text{PPh}_3$  (7.5), and values of the forward rate constant  $10^4 k_f$  ( $\text{s}^{-1}$ ) vary slightly (at 5 °C):  $\text{SbPh}_3$  (0.27) <  $\text{AsPh}_3$  (0.87) <  $\text{PMe}_2\text{Ph}$  (1.1) <  $\text{PBU}_3$  (1.4) <  $\text{P(O-}i\text{-Pr)}_3$  (1.9) <  $\text{PMePh}_2$  (2.7)  $\approx$   $\text{PPh}_3$  (2.7)  $\lesssim$   $\text{P(OPh)}_3$  (2.8) <  $\text{P(OMe)}_3$  (3.6) <  $\text{PCyc}_3$ . These trends indicate that both steric and electronic factors are important,  $K_{eq}$  and  $k_f$  increasing as the size and hardness of L increase. Activation parameters for  $k_f$  for rearrangement of  $(\mu\text{-H})\text{M}_3(\mu\text{-CNMe}_2)(\text{CO})_9(\text{AsPh}_3)$  are  $\Delta H^\ddagger = 20.7$  (M = Ru) and 15.5 kcal/mol (M = Os) and  $\Delta S^\ddagger = -3.2$  (M = Ru) and -27 eu (M = Os). The deuterium isotope effect  $^{\text{H}}k_f/{}^{\text{D}}k_f$  for the Ru complex is 1.24. The proposed mechanism involves migration of hydride, methylidyne, and carbonyl ligands through pairwise bridge opening to form intermediates having only terminally bound ligands.

One of the most active areas of research concerning metal cluster chemistry has been ligand migrations, most commonly involving carbonyls, hydrides, or hydrocarbon fragments, the rates of which are frequently rapid on the NMR time scale.<sup>1</sup> It has been recognized for some time that ligand migration may play an important role in ligand substitution or other reactions of metal clusters,<sup>2</sup> but because ligand migration processes are frequently orders of magnitude faster than substitutions of strongly bound ligands such as CO, there has been little definitive evidence regarding this.

We have shown that  $(\mu\text{-H})\text{Ru}_3(\mu\text{-CNMe}_2)(\text{CO})_9\text{L}$  (L = py,  $\text{PPh}_3$ , and other group 15 donor ligands) exist in solution as three isomeric forms in which the ligand L is

coordinated (1) on a bridged metal atom in the axial position trans to the  $\text{CNMe}_2$  ligand (Figure 1, bridged-axial (b-a) isomer), (2) on a bridged metal atom in the equatorial position trans to the  $\text{Ru}(\text{CO})_4$  unit (Figure 1, bridged-equatorial (b-e) isomer), or (3) on the nonbridged metal atom in the equatorial position (Figure 1, nonbridged-equatorial (n-e) isomer).<sup>3,4</sup> The only cluster for which the b-a isomer has been found to be the most stable is  $(\mu\text{-H})\text{Ru}_3(\mu\text{-CNMe}_2)(\text{CO})_9(\text{py})$ . In general, when L is a phosphine, phosphite, arsine, or stibine, the b-e and n-e isomers are both present in solution, and thermally induced substitution on  $(\mu\text{-H})\text{Ru}_3(\mu\text{-CNMe}_2)(\text{CO})_{10}$  by L produces the equilibrium mixture. However, the kinetic product from replacement of py from  $(\mu\text{-H})\text{Ru}_3(\mu\text{-CNMe}_2)(\text{CO})_9(\text{py})$  by L at 25 °C is exclusively the n-e

(1) (a) Band, E.; Muetterties, E. L. *Chem. Rev.* 1978, 78, 639. (b) Evans, J. *Adv. Organomet. Chem.* 1977, 16, 319.

(2) (a) Sonnenberger, D.; Atwood, J. D. *J. Am. Chem. Soc.* 1980, 102, 3484. (b) Sonnenberger, D. C.; Atwood, J. D. *Ibid.* 1982, 104, 2113. (c) Sonnenberger, D. C.; Atwood, J. D. *Organometallics* 1982, 1, 694. (d) Atwood, J. D.; Brown, T. L. *J. Am. Chem. Soc.* 1976, 98, 3160.

(3) Dalton, D. M.; Barnett, D. J.; Duggan, T. P.; Keister, J. B.; Malik, P. T.; Modi, S. P.; Shaffer, M. R.; Smesko, S. A. *Organometallics* 1985, 4, 1854.

(4) Churchill, M. R.; Fettingner, J. C.; Keister, J. B. *Organometallics* 1985, 4, 1867.



Table I.  $^1\text{H}$  NMR Spectral Data of  $(\mu\text{-H})\text{M}_3(\mu\text{-CNMe}_2)(\text{CO})_9\text{L}^a$ 

	L	isomer	resonances, ppm	
			hydride	N-methyl
Ru	PPh <sub>3</sub>	n-e	-14.15 (d, $J = 3.0$ Hz)	3.72 (s, 6 H)
		b-e	-14.25 (d, $J = 8.2$ Hz)	3.58 (d, 3 H, $J_{\text{PH}} = 1.3$ Hz) 2.80 (s, 3 H)
Ru	PMePh <sub>2</sub>	n-e	-14.40 (d, $J = 2.9$ Hz)	3.72 (s, 6 H)
		b-e	-14.70 (d, $J = 9.5$ Hz)	3.56 (d, 3 H, $J_{\text{PH}} = 1.5$ Hz) 2.99 (s, 3 H)
Ru	PMe <sub>2</sub> Ph	n-e	-14.40 (d, $J = 2.9$ Hz)	3.75 (s, 6 H)
		b-e	-14.70 (d, $J = 9.5$ Hz)	3.63 (d, 3 H, $J_{\text{PH}} = 1.5$ Hz) 3.13 (s, 3 H)
Ru	PBu <sub>3</sub>	n-e	-14.26 (d, $J = 2.9$ Hz)	
Ru	PCyc <sub>3</sub>	b-e	-14.81 (d, $J = 9.5$ Hz)	
		n-e	-14.83 (s)	3.81 (s, 6 H)
Ru	P(O <i>i</i> -Pr) <sub>3</sub>	b-e	-14.66 (d, $J = 7.7$ Hz)	3.76 (s, 3 H)
		n-e		3.73 (s, 3 H)
Ru	P(OMe) <sub>3</sub>	n-e	-14.60 (d, $J = 5.1$ Hz)	
		b-e	-15.09 (d, $J = 10.3$ Hz)	
Ru	P(O <i>i</i> -Pr) <sub>3</sub>	n-e	-14.49 (d, $J = 4.4$ Hz)	
		b-e	-14.98 (d, $J = 10.3$ Hz)	
Ru	P(OPh) <sub>3</sub>	n-e	-14.61 (d, $J = 6.6$ Hz)	
		b-e	-15.17 (d, $J = 11.0$ Hz)	
Ru	AsPh <sub>3</sub>	n-e	-14.28 (s)	3.80 (s, 6 H)
		b-e	-14.28 (s)	3.60 (s, 3 H) 2.90 (s, 3 H)
Ru	SbPh <sub>3</sub>	n-e	-14.47 (s)	3.72 (s, 3 H) 3.67 (s, 3 H)
		b-e	-14.62 (s)	3.44 (s, 3 H) 3.01 (s, 3 H)
Os	AsPh <sub>3</sub>	n-e	-16.04 (s)	3.78 (s, 6 H)
		b-e	-16.36 (s)	3.59 (s, 3 H)
Os	NCMe <sup>b</sup>			2.89 (s, 3 H)
				3.79 (s, 6 H)

<sup>a</sup>In deuteriochloroform at 21 °C unless otherwise noted. <sup>b</sup>Other resonances:  $\delta$  2.58 (s, 3 H, NCMe).

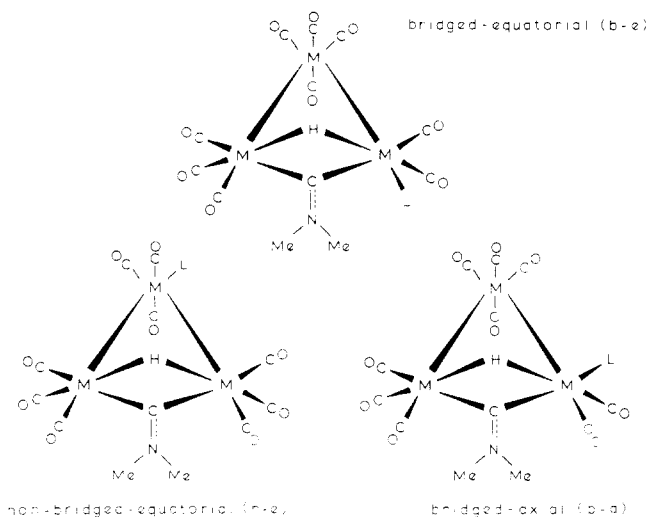


Figure 1. Structures of bridged-axial, bridged-equatorial, and nonbridged-equatorial isomers  $(\mu\text{-H})\text{M}_3(\mu\text{-CNMe}_2)(\text{CO})_9\text{L}$ .

isomer. Rearrangement of the n-e isomer to the n-e/b-e equilibrium mixture occurs at a rate conveniently followed by NMR spectroscopy. Since relatively few studies of nondegenerate rearrangements of ligands on clusters have been conducted and few in which the effects of changing the steric and electronic properties of the ligands have been examined, we have undertaken a study of the kinetics of interconversion of these isomeric clusters. These results have implications for other reactions, such as alkyne-alkylidyne coupling, which proceed through  $\text{HRu}_3(\mu\text{-CX})(\text{CO})_9\text{L}$  intermediates.<sup>5</sup>

(5) (a) Beanan, L. R.; Abdul Rahman, Z.; Keister, J. B. *Organometallics* 1983, 2, 1062. (b) Beanan, L. R.; Keister, J. B. *Organometallics* 1985, 4, 1713.

## Experimental Section

**Chemicals.**  $(\mu\text{-H})\text{Ru}_3(\mu\text{-CNMe}_2)(\text{CO})_{10}$ ,<sup>3</sup>  $(\mu\text{-H})\text{Ru}_3(\mu\text{-CNMe}_2)(\text{CO})_9(\text{py})$ ,<sup>3</sup>  $(\mu\text{-H})\text{Os}_3(\mu\text{-CNMe}_2)(\text{CO})_{10}$ ,<sup>6</sup> PMe<sub>2</sub>Ph,<sup>7</sup> and PMePh<sub>2</sub><sup>7</sup> were prepared according to previously reported procedures. Solvents and all other ligands were obtained from commercial sources and were used as received.

**Characterization of Compounds.** Characterizations of  $(\mu\text{-H})\text{Ru}_3(\mu\text{-CNMe}_2)(\text{CO})_9\text{L}$  (L = PPh<sub>3</sub>, AsPh<sub>3</sub>, SbPh<sub>3</sub>, PBu<sub>3</sub>, PCyc<sub>3</sub>, and py)<sup>3,4</sup> and  $(\mu\text{-H})\text{Os}_3(\mu\text{-COMe})(\text{CO})_9(\text{PPh}_3)$ <sup>8</sup> were reported previously. All new compounds reported here were characterized by comparison of the infrared (Perkin-Elmer 457 spectrophotometer) and  $^1\text{H}$  NMR (JEOL FX-90Q instrument) spectra with those of the other derivatives. Infrared spectral data are available as supplementary material (Table A), and  $^1\text{H}$  NMR data are given in Table I. The phosphite complexes decomposed during chromatography and characterization is of the crude products.

**$(\mu\text{-D})\text{Ru}_3(\mu\text{-CNMe}_2)(\text{CO})_{10}$ .** A solution of  $\text{Ru}_3(\text{CO})_{12}$  (84 mg, 0.13 mmol), triethylamine (2 mL, dried over potassium hydroxide and freshly distilled), and  $\text{D}_2\text{O}$  (2 mL) in dry THF was placed in a 50-mL Schlenk flask equipped with a reflux condenser, nitrogen gas inlet, and stir bar. The solution was heated at 60–70 °C for 1 h. After the solution was cooled, a solution of tetraethylammonium bromide (250 mg) in  $\text{D}_2\text{O}$  was added and then the volatile components were removed by vacuum transfer until only the water and the purple precipitate  $[\text{NET}_4][\text{DRu}_3(\text{CO})_{11}]$  remained. The water was removed by pipet, and the precipitate was washed three times with water (10 mL) and dried with vacuum. Next a solution of methyl iodide (80  $\mu\text{L}$ ) in dichloromethane (5 mL) was added, and to this purple solution was added dropwise with stirring a solution of methyl isocyanide (10  $\mu\text{L}$ ) in dichloromethane (10 mL) until the solution turned yellow. Next the solution was evaporated to dryness on a rotary evaporator, and the residue was purified by thin-layer chromatography on

(6) Keister, J. B. Ph.D. Dissertation, University of Illinois, Urbana, IL, 1978.

(7) Mathur, M. A.; Myers, W. H.; Sisler, H. H.; Ryschkewitsch, G. E. *Inorg. Synth.* 1974, 15, 128.

(8) Bavaro, L. M.; Keister, J. B. *J. Organomet. Chem.* 1985, 287, 357.

silica eluting with cyclohexane. The second yellow band was extracted with dichloromethane; evaporation yielded the product as a yellow solid (31 mg, 37%). The  $^1\text{H}$  NMR spectrum indicated that the product contained 98% deuterium in the hydride position.

$(\mu\text{-H})\text{Os}_3(\mu\text{-CNMe}_2)(\text{CO})_9(\text{NCMe})$ . To a stirred solution of  $(\mu\text{-H})\text{Os}_3(\mu\text{-CNMe}_2)(\text{CO})_{10}$  (31 mg, 0.034 mmol) in acetonitrile (10 mL) under a nitrogen atmosphere was added dropwise with stirring from a pressure-equalizing dropping funnel a solution of trimethylamine *N*-oxide dihydrate (4 mg, 0.036 mmol) in acetonitrile (10 mL). After addition was complete, the solvent was removed by vacuum transfer. The  $^1\text{H}$  NMR spectrum of the residue indicated that the only cluster products were  $(\mu\text{-H})\text{Os}_3(\mu\text{-CNMe}_2)(\text{CO})_9\text{L}$  and unreacted starting material.

The compound is unstable in solution. Recrystallization from acetonitrile gave yellow crystals. Anal. Calcd for  $\text{C}_{14}\text{H}_{10}\text{N}_2\text{O}_9\text{Os}_3$ ; C, 18.26; H, 1.09; N, 3.04. Found: C, 18.46; H, 1.33; N, 2.84.

$(\mu\text{-H})\text{Os}_3(\mu\text{-CNMe}_2)(\text{CO})_9(\text{AsPh}_3)$ . This product was prepared by addition of a slight excess of  $\text{AsPh}_3$  to a solution of  $(\mu\text{-H})\text{Os}_3(\mu\text{-CNMe}_2)(\text{CO})_9(\text{NCMe})$  in deuteriochloroform. The compound was purified by thin-layer chromatography on silica eluting with 10% dichloromethane in cyclohexane. The product was characterized by comparison of its  $^1\text{H}$  NMR and IR spectra with those of  $(\mu\text{-H})\text{Os}_3(\mu\text{-COMe})(\text{CO})_9(\text{AsPh}_3)$  previously reported.<sup>8</sup> The compound was recrystallized from methanol/2-propanol for analysis. Anal. Calcd for  $\text{C}_{30}\text{H}_{22}\text{NO}_9\text{AsOs}_3$ ; C, 30.38; H, 1.87. Found: C, 30.35; H, 1.92.

**Kinetic Measurements.** The progress of each isomerization was monitored by  $^1\text{H}$  NMR spectroscopy using a JEOL FX-90Q spectrometer. For each run a sample of  $(\mu\text{-H})\text{Ru}_3(\mu\text{-CNMe}_2)(\text{CO})_9(\text{py})$  or  $(\mu\text{-H})\text{Os}_3(\mu\text{-CNMe}_2)(\text{CO})_9(\text{NCMe})$  in deuteriochloroform (ca. 0.6 mL) was prepared. Then the ligand L was added and the solution transferred immediately to a 5-mm NMR tube which was placed into the probe already thermostated at the desired temperature ( $\pm 1$  °C, temperature measured using the methanol chemical shift method<sup>9</sup>). Spectra were recorded automatically at regular intervals using the STACK routine. Equilibrium constants  $K_{\text{eq}} = k_f/k_r$  were determined by integration of the *N*-methyl or hydride resonances due to each isomer at 21°. Error limits are given as the standard deviation from the mean for three determinations.

The rate constant  $k_{\text{obsd}}$  for the isomerization to equilibrium was determined from a plot of  $\ln\{m_t - m_{\text{eq}}\}$  vs. time *t*. The quantity *m* represents the mole fraction due to the *n*-e isomer, which was measured by the function  $m = h_n/(h_n + 2h_b)$ , where  $h_n$  and  $h_b$  are the peak heights of the methyl resonance due to the *n*-e isomer and the upfield methyl resonance due to the *b*-e isomer, respectively, or which was measured by the function  $m = h_n/(h_n + h_b)$ , where  $h_n$  and  $h_b$  are the peak heights of the hydride resonances of the *n*-e and *b*-e isomers. Although peak areas should be more properly used, satisfactory measurements could be made by using peak heights much more quickly. Equilibrium constants calculated from both peak height and area measurements were in good agreement. Good linear plots were obtained over 2–3 half-lives. A computer-calculated least-squares procedure was used to determine the slope of the plot for each run. Error limits of one standard deviation were also computer calculated. Two to three runs were made at each temperature and the average value used as the best number for the rate constant  $k_{\text{obsd}}$ .

Forward and reverse rate constants were calculated from  $k_f = k_{\text{obsd}}/(1 + K_{\text{eq}})$  and  $k_r = k_{\text{obsd}} - k_f$ . There was no measurable variation in  $K_{\text{eq}}$  with temperature over the range examined.

Activation parameters for rearrangements of  $(\mu\text{-H})\text{M}_3(\mu\text{-CNMe}_2)(\text{CO})_9(\text{AsPh}_3)$  (*M* = Ru and Os) were obtained from plots of  $\ln\{k_f/T\}$  vs.  $1/T$  using a computer-calculated least-squares procedure. Error limits are given as the computer-calculated standard deviation.

## Results

The structure of  $(\mu\text{-H})\text{Ru}_3(\mu\text{-CNMe}_2)(\text{CO})_9(\text{py})$  in solution and in the solid state contains py coordinated in the bridged-axial position (Figure 1). The structure of  $(\mu\text{-H})\text{Os}_3(\mu\text{-CNMe}_2)(\text{CO})_9(\text{NCMe})$  is unknown. The  $^1\text{H}$  NMR

spectrum of the latter (Table I) is consistent with NCMe coordination on the nonbridged metal atom and in an axial position, as was shown for  $(\mu\text{-H})\text{Os}_3(\mu\text{-COMe})(\text{CO})_9(\text{CNCMe}_3)$ ,<sup>10</sup> since this is the only isomer containing equivalent *N*-methyl groups. However, the *N*-methyl resonances may be coincidentally isochronous; the chemical shifts of the two *N*-methyl resonances of  $(\mu\text{-H})\text{Ru}_3(\mu\text{-CNMe}_2)(\text{CO})_9(\text{py})$  are not very different from one another.

As we have previously reported, the kinetic product formed upon mixing  $(\mu\text{-H})\text{Ru}_3(\mu\text{-CNMe}_2)(\text{CO})_9(\text{py})$  and L =  $\text{PR}_3$ ,  $\text{AsPh}_3$ , or  $\text{SbPh}_3$  is the *n*-e isomer  $(\mu\text{-H})\text{Ru}_3(\mu\text{-CNMe}_2)(\text{CO})_9\text{L}$ .<sup>3</sup> The *n*-e isomer is also the kinetic product from replacement of NCMe on  $(\mu\text{-H})\text{Os}_3(\mu\text{-CNMe}_2)(\text{CO})_9(\text{NCMe})$  by  $\text{AsPh}_3$ . Rearrangement to the equilibrium mixture of *n*-e and *b*-e isomers occurs with a rate conveniently measured by using  $^1\text{H}$  NMR spectroscopy. Unless noted otherwise, all experiments concern deuteriochloroform solutions.

The *n*-e and *b*-e isomers are easily differentiated in the NMR spectrum (Table I). When L is a phosphorus donor ligand, the  $^{31}\text{P}$ -hydride coupling constant is 0–6 Hz for the *n*-e isomer and always a larger value, 7–11 Hz, for the *b*-e form. For complexes of ligands having phenyl substituents, the *N*-methyl resonances have very similar chemical shifts for the *n*-e form but are separated by ca. 0.6 ppm for the *b*-e isomer. In previous papers we have fully characterized these isomers by  $^1\text{H}$  and  $^{13}\text{C}$  NMR spectroscopy, mass spectrometry, elemental analysis, and X-ray crystallography for representative examples.<sup>3,4</sup>

The value of the equilibrium constant for the *n*-e to *b*-e rearrangement (Table II) depends upon the steric and electronic properties of L. Comparison of the values of  $K_{\text{eq}}$  for L =  $\text{PCyc}_3$  (7.2) and  $\text{PBu}_3$  (0.67) suggests that large ligands stabilize the *b*-e isomer relative to the *n*-e isomer. We have previously proposed that the *b*-e form is the most favorable on steric grounds.<sup>4</sup> However, the values of  $K_{\text{eq}}$  for L =  $\text{EPh}_3$  (*E* = P (7.5), As (2.5), and Sb (0.4)), ligands which have very similar cone angles,<sup>27</sup> suggest that electronic effects are also important.

The kinetics of rearrangement from the *n*-e isomer of  $(\mu\text{-H})\text{Ru}_3(\mu\text{-CNMe}_2)(\text{CO})_9\text{L}$  to the equilibrium mixture were measured from the relative peak heights of the resonances due to each isomer, either the methyl or hydride resonances. For relaxation to equilibrium first order kinetics are observed and the first-order rate constant,  $k_{\text{obsd}}$ , is equal to the sum of the forward and reverse rate constants,  $k_f + k_r$ . The equilibrium constant,  $K_{\text{eq}}$ , is given by  $k_f/k_r$ , and was determined from the relative amounts of the *n*-e and *b*-e isomers at equilibrium. Therefore, we were able to determine values for  $k_f$  and  $k_r$  (Table II).

The isomerization does not proceed by dissociation of L since there is no formation of  $(\mu\text{-H})\text{Ru}_3(\mu\text{-CNMe}_2)(\text{CO})_9(\text{PPh}_3)$  during the isomerization of  $(\mu\text{-H})\text{Ru}_3(\mu\text{-CNMe}_2)(\text{CO})_9(\text{AsPh}_3)$  in the presence of added  $\text{PPh}_3$ , even though exchange is noted over longer time periods. Furthermore, the forward rate constant  $k_f$  of  $3.6 \times 10^{-4} \text{ s}^{-1}$  at 17 °C for isomerization of  $(\mu\text{-H})\text{Ru}_3(\mu\text{-CNMe}_2)(\text{CO})_9(\text{AsPh}_3)$  is 240 times larger than the rate constant for replacement of  $\text{AsPh}_3$  by CO ( $1.6 \times 10^{-6} \text{ s}^{-1}$ , extrapolated from 40 °C).<sup>3</sup> We can also rule out CO dissociation as the mechanism since the rate constant for the second ligand substitution on  $(\mu\text{-H})\text{Ru}_3(\mu\text{-CNMe}_2)(\text{CO})_9(\text{PPh}_3)$  is much smaller than its rate constant for isomerization. Therefore, the isomerization is an intramolecular process.

There is only a small dependence of the values for  $k_{\text{obsd}}$ ,  $k_f$ , and  $k_r$  upon the nature of L (Table II). Both steric and

(9) Van Geet, A. L. *Anal. Chem.* 1968, 40, 2227; 1970, 42, 679.

(10) Gavens, P. D.; Mays, M. J. *J. Organomet. Chem.* 1978, 162, 389.

**Table II. Equilibrium and Rate Constants for Isomerization of  $(\mu\text{-H})\text{M}_3(\mu\text{-CNMe}_2)(\text{CO})_9\text{L}^a$** 

L	M	$K_{\text{eq}}^b$	$10^4 k_{\text{obs}}^c, \text{s}^{-1}$	$10^4 k_f^d, \text{s}^{-1}$	$10^4 k_r^d, \text{s}^{-1}$	T, °C
PPh <sub>3</sub>	Ru	7.5 (0.2)	3.1 (0.1)	2.7 (0.2)	0.36 (0.02)	+5
PBu <sub>3</sub>	Ru	0.67 (0.08)	2.9 (0.1)	1.4 (0.2)	1.5 (0.1)	+5
			1.19 (0.04)	0.6 (0.2)	0.7 (0.1)	-5
PMePh <sub>2</sub>	Ru	1.75 (0.04)	4.2 (0.1)	2.7 (0.2)	1.5 (0.2)	+5
PM <sub>2</sub> Ph	Ru	0.59 (0.04)	2.8 (0.3)	1.1 (0.2)	1.7 (0.1)	+5
P(OMe) <sub>3</sub>	Ru	3.2 (0.2)	4.8 (0.2)	3.6 (0.5)	1.2 (0.1)	+5
P(O- <i>i</i> -Pr) <sub>3</sub>	Ru	6.9 (0.7)	2.2 (0.1)	1.9 (0.2)	0.28 (0.04)	+5
P(OPh) <sub>3</sub>	Ru	4.5 (0.2)	3.4 (0.1)	2.8 (0.1)	0.62 (0.02)	+5
PCyc <sub>3</sub>	Ru	7.2 (0.2)	5.6 (0.2)	4.9 (1.0)	0.7 (0.1)	-5
AsPh <sub>3</sub>	Ru	2.5 (0.1)	0.51 (0.02)	0.36 (0.04)	0.15 (0.01)	0
			1.22 (0.02)	0.87 (0.09)	0.35 (0.02)	+5
			3.1 (0.1)	2.2 (0.2)	0.90 (0.05)	+12
			5.0 (0.1)	3.6 (0.3)	1.43 (0.07)	+17
			6.8 (0.3)	4.9 (0.4)	1.9 (0.1)	+19
SbPh <sub>3</sub>	Ru	0.37 (0.01)	0.76 (0.02)	0.27 (0.03)	0.73 (0.02)	+5
AsPh <sub>3</sub>	Os	4.4 (0.2)	0.51 (0.04)	0.42 (0.07)	0.09 (0.01)	+27
			0.90 (0.04)	0.74 (0.08)	0.16 (0.01)	+34
			1.22 (0.02)	1.0 (0.1)	0.21 (0.01)	+39
			2.0 (0.1)	1.63 (0.02)	0.37 (0.03)	+44
			3.14 (0.05)	2.60 (0.03)	0.54 (0.03)	+49

<sup>a</sup>In deuteriochloroform solution unless otherwise indicated. <sup>b</sup>Measured at 21 °C. Error limits are the standard deviation for three measurements. <sup>c</sup>Error limits are the computer-calculated standard deviation. <sup>d</sup>Error limits are calculated from those for  $K_{\text{eq}}$  and  $k_{\text{obsd}}$ .

electronic properties of L seem important. The trend in the values of  $k_{\text{obsd}}$  parallels the trend in the values of  $K_{\text{eq}}$ . It appears that  $k_f$  is somewhat more sensitive to the identity of L than  $k_r$ . Comparison of the values of  $k_f$  for L = PCyc<sub>3</sub> ( $4.9 \times 10^{-4} \text{ s}^{-1}$ ) and PBu<sub>3</sub> ( $0.6 \times 10^{-4} \text{ s}^{-1}$ ) at -5 °C suggests that the rate is increased by increasing the size of L. As for the values of  $K_{\text{eq}}$ , comparison of the values of  $k_f$  for L = EPh<sub>3</sub> (E = P ( $2.7 \times 10^{-4} \text{ s}^{-1}$ ), As ( $0.9 \times 10^{-4} \text{ s}^{-1}$ ), and Sb ( $0.3 \times 10^{-4} \text{ s}^{-1}$ )) indicate that electronic effects are also important.

A small but normal deuterium kinetic isotope effect is observed. The values of  $^{\text{H}}k_{\text{obsd}}/^{\text{D}}k_{\text{obsd}}$  and  $^{\text{H}}k_f/^{\text{D}}k_f$  for  $(\mu\text{-H})\text{Ru}_3(\mu\text{-CNMe}_2)(\text{CO})_9(\text{AsPh}_3)$  at 13 °C are both 1.24 ± 0.10.

Activation parameters were determined for rearrangements of  $(\mu\text{-H})\text{M}_3(\mu\text{-CNMe}_2)(\text{CO})_9(\text{AsPh}_3)$  (M = Ru and Os). For the Ru cluster values of  $\Delta H^\ddagger = 20.7 \pm 1.0 \text{ kcal}$  and  $\Delta S^\ddagger = -3.2 \pm 0.2 \text{ eu}$  were found, while values for the Os analogue were  $15.5 \pm 1.3 \text{ kcal}$  and  $-27 \pm 5 \text{ eu}$ , respectively.

Only a small influence of the solvent upon the rate constants or equilibrium constants was noted. The equilibrium constants for  $(\mu\text{-H})\text{Ru}_3(\mu\text{-CNMe}_2)(\text{CO})_9(\text{AsPh}_3)$  in benzene, chloroform, and acetone were 2.2, 2.5, and 2.8, respectively. Rate constants  $k_{\text{obsd}}$  for n-e to b-e rearrangement at 19 °C in chloroform and in acetone were  $6.8 \times 10^{-4}$  and  $4.9 \times 10^{-4} \text{ s}^{-1}$ , respectively, not significantly different.

## Discussion

The isomerization of  $(\mu\text{-H})\text{M}_3(\mu\text{-CNMe}_2)(\text{CO})_9\text{L}$  from the n-e form to the equilibrium mixture is an intramolecular process. Evidence for this includes the lack of exchange with PPh<sub>3</sub> during the isomerization of  $(\mu\text{-H})\text{Ru}_3(\mu\text{-CNMe}_2)(\text{CO})_9(\text{AsPh}_3)$ , the much greater rate for isomerization of this cluster than for dissociation of AsPh<sub>3</sub>, the negative values of the entropies of activation (inconsistent with a dissociative process), and the very small dependence of the rate constant upon the identity of L. This last point and the fact that there are no examples of intramolecular migrations of phosphine ligands suggest that the ligand L remains attached to the same metal atom during the rearrangement. Then the isomerization requires that both the hydride ligand and the methylidyne ligand move. Although there is little information concerning the migratory aptitudes of methylidyne ligands, carbonyl and

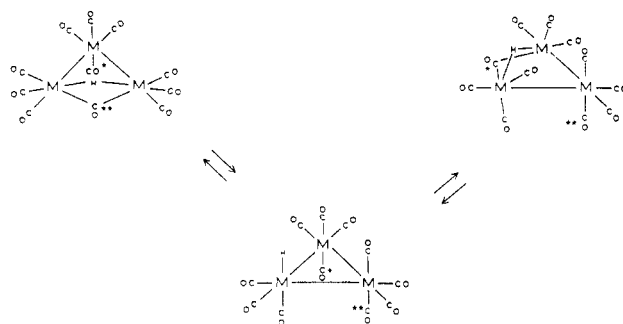


**Figure 2.** Proposed mechanism of carbonyl fluxionality on  $(\mu\text{-H})\text{M}_3(\mu\text{-CO})(\text{CO})_{10}^{1-}$  (M = Fe, Ru, Os).

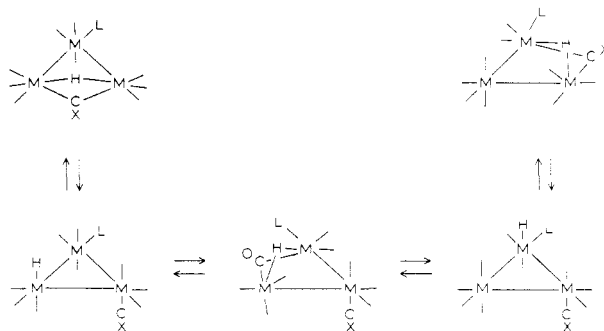


**Figure 3.** Proposed mechanism for isomerization of  $(\mu\text{-H})\text{M}_3(\mu\text{-CX})(\text{CO})_9\text{L}$  (X = CNMe<sub>2</sub>).

hydride migrations for the isoelectronic and isostructural clusters  $(\mu\text{-H})\text{M}_3(\mu\text{-CO})(\text{CO})_{10}^{1-}$  (M = Fe, Ru, or Os) have been established.<sup>11-13</sup>

The proposed mechanism for carbonyl migration on  $(\mu\text{-H})\text{M}_3(\mu\text{-CO})(\text{CO})_{10}^{1-}$  is shown in Figure 2.<sup>11,14</sup> Simul-

(11) Wilkinson, J. R.; Todd, L. J. *J. Organomet. Chem.* **1976**, *118*, 199.

(12) (a) Ungermann, C.; Landis, V.; Moya, S. A.; Cohen, H.; Walker, H.; Pearson, R. G.; Ford, P. C. *J. Am. Chem. Soc.* **1979**, *101*, 5922. (b) Johnson, B. F. G.; Lewis, J.; Raithby, P. R.; Suss, G. *J. Chem. Soc., Dalton Trans.* **1979**, 1356.

(13) Eady, C. R.; Johnson, B. F. G.; Lewis, J.; Malatesta, M. C. *J. Chem. Soc., Dalton Trans.* **1978**, 1358.

(14) Although a different mechanism for carbonyl fluxionality for  $(\mu\text{-H})\text{Ru}_3(\mu\text{-CO})(\text{CO})_{10}^{1-}$  was proposed by Johnson, Lewis, Raithby, and Suss,<sup>7b</sup> the correct assignment of the <sup>13</sup>C NMR spectrum by Ford and co-workers<sup>7a</sup> leads us to the conclusion that the lowest energy process is the same as that observed for the Fe analogue.<sup>11</sup>

taneous opening of the hydride and carbonyl bridges leads to a structure having only terminal ligands. Then closing of the hydride bridge to a different metal atom, in conjunction with formation of a carbonyl bridge, exchanges the carbonyl ligands. Similar mechanisms have been proposed for carbonyl exchange on  $\text{Fe}_3(\mu\text{-CO})_2(\text{CO})_9\text{L}^{15}$  and  $\text{Ru}_3(\mu\text{-CH}_2)(\mu\text{-CO})(\text{CO})_{10}^{16}$ .

We propose the mechanism in Figure 3 for isomerization of  $(\mu\text{-H})\text{M}_3(\mu\text{-CNMe}_2)(\text{CO})_9\text{L}$ . Opening of the methylidyne and hydride bridges of the n-e isomer produces an intermediate containing only terminally coordinated ligands. Closing of carbonyl and hydride bridges across a second metal-metal vector while retaining the terminally bound methylidyne generates a new dibridged cluster isostructural with the ground-state structures but having exchanged positions of carbonyl and methylidyne ligands. Opening of the hydride and carbonyl bridges positions the hydride on the L-substituted metal atom. Finally, closing hydride and methylidyne bridges across the third metal-metal vector generates the b-e isomer. Although there is no direct evidence for this mechanism, the small normal deuterium kinetic isotope effect is consistent with hydride bridge opening and the order of decreasing ease of carbonyl fluxionality for  $(\mu\text{-H})\text{Ru}_3(\mu\text{-CX})(\text{CO})_{10}$  ( $\text{X} = \text{O}^- > \text{OMe} > \text{NMe}_2$ ),<sup>3,13,17</sup> which would be expected to be the order of decreasing migratory aptitude of the methylidyne ligand (vide infra), is consistent with this mechanism. Deuterium kinetic isotope effects of 1.5 and 1.8 were found for hydride fluxionality on  $\text{H}_2\text{Os}_3(\text{CO})_{10}(\text{PPh}_3)$  and  $\text{H}_2\text{Ru}_3(\text{CO})_9(\text{HC}=\text{CCMe}_3)^{2+}$ , respectively.<sup>18</sup>

While there has been no direct comparison of the migratory abilities of CO,  $\text{COMe}^+$ , and  $\text{CNMe}_2^+$  ligands, analogy to related systems suggests the order  $\text{CO} > \text{COMe}^+ > \text{CNMe}_2^+$ . Cis-trans isomerization and carbonyl fluxionality of  $\text{Cp}_2\text{M}_2(\text{CO})_2(\mu\text{-CO})_2$  ( $\text{M} = \text{Fe}, \text{Ru}$ )<sup>19</sup> have been shown to proceed via bridge-terminal carbonyl exchange through an intermediate having only terminal carbonyls. Comparison of  $\text{Cp}_2\text{Fe}_2(\text{CO})_2(\mu\text{-CO})_2$  and  $\text{Cp}_2\text{Fe}_2(\text{CO})_2(\mu\text{-CO})(\mu\text{-CNPh})^{20}$  finds that the latter isomerizes at a slower rate, presumably because of the larger activation energy required to convert the isocyanide ligand to the terminal coordination mode. Finally, O-coordination of Lewis acids such as  $\text{AlEt}_3$  to the bridging carbonyl has been shown to increase the barrier to isomerization of  $\text{Cp}_2\text{Fe}_2(\text{CO})_2(\mu\text{-CO})_2$ ;<sup>21</sup> this is presumably because O-coordination stabilizes the bridged coordination mode relative to the terminal mode.<sup>22</sup> Since  $\text{COMe}^+$  and  $\text{CNMe}_2^+$  may be considered to be adducts of the Lewis acid  $\text{Me}^+$  with CO and CNMe, respectively, this suggests that the barrier to bridge-terminal ligand interconversion should increase in the order  $\text{CO} < \text{COMe}^+ < \text{CNMe}_2^+$ . Wilkinson and Todd have attributed the decrease in rate of carbonyl

fluxionality for  $(\mu\text{-H})\text{Fe}_3(\mu\text{-CO})(\text{CO})_{10}^{1-}$  in the presence of  $\text{BF}_3$  to O-coordination.<sup>11</sup>

Other mechanisms, such as ones involving  $\mu_3\text{-CNMe}_2$ ,  $\mu_3\text{-H}$ , and/or  $\mu_3\text{-CO}$  ligands, may be postulated which are consistent with our data, but these are intuitively less attractive on the basis of electron counting and are without precedent in analogous  $\text{HM}_3(\mu\text{-X})(\text{CO})_{10}$  systems. These mechanisms also require several intermediates to convert the n-e isomer to the b-e isomer.

Few studies of ligand effects upon fluxional processes on clusters have appeared,<sup>1</sup> but a number of studies of fluxional processes at single metal centers have found that the energy barrier to ligand rearrangement increases as the size of the ligand increases. For example, the free energy of activation for intramolecular CO rearrangement on  $\text{Co}(\text{CO})_4(\text{EX}_3)$  increases in the order  $\text{EX}_3 = \text{SiF}_3 < \text{SiCl}_3 < \text{SiPh}_3$ ,<sup>23</sup> and for intramolecular cis-trans isomerization of  $\text{M}(\text{CO})_4(^{13}\text{CO})(\text{PR}_3)$  ( $\text{M} = \text{Cr}, \text{Mo}, \text{W}$ ) the barrier increases in the order  $\text{PR}_3 = \text{PMe}_3 < \text{PEt}_3 < \text{P}(i\text{-Pr})_3$ .<sup>24</sup> Activation entropies for these isomerizations are generally negative, as found here for n-e to b-e isomerization, and it is interesting that the slower rate for isomerization of  $\text{W}(\text{CO})_4(^{13}\text{CO})(\text{PR}_3)$  compared to the Cr analogue is due to a more negative entropy of activation (-54.9 vs. +1.8 eu), as is the case for the Os and Ru clusters. However, these studies of isomerizations at a single metal center are not directly related to ligand exchange between different metal centers reported here because of the different mechanisms, trigonal twist for the former and bridge-terminal ligand interconversion for the latter. Furthermore, the electronic effects upon isomerizations of mononuclear complexes and clusters are different, the free energies of activation for fluxionality for  $\text{Co}(\text{CO})_4(\text{EPh}_3)$  decreasing as the atomic numbers of the donor atoms increase ( $E = \text{Si} (9.5 \text{ kcal}) > \text{Ge} (8.8) > \text{Sn} (7.2) > \text{Pb} (6.6)$ ),<sup>14</sup> in contradistinction to the trend seen for the isomerization of  $(\mu\text{-H})\text{M}_3(\mu\text{-CNMe}_2)(\text{CO})_9\text{L}$ .

The variation of  $K_{\text{eq}}$  with the steric properties of L is explained by the fact that the b-e coordination site is less sterically hindered than the n-e site.<sup>4</sup> Thus, the b-e isomer becomes more stable relative to the n-e form as the size of L increases.

The dependence of  $K_{\text{eq}}$  upon the electronic properties of L is more difficult to rationalize. The trend in  $K_{\text{eq}}$  for ligands of similar cone angle,<sup>27</sup>  $\text{L} = \text{PPh}_3 > \text{AsPh}_3 > \text{SbPh}_3$  and  $\text{L} = \text{P}(\text{OPh})_3 > \text{PBU}_3$ , can be analyzed in terms of a number of ligand properties— $\pi$ -acceptor ability,  $\sigma$ -donor ability, basicity, polarizability, and others. We have chosen to rationalize the variation in  $K_{\text{eq}}$  in terms of the "softness" of L.<sup>28</sup> The problem can be analyzed in terms of the formation of the most favorable acid-base combinations— $(\text{Ru}(\text{n-e})\text{-L}, \text{Ru}(\text{b-e})\text{-CO})$  or  $(\text{Ru}(\text{n-e})\text{-CO}, \text{Ru}(\text{b-e})\text{-L})$ . According to the HSAB theory<sup>25</sup> the most favorable combination will pair the softer metal site with the softer ligand and the harder metal site with the harder ligand. Of the two metal sites we propose that the non-bridged metal atom is in the lower oxidation state and is thus the softer; in support of this, a study of  $\text{HOs}_3(\mu\text{-X})(\text{CO})_{10}$  ( $\text{X} = \text{Cl}, \text{Br}, \text{and I}$ ) found that in each case the

(15) (a) Benfield, R. E.; Gavens, P. D.; Johnson, B. F. G.; Mays, M. J.; Aime, S.; Milone, L.; Osella, D. *J. Chem. Soc., Dalton Trans.* 1981, 1535. (b) Cotton, F. A.; Troup, J. M. *J. Am. Chem. Soc.* 1974, 96, 4155.

(16) Holmgren, J. S.; Shapley, J. R. *Organometallics* 1985, 4, 793.

(17) Johnson, B. F. G.; Lewis, J.; Orpen, A. G.; Raithby, P. R.; Suss, G. *J. Organomet. Chem.* 1983, 173, 187.

(18) Rosenberg, E.; Anslyn, E. V.; Barner-Thorsen, C.; Aime, S.; Osella, D.; Gobetto, R.; Milone, L. *Organometallics* 1984, 3, 1790.

(19) (a) Bullitt, J. G.; Cotton, F. A.; Marks, T. J. *J. Am. Chem. Soc.* 1970, 92, 2155. (b) Gansow, O. A.; Burke, A. R.; Vernon, W. D. *J. Am. Chem. Soc.* 1972, 94, 2550. (c) Adams, R. D.; Cotton, F. A. *J. Am. Chem. Soc.* 1973, 95, 6589. (d) Cotton, F. A.; Hunter, D. L.; Lahuerta, P.; White, A. J. *Inorg. Chem.* 1976, 15, 557. (e) Cotton, F. A.; Kruczyński, L.; White, A. J. *Inorg. Chem.* 1974, 13, 1402.

(20) Howell, J. A. S.; Matheson, T. W.; Mays, M. J. *J. Chem. Soc., Chem. Commun.* 1975, 865.

(21) Alich, A.; Nelson, N. J.; Strope, D.; Shriver, D. F. *Inorg. Chem.* 1972, 11, 2976.

(22) Horwitz, C. P.; Shriver, D. F. *Adv. Organomet. Chem.* 1984, 23, 219.

(23) Lichtenberger, D. L.; Brown, T. L. *J. Am. Chem. Soc.* 1977, 99, 8187.

(24) Darensbourg, D. J.; Gray, R. L. *Inorg. Chem.* 1984, 23, 2993.

(25) Pearson, R. G. In "Survey of Progress in Chemistry"; Scott, A., Ed.; Academic Press: New York, 1969; Vol. 5, pp 1-52.

(26) Chesky, P. T.; Hall, M. B. *Inorg. Chem.* 1983, 22, 3327.

(27) Tolman, C. A. *Chem. Rev.* 1977, 77, 313.

(28) Few studies have compared the softness of various phosphine, arsine, and stibine ligands. Klopman<sup>29</sup> has proposed a softness parameter which is related to the electronegativity of the donor atom.

(29) Klopman, G. *J. Am. Chem. Soc.* 1968, 90, 223.

gross atomic charges on the bridged Os atoms are positive while the charge on the nonbridged metal atom is negative.<sup>26</sup> By this argument the softer the ligand L, the more favorable should be the n-e isomer. This is also consistent with the observation that py, a harder ligand, coordinates to a bridged metal atom<sup>3,4</sup> but the softer isocyanide ligands coordinate to the nonbridged atom (e.g.,  $(\mu\text{-H})\text{Os}_3(\mu\text{-COMe})(\text{CO})_9(\text{CNCMe}_3)^{10}$ ).  $\pi$ -Bonding arguments do not explain these observations.

**Acknowledgment.** This work has been supported by the National Science Foundation (Grant No. CHE-8121059).

**Registry No.**  $(\mu\text{-H})\text{Ru}_3(\mu\text{-CNMe}_2)(\text{CO})_9(\text{PPh}_3)$  (n-e), 98065-42-0;  $(\mu\text{-H})\text{Ru}_3(\mu\text{-CNMe}_2)(\text{CO})_9(\text{PPh}_3)$  (b-e), 98065-41-9;  $(\mu\text{-H})\text{Ru}_3(\mu\text{-CNMe}_2)(\text{CO})_9(\text{PMePh}_2)$  (n-e), 99921-89-8;  $(\mu\text{-H})\text{Ru}_3(\mu\text{-CNMe}_2)(\text{CO})_9(\text{PMePh}_2)$  (b-e), 99901-46-9;  $(\mu\text{-H})\text{Ru}_3(\mu\text{-CNMe}_2)(\text{CO})_9(\text{PMe}_2\text{Ph})$  (n-e), 99921-90-1;  $(\mu\text{-H})\text{Ru}_3(\mu\text{-CNMe}_2)(\text{CO})_9(\text{PMe}_2\text{Ph})$  (b-e), 99901-47-0;  $(\mu\text{-H})\text{Ru}_3(\mu\text{-CNMe}_2)(\text{CO})_9(\text{PBu}_3)$  (n-e), 98065-48-6;  $(\mu\text{-H})\text{Ru}_3(\mu\text{-CNMe}_2)(\text{CO})_9(\text{PBu}_3)$  (b-e), 98065-47-5;  $(\mu\text{-H})\text{Ru}_3(\mu\text{-CNMe}_2)(\text{CO})_9(\text{PCy}_3)$  (n-e), 98065-46-4;  $(\mu\text{-H})\text{Ru}_3(\mu\text{-CNMe}_2)(\text{CO})_9(\text{PCy}_3)$  (b-e), 98065-45-3;  $(\mu\text{-H})\text{Ru}_3(\mu\text{-CNMe}_2)(\text{CO})_9(\text{P}(\text{OMe})_3)$  (n-e), 99901-43-6;  $(\mu\text{-H})\text{Ru}_3(\mu\text{-CNMe}_2)(\text{CO})_9(\text{P}(\text{OMe})_3)$  (b-e), 99901-48-1;  $(\mu\text{-H})\text{Ru}_3(\mu\text{-CNMe}_2)(\text{CO})_9(\text{P}(\text{O}-i\text{-Pr})_3)$  (n-e), 99901-44-7;  $(\mu\text{-H})\text{Ru}_3(\mu\text{-CNMe}_2)(\text{CO})_9(\text{P}(\text{O}-i\text{-Pr})_3)$  (b-e), 99901-49-2;  $(\mu\text{-H})\text{Ru}_3(\mu\text{-CNMe}_2)(\text{CO})_9(\text{P}(\text{OPh})_3)$  (n-e), 99901-45-8;  $(\mu\text{-H})\text{Ru}_3(\mu\text{-CNMe}_2)(\text{CO})_9(\text{P}(\text{OPh})_3)$  (b-e), 99901-50-5;  $(\mu\text{-H})\text{Ru}_3(\mu\text{-CNMe}_2)(\text{CO})_9(\text{AsPh}_3)$  (n-e), 98065-40-8;  $(\mu\text{-H})\text{Ru}_3(\mu\text{-CNMe}_2)(\text{CO})_9(\text{AsPh}_3)$  (b-e), 98065-39-5;  $(\mu\text{-H})\text{Ru}_3(\mu\text{-CNMe}_2)(\text{CO})_9(\text{SbPh}_3)$  (n-e), 98065-44-2;  $(\mu\text{-H})\text{Ru}_3(\mu\text{-CNMe}_2)(\text{CO})_9(\text{SbPh}_3)$  (b-e), 98065-43-1;  $(\mu\text{-H})\text{Os}_3(\mu\text{-CNMe}_2)(\text{CO})_9(\text{AsPh}_3)$  (n-e), 99921-91-2;  $(\mu\text{-H})\text{Os}_3(\mu\text{-CNMe}_2)(\text{CO})_9(\text{AsPh}_3)$  (b-e), 99901-53-8;  $(\mu\text{-H})\text{Os}_3(\mu\text{-CNMe}_2)(\text{CO})_9(\text{NCMe})$ , 99901-51-6;  $(\mu\text{-D})\text{Ru}_3(\mu\text{-CNMe}_2)(\text{CO})_{10}$ , 99901-52-7;  $\text{Ru}_3(\text{CO})_{12}$ , 15243-33-1;  $(\mu\text{-H})\text{Ru}_3(\mu\text{-CNMe}_2)(\text{CO})_9(\text{py})$ , 97415-87-7;  $\text{D}_2$ , 7782-39-0; Os, 7440-04-2; Ru, 7440-18-8.

**Supplementary Material Available:** Infrared spectral data for  $(\mu\text{-H})\text{M}_3(\mu\text{-CNMe}_2)(\text{CO})_9\text{L}$  (1 page). Ordering information is given on any current masthead page.

## Synthesis and Structural Characterization of Binuclear Gold(I) Complexes Derived from Two New A-Frame Ligands

H. Schmidbaur,\*† Th. Pollok,† R. Herr,† F. E. Wagner,‡ R. Bau,§,¶ J. Riede,† and G. Müller†

*Anorganisch-Chemisches Institut und Physik-Department der Technischen Universität München, D-8046 Garching, West Germany, and Department of Chemistry, University of Southern California, Los Angeles, California*

Received July 18, 1985

The molecular structure of the potential A-frame ligand cyclopropylidenebis(diphenylphosphine), cdpp, has been determined by an X-ray diffraction analysis. The ground-state conformation in the crystal is a rotamer with the lone pairs of electrons at phosphorus in cis and trans (*Z* or *E*) positions relative to the cyclopropane plane. This ligand forms 1:2 complexes with AuCl, AuI, and AuCH<sub>3</sub>. The 1:1 complex with AuCl (**7b**) has the expected eight-membered ring structure, as determined by an X-ray diffraction study of the trimethanol solvate, but one of the chloro ligands is found to be dissociated from the gold(I) centers. In the remaining dinuclear cation with an Au–Au contact of 2.907 (1) Å, the residual chloro ligand is positioned above one gold atom with an Au1–Au2–Cl1 angle of only 75.4 (1)°. The structural inequivalence of the metal atoms in the solid is confirmed by <sup>197</sup>Au Mössbauer data. Solution NMR data in CDCl<sub>3</sub> indicate a virtually symmetrical structure due to exchange processes. A related autodissociation of only one chloro ligand from a dinuclear gold(I) complex was also found in the X-ray analysis of the 1:1 complex of AuCl with 2-methoxyethylidenebis(diphenylphosphine) (**3b**). In this complex, obtained by methanol addition to the vinylidene precursor as the tetramethanol solvate, the residual chlorine is attached to one gold atom on the projection of the Au–Au axis (Au1–Au2 = 3.002 (1) Å; Au1–Cl3 = 2.963 (3) Å; Au2–Au1–Cl3 = 176.2 (1)°). The methoxy groups of the two side chains are oriented toward Au2. These peculiar interactions lead to very uncommon coordination spheres for both gold(I) centers in the cation of **3b**. Au Mössbauer data of the solid and NMR spectra of the solution are again in agreement with an unsymmetrical and symmetrical structure, respectively. Crystal data for cdpp: *C*2/*c*, *a* = 27.064 (6) Å, *b* = 10.146 (2) Å, *c* = 17.562 (4) Å,  $\beta$  = 114.30 (2)°, *V* = 4395.1 Å<sup>3</sup>, *Z* = 8, *R*<sub>w</sub> = 0.041 for 262 refined parameters and 2437 reflections with *F*<sub>o</sub> ≥ 4σ(*F*<sub>o</sub>). Crystal data for **7b**: *P*2<sub>1</sub>/*c*, *a* = 17.283 (4) Å, *b* = 17.027 (4) Å, *c* = 19.284 (4) Å,  $\beta$  = 108.75 (2)°, *V* = 5373.7 Å<sup>3</sup>, *Z* = 4, *R*<sub>w</sub> = 0.044 for 343 parameters and 6045 observed data. Crystal data for **3b**: *P*2<sub>1</sub>2<sub>1</sub>2<sub>1</sub>, *a* = 11.388 (2) Å, *b* = 22.588 (5) Å, *c* = 22.737 (5) Å, *V* = 5840.9 Å<sup>3</sup>, *R*<sub>w</sub> = 0.042 for 378 parameters and 4549 observed reflections.

### Introduction

Bis(diphenylphosphino)methane (dppm) is the prototype of a class of difunctional phosphines known to favor

the construction of binuclear complexes with short metal–metal contacts.<sup>1</sup> This close metal–metal proximity is responsible for a variety of novel addition reactions which result in a geometrical situation designated as an "A-frame" structure. Many of these reactions are at least partially reversible as other substrates are added to the system, and

\* Anorganisch-Chemisches Institut.

† Physik-Department der Technischen Universität München.

‡ University of Southern California.

§ A. v. Humboldt Awardee, 1985, Technical University of Munich.

(1) Puddephatt, R. J. *Chem. Soc. Rev.* 1983, 12, 99.

gross atomic charges on the bridged Os atoms are positive while the charge on the nonbridged metal atom is negative.<sup>26</sup> By this argument the softer the ligand L, the more favorable should be the n-e isomer. This is also consistent with the observation that py, a harder ligand, coordinates to a bridged metal atom<sup>3,4</sup> but the softer isocyanide ligands coordinate to the nonbridged atom (e.g., ( $\mu$ -H)Os<sub>3</sub>( $\mu$ -COMe)(CO)<sub>9</sub>(CNCMe<sub>3</sub>)<sup>10</sup>).  $\pi$ -Bonding arguments do not explain these observations.

**Acknowledgment.** This work has been supported by the National Science Foundation (Grant No. CHE-8121059).

**Registry No.** ( $\mu$ -H)Ru<sub>3</sub>( $\mu$ -CNMe<sub>2</sub>)(CO)<sub>9</sub>(PPh<sub>3</sub>) (n-e), 98065-42-0; ( $\mu$ -H)Ru<sub>3</sub>( $\mu$ -CNMe<sub>2</sub>)(CO)<sub>9</sub>(PPh<sub>3</sub>) (b-e), 98065-41-9; ( $\mu$ -H)Ru<sub>3</sub>( $\mu$ -CNMe<sub>2</sub>)(CO)<sub>9</sub>(PMePh<sub>2</sub>) (n-e), 99921-89-8; ( $\mu$ -H)Ru<sub>3</sub>( $\mu$ -CNMe<sub>2</sub>)(CO)<sub>9</sub>(PMePh<sub>2</sub>) (b-e), 99901-46-9; ( $\mu$ -H)Ru<sub>3</sub>( $\mu$ -CNMe<sub>2</sub>)(CO)<sub>9</sub>(PMe<sub>2</sub>Ph) (n-e), 99921-90-1; ( $\mu$ -H)Ru<sub>3</sub>( $\mu$ -CNMe<sub>2</sub>)(CO)<sub>9</sub>(PMe<sub>2</sub>Ph) (b-e), 99901-47-0; ( $\mu$ -H)Ru<sub>3</sub>( $\mu$ -

CNMe<sub>2</sub>)(CO)<sub>9</sub>(PBu<sub>3</sub>) (n-e), 98065-48-6; ( $\mu$ -H)Ru<sub>3</sub>( $\mu$ -CNMe<sub>2</sub>)(CO)<sub>9</sub>(PBu<sub>3</sub>) (b-e), 98065-47-5; ( $\mu$ -H)Ru<sub>3</sub>( $\mu$ -CNMe<sub>2</sub>)(CO)<sub>9</sub>(PCy<sub>3</sub>) (n-e), 98065-46-4; ( $\mu$ -H)Ru<sub>3</sub>( $\mu$ -CNMe<sub>2</sub>)(CO)<sub>9</sub>(PCy<sub>3</sub>) (b-e), 98065-45-3; ( $\mu$ -H)Ru<sub>3</sub>( $\mu$ -CNMe<sub>2</sub>)(CO)<sub>9</sub>(P(OMe)<sub>3</sub>) (n-e), 99901-43-6; ( $\mu$ -H)Ru<sub>3</sub>( $\mu$ -CNMe<sub>2</sub>)(CO)<sub>9</sub>(P(OMe)<sub>3</sub>) (b-e), 99901-48-1; ( $\mu$ -H)Ru<sub>3</sub>( $\mu$ -CNMe<sub>2</sub>)(CO)<sub>9</sub>(P(O-*i*-Pr)<sub>3</sub>) (n-e), 99901-44-7; ( $\mu$ -H)Ru<sub>3</sub>( $\mu$ -CNMe<sub>2</sub>)(CO)<sub>9</sub>(P(O-*i*-Pr)<sub>3</sub>) (b-e), 99901-49-2; ( $\mu$ -H)Ru<sub>3</sub>( $\mu$ -CNMe<sub>2</sub>)(CO)<sub>9</sub>(P(OPh)<sub>3</sub>) (n-e), 99901-45-8; ( $\mu$ -H)Ru<sub>3</sub>( $\mu$ -CNMe<sub>2</sub>)(CO)<sub>9</sub>(P(OPh)<sub>3</sub>) (b-e), 99901-50-5; ( $\mu$ -H)Ru<sub>3</sub>( $\mu$ -CNMe<sub>2</sub>)(CO)<sub>9</sub>(AsPh<sub>3</sub>) (n-e), 98065-40-8; ( $\mu$ -H)Ru<sub>3</sub>( $\mu$ -CNMe<sub>2</sub>)(CO)<sub>9</sub>(AsPh<sub>3</sub>) (b-e), 98065-39-5; ( $\mu$ -H)Ru<sub>3</sub>( $\mu$ -CNMe<sub>2</sub>)(CO)<sub>9</sub>(SbPh<sub>3</sub>) (n-e), 98065-44-2; ( $\mu$ -H)Ru<sub>3</sub>( $\mu$ -CNMe<sub>2</sub>)(CO)<sub>9</sub>(SbPh<sub>3</sub>) (b-e), 98065-43-1; ( $\mu$ -H)Os<sub>3</sub>( $\mu$ -CNMe<sub>2</sub>)(CO)<sub>9</sub>(AsPh<sub>3</sub>) (n-e), 99921-91-2; ( $\mu$ -H)Os<sub>3</sub>( $\mu$ -CNMe<sub>2</sub>)(CO)<sub>9</sub>(AsPh<sub>3</sub>) (b-e), 99901-53-8; ( $\mu$ -H)Os<sub>3</sub>( $\mu$ -CNMe<sub>2</sub>)(CO)<sub>9</sub>(NCMe), 99901-51-6; ( $\mu$ -D)Ru<sub>3</sub>( $\mu$ -CNMe<sub>2</sub>)(CO)<sub>10</sub>, 99901-52-7; Ru<sub>3</sub>(CO)<sub>12</sub>, 15243-33-1; ( $\mu$ -H)Ru<sub>3</sub>( $\mu$ -CNMe<sub>2</sub>)(CO)<sub>9</sub>(py), 97415-87-7; D<sub>2</sub>, 7782-39-0; Os, 7440-04-2; Ru, 7440-18-8.

**Supplementary Material Available:** Infrared spectral data for ( $\mu$ -H)M<sub>3</sub>( $\mu$ -CNMe<sub>2</sub>)(CO)<sub>9</sub>L (1 page). Ordering information is given on any current masthead page.

## Synthesis and Structural Characterization of Binuclear Gold(I) Complexes Derived from Two New A-Frame Ligands

H. Schmidbaur,\*† Th. Pollok,† R. Herr,† F. E. Wagner,‡ R. Bau,§,¶ J. Riede,† and G. Müller†

*Anorganisch-Chemisches Institut und Physik-Department der Technischen Universität München, D-8046 Garching, West Germany, and Department of Chemistry, University of Southern California, Los Angeles, California*

Received July 18, 1985

The molecular structure of the potential A-frame ligand cyclopropylidenebis(diphenylphosphine), cdpp, has been determined by an X-ray diffraction analysis. The ground-state conformation in the crystal is a rotamer with the lone pairs of electrons at phosphorus in *cis* and *trans* (*Z* or *E*) positions relative to the cyclopropane plane. This ligand forms 1:2 complexes with AuCl, AuI, and AuCH<sub>3</sub>. The 1:1 complex with AuCl (**7b**) has the expected eight-membered ring structure, as determined by an X-ray diffraction study of the trimethanol solvate, but one of the chloro ligands is found to be dissociated from the gold(I) centers. In the remaining dinuclear cation with an Au–Au contact of 2.907 (1) Å, the residual chloro ligand is positioned above one gold atom with an Au1–Au2–Cl1 angle of only 75.4 (1)°. The structural inequivalence of the metal atoms in the solid is confirmed by <sup>197</sup>Au Mössbauer data. Solution NMR data in CDCl<sub>3</sub> indicate a virtually symmetrical structure due to exchange processes. A related autodissociation of only one chloro ligand from a dinuclear gold(I) complex was also found in the X-ray analysis of the 1:1 complex of AuCl with 2-methoxyethylidenebis(diphenylphosphine) (**3b**). In this complex, obtained by methanol addition to the vinylidene precursor as the tetramethanol solvate, the residual chlorine is attached to one gold atom on the projection of the Au–Au axis (Au1–Au2 = 3.002 (1) Å; Au1–Cl3 = 2.963 (3) Å; Au2–Au1–Cl3 = 176.2 (1)°). The methoxy groups of the two side chains are oriented toward Au2. These peculiar interactions lead to very uncommon coordination spheres for both gold(I) centers in the cation of **3b**. Au Mössbauer data of the solid and NMR spectra of the solution are again in agreement with an unsymmetrical and symmetrical structure, respectively. Crystal data for cdpp: *C*2/*c*, *a* = 27.064 (6) Å, *b* = 10.146 (2) Å, *c* = 17.562 (4) Å,  $\beta$  = 114.30 (2)°, *V* = 4395.1 Å<sup>3</sup>, *Z* = 8, *R*<sub>w</sub> = 0.041 for 262 refined parameters and 2437 reflections with *F*<sub>o</sub> ≥ 4σ(*F*<sub>o</sub>). Crystal data for **7b**: *P*2<sub>1</sub>/*c*, *a* = 17.283 (4) Å, *b* = 17.027 (4) Å, *c* = 19.284 (4) Å,  $\beta$  = 108.75 (2)°, *V* = 5373.7 Å<sup>3</sup>, *Z* = 4, *R*<sub>w</sub> = 0.044 for 343 parameters and 6045 observed data. Crystal data for **3b**: *P*2<sub>1</sub>2<sub>1</sub>2<sub>1</sub>, *a* = 11.388 (2) Å, *b* = 22.588 (5) Å, *c* = 22.737 (5) Å, *V* = 5840.9 Å<sup>3</sup>, *R*<sub>w</sub> = 0.042 for 378 parameters and 4549 observed reflections.

### Introduction

Bis(diphenylphosphino)methane (dppm) is the prototype of a class of difunctional phosphines known to favor

the construction of binuclear complexes with short metal–metal contacts.<sup>1</sup> This close metal–metal proximity is responsible for a variety of novel addition reactions which result in a geometrical situation designated as an "A-frame" structure. Many of these reactions are at least partially reversible as other substrates are added to the system, and

\* Anorganisch-Chemisches Institut.

† Physik-Department der Technischen Universität München.

‡ University of Southern California.

§ A. v. Humboldt Awardee, 1985, Technical University of Munich.

(1) Puddephatt, R. J. *Chem. Soc. Rev.* 1983, 12, 99.

Table I. Crystallographic Data for cdpp, 7b, and 3b

	cdpp	7b	3b
formula	C <sub>27</sub> H <sub>24</sub> P <sub>2</sub>	C <sub>57</sub> H <sub>60</sub> Au <sub>2</sub> Cl <sub>2</sub> O <sub>3</sub> P <sub>4</sub>	C <sub>58</sub> H <sub>68</sub> Au <sub>2</sub> Cl <sub>2</sub> O <sub>6</sub> P <sub>2</sub>
fw	410.44	1381.85	1449.92
cryst system	monoclinic	monoclinic	orthorhombic
space group	C2/c	P2 <sub>1</sub> /c	P2 <sub>1</sub> 2 <sub>1</sub> 2 <sub>1</sub>
a, Å	27.064 (6)	17.283 (4)	11.388 (2)
b, Å	10.146 (2)	17.027 (4)	22.558 (5)
c, Å	17.562 (4)	19.284 (4)	22.737 (5)
α, deg	90	90	90
β, deg	114.30 (2)	108.75 (2)	90
γ, deg	90	90	90
V, Å <sup>3</sup>	4395.13	5373.69	5840.92
Z	8	4	4
ρ(calcd), g/cm <sup>3</sup>	1.240	1.708	1.649
μ, cm <sup>-1</sup>	2.0	57.0	52.5
F(000), e	1728	2712	2864
T, °C	-35	-40	-40
radiatn		Mo Kα, λ = 0.710 69 Å	
scan mode	ω	ω	ω
scan rate, deg/min		0.9-29.3	
scan width, deg	0.9	0.8	0.8
(sin θ)/λ <sub>max</sub>	0.572	0.581	0.572
reflections measd	3742	8031	5080
reflections unique	3448	7485	5080
R <sub>int</sub> <sup>a</sup>	0.033	0.031	
obsd data			
[F <sub>o</sub> ≥ 4.0σ(F <sub>o</sub> )]	2437	6045	4549
absorptn correctn		empirical	empirical
no. of refined variables	262	343	378
R <sup>b</sup>	0.050	0.044	0.038
R <sub>w</sub> <sup>c</sup>	0.041	0.044	0.042
k (last cycle)	1.6	2.9	1.9
(shift/error) <sub>max</sub>	0.001	0.110	0.02
Δρ (final), e/Å <sup>3</sup>	+0.30/-0.31	+1.50/-1.06	+1.22/-0.86

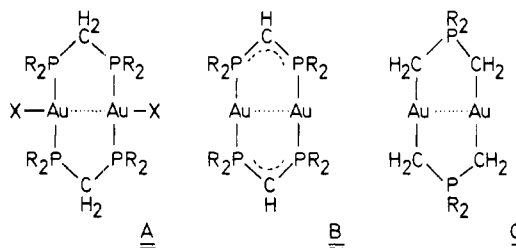
$$^a R_{\text{int}} = [\sum(N\sum_n w(\langle F \rangle - F)^2) / \sum((N-1)\sum_n wF^2)]^{1/2}. \quad ^b R = \sum(|F_o| - |F_c|) / \sum|F_o|. \quad ^c R_w = [\sum w(|F_o| - |F_c|)^2 / \sum wF_o^2]^{1/2}, \quad w = k/\sigma^2(F_o).$$

thus catalytic cycles can be induced with these complexes as active species or as precursors to reactive intermediates. One metal thereby is functioning as an activating neighboring group for the second metal center through reversible transannular interactions.<sup>1</sup>

These effects are quite pronounced also in a number of gold(I) complexes of dppm-type ligands<sup>2-5</sup> (A), or, e.g., related 1,3-difunctional phosphinobis(methylidene) metalacycles (C).<sup>6-11</sup> Oxidation with equivalent quantities of halogen leads to some of the very few species with gold in the oxidation state +II containing an Au-Au bond.<sup>5,8-11</sup> With dihalomethane, stepwise oxidative addition takes place leading eventually to methylene bridging between Au(III) centers.<sup>12,13</sup>

For the gold(I) complexes of type A-C, X-ray structure data,<sup>2,3,6,14</sup> UV/vis spectra,<sup>15</sup> and <sup>197</sup>Au Mössbauer re-

sults<sup>4,5,16</sup> have indicated that Au-Au interactions are not negligible, since, e.g., the two metal atoms have even shorter interatomic distances than the dimensions imposed by the ligand bite. The nature of this interaction has been the subject of very recent discussions, as experimental evidence is rapidly increasing not only for the limited field of A-frame complexes.<sup>17</sup>



(2) Schmidbaur, H.; Wohlleben, A.; Wagner, F.; Orama, O.; Huttner, G. *Chem. Ber.* 1977, 110, 1748.

(3) Schmidbaur, H.; Wohlleben, A.; Schubert, U.; Frank, A.; Huttner, G. *Chem. Ber.* 1977, 110, 2751.

(4) Schmidbaur, H.; Wohlleben, A.; Wagner, F.; van de Vondel, D. F.; van der Kelen, G. P. *Chem. Ber.* 1977, 110, 2758.

(5) Schmidbaur, H.; Wagner, F.; Wohlleben-Hammer, A. *Chem. Ber.* 1979, 112, 496.

(6) Schmidbaur, H. *Acc. Chem. Res.* 1975, 8, 62; *Angew. Chem.* 1983, 95, 980; *Angew. Chem., Int. Ed. Engl.* 1983, 22, 907.

(7) Fackler, J. P.; Basil, J. D. *Organometallics* 1982, 1, 871. Murray, H. H.; Mazany, A. M.; Fackler, J. P. *Ibid.* 1985, 4, 154. Knachel, H. C.; Dudis, D. S.; Fackler, J. P. *Ibid.* 1984, 3, 1312.

(8) Schmidbaur, H.; Mandl, J. R.; Frank, A.; Huttner, G. *Chem. Ber.* 1976, 109, 466.

(9) Schmidbaur, H.; Jandik, P. *Inorg. Chim. Acta* 1983, 74, 97.

(10) Schmidbaur, H.; Mandl, J. R. *Naturwissenschaften* 1976, 63, 585.

(11) Fackler, J. P.; Murray, H. H.; Basil, J. D. *Organometallics* 1984, 3, 821.

(12) Jandik, P.; Schubert, U.; Schmidbaur, H. *Angew. Chem.* 1982, 94, 74; *Angew. Chem., Int. Ed. Engl.* 1982, 21, 78; *Angew. Chem. Suppl.* 1982, 1.

(13) Murray, H. H.; Fackler, J. P.; Mazany, A. M. *Organometallics* 1984, 3, 1310.

(14) Schmidbaur, H.; Mandl, J. R.; Richter, W.; Bejenke, V.; Frank, A.; Huttner, G. *Chem. Ber.* 1977, 110, 2236.

(15) Meyer, W. W. Dissertation, Universität Zürich, 1981. Kozelka, J. Dissertation, Universität Zürich, 1983.

(16) Schmidbaur, H.; Mandl, J. R.; Wagner, F.; van de Vondel, D. F.; van der Kelen, G. P. *J. Chem. Soc., Chem. Commun.* 1976, 170.

(17) Hoffmann, R.; Jiang, Y.; Alvarez, S. *Inorg. Chem.* 1985, 24, 749. Kubiak, C. P.; Eisenberg, R. *Ibid.* 1980, 19, 2726.

(18) Schmidbaur, H.; Herr, R.; Müller, G.; Riede, J. *Organometallics* 1985, 4, 1208.



**Table II. Fractional Atomic Coordinates and Equivalent Isotropic Thermal Parameters for cdpp<sup>a</sup>**

atom	<i>x/a</i>	<i>y/b</i>	<i>z/c</i>	<i>U(eq)</i> , Å <sup>2</sup>
P1	0.3969 (0)	0.1001 (1)	0.7035 (1)	0.028
P2	0.3613 (0)	0.0422 (1)	0.8508 (1)	0.028
C1	0.4098 (1)	0.0153 (3)	0.8025 (2)	0.026
C11	0.4698 (1)	-0.0135 (3)	0.8551 (2)	0.032
C12	0.4345 (1)	-0.1201 (3)	0.8026 (2)	0.034
C2	0.3815 (1)	0.2701 (3)	0.7212 (2)	0.027
C21	0.3332 (1)	0.3122 (3)	0.7224 (2)	0.032
C22	0.3253 (2)	0.4431 (4)	0.7380 (2)	0.043
C23	0.3657 (2)	0.5347 (4)	0.7504 (3)	0.048
C24	0.4137 (2)	0.4961 (4)	0.7488 (3)	0.044
C25	0.4218 (1)	0.3645 (4)	0.7336 (2)	0.039
C3	0.3301 (1)	0.0376 (3)	0.6335 (2)	0.025
C31	0.3029 (1)	0.1028 (3)	0.5570 (2)	0.029
C32	0.2554 (1)	0.0514 (4)	0.4968 (2)	0.036
C33	0.2345 (1)	-0.0654 (4)	0.5114 (2)	0.036
C34	0.2599 (1)	-0.1307 (4)	0.5869 (2)	0.038
C35	0.3081 (1)	-0.0798 (3)	0.6477 (2)	0.032
C4	0.3976 (1)	0.1528 (3)	0.9389 (2)	0.025
C41	0.4401 (1)	0.2348 (3)	0.9442 (2)	0.032
C42	0.4633 (1)	0.3242 (4)	1.0092 (2)	0.036
C43	0.4443 (2)	0.3315 (3)	1.0714 (2)	0.037
C44	0.4016 (2)	0.2509 (4)	1.0672 (2)	0.037
C45	0.3787 (1)	0.1633 (3)	1.0017 (2)	0.033
C5	0.3649 (1)	-0.1151 (3)	0.9047 (2)	0.026
C51	0.4075 (1)	-0.1534 (4)	0.9790 (2)	0.034
C52	0.4083 (1)	-0.2782 (4)	1.0117 (2)	0.037
C53	0.3660 (2)	-0.3658 (4)	0.9712 (3)	0.039
C54	0.3231 (2)	-0.3279 (4)	0.8994 (2)	0.037
C55	0.3224 (1)	-0.2031 (3)	0.8658 (2)	0.029

<sup>a</sup>  $U(eq) = (U(1)U(2)U(3))^{1/3}$ , where  $U(1)$ ,  $U(2)$ , and  $U(3)$  are the eigenvalues of the  $U(i, j)$  matrix. Esd's are in parentheses.

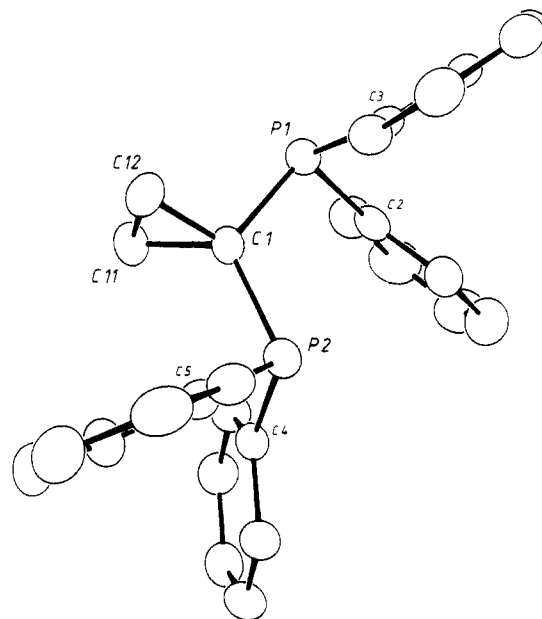
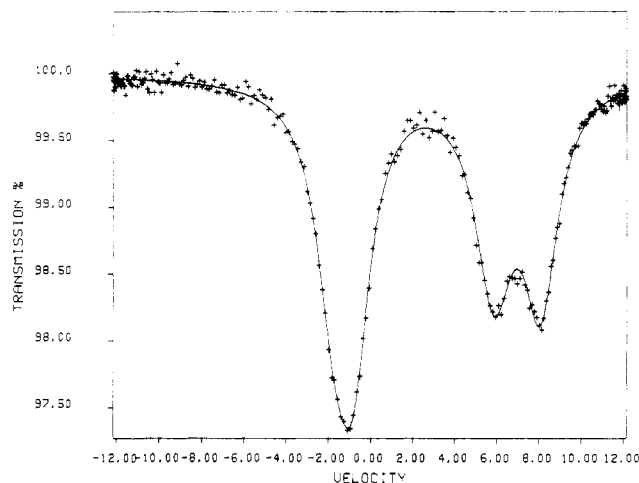
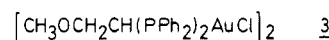
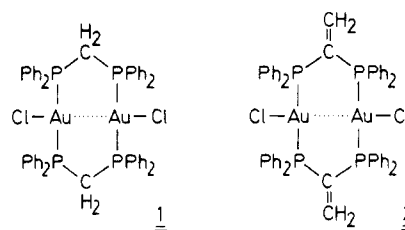
**Table III. Selected Bond Distances (Å), Bond Angles (deg), and Dihedral Angles (deg) in the Free cdpp Ligand (See Figure 1 for Atomic Numbering)<sup>a</sup>**

P1...P2	3.167 (3)	P1-C1-P2	118.0 (2)
C1-C11	1.530 (4)	C11-C1-C12	58.1 (2)
C1-C12	1.527 (4)	C1-C11-C12	60.8 (2)
C11-C12	1.485 (5)	C1-C12-C11	61.0 (2)
P1-C1	1.840 (3)	C1-P1-C2	104.3 (1)
P2-C1	1.854 (3)	C1-P1-C3	102.9 (1)
P1-C2	1.832 (4)	C2-P1-C3	102.0 (1)
P1-C3	1.831 (3)	C1-P2-C4	104.0 (1)
P2-C4	1.835 (3)	C1-P2-C5	102.1 (1)
P2-C5	1.837 (3)	C4-P2-C5	101.6 (1)
E1-P1-C1-P2	173.3	C1-P1-E1	114.4
E2-P2-C1-P1	21.8	C1-P2-E2	114.9

<sup>a</sup> P1-E1 and P2-E2 designate the main vector of the lone pairs of electrons. Points E1/E2, the missing vertices of the coordination tetrahedra around P1 and P2 (i.e., the lone pair positions E1 and E2), were placed so that the sum of unit vectors along the four "bonds" from the central atom is zero.

molecular geometries of complexes 1 and 2 are remarkably similar, with the Au-Au distances increasing only slightly, from 2.962 (1) to 2.977 (1) Å. The chlorine ligands are located above and below the eight-membered rings with a T-shaped coordination at gold. The rings both have a chair conformation as far as the arrangements of the CH<sub>2</sub> and C=CH<sub>2</sub> groups are concerned, respectively. (A crystallographic center of symmetry is present in both structures.)

During investigations of the chemical properties of the vdpp complex, a facile addition of methanol to the C=C bonds was observed. The resulting product 3 is formally a derivative of the saturated dppm prototype and was therefore assigned a similar structure. In an X-ray diffraction and Mössbauer study it could now be shown, however, that the situation, unexpectedly, is more complicated.

**Figure 1.** Molecular structure of the ligand cdpp with numbering of principal atoms. Hydrogen atoms are omitted for clarity (ORTEP, thermal ellipsoids at the 50% probability level).**Figure 2.** <sup>197</sup>Au Mössbauer spectrum of complex 7b (at 4 K).

Intrigued and encouraged by these results (see below) an investigation of the cyclopropylidenebis(diphenylphosphine) (cdpp) complex was also initiated. A preliminary communication of the synthesis of this new ligand has appeared.<sup>19</sup> Its molecular structure and the preparation of some coordination compounds, including another eight-membered ring gold(I) complex, the structure of which has also been determined, are presented in this paper.

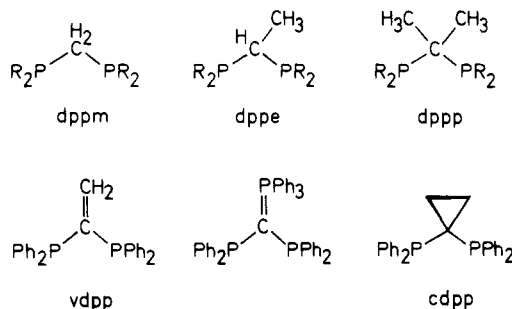
Table IV.  $^{197}\text{Au}$  Mössbauer Data (at 4 K) for Complexes 3b, 6, and 7b and Two vdpp Reference Compounds

	IS, mm s <sup>-1</sup>	QS, mm s <sup>-1</sup>
(CH <sub>3</sub> ) <sub>2</sub> C[PPh <sub>2</sub> AuCH <sub>3</sub> ] <sub>2</sub> (6)	4.67	9.45
{Au <sub>2</sub> [Ph <sub>2</sub> PC(CH <sub>2</sub> ) <sub>2</sub> PPh <sub>2</sub> ] <sub>2</sub> Cl <sup>+</sup> Cl <sup>-</sup> (7b)	2.04	7.62
	3.62	8.91
CH <sub>2</sub> =C[PPh <sub>2</sub> AuCl] <sub>2</sub>	2.47	7.08
[CH <sub>2</sub> =C(PPh <sub>2</sub> ) <sub>2</sub> AuCl] <sub>2</sub>	1.09	7.11
{Au <sub>2</sub> [Ph <sub>2</sub> PCH(CH <sub>2</sub> OCH <sub>3</sub> )PPh <sub>2</sub> ] <sub>2</sub> Cl <sup>+</sup> Cl <sup>-</sup> (3b)	4.45	8.89
	3.91	7.82

Other important reference compounds are the neutral dimeric gold(I) bis(diphenylphosphino)methanides<sup>20-23</sup> (B) and the oligomeric silver(I) and copper(I) dppm complexes, for which a large amount of structural data are available.<sup>1,24</sup> Metal-metal interactions appear to play a minor role for the lighter coinage metals, however.

### Molecular Structure of Cyclopropylidenebis(diphenylphosphine) (cdpp)

In the series methylene-, ethylidene-, 2-propylidene-, vinylidene-, (triphenylphosphoranylidene)methylene-, and cyclopropylidenebis(diphenylphosphine), the last three members are most likely to show pronounced structural differences from the first three, as an sp<sup>2</sup>-hybridized carbon or the specific cyclopropane bonding, respectively, strongly



favor 120° P-C-P bond angles, as compared to the tetrahedral angle in the remaining cases. The structure of cdpp was therefore determined in order to assess the strain-free P-P span in the free ligand, which was to be compared with the situation in binuclear cdpp bridged complexes. The structure was also of interest regarding the conformational ground state in the crystal. In Ph<sub>3</sub>P=C(MPh<sub>2</sub>)<sub>2</sub> molecules (M = P, As, Sb) and vdpp a preference for an opposite (syn/anti or E/Z) orientation of the two lone pairs of electrons with respect to the C=C bond was encountered.<sup>25-28</sup>

A sample of cdpp was prepared following the published procedure<sup>19</sup> and crystallized from ethanol. A single-crystal X-ray diffraction study (Tables II and III and Figure 1)

(20) Schmidbaur, H.; Schnatterer, S.; Dash, K. C.; Aly, A. A. M. Z. *Naturforsch., B: Anorg. Chem., Org. Chem.* **1983**, *38B*, 62. Schmidbaur, H.; Mandl, J. R.; Bassett, J. M.; Blaschke, G.; Zimmer-Gasser, B. *Chem. Ber.* **1981**, *114*, 433. Schmidbaur, H.; Mandl, J. R. *Angew. Chem.* **1977**, *89*, 679; *Angew. Chem., Int. Ed. Engl.* **1977**, *16*, 640.

(21) Briant, C. E.; Hall, K. P.; Mingos, D. M. P. *J. Organomet. Chem.* **1982**, *229*, C5.

(22) Uson, R.; Laguna, A.; Laguna, M.; Manzano, B. R.; Jones, P. G.; Sheldrick, G. M. *J. Chem. Soc., Dalton Trans.* **1984**, 839.

(23) Van der Velden, J. W. A.; Bour, J. J.; Vollenbrock, F. A.; Beurskens, P. T.; Smits, J. M. M. *J. Chem. Soc., Chem. Commun.* **1979**, 1162.

(24) (a) Ho, D. M.; Bau, R. *Inorg. Chem.* **1983**, *22*, 4073. (b) Ho, D. M.; Bau, R. *Inorg. Chem.* **1983**, *22*, 4079.

(25) Schmidbaur, H.; Deschler, U.; Milewski-Mahrla, B. *Chem. Ber.* **1983**, *116*, 1393.

(26) Schmidbaur, H.; Milewski-Mahrla, B.; Müller, G.; Krüger, C. *Organometallics* **1984**, *3*, 38.

(27) Schmidbaur, H.; Nußstein, P.; Müller, G. Z. *Naturforsch., B: Anorg. Chem. Org. Chem.* **1984**, *39B*, 1456.

(28) Schmidbaur, H.; Herr, R.; Riede, J. *Chem. Ber.* **1984**, *117*, 2322.

Table V. Fractional Atomic Coordinates and Equivalent Isotropic Thermal Parameters for Complex 7b

atom	x/a	y/b	z/c	U(eq), Å <sup>2</sup>
Au1	0.2899 (0)	0.1176 (0)	0.1394 (0)	0.019
Au2	0.2653 (0)	0.1519 (0)	0.2785 (0)	0.019
C11	0.4357 (2)	0.1499 (2)	0.3106 (1)	0.031
C12	0.8683 (2)	0.1709 (2)	0.2679 (2)	0.050
P1	0.3004 (2)	0.2480 (1)	0.1100 (1)	0.020
P2	0.2897 (2)	-0.0168 (1)	0.1565 (1)	0.019
P3	0.2547 (2)	0.0178 (1)	0.2998 (1)	0.018
P4	0.2373 (2)	0.2814 (1)	0.2385 (1)	0.018
C1	0.3118 (6)	-0.0421 (5)	0.2536 (5)	0.022
C2	0.4017 (6)	-0.0576 (6)	0.2950 (5)	0.024
C3	0.3422 (6)	-0.1223 (6)	0.2822 (5)	0.029
C4	0.3037 (6)	0.3139 (6)	0.1861 (5)	0.021
C5	0.3873 (6)	0.3429 (6)	0.2344 (5)	0.025
C6	0.3288 (6)	0.3998 (5)	0.1821 (5)	0.022
C11	0.3959 (6)	0.2598 (5)	0.0912 (5)	0.020
C12	0.4005 (6)	0.2965 (5)	0.0275 (5)	0.023
C13	0.4761 (6)	0.3009 (6)	0.0144 (5)	0.029
C14	0.5445 (6)	0.2705 (6)	0.0633 (5)	0.029
C15	0.5398 (6)	0.2316 (6)	0.1261 (5)	0.031
C16	0.4671 (6)	0.2255 (6)	0.1391 (5)	0.026
C21	0.2174 (6)	0.2800 (5)	0.0292 (5)	0.022
C22	0.1606 (6)	0.2247 (6)	-0.0049 (5)	0.033
C23	0.0932 (6)	0.2457 (6)	-0.0667 (6)	0.037
C24	0.0864 (6)	0.3227 (6)	-0.0940 (6)	0.036
C25	0.1449 (6)	0.3778 (6)	-0.0582 (6)	0.038
C26	0.2102 (6)	0.3576 (6)	0.0031 (5)	0.029
C31	0.3714 (6)	-0.0604 (6)	0.1275 (5)	0.027
C32	0.3732 (6)	-0.1418 (6)	0.1161 (5)	0.034
C33	0.4354 (6)	-0.1721 (6)	0.0923 (6)	0.043
C34	0.4917 (6)	-0.1222 (6)	0.0786 (6)	0.045
C35	0.4901 (8)	-0.0445 (6)	0.0906 (6)	0.048
C36	0.4299 (6)	-0.0119 (6)	0.1158 (6)	0.037
C41	0.1956 (6)	-0.0642 (6)	0.0997 (5)	0.031
C42	0.1467 (6)	-0.0220 (6)	0.0409 (5)	0.033
C43	0.0781 (6)	-0.0590 (6)	-0.0085 (6)	0.042
C44	0.0576 (6)	-0.1345 (6)	0.0044 (6)	0.041
C45	0.1060 (6)	-0.1754 (6)	0.0636 (6)	0.047
C46	0.1783 (6)	-0.1425 (6)	0.1122 (5)	0.032
C51	0.2968 (6)	-0.0112 (5)	0.3956 (5)	0.021
C52	0.2626 (6)	-0.0711 (6)	0.4263 (5)	0.031
C53	0.3017 (6)	-0.0914 (6)	0.4990 (6)	0.044
C54	0.3723 (6)	-0.0565 (6)	0.5409 (6)	0.037
C55	0.4052 (6)	0.0048 (6)	0.5120 (6)	0.037
C56	0.3664 (6)	0.0271 (6)	0.4391 (5)	0.025
C61	0.1502 (6)	-0.0197 (5)	0.2681 (5)	0.017
C62	0.1343 (6)	-0.0998 (6)	0.2547 (5)	0.033
C63	0.0535 (6)	-0.1253 (6)	0.2284 (6)	0.035
C64	-0.0097 (8)	-0.0738 (6)	0.2169 (6)	0.044
C65	0.0064 (6)	0.0053 (6)	0.2315 (6)	0.048
C66	0.0863 (6)	0.0325 (6)	0.2550 (5)	0.034
C71	0.1320 (6)	0.2955 (5)	0.1794 (5)	0.021
C72	0.1099 (6)	0.3540 (6)	0.1285 (5)	0.029
C73	0.0264 (6)	0.3639 (6)	0.0873 (6)	0.041
C74	-0.0310 (8)	0.3136 (6)	0.1010 (6)	0.044
C75	-0.0075 (6)	0.2567 (6)	0.1525 (6)	0.041
C76	0.0737 (6)	0.2462 (6)	0.1918 (5)	0.030
C81	0.2505 (6)	0.3549 (6)	0.3103 (5)	0.023
C82	0.2935 (6)	0.3337 (6)	0.3821 (5)	0.029
C83	0.3088 (6)	0.3889 (6)	0.4378 (5)	0.032
C84	0.2782 (6)	0.4636 (6)	0.4235 (5)	0.030
C85	0.2344 (6)	0.4856 (6)	0.3511 (6)	0.036
C86	0.2210 (6)	0.4301 (6)	0.2960 (5)	0.027
O1	-0.2366 (6)	0.1225 (5)	0.1225 (55)	0.075
O2	0.1636 (6)	0.5371 (6)	0.1411 (6)	0.089
O3	0.7022 (8)	0.1983 (8)	0.3026 (6)	0.120
CO1	-0.2421 (9)	0.1917 (8)	0.0669 (6)	0.063
CO2	0.1189 (9)	0.5616 (9)	0.0696 (6)	0.074
CO3	0.6539 (10)	0.1285 (9)	0.2889 (9)	0.085

showed the presence of individual molecules possessing no crystallographic symmetry.

The cyclopropane ring C1-C11-C12 has the shape of an isosceles triangle with the shortest bond between C11 and C12. The distances to the geminal phosphorus atoms are virtually equivalent and form an angle of 118.0 (2)°. As

**Table VI. Selected Bond Distances (Å) and Bond Angles (deg) of Complex 7b (See Figure 3 for Atomic Numbering)**

Au1-Au2	2.907 (1)	P1-Au1-P2	171.5 (1)
P1...P4	3.063 (8)	P3-Au2-P4	163.9 (1)
P2...P3	3.070 (8)	P1-C4-P4	113.0 (5)
Au1-P1	2.312 (2)	P2-C1-P3	113.3 (5)
Au1-P2	2.312 (2)	C2-C1-C3	58.2 (6)
Au2-P3	2.339 (2)	C1-C2-C3	60.1 (6)
Au2-P4	2.334 (2)	C1-C3-C2	61.6 (7)
Au2-Cl1	2.807 (3)	C5-C4-C6	59.8 (6)
P1-C4	1.834 (9)	C4-C5-C6	60.4 (6)
P4-C4	1.841 (10)	C4-C6-C5	59.9 (6)
P2-C1	1.839 (9)	C4-P1-C11	107.2 (4)
P3-C1	1.837 (9)	C4-P1-C21	108.2 (4)
C1-C2	1.52 (1)	C11-P1-C21	108.1 (4)
C1-C3	1.50 (1)	C1-P2-C31	106.7 (4)
C2-C3	1.47 (1)	C1-P2-C41	111.1 (5)
C4-C5	1.53 (1)	C31-P2-C41	105.2 (5)
C4-C6	1.53 (1)	C1-P3-C51	103.8 (4)
C5-C6	1.53 (1)	C1-P3-C61	105.8 (4)
P1-C11	1.810 (10)	C51-P3-C61	105.9 (4)
P1-C21	1.830 (9)	C4-P4-C71	106.9 (4)
P2-C31	1.835 (10)	C4-P4-C81	105.2 (4)
P2-C41	1.831 (10)	C71-P4-C81	103.8 (4)
P3-C51	1.822 (9)	C4-P1-Au1	112.2 (3)
P3-C61	1.826 (9)	C4-P4-Au2	111.4 (3)
P4-C71	1.826 (9)	C1-P2-Au1	111.6 (3)
P4-C81	1.826 (9)	C1-P3-Au2	111.8 (3)
		Au1-Au2-Cl1	75.4 (1)

a more detailed description of the cdpp structure will be given in a forthcoming paper, only those structural aspects pertinent to the complexation chemistry are discussed here.

Both phosphorus atoms have a similar pyramidal configuration in cdpp. Positions E were calculated to indicate the directions of the lone pairs of electrons defined as missing vertices of coordination tetrahedra around P1 and P2 (Table III). The phosphino groups are rotated about the P1-C1 or P2-C1 bond, respectively, into positions which can be described as quasi cis and trans (*Z* or *E*) relative to the cyclopropane plane. This rotation is best illustrated by the dihedral angles E1-P1-C1-P2 = 173.3° and E2-P2-C1-P1 = 21.8°. The molecular ground state in the crystal is therefore not the conformation predestined for chelation or metal bridging, and the P1...P2 distance (formally the ligand "bite") of 3.167 (3) Å is not a meaningful value. Since the angle P1-C1-P2 is likely to change as Ph<sub>2</sub>P1 is rotated into the "chelate position", a reduction of the P1...P2 distance is also to be expected.

### Gold(I) Complexes of cdpp

The reaction of the ligand with 2 equiv of carbonylchlorogold(I) in toluene affords a colorless precipitate of the expected 1:2 complex 4 in almost quantitative yield. CO is evolved in the process. The compound is air-stable and melts with decomposition at 270 °C. It is easily characterized by its <sup>1</sup>H, <sup>13</sup>C, and <sup>31</sup>P NMR spectra, which indicate the equivalence of the two CH<sub>2</sub> and the two Ph<sub>2</sub>PAuCl groups in solution.

Exchange of iodide for chloride yields an air-stable diiodide 5. The chloride ligands can also be substituted by methyl groups in the reaction with methylolithium in tetrahydrofuran. The product 6 is appreciably more soluble in organic solvents than the chloride precursor. The analytical and spectroscopic data are summarized in the Experimental Section.

The addition of the second equivalent of cdpp to 4 or the reaction of equimolar quantities of cdpp and (CO)AuCl give the 1:1 complex 7 in quantitative yield. The material has a light yellow-green color in the solid and in organic solvents (CHCl<sub>3</sub>, CH<sub>2</sub>Cl<sub>2</sub>, CH<sub>3</sub>OH). Its solution NMR

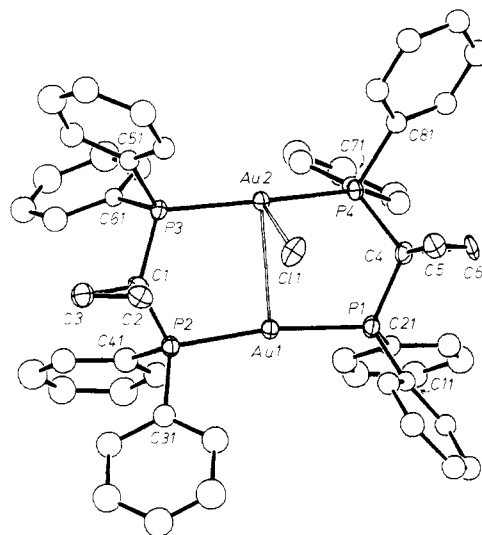
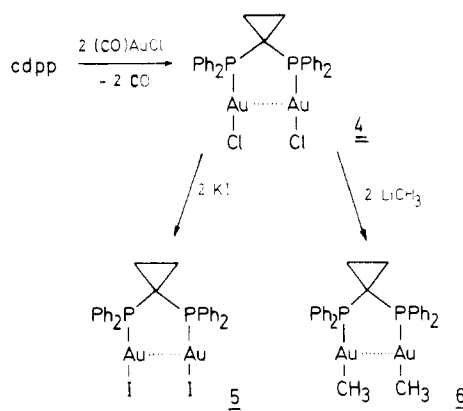


**Figure 3.** Molecular structure of the [Au<sub>2</sub>(Ph<sub>2</sub>PC(CH<sub>2</sub>)<sub>2</sub>PPh<sub>2</sub>)<sub>2</sub>Cl]<sup>+</sup> cation in complex 7b. Hydrogen atoms are omitted (ORTEP, thermal ellipsoids 50%, root-mean-square deviation used as radius for isotropic phenyl carbon atoms).



spectra are in agreement with the symmetrical formula 7a in that full equivalence of PPh<sub>2</sub> and CH<sub>2</sub> groups is suggested (virtual symmetry *D*<sub>2h</sub>).

According to molecular mass and conductivity data, 7 is partially dissociated in solution, but this dynamic dissociation equilibrium apparently renders the structural units NMR equivalent (7a-c). In contrast to these findings, the <sup>197</sup>Au Mössbauer spectrum of solid 7 at 4 K clearly indicated two nonequivalent isomeric gold centers in the molecule with grossly different isomeric shifts and quadrupole splittings (Figure 2 and Table IV). In order to clarify this inconsistency an X-ray structure analysis was carried out.

### Crystal and Molecular Structure of the Gold Complex 7b

Crystals of the complex could be grown from ether/methanol, which represented a trimethanol solvate, (cdppAuCl)<sub>2</sub>·3CH<sub>3</sub>OH. The structure determination (Tables V and VI and Figures 3 and 4) revealed the presence of the unsymmetrical structure 7b in which only one chlorine ligand is attached to one of the gold atoms, whereas the second halogen exists as a discrete chloride anion in the crystal (Figure 3).

The eight-membered ring is in a boat conformation. While one of the P-Au-P axes is roughly linear (P1-Au1-P2 = 171.5 (1)°), the second one is more strongly bent (P3-Au2-P4 = 163.9 (1)°). It is this Au atom whose coordination sphere is completed by the undissociated Cl atom lying above the eight-membered ring (Figure 4).

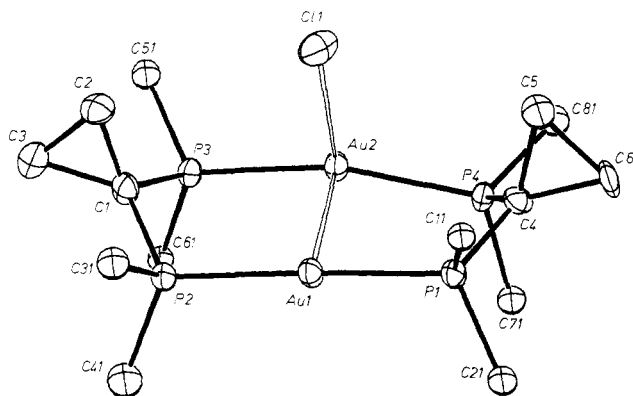
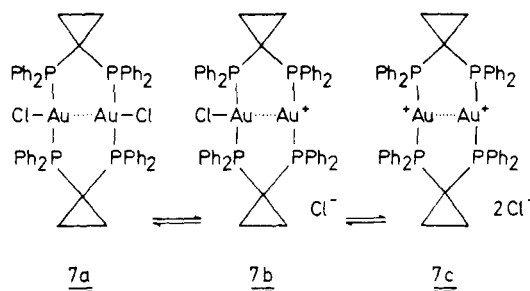
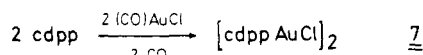


**Figure 4.** The central core of the cation in complex **7b** showing the orientation of the cyclopropyl rings and the coordination of the chlorine atom. Hydrogen atoms and phenyl carbon atoms (except C-*ipso*) are omitted for clarity (ORTEP, thermal ellipsoids 50%).



Judged from the Au2–Cl1 distance of 2.807 (3) Å, the gold chlorine coordination must appear rather weak. (In **1**, **2**, and **3** the Au–Cl distances are 2.771 (4),<sup>3</sup> 2.723 (2),<sup>18</sup> and 2.963 (4) Å (see below), respectively, but 2.288 (1) Å in CH<sub>2</sub>(PPh<sub>2</sub>AuCl)<sub>2</sub>.<sup>2</sup>) Nevertheless the Au–Cl interaction is strong enough to lead to a quasi-trigonal-planar coordination of Au2 as compared to the more linear coordination of Au1 in the same molecule. It is similar, however, to the T-shaped geometries of **1** and **2**. The Au–P bonds are also affected by the chlorine coordination. With bond lengths Au2–P3 = 2.339 (2) Å and Au2–P4 = 2.334 (2) Å they are some 0.02 Å longer than their Au1 counterparts (2.312 (2) Å). The interaction is also strong enough to give significant differences in the Mössbauer parameters (above). Thus it cannot really be considered a negligible secondary type of bonding. The orientation of the Au–Cl bond toward the side of the ring accommodating the cyclopropylidene groups is most probably due to steric factors. The opposite side appears to be more crowded by the four “axial” phenyl groups. It should be mentioned at this point already that—while this Au–Cl positioning is common to **1**, **2**, and **7b**—a completely different orientation is found for crystalline **3** (**3b** below), where a single chlorine ligand is attached to one of the gold atoms on a projection of the Au–Au axis. In **7b** the Au2–Cl1 vector forms an angle of only 75.4 (1)° with the line connecting the two gold atoms. The chlorine is thus shifted slightly toward Au1, away from the position at a right angle above Au2. A symmetrically bridging position (equidistant from Au1 and Au2) is not reached, however.

The Au–Au distance in **7b** is 2.907 (1) Å long, as compared to the distances of 2.962 (1) and 2.977 (1) Å already mentioned for **1** and **2**, respectively. The P...P distances are 3.063 (8) and 3.070 (8) Å, some 0.1 Å shorter than the

**Table VII.** Fractional Atomic Coordinates and Equivalent Isotropic Thermal Parameters for Complex **3b**

atom	<i>x/a</i>	<i>y/b</i>	<i>z/c</i>	<i>U</i> (eq), Å <sup>2</sup>
Au1	-0.3963 (0)	-0.0251 (0)	-0.8885 (0)	0.017
Au2	-0.1330 (0)	-0.0190 (0)	-0.8862 (0)	0.017
Cl3	-0.6550 (3)	-0.0356 (2)	-0.8982 (2)	0.037
Cl4	-0.2457 (3)	-0.1559 (1)	-0.6241 (1)	0.028
P5	-0.3995 (3)	0.0294 (2)	-0.9757 (1)	0.018
P6	-0.3914 (3)	-0.0687 (2)	-0.7953 (1)	0.020
P7	-0.1416 (3)	0.0579 (1)	-0.9526 (1)	0.016
P8	-0.1342 (3)	-0.0943 (1)	-0.8177 (1)	0.018
O12	-0.2040 (9)	-0.0571 (4)	-1.0215 (4)	0.023
O16	-0.1882 (9)	0.0225 (4)	-0.7542 (4)	0.025
C10	-0.2523 (12)	0.0461 (6)	-1.0100 (5)	0.016
C11	-0.2170 (12)	-0.0031 (6)	-1.0534 (6)	0.018
C13	-0.1869 (19)	-0.1055 (6)	-1.0626 (8)	0.024
C14	-0.2430 (11)	-0.0799 (6)	-0.7602 (5)	0.014
C15	-0.2076 (12)	-0.0283 (6)	-0.7201 (6)	0.024
C17	-0.1671 (19)	0.0755 (6)	-0.7170 (8)	0.034
O101	-0.1638 (9)	-0.2776 (5)	-0.6697 (5)	0.040
C102	-0.0749 (17)	-0.2915 (9)	-0.6280 (8)	0.067
O201	-0.1853 (12)	-0.3750 (6)	-0.7421 (6)	0.072
C202	-0.1708 (18)	-0.4279 (8)	-0.7081 (9)	0.065
O301	-0.2871 (15)	-0.3638 (8)	-0.0412 (6)	0.099
C302	-0.3773 (2)	-0.3953 (12)	-0.0102 (11)	0.105
O401	-0.3241 (17)	-0.2510 (8)	-0.0733 (8)	0.029
C402	-0.3714 (41)	-0.2425 (20)	-0.1309 (12)	0.084
O501	-0.3236 (24)	-0.1949 (12)	-0.1609 (13)	0.075
C502	-0.4030 (34)	-0.2240 (18)	-0.2000 (17)	0.073
C21	-0.5163 (13)	-0.0386 (6)	-0.6904 (6)	0.032
C22	-0.5736 (13)	-0.0008 (6)	-0.6550 (8)	0.037
C23	-0.5870 (13)	0.0569 (6)	-0.6699 (6)	0.039
C24	-0.5392 (15)	0.0768 (8)	-0.7232 (8)	0.044
C25	-0.4816 (13)	0.0378 (8)	-0.7598 (8)	0.039
C26	-0.4712 (10)	-0.0207 (6)	-0.7446 (6)	0.018
C31	-0.4568 (13)	0.1499 (6)	-1.0008 (6)	0.027
C32	-0.5151 (13)	0.2011 (8)	-0.9897 (8)	0.040
C33	-0.5859 (13)	0.2074 (6)	-0.9400 (6)	0.034
C34	-0.5992 (13)	0.1593 (6)	-0.9015 (6)	0.032
C35	-0.5417 (12)	0.1060 (6)	-0.9133 (6)	0.021
C36	-0.4709 (12)	0.1008 (6)	-0.9642 (6)	0.019
C41	0.1052 (12)	-0.0879 (6)	-0.8018 (6)	0.020
C42	0.2118 (13)	-0.0988 (6)	-0.7735 (6)	0.033
C43	0.2123 (13)	-0.1283 (6)	-0.7203 (6)	0.036
C44	0.1075 (13)	-0.1492 (6)	-0.6957 (6)	0.034
C45	0.0023 (13)	-0.1375 (6)	-0.7236 (6)	0.031
C46	0.0005 (12)	-0.1089 (6)	-0.7780 (6)	0.025
C51	-0.0045 (13)	0.1134 (6)	-1.0400 (6)	0.030
C52	0.1022 (13)	0.1283 (6)	-1.0650 (6)	0.031
C53	0.2049 (13)	0.1061 (6)	-1.0421 (6)	0.032
C54	0.2029 (12)	0.0686 (6)	-0.9953 (6)	0.028
C55	0.0975 (12)	0.0531 (6)	-0.9692 (6)	0.022
C56	-0.0075 (11)	0.0760 (6)	-0.9907 (6)	0.021
C61	-0.5170 (12)	-0.1622 (6)	-0.8437 (6)	0.030
C62	-0.5664 (13)	-0.2177 (6)	-0.8447 (6)	0.036
C63	-0.5577 (15)	-0.2537 (6)	-0.7950 (6)	0.043
C64	-0.4962 (15)	-0.2359 (8)	-0.7458 (8)	0.039
C65	-0.4493 (13)	-0.1798 (6)	-0.7434 (6)	0.027
C66	-0.4569 (12)	-0.1416 (6)	-0.7939 (6)	0.020
C71	-0.4997 (13)	-0.0654 (8)	-1.0301 (8)	0.037
C72	-0.5600 (17)	-0.0964 (8)	-1.0754 (8)	0.052
C73	-0.6010 (15)	-0.0661 (6)	-1.1242 (6)	0.047
C74	-0.5841 (16)	-0.0039 (6)	-1.1266 (6)	0.046
C75	-0.5229 (12)	0.0247 (6)	-1.0825 (6)	0.031
C76	-0.4810 (12)	-0.0059 (6)	-1.0352 (6)	0.021
C81	-0.2128 (15)	-0.1640 (6)	-0.9092 (6)	0.041
C82	-0.2526 (18)	-0.2179 (8)	-0.9358 (8)	0.055
C83	-0.2614 (16)	-0.2681 (6)	-0.9022 (6)	0.048
C84	-0.2302 (13)	-0.2668 (6)	-0.8430 (6)	0.038
C85	-0.1927 (13)	-0.2174 (6)	-0.8167 (6)	0.033
C86	-0.1811 (12)	-0.1633 (6)	-0.8503 (6)	0.024
C91	-0.2278 (13)	0.1233 (6)	-0.8586 (6)	0.027
C92	-0.2698 (15)	0.1722 (6)	-0.8319 (6)	0.042
C93	-0.2791 (13)	0.2271 (6)	-0.8613 (6)	0.035
C94	-0.2419 (15)	0.2286 (6)	-0.9201 (6)	0.033
C95	-0.1992 (13)	0.1784 (6)	-0.9487 (6)	0.034
C96	-0.1900 (12)	0.1255 (6)	-0.9170 (6)	0.018

value P1...P2 = 3.167 (3) Å in the free ligand cdpp, but in the latter this distance refers to a different conformation

**Table VIII. Selected Bond Distances (Å) and Angles (deg) for Complex 3b (See Figure 5 for Atomic Numbering)**

Bond Distances			
Au1-Au2	3.002 (1)	Au1-Cl3	2.963 (4)
Au1-P5	2.333 (3)	Au2-P7	2.301 (3)
Au1-P6	2.337 (3)	Au2-P8	2.305 (3)
P5-C10	1.887 (14)	P7-C10	1.833 (13)
P5-C36	1.824 (13)	P7-C56	1.803 (14)
P5-C76	1.824 (14)	P7-C96	1.811 (13)
P6-C14	1.885 (13)	P8-C14	1.830 (13)
P6-C26	1.823 (14)	P8-C46	1.810 (15)
P6-C66	1.807 (13)	P8-C86	1.806 (14)
C10-C11	1.537 (17)	C14-C15	1.532 (19)
C11-O12	1.426 (15)	C15-O16	1.402 (17)
O12-C13	1.450 (16)	O16-C17	1.483 (17)

Bond Angles			
Au2-Au1-Cl3	176.2 (1)	Au1-Au2-P7	88.9 (1)
Au2-Au1-P5	90.3 (1)	Au1-Au2-P8	88.4 (1)
Au2-Au1-P6	88.8 (1)	P7-Au2-P8	176.9 (1)
Cl3-Au1-P5	87.9 (1)	P5-Au1-P6	173.0 (1)
Cl3-Au1-P6	93.3 (1)		
Au1-P5-C10	116.2 (4)	Au2-P7-C10	112.7 (4)
Au1-P5-C36	110.6 (5)	Au2-P7-C56	116.8 (5)
Au1-P5-C76	114.1 (5)	Au2-P7-C96	110.8 (4)
C10-P5-C36	106.2 (6)	C10-P7-C56	105.9 (6)
C10-P5-C76	103.4 (6)	C10-P7-C96	103.4 (6)
C36-P5-C76	105.4 (6)	C56-P7-C96	106.3 (6)
Au1-P6-C14	117.5 (4)	Au2-P8-C14	110.8 (4)
Au1-P6-C26	108.2 (5)	Au2-P8-C46	117.8 (5)
Au1-P6-C66	112.8 (5)	Au2-P8-C86	111.1 (5)
C14-P6-C66	103.9 (6)	C14-P8-C86	104.3 (6)
C26-P6-C66	108.9 (6)	C46-P8-C86	107.3 (7)
P5-C10-P7	110.2 (6)	P6-C14-P8	109.2 (6)
P5-C10-C11	110.7 (9)	P6-C14-C15	112.7 (9)
P7-C10-C11	112.5 (9)	P8-C14-C15	112.5 (9)
C10-C11-O12	108.5 (10)	C14-C15-O16	109.5 (10)
C11-O12-C13	109.3 (1)	C15-O16-C17	111.7 (11)

(above). The cyclopropane moieties are again nearly isosceles triangles with dimensions similar to those in the free cdpp ligand. All P-C distances and C-P-C angles are remarkably close to standard literature values. Even the C-P-Au angles show surprisingly little variation ( $111.8 \pm 0.5^\circ$ ). The NMR spectra of solutions of **7** in chloroform show equivalent phosphorus atoms and equivalent phenyl groups. Due to a reversible chlorine dissociation ( $7a \rightleftharpoons 7b \rightleftharpoons 7c$ ), rapid on the NMR time scale, quasi- $D_{2h}$  symmetry is reached. A rapid chair/boat interconversion must be part of this equilibration process, as proven by the single  $^{13}\text{C}$  signal of the  $\text{CH}_2$  groups (Experimental Section).

### Crystal and Molecular Structure and the $^{197}\text{Au}$ Mössbauer Spectrum of the Gold Complex **3b**

The vdpp complex **2**, whose crystal structure has been determined, undergoes an addition reaction in methanol at room temperature.<sup>18</sup> Colorless crystals obtained from this solvent were shown to represent a tetramethanol solvate of the partially dissociated species **3b** by X-ray structure analysis. Like in the **7b** case, only one chlorine atom is attached to the heterocycle in the crystal whereas the second one is positioned in the lattice without any contact to the cation formed in the dissociation (Tables VII and VIII and Figures 5 and 6).

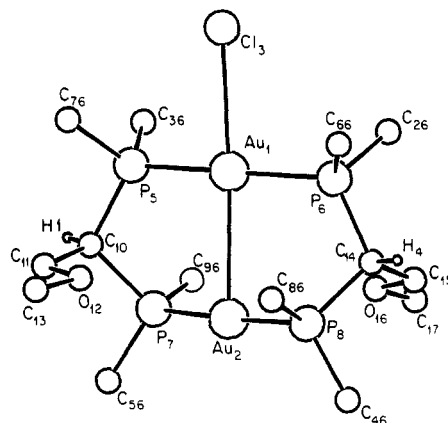
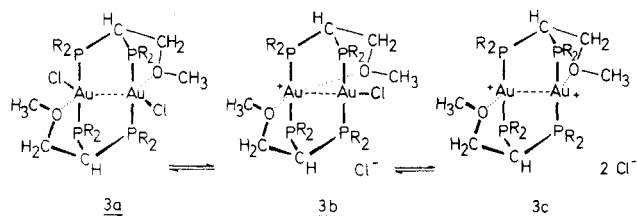


**Figure 5.** A molecular plot of the  $\text{Au}_2[\text{Ph}_2\text{PCH}(\text{CH}_2\text{OCH}_3)_2\text{PPh}_2]_2\text{Cl}^+$  core of the cation in complex **3b**, viewed approximately normal to the  $\text{Au}_2\text{P}_4\text{Cl}$  plane. (ORTEP, arbitrary radii).

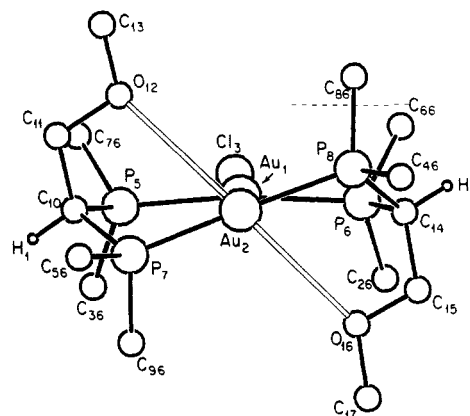


**Figure 6.** An alternative view of the central core of the complex cation in compounds **3b**, showing the weak coordination of the two ether-type oxygen atoms to the gold atom Au2. In this and the previous plot (Figure 5), all carbon atoms except the ipso carbons of the phenyl rings have been omitted for clarity (ORTEP, arbitrary radii).

Contrary to the situation in **7b**, the metallacycle is in a chair configuration, very similar to that in **1** or in the precursor **2**. The only unusual feature in the structure of **3b** is therefore the coordination mode of the chloride ion, which appears on the Au2-Au1 axis. Thus the overall molecular symmetry comes close to  $C_2$  with the (non-crystallographic) twofold axis passing through Cl3, Au1, and Au2. Even the relative conformation of the phenyl rings is in accord with this description. Because of its inherent dissymmetry the cation in **3b** exists in two conformations in the solid state which are optical antipodes. Due to the noncentrosymmetric space group only one conformation is present in a single crystal. The square-planar ligand array around Au1 (Cl3, P5, P6, Au2) is unprecedented for gold in its oxidation state +I. The Au1-Cl3 distance of 2.963 (3) Å is extremely long, however, and suggests very weak interactions. The P5-Au1-P6 angle is not distorted by the proximity of Cl and is obviously balanced by the transannular interaction of the gold atoms at Au1-Au2 = 3.002 (1) Å (Figure 5).

On close inspection of the model, an explanation can be offered for the dissociation of the chloride ion from Au2: As clearly shown in a projection roughly down the Au2-Au1-Cl3 axis (Figure 6), the two methoxy groups (which are located on different sides of the metallacycle, i.e., in trans positions) are folded back toward Au2 and are able to complement the coordination sphere of this gold atom. The distances of Au2-O16 = 3.209 (6) and Au2-O12 =

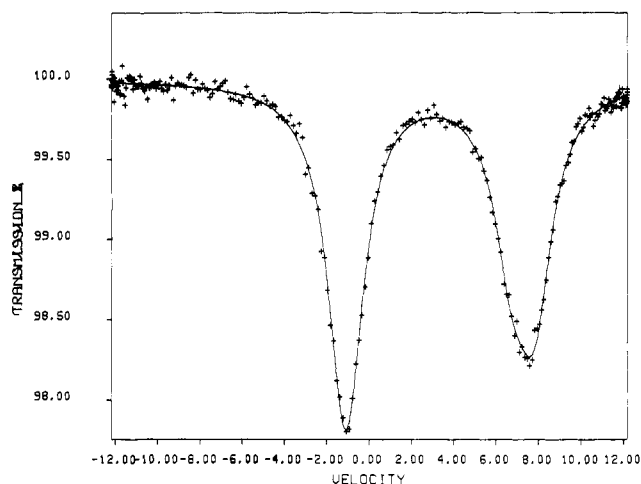


Figure 7.  $^{197}\text{Au}$  Mössbauer spectrum of complex **3b** (at 4 K).

3.294 (6) Å are, of course, exceedingly long, but there can be no doubt that both alkoxy chain ends are oriented toward the same gold atom (Au2), while Au1 is associated with Cl3. To allow such an interaction to optimize, the P7–Au2–P8 axis is clearly rotated against the P5–Au2–P6 axis (Figure 6). No such rotation is noticed in **1**, **2**, or **7b**.

If the Au1–Au2 contact is included, the array of ligands around Au2 is a very distorted tetragonal pyramid. Considering the exceedingly long distance, however, such a description may not be very meaningful. Interestingly enough, the Au–P distances around the “methoxy-supported” gold atom Au2 are still significantly shorter than those of the chlorine-coordinated Au1 atom as was also found in **7b**. There is clearly no straightforward explanation for these unusual structural data, and it was hoped that other techniques could contribute to the open discussion of the phenomena.

Unexpectedly, the  $^{197}\text{Au}$  Mössbauer spectrum proved not very decisive (Figure 7). Isomeric shifts and quadrupole splittings are very close and barely resolved (Table IV). A compensation of counteracting effects is probably responsible for this coincidence of numerical data. On the basis of the Mössbauer spectrum alone, a more symmetrical structure might have been predicted for **3b**, while for **7b** gross structural dissymmetry could be expected already from its spectral features. The spectra of the two symmetrical reference compounds  $\text{vdpp}(\text{AuCl})_2$  and  $[\text{vdppAuCl}]_2$  show only one Mössbauer doublet (Table IV).

As for **7b**, NMR data of solutions of **3b** in chloroform/methanol indicate a more symmetrical structure with equivalent phosphorus atoms, resulting from complete or reversible partial chloride dissociation following the scheme  $3\mathbf{a} = 3\mathbf{b} = 3\mathbf{c}$ .<sup>18</sup>

In summary, the structures of **3b** and **7b** are probably good examples for surprisingly large structural effects originating from very subtle changes in ligand geometry and functionality. Gold(I) seems to be particularly sensitive to these second-order interactions since ligands in excess of the coordination number 2 are only weakly bonded, but structurally quite effective.

### Experimental Section

The experiments were carried out under dry, purified nitrogen. Solvents and glassware were dried and saturated or filled with nitrogen, respectively.

**Vinylidenebis(diphenylphosphine) (vdpp) and cyclopropylidenebis(diphenylphosphine) (cdpp)** were prepared according to literature methods.<sup>19,28</sup>

**Cyclopropylidenebis[(diphenylphosphino)chlorogold(I)] (4)**. A mixture of 1.61 g of carbonylchlorogold(I) (6.18 mmol) and

1.27 g of cdpp (3.09 mmol) in 35 mL of anhydrous toluene was stirred for 90 min at 20 °C. The precipitate was filtered, washed with toluene and pentane, and dried in vacuo to yield 2.66 g (98%); mp 270 °C with decomposition; colorless microcrystalline solid; soluble in  $\text{CH}_2\text{Cl}_2$ ;  $^1\text{H}$  NMR ( $\text{CD}_2\text{Cl}_2$ )  $\delta$  1.1 (t,  $\text{A}_2\text{A}_2'\text{XX}'$ ,  $N = 19.4$  Hz, 4 H,  $\text{CH}_2$ ), 7.1–7.9 (m, 20 H,  $\text{C}_6\text{H}_5$ );  $^{13}\text{C}$  NMR ( $\text{CD}_2\text{Cl}_2$ )  $\delta$  10.7 (t,  $^1J(\text{PC}) = 39.1$  Hz,  $\text{CP}_2$ ), 13.3 (br s,  $\text{CH}_2$ ), 126.4, 129.5, and 134.8 (t,  $\text{AA}'\text{X}$  each with  $N = 64.4$ , 12.7, and 13.7 Hz, respectively, C1–C3), 132.9 (s, C4);  $^{31}\text{P}$  NMR ( $\text{CD}_2\text{Cl}_2$ )  $\delta$  39.9 (s); IR (KBr) 340  $\text{cm}^{-1}$  [ $\nu(\text{AuCl})$ ]. Anal. Calcd for  $\text{C}_{27}\text{H}_{24}\text{Au}_2\text{Cl}_2\text{P}_2$  (875.27): C, 37.05; H, 2.76. Found: C, 38.07; H, 2.86.

**Cyclopropylidenebis[(diphenylphosphino)iodogold(I)] (5)**. A solution of 0.17 g (0.194 mmol) of **4** was treated with 0.6 g of potassium iodide (3.6 mmol, excess) in 100 mL of acetone at reflux. After 150 min the KCl precipitate was filtered. The solvent was evaporated from the filtrate, and the residue was washed with water, dissolved in  $\text{CH}_2\text{Cl}_2$ , and precipitated by addition of pentane. The product can be crystallized from acetone: mp 259 °C with decomposition; 0.16 g (78%) yield;  $^1\text{H}$  NMR ( $\text{CD}_2\text{Cl}_2$ )  $\delta$  1.2 (t,  $\text{A}_2\text{A}_2'\text{XX}'$ ,  $N = 19.6$  Hz, 4 H,  $\text{CH}_2$ ), 7.2–7.9 (m, 20 H,  $\text{C}_6\text{H}_5$ );  $^{31}\text{P}$  NMR ( $\text{CD}_2\text{Cl}_2$ )  $\delta$  42.9 (s). Anal. Calcd for  $\text{C}_{27}\text{H}_{24}\text{Au}_2\text{I}_2\text{P}_2$  (1058.18): C, 30.65; H, 2.29; Au, 37.23. Found: C, 30.69; H, 2.50; Au, 36.70.

**Cyclopropylidenebis[(diphenylphosphino)methylgold(I)] (6)**. **4** (2.56 g, 2.92 mmol) was suspended in 40 mL of tetrahydrofuran and treated at –60 °C with 5.9 mmol of methyllithium (in ether). The reaction mixture was allowed to warm to room temperature. The resulting clear solution was hydrolyzed, the product was extracted with ether and crystallized from benzene/hexane (2:1): mp 203 °C with decomposition; 1.75 g (72%) yield;  $^1\text{H}$  NMR ( $\text{CDCl}_3$ )  $\delta$  0.34 (t,  $\text{A}_3\text{A}_3'\text{XX}'$ ,  $N = 7.8$  Hz, 6 H,  $\text{CH}_3$ ), 1.22 (t,  $\text{A}_2\text{A}_2'\text{XX}'$ ,  $N = 18.0$  Hz, 4 H,  $\text{CH}_2$ ), 7.3–8.0 (m, 20 H,  $\text{C}_6\text{H}_5$ );  $^{13}\text{C}$  NMR ( $\text{CDCl}_3$ )  $\delta$  5.7 ( $\text{AA}'\text{X}$ ,  $N = 95.7$  Hz,  $\text{CH}_3$ ), 11.7 (t,  $^1J(\text{PC}) = 21.5$  Hz,  $\text{CP}_2$ ), 12.7 (s,  $\text{CH}_2$ ), 128.6, 130.1, 134.6 ( $\text{AA}'\text{X}$  each with  $N = 10.7$ , 48.8, and 14.7 Hz, respectively, C1–C3), 131.1 (s, C4);  $^{31}\text{P}$  NMR ( $\text{CDCl}_3$ )  $\delta$  54.3 (s). Anal. Calcd for  $\text{C}_{29}\text{H}_{30}\text{Au}_2\text{P}_2$  (834.44): C, 41.74; H, 3.62; Au, 47.21. Found: C, 41.47; H, 3.61; Au, 48.30.

**$\mu, \mu'$ -Bis[cyclopropylidenebis(diphenylphosphino)-P,P']-dichlorogold(I) (7)**. A suspension of 2.12 g of  $(\text{CO})\text{AuCl}$  (8.14 mmol) in 20 mL of tetrahydrofuran was treated with 3.35 g of cdpp (8.16 mmol, dissolved in 20 mL of THF) for 3 h at reflux. A precipitate was formed, which was crystallized from a 1:1:1 mixture of methanol, ether, and hexane. A yellow-green product was obtained in 74% yield (3.85 g): mp 150–155 °C;  $^1\text{H}$  NMR ( $\text{CDCl}_3$ )  $\delta$  1.42–1.90 (m, 4 H,  $\text{CH}_2$ ), 7.2–8.3 (m, 20 H,  $\text{C}_6\text{H}_5$ );  $^{13}\text{C}$  NMR ( $\text{CDCl}_3$ )  $\delta$  11.5 (s,  $\text{CH}_2$ ), 14.8 (m,  $\text{CP}_2$ ),  $\delta$  125.2 (m, C1), 128.8, 132.4, and 135.1 (s, C2–C4). Anal. Calcd for  $\text{C}_{54}\text{H}_{48}\text{Au}_2\text{Cl}_2\text{P}_4$  (1285.7): C, 50.45; H, 3.76; Au, 30.64. Found: C, 49.41; H, 3.76; Au, 30.10.

**X-ray Structure Analyses of  $\text{Ph}_2\text{PC}(\text{CH}_2)_2\text{PPh}_2$ , cdpp,  $(\text{Au}_2[\text{Ph}_2\text{PC}(\text{CH}_2)_2\text{PPh}_2]_2\text{Cl})^+\text{Cl}^-$  (**7b**), and  $(\text{Au}_2[\text{Ph}_2\text{PCH}(\text{CH}_2\text{OCH}_3)\text{PPh}_2]_2\text{Cl})^+\text{Cl}^-$  (**3b**)**. Suitable single crystals of the compounds were sealed into glass capillaries at dry ice temperature under an atmosphere of argon. After centering on an automatic four-circle diffractometer (Syntex P2<sub>1</sub>), preliminary measurements indicated the respective crystal systems listed in Table I which were confirmed by axial photographs and reductions of the unit cell (TRACER<sup>29</sup>). Exact cell constants were calculated by a least-squares fit of the parameters of the orientation matrix to the setting angles of 15 high order reflections from various parts of reciprocal space centered on the diffractometer. A summary of the crystal data as well as numerical data of the intensity data collection and structure refinement for all three compounds are given in Table I. Intensity data were collected by a variable speed moving crystal-stationary counter technique where the peak height at the calculated peak position served to determine the final scan speed. The time spent to measure the background at each end of the scan interval was half that taken to measure the peak ( $I = k(S - B/\beta)$ ,  $\sigma(I) = k[S + B/\beta^2]^{1/2}$ , where  $S$  is the total scan counts,  $B$  the total background counts,  $\beta$  the time ratio of total background to scan, and  $k$  a constant which depends on the scanning speed).

For **7b** and **3b** semiempirical absorption corrections were carried

(29) Lawton, S. L.; Jacobson, R. A. TRACER, A General Fortran Lattice Transformation - Cell Reduction Program, Iowa State University, 1965.

out by recording scans at intervals of  $10^\circ$  around the diffraction vectors of eight reflections near  $\chi = 90^\circ$ , which served to evaluate the transmission curves (Syntex XTL). After  $Lp$  corrections ( $F_o = (I/Lp)^{1/2}$ ,  $\sigma(F_o) = \sigma(I)/(2F_o Lp)$ ), removal of systematically extinct reflections, and merging of equivalent data, structure factors with  $F_o \leq 4.0\sigma(F_o)$  were deemed statistically insignificant and not used for all further calculations.

**Structure Solution and Refinement.** **cdpp.** The structure was solved by direct methods (MULTAN 80<sup>30</sup>) which yielded the core of the molecule as well as parts of the phenyl rings. After completion of the structure by difference Fourier syntheses all non-hydrogen atoms were refined to convergence first with isotropic and then with anisotropic thermal parameters. At this stage all the H atom positions were revealed in a difference map. In subsequent cycles they were kept constant ( $U_{iso} = 0.05 \text{ \AA}^2$ ). At convergence the residual electron density maps were essentially featureless with the maxima near the P atoms. The function minimized was  $\sum w(|F_o| - |F_c|)^2$  with  $w = k/\sigma^2(F_o)$  (SHELX-76<sup>31</sup>). Scattering factors for neutral spherical atoms were taken from Cromer and Waber.<sup>32</sup> Those for hydrogen were based on a bonded spherical atom model as given by Stewart, Davidson, and Simpson.<sup>33</sup> Corrections for  $\Delta f'$  and  $\Delta f''$  were applied to all atoms.<sup>34</sup> Table II contains the final coordinates of the non-hydrogen atoms with equivalent isotropic temperature factors. Table III summarizes important bond lengths and angles. Figure 1 gives a view of the molecule (ORTEP<sup>35</sup>).

**7b.** The structure was solved by analysis of a Patterson synthesis and completed by Fourier methods. After refinement of the non-hydrogen atoms (phenyl C atoms with isotropic temperature factors and all others with anisotropic), the positions of the solvate methanol molecules were taken from a difference map. Although the majority of hydrogens could be identified at this stage, they showed major deviations from their expected positions. Therefore they were introduced at idealized geometrical positions (XANADU<sup>36</sup>). In subsequent refinement cycles they were treated together with the carbon atoms they are bonded to as a

riding model with fixed C-H distance (1.08 Å) and  $U_{iso} = 0.05 \text{ \AA}^2$ . The phenyl C atoms again were treated isotropically as were the methanol atoms. The latter were constrained to a standard distance of  $1.428 \pm 0.01 \text{ \AA}$ , and their H atoms were not included. All other atoms were allowed anisotropic thermal motion. A final difference map had maxima near the solvate molecules as well as near the Au and Cl1 centers. Table V lists the fractional coordinates and equivalent isotropic temperature factors, and Table VI contains important structure parameters. Figures 3 and 4 depict the molecular structure of the cation.

**3b.** The positions of the two gold atoms were located by using direct methods (MULTAN 80<sup>30</sup>), and the rest of the structure gradually built up via a series of structure factor calculation/difference Fourier cycles: first the phosphorus and chlorine atoms, then the phenyl rings and the CH-CH<sub>2</sub>-O-CH<sub>3</sub> side chains, and finally the methanol molecules of crystallization. The Au, Cl, P, and C-C-O-C side chain atoms were refined anisotropically, while all other atoms (phenyl carbons and methanol C's and O's) were assigned isotropic thermal parameters. Calculated H atom positions were included (but not refined) for all C atoms except those of the methyl groups. The C-O distances of the CH<sub>3</sub>OH molecules of crystallization were constrained at a standard value ( $1.428 \pm 0.01 \text{ \AA}$ ). The fourth CH<sub>3</sub>OH solvent molecule presented some minor difficulties due to disorder and had to be refined as two half methanols with 50% occupancy.

Because space group  $P2_12_12_1$  is noncentrosymmetric, both sets of enantiomeric coordinates were refined, with one set giving a substantially better fit (an  $R$  factor improvement of about 2%). Exhaustive least-squares refinement of the structure yielded final agreement factors of  $R = 3.8\%$  and  $R_w = 3.4\%$  for 4548 reflections. For the last cycle of refinement, the maximum shift/esd ratio was about 1%. Final atomic coordinates are presented in Table VII, and selected distances and angles are given in Table VIII. Figures 5 and 6 show views of the molecular geometry of the cation.

**Acknowledgment.** We acknowledge support from Deutsche Forschungsgemeinschaft, Bonn-Bad Godesberg, and Fonds der Chemischen Industrie, Frankfurt am Main. Degussa AG is thanked for a generous loan of chemicals. R.B. thanks the Humboldt Foundation for a Senior U.S. Scientist Award.

**Registry No.** **3b**·4MeOH, 99665-61-9; **4**, 99665-62-0; **5**, 99665-63-1; **6**, 99665-64-2; **7b**, 99665-65-3; (CO)AuCl, 50960-82-2; cdpp, 96921-88-9; Au, 7440-57-5.

**Supplementary Material Available:** Tables of additional crystal structure data, anisotropic temperature factors, H atom coordinates, and observed and calculated structure factor amplitudes for cdpp, **7b**, and **3b** (86 pages). Ordering information is given on any current masthead page.

(30) Main, P.; Fiske, S. J.; Hull, S. E.; Lessinger, L.; Germain, G.; Declercq, J.-P.; Woolfson, M. M. MULTAN 80, A System of Computer Programs for the Automatic Solution of Crystal Structures from X-ray Diffraction Data, Universities of York, England, and Louvain, Belgium, 1980.

(31) Sheldrick, G. M. SHELX-76, Program for Crystal Structure Determination, University of Cambridge, England, 1976.

(32) Cromer, D. T.; Waber, J. T. *Acta Crystallogr.* **1965**, *18*, 104.

(33) Stewart, R. F.; Davidson, E. R.; Simpson, W. T. *J. Chem. Phys.* **1965**, *42*, 3175.

(34) "International Tables for X-ray Crystallography"; Vol. IV, Birmingham: Kynoch Press, 1974.

(35) Johnson, C. K. ORTEP II, Report ORNL-5138, Oak Ridge National Laboratory, Oak Ridge, TN, 1976.

(36) Roberts, P.; Sheldrick, G. M. XANADU, University of Cambridge, England, 1975.



# Chemistry of $(\eta^5\text{-C}_5\text{Me}_5)\text{Ir}(\text{CO})_2$ . 1. Metal-Metal Bond Formation Employing a Basic Metal Center

A. A. Del Paggio,\*† E. L. Muettterties,† D. M. Heinekey,‡ V. W. Day,§ and C. S. Day¶

Departments of Chemistry, University of California, Berkeley, California 94720, and University of Nebraska, Lincoln, Nebraska 68588, and The Crystallitics Company, P.O. Box 82286, Lincoln, Nebraska 68501

Received June 10, 1985

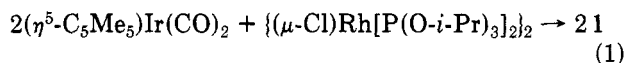
The binuclear complex  $(\eta^5\text{-C}_5\text{Me}_5)(\text{OC})[(i\text{-PrO})_3\text{P}]\text{IrRhCl}(\text{CO})[\text{P}(\text{O}-i\text{-Pr})_3]$  (**1**) has been prepared by the reaction of  $(\eta^5\text{-C}_5\text{Me}_5)\text{Ir}(\text{CO})_2$  with  $\{(\mu\text{-Cl})\text{Rh}[\text{P}(\text{O}-i\text{-Pr})_3]_2\}_2$  at 90 °C in toluene. The structure of **1** has been determined by single-crystal X-ray diffraction. Compound **1** crystallizes in the monoclinic space group  $P2_1/n-C_{2h}^5$  (no. 14) with four molecules in a unit cell of dimensions  $a = 11.463$  (4) Å,  $b = 15.888$  (6) Å,  $c = 22.417$  (6) Å, and  $\beta = 99.01$  (2)°. Least-squares refinement led to a value for the conventional  $R$  index (on  $F$ ) of 0.045 for 5093 independent reflections having  $2\theta_{\text{MoK}\alpha} < 55.0^\circ$  and  $I > 3\sigma(I)$ . The crystallographic investigation confirmed the formulation of **1** as a heterobimetallic complex possessing an unsupported Ir-Rh bond of 2.797 (1) Å. Spectroscopic investigations indicate the metal-metal bond remains intact in solution, but it is susceptible to cleavage by ligands, L, affording  $(\eta^5\text{-C}_5\text{Me}_5)\text{Ir}(\text{CO})[\text{P}(\text{O}-i\text{-Pr})_3]$  and *trans*-ClRh(L)(L')[P(O-*i*-Pr)<sub>3</sub>] (where L = P-*i*-Pr<sub>3</sub>, L' = CO and L = *t*-BuNC, L' = *t*-BuNC). Reaction of  $(\eta^5\text{-C}_5\text{Me}_5)\text{Ir}(\text{CO})_2$  with  $\{(\mu\text{-Cl})\text{Rh}[\text{P}(\text{OR})_3]_2\}_2$  (R = Me, Et, Ph) did not yield binuclear analogues of **1** but instead gave  $(\eta^5\text{-C}_5\text{Me}_5)\text{Ir}(\text{CO})[\text{P}(\text{OR})_3]$  and  $\{(\mu\text{-Cl})\text{Rh}(\text{CO})[\text{P}(\text{OR})_3]_2\}_2$ .

## Introduction

The synthesis of heterobimetallic complexes has been the subject of considerable recent interest due to their potential for novel stoichiometric and catalytic chemistry across an asymmetric metal-metal bond.<sup>2a,b</sup> Although several synthetic methodologies have been employed previously,<sup>3</sup> one potentially general method which has received relatively little attention is the use of neutral electron-rich transition-metal complexes as ligands to other metal centers in the formation of metal-metal bonds between dissimilar metals. This method usually proceeds under mild conditions for a variety of basic metal complexes such as  $(\eta^5\text{-C}_5\text{H}_5)\text{Co}(\text{PMe}_2)_2$ ,<sup>4</sup>  $(\eta^5\text{-C}_5\text{H}_5)\text{Rh}(\text{CO})_2$ ,<sup>5</sup>  $\text{Os}(\text{CO})_5$ ,<sup>6a,b</sup> and  $\text{Os}(\text{CO})_4\text{PMe}_3$ .<sup>7a,b</sup> We have investigated the reaction of the basic metal complex  $(\eta^5\text{-C}_5\text{Me}_5)\text{Ir}(\text{CO})_2$ <sup>8</sup> with various halide-bridged species of the type  $\{(\mu\text{-X})\text{Rh}[\text{P}(\text{OR})_3]_2\}_2$  (X = Cl, Br, I; R = Me, Et, *i*-Pr, Ph). The  $(\eta^5\text{-C}_5\text{Me}_5)\text{Ir}(\text{CO})_2$  molecule was selected for study by virtue of its demonstrated basicity which is greater than either the cobalt or rhodium analogues.<sup>9</sup> This led to the isolation of  $(\eta^5\text{-C}_5\text{Me}_5)(\text{OC})[(i\text{-PrO})_3\text{P}]\text{IrRhCl}(\text{CO})[\text{P}(\text{O}-i\text{-Pr})_3]$  (**1**) which has been structurally characterized by a single-crystal X-ray diffraction study.

## Results and Discussion

Reaction of  $(\eta^5\text{-C}_5\text{Me}_5)\text{Ir}(\text{CO})_2$  with  $\{(\mu\text{-Cl})\text{Rh}[\text{P}(\text{O}-i\text{-Pr})_3]_2\}_2$  in toluene at 90 °C affords **1** in 65% yield (eq 1).



The formulation of **1** as a heterobimetallic complex was confirmed by a single-crystal X-ray diffraction study. Atomic positions for non-hydrogen atoms are contained in Table I, anisotropic thermal parameters are in Table II, and selected bond angles and bond lengths are contained in Table IV. Hydrogen atom positions (Table III) and a complete listing of the bond angles and bond lengths involving hydrogen atoms in **1** (Table V) have been de-

posited as supplementary material. ORTEP diagrams showing the entire molecule as well as the immediate coordination spheres of the metals are shown in Figures 1 and 2, respectively. The molecular structure of **1** may be described as being composed of the neutral 18-electron complex  $(\eta^5\text{-C}_5\text{Me}_5)\text{Ir}(\text{CO})[\text{P}(\text{O}-i\text{-Pr})_3]$  acting as a Lewis base donating an electron pair to the 14-electron Lewis acid  $\text{Rh}(\text{Cl})(\text{CO})[\text{P}(\text{O}-i\text{-Pr})_3]$ . This interaction results in a direct metal-metal bond which is unsupported by halide or carbonyl ligands.<sup>5,10a-c</sup> In addition, a ligand exchange reaction (CO for P(O-*i*-Pr)<sub>3</sub>) has occurred between the metal centers<sup>6b</sup> at some point in the synthetic pathway (eq 1). If the pentamethylcyclopentadienyl ligand is considered to occupy three coordination sites, the iridium(I) center is situated in a roughly octahedral environment. The coordination geometry about the rhodium(I) center is square planar with the two largest ligands  $(\eta^5\text{-C}_5\text{Me}_5)\text{Ir}(\text{CO})[\text{P}(\text{O}-i\text{-Pr})_3]$  and P(O-*i*-Pr)<sub>3</sub> disposed in a trans

(1) Correspondence should be addressed to Professor R. A. Andersen, Department of Chemistry, University of California, Berkeley, CA 94720.

(2) (a) Masters, C. *Adv. Organomet. Chem.* 1979, 17, 61. (b) For a review of heterometallic clusters including dimers, see: Geoffroy, G. L.; Roberts, D. A. In "Comprehensive Organometallic Chemistry"; Abel E. W.; Stone, F. G. A., Wilkinson, G., Eds.; Pergamon Press: Oxford, 1982; Chapter 40.

(3) These include the use of difunctional bridging ligands; phosphide, sulfide, or mercaptide bridging ligands, or reaction of anionic metal salts with metal halides.

(4) Leonard, K.; Werner, H. *Angew. Chem., Int. Ed. Engl.* 1977, 16, 649.

(5) Aldridge, M. L.; Green, M.; Howard, J. A. K.; Pain, G.; Porter, S. J.; Stone, F. G. A. *J. Chem. Soc., Dalton Trans.* 1982, 1333.

(6) (a) Einstein, F. W. B.; Pomeroy, R. K.; Rushman, P.; Willis, A. C. *J. Chem. Soc., Chem. Commun.* 1983, 854. (b) Fleming, M. M.; Pomeroy, R. K.; Rushman, P. *J. Organomet. Chem.* 1984, C33.

(7) (a) Einstein, F. W. B.; Pomeroy, R. K.; Rushman, P. *J. Am. Chem. Soc.* 1984, 106, 2707. (b) Einstein, F. W. B.; Martin, L. R.; Pomeroy, R. K.; Rushman, P. *J. Chem. Soc., Chem. Commun.* 1985, 345.

(8) During the course of this work, we became aware of closely related research which was carried out by R. K. Pomeroy and co-workers. This work was subsequently published. Einstein, F. W. B.; Pomeroy, R. K.; Rushman, P.; Willis, A. C. *Organometallics* 1985, 4, 250.

(9) Herrmann, W. A.; Planck, J.; Bauer, C.; Ziegler, M. L.; Guggolz, E.; Alt, R. *Z. Anorg. Allg. Chem.* 1982, 487, 85.

(10) In heterobimetallic complexes containing carbonyl ligands, the carbonyl ligands are usually in predominantly bridging positions: (a) Werner, H.; Juthani, B. *J. Organomet. Chem.* 1981, 209. (b) Faraone, F.; Bruno, G.; Lo Schiavo, S.; Piraino, P.; Bombieri, G. *J. Chem. Soc., Dalton Trans.* 1983, 1819. (c) Barr, R. D.; Marder, T. B.; Orpen, A. G.; Williams, I. D. *J. Chem. Soc., Chem. Commun.* 1984, 112.

\* Deceased January 12, 1984.

† University of California.

‡ University of Nebraska.

§ The Crystallitics Co.

**Table 1. Atomic Coordinates for Non-Hydrogen Atoms in  $[\eta^5\text{-}(\text{CH}_3)_5\text{C}_5\text{Ir}(\text{CO})[\text{P}(\text{O}-i\text{-C}_3\text{H}_7)_3]\text{RhCl}(\text{CO})[\text{P}(\text{O}-i\text{-C}_3\text{H}_7)_3]_2$** 

atom type <sup>b</sup>	$10^4x$	$10^4y$	$10^4z$	$B_i$ , Å <sup>2</sup>
Ir	-16.7 (3)	2819.9 (2)	286.9 (2)	4.00 (1)
Rh	1112.5 (6)	2114.8 (6)	-613.7 (3)	4.58 (2)
Cl	-31 (3)	2943 (2)	-1383 (1)	6.50 (9)
P <sub>1</sub>	1543 (2)	2956 (2)	1003 (1)	4.39 (6)
P <sub>2</sub>	2067 (3)	1565 (2)	-1292 (1)	5.68 (9)
O <sub>1</sub>	817 (6)	4337 (5)	-300 (3)	6.4 (2)
O <sub>2</sub>	2274 (7)	912 (4)	275 (3)	7.0 (3)
O <sub>11</sub>	1856 (6)	2120 (4)	1366 (3)	5.5 (2)
O <sub>12</sub>	2738 (6)	3363 (4)	879 (3)	6.0 (2)
O <sub>13</sub>	1333 (6)	3553 (4)	1550 (3)	5.7 (2)
O <sub>21</sub>	2594 (6)	2190 (5)	-1725 (3)	7.2 (2)
O <sub>22</sub>	1433 (7)	919 (5)	-1789 (3)	6.8 (2)
O <sub>23</sub>	3132 (6)	998 (5)	-996 (3)	7.1 (3)
C <sub>1</sub>	477 (8)	3702 (7)	-92 (5)	5.6 (3)
C <sub>2</sub>	1850 (9)	1402 (5)	-64 (5)	5.1 (3)
C <sub>11</sub>	2722 (9)	2062 (7)	1928 (5)	6.3 (3)
C <sub>12</sub>	2036 (11)	2015 (10)	2455 (5)	9.9 (6)
C <sub>13</sub>	3458 (13)	1312 (8)	1885 (7)	9.5 (5)
C <sub>14</sub>	3373 (9)	3255 (7)	372 (5)	6.0 (3)
C <sub>15</sub>	4310 (9)	2614 (7)	530 (6)	7.7 (4)
C <sub>16</sub>	3846 (12)	4105 (8)	261 (7)	8.5 (5)
C <sub>17</sub>	843 (10)	4372 (7)	1479 (5)	6.7 (4)
C <sub>18</sub>	225 (14)	4563 (10)	2007 (7)	11.9 (7)
C <sub>19</sub>	1730 (13)	5014 (8)	1417 (7)	9.9 (6)
C <sub>21</sub>	2947 (12)	3063 (9)	-1549 (6)	8.7 (5)
C <sub>22</sub>	4229 (12)	3107 (13)	-1449 (9)	14.3 (9)
C <sub>23</sub>	2422 (14)	3633 (10)	-2057 (7)	11.6 (7)
C <sub>24</sub>	472 (11)	1146 (7)	-2244 (5)	6.8 (4)
C <sub>25</sub>	863 (18)	1177 (16)	-2835 (7)	17.5 (11)
C <sub>26</sub>	-452 (17)	589 (15)	-2231 (8)	17.6 (10)
C <sub>27</sub>	3912 (10)	512 (9)	-1330 (6)	9.0 (5)
C <sub>28</sub>	3576 (14)	-405 (10)	-1287 (10)	14.9 (9)
C <sub>29</sub>	5137 (13)	688 (13)	-1069 (10)	16.2 (10)
C <sub>p1</sub>	-1262 (10)	2305 (8)	873 (5)	6.0 (3)
C <sub>p2</sub>	-1913 (8)	2958 (7)	509 (5)	5.9 (3)
C <sub>p3</sub>	-1974 (8)	2643 (7)	-83 (6)	6.1 (4)
C <sub>p4</sub>	-1454 (8)	1843 (7)	-97 (6)	5.6 (3)
C <sub>p5</sub>	-969 (10)	1659 (7)	497 (6)	6.4 (4)
C <sub>m1</sub>	-1098 (11)	2302 (9)	1575 (5)	8.1 (4)
C <sub>m2</sub>	-2427 (10)	3740 (7)	718 (7)	8.4 (5)
C <sub>m3</sub>	-2627 (10)	3114 (9)	-627 (6)	9.2 (5)
C <sub>m4</sub>	-1537 (11)	1280 (8)	-630 (6)	8.3 (5)
C <sub>m5</sub>	-461 (12)	826 (7)	724 (6)	8.2 (5)

<sup>a</sup> Numbers in parentheses are the estimated standard deviations in the last significant digit. <sup>b</sup> Atoms are labeled in agreement with Figure 1. <sup>c</sup> Equivalent isotropic thermal parameter. This is one-third of the trace of the orthogonalized  $B_{ij}$  tensor.

configuration in order minimize nonbonded repulsions between them.

The carbon framework of pentamethylcyclopentadienyl ligand contains no peculiarities in its bond angles or bond lengths. Likewise, there are no large differences in the ring carbon-to-iridium bond lengths, indicating the pentamethylcyclopentadienyl ligand is symmetrically bound; i.e., it has fivefold symmetry. Complexes of the type  $(\text{C}_5\text{R}_5)\text{-M}(\text{L})_2$  ( $\text{R} = \text{H}, \text{Me}; \text{M} = \text{Co}, \text{Rh}; \text{L} = \text{any two-electron ligand}$ ) generally do not possess cyclopentadienyl ligands that have pseudo- $\text{C}_5$  axis; instead the ring is distorted to an allyl-ene structure with only mirror symmetry.<sup>11a-e</sup> This phenomenon may be interpreted in a very simple manner using frontier molecular orbitals.<sup>12</sup> The HOMO in  $(\eta^5\text{-C}_5\text{Me}_5)\text{Ir}(\text{CO})_2$  is metal-ring antibonding<sup>11d-f</sup> (see Figure 3). Distortion of the geometry about the iridium center upon coordination of it to the  $\text{Rh}(\text{Cl})(\text{CO})[\text{P}(\text{O}-i-$

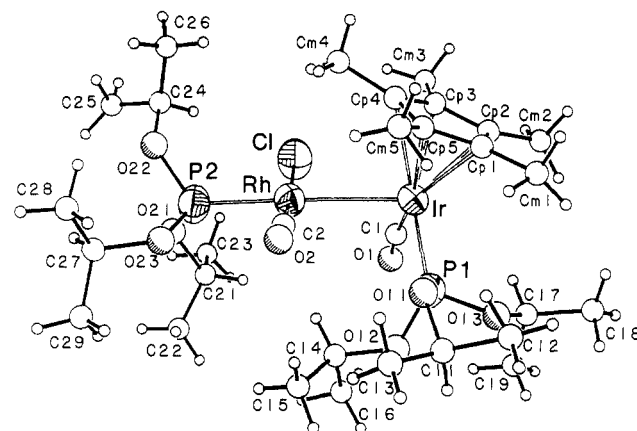


**Figure 1.** ORTEP drawing of 1. Dummy spheres of arbitrary radii have been introduced for all carbon and oxygen atoms. The introduction of these spheres was done to allow a less obstructed view of 1 despite large thermal motion of the methyl groups of each phosphite ligand.

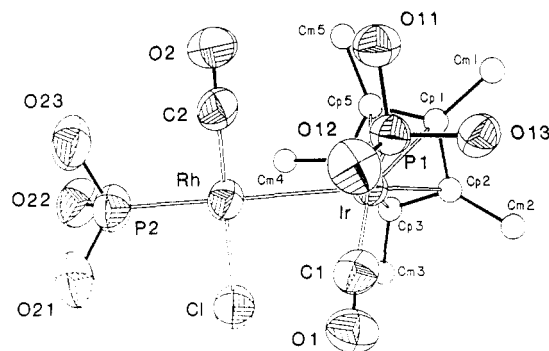


**Figure 2.** ORTEP drawing of 1 showing the immediate coordination spheres of both metal centers.

$\text{Pr}_3$ ] fragment stabilizes the iridium-to-cyclopentadienyl ring bonding by depopulating the HOMO of  $(\eta^5\text{-C}_5\text{Me}_5)\text{-Ir}(\text{CO})_2$  and localizing electron density in an orbital of a symmetry. The removal of electrons from the HOMO of  $(\eta^5\text{-C}_5\text{Me}_5)\text{Ir}(\text{CO})_2$  (which is metal-ring antibonding) results in a planar cyclopentadienyl ligand of pseudo- $\text{C}_5$  symmetry. The LUMO of the  $\text{ClRh}(\text{CO})[\text{P}(\text{O}-i\text{-Pr})_3]$  fragment is generated by removal of one ligand from a square-planar  $d^8 \text{ML}_4$  complex to form a T-shaped fragment of idealized  $\text{C}_{2v}$  symmetry. This orbital is also of a symmetry and, in addition, M-L  $\sigma$ -antibonding. Since the donor orbital on the iridium center and the acceptor orbital of the rhodium fragment are of like symmetry, 1 may be regarded as a classic donor-acceptor complex, similar to  $\text{L-BH}_3$ .

This complexation may alternatively be viewed as an oxidation of the iridium center, removing the pair of electrons from the HOMO of  $(\eta^5\text{-C}_5\text{Me}_5)\text{Ir}(\text{CO})_2$  and placing them into the LUMO of the  $\text{Rh}(\text{Cl})(\text{CO})[\text{P}(\text{O}-i\text{-Pr})_3]$  fragment, thereby reducing it. Since the electron pair now "resides" in an M-L  $\sigma$ -antibonding orbital, the Rh-P distance should be relatively long. In  $\{(\mu\text{-Cl})\text{Rh}[\text{P}(\text{O}-i\text{-Pr})_3]_2\}$ <sup>13</sup> the Rh-P distances range from 2.159 (1) to 2.171 (2) Å. In 1, the Rh-P distance is 2.189 (3) Å, one of the longest rhodium-phosphite distances known.

The steric congestion about the metal centers in 1 can be revealed by several observations. First, the methyl group of the pentamethylcyclopentadienyl ligand lying directly over the rhodium atom ( $\text{C}_{m4}$ ) is distorted such that it lies further away from the rhodium atom than if it were

(11) (a) Guggenberger, L. J.; Cramer, R. *J. Am. Chem. Soc.* **1972**, *94*, 3779. (b) Porzio, W.; Zocchi, M. *J. Am. Chem. Soc.* **1978**, *100*, 2048. (c) Byers, L. R.; Dahl, L. F. *Inorg. Chem.* **1980**, *19*, 277. (d) Harlow, R. L.; McKinney, R. J.; Whitney, J. F. *Organometallics* **1983**, *2*, 1839. (e) Lichtenberger, D. L.; Blevins, C. H.; Ortega, R. B. *Organometallics* **1984**, *3*, 1614.

(12) Albright, T. A.; Burdett, J. K.; Whangbo, M. H. "Orbital Interaction in Chemistry"; Wiley: New York, 1985.

(13) Del Paggio, A. A.; Muetterties, E. L.; Day, V. W.; Day, C. S., unpublished results.

Table II. Anisotropic Thermal Parameters ( $\text{\AA}^2$ ) for Non-Hydrogen Atoms in Crystalline  $[\eta^5\text{-(CH}_3)_5\text{C}_5\text{]Ir}(\text{CO})[\text{P}(\text{O-}i\text{-C}_3\text{H}_7)_3]\text{RhCl}(\text{CO})[\text{P}(\text{O-}i\text{-C}_3\text{H}_7)_3]^a$

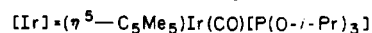
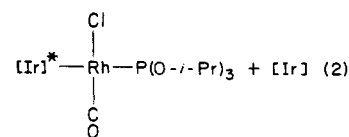
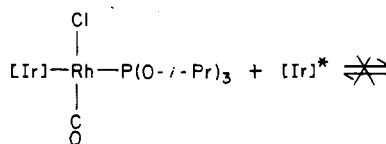
atom type <sup>b</sup>	$B_{11}$	$B_{22}$	$B_{33}$	$B_{12}$	$B_{13}$	$B_{23}$
Ir	3.77 (2)	4.06 (2)	4.21 (2)	0.15 (2)	0.76 (1)	0.21 (2)
Rh	4.26 (3)	4.89 (4)	4.56 (4)	0.55 (3)	0.62 (2)	-0.36 (4)
Cl	6.6 (1)	7.7 (2)	5.0 (1)	2.1 (1)	0.2 (1)	0.3 (1)
P <sub>1</sub>	4.7 (1)	4.3 (1)	4.2 (1)	0.1 (1)	0.6 (1)	0.1 (1)
P <sub>2</sub>	5.6 (1)	6.7 (2)	4.7 (1)	1.2 (1)	0.7 (1)	-0.8 (1)
O <sub>1</sub>	6.9 (4)	6.2 (4)	5.7 (4)	-0.8 (3)	-0.1 (3)	0.7 (3)
O <sub>2</sub>	8.9 (5)	5.6 (4)	6.3 (4)	1.5 (4)	0.7 (4)	1.0 (3)
O <sub>11</sub>	5.9 (3)	5.1 (3)	5.2 (3)	0.4 (3)	0.1 (3)	0.5 (3)
O <sub>12</sub>	5.1 (3)	6.9 (4)	5.7 (4)	-0.8 (3)	-0.1 (3)	-0.6 (3)
O <sub>13</sub>	7.9 (4)	4.1 (3)	4.8 (3)	1.0 (3)	0.1 (3)	-0.4 (3)
O <sub>21</sub>	7.5 (4)	8.9 (5)	5.5 (4)	0.6 (4)	2.3 (3)	-1.5 (4)
O <sub>22</sub>	7.2 (4)	7.3 (4)	5.5 (4)	1.5 (4)	-0.3 (3)	-1.5 (3)
O <sub>23</sub>	5.9 (4)	9.9 (4)	5.5 (4)	2.9 (4)	0.6 (3)	-0.9 (4)
C <sub>1</sub>	4.6 (5)	6.3 (5)	5.2 (5)	1.4 (4)	-1.1 (4)	-0.0 (5)
C <sub>2</sub>	6.2 (5)	3.5 (4)	5.9 (6)	-0.3 (4)	1.2 (4)	-0.6 (4)
C <sub>11</sub>	5.8 (5)	7.2 (7)	5.5 (5)	-0.7 (5)	-0.1 (5)	0.6 (5)
C <sub>12</sub>	10.2 (9)	14.8 (13)	4.2 (6)	3.6 (9)	-0.5 (6)	0.7 (8)
C <sub>13</sub>	10.7 (10)	8.9 (9)	8.4 (9)	4.4 (8)	0.2 (7)	1.7 (8)
C <sub>14</sub>	5.0 (5)	7.6 (6)	5.5 (6)	-0.9 (5)	0.9 (4)	-0.6 (5)
C <sub>15</sub>	6.0 (6)	8.1 (8)	9.0 (8)	-1.4 (6)	0.7 (5)	-1.0 (6)
C <sub>16</sub>	7.6 (8)	8.2 (8)	9.9 (10)	-1.2 (7)	1.8 (7)	0.4 (8)
C <sub>17</sub>	7.6 (7)	5.8 (6)	6.3 (7)	1.8 (5)	-0.2 (5)	-1.4 (5)
C <sub>18</sub>	11.8 (11)	10.6 (10)	14.7 (14)	-1.1 (9)	6.6 (10)	-6.2 (10)
C <sub>19</sub>	13.4 (12)	5.1 (6)	11.5 (11)	2.3 (7)	2.4 (10)	-0.3 (7)
C <sub>21</sub>	10.0 (9)	10.3 (10)	6.3 (7)	-2.0 (7)	3.1 (7)	-0.6 (7)
C <sub>22</sub>	7.8 (9)	17.8 (17)	16.3 (16)	-3.6 (11)	-1.0 (10)	1.5 (13)
C <sub>23</sub>	14.4 (14)	10.4 (11)	11.4 (12)	-0.4 (10)	6.4 (11)	1.9 (10)
C <sub>24</sub>	7.9 (7)	6.4 (6)	5.9 (7)	0.4 (5)	0.0 (5)	-1.4 (5)
C <sub>25</sub>	15.9 (16)	31.4 (28)	4.9 (8)	-4.0 (17)	0.7 (9)	0.6 (13)
C <sub>26</sub>	15.3 (16)	24.1 (22)	11.3 (14)	-10.9 (16)	-4.5 (12)	4.0 (15)
C <sub>27</sub>	6.6 (7)	12.2 (10)	7.8 (8)	3.8 (7)	0.2 (6)	-2.9 (8)
C <sub>28</sub>	9.0 (11)	11.8 (12)	24.7 (22)	2.6 (10)	5.0 (12)	-6.3 (14)
C <sub>29</sub>	6.7 (9)	17.6 (16)	24.0 (21)	3.4 (11)	1.4 (11)	-8.8 (15)
C <sub>p1</sub>	6.6 (6)	6.4 (6)	5.0 (5)	-2.0 (5)	1.2 (4)	0.1 (5)
C <sub>p2</sub>	4.3 (4)	6.7 (6)	7.0 (6)	-0.1 (4)	2.5 (4)	0.8 (6)
C <sub>p3</sub>	3.1 (4)	7.3 (7)	7.8 (7)	-0.2 (4)	0.4 (4)	0.7 (6)
C <sub>p4</sub>	3.6 (4)	6.0 (5)	7.1 (7)	-0.7 (4)	0.8 (4)	-1.0 (5)
C <sub>p5</sub>	6.8 (7)	4.7 (5)	7.7 (8)	-0.1 (5)	1.2 (6)	1.7 (5)
C <sub>m1</sub>	8.5 (7)	10.1 (9)	6.2 (7)	-1.7 (7)	3.0 (6)	1.2 (7)
C <sub>m2</sub>	5.8 (6)	7.7 (8)	12.1 (11)	0.4 (6)	3.1 (6)	0.7 (8)
C <sub>m3</sub>	4.2 (5)	12.9 (11)	9.8 (9)	0.6 (6)	-0.9 (5)	3.0 (8)
C <sub>m4</sub>	7.4 (7)	10.3 (9)	7.0 (8)	-3.4 (7)	0.6 (6)	-2.3 (7)
C <sub>m5</sub>	9.5 (9)	5.4 (6)	10.1 (10)	-1.0 (6)	3.0 (7)	1.6 (6)

<sup>a</sup> Numbers in parentheses are the estimated standard deviations in the last significant digit. The form of the anisotropic thermal parameter is  $\exp[-0.25(B_{11}h^2a^{*2} + B_{22}k^2b^{*2} + B_{33}l^2c^{*2} + 2B_{12}hka^{*}b^{*} + 2B_{13}hla^{*}c^{*} + 2B_{23}klb^{*}c^{*})]$ . <sup>b</sup> Atoms are labeled in agreement with Table I and Figure 1.

lying in the mean plane determined by the other four (C<sub>m1</sub>, C<sub>m2</sub>, C<sub>m3</sub>, C<sub>m5</sub>). This suggests a slight nonbonded repulsion between it and the rhodium atom beneath it.<sup>14</sup> Secondly, the iridium-rhodium vector is displaced approximately 12° from the normal to the plane determined by the atoms C<sub>1</sub>, Ir, and P<sub>1</sub>. This deviation is in a direction away from the phosphite ligand coordinated to the iridium center and, therefore, probably reflects a repulsive interaction between the isopropyl groups of the two phosphite ligands rather than indicating any incipient bridging interaction of the carbonyl ligand containing carbon atom C<sub>1</sub>.

The <sup>1</sup>H, <sup>31</sup>P{<sup>1</sup>H}, and <sup>13</sup>C{<sup>1</sup>H} NMR spectra (see Experimental Section) of 1 showed each of the two phosphite ligands to be chemically nonequivalent. The <sup>31</sup>P{<sup>1</sup>H} NMR spectrum of 1 at room temperature showed a singlet due to the iridium-bound phosphite (A) and a doublet ( $J_{\text{PRh}} = 269$  Hz) due to the rhodium-bound phosphite (B). The observed spectrum suggests that both <sup>3</sup>J<sub>AB</sub> and <sup>2</sup>J<sub>ARh</sub> are very small. No evidence for the dissociation of the iridium complex, however, was observed in any of the following experiments. The appearance of the spectrum remains constant, independent of temperature and solvent. Ad-

dition of 1 molar equiv of  $(\eta^5\text{-C}_5\text{Me}_5)\text{Ir}(\text{CO})[\text{P}(\text{O-}i\text{-Pr})_3]$  failed to modify the appearance of the spectrum, and likewise, addition of  $(\eta^5\text{-C}_5\text{Me}_5)\text{Ir}(\text{CO})[\text{P}(\text{OMe})_3]$  (a sterically less demanding ligand) failed to produce crossover products upon standing for several weeks at room temperature. These experiments strongly suggest that 1 does not undergo exchange by way of a dissociative equilibrium (eq 2) and that both <sup>3</sup>J<sub>AB</sub> and <sup>2</sup>J<sub>ARh</sub> are indeed small.



Further, the two chemically nonequivalent carbonyl ligands do not undergo site exchange even at +60 °C. This is in contrast to the related systems studied by Pomeroy<sup>7a,b,8</sup> which undergo carbonyl site exchange at room temperature.

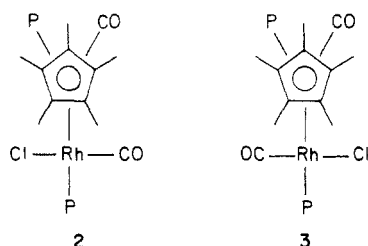
(14) The carbon atom C<sub>m4</sub> lies approximately 0.1 Å out of the mean plane determined by C<sub>m1</sub>, C<sub>m2</sub>, C<sub>m3</sub> and C<sub>m5</sub>.

**Table IV. Bond Lengths and Angles in Coordination Groups of  $(\eta^5\text{-C}_5\text{Me}_5)(\text{OC})[i\text{-Pr-O}]_3\text{P}[\text{IrRhCl}(\text{CO})[\text{P}(\text{O}-i\text{-Pr})_3]_2$**

parameter <sup>b</sup>	value	parameter <sup>b</sup>	value
Bond Lengths, Å			
Ir-Rh	2.797 (1)	Ir-C <sub>p1</sub>	2.240 (12)
		Ir-C <sub>p2</sub>	2.314 (10)
Rh-Cl	2.391 (3)	Ir-C <sub>p3</sub>	2.284 (9)
Rh-P <sub>2</sub>	2.189 (3)	Ir-C <sub>p4</sub>	2.329 (10)
Rh-C <sub>2</sub>	1.787 (9)	Ir-C <sub>p5</sub>	2.230 (12)
Ir-P <sub>1</sub>	2.219 (2)		
Ir-C <sub>1</sub>	1.777 (10)	C <sub>p1</sub> -C <sub>p2</sub>	1.45 (2)
Ir-C <sub>g</sub> <sup>c</sup>	1.938 (...)	C <sub>p2</sub> -C <sub>p3</sub>	1.41 (2)
		C <sub>p3</sub> -C <sub>p4</sub>	1.41 (2)
C <sub>1</sub> -O <sub>1</sub>	1.20 (1)	C <sub>p4</sub> -C <sub>p5</sub>	1.39 (2)
C <sub>2</sub> -O <sub>2</sub>	1.14 (1)	C <sub>p1</sub> -C <sub>p5</sub>	1.40 (2)
Bond Angles, deg			
C <sub>g</sub> -Ir-C <sub>1</sub>	136.8	Ir-Rh-Cl	92.1 (1)
C <sub>g</sub> -Ir-Rh	112.5	Ir-Rh-P <sub>2</sub>	177.6 (1)
C <sub>g</sub> -Ir-P <sub>1</sub>	128.3	Ir-Rh-C <sub>2</sub>	88.8 (3)
C <sub>1</sub> -Ir-P <sub>1</sub>	89.3 (3)	Cl-Rh-P <sub>2</sub>	89.7 (1)
C <sub>1</sub> -Ir-Rh	75.7 (3)	Cl-Rh-C <sub>2</sub>	173.5 (3)
P <sub>1</sub> -Ir-Rh	98.6 (1)	C <sub>2</sub> -Rh-P <sub>2</sub>	89.6 (4)
Ir-C <sub>1</sub> -O <sub>1</sub>	174.2 (9)	Rh-C <sub>2</sub> -O <sub>2</sub>	176.0 (8)

<sup>a</sup> Numbers in parentheses are the estimated standard deviations in the last significant digit. <sup>b</sup> Atoms are labeled in agreement with Figures 1 and 2. <sup>c</sup> C<sub>g</sub> refers to the center of gravity of the five-carbon ring of the (C<sub>5</sub>Me<sub>5</sub>) ligand.

The solution infrared spectrum of 1 in pentane shows four sharp intense CO absorptions at 2024, 2014, 1958, and 1934 cm<sup>-1</sup>. Figure 1 shows that the methyl groups of both the P(O-*i*-Pr)<sub>3</sub><sup>15</sup> and (η<sup>5</sup>-C<sub>5</sub>Me<sub>5</sub>) ligands<sup>14</sup> extend nearly across the Cl-Rh-C≡O fragment, imposing a slight barrier to rotation. This could give rise to significant populations of the rotamers 2 and 3 in solution, each of which will have two infrared-active CO stretching frequencies. These rotamers were not observed in the low-



temperature <sup>31</sup>P{<sup>1</sup>H} NMR spectrum. This would suggest that interconversion between 2 and 3 is rapid on the NMR time scale. A similar phenomena has been observed previously in the infrared spectra of the related (η<sup>5</sup>-C<sub>5</sub>H<sub>5</sub>)(OC)XC<sub>5</sub>MRX<sub>2</sub> and (η<sup>5</sup>-C<sub>5</sub>H<sub>5</sub>)(OC)Co(MRX<sub>2</sub>)<sub>2</sub> (M = Ge, Sn; X = Cl, Br, I) systems studied by Graham and Kummer.<sup>16</sup>

The scope of the reaction shown in eq 1 is extremely limited. Reaction of (η<sup>5</sup>-C<sub>5</sub>Me<sub>5</sub>)Ir(CO)<sub>2</sub> with {(μ-X)Rh[P(O-*i*-Pr)<sub>3</sub>]<sub>2</sub>} (X = Br, I) gives only products derived from ligand exchange as indicated in eq 3. Further, the iridium (η<sup>5</sup>-C<sub>5</sub>Me<sub>5</sub>)Ir(CO)<sub>2</sub> + {(μ-X)Rh[P(O-*i*-Pr)<sub>3</sub>]<sub>2</sub>} → (η<sup>5</sup>-C<sub>5</sub>Me<sub>5</sub>)Ir(CO)[P(O-*i*-Pr)<sub>3</sub>] + {(μ-X)Rh(CO)[P(O-*i*-Pr)<sub>3</sub>]<sub>2</sub>} (3)

(15) The large number of rotational degrees of freedom allowed the P(O-*i*-Pr)<sub>3</sub> ligand makes its solution steric requirements difficult to adequately describe. To allow free rotation of the Rh-C≡O<sub>2</sub> unit, however, the closest nonbonded contact between Rh and a carbon or hydrogen atom must exceed 3.201 (22) Å. In the case of H<sub>14</sub>, a nonbonded distance of 2.728 Å exists and would create a barrier to rotation if it were stationary in solution while the Cl-Rh-C≡O<sub>2</sub> unit were allowed to rotate about the Rh-Ir bond.

(16) Graham, W. A. G.; Kummer, R. *Inorg. Chem.* 1968, 7, S23.

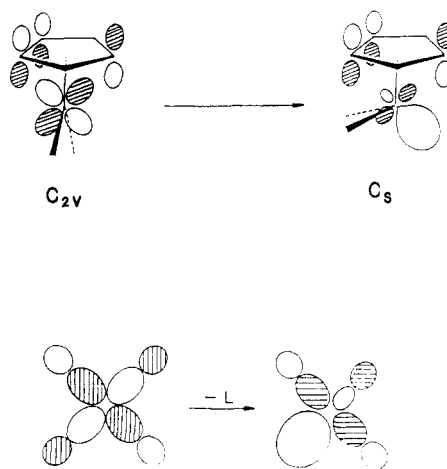
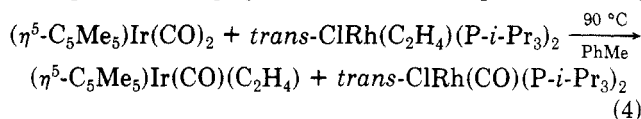


**Figure 3.** Top: changes in the HOMO of (η<sup>5</sup>-C<sub>5</sub>Me<sub>5</sub>)Ir(CO)<sub>2</sub> created by deforming the coordination geometry about iridium from idealized C<sub>2v</sub> symmetry to C<sub>s</sub> symmetry. Note that the metal-ring antibonding character of this donor orbital has been reduced, thereby restoring the pseudo-C<sub>5</sub> axis to the cyclopentadienyl ligand. Bottom: generation of the acceptor orbital on rhodium by removal of a ligand from a square-planar d<sup>8</sup> ML<sub>4</sub> complex forming a fragment of idealized C<sub>2v</sub> symmetry.

complex reacts with *trans*-ClRh(C<sub>2</sub>H<sub>4</sub>)(P-*i*-Pr)<sub>3</sub><sub>2</sub> to give the ligand exchange products shown in eq 4. Likewise,



the rhodium complex (η<sup>5</sup>-C<sub>5</sub>Me<sub>5</sub>)Rh(CO)<sub>2</sub> does not give Rh-Rh bonded compounds with {(μ-X)Rh[P(O-*i*-Pr)<sub>3</sub>]<sub>2</sub>}<sub>2</sub> (X = Cl, Br, I) but instead yields the products shown in eq 5.

The product distributions in eq 5 illustrate the greater tendency for (η<sup>5</sup>-C<sub>5</sub>Me<sub>5</sub>)Rh(CO)<sub>2</sub> to donate a carbonyl ligand compared to its iridium analogue. This is not unexpected in view of the fact that the CO ligand in these complexes is bound more weakly by rhodium than iridium.<sup>17</sup> An additional driving force for the CO donation by rhodium is undoubtedly the formation of metal-metal multiple bonds in the very stable [(η<sup>5</sup>-C<sub>5</sub>Me<sub>5</sub>)Rh(μ-CO)]<sub>2</sub> molecule,<sup>18a</sup> the structure of which has been reported.<sup>18b</sup>

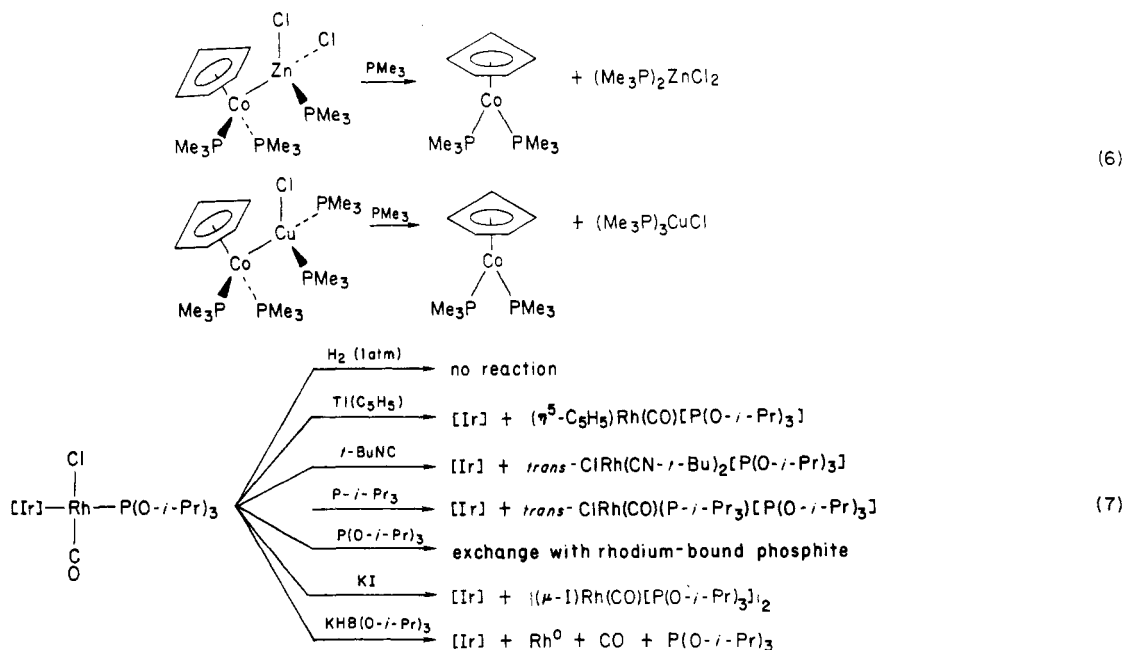
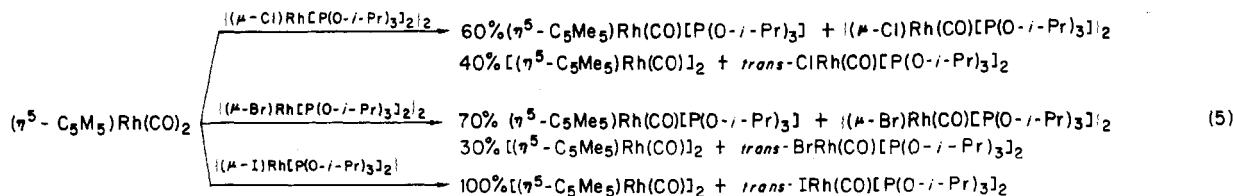
**Reactivity of 1.** The reaction of small ligands, L, with heterobimetallic complexes containing donor-acceptor metal-metal bonds is dominated almost exclusively by fragmentation. Werner and co-workers<sup>4,19</sup> have shown that 1 equiv of PMe<sub>3</sub> will quantitatively displace (η<sup>5</sup>-C<sub>5</sub>H<sub>5</sub>)Co(PMe<sub>3</sub>)<sub>2</sub> from Cu(I) and Zn(II) adducts of this complex (eq 6). By incorporating heavier congeners of the group VIII B (8-10<sup>28</sup>) metals, namely, rhodium and iridium, it was hoped the strength of the metal-metal bond could be increased sufficiently to prevent its cleavage by ligands. The reaction of 1 with some representative ligands, L, is summarized in eq 7. Each reaction shown in eq 7 was performed at 0 °C, and the yields were quantitative.

The ligand P-*i*-Pr<sub>3</sub> was found to cleave the metal-metal bond of 1 to produce the mononuclear complexes (η<sup>5</sup>-

(17) This can be inferred from the values of the symmetric and asymmetric CO stretching frequencies in the solution infrared spectrum. ν<sub>sym</sub> for Rh is 2030 cm<sup>-1</sup> and ν<sub>asym</sub> for Rh is 1968 cm<sup>-1</sup> while the corresponding values for Ir are 2023 and 1956 cm<sup>-1</sup>, respectively. Also, reaction of Me<sub>3</sub>N<sup>+</sup>O<sup>-</sup> with (η<sup>5</sup>-C<sub>5</sub>Me<sub>5</sub>)Rh(CO)<sub>2</sub> yields [(η<sup>5</sup>-C<sub>5</sub>Me<sub>5</sub>)Rh(μ-CO)]<sub>2</sub> while (η<sup>5</sup>-C<sub>5</sub>Me<sub>5</sub>)Ir(CO)<sub>2</sub> is unreactive toward this reagent under similar conditions.

(18) (a) Maitlis, P. M.; Nutton, A. *J. Organomet. Chem.* 1979 166, C21. (b) Green, M.; Hankey, D. R.; Howard, J. A. K.; Louca, P.; Stone, F. G. A. *J. Chem. Soc. Chem. Commun.* 1983, 14, 757.

(19) Werner, H. *Chem. Ber.* 1979, 112 (3), 823.



$\text{C}_5\text{Me}_5\text{Ir}(\text{CO})[\text{P}(\text{O-}i\text{-Pr})_3]$  and  $\text{trans-ClRh}(\text{CO})(\text{P-}i\text{-Pr})_3[\text{P}(\text{O-}i\text{-Pr})_3]$ . Addition of 1 equiv of  $\text{P}(\text{O-}i\text{-Pr})_3$  gave rise to chemical exchange between the free and rhodium-bound phosphite ligand in 1. The two resonances in the  $^{31}\text{P}\{^1\text{H}\}$  spectrum coalesced at  $-50^\circ\text{C}$  and failed to yield a low-temperature limiting spectrum as low as  $-85^\circ\text{C}$ .

Addition of the ligand  $t\text{-BuNC}$  followed a somewhat different course. The initial cleavage of the metal-metal bond was apparently followed by a second, more facile displacement of CO from the assumed  $\text{trans-ClRh}(\text{CN-}t\text{-Bu})(\text{CO})[\text{P}(\text{O-}i\text{-Pr})_3]$  intermediate to yield a product consistent with the formulation  $\text{trans-ClRh}(\text{CN-}t\text{-Bu})_2[\text{P}(\text{O-}i\text{-Pr})_3]$ . With the addition of 1 equiv of  $t\text{-BuNC}$  per binuclear, the observed products included 50%  $\text{trans-ClRh}(\text{CN-}t\text{-Bu})_2[\text{P}(\text{O-}i\text{-Pr})_3]$  and 50% unreacted 1.

Attempts to metathesize the halide ligand were unsuccessful. For example, reaction of 1 with  $\text{KHB}(\text{O-}i\text{-Pr})_3$  in THF at  $0^\circ\text{C}$  resulted in reduction of the rhodium fragment, a rhodium mirror being deposited over several minutes. Examination of the products from this reaction indicated both CO and  $\text{P}(\text{O-}i\text{-Pr})_3$  had been released. The other product from this reduction was the neutral complex  $(\eta^5\text{-C}_5\text{Me}_5)\text{Ir}(\text{CO})[\text{P}(\text{O-}i\text{-Pr})_3]$ . Reaction of 1 with excess KI in acetone resulted in displacement of the  $(\eta^5\text{-C}_5\text{Me}_5)\text{Ir}(\text{CO})[\text{P}(\text{O-}i\text{-Pr})_3]$  ligand with concomitant dimerization of the rhodium fragment to form  $\{(\mu\text{-I})\text{Rh}(\text{CO})[\text{P}(\text{O-}i\text{-Pr})_3]_2\}$ .

The fact that each ligand, including  $\text{I}^-$ , displaced the basic iridium complex from the binuclear complex 1 clearly indicates that  $(\eta^5\text{-C}_5\text{Me}_5)\text{Ir}(\text{CO})[\text{P}(\text{O-}i\text{-Pr})_3]$  is by far the most weakly bound ligand. In fact, the binuclear complex 1 is a very convenient source of the  $\text{ClRh}(\text{CO})[\text{P}(\text{O-}i\text{-Pr})_3]$  fragment and therefore constitutes a useful preparation of complexes  $\text{trans-ClRh}(\text{CO})(\text{L})[\text{P}(\text{O-}i\text{-Pr})_3]$ . In this respect, the heavier group VIII metals display the same chemistry initially observed for  $(\eta^5\text{-C}_5\text{H}_5)\text{Co}(\text{PMe}_3)_2$ <sup>4,19</sup> and its respective Lewis acid adducts.

## Experimental Section

**Reagents and Solvents.** All compounds were handled under a dry dinitrogen atmosphere in a Vacuum Atmospheres drybox or under a dinitrogen atmosphere using conventional Schlenk techniques. Pentane, toluene, and tetrahydrofuran solvents were vacuum distilled from sodium benzophenone ketyl directly into dry reaction vessels. Deuterated NMR solvents were purchased from Stohler Isotope Chemicals, stored over sodium benzophenone ketyl or Na/Pb alloy ( $\text{CD}_2\text{Cl}_2$ ), and vacuum distilled directly into sample tubes as needed. Pentamethylcyclopentadiene was purchased from Strem Chemicals and used without further purification. All phosphine and phosphite ligands were vacuum distilled from sodium mirrors.  $(\eta^5\text{-C}_5\text{Me}_5)\text{Ir}(\text{CO})_2$ <sup>20</sup> and  $(\eta^5\text{-C}_5\text{Me}_5)\text{Rh}(\text{CO})_2$ <sup>9,20</sup> were prepared by literature methods. These complexes were enriched in  $^{13}\text{C}$  by stirring pentane solutions of them at ambient temperature under an atmosphere containing several equivalents of  $^{13}\text{CO}$ . The incorporation of  $^{13}\text{C}$  under these conditions was found to be rapid.

**Spectroscopic and Analytical Methods.** All NMR spectra were recorded on an instrument comprising a 200-MHz ( $^1\text{H}$ ) Oxford superconducting magnet interfaced with Nicolet 1180 computer. Chemical shifts ( $^1\text{H}$ ,  $^{13}\text{C}$ ) are reported relative to tetramethylsilane, and  $^{31}\text{P}$  chemical shifts are reported relative to external 85%  $\text{H}_3\text{PO}_4$  with all chemical shifts positive to higher frequency.

Microanalyses were performed by Mr. Vazken H. Tashinian in the microanalytical laboratory at the University of California, Berkeley.

**Preparation of  $\{(\mu\text{-Cl})\text{Rh}[\text{P}(\text{OR})_3]_2\}_2$ .** A solution of 4.04 mmol of  $\text{P}(\text{OR})_3$  in 10 mL of THF was added dropwise to a solution of 0.50 g (1.0 mmol) of  $\{(\mu\text{-Cl})\text{Rh}(\text{C}_2\text{H}_4)_2\}_2$ <sup>21</sup> in 30 mL of THF at room temperature. Ethylene evolution proceeded smoothly, and the color of the solution changed from orange to yellow. The solvent was removed in vacuo to yield a yellow powder. Crystallization from either pentane ( $\text{R} = \text{Et}$ ,  $i\text{-Pr}$ ,  $\text{Ph}$ ) or toluene ( $\text{R} = \text{Me}$ ) at  $-40^\circ\text{C}$  afforded yellow crystals of  $\{(\mu\text{-Cl})\text{Rh}[\text{P}(\text{OR})_3]_2\}_2$  in yields of 85–95%.

(20) Maitlis, P. M.; Kang, J. W.; Moseley, K. J. *J. Am. Chem. Soc.* **1969**, *91*, 5970.

(21) Cramer, R. *Inorg. Synth.* **1974**, *15*, 14.

$\{(\mu\text{-Cl})\text{Rh}[\text{P}(\text{OMe})_3]_2\}_2$ :  $^1\text{H}$  NMR (20 °C, THF- $d_6$ )  $\delta$  3.68 (virtual triplet,  $^3J_{\text{HP}} + ^5J_{\text{HP}} = 11$  Hz,  $\text{P}(\text{OCH}_3)_3$ );  $^{31}\text{P}\{^1\text{H}\}$  NMR  $\delta$  139.5 (d,  $J_{\text{PRh}} = 295$  Hz). Anal. Calcd for  $\text{C}_{12}\text{H}_{36}\text{O}_{12}\text{P}_4\text{Cl}_2\text{Rh}_2$ : C, 18.6; H, 4.66; P, 16.0. Found: C, 18.6; H, 4.61; P, 16.0.

$\{(\mu\text{-Cl})\text{Rh}[\text{P}(\text{OEt})_3]_2\}_2$ :  $^1\text{H}$  NMR (20 °C,  $\text{C}_6\text{D}_6$ )  $\delta$  4.29 (m, 2 H,  $\text{P}(\text{OCH}_2\text{CH}_3)_3$ ), 1.22 (t, 3 H,  $^3J_{\text{HH}} = 7.1$  Hz,  $\text{P}(\text{OCH}_2\text{CH}_3)_3$ );  $^{31}\text{P}\{^1\text{H}\}$  NMR  $\delta$  134.64 (d,  $J_{\text{PRh}} = 294$  Hz);  $^{13}\text{C}\{^1\text{H}\}$  NMR  $\delta$  60.75 (d,  $^2J_{\text{CP}} = 4.4$  Hz,  $\text{P}(\text{OCH}_2\text{CH}_3)_3$ ), 16.54 (s,  $\text{P}(\text{OCH}_2\text{CH}_3)_3$ ). Anal. Calcd for  $\text{C}_{24}\text{H}_{60}\text{O}_{12}\text{P}_4\text{Cl}_2\text{Rh}_2$ : C, 30.6; H, 6.38; P, 13.2. Found: C, 30.7; H, 6.50; P, 13.1.

$\{(\mu\text{-Cl})\text{Rh}[\text{P}(\text{O-}i\text{-Pr})_3]_2\}_2$ :  $^1\text{H}$  NMR (20 °C,  $\text{C}_6\text{D}_6$ )  $\delta$  5.26 (m, 1 H,  $\text{P}(\text{OCH}(\text{CH}_3)_2)_3$ ), 1.38 (d, 6 H,  $^3J_{\text{HH}} = 6.2$  Hz,  $\text{P}(\text{OCH}(\text{CH}_3)_2)_3$ );  $^{13}\text{C}\{^1\text{H}\}$  NMR  $\delta$  69.53 (s,  $\text{P}(\text{OCH}(\text{CH}_3)_2)_3$ ), 24.77 (s,  $\text{P}(\text{OCH}(\text{CH}_3)_2)_3$ );  $^{31}\text{P}\{^1\text{H}\}$  NMR  $\delta$  131.9 (d,  $J_{\text{PRh}} = 295$  Hz). Anal. Calcd for  $\text{C}_{36}\text{H}_{84}\text{O}_{12}\text{P}_4\text{Cl}_2\text{Rh}_2$ : C, 38.9; H, 7.57; P, 11.2. Found: C, 39.3; H, 7.63; P, 11.1.

$\{(\mu\text{-Cl})\text{Rh}[\text{P}(\text{OPh})_3]_2\}_2$ :  $^1\text{H}$  NMR (20 °C, THF- $d_8$ )  $\delta$  7.1–7.5 (m);  $^{31}\text{P}\{^1\text{H}\}$  NMR  $\delta$  124.2 (d,  $J_{\text{PRh}} = 309$  Hz). Anal. Calcd for  $\text{C}_{72}\text{H}_{60}\text{O}_{12}\text{P}_4\text{Cl}_2\text{Rh}_2$ : C, 57.0; H, 3.96; P, 8.17. Found: C, 57.3; H, 3.99; P, 8.15.

**Preparation of  $\{(\mu\text{-X})\text{Rh}[\text{P}(\text{O-}i\text{-Pr})_3]_2\}_2$  (X = Br, I).**  $\{(\mu\text{-Cl})\text{Rh}[\text{P}(\text{O-}i\text{-Pr})_3]_2\}_2$  (600 mg, 0.54 mmol) was dissolved in 40 mL of dry acetone, and 1.0 g (excess) of finely ground KX was added. The solution rapidly changed color from yellow to orange (X = Br) or deep red (X = I). The suspension was stirred for 3 h, the solvent was removed in vacuo, and the product was extracted with pentane. Crystallization from pentane at  $-40$  °C afforded well-formed crystals of the product.

$\{(\mu\text{-Br})\text{Rh}[\text{P}(\text{O-}i\text{-Pr})_3]_2\}_2$  was isolated as large orange crystals in 91% (0.59 g) yield.  $^1\text{H}$  NMR (20 °C,  $\text{C}_6\text{D}_6$ ):  $\delta$  5.36 (m, 1 H,  $\text{P}(\text{OCH}(\text{CH}_3)_2)_3$ ), 1.36 (d, 6 H,  $^3J_{\text{HH}} = 6.2$  Hz,  $\text{P}(\text{OCH}(\text{CH}_3)_2)_3$ );  $^{13}\text{C}\{^1\text{H}\}$  NMR  $\delta$  69.06 (s,  $\text{P}(\text{OCH}(\text{CH}_3)_2)_3$ ), 24.66 (s,  $\text{P}(\text{OCH}(\text{CH}_3)_2)_3$ );  $^{31}\text{P}\{^1\text{H}\}$  NMR  $\delta$  133.2 (d,  $J_{\text{PRh}} = 293$  Hz). Anal. Calcd for  $\text{C}_{36}\text{H}_{84}\text{O}_{12}\text{P}_4\text{Br}_2\text{Rh}_2$ : C, 36.1; H, 7.01; P, 10.4; Br, 13.4. Found: C, 36.2; H, 6.98; P, 10.4; Br, 13.2.

$\{(\mu\text{-I})\text{Rh}[\text{P}(\text{O-}i\text{-Pr})_3]_2\}_2$  was isolated as large burgundy bricks in 91% (0.64 g) yield.  $^1\text{H}$  NMR (24 °C,  $\text{C}_6\text{D}_5\text{CD}_3$ )  $\delta$  5.27 (d sept, 1 H),  $^3J_{\text{HP}} = 10.2$  Hz,  $^3J_{\text{HH}} = 6.2$  Hz,  $\text{P}(\text{OCH}(\text{CH}_3)_2)_3$ ); 1.35 (d, 6 H,  $^3J_{\text{HH}} = 6.2$  Hz,  $\text{P}(\text{OCH}(\text{CH}_3)_2)_3$ );  $^{13}\text{C}\{^1\text{H}\}$  NMR  $\delta$  68.95 (s,  $\text{P}(\text{OCH}(\text{CH}_3)_2)_3$ ), 24.53 (s,  $\text{P}(\text{OCH}(\text{CH}_3)_2)_3$ );  $^{31}\text{P}\{^1\text{H}\}$  NMR  $\delta$  132.1 (d,  $J_{\text{PRh}} = 296$  Hz). Anal. Calcd for  $\text{C}_{36}\text{H}_{84}\text{O}_{12}\text{P}_4\text{Rh}_2\text{I}_2$ : C, 33.5; H, 6.51; P, 9.61; I, 19.5. Found: C, 33.6; H, 6.48; P, 9.70; I, 19.6.

**Preparation of  $\text{ClRh}(\text{C}_2\text{H}_4)(\text{P-}i\text{-Pr})_2$ .** This preparation is a simplification of an earlier procedure.<sup>22</sup> A solution of 1.52 g (4.74 mmol) of  $\text{P-}i\text{-Pr}_3$  in 5 mL of pentane was added rapidly to a suspension of 0.92 g (2.4 mmol) of  $\{(\mu\text{-Cl})\text{Rh}(\text{C}_2\text{H}_4)_2\}_2$  in 50 mL of pentane. After the addition of  $\text{P-}i\text{-Pr}_3$  was complete, 20 mL of THF was added, the reaction vessel sealed, and the orange solution allowed to stir overnight. The solvent was removed in vacuo, and the resultant orange powder was extracted with 75 mL of toluene and filtered. Concentration of the filtrate in vacuo gave 1.8 g (78%) of orange-yellow crystals:  $^1\text{H}$  NMR (20 °C,  $\text{CD}_2\text{Cl}_2$ )  $\delta$  2.33 (br sept, 6 H,  $^3J_{\text{HH}} = 7$  Hz,  $\text{P}(\text{CH}(\text{CH}_3)_2)_3$ ), 2.46 (m, 4 H,  $\text{C}_2\text{H}_4$ ), 1.31 (m, 18 H,  $\text{P}(\text{CH}(\text{CH}_3)_2)_3$ );  $^{31}\text{P}\{^1\text{H}\}$  NMR  $\delta$  33.8 (d,  $J_{\text{PRh}} = 118.8$  Hz). Anal. Calcd for  $\text{C}_{20}\text{H}_{46}\text{P}_2\text{ClRh}$ : C, 49.4; H, 9.45; P, 12.7; Cl, 7.29. Found: C, 49.2; H, 9.51; P, 12.4; Cl, 7.21.

**Preparation of  $(\eta^5\text{-C}_5\text{Me}_5)(\text{OC})[(i\text{-PrO})_3\text{P}]\text{IrRhCl}(\text{CO})[\text{P}(\text{O-}i\text{-Pr})_3]$  (1).**  $\{(\mu\text{-Cl})\text{Rh}[\text{P}(\text{O-}i\text{-Pr})_3]_2\}_2$  (300 mg, 0.270 mmol) and 207 mg (0.540 mmol) of  $(\eta^5\text{-C}_5\text{Me}_5)\text{Ir}(\text{CO})_2$  were placed in a dry 50-mL reactor. Toluene (20 mL) was vacuum distilled into the reactor, the stopcock was closed, and the tube was slowly heated to 90 °C and kept at this temperature for 3 h. After the solution was cooled to room temperature, the solvent was removed in vacuo, affording an orange-brown residue which was dissolved in a minimum amount of pentane and filtered. Cooling to  $-40$  °C yielded 329 mg (65%) of 1 as large orange rhombohedra:  $^1\text{H}$  NMR (20 °C,  $\text{C}_6\text{D}_6$ )  $\delta$  5.15 (d, sept, 1 H,  $^3J_{\text{HP}} = 9.63$  Hz,  $^3J_{\text{HH}} = 6.2$  Hz,  $\text{RhP}(\text{OCH}(\text{CH}_3)_2)_3$ ), 4.82 (d sept,  $^3J_{\text{HP}} = 10.2$  Hz,  $^3J_{\text{HH}} = 6.2$  Hz,  $\text{IrP}(\text{OCH}(\text{CH}_3)_2)_3$ ), 2.06 (d, 5 H,  $^3J_{\text{HP}} = 2.1$  Hz,  $\text{C}_5(\text{CH}_3)_5$ ), 1.22 (d, 6 H,  $^3J_{\text{HH}} = 6.2$  Hz,  $\text{P}(\text{OCH}(\text{CH}_3)_2)_3$ ), 1.21 (d, 6 H,  $^3J_{\text{HH}} = 6.2$  Hz,  $\text{P}(\text{OCH}(\text{CH}_3)_2)_3$ );  $^{13}\text{C}\{^1\text{H}\}$  NMR  $\delta$  184.7 (dd,  $^1J_{\text{CRh}} = 82.6$  Hz,  $^2J_{\text{CP}} = 17.4$  Hz,  $\text{Rh}(\text{CO})$ ), 180.96 (d,  $^2J_{\text{CP}} = 23$  Hz,  $\text{Ir}(\text{CO})$ ),

94.94 (d,  $^2J_{\text{CP}} = 2.7$  Hz,  $\text{C}_5(\text{CH}_3)_5$ ), 71.51 (s,  $\text{IrP}(\text{OCH}(\text{CH}_3)_2)_3$ ), 69.56 (d,  $^2J_{\text{CP}} = 2.0$  Hz,  $\text{RhP}(\text{OCH}(\text{CH}_3)_2)_3$ ), 24.11 (d,  $^3J_{\text{CP}} = 3$  Hz,  $\text{P}(\text{OCH}(\text{CH}_3)_2)_3$ ), 24.05 (d,  $^3J_{\text{CP}} = 4.1$  Hz,  $\text{P}(\text{OCH}(\text{CH}_3)_2)_3$ ), 10.90 (s,  $\text{C}_5(\text{CH}_3)_5$ );  $^{31}\text{P}\{^1\text{H}\}$  NMR  $\delta$  93.0 (s,  $\text{IrP}$ ), 114.96 (d,  $J_{\text{PRh}} = 269$  Hz,  $\text{RhP}$ ); IR (solution, pentane)  $\nu_{\text{CO}}$  2024, 2014, 1958, 1934. Anal. Calcd for  $\text{C}_{36}\text{H}_{57}\text{O}_8\text{P}_2\text{ClIrRh}$ : C, 38.4; H, 6.08; P, 6.61; Cl, 3.79. Found: C, 38.5; H, 5.97; P, 6.65; Cl, 3.78.

**Preparation of  $(\eta^5\text{-C}_5\text{Me}_5)\text{Ir}(\text{CO})\text{PR}_3$  (R = OMe, Et, O-*i*-Pr).**  $(\eta^5\text{-C}_5\text{Me}_5)\text{Ir}(\text{CO})_2$  (380 mg, 0.98 mmol) was dissolved in 25 mL of dry toluene, and 1 molar equiv of a phosphine or phosphite was added via a microliter syringe, and the solution was refluxed for 6 h. Removal of the solvent and crystallization from pentane at  $-40$  °C yielded the compounds as pale yellow crystals.

$(\eta^5\text{-C}_5\text{Me}_5)\text{Ir}(\text{CO})[\text{P}(\text{OMe})_3]$ :  $^1\text{H}$  NMR (20 °C,  $\text{C}_6\text{D}_6$ )  $\delta$  3.36 (d, 9 H,  $^3J_{\text{HP}} = 12.8$  Hz,  $\text{P}(\text{OCH}_3)_3$ ), 2.01 (d, 15 H,  $^4J_{\text{HP}} = 2.2$  Hz,  $\text{C}_5(\text{CH}_3)_5$ );  $^{31}\text{P}\{^1\text{H}\}$  NMR  $\delta$  111.1 (s); IR (solution, pentane) 1944  $\text{cm}^{-1}$ . Anal. Calcd for  $\text{C}_4\text{H}_{24}\text{O}_4\text{PIr}$ : C, 35.1; H, 5.01; P, 6.47. Found: C, 35.2; H, 5.06; P, 6.51.

$(\eta^5\text{-C}_5\text{Me}_5)\text{Ir}(\text{CO})(\text{PEt}_3)$ :  $^1\text{H}$  NMR ( $-20$  °C,  $\text{C}_6\text{D}_5\text{CD}_3$ )  $\delta$  1.99 (d, 15 H,  $^4J_{\text{HP}} = 1$  Hz,  $\text{C}_5(\text{CH}_3)_5$ ), 1.42 (q, 6 H,  $^3J_{\text{HH}} = ^2J_{\text{HP}} = 7.8$  Hz,  $\text{P}(\text{CH}_2\text{CH}_3)_3$ ), 0.84 (dt,  $^3J_{\text{HP}} = 16.2$  Hz,  $^3J_{\text{HH}} = 7.8$  Hz,  $\text{P}(\text{CH}_2\text{CH}_3)_3$ );  $^{31}\text{P}\{^1\text{H}\}$  NMR  $\delta$  2.44 (s);  $^{13}\text{C}\{^1\text{H}\}$  NMR  $\delta$  93.5 (s,  $\text{C}_5(\text{CH}_3)_5$ ), 11.29 (s,  $\text{C}_5(\text{CH}_3)_5$ ), 10.37 (s,  $\text{P}(\text{CH}_2\text{CH}_3)_3$ ), 8.25 (s,  $\text{P}(\text{CH}_2\text{CH}_3)_3$ ). Anal. Calcd for  $\text{C}_{17}\text{H}_{30}\text{OPIr}$ : C, 43.2; H, 6.34; P, 6.55. Found: C, 43.4; H, 6.38; P, 6.43.

$(\eta^5\text{-C}_5\text{Me}_5)\text{Ir}(\text{CO})[\text{P}(\text{O-}i\text{-Pr})_3]$ :  $^1\text{H}$  NMR (20 °C,  $\text{C}_6\text{D}_6$ ) 4.69 (d sept, 3 H,  $^3J_{\text{HP}} = 10.1$  Hz,  $^3J_{\text{HH}} = 6.2$  Hz,  $\text{P}(\text{OCH}(\text{CH}_3)_2)_3$ ), 2.08 (d, 15 H,  $^4J_{\text{HP}} = 2.1$  Hz,  $\text{C}_5(\text{CH}_3)_5$ ), 1.22 ppm (d, 18 H,  $^3J_{\text{HH}} = 6.2$  Hz,  $\text{P}(\text{OCH}(\text{CH}_3)_2)_3$ );  $^{13}\text{C}\{^1\text{H}\}$  NMR (20 °C, THF- $d_3$ )  $\delta$  181.07 (d,  $^2J_{\text{CP}} = 23.2$  Hz,  $\text{IrCO}$ ), 95.41 (d,  $^2J_{\text{C}} = 3.8$  Hz,  $\text{C}_5(\text{CH}_3)_5$ ), 70.06 (d,  $^2J_{\text{CP}} = 2.2$  Hz,  $\text{P}(\text{OCH}(\text{CH}_3)_2)_3$ ), 24.23 (s,  $\text{P}(\text{OCH}(\text{CH}_3)_2)_3$ ), 10.95 (s,  $\text{C}_5(\text{CH}_3)_5$ );  $^{31}\text{P}\{^1\text{H}\}$  NMR  $\delta$  97.6 (s); IR (solution, pentane) 1939  $\text{cm}^{-1}$ . Anal. Calcd for  $\text{C}_{20}\text{H}_{36}\text{O}_4\text{PIr}$ : C, 42.7; H, 6.39; P, 5.50. Found: C, 42.5; H, 6.39; P, 5.57.

**Reaction of 1 with  $\text{TICl}_5\text{H}_5$ .** 1 (94 Mg, 0.10 mmol) and 38 mg (0.10 mmol) of freshly sublimed  $\text{TICl}_5\text{H}_5$  were placed in a reactor, and approximately 10 mL of THF was vacuum distilled in at 0 °C. The reaction mixture was stirred at 0 °C, and a precipitate of  $\text{TICl}$  quickly formed. The solvent was removed in vacuo, and the products were extracted with pentane. The products were separated by fractional crystallization and identified as  $(\eta^5\text{-C}_5\text{Me}_5)\text{Ir}(\text{CO})[\text{P}(\text{O-}i\text{-Pr})_3]$  (by its  $^1\text{H}$  and  $^{31}\text{P}\{^1\text{H}\}$  NMR spectra) and  $(\eta^5\text{-C}_5\text{H}_5)\text{Rh}(\text{CO})[\text{P}(\text{O-}i\text{-Pr})_3]$ :  $^1\text{H}$  NMR (20 °C, THF- $d_3$ )  $\delta$  5.28 (dd, 5 H,  $^2J_{\text{HRh}} = ^3J_{\text{HP}} = 0.7$  Hz,  $\text{C}_5\text{H}_5$ ), 4.70 (d sept, 3 H,  $^3J_{\text{HP}} = 10.2$  Hz,  $^3J_{\text{HH}} = 6.2$  Hz,  $\text{P}(\text{OCH}(\text{CH}_3)_2)_3$ ), 1.23 (d, 18 H,  $^3J_{\text{HH}} = 6.2$  Hz,  $\text{P}(\text{OCH}(\text{CH}_3)_2)_3$ );  $^{13}\text{C}\{^1\text{H}\}$  NMR  $\delta$  87.4 (s), 71.5 (s,  $\text{P}(\text{OCH}(\text{CH}_3)_2)_3$ ), 24.3 (s,  $\text{P}(\text{OCH}(\text{CH}_3)_2)_3$ );  $^{31}\text{P}\{^1\text{H}\}$  NMR  $\delta$  137.7 (d,  $J_{\text{PRh}} = 294$  Hz). Anal. Calcd for  $\text{C}_{15}\text{H}_{26}\text{O}_4\text{PRh}$ : C, 44.6; H, 6.43; P, 7.67. Found: C, 44.6; H, 6.40; P, 7.63.

**Reaction of 1 with  $\text{P-}i\text{-Pr}_3$ .** 1 (94 Mg, 0.10 mmol) was dissolved in 10 mL of dry toluene, and the solution was cooled to 0 °C. The  $\text{P-}i\text{-Pr}_3$  (16 mg, 20  $\mu\text{L}$ , 0.10 mmol) was added to this stirred solution via microliter syringe and the system allowed to warm to room temperature. The solvent was removed in vacuo, and the products were crystallized from pentane. The  $\text{ClRh}(\text{CO})(\text{P-}i\text{-Pr}_3)[\text{P}(\text{O-}i\text{-Pr})_3]$  obtained had the two phosphorus nuclei strongly coupled in the  $^{31}\text{P}\{^1\text{H}\}$  NMR spectrum and was therefore assigned a stereochemistry having these two ligands trans to one another:  $^1\text{H}$  NMR ( $-40$  °C,  $\text{C}_6\text{D}_5\text{CD}_3$ ) 5.31 (dd sept, 3 H,  $^3J_{\text{HP}} = 10.1$  Hz,  $^3J_{\text{HH}} = 6.1$  Hz,  $^5J_{\text{HP}} = 3.1$  Hz,  $\text{P}(\text{OCH}(\text{CH}_3)_2)_3$ ), 2.39 (br, 3 H,  $\text{P}(\text{CH}(\text{CH}_3)_2)_3$ ), 1.32 (br d, 18 H,  $^3J_{\text{HH}} = 5.9$  Hz (small HP coupling unresolved),  $\text{P}(\text{CH}(\text{CH}_3)_2)_3$ ), 1.21 ppm (d, 18 H,  $^3J_{\text{HH}} = 6.1$  Hz,  $\text{P}(\text{OCH}(\text{CH}_3)_2)_3$ );  $^{31}\text{P}\{^1\text{H}\}$  NMR  $\delta$  120.9 (dd,  $J_{\text{PRh}} = 199.4$  Hz (phosphite, denoted P),  $^2J_{\text{PP}} = 486.5$  Hz), 45.8 (dd,  $J_{\text{PRh}} = 114$  Hz,  $^2J_{\text{PP}} = 486.5$  Hz (phosphine, P'));  $^{13}\text{C}\{^1\text{H}\}$  NMR  $\delta$  187.6 (ddd,  $^1J_{\text{CRh}} = 74.3$  Hz,  $^2J_{\text{CP}} = 16.1$  Hz,  $^2J_{\text{CP}} = 14.1$  Hz,  $\text{RhCO}$ ), 69.3 (s,  $\text{P}(\text{OCH}(\text{CH}_3)_2)_3$ ), 25.4 (s,  $\text{P}(\text{OCH}(\text{CH}_3)_2)_3$ ), 24.06 (d,  $^2J_{\text{CP}} = 4.3$  Hz,  $\text{P}(\text{CH}(\text{CH}_3)_2)_3$ ), 19.54 (s,  $\text{P}(\text{CH}(\text{CH}_3)_2)_3$ ). Anal. Calcd for  $\text{C}_{19}\text{H}_{42}\text{O}_4\text{P}_2\text{ClRh}$ : C, 42.7; H, 7.86; Cl, 6.64. Found: C, 42.5; H, 7.88; Cl, 6.61.

**X-ray Crystallographic Study<sup>23</sup> of  $(\eta^5\text{-C}_5\text{Me}_5)(\text{OC})[(i\text{-PrO})_3\text{P}]\text{IrRhCl}(\text{CO})[\text{P}(\text{O-}i\text{-Pr})_3]$  (1).** Air-sensitive single crystals of 1 were obtained as described above by isothermal

(22) Busetto, C.; D'Alfonso, A.; Maspero, F.; Perogo, G.; Zazzetta, A. *J. Chem. Soc., Dalton Trans.* 1977, 1828.

(23) See paragraph at end of paper for information regarding supplementary material.

evaporation of a saturated pentane solution at  $-40^\circ\text{C}$ . They are,  $20 \pm 1^\circ\text{C}$ , monoclinic with  $a = 11.463(4)\text{ \AA}$ ,  $b = 15.888(6)\text{ \AA}$ ,  $c = 22.417(6)\text{ \AA}$ ,  $\beta = 99.01(2)^\circ$ , and  $Z = 4$  ( $\mu_a(\text{Mo K}\alpha)^{24a} = 3.871\text{ mm}^{-1}$ ;  $\rho(\text{calcd}) = 1.545\text{ g cm}^{-3}$ ). The systematically absent reflections in the diffraction pattern were those for the uniquely determined centrosymmetric space group  $P2_1/n$  (an alternate setting of  $P2_1/c\text{-C}_{2h}^{5h}$  (no. 14)).<sup>25</sup>

Intensity measurements were made on a Nicolet PI autodiffractometer using  $1.0^\circ$  wide  $\omega$  scans and graphite-monochromated  $\text{Mo K}\alpha$  radiation for a specimen having the shape of a rectangular parallelepiped with dimensions of  $0.25 \times 0.50 \times 0.55\text{ mm}$ . This crystal was glued with epoxy cement to the inside of a thin-walled glass capillary which was then sealed under an  $\text{N}_2$  atmosphere before mounting on a goniometer head with its longest edge nearly parallel to the  $\phi$  axis of the diffractometer. A total of 9247 independent reflections having  $2\theta_{\text{MoK}\alpha} < 55^\circ$  (the equivalent of 1.0 limiting  $\text{Cu K}\alpha$  spheres) were measured in two concentric shells of increasing  $2\theta$ , each of which contained approximately 4600 reflections. A scanning rate of  $8^\circ/\text{min}$  was used to measure intensities for reflections having  $3^\circ \geq 2\theta \geq 43.0^\circ$  and a rate of  $4^\circ/\text{min}$  was used for all others. Each of these  $1.0^\circ$  wide scans were divided into 17 equal (time) intervals, and those 13 continuous intervals which had the highest single accumulated count at their midpoint were used to calculate the net intensity from scanning. Background counts, each lasting for one-fourth the total time used for the net scan (13/17 of the total scan time), were measured at settings  $1.0^\circ$  above and below the calculated  $\text{K}\alpha$  doublet value for each reflection. The intensity data were corrected empirically for variable absorption effects using scans for six reflections having  $2\theta$  between  $11.2^\circ$  and  $34.6^\circ$  (range of relative transmission factors 0.35–1.00) before reducing them to relative squared amplitudes,  $|F_o|^2$ , by means of standard Lorentz and polarization corrections.

The structure was solved by using the "heavy-atom" technique. Counting-statistics weighted cascade block diagonal least-squares refinement which utilized anisotropic thermal parameters for all 43 crystallographically independent non-hydrogen atoms converged to  $R_1$  (unweighted based on  $F$ )<sup>26</sup> = 0.044 and  $R_2$  (weighted, based on  $F$ )<sup>26</sup> = 0.050 for 3169 independent reflections having  $2\theta_{\text{MoK}\alpha} < 43^\circ$  and  $I > 3\sigma(I)$ . A difference Fourier synthesis at this point permitted the location of most of the 57 hydrogen atoms in the asymmetric unit. These difference Fourier positions were used as a starting point for refining the 17 terminal methyl groups as rigid rotors with idealized  $\text{sp}^3$ -hybridized geometry and a C–H bond length of  $0.96\text{ \AA}$ ; the final orientation of each group was determined by three variable rotational parameters. The re-

maining hydrogen atoms were included in subsequent structure factor calculations as idealized atoms (assuming  $\text{sp}^3$  hybridization of the carbon and a C–H bond length of  $0.96\text{ \AA}$ ) "riding" on their respective carbon atoms. The isotropic thermal parameter of each hydrogen atom was fixed at 1.2 times the equivalent isotropic thermal parameter of the carbon atom to which it is covalently bonded. All additional least-squares refinement cycles employed cascade block diagonal techniques and weights derived from counting statistics; hydrogen atoms were modeled with isotropic thermal parameters and non-hydrogen atoms with anisotropic thermal parameters. Additional refinement cycles for 1 gave  $R_1 = 0.038$  and  $R_2 = 0.041$  with 3169 reflections. The final cycles of weighted cascade block diagonal least-squares refinement employed the more complete ( $2\theta_{\text{MoK}\alpha} < 55^\circ$ ) data set and a least-squares refineable extinction correction<sup>27</sup> and gave  $R_1 = 0.045$  and  $R_2 = 0.056$  for 5093 independent absorption-corrected reflections having  $2\theta_{\text{MoK}\alpha} < 55^\circ$  and  $I > 3\sigma(I)$ .

All the structure factor calculations employed recent tabulations of atomic form factors<sup>24b</sup> and anomalous dispersion corrections<sup>24c</sup> to the scattering factors of the Ir, Rh, Cl, and P atoms. All calculations were performed on a Data General Eclipse S-200 computer with 64K of 16-bit words, a floating point processor for 32- and 64-bit arithmetic, and versions of the Nicolet E-XTL or SHELXTL interactive crystallography software package as modified at The Crystallography Co.

**Acknowledgment.** We wish to acknowledge the generous support of the National Science Foundation Grant No. CHE 8307159 for this research. Additionally, A.A.D.P. wishes to acknowledge the support of the NSF in the form of a predoctoral fellowship.

**Registry No.** 1, 99643-13-7;  $(\mu\text{-Cl})\text{Rh}(\text{C}_2\text{H}_4)_2$ , 12081-16-2;  $(\mu\text{-Cl})\text{Rh}[\text{P}(\text{Ome})_3]_2$ , 49634-27-7;  $(\mu\text{-Cl})\text{Rh}[\text{P}(\text{OEt})_3]_2$ , 65363-82-8;  $(\mu\text{-Cl})\text{Rh}[\text{P}(\text{O-}i\text{-Pr})_3]_2$ , 65363-84-0;  $(\mu\text{-Cl})\text{Rh}[\text{P}(\text{OPh})_3]_2$ , 25966-16-9;  $(\mu\text{-Br})\text{Rh}[\text{P}(\text{O-}i\text{-Pr})_3]_2$ , 99643-14-8;  $(\mu\text{-I})\text{Rh}[\text{P}(\text{O-}i\text{-Pr})_3]_2$ , 99643-15-9; *trans*- $\text{ClRh}(\text{C}_2\text{H}_4)(\text{P-}i\text{-Pr})_2$ , 65165-43-7;  $(\eta^5\text{-C}_5\text{Me}_5)\text{Ir}(\text{CO})_2$ , 32660-96-1;  $(\eta^5\text{-C}_5\text{Me}_5)\text{Ir}(\text{CO})\text{P}(\text{Ome})_3$ , 99655-33-1;  $(\eta^5\text{-C}_5\text{Me}_5)\text{Ir}(\text{CO})\text{Pet}_3$ , 99643-16-0;  $(\eta^5\text{-C}_5\text{Me}_5)\text{Ir}(\text{CO})[\text{P}(\text{O-}i\text{-Pr})_3]$ , 99643-17-1;  $\text{TiC}_5\text{H}_5$ , 34822-90-7;  $(\text{C}_5\text{H}_5)\text{Rh}(\text{CO})[\text{P}(\text{O-}i\text{-Pr})_3]$ , 99643-18-2; *trans*- $\text{ClRh}(\text{CO})(\text{P-}i\text{-Pr})_3[\text{P}(\text{O-}i\text{-Pr})_3]$ , 99643-19-3; Ir, 7439-88-5; Rh, 7440-16-6.

**Supplementary Material Available:** Crystal structure analysis report, Table III, hydrogen atom coordinates, Table V, bond lengths and angles, and a listing of structure factors for  $(\eta^5\text{-C}_5\text{Me}_5)(\text{OC})[(i\text{-PrO})_3\text{P}]\text{IrRhCl}(\text{CO})[\text{P}(\text{O-}i\text{-Pr})_3]$  (32 pages). Ordering information is given on any current masthead page.

(24) (a) "International Tables for X-Ray Crystallography"; Kynoch Press: Birmingham, England, 1974; Vol. IV, pp 55–66. (b) *Ibid.*, pp 99–101. (c) *Ibid.*, pp 149–150.

(25) "International Tables for X-Ray Crystallography"; Kynoch Press: Birmingham, England, 1969; Vol. 1, p 99.

(26) The  $R$  values are defined as  $R_1 = \sum ||F_o| - |F_c|| / \sum |F_o|$  and  $R_2 = \{\sum w(|F_o| - |F_c|)^2 / \sum w|F_o|^2\}^{1/2}$  where  $w$  is the weight assigned to each reflection. The function which is minimized is  $\sum w(|F_o| - K|F_c|)^2$ .  $K$  is the scale factor.

(27) Larson, A. C. *Acta Crystallogr.* 1967, 23, 664.

(28) In this paper the periodic group notation in parentheses is in accord with recent actions by IUPAC and ACS nomenclature committees. A and B notation is eliminated because of wide confusion. Groups IA and IIA become groups 1 and 2. The d-transition elements comprise groups 3 through 12, and the p-block elements comprise groups 13 through 18. (Note that the former Roman number designation is preserved in the last digit of the new numbering: e.g., III  $\rightarrow$  3 and 13.)



# Communications

## Carbonyl Substitution and Ring Slippage upon Reaction of Trialkylphosphines with (Fulvalene)diruthenium Tetracarbonyl. X-ray Structural Analysis of $(\eta^0:\eta^4\text{-C}_{10}\text{H}_8)\text{Ru}(\text{PMe}_3)_2\text{CO}$ and Fluxional Behavior of $(\eta^5:\eta^5\text{-C}_{10}\text{H}_8)\text{Ru}_2(\text{CO})_3\text{L}$ (L = Phosphine)

Roland Boese,<sup>†</sup> William B. Tolman, and K. Peter C. Vollhardt<sup>\*‡</sup>

Department of Chemistry, University of California, Berkeley and the Materials and Molecular Research Division Lawrence Berkeley Laboratory Berkeley, California 94720 and the Institut für Anorganische Chemie Universität Essen-GHS

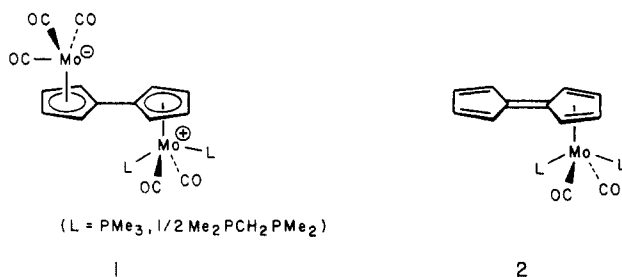
D-4300 Essen-1, Postfach 103764, West Germany

Received September 30, 1985

**Summary:** Treatment of  $(\eta^5:\eta^5\text{-fulvalene})\text{diruthenium}$  tetracarbonyl [ $\text{FvRu}_2(\text{CO})_4$ , **3**] with a large excess (8–10 equiv) of  $\text{PMe}_3$  at 120 °C provides *trans*- $\text{Ru}(\text{CO})_3(\text{PMe}_3)_2$  (**7**) and  $\text{FvRu}(\text{PMe}_3)_2(\text{CO})$  (**6**), in which only one Cp ring is bonded to Ru. Complex **6** was characterized by X-ray crystallography: orthorhombic,  $a = 1464.3$  (4) pm,  $b = 1535.1$  (2) pm,  $c = 1691.6$  (4) pm, space group *Pbca*. Reaction of **3** with 2–3 equiv of  $\text{PMe}_3$  or excess (5 equiv)  $\text{PEt}_3$  gives  $\text{FvRu}_2(\text{CO})_3\text{L}$  (**4**, **5**). Both substitution products are fluxional on the NMR time scale and a mechanism involving reversible terminal to bridged carbonyl exchange is proposed. Activation parameters for the process were determined from a line-shape analysis of variable-temperature  $^{13}\text{C}$  NMR spectra of  $^{13}\text{C}$ -labeled **5**.

The ligand-induced cyclopentadienyl (Cp) ring slippage reaction has only recently been unambiguously established.<sup>1</sup> We have been interested in the chemistry of carbonyl  $(\eta^5:\eta^5\text{-fulvalene})\text{dimetal}$  ( $\text{FvM}_2$ ) complexes,<sup>2</sup> in which linked Cps bridge the two metals. We have reported on the reaction of strongly donating phosphines ( $\text{PMe}_3$ ,  $\text{Me}_2\text{PCH}_2\text{PMe}_2$ ) with  $\text{FvMo}_2(\text{CO})_6$ .<sup>2d</sup> The initial product, the novel dinuclear organometallic zwitterion **1** (characterized by X-ray analysis), was found to convert further with phosphines to yield compounds **2** (characterized spectroscopically), which contain a fulvalene ligand with an uncomplexed Cp ring. Here we report the thermal reactions of trialkylphosphines ( $\text{PR}_3$ ; R = Me, Et) with  $\text{FvRu}_2(\text{CO})_4$  (**3**)<sup>2a</sup> to give the substitution products **4** and **5** as well as the decomplexed system  $\text{FvRu}(\text{PMe}_3)_2\text{CO}$  (**6**), the first of its kind to have been characterized by an X-ray structural investigation.

Whereas  $\text{FvMo}_2(\text{CO})_6$  readily reacts with  $\text{PMe}_3$  at room temperature<sup>2d</sup> to give **1**, **3** transforms only under more vigorous conditions (8–10 equiv of  $\text{PMe}_3$ , ~0.3 M, 120 °C, THF, sealed tube, 22 h) to give two major products, *trans*- $\text{Ru}(\text{PMe}_3)_2(\text{CO})_3$  (**7**)<sup>3</sup> and **6** (1:1, 89% yield),<sup>4</sup> and a small amount (<5%) of  $\text{FvRu}_2(\text{CO})_3(\text{PMe}_3)$  (**4**)<sup>4</sup> (Scheme



I). When the reaction was monitored by  $^1\text{H}$  NMR spectroscopy, only starting material and products were observed; there was no evidence for the expected<sup>2d</sup> zwitterion [ $\text{Fv}[\text{Ru}(\text{CO})_2][\text{Ru}(\text{PMe}_3)_2\text{CO}^+]$ . To test whether **4** is an intermediate in the formation of **6**, **4** was subjected to the same reaction conditions and did indeed give **6**, albeit at a lower rate (50% conversion after 22 h;  $^1\text{H}$  NMR). Moreover, in addition to **6**,  $\text{Ru}(\text{PMe}_3)_3(\text{CO})_2$  (**8**)<sup>4</sup> formed instead of **7**, indicating that **4** cannot be a primary intermediate between **3** and **6**.

Compound **6** can be formulated as a  $\text{Ru}(\text{O})$  diene complex (a, Scheme I) or, in the other extreme, as a dipolar species (b) containing a cyclopentadienide ring and a cationic  $\text{Ru}(\text{II})$  fragment. The average position of the uncomplexed ring resonances in the  $^{13}\text{C}$  NMR spectrum (120 ppm) is intermediate between those of fulvalene (135 ppm)<sup>5</sup> and the cyclopentadienide anion (103 ppm),<sup>6</sup> suggesting contributions from both resonance forms. In addition, the observation of facile H–D exchange (room temperature, acetone- $d_6$ ) into the uncomplexed ring supports a significant contribution of **6b**. Because of its novelty, an X-ray structural investigation was performed on **6**<sup>4</sup> (Figure 1).

The intermediate nature of **6** between extremes **6a** and **6b** is also reflected in its structural details. Consistent with a  $\text{Ru}(\text{O})$  diene complex, the atoms C(2), C(3), C(4), and C(5) are within a plane with C(1) 15 pm above it and with an envelope angle of 8.3°. There is a slip of 19 pm of Ru(1) toward C(3) and C(4) relative to the idealized midpoint of the coordinated ring. Consequently the Ru(1)–C(1) bond is the longest ruthenium–carbon bond of the ring. The planar noncoordinated Cp and the plane C(1), C(2), C(5) are close to coplanar with a twist angle of 6.2°. Additionally, the C(1)–C(6) bond length (142.7 pm) is shorter than a C–C single bond. Nevertheless, in a pure diene

(1) Casey, C. P.; O'Connor, J. M.; Haller, K. J. *J. Am. Chem. Soc.* **1985**, *107*, 1241 and references therein.

(2) (a) Vollhardt, K. P. C.; Weidman, T. W. *J. Am. Chem. Soc.* **1983**, *105*, 1676; *Organometallics* **1984**, *3*, 82. (b) Drage, J. S.; Tilset, M.; Vollhardt, K. P. C.; Weidman, T. W. *Organometallics* **1984**, *3*, 812. (c) Drage, J. S.; Vollhardt, K. P. C. *Ibid.* **1985**, *4*, 191, and in press. (d) Tilset, M.; Vollhardt, K. P. C. *Ibid.*, in press.

(3) Jones, R. A.; Wilkinson, G.; Galas, A. M. R.; Hursthouse, M. B.; Malik, K. M. A. *J. Chem. Soc., Dalton Trans.* **1980**, 1771.

(4) All new compounds gave satisfactory spectral and analytical data (see supplementary material). X-ray determination of **6**: crystal size 0.32 × 0.27 × 0.20 mm, orthorhombic Laue symmetry, space group *Pbca*,  $a = 1464.3$  (4) pm,  $b = 1535.1$  (2) pm,  $c = 1691.6$  (4) pm,  $\alpha = \beta = \gamma = 90^\circ$ ,  $V = 3.803$  (1) × 10<sup>9</sup> pm<sup>3</sup>,  $\mu_{\text{calcd}} = 9.71 \text{ cm}^{-1}$ ,  $d_{\text{calcd}} = 1.43 \text{ g cm}^{-3}$ , radiation Mo K $\alpha$  ( $\lambda = 0.71073 \text{ \AA}$ ), scan range  $3^\circ \leq 2\theta \leq 65^\circ$ , reflections collected 6667, unique 3486 with  $F_o \geq 2.5\sigma(F)$  empirical absorption correlation applied,  $R = 0.051$ ,  $R_w = 0.044$ .

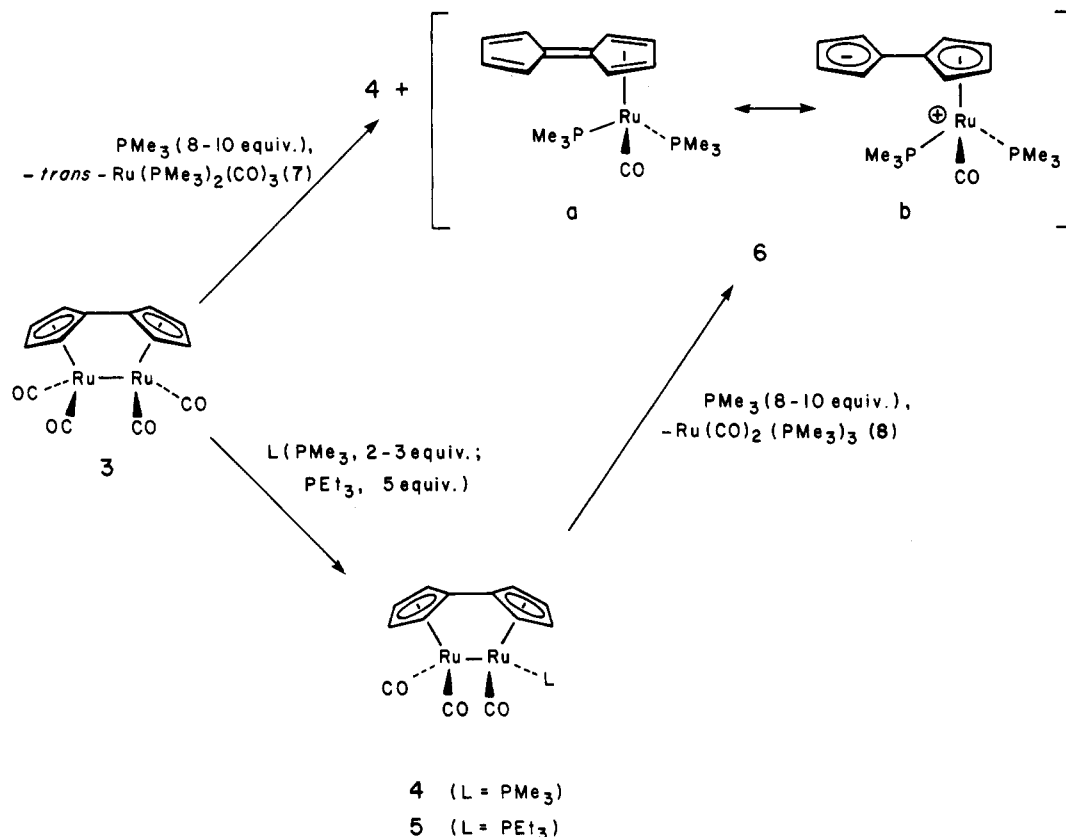
(5) Rutsch, W.; Escher, A.; Neuenschwander, M. *Chimia* **1983**, *37*, 160.

(6) Spiessicke, H.; Schneider, W. G. *Tetrahedron Lett.* **1961**, 468.

<sup>†</sup> Universität Essen-GHS.

<sup>‡</sup> University of California, Berkeley.

Scheme I



Scheme II

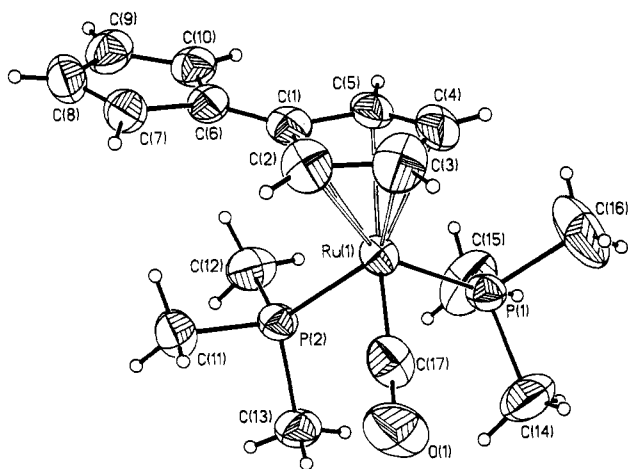
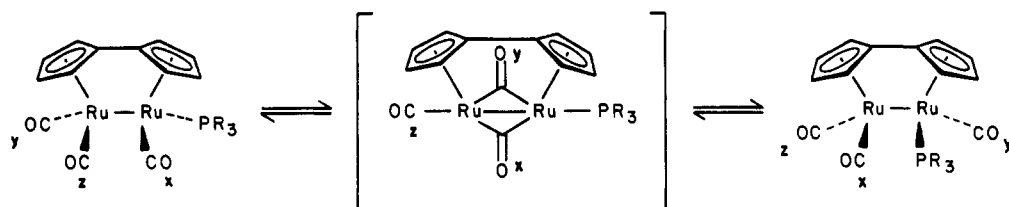


**Figure 1.** SHELXTL drawing of 6. Ellipsoids are scaled to represent the 50% probability surface.

complex, the C-C distances would have been expected to show greater alternation.<sup>7</sup> Similar to ring slippage in ordinary Cp complexes, that in 3 is reversible leading to new heterobimetallic fulvalenes.<sup>2d,5</sup>

Table I. Selected Bond Distances in 6 (pm)

Ru(1)-C(1)	242.8 (4)	C(1)-C(6)	142.7 (5)
Ru(1)-C(2)	225.6 (4)	C(1)-C(2)	142.7 (6)
Ru(1)-C(5)	227.3 (4)	C(1)-C(5)	143.3 (6)
Ru(1)-C(4)	220.6 (4)	C(2)-C(3)	141.3 (8)
Ru(1)-C(3)	219.9 (5)	C(4)-C(5)	142.0 (7)
Ru(1)-C(17)	183.7 (4)	C(3)-C(4)	138.0 (8)
Ru(1)-P(1)	231.1 (1)	C(6)-C(7)	142.0 (5)
Ru(1)-P(2)	231.1 (1)	C(6)-C(10)	141.4 (6)
C(17)-O(1)	115.3 (5)	C(7)-C(8)	135.8 (7)
P-C(av)	180.3	C(9)-C(10)	138.1 (7)
		C(8)-C(9)	139.1 (7)

Reaction of 3 with  $\text{PMe}_3$  (2-3 equiv,  $\sim 0.1 \text{ M}$ ,  $120^\circ\text{C}$ ) or  $\text{PEt}_3$  (5 equiv,  $\sim 0.2 \text{ M}$ ,  $120^\circ\text{C}$ ) gave moderate yields of 4 (44%) and 5 (58%), respectively.<sup>4</sup> Their room-temperature  $^1\text{H}$  NMR spectra exhibit only four multiplets in the Fv region instead of the expected eight, suggesting fluxional behavior. Indeed, at  $-78^\circ\text{C}$  significant broadening of the three lowest field peaks and the splitting of the fourth into two multiplets was observed.

A possible explanation for this finding might be the exchange of two carbonyl ligands between the two metals via pairwise shifts between terminal and bridged bonding modes<sup>9</sup> (Scheme II), as observed for cyclopentadienylmetal

(7) Compare to the structures of  $\eta^4$ - and  $\eta^6$ -fulvene complexes: Edelman, F.; Lubke, B.; Behrens, M. *Chem. Ber.* 1982, 115, 1325; 1984, 117, 3463. Dauter, Z.; Hansen, L. K.; Mawby, R. J.; Probits, E. J.; Reynolds, C. D. *Acta Crystallogr., Sect. C: Cryst. Struct. Commun.* 1985, C41, 850 and references therein.

(8) Huffman, M. A.; Newman, D. A.; Tilstet, M.; Tolman, W. B.; Vollhardt, K. P. C., to be submitted for publication.

carbonyl dimers.<sup>9,10</sup> An important consequence of this mechanism is that only two of the carbonyls (*x* and *y*, Scheme II) exchange between the two metals while the third (*z*) remains terminally bound in a position "trans" to the phosphine. Thus, in the <sup>13</sup>C NMR spectrum, carbonyl *x* and *y* should give rise to a singlet and a doublet ( $J_{CP}$ ) at the low-temperature limit and to a doublet ( $J \approx 1/2 J_{CP}$ ) at high temperature, while carbonyl *z* should remain a singlet throughout. Confirmation of these predictions was accomplished by acquisition of variable-temperature (-75 °C to +55 °C) <sup>13</sup>C NMR data for <sup>13</sup>CO-labeled **5**.<sup>11</sup> Line-shape analysis<sup>12</sup> of the four spin system, assuming exchange between only two spins as dictated by the proposed mechanism, allowed calculation of the activation parameters for the fluxional process:  $\Delta G^\ddagger_{298} = +12.0$  (1) kcal mol<sup>-1</sup>,  $\Delta H^\ddagger = +8.8$  (2) kcal mol<sup>-1</sup>, and  $\Delta S^\ddagger = -10.6$  (1.0) eu.

A bridging dicarbonyl intermediate or transition state of the type depicted in Scheme II has never been observed in any of the other known carbonyl FvM<sub>2</sub> complexes, unlike the situation encountered in the Cp<sub>2</sub>M<sub>2</sub>(CO)<sub>4</sub> (M = Fe, Ru) dimers where it is thermodynamically stable.<sup>10a</sup>

**Acknowledgment.** This work was supported by the Director, Office of Energy Research, Office of Basic Energy Sciences, Chemical Sciences Division of the U.S. Department of Energy, under Contract DE-AC03-76SF00098. W.B.T. is the recipient of a W. R. Grace Fellowship (1984-1985) and K.P.C.V. is a Miller Research Professor in Residence (1985-1986). Support from Nicolet Instruments, Madison, WI, is gratefully acknowledged by R.B. as well as the assistance of D. Bläser (University of Essen).

**Supplementary Material Available:** Listings of positional and thermal parameters, bond lengths and angles, and structure factors of **6**, variable-temperature <sup>13</sup>C NMR spectra of <sup>13</sup>CO-labeled **5**, and melting point, spectral, and analytical data on **4-6** and **8** (48 pages). Ordering information is given on any current masthead page.

(9) Adams, R. D.; Cotton, F. A. *J. Am. Chem. Soc.* **1973**, *95*, 6589.

(10) (a) Gansow, O. A.; Burke, A. R.; Vernon, W. D. *J. Am. Chem. Soc.* **1976**, *98*, 5817. (b) Haines, R. J.; DuPreez, A. L. *Inorg. Chem.* **1969**, *8*, 1459. Adams, R. D.; Brice, M.; Cotton, F. A. *J. Am. Chem. Soc.* **1973**, *95*, 6594. Kirchner, R. M.; Marks, T. J.; Kristoff, J. S.; Ibers, J. A. *Ibid.* **1973**, *95*, 6602. Howell, J. A. S.; Rowan, A. J. *J. Chem. Soc., Dalton Trans.* **1980**, 1845.

(11) <sup>13</sup>CO-labeled **5** was prepared via the reaction of PEt<sub>3</sub> with <sup>13</sup>CO-labeled **3**, which was in turn synthesized from the reaction of <sup>13</sup>CO with **3** (50 psi of <sup>13</sup>CO, 130 °C, THF, 50 h, approximately 20% incorporation by IR and <sup>13</sup>C NMR).

(12) Line-shape analysis was performed at the UCB Computer Center using DYNAMAR, a modified version of a program developed by: Meakin, P.; Muettterties, E. L.; Tebbe, F. N.; Jesson, J. P. *J. Am. Chem. Soc.* **1971**, *93*, 4701. Jesson, J. P.; Meakin, P. *Acc. Chem. Res.* **1973**, *6*, 269. Data were plotted according to the Eyring equation  $\ln(nhk/k_0T) = -\Delta H^\ddagger/RT + S^\ddagger/R$  and fitted to a straight line using linear least-squares program ACTPAR, a modified version of a program developed by: Binsch, G.; Kessler, H. *Angew. Chem., Int. Ed. Engl.* **1980**, *19*, 411.

## Reaction of a $\mu$ -Ethenylidene Diron Complex with Ethyl Diazoacetate

Charles P. Casey\* and Edwin A. Austin

Department of Chemistry, University of Wisconsin  
Madison, Wisconsin 53706

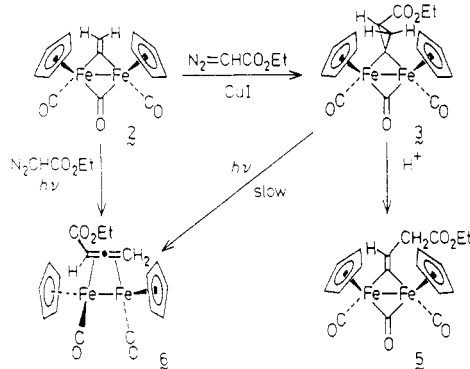
Received October 8, 1985

**Summary:** The  $\mu$ -ethenylidene complex [(C<sub>5</sub>H<sub>5</sub>)(CO)-Fe]<sub>2</sub>( $\mu$ -C=CH<sub>2</sub>) (**2**) reacted with ethyl diazoacetate in the presence of CuI to produce the cyclopropylidene com-

plex [(C<sub>5</sub>H<sub>5</sub>)(CO)Fe]<sub>2</sub>( $\mu$ -CO)( $\mu$ -CCH<sub>2</sub>CHCO<sub>2</sub>Et) (**3**). Cyclopropylidene complex **3** underwent acid-catalyzed ring opening to give  $\mu$ -alkenylidene compound [(C<sub>5</sub>H<sub>5</sub>)(CO)-Fe]<sub>2</sub>( $\mu$ -C=CHCH<sub>2</sub>CO<sub>2</sub>Et) (**5**). Photolysis of **2** and ethyl diazoacetate gave the allene complex [(C<sub>5</sub>H<sub>5</sub>)(CO)Fe]<sub>2</sub>( $\mu$ -CH<sub>2</sub>=C=CHCO<sub>2</sub>Et) (**6**).

For the past several years, we have been studying new carbon-carbon bond-forming reaction of diiron complexes with bridging hydrocarbon ligands. We discovered the addition of the C-H bond of the cationic bridging methylydene complex [(C<sub>5</sub>H<sub>5</sub>)(CO)Fe]<sub>2</sub>( $\mu$ -CO)( $\mu$ -CH)<sup>+</sup> (**1**) across the carbon-carbon double bond of alkenes which produces new  $\mu$ -alkylidene complexes.<sup>1,2</sup> We have also found that neutral  $\mu$ -alkenylidene complexes (in equilibrium with cationic  $\mu$ -alkylidene complexes) condense with aldehydes under acidic conditions to produce vinylcarbyne diiron complexes.<sup>3</sup> Hoel's recent report<sup>4</sup> of the copper-catalyzed cyclopropanation of the  $\mu$ -ethenylidene complex (C<sub>5</sub>H<sub>5</sub>)<sub>2</sub>(CO)<sub>2</sub>Fe<sub>2</sub>( $\mu$ -CO)( $\mu$ -C=CH<sub>2</sub>) (**2**) with diazomethane sparked our interest in the reactions of diazoesters with  $\mu$ -alkenylidene complexes. Here we report three different selective reaction pathways for the reaction of  $\mu$ -ethenylidene complex **2** with ethyl diazoacetate that lead to bridging cyclopropylidene, alkenylidene, and allene complexes.

Ethenylidene complex **2** reacts with ethyl diazoacetate only in the presence of a copper catalyst or upon photolysis. Ethenylidene complex **2** (250 mg, 0.71 mmol), excess ethyl diazoacetate (2.8 mmol), and CuI (1.3 mmol) were heated in 50 mL of refluxing CH<sub>2</sub>Cl<sub>2</sub> for 19 h. After filtration and evaporation of solvent the oily residue was crystallized from hexane-CH<sub>2</sub>Cl<sub>2</sub> to give a single isomer of the cyclopropylidene complex **3** (185 mg, 60%).<sup>5</sup> In the <sup>1</sup>H NMR of **3**, the ABC pattern of the cyclopropane hydrogens ( $J_{cis} = 8.0$  Hz,  $J_{trans} = 4.5$  Hz,  $J_{gem} = -8.5$  Hz) helped to establish the structure of **3**. In the IR spectrum



(1) Casey, C. P.; Fagan, P. J. *J. Am. Chem. Soc.* **1982**, *104*, 4950.

(2) Casey, C. P.; Fagan, P. J.; Miles, W. H.; Marder, S. R. *J. Mol. Catal.* **1983**, *21*, 173.

(3) Casey, C. P.; Konings, M. S.; Palermo, R. E.; Colborn, R. E. *J. Am. Chem. Soc.* **1985**, *107*, 5296.

(4) Hoel, E. L.; Ansell, G. B.; Leta, S. *Organometallics* **1984**, *3*, 1633.

(5) **3**, major isomer: <sup>1</sup>H NMR (acetone-*d*<sub>6</sub>, 270 MHz)  $\delta$  4.84 (s, C<sub>5</sub>H<sub>5</sub>), 4.80 (s, C<sub>5</sub>H<sub>5</sub>), 4.05 (dq,  $J = 11.0, 7.2$  Hz, OCHHCH<sub>3</sub>), 3.94 (dq,  $J = 11.0, 7.2$  Hz, OCHHCH<sub>3</sub>), 2.67 (dd,  $J = 8.0, 4.5$  Hz, CHCO<sub>2</sub>Et), 2.56 (dd,  $J = -8.5, 8.0$  Hz, CHHCHCO<sub>2</sub>Et), 2.53 (dd,  $J = -8.5, 4.5$  Hz, CHHCO<sub>2</sub>Et), 1.13 (t,  $J = 7.2$  Hz, CH<sub>3</sub>). <sup>13</sup>C NMR (acetone-*d*<sub>6</sub>, 0.07 M Cr(acac)<sub>3</sub>, 50.1 MHz)  $\delta$  269.9 ( $\mu$ -CO), 213.0 (CO), 212.3 (CO), 175.2 (CO<sub>2</sub>), 155.9 ( $\mu$ -C), 89.8 (d,  $J = 183$  Hz, C<sub>5</sub>H<sub>5</sub>), 89.5 (d,  $J = 180$  Hz, C<sub>5</sub>H<sub>5</sub>), 5.97 (t,  $J = 148$  Hz, CH<sub>2</sub>CH<sub>3</sub>), 34.0 (t,  $J = 165$  Hz, CCH<sub>2</sub>CH), 32.7 (d,  $J = 170$  Hz, CHCO<sub>2</sub>Et), 14.3 (q,  $J = 125$  Hz, CH<sub>3</sub>); IR (CH<sub>2</sub>Cl<sub>2</sub>) 1999 (s), 1957 (m), 1788 (m), 1704 (m) cm<sup>-1</sup>; HRMS calcd for C<sub>19</sub>H<sub>18</sub>Fe<sub>2</sub>O<sub>3</sub> 437.9847, found 437.9852.

**4**, minor isomer: <sup>1</sup>H NMR (acetone-*d*<sub>6</sub>, 270 MHz)  $\delta$  4.75 (s, C<sub>5</sub>H<sub>5</sub>), 4.70 (s, C<sub>5</sub>H<sub>5</sub>), 4.14 (m, OCH<sub>2</sub>), 2.95 (dd,  $J = 8.5, 4.9$  Hz, 1 H), 2.48 (dd,  $J = 8.5, 4.9$  Hz, 1 H), 2.37 (t,  $J = 8.5$  Hz, 1 H), 1.20 (t,  $J = 6.8$  Hz, CH<sub>3</sub>).

carbonyl dimers.<sup>9,10</sup> An important consequence of this mechanism is that only two of the carbonyls (*x* and *y*, Scheme II) exchange between the two metals while the third (*z*) remains terminally bound in a position "trans" to the phosphine. Thus, in the <sup>13</sup>C NMR spectrum, carbonyl *x* and *y* should give rise to a singlet and a doublet ( $J_{CP}$ ) at the low-temperature limit and to a doublet ( $J \approx 1/2 J_{CP}$ ) at high temperature, while carbonyl *z* should remain a singlet throughout. Confirmation of these predictions was accomplished by acquisition of variable-temperature (-75 °C to +55 °C) <sup>13</sup>C NMR data for <sup>13</sup>CO-labeled **5**.<sup>11</sup> Line-shape analysis<sup>12</sup> of the four spin system, assuming exchange between only two spins as dictated by the proposed mechanism, allowed calculation of the activation parameters for the fluxional process:  $\Delta G^\ddagger_{298} = +12.0$  (1) kcal mol<sup>-1</sup>,  $\Delta H^\ddagger = +8.8$  (2) kcal mol<sup>-1</sup>, and  $\Delta S^\ddagger = -10.6$  (1.0) eu.

A bridging dicarbonyl intermediate or transition state of the type depicted in Scheme II has never been observed in any of the other known carbonyl FvM<sub>2</sub> complexes, unlike the situation encountered in the Cp<sub>2</sub>M<sub>2</sub>(CO)<sub>4</sub> (M = Fe, Ru) dimers where it is thermodynamically stable.<sup>10a</sup>

**Acknowledgment.** This work was supported by the Director, Office of Energy Research, Office of Basic Energy Sciences, Chemical Sciences Division of the U.S. Department of Energy, under Contract DE-AC03-76SF00098. W.B.T. is the recipient of a W. R. Grace Fellowship (1984-1985) and K.P.C.V. is a Miller Research Professor in Residence (1985-1986). Support from Nicolet Instruments, Madison, WI, is gratefully acknowledged by R.B. as well as the assistance of D. Bläser (University of Essen).

**Supplementary Material Available:** Listings of positional and thermal parameters, bond lengths and angles, and structure factors of **6**, variable-temperature <sup>13</sup>C NMR spectra of <sup>13</sup>CO-labeled **5**, and melting point, spectral, and analytical data on **4-6** and **8** (48 pages). Ordering information is given on any current masthead page.

(9) Adams, R. D.; Cotton, F. A. *J. Am. Chem. Soc.* **1973**, *95*, 6589.

(10) (a) Gansow, O. A.; Burke, A. R.; Vernon, W. D. *J. Am. Chem. Soc.* **1976**, *98*, 5817. (b) Haines, R. J.; DuPreez, A. L. *Inorg. Chem.* **1969**, *8*, 1459. Adams, R. D.; Brice, M.; Cotton, F. A. *J. Am. Chem. Soc.* **1973**, *95*, 6594. Kirchner, R. M.; Marks, T. J.; Kristoff, J. S.; Ibers, J. A. *Ibid.* **1973**, *95*, 6602. Howell, J. A. S.; Rowan, A. J. *J. Chem. Soc., Dalton Trans.* **1980**, 1845.

(11) <sup>13</sup>CO-labeled **5** was prepared via the reaction of PEt<sub>3</sub> with <sup>13</sup>CO-labeled **3**, which was in turn synthesized from the reaction of <sup>13</sup>CO with **3** (50 psi of <sup>13</sup>CO, 130 °C, THF, 50 h, approximately 20% incorporation by IR and <sup>13</sup>C NMR).

(12) Line-shape analysis was performed at the UCB Computer Center using DYNAMAR, a modified version of a program developed by: Meakin, P.; Muettterties, E. L.; Tebbe, F. N.; Jesson, J. P. *J. Am. Chem. Soc.* **1971**, *93*, 4701. Jesson, J. P.; Meakin, P. *Acc. Chem. Res.* **1973**, *6*, 269. Data were plotted according to the Eyring equation  $\ln(nhk/k_0T) = -\Delta H^\ddagger/RT + S^\ddagger/R$  and fitted to a straight line using linear least-squares program ACTPAR, a modified version of a program developed by: Binsch, G.; Kessler, H. *Angew. Chem., Int. Ed. Engl.* **1980**, *19*, 411.

## Reaction of a $\mu$ -Ethenylidene Diiron Complex with Ethyl Diazoacetate

Charles P. Casey\* and Edwin A. Austin

Department of Chemistry, University of Wisconsin  
Madison, Wisconsin 53706

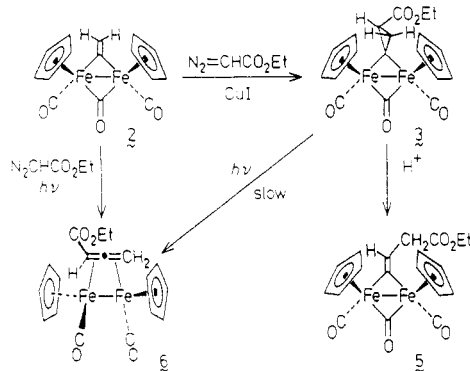
Received October 8, 1985

**Summary:** The  $\mu$ -ethenylidene complex [(C<sub>5</sub>H<sub>5</sub>)(CO)-Fe]<sub>2</sub>( $\mu$ -C=CH<sub>2</sub>) (**2**) reacted with ethyl diazoacetate in the presence of CuI to produce the cyclopropylidene com-

plex [(C<sub>5</sub>H<sub>5</sub>)(CO)Fe]<sub>2</sub>( $\mu$ -CO)( $\mu$ -CCH<sub>2</sub>CHCO<sub>2</sub>Et) (**3**). Cyclopropylidene complex **3** underwent acid-catalyzed ring opening to give  $\mu$ -alkenylidene compound [(C<sub>5</sub>H<sub>5</sub>)(CO)-Fe]<sub>2</sub>( $\mu$ -C=CHCH<sub>2</sub>CO<sub>2</sub>Et) (**5**). Photolysis of **2** and ethyl diazoacetate gave the allene complex [(C<sub>5</sub>H<sub>5</sub>)(CO)Fe]<sub>2</sub>( $\mu$ -CH<sub>2</sub>=C=CHCO<sub>2</sub>Et) (**6**).

For the past several years, we have been studying new carbon-carbon bond-forming reaction of diiron complexes with bridging hydrocarbon ligands. We discovered the addition of the C-H bond of the cationic bridging methylydene complex [(C<sub>5</sub>H<sub>5</sub>)(CO)Fe]<sub>2</sub>( $\mu$ -CO)( $\mu$ -CH)<sup>+</sup> (**1**) across the carbon-carbon double bond of alkenes which produces new  $\mu$ -alkylidene complexes.<sup>1,2</sup> We have also found that neutral  $\mu$ -alkenylidene complexes (in equilibrium with cationic  $\mu$ -alkylidene complexes) condense with aldehydes under acidic conditions to produce vinylcarbyne diiron complexes.<sup>3</sup> Hoel's recent report<sup>4</sup> of the copper-catalyzed cyclopropanation of the  $\mu$ -ethenylidene complex (C<sub>5</sub>H<sub>5</sub>)<sub>2</sub>(CO)<sub>2</sub>Fe<sub>2</sub>( $\mu$ -CO)( $\mu$ -C=CH<sub>2</sub>) (**2**) with diazomethane sparked our interest in the reactions of diazoesters with  $\mu$ -alkenylidene complexes. Here we report three different selective reaction pathways for the reaction of  $\mu$ -ethenylidene complex **2** with ethyl diazoacetate that lead to bridging cyclopropylidene, alkenylidene, and allene complexes.

Ethenylidene complex **2** reacts with ethyl diazoacetate only in the presence of a copper catalyst or upon photolysis. Ethenylidene complex **2** (250 mg, 0.71 mmol), excess ethyl diazoacetate (2.8 mmol), and CuI (1.3 mmol) were heated in 50 mL of refluxing CH<sub>2</sub>Cl<sub>2</sub> for 19 h. After filtration and evaporation of solvent the oily residue was crystallized from hexane-CH<sub>2</sub>Cl<sub>2</sub> to give a single isomer of the cyclopropylidene complex **3** (185 mg, 60%).<sup>5</sup> In the <sup>1</sup>H NMR of **3**, the ABC pattern of the cyclopropane hydrogens ( $J_{cis} = 8.0$  Hz,  $J_{trans} = 4.5$  Hz,  $J_{gem} = -8.5$  Hz) helped to establish the structure of **3**. In the IR spectrum



(1) Casey, C. P.; Fagan, P. J. *J. Am. Chem. Soc.* **1982**, *104*, 4950.

(2) Casey, C. P.; Fagan, P. J.; Miles, W. H.; Marder, S. R. *J. Mol. Catal.* **1983**, *21*, 173.

(3) Casey, C. P.; Konings, M. S.; Palermo, R. E.; Colborn, R. E. *J. Am. Chem. Soc.* **1985**, *107*, 5296.

(4) Hoel, E. L.; Ansell, G. B.; Leta, S. *Organometallics* **1984**, *3*, 1633.

(5) **3**, major isomer: <sup>1</sup>H NMR (acetone-*d*<sub>6</sub>, 270 MHz)  $\delta$  4.84 (s, C<sub>5</sub>H<sub>5</sub>), 4.80 (s, C<sub>5</sub>H<sub>5</sub>), 4.05 (dq,  $J = 11.0, 7.2$  Hz, OCHHCH<sub>3</sub>), 3.94 (dq,  $J = 11.0, 7.2$  Hz, OCHHCH<sub>3</sub>), 2.67 (dd,  $J = 8.0, 4.5$  Hz, CHCO<sub>2</sub>Et), 2.56 (dd,  $J = -8.5, 8.0$  Hz, CHHCHCO<sub>2</sub>Et), 2.53 (dd,  $J = -8.5, 4.5$  Hz, CHHCO<sub>2</sub>Et), 1.13 (t,  $J = 7.2$  Hz, CH<sub>3</sub>). <sup>13</sup>C NMR (acetone-*d*<sub>6</sub>, 0.07 M Cr(acac)<sub>3</sub>, 50.1 MHz)  $\delta$  269.9 ( $\mu$ -CO), 213.0 (CO), 212.3 (CO), 175.2 (CO<sub>2</sub>), 155.9 ( $\mu$ -C), 89.8 (d,  $J = 183$  Hz, C<sub>5</sub>H<sub>5</sub>), 89.5 (d,  $J = 180$  Hz, C<sub>5</sub>H<sub>5</sub>), 5.97 (t,  $J = 148$  Hz, CH<sub>2</sub>CH<sub>3</sub>), 34.0 (t,  $J = 165$  Hz, CCH<sub>2</sub>CH), 32.7 (d,  $J = 170$  Hz, CHCO<sub>2</sub>Et), 14.3 (q,  $J = 125$  Hz, CH<sub>3</sub>); IR (CH<sub>2</sub>Cl<sub>2</sub>) 1999 (s), 1957 (m), 1788 (m), 1704 (m) cm<sup>-1</sup>; HRMS calcd for C<sub>19</sub>H<sub>18</sub>Fe<sub>2</sub>O<sub>5</sub> 437.9847, found 437.9852.

**4**, minor isomer: <sup>1</sup>H NMR (acetone-*d*<sub>6</sub>, 270 MHz)  $\delta$  4.75 (s, C<sub>5</sub>H<sub>5</sub>), 4.70 (s, C<sub>5</sub>H<sub>5</sub>), 4.14 (m, OCH<sub>2</sub>), 2.95 (dd,  $J = 8.5, 4.9$  Hz, 1 H), 2.48 (dd,  $J = 8.5, 4.9$  Hz, 1 H), 2.37 (t,  $J = 8.5$  Hz, 1 H), 1.20 (t,  $J = 6.8$  Hz, CH<sub>3</sub>).

of **3**, an intense band at 1999  $\text{cm}^{-1}$  and a weak band at 1957  $\text{cm}^{-1}$  established the presence of cis terminal carbonyl groups. **3** is most likely the stereoisomer shown since this structure has the ester group in the least congested site. When the conversion of **1** to **3** was followed by NMR, a second diastereomer, **4**,<sup>5</sup> was seen at early times but it was eventually converted to **3**.

Cyclopropylidene complex **3** undergoes regiospecific acid-catalyzed cyclopropane ring opening upon exposure to acidic conditions. For example, attempted chromatography of **3** on silica gel led to isolation of alkylidene complex **5**<sup>6</sup> in 45% yield from **2**. Treatment of **3** with  $\text{HBF}_4$  in diethyl ether also led to ring opening to **5**. This regiospecific ring opening is best explained by initial protonation at the ester carbonyl group.

Photolysis of a solution of **2** (20 mg, 0.57 mmol) and ethyl diazoacetate (3.4 mmol) in  $\text{CH}_2\text{Cl}_2$  at 0 °C for 4 h gave no detectable cyclopropylidene complex **3**. Instead, the only product seen by IR and by  $^1\text{H}$  NMR was the novel allene complex **6**.<sup>7</sup> In the formation of **6**, one CO is lost. The complex contains only terminal CO groups [IR ( $\text{C}-\text{H}_2\text{Cl}_2$ ) 1974 (s), 1921 (s), 1693 (s)  $\text{cm}^{-1}$ ]. In the  $^1\text{H}$  NMR of **6**, the hydrogens on the complexed allene give rise to three separate doublets of doublets at  $\delta$  3.29 ( $J = 1.2, 2.3$  Hz), 3.49 ( $J = 4.1, 2.3$  Hz), and 3.84 ( $J = 4.1, 1.2$  Hz). Related dimanganese,<sup>8</sup> dimolybdenum,<sup>9</sup> and diiron complexes<sup>10</sup> are known.

The possibility that photolysis of **2** and ethyl diazoacetate initially produces cyclopropylidene complex **3** which then photolytically ring opens to give allene complex **6** can be rejected on the basis of two observations. First, during the photolysis of **2** and the diazo ester, none of the cyclopropylidene complex **3** was detected by  $^1\text{H}$  NMR. Second, while photolysis of the cyclopropylidene complex **3** slowly produces allene complex **6**, the rate of conversion of **3** to **6** is much slower than the rate of formation of allene complex **6** from **2**. We suggest that under photolysis **2** loses CO prior to reaction with ethyl diazoacetate to generate a complex containing a carbomethoxy carbene ligand and an ethenylidene ligand which then couple to produce a complexed allene.

**Acknowledgment.** Support from the National Science Foundation is gratefully acknowledged. We thank Dr. Elvin Hoel for keeping us informed of his related studies.

**Registry No.** **2**, 86420-26-0; **3**, 99326-80-4; **4**, 99395-44-5; **5**, 99326-81-5; **6**, 99326-82-6;  $\text{N}_2=\text{CHCO}_2\text{Et}$ , 623-73-4;  $\text{CuI}$ , 7681-65-4.

(6) **5**:  $^1\text{H}$  NMR (acetone- $d_6$ , 270 MHz)  $\delta$  7.16 (dd,  $J = 7.9, 6.8$  Hz,  $\text{C}=\text{CH}$ ), 5.04 (s,  $\text{C}_5\text{H}_5$ ), 4.93 (s,  $\text{C}_5\text{H}_5$ ), 4.16 (q,  $J = 7.1$  Hz,  $\text{OCH}_2$ ), 3.74 (dq,  $J = 15.2, 7.9$  Hz,  $\text{CHCHH}$ ), 3.62 (dq,  $J = 15.2, 6.8$  Hz,  $\text{CHCHH}$ ), 1.26 (t,  $J = 7.1$  Hz,  $\text{CH}_3$ );  $^{13}\text{C}\{^1\text{H}\}$  NMR (acetone- $d_6$ , 0.07 M  $\text{Cr}(\text{acac})_3$ , 50.1 MHz)  $\delta$  270.4 ( $\mu\text{-CO}$ ), 270.1 ( $\mu\text{-C}$ ), 212.7 (CO), 212.5 (CO), 173.3 ( $\text{CO}_2$ ), 131.6 (CH), 89.0 ( $\text{C}_5\text{H}_5$ ), 88.2 ( $\text{C}_5\text{H}_5$ ), 60.6 ( $\text{CH}_2\text{CH}_3$ ), 42.7 ( $\text{CHCH}_2$ ), 14.7 ( $\text{CH}_3$ ); IR ( $\text{CH}_2\text{Cl}_2$ ) 2000 (s), 1962 (m), 1790 (s), 1720 (m)  $\text{cm}^{-1}$ ; HRMS calcd for  $\text{C}_{19}\text{H}_{18}\text{Fe}_2\text{O}_5$  437.9847, found 437.9853.

(7) **6**:  $^1\text{H}$  NMR (acetone- $d_6$ , 200 MHz)  $\delta$  4.39 (s,  $\text{C}_5\text{H}_5$ ), 4.28 (s,  $\text{C}_5\text{H}_5$ ), 4.06 (q,  $J = 7.1$  Hz,  $\text{OCH}_2$ ), 3.84 (dd,  $J = 4.1, 1.2$  Hz, 1 H), 3.49 (dd,  $J = 4.1, 2.3$  Hz, 1 H), 3.29 (dd,  $J = 1.2, 2.3$  Hz, 1 H), 1.24 (t,  $J = 7.2$  Hz,  $\text{CH}_3$ );  $^{13}\text{C}$  NMR (acetone- $d_6$ , 0.07 M  $\text{Cr}(\text{acac})_3$ , 50.1 MHz)  $\delta$  227.8 (CO), 226.5 (CO), 219.3 ( $\mu\text{-C}$ ), 173.2 ( $\text{CO}_2$ ), 83.6 (d,  $J = 176$  Hz,  $\text{C}_5\text{H}_5$ ), 59.9 (t,  $J = 146$  Hz,  $\text{CH}_2\text{CH}_3$ ), 36.2 (t,  $J = 150$  Hz,  $=\text{CH}_2$ ), 34.6 (d,  $J = 168$  Hz,  $=\text{CHCO}_2$ ), 15.0 (q,  $J = 128$  Hz,  $\text{CH}_3$ ); IR ( $\text{CH}_2\text{Cl}_2$ ) 1947 (s), 1921 (s), 1693 (s)  $\text{cm}^{-1}$ ; HRMS calcd for  $\text{C}_{18}\text{H}_{18}\text{Fe}_2\text{O}_4$  409.9904, found 409.9911.

(8) Lewis, L. N.; Huffman, J. C.; Caulton, K. G. *J. Am. Chem. Soc.* **1980**, *102*, 403.

(9) Bailey, W. I., Jr.; Chisholm, M. H.; Cotton, F. A.; Murillo, C. A.; Rankel, L. A. *J. Am. Chem. Soc.* **1978**, *100*, 802. Doherty, N. M.; Eilschenbroich, C.; Kneuper, H.-J.; Knox, S. A. R. *J. Chem. Soc., Chem. Commun.* **1985**, 170.

(10) Hoel, E. L.; Ansell, G. B.; Leta, S. *Organometallics*, following paper in this issue.

## Thermal and Photochemical Rearrangements of a Bridging Cyclopropylidene Ligand to Allene in a Diiron Complex

Elvin L. Hoel,\* Gerald B. Ansell,<sup>†</sup> and Susan Leta<sup>†</sup>

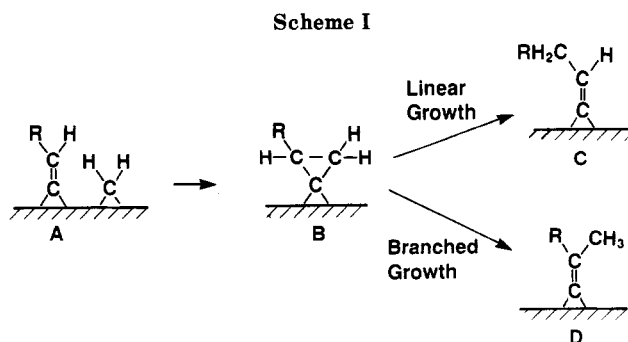
Corporate Research Science Laboratories  
and Analytical Division  
Exxon Research and Engineering Company  
Annandale, New Jersey 08801

Received October 21, 1985

**Summary:** The bridging cyclopropylidene ligand in  $\text{Cp}_2\text{Fe}_2(\text{CO})_2(\mu\text{-CCH}_2\text{CH}_2)$  ( $\text{Cp} = \eta^5\text{-C}_5\text{H}_5$ ) rearranges at 100 °C or photochemically at 10 °C to the thermally unstable allene complex  $\text{Cp}_2\text{Fe}_2(\text{CO})_2(\mu\text{-CH}_2\text{C}=\text{C}=\text{CH}_2)$ . The relevance of this chemistry to a recently proposed Fischer-Tropsch mechanism is discussed.

We recently prepared diiron cyclopropylidene complexes so that the chemistry of the previously unknown cyclopropylidene ligand could be studied as a model for the novel methylene/vinylidene Fischer-Tropsch mechanism proposed by McCandlish (Scheme I).<sup>1</sup> The complexes **1c** and **1t** (with CO and Cp ( $\text{Cp} = \eta^5\text{-C}_5\text{H}_5$ ) ligands cis and trans, respectively, to the plane of the metal atoms and bridging ligands) were prepared by reaction of the corresponding  $\mu$ -vinylidene complexes **2c** and **2t** with diazomethane in the presence of  $\text{CuCl}$ ,<sup>2</sup> a synthesis formally equivalent to  $\text{A} \rightarrow \text{B}$ . We find that the thermal and photochemistry of **1** do not support the proposed mechanism; however, as detailed in the accompanying communication, hydrocarbon chains can be grown via cyclopropylidene intermediates by using protonation/deprotonation chemistry to effect the rearrangement of the homologous vinylidene ligand.<sup>3</sup>

Solutions of **1c** or **1t** in octane were heated under argon and the course of reaction was followed by IR spectroscopy. The first observed change was interconversion of the cis and trans isomers, beginning at about 60 °C. An equilibrium appeared to be established after about 30 min at 80 °C. At about 100 °C two new peaks, subsequently identified as belonging to **3** (see below), began to show at 1939 (m) and 1919 (s)  $\text{cm}^{-1}$ . At 125 °C, bands due to  $\text{Cp}_2\text{Fe}_2(\text{CO})_4$  (2006 (w), 1959 (s), 1793 (s)  $\text{cm}^{-1}$ ) (**4**) began to appear. The bands for **3** appeared to reach a steady-state concentration while the bands for **1** disappeared and those for **4** grew. After several hours at 125 °C the only significant carbonyl bands were those for **4**. Upon cooling, **4** crystallizes from the solution and could be isolated in



\* Corporate Research Science Laboratories.

<sup>†</sup> Analytical Division.

of **3**, an intense band at 1999  $\text{cm}^{-1}$  and a weak band at 1957  $\text{cm}^{-1}$  established the presence of cis terminal carbonyl groups. **3** is most likely the stereoisomer shown since this structure has the ester group in the least congested site. When the conversion of **1** to **3** was followed by NMR, a second diastereomer, **4**,<sup>5</sup> was seen at early times but it was eventually converted to **3**.

Cyclopropylidene complex **3** undergoes regiospecific acid-catalyzed cyclopropane ring opening upon exposure to acidic conditions. For example, attempted chromatography of **3** on silica gel led to isolation of alkylidene complex **5**<sup>6</sup> in 45% yield from **2**. Treatment of **3** with  $\text{HBF}_4$  in diethyl ether also led to ring opening to **5**. This regiospecific ring opening is best explained by initial protonation at the ester carbonyl group.

Photolysis of a solution of **2** (20 mg, 0.57 mmol) and ethyl diazoacetate (3.4 mmol) in  $\text{CH}_2\text{Cl}_2$  at 0 °C for 4 h gave no detectable cyclopropylidene complex **3**. Instead, the only product seen by IR and by  $^1\text{H}$  NMR was the novel allene complex **6**.<sup>7</sup> In the formation of **6**, one CO is lost. The complex contains only terminal CO groups [IR ( $\text{C}-\text{H}_2\text{Cl}_2$ ) 1974 (s), 1921 (s), 1693 (s)  $\text{cm}^{-1}$ ]. In the  $^1\text{H}$  NMR of **6**, the hydrogens on the complexed allene give rise to three separate doublets of doublets at  $\delta$  3.29 ( $J = 1.2, 2.3$  Hz), 3.49 ( $J = 4.1, 2.3$  Hz), and 3.84 ( $J = 4.1, 1.2$  Hz). Related dimanganese,<sup>8</sup> dimolybdenum,<sup>9</sup> and diiron complexes<sup>10</sup> are known.

The possibility that photolysis of **2** and ethyl diazoacetate initially produces cyclopropylidene complex **3** which then photolytically ring opens to give allene complex **6** can be rejected on the basis of two observations. First, during the photolysis of **2** and the diazo ester, none of the cyclopropylidene complex **3** was detected by  $^1\text{H}$  NMR. Second, while photolysis of the cyclopropylidene complex **3** slowly produces allene complex **6**, the rate of conversion of **3** to **6** is much slower than the rate of formation of allene complex **6** from **2**. We suggest that under photolysis **2** loses CO prior to reaction with ethyl diazoacetate to generate a complex containing a carbomethoxy carbene ligand and an ethenylidene ligand which then couple to produce a complexed allene.

**Acknowledgment.** Support from the National Science Foundation is gratefully acknowledged. We thank Dr. Elvin Hoel for keeping us informed of his related studies.

**Registry No.** **2**, 86420-26-0; **3**, 99326-80-4; **4**, 99395-44-5; **5**, 99326-81-5; **6**, 99326-82-6;  $\text{N}_2=\text{CHCO}_2\text{Et}$ , 623-73-4; CuI, 7681-65-4.

(6) **5**:  $^1\text{H}$  NMR (acetone- $d_6$ , 270 MHz)  $\delta$  7.16 (dd,  $J = 7.9, 6.8$  Hz, C=CH), 5.04 (s,  $\text{C}_5\text{H}_5$ ), 4.93 (s,  $\text{C}_5\text{H}_5$ ), 4.16 (q,  $J = 7.1$  Hz, OCH<sub>2</sub>), 3.74 (dq,  $J = 15.2, 7.9$  Hz, CHCHH), 3.62 (dq,  $J = 15.2, 6.8$  Hz, CHCHH), 1.26 (t,  $J = 7.1$  Hz, CH<sub>3</sub>);  $^{13}\text{C}\{^1\text{H}\}$  NMR (acetone- $d_6$ , 0.07 M Cr(acac)<sub>3</sub>, 50.1 MHz)  $\delta$  270.4 ( $\mu\text{-CO}$ ), 270.1 ( $\mu\text{-C}$ ), 212.7 (CO), 212.5 (CO), 173.3 (CO<sub>2</sub>), 131.6 (CH), 89.0 ( $\text{C}_5\text{H}_5$ ), 88.2 ( $\text{C}_5\text{H}_5$ ), 60.6 (CH<sub>2</sub>CH<sub>3</sub>), 42.7 (CHCH<sub>2</sub>), 14.7 (CH<sub>3</sub>); IR ( $\text{CH}_2\text{Cl}_2$ ) 2000 (s), 1962 (m), 1790 (s), 1720 (m)  $\text{cm}^{-1}$ ; HRMS calcd for  $\text{C}_{19}\text{H}_{18}\text{Fe}_2\text{O}_5$  437.9847, found 437.9853.

(7) **6**:  $^1\text{H}$  NMR (acetone- $d_6$ , 200 MHz)  $\delta$  4.39 (s,  $\text{C}_5\text{H}_5$ ), 4.28 (s,  $\text{C}_5\text{H}_5$ ), 4.06 (q,  $J = 7.1$  Hz, OCH<sub>2</sub>), 3.84 (dd,  $J = 4.1, 1.2$  Hz, 1 H), 3.49 (dd,  $J = 4.1, 2.3$  Hz, 1 H), 3.29 (dd,  $J = 1.2, 2.3$  Hz, 1 H), 1.24 (t,  $J = 7.2$  Hz, CH<sub>3</sub>);  $^{13}\text{C}$  NMR (acetone- $d_6$ , 0.07 M Cr(acac)<sub>3</sub>, 50.1 MHz)  $\delta$  227.8 (CO), 226.5 (CO), 219.3 ( $\mu\text{-C}$ ), 173.2 (CO<sub>2</sub>), 83.6 (d,  $J = 176$  Hz,  $\text{C}_5\text{H}_5$ ), 59.9 (t,  $J = 146$  Hz, CH<sub>2</sub>CH<sub>3</sub>), 36.2 (t,  $J = 150$  Hz, =CH<sub>2</sub>), 34.6 (d,  $J = 168$  Hz, =CHCO<sub>2</sub>), 15.0 (q,  $J = 128$  Hz, CH<sub>3</sub>); IR ( $\text{CH}_2\text{Cl}_2$ ) 1947 (s), 1921 (s), 1693 (s)  $\text{cm}^{-1}$ ; HRMS calcd for  $\text{C}_{18}\text{H}_{18}\text{Fe}_2\text{O}_4$  409.9904, found 409.9911.

(8) Lewis, L. N.; Huffman, J. C.; Caulton, K. G. *J. Am. Chem. Soc.* **1980**, *102*, 403.

(9) Bailey, W. I., Jr.; Chisholm, M. H.; Cotton, F. A.; Murillo, C. A.; Rankel, L. A. *J. Am. Chem. Soc.* **1978**, *100*, 802. Doherty, N. M.; Eilschenbroich, C.; Kneuper, H.-J.; Knox, S. A. R. *J. Chem. Soc., Chem. Commun.* **1985**, 170.

(10) Hoel, E. L.; Ansell, G. B.; Leta, S. *Organometallics*, following paper in this issue.

## Thermal and Photochemical Rearrangements of a Bridging Cyclopropylidene Ligand to Allene in a Diiron Complex

Elvin L. Hoel,\* Gerald B. Ansell,<sup>†</sup> and Susan Leta<sup>‡</sup>

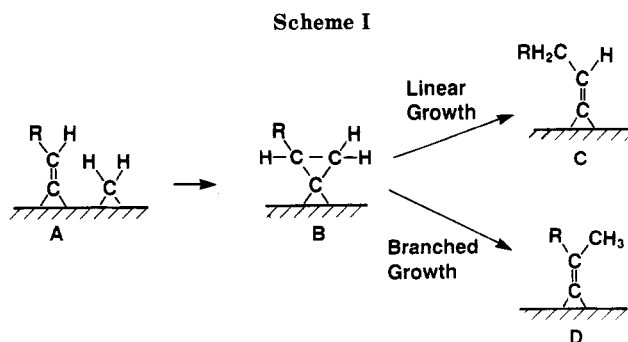
Corporate Research Science Laboratories  
and Analytical Division  
Exxon Research and Engineering Company  
Annandale, New Jersey 08801

Received October 21, 1985

**Summary:** The bridging cyclopropylidene ligand in  $\text{Cp}_2\text{Fe}_2(\text{CO})_2(\mu\text{-CCH}_2\text{CH}_2)$  ( $\text{Cp} = \eta^5\text{-C}_5\text{H}_5$ ) rearranges at 100 °C or photochemically at 10 °C to the thermally unstable allene complex  $\text{Cp}_2\text{Fe}_2(\text{CO})_2(\mu\text{-CH}_2\text{C}=\text{C}=\text{CH}_2)$ . The relevance of this chemistry to a recently proposed Fischer-Tropsch mechanism is discussed.

We recently prepared diiron cyclopropylidene complexes so that the chemistry of the previously unknown cyclopropylidene ligand could be studied as a model for the novel methylene/vinylidene Fischer-Tropsch mechanism proposed by McCandlish (Scheme I).<sup>1</sup> The complexes **1c** and **1t** (with CO and Cp ( $\text{Cp} = \eta^5\text{-C}_5\text{H}_5$ ) ligands cis and trans, respectively, to the plane of the metal atoms and bridging ligands) were prepared by reaction of the corresponding  $\mu$ -vinylidene complexes **2c** and **2t** with diazomethane in the presence of CuCl,<sup>2</sup> a synthesis formally equivalent to  $\text{A} \rightarrow \text{B}$ . We find that the thermal and photochemistry of **1** do not support the proposed mechanism; however, as detailed in the accompanying communication, hydrocarbon chains can be grown via cyclopropylidene intermediates by using protonation/deprotonation chemistry to effect the rearrangement of the homologous vinylidene ligand.<sup>3</sup>

Solutions of **1c** or **1t** in octane were heated under argon and the course of reaction was followed by IR spectroscopy. The first observed change was interconversion of the cis and trans isomers, beginning at about 60 °C. An equilibrium appeared to be established after about 30 min at 80 °C. At about 100 °C two new peaks, subsequently identified as belonging to **3** (see below), began to show at 1939 (m) and 1919 (s)  $\text{cm}^{-1}$ . At 125 °C, bands due to  $\text{Cp}_2\text{Fe}_2(\text{CO})_4$  (2006 (w), 1959 (s), 1793 (s)  $\text{cm}^{-1}$ ) (**4**) began to appear. The bands for **3** appeared to reach a steady-state concentration while the bands for **1** disappeared and those for **4** grew. After several hours at 125 °C the only significant carbonyl bands were those for **4**. Upon cooling, **4** crystallizes from the solution and could be isolated in



\* Corporate Research Science Laboratories.

<sup>†</sup> Analytical Division.





in this soluble diiron complex is not necessarily the same as that which could occur on heterogeneous Fischer-Tropsch synthesis catalysts. Nonetheless, the availability of a low-energy, thermal pathway to allene reduces the likelihood that the cyclopropylidene pathway is a major contributor to Fischer-Tropsch synthesis. Further investigations to define the general scope of this chemistry and mechanistic details for the thermal, photochemical, and protonation/deprotonation pathways for hydrocarbon ligand rearrangements are in progress, not only for the diiron system but also for similar diruthenium and dicobalt cyclopropylidene complexes.

**Acknowledgment.** We are indebted to Dr. Larry McCandlish and Prof. John Bercaw for helpful discussions. The laboratory assistance of E. G. Habeeb is also gratefully acknowledged.

**Registry No.** 1c, 91547-48-7; 1t, 91443-97-9; 3, 100021-54-3; 4, 12154-95-9; Fe, 7439-89-6; H<sub>2</sub>C=C=CH<sub>2</sub>, 463-49-0.

**Supplementary Material Available:** Preliminary crystal structure results for 3 and tables of atomic positional and thermal parameters, bond lengths, bond angles, and structure factor amplitudes (16 pages). Ordering information is given on any current masthead page.

### Protonation/Deprotonation Rearrangements of Bridging Cyclopropylidene Ligands in Diiron Complexes. Stepwise Hydrocarbon Chain Growth via Cyclopropylidene Intermediates

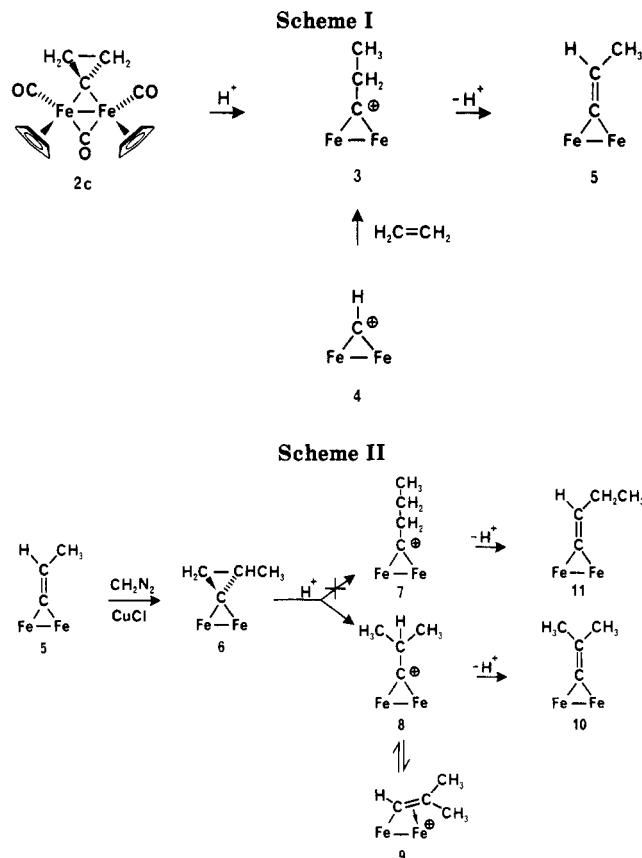
Elvin L. Hoel

Corporate Research Science Laboratories  
Exxon Research and Engineering Company  
Annandale, New Jersey 08801

Received October 21, 1985

**Summary:** Protonation of the bridging cyclopropylidene ligand in Cp<sub>2</sub>Fe<sub>2</sub>(CO)<sub>2</sub>(μ-CCH<sub>2</sub>CH<sub>2</sub>) leads to the bridging propylidyne complex [Cp<sub>2</sub>Fe<sub>2</sub>(CO)<sub>2</sub>(μ-CCH<sub>2</sub>CH<sub>3</sub>)]<sup>+</sup> which when deprotonated provides the methylvinylidene Cp<sub>2</sub>Fe<sub>2</sub>(CO)<sub>2</sub>(μ-C=CHCH<sub>3</sub>). Cyclopropanation of this vinylidene ligand followed by protonation/deprotonation leads exclusively to the dimethylvinylidene complex; none of the linear ethylvinylidene is formed.

In the preceding communication,<sup>1</sup> we reported on the thermal and photochemical rearrangement chemistry of the bridging cyclopropylidene ligand in Cp<sub>2</sub>Fe<sub>2</sub>(CO)<sub>2</sub>(μ-CO)(μ-CCH<sub>2</sub>CH<sub>2</sub>) (2) (Cp = η<sup>5</sup>-C<sub>5</sub>H<sub>5</sub>) which was synthesized from the reaction of diazomethane with Cp<sub>2</sub>Fe<sub>2</sub>(CO)<sub>2</sub>(μ-CO)(μ-C=CH<sub>2</sub>) (1)<sup>2</sup> to model the novel methylene/vinylidene Fischer-Tropsch mechanism proposed by McCandlish.<sup>3</sup> Although the thermal and photochemistry of 2 do not support the proposed mechanism, we find that hydrocarbon chains can be grown via cyclopropylidene intermediates, by using protonation/deprotonation chemistry to effect the rearrangement to the homologous vi-



nylidene ligand. Employment of this route through several stepwise cycles, however, results in the exclusive formation of the branched hydrocarbon chain, in contrast to the primarily linear chain growth observed in Fischer-Tropsch synthesis.<sup>3,4</sup>

Protonation of 2 with strong acids such as HBF<sub>4</sub> or CF<sub>3</sub>COOH gives the propylidyne complex 3 in high yield. This is consistent with Casey's suggestion that an edge- or corner-protonated form of 2 might be a possible intermediate in the hydrocarbation reaction of ethylene with the methylidyne complex 4.<sup>5</sup> NMR experiments with CF<sub>3</sub>COOD as the proton source confirm that the added proton ends up on the methyl of the propylidyne ligand. Bridging alkylidyne complexes in this system are readily deprotonated with a variety of bases to give the bridging vinylidene complexes.<sup>5,6</sup> In this instance, 3 is deprotonated to yield the methylvinylidene complex 5,<sup>7</sup> which is the rearranged hydrocarbon species equivalent to C in Scheme I of the preceding communication.<sup>1</sup> Thus, although the cyclopropylidene ligand does not rearrange to the homologous vinylidene either thermally or photochemically, it does so rearrange via a protonation/deprotonation sequence.<sup>8</sup>

(4) Pichler, H.; Schulz, H.; Kuhne, D. *Brennst.-Chem.* 1968, 49, 344.  
(5) (a) Casey, C. P.; Fagan, P. J. *J. Am. Chem. Soc.* 1982, 104, 4950-4951. (b) Casey, C. P.; Fagan, P. J.; Miles, W. H.; Marder, S. R. *J. Mol. Catal.* 1983, 21, 173-188.

(6) (a) Dawkins, G. M.; Green, M.; Jeffery, J. C.; Sambale, C.; Stone, F. G. A. *J. Chem. Soc., Dalton Trans.* 1983, 499-506. (b) Kao, S. C.; Lu, P. P. Y.; Pettit, R. *Organometallics* 1982, 1, 911-918. (c) Diazomethane also deprotonates 3 to give 5; Hoel, E. L., unpublished results.

(7) *cis*-Cp<sub>2</sub>Fe<sub>2</sub>(CO)<sub>2</sub>(μ-CO)(μ-C=CHCH<sub>3</sub>) (5): IR (hexane) 2000 (vs), 1966 (m), 1805 (s), 1612 (w) cm<sup>-1</sup>; <sup>1</sup>H NMR (400 MHz, CDCl<sub>3</sub>) δ 7.14 (q, J = 6.6 Hz, 1 H, =CH-), 4.83 (s, 5 H, Cp), 4.75 (s, 5 H, Cp), 2.38 (d, J = 6.6 Hz, 3 H, CH<sub>3</sub>). Anal. Calcd for C<sub>16</sub>H<sub>14</sub>O<sub>3</sub>Fe<sub>2</sub>: C, 52.51; H, 3.86; Fe, 30.52. Found: C, 52.31; H, 3.72; Fe, 30.33.

(8) A substituted cyclopropylidene complex has been prepared from 1 and ethyl diazoacetate. This complex readily rearranges over silica gel to the linear vinylidene, presumably via a protonation/deprotonation pathway. Casey, C. P.; Austin, E. *Organometallics*, first of three papers in this issue.

(1) Hoel, E. L.; Ansell, G. B.; Leta, S. *Organometallics*, second of three papers in this issue.

(2) Hoel, E. L.; Ansell, G. B.; Leta, S. *Organometallics* 1984, 3, 1633-1637.

(3) McCandlish, L. E. *J. Catal.* 1983, 83, 362-370.

in this soluble diiron complex is not necessarily the same as that which could occur on heterogeneous Fischer-Tropsch synthesis catalysts. Nonetheless, the availability of a low-energy, thermal pathway to allene reduces the likelihood that the cyclopropylidene pathway is a major contributor to Fischer-Tropsch synthesis. Further investigations to define the general scope of this chemistry and mechanistic details for the thermal, photochemical, and protonation/deprotonation pathways for hydrocarbon ligand rearrangements are in progress, not only for the diiron system but also for similar diruthenium and dicobalt cyclopropylidene complexes.

**Acknowledgment.** We are indebted to Dr. Larry McCandlish and Prof. John Bercaw for helpful discussions. The laboratory assistance of E. G. Habeeb is also gratefully acknowledged.

**Registry No.** 1c, 91547-48-7; 1t, 91443-97-9; 3, 100021-54-3; 4, 12154-95-9; Fe, 7439-89-6; H<sub>2</sub>C=C=CH<sub>2</sub>, 463-49-0.

**Supplementary Material Available:** Preliminary crystal structure results for 3 and tables of atomic positional and thermal parameters, bond lengths, bond angles, and structure factor amplitudes (16 pages). Ordering information is given on any current masthead page.

### Protonation/Deprotonation Rearrangements of Bridging Cyclopropylidene Ligands in Diiron Complexes. Stepwise Hydrocarbon Chain Growth via Cyclopropylidene Intermediates

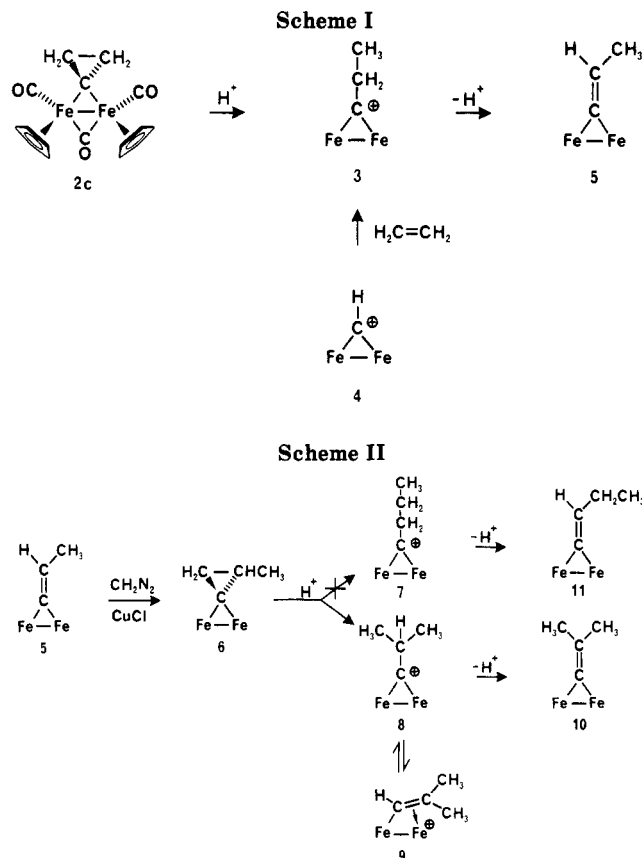
Elvin L. Hoel

Corporate Research Science Laboratories  
Exxon Research and Engineering Company  
Annandale, New Jersey 08801

Received October 21, 1985

**Summary:** Protonation of the bridging cyclopropylidene ligand in Cp<sub>2</sub>Fe<sub>2</sub>(CO)<sub>2</sub>(μ-CCH<sub>2</sub>CH<sub>2</sub>) leads to the bridging propylidyne complex [Cp<sub>2</sub>Fe<sub>2</sub>(CO)<sub>2</sub>(μ-CCH<sub>2</sub>CH<sub>3</sub>)]<sup>+</sup> which when deprotonated provides the methylvinylidene Cp<sub>2</sub>Fe<sub>2</sub>(CO)<sub>2</sub>(μ-C=CHCH<sub>3</sub>). Cyclopropanation of this vinylidene ligand followed by protonation/deprotonation leads exclusively to the dimethylvinylidene complex; none of the linear ethylvinylidene is formed.

In the preceding communication,<sup>1</sup> we reported on the thermal and photochemical rearrangement chemistry of the bridging cyclopropylidene ligand in Cp<sub>2</sub>Fe<sub>2</sub>(CO)<sub>2</sub>(μ-CO)(μ-CCH<sub>2</sub>CH<sub>2</sub>) (2) (Cp = η<sup>5</sup>-C<sub>5</sub>H<sub>5</sub>) which was synthesized from the reaction of diazomethane with Cp<sub>2</sub>Fe<sub>2</sub>(CO)<sub>2</sub>(μ-CO)(μ-C=CH<sub>2</sub>) (1)<sup>2</sup> to model the novel methylene/vinylidene Fischer-Tropsch mechanism proposed by McCandlish.<sup>3</sup> Although the thermal and photochemistry of 2 do not support the proposed mechanism, we find that hydrocarbon chains can be grown via cyclopropylidene intermediates, by using protonation/deprotonation chemistry to effect the rearrangement to the homologous vi-



nylidene ligand. Employment of this route through several stepwise cycles, however, results in the exclusive formation of the branched hydrocarbon chain, in contrast to the primarily linear chain growth observed in Fischer-Tropsch synthesis.<sup>3,4</sup>

Protonation of 2 with strong acids such as HBF<sub>4</sub> or CF<sub>3</sub>COOH gives the propylidyne complex 3 in high yield. This is consistent with Casey's suggestion that an edge- or corner-protonated form of 2 might be a possible intermediate in the hydrocarbation reaction of ethylene with the methylidyne complex 4.<sup>5</sup> NMR experiments with CF<sub>3</sub>COOD as the proton source confirm that the added proton ends up on the methyl of the propylidyne ligand. Bridging alkylidyne complexes in this system are readily deprotonated with a variety of bases to give the bridging vinylidene complexes.<sup>5,6</sup> In this instance, 3 is deprotonated to yield the methylvinylidene complex 5,<sup>7</sup> which is the rearranged hydrocarbon species equivalent to C in Scheme I of the preceding communication.<sup>1</sup> Thus, although the cyclopropylidene ligand does not rearrange to the homologous vinylidene either thermally or photochemically, it does so rearrange via a protonation/deprotonation sequence.<sup>8</sup>

(4) Pichler, H.; Schulz, H.; Kuhne, D. *Brennst.-Chem.* 1968, 49, 344.

(5) (a) Casey, C. P.; Fagan, P. J. *J. Am. Chem. Soc.* 1982, 104, 4950-4951. (b) Casey, C. P.; Fagan, P. J.; Miles, W. H.; Marder, S. R. *J. Mol. Catal.* 1983, 21, 173-188.

(6) (a) Dawkins, G. M.; Green, M.; Jeffery, J. C.; Sambale, C.; Stone, F. G. A. *J. Chem. Soc., Dalton Trans.* 1983, 499-506. (b) Kao, S. C.; Lu, P. P. Y.; Pettit, R. *Organometallics* 1982, 1, 911-918. (c) Diazomethane also deprotonates 3 to give 5; Hoel, E. L., unpublished results.

(7) *cis*-Cp<sub>2</sub>Fe<sub>2</sub>(CO)<sub>2</sub>(μ-CO)(μ-C=CHCH<sub>3</sub>) (5): IR (hexane) 2000 (vs), 1966 (m), 1805 (s), 1612 (w) cm<sup>-1</sup>; <sup>1</sup>H NMR (400 MHz, CDCl<sub>3</sub>) δ 7.14 (q, J = 6.6 Hz, 1 H, =CH-), 4.83 (s, 5 H, Cp), 4.75 (s, 5 H, Cp), 2.38 (d, J = 6.6 Hz, 3 H, CH<sub>3</sub>). Anal. Calcd for C<sub>16</sub>H<sub>14</sub>O<sub>3</sub>Fe<sub>2</sub>: C, 52.51; H, 3.86; Fe, 30.52. Found: C, 52.31; H, 3.72; Fe, 30.33.

(8) A substituted cyclopropylidene complex has been prepared from 1 and ethyl diazoacetate. This complex readily rearranges over silica gel to the linear vinylidene, presumably via a protonation/deprotonation pathway. Casey, C. P.; Austin, E. *Organometallics*, first of three papers in this issue.

(1) Hoel, E. L.; Ansell, G. B.; Leta, S. *Organometallics*, second of three papers in this issue.

(2) Hoel, E. L.; Ansell, G. B.; Leta, S. *Organometallics* 1984, 3, 1633-1637.

(3) McCandlish, L. E. *J. Catal.* 1983, 83, 362-370.

The cycloprotonation process can be repeated to give the methylcyclopropylidene complex **6**.<sup>9</sup> At this point, protonation might possibly lead to either the linear (**7**) or the branched (**8**) alkylidyne complex, or both, depending on the selectivity of the proton attack. As shown in Scheme II, we find that attack is selectively at the less substituted carbon, none of the linear isomer is visible in the <sup>1</sup>H NMR spectrum of a solution obtained by addition of CF<sub>3</sub>COOH to **6** in CDCl<sub>3</sub>. The isobutylidyne complex is seen to be in equilibrium with the dimethylvinyl complex **9**,<sup>10</sup> with an equilibrium ratio of 8:9 = 2:3. Casey found this equilibration to be a general feature of alkylidyne complexes with tertiary carbons next to the bridging carbon atom.<sup>11</sup> Deprotonation of the mixture of cationic complexes led exclusively to the branched vinylidene complex **10**<sup>12</sup>—none of the linear isomer **11** could be detected by <sup>1</sup>H NMR. The pentylidyne analogue of **7**, prepared by different routes, has been shown to deprotonate smoothly to the linear vinylidene without rearrangement.<sup>11,13</sup>

Further investigations to define the general scope of this chemistry and mechanistic details for the thermal, photochemical, and protonation/deprotonation pathways for hydrocarbon ligand rearrangements are in progress, not only for the diiron system but also for similar diruthenium and dicobalt cyclopropylidene complexes. However, the facile, low-energy chemistry of the cyclopropylidene ligand in this diiron system, rearranging readily to allene via thermal and photochemical processes<sup>1</sup> and leading exclusively to branched vinylidene ligands via the protonation/deprotonation pathway, argues against the cyclopropylidene pathway as a major contributor to a Fischer-Tropsch synthesis on heterogeneous catalysts.

**Acknowledgment.** We are indebted to Dr. Larry McCandlish, Dr. Tom Upton, and Prof. John Bercaw for helpful discussions. The laboratory assistance of E. G. Habeeb is also gratefully acknowledged.

**Registry No.** **2**, 91547-48-7; **3**, 82621-28-1; **5**, 99923-10-1; **6**, 99923-11-2; **8**, 99923-07-6; **9**, 99923-09-8; **10**, 99923-12-3.

## Cobalt-Mediated Diene Activation: Facile Addition of Nucleophiles to [( $\eta^4$ -1,3-Butadiene)Co(CO)<sub>3</sub>]BF<sub>4</sub>

Lucio S. Barinelli, Ke Tao, and Kenneth M. Nicholas\*

Department of Chemistry, University of Oklahoma  
Norman, Oklahoma 73019

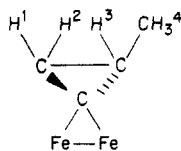
Received October 8, 1985

**Summary:** [( $\eta^4$ -1,3-Butadiene)Co(CO)<sub>3</sub>]BF<sub>4</sub> (**1**) reacts regioselectively by attack at the diene C-1 under mild conditions with a variety of nucleophiles including NaBH<sub>3</sub>CN(H<sup>-</sup>), pyridine, PhMgBr, and PMe<sub>3</sub> to give (*anti*- $\eta^3$ -CH<sub>2</sub>CHCHCH<sub>2</sub>Nu)Co(CO)<sub>3</sub> (**2**). Regio- and stereospecific 1,4-difunctionalization of butadiene can be achieved by sequential double nucleophilic addition to **1**.

Although metal carbonyl  $\pi$ -complexes of conjugated dienes are among the oldest of organo-transition-metal compounds,<sup>1</sup> their reactivities have been surprisingly little studied. In this context it is particularly interesting to contrast recent reports of selective C-2 attack by nucleophiles on ( $\eta^4$ -diene)Fe(CO)<sub>3</sub><sup>2</sup> with those of selective C-1 attack on [CpMo( $\eta^4$ -diene)(CO)<sub>2</sub>]<sup>+</sup>.<sup>3</sup> Described herein are nucleophilic reactions of the parent compound ( $\eta^4$ -butadiene)Co(CO)<sub>3</sub>BF<sub>4</sub> (**1**),<sup>4</sup> isoelectronic with the prototypical diene complex ( $\eta^4$ -butadiene)Fe(CO)<sub>3</sub>.

[( $\eta^4$ -Butadiene)Co(CO)<sub>3</sub>]BF<sub>4</sub> (**1**) was prepared by an improved route via oxidation of [( $\eta^4$ -butadiene)Co(CO)<sub>2</sub>]<sub>2</sub> with (C<sub>5</sub>H<sub>5</sub>)<sub>2</sub>FeBF<sub>4</sub>.<sup>5</sup> The high reactivity of **1** toward nucleophiles was foreshadowed by remarkably high  $\nu$ (CO) = 2150 and 2102 cm<sup>-1</sup> (cf.  $\nu$ (free CO) = 2143 cm<sup>-1</sup>). Indeed, treatment of CH<sub>3</sub>NO<sub>2</sub> solutions or THF or CH<sub>2</sub>Cl<sub>2</sub> suspensions of **1** with various prospective nucleophiles at -78 → 0 °C caused generally rapid (min) disappearance of the IR bands at 2150 and 2102 cm<sup>-1</sup> and their clean replacement with two new bands at ca. 2060 and 1995 cm<sup>-1</sup>, typical for ( $\eta^3$ -allyl)Co(CO)<sub>3</sub> derivatives.<sup>7</sup> Nucleophiles found to react include pyridine, NaBH<sub>3</sub>CN(H<sup>-</sup>), PhMgBr, PMe<sub>3</sub>, PPh<sub>3</sub>, P(OMe)<sub>3</sub>, NaCH(CO<sub>2</sub>Me)<sub>2</sub>, (allyl)SiMe<sub>3</sub>, 1-(trimethylsilyloxy)cyclohexene, and MeOH. Somewhat unstable adducts of **1** with the first four nucleophiles have been isolated in moderate to good yields, and their structures

(9) (a) *cis*-Cp<sub>2</sub>Fe<sub>2</sub>(CO)<sub>2</sub>( $\mu$ -CO)( $\mu$ -C(CH<sub>3</sub>)<sub>2</sub>CHCH<sub>3</sub>) (**6**): IR (hexane) 1993 (vs), 1958 (m), 1798 (s) cm<sup>-1</sup>; <sup>1</sup>H NMR (400 MHz, CDCl<sub>3</sub>)  $\delta$  4.60 (s, 5 H, Cp), 4.56 (s, 5 H, Cp), 2.08 (dd, *J*<sub>1,2</sub> = -7.9, *J*<sub>1,3</sub> = 9.7 Hz, 1 H, H<sup>1</sup>), 1.82 (ddq, *J*<sub>1,3</sub> = 9.7, *J*<sub>2,3</sub> = 5.5, *J*<sub>3,4</sub> = 6.2 Hz, 1 H, H<sup>3</sup>), 1.49 (d, *J*<sub>3,4</sub> = 6.2 Hz, 3 H, H<sup>4</sup>), 1.38 (dd, *J*<sub>1,2</sub> = -7.9, *J*<sub>2,3</sub> = 5.5 Hz, 1 H, H<sup>2</sup>). Anal. Calcd for C<sub>17</sub>H<sub>16</sub>O<sub>5</sub>Fe<sub>2</sub>: C, 53.73; H, 4.24; Fe, 29.39. Found: C, 53.55; H, 4.24; Fe, 29.62.



(b) The X-ray crystal structure has been published: Ansell, G. B.; Leta, S.; Hoel, E. L.; Habeeb, E. G. *Acta Crystallogr., Sect. C: Cryst. Struct. Commun.*, in press.

(10) (a) [Cp<sub>2</sub>Fe<sub>2</sub>(CO)<sub>2</sub>( $\mu$ -CO)( $\mu$ -C(CH<sub>3</sub>)<sub>2</sub>)]<sup>+</sup>[CF<sub>3</sub>COO]<sup>-</sup> (**8**): <sup>1</sup>H NMR (400 MHz, CDCl<sub>3</sub>)  $\delta$  5.30 (s, 10 H, Cp), 1.80 (d, *J* = 7 Hz, 6 H, CH<sub>3</sub>), septet for tertiary hydrogen not observed, presumed to be under Cp resonances. (b) [Cp<sub>2</sub>Fe<sub>2</sub>(CO)<sub>2</sub>( $\mu$ -CO)( $\mu$ -CH=C(CH<sub>3</sub>)<sub>2</sub>)]<sup>+</sup>[CF<sub>3</sub>COO]<sup>-</sup> (**9**): <sup>1</sup>H NMR (400 MHz, CDCl<sub>3</sub>)  $\delta$  11.36 (s, 1 H, -CH=), 5.24 (s, 10 H, Cp), 2.31 (s, 3 H, CH<sub>3</sub>), 1.47 (s, 3 H, CH<sub>3</sub>). The presence of only one Cp resonance implies rapid oscillation of the  $\mu$ -vinyl bonding between the metal atoms at 20 °C.<sup>5</sup>

(11) Casey, C. P.; Marder, S. R.; Fagan, P. J. *J. Am. Chem. Soc.* **1983**, *105*, 7197-7198.

(12) *cis*-Cp<sub>2</sub>Fe<sub>2</sub>(CO)<sub>2</sub>( $\mu$ -CO)( $\mu$ -C=C(CH<sub>3</sub>)<sub>2</sub>) (**10**): IR (hexane): 1999 (vs), 1965 (m), 1804 (s), 1630 (w) cm<sup>-1</sup>; <sup>1</sup>H NMR (400 MHz, CDCl<sub>3</sub>)  $\delta$  4.80 (s, 10 H, Cp), 2.47 (s, 6 H, CH<sub>3</sub>).

(13) Hoel, E. L., unpublished results.

(1) Riehlen, H.; Gruhl, A.; Von Hessling, G.; Pfengle, O. *Justus Liebig's Ann. Chem.* **1930**, *482*, 161.

(2) (a) Semmelhack, M. F.; Herndon, J. W. *J. Organomet. Chem.* **1984**, *265*, C15. (b) Semmelhack, M. F.; Herndon, J. W.; Springer, J. P. *J. Am. Chem. Soc.* **1983**, *105*, 2497. (c) Semmelhack, M. F.; Herndon, J. W. *Organometallics* **1983**, *2*, 363.

(3) (a) Green, M. L. H.; Mitchard, L. C.; Silverthorn, W. E. *J. Chem. Soc. Dalton Trans.* **1973**, 1952. (b) Faller, J. W.; Rosan, A. M. *J. Am. Chem. Soc.* **1977**, *99*, 4858. Faller, J. W.; Murray, H. H.; White, D. L.; Chao, K. H. *Organometallics* **1983**, *2*, 400. (c) Pearson, A. J.; Khan, M. N. I.; Clardy, J. C.; Cun-heng, H. *J. Am. Chem. Soc.* **1985**, *107*, 2748.

(4) Chaudury, F. M.; Pauson, P. L. *J. Organomet. Chem.* **1974**, *69*, C31.

(5) Stirring a CH<sub>2</sub>Cl<sub>2</sub> solution of [(butadiene)Co(CO)<sub>2</sub>]<sub>2</sub> (prepared from Co<sub>2</sub>(CO)<sub>8</sub> + butadiene in 90% yield according to ref 6) with 2 molar equiv of (C<sub>5</sub>H<sub>5</sub>)<sub>2</sub>FeBF<sub>4</sub> at 20 °C (for 4-6 h) under N<sub>2</sub> followed by filtration and reprecipitation of the solid (2-3 times) from CH<sub>3</sub>NO<sub>2</sub>/Et<sub>2</sub>O affords **1** as a moisture sensitive yellow solid (30-40%). Because of the deficiency of CO's, 50% is the maximum possible yield of **1** from [(C<sub>4</sub>H<sub>6</sub>)Co(CO)<sub>2</sub>]<sub>2</sub>. Running the reaction under 15-200 psi of CO had no effect on the yield. Comparable results have been obtained in the preparation of (isoprene- and (1,3-cyclohexadiene)Co(CO)<sub>3</sub>BF<sub>4</sub>. More efficient routes to **1** are being examined. **1**: IR (CH<sub>3</sub>NO<sub>2</sub>) 2150, 2102 (MC=O), 1050 (BF<sub>4</sub><sup>-</sup>) cm<sup>-1</sup>; <sup>1</sup>H NMR (CD<sub>3</sub>NO<sub>2</sub>)  $\delta$  6.7 (m, 2 H), 3.6 (dd, *J* = 3.5 Hz, 2 H), 2.5 (dd, *J* = 3, 10 Hz, 2 H).

(6) Fischer, E. O.; Kuzel, P.; Fritz, H. P. *Z. Naturforsch., B: Anorg. Chem., Org. Chem., Biochem., Biophys., Biol.* **1961**, *16B*, 138.

(7) Heck, R. F.; Breslow, D. S. *J. Am. Chem. Soc.* **1961**, *83*, 1097.

The cycloprotonation process can be repeated to give the methylcyclopropylidene complex **6**.<sup>9</sup> At this point, protonation might possibly lead to either the linear (**7**) or the branched (**8**) alkylidyne complex, or both, depending on the selectivity of the proton attack. As shown in Scheme II, we find that attack is selectively at the less substituted carbon, none of the linear isomer is visible in the <sup>1</sup>H NMR spectrum of a solution obtained by addition of CF<sub>3</sub>COOH to **6** in CDCl<sub>3</sub>. The isobutylidyne complex is seen to be in equilibrium with the dimethylvinyl complex **9**,<sup>10</sup> with an equilibrium ratio of 8:9 = 2:3. Casey found this equilibration to be a general feature of alkylidynes with tertiary carbons next to the bridging carbon atom.<sup>11</sup> Deprotonation of the mixture of cationic complexes led exclusively to the branched vinylidene complex **10**<sup>12</sup>—none of the linear isomer **11** could be detected by <sup>1</sup>H NMR. The pentylidyne analogue of **7**, prepared by different routes, has been shown to deprotonate smoothly to the linear vinylidene without rearrangement.<sup>11,13</sup>

Further investigations to define the general scope of this chemistry and mechanistic details for the thermal, photochemical, and protonation/deprotonation pathways for hydrocarbon ligand rearrangements are in progress, not only for the diiron system but also for similar diruthenium and dicobalt cyclopropylidene complexes. However, the facile, low-energy chemistry of the cyclopropylidene ligand in this diiron system, rearranging readily to allene via thermal and photochemical processes<sup>1</sup> and leading exclusively to branched vinylidene ligands via the protonation/deprotonation pathway, argues against the cyclopropylidene pathway as a major contributor to a Fischer-Tropsch synthesis on heterogeneous catalysts.

**Acknowledgment.** We are indebted to Dr. Larry McCandlish, Dr. Tom Upton, and Prof. John Bercaw for helpful discussions. The laboratory assistance of E. G. Habeeb is also gratefully acknowledged.

**Registry No.** **2**, 91547-48-7; **3**, 82621-28-1; **5**, 99923-10-1; **6**, 99923-11-2; **8**, 99923-07-6; **9**, 99923-09-8; **10**, 99923-12-3.

## Cobalt-Mediated Diene Activation: Facile Addition of Nucleophiles to [( $\eta^4$ -1,3-Butadiene)Co(CO)<sub>3</sub>]BF<sub>4</sub>

Lucio S. Barinelli, Ke Tao, and Kenneth M. Nicholas\*

Department of Chemistry, University of Oklahoma  
Norman, Oklahoma 73019

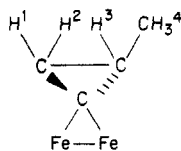
Received October 8, 1985

**Summary:** [( $\eta^4$ -1,3-Butadiene)Co(CO)<sub>3</sub>]BF<sub>4</sub> (**1**) reacts regioselectively by attack at the diene C-1 under mild conditions with a variety of nucleophiles including NaBH<sub>3</sub>CN(H<sup>-</sup>), pyridine, PhMgBr, and PMe<sub>3</sub> to give (*anti*- $\eta^3$ -CH<sub>2</sub>CHCHCH<sub>2</sub>Nu)Co(CO)<sub>3</sub> (**2**). Regio- and stereospecific 1,4-difunctionalization of butadiene can be achieved by sequential double nucleophilic addition to **1**.

Although metal carbonyl  $\pi$ -complexes of conjugated dienes are among the oldest of organo-transition-metal compounds,<sup>1</sup> their reactivities have been surprisingly little studied. In this context it is particularly interesting to contrast recent reports of selective C-2 attack by nucleophiles on ( $\eta^4$ -diene)Fe(CO)<sub>3</sub><sup>2</sup> with those of selective C-1 attack on [CpMo( $\eta^4$ -diene)(CO)<sub>2</sub>]<sup>+</sup>.<sup>3</sup> Described herein are nucleophilic reactions of the parent compound ( $\eta^4$ -butadiene)Co(CO)<sub>3</sub>BF<sub>4</sub> (**1**),<sup>4</sup> isoelectronic with the prototypical diene complex ( $\eta^4$ -butadiene)Fe(CO)<sub>3</sub>.

[( $\eta^4$ -Butadiene)Co(CO)<sub>3</sub>]BF<sub>4</sub> (**1**) was prepared by an improved route via oxidation of [( $\eta^4$ -butadiene)Co(CO)<sub>2</sub>]<sub>2</sub> with (C<sub>5</sub>H<sub>5</sub>)<sub>2</sub>FeBF<sub>4</sub>.<sup>5</sup> The high reactivity of **1** toward nucleophiles was foreshadowed by remarkably high  $\nu$ (CO) = 2150 and 2102 cm<sup>-1</sup> (cf.  $\nu$ (free CO) = 2143 cm<sup>-1</sup>). Indeed, treatment of CH<sub>3</sub>NO<sub>2</sub> solutions or THF or CH<sub>2</sub>Cl<sub>2</sub> suspensions of **1** with various prospective nucleophiles at -78 → 0 °C caused generally rapid (min) disappearance of the IR bands at 2150 and 2102 cm<sup>-1</sup> and their clean replacement with two new bands at ca. 2060 and 1995 cm<sup>-1</sup>, typical for ( $\eta^3$ -allyl)Co(CO)<sub>3</sub> derivatives.<sup>7</sup> Nucleophiles found to react include pyridine, NaBH<sub>3</sub>CN(H<sup>-</sup>), PhMgBr, PMe<sub>3</sub>, PPh<sub>3</sub>, P(OMe)<sub>3</sub>, NaCH(CO<sub>2</sub>Me)<sub>2</sub>, (allyl)SiMe<sub>3</sub>, 1-(trimethylsilyloxy)cyclohexene, and MeOH. Somewhat unstable adducts of **1** with the first four nucleophiles have been isolated in moderate to good yields, and their structures

(9) (a) *cis*-Cp<sub>2</sub>Fe<sub>2</sub>(CO)<sub>2</sub>( $\mu$ -CO)( $\mu$ -C(CH<sub>3</sub>)<sub>2</sub>CHCH<sub>3</sub>) (**6**): IR (hexane) 1993 (vs), 1958 (m), 1798 (s) cm<sup>-1</sup>; <sup>1</sup>H NMR (400 MHz, CDCl<sub>3</sub>)  $\delta$  4.60 (s, 5 H, Cp), 4.56 (s, 5 H, Cp), 2.08 (dd, *J*<sub>1,2</sub> = -7.9, *J*<sub>1,3</sub> = 9.7 Hz, 1 H, H<sup>1</sup>), 1.82 (ddq, *J*<sub>1,3</sub> = 9.7, *J*<sub>2,3</sub> = 5.5, *J*<sub>3,4</sub> = 6.2 Hz, 1 H, H<sup>3</sup>), 1.49 (d, *J*<sub>3,4</sub> = 6.2 Hz, 3 H, H<sup>4</sup>), 1.38 (dd, *J*<sub>1,2</sub> = -7.9, *J*<sub>2,3</sub> = 5.5 Hz, 1 H, H<sup>2</sup>). Anal. Calcd for C<sub>17</sub>H<sub>16</sub>O<sub>5</sub>Fe<sub>2</sub>: C, 53.73; H, 4.24; Fe, 29.39. Found: C, 53.55; H, 4.24; Fe, 29.62.



(b) The X-ray crystal structure has been published: Ansell, G. B.; Leta, S.; Hoel, E. L.; Habeeb, E. G. *Acta Crystallogr., Sect. C: Cryst. Struct. Commun.*, in press.

(10) (a) [Cp<sub>2</sub>Fe<sub>2</sub>(CO)<sub>2</sub>( $\mu$ -CO)( $\mu$ -C(CH<sub>3</sub>)<sub>2</sub>)]<sup>+</sup>[CF<sub>3</sub>COO]<sup>-</sup> (**8**): <sup>1</sup>H NMR (400 MHz, CDCl<sub>3</sub>)  $\delta$  5.30 (s, 10 H, Cp), 1.80 (d, *J* = 7 Hz, 6 H, CH<sub>3</sub>), septet for tertiary hydrogen not observed, presumed to be under Cp resonances. (b) [Cp<sub>2</sub>Fe<sub>2</sub>(CO)<sub>2</sub>( $\mu$ -CO)( $\mu$ -CH=C(CH<sub>3</sub>)<sub>2</sub>)]<sup>+</sup>[CF<sub>3</sub>COO]<sup>-</sup> (**9**): <sup>1</sup>H NMR (400 MHz, CDCl<sub>3</sub>)  $\delta$  11.36 (s, 1 H, -CH=), 5.24 (s, 10 H, Cp), 2.31 (s, 3 H, CH<sub>3</sub>), 1.47 (s, 3 H, CH<sub>3</sub>). The presence of only one Cp resonance implies rapid oscillation of the  $\mu$ -vinyl bonding between the metal atoms at 20 °C.<sup>5</sup>

(11) Casey, C. P.; Marder, S. R.; Fagan, P. J. *J. Am. Chem. Soc.* **1983**, *105*, 7197-7198.

(12) *cis*-Cp<sub>2</sub>Fe<sub>2</sub>(CO)<sub>2</sub>( $\mu$ -CO)( $\mu$ -C=C(CH<sub>3</sub>)<sub>2</sub>) (**10**): IR (hexane): 1999 (vs), 1965 (m), 1804 (s), 1630 (w) cm<sup>-1</sup>; <sup>1</sup>H NMR (400 MHz, CDCl<sub>3</sub>)  $\delta$  4.80 (s, 10 H, Cp), 2.47 (s, 6 H, CH<sub>3</sub>).

(13) Hoel, E. L., unpublished results.

(1) Riehlen, H.; Gruhl, A.; Von Hessling, G.; Pfengle, O. *Justus Liebig's Ann. Chem.* **1930**, *482*, 161.

(2) (a) Semmelhack, M. F.; Herndon, J. W. *J. Organomet. Chem.* **1984**, *265*, C15. (b) Semmelhack, M. F.; Herndon, J. W.; Springer, J. P. *J. Am. Chem. Soc.* **1983**, *105*, 2497. (c) Semmelhack, M. F.; Herndon, J. W. *Organometallics* **1983**, *2*, 363.

(3) (a) Green, M. L. H.; Mitchard, L. C.; Silverthorn, W. E. *J. Chem. Soc. Dalton Trans.* **1973**, 1952. (b) Faller, J. W.; Rosan, A. M. *J. Am. Chem. Soc.* **1977**, *99*, 4858. Faller, J. W.; Murray, H. H.; White, D. L.; Chao, K. H. *Organometallics* **1983**, *2*, 400. (c) Pearson, A. J.; Khan, M. N. I.; Clardy, J. C.; Cun-heng, H. *J. Am. Chem. Soc.* **1985**, *107*, 2748.

(4) Chaudury, F. M.; Pauson, P. L. *J. Organomet. Chem.* **1974**, *69*, C31.

(5) Stirring a CH<sub>2</sub>Cl<sub>2</sub> solution of [(butadiene)Co(CO)<sub>2</sub>]<sub>2</sub> (prepared from Co<sub>2</sub>(CO)<sub>8</sub> + butadiene in 90% yield according to ref 6) with 2 molar equiv of (C<sub>5</sub>H<sub>5</sub>)<sub>2</sub>FeBF<sub>4</sub> at 20 °C (for 4-6 h) under N<sub>2</sub> followed by filtration and reprecipitation of the solid (2-3 times) from CH<sub>3</sub>NO<sub>2</sub>/Et<sub>2</sub>O affords **1** as a moisture sensitive yellow solid (30-40%). Because of the deficiency of CO's, 50% is the maximum possible yield of **1** from [(C<sub>4</sub>H<sub>6</sub>)Co(CO)<sub>2</sub>]<sub>2</sub>. Running the reaction under 15-200 psi of CO had no effect on the yield. Comparable results have been obtained in the preparation of (isoprene- and (1,3-cyclohexadiene)Co(CO)<sub>3</sub>BF<sub>4</sub>. More efficient routes to **1** are being examined. **1**: IR (CH<sub>3</sub>NO<sub>2</sub>) 2150, 2102 (MC=O), 1050 (BF<sub>4</sub><sup>-</sup>) cm<sup>-1</sup>; <sup>1</sup>H NMR (CD<sub>3</sub>NO<sub>2</sub>)  $\delta$  6.7 (m, 2 H), 3.6 (dd, *J* = 3.5 Hz, 2 H), 2.5 (dd, *J* = 3, 10 Hz, 2 H).

(6) Fischer, E. O.; Kuzel, P.; Fritz, H. P. *Z. Naturforsch., B: Anorg. Chem., Org. Chem., Biochem., Biophys., Biol.* **1961**, *16B*, 138.

(7) Heck, R. F.; Breslow, D. S. *J. Am. Chem. Soc.* **1961**, *83*, 1097.

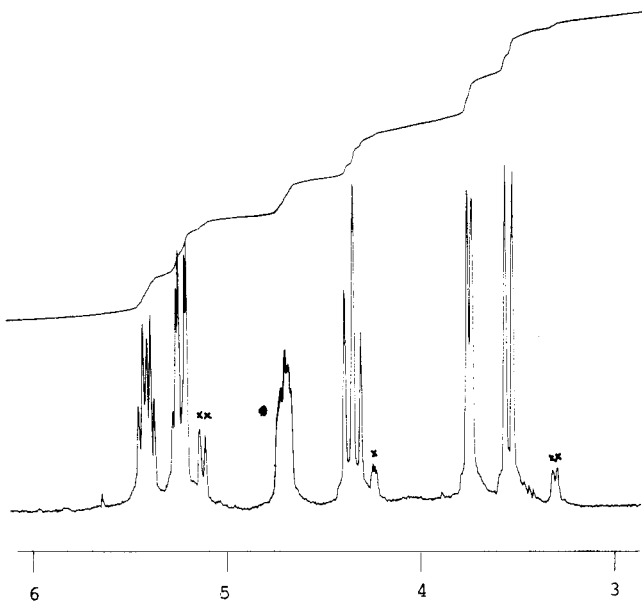
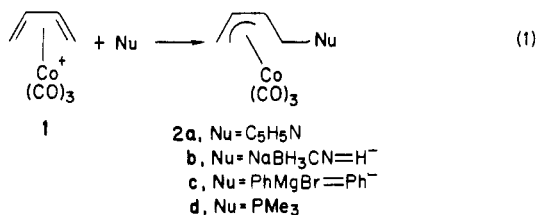


**Figure 1.**  $^1\text{H}$  NMR spectrum of **2a** (acetone- $d_6$ , 300 MHz). The double x (xx) indicates impurities.

have been established unambiguously by  $^1\text{H}$  NMR as the *anti*-( $\eta^3$ -1-substituted allyl)Co(CO) $_3$  derivatives **2a-d** (eq



1).<sup>8</sup> The spectrum of the pyridine adduct shown in Figure 1 is representative, exhibiting a nearly first-order splitting pattern for the ABCDEE' spin system of the butenyl fragment with chemical shifts in the typical range for substituted allyl complexes;<sup>9</sup> proton assignments for **2a-d** were confirmed by complete homonuclear spin decoupling experiments. Furthermore, the spectrum of *anti*-( $\eta^3$ -1-methylallyl)Co(CO) $_3$  (**2b**) prepared according to eq 1 was identical with that reported previously.<sup>9b</sup>

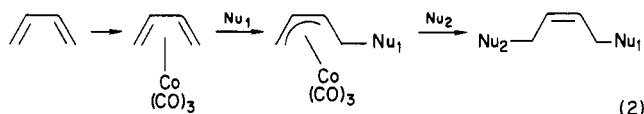
Several aspects of the observed regio- and stereospecificity of these reactions are especially noteworthy. First,

(8) **2a**: from **1** + pyridine (1.1 equiv) in  $\text{CH}_2\text{Cl}_2$ /-78 °C/15 min; precipitated as a yellow solid (79%) from  $\text{CH}_2\text{Cl}_2/\text{Et}_2\text{O}$ ; IR ( $\text{CH}_2\text{Cl}_2$ ) 2070, 2005, 1050  $\text{cm}^{-1}$ ;  $^1\text{H}$  NMR [( $\text{CD}_3$ ) $_2\text{CO}$ , Figure 1]  $\delta$  9.13 (d,  $J$  = 11 Hz, 2 H, ortho), 8.76 (t,  $J$  = 7 Hz, 1 H, para), 8.29 (t,  $J$  = 7 Hz, 1 H, meta), 5.41 (m, 1 H,  $\text{H}_c$ ), 5.23 (dd,  $J$  = 14, 3 Hz,  $\text{H}_e$ ), 4.69 (m, 1 H,  $\text{H}_a$ ), 4.35 (apparent t,  $J$  = 14, 14 Hz, 1 H,  $\text{H}_b$ ), 3.74 (d,  $J$  = 7 Hz, 1 H,  $\text{H}_b$ ), 3.53 (d,  $J$  = 11 Hz,  $\text{H}_a$ ). Anal. Calcd for  $\text{C}_{12}\text{H}_{11}\text{BCO}_4\text{NO}_3$ : C, 39.70; H, 3.03. Found: C, 39.48; H, 3.2. **2b**: from **1** +  $\text{NaBH}_3\text{CN}$  (1.1 equiv) in  $\text{CH}_3\text{NO}_2/\text{O}^\circ\text{C}/10$  min; extraction with pentane followed by solvent evaporation gave **2b** (50%) as a volatile yellow liquid; IR (pentane) 2060, 1990  $\text{cm}^{-1}$ ;  $^1\text{H}$  NMR ( $\text{C}_6\text{D}_6$ )  $\delta$  4.38 (m, 1 H,  $\text{H}_c$ ), 3.83 (m, 1H,  $\text{H}_a$ ), 2.89 (d,  $J$  = 5 Hz, 1 H,  $\text{H}_b$ ), 2.44 (d,  $J$  = 11 Hz, 1 H,  $\text{H}_a$ ), 0.80 (d,  $J$  = 7 Hz, 3 H,  $\text{CH}_3$ ); lit. NMR ref 9b. **2c**: from **1** +  $\text{PhMgBr}$  (1.1 equiv) in  $\text{Et}_2\text{O}$ /-78 °C/30 min; solvent evaporated and residue chromatographed through alumina to give **2c** (60%) as a somewhat unstable yellow solid; IR ( $\text{Et}_2\text{O}$ ) 2060, 1990  $\text{cm}^{-1}$ ;  $^1\text{H}$  NMR ( $\text{C}_6\text{D}_6$ )  $\delta$  7.3 (m, 5 H,  $\text{C}_6\text{H}_5$ ), 4.32 (m, 1 H,  $\text{H}_c$ ), 3.93 (m, 1 H,  $\text{H}_d$ ), 2.87 (d,  $J$  = 6 Hz, 1 H,  $\text{H}_b$ ), 2.54 (dd,  $J$  = 14, 4 Hz,  $\text{H}_e$ ), 2.45 (d,  $J$  = 11 Hz, 1 H,  $\text{H}_a$ ), 2.00 (dd,  $J$  = 14, 11 Hz,  $\text{H}_e$ ); MS (12 eV),  $m/e$  274 ( $\text{M}^+$ ), 246 ( $\text{M} - \text{CO}$ ), 218 ( $\text{M} - 2\text{CO}$ ), 190 ( $\text{M} - 3\text{CO}$ ), 131 ( $\text{M} - \text{Co}(\text{CO})_3$ ). **2d**: from **1** +  $\text{PMe}_3$  (1.0 equiv) in  $\text{CH}_3\text{NO}_2$ /-45 °C/15 min; addition of  $\text{Et}_2\text{O}$  caused precipitation of yellow solid **2d** (35%); IR ( $\text{CH}_2\text{Cl}_2$ ) 2070, 2000, 1070  $\text{cm}^{-1}$ ;  $^1\text{H}$  NMR (acetone- $d_6$ )  $\delta$  5.42 (m, 1 H,  $\text{H}_c$ ), 4.40 (m, 1 H,  $\text{H}_d$ ), 3.67 (d,  $J$  = 7 Hz, 1 H,  $\text{H}_b$ ), 3.27 (d,  $J$  = 11 Hz, 1 H,  $\text{H}_a$ ), 3.13 (apparent q,  $J_{\text{HH}} = 14, 7$  Hz,  $J_{\text{PH}} = 14$  Hz, 1 H,  $\text{H}_e$ ), 2.10 (d,  $J_{\text{PH}} = 14$  Hz, 9 H,  $\text{PMe}_3$ ).

(9) (a) Chatani, N.; Yamasaki, Y.; Murai, S.; Sonada, N. *Tetrahedron Lett.* 1983, 24, 5649. (b) Bertrand, J. A.; Jonassen H. B.; Moore, D. W. *Inorg. Chem.* 1963, 2, 601.

the preference for C-1 attack parallels the reported behavior of the CpMo(diene)(CO) $_2^+$  systems<sup>3</sup> but stands in contrast with the C-2 selectivity (kinetic) of the *neutral*, isoelectronic iron system.<sup>2</sup> IR monitoring gave no evidence of the formation of any transient intermediates in these reactions. We suspect that the basis for the differing regioselectivities derives from the charge differences in the systems, a hypothesis which is currently being tested experimentally and theoretically.<sup>10</sup> Not surprisingly, the cationic cobalt derivatives **1** are far more reactive than the neutral iron tricarbonyl compounds. The *anti* stereoselectivity which retains the cisoid geometry of the original coordinated diene is also noteworthy in view of the facile *anti*  $\rightarrow$  *syn* isomerization known for ( $\eta^3$ -allyl)Co(CO) $_3$  complexes.<sup>9b</sup> This feature makes eq 1 an attractive, general route to the rather inaccessible *anti*- $\eta^3$ -allyl derivatives.

The potential for subsequent selective functionalization of the ( $\eta^3$ -allyl)Co(CO) $_3$  species resulting from eq 1 is an especially appealing feature of the present system. Recently reported<sup>11</sup> and emerging<sup>12</sup> chemistry of the allyl complexes **2** provides a scheme for regio- and stereoselective 1,4-functionalization of dienes (eq 2) by means of



sequential *double nucleophilic addition*. As an illustration of this process, one-pot treatment of a suspension of **1** in THF, first with  $\text{NaBH}_3\text{CN}$  (1.0 equiv, 0 °C, 10 min) and then with  $\text{NaCH}(\text{CO}_2\text{Me})_2$  (1.0 equiv in THF, 20 °C, 20 h) led, after aqueous workup, to a 6:1 mixture of (*Z*)-2-butenyl dimethylmalonate and (2-methyl-2-propenyl)dimethylmalonate (33%;<sup>13</sup> eq 2,  $\text{Nu}_1 = \text{H}^-$ ,  $\text{Nu}_2 = ^-\text{CH}(\text{CO}_2\text{Me})$ ).<sup>14</sup> Similarly, addition to **1** of 2 equiv of  $\text{NaCH}(\text{CO}_2\text{Me})_2$  afforded 1,1,6,6-tetracarboxymethoxy (*Z*)-3-hexene (eq 2,  $\text{Nu}_1 = \text{Nu}_2 = ^-\text{CH}(\text{CO}_2\text{Me})_2$ ) as the exclusive product (35%).<sup>13</sup> Particularly significant in the present cobalt system is the ability to add a second nucleophile without necessarily reactivating the  $\eta^3$ -allyl complex by  $\text{NO}^+$  or  $\text{Ph}_3\text{C}^+$ , as required in the Mo( $\eta^4/\eta^3$ ) series<sup>3b,c</sup> and in most other  $\eta^n/\eta^{n-1}$  couples.<sup>14-16</sup> The present method also complements nicely the selective 1,2-difunctionalization of dienes mediated by  $-\text{Fe}(\text{CO})_3$  complexation.<sup>17</sup>

Studies are currently underway to explore the full scope and generality of cobalt-mediated diene functionalization and to elucidate further the factors controlling the regio- and stereochemical course of these reactions.

**Acknowledgment.** We are grateful for financial support provided by the National Institutes of Health (GM 26760 and GM 34799).

**Registry No.** **1**, 90502-48-0; **2a**, 99922-86-8; **2b**, 31627-45-9; **2c**, 99922-87-9; **2d**, 99946-54-0; [(butadiene)Co(CO) $_2$ ] $_2$ , 53494-67-0;

(10) Theoretical analyses of the reactions of ( $\eta^4$ -diene)M(CO) $_3^+$ (0) with nucleophiles are being conducted by Profs. D. A. Brown (U. Dublin) and O. Eisenstein (U. Paris, Sud) using perturbational Huckel methods.

(11) Hegedus, L. S.; Perry, R. J. *J. Org. Chem.* 1984, 49, 2570. Hegedus, L. S.; Inoue, Y. *J. Am. Chem. Soc.* 1982, 104, 4917.

(12) Barinelli, L. S.; Nicholas, K. M., unpublished results, 1985.

(13) Yields are unoptimized.

(14) Structures established by comparison with authentic samples.

(15) See, e.g.: Chung, Y. K.; Choi, H. S.; Sweigart, D. A. *J. Am. Chem. Soc.* 1982, 104, 4245. Pearson, A. J. *J. Chem. Soc., Chem. Commun.* 1980, 488. Pearson, A. J.; Ong, C. W. *J. Org. Chem.* 1982, 47, 3780.

(16) Palladium-catalyzed 1,4-addition has been reported recently,<sup>17</sup> but, in contrast to the Co-based methodology, acyclic dienes are converted to *E*-substituted olefins.

(17) Bäckvall, J.-E.; Nyström, J.-E.; Nordberg, R. E. *J. Am. Chem. Soc.* 1985, 107, 3676. Akermark, B.; Ljungqvist, A.; Panunzio, M. *Tetrahedron Lett.* 1981, 22, 1055.

(C<sub>5</sub>H<sub>5</sub>)<sub>2</sub>FeBF<sub>4</sub>, 1282-37-7; C<sub>5</sub>H<sub>5</sub>N, 110-86-1; NaBH<sub>3</sub>CN, 25895-60-7; PhMgBr, 100-58-3; PMe<sub>3</sub>, 594-09-2; PPh<sub>3</sub>, 603-35-0; P(OMe)<sub>3</sub>, 512-56-1; NaCH(CO<sub>2</sub>Me)<sub>2</sub>, 18424-76-5; (allyl)SiMe<sub>3</sub>, 762-72-1; MeOH, 67-56-1; 1-(trimethylsilyloxy)cyclohexene, 6651-36-1; (Z)-2-butenyl dimethylmalonate, 99922-88-0; dimethylmalonate, 64963-86-6; 1,1,6,6-tetracarboxymethoxy-(z)-3-hexene, 93915-00-5.

### The Activation of Methane by Rhenium. Catalytic H/D Exchange in Alkanes with CpRe(PPh<sub>3</sub>)<sub>2</sub>H<sub>2</sub>

William D. Jones\*<sup>†</sup> and John A. Maguire

Department of Chemistry, University of Rochester  
Rochester, New York 14627

Received October 1, 1985

**Summary:** The complex CpRe(PPh<sub>3</sub>)<sub>2</sub>H<sub>2</sub> is found to undergo photochemical loss of phosphine. The intermediate formed is capable of catalyzing H/D exchange between benzene, THF, and a variety of alkanes including methane.

In recent years several metal complexes that are capable of activating alkanes have been discovered in which the C-H cleavage reaction proceeds by either an electrophilic<sup>1-4</sup> or nucleophilic<sup>5-10</sup> pathway. In a few of these cases methane has been observed to undergo C-H bond cleavage to give a metal-methyl complex.<sup>1-4,7,8,10</sup> Not since the first reports of alkane activation with Pt(II) by Shilov<sup>11</sup> and Webster<sup>12</sup> have H/D exchange reactions with alkanes been observed. We report here the catalytic exchange of deuterium from C<sub>6</sub>D<sub>6</sub> and THF-d<sub>8</sub> into alkanes upon photochemical activation of CpRe(PPh<sub>3</sub>)<sub>2</sub>H<sub>2</sub>.

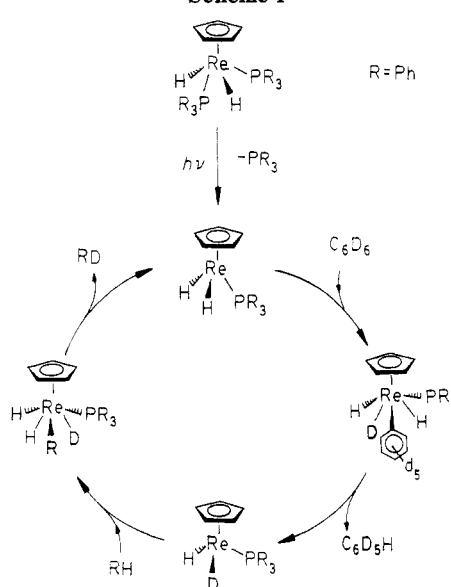
As an analogue of the known (C<sub>5</sub>Me<sub>5</sub>)M(PMe<sub>3</sub>)H<sub>2</sub> (M = Ir, Rh) complexes that lose H<sub>2</sub> upon irradiation and undergo oxidative addition of alkanes,<sup>7,9</sup> we have examined the photochemical behavior of the complexes CpRe-

**Table I. Turnover Numbers and Rates for Exchange of Deuterium from C<sub>6</sub>D<sub>6</sub> into Alkanes by CpRe(PPh<sub>3</sub>)<sub>2</sub>H<sub>2</sub><sup>a</sup>**

alkane	[alkane], M	irradiation time, min	no. of turnovers
methane	~0.4	180	68
ethane	2	300	33
propane	2	60	51, <sup>c</sup> 2.5 <sup>d</sup>
		120	72, <sup>c</sup> 4.0 <sup>d</sup>
		180	77, <sup>c</sup> 4.0 <sup>d</sup>
cyclopropane	5	40	250
		70	369
		120	409
		180	423
cyclopentane	1.2	30	42
		70	74
		120	87
		300	90
THF <sup>b</sup>	6.2	60	488, <sup>e</sup> 840 <sup>f</sup>
		100	520, <sup>e</sup> 895 <sup>f</sup>

<sup>a</sup> [CpRe(PPh<sub>3</sub>)<sub>2</sub>H<sub>2</sub>] = 1.2 mM. <sup>b</sup> [CpRe(PPh<sub>3</sub>)<sub>2</sub>H<sub>2</sub>] = 0.6 mM. <sup>c</sup> Primary exchange. <sup>d</sup> Secondary exchange. <sup>e</sup> β exchange. <sup>f</sup> α exchange.

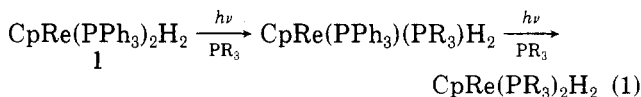
**Scheme I**



<sup>†</sup> Alfred P. Sloan Fellow, 1984-1986. Camille and Henry Dreyfus Teacher-Scholar, 1985-1986.

- (1) Watson, P. L. *J. Am. Chem. Soc.* **1983**, *105*, 6491-6493.
- (2) Thompson, M. E.; Bercaw, J. E. *Pure Appl. Chem.* **1984**, *56*, 1-11.
- (3) Bruno, J. W.; Marks, T. J.; Day, V. W. *J. Am. Chem. Soc.* **1982**, *104*, 7357-7360. Fendrick, C. M.; Marks, T. J. *J. Am. Chem. Soc.* **1984**, *106*, 2214-2216.
- (4) Kitajima, N.; Schwartz, J. J. *J. Am. Chem. Soc.* **1984**, *106*, 2220-2222.
- (5) Crabtree, R. H.; Mihelcic, J. M.; Quirk, J. M. *J. Am. Chem. Soc.* **1979**, *101*, 7738-7740. Crabtree, R. H.; Mellea, M. F.; Mihelcic, J. M.; Quirk, J. M. *J. Am. Chem. Soc.* **1982**, *104*, 107-113. Crabtree, R. H.; Demou, P. C.; Eden, D.; Mihelcic, J. M.; Parnell, C. A.; Quirk, J. M.; Morris, G. E. *J. Am. Chem. Soc.* **1982**, *104*, 6994-7001.
- (6) Baudry, D.; Ephritikhine, M.; Felkin, H. *J. Chem. Soc., Chem. Commun.* **1980**, 1243-1244. Felkin, H.; Fillebeen-Khan, T.; Gault, Y.; Holmes-Smith, R.; Zakrzewski, J. *Tetrahedron Lett.* **1984**, *25*, 1279-1282. Baudry, D.; Ephritikhine, M.; Felkin, H.; Zakrzewski, J. *Tetrahedron Lett.* **1984**, *25*, 1283-1284.
- (7) Janowicz, A. H.; Bergman, R. G. *J. Am. Chem. Soc.* **1982**, *104*, 352-354. Bergman, R. G.; Janowicz, A. H. *J. Am. Chem. Soc.* **1983**, *105*, 3929-3939. Wax, M. J.; Stryker, J. M.; Buchanan, J. M.; Kovac, C. A.; Bergman, R. G. *J. Am. Chem. Soc.* **1984**, *106*, 1121-1122.
- (8) Hoyano, J. K.; Graham, W. A. G. *J. Am. Chem. Soc.* **1982**, *104*, 3723-3725. Hoyano, J. K.; McMaster, A. D.; Graham, W. A. G. *J. Am. Chem. Soc.* **1983**, *105*, 7190-7191. Rest, A. J.; Whitwell, I.; Graham, W. A. G.; Hoyano, J. K.; McMaster, A. D. *J. Chem. Soc., Chem. Commun.* **1984**, 624-626.
- (9) Jones, W. D.; Feher, F. J. *Organometallics* **1983**, *2*, 562-563. Jones, W. D.; Feher, F. J. *J. Am. Chem. Soc.* **1984**, *106*, 1650-1663. Jones, W. D.; Feher, F. J. *J. Am. Chem. Soc.* **1985**, *107*, 620-631.
- (10) Bergman, R. G.; Seidler, P. F.; Wenzel, T. T. *J. Am. Chem. Soc.* **1985**, *107*, 4358-4359.
- (11) Gol'dshleger, N. F.; Tyabin, M. B.; Shilov, A. E.; Shteinman, A. A. *Russ. J. Phys. Chem. (Engl. Trans)* **1969**, *43*, 1222-1223.
- (12) Hodges, R. J.; Webster, D. E.; Wells, P. B. *J. Chem. Soc., Chem. Commun.* **1971**, 462-463.

(PR<sub>3</sub>)<sub>2</sub>H<sub>2</sub> (R = alkyl, aryl). Contrary to the behavior of the rhodium and iridium complexes, the dihydride CpRe(PPh<sub>3</sub>)<sub>2</sub>H<sub>2</sub> (1) loses PPh<sub>3</sub> rather than H<sub>2</sub> upon photolysis,<sup>13</sup> apparently due to the trans disposition of the hydride ligands.<sup>14</sup> Irradiation of 1 in THF solution in the presence of other phosphines results in the stepwise formation of CpRe(PPh<sub>3</sub>)(PR<sub>3</sub>)H<sub>2</sub> and CpRe(PR<sub>3</sub>)<sub>2</sub>H<sub>2</sub> (R = *p*-tolyl, methyl, C<sub>6</sub>D<sub>5</sub>) in quantitative yield (eq 1).<sup>15</sup>



(13) Photochemical phosphine loss has been observed previously: (a) Green, M. A.; Huffman, J. C.; Caulton, K. G.; Rybak, W. K.; Ziolkowski, J. J. *J. Organomet. Chem.* **1981**, *218*, C39-C43. (b) Roberts, D. A.; Geoffroy, G. L. *J. Organomet. Chem.* **1981**, *214*, 221-231.

(14) Preliminary X-ray studies of CpRe(PPh<sub>3</sub>)<sub>2</sub>H<sub>2</sub>·C<sub>6</sub>H<sub>6</sub> show a symmetrical trans disposition of the two PPh<sub>3</sub> ligands.

(15) The UV spectrum of 1 displays a well-resolved absorption with λ<sub>max</sub> = 328 nm. <sup>1</sup>H NMR (C<sub>6</sub>D<sub>6</sub>): 1, δ 4.268 (s, 5 H), 7.621 (m, 12 H), 6.973 (m, 18 H), -9.953 (t, J = 40.1 Hz, 2 H); CpRe(PMe<sub>3</sub>)<sub>2</sub>H<sub>2</sub>, δ 4.553 (s, 5 H), 1.537 (d, J = 7.3 Hz, 18 H), -12.130 (t, J = 43.6 Hz, 2 H); CpRe[P(*p*-tolyl)]<sub>2</sub>H<sub>2</sub>, δ 4.404 (s, 5 H), 7.641 (t, J = 9.0 Hz, 12 H), 6.902 (d, J = 9.0 Hz, 12 H), 2.031 (s, 18 H), -9.901 (t, J = 40.2 Hz, 2 H); CpRe(PMe<sub>3</sub>)(PPh<sub>3</sub>)H<sub>2</sub>, δ 4.531 (s, 5 H), 7.800 (m, 6 H), 7.060 (m, 9 H), 1.218 (d, J = 8.9 Hz, 9 H), -11.186 (dd, J = 44.7, 40.7 Hz, 2 H); CpRe[P(*p*-tolyl)]<sub>2</sub>(PPh<sub>3</sub>)H<sub>2</sub>, δ 4.342 (s, 5 H), 7.680 (m, 6 H), 7.35 (m, 6 H), 6.95 (m, 15 H), 2.040 (s, 9 H), -9.923 (t, J = 40.1 Hz, 2 H).

(C<sub>5</sub>H<sub>5</sub>)<sub>2</sub>FeBF<sub>4</sub>, 1282-37-7; C<sub>5</sub>H<sub>5</sub>N, 110-86-1; NaBH<sub>3</sub>CN, 25895-60-7; PhMgBr, 100-58-3; PMe<sub>3</sub>, 594-09-2; PPh<sub>3</sub>, 603-35-0; P(OMe)<sub>3</sub>, 512-56-1; NaCH(CO<sub>2</sub>Me)<sub>2</sub>, 18424-76-5; (allyl)SiMe<sub>3</sub>, 762-72-1; MeOH, 67-56-1; 1-(trimethylsilyloxy)cyclohexene, 6651-36-1; (Z)-2-butenyl dimethylmalonate, 99922-88-0; dimethylmalonate, 64963-86-6; 1,1,6,6-tetracarboxymethoxy-(z)-3-hexene, 93915-00-5.

### The Activation of Methane by Rhenium. Catalytic H/D Exchange in Alkanes with CpRe(PPh<sub>3</sub>)<sub>2</sub>H<sub>2</sub>

William D. Jones\*<sup>†</sup> and John A. Maguire

Department of Chemistry, University of Rochester  
Rochester, New York 14627

Received October 1, 1985

**Summary:** The complex CpRe(PPh<sub>3</sub>)<sub>2</sub>H<sub>2</sub> is found to undergo photochemical loss of phosphine. The intermediate formed is capable of catalyzing H/D exchange between benzene, THF, and a variety of alkanes including methane.

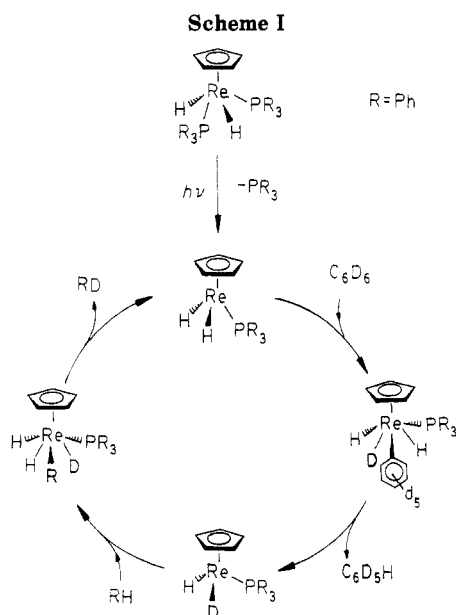
In recent years several metal complexes that are capable of activating alkanes have been discovered in which the C-H cleavage reaction proceeds by either an electrophilic<sup>1-4</sup> or nucleophilic<sup>5-10</sup> pathway. In a few of these cases methane has been observed to undergo C-H bond cleavage to give a metal-methyl complex.<sup>1-4,7,8,10</sup> Not since the first reports of alkane activation with Pt(II) by Shilov<sup>11</sup> and Webster<sup>12</sup> have H/D exchange reactions with alkanes been observed. We report here the catalytic exchange of deuterium from C<sub>6</sub>D<sub>6</sub> and THF-d<sub>8</sub> into alkanes upon photochemical activation of CpRe(PPh<sub>3</sub>)<sub>2</sub>H<sub>2</sub>.

As an analogue of the known (C<sub>5</sub>Me<sub>5</sub>)M(PMe<sub>3</sub>)H<sub>2</sub> (M = Ir, Rh) complexes that lose H<sub>2</sub> upon irradiation and undergo oxidative addition of alkanes,<sup>7,9</sup> we have examined the photochemical behavior of the complexes CpRe-

**Table I. Turnover Numbers and Rates for Exchange of Deuterium from C<sub>6</sub>D<sub>6</sub> into Alkanes by CpRe(PPh<sub>3</sub>)<sub>2</sub>H<sub>2</sub><sup>a</sup>**

alkane	[alkane], M	irradiation time, min	no. of turnovers
methane	~0.4	180	68
ethane	2	300	33
propane	2	60	51, <sup>c</sup> 2.5 <sup>d</sup>
		120	72, <sup>c</sup> 4.0 <sup>d</sup>
		180	77, <sup>c</sup> 4.0 <sup>d</sup>
cyclopropane	5	40	250
		70	369
		120	409
		180	423
cyclopentane	1.2	30	42
		70	74
		120	87
		300	90
THF <sup>b</sup>	6.2	60	488, <sup>e</sup> 840 <sup>f</sup>
		100	520, <sup>e</sup> 895 <sup>f</sup>

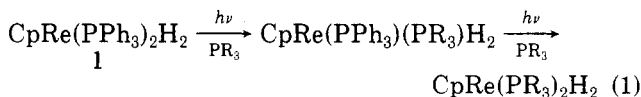
<sup>a</sup> [CpRe(PPh<sub>3</sub>)<sub>2</sub>H<sub>2</sub>] = 1.2 mM. <sup>b</sup> [CpRe(PPh<sub>3</sub>)<sub>2</sub>H<sub>2</sub>] = 0.6 mM. <sup>c</sup> Primary exchange. <sup>d</sup> Secondary exchange. <sup>e</sup> β exchange. <sup>f</sup> α exchange.



<sup>†</sup> Alfred P. Sloan Fellow, 1984-1986. Camille and Henry Dreyfus Teacher-Scholar, 1985-1986.

- (1) Watson, P. L. *J. Am. Chem. Soc.* **1983**, *105*, 6491-6493.
- (2) Thompson, M. E.; Bercaw, J. E. *Pure Appl. Chem.* **1984**, *56*, 1-11.
- (3) Bruno, J. W.; Marks, T. J.; Day, V. W. *J. Am. Chem. Soc.* **1982**, *104*, 7357-7360. Fendrick, C. M.; Marks, T. J. *J. Am. Chem. Soc.* **1984**, *106*, 2214-2216.
- (4) Kitajima, N.; Schwartz, J. J. *J. Am. Chem. Soc.* **1984**, *106*, 2220-2222.
- (5) Crabtree, R. H.; Mihelcic, J. M.; Quirk, J. M. *J. Am. Chem. Soc.* **1979**, *101*, 7738-7740. Crabtree, R. H.; Mellea, M. F.; Mihelcic, J. M.; Quirk, J. M. *J. Am. Chem. Soc.* **1982**, *104*, 107-113. Crabtree, R. H.; Demou, P. C.; Eden, D.; Mihelcic, J. M.; Parnell, C. A.; Quirk, J. M.; Morris, G. E. *J. Am. Chem. Soc.* **1982**, *104*, 6994-7001.
- (6) Baudry, D.; Ephritikhine, M.; Felkin, H. *J. Chem. Soc., Chem. Commun.* **1980**, 1243-1244. Felkin, H.; Fillebeen-Khan, T.; Gault, Y.; Holmes-Smith, R.; Zakrzewski, J. *Tetrahedron Lett.* **1984**, *25*, 1279-1282. Baudry, D.; Ephritikhine, M.; Felkin, H.; Zakrzewski, J. *Tetrahedron Lett.* **1984**, *25*, 1283-1284.
- (7) Janowicz, A. H.; Bergman, R. G. *J. Am. Chem. Soc.* **1982**, *104*, 352-354. Bergman, R. G.; Janowicz, A. H. *J. Am. Chem. Soc.* **1983**, *105*, 3929-3939. Wax, M. J.; Stryker, J. M.; Buchanan, J. M.; Kovac, C. A.; Bergman, R. G. *J. Am. Chem. Soc.* **1984**, *106*, 1121-1122.
- (8) Hoyano, J. K.; Graham, W. A. G. *J. Am. Chem. Soc.* **1982**, *104*, 3723-3725. Hoyano, J. K.; McMaster, A. D.; Graham, W. A. G. *J. Am. Chem. Soc.* **1983**, *105*, 7190-7191. Rest, A. J.; Whitwell, I.; Graham, W. A. G.; Hoyano, J. K.; McMaster, A. D. *J. Chem. Soc., Chem. Commun.* **1984**, 624-626.
- (9) Jones, W. D.; Feher, F. J. *Organometallics* **1983**, *2*, 562-563. Jones, W. D.; Feher, F. J. *J. Am. Chem. Soc.* **1984**, *106*, 1650-1663. Jones, W. D.; Feher, F. J. *J. Am. Chem. Soc.* **1985**, *107*, 620-631.
- (10) Bergman, R. G.; Seidler, P. F.; Wenzel, T. T. *J. Am. Chem. Soc.* **1985**, *107*, 4358-4359.
- (11) Gol'dshleger, N. F.; Tyabin, M. B.; Shilov, A. E.; Shteinman, A. A. *Russ. J. Phys. Chem. (Engl. Trans)* **1969**, *43*, 1222-1223.
- (12) Hodges, R. J.; Webster, D. E.; Wells, P. B. *J. Chem. Soc., Chem. Commun.* **1971**, 462-463.

(PR<sub>3</sub>)<sub>2</sub>H<sub>2</sub> (R = alkyl, aryl). Contrary to the behavior of the rhodium and iridium complexes, the dihydride CpRe(PPh<sub>3</sub>)<sub>2</sub>H<sub>2</sub> (1) loses PPh<sub>3</sub> rather than H<sub>2</sub> upon photolysis,<sup>13</sup> apparently due to the trans disposition of the hydride ligands.<sup>14</sup> Irradiation of 1 in THF solution in the presence of other phosphines results in the stepwise formation of CpRe(PPh<sub>3</sub>)(PR<sub>3</sub>)H<sub>2</sub> and CpRe(PR<sub>3</sub>)<sub>2</sub>H<sub>2</sub> (R = *p*-tolyl, methyl, C<sub>6</sub>D<sub>5</sub>) in quantitative yield (eq 1).<sup>15</sup>



(13) Photochemical phosphine loss has been observed previously: (a) Green, M. A.; Huffman, J. C.; Caulton, K. G.; Rybak, W. K.; Ziolkowski, J. J. *J. Organomet. Chem.* **1981**, *218*, C39-C43. (b) Roberts, D. A.; Geoffroy, G. L. *J. Organomet. Chem.* **1981**, *214*, 221-231.

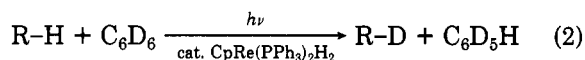
(14) Preliminary X-ray studies of CpRe(PPh<sub>3</sub>)<sub>2</sub>H<sub>2</sub>·C<sub>6</sub>H<sub>6</sub> show a symmetrical trans disposition of the two PPh<sub>3</sub> ligands.

(15) The UV spectrum of 1 displays a well-resolved absorption with λ<sub>max</sub> = 328 nm. <sup>1</sup>H NMR (C<sub>6</sub>D<sub>6</sub>): 1, δ 4.268 (s, 5 H), 7.621 (m, 12 H), 6.973 (m, 18 H), -9.953 (t, J = 40.1 Hz, 2 H); CpRe(PMe<sub>3</sub>)<sub>2</sub>H<sub>2</sub>, δ 4.553 (s, 5 H), 1.537 (d, J = 7.3 Hz, 18 H), -12.130 (t, J = 43.6 Hz, 2 H); CpRe[P(*p*-tolyl)]<sub>2</sub>H<sub>2</sub>, δ 4.404 (s, 5 H), 7.641 (t, J = 9.0 Hz, 12 H), 6.902 (d, J = 9.0 Hz, 12 H), 2.031 (s, 18 H), -9.901 (t, J = 40.2 Hz, 2 H); CpRe(PMe<sub>3</sub>)(PPh<sub>3</sub>)H<sub>2</sub>, δ 4.531 (s, 5 H), 7.800 (m, 6 H), 7.060 (m, 9 H), 1.218 (d, J = 8.9 Hz, 9 H), -11.186 (dd, J = 44.7, 40.7 Hz, 2 H); CpRe[P(*p*-tolyl)]<sub>2</sub>(PPh<sub>3</sub>)H<sub>2</sub>, δ 4.342 (s, 5 H), 7.680 (m, 6 H), 7.35 (m, 6 H), 6.95 (m, 15 H), 2.040 (s, 9 H), -9.923 (t, J = 40.1 Hz, 2 H).



Irradiation of 1 in C<sub>6</sub>D<sub>6</sub> solvent containing an excess of alkane results in the catalytic scrambling of deuterium between the benzene and the alkane (eq 2). In a typical experiment, 5 mg of 1 in 0.4 mL of C<sub>6</sub>D<sub>6</sub> along with ~300 equiv of methane were sealed in an NMR tube under vacuum.<sup>16</sup> Upon irradiation (200-W Hg lamp, Pyrex filter) the appearance of CH<sub>3</sub>D is observed by <sup>2</sup>H NMR spectroscopy at δ 0.115. The quartet nature of the resonance (*J* = 2.0 Hz) is consistent with a single H/D exchange per encounter and is identical with the <sup>2</sup>H NMR spectrum of authentic CH<sub>3</sub>D. Added *c*-C<sub>6</sub>D<sub>12</sub> as an internal standard (2 equiv relative to Re) shows 68 turnovers after 3 h of irradiation. During this period, the appearance of free PPh<sub>3</sub> is observed in the <sup>1</sup>H NMR as well as a new unidentified rhenium side product (20%) displaying a cyclopentadienyl singlet at δ 4.47.

Details of the turnover numbers and rates based on similar experiments with ethane, propane, cyclopropane, cyclopentane, and THF are shown in Table I. As the irradiation proceeds, 1 is depleted, free PPh<sub>3</sub> appears, and the initial turnover rates are observed to drop off. Irradiation of 1 in THF-*d*<sub>8</sub> solvent also serves as an efficient method for exchanging deuterium into alkanes. Methane is readily deuterated upon photolysis in this solvent. Turnover numbers for C<sub>6</sub>D<sub>6</sub>/THF H/D exchange exceed 1000.



The loss of PPh<sub>3</sub> from 1 appears to generate the species [CpRe(PPh<sub>3</sub>)H<sub>2</sub>] that is active in the H/D exchange. The addition of 3 equiv of PPh<sub>3</sub> completely inhibits the isotopic scrambling between C<sub>6</sub>D<sub>6</sub> and ethane. Slow photochemical decomposition of 1 also produces free PPh<sub>3</sub>, accounting for the inhibition of the reaction upon prolonged photolysis. Added O<sub>2</sub> (20 equiv) has little effect upon the scrambling rate or products, suggesting that alkyl radicals are not involved. A proposed mechanism for the reaction is suggested in Scheme I, in which the intermediates CpRe(PPh<sub>3</sub>)H<sub>3</sub>R are similar to the known CpRe(PPh<sub>3</sub>)H<sub>4</sub>.<sup>13a</sup>

The kinetic selectivity of the reactive intermediate was investigated by photolysis of C<sub>6</sub>D<sub>6</sub> solutions of 1 containing both an alkane and methane. Integration of the R-D resonances in the <sup>2</sup>H NMR spectrum corrected for the relative amounts of alkane present showed only small preferences for methane over ethane (2.0:1) and methane over cyclopentane (1.6:1). The preference for primary over secondary activation in propane was observed to be 20:1. THF displayed a 1.7:1 ratio of α:β exchange. Competition between propane and benzene in THF-*d*<sub>8</sub> solvent shows an 8.2:1 ratio of arene:alkane H/D exchange, indicating comparable reactivity between aromatic and primary aliphatic C-H bonds.

There are two interesting features of this system. First, the recent studies by Bergman and co-workers<sup>10</sup> using CpRe(PMe<sub>3</sub>)<sub>3</sub> and derivatives provides a means of circumventing the inability to labilize H<sub>2</sub> in CpRe(PPh<sub>3</sub>)<sub>2</sub>H<sub>2</sub>. Photochemical loss of PMe<sub>3</sub> from this compound resulted in the formation of alkane oxidative addition adducts in which it is not possible to exchange hydrogen and deuterium between C-H and C-D containing substrates. The intermediate species responsible for alkane activation in the system reported here must contain at least one hydrogen ligand and therefore has to be fundamentally

different from the one reported by Bergman.

Second, the presence of more than one hydrogen combined with the assumption that an even-electron intermediate is involved means that a Re(III)/Re(V) couple is probably responsible for the alkane activation. Felkin also proposed a Re(III)/Re(V) couple for the activation of alkanes by Re(PPh<sub>3</sub>)<sub>2</sub>H<sub>7</sub>.<sup>6</sup> The catalytic H/D exchange by CpRe(PPh<sub>3</sub>)<sub>2</sub>H<sub>2</sub> represents C-H bond activation by a complex in an intermediate oxidation state, probably involving an intermediate that is neither electrophilic nor nucleophilic in nature.

**Acknowledgment.** We thank the U.S. Department of Energy (83ER13095) for their support of this work.

**Registry No.** 1, 81422-70-0; CpRe(PMe<sub>3</sub>)<sub>2</sub>H<sub>2</sub>, 97577-92-9; CpRe[P(*p*-tolyl)<sub>3</sub>]<sub>2</sub>H<sub>2</sub>, 100164-66-7; CpRe(PMe<sub>3</sub>)(PPh<sub>3</sub>)<sub>2</sub>H<sub>2</sub>, 100082-36-8; CpRe[P(*p*-toy)]<sub>3</sub>(PPh<sub>3</sub>)H<sub>2</sub>, 100082-37-9; THF, 109-99-9; THF-*d*<sub>8</sub>, 1693-74-9; C<sub>6</sub>D<sub>6</sub>, 1076-43-3; methane, 74-82-8; ethane, 74-84-0; propane, 74-98-6; cyclopropane, 75-19-4; cyclopentane, 287-92-3.

### Transformation of an η<sup>4</sup>-Cycloocta-1,5-diene (cod) Ligand into an η<sup>1</sup>-Alkenyl Group from Reactions of CpRuH(cod) (Cp = η<sup>5</sup>-C<sub>5</sub>H<sub>5</sub>) with Diphosphines: The X-ray Structural Determination of the Orange and Yellow Forms of CpRu(1-σ-C<sub>8</sub>H<sub>13</sub>)(Ph<sub>2</sub>PCH<sub>2</sub>PPh<sub>2</sub>)

David C. Liles, Hester E. Oosthuizen, Alan Shaver,<sup>†</sup> Eric Singleton,\* and Manfred B. Wiege

National Chemical Research Laboratory  
Council for Scientific and Industrial Research  
Pretoria 0001, Republic of South Africa

Received November 5, 1985

**Summary:** Treatment of [RuH(cod)(NH<sub>2</sub>NMe<sub>2</sub>)<sub>3</sub>]PF<sub>6</sub> (cod = cycloocta-1,5-diene) with TICp (Cp = η<sup>5</sup>-C<sub>5</sub>H<sub>5</sub>) gave the novel hydride complex CpRuH(cod). With monodentate ligands, hydride migration occurred to give the η<sup>3</sup>-allyl complexes CpRuL(η<sup>3</sup>-C<sub>8</sub>H<sub>13</sub>) (L = PPh<sub>3</sub>, CNxylyl; xylyl = 2,6-dimethylphenyl) whereas with chelating diphosphines transformation of the hydride complex to the alkenyl derivative CpRuL<sub>2</sub>(1-σ-C<sub>8</sub>H<sub>13</sub>) was found to take place. Restricted rotation about the Ru-C bond in CpRu(Ph<sub>2</sub>PCH<sub>2</sub>PPh<sub>2</sub>)(1-σ-C<sub>8</sub>H<sub>13</sub>) produces yellow and orange forms of this compound, both of which have been characterized by X-ray diffraction.

The chemistry of half-sandwich complexes of ruthenium(II) and osmium(II) received considerable impetus with recent reports<sup>1</sup> of new high yield syntheses of CpRuCl(cod) and Cp'MCl(cod) (M = Ru, Os; Cp' = η<sup>5</sup>-C<sub>5</sub>Me<sub>5</sub>; cod = cycloocta-1,5-diene). The cyclooctadiene and chloro ligands in these compounds are highly labile, providing facile routes into a wealth of cyclopentadienyl and pentamethylcyclopentadienyl derivatives of ruthenium and osmium. In this paper we wish to report the synthesis of the

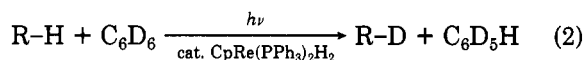
<sup>†</sup>Senior Visiting Scientist from the Department of Chemistry, McGill University, Montreal, Quebec, Canada.

(16) The pressure of methane in the NMR tube exceeds 10 atm under these conditions, and great care must be exercised in handling the sample to avoid explosion.

(1) (a) Albers, M. O.; Oosthuizen, H. E.; Robinson, D. J.; Shaver, A.; Singleton, E. *J. Organomet. Chem.* 1985, 282, C49. (b) Oshima, N.; Suzuki, H.; Moro-oka, Y. *Chem. Lett.* 1984, 1161. (c) Liles, D. C.; Shaver, A.; Singleton, E.; Wiege, M. B. *J. Organomet. Chem.* 1985, 288, C33.

Irradiation of 1 in C<sub>6</sub>D<sub>6</sub> solvent containing an excess of alkane results in the catalytic scrambling of deuterium between the benzene and the alkane (eq 2). In a typical experiment, 5 mg of 1 in 0.4 mL of C<sub>6</sub>D<sub>6</sub> along with ~300 equiv of methane were sealed in an NMR tube under vacuum.<sup>16</sup> Upon irradiation (200-W Hg lamp, Pyrex filter) the appearance of CH<sub>3</sub>D is observed by <sup>2</sup>H NMR spectroscopy at δ 0.115. The quartet nature of the resonance (*J* = 2.0 Hz) is consistent with a single H/D exchange per encounter and is identical with the <sup>2</sup>H NMR spectrum of authentic CH<sub>3</sub>D. Added *c*-C<sub>6</sub>D<sub>12</sub> as an internal standard (2 equiv relative to Re) shows 68 turnovers after 3 h of irradiation. During this period, the appearance of free PPh<sub>3</sub> is observed in the <sup>1</sup>H NMR as well as a new unidentified rhenium side product (20%) displaying a cyclopentadienyl singlet at δ 4.47.

Details of the turnover numbers and rates based on similar experiments with ethane, propane, cyclopropane, cyclopentane, and THF are shown in Table I. As the irradiation proceeds, 1 is depleted, free PPh<sub>3</sub> appears, and the initial turnover rates are observed to drop off. Irradiation of 1 in THF-*d*<sub>8</sub> solvent also serves as an efficient method for exchanging deuterium into alkanes. Methane is readily deuterated upon photolysis in this solvent. Turnover numbers for C<sub>6</sub>D<sub>6</sub>/THF H/D exchange exceed 1000.



The loss of PPh<sub>3</sub> from 1 appears to generate the species [CpRe(PPh<sub>3</sub>)H<sub>2</sub>] that is active in the H/D exchange. The addition of 3 equiv of PPh<sub>3</sub> completely inhibits the isotopic scrambling between C<sub>6</sub>D<sub>6</sub> and ethane. Slow photochemical decomposition of 1 also produces free PPh<sub>3</sub>, accounting for the inhibition of the reaction upon prolonged photolysis. Added O<sub>2</sub> (20 equiv) has little effect upon the scrambling rate or products, suggesting that alkyl radicals are not involved. A proposed mechanism for the reaction is suggested in Scheme I, in which the intermediates CpRe(PPh<sub>3</sub>)H<sub>3</sub>R are similar to the known CpRe(PPh<sub>3</sub>)H<sub>4</sub>.<sup>13a</sup>

The kinetic selectivity of the reactive intermediate was investigated by photolysis of C<sub>6</sub>D<sub>6</sub> solutions of 1 containing both an alkane and methane. Integration of the R-D resonances in the <sup>2</sup>H NMR spectrum corrected for the relative amounts of alkane present showed only small preferences for methane over ethane (2.0:1) and methane over cyclopentane (1.6:1). The preference for primary over secondary activation in propane was observed to be 20:1. THF displayed a 1.7:1 ratio of α:β exchange. Competition between propane and benzene in THF-*d*<sub>8</sub> solvent shows an 8.2:1 ratio of arene:alkane H/D exchange, indicating comparable reactivity between aromatic and primary aliphatic C-H bonds.

There are two interesting features of this system. First, the recent studies by Bergman and co-workers<sup>10</sup> using CpRe(PMe<sub>3</sub>)<sub>3</sub> and derivatives provides a means of circumventing the inability to labilize H<sub>2</sub> in CpRe(PPh<sub>3</sub>)<sub>2</sub>H<sub>2</sub>. Photochemical loss of PMe<sub>3</sub> from this compound resulted in the formation of alkane oxidative addition adducts in which it is not possible to exchange hydrogen and deuterium between C-H and C-D containing substrates. The intermediate species responsible for alkane activation in the system reported here must contain at least one hydrogen ligand and therefore has to be fundamentally

different from the one reported by Bergman.

Second, the presence of more than one hydrogen combined with the assumption that an even-electron intermediate is involved means that a Re(III)/Re(V) couple is probably responsible for the alkane activation. Felkin also proposed a Re(III)/Re(V) couple for the activation of alkanes by Re(PPh<sub>3</sub>)<sub>2</sub>H<sub>7</sub>.<sup>6</sup> The catalytic H/D exchange by CpRe(PPh<sub>3</sub>)<sub>2</sub>H<sub>2</sub> represents C-H bond activation by a complex in an intermediate oxidation state, probably involving an intermediate that is neither electrophilic nor nucleophilic in nature.

**Acknowledgment.** We thank the U.S. Department of Energy (83ER13095) for their support of this work.

**Registry No.** 1, 81422-70-0; CpRe(PMe<sub>3</sub>)<sub>2</sub>H<sub>2</sub>, 97577-92-9; CpRe[P(*p*-tolyl)<sub>3</sub>]<sub>2</sub>H<sub>2</sub>, 100164-66-7; CpRe(PMe<sub>3</sub>)(PPh<sub>3</sub>)<sub>2</sub>H<sub>2</sub>, 100082-36-8; CpRe[P(*p*-toy)]<sub>3</sub>(PPh<sub>3</sub>)H<sub>2</sub>, 100082-37-9; THF, 109-99-9; THF-*d*<sub>8</sub>, 1693-74-9; C<sub>6</sub>D<sub>6</sub>, 1076-43-3; methane, 74-82-8; ethane, 74-84-0; propane, 74-98-6; cyclopropane, 75-19-4; cyclopentane, 287-92-3.

### Transformation of an η<sup>4</sup>-Cycloocta-1,5-diene (cod) Ligand into an η<sup>1</sup>-Alkenyl Group from Reactions of CpRuH(cod) (Cp = η<sup>5</sup>-C<sub>5</sub>H<sub>5</sub>) with Diphosphines: The X-ray Structural Determination of the Orange and Yellow Forms of CpRu(1-σ-C<sub>8</sub>H<sub>13</sub>)(Ph<sub>2</sub>PCH<sub>2</sub>PPh<sub>2</sub>)

David C. Liles, Hester E. Oosthuizen, Alan Shaver,<sup>†</sup> Eric Singleton,\* and Manfred B. Wiege

National Chemical Research Laboratory  
Council for Scientific and Industrial Research  
Pretoria 0001, Republic of South Africa

Received November 5, 1985

**Summary:** Treatment of [RuH(cod)(NH<sub>2</sub>NMe<sub>2</sub>)<sub>3</sub>]PF<sub>6</sub> (cod = cycloocta-1,5-diene) with TICp (Cp = η<sup>5</sup>-C<sub>5</sub>H<sub>5</sub>) gave the novel hydride complex CpRuH(cod). With monodentate ligands, hydride migration occurred to give the η<sup>3</sup>-allyl complexes CpRuL(η<sup>3</sup>-C<sub>8</sub>H<sub>13</sub>) (L = PPh<sub>3</sub>, CNxylyl; xylyl = 2,6-dimethylphenyl) whereas with chelating diphosphines transformation of the hydride complex to the alkenyl derivative CpRuL<sub>2</sub>(1-σ-C<sub>8</sub>H<sub>13</sub>) was found to take place. Restricted rotation about the Ru-C bond in CpRu(Ph<sub>2</sub>PCH<sub>2</sub>PPh<sub>2</sub>)(1-σ-C<sub>8</sub>H<sub>13</sub>) produces yellow and orange forms of this compound, both of which have been characterized by X-ray diffraction.

The chemistry of half-sandwich complexes of ruthenium(II) and osmium(II) received considerable impetus with recent reports<sup>1</sup> of new high yield syntheses of CpRuCl(cod) and Cp'MCl(cod) (M = Ru, Os; Cp' = η<sup>5</sup>-C<sub>5</sub>Me<sub>5</sub>; cod = cycloocta-1,5-diene). The cyclooctadiene and chloro ligands in these compounds are highly labile, providing facile routes into a wealth of cyclopentadienyl and pentamethylcyclopentadienyl derivatives of ruthenium and osmium. In this paper we wish to report the synthesis of the

<sup>†</sup>Senior Visiting Scientist from the Department of Chemistry, McGill University, Montreal, Quebec, Canada.

(16) The pressure of methane in the NMR tube exceeds 10 atm under these conditions, and great care must be exercised in handling the sample to avoid explosion.

(1) (a) Albers, M. O.; Oosthuizen, H. E.; Robinson, D. J.; Shaver, A.; Singleton, E. *J. Organomet. Chem.* 1985, 282, C49. (b) Oshima, N.; Suzuki, H.; Moro-oka, Y. *Chem. Lett.* 1984, 1161. (c) Liles, D. C.; Shaver, A.; Singleton, E.; Wiege, M. B. *J. Organomet. Chem.* 1985, 288, C33.

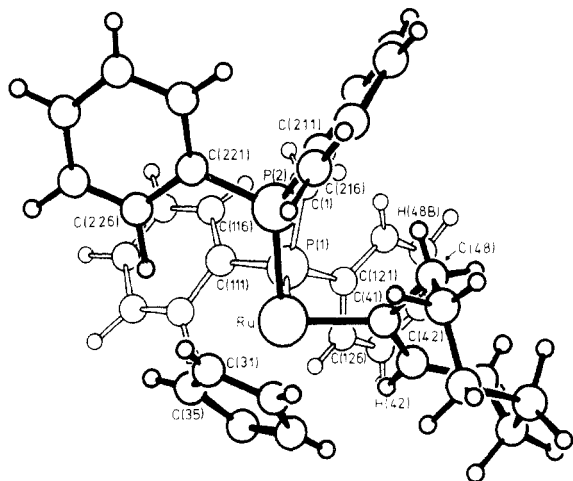


**Figure 1.** **3a** viewed perpendicular to the Ru-C(cyclooctenyl) bond, showing the atom numbering scheme. Selected bond lengths (Å) and angles (deg): Ru-P(1) = 2.258 (1), Ru-P(2) = 2.253 (1), Ru-C(Cp) (mean) = 2.259 (7), Ru-C(41) = 2.101 (6), P(1)-C(1) = 1.846 (5), P(2)-C(1) = 1.838 (6), P-C(Ph) (mean) = 1.836 (8), C(41)-C(42) = 1.352 (9), C(42)-C(43) = 1.516 (12), C(43)-C(44) = 1.508 (11), C(44)-C(45) = 1.536 (9), C(45)-C(46) = 1.543 (13), C(46)-C(47) = 1.517 (11), C(47)-C(48) = 1.516 (10), C(48)-C(41) = 1.515 (6); P(1)-Ru-P(2) = 70.8 (1), P(1)-Ru-C(41) = 85.3 (2), P(2)-Ru-C(41) = 94.1 (1), Ru-C(41)-C(42) = 118.1 (4), Ru-C(41)-C(48) = 125.1 (4), C(42)-C(41)-C(48) = 116.4 (6).

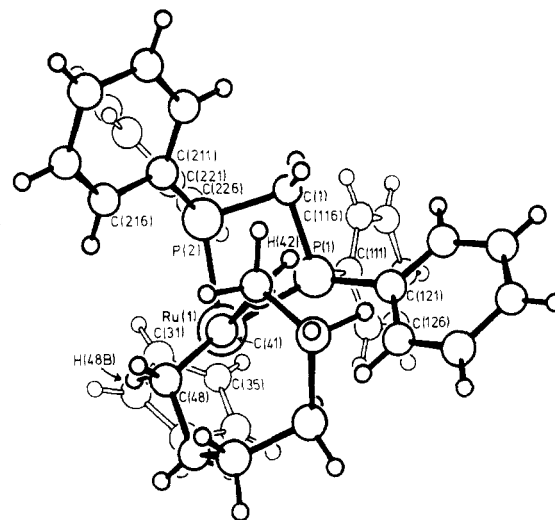


**Figure 2.** The first molecule of **3b** viewed along the Ru-C(cyclooctenyl) bond, showing the atom numbering scheme. Selected bond lengths (Å) and angles (deg): Ru(1)-P(1) = 2.259 (2), Ru(1)-P(2) = 2.250 (2), Ru(1)-C(Cp) (mean) = 2.262 (7), Ru(1)-C(41) = 2.124 (6), P(1)-C(1) = 1.838 (6), P(2)-C(1) = 1.854 (6), P-C(Ph) (mean) = 1.827 (6), C(41)-C(42) = 1.323 (10), C(42)-C(43) = 1.509 (10), C(43)-C(44) = 1.514 (12), C(44)-C(45) = 1.586 (15), C(45)-C(46) = 1.513 (14), C(46)-C(47) = 1.529 (12), C(47)-C(48) = 1.528 (11), C(48)-C(41) = 1.541 (9); P(1)-Ru(1)-P(2) = 71.9 (1), P(1)-Ru(1)-C(41) = 94.6 (2), P(2)-Ru(1)-C(41) = 85.1 (2), Ru(1)-C(41)-C(42) = 128.8 (5), Ru(1)-C(41)-C(48) = 115.3 (5), C(42)-C(41)-C(48) = 115.7 (6).

new highly reactive complex CpRuH(cod) (**1**) and to demonstrate one of its unusual reactivity patterns arising from reactions of **1** with chelating diphosphines.

The hydride complex **1**<sup>2</sup> is readily prepared in 88% yield as a white solid by stirring an acetone solution of [RuH(cod)(NH<sub>2</sub>NMe<sub>2</sub>)<sub>3</sub>]PF<sub>6</sub><sup>3</sup> with TICp for 2 h. Treatment of **1** with monodentate ligands effected hydride migration to the cod ligand to give the η<sup>3</sup>-allyl complexes CpRuL(η<sup>3</sup>-C<sub>3</sub>H<sub>3</sub>) (**2**; L = PPh<sub>3</sub>, CNxylyl; xylyl = 2,6-dimethylphenyl)<sup>4</sup> as yellow air-stable solids (>70% yields). This migration thus follows numerous precedents<sup>5</sup> established for intramolecular hydride transfers in a variety of transition-metal diene hydrides.

In contrast, the chelating diphosphine Me<sub>2</sub>PCH<sub>2</sub>CH<sub>2</sub>PMe<sub>2</sub> reacts with **1** in acetone under reflux (2 h) to give an air-stable yellow solid in high yield and which contains a triplet at δ 5.0 in its <sup>1</sup>H NMR spectrum. This feature we ascribe to the α-hydrogen atom on a ruthenium-vinyl group, thus deducing this structure of the product to be CpRuL<sub>2</sub>(1-σ-C<sub>3</sub>H<sub>3</sub>) (**3**; L<sub>2</sub> = Me<sub>2</sub>PCH<sub>2</sub>CH<sub>2</sub>PMe<sub>2</sub>). The reaction of **1** with the more sterically demanding Ph<sub>2</sub>PCH<sub>2</sub>PPh<sub>2</sub> ligand formed initially a yellow complex which slowly converted to an orange product on standing in acetone (2 h). Both forms corre-

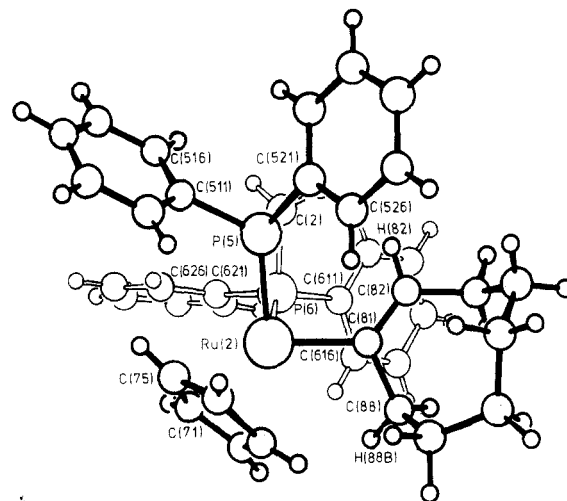


**Figure 3.** The second molecule of **3b** viewed perpendicular to the Ru-C(cyclooctenyl) bond, showing the atom numbering scheme. Selected bond lengths (Å) and angles (deg): Ru(2)-P(5) = 2.244 (2), Ru(2)-P(6) = 2.252 (2), Ru(2)-C(Cp) (mean) = 2.246 (7), Ru(2)-C(81) = 2.119 (6), P(5)-C(2) = 1.842 (6), P(6)-C(2) = 1.859 (6), P-C(Ph) (mean) = 1.839 (7), C(81)-C(82) = 1.330 (9), C(82)-C(83) = 1.515 (10), C(83)-C(84) = 1.512 (13), C(84)-C(85) = 1.538 (13), C(85)-C(86) = 1.501 (12), C(86)-C(87) = 1.515 (12), C(87)-C(88) = 1.530 (11), C(88)-C(81) = 1.537 (8); P(5)-Ru(2)-P(6) = 72.0 (6), P(5)-Ru(2)-C(81) = 94.5 (2), P(6)-Ru(2)-C(81) = 84.5 (2), Ru(2)-C(81)-C(82) = 128.9 (4), Ru(2)-C(81)-C(88) = 115.8 (4), C(82)-C(81)-C(88) = 115.1 (6).

(2) Spectral data of **1**: IR (Nujol) ν(Ru-H) 2000 cm<sup>-1</sup>; <sup>1</sup>H NMR (500 MHz, toluene-d<sub>6</sub>) δ -5.25 (s, 1 H, Ru-H), 1.4-2.3 (m, 8 H, CH<sub>2</sub>), 3.11 (m, 2 H, CH), 3.68 (m, 2 H, CH), 4.91 (s, 5 H, Cp); <sup>13</sup>C NMR (123 MHz, toluene-d<sub>6</sub>) δ 32.7 (s), 34.1 (s), 57.0 (s), 59.4 (s), 83.5 (s, Cp); mp 69 °C. Anal. Calcd for C<sub>13</sub>H<sub>18</sub>Ru: C, 56.71; H, 6.59. Found: C, 56.43; H, 6.35.

(3) Ashworth, T. V.; Singleton, E.; Hough, J. J. *J. Chem. Soc., Dalton Trans.* 1977, 1809.

(4) Spectral data for **2** (CNxylyl derivative): IR (KBr) ν(N≡C) 2040 cm<sup>-1</sup>; <sup>1</sup>H NMR (500 MHz, CD<sub>2</sub>Cl<sub>2</sub>) δ 1.2-2.2 (m, 10 H, CH<sub>2</sub>), 2.38 (s, 6 H, CH<sub>3</sub>), 3.85 (dt, 2 H, anti allyl protons), 4.19 (t, 1 H, central allyl proton), 4.86 (s, 5 H, Cp), 6.9-7.1 (m, 3 H, aromatic); <sup>13</sup>C NMR (123 MHz, CD<sub>2</sub>Cl<sub>2</sub>) δ 19.7 (s, CH<sub>3</sub>), 26.1, 30.7, 33.6 (3 × s, aliphatic C), 48.4 (s, allyl), 69.0 (s, allyl), 80.8 (s, Cp), 125.6, 128.0, 134.0 (3 × s, aromatic C); mp 126 °C. Anal. Calcd for C<sub>22</sub>H<sub>27</sub>NRu: C, 65.0; H, 6.69; N, 3.45. Found: C, 64.84; H, 6.92; N, 3.44. Satisfactory spectral data and elementary analysis were obtained for **2** (PPh<sub>3</sub> derivative) and are given in the supplementary material.

(5) Ashworth, T. V.; Chalmers, A. A.; Meintjies, E.; Oosthuizen, H. E.; Singleton, E. *Organometallics* 1984, 3, 1485 and references therein.

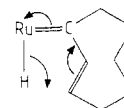


**Figure 4.**

spond to the stoichiometry **3** (L<sub>2</sub> = Ph<sub>2</sub>PCH<sub>2</sub>PPh<sub>2</sub>; yellow, **3a**; orange, **3b**) but differ in their <sup>1</sup>H NMR in the relative chemical shifts of the vinyl hydrogen atoms and asymmetric diphosphine methylene hydrogens.<sup>6</sup> These dif-

ferences indicated variations in the orientation of the  $\eta^1\text{-C}_8\text{H}_{13}$  ring in the molecule due to restricted rotation about the Ru-C bond, which was confirmed by the determination of the crystal and molecular structures of **3a** and **3b** by X-ray diffraction.<sup>7</sup>

The X-ray structure analysis of **3a** and **3b** shows them to be chemically equivalent and confirms the novel Ru-(1- $\sigma\text{-C}_8\text{H}_{13}$ ) linkages. More importantly, however, the molecular structures of **3a** and **3b** confirm and quantify the different orientation and conformations of the cyclooctenyl ligand. In **3a** the conformation of the cyclooctenyl ligand and its orientation with respect to the rest of the molecule are such that the vinyl hydrogen atom, H(42), is directed away from the phenyl groups of the  $\text{Ph}_2\text{PCH}_2\text{PPh}_2$  ligand (Figure 1). The orange form has two independent, but structurally almost identical, molecules in the asymmetric unit,<sup>8</sup> and in these the vinyl hydrogen atom, H(42) or H(82), is directed between two of the diphosphine phenyl groups (Figures 2 and 3). This accounts for the upfield chemical shift observed for this hydrogen in the  $^1\text{H}$  NMR of **3b**. Calculations and inspection of space-filling models show that interconversion of the two molecular structures in **3a** and **3b** is restricted by close contacts during the transition state between the hydrogen atoms of the  $\eta^1\text{-C}_8\text{H}_{13}$  ring and the two nearest diphosphine phenyl groups. In particular, rotations of the  $\eta^1\text{-C}_8\text{H}_{13}$  ring about Ru-C produces minimum contact distances between H(42) [H(82)] or H(48B) [H(88B)] and C(121) [C(51)] or C(126) [C(516)] of between 1.31 and 1.62 Å, depending upon the direction of rotation and the specific molecule.

The conversion of a diene hydride into a metal vinyl complex is, to our knowledge, without precedent, although the reverse reaction, namely, the formation of an  $\eta^3$ -allyl ligand in vinylzirconium, -molybdenum, -ruthenium, and -iridium complexes has been observed.<sup>9</sup> Hydrido allene intermediates were preferred in the Zr, Mo and Ir systems,

leading to speculation from the present system that the stepwise isomerization of 1,5-cod to the thermodynamically favoured 1,3-cod could extend to 1,2-cod. However, our recent isolation<sup>10</sup> of  $\text{CpRuCl}_2(\eta^3\text{-CH}_2\text{C}(\text{Me})\text{CH}_2)$  from oxidative addition of  $\text{Me}_2\text{C}=\text{CHCl}$  to  $\text{CpRuCl}(\text{cod})$  casts some doubt on a hydrido allene intermediate and has led us to consider other intermediates<sup>11</sup> in this process. For example, the  $\alpha$ -hydrogen shifts in tungsten-methyl complexes<sup>12</sup> had led us to consider a hydrido carbene complex (Figure 4) as an intermediate in the  $\eta^3$ -allyl  $\rightarrow$   $\eta^1$ -vinyl conversion. Evidence for this intermediate is now being sought from deprotonation reactions of Ru- $\eta^1$ -allyl complexes, similar to those recently reported in rhenium-alkyl systems.<sup>13</sup>

**Acknowledgment.** An International Scientific Collaboration Award to A.S. from the National Sciences and Engineering Research Council of Canada is gratefully acknowledged.

**Registry No.** 1, 97913-64-9; (L =  $\text{PPh}_3$ ), 100082-24-4; (L =  $\text{CNxyllyl}$ ), 100082-26-6; **3**, 100082-25-5;  $[\text{RuH}(\text{cod})\text{-(NH}_2\text{NMe}_2)_3]\text{PF}_6$ , 61042-65-7;  $\text{TICp}$ , 34822-90-7.

**Supplementary Material Available:** Tables of atomic coordinates, anisotropic temperature factors, bond lengths and angles, and observed and calculated structure factors for **3a** and **3b** and  $^1\text{H}$  NMR and analytical data for **2** ( $\text{PPh}_3$  derivative) and **3** ( $\text{L}_2 = \text{Me}_2\text{PCH}_2\text{CH}_2\text{PMe}_2$ ) (76 pages). Ordering information is given on any current masthead page.

(10) Albers, M. O.; Robinson, D. J.; Singleton, E., unpublished results.

(11) Bonding of an allyl to a transition-metal complex can open a migration corridor for the allyl  $\alpha$ -hydrogen atom to travel intramolecularly across the suprafacial arch of the allyl ligand. There are, however, no unequivocal precedents for this type of migration. See, for example: (a) Mango, F. D. *Adv. Catal.* 1969, 20, 291. (b) Mango, F. D. *Coord. Chem. Rev.* 1975, 15, 109. (c) Slutsky, J.; Kwart, H. *J. Am. Chem. Soc.* 1973, 95, 8678.

(12) Cooper, N. J.; Green, M. L. H. *J. Chem. Soc., Dalton Trans.* 1979, 1122.

(13) Crocco, G. L.; Gladysz, J. A. *J. Am. Chem. Soc.* 1985, 107, 4103.

(6) Spectral data for **3a**:  $^1\text{H}$  NMR (500 MHz,  $(\text{CD}_3)_2\text{CO}$ )  $\delta$  1.37-2.34 (m, 12 H,  $\text{CH}_2$ ), 4.37 (dt,  $\text{PCH}_2\text{P}$ ,  $J(\text{HP}) = 10.8$  Hz,  $J(\text{HH}) = 13.3$  Hz), 4.61 (dt,  $\text{PCH}_2\text{P}$ ,  $J(\text{HP}) = 9.6$  Hz,  $J(\text{HH}) = 13.3$  Hz), 5.02 (s, Cp), 5.06 (t,  $=\text{CH}$ ,  $J(\text{HH}) = 7.8$  Hz), 6.8-7.6 (m, aromatic H);  $^{13}\text{C}$  NMR (123 MHz,  $\text{CDCl}_3$ )  $\delta$  26.6, 27.3, 29.2, 29.5, 30.5, 41.8 (6  $\times$  s, aliphatic C), 48.6 (t,  $\text{CH}_2\text{P}$ ,  $J(\text{PC}) = 20$  Hz), 80.4 (s, Cp), 127-132 (aromatic C), 137.3 (t, ipso aromatic C,  $J(\text{PC}) = 20$  Hz), 139.2 (t,  $=\text{CH}$ ,  $J(\text{PH}) = 7$  Hz), 140.8 (t, ipso aromatic C,  $J(\text{PH}) = 20$  Hz), 146.7 (t, Ru-C,  $J(\text{PH}) = 15$  Hz); mp 156 °C. Anal. Calcd for  $\text{C}_{38}\text{H}_{40}\text{P}_2\text{Ru}$ : C, 69.18; H, 6.11. Found: C, 69.35; H, 6.48. Spectral data for **3b**:  $^1\text{H}$  NMR (500 MHz,  $(\text{CD}_3)_2\text{CO}$ )  $\delta$  1.0-2.1 (m, 12 H,  $\text{CH}_2$ ), 4.36 (dt,  $\text{PH}_2\text{P}$ ,  $J(\text{HP}) = 11.1$  Hz,  $J(\text{HH}) = 13.5$  Hz), 4.77 (t,  $=\text{CH}$ ,  $J(\text{HH}) = 7.7$  Hz), 4.89 (s, Cp), 4.97 (dt,  $\text{PH}_2\text{P}$ ,  $J(\text{HP}) = 9.5$  Hz,  $J(\text{HH}) = 13.8$  Hz), 6.8-7.6 (m, aromatic H);  $^{13}\text{C}$  NMR (123 MHz,  $\text{CDCl}_3$ ) same as for **3a**; mp 108 °C. Anal. Calcd for  $\text{C}_{38}\text{H}_{40}\text{P}_2\text{Ru}$ : C, 69.18; H, 6.11. Found: C, 69.42; H, 6.39.

(7) Crystal data for **3a**: monoclinic, space group  $\text{P}2_1/n$ ;  $a = 11.540$  (2) Å,  $b = 27.731$  (5) Å,  $c = 11.541$  (2) Å,  $\beta = 118.44$  (2)°,  $U = 3247.5$  Å<sup>3</sup>,  $Z = 4$ ,  $D_{\text{calcd}} = 1.349$  Mg m<sup>-3</sup>,  $F(000) = 1368$ , Philips PW1100 diffractometer, Mo K $\alpha$  radiation,  $\lambda = 0.71069$  Å,  $\mu(\text{Mo K}\alpha) = 0.532$  mm<sup>-1</sup>. Crystal data for **3b**: triclinic, space group  $\text{P}\bar{1}$ ;  $a = 10.671$  (4) Å,  $b = 14.269$  (2) Å,  $c = 21.106$  (5) Å,  $\alpha = 98.17$  (2)°,  $\beta = 91.03$  (3)°,  $\gamma = 98.81$  (2)°,  $U = 3140.9$  Å<sup>3</sup>,  $Z = 4$ ,  $D_{\text{calcd}} = 1.395$  Mg m<sup>-3</sup>,  $F(000) = 1368$ , Enraf-Nonius CAD4 diffractometer, Mo K $\alpha$  radiation,  $\mu(\text{Mo K}\alpha) = 0.550$  mm<sup>-1</sup>. The structures were solved by normal heavy-atom methods and were refined by weighted least squares [ $\sum w(|F_o| - |F_c|)^2$  minimized,  $w = \sigma^{-2}(F_o)$ ]. Anisotropic temperature factors were used for all non-hydrogen atoms. For **3a** all hydrogen atoms were located and refined; for **3b** only the hydrogen atoms of the cyclooctenyl ligands were refined; all other hydrogen atoms were added in calculated positions ( $d_{\text{C-H}} = 0.95$  Å). The refinements converged with  $R = 0.0470$  and  $R_w = 0.0454$  for 3668 unique reflections with  $F_o \geq 4\sigma(F_o)$  (**3a**) and  $R = 0.0482$  and  $R_w = 0.0440$  for 6256 unique reflections with  $F_o \geq 4\sigma(F_o)$  (**3b**).

(8) One molecule and the enantiomer of the second are almost superimposable.

(9) (a) McGrady, N. D.; McDade, C.; Bercaw, J. E. In "Organometallic Compounds"; Shapiro, B. L., Ed.; Texas A&M University Press: Texas, 1983. (b) Allen, A. R.; Baker, P. K.; Barnes, S. G.; Bottrill, M.; Green, M.; Orpen, A. G.; Williams, I. D. *J. Chem. Soc., Dalton Trans.* 1983, 927. (c) Ashworth, T. V.; Singleton, E., unpublished results. (d) Schwartz, J.; Hart, D. W.; McGiffert, B. *J. Am. Chem. Soc.* 1974, 96, 5613.

## Synthesis of a Phosphavinyl Complex via Shift of a Pentamethylcyclopentadienyl from Phosphorus to Iron

Dietrich Gudat and Edgar Niecke\*

Fakultät für Chemie der Universität, Postfach 8640  
D-4800 Bielefeld, West Germany

Atta M. Arif, Alan H. Cowley,\* and Sapé Quashie

Department of Chemistry, The University of Texas at Austin  
Austin, Texas 78712

Received October 29, 1985

**Summary:** The reaction of the phosphalkene ( $\eta^1\text{-Me}_5\text{C}_5\text{P}=\text{C}(\text{SiMe}_3)_2$ ) with  $\text{Fe}_2(\text{CO})_9$  affords the  $\eta^1$  (P-bonded) complex ( $\eta^1\text{-Me}_5\text{C}_5\text{P}[(\text{CO})_4\text{Fe}]\text{P}=\text{C}(\text{SiMe}_3)_2$ ) (**4**). Photolysis of **4** produces the phosphavinyl complex [ $\text{Fe}\{\eta^1\text{-P}=\text{C}(\text{SiMe}_3)_2\}(\eta^5\text{-Me}_5\text{C}_5)(\text{CO})_2$ ] (**5**). Compound **5** can also be prepared via the metathetical reaction of  $(\text{Me}_3\text{Si})_2\text{C}=\text{PCl}$  with  $\text{K}[\text{Fe}(\eta^5\text{-Me}_5\text{C}_5)(\text{CO})_2]$ . The structure of **5** has been determined by X-ray crystallography.

Phosphalkenes,  $\text{RP}=\text{CR}_2$ ,<sup>1</sup> are proving to be remarkably versatile ligands. As intact units, they can coordinate

(1) (a) Klebach, T. C.; Lourens, R.; Bickelhaupt, F.; Stam, C. H.; Van Herk, A. *J. Organomet. Chem.* 1981, 210, 211. (b) Kroto, H. W.; Nixon, J. F.; Taylor, M. J.; Frew, A. A.; Muir, K. W. *Polyhedron* 1982, 1, 89. (c) Neilson, R. H.; Thoma, R. J.; Vickovic, I.; Watson, W. A. *Organometallics* 1984, 3, 1132.

ferences indicated variations in the orientation of the  $\eta^1\text{-C}_8\text{H}_{13}$  ring in the molecule due to restricted rotation about the Ru-C bond, which was confirmed by the determination of the crystal and molecular structures of **3a** and **3b** by X-ray diffraction.<sup>7</sup>

The X-ray structure analysis of **3a** and **3b** shows them to be chemically equivalent and confirms the novel Ru-(1- $\sigma\text{-C}_8\text{H}_{13}$ ) linkages. More importantly, however, the molecular structures of **3a** and **3b** confirm and quantify the different orientation and conformations of the cyclooctenyl ligand. In **3a** the conformation of the cyclooctenyl ligand and its orientation with respect to the rest of the molecule are such that the vinyl hydrogen atom, H(42), is directed away from the phenyl groups of the  $\text{Ph}_2\text{PCH}_2\text{PPh}_2$  ligand (Figure 1). The orange form has two independent, but structurally almost identical, molecules in the asymmetric unit,<sup>8</sup> and in these the vinyl hydrogen atom, H(42) or H(82), is directed between two of the diphosphine phenyl groups (Figures 2 and 3). This accounts for the upfield chemical shift observed for this hydrogen in the  $^1\text{H}$  NMR of **3b**. Calculations and inspection of space-filling models show that interconversion of the two molecular structures in **3a** and **3b** is restricted by close contacts during the transition state between the hydrogen atoms of the  $\eta^1\text{-C}_8\text{H}_{13}$  ring and the two nearest diphosphine phenyl groups. In particular, rotations of the  $\eta^1\text{-C}_8\text{H}_{13}$  ring about Ru-C produces minimum contact distances between H(42) [H(82)] or H(48B) [H(88B)] and C(121) [C(51)] or C(126) [C(516)] of between 1.31 and 1.62 Å, depending upon the direction of rotation and the specific molecule.

The conversion of a diene hydride into a metal vinyl complex is, to our knowledge, without precedent, although the reverse reaction, namely, the formation of an  $\eta^3$ -allyl ligand in vinylzirconium, -molybdenum, -ruthenium, and -iridium complexes has been observed.<sup>9</sup> Hydrido allene intermediates were preferred in the Zr, Mo and Ir systems,

leading to speculation from the present system that the stepwise isomerization of 1,5-cod to the thermodynamically favoured 1,3-cod could extend to 1,2-cod. However, our recent isolation<sup>10</sup> of  $\text{CpRuCl}_2(\eta^3\text{-CH}_2\text{C}(\text{Me})\text{CH}_2)$  from oxidative addition of  $\text{Me}_2\text{C}=\text{CHCl}$  to  $\text{CpRuCl}(\text{cod})$  casts some doubt on a hydrido allene intermediate and has led us to consider other intermediates<sup>11</sup> in this process. For example, the  $\alpha$ -hydrogen shifts in tungsten-methyl complexes<sup>12</sup> had led us to consider a hydrido carbene complex (Figure 4) as an intermediate in the  $\eta^3$ -allyl  $\rightarrow$   $\eta^1$ -vinyl conversion. Evidence for this intermediate is now being sought from deprotonation reactions of Ru- $\eta^1$ -allyl complexes, similar to those recently reported in rhenium-alkyl systems.<sup>13</sup>

**Acknowledgment.** An International Scientific Collaboration Award to A.S. from the National Sciences and Engineering Research Council of Canada is gratefully acknowledged.

**Registry No.** 1, 97913-64-9; (L =  $\text{PPh}_3$ ), 100082-24-4; (L =  $\text{CNxyllyl}$ ), 100082-26-6; **3**, 100082-25-5;  $[\text{RuH}(\text{cod})\text{-(NH}_2\text{NMe}_2)_3]\text{PF}_6$ , 61042-65-7;  $\text{TICp}$ , 34822-90-7.

**Supplementary Material Available:** Tables of atomic coordinates, anisotropic temperature factors, bond lengths and angles, and observed and calculated structure factors for **3a** and **3b** and  $^1\text{H}$  NMR and analytical data for **2** ( $\text{PPh}_3$  derivative) and **3** ( $\text{L}_2 = \text{Me}_2\text{PCH}_2\text{CH}_2\text{PMe}_2$ ) (76 pages). Ordering information is given on any current masthead page.

(10) Albers, M. O.; Robinson, D. J.; Singleton, E., unpublished results.

(11) Bonding of an allyl to a transition-metal complex can open a migration corridor for the allyl  $\alpha$ -hydrogen atom to travel intramolecularly across the suprafacial arch of the allyl ligand. There are, however, no unequivocal precedents for this type of migration. See, for example: (a) Mango, F. D. *Adv. Catal.* 1969, 20, 291. (b) Mango, F. D. *Coord. Chem. Rev.* 1975, 15, 109. (c) Slutsky, J.; Kwart, H. *J. Am. Chem. Soc.* 1973, 95, 8678.

(12) Cooper, N. J.; Green, M. L. H. *J. Chem. Soc., Dalton Trans.* 1979, 1122.

(13) Crocco, G. L.; Gladysz, J. A. *J. Am. Chem. Soc.* 1985, 107, 4103.

(6) Spectral data for **3a**:  $^1\text{H}$  NMR (500 MHz,  $(\text{CD}_3)_2\text{CO}$ )  $\delta$  1.37-2.34 (m, 12 H,  $\text{CH}_2$ ), 4.37 (dt,  $\text{PCH}_2\text{P}$ ,  $J(\text{HP}) = 10.8$  Hz,  $J(\text{HH}) = 13.3$  Hz), 4.61 (dt,  $\text{PCH}_2\text{P}$ ,  $J(\text{HP}) = 9.6$  Hz,  $J(\text{HH}) = 13.3$  Hz), 5.02 (s, Cp), 5.06 (t,  $=\text{CH}$ ,  $J(\text{HH}) = 7.8$  Hz), 6.8-7.6 (m, aromatic H);  $^{13}\text{C}$  NMR (123 MHz,  $\text{CDCl}_3$ )  $\delta$  26.6, 27.3, 29.2, 29.5, 30.5, 41.8 (6  $\times$  s, aliphatic C), 48.6 (t,  $\text{CH}_2\text{P}$ ,  $J(\text{PC}) = 20$  Hz), 80.4 (s, Cp), 127-132 (aromatic C), 137.3 (t, ipso aromatic C,  $J(\text{PC}) = 20$  Hz), 139.2 (t,  $=\text{CH}$ ,  $J(\text{PH}) = 7$  Hz), 140.8 (t, ipso aromatic C,  $J(\text{PH}) = 20$  Hz), 146.7 (t, Ru-C,  $J(\text{PH}) = 15$  Hz); mp 156 °C. Anal. Calcd for  $\text{C}_{38}\text{H}_{40}\text{P}_2\text{Ru}$ : C, 69.18; H, 6.11. Found: C, 69.35; H, 6.48. Spectral data for **3b**:  $^1\text{H}$  NMR (500 MHz,  $(\text{CD}_3)_2\text{CO}$ )  $\delta$  1.0-2.1 (m, 12 H,  $\text{CH}_2$ ), 4.36 (dt,  $\text{PH}_2\text{P}$ ,  $J(\text{HP}) = 11.1$  Hz,  $J(\text{HH}) = 13.5$  Hz), 4.77 (t,  $=\text{CH}$ ,  $J(\text{HH}) = 7.7$  Hz), 4.89 (s, Cp), 4.97 (dt,  $\text{PH}_2\text{P}$ ,  $J(\text{HP}) = 9.5$  Hz,  $J(\text{HH}) = 13.8$  Hz), 6.8-7.6 (m, aromatic H);  $^{13}\text{C}$  NMR (123 MHz,  $\text{CDCl}_3$ ) same as for **3a**; mp 108 °C. Anal. Calcd for  $\text{C}_{38}\text{H}_{40}\text{P}_2\text{Ru}$ : C, 69.18; H, 6.11. Found: C, 69.42; H, 6.39.

(7) Crystal data for **3a**: monoclinic, space group  $\text{P}2_1/n$ ;  $a = 11.540$  (2) Å,  $b = 27.731$  (5) Å,  $c = 11.541$  (2) Å,  $\beta = 118.44$  (2)°,  $U = 3247.5$  Å<sup>3</sup>,  $Z = 4$ ,  $D_{\text{calcd}} = 1.349$  Mg m<sup>-3</sup>,  $F(000) = 1368$ , Philips PW1100 diffractometer, Mo K $\alpha$  radiation,  $\lambda = 0.71069$  Å,  $\mu(\text{Mo K}\alpha) = 0.532$  mm<sup>-1</sup>. Crystal data for **3b**: triclinic, space group  $\text{P}\bar{1}$ ;  $a = 10.671$  (4) Å,  $b = 14.269$  (2) Å,  $c = 21.106$  (5) Å,  $\alpha = 98.17$  (2)°,  $\beta = 91.03$  (3)°,  $\gamma = 98.81$  (2)°,  $U = 3140.9$  Å<sup>3</sup>,  $Z = 4$ ,  $D_{\text{calcd}} = 1.395$  Mg m<sup>-3</sup>,  $F(000) = 1368$ , Enraf-Nonius CAD4 diffractometer, Mo K $\alpha$  radiation,  $\mu(\text{Mo K}\alpha) = 0.550$  mm<sup>-1</sup>. The structures were solved by normal heavy-atom methods and were refined by weighted least squares [ $\sum w(|F_o| - |F_c|)^2$  minimized,  $w = \sigma^{-2}(F_o)$ ]. Anisotropic temperature factors were used for all non-hydrogen atoms. For **3a** all hydrogen atoms were located and refined; for **3b** only the hydrogen atoms of the cyclooctenyl ligands were refined; all other hydrogen atoms were added in calculated positions ( $d_{\text{C-H}} = 0.95$  Å). The refinements converged with  $R = 0.0470$  and  $R_w = 0.0454$  for 3668 unique reflections with  $F_o \geq 4\sigma(F_o)$  (**3a**) and  $R = 0.0482$  and  $R_w = 0.0440$  for 6256 unique reflections with  $F_o \geq 4\sigma(F_o)$  (**3b**).

(8) One molecule and the enantiomer of the second are almost superimposable.

(9) (a) McGrady, N. D.; McDade, C.; Bercaw, J. E. In "Organometallic Compounds"; Shapiro, B. L., Ed.; Texas A&M University Press: Texas, 1983. (b) Allen, A. R.; Baker, P. K.; Barnes, S. G.; Bottrill, M.; Green, M.; Orpen, A. G.; Williams, I. D. *J. Chem. Soc., Dalton Trans.* 1983, 927. (c) Ashworth, T. V.; Singleton, E., unpublished results. (d) Schwartz, J.; Hart, D. W.; McGiffert, B. *J. Am. Chem. Soc.* 1974, 96, 5613.

## Synthesis of a Phosphavinyl Complex via Shift of a Pentamethylcyclopentadienyl from Phosphorus to Iron

Dietrich Gudat and Edgar Niecke\*

Fakultät für Chemie der Universität, Postfach 8640  
D-4800 Bielefeld, West Germany

Atta M. Arif, Alan H. Cowley,\* and Sapé Quashie

Department of Chemistry, The University of Texas at Austin  
Austin, Texas 78712

Received October 29, 1985

**Summary:** The reaction of the phosphalkene ( $\eta^1\text{-Me}_5\text{C}_5\text{P}=\text{C}(\text{SiMe}_3)_2$ ) with  $\text{Fe}_2(\text{CO})_9$  affords the  $\eta^1$  (P-bonded) complex ( $\eta^1\text{-Me}_5\text{C}_5\text{P}[(\text{CO})_4\text{Fe}]\text{P}=\text{C}(\text{SiMe}_3)_2$ ) (**4**). Photolysis of **4** produces the phosphavinyl complex [ $\text{Fe}\{\eta^1\text{-P}=\text{C}(\text{SiMe}_3)_2\}(\eta^5\text{-Me}_5\text{C}_5)(\text{CO})_2$ ] (**5**). Compound **5** can also be prepared via the metathetical reaction of  $(\text{Me}_3\text{Si})_2\text{C}=\text{PCl}$  with  $\text{K}[\text{Fe}(\eta^5\text{-Me}_5\text{C}_5)(\text{CO})_2]$ . The structure of **5** has been determined by X-ray crystallography.

Phosphalkenes,  $\text{RP}=\text{CR}_2$ ,<sup>1</sup> are proving to be remarkably versatile ligands. As intact units, they can coordinate

(1) (a) Klebach, T. C.; Lourens, R.; Bickelhaupt, F.; Stam, C. H.; Van Herk, A. *J. Organomet. Chem.* 1981, 210, 211. (b) Kroto, H. W.; Nixon, J. F.; Taylor, M. J.; Frew, A. A.; Muir, K. W. *Polyhedron* 1982, 1, 89. (c) Neilson, R. H.; Thoma, R. J.; Vickovic, I.; Watson, W. A. *Organometallics* 1984, 3, 1132.

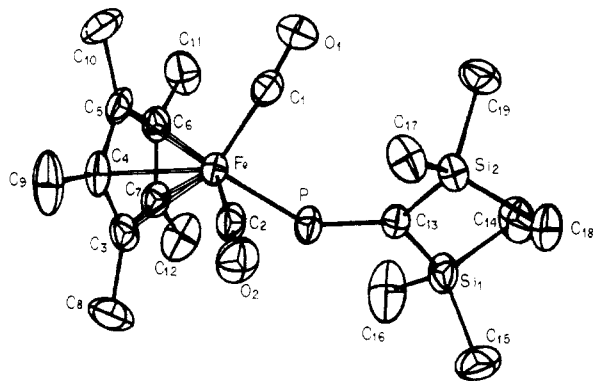
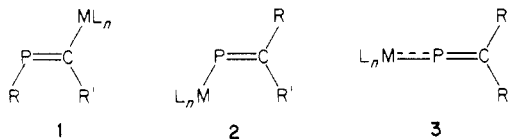


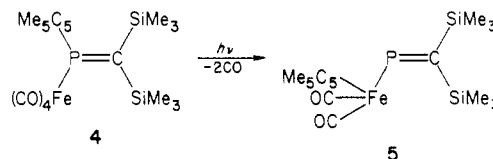
**Figure 1.** ORTEP drawing of  $[\text{Fe}(\eta^1\text{-P}=\text{C}(\text{SiMe}_3)_2)(\eta^5\text{-Me}_5\text{C}_5)(\text{CO})_2]$  (**5**) showing the atom numbering scheme. Important structural parameters: P-Fe = 2.256 (2) and P-C(13) = 1.680 (9) Å; Fe-P-C(13) = 126.2 (3), P-C(13)-Si(1) = 107.1 (5), P-C(13)-Si(2) = 134.4 (5), and Si(1)-C(13)-Si(2) = 118.4 (5)°.

in an  $\eta^1$  (P donor)<sup>1</sup> or an  $\eta^2$  (P=C donor)<sup>2</sup> fashion. Combinations of  $\eta^1$  and  $\eta^2$  ligation have also been observed<sup>3</sup> as has equilibration between these bonding modes.<sup>4</sup> Further elaboration of this chemistry has become possible by the incorporation of organometallic substituents. Thus, monometalation at carbon produces **1**<sup>5</sup> while P-metalation results in either phosphavinyl (**2**)<sup>6</sup> or phosphavinylidene (**3**)<sup>7</sup> complexes depending on whether the phosphorus atom functions as a one- or three-electron donor. We report a novel synthesis of a phosphavinyl complex via migration of a  $\text{C}_5\text{Me}_5$  group from phosphorus to iron.



Treatment of 3.24 g (10 mmol) of  $(\eta^1\text{-Me}_5\text{C}_5)\text{P}=\text{C}(\text{SiMe}_3)_2$ <sup>8</sup> with an equimolar quantity of  $\text{Fe}_2(\text{CO})_9$  for 3 days at 25 °C produced a dark red solution. After filtration and removal of the solvent and volatiles, the resulting red oil was recrystallized from 20 mL of (2:3) toluene/acetonitrile at -30 °C. The red-black crystals (mp 79 °C), which were isolated in 41% yield, were identified as the  $\eta^1$ -phosphaalkene complex **4** on the basis of analytical and spectroscopic data.<sup>9</sup> Of particular significance is the <sup>31</sup>P

chemical shift (371.5 ppm) which falls in the region typical of P-bonded phosphaalkene complexes.<sup>1</sup>



Photolysis of a *n*-hexane solution of **4** with a Hanau TQ-718 mercury lamp caused immediate gas evolution. After 3 h the carbonyl bands of **4** (2055, 1975, and 1959  $\text{cm}^{-1}$ ) disappeared and were replaced with absorptions at 1942 and 1988  $\text{cm}^{-1}$  which are attributable to **5**. <sup>31</sup>P NMR spectroscopic assay indicated that the reaction mixture contained **5** (s, 641.5 ppm) and traces of  $(\eta^1\text{-Me}_5\text{C}_5)\text{P}=\text{C}(\text{SiMe}_3)_2$  (s, 374.5 ppm).<sup>8</sup> Compound **5** can also be prepared by treatment of  $(\text{Me}_3\text{Si})_2\text{C}=\text{P}\text{Cl}$ <sup>10</sup> with  $\text{K}[\text{Fe}(\eta^5\text{-Me}_5\text{C}_5)(\text{CO})_2]$  in THF solution (-20 °C), and purified by recrystallization from *n*-hexane solution at -20 °C (yield 57.7%). The composition of brown, crystalline **5** (mp 117–123 °C) was established on the basis of analytical and spectroscopic data,<sup>11</sup> and its structure (Figure 1) was elucidated by single-crystal X-ray diffraction methods.<sup>12</sup> The phosphorus-carbon bond length (1.680 (9) Å) is similar to those of unmetalated phosphaalkenes;<sup>2d,13</sup> moreover, the sum of bond angles at C(13) is 360° within experimental error. The phosphorus-iron bond length (2.256 (2) Å) and the Fe-P-C bond angle (126.2 (3)°) indicate that the phosphorus lone pair is not involved in bonding to the metal. The fact that the Fe-P-C angle is ~15° larger than those of unmetalated phosphaalkenes seems to be a consequence of steric effects because the P-C(13)-Si(2) angle (134.4 (5)°) is considerably larger than the P-C(13)-Si(1) angle (107.1(5)°).

The scope of the  $\text{Me}_5\text{C}_5$  (and  $\text{C}_5\text{H}_5$ ) main-group/transition-metal shift reaction is presently being studied as is the reactivity of **5**.

**Acknowledgment.** We are grateful to the Deutsche Forschungsgemeinschaft, the Fonds der Chemischen Industrie, the National Science Foundation, and the Robert A. Welch Foundation.

**Registry No.** **4**, 100082-33-5; **5**, 100082-34-6;  $\text{K}[\text{Fe}(\eta^5\text{-Me}_5\text{C}_5)(\text{CO})_2]$ , 59654-59-0;  $\text{Fe}_2(\text{CO})_9$ , 15321-51-4;  $(\eta^1\text{-Me}_5\text{C}_5)\text{P}=\text{C}(\text{SiMe}_3)_2$ , 100082-32-4;  $(\text{Me}_3\text{Si})_2\text{C}=\text{P}\text{Cl}$ , 79454-85-6.

(2) (a) Cowley, A. H.; Jones, R. A.; Stewart, C. A.; Stuart, A. L.; Atwood, J. L.; Hunter, W. E.; Zhang, H.-M. *J. Am. Chem. Soc.* **1983**, *105*, 3737. (b) Al-Resayes, A. I.; Klein, S. I.; Kroto, H. W.; Meidine, M. F.; Nixon, J. F. *J. Chem. Soc., Chem. Commun.* **1983**, 930. (c) Van der Knaap, Th. A.; Jennekens, L. W.; Meerwissen, H. J.; Bickelhaupt, F.; Walther, D.; Dinjus, E.; Uhlig, E.; Spek, A. L. *J. Organomet. Chem.* **1983**, *254*, C33. (d) Cowley, A. H.; Jones, R. A.; Lasch, J. G.; Norman, N. C.; Stewart, C. A.; Stuart, A. L.; Atwood, J. L.; Hunter, W. E.; Zhang, H.-M. *J. Am. Chem. Soc.* **1984**, *106*, 7015. (e) Werner, H.; Paul, W.; Zolk, R. *Angew. Chem., Int. Ed. Engl.* **1984**, *23*, 626.

(3) (a) Knoll, K.; Huttner, G.; Wasiucionek, M.; Zsolnai, L. *Angew. Chem., Int. Ed. Engl.* **1984**, *23*, 739. (b) Holland, S.; Charrier, C.; Mathey, F.; Fischer, J.; Mitschler, A. *J. Am. Chem. Soc.* **1984**, *106*, 826. (c) Appel, R.; Casser, C.; Knoch, F. *J. Organomet. Chem.* **1985**, *293*, 213.

(4) (a) Van der Knaap, Th. A.; Bickelhaupt, F.; van der Poel, H.; van Koten, G.; Stam, C. H. *J. Am. Chem. Soc.* **1982**, *104*, 1756. Kroto, H. W.; Klein, S. I.; Meidine, M. F.; Nixon, J. F.; Harris, R. K.; Packer, K. J.; Reams, P. *J. Organomet. Chem.* **1985**, *280*, 281.

(5) Weber, L.; Reizig, K. *Angew. Chem., Int. Ed. Engl.* **1985**, *24*, 53.

(6) Weber, L.; Reizig, K.; Boese, R.; Polk, M. *Angew. Chem., Int. Ed. Engl.* **1985**, *24*, 604.

(7) Cowley, A. H.; Norman, N. C.; Quashie, S. *J. Am. Chem. Soc.* **1984**, *106*, 5007.

(8) Gudat, D.; Niecke, E.; Krebs, B.; Dartmann, M. *Chimia* **1985**, *39*, 277.

(9) Anal. Calcd for  $\text{C}_{21}\text{H}_{33}\text{FePO}_4\text{Si}_2$ : C, 51.22; H, 6.75. Found: C, 51.06; H, 6.97. MS (EI, 70 eV): *m/e* (relative intensity) 492 ( $\text{M}^+$ , 0.4), 477 ( $\text{M}^+ - \text{CH}_3$ , 0.4), 436 ( $\text{M}^+ - 2\text{CO}$ , 2.7), 408 ( $\text{M}^+ - 3\text{CO}$ , 27.1), 380 ( $\text{M}^+ - 4\text{CO}$ , 76.2), 73 ( $\text{SiMe}_3^+$ , 100). <sup>13</sup>C{<sup>1</sup>H} NMR: ( $\text{C}_6\text{D}_6$ , 28°C): 4.2 (d, *J* = 8.2 Hz,  $\text{SiC}_3$ ), 5.1 (d, *J* = 4.8 Hz,  $\text{SiC}_3$ ), 11.8 (broad,  $\text{CCH}_3$ ), 136.5 and 142.8 (very broad,  $\text{CCH}_3$ ), 187.8 (d, *J* = 24.5 Hz, P=C), 216.1 (d, *J* = 15 Hz, CO).

(10) Appel, R.; Westerhaus, A. *Tetrahedron Lett.* **1984**, *22*, 2159.

(11) Anal. Calcd for  $\text{C}_{19}\text{H}_{33}\text{FePO}_2\text{Si}_2$ : C, 52.29; H, 7.62. Found: C, 50.84; H, 7.72. MS (EI, 70 eV): *m/e* (relative intensity) 436 ( $\text{M}^+$ , 2.9), 408 ( $\text{M}^+ - \text{CO}$ , 44.0), 380 ( $\text{M}^+ - 2\text{CO}$ , 100), 73 ( $\text{SiMe}_3^+$ , 72.5). <sup>13</sup>C{<sup>1</sup>H} NMR ( $\text{CD}_2\text{Cl}_2$ , 28 °C): 3.5 (s,  $\text{SiC}_3$ ), 3.9 (d, *J* = 15.6 Hz,  $\text{SiC}_3$ ), 9.3 (d, *J* = 9.2 Hz,  $\text{CCH}_3$ ), 98.9 (s,  $\text{CCH}_3$ ), 208.9 (d, *J* = 106.1 Hz, P=C), 217.6 ppm (s, CO).

(12) A single crystal of **5** with dimensions 0.35 × 0.35 × 0.20 mm was sealed under dry nitrogen in a Lindemann capillary. Some crystal data for **5** are as follows:  $\text{C}_{19}\text{H}_{33}\text{FeO}_2\text{PSi}_2$ , *M* = 436.47, monoclinic, space group  $P2_1/n$  (No. 14); *a* = 12.807 (2) Å, *b* = 9.364 (3) Å, *c* = 20.328 (3) Å,  $\beta$  = 103.55 (1)°; *V* = 2370 Å<sup>3</sup>; *Z* = 4; *D*(calcd) = 1.223 g cm<sup>-3</sup>, and  $\mu$  = 8.1 cm<sup>-1</sup>. A total of 3720 symmetry-independent reflections were recorded by using  $\omega$ - $2\theta$  scans in the range 3.0 <  $2\theta$  < 48.0° using graphite-monochromated Mo K $\alpha$  X-radiation with  $\lambda$  = 0.71069 Å. Of these, 2339 reflections (*I* > 3.0  $\sigma(I)$ ) were used to solve (SIMPDEL) and refine (full matrix, least squares) the structure of **5**. Final least-squares refinement gave *R* = 0.0572 and *R*<sub>w</sub> = 0.0746.

(13) For a review, see: Appel, R.; Knoll, F.; Ruppert, I. *Angew. Chem., Int. Ed. Engl.* **1984**, *20*, 731.



**Supplementary Material Available:** Tables of bond lengths, bond angles, atomic coordinates, thermal parameters, and structure factors for 5 (17 pages). Ordering information is given on any current masthead page.

## Organometallic Chemistry of the Transition Elements. 7. A 2+ State of Bis(arene)chromium Complexes<sup>1</sup>

Richard J. Markle and J. J. Lagowski\*

Department of Chemistry  
The University of Texas at Austin  
Austin, Texas 78712

Received October 29, 1985

**Summary:** A new, stable oxidation state of a bis( $\eta^6$ -arene)chromium complex is reported in THF. Two one-electron oxidation-reduction processes are observed for bis(hexamethylbenzene)chromium(0) at  $-1.630$  V (reversible 1+/0 redox couple) and at  $-0.160$  V (quasi-reversible 2+/1+ redox couple), both being measured in the presence of TBAPF<sub>6</sub> against the Ag/AgNO<sub>3</sub> couple.

The reversible or quasi-reversible oxidation-reduction processes of bis(arene)chromium(0) complexes and their corresponding bis(arene)chromium(1+) ions are well-known.<sup>2,3</sup> Some bis(arene)chromium redox couples are stable and sufficiently reproducible that they have been recommended as references for nonaqueous solvent systems.<sup>4</sup> Up to now attempts to oxidize bis(arene)chromium monocations to higher oxidation states, however, have led to irreversible oxidations and/or ligand disproportionation.<sup>2,5</sup>

Our work in the effects of methyl substitution on magnetic and electrochemical properties of bis(arene)chromium(0) complexes<sup>6</sup> has also resulted in the discovery of a new, stable, quasi-reversible oxidation state for such a complex. We report here the first example of a quasi-reversible 2+/1+ oxidation process for bis(hexamethylbenzene)chromium(0) which exhibits two redox potentials in THF.

**Synthesis of Bis(hexamethylbenzene)chromium(0).** Bis(hexamethylbenzene)chromium(0) was prepared by using the rotating reactor system described previously.<sup>6,7</sup> Chromium metal was evaporated into neat hexamethylbenzene. After workup, bis(hexamethylbenzene)chromium(0) [mp 339-340 °C dec (lit.<sup>8</sup> mp 400 °C dec)] was collected by sublimation [110 °C at 10<sup>-3</sup> torr]. Total yield was 0.294 g or 3.66%, based on metal evaporated (HRMS calcd 376.222 20, found 376.223 13).

**Electrochemical Cell and Analyses.** The electrochemistry of bis(hexamethylbenzene)chromium was established by cyclic voltammetry using the apparatus illustrated in Figure 1 as described briefly here and in greater detail elsewhere.<sup>6</sup> The solvent THF was purified and dried by refluxing and distilling from a mixture of potassium and benzophenone and transferred to a primary

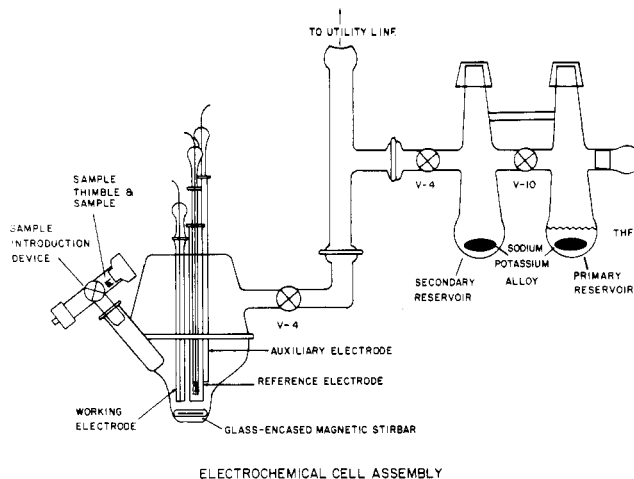


**Figure 1.** Electrochemical cell and related assembly used for cyclic voltammetric studies.

reservoir by using standard Schlenk techniques. The THF was stored over a 1:1 mole ratio of a sodium-potassium alloy and degassed by standard freeze-pump-thaw techniques. The THF in the reservoir was kept under static vacuum at  $-30$  °C while the cell was dried and deoxygenated.

The supporting electrolyte, tetra-*n*-butylammonium hexafluorophosphate (TBAPF<sub>6</sub>), was prepared by mixing equal molar aqueous solutions of tetra-*n*-butylammonium hydroxide and ammonium hexafluorophosphate. The product was collected, recrystallized twice from ethanol, recrystallized once from ethyl acetate, dried under vacuum, ground and dried at 140 °C, cooled, and stored in a desiccator (mp 235-237 °C, standard reference sample mp 236-238 °C). Sufficient supporting electrolyte was used in all chambers of the electrochemical cell to produce a 1.5 M solution when the appropriate amount of solvent was introduced.

The working electrode was a platinum disk (1.950-mm diameter) mounted in Pyrex glass. The platinum surface was polished to the point where no major imperfections could be observed at 50 $\times$  magnification.

The reference electrode was a silver wire immersed in a solution containing TBAPF<sub>6</sub> and saturated with AgNO<sub>3</sub>, the mixture being contained within a small fritted tube. A second, slightly larger fritted tube surrounded the reference electrode and contained a solution of TBAPF<sub>6</sub> in THF. The Ag/AgNO<sub>3</sub> reference electrode was thus separated from the solution containing the arene complex by two concentric fritted tubes. This reference electrode was extremely stable with reproducible potentials. Similar systems have been described by others.<sup>3,5</sup>

In a typical experiment, the electrochemical cell and supporting electrolyte were assembled and then dried and deoxygenated by heating under vacuum. After cooling, standard anaerobic and anhydrous handling techniques were used to incorporate the dry AgNO<sub>3</sub>, the sample introduction device (and the sample), and the THF reservoir system. The assembled apparatus was then reevacuated. The solvent (THF) was flash distilled sequentially from the primary reservoir to the secondary reservoir, the secondary reservoir was isolated, and then the THF was distilled from the secondary reservoir into the electrochemical cell. Supporting electrolyte was dissolved completely and the solution allowed to equilibrate at room temperature.

All electrochemical measurements were made by using an EG&G PAR Model 175 Universal Programmer, an EG&G PAR Model 173 Potentiostat/Galvanostat, and a

(1) Paper 6 in this series: Pettijohn, T.; Shepherd, M.; Chinn, J.; Lagowski, J. J., submitted for publication.

(2) Valcher, S.; Casalbore, G.; Mastragostino, M. J. *Electroanal. Chem. Interfacial Electrochem.* 1974, 51, 226.

(3) Ito, N.; Saji, T.; Suga, K.; Aoyagui, S. *J. Organomet. Chem.* 1982, 229, 43.

(4) Gritzner, G.; Kuta, J. *Pure Appl. Chem.* 1984, 56, 461.

(5) Bailey, S.; Leung, W.; Ritchie, F. *Electrochim. Acta* 1985, 30, 861.

(6) Markle, R. Master's Thesis, The University of Texas at Austin, 1985.

(7) Markle, R.; Pettijohn, T.; Lagowski, J. J. *Organometallics* 1985, 4, 1529.

(8) Fischer, E.; Hafner, W. Brit. Pat. 829 574, 1960.



**Supplementary Material Available:** Tables of bond lengths, bond angles, atomic coordinates, thermal parameters, and structure factors for 5 (17 pages). Ordering information is given on any current masthead page.

## Organometallic Chemistry of the Transition Elements. 7. A 2+ State of Bis(arene)chromium Complexes<sup>1</sup>

Richard J. Markle and J. J. Lagowski\*

Department of Chemistry  
The University of Texas at Austin  
Austin, Texas 78712

Received October 29, 1985

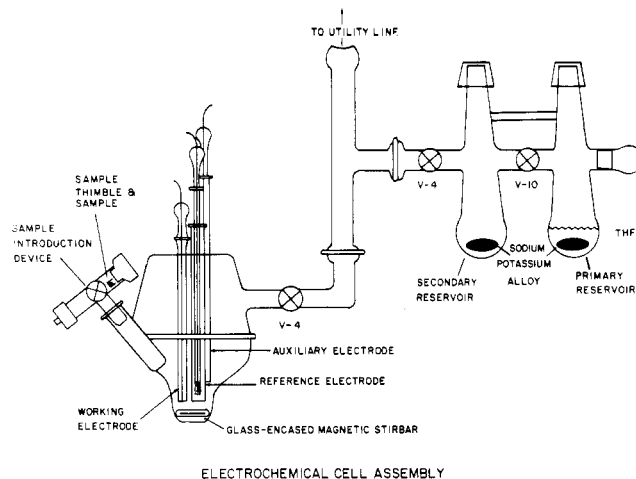
**Summary:** A new, stable oxidation state of a bis( $\eta^6$ -arene)chromium complex is reported in THF. Two one-electron oxidation-reduction processes are observed for bis(hexamethylbenzene)chromium(0) at  $-1.630$  V (reversible 1+/0 redox couple) and at  $-0.160$  V (quasi-reversible 2+/1+ redox couple), both being measured in the presence of TBAPF<sub>6</sub> against the Ag/AgNO<sub>3</sub> couple.

The reversible or quasi-reversible oxidation-reduction processes of bis(arene)chromium(0) complexes and their corresponding bis(arene)chromium(1+) ions are well-known.<sup>2,3</sup> Some bis(arene)chromium redox couples are stable and sufficiently reproducible that they have been recommended as references for nonaqueous solvent systems.<sup>4</sup> Up to now attempts to oxidize bis(arene)chromium monocations to higher oxidation states, however, have led to irreversible oxidations and/or ligand disproportionation.<sup>2,5</sup>

Our work in the effects of methyl substitution on magnetic and electrochemical properties of bis(arene)chromium(0) complexes<sup>6</sup> has also resulted in the discovery of a new, stable, quasi-reversible oxidation state for such a complex. We report here the first example of a quasi-reversible 2+/1+ oxidation process for bis(hexamethylbenzene)chromium(0) which exhibits two redox potentials in THF.

**Synthesis of Bis(hexamethylbenzene)chromium(0).** Bis(hexamethylbenzene)chromium(0) was prepared by using the rotating reactor system described previously.<sup>6,7</sup> Chromium metal was evaporated into neat hexamethylbenzene. After workup, bis(hexamethylbenzene)chromium(0) [mp 339-340 °C dec (lit.<sup>8</sup> mp 400 °C dec)] was collected by sublimation [110 °C at 10<sup>-3</sup> torr]. Total yield was 0.294 g or 3.66%, based on metal evaporated (HRMS calcd 376.222 20, found 376.223 13).

**Electrochemical Cell and Analyses.** The electrochemistry of bis(hexamethylbenzene)chromium was established by cyclic voltammetry using the apparatus illustrated in Figure 1 as described briefly here and in greater detail elsewhere.<sup>6</sup> The solvent THF was purified and dried by refluxing and distilling from a mixture of potassium and benzophenone and transferred to a primary



ELECTROCHEMICAL CELL ASSEMBLY

**Figure 1.** Electrochemical cell and related assembly used for cyclic voltammetric studies.

reservoir by using standard Schlenk techniques. The THF was stored over a 1:1 mole ratio of a sodium-potassium alloy and degassed by standard freeze-pump-thaw techniques. The THF in the reservoir was kept under static vacuum at  $-30$  °C while the cell was dried and deoxygenated.

The supporting electrolyte, tetra-*n*-butylammonium hexafluorophosphate (TBAPF<sub>6</sub>), was prepared by mixing equal molar aqueous solutions of tetra-*n*-butylammonium hydroxide and ammonium hexafluorophosphate. The product was collected, recrystallized twice from ethanol, recrystallized once from ethyl acetate, dried under vacuum, ground and dried at 140 °C, cooled, and stored in a desiccator (mp 235-237 °C, standard reference sample mp 236-238 °C). Sufficient supporting electrolyte was used in all chambers of the electrochemical cell to produce a 1.5 M solution when the appropriate amount of solvent was introduced.

The working electrode was a platinum disk (1.950-mm diameter) mounted in Pyrex glass. The platinum surface was polished to the point where no major imperfections could be observed at 50 $\times$  magnification.

The reference electrode was a silver wire immersed in a solution containing TBAPF<sub>6</sub> and saturated with AgNO<sub>3</sub>, the mixture being contained within a small fritted tube. A second, slightly larger fritted tube surrounded the reference electrode and contained a solution of TBAPF<sub>6</sub> in THF. The Ag/AgNO<sub>3</sub> reference electrode was thus separated from the solution containing the arene complex by two concentric fritted tubes. This reference electrode was extremely stable with reproducible potentials. Similar systems have been described by others.<sup>3,5</sup>

In a typical experiment, the electrochemical cell and supporting electrolyte were assembled and then dried and deoxygenated by heating under vacuum. After cooling, standard anaerobic and anhydrous handling techniques were used to incorporate the dry AgNO<sub>3</sub>, the sample introduction device (and the sample), and the THF reservoir system. The assembled apparatus was then reevacuated. The solvent (THF) was flash distilled sequentially from the primary reservoir to the secondary reservoir, the secondary reservoir was isolated, and then the THF was distilled from the secondary reservoir into the electrochemical cell. Supporting electrolyte was dissolved completely and the solution allowed to equilibrate at room temperature.

All electrochemical measurements were made by using an EG&G PAR Model 175 Universal Programmer, an EG&G PAR Model 173 Potentiostat/Galvanostat, and a

(1) Paper 6 in this series: Pettijohn, T.; Shepherd, M.; Chinn, J.; Lagowski, J. J., submitted for publication.

(2) Valcher, S.; Casalbore, G.; Mastragostino, M. J. *Electroanal. Chem. Interfacial Electrochem.* 1974, 51, 226.

(3) Ito, N.; Saji, T.; Suga, K.; Aoyagui, S. *J. Organomet. Chem.* 1982, 229, 43.

(4) Gritzner, G.; Kuta, J. *Pure Appl. Chem.* 1984, 56, 461.

(5) Bailey, S.; Leung, W.; Ritchie, F. *Electrochim. Acta* 1985, 30, 861.

(6) Markle, R. Master's Thesis, The University of Texas at Austin, 1985.

(7) Markle, R.; Pettijohn, T.; Lagowski, J. J. *Organometallics* 1985, 4, 1529.

(8) Fischer, E.; Hafner, W. Brit. Pat. 829 574, 1960.

Table I. Electrochemical Values for Bis(hexamethylbenzene)chromium 1+/0 and 1+/2+ Room-Temperature Redox Processes<sup>a</sup>

ox. step	peak position V		peak height $\mu\text{A}$		scan rate, mV/s	$\Delta E_p$ , mV	$i_{pc}/i_{pa}$	$E_{1/2}$ , V
	$E_p$ cathodic	$E_p$ anodic	$i_p$ cathodic	$i_p$ anodic				
1+/0	-1.661	-1.600	0.40	0.35	50	61	1.03	-1.630
2+/1+	-0.195	-0.124	0.16	0.36	200	71	0.44	-0.160

<sup>a</sup> Concentration = 7.97 mM.

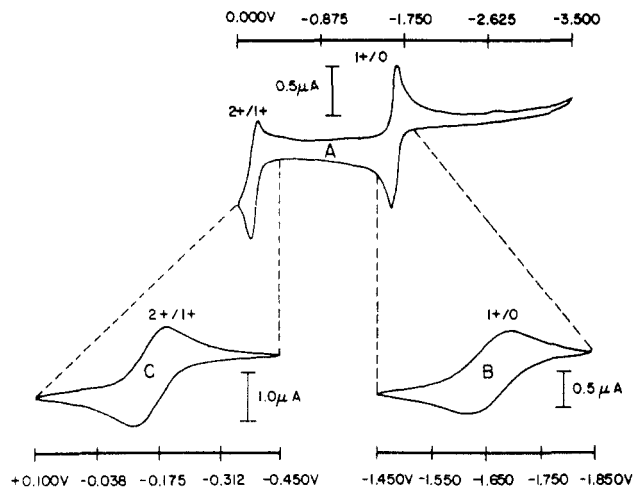


Figure 2. A typical current-voltage curve of bis(hexamethylbenzene)chromium recorded at (a) 50 mV/s over the full range exhibiting both 1+/0 and 2+/1+ redox couples, (b) 50 mV/s over the range exhibiting the 1+/0 redox couple, and (c) 200 mV/s over the range exhibiting the 2+/1+ redox couple.

Model RE 0074 X-4 Recorder. After the sample (0.03 g, 7.97 mM) was introduced into the electrochemical cell a cyclic voltammogram, CV, containing both redox potentials was recorded. Each redox couple was then individually investigated. Both the 1+/0 and 2+/1+ redox couples were recorded separately at 50, 100, 200, 500, and 1,000 mV/s to test for peak position/scan rate dependency. The anodic peak position for each individual CV was essentially unaffected by and independent of the scan rate. Peak currents were dependent on the scan rate. Scan rates of each individual CV used in the determination of electrochemical parameters were chosen to maximize the peak currents and cathodic and anodic peak height parity.

Figure 2 represents (a) a cyclic voltammogram (CV) recorded at a scan rate of 50 mV/s and exhibiting both redox processes, (b) a detailed CV of the 1+/0 redox couple recorded at 50 mV/s, and (c) a detailed CV of the 2+/1+ redox couple recorded at 200 mV/s. Table I summarizes the electrochemical parameters obtained.

**Electron Spin Resonance.** A saturated solution of bis(hexamethylbenzene)chromium in methanol was recorded on a Varian E-9 EPR spectrometer with a Varian E-101 Microwave bridge operated at room temperature. The ESR spectrum of bis(hexamethylbenzene)chromium(1+) was consistent with that reported by Brubaker.<sup>9</sup> The  $g$  value was 1.9893 (lit.<sup>9</sup>  $g = 1.9867$ ). The observation confirms that our bis(hexamethylbenzene)chromium sample forms the expected stable 1+ cation in solution.

The 1+/0 and 2+/1+ redox potentials have peak separations,  $\Delta E_p$ , of 61 and 71 mV, respectively. These values are well within those expected for a one-electron Nernstian process at room temperature. For example, Saji<sup>3</sup> and Treichel<sup>10</sup> report the 1+/0 redox couple for bis(benz-

ene)chromium in acetonitrile at 58 and 114 mV, respectively.

Peak separation, the effect of the scan rate, and the ratio of cathodic peak current,  $i_{pc}$ , to anodic peak current,  $i_{pa}$ , form the basis of the argument for the reversibility for the 1+/0 couple of bis(hexamethylbenzene)chromium and the quasi-reversibility of the corresponding 2+/1+ couple. The peak current ratio for the 2+/1+ redox couple is less than unity. It is not unexpected that at moderate scan rates of 200 mV/s at room temperature that some of the 2+ cation might disproportionate before the return scan occurs because this chromium species is highly unstable under normal conditions.

We can speculate that the presence of the 12 electron-releasing methyl groups on the two complexed rings provides sufficient electron density to the chromium cation to permit the formal, further oxidation of the 1+ species in a potential range that can be attained in this solvent system. Unpublished work from these laboratories on the electrochemistry of the monocations and magnetic properties of progressively methylated derivatives of bis(benzene)chromium(0) seems to support this general conclusion. Work in the extension of the range of oxidation states for bis(arene)chromium complexes continues.

**Acknowledgment.** We thank Mr. Ted Pettijohn for his assistance with the ESR experiments. The Robert A. Welch Foundation and the National Science Foundation provided generous support.

**Registry No.** Bis(hexamethylbenzene)chromium (0), 12156-66-0; bis(hexamethylbenzene)chromium (1+), 12243-39-9.

### Influence of Dienes on the Cobalt Carbonyl Catalyzed Reaction of Mercaptans with Carbon Monoxide

Shlomo Antebi and Howard Alper\*†

Ottawa-Carleton Chemistry Institute  
Department of Chemistry, University of Ottawa  
Ottawa, Ontario, Canada K1N 9B4

Received October 29, 1985

**Summary:** Thio esters are obtained in good to excellent yields by the cobalt carbonyl catalyzed carbonylation of mercaptans in the presence of 2,3-dimethyl-1,3-butadiene or 2,3-dimethoxy-1,3-butadiene. Diene-cobalt carbonyl complexes [i.e., (diene-Co(CO)<sub>2</sub>)<sub>2</sub>] are probably the key catalytic species in these reactions.

Many investigations have been carried out on metal-catalyzed reactions of substrates bearing nitrogen and oxygen atoms. Examples include the cobalt carbonyl catalyzed reductive carbonylation of Schiff bases with organoboranes,<sup>1</sup> the conversion of amines to formamides

(9) Brubaker, C.; Li, T.; Kung, W.; Ward, D.; McCulloch, B. *Organometallics* 1982, 1, 1229.

(10) Treichel, P.; Essensmacher, G.; Efner, H.; Klabunde, K. *Inorg. Chim. Acta* 1981, 48, 41.

\* John Simon Guggenheim Fellow, 1985-1986.

(†) Alper, H.; Amaratunga, S. *J. Org. Chem.* 1982, 47, 3593.

Table I. Electrochemical Values for Bis(hexamethylbenzene)chromium 1+/0 and 1+/2+ Room-Temperature Redox Processes<sup>a</sup>

ox. step	peak position V		peak height $\mu\text{A}$		scan rate, mV/s	$\Delta E_p$ , mV	$i_{pc}/i_{pa}$	$E_{1/2}$ , V
	$E_p$ cathodic	$E_p$ anodic	$i_p$ cathodic	$i_p$ anodic				
1+/0	-1.661	-1.600	0.40	0.35	50	61	1.03	-1.630
2+/1+	-0.195	-0.124	0.16	0.36	200	71	0.44	-0.160

<sup>a</sup> Concentration = 7.97 mM.

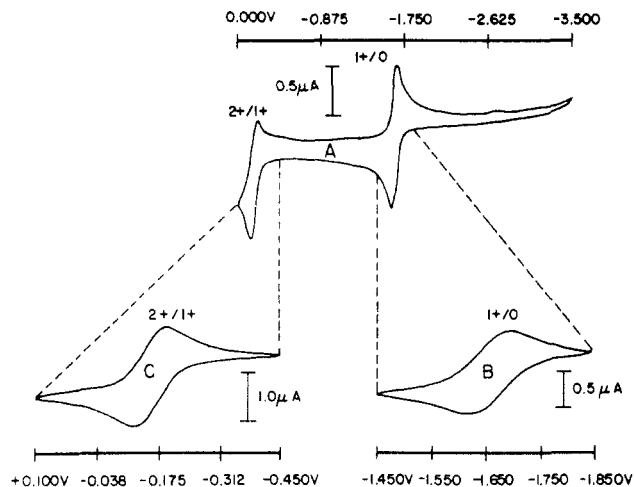


Figure 2. A typical current-voltage curve of bis(hexamethylbenzene)chromium recorded at (a) 50 mV/s over the full range exhibiting both 1+/0 and 2+/1+ redox couples, (b) 50 mV/s over the range exhibiting the 1+/0 redox couple, and (c) 200 mV/s over the range exhibiting the 2+/1+ redox couple.

Model RE 0074 X-4 Recorder. After the sample (0.03 g, 7.97 mM) was introduced into the electrochemical cell a cyclic voltammogram, CV, containing both redox potentials was recorded. Each redox couple was then individually investigated. Both the 1+/0 and 2+/1+ redox couples were recorded separately at 50, 100, 200, 500, and 1,000 mV/s to test for peak position/scan rate dependency. The anodic peak position for each individual CV was essentially unaffected by and independent of the scan rate. Peak currents were dependent on the scan rate. Scan rates of each individual CV used in the determination of electrochemical parameters were chosen to maximize the peak currents and cathodic and anodic peak height parity.

Figure 2 represents (a) a cyclic voltammogram (CV) recorded at a scan rate of 50 mV/s and exhibiting both redox processes, (b) a detailed CV of the 1+/0 redox couple recorded at 50 mV/s, and (c) a detailed CV of the 2+/1+ redox couple recorded at 200 mV/s. Table I summarizes the electrochemical parameters obtained.

**Electron Spin Resonance.** A saturated solution of bis(hexamethylbenzene)chromium in methanol was recorded on a Varian E-9 EPR spectrometer with a Varian E-101 Microwave bridge operated at room temperature. The ESR spectrum of bis(hexamethylbenzene)chromium(1+) was consistent with that reported by Brubaker.<sup>9</sup> The  $g$  value was 1.9893 (lit.<sup>9</sup>  $g = 1.9867$ ). The observation confirms that our bis(hexamethylbenzene)chromium sample forms the expected stable 1+ cation in solution.

The 1+/0 and 2+/1+ redox potentials have peak separations,  $\Delta E_p$ , of 61 and 71 mV, respectively. These values are well within those expected for a one-electron Nernstian process at room temperature. For example, Saji<sup>3</sup> and Treichel<sup>10</sup> report the 1+/0 redox couple for bis(benz-

ene)chromium in acetonitrile at 58 and 114 mV, respectively.

Peak separation, the effect of the scan rate, and the ratio of cathodic peak current,  $i_{pc}$ , to anodic peak current,  $i_{pa}$ , form the basis of the argument for the reversibility for the 1+/0 couple of bis(hexamethylbenzene)chromium and the quasi-reversibility of the corresponding 2+/1+ couple. The peak current ratio for the 2+/1+ redox couple is less than unity. It is not unexpected that at moderate scan rates of 200 mV/s at room temperature that some of the 2+ cation might disproportionate before the return scan occurs because this chromium species is highly unstable under normal conditions.

We can speculate that the presence of the 12 electron-releasing methyl groups on the two complexed rings provides sufficient electron density to the chromium cation to permit the formal, further oxidation of the 1+ species in a potential range that can be attained in this solvent system. Unpublished work from these laboratories on the electrochemistry of the monocations and magnetic properties of progressively methylated derivatives of bis(benzene)chromium(0) seems to support this general conclusion. Work in the extension of the range of oxidation states for bis(arene)chromium complexes continues.

**Acknowledgment.** We thank Mr. Ted Pettijohn for his assistance with the ESR experiments. The Robert A. Welch Foundation and the National Science Foundation provided generous support.

**Registry No.** Bis(hexamethylbenzene)chromium (0), 12156-66-0; bis(hexamethylbenzene)chromium (1+), 12243-39-9.

### Influence of Dienes on the Cobalt Carbonyl Catalyzed Reaction of Mercaptans with Carbon Monoxide

Shlomo Antebi and Howard Alper\*†

Ottawa-Carleton Chemistry Institute  
Department of Chemistry, University of Ottawa  
Ottawa, Ontario, Canada K1N 9B4

Received October 29, 1985

**Summary:** Thio esters are obtained in good to excellent yields by the cobalt carbonyl catalyzed carbonylation of mercaptans in the presence of 2,3-dimethyl-1,3-butadiene or 2,3-dimethoxy-1,3-butadiene. Diene-cobalt carbonyl complexes [i.e., (diene-Co(CO)<sub>2</sub>)<sub>2</sub>] are probably the key catalytic species in these reactions.

Many investigations have been carried out on metal-catalyzed reactions of substrates bearing nitrogen and oxygen atoms. Examples include the cobalt carbonyl catalyzed reductive carbonylation of Schiff bases with organoboranes,<sup>1</sup> the conversion of amines to formamides

(9) Brubaker, C.; Li, T.; Kung, W.; Ward, D.; McCulloch, B. *Organometallics* 1982, 1, 1229.

(10) Treichel, P.; Essensmacher, G.; Efner, H.; Klabunde, K. *Inorg. Chim. Acta* 1981, 48, 41.

\* John Simon Guggenheim Fellow, 1985-1986.

(†) Alper, H.; Amaratunga, S. *J. Org. Chem.* 1982, 47, 3593.

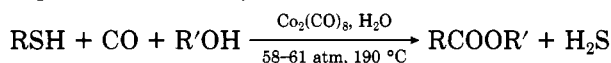
Table I. Products Obtained from the Reaction of Mercaptans with Diene, CO, and Co<sub>2</sub>(CO)<sub>8</sub>

RSH, R =	diene <sup>a</sup>	products, % yield <sup>b</sup>			
		thio ester	disulfide	addition product	sulfide
Ph	CHD	20	10		
	DME	87	3		
<i>p</i> -CH <sub>3</sub> C <sub>6</sub> H <sub>4</sub>	CHD	22	16	6	
	CHD(N <sub>2</sub> ) <sup>c</sup>	8		35	12
	CHD(N <sub>2</sub> ) <sup>d</sup>			87	
	In	37	15	20	
	I	13			
<i>p</i> -CH <sub>3</sub> OC <sub>6</sub> H <sub>4</sub>	DM	61	5	3	
	DME	82	4		
	CHD	24	27		
<i>p</i> -BrC <sub>6</sub> H <sub>4</sub>	CHD	14			18
	DM	55	4	12	
<i>p</i> -FC <sub>6</sub> H <sub>4</sub>	CHD	24	5		
	DME	84	5		
2-C <sub>10</sub> H <sub>7</sub>	CHD	24	27		
	DM	63		14	
	DME	85	2		
<i>p</i> -CH <sub>3</sub> OC <sub>6</sub> H <sub>4</sub> CH <sub>2</sub>	CHD	13	5		55
	DME	59	12	3	
<i>p</i> -CH <sub>3</sub> C <sub>6</sub> H <sub>4</sub> CH <sub>2</sub>	CHD	5	18	15	

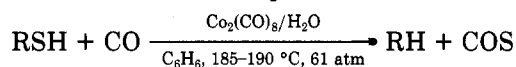
<sup>a</sup>CHD = 1,3-cyclohexadiene; I = isoprene; In = indene; DM = 2,3-dimethyl-1,3-butadiene; DME = 2,3-dimethoxy-1,3-butadiene.

<sup>b</sup>Products were identified by comparison of boiling points and spectral data (IR, NMR [<sup>1</sup>H, <sup>13</sup>C], MS) with literature values. Yields are of pure materials. <sup>c</sup>N<sub>2</sub> atmosphere. <sup>d</sup>Without Co<sub>2</sub>(CO)<sub>8</sub>.

or ureas induced by various metal complexes,<sup>2</sup> and the ruthenium complex catalyzed carbonylation of methyl ether to methyl acetate.<sup>3</sup> Few examples are known of catalytic processes in which one of the reactants contains sulfur as the heteroatom, since the presence of such a heteroatom frequently poisons the catalyst. Recently, we found that cobalt carbonyl is a fine catalyst for the desulfurization and carbonylation of benzylic mercaptans and thiophenols to carboxylic esters.<sup>4</sup>

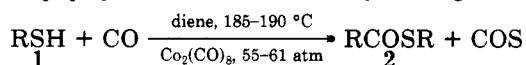


Hydrocarbons were formed when the reaction was effected in benzene instead of aqueous alcohol.<sup>5</sup> The byproduct is carbonyl sulfide, while hydrogen sulfide was the gaseous product of the reaction in aqueous alcohol.



It seemed of value to attempt the mercaptan reaction with carbon monoxide in benzene, in the presence of conjugated dienes. Conceptually, the diene can complex to the cobalt catalyst to generate a new perhaps more active catalytic species, intercept an organocobalt intermediate, or experience addition of the mercaptan affording an unsaturated sulfide.<sup>6</sup> We now wish to report that the presence of a diene causes a dramatic change in reaction course and that the product yields are sensitive to the nature of substituent groups on the diene.

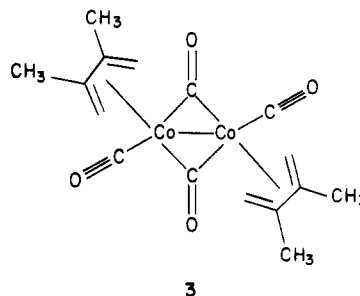
When *p*-toluenethiol (1, R = *p*-CH<sub>3</sub>C<sub>6</sub>H<sub>4</sub>) was carbonylated in the presence of 1,3-cyclohexadiene and cobalt carbonyl, at 58 atm and 185–190 °C, the thio ester 2, R = *p*-CH<sub>3</sub>C<sub>6</sub>H<sub>4</sub>, was formed in 22% yield together with



*p*-tolyl disulfide (16% yield) and a product (6% yield) resulting from 1,2-addition of the thiol to 1,3-cyclohexadiene. The latter adduct could be obtained in high yield, in the absence of cobalt carbonyl, by using a nitrogen atmosphere.<sup>6</sup> The yield of thio ester in these reactions is dependent on the structure of the diene. While indene and 2-methyl-1,3-butadiene (isoprene) are somewhat less or more effective than 1,3-cyclohexadiene, 2,3-dimethyl-1,3-butadiene affords thio esters in improved yields (55–63%). Even better is 2,3-dimethoxy-1,3-butadiene, since thio esters are obtained in excellent yields (82–87%) when the mercaptan carbonylation is run in the presence of this diene.

The carbonylation reaction is applicable to a variety of thiophenols and benzylic mercaptans (see Table I for yields of pure products), but alkanethiols are inert under these reaction conditions. Note that hydrocarbons were not isolated in these reactions. Carbonyl sulfide was the gaseous product, confirmed by mass spectrometric analysis of the evolved gases (intense signal at *m/e* 60).

It is likely that diene-cobalt carbonyl complexes are the true catalysts in the carbonylation reaction. Such complexes are known and are easily prepared by the reaction of the diene with Co<sub>2</sub>(CO)<sub>8</sub>.<sup>7,8</sup> Complex 3, synthesized



according to Winkhaus and Wilkinson,<sup>7</sup> was employed as the catalyst for the carbonylation of *p*-methoxybenzenethiol in benzene [in the absence of diene and Co<sub>2</sub>(CO)<sub>8</sub>]. The thio ester was obtained in 48% yield, which compared

(2) Sheldon, R. A. "Chemicals from Synthesis Gas"; D. Reidel Publishing Co.; Dordrecht, Holland, 1983; pp 167–184.

(3) Braca, G.; Sbrana, G.; Valentini, G.; Andrich, G.; Gregorio, G. *J. Am. Chem. Soc.* **1978**, *100*, 6238.

(4) Shim, S. C.; Antebi, S.; Alper, H. *J. Org. Chem.* **1985**, *50*, 147.

(5) Shim, S. C.; Antebi, S.; Alper, H. *Tetrahedron Lett.* **1985**, *26*, 1935.

(6) E.g.: Claisse, J. A.; Davies, D. I. *J. Chem. Soc.* **1965**, 4894. Saville, B. *J. Chem. Soc.* **1962**, 5040.

(7) Winkhaus, G.; Wilkinson, G. *J. Chem. Soc.* **1961**, 602.

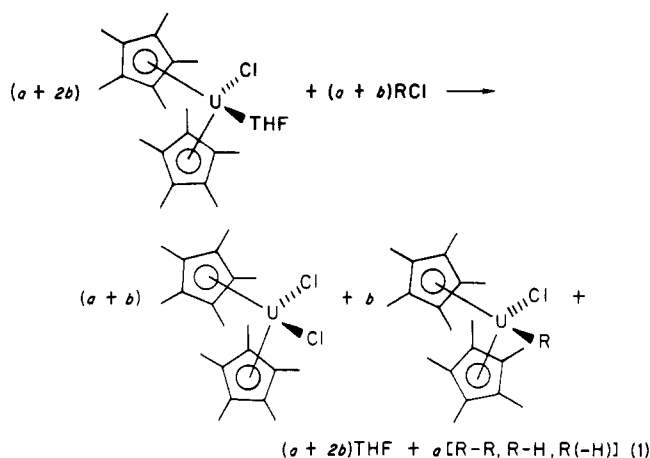
(8) McArdle, P.; Manning, A. R. *J. Chem. Soc. A* **1970**, 2123.





$a(\text{C}_5\text{Me}_5)_2\text{Yb}^{\text{III}}\text{-X} + a(\text{C}_5\text{Me}_5)_2\text{Yb}^{\text{III}}\text{X}_2 + 1.0\text{Et}_2\text{O} + a\text{C}_5\text{Me}_5\text{R} + 0.5[\text{R-R}, \text{R-H (alkanes)}, \text{R(-H) (olefins)}]$ , if RX is added until excess is present. The differences in the organolanthanide,  $(\text{C}_5\text{Me}_5)_2\text{Yb}^{\text{II}}\cdot\text{OEt}_2$ , stoichiometries compared to their previously studied organoactinide,  $(\text{C}_5\text{Me}_5)_2\text{UCl}\cdot\text{THF}$ , counterparts are accounted for by the presence of  $(\text{C}_5\text{Me}_5)_2\text{Yb}^{\text{III}}\text{-R}$  as a metastable intermediate which, along with  $(\text{C}_5\text{Me}_5)_2\text{Yb}^{\text{III}}\text{-Cl}$ , undergoes "Yb<sup>III</sup> Grignard" reactions to yield R-R,  $\text{C}_5\text{Me}_5\text{R}$ , and  $(\text{C}_5\text{Me}_5)\text{-YbCl}_2$  products. The results are summarized in a minimum number of steps (minimum mechanistic scheme) necessary to account for the observed results.

Oxidative additions are an important class of reactions which have been widely investigated in d-block transition metals.<sup>1</sup> In contrast, systematic and detailed studies of f-block organotransition-metal oxidative-addition reactions<sup>2,3</sup> were not reported until our discovery<sup>4a</sup> and mechanistic investigation<sup>4b</sup> of  $(\text{C}_5\text{Me}_5)_2\text{UCl}\cdot\text{THF} + \text{RX}$  (R = alkyl, aryl) organoactinide oxidative additions (eq 1).



(1) Collman, J. P.; Hegedus, L. S. "Principles and Applications of Organotransition Metal Chemistry"; University Science Books: Mill Valley, CA, 1980.

(2) A few scattered reports, often involving reaction with  $\text{CH}_2\text{Cl}_2$  or  $\text{CHCl}_3$  solvent, exist. (a) Watson, P. L. *J. Chem. Soc., Chem. Commun.* 1980, 652. (b) Tilley, T. D.; Andersen, R. A.; Zalkin, A. *Inorg. Chem.* 1983, 22, 856. (c) Tilley, T. D.; Andersen, R. A. *Ibid.* 1981, 20, 3267. (d) Dolgoplosk, B. A.; Tinyakova, E. I.; Markevich, I. N.; Soboleva, T. V.; Chernrenko, G. M.; Sharaev, O. K.; Yakovlev, V. A. *J. Organomet. Chem.* 1983, 255, 71. (e) Deacon, G. B.; MacKinnon, P. I. *Tetrahedron Lett.* 1984, 25, 783. (f) The use of Ln(II) to Ln(III) reactions in organic synthesis has been investigated: Natale, N. R. *Org. Prep. Proced. Int.* 1983, 15, 387. Imamoto, T.; Tawarayama, Y.; Kusumoto, T.; Yokoyama, M. *J. Synth. Org. Chem. Jpn.* 1984, 42, 143. Yokoo, K.; Fukagawa, T.; Yamanao, Y.; Taniguchi, H.; Fujiwara, Y. *J. Org. Chem.* 1984, 49, 3237. Girard, P.; Namy, J. L.; Kagan, H. B. *J. Am. Chem. Soc.* 1980, 102, 2693. Soupe, J.; Danon, L.; Namy, J. L.; Kagan, H. B. *J. Organomet. Chem.* 1983, 250, 227. Yokoo, K.; Kijime, Y.; Fujiwara, Y.; Taniguchi, H. *Chem. Lett.* 1984, 1321. Soupe, J.; Namy, J. L.; Kagan, H. B. *Tetrahedron Lett.* 1984, 25, 2869. Deacon, G. B.; Tuong, T. D. *J. Organomet. Chem.* 1981, 205, C4. Molander, G. A.; Etter, J. B. *Tetrahedron Lett.* 1984, 25, 3281.

(3) Organoactinide and organolanthanide reactions involving metal oxidation state changes<sup>2,3a</sup> are less well studied in general compared to their nonredox reactions such as insertion.<sup>3b</sup> (a) Brennan, J. G.; Anderson, R. A. *J. Am. Chem. Soc.* 1985, 107, 514. Boncella, J. M.; Anderson, R. A. *J. Chem. Soc., Chem. Commun.* 1984, 809. Tilley, T. D.; Anderson, R. A. *J. Am. Chem. Soc.* 1982, 104, 1772. Deacon, G. B.; Fallon, G. D.; MacKinnon, P. I.; Newham, R. H.; Pain, G. N.; Tuong, T. D.; Wilkinson, D. L. *J. Organomet. Chem.* 1984, 227, C1. Mikheev, N. B. *Inorg. Chim. Acta* 1984, 94, 241. (b) Marks, T. J. *Science (Washington, D.C.)* 1982, 217, 989. Cramer, R. E.; Higa, K. T.; Gilje, J. W. *J. Am. Chem. Soc.* 1984, 106, 7245 and earlier references in this series. Moloy, K. G.; Marks, T. J. *J. Am. Chem. Soc.* 1984, 106, 7051. Evans, W. J.; Wayda, A. L.; Hunter, W. E.; Atwood, J. L. *J. Chem. Soc., Chem. Commun.* 1981, 706. Katahira, D. A.; Moloy, K. G.; Marks, T. J. *Organometallics* 1982, 1, 1723. Evans, W. J.; Atwood, J. L.; Meadows, J. H.; Hunter, W. E. *Organometallics* 1983, 2, 1252. Evans, W. J.; Grate, J. W.; Doedens, R. J. *J. Am. Chem. Soc.* 1985, 107, 1671.

These one-electron U<sup>III</sup> to U<sup>IV</sup> reactions proceed according to the generalized stoichiometry<sup>4a</sup> in eq 1, involve an inner-sphere halogen atom abstraction to yield an R· intermediate, and proceed at rates  $10^4\text{--}10^7$  faster than typical d-block oxidative additions.<sup>4b</sup>

Herein we provide the results of an initial investigation<sup>5</sup> of organolanthanide oxidative-addition reactions  $(\text{C}_5\text{Me}_5)_2\text{Yb}^{\text{II}}\cdot\text{OEt}_2 + \text{RX}$ , reactions which give distinctive products and stoichiometries relative to their organoactinide counterparts.

Green, crystalline  $(\text{C}_5\text{Me}_5)_2\text{Yb}^{\text{II}}\cdot\text{OEt}_2$  was prepared from  $\text{KC}_5\text{Me}_5 + \text{YbBr}_2$  as previously described.<sup>2a,6a</sup> In preliminary kinetic studies,<sup>6b</sup> the rate of  $n\text{-BuCl} + (\text{C}_5\text{Me}_5)_2\text{Yb}^{\text{II}}\cdot\text{OEt}_2$  oxidative addition was determined by monitoring the loss of  $[\text{Yb}^{\text{II}}]_T$  at 680 nm (22.0 °C). The observed rate constant<sup>12a</sup>  $k_{2(\text{obsd})}$  (toluene) =  $3.6 \pm 0.6 \text{ M}^{-1} \text{ s}^{-1}$  is only 5.6 times slower than the corresponding reaction of  $(\text{C}_5\text{Me}_5)_2\text{UCl}\cdot\text{THF}$ ,  $k_{2(\text{obsd})}$  (22.0 °C, benzene) =  $20 \pm 1 \text{ M}^{-1} \text{ s}^{-1}$ , demonstrating that these f-block organolanthanide oxidative additions are also  $10^3\text{--}10^6$  times faster than their d-block counterparts.<sup>4b</sup>

Following examination of 15 alkyl and aryl halides, benzyl chloride emerged as a typical and convenient substrate for <sup>1</sup>H NMR product and stoichiometry studies. The product assignments provided below were made by comparison to authentic bibenzyl and to independently prepared, fully characterized  $\text{C}_5\text{Me}_5\text{CH}_2\text{Ph}$ ,<sup>7</sup>  $(\text{C}_5\text{Me}_5)\text{-YbCl}_2$ ,<sup>8</sup> and  $(\text{C}_5\text{Me}_5)_2\text{Yb}(\text{Cl})(\text{OEt}_2)$ .<sup>9</sup> In addition, independently prepared mixtures of the  $(\text{C}_5\text{Me}_5)_x\text{YbCl}_y$  complexes were necessary to verify the chemical shift(s) of what

(4) (a) Finke, R. G.; Gaughan, G.; Hirose, Y. *J. Chem. Soc., Chem. Commun.* 1981, 232. (b) Finke, R. G.; Schiraldi, D. A.; Hirose, Y. *J. Am. Chem. Soc.* 1981, 103, 1875.

(5) (a) Our goal is to compare a series of organolanthanides of different f<sup>n</sup> configuration, reduction potential ( $E_{1/2}$ ), and ionic radius, specifically:  $(\text{C}_5\text{Me}_5)_2\text{Yb}^{\text{II}}$  solvent, 4f<sup>14</sup>,  $E_{1/2} = -1.78$  (vs.  $\text{FeCp}_2/\text{FeCp}_2^+$ ) in acetonitrile,<sup>5c,d</sup> ionic radius<sup>5b</sup> = 1.1–1.2 Å;  $(\text{C}_5\text{Me}_5)_2\text{Sm}^{\text{II}}$ -solvent, 4f<sup>6</sup>,  $E_{1/2}$  (estimated) =  $-2.4$  V (vs.  $\text{FeCp}_2/\text{FeCp}_2^+$ ) in acetonitrile,<sup>5c,d</sup> ionic radius<sup>5b</sup> = 1.2–1.3 Å;  $(\text{C}_5\text{Me}_5)_2\text{Eu}^{\text{II}}$ -solvent, 4f<sup>7</sup>,  $E_{1/2}$  (estimated) =  $-1.22$  V (vs.  $\text{FeCp}_2/\text{FeCp}_2^+$ ) in acetonitrile,<sup>5c,d</sup> ionic radius<sup>5b</sup> = 1.2–1.4 Å. (b) Shannon, R. D. *Acta Crystallogr., Sect. A Cryst. Phys., Diffraction, Theor. Gen. Crystallogr.* 1976, A32, 751. (c) Watson, P. L., unpublished results. (d) Varlashkin, P. G.; Peterson, J. R. *J. Less-Common Met.* 1983, 94, 333. (e) For determinations of these reduction potentials under other conditions see: Mikheev, N. B. *Inorg. Chim. Acta* 1984, 94, 241. Morss, L. R. *Chem. Rev.* 1976, 76, 827. Johnson, D. A. *J. Chem. Soc., Dalton Trans.* 1974, 1671. Bratsch, S. G.; Lagowski, J. J. *J. Phys. Chem.* 1985, 89, 3317.

(6) (a) Green  $(\text{C}_5\text{Me}_5)_2\text{Yb}(\text{OEt}_2)$  shows  $\lambda_{\text{max}} = 680$  nm and obeys Beer's law over the concentration range examined:  $(3.42\text{--}9.77) \times 10^{-3} \text{ M}$ ;  $\epsilon_{680} = 214 \pm 20 \text{ M}^{-1} \text{ cm}^{-1}$ ; <sup>1</sup>H NMR (benzene-*d*<sub>6</sub>)  $\delta$  2.98 (q, 4 H,  $lw_{1/2} = 6$  Hz), 2.07 (s, 30 H,  $lw_{1/2} = 14$  Hz), 0.92 (t, 6 H,  $lw_{1/2} = 6$  Hz). (b) Second-order kinetic plots are typically linear over 80–90% of the reaction<sup>12a</sup> for  $(7.8\text{--}8.5) \times 10^{-3} \text{ M}$   $(\text{C}_5\text{Me}_5)_2\text{Yb}^{\text{II}}\cdot\text{OEt}_2$  (with the [RX] 20% higher than the  $[\text{Yb}^{\text{II}}]_{\text{T}}$ )<sup>12a</sup> establishing that the reaction is first-order each in  $[\text{Yb}^{\text{II}}]_T$  and [RX]. An inverse dependence on  $[\text{Et}_2\text{O}]$  (indicating the reaction is inner sphere)<sup>4b</sup> is also observed, analogous to the [THF] dependence determined for reactions of  $(\text{C}_5\text{Me}_5)_2\text{UCl}\cdot\text{THF}$  with RX. Full details of our kinetic and mechanistic studies will be forthcoming.<sup>13</sup>

(7) (a)  $\text{C}_5\text{Me}_5\text{Benzyl}$  was prepared from benzyl bromide and  $(\text{C}_5\text{Me}_5)\text{MgCl}^{\text{Ib}}$  in THF: <sup>1</sup>H NMR (benzene-*d*<sub>6</sub>)  $\delta$  2.65 (s, 2 H), 1.77 (s, 6 H), 1.57 (s, 6 H), 0.98 (s, 3 H), 7.03 (m, 5 H). Anal. Calcd for  $\text{C}_{17}\text{H}_{20}$ : C, 90.18; H, 9.82. Found: C, 89.94; H, 9.76. MS mass for  $\text{C}_{17}\text{H}_{20}$ : calcd, 226; found, 226. (b) Threlkel, R. S.; Bercaw, J. E. *J. Organomet. Chem.* 1977, 136, 1.

(8) Blue  $(\text{C}_5\text{Me}_5)\text{YbCl}_2$  exhibits the following <sup>1</sup>H NMR (benzene-*d*<sub>6</sub>)  $\delta$  19.17 (b s, 15 H,  $lw_{1/2} = 45$  Hz), in the absence of any  $\text{Yb}^{\text{II}}$ ,  $\text{Yb}^{\text{III}}$ , and/or  $\text{Et}_2\text{O}$ . In the presence of any of the latter, the resonance is broadened and undetectable. UV/visible:  $\lambda_{\text{max}} = 740$  and 380 nm. This complex obeys Beer's law over the concentration range examined:  $(6.0\text{--}1.6) \times 10^{-2} \text{ M}$ ;  $\epsilon_{680} = 74 \pm 6 \text{ M}^{-1} \text{ cm}^{-1}$ . Anal. Calcd for  $\text{C}_{10}\text{H}_{15}\text{YbCl}_2$ : Yb, 45.6; C, 31.7; H, 4.0; Cl, 18.7. Found: Yb, 45.8; C, 31.4; H, 3.8; Cl, 18.8.

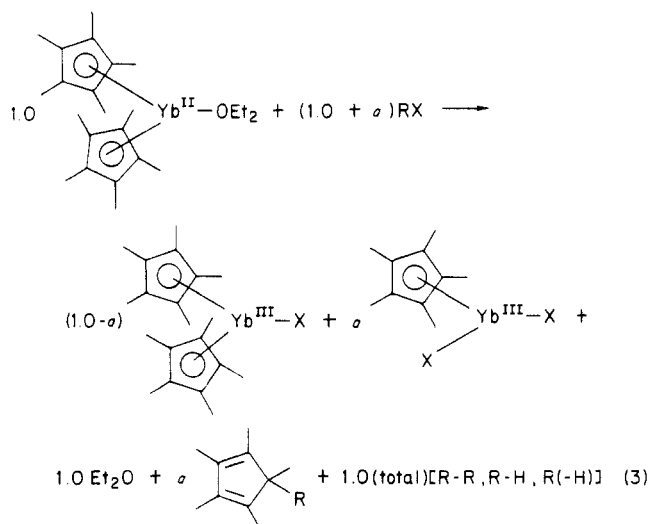
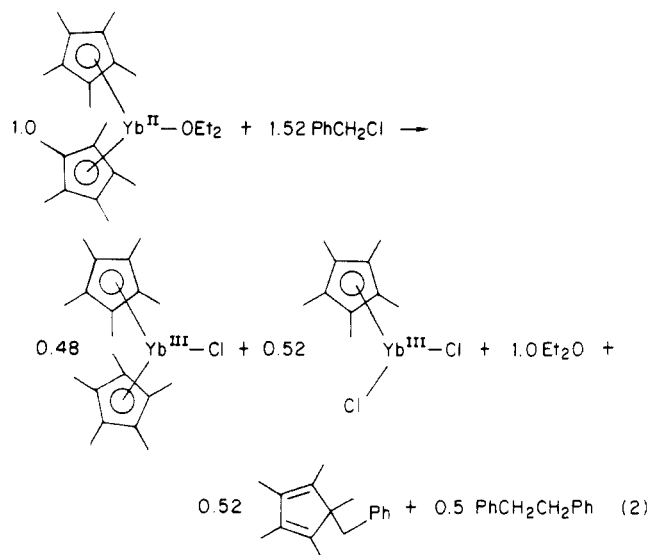
(9) Purple  $(\text{C}_5\text{Me}_5)_2\text{Yb}(\text{Cl})(\text{OEt}_2)$  was prepared by reaction of  $(\text{C}_5\text{Me}_5)_2\text{Yb}^{\text{II}}\cdot\text{OEt}_2$  with  $\text{CHCl}_3$  in  $\text{Et}_2\text{O}$ . The UV/visible spectrum shows  $\lambda_{\text{max}} = 550$  nm, and the compound obeys Beer's law over the concentration range examined:  $(2.26\text{--}9.04) \times 10^{-3} \text{ M}$ ;  $\epsilon_{550} = 176 \pm 2 \text{ M}^{-1} \text{ cm}^{-1}$ . The <sup>1</sup>H NMR (benzene-*d*<sub>6</sub>) spectrum is highly variable depending upon the initial concentration and upon the presence of  $\text{Et}_2\text{O}$ ;  $(\text{C}_5\text{Me}_5)_2\text{Yb}^{\text{III}}\cdot(\text{Cl})(\text{OEt}_2)$  alone exhibits a broad resonance in the region  $\delta$  12.9 (30 H,  $lw_{1/2} = 50$  Hz).



proved (*vide infra*) to be a composite  $C_5Me_5$  peak during the different stages of the reaction.

In a typical reaction,  $(C_5Me_5)_2Yb^{II} \cdot OEt_2$  (20 mg, 0.04 mmol), hexamethylbenzene (2 mg, 0.02 mmol) as an internal standard, benzene- $d_6$  (0.4 mL), and benzyl chloride were combined in an NMR tube. The  $PhCH_2Cl$  (0.25 equiv at a time) was added via gas-tight syringe until it was no longer consumed and the excess was observable by  $^1H$  NMR. During the course of addition of the first 0.75 equiv of  $PhCH_2Cl$ , the  $^1H$  NMR  $C_5Me_5$  resonance of the green<sup>6a</sup>  $(C_5Me_5)_2Yb^{II} \cdot OEt_2$  solution shifts downfield from its initial  $\delta$  2.07 position, appearing as a broad, composite  $\delta$  6.12 peak due to the  $C_5Me_5$  groups of the bis  $C_5Me_5$  complexes  $(C_5Me_5)_2Yb^{II}$  and  $(C_5Me_5)_2Yb^{III}-Cl$ .<sup>10</sup> Concomitantly, the solution turns a purple hue, confirming the formation of  $(C_5Me_5)_2Yb^{III}-Cl$ .<sup>9</sup> At this intermediate state of the reaction, only  $87 \pm 7\%$  of the starting  $(C_5Me_5)_2Yb^{II} \cdot OEt_2$  can be accounted for, and the missing mass is consistent with the presence of a Yb alkyl,  $(C_5Me_5)_2Yb-CH_2Ph$ , intermediate (*vide infra*). With the addition of further  $PhCH_2Cl$  ( $4 \times 0.25$  equiv; 1.75 equiv total) the missing 13%  $C_5Me_5$  is observed as additional  $C_5Me_5CH_2Ph$ ,  $(C_5Me_5)_2YbCl$ , and  $(C_5Me_5)YbCl_2$ . A new composite  $^1H$  NMR  $C_5Me_5$  resonance for the bis  $C_5Me_5$  products is now observed 1 ppm upfield at  $\delta$  5.1, and excess (free)  $PhCH_2Cl$  is seen. The solution also turns dark blue within 5 min following this second addition of  $PhCH_2Cl$  (the  $4 \times 0.25$  equiv), indicating the formation of the mono  $C_5Me_5$  product  $(C_5Me_5)Yb^{III}Cl_2$ .<sup>8</sup> This mono  $C_5Me_5$  product was detected separately and quantified by a  $\delta$  -1.42 resonance indicative of  $(C_5Me_5)Yb^{III}Cl_2$  in the presence of  $(C_5Me_5)_2Yb^{II} \cdot OEt_2$ .<sup>11</sup>

The resultant  $PhCH_2Cl$  oxidative-addition stoichiometry, observed when a slight excess of  $PhCH_2Cl$  has been added, is shown in eq 2 and accounts for  $98 \pm 5\%$  of the reactants. In fact, a generalized version of this stoichiometry<sup>12</sup> (eq 3) is obeyed by  $PhCH_2Cl$  ( $a = 0.52$ ),  $MeI$  ( $a = 0$ ),  $n-BuCl$  ( $a = 0.35$ ),  $PhI$  ( $a = 0.41$ ), and the other 15 total alkyl and aryl halides examined as long as  $RX$  is added until a slight excess is present. Mass balances in the range of 90–100% ( $\pm 10\%$ ) by NMR are generally observed, two exceptions being  $n-BuCl$  and  $PhCH_2CH_2Cl$ , which exhibited mass balances of approximately 75 and 70% respectively.<sup>13</sup>



The  $(C_5Me_5)_2Yb^{II} \cdot OEt_2$  oxidative-addition stoichiometry (eq 2 and 3) differs from its organoactinide  $(C_5Me_5)_2YbCl \cdot THF$  counterpart (eq 1) in three respects: the presence of  $(C_5Me_5)YbX_2 + C_5Me_5R$  products, the observation of a  $(C_5Me_5)_2Yb^{II} \cdot OEt_2/RX$  ratio of  $\leq 1.0$  (due to the formation of these products), and the lack of a *stable*  $(C_5Me_5)_2Yb-R$  product when excess  $RX$  is present. However, these differences can be accounted for in part (*vide*

(10) In the same reaction the movement of the  $Et_2O$  resonances is even more dramatic. For example, the  $O(CH_2CH_3)_2$  resonance, initially a sharp quartet at  $\delta$  2.98, broadens considerably ( $lw_{1/2} \geq 150$  Hz) shifting downfield to approximately  $\delta$  10.8 when the solution is purple, moving back upfield to  $\delta$  0.1 ( $lw_{1/2} = 40$  Hz) as the reaction proceeds, finally settling at approximately  $\delta$  2.8 ( $lw_{1/2} = 30$  Hz) when the solution is blue.

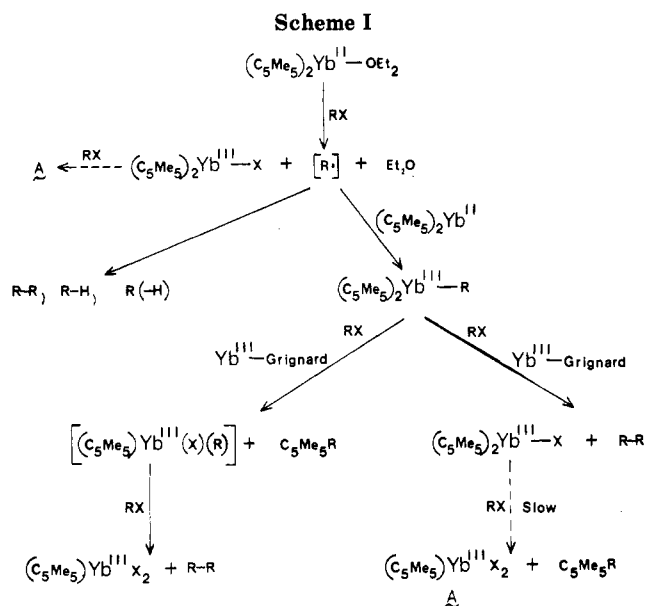
(11) This method of  $^1H$  NMR detection of the  $(C_5Me_5)YbCl_2$  product was discovered during the course of the benzyl chloride reaction, where a transient NMR resonance is observed at  $\delta$  -1.42 (s, 15 H,  $lw_{1/2} = 6$  Hz) as long as unreacted  $Yb^{II}$  is present. A control consisting of a 1:1 mixture of  $(C_5Me_5)_2Yb^{II} \cdot OEt_2$  and authentic  $(C_5Me_5)YbCl_2$  shows the same sharp resonance at  $\delta$  -1.42 (the two  $C_5Me_5$  ligands attached to  $Yb^{II}$  appear as a broad resonance centered at approximately  $\delta$  5.5), providing a method for quantification of this product. In the absence of  $Yb^{II}$  and in the presence of any  $Et_2O$  or  $(C_5Me_5)_2Yb(Cl)(OEt_2)$ , the  $(C_5Me_5)YbCl_2$  resonance broadens and shifts to the point where it is no longer independently identifiable.<sup>5</sup>

(12) (a) This  $k_{2(obsd)}$  value is probably less certain than the observed error bars indicate due to the requirement for, and the present uncertainty in, the stoichiometry coefficient<sup>12b</sup>  $a$  (eq 1) under the *exact conditions* of the second-order kinetic experiment.<sup>6b</sup> A tentative value<sup>19</sup> of  $a = 1.0$  was used to obtain  $k_{2(obsd)} = 3.6 M^{-1} s^{-1}$  since it gave linear second-order kinetic plots. (b) Added ligands (especially  $Et_2O$ ), the concentration, rate and method of addition of  $RX$  (four aliquots of 0.25 equiv vs. a single addition of 1.0 equiv for example), and the amount of any  $(C_5Me_5)_2Yb(Cl)(OEt_2)$  added prior to initiating the reaction all affect the observed stoichiometries.

(13) The volatility of the organic products, butane and butene, and the consumption of the olefin products (particularly the styrene from  $PhCH_2CH_2Cl$  reactions) increases the uncertainty in the mass balance to  $\geq 20\%$ .

(14) (a) It is interesting that  $(C_5Me_5)_2Yb^{III}-R$ ,  $R = CH_2Ph$ , is not seen by  $^1H$  NMR in contrast to some recently synthesized  $(C_5H_5)_2Yb-R$  analogues.<sup>14c</sup> However, an authentic sample of the red crystalline methyl complex  $(C_5Me_5)_2Yb(CH_3)(OEt_2)$  is undetectable under the same conditions of concentration, solvent, and temperature. (b) The required study of the  $(C_5Me_5)_2YbR$  ( $R = CH_3$ ,  $PhCH_2$ , and  $n-Bu$ ) alkyls and their reactions with  $RX$  ( $CH_3I$ ,  $PhCH_2Cl$ ,  $n-BuCl$ , respectively) to form  $R-R$  and/or  $C_5Me_5R$  is in progress. (c) Schumann, H.; Genthe, W.; Bruns, N.; Pickardt, J. *Organometallics* **1982**, *1*, 1194. Deacon, G. B.; Fallon, G. D.; MacKinnon, P. I.; Newham, R. H.; Plain, G. N.; Tuong, T. D.; Wilkinson, D. L. *J. Organomet. Chem.* **1984**, *277*, C21.

(15) The behavior of organolanthanide compounds as Grignard reagents is amply precedented for  $Yb^{II}$  complexes such as "RYbX"<sup>15a,c</sup> "RYbR"<sup>15b</sup> and  $X_2Ln^{III}-R$ <sup>15e</sup>, but not specifically for  $(C_5Me_5)_2Yb^{III}-R$  or  $(C_5Me_5)_2Yb^{III}-X$ . (a) Reference 2f. (b) Evans, D. F.; Fazakerly, G. V.; Phillips, R. F. *J. Chem. Soc. A* **1971**, 1931. (c) Deacon, G. B.; Tuong, T. D. *J. Organomet. Chem.* **1981**, *205*, C4. (d) A related reductive radical trapping by  $SmI_2(THF)_n$  in Kagan's chemistry has been postulated although its probable inner-sphere mechanism<sup>4b,6b</sup> was not previously appreciated: Kagan, H. B.; Namy, J. L.; Girard, P. *Tetrahedron, Suppl.* **1981**, *No. 9*, 175. Interestingly,  $Ln^0$  reductive capture of  $CH_3$  provided the first evidence for the formation of Ln alkyls: Schumann, H. *Angew. Chem., Int. Ed., Engl.* **1984**, *23*, 474. (e) Kauffmann, T.; Pahde, C.; Tannert, A.; Wingbermuehle, D.; *Tetrahedron* **1985**, *26*, 4063.



infra, by a metastable and reactive  $(C_5Me_5)_2Yb^{III}-R$  intermediate<sup>14</sup> that undergoes a "Yb<sup>III</sup> Grignard"<sup>15</sup> reaction with excess RX to give  $C_5Me_5R$  and/or R-R (plus Yb products). Three lines of evidence support the presence of such a  $(C_5Me_5)_2Yb^{III}-R$  intermediate. First, the <sup>1</sup>H NMR determined difference in mass balance between reactions with excess PhCH<sub>2</sub>Cl (1.6 equiv) and those with only 0.68 equiv of PhCH<sub>2</sub>Cl requires formation of ca. 25% of an intermediate of unknown structure but of net composition  $(C_5Me_5)_{1.9\pm 0.4}Yb_{1.0\pm 0.2}(CH_2Ph)_{1.0\pm 0.4}$ . (The precision of this experiment is limited by overlapping resonances in the <sup>1</sup>H NMR). Second, independent evidence for such an intermediate was obtained by quenching the 0.68 equiv of PhCH<sub>2</sub>Cl reaction with MeOH followed by GLC analysis for toluene, which yields  $82 \pm 8\%$  of the expected toluene (0.20 equiv based on PhCH<sub>2</sub>Cl). Third, a reaction to maximize the apparent trapping of PhCH<sub>2</sub>· by  $(C_5Me_5)_2Yb^{II}$  was performed by using a 12-fold excess of  $(C_5Me_5)_2Yb/PhCH_2Cl$  at  $[PhCH_2Cl] = 8.7 \times 10^{-3} M$ , followed by MeOH quench and GLC analysis for toluene. The increased amount of toluene observed in this experiment,  $62 \pm 8\%$  based on PhCH<sub>2</sub>Cl, provides strong evidence for  $(C_5Me_5)_2Yb^{III}-CH_2Ph$  formation by the novel PhCH<sub>2</sub>· radical trapping reaction by diamagnetic  $4f^{14} Yb^{II}$ ,  $(C_5Me_5)_2Yb^{II} + PhCH_2\cdot \rightarrow (C_5Me_5)_2Yb-CH_2Ph$ , probably by an inner-sphere, electron-transfer reaction.<sup>15d</sup> Under these conditions (excess  $(C_5Me_5)_2Yb^{II}\cdot OEt_2$ ), the initial limiting stoichiometry approaches the limiting stoichiometry previously observed<sup>4</sup> for  $(C_5Me_5)_2UCl\cdot THF$  when all the R· is captured by the metal, i.e.,  $2(C_5Me_5)_2Yb^{II}\cdot OEt_2 + RX \rightarrow (C_5Me_5)_2YbX + (C_5Me_5)_2Yb-R$ . Subsequent, follow-up Grignard reactions of the  $(C_5Me_5)_2Yb-CH_2Ph$  intermediate with additional PhCH<sub>2</sub>Cl are summarized in the bottom half of Scheme I, the formation of blue  $(C_5Me_5)_2YbCl_2$  accounting for the purple to blue color change in the reactions of Yb<sup>II</sup> with excess PhCH<sub>2</sub>Cl.

We probed another possible "Yb<sup>III</sup> Grignard" reaction by verifying that  $(C_5Me_5)_2Yb^{III}(Cl)(OEt_2)$  with 1.0 equiv

of PhCH<sub>2</sub>Cl cleanly yields 1.0 equiv each of  $(C_5Me_5)_2YbCl_2$  and  $C_5Me_5CH_2Ph$ . The observed rate constant, from the disappearance of  $[Yb^{III}]_T$  at 550 nm (22.0 °C) in toluene, is  $k_{2(obsd)} = (6.5 \pm 1.5) \times 10^{-2} M^{-1} s^{-1}$ .<sup>16a</sup> This is at least 300 times slower than the observed  $(C_5Me_5)_2Yb^{II}\cdot OEt_2 + PhCH_2Cl$  reaction ( $k_{2(obsd)} \geq 20 M^{-1} s^{-1}$ ) and ca. 7 times slower than the  $(C_5Me_5)_2Yb^{III}-R + PhCH_2Cl$  reaction.<sup>17</sup> Participation of this specific Yb<sup>III</sup> Grignard pathway in the observed reaction is therefore negligible except toward the end of reactions and unless excess PhCH<sub>2</sub>Cl is present. Interestingly, this latter Yb<sup>III</sup> Grignard reaction is 200 times slower in Et<sub>2</sub>O than toluene,<sup>16b</sup> suggesting it proceeds via prior coordination and an inner-sphere mechanism. Also, a free radical mechanism is not involved since  $(C_5Me_5)_2Yb^{III}-Cl + (bromomethyl)cyclopropane$  yields only the closed-ring ( $\geq 98\%$ ), nonradical<sup>18a</sup>  $C_5Me_5CH_2CHCH_2CH_2$  product. None ( $\leq 2\%$ ) of the open-ring  $C_5Me_5CH_2CH_2CH=CH_2$  product is observed by glc comparison to authentic materials.<sup>18</sup>

Scheme I presents the minimum steps necessary to account for the products, stoichiometries, and other observations (for example, those supporting the presence of a R· intermediate<sup>19</sup>). When the  $(C_5Me_5)_2Yb-R$  and  $(C_5Me_5)_2Yb^{III}-Cl$  "Grignard" reactions are taken into account, the differences in the Yb<sup>II</sup> stoichiometry relative to U<sup>III</sup> disappear, with Yb<sup>II</sup> behaving very similarly to U<sup>III</sup> for both the rate of the initial atom abstraction reaction and the initial reaction stoichiometry.

The present studies raise a number of interesting mechanistic questions, especially the inner vs. outer-sphere nature of the initial atom abstraction reaction and why the rates of the diamagnetic  $4f^{14} Yb^{II}$  organolanthanide are so similar to those of the  $5f^3 U^{III}$  organoactinide triradical—a result which seems to demand a single electron-transfer (SET) component in these "atom abstraction" reactions.<sup>20</sup> These and other questions<sup>14b</sup> will be the focus of a subsequent kinetic and mechanistic paper.<sup>19</sup>

**Acknowledgment.** Support from NSF Grant CHE-8313459, donors of the Petroleum Research Fund, administered by the American Chemical Society, and Dreyfus Teacher-Scholar and Alfred P. Sloan Fellowships to R.G.F. are gratefully acknowledged.

**Registry No.**  $(C_5Me_5)_2Yb^{II}\cdot OEt_2$ , 74282-47-6;  $(C_5Me_5)_2Yb^{III}Cl$ , 75750-86-6;  $(C_5Me_5)_2Yb^{III}Cl_2$ , 99642-75-8;  $(C_5Me_5)_2Yb^{III}(Cl)(OEt_2)$ , 99642-76-9.

(17) Preliminary kinetic studies of impure samples of independently prepared  $(C_5Me_5)_2Yb(CH_2Ph)$  with PhCH<sub>2</sub>Cl yield a rate of reaction of ca.  $0.5 M^{-1} s^{-1}$ .<sup>20</sup>

(18) (a) Griller, D.; Ingold, K. U. *Acc. Chem. Res.* **1980**, *13*, 317. Maillard, B.; Forrest, D.; Ingold, K. U. *J. Am. Chem. Soc.* **1976**, *98*, 7024.

(b)  $C_5Me_5CH_2CHCH_2CH_2$  was prepared by reaction of (bromomethyl)cyclopropane with  $(C_5Me_5)MgCl$  in THF: <sup>1</sup>H NMR (benzene-*d*<sub>6</sub>)  $\delta$  1.8 (apparent doublet, 12 H), 1.51 (d, 2 H, *J* = 5 Hz), 1.36 (pt, 2 H), 0.93 (s, 3 H), 0.23 (m, 2 H), -0.06 (m, 1 H). Anal. Calcd for C<sub>14</sub>H<sub>24</sub>: C, 88.3; H, 11.7. Found: C, 88.4; H, 11.8. MS mass for C<sub>14</sub>H<sub>24</sub>: calcd, 190; found, 190. (c)  $C_5Me_5CH_2CH_2CH=CH_2$  was prepared by reaction of 4-bromo-1-butene with  $(C_5Me_5)MgCl$  in THF: <sup>1</sup>H NMR (benzene-*d*<sub>6</sub>)  $\delta$  5.84 (m, 2 H), 5.04 (pt, 1 H), 1.76 (s, 6 H), 1.68 (s, 6 H), 1.54 (m, 4 H), 0.94 (s, 3 H). Anal. Calcd for C<sub>14</sub>H<sub>24</sub>: C, 88.3; H, 11.7. Found: C, 87.9; H, 11.9. MS mass for C<sub>14</sub>H<sub>24</sub>: calcd, 190; found, 190.

(19) Finke, R. G.; Keenan, S. R.; Watson, P. L., manuscript in preparation.

(20) Evidence for a single electron-transfer component in d-block transition metal and main-group "atom abstraction" reactions has appeared: Blackburn, E. V.; Tanner, D. D. *J. Am. Chem. Soc.* **1980**, *102*, 692. Tamblin, W. H.; Volger, E. A.; Kochi, J. K. *J. Org. Chem.* **1980**, *45*, 3912. Menapace, C. W.; Kuivila, H. G. *J. Am. Chem. Soc.* **1964**, *86*, 3047. Chatgililoglu, C.; Ingold, K. U.; Sciano, J. C. *Ibid.* **1982**, *104*, 5123.

(16) (a) For the reaction of benzyl chloride with  $(C_5Me_5)_2Yb(Cl)(OEt_2)$  in toluene at 22.0 °C, monitoring 550 nm,  $[Yb^{III}] = (8.5-9.8) \times 10^{-3} M$  and  $[PhCH_2Cl] = 0.073-0.212 M$ . (b) For  $(C_5Me_5)_2Yb(Cl)(OEt_2) + PhCH_2Cl$  in Et<sub>2</sub>O,  $[Yb^{III}] = 6.7 \times 10^{-3} M$ ,  $[PhCH_2Cl] = 0.115 M$ , and  $k_{2(obsd)}(22.0^\circ C, Et_2O) = (3.5 \pm 0.4) \times 10^{-4} M^{-1} s^{-1}$ .  $(C_5Me_5)_2YbCl_2$  also reacts with PhCH<sub>2</sub>Cl forming YbCl<sub>3</sub> (green-yellow, insoluble) +  $C_5Me_5CH_2Ph$ , but at a rate approximately  $10^2$  slower than the corresponding reaction of  $(C_5Me_5)_2Yb(Cl)(OEt_2)$ .

## An Unexpected Carbon-Carbon Bond Formation in the Reaction between $\text{Mo}_2(\text{ONp})_6(\mu\text{-NCNEt}_2)$ and $\text{MeC}\equiv\text{CMe}$

Malcolm H. Chisholm,\* Kirsten Folting,  
John C. Huffman, and Nancy S. Marchant

Department of Chemistry and Molecular Structure Center  
Indiana University, Bloomington, Indiana 47405

Received December 13, 1985

**Summary:**  $\text{Mo}_2(\text{ONp})_6(\mu\text{-NCNEt}_2)$  (I) and  $\text{MeC}\equiv\text{CMe}$  react in hydrocarbon solution at room temperature and below to give  $\text{Mo}_2(\text{ONp})_6(\mu\text{-C}_4\text{Me}_4)(\text{NCNEt}_2)$  (II) which at +60 °C reacts further to give a novel compound,  $\text{Mo}_2(\text{ONp})_6(\mu\text{-C}_4\text{Me}_3\text{CH}_2\text{C}(\text{NH})\text{NEt}_2)$  (III), containing two connected five-membered rings bonded to the  $\text{Mo}_2$  centers.

Following the discovery that  $\text{W}_2(\text{OR})_6(\text{py})_n(\mu\text{-C}_2\text{R}'_2)$  compounds and nitriles reacted under mild conditions to give  $\text{W}_2$ -containing compounds with bridging ligands formed by the coupling of the  $\mu\text{-C}_2\text{R}'_2$  and  $\text{R}'\text{CN}$  groups, e.g.,  $\text{W}_2(\text{O}-t\text{-Bu})_6(\mu\text{-CHCHCPhN})$  and  $\text{W}_2(\text{ONp})_6(\mu\text{-N}(\text{CMe})_4\text{N})$ ,<sup>1</sup> we examined the reactivity of  $\text{Mo}_2(\text{ONp})_6(\mu\text{-NCNEt}_2)$  (I) toward alkynes. Compound I has a cyanamide unit which bridges parallel to the dimetal center,<sup>2</sup> and one would anticipate that similar C-C bond-forming reactions might result.

Contrary to this expectation hydrocarbon solutions of I react with  $\text{MeC}\equiv\text{CMe}$  at ambient temperatures and below (ca. -30 °C) to give  $\text{Mo}_2(\text{ONp})_6(\mu\text{-C}_4\text{Me}_4)(\text{NCNEt}_2)$  (II) in which the  $\mu\text{-NCNEt}_2$  ligand becomes terminally bound (Figure 1).<sup>3</sup> Compound II is closely related to the previously characterized pyridine adduct  $\text{Mo}_2(\text{ONp})_6(\mu\text{-C}_4\text{H}_4\text{py})$ ,<sup>4</sup> and addition of pyridine to II leads to the formation of  $\text{Mo}_2(\text{ONp})_6(\mu\text{-C}_4\text{Me}_4)(\text{py})$ . II is fluxional on the NMR time scale in toluene- $d_8$  at room temperature. Upon raising the temperature to +60 °C, II reacts to give compound III which is stereochemically rigid and lacking any elements of symmetry (by NMR spectroscopy).

Of particular note in the <sup>1</sup>H NMR spectrum of III was the presence of seven AB quartets of equal intensity and only three Me signals derived from the  $\mu\text{-C}_4\text{Me}_4$  ligand of II. Reactions employing <sup>13</sup>C NMR revealed that the high-field AB quartet showed coupling to <sup>13</sup>C, <sup>2</sup>J<sub>C-H</sub> = 6.1 Hz, suggestive of C-C bond formation involving the

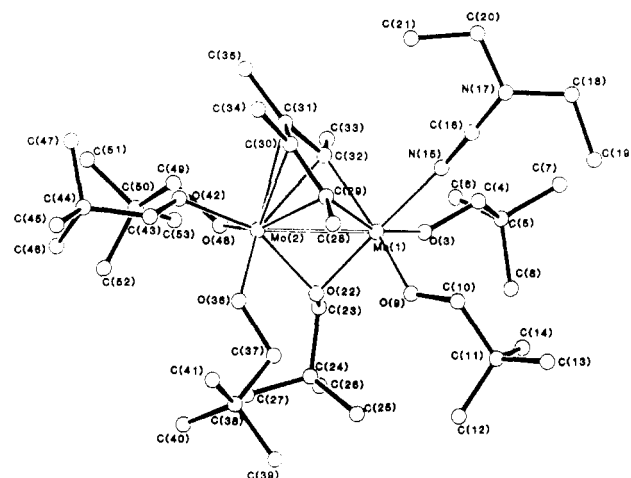


**Figure 1.** A view of the  $\text{Mo}_2(\text{ONp})_6(\mu\text{-C}_4\text{Me}_4)(\text{NCNEt}_2)$  molecule. Pertinent distance (Å) are Mo-Mo = 2.639 (1), Mo(1)-O(3) = 1.959 (4), Mo(1)-O(9) = 1.918 (5), Mo(1)-O(22) = 2.073 (4), Mo(1)-N(15) = 2.168 (6), Mo(1)-C(29) = 2.158 (7), Mo(1)-C(32) = 2.131 (6), Mo(2)-O(22) = 2.150 (4), Mo(2)-O(36) = 1.922 (5), Mo(2)-O(42) = 2.015 (4), Mo(2)-O(48) = 1.941 (4), Mo(2)-C(29) = 2.295 (7), Mo(2)-C(30) = 2.432 (6), Mo(2)-C(31) = 2.407 (7), and Mo(2)-C(32) = 2.369 (6).

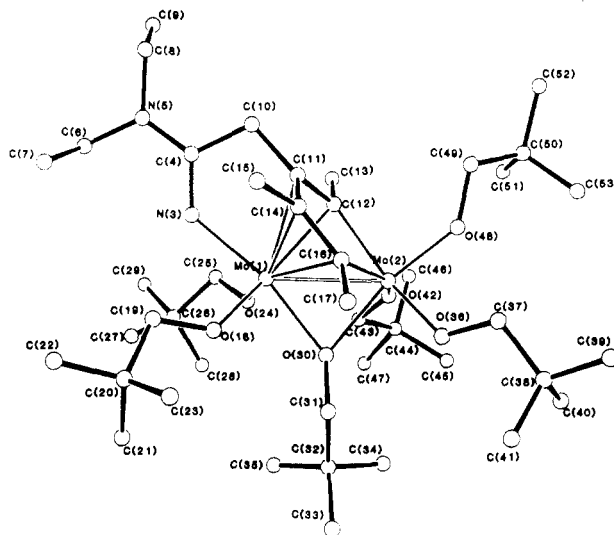


**Figure 2.** A view of the  $\text{Mo}_2(\text{ONp})_6(\text{C}_4\text{Me}_3\text{CH}_2(\text{NEt}_2)\text{NH})$  molecule. Pertinent bond distances (Å) are Mo-Mo = 2.711 (2), Mo(1)-O(18) = 1.938 (5), Mo(1)-O(24) = 1.944 (5), Mo(1)-O(30) = 2.135 (5), Mo(1)-N(3) = 2.167 (7), Mo(1)-C(11) = 2.335 (8), Mo(1)-C(12) = 2.319 (8), Mo(1)-C(14) = 2.264 (8), Mo(1)-C(16) = 2.299 (8), Mo(2)-O(30) = 2.127 (5), Mo(2)-O(36) = 1.950 (5), Mo(2)-O(42) = 1.890 (6), Mo(2)-O(48) = 1.920 (6), Mo(2)-C(12) = 2.118 (8), and Mo(2)-C(16) = 2.164 (8).

<sup>13</sup>C NMR carbon. A broad singlet at  $\delta$  5.07, together with a band at 3358  $\text{cm}^{-1}$  in the infrared spectrum was also indicative of the formation of a  $\text{CH}_2\text{C}(\text{NH})\text{NEt}_2$  unit.

Coordination of the NH function to a Mo atom was anticipated but to which molybdenum atom was uncertain. Furthermore which methyl group of the  $\mu\text{-C}_4\text{Me}_4$  ligand ( $\alpha$  or  $\beta$ ) had reacted could not be ascertained. The molecular structure of III was accordingly determined<sup>3</sup> and is shown in Figure 2. To our knowledge the two connected five-membered rings coordinated to the dimetal center is without precedent.

A possible reaction pathway leading to the formation of III may be based on the "tuck-in" chemistry established for  $(\text{C}_5\text{Me}_5)_2\text{ZrH}_2$  chemistry.<sup>4</sup> In the present instance loss of  $\text{Et}_2\text{NCN}$  from II would lead to an unsaturated intermediate which could undergo H abstraction from the  $\text{C}_4\text{Me}_3$  ring. The cyanamide would then insert into either

(1) Chisholm, M. H.; Hoffman, D. M.; Huffman, J. C. *J. Am. Chem. Soc.* 1984, 106, 6815.

(2)  $\text{Mo}_2(\text{ONp})_6(\text{Et}_2\text{NCN})$  was characterized spectroscopically and found to be structurally analogous to other  $\text{Mo}_2(\text{OR})_6\text{R}'_2\text{NCN}$  compounds. (a) Chisholm, M. H.; Kelly, R. L. *Inorg. Chem.* 1979, 18, 2321. (b) Chisholm, M. H.; Huffman, J. C.; Marchant, N. S. *J. Am. Chem. Soc.* 1983, 105, 6162.

(3) Summary of crystal data. (i)  $\text{Mo}_2(\text{ONp})_6(\mu\text{-C}_4\text{Me}_4)(\text{NCNEt}_2)$  at -159 °C:  $a = 11.892$  (5) Å,  $b = 32.487$  (18) Å,  $c = 13.919$  (6) Å,  $\beta = 111.38$  (2)°,  $d_{\text{calc}} = 1.21$   $\text{g cm}^{-3}$ , and space group  $P2_1/a$ . Of 7199 reflections collected (Mo K $\alpha$ ,  $6^\circ < 2\theta < 45^\circ$ ), 6560 reflections were unique and the 4486 reflections having  $F > 3\sigma(F)$  were used in the full-matrix least-squares refinement. Hydrogen atoms were refined by using fixed idealized positions. Final residuals are  $R(F) = 0.049$  and  $R_w(F) = 0.049$ . (ii)  $\text{Mo}_2(\text{ONp})_6(\text{C}_4\text{Me}_3\text{CH}_2\text{C}(\text{NEt}_2)\text{NH})$  at -153 °C:  $a = 11.101$  (4) Å,  $b = 17.177$  (9) Å,  $c = 25.766$  (14) Å,  $d_{\text{calc}} = 1.24$   $\text{g cm}^{-3}$ , and space group  $P2_12_1$ . Of the 3716 reflections collected (Mo K $\alpha$ ,  $6^\circ < 2\theta < 45^\circ$ ), 3631 reflections were unique and 3200 reflections having  $F > 3\sigma(F)$  were used in the full-matrix least-squares refinement. Hydrogen atoms were included in fixed calculated positions. Final residuals are  $R(F) = 0.042$  and  $R_w(F) = 0.043$ .

(4) Chisholm, M. H.; Folting, K.; Huffman, J. C.; Rothwell, I. P. *J. Am. Chem. Soc.* 1982, 104, 4389.

(5) Bercaw, J. E. *Adv. Chem. Ser.* 1978, No. 167, 135 (Transition Metal Hydrides, Bau, Ed.).

the M-H bond or the "tucked-in" position of the  $C_4Me_4$  ligand. Evidence in support of this mechanism is that (1) the cyanamide ligand in II is easily replaced by py and (2) that  $Mo_2(ONp)_6(\mu-C_4Me_4)(py)$  in the presence of  $Et_2NCN$  will also form III at slightly higher temperatures. Further kinetic studies are in progress in order to gain a better understanding of this unusual reaction.<sup>6</sup>

**Supplementary Material Available:** Tables of fractional coordinates and isotropic thermal parameters, anisotropic thermal parameters, bond distances, bond angles, and structure factor amplitudes for compounds I and II (52 pages). Ordering information is given on any current masthead page.

(6) We thank the Department of Energy, Office of Basic Sciences, Chemical Division for support of this work.

### Mercury in Organic Chemistry. 32. Bromination and Iodination of Allenic and Propargylic Organomercurials: A Convenient Synthesis of 3-Halo-1,2-alkadienes

Richard C. Larock\* and Min-Shine Chow

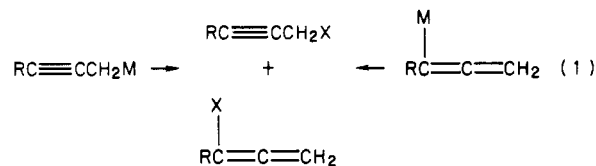
Department of Chemistry, Iowa State University  
Ames, Iowa 50011

Received November 12, 1985

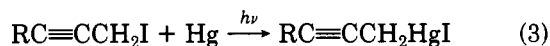
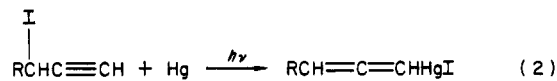
**Summary:** The bromination (pyridinium hydrobromide perbromide) and iodination (iodine) of allenic and propargylic organomercuric halides in pyridine proceeds with rearrangement to afford the corresponding propargylic and allenic halides, respectively. This procedure provides a convenient, new route to 3-bromo- and 3-iodo-1,2-alkadienes useful in organic synthesis.

While there has been considerable recent interest in the application of allenic and propargylic organometallics in organic synthesis, two major problems in this area remain. Few of the organometallics so far studied accommodate many important functional groups, and the majority of the

synthetic applications of these organometallics reported to date result in mixtures of allenic and propargylic products (eq 1). Our recent discovery of a convenient new



route to allenic and propargylic organomercuric halides (eq 2 and 3)<sup>1</sup> appeared to offer possible solutions to both of



these problems, since these organometallics do not appear to equilibrate and their method of synthesis readily accommodates functionality. At this time we wish to report our preliminary results on the bromination and iodination of these organometallics. Our results to date are summarized in Table I.

All halogenation reactions were carried out by using the following general procedure. The halogenating agent (0.5 mmol) dissolved in 5 mL of pyridine was added to a solution of the organomercurial (0.5 mmol) in 5 mL of pyridine at the appropriate temperature. After 5-min reaction time, methylene chloride was added and the organic layer was washed successively with 3 M  $Na_2S_2O_3$ , water, 1 N HCl, and water. After the solution was dried over  $MgSO_4$ , the solvent was removed affording essentially pure organic halide. The purity and ratio of organic halides was established by  $^1H$  NMR spectroscopy. The structure of the products was confirmed by IR spectroscopy, high-resolution mass spectrometry, and comparison with literature data.

The reaction of both the allenic and propargylic organomercurials with iodine proceeds readily at room temperature to  $-40^\circ C$  in pyridine to afford the corresponding rearranged propargylic or allenic iodides respectively. No more than minor amounts of the products of retention were observed. The use of solvents other than pyridine

Table I. Halogenation of Allenic and Propargylic Organomercurials

entry	organomercurial	halogenating agent	reactn temp, °C	product(s)	yield, %	ratio of allenic to propargylic halide
1	$\begin{array}{c} CH_3 \\   \\ C=C=C \\   \quad   \\ H \quad HgI \end{array}$	$I_2$	-40	$CH_3CHIC\equiv CH$	85	<2/98
2		$C_5H_5NHBr_3$	-40	$CH_3CHXC\equiv CH$ (X: Br/I = 93/7)	82	0/100
3	$\begin{array}{c} CH_3 \\   \\ C=C=C \\   \quad   \\ H \quad C_6H_5 \\ \quad \quad   \\ \quad \quad HgI \end{array}$	$I_2$	-40	$CH_3CHIC\equiv CC_6H_5$	95	<2/98
4	$CH_3C\equiv CCH_2HgI$	$I_2$	25	$CH_3CI=C=CH_2$	77	98/2
5		$C_5H_5NHBr_3$	-40	$CH_3CX=C=CH_2$ (X: Br/I = 92/8)	71	~100/0
6	$C_6H_5C\equiv CCH_2HgI$	$I_2$	25	$C_6H_5CI=C=CH_2$	100	92/8
7		$C_5H_5NHBr_3$	25	$C_6H_5CX=C=CH_2$ (X: Br/I = 99/1)	94	~100/0
8	$C_6H_5C\equiv CCH_2HgBr$	$C_5H_5NHBr_3$	25	$C_6H_5CBr=C=CH_2$	94	99/1
9	$CH_3O_2C(CH_2)_3C\equiv CCH_2HgI$	$I_2$	25	$CH_3O_2C(CH_2)_3CI=C=CH_2$	97	100/0
10		$C_5H_5NHBr_3$	-40	$CH_3O_2C(CH_2)_3CX=C=CH_2$ (X: Br/I = 44/56)	82	100/0

the M-H bond or the "tucked-in" position of the  $C_4Me_4$  ligand. Evidence in support of this mechanism is that (1) the cyanamide ligand in II is easily replaced by py and (2) that  $Mo_2(ONp)_6(\mu-C_4Me_4)(py)$  in the presence of  $Et_2NCN$  will also form III at slightly higher temperatures. Further kinetic studies are in progress in order to gain a better understanding of this unusual reaction.<sup>6</sup>

**Supplementary Material Available:** Tables of fractional coordinates and isotropic thermal parameters, anisotropic thermal parameters, bond distances, bond angles, and structure factor amplitudes for compounds I and II (52 pages). Ordering information is given on any current masthead page.

(6) We thank the Department of Energy, Office of Basic Sciences, Chemical Division for support of this work.

### Mercury in Organic Chemistry. 32. Bromination and Iodination of Allenic and Propargylic Organomercurials: A Convenient Synthesis of 3-Halo-1,2-alkadienes

Richard C. Larock\* and Min-Shine Chow

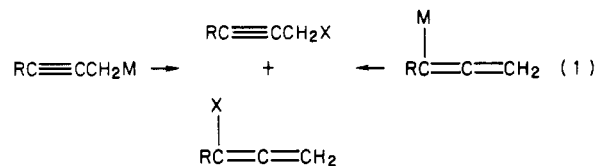
Department of Chemistry, Iowa State University  
Ames, Iowa 50011

Received November 12, 1985

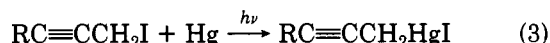
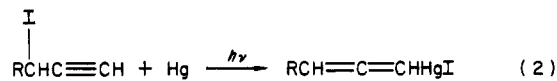
**Summary:** The bromination (pyridinium hydrobromide perbromide) and iodination (iodine) of allenic and propargylic organomercuric halides in pyridine proceeds with rearrangement to afford the corresponding propargylic and allenic halides, respectively. This procedure provides a convenient, new route to 3-bromo- and 3-iodo-1,2-alkadienes useful in organic synthesis.

While there has been considerable recent interest in the application of allenic and propargylic organometallics in organic synthesis, two major problems in this area remain. Few of the organometallics so far studied accommodate many important functional groups, and the majority of the

synthetic applications of these organometallics reported to date result in mixtures of allenic and propargylic products (eq 1). Our recent discovery of a convenient new



route to allenic and propargylic organomercuric halides (eq 2 and 3)<sup>1</sup> appeared to offer possible solutions to both of



these problems, since these organometallics do not appear to equilibrate and their method of synthesis readily accommodates functionality. At this time we wish to report our preliminary results on the bromination and iodination of these organometallics. Our results to date are summarized in Table I.

All halogenation reactions were carried out by using the following general procedure. The halogenating agent (0.5 mmol) dissolved in 5 mL of pyridine was added to a solution of the organomercurial (0.5 mmol) in 5 mL of pyridine at the appropriate temperature. After 5-min reaction time, methylene chloride was added and the organic layer was washed successively with 3 M  $Na_2S_2O_3$ , water, 1 N HCl, and water. After the solution was dried over  $MgSO_4$ , the solvent was removed affording essentially pure organic halide. The purity and ratio of organic halides was established by  $^1H$  NMR spectroscopy. The structure of the products was confirmed by IR spectroscopy, high-resolution mass spectrometry, and comparison with literature data.

The reaction of both the allenic and propargylic organomercurials with iodine proceeds readily at room temperature to  $-40^\circ C$  in pyridine to afford the corresponding rearranged propargylic or allenic iodides respectively. No more than minor amounts of the products of retention were observed. The use of solvents other than pyridine

Table I. Halogenation of Allenic and Propargylic Organomercurials

entry	organomercurial	halogenating agent	reactn temp, °C	product(s)	yield, %	ratio of allenic to propargylic halide
1	$\begin{array}{c} CH_3 \\   \\ C=C=C \\   \quad   \\ H \quad HgI \end{array}$	$I_2$	-40	$CH_3CHIC\equiv CH$	85	<2/98
2		$C_5H_5NHBr_3$	-40	$CH_3CHXC\equiv CH$ (X: Br/I = 93/7)	82	0/100
3	$\begin{array}{c} CH_3 \\   \\ C=C=C \\   \quad   \\ H \quad C_6H_5 \\ \quad \quad   \\ \quad \quad HgI \end{array}$	$I_2$	-40	$CH_3CHIC\equiv CC_6H_5$	95	<2/98
4	$CH_3C\equiv CCH_2HgI$	$I_2$	25	$CH_3CI=C=CH_2$	77	98/2
5		$C_5H_5NHBr_3$	-40	$CH_3CX=C=CH_2$ (X: Br/I = 92/8)	71	~100/0
6	$C_6H_5C\equiv CCH_2HgI$	$I_2$	25	$C_6H_5CI=C=CH_2$	100	92/8
7		$C_5H_5NHBr_3$	25	$C_6H_5CX=C=CH_2$ (X: Br/I = 99/1)	94	~100/0
8	$C_6H_5C\equiv CCH_2HgBr$	$C_5H_5NHBr_3$	25	$C_6H_5CBr=C=CH_2$	94	99/1
9	$CH_3O_2C(CH_2)_3C\equiv CCH_2HgI$	$I_2$	25	$CH_3O_2C(CH_2)_3CI=C=CH_2$	97	100/0
10		$C_5H_5NHBr_3$	-40	$CH_3O_2C(CH_2)_3CX=C=CH_2$ (X: Br/I = 44/56)	82	100/0

generally led to more complicated mixtures of allenic and propargylic iodides.

Bromination of these same organomercurials is best effected by using pyridinium hydrobromide perbromide at  $-40$  to  $25$  °C in pyridine for 5 min. Bromine itself tended to give large amounts of polybrominated products, and mixtures of organic bromides and iodides were obtained when organomercury iodides were employed. The former problem can generally be circumvented by using the pyridinium reagent, but mixtures of organic bromides and iodides are still observed. Organomercuric bromides, however, brominate cleanly with the pyridinium reagent.

While a number of ways of preparing allenic halides are known,<sup>2</sup> relatively little work has been reported on the halogenation of allenic or propargylic organometallics. Allenylsilver compounds, though of limited availability, have been reported to react with *N*-chloro- or *N*-bromosuccinimide, cyanogen bromide and iodine to afford the corresponding 1-halo-1,2-alkadienes.<sup>3</sup> Allenic and propargylic tin compounds iodinate with rearrangement to yield propargyl iodides and 1-iodo-1,2-alkadienes respectively.<sup>4</sup> Finally, propargylic silanes react with bromine

and iodine to generate 3-halo-1,2-alkadienes, a class of compounds apparently not available by any other route.<sup>5</sup> This latter approach has found considerable recent use in eicosanoid synthesis.<sup>6-9</sup> While the halogenation of organomercurials has been extensively studied,<sup>10</sup> there are no previous reports of the halogenation of the virtually unknown allenic and propargylic mercurials. We believe that our propargylic mercurial halogenation procedure provides a useful alternative to the silane approach to 3-halo-1,2-alkadienes due to the ready availability of the mercurials and their ability to accommodate considerable functionality. This is illustrated by the ease with which we have been able to prepare intermediates useful in prostaglandin synthesis (see entries 9 and 10 in Table I).

We are presently studying other potential applications of allenic and propargylic mercurials in organic synthesis and hope to report on these shortly.

**Acknowledgment.** We gratefully acknowledge the National Institutes of Health (GM 24254) and the American Heart Association, Iowa Affiliate, for their generous financial support of this research.

---

(1) Larock, R. C.; Chow, M.-S. *Tetrahedron Lett.* **1984**, *25*, 2727.  
(2) "The Chemistry of the Allenes"; Landor, S. R., Ed.; Academic Press: 1982; Vol. 1, pp 75-93.  
(3) Westmijze, H.; Kleijn, H.; Bos, H. J. T.; Vermeer, P. *J. Organomet. Chem.* **1980**, *199*, 293.  
(4) Simo, M.; Sipeuhou, J. A.; Lequan, M. *J. Organomet. Chem.* **1972**, *35*, C23.

---

(5) Flood, T.; Peterson, P. E. *J. Org. Chem.* **1980**, *45*, 5006.  
(6) Corey, E. J.; Kang, J. *J. Am. Chem. Soc.* **1981**, *103*, 4618.  
(7) Corey, E. J.; Kang, J. *Tetrahedron Lett.* **1982**, *23*, 1651.  
(8) Corey, E. J.; Raju, N. *Tetrahedron Lett.* **1983**, *24*, 5571.  
(9) Corey, E. J.; De, B. *J. Am. Chem. Soc.* **1984**, *106*, 2735.  
(10) Larock, R. C. "Organomercury Compounds in Organic Synthesis"; Springer-Verlag: New York, 1985; Chapter 3.

# Additions and Corrections

A. L. Wayda,\* J. L. Dye, and R. D. Rogers: Divalent Lanthanoid Synthesis in Liquid Ammonia. 1. The Synthesis and X-ray Crystal Structure of  $(C_5Me_5)_2Yb(NH_3)(THF)$ . 1984, 3, 1605-1610.

Several minus signs have been inadvertently omitted from the published coordinates in Table II, page 1608. The corrected table is given below.

**Table II. Final Fractional Coordinates for  $(C_5Me_5)_2Yb(NH_3) \cdot OC_4H_8$**

atom	<i>x/a</i>	<i>y/h</i>	<i>z/c</i>
Yb(1)	0.39318 (5)	0.43895 (8)	0.5000
Yb(2)	0.62487 (5)	0.03094 (8)	0.4550 (1)
X(1) <sup>a</sup>	0.360 (1)	0.470 (2)	0.342 (2)
X(2)	0.450 (1)	0.482 (2)	0.501 (3)
O(2)	0.643 (1)	0.103 (2)	0.598 (2)
N(2)	0.548 (1)	0.146 (2)	0.424 (2)
C(1)	0.441 (2)	0.280 (2)	0.533 (2)
C(2)	0.437 (2)	0.278 (2)	0.440 (2)
C(3)	0.477 (2)	0.344 (3)	0.404 (3)
C(4)	0.506 (1)	0.377 (2)	0.475 (2)
C(5)	0.481 (2)	0.334 (3)	0.560 (3)
C(6)	0.410 (2)	0.208 (3)	0.587 (3)
C(7)	0.396 (2)	0.219 (3)	0.380 (3)
C(8)	0.491 (2)	0.355 (3)	0.312 (3)
C(9)	0.558 (2)	0.428 (3)	0.467 (3)
C(10)	0.508 (3)	0.349 (4)	0.659 (4)
C(11)	0.276 (2)	0.466 (3)	0.531 (3)
C(12)	0.291 (2)	0.396 (3)	0.582 (3)
C(13)	0.325 (2)	0.415 (3)	0.653 (3)
C(14)	0.334 (2)	0.500 (3)	0.653 (3)
C(15)	0.311 (2)	0.540 (3)	0.590 (3)
C(16)	0.236 (4)	0.524 (6)	0.466 (8)
C(17)	0.258 (3)	0.307 (4)	0.529 (6)
C(18)	0.340 (3)	0.377 (5)	0.741 (6)
C(19)	0.360 (3)	5.553 (4)	0.731 (5)
C(20)	0.293 (4)	0.634 (6)	0.573 (7)
C(21)	0.339 (4)	0.415 (6)	0.284 (6)
C(22)	0.340 (3)	0.454 (4)	0.197 (5)
C(23)	0.328 (3)	0.545 (5)	0.219 (5)
C(24)	0.358 (3)	0.559 (5)	0.298 (5)
C(21)	0.479 (4)	0.613 (6)	0.413 (6)
C(22)	0.479 (4)	0.713 (7)	0.445 (8)
C(23)	0.509 (4)	0.681 (6)	0.551 (7)
C(24)	0.469 (3)	0.626 (5)	0.569 (5)
C(25)	0.603 (1)	-0.121 (2)	0.544 (3)
C(26)	0.601 (1)	-0.142 (2)	0.453 (3)
C(27)	0.551 (2)	-0.107 (2)	0.409 (3)
C(28)	0.521 (1)	-0.060 (2)	0.485 (3)
C(29)	0.550 (2)	-0.071 (2)	0.563 (3)
C(30)	0.647 (2)	-0.162 (3)	0.617 (4)
C(31)	0.640 (2)	-0.207 (3)	0.401 (3)
C(32)	0.534 (2)	-0.115 (3)	0.313 (4)
C(33)	0.461 (2)	-0.019 (3)	0.446 (4)
C(34)	0.532 (2)	-0.043 (3)	0.659 (3)
C(35)	0.673 (2)	0.097 (3)	0.296 (3)
C(36)	0.695 (2)	0.149 (3)	0.363 (3)
C(37)	0.733 (2)	0.102 (2)	0.417 (3)
C(38)	0.731 (2)	0.016 (3)	0.378 (3)
C(39)	0.692 (2)	0.018 (3)	0.300 (3)
C(40)	0.631 (2)	0.132 (4)	0.225 (4)
C(41)	0.685 (2)	0.250 (3)	0.381 (3)
C(42)	0.775 (2)	0.128 (3)	0.490 (4)
C(43)	0.779 (3)	-0.058 (4)	0.392 (5)
C(44)	0.687 (2)	-0.050 (3)	0.232 (4)
C(45)	0.614 (2)	0.185 (3)	0.631 (3)
C(46)	0.624 (4)	0.185 (5)	0.731 (6)
C(47)	0.653 (5)	0.108 (7)	0.762 (8)
C(48)	0.672 (2)	0.076 (4)	0.677 (4)
C(46)	0.649 (3)	0.216 (5)	0.701 (6)
C(47)	0.681 (4)	0.150 (6)	0.721 (6)

<sup>a</sup> X(1) and X(2) correspond to the two disordered O and N positions in molecule 1 (see Experimental Section).



# Additions and Corrections

A. L. Wayda,\* J. L. Dye, and R. D. Rogers: Divalent Lanthanoid Synthesis in Liquid Ammonia. 1. The Synthesis and X-ray Crystal Structure of  $(C_5Me_5)_2Yb(NH_3)(THF)$ . 1984, 3, 1605-1610.

Several minus signs have been inadvertently omitted from the published coordinates in Table II, page 1608. The corrected table is given below.

**Table II. Final Fractional Coordinates for  $(C_5Me_5)_2Yb(NH_3) \cdot OC_4H_8$**

atom	<i>x/a</i>	<i>y/h</i>	<i>z/c</i>
Yb(1)	0.39318 (5)	0.43895 (8)	0.5000
Yb(2)	0.62487 (5)	0.03094 (8)	0.4550 (1)
X(1) <sup>a</sup>	0.360 (1)	0.470 (2)	0.342 (2)
X(2)	0.450 (1)	0.482 (2)	0.501 (3)
O(2)	0.643 (1)	0.103 (2)	0.598 (2)
N(2)	0.548 (1)	0.146 (2)	0.424 (2)
C(1)	0.441 (2)	0.280 (2)	0.533 (2)
C(2)	0.437 (2)	0.278 (2)	0.440 (2)
C(3)	0.477 (2)	0.344 (3)	0.404 (3)
C(4)	0.506 (1)	0.377 (2)	0.475 (2)
C(5)	0.481 (2)	0.334 (3)	0.560 (3)
C(6)	0.410 (2)	0.208 (3)	0.587 (3)
C(7)	0.396 (2)	0.219 (3)	0.380 (3)
C(8)	0.491 (2)	0.355 (3)	0.312 (3)
C(9)	0.558 (2)	0.428 (3)	0.467 (3)
C(10)	0.508 (3)	0.349 (4)	0.659 (4)
C(11)	0.276 (2)	0.466 (3)	0.531 (3)
C(12)	0.291 (2)	0.396 (3)	0.582 (3)
C(13)	0.325 (2)	0.415 (3)	0.653 (3)
C(14)	0.334 (2)	0.500 (3)	0.653 (3)
C(15)	0.311 (2)	0.540 (3)	0.590 (3)
C(16)	0.236 (4)	0.524 (6)	0.466 (8)
C(17)	0.258 (3)	0.307 (4)	0.529 (6)
C(18)	0.340 (3)	0.377 (5)	0.741 (6)
C(19)	0.360 (3)	5.553 (4)	0.731 (5)
C(20)	0.293 (4)	0.634 (6)	0.573 (7)
C(21)	0.339 (4)	0.415 (6)	0.284 (6)
C(22)	0.340 (3)	0.454 (4)	0.197 (5)
C(23)	0.328 (3)	0.545 (5)	0.219 (5)
C(24)	0.358 (3)	0.559 (5)	0.298 (5)
C(21)	0.479 (4)	0.613 (6)	0.413 (6)
C(22)	0.479 (4)	0.713 (7)	0.445 (8)
C(23)	0.509 (4)	0.681 (6)	0.551 (7)
C(24)	0.469 (3)	0.626 (5)	0.569 (5)
C(25)	0.603 (1)	-0.121 (2)	0.544 (3)
C(26)	0.601 (1)	-0.142 (2)	0.453 (3)
C(27)	0.551 (2)	-0.107 (2)	0.409 (3)
C(28)	0.521 (1)	-0.060 (2)	0.485 (3)
C(29)	0.550 (2)	-0.071 (2)	0.563 (3)
C(30)	0.647 (2)	-0.162 (3)	0.617 (4)
C(31)	0.640 (2)	-0.207 (3)	0.401 (3)
C(32)	0.534 (2)	-0.115 (3)	0.313 (4)
C(33)	0.461 (2)	-0.019 (3)	0.446 (4)
C(34)	0.532 (2)	-0.043 (3)	0.659 (3)
C(35)	0.673 (2)	0.097 (3)	0.296 (3)
C(36)	0.695 (2)	0.149 (3)	0.363 (3)
C(37)	0.733 (2)	0.102 (2)	0.417 (3)
C(38)	0.731 (2)	0.016 (3)	0.378 (3)
C(39)	0.692 (2)	0.018 (3)	0.300 (3)
C(40)	0.631 (2)	0.132 (4)	0.225 (4)
C(41)	0.685 (2)	0.250 (3)	0.381 (3)
C(42)	0.775 (2)	0.128 (3)	0.490 (4)
C(43)	0.779 (3)	-0.058 (4)	0.392 (5)
C(44)	0.687 (2)	-0.050 (3)	0.232 (4)
C(45)	0.614 (2)	0.185 (3)	0.631 (3)
C(46)	0.624 (4)	0.185 (5)	0.731 (6)
C(47)	0.653 (5)	0.108 (7)	0.762 (8)
C(48)	0.672 (2)	0.076 (4)	0.677 (4)
C(46)	0.649 (3)	0.216 (5)	0.701 (6)
C(47)	0.681 (4)	0.150 (6)	0.721 (6)

<sup>a</sup> X(1) and X(2) correspond to the two disordered O and N positions in molecule 1 (see Experimental Section).